NBS SPECIAL PUBLICATION 581

U.S. DEPARTMENT OF COMMERCE / National Bureau of Standards

Radon in Buildings

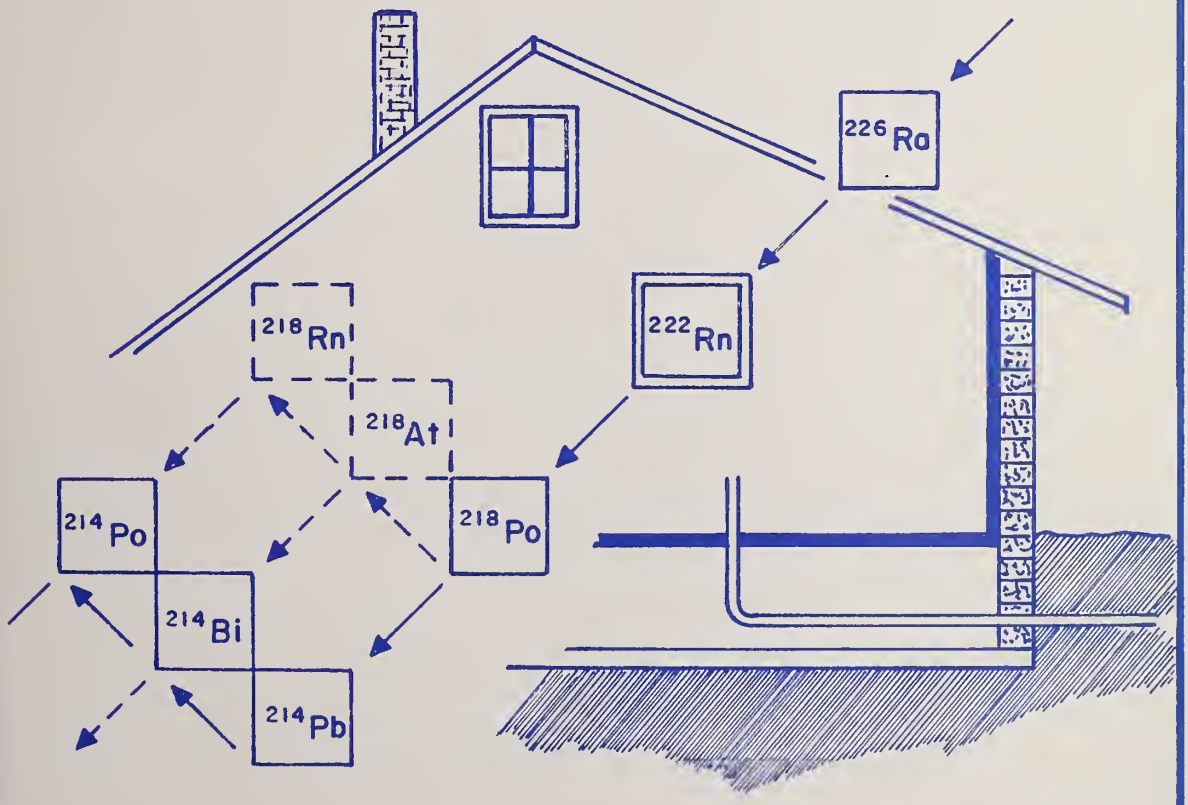

NATIONAL BUREAU OF STANDARDS

The National Bureau of Standards[1] was established by an act of Congress on March 3, 1901. The Bureau's overall goal is to strengthen and advance the Nation's science and technology and facilitate their effective application for public benefit. To this end, the Bureau conducts research and provides: (1) a basis for the Nation's physical measurement system, (2) scientific and technological services for industry and government, (3) a technical basis for equity in trade, and (4) technical services to promote public safety. The Bureau's technical work is performed by the National Measurement Laboratory, the National Engineering Laboratory, and the Institute for Computer Sciences and Technology.

THE NATIONAL MEASUREMENT LABORATORY provides the national system of physical and chemical and materials measurement; coordinates the system with measurement systems of other nations and furnishes essential services leading to accurate and uniform physical and chemical measurement throughout the Nation's scientific community, industry, and commerce; conducts materials research leading to improved methods of measurement, standards, and data on the properties of materials needed by industry, commerce, educational institutions, and Government; provides advisory and research services to other Government agencies; develops, produces, and distributes Standard Reference Materials; and provides calibration services. The Laboratory consists of the following centers:

Absolute Physical Quantities[2] — Radiation Research — Thermodynamics and Molecular Science — Analytical Chemistry — Materials Science.

THE NATIONAL ENGINEERING LABORATORY provides technology and technical services to the public and private sectors to address national needs and to solve national problems; conducts research in engineering and applied science in support of these efforts; builds and maintains competence in the necessary disciplines required to carry out this research and technical service; develops engineering data and measurement capabilities; provides engineering measurement traceability services; develops test methods and proposes engineering standards and code changes; develops and proposes new engineering practices; and develops and improves mechanisms to transfer results of its research to the ultimate user. The Laboratory consists of the following centers:

Applied Mathematics — Electronics and Electrical Engineering[2] — Mechanical Engineering and Process Technology[2] — Building Technology — Fire Research — Consumer Product Technology — Field Methods.

THE INSTITUTE FOR COMPUTER SCIENCES AND TECHNOLOGY conducts research and provides scientific and technical services to aid Federal agencies in the selection, acquisition, application, and use of computer technology to improve effectiveness and economy in Government operations in accordance with Public Law 89-306 (40 U.S.C. 759), relevant Executive Orders, and other directives; carries out this mission by managing the Federal Information Processing Standards Program, developing Federal ADP standards guidelines, and managing Federal participation in ADP voluntary standardization activities; provides scientific and technological advisory services and assistance to Federal agencies; and provides the technical foundation for computer-related policies of the Federal Government. The Institute consists of the following centers:

Programming Science and Technology — Computer Systems Engineering.

[1]Headquarters and Laboratories at Gaithersburg, MD, unless otherwise noted; mailing address Washington, DC 20234.
[2]Some divisions within the center are located at Boulder, CO 80303.

Radon in Buildings

Proceedings of a Roundtable Discussion of Radon in Buildings held at the National Bureau of Standards, Gaithersburg, Maryland, June 15, 1979

Edited by

R. Collé

Center for Radiation Research
National Measurement Laboratory
National Bureau of Standards
Washington, D.C. 20234

Preston E. McNall, Jr.

Center for Building Technology
National Engineering Laboratory
National Bureau of Standards
Washington, D.C. 20234

Organized by
National Bureau of Standards

U.S. DEPARTMENT OF COMMERCE, Philip M. Klutznick, Secretary

Luther H. Hodges, Jr., Deputy Secretary
Jordan J. Baruch, Assistant Secretary for Productivity, Technology and Innovation

NATIONAL BUREAU OF STANDARDS, Ernest Ambler, Director

Issued June 1980

Library of Congress Catalog Card Number: 80-600069

National Bureau of Standards Special Publication 581
Nat. Bur. Stand. (U.S.), Spec. Publ. 581, 84 pages (June 1980)
CODEN: XNBSAV

U.S. GOVERNMENT PRINTING OFFICE
WASHINGTON: 1980

For sale by the Superintendent of Documents, U.S. Government Printing Office, Washington, D.C. 20402
Price $3.75
(Add 25 percent additional for other than U.S. mailing)

PREFACE

During the past few years, potential health hazards of radiation exposure due to radon in buildings have received increasing attention. Many studies have indicated that indoor concentrations of radon and its radioactive-daughter products are frequently higher than outdoor concentrations. At the same time, there is an increasing interest in energy conservation in buildings including strategies such as reducing air exchange rates which may result in elevated radiation levels. It is becoming clear that radiation protection and building technology are in some cases interdependent. Radiation protection should be considered in building designs; similarly, known building technologies should be considered in the control of elevated indoor radon levels.

As a result of these concerns, a Roundtable Discussion of Radon in Buildings, jointly organized by the NBS Center for Radiation Research and the Center for Building Technology, was held June 15, 1979 at the National Bureau of Standards in Gaithersburg, Maryland. Participants included individuals with programmatic as well as scientific and technical expertise in radiation protection, radiation measurement and building technology areas. They represented a wide range of private and government institutions with diverse radiation and building technology interests.

The objective of the meeting was to bring together these participants to exchange information and to draw attention to some of the problems and research needs, and provide a forum for a general discussion of radon in buildings. Topics that were considered include: (1) the sources and pathways of radon in buildings; (2) diffusion and interaction properties and the distribution of daughter products on aerosols; (3) the biological and health effects; (4) measurement methods; and (5) strategies to minimize indoor levels of radon, such as increased ventilation and selection and treatment of building materials.

The program consisted of five review papers, twenty brief reports from some of the participants on their current research activities and interests, and the roundtable discussion. This publication contains the review papers, summaries of the brief reports, and edited summary of the roundtable discussion. The papers and summaries are printed in the order in which they were presented. The roundtable discussion session of the meeting was recorded for subsequent analysis and use in preparing the summary. Apart from a few minor changes, the papers and summaries are essentially those submitted by the speakers as the final versions of their presentations. The editors apologize for any inadvertent mistakes. For additional information on the presentations, contact the speakers directly.

Certain commercial equipment, instruments and materials are identified in this report in order to adequately specify experimental procedure. In no case does such identification imply recommendation or endorsement by the National Bureau of Standards, nor does it imply that the material or equipment identified is necessarily the best available for the purpose.

The roundtable discussion and this subsequent report would not have been possible without the guidance and encouragement of Elmer H. Eisenhower. The editors also gratefully acknowledge the excellent secretarial assistance of Karen Fritz, Jennifer Wright and Edythe Kramer in organizing and arranging the meeting and in preparing this report, and the assistance of the National Bureau of Standards Technical Information and Publications Division in the preparation and publication of this report. Lastly, the editors wish to thank the authors and participants of the roundtable discussion for their enthusiasm, lively discussion, and contributions to this report.

R. Collé
Center for Radiation Research

Preston E. McNall, Jr.
Center for Building Technology

ABSTRACT

This is the proceedings of a Roundtable Discussion of Radon in Buildings held June 15, 1979 at the National Bureau of Standards in Gaithersburg, Maryland. The meeting brought together a number of participants with diverse interdisciplinary interests in radiation protection, radiation measurement and building technology, provided a forum to exchange information, and drew attention to some of the problems and research needs associated with radiation exposure due to radon in buildings. Emphasis was placed on (1) the characterization of the sources and pathways of radon in buildings; (2) the biological and health effects; (3) measurement considerations; and (4) strategies and control technologies to minimize indoor radiation exposure.

Key Words: Buildings; environment; health; measurements; radiation; radon; radon daughters; ventilation.

TABLE OF CONTENTS

LIST OF PARTICIPANTS

P. R. Achenbach
Center for Building Technology
National Bureau of Standards
Washington, DC 20234

H. Ward Alter
Terradex Corp.
Walnut Creek, CA 94598

Jan Beyea
Center for Environmental Studies
Princeton University
Princeton, NJ 08540

David E. Brackett
Gypsum Association
1120 Connecticut Ave., NW
Suite 940
Washington, DC 20036

A. J. Breslin
Environmental Measurements Laboratory
Department of Energy
376 Hudson St.
New York, NY 10014

L. Cavallo
Center for Radiation Research
National Bureau of Standards
Washington, DC 20234

Olivia Chatard
National Measurements Laboratory
National Bureau of Standards
Washington, DC 20234

R. Collé
Center for Radiation Research
National Bureau of Standards
Washington, DC 20234

Arthur E. Desrosiers
Radiation Standards and Engineering
Battelle Pacific Northwest Laboratories
Battelle Boulevard
Richland, WA 99352

Roger S. Eaton
Radioactivity Remedial Action Group
Atomic Energy Control Board
P.O. Box 1046
Ottawa, Canada K1P 5S9

Norman Eisenberg
Office of Standards Development
Nuclear Regulatory Commission
Washington, D.C. 20555

E. H. Eisenhower
Center for Radiation Research
National Bureau of Standards
Washington, DC 20234

Stewart Farber
Nuclear Information Department
New England Power
280 Melrose Street
Providence, RI 02901

W. O. Findlay
DSMA/Acres
c/o 27 Columbia Walk
Elliot Lake
Ontario, Canada

James A. Frazier
National Research Council-National
Academy of Sciences
2101 Constitution Avenue, NW
Washington, DC 20418

Thomas F. Gesell
University of Texas School of Public Health
P. O. Box 20186
Houston, TX 77025

Daniel Golas
Center for Radiation Research
National Bureau of Standards
Washington, DC 20234

Peter G. Groer
Institute for Energy Analysis
P. O. Box 117
Oak Ridge, TN 37830

Fred Haywood
Building 7505
P. O. Box X
Oak Ridge National Laboratory
Oak Ridge, TN 37830

Thomas Hess
Department of Physics
Bennett Hall
University of Maine
Orono, ME 04469

Robert Horton
Health Effects Research Laboratory
Environmental Protection Agency, MD-70
Research Triangle Park, NC 27711

Charles M. Hunt
Center for Building Technology
National Bureau of Standards
Washington, DC 20234

Ken G. W. Inn
Center for Radiation Research
National Bureau of Standards
Washington, D.C. 20234

Raymond Johnson
Environmental Protection Agency
Office of Radiation Programs
401 M Street, SW
ANR-461
Washington, DC 20460

Neils Jonassen
Laboratory of Applied Physics
Technical University of Denmark
Building 307
DK-2800 Lyngby, Denmark

Harlan W. Keaton
Polk County Health Department
P. O. Box 1480
Winter Haven, FL 33880

Donald J. Keefe
Electronics Division (Bldg. 818)
Argonne National Laboratory
9700 South Cass Avenue
Argonne, IL 60439

Tamami Kusuda
Center for Building Technology
National Bureau of Standards
Washington, DC 20234

Wayne M. Lowder
Department of Energy
Office of Health and Environmental Research
Washington, D.C. 20545
and
Environmental Measurements Laboratory
New York, NY 10014

Gene McDowell
Center for Consumer Product Technology
National Bureau of Standards
Washington, DC 20234

Preston E. McNall, Jr.
Center for Building Technology
National Bureau of Standards
Washington, DC 20234

Donald A. Morken
Department of Radiation Biology and Biophysics
University of Rochester
Rochester, NY 14627

Sallie S. Morse
Geomet, Inc.
15 Firstfield Road
Gaithersburg, MD 20760

Chuck Muller
Purifill, Inc.
P. O. Box 3103
Wayne, NJ 07470
Corp Hdqtrs:
P. O. Box 80434
Chamblee, GA 30341

John Nagy
Biomedical and Environmental
Assessment Division
Brookhaven National Laboratory
Upton, NY 11973

Neal Nelson
Criteria and Standards Division
Office of Radiation Programs
Environmental Protection Agency
Washington, DC 20460

William Nazaroff
Ventilation Program
Lawrence Berkeley Laboratory
Building 90, Room 3058
Berkeley, CA 94720

James R. Noyce
Center for Radiation Research
National Bureau of Standards
Washington, DC 20234

K. Ochifuji
Center for Building Technology
National Bureau of Standards
Washington, DC 20234

Charles R. Phillips
Eastern Environmental Radiation Facility
Office of Radiation Programs
Environmental Protection Agency
P. O. Box 3009
Mongtomery, AL 36109

Allan C. B. Richardson
Federal Guidance Branch
Criteria and Standards Division
Office of Radiation Programs
Environmental Protection Agency
Washington, DC 20460

Charles E. Roessler
Department of Environmental Engineering Sciences
University of Florida
Gainesville, FL 32611

John Rundo
Radiological and Environmental Research
Argonne National Laboratory
9700 South Cass Avenue
Argonne, IL 60439

Samuel Silberstein
Center for Building Technology
National Bureau of Standards
Washington, DC 20234

Zachary A. Smith
Department of Environmental Engineering Sciences
University of Florida
Gainesville, FL 32601

Jan A. J. Stolwijk
J.B. Pierce Foundation
Yale University
290 Congress Ave.
New Haven, CT 06519

George T. Tamura
Division of Building Research
National Research Council of Canada
Ottawa, Ont., Canada K1A OR6

George Winzer
Department of Housing and Urban Development
Environmental Research
451 7th Street, SW
Washington, DC 20410

James E. Woods
Department of Mechanical Engineering
Iowa State University
Ames, IA 50011

National Bureau of Standards Special Publication 581, Proceedings of a Roundtable Discussion of Radon in Buildings held at NBS, Gaithersburg, Maryland, June 15, 1979. Issued June 1980

THE PHYSICS AND INTERACTION PROPERTIES OF RADON AND ITS PROGENY

R. Collé

Center for Radiation Research
National Bureau of Standards
Washington, D.C. 20234

This review summarizes the elementary physical and chemical properties of radon and its radioactive decay products. These properties govern their behavior in the environment and in buildings where they may concentrate and create potential human health hazards. Radon and its progeny, as intermediate decay products in the naturally-occurring long-lived primordial radioactive series, are characterized by a unique and complex behavior. The characteristics and properties are considered in describing the natural and "technologically enhanced" sources of radon, the radioactive decay relationships involved, the type and energy of the radiations emitted in the decay of radon, and the interactions of radon and its progeny in natural and building environments.

The element radon is a noble gas which has three naturally-occurring isotopes with mass numbers of 219, 220 and 222. All three are radioactive and have short halflives: ^{219}Rn, 3.96 seconds; ^{220}Rn, 55.6 seconds; ^{222}Rn, 3.82 days. Historically, they were named "actinon", "thoron" and "radium emanation", respectively[1]. The three radon isotopes occur in nature as intermediate decay products in the three radioactive series headed by the long-lived primordial radionuclides uranium-235 ("actinium"), thorium-232 and uranium-238. The ^{232}Th and ^{238}U decay series are illustrated in Figures 1 and 2. Natural uranium consists of 99.27 percent (by weight) ^{238}U and 0.73 percent ^{235}U. For this reason, the ^{235}U series is less important. Additionally, the decay products of ^{235}U, i.e., the subsequent radionuclides of the series (sometimes called

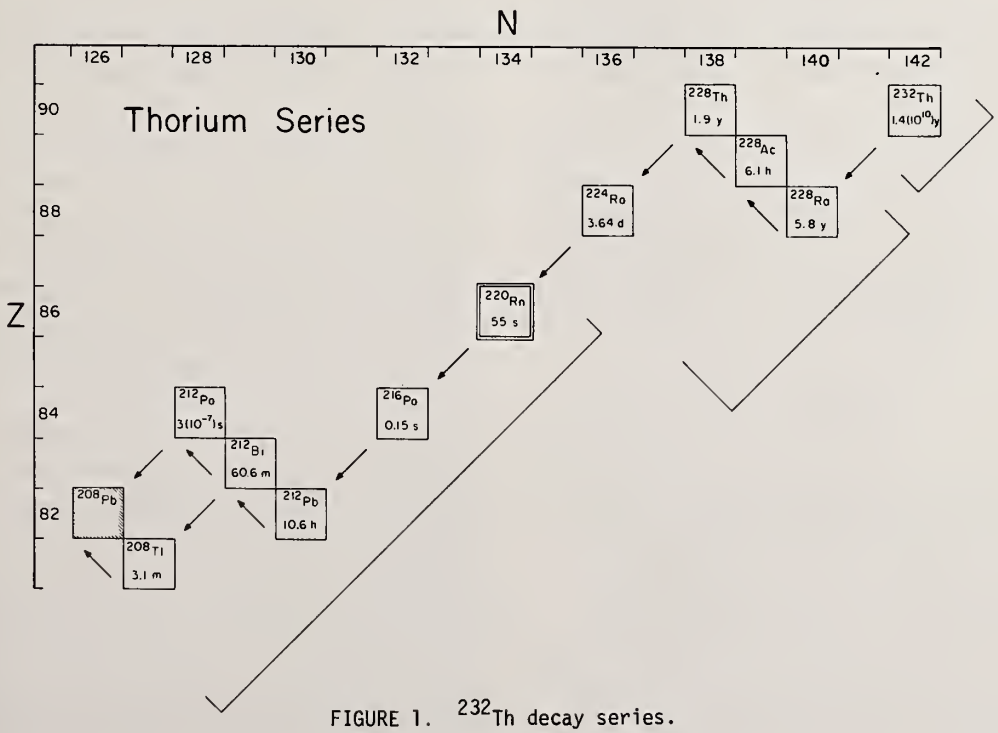

FIGURE 1. ^{232}Th decay series.

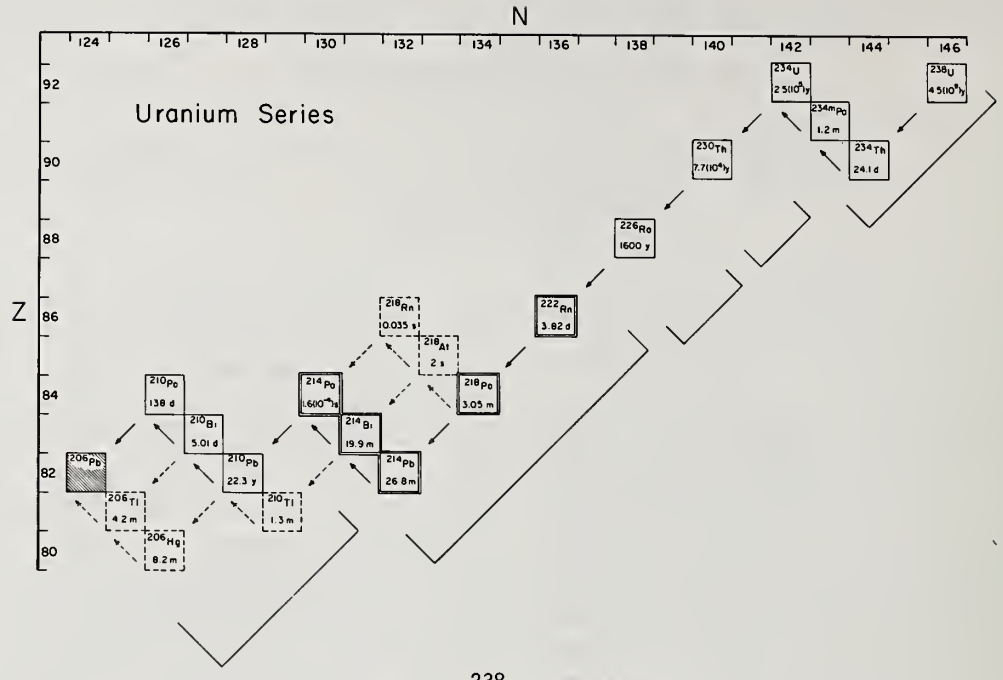

FIGURE 2. ^{238}U decay series.

decay "daughters" or "progeny"), have relatively short halflives and do not appear in the environment in significant concentrations[2]. Natural thorium consists entirely (100% abundance) of the isotope ^{232}Th. Therefore, both the decay series of ^{232}Th and ^{238}U are of importance as natural sources of radon.

The complexity of the naturally-occurring radioactive series arises because every isotope of every element with an atomic number greater than 83 (bismuth) is radioactive and decays primarily by either alpha or beta decay. Alpha decay (α) decreases the atomic number (Z) by two and the mass number (Z + N) by four units. Beta decay (β^-) increases the atomic number by one, but does not change the mass number (see Figures 1 and 2). Thus, the nucleus ^{232}Th with an atomic number of 90 and mass 232 emits 6 alpha particles and 4 β^- particles before it achieves stability and results in the stable lead isotope ^{208}Pb. This progression toward stability illustrated in Figures 1 and 2 is further complicated by branching decay so that the complete series, ignoring isomers, consist of 12 distinct nuclear species for the ^{232}Th series, and 20 for the ^{238}U series.

In alpha decay, the nucleus emits one or more α particles with discrete energies. Usually, an α particle of one energy value predominates. In β^- decay, on the other hand, the nucleus emits β^- particles which have a continuous spectrum of energies, ranging from near zero to a maximum value which is characteristic of the particular radionuclide. In either case, the decaying nucleus may not release all of the available decay energy, but may leave the product nucleus in an excited state from which it decays by some form of electromagnetic transition which is primarily by the emission of gamma rays. Thus, the decay of radionuclides in a naturally-occurring series may involve the emission of many different α particles, β^- particles and gamma rays. For example, the decay of the ^{222}Rn subseries shown in Figure 3 comprises three major and at least four other less intense α-particle transitions, over 50 different β^--particle transitions, and nearly 200 distinct gamma-ray transitions. The major radiations, their energies and intensities

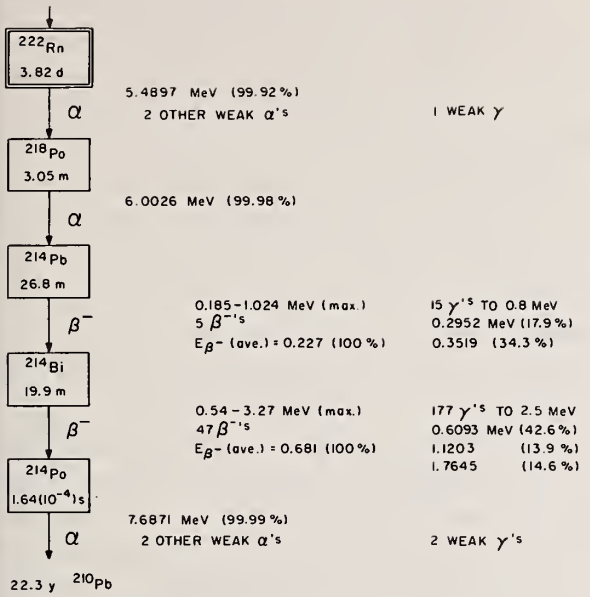

FIGURE 3. ^{222}Rn decay subseries.

for the naturally-occurring radioactive series have been summarized in a number of NCRP Reports [3, 4]. More complete tabulations are also available [5, 6].

If undisturbed by either chemical or physical processes, the radionuclides in a decay series attain a state of radioactive "equilibrium". Unlike chemical equilibrium, this state does not imply reversibility of reactions, nor does it describe a true "steady state" condition since the concentrations of the radionuclides continually change. In the case of a long-lived parent and short-lived daughter, equilibrium is achieved when the ratio of the decay rates of parent and daughter becomes constant. Contrary to what might be expected intuitively, how fast equilibrium occurs depends primarily upon the halflife of the daughter activity, and only secondarily on the halflife of the parent. Once equilibrium is established, however, both activities decay with the parent's halflife. In equilibrium, the daughter activity will be greater than the parent activity by the factor $T_1/(T_1-T_2)$ where T_1 and T_2 are the parent and daughter halflives, respectively. In the naturally-occurring radioactive series, at equilibrium, the decay rate of every radionuclide in a given series is very nearly equal to the decay rate of the radionuclide that heads the series.

The radionuclides in the ^{238}U and ^{232}Th series, however, rarely attain a state of equilibrium in the environment. The shorter-lived daughter radionuclides are more directly controlled by chemical or physical processes than by the halflife controlled genetic decay relationships. A state of "disequilibrium" in a decay chain occurs when the activities of the various radionuclides in the series exist in some arbitrary nonequilibrium ratio to each other. Such situations can arise when parent and daughter activities are chemically and physically different, and can be separated in nature by ordinary geological processes. This can include the selective leaching of minerals by ground water, the diffusion of radon, partitioning of substances in mixtures, as well as differences in electrostatic attraction, physical adsorption, and containment within minerals, rocks and soils.

The uranium series, headed by ^{238}U (Figure 2) is generally separated into five subseries[7] as a result of the different chemical and physical properties, and the sufficiently long halflives of the intermediate members. The members of the various subseries are designated in Figure 2. Within each subseries, the activities are generally near a state of radioactive equilibrium with the head of the subseries. Brief descriptions of the ^{238}U subseries, adapted from NCRP No. 45[7] follow:

(i) The first subseries consists of the two uranium isotopes ^{238}U and ^{234}U and the two intermediate radionuclides, ^{234}Th and ^{234m}Pa. The halflives of the intermediate members are too short to allow significant separation from the uranium isotopes. Although isotopic fractionation of uranium can occur in some soils and in sea water, ^{238}U and ^{234}U may be considered to be in radioactive equilibrium.

(ii) ^{230}Th comprises the second subseries. The relative chemical inertness of tetravalent thorium compounds compared to the tendency of uranium to exist in hexavalent oxidation states, and long ^{230}Th halflife permits separation from the uranium precursors. Significant disequilibrium can occur in oceans where thorium precipitates and is deposited in sedimentary layers.

(iii) The third subseries is composed of ^{226}Ra. It is frequently distributed differently than its precursors since radium is relatively mobile with respect to uranium and thorium. Except for certain ^{226}Ra "hot spots" of radium sulfate remaining from uranium deposits, radium rarely concentrates and is widely dispersed.

(iv) The fourth subseries includes ^{222}Rn and its progeny ^{218}Po, ^{214}Pb, ^{214}Bi, and ^{214}Po. Although radon accompanies radium in nature, as a noble gas, it can diffuse and migrate considerable distance from its parent. Radon is spontaneously liberated in varying extents from crystalline compounds and other solids containing radium. Relatively impervious minerals such as zircon lose very little of the radon formed in them, while open-lattice structures may lose most of their radon under natural conditions. The degree (fractional amount of radon that is missing) to which a mineral loses radon is called the "emanating power." Similarly, the rate of loss of radon from materials is called the "emanation rate". Radon is soluble in water and can be found in concentrations much greater than its radium parent. The short-lived decay products with halflives ranging from 26.8 minutes to 164 microseconds are readily ionized and attach to surfaces such as dust partices in air. Undisturbed, the subseries reaches radioactive equilibrium within a few hours.

(v) The fifth and final subseries starts with the long-lived ^{210}Pb and continues through ^{210}Bi and ^{210}Po where it finally terminates in stable ^{206}Pb.

The ^{232}Th series (Figure 1) has also been described in NCRP Report No. 45 [7]. The series is characterized by the long-lived ^{232}Th parent, and progeny which are all relatively short-lived. It may be considered in three subseries consisting of

(i) ^{232}Th itself, the least mobile radionuclide in the series;

(ii) the two radium isotopes ^{228}Ra and ^{224}Ra and the two intermediate members ^{228}Ac and ^{228}Th; and

(iii) the seven-radionuclide sequence starting with the inert noble gas ^{220}Rn and terminating in stable ^{208}Pb.

Generally, disequilibrium within the series does not occur to a large extent. Radioactive equilibrium occurs in the geologically short time of about 60 years if the members, particularly radium, do not migrate. Disequilibrium situations arise mainly at interfaces between soils, natural waters, natural gas and petroleum deposits, and the atmosphere.

The short halflife of ^{220}Rn (55 seconds) precludes significant migration from its natural sources. Therefore except in special situations where thorium-rich minerals like zircon and monazite are concentrated in placer deposits[8] such as sands on the Florida coast, ^{220}Rn (from the thorium series) is not as important as ^{222}Rn (from the uranium series) as a natural source of radon exposure. For this reason, the remainder of this review will focus on the ^{222}Rn subseries.

The naturally-occurring radionuclides in the ^{222}Rn subseries, whether undisturbed in the ambient background or technologically enhanced, can result in both external and internal exposure to human populations. As indicated in Figure 3, decay of the ^{222}Rn subseries radionuclides involves emission of both α and β^- particles as well as gamma radiation. For external exposure, the radionuclides of primary importance are ^{214}Pb and ^{214}Bi. In fact, the gamma rays of ^{214}Bi are the most abundant and energetic of the

uranium series. The greatest contribution to the external exposure is made by gamma radiation from these sources. The external radiation from α and β^- decay does not contribute significantly to the absorbed dose in the tissues and organs of man. Internal exposure, which is generally more hazardous, may arise, however, from inhalation or ingestion of the radionuclides. The major contribution to the internal dose comes from airborne α-emitting members of the ^{222}Rn subseries which account for about 45% of the alpha energy of the uranium series. Ambient air can be enriched in ^{222}Rn and its progeny because of emanation of the gaseous radon and its subsequent decay in the atmosphere. These radionuclides can be inhaled and contribute to the absorbed dose in lung tissue. Although the dose to the lung is most significant, the ^{222}Rn progeny are isotopes of lead, bismuth and polonium and can be translocated from the lung to other organs of the body [9].

Since the exposure to man from ^{222}Rn and its progeny will depend on the concentration and distribution of these radionuclides in man's environment, one must consider the radioactive decay and growth relationships involved in the ^{222}Rn subseries. The general mathematical forms of the decay and growth equations governing radioactive-series decay are often referred to as the "Bateman equations" [10]. The derivations are available in many standard texts [11], and only the results are summarized here.

The decay of a single radionuclide is given by

$$A(t) = A^{\circ} e^{-\lambda t}$$

where $A(t)$ is the activity of the radionuclide at any time t, A° is its activity at time $t=0$, and λ is the decay constant given by $\lambda = \ln 2/T$ where T is the characteristic halflife of the radionuclide. The activity of a radioactive daughter produced from decay of its parent is

$$A_2(t) = A_1^{\circ}\left[\frac{\lambda_2}{\lambda_2-\lambda_1}\right]\left(e^{-\lambda_1 t} - e^{-\lambda_2 t}\right) + A_2^{\circ} e^{-\lambda_2 t}$$

where subscripts 1 and 2 refer to parent and daughter, respectively. The second term in the above equation is that part of the daughter activity originally present at time $t=0$ which is still present at time t. If no daughter is present initially ($A_2^{\circ}=0$), this term is zero. The activity of a radioactive granddaughter can be expressed similarly. If parent 1 decays through daughter 2 to produce granddaughter 3, then (for the case of $A_2^{\circ}=A_3^{\circ}=0$) the granddaughter activity is

$$A_3(t) = A_1^{\circ}\left\{\frac{\lambda_2\lambda_3 e^{-\lambda_1 t}}{(\lambda_2-\lambda_1)(\lambda_3-\lambda_1)} + \frac{\lambda_2\lambda_3 e^{-\lambda_2 t}}{(\lambda_1-\lambda_2)(\lambda_3-\lambda_2)} + \frac{\lambda_2\lambda_3 e^{-\lambda_3 t}}{(\lambda_1-\lambda_3)(\lambda_2-\lambda_3)}\right\}$$

The above equations may be expressed generically for the $n^{\underline{th}}$ generation activity as

$$A_n(t) = A_1^{\circ}\sum_{i=1}^{n} C_i\, e^{-\lambda_i t}$$

where

$$C_i = \frac{\prod_{k=2}^{n}\lambda_k}{\prod_{j=1}^{n}(\lambda_j-\lambda_i)} \qquad (j\neq i).$$

For an initially pure source of ^{222}Rn, Figure 4 shows the growth and decay curves of the various members of the ^{222}Rn subseries computed from these equations. The daughter ^{218}Po grows in and reaches equilibrium with ^{222}Rn within about one half hour. The granddaughter ^{214}Pb

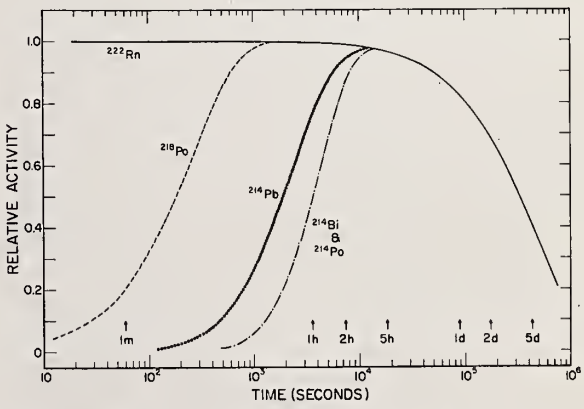

FIGURE 4. Decay of an initially pure source of Rn-222, and the subsequent growth and decay of its progeny.

achieves equilibrium within several hours, and is followed shortly thereafter by the ^{214}Bi and ^{214}Po progeny. As indicated earlier, the approach to equilibrium is controlled mainly by the half-lives of the progeny. Once equilibrium is achieved, the ^{222}Rn and progeny decay with the halflife of ^{222}Rn. From Figure 4 it is easy to see that disequilibrium activity ratios of progeny to ^{222}Rn will occur if a disturbing influence removes or depletes some of the ^{222}Rn progeny prior to the establishment of equilibrium.

Similarly, the growth and decay of the total α- and β^-- particle emission rates for an initially pure source of ^{222}Rn is illustrated in Figure 5. The decay of the ^{222}Rn subseries results in the ultimate emission of three α and two β^- particles for each ^{222}Rn radioactive decay. As a result, an undisturbed ^{222}Rn source of unit activity (s^{-1}) will achieve a maximum total α-emission rate approaching nearly 3 $\alpha \cdot s^{-1}$, and a maximum total β^--emission rate of nearly 2 $\beta^- \cdot s^{-1}$. Once equilibrium is achieved, the α- and β^--emission rates decrease with the halflife of ^{222}Rn. As before, the emission rates will also be altered by any perturbation or disturbing influence that removes or depletes the ^{222}Rn progeny.

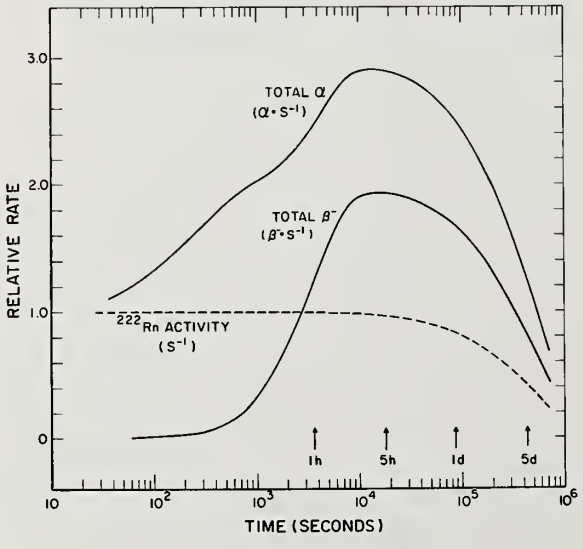

FIGURE 5. Growth and decay of the total α-and β^--particle emission rates for an initially pure source of Rn-222.

The dose to the human lung resulting from exposure to radon is predominately attributed to the α particles emitted in the decay of the ^{222}Rn progeny, and not that from the radon itself. At the same time, the occurrence of nonequilibrium mixtures of ^{222}Rn and progeny is common.[12-14] As a result, a unit of measurement called the "working level" (WL) was introduced in the late 1950s which takes account of the importance of the ^{222}Rn - progeny concentrations and the likely absence of radioactive equilibrium between ^{222}Rn and its progeny. The WL unit, which is now widely used for radiation protection, control and regulatory purposes, is defined as

> any combination of the short-lived radon progeny (^{218}Po, ^{214}Pb, ^{214}Bi and ^{214}Po) in one liter of air that will result in the ultimate emission of 1.3×10^5 MeV of alpha - particle energy.[15-16]

The numerical value of the WL (1.3×10^5 MeV per liter) is derived from the total α-particle energy ultimately emitted in the decay of the short-lived ^{222}Rn progeny that are in radioactive equilibrium with 100 picocuries of ^{222}Rn per liter of air. Table 1, adapted from Evans[16], illustrates the definition of the WL unit and the relevant numerical data. Although the numerical value of the WL unit is derived with the assumption of radioactive equilibrium (i.e., 100 $pCi \cdot L^{-1}$ of each ^{222}Rn progeny), the unit is applicable for any mixture of short-lived ^{222}Rn progeny including nonequilibrium situations. It is also important to remember that the WL is a concentration unit based on one liter of air which may be subject to density variations. The definition, interpretation and shortcomings of the WL unit have been excellently described by Evans[16]. When considering radiation exposure to the human lung from radon sources, the WL unit is presently the most useful single-parameter measure of the effective airborne radioactivity.

The relative contributions of the various progeny to the WL in an initially pure source of ^{222}Rn is shown in Figure 6. This growth in the WL can be compared to the growth of the ^{222}Rn progeny (Figure 4). The earliest contribution

TABLE 1

Definition of the "Working Level" (WL) Unit.

Nuclide	α-Particle Energy (MeV)	Half-Life	Number of Atoms per 100 pCi	Ultimate α-Particle Energy Per Atom (MeV)	Total Ultimate α-Particle Energy Per 100 pCi (MeV)	Percent of Total α-Particle Energy
^{222}Rn	5.490	3.8235 d	$1.763(10^6)$	excluded	--	--
^{218}Po	6.003	3.05 m	$9.768(10^2)$	6.003 +7.687	$0.1337(10^5)$	10.4%
^{214}Pb	0	26.8 m	$8.583(10^3)$	7.687	$0.6598(10^5)$	51.4%
^{214}Bi	0	19.9 m	$6.374(10^3)$	7.687	$0.4900(10^5)$	38.2%
^{214}Po	7.687	$1.643(10^{-4})$s	$8.770(10^{-4})$	7.687	$0.0000(10^5)$	0.0%
				TOTAL	$1.2835(10^5)$	100.0%
				CALLED	1.3×10^5 MeV	

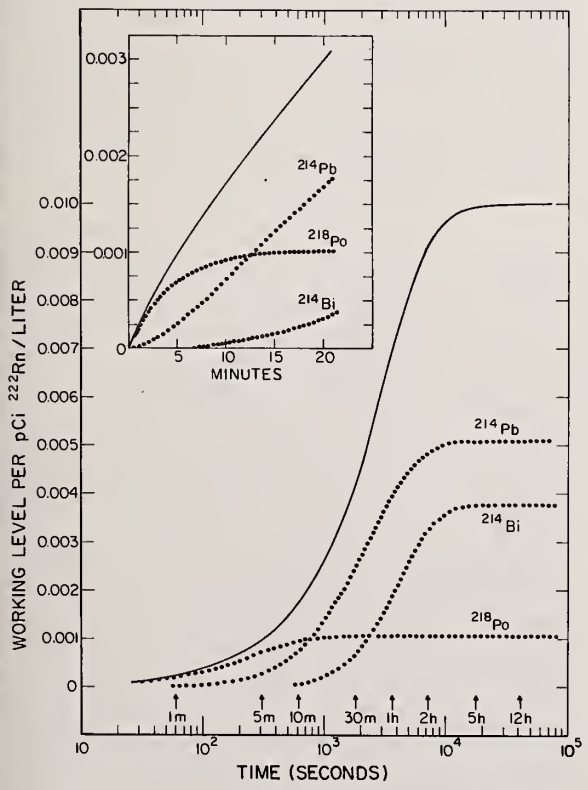

FIGURE 6. Growth of the WL for an initially pure source of Rn-222, and the relative contributions to it from the progeny.

to the WL is made by ^{218}Po, followed by ^{214}Pb, and finally by ^{214}Bi. A significant contribution to the WL by ^{214}Po is precluded by its extremely short halflife (Table 1). If the initially pure ^{222}Rn source remains undisturbed, the largest contributions to the WL are made by ^{214}Pb and ^{214}Bi which contribute 51% and 38% of the ultimate α- particle energy, respectively. As indicated in Figure 6, these relative contributions by the various progeny (last column, Table 1) will only be achieved after several hours. They may never be achieved if the radon is dispersed (such as by rapid air changes) before sufficient time has elapsed for the build-up of the progeny, or if the progeny are removed from the air (such as by filtration). In these situations, more significant contributions to the WL may be made by the first decay product, ^{218}Po. For example, Evans [16] compared the relative contribution of the ^{222}Rn progeny to the total α-particle energy for air of various "ages". The results for "3 min air" (i.e., a ^{222}Rn air sample that has had only 3 minutes in which to accumulate its radon progeny) and "10 min air" is compared to "equilibrium air" in Table 2.

TABLE 2

Percent of total α-particle energy contributed by the progeny of ^{222}Rn for various "air ages".

	^{218}Po	^{214}Pb	^{214}Bi
"3 min air"	83%	17%	0.5%
"10 min air"	54%	42%	4%
"equilib. air"*	10%	51%	38%

*See Table 1.

Before considering the factors influencing and causing these variations, as well as the important characteristics and interaction properties of the ^{222}Rn progeny, it may be useful to summarize the major sources of radon in the environment and in buildings.

Since very little radium is found in the atmosphere, essentially all radon is considered to originate from natural or disturbed terrestrial sources.[9,17] Radon, which originates from the decay of radium in soils, rocks and minerals, diffuses and emanates more or less rapidly depending on the porosity, and can become widely distributed before it decays. The vertical distribution and occurrence of ^{222}Rn and its progeny at various altitudes has been measured by many investigators (Cf., 1977 UNSCEAR report[17]). In general, radon concentrations decrease with increasing height. Based on a review of nearly 1000 measurements of the ^{222}Rn emanation rate from soils of various types at locations across the earth, Wilkening, et al[18] obtained a world-wide overall mean of 0.42 $pCi \cdot m^{-2} \cdot s^{-1}$ with a range from 0.006 to 1.4 $pCi \cdot m^{-2} \cdot s^{-1}$.

The emanation rate is influenced by the type, porosity, moisture content and temperature of the soil, and the atmospheric pressure and thermal stability of the ground air[19-25]. The rate is reduced when the ground is cold or frozen, when wet following heavy rainfall, by snow cover, and by increasing barometric pressure. Diurnal variations in the emanation rate are frequently observed with maxima at night and minima in the afternoon. The variations, which can range up to 100%, are caused by two opposing factors.[18] At night, emanation rate is increased because of upward convective flow which results from the temperature variations in the top soil layer. It can also be increased during daylight hours because of the greater turbulent mixing in the ground atmosphere. As a result, the diurnal fluctuations are considerably smoothed. Seasonal variations of the emanation rate are controlled by climatic conditions (snow cover, temperature, thermal stability, etc.).

The total world-wide release of ^{222}Rn has been estimated as 50 $Ci \cdot s^{-1}$ by Wilkening[18] and 75 $Ci \cdot s^{-1}$ by Harley[26], which leads to a total equilibrium activity of 25 to 40 million curies. Harley[26] has also calculated that this corresponds to an average surface air concentration of 70 $pCi \cdot m^{-3}$, and about 100 $pCi \cdot m^{-3}$ in the northern hemisphere. These values are in reasonable agreement with surface air measurements of ^{222}Rn concentrations (and those inferred from measurements of ^{222}Rn progeny concentrations). Average outdoor concentrations of ^{222}Rn are typically between 100 and 200 $pCi \cdot m^{-3}$[9,17,18]. in the northern hemisphere.

In addition to the truly natural sources, exposure to radon and its progeny may be enhanced by human activities or technology that redistributes the naturally-occurring terrestrial radionuclides. This source category, which has been termed "technologically enhanced natural radioactivity" (TENR)[27], is used to distinguish controllable natural radioactivity sources from those generally uncontrollable. Examples of activities that enhance naturally-occurring radiation include mining operations, well drilling and development, burning of fossil fuels, and the use of construction material containing radionuclides (e.g., granite, brick, concrete block). A number of these TENR sources of radon have been extensively studied over the past few years, and some will be briefly highlighted.

Coal[33-35]

Coal contains varying concentrations of

uranium, thorium and their radioactive progeny. In the U.S., the coal which is mined in the western states contains significantly higher amounts of uranium (0.001 to 0.1%) than coal mined in the north central and eastern regions (<0.001%).[28-30] Exposure to radon and its progeny can occur in several ways, one of which is during the mining process. Radon is released into the atmosphere during the exposure of coal seams as well as during the breakup of the coal being mined. In this case, the concentration of radon in the mine atmosphere depends not only on the uranium and thorium content of the coal, but also on the ventilation rate of the mine. The dominant area of radon emission from coal, however, occurs at power generating plants during the combustion process. With the exception of radon, which is released as a gas into the atmosphere, all other radionuclide emissions from coal combustion are associated with the discharge of fly ash.[32] This fly ash may contain radon progenitors, such as uranium or radium, which ultimately decay to radon. Other possible sources of radon dispersal include run off from fly ash storage and disposal areas, and the use of fly ash in construction material.[28]

Natural Gas[33-35]

Radon which is found in the same geological strata where natural gas production sites are located, diffuses from the strata into the wells where it is collected along with the natural gas. Based on a number of selected sites throughout the U.S., Johnson, et. al.[34] reported an overall average ^{222}Rn concentration in natural gas at production wells of 37 $pCi \cdot L^{-1}$. The natural gas processing and distribution network plays an important role in reducing the concentration of radon. The concentration is greatest at the wellhead and decreases with distance. In selected distribution lines, Johnson, et. al.[34] reported an overall average ^{222}Rn concentration of 23 $pCi \cdot L^{-1}$. Natural gas used in unvented appliances, such as kitchen ranges and space heaters, is a source of radon in buildings. Scant data exist on radon and its progeny concentrations resulting specifically from the use of natural gas in buildings.[34-35] Concentrations of radon remaining in the gas when it is used in buildings may vary widely as a result of many factors including the wellhead concentration, dilution, removal during processing, transmission time in the distribution line and reservoir storage time which reduce the concentrations by decay.[35]

Liquified Petroleum Gas[35-37]

Before natural gas is distributed to consumers it is processed to remove impurities and heavy hydrocarbons. Some of these hydrocarbons, particularly propane, are recovered and distributed under pressure as liquified petroleum gas (LPG). This process may remove up to 50% of the radon in natural gas,[35,37] but a substantial fraction of the radon will remain in the LPG which is sold by retailers for use in buildings. As in the case of natural gas, the further from the main processing areas, the lower the concentration of radon.[37]

Uranium Mining and Milling Wastes[38-49]

The two most common methods of obtaining uranium in the U.S. are by open-pit and underground mining. Open-pit mining produces the largest amount of waste because of stripping of the overburden from above the ore. For example, in Wyoming in 1974, 2.7 million tons of uranium ore were mined almost exclusively by open-pit, and 107 million tons of waste were generated. In Colorado, 1.2 million tons of ore were mined using underground methods, and only 1.2 million tons of waste were generated.[38] These waste products include solids, liquids and exhaust gases.[38,39] While underground mining produces less waste than strip or open-pit mining, it does expose miners to higher concentrations of radon and its progeny. After the ore is mined, it is sent to mills (usually located in the immediate area) where the uranium is extracted out of the ore, leaving large quantities of waste products called "mill tailings." These mill tailings contain almost all of the radium, thorium and their progeny which were originally present in the ore. Over the lifetime of a typical mill, 40 to 80 hectares (100 to 200

acres) of land may be committed to storing these tailings.[40] As of December, 1977, the magnitude of the tailings exceeded 110 million tons for the active, active standby, and inactive mills in the U.S.[38,40] Radon and radioactive particles containing radon progenitors are released into the atmosphere from the tailings piles as well as during the milling operations (from ore piles, during crushing, grinding and leaching).[38,39] In addition, radon may be dispersed into ground waters and nearby rivers by seepage from liquid waste ponds and by the leaching of tailings piles.

From 1953 to the mid 1960s, the use of uranium mill tailings for construction was common in several Colorado communities, particularly in Grand Junction and Durango. The tailings were used as landfill and backfill, and as aggregate in cement for many homes and commercial buildings. This practice was stopped in 1966 after the discovery that radon and radon-progeny levels inside these buildings were considerably elevated above those found in buildings without tailings. It became apparent that remedial action should be initiated, and guidelines were established by the Surgeon General for permissible radon-progeny levels in these buildings (Table 3).

TABLE 3

Surgeon General guidelines for buildings constructed on or with mill tailings[41].

Indoor WL	Recommendation
>0.05	remedial action indicated
0.01-0.05	remedial action may be suggested
<0.01	no action indicated

A broad survey identified 600 buildings (out of 15,000 surveyed) that have radon-progeny levels above the Surgeon General guidelines and, therefore, require removal of this material. The total cost of the remedial effort, including clean-up of mill tailings piles, will be in excess of $80 million.[42] Congressional concern prompted passage of legislation in the fall of 1978 giving the Nuclear Regulatory Commission authority to license and control mill tailings, and authorizing the Department of Energy to assist States in cleaning up a number of mill tailing sites.[43] The Canadian government has gone through similar experiences.[44]

Phosphate Mining, Milling and Reclaimed Lands[33, 50-64]

The phosphate mining and manufacturing industry as a source of radon is somewhat similar to the uranium mining situation. Phosphate rocks contain naturally occurring quantities of uranium, thorium and radium, which are redistributed among the various products, byproducts and wastes of this industry. The U.S. produces 40% of the total world production of phosphate rock and exports only 30% of the phosphate produced.[50] Over 80% of the total U.S. production occurs in central Florida with the remaining plants located primarily in the west.[51] Most of these plants produce fertilizer, phosphoric acid, and small quantities of elemental phosphorus.[52] Enhancement of natural radon levels occurs during the mining and milling operations, from the use of reclaimed lands, and from the use of various phosphate products and byproducts. These latter sources will be described in subsequent paragraphs.

Most phosphate is mined in an open-pit or strip-mining process. In order to reach the phosphate rock, miners must first remove a top layer called overburden (which ranges from a few decimeters to 12 meters thick) and a second layer known as the leach zone (which can be anywhere from a few decimeters to 1 or 2 meters).[52,53] The ore layer, or matrix, is then exposed and removed, and the top two layers are replaced but not necessarily in the order of occurrence. As a result, material from the leach zone, which has been found to have generally higher concentrations of ^{226}Ra than either the overburden or the ore matrix, is frequently placed at or near the surface[53] which results in increased radioactivity concentrations. Once the ore is removed from the ground, it is stacked, washed, and pumped in slurry form to the beneficiation plant where it is prepared for the mills by upgrading the P_2O_5 percentage. Most western phosphate does not require beneficiation, but it is necessary for

Florida ore. The beneficiation process, which is mainly by physical separation, produces marketable phosphate ore and two separated wastes: slimes which go to a slime pond for settling; and sand tailings which go to a tailings pile.[54] Approximately one ton each of slimes and tailings must be disposed of for each ton of marketable phosphate rock.[33] The rock is now ready for the milling process where it is either mixed with a solution of sulfuric acid and water to produce phosphoric acid and gypsum, or it is placed in an electric furnace along with silica and coke to form elemental phosphorus.[54] The phosphoric acid is further reacted with either ammonia or marketable phosphate rock to form ammonium phosphate or triple superphosphate, respectively, which are utilized in the production of fertilizer.

With respect to exposure to radon and its progeny, there are several problems associated with the mining and milling of phosphate ore and the subsequent redistribution of the naturally-occurring radionuclides. These problems involve the use of water, the accumulation of gypsum piles, and the disposition of reclaimed phosphate lands.

Water used in both the mining and milling processes contains significant quantities of the naturally-occurring radionuclides which are discharged along with the water into large settling ponds. During periods of heavy rains, the ponds, which are often 200 hectares (500 acres) or more, may overflow into nearby streams where the radioactivity is dispersed.

The second problem stems from the fact that phosphate milling involves the accumulation of massive gypsum piles (10 to 30 meters high).[54] This waste gypsum or phosphogypsum is currently stored at mill sites where the natural radionuclides present can be a source of exposure to the general population in much the same way as the uranium mill tailings piles. There is a potential use for this phosphogypsum in building materials, and this will be discussed shortly.

The third problem involves the use of reclaimed phosphate land for residential and commercial development. Over 40,000 hectares (100,000 acres) of land have been mined for phosphate rock in Florida. As of 1977, about 10,000 hectares (25,000 acres have been reclaimed for building purposes, farming and grazing.[51] Since the reclaimed lands are composed of overburden, leach zone material, ore matrix, sand tailings and slimes, they frequently contain ^{226}Ra concentrations of 10 to 30 $pCi \cdot g^{-1}$ which is substantially higher than the 0.1 to 3 $pCi \cdot g^{-1}$ typical of U.S. soils.[29] The increased levels of ^{226}Ra produce considerable quantities of ^{222}Rn which diffuses to the surface and through the foundations of buildings, which leads to a build-up of short-lived ^{222}Rn progeny in the indoor environments.[51] Elevated radioactivity levels on reclaimed lands and ^{222}Rn-progeny levels in buildings built on the land has been extensively investigated over the past few years by the State of Florida and the Environmental Protection Agency (EPA).[51-53, 57-59, 61-62] Recommendations for radiation protection in Florida phosphate lands have also been promulgated by the EPA.[63, 64]

Phosphate Products and Byproducts[33,50,65-68]

The use of phosphate products and byproducts constitutes another source of exposure to radon and its progeny. Two of these products-fertilizers and building materials-will be considered.

As indicated earlier, almost 80% of the phosphate rock mined in the U.S. is used to manufacture fertilizers. The use of phosphate-based fertilizers results in the redistribution of naturally-occurring radionuclides. All fertilizers contain varying quantities of radionuclides, principally members of the ^{238}U and ^{232}Th decay series. Typical radioactivity concentrations in various fertilizer materials made from Florida phosphates were reported by Guimond[50] and range from 1 to 60 $pCi \cdot g^{-1}$. In addition to occupational exposures resulting from the mining and manufacturing of the phosphate products,[55, 56, 59] there are several exposure pathways for the release of radon and radon progenitors to the environment which results from the use of fertilizers.[50, 65] These pathways include: 1) Plant uptake - There is some plant uptake of ^{238}U and ^{226}Ra depending upon solubility, crop, soil and

calcium concentration in the soil. The amount of radionuclide uptake was found to be minor.[50] The escalating use of fertilizers, however, may lead to increases in the radioactivity concentrations found in various crops. 2) Leaching and runoff - It is estimated that over four billion tons of sediment are annually lost to surface waters through erosion. About half of this loss results from agricultural uses, and contains approximately 4.5 million tons of phosphate.[50] Most of this runoff eventually reaches the oceans, but some may collect on river banks and basins where it would be available for plant uptake. Additionally, radionuclides present in the runoff may enter ground and surface water supplies. 3) Fertilizer application - Agricultural workers who apply fertilizer or who work in fields which have been recently fertilized are subject to both direct gamma radiation and to inhalation of radon and radon progeny released to the atmosphere. Considering the total amount of fertilizers applied over the last 80 years, estimates have been made of the exposure that could be received by a typical agricultural worker.[54] Certain states are heavy users of phosphate-based fertilizers[50] and both workers and the general public residing in agricultural areas in these states could receive higher exposures.

Considerable quantities of waste gypsum or phosphogypsum, one of the byproducts of the phosphate industry, are produced each year which must be disposed of in some way (one ton of marketable rock produces 0.6 ton of gypsum).[65] The estimated annual production of phosphogypsum in the U.S. from 1950 to 1973 increased from approximately 1.5 to nearly 24 million metric tons.[66] The ^{226}Ra content of this waste material is typically 30 $pCi \cdot g^{-1}$. The increased production of this waste gypsum has led to a growing interest in developing and using it in building materials. This would solve a number of disposal problems while at the same time creating new environmental ones. This phosphogypsum is being used in building materials in some European countries and Japan[66] although it is not a current practice in the U.S. Florida phosphogypsum was used in the manufacture of wallboard, partition blocks and plaster by at least one company during the eleven year period from 1935 to 1946.[66] The products were mainly distributed in northeastern states. From 1934 to December, 1978, the Tennessee Valley Authority sold waste gypsum and phosphate slag from their fertilizer facilities in Alabama to several concrete block manufacturers in southern states.[67] Annual distributions ranged from 5,000 to 70,000 tons of byproducts. Thousands of buildings in Idaho and Montana have also been reported to have been partly constructed with materials made with phosphate slags.[68]

Building Materials[33, 65, 69-71]

All building materials contain radioactivity that is inherent to the natural raw materials of which they are composed. In addition to building materials containing phosphogypsum, phosphate slag or other atypical higher-than-average concentrations of naturally-occurring radionuclides,[65] even materials of a completely natural origin (such as granite or pumice stone) are sources of radon. Concentrations of naturally-occurring radionuclides, principally ^{232}Th, ^{226}Ra and ^{40}K, in various types of building materials and their effect on indoor radiation levels has been studied in a number of countries. This literature was reviewed in 1975[71] and also summarized in the 1977 UNSCEAR report.[65]

Potable Water Supplies [33, 72-78]

^{226}Ra, ^{222}Rn and their progeny exist in varying concentrations in the groundwater throughout the country. Disequilibrium arising from migration of ^{238}U-series radionuclides via soil water was noted previously. In general, concentrations of ^{226}Ra in common groundwaters are typically 1000 times lower than ^{222}Rn because radon is relatively soluble in water.[73] The solubility of radon in water at atmospheric pressure decreases from 0.5 $L \cdot kg^{-1}$ at 0°C to approximately 0.1 $L \cdot kg^{-1}$ at 60°C.[74] Concentrations of ^{226}Ra may range from trace quantities to over 50 $pCi \cdot L^{-1}$, while ^{222}Rn may be found in concentrations exceeding 50,000 $pCi \cdot L^{-1}$,[33] Distributions of ^{222}Rn concentrations in water in the U.S. and some subregions have been

reported.[75] Population exposure to these radionuclides results from the use of private, commercial, agricultural, public and community groundwater supplies. The primary path of exposure is through ingestion by drinking the water.[75] A secondary exposure pathway is through inhalation of ^{222}Rn progeny. If the water is heated, aerated (such as in a shower head), or agitated (as in a washing machine), the radon is readily released into the atmosphere. Some limited studies have been made of ^{222}Rn-progeny concentrations in homes resulting from the use of tap water.[75-77] This subject is receiving increasing attention[78] since it may involve exposure to large segments of the population. Another possible exposure pathway is through crop uptake[73] which can result if these potable supplies are used for irrigation as they often are in small scale gardens and family farms. This pathway, however, would involve only limited segments of the population.

As indicated, there are a considerable number and variety of both natural and TENR sources of ^{222}Rn and its progeny to which man may be exposed. The primary source to the outdoor environment is by emanation of ^{222}Rn from the earth, but this may be enhanced by contributions from mill tailings piles, phosphate lands, the burning of coal, and other TENR sources. Indoors, the sources include building materials, soil surrounding the building foundation, water, natural gas, and infiltration of outdoor air.[79]

As the radon emanates from soil, water, building materials, etc. and disperses into the air, it is not accompanied by its heavy metal progeny which are relatively immobile. When the ^{222}Rn decays by α-particle emission, its daughter ^{218}Po (Figure 3) is formed as a recoiling positively-charged ion with a range in air of about 50 μm.[80] Initially, the ^{218}Po ion is most likely positively charged because of ionization of the atomic electrons by the emitted α-particle. These ions exhibit a high rate of diffusion in air,[81, 82] are fairly reactive, and interact very rapidly with water vapor, oxygen or other gases to alter their charge state or to form small molecular clusters.[79] Within a very short time, these clusters tend to become attached to aerosol particles suspended in the air (the mean lifetime existence as free unattached ions is of the order of 10 to 50 seconds).[81] The ^{218}Po may be either attached or unattached when it decays to the granddaughter ^{214}Pb. If unattached, the newly created ^{214}Pb undergoes a fate similar to that just described for the initial ^{218}Po. If the ^{218}Po is attached at the time of decay, the ^{214}Pb may, depending upon the size of the aerosol particle, either recoil deeper into the particle or disattach from the particle. This dynamic sequence of events continues throughout the progression of the ^{222}Rn-subseries decay.

The fraction of the activity of the short-lived ^{222}Rn progeny which is absorbed on aerosol particles is called the "attached fraction", and the fraction carried by the molecular clusters (or existing as free ions or atoms) is called the "unattached fraction."[79, 82] This distinction is important since the sizes of the clusters and aerosol particles are considerably different, and therefore do not deposit in the same region of the respiratory tract when inhaled.[79, 83-85] The fraction of unattached

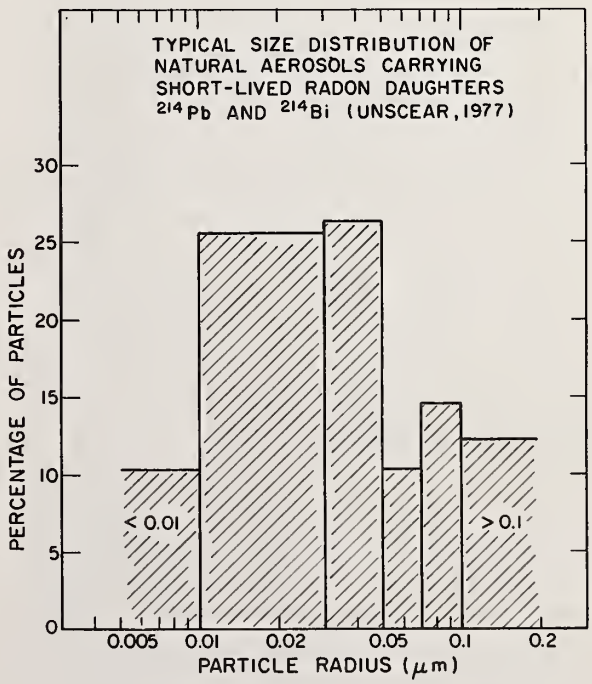

FIGURE 7.

progeny is, however, normally quite small (typically 5 to 10%).[79]

The size and specific gravity of the particles largely determine where the particles will be deposited in the respiratory system and the fate of the particles after deposition.[85] The size distribution of aerosol particles carrying ^{222}Rn progeny is dependent on the size distribution of the natural aerosol which is present. This size distribution is relatively constant[79] in both outdoor air and in the ambient atmosphere within typical buildings. The typical size distribution of aerosol particles carrying the short-lived ^{222}Rn progeny ^{214}Pb and ^{214}Bi is shown in Figure 7.[79, 86] As indicated, nearly 80% of the particles carrying the ^{214}Pb and ^{214}Bi have radii between 0.01 and 0.1 μm. These are mainly deposited in the pulmonary region,[83-85] in contrast to the progeny in the unattached fraction which are deposited in the upper respiratory tract. The implications of these particle size considerations in determining lung dose and the impact on respiratory cancer, particularly in uranium miners, have been discussed in a large number of studies.[83, 84, 87-91]

In assessing the potential radiation hazard due to ^{222}Rn and its progeny, the important factors include the degree of radioactive equilibrium between ^{222}Rn and its progeny, the relative attached and unattached fractions, and the aerosol particle size distributions. Each is time dependent and is influenced by a large number of variables. The levels of ^{222}Rn and its progeny within buildings and their dependence on both locally-dependent and time-dependent variables have been extensively studied by many investigators.[12, 16, 58, 80, 84, 92-108] Two of the most important variables are the ventilation rate[58, 84, 96, 97] and the plateout of the aerosol particles by deposition and adsorption on walls and surfaces.[90, 105, 107] Increased ventilation or high air change rates usually decreases aerosol particle concentrations within buildings, and at the same time decreases the residence time or "age" of the air. The net result is a greater degree of radioactive disequilibrium, an increase in the unattached fraction, a decrease in the WL, and a reduction in the dose to the lung. Source dependent or locally dependent factors[99], such as the type of building materials and the location of the building or rooms inside the building, also influence the levels of radon and its progeny in the room. The dependence of radon emanation rates on meteorological parameters was noted previously. These parameters, such as barometric pressure, wind speed, air and soil temperature, relative humidity, etc., similarly affect the concentrations of ^{222}Rn progeny in buildings.[92, 94, 98, 99, 103] Steinhäusler[99] evaluated the dependence on 24 meteorological variables, and found great daily and seasonal fluctuations in indoor radionuclide concentrations even under constant ventilation conditions. In general, because of the strong influence of these time dependent variables (e.g., the ventilation rate or meteorological effects), it is presently impossible to correlate the levels of radon and its progeny in buildings to the known radon sources or the locally dependent factors (e.g., the radium content of the building materials). As evidenced by just the titles of a number of studies that have been conducted in the past few years (cf., references 94-108), the effects of many of these variables have been studied either individually or several at a time. No detailed models exist, however, which can adequately predict the levels of radon and its progeny for given conditions or simultaneously treat all of the antecedent-consequent relationships that are involved.

This review has attempted to demonstrate that the sources and behavior of radon and its progeny are exceedingly complex. Inasmuch as "radon" may be the most serious problem we have in environmental radiation protection,[109] greater understanding and more complete solutions to this problem are urgently needed.

REFERENCES

1. Kirby, H.W. The Early History of Radiochemistry, Mound Laboratory Report MLM-1960, TID-4500, UC-4 Chemistry, Monsanto Research Corp., Miamisburg, Ohio, 1972.
2. National Council on Radiation Protection and Measurements, Natural Background Radiation in

the United States, NCRP Report No. 45, National Council on Radiation Protection and Measurements, Washington, D.C., 1975, pp. 3-7.

3. National Council on Radiation Protection and Measurements, Environmental Radiation Measurements, NCRP Report No. 50, National Council on Radiation Protection and Measurements, Washington, D.C., 1976, pp. 6-9.
4. National Council on Radiation Protection and Measurements. A Handbook of Radioactivity Measurements Procedures, NCRP Report No. 58, National Council on Radiation Protection and Measurements, Washington, D.C., 1978, Appendix A.3. This appendix contains a tabulation of atomic and nuclear data for some 200 radioactive nuclides from the Evaluated Nuclear Structure Data File of the Oak Ridge National Laboratory.
5. Cf., Nuclear Data Sheets, edited by Nuclear Data Project, Oak Ridge National Laboratory, Academic Press, New York, and other compilations using the Evaluated Nuclear Structure Data File (ENSDF) maintained at ORNL for the U.S. Nuclear Data Network.
6. Lederer, C.M. and Shirley, V.S. (eds.), Table of Isotopes, 7th Ed., Wiley, New York, 1978.
7. NCRP Report No. 45, op. cit., pp. 45-7.
8. Bell, K.G., Uranium and thorium in sedimentary rocks, Nuclear Geology, H. Faul (ed.), Wiley, New York, 1954, pp. 98-115.
9. NCRP Report No. 45, op. cit., p. 75f.
10. Bateman, H., The solution of a system of differential equations occurring in the theory of radioactive transformations, Proceedings Cambridge Philosophical Society 15, 423-7 (1910).
11. Evans, R.D., The Atomic Nucleus, McGraw-Hill, New York, 1955, pp. 470-510.
12. Tsivoglou, E.C., Ayer, H.E. and Holaday, D.A., Occurrence of nonequilibrium atmospheric mixtures of radon and its daughters, Nucleonics 11, No. 9, 40-5 (1953).
13. NCRP Report No. 45, op. cit., p. 83.
14. United Nations Scientific Committee on the Effects of Atomic Radiation (UNSCEAR), Sources and Effects of Ionizing Radiation, 1977 report to the General Assembly, United Nations, New York, 1977, pp. 76-8.
15. Federal Radiation Council, Guidance for the Control of Radiation Hazards in Uranium Mining, Staff Report of the Federal Radiation Council, Report No. 8 (revised), Washington, D.C., 1967, p. 11.
16. Evans, R.D., Engineers' guide to the elementary behavior of radon daughters, Health Phys. 17, 229-52 (1969).
17. UNSCEAR, 1977 report, op. cit., p. 72f.
18. Wilkening, M.H., Clements, W.E., and Stanley, D. Radon-222 flux measurements in widely separated regions, Natural Radiation Environment II, Adams, J.A.S., Lowder, W.M., and Gesell, T.F. (eds.), U.S. Energy Research and Development Administration report CONF-72-0805, Washington, D.C., 1972, pp. 717-30.
19. Pearson, J.E. and Jones, G.E., Emanation of radon-222 from soils and its use as a tracer, J. Geophys. Res. 70, 5279 (1965).
20. Israël, G.W., Meteorological influences on the thoron (Rn-220) content of the atmosphere, Tellus 18, 638 (1966).
21. Kraner, H.W., Schroeder, G.L. and Evans, R.D., Measurements of the effects of atmospheric variables on radon-222 flux and soil-gas concentrations, The Natural Radiation Environment, Adams, J.A.S. and Lowder, W.M. (eds.), Univ. Chicago Press, 1964, pp. 191-215.
22. Pritchin, B.P., Emanation of accumulated radon from heated rock minerals, Atomnaya Energiya 25, No. 4, 324-5 (1968). Translated in Soviet Atomic Energy.
23. Tanner, A.B., Radon migration in the ground: a review, The Natural Radiation Environment, op. cit., pp. 161-190.
24. Megumi, K. and Mamuro, T., Radon and thoron exhalation from the ground, J. Geophys. Res. 78, 1804-8 (1973).
25. Cox, W.M., Blanchard, R.L. and Kahn B., Relation of radon concentration in the atmosphere to total moisture detention in soil and atmospheric thermal stability,

Radionuclides in the Environment, Freiling, E.C. (ed.), Advances in Chemistry Series No. 93, American Chemical Society, Washington, D.C. (1970), pp. 436-46.

26. Harley, J.H., Environmental radon, Noble Gases, Stanley, R.E. and Moghissi, A.S. (eds.), U.S. Energy Research and Development Administration report CONF-73-0915, Washington, D.C., 1973, pp. 109-114.
27. Gesell, T.F. and Prichard, H.M., The technologically enhanced natural radiation environment, Health Phys 28, 361-6 (1975).
28. U.S. Environmental Protection Agency, Radiological Quality of the Environment in the United States: 1977, EPA 520/1-77-009, U.S. Environmental Protection Agency, Washington, D.C., 1979, pp. 90-7.
29. McBride, J.P., Moore, R.E., Witherspoon, J.P., and Blanco, R.E., Radiological impact of airborne effluents of coal and nuclear plants, Science 202, 1045-50 (1978).
30. UNSCEAR, 1977 report, op. cit., pp. 86-9.
31. Eisenbud, M., Environmental Radioactivity, 2nd. Ed., Academic Press, New York, 1973, pp. 197-8.
32. Lee, H., Peyton, T., Steele, R., and White, R., Potential Radioactive Pollutants Resulting From Expanded Energy Programs, U.S. Environmental Protection Agency report EPA-600/7-77-082, Washington, D.C., 1977.
33. Conference of Radiation Control Program Directors, Inc., Natural Radioactivity Contamination Problems, U.S. Environmental Protection Agency report EPA 520-4/77-015 Washington, D.C., 1978.
34. Johnson, Jr., R.H., Bernhardt, D.E., Nelson, N.S., Calley, Jr., H.W., Assessment of Potential Radiological Health Effects From Radon in Natural Gas, U.S. Environmental Protection Agency report EPA-520/1-73-004, Washington, D.C., 1973.
35. UNSCEAR, 1977 report, op. cit., pp. 92-3.
36. Gesell, T.F., Some radiological health aspects of radon-222 in liquified petroleum gas, Noble Gases, op. cit., pp. 612-629.
37. Gesell, T.F., Johnson, Jr. R.H. and Bernhardt, D.E., Assessment of potential radiological population health effects from radon in liquefied petroleum gas, U.S. Environmental Protection Agency report EPA-520/1-75-002, Washington, D.C., 1977.
38. EPA 520/1-77-009, op. cit., pp. 58-67; 133-142.
39. UNSCEAR, 1977 report, op. cit., pp. 166-170.
40. U.S. Environmental Protection Agency, Radiation Protection Activities, Annual Report-Office of Radiation Programs, EPA-520/4-78-003, Washington, D.C., 1978, p.9.
41. Code of Federal Regulations, Grand Junction Remedial Action, 10 CFR part 12 (1972).
42. Liverman, J.L., Testimony presented to the Senate Committee on Commerce, Science and Transportation, June 28, 1977.
43. Libassi, F.P., et. al., Report of the Interagency Task Force on the Health Effects of Ionizing Radiation, Department of Health, Education and Welfare, Washington, D.C., 1979.
44. Atomic Energy Control Board, Second Workshop on Radon and Radon Daughters in Urban Communities Associated With Uranium Mining and Processing, AECB-1164, Ottawa, Canada, 1979.
45. Shearer, Jr., S.D. and Sill, C.W., Evaluation of atmospheric radon in the vicinity of uranium mill tailings, Health Phys. 17, 77-78 (1969).
46. Bernhardt, D.E., Johns, F.B. and Kaufmann, R.F., Radon Exhalation from Uranium Mill Tailings Piles: Description and Verification of the Measurement Method, U.S. Environmental Protection Agency technical note ORP/LV-75-7, Washington, D.C., 1975.
47. Raghava, M. and Khan, A.H., Radon emanation from uranium mill tailings used as backfill in mines, Noble Gases, op. cit., pp. 269-273.
48. Langner, Jr., G.H. and Franz, G.A., Considerations and Recommendations on Methods for Determination of Eligibility (Ed. note: with regard to uranium mill tailings remedial action program), Colorado Department

of Health report, Denver, Colorado, January, 1979.

49. Busigin, A., Nathwani, J.S. and Phillips, C.R., Attenuation of radon flux from uranium mill tailings by consolidation, Health Phys. 36, 393-9 (1979).
50. Guimond, R.J., The radiological aspects of fertilizer utilization, Radioactivity in Consumer Products, Moghissi, A.A., Paras, P., Carter, M.W. and Barker, R.F. (eds.), U.S. Nuclear Regulatory Commission report NUREG/ CP-0001, Washington, D.C., 1979, pp. 380-93.
51. U.S. Environmental Protection Agency, Preliminary Findings-Radon Daughter Levels in Structures Constructed on Reclaimed Florida Phosphate land, U.S. Environmental Protection Agency report ORP.CSD-75-4, Washington, D.C., 1975.
52. Guimond, R.J. and Windham, S.T., Radioactivity Distributions in Phosphate Products, Byproducts, Effluents and Wastes, U.S. Environmental Protection Agency report ORP/ CSD-75-3, Washington, D.C., 1975.
53. Johnson, W.B., Natural radioactivity problems in Florida, unpublished paper presented at National Bureau of Standards (Jan., 1976).
54. EPA 520/1-77-009, op. cit., pp. 68-74.
55. Mills, W.A., Guimond, R.J. and Windham, S.T., Radiation exposures in the Florida phosphate industry, Fourth International Congress of the International Radiation Protection Association, Paris, France, 1977.
56. Windham, S., Partridge, J. and Horton, T., Radiation Dose Estimates to Phosphate Industry Personnel, U.S. Environmental Protection Agency report EPA-520/5-76-014, Washington, D.C., 1976.
57. Florida Department of Health and Rehabilitative Services, Study of Radon Daughter Concentrations in Structures in Polk and Hillsborough Counties, State of Florida, 1978.
58. Fitzgerald, Jr., J.E., Guimond, R.J. and Shaw, R.A., A Preliminary Evaluation of the Control of Indoor Radon Daughter Levels in New Structures, U.S. Environmental Protection Agency report EPA-520/4-76-018, Washington, D.C., 1976.
59. Partridge, J.E., Horton, T.R., Sensintaffer, E.L., and Boysen, G.A., Radiation Dose Estimates Due to Air Particulate Emissions From Selected Phosphate Industry Operations, U.S. Environmental Protection Agency report ORP/EERF-78-1, Montgomery, Alabama, 1978.
60. Boothe, G.F., The need for radiation controls in the phosphate and related industries, Health Phys. 32, 285-290 (1977).
61. Guimond, R., Ellett, W., Fitzgerald, J., Windham, S.F., and Cuny, P., Indoor Radiation Exposure Due to Radium-226 in Florida Phosphate Lands, U.S. Environmental Protection Agency report EPA 520/4-78-013, Washington, D.C., 1978.
62. Johnson, W.C., Radon daughter concentrations in Structures in Polk and Hillsborough Counties, Florida, 10th Annual National Conference on Radiation Control, HEW Publication (FDA)-79-8054, Washington, D.C., 1979, pp. 219-226.
63. U.S. Environmental Protection Agency, Florida Phosphate Lands: Interim Recommendations for Radiation Levels, Federal Register 41, 26066-8 (June 24, 1976).
64. U.S. Environmental Protection Agency, Indoor Radiation Exposure Due to Radium-226 in Florida Phosphate Lands: Radiation Protection Recommendations and Request for Comment, Federal Register 44, 38664-70 (July 2, 1979).
65. UNSCEAR, 1977 report, op. cit., pp. 90-4.
66. Fitzgerald, Jr., J.E. and Sensintaffer, E.L., Radiation exposure from construction material utilizing byproduct gypsum from phosphate mining, Radioactivity in Consumer Products, op. cit., pp. 351-68.
67. Branscome, J., Concrete blocks studied as radioactive hazard, Washington Post, Jan. 19, 1979, p. A3.
68. Sulzberger, A.O., House panel is told of radiation in Idaho and Montana buildings, New York Times, May 24, 1979, p. A16.

69. Harley, J.H., Radioactivity in building materials, Radioactivity in Consumer Products, op. cit., pp. 332-343.
70. Kolb, W., Building material induced radiation exposure of the population, Radioactivity in Consumer Products, op. cit., pp. 344-350.
71. Eadie, G.G., Radioactivity in Construction Materials: A Literature Review and Bibliography, U.S. Environmental Protection Agency report ORP/LV 75-1, Las Vegas, Nevada, 1975.
72. UNSCEAR, 1977 report, op. cit., p. 79.
73. NCRP Report No. 45, op. cit., pp. 56-8.
74. McKinley, C., An overview of the physical-chemical properties of the noble gases, Noble Gases, op. cit., pp. 391-404.
75. U.S. EPA 520/1-77-009, op. cit., pp. 74-84.
76. Gesell, T.F. and Prichard, H.M., Measurements of radon-222 in water and indoor airborne radon-222 originating in water, Radon Workshop, Breslin, A.J. (ed.), Health and Safety Laboratory report HASL-325, New York, 1977, pp. 132-140.
77. Partridge, J.E., Horton, T.R., and Sensintaffer, E.L., A Study of Radon-222 Released from Water During Typical Household Activities, U.S. Environmental Protection Agency report ORP.EERF-79-1, Montgomery, Alabama, 1979.
78. Hickey, J., Nolan, J. and Weisberg, R., Natural Radioactivity in Drinking Water Supplies in Rhode Island, New England Radiological Health Committee report, Rhode Island Department of Health, 1977.
79. UNSCEAR, 1977 report, op. cit., pp. 68f.
80. Raabe, O.G., Concerning the interactions that occur between radon decay products and aerosols, Health Phys. 17, 177-185 (1969).
81. Evans, R.D. and Goodman, C., Determination of the thoron content of air and its bearing on lung cancer hazards in industry, Journal Industrial Hygiene and Toxicology 22, 89-94 (1940).
82. Kotrappa, P., Bhanti, D.P. and Dhandayutham, R., Diffusion sampler useful for measuring diffusion coefficients and unattached fraction of radon and thoron decay products, Health Phys. 29, 155-62 (1975).
83. International Commission on Radiation Protection, Task Group on Lung Dynamics, Deposition and retention models for internal dosimetry of the human respiratory tract, Health Phys. 12, 173-207 (1966).
84. Haque, A.K.M.M. and Collinson, A.J.L., Radiation dose to the respiratory system due to radon and its daughter products, Health Phys. 13, 431-43 (1967).
85. Weidner, R.B., Hazardous particulates, Occupational Health and Safety Symposia, National Institute Occupational Safety and Health report NIOSH-76-136, Cincinnati, Ohio, 1976, pp. 209-19.
86. Mohen, V. and Stierstadt, K., Die verteilung der naturlichen radioaktivitat auf das grossenspecktrum des naturlichen aerosols, Zeitschrift fur Physik 173, 276-93 (1963).
87. Archer, V.E. and Wagoner, J.K., Lung cancer among uranium miners in the United States, Health Phys. 25, 351-71 (1973).
88. Archer, V.E., Epidemiologic studies of lung disease among miners exposed to increased levels of radon daughters, Health Effects of New Energy Technologies, Park City Conference, Society Environmental and Occupational Health, Washington, D.C., 1979.
89. Morken, D.A., The biological effects of radon on the lung, Noble Gases, op. cit., pp. 501-6.
90. Jacobi, W., Relation between cumulative exposure to radon-daughters, lung dose, and lung cancer risk, Noble Gases, op. cit., pp. 492-500.
91. Hilberg, A.W., A review of the uranium miner experience in the United States, Noble Gases, op. cit., pp. 527-31.
92. UNSCEAR, 1977 report, op. cit., pp. 77-8
93. NCRP Report No. 45, op. cit., pp. 82-3.
94. Haque, A.K.M.M., Collinson, A.J.L. and Brooke, C.O.S.B., Radon concentration in different environments and the factors influencing it, Phys. Med. Biol. 10, 505-14 (1965).
95. Lindeken, C.L., Jones, D.E. and McMillen,

R.E., Environmental radiation background variations between residences, Health Phys. 24, 81-66 (1973).

96. Jacobi, W., Activity and potential alpha-energy of ^{222}Rn and ^{220}Rn daughters in different air atmospheres, Health Phys. 22, 441-50 (1972).
97. Windham, S.T., Savage, E.D. and Phillips, C.R., The Effects of Home Ventilation Systems on Indoor Radon-Radon Daughter Levels, U.S. Environmental Protection Agency report EPA-520/5-77-011, Washington, D.C., 1978.
98. Jonassen, N., On the effect of atmospheric pressure variations on the radon-222 concentration in unventilated rooms, Health Phys. 29, 216-20 (1975).
99. Steinhäusler, F., Long-term measurements of ^{222}Rn, ^{220}Rn, ^{214}Pb and ^{212}Pb concentrations in the air of private and public buildings and their dependence on meteorological parameters, Health Phys. 29, 705-13 (1975).
100. Cliff, K.D., Assessment of airborne radon daughter concentrations in dwellings in Great Britain, Phys. Med. Biol. 23, 696-711 (1978).
101. Stranden, E., Berteig, L. and Ugletveit, F., A study of radon in dwellings, Health Phys. 36, 413-21 (1979).
102. Auxier, J.A. Shinpaugh, W.H., Kerr, G.D. and Christian, D.J., Preliminary studies of the effects of sealants on radon emanation from concrete, Health Phys. 27, 390-1 (1974).
103. Pohl-Ruling, J. and Pohl, E., The radon-222 concentration in the atmosphere of mines as a function of the barometric pressure, Health Phys. 16, 579-84 (1969).
104. Caruthers, L.T. and Waltner, A.W., Need for standards for natural airborne radioactivity (radon and daughters) concentrations in modern buildings, Health Phys. 29, 814-7 (1973).
105. Holub, R.F., Droullard, R.F., Ho, W.L., Hopke, P.K., Parsley, R. and Stukel, J.J., The reduction of airborne radon daughter concentrations by plateout on an air mixing fan, Health Phys. 36, 497-504 (1979).
106. Culot, M.V.J., Olsen, H.G. and Schaiger, K.J., Effective diffusion coefficient of radon in concrete: theory and method of measurement, Health Phys. 30, 263-70 (1976).
107. Wrenn, M.E., Rosen, J.C. and Van Pelt, W.R., Steady state solutions for diffusion equations of radon-222 daughters, Health Phys. 16, 647-656 (1969).
108. Wrenn, M.E., Costa-Ribeiro, C., Hazle, A. and Siek, R.D., Reduction of radon daughter concentrations in mines by rapid mixing without makeup air, Health Phys. 17, 405-14 (1969).
109. Anon., EPA believes radon may be the most serious problem for Clear Air Act, Nucleonics Week, July 20, 1978, pp. 8-9.

ADDENDUM

Despite the seemingly excessive number of references cited above, the author wishes to note that it is not by any means an exhaustive list. Hundreds of additional sources may be found in some of the reviews cited herein. The extensiveness of the literature is such that Harley[26], a few years ago, noted that a bibliography of a thousand references to radon and its progeny can be easily assembled. The present list has barely touched upon the vast biological, health effects and epidemological work, and has excluded the additionally extensive literature relating to various measurement methods.

National Bureau of Standards Special Publication 581, Proceedings of a Roundtable Discussion of Radon in Buildings held at NBS, Gaithersburg, Maryland, June 15, 1979. Issued June 1980

THE BIOLOGICAL AND HEALTH EFFECTS OF RADON: A REVIEW[+]

Donald A. Morken

University of Rochester
Rochester, New York

Human knowledge of radon began near the turn of this century when the discovery of radioactivity followed closely the discovery of X-rays. Thus began an exciting period in the fields of physics, chemistry and biology. Radium especially became important when its intense gamma radiation was found to be as effective as the X-ray in its interaction with, and damage to, biological systems. Radium could be sealed into a metal tube or needle and surgically implanted in living tissue to provide *in situ* irradiation of various cancers, whereas X-rays were directed to the cancerous growths from outside the body and were thus required to traverse normal tissue surrounding the growth. Medicine had acquired a new surgical tool. The physicists, in developing the decay schemes of the radioactive materials, found that it was not radium but rather one of its decay products which provided the intense gamma radiation. Radon, a gas and first decay product of radium, was parent to the needed gamma radiation and for the same intensity radon sources or seeds could be much smaller than the radium needle. Also the long half life of radium, while it permitted a constant dose rate, required that the needle be removed after treatment, whereas radon, with a short half life and consequent rapidly decreasing dose rate, could be contained in glass seeds and left *in situ* in many applications. In addition, radon became useful to the medical profession which, with its suppliers, promoted the use of radon for the common good by developing ointments and salves containing radon for topical application. Other entrepreneurs arranged to let people bathe in radon water, inhale radon, drink water which contained radon, and intravenously inject radon-containing solutions, all to promote the general good health of the people.

The physicists had been studying the decay schemes of uranium and much information was published in the scientific journals of the day. A first book on radioactivity appeared in 1904[1] and was followed over the next two decades by many others from many countries. The extensive treatment by Rutherford, Chadwick and Ellis appeared in 1930[2]. Jennings and Russ[3] have provided a description of the production and use of radon seeds.

The chemists had been busy developing the field of radiochemistry and, of interest here, there was the production of emanation sources (another name for radon, more specifically radium emanation). It was desired to have sources which could release radon continuously and this was accomplished by incorporating radium into colloids or organic structures. These sources could release nearly all the radon formed without losing radium and were essentially dry sources, therefore handy and useful. The radiochemistry of the period, as well as the production of emanation sources, has been described by Hahn[4].

The biologists began to study the toxic nature of radium, radon and X-rays soon after their discoveries and reports of small animal experiments appeared as early as 1904[5-7]. Thus began the studies of the biological effects of radon. Experiments with the X-ray and the gamma emissions from radon were designed to demonstrate the utility of the radiations in the treatment of maligant diseases, but many studies with radon were directed to the discovery and promotion of the healing powers of radon therapy. Much of the work with radium and radon was summarized by London[8].

[+]This work was supported partially under contract with the U.S. Department of Energy and partially by the U.S. Environmental Protection Agency at the University of Rochester Department of Radiation Biology and Biophysics and has been assigned Report No. UR-3490.

In 1879 Harting and Hesse[9] had described as lung cancer the illness miners contracted in the uranium mines of Schneeberg, Germany, and in those of nearby Joachimsthal, Czechoslovakia. Mortality from lung cancer was near 75 per cent, with the incidence greater for miners than for the masons and carpenters working in the mines. In 1913, Arnstein[10] reported from a new study that the lung cancer was a squamous-cell carcinoma, and in 1924 Ludewig and Lorenser[11], familiar with the carcinogenic action of X and gamma radiation, suggested that the lung cancers of the Schneeberg miners, who were now mining the uranium ore for its valuable radium content, might be caused by the radon in the mines. The radon concentrations in these mines averaged about 4×10^{-9} curie per liter, compared to levels of about 10^{-12} curie per liter far away from the mines.

Thus did radon become suspect as the cause of lung cancer in uranium miners, and from that time to the present much work has gone into studies of its carcinogenic activity as well as determinations of maximum recommended concentrations. Radon still had value as a therapeutic agent through use of radon seeds, and emanation therapy continued. The ubiquitous nature of radon was known but lung cancer was considered to be an occupational problem. Many reviews of the mine data and animal experiments are available [12-15].

Not everyone agreed that radon alone caused the lung cancer in the miners, and Lorenz[12], after reviewing the extensive literature on the subject, concluded that radon could not be the sole cause of the lung cancer in uranium miners. Lorenz mentions as contributing factors pneumoconiosis from dust in the mines, chronic irritation caused by respiratory diseases, arsenic, other radioactive substances, and perhaps a hereditary susceptibility.

Many experiments have been conducted to elicit the biological effects of radon inhalation. Most of these were acute-lethal and subacute lethal exposures so that effects might occur in reasonable periods after exposure and they had obvious ill effects on the health of the animals. Some longterm exposures did not appear to permanently affect the health of the animals despite severe transient effects. Morken has summarized most experiments and provided confirmation of the many of them as well as new information[13,16,17,19,20] and has provided new information on long term expsoures[20,21]. Scott has reported on the histopathology of mice exposed to radon, confirming much previous work and offering new information[23].

In general, sub-lethal exposures to radon produced effects on life shortening and body weight similar to those found with X or gamma radiation. Two specific differences did appear: red blood cell forming tissue was only slightly, but permanently, injured whereas the other blood cell forming tissues responded in the expected manner, and the growth pattern was altered and produced permanent stunting. Spleen evidenced the greatest early damage but also showed rapid repair, and late injury appeared in the kidney. Lung and trachea showed no lesions early after exposure but the epithelial lining of the small bronchi showed changes at 2 months, with definite injury at 7 months. Of all the effects, only the red cell depression was not proportional to dose.

In these experiments the tissue-absorbed dose was calculated from the measured activities and weights of tissues, a standard practice following the definition of absorbed dose. Whole body doses ranged from 50 to 300 rad. Although radon was shown to be toxic and could provide the kind of lesion which was thought to precede lung cancer, early experiments were generally unsuccessful in producing lung cancer. Most of these experiments used an exposure system in which only the radon was inhaled, with the decay products of radon in air having been effectively removed either deliberately or inadvertantly from the inhaled atmosphere. With the recognition and confirmation[24-26] that radon in air which contained dust produced a radioactive aerosol which could be inhaled along with the radon, the problem of the miner's lung cancer took a new turn.

Radon-222, a noble gas and decay product of radium-226, decays with a half-life of 3.82 days and the emission of an alpha particle to radium-A (RaA, Po-218), which in turn decays with a half-

life of 3.05 minutes and the emission of an alpha particle to RaB (Pb-214). RaB decays with a half-life of 26.8 minutes and the emission of a beta particle and coincident gamma ray to RaC (Bi-214). RaC decays with a half-life of 19.7 minutes primarily by beta particle emmision and coincident gamma ray to RaC' (Po-214) which decays almost instantly to RaD (Pb-210) by the emission of an alpha particle (a few RaC atoms take an alternate path through RaC'', Tl-210). The long half-life of RaD, 22 years, removes consideration of the remainder of the decay chain from the immediate problem; following RaD are RaE (Bi-210), RaF (Po-210) and finally RaG (Pb-206) a stable isotope. The products RaA through RaC' have historically been called the "active deposit" of radon because of their propensity as metallic ions to attach to any nearby surface. In normal atmosphere these products are found attached to dust particles, most frequently perhaps because the first-formed RaA will so attach. For the brief time from formation to attachment the RaA atom will exist in the unattached state and any specified volume of dust will show both attached and unattached atoms. Attached atoms will decay through the chain to produce attached RaB, RaC and RaC'. It is a consequence of the decay sequence that if the process is allowed to progress for a long time (about 4 hours for the radon series) the radioactivity of each of the isotopes will equal that of the parent radon. If competing surfaces such as walls are provided much of the active deposit may be found on those surfaces, to effectively remove them from the air.

The situation in the mines favored the attachment of the decay products to dust particles. Some of these particles when inhaled will deposit in the lung. Then in addition to the dose from inhaled radon, there will be a dose delivered from the radioactivity carried on the dust particles. Indeed, the dose from radon now waned in comparison to that from the radioactive aerosol.

The deposition of dust particles in the lung has been well studied and well reported (e.g.[27]). It is necessary to understand the morphology and respiratory physiology of the lung as well as the fluid dynamics of aerosol particles to permit a proper evaluation of the dose delivered to the lung from the decay products of radon. The lung is a complex organ mechanically, but may be divided into two major parts below the larynx for consideration of dust particle deposition. Inhaled air and dust are carried through a series of branching airways, the bronchial tree, until they reach the alveolar region where the usual gas exchange occurs. Dust is deposited along the length of the bronchial tree and in the alveolar region, with particle size separation occurring according to air flows, particle parameters of inertia and diffusion, and the branching. Larger particles deposit primarily in the upper parts of the bronchial tree and smaller particles in the deeper portions of the lung. Deposition is not total and the fraction of a given size particle which deposits in each portion of the lung has been well studied[27]. The unattached ions are almost completely removed in the region above the larynx if breathing is through the nose, but for mouth breathing these ions are likely to be deposited in the trachea and major bronchi.

Solid materials which deposit in the lung undergo removal, sometimes incomplete, by several mechanisms. The primary clearance mode in the bronchial tree is the ciliated epithelium which carries particles to the mouth and this method is rapid, total clearance being accomplished in an hour or less. Clearance from the alveolar region is less rapid, principally by dissolution for soluble dusts, a relatively rapid process, and by phagocytosis, a slow process, but other methods are thought active. Dusts can remain in the lung for long periods. The slow removal from the alveolar region, important for consideration in the dust-caused diseases of the lung, does not play a significant role because of the relatively rapid decay of the decay products of radon which may have been deposited.

The Schneeberg lung cancer, bronchogenic in nature, appeared to occur about one-third the way down the bronchial tree from the trachea. It has been a fairly simple matter to show, when suitable parameters are chosen, that the greatest dose to bronchial tissue might occur in the region of the Schneeberg lung cancer. The rapid transport of

the radioactive dust toward the trachea, the relatively short life of the radioactivity, the selectivity to particle size, the geometry of the tissue, and the ventilation rate are all considered in the calculation of the dose. The geometry of the situation involves consideration of a thick-walled tube with the activity on its inner surface. Because only alpha particle energy applies, the penetration of the alpha particle into the wall of the tube probably cannot exceed the range of the alpha particle in tissue; about 45 μm for RaA and 70 μm for RaC'. Limiting the thickness in this way results in a smaller mass in which the energy is released and promptly results in a greater dose than would otherwise be calculated; this method of calculation is justified only by the geometry involved but will result in improper comparisons with doses calculated in the normal way.

More recently, attention has focussed on a target method, in which the dose absorbed in small volume, commonly one cubic micrometer, at the presumed depth of a cell nucleus is calculated for the radiation from a particle in transit on the inner surface of the tube. From the methods proposed it appears that the dosimetry is arranged to maximize the dose in the region of the Schneeberg lung cancer.

Parker has discussed the possibilities and probablities, the failures and the successes of these various methods in light of the great biological variations which occur[28]. Walsh[29] has further reviewed these methods and others continue to improve them[30,31] with the intent to provide a firmer basis for a regulatory level for uranium mines.

Application of the methods of dosimetry to environmental situations requires changes in some parameters. Lung morphometry and physiology will remain the same, but the breathing rate, which brings in the dust, must change to allow for work, play and rest periods. Natural environmental particle sizes are generally smaller, of a size to produce greatest deposition in the alveolar region.

Hofmann et al[32] have estimated dose to the lung for various age groups and found a strong influence of age and physical activity and a slight dependence on sex and weight. Maximum dose from natural radioactivity appeared in the 5-to-9 years age group. Adult doses were received chiefly at places of employment.

In the 1940's the maximum permissible concentration of radon in air for continued human exposure was set at 10^{-11} curie per liter in equilibrium with the short-lived decay products, as recommended by a consideration of the radon exhaled from a known body burden of radium and including a factor of safety of 100[34]. In the 1950's this was raised to 10^{-10} curie per liter in equilibrium with the short-lived decay products. With consideration of the decay products only this latter level was changed to include just the alpha particle energy potentially available in one liter of air from any combination of the decay products, and was designated the Working Level (WL). This WL represented a concentration or dose rate, and exposure to 1 WL for a 168-hour work week constituted a dose for 1 Working Level Month (WLM). Reference[15] describes how these regulatory levels were derived. The annual permitted exposure was then 12 WLM, since reduced to 3 WLM. The WL is a useful air-equivalent unit of dose rate because it contains a measure of the energy available for release in the lung and is not subject to the vagaries of the lung parameters; it also does not require equilibrium of the decay products, as did the radon levels. Radioactive equilibrium rarely occurs except in a stagnant situation and even then the presence of surfaces, such as walls, removes the decay products from the air. Most mine and environmental atmospheres contain decreasing isotope radioactivities for each isotope which occurs further down the chain from radon.

Epidemiologic studies of uranium miners in this country have used the WLM as the dose unit, and these studies have been well reported[35,36]. While the evidence certainly indicates lung cancer incidence among uranium miners is greater than for non-miners, there are other possible agents in the mines. Also reported[37,40] are non-uranium mines in which the radioactivity levels are elevated above background values and sometimes equal

to those in uranium mines, but with no corresponding high incidence of lung cancer such as afflicts the uranium miner. A more recent report[38] suggests that despite strict controls on mine atmospheres for the past twenty or more years the high incidence of cancer has not abated, and a non-malignant respiratory disease in miners, thought due to diffuse parenchymal radiation damage, is approaching cancer in importance as a cause of death. Current dosimetry methods do not apply to other than the bronchogenic cancer.

Experiments with radon and dusty atmospheres have been reviewed[22]. These have been unsuccessful in producing lung cancer when the natural aerosol was used, but radon inhalation during or after exposure to a noxious dust has produced tumors and cancer, mostly pulmonary, rarely bronchogenic. It appears that once a lesion has been produced by chemical agents radon inhalation enhances the effect; radon inhalation followed by application of the noxious dust does not provide enhancement. Recalling that Lorenz[12] anticipated this result, current dosimetry concepts might not relate to present concerns with radon in environmental atmospheres.

Radon itself has not completely disappeared from the scene. Radon therapy is still being studied and applied for its health-saving properties[41,42].

References

1. Rutherford, E. Radioactivity, Cambridge University Press (1904).
2. Rutherford, E., J. Chadwick and C.D. Ellis. Radiations From Radioactive Substances, Cambridge University Press (1930).
3. Jennings, W.A. and S. Russ. Radon, its Technique and Use. John Murray, London (1948).
4. Hahn, O. Applied Radiochemistry. Cornell University Press, Itaca, New York (1936).
5. London, E.S. Uber die physiologischen Wirkungen der Emanation des Radiums. Zntrlbl. f. Physiol. 18: 185(1904).
6. Bouchard, C., P. Curie and V. Balthazard. Action physiologique de l'emanation du radiums. Compt. Rend. des Sci. 138: 1384 (1904).
7. Bouchard. C. and Balthazard, V. Action toxique et localization de l'emanation du radiums. Compt. Rend. Acad. des Sci. 143: 198 (1906).
8. London, E.S. Das Radium in der Biologie und Medizin. Akademische Verlagsgesellschaft m.b.H., Leipzig (1911).
9. Harting, F.H. and W. Hess. Der Lungenkrebs, die Bergkrankheit in den Schneeberger Gruben. Vierteljahrsschr. f. gerichtl. Med. u. offentl. Gesundheitwesen, (N.F.) 30: 296, 31: 102, 313 (1879).
10. Arnstein, A. Uber den sogenannten "Schneeberger Lungenkrebs". Verhandl. d. Deutsch. path. Gesellsch. 16: 332 (1913) also Wien. klin. Wchnschr. 26: 748 (1913).
11. Ludwig, P. and Lorenser, E. Untersuchung der Grubenluft in den Schneeberger Gruben auf den Gehalt an Radiumemanation. Ztschr. f. Phys. 22: 178 (1924); Strahlentherapie 17: 428 (1924).
12. Lorenz, E. Radioactivity and lung cancer. J. Natl. Cancer Inst. 5: 1 (1944).
13. Morken, D.A. A survey of the literature on the biological effects of radon and a determination of its acute toxicity. University of Rochester AEP Report UR-379 (1955).
14. Jackson, M.L. The biological effects of inhaled radon. Thesis, Mass. Inst. Techn., Cambridge, Mass. (1940).
15. Stewart, C.G. and S.D. Simpson. The hazards of inhaling radon-222 and its short-lived daughters: consideration of proposed maximum permissible concentrations in air. in Radiological Health and Safety in Mining and Milling of Nuclear Materials, IAEA, Vienna, (1964).
16. Morken, D.A. The effect of inhaled radon on the survival, body weight and hemogram of the mouse following single exposures. University of Rochester AEP Report UR-593 (1961).
17. Morken, D.A. The effect of inhaled radon on the survival, body weight and hemogram of the mouse following multiple exposures. University of Rochester AEP Report UR-624 (1964).

18. Morken, D.A. and J.K. Scott. The effects of continual exposure to radon and its decay products on dust. University of Rochester AEP Report UR-669 (1966).
19. Morken, D.A. The acute toxicity of radon. A.M.A. Arch. Indust. Health 12: 435 (1955).
20. Morken, D.A. The radiation dose to the kidney of the rat from inhaled radon. A.M.A. Arch. Indust. Health 20: 505 (1959).
21. Morken, D.A. The biological effects of the radioactive noble gases. Noble Gases, p. 469, ERDA TIC-CONF-730915 (1975).
22. Morken, D.A. The biological effect of radon on the lung. Noble Gases, p. 501, ERDA TIC-CONF-730915 (1975).
23. Scott, J.K. The histopathology of mice exposed to radon. University of Rochester AEP Report UR-411 (1955).
24. Control of Radon and Daughters in Uranium Mines and Calculations on Biologic Effects. USHEW-PHS Publication 494 (1957).
25. Shapiro, J. Radiation dosage from breathing radon and its daughter products. AMA Arch. Ind. Health 14: 196 (1956).
26. Chamberlain, A.C. and E.D. Dyson. The dose to the trachea and bronchi from the decay products of radon and thoron. Brit. J. Radiol, 29: 317 (1956).
27. Hatch, T. F. and P. Gross. Pulmonary Deposition and Retention of Inhaled Aerosols. Academic Press, New York (1964).
28. Parker, H.M. The dilemma of lung dosimetry. Health Physics 16: 553 (1969).
29. Walsh, P.J. Radiation dose to the respiratory tract of uranium miners--- a review of the literature. Environ. Res. 3; 14 (1970).
30. Harley, N.H. and B.S. Pasternak. Alpha absorption measurements applied to lung dose from radon daughters. Health Physics 23: 771 (1972).
31. Desrosiers, A. E. Alpha particle dose to respiratory airway epithelium. Health Physics 32: 192 (1977).
32. Hofmann, W., F. Steinhausler and E. Pohl. Age, sex and weight dependent dose distribution patterns for human organs and tissues due to inhalation of natural radioactive nuclides. Presented to the Symposium on the Natural Radiation Environment III, Houston (1978).
33. Steinhausler, F., W. Hofmann and E. Pohl. Local and temporal distribution pattern of radon and daughters in an urban environment and determination of organ dose frequency distributions with demoscopical methods. Presented at the Symposium on the Natural Radiation Environment III, Houston (1978).
34. Evans, R.D. and C. Goodman. Determination of the thoron content of air and its bearing on lung hazards in industry. J. Ind. Hyg. and Toxicol. 22: 89 (1940).
35. Archer, V.E., J.K. Wagoner and F.E. Lundin. Cancer among uranium miners in the United States. Health Physics 25: 351 (1973).
37. Jacoe, P.W. The occurrence of radon in non-uranium mines in Colorado. Arch. Ind. Hyg. and Occup. Med. 8: 118 (1953).
38. Brandom, W.F., G. Saccomanno, V.E. Archer, P.G. Archer and A.D. Bloom. Chromosome aberrations as a biological dose-response indicator of radiation exposure in uranium miners. Rad. Res. 76: 159 (1978).
39. Pohl-Ruling, j., P. Fischer and E. Pohl. Chromosome aberrations in peripheral blood lymphocytes dependent on various dose levels of natural radioactivity. in Biological and Environmental Effects of Low-Level Radiation vol. II; 317 (1976).
40. Duggan, M.J., D.M. Howell and P.J. Soilleux. Concentrations of radon-222 in coal mines in England and Scotland. Nature 219: 1149 (1968).
41. Andreev, S.V. The technique of determining the radiation doses absorbed during whole-body alpha therapy and some results for per-oral administration of radon water. Med, Radiol. 8; 69 (1963).
42. Keleinikov, G.T. and S.M. Petelin. Effectiveness of treatments of patients with paralytic forms of poliomeylitis with radicular syndrome be means of mud applications and radon baths. Nuclear Science Abstracts 33: #29625 (1976).

National Bureau of Standards Special Publication 581, Proceedings of a Roundtable Discussion of Radon in Buildings held at NBS, Gaithersburg, Maryland, June 15, 1979. Issued June 1980

TECHNIQUES FOR MEASURING RADON IN BUILDINGS

A.J. Breslin

Environmental Measurements Laboratory
U.S. Department of Energy
New York, NY 10014

INTRODUCTION

Present techniques for monitoring radon and radon daughters, although not in all cases the most convenient or efficient that might be desired, are adequate for almost anv requirement. Probably the most critical, present deficiency is the lack of commercial versions of some of the newer instruments. Much of current radon monitoring is being done with instruments that are either home-made or have been obtained by special arrangements.

There is an abundance of available techniques, each one having attributes that make it suitable to certain applications and it is necessary to be selective in satisfying the objectives of a particular mission. By confining attention to buildings, a few methods are eliminated from consideration but a formidable number remains. In the following presentation, some of the more practical methods will be identified.

Before discussing specific methods, it may be useful to touch on accuracy and precision, important considerations in connection with all measurements. The following generalization applies to most any kind of radon monitoring: errors of accuracy and precision of individual measurements are small and generally insignificant compared to errors in applying and interpreting the measurements. Like other air pollutants, radon concentration varies greatly with time and location although probably to a greater degree. The errors of most radon measuring techniques are acceptably small but it is of questionable utility to measure a particular concentration with an accuracy, say, of ±10%, recognizing that an hour later the concentration at the same location may differ by a factor of two or that the concentration in an adjoining room of a building differs substantially from the one that has been measured. Actually, radon variation is more likely to be 10-fold than 2-fold over the period of a day or longer. Generally speaking, single measurements are not very useful and one must resort to multiple measurements, either by manual or automatic means, to develop complete information.

This assertion about small instrumental errors is predicated on proper calibration. In this regard, it is vital to calibrate instruments and to intercalibrate with other groups periodically. Moreover, it is inadvisable to accept the calibration of a radon instrument as received from a commercial supplier. Occasionally, commercial instruments are brought to our laboratory by purchasers who are not obtaining correct measurements. In every instance to date, the instrument itself has been of good quality but simply was not calibrated properly at the factory. The problem usually can be corrected with a few hours of effort.

To present methods in some semblance of order, it's convenient to separate them by applications. If the mission under consideration is monitoring, one is concerned mainly with the air concentration of either radon or radon daughters or both. If there is a requirement to calculate lung doses to building occupants, additional information may be needed, adding a degree of complexity to instrumental requirements. For example, radon daughter ratios, fraction of uncombined radon daughters, and particle size distribution enter into these calculations. Taking another direction, if measurements are to be diagnostic, sources of radon and rates of radon input may be important, thus necessitating measurements of radon emanation from building surfaces and, possibly, radon concentration in water supplies which can be a substantial, even a dominant source of air radon in buildings. And finally, since air concentration is a function of ventilation rate as well as radon input rate, the rate of air exchange is a measurement of possible interest.

AIR CONCENTRATION

Measurements of air concentration can be sub-

divided into three groups: prompt (otherwise known as instantaneous or grab sampling methods) methods in which an air sample is obtained either instantaneously or over a brief sampling period of 5 to 10 minutes; continuous readout monitors that continuously sense and register the concentration; and time-integrating monitors that yield a single, average concentration for an extended time period from a few days to a week or more.

Prompt Radon

Scintillation flask. The scintillation flask,[1,2] popularly known as the Lucas flask, is one of the oldest, most reliable, and widely used methods both in the laboratory and in the field. Required equipment consists of one or more scintillation flasks and a photocathode counter, both available from commercial sources.

The scintillation flask is a small glass or plastic vessel equipped with one or two valves and lined with a phosphor (silver-activated zinc sulfide) which emits light flashes when bombarded with alpha particles. A sample of whole air is collected in the flask which is then counted with the photocathode, usually after a delay of a few hours to allow radon daughters to equilibrate with the radon. In routine use, its sensitivity is about 1 $pCi \cdot L^{-1}$ but with care and long counting periods, a sensitivity of <0.1 $pCi \cdot L^{-1}$ can be attained. Portable, battery-powered photocathode counters are available which enable the measurements to be performed entirely in the field.

Two-filter method. The two-filter method,[3] a later development than the scintillation flask, is intended primarily for the field. It requires a two-filter tube, which is not available commercially, in addition to an air sampling pump and a portable alpha counter, both of which can be obtained commercially.

The two-filter tube is a metal cylinder with a high efficiency filter at each end. Sample air is drawn through the tube for five or ten minutes. The front filter removes all particulates including radon daughters from the air stream allowing only radon to enter the tube with the air. While in-flight through the tube, some of the radon decays to radium-A, part of which is collected on the downstream filter, the rest diffusing to the wall of the cylinder. Immediately after sampling, the downstream filter is removed and alpha-counted for several minutes. Radon concentration can be calculated by a simple formula that takes into account tube dimensions and sampling and counting times.

The entire measurement is completed in the field in a total time of 15 to 20 minutes and measurements can be repeated indefinitely with the same apparatus. Sensitivity is dependent on tube volume. Concentrations on the order of 5-10 $pCi \cdot L^{-1}$ can be measured with a 1 liter tube; sensitivities as low as 0.1 $pCi \cdot L^{-1}$ can be attained with tubes of much larger volume.

Pulse-type ionization chamber. Measurement of radon by the pulse-type ionization chamber[4] has been the standard method at EML for 30 years. Its application in the field is somewhat less convenient than other methods and so it is seldom used in the field unless extreme sensitivity is needed. However, it serves as a standard for calibrating other radon instruments. It is not made commercially.

A whole air sample is collected in a one-liter glass flask and then returned to the laboratory for analysis in a pulse-ionization chamber. A separate flask, protected by a padded shipping container, is required for each measurement rendering the method awkward if more than two or three measurements are required. The method is very accurate and has a sensitivity of about 0.01 $pCi \cdot L^{-1}$.

Continuous Radon

Because of the dynamic behavior of radon in air, it is rarely sufficient to obtain a single grab sample. Any of the foregoing methods can be repeated periodically to cover a longer time span but it is far more convenient to use a monitoring instrument specifically designed for the purpose although considerably increased instrument size, complexity, and cost are necessary to attain the added convenience.

Three kinds of continuously-reading radon

monitors have been developed to serve this purpose: the continuous flask monitor; automated two-filter monitor, and a diffusion electrostatic monitor.

Continuous flask monitor. This instrument consists of a scintillation flask permanently mounted in a photocathode counter. Air is drawn continuously through the flask so that the counter tracks changes in radon concentration as they occur. The first instrument of this type was designed at the former HASL in the mid-50s[5] and similar instruments have been reported several times since by other groups. A commercial version has become available.

The fallacy in this arrangement is that even if the inlet air stream is filtered, radon daughters remain in the flask long after the radon from which they originated has passed through. Since the daughters continue to emit alpha radiation, they mask the changes in concentration which the instrument is designed to monitor. This problem persisted until two years ago when an experimental and theoretical procedure was developed at EML[6] to correct for the previously-deposited radon daughters. This procedure enables one to calculate the correct radon concentration in each measurement period by taking account of alpha activity that was registered in preceding measurement periods. Therefore, the continuous flask monitor is now a reliable instrument that is capable of detecting varying radon concentrations for an indefinite length of time. The approximate sensitivity is 0.5 $pC \cdot L^{-1}$. The instrumentation is not truly portable but can be moved and set up readily by one person.

Automated two-filter radon monitor.[7] Basically this is a two-filter tube with a scintillation-photocathode detector positioned in front of the collecting surface of the second filter. Air is pumped through the tube continuously and the detector continuously counts the accumulated radon daughters. Obviously, this technique also is vulnerable to interference from previously deposited radon daughters. But the interference either can be eliminated by providing a filter transport mechanism to replace the downstream filter periodically or it can be corrected mathematically by an equation[7] that takes the previously collected activity into account. Therefore, this instrument also is capable of recording radon concentration at selected intervals for an indefinite period. The lower limit of detection is inversely proportional to the volume of the tube and sensitivities of 0.01 $pCi \cdot L^{-1}$ have been achieved. However, the sensitivity of a unit that can be moved readily is on the order of a few tenths of a picocurie per liter.

Diffusion-electrostatic radon monitor.[8] This monitor uses a different sampling principle but the method of detection is similar to the monitors just described. The sensitive volume is a 1-liter hemisphere made of a wire screen covered by a light-tight porous foam. At the center of the hemisphere are a scintillator and photocathode detector. A high potential is applied between the wire screen and a disc of aluminized Mylar covering the scintillator. Instruments of this type have not been produced commercially.

In operation, ambient air enters the hemisphere through the porous foam by molecular diffusion. Within the hemisphere, radon decays to radium-A which, being positively charged, is drawn to the aluminized mylar cathode where it deposits and decays to radium-B and radium-C. The alpha decays are detected by the photocathode counter and recorded. The concentrations within the hemisphere follow the ambient radon concentration after a time lag. Therefore, in principle, the monitor is continuously detecting the ambient radon concentration. But, as in the case of the other continuous radon monitors, the changes in ambient radon concentration are masked by the previously deposited radon daughters. Probably, a procedure could be devised by which this phenomenon could be corrected but it has not been done and, at the moment, this effect compromises the utility of the instrument. Another deficiency is a pronounced humidity dependence of the response to radon concentration.[9]

Time-Integrating Radon Monitor

Another class of instrument that measures radon concentration over long periods of time is the time-integrating monitor. This class represents an improvement in simplicity and a lower cost with respect to the continuously-reading

radon monitor. In monitoring radon for compliance with regulations or to assess biological hazard, average concentration is the most useful measurement and time-integrating systems were developed specifically for that purpose. The first and probably most widely used time-integrating method for radon was developed by Sill[10] for studies of radon distribution around tailings piles. Field equipment consists of a 40-liter Mylar bag and an aquarium pump powered with a storage battery. A whole-air sample is collected over two days by pumping air into the bag at a very slow rate, 10 milliliter per minute. Analysis of radon is performed in the laboratory by discharging the sample from the Mylar bag through a cold charcoal trap and then transferring the radon from the charcoal to a Lucas flask for counting. The result is a 48-hour average radon concentration. The method is very sensitive, capable of measuring concentrations as low as 0.01 $pCi \cdot L^{-1}$, and it has been used with success for many years. Commercial equipment is available.

A more recent instrument, a passive environmental radon monitor,[11] was developed at EML for its own ambient radon studies. Its principle of measurement is similar to the diffusion-electrostatic monitor in that it samples by molecular diffusion and collects radium-A ions in an electrostatic field. However, instead of a photocathode counter, detection is by means of a thermoluminescent lithium fluoride chip which continuously absorbs and stores alpha decay energy for as long as the monitor is operating. After a designated monitoring period, usually one to two weeks, the chip is removed and analyzed in the laboratory. Since there are no electronic circuits, the cost of the monitor is very low. Moreover, there is no power consumption, the electrostatic field being provided by dry-cell batteries. Therefore the monitor can be placed anywhere and operated for an indefinite period of time. Sensitivity is about 0.03 $pCi \cdot L^{-1}$ in a one week measurement. A commercial instrument of this general type has been advertised but it is much less sensitive than the EML design and is humidity dependent.

Prompt Radon Daughters

Methods are available to measure radon daughters either in terms of working level or in terms of the individual concentrations of RaA, RaB and RaC.

Kusnetz method. The most practical and popular method for measuring working level was developed by Howard Kusnetz[12] for uranium mines in the mid 1950s. Apparatus consists of a portable air filter sampler and a portable alpha counter, both of which are commercial instruments. Air is sampled through a small-diameter filter for five minutes and then after a delay of from 40 to 90 minutes, the filter is counted for gross alpha activity. Working level is calculated by a formula involving the count rate, sample volume, and a correction factor for decay. In the original method, the alpha activity on the filter was measured with a simple ratemeter but as radon daughter concentrations in mines later were reduced by increased ventilation, it became necessary to substitute a scaler for the ratemeter to achieve better sensitivity. Scalers are used almost exclusively today and concentrations as low as 0.0005 WL can be measured with little difficulty.

Several variations in the basic method have appeared since Kusnetz introduced it, the one attracting the most attention being described by Rolle.[13] The main difference in Rolle's method is that the alpha count is made after a delay of only 5 to 10 minutes after sampling.

Tsivoglou method. The individual concentrations of radon daughters can be measured by either the Tsivoglou method or by alpha spectrometry. Tsivoglou,[14] a colleague of Kusnetz, also developed his method for use in uranium mines in the days when concentrations were orders of magnitude higher than today. The method uses identical equipment. The sampling procedure also is the same but the collected alpha activity is measured three times at prescribed intervals in the 30 minutes immediately after sampling. From the three counts, the concentrations of RaA, RaB, and RaC, can be calculated with three equations and, of course, working level also be calculated.

Like the original Kusnetz method, the original Tsivoglou method used a ratemeter but sensitivity is improved tremendously by substituting a scaler. In the modified Tsivoglou method introduced by Thomas[15] about 8 years ago, the alpha activity is measured by means of a scaler in three intervals over 30 minutes. This method is adequate for concentrations on the order of a few tenths of a picocurie per liter.

Another variation on the Tsivoglou method has been described by Raabe and Wrenn.[16] Again, sampling is the same as in the Kusnetz method but alpha counts are made repeatedly at closely-spaced intervals beginning immediately after sampling and continuing for almost any desired period from 15 to 20 minutes to an hour or more. Calculation of radon daughter concentrations involves fitting the resultant alpha decay curve by a least-squares technique.

Alpha spectrometry. Still another variation of the Tsivoglou method employs alpha spectrometry to count RaA and RaC' separately.[17] Sampling equipment and procedure remain the same as in the previous method but filter counting is performed with a two-channel alpha analyzer. Usually two counts are made in the first 20 minutes after collection.

Conceptually, this method affords better precision than methods that rely on gross alpha counting but in practice, the air sample is sharply limited compared to the other methods because solid state detectors, which are used for alpha spectrometry, are very small. Hence, the methods based on total alpha counting, not being limited in sample volume, are capable of much better sensitivity.

Working level meter. Finally, there is a class of instruments popularly known as working level meters.[18,19,20] Several measure working level only whereas one type measures the individual concentrations of RaA, RaB, and RaC. The first type of instrument is available commercially; the second is not. These instruments more-or-less automatically perform the measurement and register a result in a span of 5 to 10 minutes.

The original versions, developed for use in uranium mines, were not sensitive enough for measurements at natural levels above ground; both types of instrument are now available in models that could be used in buildings.

Continuous Radon Daughters

Proposed methods for measuring radon daughters continuously have not yet been shown to be reliable. Fixed filter samplers have been developed with either alpha or beta detectors that continuously count the deposited radon daughters but the problem of previously-deposited radon daughters, mentioned in connection with continuous radon monitors, has not been solved.

Time-Integrating Radon Daughter Monitor

There are two techniques which have been developed for time-integrated measurements of radon daughter concentration in air. Both give results in terms of working level. One method has been shown to be reliable and practical over many years of use whereas the other, although offering promise, has not yet been perfected for monitoring at low concentration.

The first method, developed by Schiager at Colorado State University,[21] uses a thermoluminescent (TLD) detector in an active air sampling system. The monitor consists essentially of a membrane filter and holder containing a TLD and a low-volume air pump. Air is drawn through the filter continuously at 100 milliliter per minute for a total sampling period of about one week. The TLD is positioned in front of the filter where it absorbs and stores alpha decay energy. At the end of sampling, the TLD is removed and analyzed in the laboratory.

Instruments of this type have been used extensively in Grand Junction, in investigations of tailings piles, and various other situations. We have used our own version[22] in studies of ambient radon daughters in buildings and in outside air. Sensitivity is about 0.0005 WL in 168 hours. Commercial versions have not been produced.

The other system uses track-etch film in a completely passive mode of measurement.[23] One centimeter square pieces of cellulose nitrate film are suspended for a long period of time in the air to be monitored. An alpha particle, upon striking the film, damages the surface. Each point of impact can be enlarged by etching the film in an alkaline solution. The resultant pits are counted with a microscope.

The potential advantages of track-etch film are low cost, simplicity, and the feasibility of extensive coverage, if needed. So far it has not been widely used because of inaccuracy and poor sensitivity. For example, year-long exposures are needed to obtain sufficient track densities at concentrations on the order of 0.01 WL. At that concentration, the precision of measurement is about ±50%.

UNCOMBINED FRACTION AND PARTICLE SIZE OF RADON DAUGHTERS

Measurements of uncombined fractions of radon daughters and of the particle size distributions of radon daughters are obtained by prompt sampling methods.

Uncombined radon daughters, which are single atoms or molecules in air, are measured by diffusion techniques. We have used the diffusion cell,[24] developed by Mercer at the University of Rochester, and the wire screen method,[25] developed by George at EML, with equal success. In both methods, two measurements are made simultaneously, one of the uncombined radon daughters alone and the other of total radon daughters. The ratio of the two measurements is the uncombined fraction. Both the diffusion cell and the wire screen collect uncombined daughters with good efficiency while allowing combined daughters to penetrate freely. The collection efficiency for uncombined daughters must be determined experimentally and typically is in the range of 60 to 90% for a screen of 60 mesh size. The collection efficiency need not be very high but it must be reproducible.

Total daughter concentration is obtained by conventional filter sampling. Immediately after sampling, both the filter sample and either the diffusion cell or wire screen, depending on which is used, are alpha-counted by either the modified Tsivoglou or the Raabe-Wrenn method.

Neither the Mercer cell nor the wire screen device are available commercially but the wire screen device can be assembled readily from conventional air sampling components. The Mercer cell must be machined to rigid specifications.

Radon daughter particle sizes are most readily measured with diffusion batteries.[26] Several different types of diffusion battery that are suitable for measuring radon daughters have been developed but none is available commercially.

In passing through a diffusion battery, a portion of the radon daughters deposits on the battery walls in an amount that is inversely related to particle size. Thus, the smallest particles penetrate least through the battery whereas large particles penetrate much more freely. Collection efficiency as a function of particle size can be calculated accurately by means of diffusion equations. By measuring the penetration of radon daughters simultaneously through several batteries each with a different collection efficiency, a rough size distribution can be determined. Typically we use three batteries and a reference filter, four air pumps, and four alpha counters.

RADON EMANATION

Two methods are in common use for measuring radon flux from soil and from building surfaces, the accumulator method and the charcoal canister method.

The accumulator method,[27] also known as the flux can method, has been in use for 20 or 30 years and enjoys universal acceptance. A can of nominal size (20-100 liters), open at one end, is placed open-side-down on the emanating surface and sealed. After a brief period, usually no more than 30 minutes, radon which has collected in the can is sampled through a valve with a scintillation flask and measured. Radon flux can be calculated from the increase in radon concentration, the time of collection, and the dimensions of the can.

The can, itself, can be constructed very easily; the method is simple, reliable, and quite sensitive. Since the measurement is performed

in a brief period, it is analogous to the prompt sampling methods for air concentration.

In the charcoal canister method,[28] a fairly recent development, a canister from a conventional personal respirator is modified by removing the metal casing from one face. In making a measurement, the canister is placed, open-side-down, on the emanating surface, sealed, and left in place for 1 to 2 days. Emanating radon is absorbed completely in the charcoal. After collection, the canister is analyzed in a gamma spectrometer for the radon daughters which have grown to equilibrium with the radon.

This method is simple, sensitive, and reliable. It is easy to apply in the field and because of the low cost and convenient size of the canisters, many measurements can be obtained simultaneously with little effort. Since the collecting period is one day or longer, the method is analogous to the time-integrating methods for air concentration.

RADON IN WATER

The simplest way to measure the concentration of radon in water is to collect the water in a plastic container and count the radon daughter activity in a gamma spectrometer. This technique was reported 15 years ago by Lucas.[29] Using a conventional 1 quart polyethylene bottle, he obtained a sensitivity of about 100 $pCi \cdot L^{-1}$.

The sensitivity of Lucas' method can be improved by using a modified Marinelli beaker for sample collection and counting.[30] The Marinelli beaker has a recess that fits over the crystal in a gamma-counter, resulting in a much better counting geometry. A sensitivity of about 30 $pCi \cdot L^{-1}$ can be obtained for a 10-minute count.

For still better sensitivity, one must turn to liquid scintillation counting which has been described by Prichard and Gessel[31] and others. In this method, a 10 ml water sample is collected in a syringe and later injected into a 20 mL glass scintillation vial along with 5 mL of scintillation fluid. The vial is then counted in a liquid scintillation counter. A sensitivity of 10 $pCi \cdot L^{-1}$ is obtained in a 10-minute count. Because the syringes are small, many samples can be collected conveniently. Also, the use of an automatic counter simplifies analyses in the laboratory.

VENTILATION

The classic method for measuring ventilation rate in a building employs a tracer gas. Many gases have been used; we have used helium and radon itself, while others have used krypton-85, sulfur hexafluoride, hydrogen and ethane. One approach is to inject a slug of gas into a room, mix it thoroughly, and then monitor the reduction of concentration with time. Ideally, the reduction is exponential and the rate of air exchange can be obtained directly from the slope of the curve.

Another approach, which seems to be gaining in popularity, is to inject the gas at a slow, uniform rate until a steady-state concentration is attained. The ventilation rate in that case is calculated from the rate of gas input and the resultant air concentration.

The tracer gas technique has been verified by ventilation engineers in decades of use but its use in connection with radon studies must be cautious because the sources and distribution of radon are complex.

SUMMARY

Sufficiently varied techniques have been developed to meet most of the requirements for monitoring radon that are likely to be encountered. Unfortunately, the availability of commercial instrumentation is lagging behind the technological advances, often necessitating procurement from non-commercial sources, an inefficient and time-consuming procedure.

Since radon monitoring techniques differ in their capabilities, selection must be based on the needs of the particular mission. A basic decision is whether to measure radon or radon daughters. Other questions to be decided concern the duration of monitoring and whether time-variation of concentration or average concentration is needed.

Time variation and spatial variation, inherent characteristics of radon both indoors and in outside air, must be taken into account in the conduct of any monitoring program. In the measurements of average concentration, they are

much greater sources of error than instrument error which usually is small.

REFERENCES

1. Lucas, H.F. Improved low-level alpha scintillation counter for radon. Rev. Sci. Instru. 28, 680 (1957).
2. George, A.C. Scintillation flasks for the determination of low level concentrations of radon. Proceedings of Ninth Midyear Health Physics Symp., Denver, CO, Feb. 1976.
3. Thomas, J.W. and LeClare, P.C. A study of the two-filter method for radon-222. Health Phys. 18, 113 (1970).
4. J.H. Harley, Editor. EML Procedures Manual. U.S. Department of Energy, HASL-300, New York, revised annually, 1979.
5. Harris, W.B., LeVine, H.D. and Watnick, S.I. Portable radon detector for continuous air monitoring. AMA Arch. Ind. Health 6, 493 (1957).
6. Countess, R.J. and Thomas, J.W. Radon flask monitor. US ERDA Report, HASL-330 (1977).
7. Thomas, J.W., personal communication, 1975.
8. Spitz, H. and Wrenn, M.E. Design and application of a continuous, digital-output, environmental radon measuring instrument, p. 48. Radon Workshop, edited by A.J. Breslin, US ERDA Report, HASL-325, Feb. (1977).
9. Graveson, R., personal communication, 1978.
10. Sill, C.W. An integrating air sampler for determination of radon-222. Health Phys. 16, 371 (1969).
11. George, A.C. and Breslin, A.J. Measurements of environmental radon with integrating instruments. Workshop of Methods for Measuring Radon in and Around Uranium Mills, edited by E. D. Harward, Atomic Industrial Forum, Inc., Program Report, Vol. 3, No. 9 (1977).
12. Kusnetz, H.L. Radon daughters in mine atmospheres - A field method for determining concentrations. AIHA J. 17, 85, (1965).
13. Rolle, R. Rapid working level monitoring. Health Phys. 22, 223 (1972).
14. Tsivoglou, E.C., Ayer, H.E. and Holaday, D.A. Occurence of nonequilibrium atmospheric mixtures of radon and its daughters. Nucleonics 1, 40 (1953).
15. Thomas, J.W. Measurement of radon daughters in air. Health Phys. 23, 783 (1972).
16. Raabe, O.G. and Wrenn, M.E. Analysis of the activity of radon daughter samples by weighted least squares. Health Phys. 17, 593 (1969).
17. Martz, D.E., Holleman, D.F., McCurdy, D.E. and Schiager, K.J. Analysis of atmospheric concentrations of RaA, RaB and RaC by alpha spectroscopy. Health Phys. 17, 131 (1969).
18. Groer, P.G., Keefe, D.J., McDowell, W.P. and Selman, R.F. Rapid determination of radon daughter concentrations and working level with the instant working level meter. CONF 740935-1, International Symp. on Radiation Protection in Mining and Milling of Uranium and Thorium, Bordeaux, France (1974).
19. Shreve, J.D. Protection of workers in radon-rich atmospheres: the mandate for quick determination of radon daughter concentrations and a solution. Proceedings of the NEA Specialist Meeting on Personal Dosimetry and Area monitoring Suitable for Radon and Daughter Products, Elliot Lake, Canada, Oct. 4-8, 1976.
20. Hill, A. Rapid measurement of radon, decay products, unattached fractions, and working level values of mine atmospheres. Health Phys. 28, 472 (1975).
21. Schiager, K.J. The evaluation of radon progeny exposures in buildings. Colorado State University Report, March 15, 1971.
22. Breslin, A.J. Two area monitors with potential application in uranium mines. Proceedings of NEA Specialist Meeting on Personal Dosimetry and Area Monitoring Suitable for Radon and Daughter Products, Elliot Lake, Canada, Oct. 4-8, 1976.
23. Countess, R.J. Quantitative measurement of alpha activity using alpha track-etch film. Proceedings of the Ninth Midyear Topical Symposium of the Health Physics Society, Denver, CO, Feb. 9-12, 1976.

24. Mercer, T.T. and Stowe, W.A. Deposition of unattached radon decay products in an impactor stage. Health Phys. 17, 259 (1969).
25. George, A.C. Measurement of the uncombined fraction of radon daughters with wire screens. Health Phys. 23, 390 (1972).
26. Sinclair, D., George, A.C. and Knutson, E.O. Application of diffusion batteries to measurement of submicron radioactive aerosols. American Nuclear Society National Meeting Papers, Winter Meeting, San Francisco, CA, Nov. 28 - Dec. 2, 1977.
27. Wilkening, M. Measurements of radon flux by the accumulation method. Workshop of Methods for Measuring Radon in and Around Uranium Mills, edited by E. D. Harward, Atomic Industrial Forum, Inc., Program Report, Vol. 3, No. 9 (1977)
28. Countess, R.J. Measurement of radon flux with charcoal canisters. ibid.
29. Lucas, H.F. A fast and accurate survey technique for both radon-222 and radium-226. The Natural Radiation Environment, edited by J.A.S. Adams and W.M. Lowder, University of Chicago Press, 1964.
30. Countess, R.J. Measurement of radon-222 in water. Health Phys. 34, 389, 1978.
31. Prichard, H.M. and Gesell, T.F. Rapid measurements of radon-222 concentration in water with a commercial liquid scintillation counter. Health Phys. 33, 577, (1977).

National Bureau of Standards Special Publication 581, Proceedings of a Roundtable Discussion of Radon in Buildings held at NBS, Gaithersburg, Maryland, June 15, 1979. Issued June 1980

RADON AND RADON DAUGHTERS IN BUILDINGS: A SURVEY OF PAST EXPERIENCE

Charles R. Phillips
Sam T. Windham
Jon A. Broadway

U. S. Environmental Protection Agency
Office of Radiation Programs
Eastern Environmental Radiation Facility
Montgomery, AL 36109

INTRODUCTION

The potential for elevated levels of radon and progeny in inhabited structures has been recognized for many years. This potential has been realized in several locations when materials bearing relatively high levels of radium have been incorporated into building or fill materials in, under and around structures. Noteworthy of these situations are Grand Junction, Colorado, the phosphate mining area of Central Florida, Elliot Lake, Ontario, and many instances of the incorporation of natural activity in building materials[1,2]. In addition, recent studies have called attention to elevated radon and progeny levels in structures due to the release of radon from water used in the structure[3-5].

There are considerable radon and progeny data available on individual structures in these and other areas. However, the amount on information available on the factors which combine to establish the measured radon and progeny levels is sparse at best. In particular, the things which are of most interest to this forum, i.e. data on deterministically relating structural characteristics to radon and progeny levels in buildings are largely nonexistent. This information is becoming increasingly important as health effects data suggest establishing exposure guidance at relatively low levels.

Since energy conservative designs or certain building materials may contribute to radon guidelines being exceeded, this clearly indicates the need for a predictive model including all pertinent parameters.

PAST EXPERIENCE

This presentation will focus mainly on the studies conducted in the Central Florida phosphate mining area. This is due to the limited time available for this presentation and because results of the previously mentioned studies have been available for quite some time.

Florida Phosphate Studies

In June 1975, the Environmental Protection Agency, in conjunction with the Florida Department of Health and Rehabilitative Services (DHRS) and the Polk County Health Department, initiated a pilot study to examine the radiological impact of structures built on reclaimed phosphate land. The results of these studies have been reported in various publications[6-8].

The phosphate ore in the Central Florida land-pebble phosphate area contains between 40 and 50 pCi of radium-226 per gram of ore. The ore is normally covered with a sand overburden approximately 3 to 15 m thick, containing from 1 to 2 pCi/g of radium-226.

The standard mining practice in the Florida land-pebble phosphate fields is to strip the overburden and mine the phosphate ore with drag-lines. The reclamation process consists of filling the strip-mined areas with overburden removed from adjacent areas and some byproducts of the ore beneficiation process. The land area thus reclaimed may contain from 1 to 50 pCi/g of radium-226 depending on reclamation techniques employed. The radium concentrations in reclaimed land have been found to vary widely both horizontally and vertically within relatively small areas.

The amount of reclaimed phosphate mining land in Florida has been estimated at approximately 25,000 acres (100 km^2). Approximately 30% of this land contains residential structures and 8% commercial structures. The remainder is used for parks, farming, and grazing. It has been estimated that an additional 70,000 acres (280 km^2) of reclaimed land may become available within the next 30 years. In addition, there may be a large area of land where phosphate deposits containing radium exist near the surface.

Two measurement techniques were employed in the Florida phosphate studies, namely, the Radon Progeny Integrating Sampling Units (RPISU) [9] and Track Etch* films[10].

The land on which the tested structures were constructed was classified according to four categories: non-mineralized (no deposits), mineralized (deposits present but unmined), reclaimed, and other (missing or incomplete information). Table 1 gives the results of the EPA-DHRS results for RPISU data for the 133 occupied structures[7]. (Over 200 structures were studied, but for various reasons only 133 were selected for analysis.)

Table 1

EPA and DHRS Radon Progeny Levels and Distribution by Land Category

Working Level (gross)	No. of Structures	%
> 0.05	8	6
0.03-0.05	12	9
0.01-0.03	26	20
< 0.01	87	65

Land Use	Mean WL	N	WL< 0.01	0.01<WL <0.03	0.03<WL <0.05	WL> 0.05
Reclaimed	0.017	93	61%	18%	13%	8%
Mineralized	0.015	9	56%	33%	11%	0%
Non-Mineralized	0.003	29	97%	3%	0%	0%
Unknown	0.009	2	0%	100%	0%	0%

A statistical analysis of these data indicate that working levels in the structures on non-mineralized land are different from those on reclaimed land at the 99% confidence level. Further, working levels in structures on mineralized land are not different from reclaimed land at the 90% confidence level.

The track etch data from the phosphate study have been analyzed by Robinson[11] to draw some tentative conclusions on the manner in which certain structural characteristics affect radon progeny levels. Since the study was not designed to provide the data for such a correlation, the tentative nature of this analysis must be emphasized. Table 2 summarizes the data used in this analysis. Because 90% of the structures studied were single-family residences only those structures are analyzed. The track etch data were regressed against external gamma exposure rates measured at each tested structure in order to account for the

Table 2

Summary of Relevant Characteristics for Single-Family Residences

	No.	%	Track Etch Data: Mean Tracks-hr mm^2	Track Etch Data: Standard Deviation Tracks-hr mm^2
Total	182	100	0.0025	0.0028
BUILDING STRUCTURE				
Basement or multi-level	11	6	0.0009	0.0011
Single-level slab	148	81	0.0029	0.0029
Single-level crawl space	15	8	0.0005	0.0004
Multi-level crawl space	3	2	0.002	0.0006
Trailer	3	2	0.001	0.0005
Unknown	2	1	0.004	0.0003
BUILDING MATERIALS				
Masonry	161	88	0.0028	0.0029
Non-Masonry	16	9	0.0009	0.0008
Trailer	3	2	0.0010	0.0005
Unknown	2	1	0.0004	0.0003
AIR CONDITIONING				
Yes	147	81	0.0029	0.0029
No	33	18	0.0008	0.0009
Unknown	2	1	0.0033	0.0011

* Service mark, General Electric Company

fact that structures with particular characteristics are built on lands with varying amounts of radium-226. The external gamma exposure should be an indication of soil radium-226. The regressions include a binary variable to represent the housing characteristic of interest.

Table 3 summarizes the results of these analyses.

Table 3

Effect of Working Levels of Indicated Housing Characteristics

	Significant?	
Crawl Space vs Slab-on-Grade	Yes	Lower WL for Crawl Space
Multi-Level vs Single-Level	Yes	Lower WL for Multi-Story
Air Conditioning vs Non-A/C	Yes	Lower WL for Non-A/C
Masonry vs Non-Masonry	Yes	Lower WL for Non-Masonry

Due to the limitations of study design, the small number of structures having some characteristics and the "looseness" of some of the regressions, these correlations must be tentative. However, these analyses do verify effects expected from physical principles.

Structures built with crawl spaces appear to have lower radon progeny levels than slab-on-grade ones. This would be expected due to the dilution of radon concentration prior to diffusion into the structure.

Multi-level structures apparently have lower working levels than single level ones. The radon input per unit time into a structure should be proportional to the product of the radon flux of the soil on which it is constructed and ground floor area of that structure. With adequate mixing, the radon (progeny) concentration is then proportional to the radon input and the volume of the structure, for a constant ventilation rate. Thus, a multi-level structure with a higher volume-to-foundation ratio would be expected to exhibit lower radon progeny levels than a single-level one.

The warm, humid climate in the area of this study makes it necessary to cool structures a large portion of the year. If the house is not air-conditioned it is probable that the cooling is provided by natural or forced ventilation. The fact that the working levels in air-conditioned structures appear to be higher than non-air-conditioned is an expected result due to the increased ventilation in non-air-conditioned houses.

There are many reports of increased radon and progeny levels in structures of masonry type materials. These reports tend to support this effect in the studied structures.

Environmental Measurements Laboratory Study - New Jersey - New York Area [3,12]

This study was performed by George and Breslin over a two-year period in 21 residences, mostly single-family one- or two-story wood-frame or brick construction with full basements (majority finished). These houses were built on land with radium-226 concentrations of approximately 1 pCi/g which is within the range of "background" (unenhanced) values. The houses were occupied during the study. The mean working level in the cellars of the studied structures range from approximately 0.002 to 0.026 WL. The first floor values range from 0.002 to 0.013 WL.

Simultaneous week-long measurements of radon and progeny were made in the cellars and on the other floors. These measurements were made periodically and distributed over the study duration. The average first floor to cellar radon concentration ratio of individual paired values was 0.53 ± 0.22. The average ratio of individual paired values of working levels for first floor to cellar was 0.56 ± 0.30. The average ratio of second to first floor working level was 1.06 ± 0.29.

These week-long measurements were highly variable, reemphasizing the need for long-term rather than "grab-sample" type monitoring in occupied structures.

A more recent publication for this study[3] shows that average radon concentrations in cellars are correlated with measured radon exhalation from cellar floors. It is further suggested that radon released from water used in the structure has a discernible effect on cellar radon concentrations.

Other Studies

Many other studies of measurements of radon and progeny in structures have been reported [13-

19]. Many of these studies have been summarized by Harley[2]. The source of radon exposure in most of these studies is from radium-226 in the construction materials. A wide range of materials has been implicated and resulting radon progeny levels above the anticipated guidance level have been reported. In most cases, these studies have one or more of the following limitations:

a) They were conducted under artificial ventilation conditions;
b) Measurements were of short-term or grab grab samples; and
c) They were directed only toward the effects of a given construction material with insufficient detail for general applicability.

VENTILATION AND INFILTRATION

For a given radon input into a structure the radon and progeny concentrations in that structure are highly dependent upon the ventilation and infiltration (henceforth called ventilation) rates within that structure as shown in Figure 1. The magnitude of these rates is a function of wind speed, pressure difference between inside and outside, type of construction, workmanship, condition of the building and the activities of the occupants.

The most common method of determining ventilation rate is by releasing a tracer gas into the structure and measuring its concentration as a function of time. A literature survey of published data was performed by Handley and Barton [20]. They found the average annual ventilation rate of most occupied single-family houses falls in the range 0.5 to 1.5 air changes per hour.

Ventilation measurements made in a modern test house, constructed to minimize infiltration, indicate ventilation rates from 0.22 to 0.4 air changes per hour, depending on wind speed [21]. The test house was unoccupied; however, utility usage was simulated. Other unpublished measurements on similarly constructed "energy-conservative" houses indicate ventilation rates of from 0.1 to 0.2 air changes per hour.

Figure 1

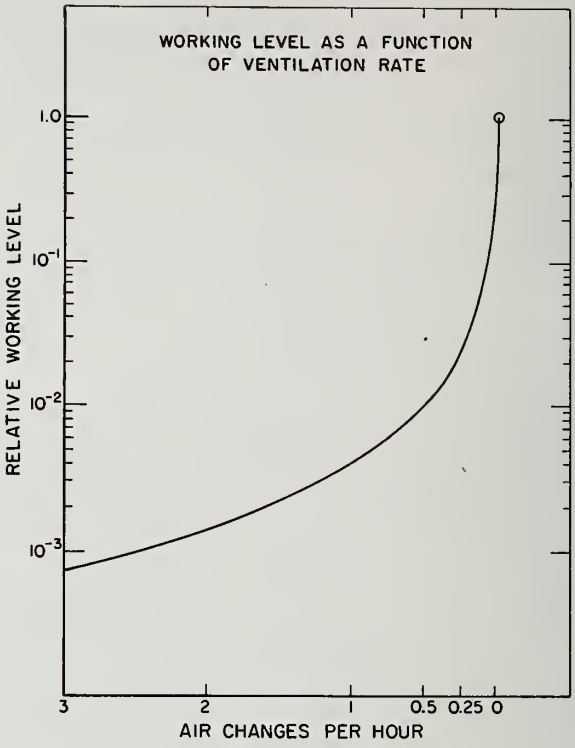

Occupancy factors must not be ignored when making ventilation measurements or in using some published value for calculation purposes. For example, in a test house in Florida, the central air-conditioning fan was allowed to operate continuously for three hours. There was a subsequent reduction in working level by a factor of ten and a reduction in radon by a factor of five from that of a closed, unoccupied condition. This represented an effective ventilation rate change from 0.5 to 2.5 air changes per hour [8].

CONTROL TECHNOLOGY

A study funded by the Colorado Department of Health evaluated radon progeny control measures including dilution by ventilation, air cleaning with HEPA filters and air cleaning by electrostatic precipitation[22]. This report concluded that dilution by ventilation provides the most cost-effective method for radon progeny reduction, closely followed by elastrostatic precipitation.

Fitzgerald et al.[23] evaluated various radon progeny control measures applicable to the Florida phosphate situation, i.e. radon entry through structure floor.

The criteria for selection of an optimal control measure were: (1) operative passivity; (2) uniform effectiveness over the lifetime of a structure; (3) a one-time reasonable cost upon implementation; and (4) minimum impact on the lives of future occupants.

The evaluation is primarily, of necessity, based on theoretical predictions as very little experimental data exists which is directly applicable to the control of radon and progeny in structures. An exception to this lack of experimental efficacy verification is for the polymeric sealants [24, 25].

Table 4 summarizes the control measures considered in Ref. 23 with the authors' listing of advantages and disadvantages.

Table 4

CONTROL MEASURES: ADVANTAGES AND DISADVANTAGES

CONTROL MEASURE	ADVANTAGES	DISADVANTAGES
FULL MEASURES		
VENTILATED CRAWL SPACE	1-PASSIVE, LIFE-OF-HOUSE MEASURE 2-HIGH EFFECTIVENESS WITH PROPER VENTILATION	1-EXPENSE ASSOCIATED W/CHANGES IN HOME'S STRUCTURAL SPECIFICATIONS 2-BUYER'S OBJECTIONS ON AESTHETIC OR OTHER GROUNDS 3-HIGHER ELECTRICAL COST FROM INFILTRATION
POLYMERIC SEALANT	1-PASSIVE MEASURE 2-WITH PROPER APPLICATION, HIGH EFFECTIVENESS ACHIEVED AT RELATIVELY LOW COSTS 3-SEALANT PROVIDES ADDITIONAL WATER-PROOFING	1-UNCERTAINTY AS TO LONGEVITY OF SEALANT EFFECTIVENESS 2-THOROUGH APPLICATION NECESSARY FOR EFFICIENT RADON REDUCTION
EXCAVATION AND FILL (W/NOMINAL FILL COST)	1-PASSIVE, LIFE-OF-HOUSE MEASURE 2-NO ALTERATION IN HOUSE PLANS OR CONSTRUCTION PROCEDURES NECESSARY	1-EFFECTIVENESS BASED ON THEORY ALONE 2-PROBLEMS ASSOCIATED WITH IMPROPER COMPACTION OF FILL 3-RADON INFILTRATION ALONG PIPING LAID UNDER SLAB
EXCAVATION AND FILL (AT COMMERCIAL RATES)	SAME AS ABOVE	SAME AS ABOVE EXCEPT FOR HIGH COST ASSOCIATED WITH FILL
ELECTRONIC & AIR EXCHANGER	1-SYSTEM DURABLE 2-LITTLE MAINTENANCE REQUIRED 3-PARTICULATE CONCENTRATION REDUCED IN HOME	1-NON-PASSIVE 2-HIGH COST INVOLVED WITH OPERATION 3-OZONE RELEASED BY PRECIPITATOR
IMPROVED SLAB CONSTRUCTION (8" SLAB)	1-PASSIVE, LIFE-OF-HOUSE MEASURE 2-VERY LITTLE ALTERATION IN CONSTRUCTION PLANS REQUIRED	1-CRACKING IF IT OCCURS, WOULD NEGATE MUCH OF EFFECTIVENESS
LIMITED MEASURES		
ELECTRONIC AIR CLEANER	1-MINIMAL ELECTRICAL COST AND MAINTENANCE NECESSARY 2-PARTICULATE CONCENTRATION REDUCED IN HOME	1-NON-PASSIVE 2-OZONE RELEASED BY PRECIPITATOR
HEPA FILTERS	1-EFFECTIVE AT SMALL PARTICLE SIZE RANGE 2-NON MECHANICAL PARTS, NO MAINTENANCE NECESSARY	1-NON-PASSIVE 2-HIGH COST OF FILTERS 3-HIGH PRESSURE DROP (AS AIR FLOW RATE INCREASES, EFFICIENCY DECREASES)

Table 5 gives the authors' estimated efficacy and costs for the considered techniques. The authors conclude that the inclusion of crawlspace in the construction of a residence is the most cost-effective technique which satisfies the criteria for optimal radon progeny control.

This study by Fitzgerald et al. also calls attention to the potential for increasing lung doses due to increased free ion fractions with techniques employing high air exchange rates or selective removal of aerosols through filtration.

When using control techniques that decrease the diffusion of radon through the floor, the potential increase in whole-body gamma exposure due to radon daughter build-up and decay in and under the floor must be considered[26].

CONCLUSION

This paper has attempted to review the literature on the factors that affect the radon and progeny levels in structures. Although a seemingly large volume of data is available on this subject, it falls far short of being sufficient, in this author's opinion. We know only in a qualitative sense the deterministic factors affecting these levels. We are not able to answer the principal question: "What will be the radon progeny concentration in a structure constructed of given materials, in a given manner on a known location?" Hopefully, this meeting is the needed impetus to begin to address this question.

Table 5

AVERAGE COST PER PERCENT REDUCTION OF RADON DAUGHTER LEVELS

CONTROL MEASURE	ESTIMATED PERCENT RADON PROGENY REDUCTION	TOTAL COST (30–50 YRS)*	AVERAGE COST/PERCENT REDUCTION	RANK FULL MEASURE**	RANK LIMITED MEASURES
AIR CLEANERS:					
HEPA	40%	$1725–1925	$43–48($45)	–	5
ELECTRONIC	40%	800– 900	20–23($21)	–	2
ELECTRONIC & AIR EXCHANGE	60%	3000–3325	50–55($52)	5	6
VENTILATED CRAWL SPACE	80%+	450	6($ 6)	1	1
POLYMERIC SEALANT	80%	400–1300	5– 16($ 10)	2	3
EXCAVATION AND FILL (TO 10' DEPTH):					
COMMERCIAL FILL RATE	80%	2100–3700	26– 46($ 36)	4	–
W/NOMINAL FILL COST	80%	1595–1850	20– 23($ 22)	3	–
(TO 5' DEPTH):					
COMMERCIAL FILL RATE	40%	1100–1900	28– 48($ 38)	–	4
W/NOMINAL FILL COST	40%	800– 950	20– 24($ 22)	–	2
IMPROVED SLAB CONSTRUCTION	80%+	450	6($ 6)	1	1

*WITH 6% DISCOUNT RATE.
**MEASURES WITH ESTIMATED REDUCTION OF EFFICIENCIES OF 50% OR MORE.

REFERENCES

1. Eadie, G.G., Radioactivity in construction materials, a literature review and bibliography. Technical Note ORP/LV-75-1, U.S. Environmental Protection Agency (1975).
2. Harley, J.H., Radioactivity in building materials, in Radioactivity in Consumer Products, Moghissi, A.A. Moghissy et al., eds., p. 336. Pergamon Press, New York (1978).
3. Breslin, A.J., Knutson, E.O. and George, A.C., Correlation of air concentration of radon with sources in residential buildings, presented at NEA Specialist Meeting on Personal Dosimetry and Area Monitoring Suitable for Radon and Daughter Products. Paris (Nov. 20-22, 1978).
4. Gessell, T.F. and Prichard, H.M., The contribution of radon in tap water to indoor radon concentration, in Book of Summaries, The Natural Radiation Environment III. Houston (April 1978).
5. Partridge, J.E., Horton, T.R. and Sensintaffar, E.L., A study of radon-222 released from water during typical household activities. U.S. Environmental Protection Agency Technical Note ORP/EERF-79-1 (1979).
6. Study of radon daughter concentration in structures in Polk and Hillsboro Counties. Florida Department of Health and Rehabilitation Services (January 1978).
7. Guimond, R.J., Ellett, W.H., Fitzgerald, J.E., Windham, S.T. and Cuny, P.A., Indoor radiation exposure due to radium-226 in Florida phosphate lands. U.S. Environmental Protection Agency report 520/4-78-013 (1979).
8. Windham, S.T., Savage, E.D. and Phillips, C.R., The effects of home ventilation systems on indoor radon-radon daughter levels. U.S. Environmental Protection Agency report EPA-520/577-011 (1978).
9. Schiager, K.J., Integrating radon progeny air sampler. Am. Ind. Hyg. Assoc. J. 35, 165-174 (1974).
10. Lovett, D.B., Track etch detectors for alpha exposure estimates. Health Phys. 16, 623-628 (1969).
11. Robinson, D.P., Draft report of statistical analysis of indoor working levels for house on Florida phosphate lands. (To be published in 1979).
12. George, A.C. and Breslin, A.J., Distribution of ambient radon and radon daughters in residential buildings in the New Jersey-New York area, in The Natural Radiation Environment III (1978).
13. Hultquist, G., Studies of naturally occurring ionization radiations with special reference to radiation doses in Swedish houses of various types. Kungl. Svenska Venlenskysakrad Handlinger 6, 125-129 (1956).
14. Steinhausler, F., Long-term measurements of ^{222}Rn, ^{220}Rn, ^{214}Pb and ^{212}Pb concentrations in the air of private and public buildings and their dependence on meterological parameters. Health Phys. 29, 705-713 (1975).
15. Yeates, D.B., Goldin, A.S. and Moeller, D.W., Natural radiation in the urban environment. Nuclear Safety 13, 275-286. (1972).
16. Toth, A., Determining the respiratory dosage from RaA, RaB and RaC inhaled by the population in Hungary. Health Phys. 23, 281-289 (1972).
17. Gemesi, J., Gzy, D. and Toth, A., Radon-222 content in the internal atmosphere of Hungarian residential buildings, in The Natural Radiation Environment II, 751-756 (1972).
18. Eadie, G.G., Kaufmann, R.F., Markley, D.J. and Williams, R., Report of ambient outdoor radon and indoor radon progeny concentrations during November 1975 at selected locations in the Grants Mineral Belt, New Mexico. U.S. Environmental Protection Agency Technical Note ORP/LV-76-4 (1976).
19. Douglas, R.L., Han, Sr., J.M. and Wolff, T.A., Working level screening survey of structures constructed of materials containing pumice. U.S. Environmental Protection Agency report ORP/LV-78-6 (1978).
20. Handley, T.H. and Barton, C.J., Home ventilation rates: a literature survey. AEC Report ORNL-TM-4318 (1973).

21. Haywood, F.F., Hawthorne, A.R. and Stone, D.R., Measurements of airborne pollutant concentrations inside a well insulated structure with low ventilation rate, in highlights of an ORNL report to be published (1979).
22. Carr, G. and Tappan, T., Phase I demonstration and study of ventilation/filtration techniques as a uranium mill tailings remedial action, in a report by Nelson, Haley, Patterson and Quick, Inc. (September 1976).
23. Fitzgerald, J.E., Guimond, R.J. and Shaw, R.A., A preliminary evaluation of the control of indoor radon daughter levels in new structures. U.S. Environmental Protection Agency report EPA-520/4-76-018 (1976).
24. Culot, M.V.J., Olson, H.G. and Schiager, K.J., Effective diffusion coefficient of radon in concrete; theory and method for field measurements. Health Phys. 30, 263-270 (1976).
25. Auxier, J.A., Shinpaugh, W.H., Derr, G.D. and Christian, D.J., Preliminary studies of the effects of sealants on radon emanation from concrete. Health Phys. 27, 390-392 (1974).
26. Culot, M.V.J., Schiager, K.J. and Olson, H.G., Prediction of increased gamma fields after application of a radon barrier on concrete surfaces. Health Phys. 35, 375-380 (1976).

National Bureau of Standards Special Publication 581, Proceedings of a Roundtable Discussion of Radon in Buildings held at NBS, Gaithersburg, Maryland, June 15, 1979. Issued June 1980

RESIDENTIAL BUILDING TECHNOLOGY TRENDS AND INDOOR RADON AND RADON DAUGHTER CONCENTRATIONS

P. E. McNall, Jr. and S. Silberstein

Center for Building Technology
National Bureau of Standards
Washington, D.C. 20234

ABSTRACT

Radon-222, a radioactive gas, is a decay product of naturally occurring Ra-226. Small amounts of Rn-222 and its further decay products are present in the indoor and outdoor environments. Since the energy crisis of 1973-74, residential building trends have been in the direction of providing more energy-conserving residences. In addition, higher energy costs and energy supply uncertainties have motivated occupants to operate residences in more energy-conserving ways. This paper surveys several of these trends as they relate to the resulting concentrations of Rn-222 and its daughters in the residential environment. It is concluded that energy-conserving measures tend to increase indoor potential alpha energy levels associated with radon progeny up to 10 times those typical of pre-energy crisis construction and operational strategies. These higher levels may indicate a future additional human health hazard.

Key words: Construction materials; earth berms; energy conservation; indoor air quality; natural gas; passive solar energy; radioactivity; radon; ventilation

INTRODUCTION

Radium-226 is widely distributed in minerals over the earth. It has a half-life of 1600 years so, for practical purposes, its activity is invariant with time. Ra-226 decays to gaseous radon-222, which can diffuse through many materials and become airborne. Rn-222, in turn, decays to give a chain of solid decay products, with short half-lives until Pb-210, which has a 22-year half-life. Table 1 lists these decay products.[1]

Table 1. Relevant Ra-226 Decay Products[1]

Radionuclide		Half-life	Potential alpha energy per atom (MeV)
Radon	Rn-222 ↓α	3.8 d	-
Polonium	Po-218 ↓α	3.1 min	13.68
Lead	Pb-214 ↓β	27 min	7.68
Bismuth	Bi-214 ↓β	20 min	7.68
Polonium	Po-214 ↓α	<1 s	7.68
Lead	Pb-210	22 y	-

Thus, if Rn-222 diffuses into indoor air, these radioactive progeny may remain airborne by becoming attached to dust particles, which could be deposited in the lungs of exposed persons. Alpha particles emitted by attached or unattached (to aerosol) radon progeny could be health hazards depending on their concentrations in the body.

The health effects of radon daughters depend on the form in which they occur since the form affects their penetration into the lungs. They are found in two distinct fractions[2]: an unattached fraction composed of free ions and atoms, and an attached fraction of daughters associated with aerosols. Most of the respired unattached fraction (60-70%)[3] is removed by nasal deposition but part can penetrate as far as the bronchial region. Because of the high diffusion coefficient, any remaining unattached daughters deposit on the bronchi, and there is little deeper penetration into the lung. The unattached fraction may be a cause of lung

cancer in uranium miners, which presumably originates in the underlying basal cells of the bronchi.[4]

The attached fraction is found predominantly on respirable particulates (activity median diameter between 0.1 and 0.2 μm).[2] Very little of this fraction is removed by the nose, and the particles can penetrate into the pulmonary region of the lung.[5,6]

A measure of potential alpha energy is the working level (WL), defined is any combination of short-lived radon daughters per liter of air yielding 1.3×10^5 MeV of alpha energy upon decay to Pb-210. If Rn-222 and its daughters were in equilibrium, this would correspond to 100 pCi/L (3700 Bq/m^3) of Rn-222. The equilibrium factor (F) is used to convert between Rn-222 concentration and potential energy. It is defined as the ratio of actual potential alpha energy to that if daughters were in equilibrium with Rn-222.

$$F = (100\ pCi \cdot L^{-1}/WL \text{ or } 3700\ Bq/m^3) \times \frac{\text{potential alpha energy}}{\text{Rn-222 concentration}}$$

Atmospheric diffusion and wind dilute Rn-222 and progeny activities in outdoor air. Rn-222 in indoor air is diluted by air leakage (infiltration) and ventilation. Fallout of dust particles with attached daughter products may also decrease airborne activity.

There are four identifiable sources of Rn-222 gas which can be introduced into indoor air and would increase the indoor activity with respect to that outdoors:[1]

1. Soil-produced Rn-222 in the ground in contact with a residence. Rn-222 can diffuse through the earth, basement walls and floors at a rate determined by soil Ra-226, U-238 (an "ancestor" of Ra-226) and moisture content, porosity, and temperature.
2. Construction materials. Concrete, brick, stone, plaster, sand and gravel contain Ra-226 in varying concentrations. Wood products do not contain sufficient amounts of Ra-226.
3. Residential water supplies from ground water. Such water contains dissolved Rn-222 which can outgas in the residence as the water is used. Bathing, and washing of clothes and dishes release a significant fraction of the Rn-222 into the air.
4. Natural gas. Natural gas contains varying concentrations of Rn-222. Gas cooking and unvented space heating are the significant sources. Vented gas appliances would presumably also vent most of the Rn-222 and daughters from this source from the residence.

Commonly accepted building construction in the past has resulted in infiltration rates in residences sufficiently high that no indoor health hazards have been identified, with the exception of a few cases where houses were built unusually radioactive material obtained from uranium mill tailings[7] or phosphate ores.

POST-ENERGY CRISIS TRENDS

Tighter Construction

Construction practices prior to 1973-74 resulted in uncontrolled air leakage (infiltration) of about 0.5 to 1.5 air changes per hour (ach).[10] Air exchange rates increase with increasing wind velocity and increasing indoor-outdoor temperature difference for any building. Air exchange rates below 0.5 ach can occur even in buildings with loosely constructed envelopes if there is little indoor-outdoor temperature difference and low wind speed, but less frequently than in tighter buildings. Construction details and workmanship are responsible for significant variations among residences.

Infiltration may account for approximately 25% of the heating and cooling cost of a residence[11] but its share would increase if insulation levels were increased without a corresponding reduction in air leakage. Thus application of current technology also results in lower infiltration rates, and this trend will undoubtedly continue. One practical technique to reduce infiltration is to wrap the framing of the residential exterior walls and ceiling with a polyethylene film and apply interior dry wall or other surfacing over it. Another trend is toward more effective weatherstripping of doors and windows to reduce infiltration. Homes have been built which have measured infiltration rates as low as 0.1 ach, and perhaps 0.5 ach will oe a

future accepted norm partly because water condensation may be a problem at lower air exchange rates.

If air exchange rates in residences were reduced from about 1 to 0.25-0.5 ach, Rn-222 activities could increase 2- to 4-fold. Decreased air exchange rates also affect total potential alpha energy, the equilibrium factor, the attached fraction/unattached fraction ratio, and the rate of particulate removal by surfaces: walls, floors and furniture.[12-14] Predicting the extent of the changes in these parameters is not simple.

Fig. 1 shows the effect of changing ventilation on total potential alpha activity in a residence, as calculated by a computer model developed at the Center for Building Technology of the National Bureau of Standards.[15] The model assumes typical indoor Rn-222 emanation rates, typical outdoor Rn-222 and daughter levels,[11] and includes the increase in equilibrium factor indoors due to lowered ventilation rates, but does not include particulate settling. (The equilibrium factor increases with decreased ventilation because more of the Rn-222 has a chance to decay before being exhausted from the building). Since most of the potential alpha activity is associated with the attached fraction, and this fraction closely parallels total activity, the figure shows very well the increased dose to the pulmonary region in the absence of any air cleaning.[11]

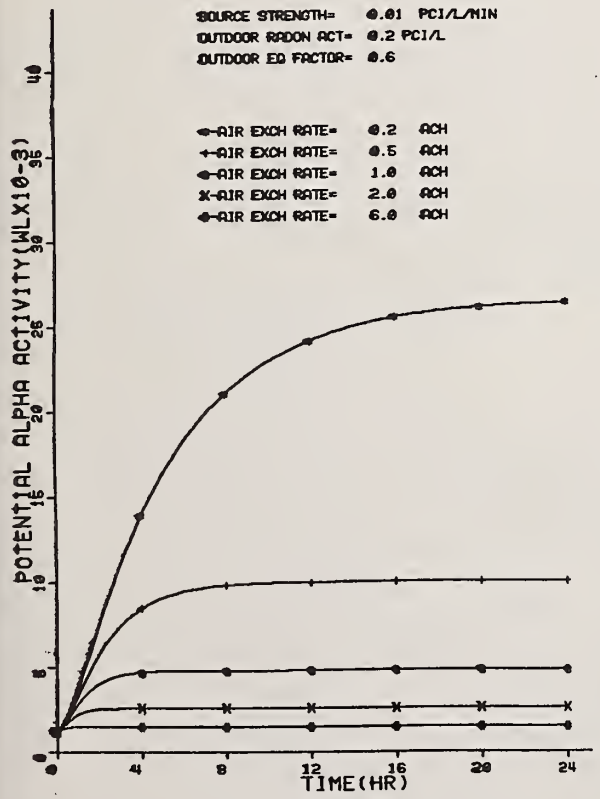

Figure 1. Time course of potential alpha activity at several air exchange rates.

When the air exchange rate is reduced from 1 to 0.5 ach, steady-state potential alpha activity increases 2.1-fold. A reduction to 0.2 ach causes a further 2.1-fold increase (the 8-hour, not the steady-state, value is used for 0.2 ach because it is doubtful that the air exchange rate would remain constant any longer). Potential alpha activity increases from 0.0048 WL at 1 ach to 0.010 WL at 0.5 ach, and to 0.021 WL at 0.2 ach. The Surgeon General of the U. S. Public Health Service recommended remedial action at Grand Junction, Colorado, at levels between 0.01 and 0.05 WL above background.[1]

Although total daughter activities rise markedly when air exchange rates are lowered, increased aerosol levels and residence times of air in buildings also could greatly reduce the unattached fraction[14] so it is difficult to predict whether the unattached progeny concentration would increase or decrease.

Homeowners might be encouraged to replace combustion-fired with electric appliances, or to install air-cleaning equipment like electrostatic precipitators or other high-efficiency filters. These measures might reduce total potential alpha activity in the unattached fraction. Table 2 summarizes what is known about the effects of decreased ventilation on radon levels in indoor air.

Table 2

Effects of Air Cleaning on Radioactivity due to Radon-222 and Progeny

	Air Cleaning	No Air Cleaning
Total potential α energy	unknown	increases
Equilibrium factor	unknown	increases
Unattached fraction	increases	decreases
Total potential α energy on unattached fraction (and effect on tracheo-bronchial region)	unknown	unknown
Attached fraction	decreases	increases
Total potential α energy on attached fraction (and effect on pulmonary region)	unknown	unknown

Increased Use of Thermal Storage

It is expected that much more use will be made of thermal storage in homes to save energy. Solar-heating systems and possible off-peak power-pricing strategies could encourage use of thermal storage. Massive concrete, brick or stone walls, floors, and room dividers are likely to find increased use in residences. These may significantly increase Rn-222 activity inside homes.

Since building materials often emit less Rn-222 than soil,[1] the main effect of increased use of massive concrete, brick and stone walls on indoor Rn-222 levels may be through the tighter envelopes that result. Figure 2 shows the results on potential alpha energy levels when the source strength is doubled from 0.01 to 0.02 pCi/L·min (6×10^{-3} to 0.012 Bq/m^3·sec) and and the air exchange rate is halved from 1 to 0.5 ach.

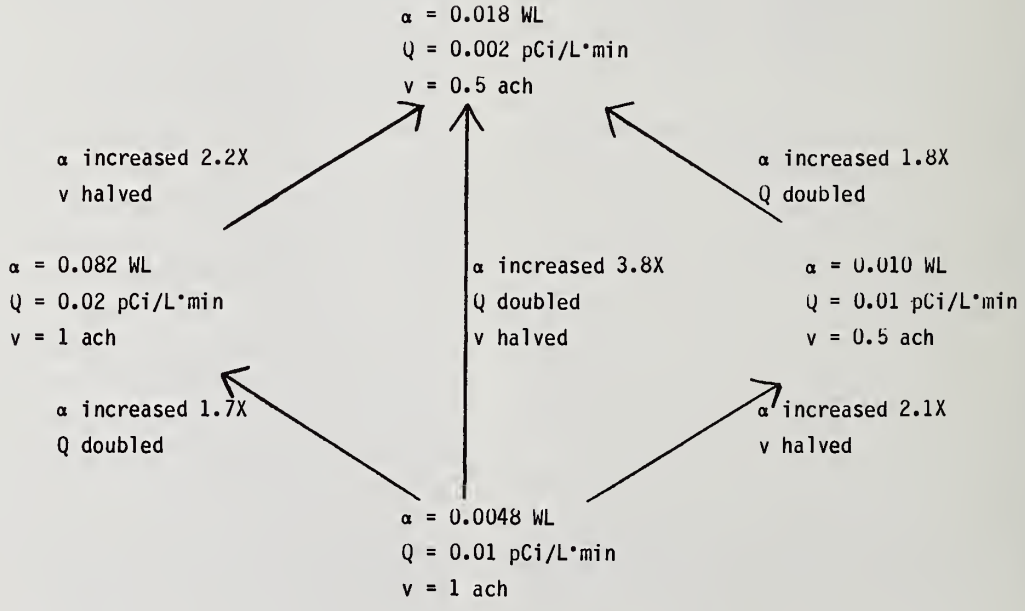

Figure 2. Increase in potential alpha energy (α, WL) with increasing source strength (Q, pCi/L·min) and decreasing air exhcange rate (v, ach).

The effects of changes in building materials are illustrated by Swedish experience.[17] Homes built before 1930 had average Rn-222 activity levels of about 0.54 pCi/L (20 Bq/m^3) compared to 0.86 pCi/L (32 Bq/m^3) for those built between 1941 and 1950 and 2.9 pCi/L (107 Bq/m^3) for those built between 1971 and 1975. Most of the 3.3-fold increase between 1941-50 and 1971-75 can be attributed to the reduction in average air exchange rates from 0.8-0.9 to 0.3-0.45 ach, but some of it is due to changes in building materials. The contribution of building materials is seen more clearly in the 1.5-fold increase in Rn-222 activity between houses built before 1930 and those built in the period 1941-50. There was little difference in air exchange rates between these two groups of houses.

Earth berms

Another strategy which can save energy in buildings is partial burying to take advantage of the earth's insulating value and thermal storage. Many experimental buildings have been built where entire walls and even roofs are banked with earth. Partially buried walls would presumably be more common. In any case, increased earth in proximity to the building shell could increase Ra-226 activity near the shell, and larger quantities of Rn-222 could diffuse inward.

Economic Considerations

Higher energy costs as well as general inflation may cause a future reduction in residential size. If this occurs, the ratio of surface area to volume of the residence will increase, causing an increase in indoor Rn-222 activity arising from subsoil or building material. The increase in Rn-222 activity from decreased floor area and volume is calculated in Appendix A. Rn-222 emanation rates from building materials per unit volume increase about 11% for the extreme case of a 1-story house with no attic or basement where walls and floors contribute equal activities of Rn-222 per unit time and area, and the house volume (or floor surface) is decreased by 1/3 from 150 to 100 m^2.

In areas where the main Rn-222 source is natural gas or water, the effect of decreasing house size would be greater. If the same quantities of these materials were used inside the two houses above, there would be a 50% increase in Rn-222 activity from these sources. If the equilibrium factor were also raised, then the increase in potential alpha activity would be still greater. Occupants of residences could also be expected to alter their behavior to save energy and money, for example by reducing operation of the usually present ventilating fans in bathrooms and kitchens, or by not opening windows. These actions would reduce venting of Rn-222 and its daughters from water and natural gas sources and therefore increase indoor radioactivity levels.

POSSIBLE CONTROL STRATEGIES

If Rn-222 activity levels are known to be hazardous, there are several possible controls, but with economic penalties. For example, additional natural or mechanical ventilation air could be provided at the expense of additional energy use. Heat exchangers now being introduced in Europe, which transfer heat from the exhaust to incoming ventilation air, could also be employed at a capital cost penalty. High-efficiency air cleaners used on recirculated air could reduce levels of particulates and attached radioactivity. These air cleaners are currently available, but are rather costly for widespread residential use. Surface coatings impervious to Rn-222 for basement walls and floors are being developed and tested.[18] Other architectural strategies might also be developed.

CONCLUSION

Several trends in housing construction and occupant strategy are likely to become permanent changes due to to increased costs and uncertain availability of energy. These trends suggest that higher activity levels of Rn-222 and its progeny will occur in future residences than in those built with pre-energy crisis practice. It is calculated that, under the most extreme circumstances, future potential alpha activities up to 10 times past levels may occur. Therefore, this problem should be investigated to obtain more quantitative data to further assess health hazards.

APPENDIX A

RN-222 EMMISSION AND REDUCTION OF HOUSE VOLUME OR FLOOR SURFACE

Let A_i = floor area (m^2) of house i. A_i is proportional to volume because height is assumed constant.

E_i = total Rn-222 emanation rate from exterior walls and floors per unit volume (pCi/L·min)

S_f = Rn-222 emanation rate per unit floor surface (pCi/min·m^2)

S_w = Rn-222 emanation rate per unit wall surface (pCi/min·m^2)

w_i = width (m) of house i

l_i = length (m) of house i

h = height (m) of house = 2.5 m

$\gamma = l_i/w_i$ = length/width ratio

$\delta = w_2/w_1 = l_2/l_1$ = ratio of linear dimensions of house 2 to house 1.

A_f = floor surface area (m^2)

A_w = exterior wall surface area (m^2)

V = volume (m^3)

h, γ and δ are assumed constant when floor surface is reduced, i.e. the floors of both houses are assumed to retain the same geometry. The ceiling and interior wall partitions are assumed to contribute a negligible amount of Rn-222 activity since they probably contain little concrete.

$$E_i = \frac{A_f S_f + A_w S_w}{V}$$

$$= \frac{w_i l_i S_f + 2h(w_i + l_i) S_w}{w_i l_i h}$$

$$= \frac{1}{h} S_f + 2\left(\frac{1}{l_i} + \frac{1}{w_i}\right) S_w$$

$$= \frac{1}{h} S_f + 2\left(\frac{1}{\gamma} + 1\right) \frac{1}{w_i} S_w$$

Therefore:

$$\frac{E_2}{E_1} = \frac{1 + 2\left(\frac{1}{\gamma} + 1\right) \frac{h}{\delta w_1} \frac{S_w}{S_f}}{1 + 2\left(\frac{1}{\gamma} + 1\right) \frac{h}{w_1} \frac{S_w}{S_f}}$$

Let γ = 4/5, corresponding to a reduction in V of about 1/3. Assume A_1 = 150 m^3, then $A_2 \approx 100$ m^3. Usually, $S_w < S_f$.[1] If S_w is very small, then $E_2/E_1 \approx 1$. Take $S_w/S_f = 1$ as an extreme case. Three cases are γ = 1 (square house), γ = 1.5 (length = 1.5 x width), and γ = 2 (length = 2 x width). These yield increased radon concentrations due to the structure itself of 11.2, 11.3 and 11.6%, respectively. A sample calculation is given for the first case:

$A_1 = w^2$

w_1 = 12.247 m

h/w_1 = 0.204

E_2/E_1 = 1.112

REFERENCES

1. Sources and effects of ionizing radiation. United Nations Scientific Committee on the effects of atomic radiation 1977 report to the General Assembly, with Annexes, United Nations Publication, New York (1977).
2. George, A. C., and Breslin, A. J., The distribution of ambient radon and radon daugthers in residential buildings in the New Jersey-New York area. Symposium on the Natural Radiation Environment III, Houston (1978).
3. George, A. C., And Breslin, A. J., Deposition of radon daughters in humans exposed to uranium mine atmospheres. Health Phys. 17, 115-124 (1969).
4. Lundin, F. E., Jr., Wagoner, J. K., and Archer, V. E., Radon daugthers and respiratory cancer, quantitative and temporal aspects. U.S. Department of Health, Education and Welfare joint monograph no. 1 (1971).
5. Jacobi, W., Relations between the inhaled potential alpha-energy of ^{222}Rn and ^{220}Rn daughters and the absorbed alpha-energy in the bronchial and pulmonary region. Health Phys. 23, 3-11 (1972).
6. Jacobi, W., Relation between cumulative exposure to radon daugthers, lung dose and lung cancer risk, p. 492-500 in Noble Gases, R. E. Stanley and A. A. Moghissi, eds., U.S. Energy Research and Development Administration report CONF-730915 (1973).
7. Schiager, K. J., Analysis of radiation exposures on or near uranium mill tailing piles. Report prepared for the Silver Corporation, Salt Lake City (1973).
8. A preliminary evaluation of the control of indoor radon daughter levels in new structures. U.S. Environmental Protection Agency report EPA-520/4-76-018, Washington (1976).

9. Indoor radiation exposure due to radium-226 in Florida phosphate lands. U.S. Environmental Protection Agency report EPA-520/4-78-013, Washington, (1979).
10. Handley, T. H. and Barton, C. J., Home ventilation rates: a literature survey, AEC report ORNL-TM-4318 (1973).
11. Sinden, F. W., A two-thirds reduction in the space heat requirement of a Twin River townhouse. Center for Environmental Studies report no. 56, Princeton (1977).
12. Harris, R. L. and Bales, R. E., Protection of workers against radioactive gas and dust, p. 61-82 in Proceedings of the symposium on radiological health and safety in mining and milling of nuclear materials 1963, vol. II, IAEA publication STI/PUB/78, Vienna (1964).
13. Wrenn, M. E., Rosen, J. C. and Van Pelt, W.R., Steady-state solutions for the diffusion equations of radon-222 daughters, Health Phys. 16, 647-656 (1969).
14. Jacobi, W., Activity and potential alpha-energy of ^{222}Rn and ^{220}Rn daughters in different air atmospheres. Health Phys. 22, 441-450 (1972).
15. Kusuda, T., Silberstein, S. and McNall, P.E. Jr., Modeling of radon-daughter concentrations in ventilated spaces, in prep.
16. 10 CFR 12 (1972).
17. Swedjemark, G. A., Radon in dwellings in Sweden. Symposium on Natural Radiation Environment III, Houston (1978).
18. Auxier, J. A., Shinpaugh, W. H., Derr, G. D., and Christian, D. J., Preliminary studies of the effects of sealants on radon emanation from concrete. Health Phys. 27, 390-392 (1974).

EPA APPROACH TO ESTIMATING HEALTH RISKS OF RADON/RADON DAUGHTER EXPOSURE

Neal S. Nelson

Bioeffects Analysis Branch
Criteria and Standards Division
Office of Radiation Programs
Environmental Protection Agency
Washington, D.C. 20460

The EPA has used the results of epidemiological studies of uranium and other underground miners to obtain risk coefficients for estimating the health impact (fatal lung cancer) due to radon/radon daughter exposure. Animal exposure data, although now showing a dose response curve, is of little help due to differences in human-animal lung morphometrics, dosimetry and the cells of origin of lung cancer. It is not always appreciated that animal lung cancers differ in histological classification from common human lung cancers. U.S. uranium miner data is likewise of little use since exposures generally greatly exceeded several hundred cumulative working level months (CWLM).

EPA has derived an average relative risk coefficient of 3% increase in lung cancer per CWLM exposure from an evaluation of Ontario, Czech, and Swedish miner data. These data, aggregated for all ages of miners, show for exposures less than a few hundred CWLM a linear dose response curve. Apparent increases in fatal lung cancer range from 1% per CWLM at high CWLM to 4% or more per CWLM at low CWLM exposures.

Since published data show no striking differences between aerosol characteristics in mines, outdoors, or inside, the major difference in exposure between miners and a general population is the volume of air respired. A miner engaged in a mixture of light and heavy work inhales about 3×10^5 liters of air a month, a reference adult in the population about 2.2 times greater volume. In a 1 WL atmosphere, a miner would be exposed to 12 CWLM per year, a reference adult about 27 CWLM. However, Americans spend only about 75% of their time in their residence; so a residential exposure to 1 WL indoor radon/radon daughter concentration corresponds to 20 CWLM per year.

Using a 3% CWLM relative risk model and residential exposure to 0.02 WL, the following population risk estimates were made in an EPA report.[1]

Lifetime Risk of Lung Cancer per 100,000 Persons
Due to Lifetime Residency in Structures with
an Average Radon Daughter Concentration of 0.02 WL

Relative Risk	Excess Cancer Deaths	Total Years of Life Lost
Adult and Child Sensitivity Equal	2,000	30,000
Child Sensitivity 3 times Adult	3,000	50,000
Absolute Risk (10 deaths/CWLM for 10^6 person-years at risk)	1,000	27,000

In perspective, the expected lifetime lung cancer mortality in the U.S. population is 2,900 per 100,000 persons in a population having the age specific mortality pattern of the 1970 U.S. population.

A detailed analysis of the rationale for estimating radon/radon daughter health effects is given in the EPA publication. [1]

---

[1] Guimond, R., Ellett, W., Fitzgerald, J., Windham, S.F., and Cuny, P., Indoor Radiation Exposure Due to Radium-226 in Florida Phosphate Lands, Environmental Protection Agency, EPA 520/4-78-013 (1978).

* *

THE ENVIRONMENTAL WORKING LEVEL MONITOR (EWLM)

D.J. Keefe, W.P. McDowell and P.G. Groer*

Electronic Division
Argonne National Laboratory
Argonne, IL 60439

The Environmental Working Level Monitor (EWLM), designed and developed at Argonne National Laboratory for the EPA, is a fully automated, microprocessor- controlled, portable instrument, which allows monitoring of airborne radon-daughter concentrations and the Working Level (WL). It has a monitoring range of 10^{-3} to 10 WL or a lower limit of approximately 0.1 pCi per liter for the radon-daughter concentrations. Thus the instrument is capable of measuring the normal background levels of these nuclides. The EWLM requires 9 minutes to make and record a measurement. It can be programmed to automatically take and record 192 measurements at a minimum time interval of one measurement every 10 minutes. The time interval between measurements can be programmed for any period of time greater than 10 minutes, such as one measurement every hour for 8 days. The starting time and completion time are also programmable.

To provide these measurements, the EWLM uses a diffused junction detector for the alpha particles and a NE102 scintillator optically coupled with a 10-stage photomultiplier for the beta particles.

A single channel analyzer resolves the 6.0 MeV RaA (^{218}Po) from the 7.69 MeV RaC' (^{214}Po) alpha particles. The separated RaA and RaC' (^{218}Po and ^{214}Po) counts are stored in the computer memory along with the total (beta and gamma) counts from RaB and RaC (^{214}Pb and ^{214}Bi). These three stored counts are used by the internal computer to calculate the radon-daughter concentrations and the WL. The EWLM method does not make any assumptions about the equilibrium conditions between the radon daughters, but does assume, like all other methods, that the airborne radon-daughter concentrations are constant during the sampling period of three minutes.

The calibration of the instrument is quite complex. Briefly, it requires analysis of the same air sample by the EWLM method and by other methods which determine the radon-daughter concentrations and the WL from alpha counts observed during three different counting intervals.

The flexibility of this instrument with its computer-programmable options makes it a useful tool to study the effects of ventilation on the radon-daughter concentrations in buildings.

---

* Institute for Energy Analysis, Oak Ridge, Tenn.

TRACK ETCH TECHNIQUES FOR RADON MEASUREMENTS

H. Ward Alter

Terradex Corporation
Walnut Creek, CA 94598

The Terradex Corporation has supplied several hundred thousand Track Etch® cups to the mining industry to measure radon levels in soil gas as a tool in uranium exploration. The Track Etch technique involves a simple dielectric detector which responds to alpha particle radiation damage tracks from radon and its daughters. The tracks are subsequently etched and counted to give a measure of the integrated alpha dose to the detector. Detectors can measure the integrated dose over exposure periods ranging from about one day to one year.

The Track Etch technique, originally invented for environmental measurements, has recently been significantly improved. New materials allow increased sensitivity, automatic readout and high resistance to environmental factors such as temperature and humidity. Membrane filters permit the exclusion of thoron gas from the cup and also of particulate radon daughters in the ambient atmosphere. Calibration of the Track Etch response to the standard radon atmospheres at the Environmental Measurements Laboratory in New York, have shown good reproducibility and will allow the Track Etch response to be reported directly in picocuries per liter.

The improved Track Etch system has the sensitivity and simplicity for inexpensive large scale screening of structures for radon levels.

* *

EPA RADIATION PROTECTION GUIDANCE FOR PHOSPHATE LANDS

Allan C.B. Richardson

Federal Guidance Branch
Criteria and Standards Division
Office of Radiation Programs
Environmental Protection Agency
Washington, D.C. 20460

Ed. note: The speaker did not submit a summary for inclusion in this report. The EPA letter to the Governor of Florida setting forth the findings of its investigation of indoor radiation exposure due to radium-226 in Florida phosphate lands, and the recommendations for radiation protection of persons residing on phosphate lands has been published in the Federal Register, Vol. 44, 38664-70 (July 2, 1979). For further information, contact the speaker directly.

* *

RADON IN BUILDINGS: UNIVERSITY OF FLORIDA INTEREST AND ACTIVITIES

C.E. Roessler and Z.A. Smith

Department of Environmental Engineering Sciences
University of Florida
Gainesville, FL 32611

Efforts are directed primarily to indoor radon associated with phosphate mining, land reclamation and by-product use. Emphasis areas include:

1. Developing a general overview of the situation;
2. Determining the relationship of indoor radon and radon progeny levels to land and materials history;
3. Development of methods for predicting future indoor levels for currently undeveloped lands; and
4. Proposing and verifying mining and land reclamation methods that minimize future radiological impact.

From the standpoint of developing criteria and remedial measures, three distinct situations exist:

1. Radioactivity in existing structures,
2. Future construction over existing mined but undeveloped land, and
3. Mining, reclamation and future development of currently unmined land.

Lands can be classified according to history - undisturbed, tailings reclaimed, low activity overburden, high activity overburden, etc. Each has its characteristic distribution of soil radium concentrations, and structure-land type categories have characteristic distributions of indoor radon progeny concentrations.

By estimating the number of structures in various land-structure type categories and summing distributions across categories, the distribution of indoor radon progeny concentrations was estimated for Polk County in the Central Florida phosphate mining region.

Predicting future indoor levels expected for currently undeveloped land is complicated by the many variables in this relationship. Soil surface radon flux, soil radium distribution and gamma radiation levels are being examined for sensitivity and usefulness as predictors.

For the case of currently unmined lands, the opportunity exists for limiting future indoor radon levels by measures applied during mining and reclamation. Mining companies are being encouraged to examine the feasibility of mining and reclaiming in a fashion that simulates the natural soil radium distribution - i.e. selectively placing the higher activity spoils and wastes under a cover of lower activity overburden. Future work will include field testing of the effectiveness of such procedures.

* *

PROPOSED PROJECT TO STUDY REDUCTION OF INDOOR RADON -222 CONCENTRATIONS THROUGH IMPROVED CONSTRUCTION TECHNIQUES

Harlan Keaton

Polk County Health Department
Winter Haven, FL 33880

Large areas of Central Florida, located primarily in Polk and Hillsboro Counties have been mined for phosphate bearing ore. Associated with this ore are significantly elevated concentrations of uranium and its decay products (about 30 to 60 times greater than those found in average soil and rock). As this ore is recovered large areas of waste land containing water filled trenches (phosphate pits), overburden, tailings and slimes from processing the ore are left behind. Much of the uranium and its decay products either remain in this waste land or are returned to it with the process wastes after the phosphate has been removed. A significant amount of this waste land has been and will be converted into beneficial and productive land for use in agricultural production, recreational and housing needs. Much of this land borders relatively large populated areas and is needed for home construction. In fact many homes have already be built on this reclaimed phosphate land and many are being built. There has been a great deal of data compiled by several government and private organizations concerning the problems associated with this construction. The major one being risk of increased cancer rates due to exposure to radon-222 daughter products. In the latest Environmental Protection Agency publication concerning the subject entitled Indoor Radiation Exposure Due To Radium -226 In Florida Phosphate Lands, the subject of control measures is discussed, and the following five types of control methods to reduce radon in homes are analyzed:

(1) Air particulate removal;
(2) Polymeric sealants;
(3) Ventilated crawl spaces;
(4) Excavation and fill methods; and
(5) Improved slab construction.

The five methods evaluated indicate an average probable reduction of radon decay product air concentration by about 80% but as of this date there have been no test structures built or tests performed to confirm any reduction figures.

The Polk County Health Department, with the cooperation of a local builder-contractor, has begun a project that should supply data on a number of control techniques to reduce radon concentrations in homes built on reclaimed phosphate lands. Several test homes will be built on a proposed tract of reclaimed phosphate land. The models will be of the following types:

(1) Improved slab construction - monolithic slab;.
(2) Monolithic slab with ventilation pipes to allow ventilation from under the slab to the exterior;
(3) Ventilated crawl space with wooden flooring at least twelve inches above ground surface; and
(4) Ventilated crawl space with prestress concrete floor at least twelve inches above ground surface.

Measurements taken at structure sites and in structures will include:

(1) Radium-226 analysis in the soil before construction;
(2) Radon exhalation rates from soil before construction;
(3) Soil density measurements before construction;
(4) Soil moisture measurements in conjunction with Radon exhalation rates;
(5) Radon exhalation rates after construction (near structures and underneath structures with crawl spaces);
(6) Radon concentrations in ventilated crawl spaces;
(7) Equilibrium measurements in crawl spaces;
(8) Radon concentrations in structures;
(9) Equilibrium measurements in structures;
(10) Working level concentrations in structures; and
(11) Gamma survey done over entire tract of land.

Upon completion of this project we hope to have identified at least one or two construction types that will reduce radon daughter concentrations to a level low enough to allow contractors and home builders to utilize the reclaimed phosphate land for further residential use.

* *

NRC INTEREST IN RADON IN BUILDINGS

N.A. Eisenberg

Transportation and Products Standards Branch
Office of Standards Development
Nuclear Regulatory Commission
Washington, D.C. 20555

NRC interest in the issue of radon in buildings may be divided into three categories:

1. In the event that NRC is given the responsibility for regulating NARM (naturally occurring and accelerator-produced radioactive materials), the NRC staff may need to issue regulatory guidance to enhance human safety related to radon in buildings;
2. NRC licensing of consumer products used in buildings may need to take account of the elevated background population exposure due to radon in buildings and;
3. Models used to analyze radon in buildings may have application to analyses performed by NRC (for consumer products, transportation incidents, reactor accidents) and vice versa.

In July 1977, NRC published a task force report, "Regulation of Naturally Occurring and Accelerator-Produced Radioactive Materials," NUREG-0301. The task force recommended that the NRC seek legislative authority to regulate NARM, since these materials present significant radiation exposure potential and present controls are fragmentary and non-uniform at both the State and Federal level.

In the process of licensing consumer products such as ionization-type smoke detectors, tritium backlighted watches, and spark eliminators, the elevated radiation exposure levels in enclosed, interior spaces may need to be taken into account to avoid unnecessarily excessive cumulative exposures.

The NRC staff often needs to estimate the dose received by people in buildings resulting from sources of radioactive gases or aerosols--the source of which is either internal to the building (such as consumer products, defective products, or storage facilities) or external to the buildings (such as transportation or reactor incidents). One model used for transporation accidents[1] relates dose to an individual inside the building to the dose to an individual outside using parameters such as deposition, filtration, radioactive decay, air-recirculation, and infiltration factors. Another model[2] used for hazardous material spills relates the time history of concentration inside a building to the time history of concentration outside in terms of building volume and air change rate.

---

[1] A. R. Ducharme, et. al., "Transport of Radionuclides in Urban Environs: a Working Draft Assessment", SAND 77-1927, May 1978, p. A-203.

[2] A. H. Rausch, et. al., "Continuing Development of the Vulnerability Model", CG-D-53-77, February 1977, Chapter 8.

* *

REPORT ON INTERESTS AT BROOKHAVEN NATIONAL LABORATORY

John Nagy

Biomedical and Environmental Assessment Division
Brookhaven National Laboratory
Upton, NY 11973

The Biomedical and Environmental Assessment Division (BEAD) is part of the Brookhaven National Laboratory in Upton, New York. Most of the support of the division comes from the Office of the Assistant Secretary for the Environment of the Department of Energy. The division's mission is to help evaluate the human health and ecological impacts of alternative energy supply and use strategies.

The BEAD's interest in radon arises from two separate energy strategies only one of which is directly related to the subject of this discussion.

(1) Some building energy conservation methods will increase indoor levels of radon and its daughters. A former staff member of BEAD published work relating to the general problem of increased levels of indoor pollution before joining the National Bureau of Standards. No work has since been done at BEAD, nor is any contempleted, to pursue the specific topic of indoor radon health effects. Work does continue on general problems related to building energy conservation, indoor air pollution, and methods of monitoring exposure to indoor air pollution.

(2) Uranium mining, active mills, and mill tailings produce radon gas which raises outdoor levels. A paper is in preparation reviewing current knowledge about and estimates of the health effects from this source.

HEALTH TRADE-OFFS INVOLVED IN TIGHTENING HOUSES: INCREASED RADON EXPOSURE VS. DECREASED EXTERNAL AIR POLLUTION

Jan Beyea

Center for Energy and Environmental Studies
Princeton University
Princeton, NJ 08544

Ed. note: The speaker withdrew the summary submitted for inclusion in this report. For further information, contact the author directly.

* *

INDOOR RADON STUDIES AT LAWRENCE BERKELEY LABORATORY

W.W. Nazaroff, C.D. Hollowell and J.V. Berk

Energy and Environment Division
Lawrence Berkeley Laboratory
Berkeley, CA 94720

Space heating and air conditioning account for roughly 20% of the primary energy used in the United States. Rising costs and supply uncertainties are motivating builders and owners to reduce building energy consumption. Substantial energy savings can be achieved by reducing the rate at which outside air enters a building. This can lead to increased exposures to radon daughters and other indoor generated contaminants. The Building Ventilation and Indoor Air Quality Group at Lawrence Berkeley Laboratory is studying the impact of energy conservation in builings on indoor air quality.

Work at LBL on radon in buildings began in 1978. We have focused initially on the following tasks:

1. Review radon literature;
2. Enter radon information into LBL ventilation data base;
3. Develop a quick and sensitive technique for measuring the exhalation rate and diffusion length of radon in concrete and rock samples; and
4. Measure radon concentrations and ventilation rates in energy efficient buildings.

Interim results of this project will be presented.

The ultimate goals of the LBL indoor radon project are to:

1. Measure radon and radon daughter concentrations in conventional buildings and energy-efficient buildings;
2. Characterize sources of indoor radon;
3. Establish relationship between radon levels and building design parameters;
4. Evaluate control strategies; and
5. Estimate U.S. populations at risk to indoor radon in conventional buildings and proposed energy-efficient buildings.

THE EFFECTS OF VENTILATION ON RADON AND DAUGHTER ACTIVITIES

Samuel Silberstein

Building Thermal and Service Systems Divisions
Center for Building Technology
National Bureau of Standards
Washington, D.C. 20234

The dependence of indoor potential alpha energy concentration on ventilation rate, source strenyth and outdoor Radon-222 concentration was studied usiny a computer program developed at the Center for Building Technology of the National Bureau of Standards. As an example, Fiyure 1 shows potential energy time courses for various source strengths; it is believed that 0.01 pCi/L min is a common value.

The model developed at NBS lends itself to simulation of source strenyths and ventilation rates changing at intervals of 1 or 2 hours. It can also be modified to account for settling out of particulates. Steady-state conditions have usually been assumed to study Radon-222 and daughter levels but are inappropriate because of changing air exchange rates and source strengths, and because they take several hours to reach at low air exchange rates.

A complete description of the program is presented in the forthcoming paper "Modeling of Radon-Daughter Concentrations in Ventilated Spaces" by T. Kusuda, S. Silberstein and P. E. McNall, Jr.

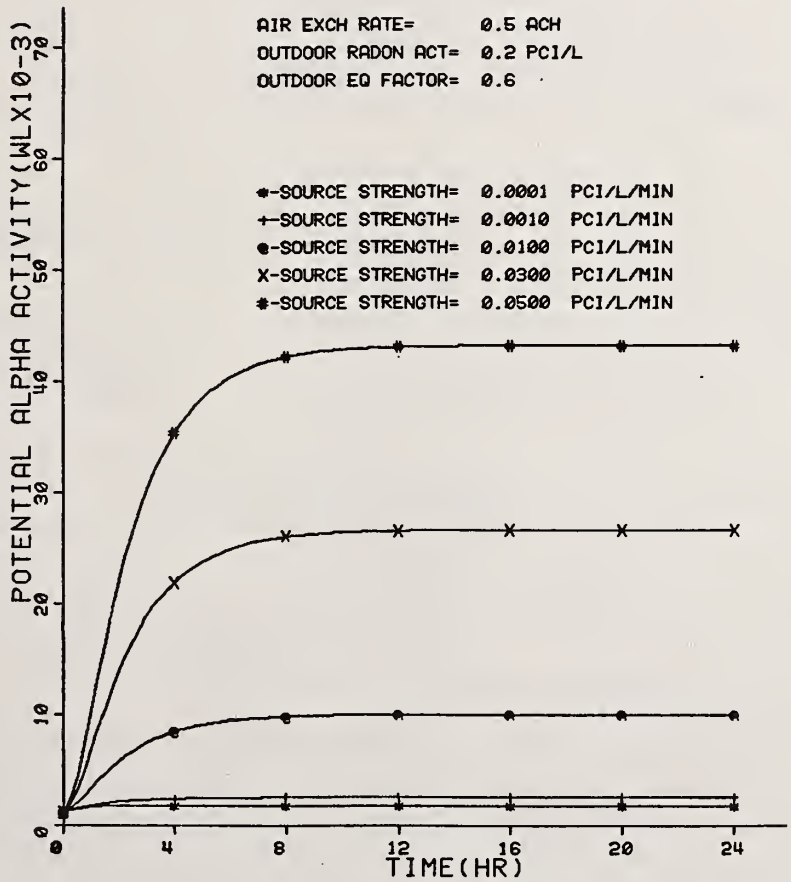

Figure 1. Potential alpha activity for various source strengths. Initial radionuclide concentrations equal outdoor levels.

* *

THE RADIOLOGICAL HEALTH ASPECTS OF SOLAR HOME HEATING

A.E. Desrosiers

Battelle Memorial Institute
Pacific Northwest Laboratory
Richland, WA 99352

and

Stewart A. Farber

New England Power Company
Providence, RI 02901

Some active solar heating systems use a heat storage reservoir which consists of approximately 30 tons of granite. Air-cooled solar collectors transfer radiant energy to a bed of crushed granite, where the heated rock serves as a storage medium. The granite bed is usually in a basement of subterranean space; the rock is crushed to 1" - 1 1/2" diameter pieces. A conventional hot air heating system then extracts energy from the rock to maintain temperatures in the living space.

The hot granite also emanates ^{222}Rn. Preliminary calculations indicate that the granite bed may release 140,000 pCi per hour of ^{222}Rn. Allowing for losses of radon daughter products through leakage and filtration, an 1800-ft^2 home would maintain a level of 9 pCi per liter of ^{222}Rn and its daughter products or 76 cumulative working level months of exposure per year. This exceeds EPA's regulations for ^{222}Rn in homes. The zero-intercept, linear hypothesis model of the BEIR report suggests that continuous exposure of the US population at these levels would result in 26,000 to 56,000 cancer deaths per year.

Clearly, the potential health aspects of this energy technology have not been well examined. We suggest a three-part program of investigation:

1. Develop a complete analytical model which will examine the radiological influence of each design parameter of the solar heating system;
2. Inaugurate a measurement program which will test and verify the model; and
3. Select a solar heating design which will minimize radiological health impacts and also examine the tradeoff of radiation versus cost for a number of intermediate designs.

With only minor modifications this proposed model will be applicable to evaluation of the radiological health aspects of any type of solar heating design which employs masonry or stone heat storage media. This includes passive solar heating concepts, such as Trombe walls, masonry lined atria or greenhouses. In passive solar heating systems the radon emanation may be significantly lower; however, direct radiation from naturally occuring radionuclides in masonry materials is expected to be larger and may be as significant as the radon emanations from those active systems using rock storage beds. Consequently, the modifications to our model will include calculations of the direct radiation components.

The radiological health impacts of some solar home heating concepts or designs are potentially greater than other energy technologies. This is because radiation is released within the home rather than from a distant central power source. A single central power source may be more effectively and economically controlled than the dispersed sources which are inherent in a widespread deployment of solar space heating technology. Therefore, the radiological health implications of solar home heating must be factored into the research and development of this energy technology at the earliest possible stage.

* *

SOME DETERMINATIONS AT ARGONNE NATIONAL LABORATORY OF RADON IN HOUSES*

J. Rundo, F. Markun and N.J. Plondke

Center for Human Radiobiology
Argonne National Laboratory
Argonne, IL 60439

The chance observation of a radon concentration of 26 $pCi \cdot L^{-1}$ in the bedroom air of a frame house has led to the discovery that such levels can arise as a result of emanation of radon from bare soil in a "crawl space" under part or all of the house. They are not a consequence of "technologically enhanced" radioactivity in building materials. In a total of 23 houses investigated, the air of ten showed concentrations of radon of 5 $pCi \cdot L^{-1}$ or more; of these, six had radon concentrations of 10 $pCi \cdot L^{-1}$ or more. It should also be mentioned that a concentration as low as 0.2 $pCi \cdot L^{-1}$ was observed in one of these houses. The presence or absence of plastic vapor barriers seems to be one important factor in determing the level, but certainly not the only one.

During July and August 1978, an Environmental Working Level Monitor that was returned to A.N.L. for repair and testing was used to determine the concentrations of radon daughters during a total of three periods, each of about 100 hours' duration, in two of the houses. Mean values of 0.008 WL and 0.023 WL were observed in the first, and of 0.008 WL for the second.

On the basis of such limited data it is obviously not possible to generalize on the average concentration of radon daughters in these houses. However, it is conceivable that the average concentration might be in the region of 0.01 WL; exposure at this level for a year (say of a small child) would result in a radiation dose equivalent of 2.6 rem to the bronchial epithelium (derived from 5 rem per WLM, for a 170-hour working month).

---

*Work supported by the United States Department of Energy

* *

REPORT ON ACTIVITIES AT THE TECHNICAL UNIVERSITY OF DENMARK

Niels Jonassen

Laboratory of Applied Physics I
Technical University of Denmark
Lyngby, Denmark

The radon-oriented work at our laboratory is presently concentrated around three topics:

1. EXHALATION OF RADON FROM BUILDING MATERIALS

As a part of the Danish Ministry of Commerce' energy saving projects a number of building materials are being checked for radon exhalation. The materials are being placed in closed containers and the build-up of radon activity in the containers measured as a function of time.

2. EFFECT OF IMPROVED INSULATION OF HOUSES ON INDOOR RADON LEVELS

As a part of the projects mentioned above the concentrations of radon and its daughter products are being measured in houses with very low ventilation rates. This will be done in newly constructed, so-called low-energy houses as well as in older houses and apartments, which have had their insulation improved. The radon measurements will be supplemented by the measurements of other indoor climatic parameters, such as temperature, humidity, ventilation rate and concentration of various (organic) vapors.

3. REMOVAL OF RADON DAUGHTERS BY ELECTRIC FIELDS

The effect of an electric field on the concentration of radon daughters in a closed room is being studied by keeping a wire or arrangement of wires at various positive and negative potentials with respect to ground. Preliminary measurements indicate that the working level may be lowered to about half of its undisturbed value by a single wire kept at a negative voltage of a few kV. The effect seems primarily to be due to a decrease in the concentrations of ^{214}Pb, ^{214}Bi and ^{214}Po, while the concentration of ^{218}Po remains almost constant, although ^{218}Po is the predominant element in the deposit on the wire. Work is planned to clear this problem as well as to study the relation between wire voltage and WL-lowering. Also the possible effect of a corona discharge on the depletion of the radon daughters will be studied.

* *

MEASUREMENTS OF AIRBORNE POLLUTANT CONCENTRATIONS INSIDE A WELL-INSULATED STRUCTURE WITH LOW VENTILATION RATE

F.F. Haywood, A.R. Hawthorne and D.R. Stone*

Health and Safety Research Division
Oak Ridge National Laboratory
Oak Ridge, TN 37830

A series of pollutant concentration measurements has been made in a residential structure designed to reflect current concepts in energy conservation. The residence was constructed with ordinary building materials, but special attention was given to minimizing heat losses to the outside by air infiltration and surface convection. The house represents a typical eastern Tennessee dwelling: single family, two story, light frame, recirculated air, electric heat, and ventilated crawl space below the first floor. The structure is one of the three test houses (control house) included in the Tennessee Energy Conservation in Housing (TECH) project in Knoxville, Tennessee.

Measurements were made over a period of five days in September 1978. These included such determinations as concentration of indoor gaseous pollutants by mass spectrometry; indoor and outdoor radon concentration; indoor radon daughter concentration; radon flux through floors, walls and ground; airborne dust concentration; and ventilation rate in four rooms of the house. In addition to these measurements, samples of soil which were obtained from the crawl space beneath the house and from the lawn surrounding the house were analyzed for radionuclides in the uranium and thorium decay series. In order to make correlations between observed pollutant concentrations and meteorological conditions, data were obtained from existing TECH project instrumentation and included wind speed and direction, solar flux, temperature, and barometric pressure. Facilities and equipment used for this study included those of the Health and Safety Research Division's Off-Site Pollutant Measurements Group and the Monitoring Technology and Instrumentation Group.

Results of this study represent a baseline situation. In searching for nonradioactive airborne pollutants, no mass peaks above detection limit were observed. The detection limit for most mass peaks is 0.5 ppm. The low concentration of airborne pollutants is attributed to the fact that no one lives in the house; utility usage is simulated solely for purposes of economic studies. The mass spectrometer was useful for measuring the concentration of a tracer gas (CO_2) used to determine the structure's ventilation rate. This latter parameter was found to be dependent on external driving forces - notably wind speed. For example, whenever the wind speed was below about 10 kilometers per hour, the ventilation rate was approximately 0.22 air changes per hour (ach); however, as the wind speeds increased to about 15-17 $km \cdot h^{-1}$, the ventilation rate increased to 0.4 ach.

Continuous indoor radon measurements at four locations showed concentrations ranging from less than 0.1 $pCi \cdot L^{-1}$ to as high as 0.93 $pCi \cdot L^{-1}$. Most values fell within the 0.2 to 0.4 $pCi \cdot L^{-1}$ range. Simultaneously, continuous outdoor measurements ranged from 0.02 to 1.21 $pCi \cdot L^{-1}$ at two nearby locations. The indoor radon concentration was generally lower (20-50%) than the outdoor concentration. This reversal from the usual pattern may be attributed to the typically low ^{226}Ra concentration in building materials used in light frame structures of this type. Furthermore, the ventilated crawl space beneath the floor prevents soil-borne radon from readily diffusing into the structure. Other typical household sources of radon such as tapwater and natural gas result in limited contributions (none for natural gas) through simulated occupancy. Thus, most of the indoor radon originates from outdoor air entering the structure. For example, as the wind speed increased one day, the structure ventilation rate was observed to increase from 0.22 to 0.41 ach. The indoor radon concentration increased and approached that outside, but lagged the increase in exchange rate by three to four hours. This behavior was expected since outside air was the major source of radon. For structures coupled to the ground (i.e. slab on grade, or basement) constructed with materials known to bear ^{226}Ra (concrete, cinder block, brick, etc.), the reverse situation would be expected. That is, when the major source of indoor radon consists of that from construction materials and the ground, a reduction in ventilation rate would increase the indoor concentration. Results of radon daughter measurements at the four radon monitoring locations indicated that the degree of equilibrium between radon and its daughters ranged from 40 to 70% - a little less than would be expected at these air exchange rates.

The report contains all pertinent data collected during this study and includes tabular and graphical presentations of radiological and meteorological data as a function of time and location.

---

*Consultant.

+Operated by Union Carbide Corporation under contract W-7405-eng-26 with the U.S. Department of Energy.

* *

RADON CONTROL IN HOUSING IN CANADA

R.S. Eaton

Atomic Energy Control Board
Ottawa, Canada

The Canadian government using the Atomic Energy Control Board as the executive agent of a Federal Provincial Task Force on Radioactivity has undertaken a program of decontamination and radon concentration reduction in a number of communities in Canada associated with the nuclear fuel cycle.

One town, Port Hope, Ontario, is the site of the Canadian facility where yellowcake is presently refined. Contamination in the town can be traced back over forty years from when this facility was used for radium extraction from pitchblende. Radon control in private, commercial and public buildings is primarily achieved by digging up and removing the contaminating soil from under and adjacent to those buildings where the radon/radon daughter concentration is found to be greater than the Task Force established criteria.

Three uranium mining towns, Elliot Lake and Bancroft in Ontario and Uranium City, Saskatchewan are also contaminated to some degree, in this case, by waste mine rock. However, the radon is mainly from natural sources and is transported underground by soil gas. All three towns are built on alluvial sands in proximity to uranium-bearing bedrock and our evidence suggests that there is a good

correlation between such porous soils and radon in structures. However we do not know the driving force that moves the gas. Clay will not permit long distance transportation of radon; unbroken bedrock does not emanate radon quickly enough to be a source for those buildings constructed directly on such rock formations.

Two remedial techniques have been developed:

(a) a sub-floor ventilation system; and

(b) the sealing of a foundation and the trapping of services which penetrate the foundation.

The latter approach is preferred as it causes minimum disruption to structures already in place. Application to new structures has been proven and the techniques can be made available to contractors as only the adaptation of standard building practices is involved.

* *

APPLICATION OF RADON STANDARDS TO NEW AND EXISTING HOUSING IN ELLIOT LAKE, ONTARIO

W.O. Findlay

Elliot Lake Project*
DSMA/ACRES
Elliot Lake, Ontario

A program to identify houses with radon daughter levels greater than acceptable (0.02 WL) and to take appropriate remedial action has been underway in Elliot Lake, Ontario, since mid 1977. The work is under the direction of DSMA/ACRES acting for the Atomic Energy Control Board (of Canada).

To date 671 houses have been surveyed and 117 have been identified as requiring remedial treatment. Of these, 74 have been brought to below the AECB criterion of 0.02 WL and work is proceeding on the remaining 43.

An exploration program extending over 6 months and culminating in a remedial demonstration program showed that the source of the radon was from the emanating fraction of naturally occurring radium in the soil and that the radon moved into the houses as a component of soil gas.

Investigation and testing techniques have been developed to locate the routes of entry of soil gas containing radon in finished and unfinished areas of all forms of house base construction, including poured concrete and block basement, slab on grade, and ventilated and unventilated crawl space.

Materials and methods for remedial treatment have been tested in the laboratory and in the field before being selected on a cost effective basis for specific application.

The National Building Code has been amended to provide that all new houses in Elliot Lake must be below 0.02 WL before occupancy is allowed. To assist contractors, three methods of construction have been developed; firstly a sub-floor mechanically-vented collector system which is incorporated into all mine owned homes; secondly, a passive system in which the design precludes the entry of radon into the houses and which is favoured by private purchasers; and thirdly a ventilated crawl space.

Direction of remedial work and the construction of new homes has shown that it is extremely difficult for an unsupervised contractor to construct a building without numerous unplanned openings. All failures to date have been caused by the inadequate levels of workmanship common to normal construction practices.

The order of magnitude of remedial and preventative construction work to date is:

Remedial Treatment	
Sealing of Single Route of Entry	$ 500.00
Fully Finished Basement including Apartment	$12,000.00
Average Cost of 74 Homes	$ 2,600.00
New Construction	
Under Floor System	$ 2,000.00
Sealed Basement	$ 500.00
Remedial Treatment on Unsupervised Construction	$ 2,400.00

*Dilworth, Secord, Meagher and Associates Limited, Elliot Lake Project in Consultation with Acres Consulting Services Limited.

* *

RADON STUDIES AT THE UNIVERSITY OF TEXAS

Thomas F. Gesell

School of Public Health
University of Texas
Houston, Texas 77025

Ed note: The speaker did not submit a summary for inclusion in this report. For further information contact him directly.

LEVELS OF RADON-222 IN MAINE AND NEW ENGLAND BUILDINGS ARISING FROM POTABLE WATER SUPPLIES

C.T. Hess, S.A. Norton, W.F. Brutsaert, R.E. Casparius and E.G. Coombs

University of Maine at Orono
Orono, ME 04469

During the past two years, the authors have been studying the gas ^{222}Rn in approximately 2000 groundwater supplies in Maine and 50 additional supplies elsewhere in New England. Levels of ^{222}Rn have been compared to physical, chemical, geological, and hydrological characteristics for 350 of the 2000 supplies. Levels of ^{222}Rn gas have been measured for several experiments in 10 homes and public buildings to determine the transfer from radon in water to air. Radon daughters have been determined to calculate the plate-out or loss from secular equilibrium and to enable dose calculations. Geographical distributions of ^{222}Rn levels in Maine private wells and utilities are given. Results of shower experiments for radon transfer into air and two day radon level measurements are given. The resulting variations of radon with time and water usage provide building ventilation time constants. Radon daughters in air are measured to be a factor of thirty lower than measured radon in air.

* *

CONTROL OF RADIOACTIVE HAZARDOUS WASTES PURSUANT TO THE RESOURCE CONSERVATION AND RECOVERY ACT (RCRA)

Allan C.B. Richardson

Federal Guidance Branch
Criteria and Standards Division
Office of Radiation Programs
Environmental Protection Agency
Washington, D.C. 20460

Ed. note: The speaker did not submit a summary for inclusion in this report. For further information, contact him directly.

ROUNDTABLE DISCUSSION

Summary

This summary of the roundtable discussion attempts to accurately reflect many views and opinions that were expressed during the course of the discussion. It must be emphasized that it does not represent a consensus of the participants. Whenever possible, the summary maintains the chronological sequence of the discussion, but greater emphasis was placed on topically arranging the subject material. In all cases, contributions to the discussion are summarized or quoted without attributing them to a specific participant.

The roundtable discussion focused on four very broad, interrelated topics:

1. the existence of a potential health hazard and the scope of the problem;
2. sources of radon in buildings and characterization of those sources;
3. the adequacy of existing measurement methods; and
4. appropriate strategies and building technologies to reduce or control indoor radiation levels.

For each of these topics the participants were asked to address and, if possible, identify what is known, what are some of the suspected or possibly exogenous factors that may be involved, and what further research is needed.

* * * * *

Potential Health Hazard

The first topic focused on whether there indeed is a real problem arising from radiation exposure due to radon in buildings, and in particular, on whether the present concern over the health hazards is realistic. One participant noted that many of the existing conditions and sources of radon exposure have existed for many years, yet the regulatory agencies "seem to be on a red alert and gearing up" for treating these as problems. Is there really a significant problem, however, from the biological point of view? As an example, concern was voiced as to whether there is a public health hazard for residents of Maine who live in areas with naturally high concentrations of radon in their water supplies. In regard to this specific situation, it was reported that in looking at geographical areas in Maine with known concentrations of radon in water supplies and at cancer incidence in these areas (using National Cancer Institute data) some crude geographical correlations have been found. In some cases, such as lung cancer in women, the correlations are significant at very high significance levels ($p=0.001$). Less striking, but significant correlations have also been observed for lung cancer in men, female brain cancer, and male reproductive cancer. It was emphasized, however, that these results do not imply causality since many other factors could also cause cancer. Each of these factors would have to be considered before any conclusion as to the role of radon could be made.

Since available evidence does not exclude the possibility of a health hazard, the prudent view, as expressed by several of the participants, is to treat these situations as potential hazards with some associated risk. As a result, the estimated risk or risk estimator is of primary importance. One participant observed, however, that risk estimates are confounded by two very important considerations: (1) the cumulative level of exposure, and (2) exposure to other pollutants.

The first consideration involves the calculation of any cumulative unit of a radiation quantity, such as the Working Level Month (WLM), which is used as an indicator of the dose. Since one does not have an understanding of the cancer-induction mechanism, the last event that induces the cancer cannot be determined, and it is impossible to know when to stop the accumulation of dose in the calculation. Should one stop at death, at the time of diagnosis of the cancer, or should one try to account for some latent period? One participant indicated that all epidemiological data use WLM values that have been calculated up to the time of death. Risk estimates, therefore, are probably underestimated since some exposure occurs after the cancer was induced. It was noted that the risk estimates may increase if they are recalculated after uniformly subtracting the dose received during some assumed induction-latent period.

The second important consideration involves the problem of combined effects of radiation and exposure to other carcinogenic agents. Since exposure to radon daughters always occurs in the presence of other pollutants, we are never exposed to one risk at a time, and it is exceedingly difficult to extrapolate the results from one group to another. It was emphasized that it may be misleading to provide any risk estimate without further specifying the presence or absence of other agents. None of the current risk estimates considers combined effects. It was further noted that most of the lung-cancer mortality observed in uranium miners occurred in miners who smoked. The additional point was made that epidemiological data on bronchogenic cancers which were characteristic of miners in old uranium mines may not be applicable to populations exposed in non-mine environmental settings. Furthermore, there was a suggestion that some of the radon concentration data from uranium mines in this country and in Europe may be suspect. One participant said "I've been to many mines and as soon as I arrive I can hear the air pumps being turned on. By the time I get into the mine the working level is about 1 WL, but it was probably 10 WL before I got there."

Considerable discussion was devoted to the various extant estimates of lung cancer mortality resulting from exposure to radon daughters in residences. These mortality estimates range from a few percent to over 20% of all lung cancer deaths. Nearly all of them are derived in part using the risk estimators of the UNSCEAR* and BEIR** reports along with other assumptions about activity levels, occupancy and intake factors. Several conflicting arguments were made regarding the validity of some of the mortality estimates. In all cases, these conflicts involved the underlying assumptions employed in the calculations. It was observed, for example, that most indoor levels are five to ten times smaller than the value of 0.02 WL assumed in one estimate. Another participant concluded that one cannot use current exposure levels to predict current incidence rates since houses were leakier in the past than now, and lung cancers have latent periods of 20 to 30 years. Therefore past levels should be used to predict current rates, and present levels for future rates. Additionally, the assumed equilibrium factors for the daughter activities in houses may not be correct. The daughters ^{214}Pb, ^{214}Bi, and ^{214}Po contribute significantly to the dose, and their concentrations may differ by a factor of ten in a residence. This effect alone introduces considerable uncertainty to the mortality estimates. Perhaps the most telling point was made by the participant who suggested that an entire meeting "lasting a week or even a month" could be devoted exclusively to the topic of "what are the best values [of the risk estimators] to use."

An entirely different aspect of this question as to the existence of a problem was subsequently raised in a later part of the discussion by a participant who suggested that the true scope of

---

*United Nations Scientific Committee on the Effects of Atomic Radiation (UNSCEAR), "Sources and Effects of Ionizing Radiation", 1977 Report to the General Assembly, United Nations (1977).

**"The Effects on Populations of Exposure to low Levels of Ionizing Radiation", National Academy of Sciences, Advisory Committee on the Biological Effects of Ionizing Radiation (1972).

the problem will remain unknown until more field studies are conducted. Only then will we be able to say what the effects are, and be able to derive some maximum estimate of the risk. He then expressed the hope that we will be able to evaluate these risks on an equivalent basis with other radiation risks. "From the public health point of view, in the best of all possible worlds, we would hopefully be able to spend our money to reduce radiation exposure in ways which will do the most good." That is, in ways that will result in the quickest and largest reduction for the money spent to maximize the risk reduction per dollar. He lamented that political factors and misinformed public perceptions of the various risks play a more important role than the magnitude of the risk. As an example he offered the case of natural gas, which is a source of radon in buildings when used in unvented space heaters and appliances. The Environmental Protection Agency (EPA) six years ago estimated that this source results in a population dose commitment of 2.7 million person-rem per year, resulting in an estimated 95 lung cancer fatalities per year. He suggested that this has been completely ignored while billions of dollars are spent in the nuclear power industry to reduce dose commitments as low as 0.05 million person-rem per year. A participant from EPA concurred and stated that the nuclear power industry has indeed spent on the order of hundreds of thousands of dollars per life saved for public exposures and much larger sums for occupational exposures. "One of the things that is encouraging about this conference.....is that we are now focusing on a radiation problem where the returns per dollar spent are much, much greater." He provided, as an example, the implications of the EPA recommendations for Florida [subsequently published in Federal register 44, 38774-70 (July 2, 1979)]. It has been calculated that exposure to 0.02 WL in an average house results in a 2% risk of lung cancer per individual for lifetime occupancy. If remedial measures costing approximately $1000 per house are made, it is estimated that we will be spending at a rate of $12,000 per health effect averted (assuming 4 occupants per house). This may be contrasted to the hundreds of thousands or millions of dollars spend in the nuclear industry. He suggested that by focusing on these areas great returns can be achieved, and will result in more equity in the treatment of radiation risks.

The issue of equity was addressed by another participant who noted that although this dispassionate approach may be intellectually satisfying and the altruistic ideal, it is not realistic in a democratic society. We stress the risks the public or body politic wishes to stress. "If the public is more concerned about a microrad from a nuclear power plant than a millirad from radon, then we are going to be worried about nuclear power plants."

Subsequent to the conclusion of the roundtable discussion, the question of whether there is a problem was summarized by a participant who concluded that "there is indeed a problem and that it is quite simply this - what is the average radiation dose from radon daughters to the lung experienced by the population of the U.S.A., how does it vary with type and location of house, and what can be predicted about future trends of that dose as houses are built with less ventilation, or with additional sources of radon (underground houses, houses in caves, houses with thermal storage in rock, etc.)? This is the real issue and it is an extremely important one in view of the great public concern about tiny and probably inconsequential increments of radiation dose from nuclear power, either as a result of normal operation or of accidental releases (e.g., Three Mile Island)."

* * * * *

Source Characterization

The second major topic of discussion focused on the sources of radon in buildings and characterization of these sources. It was noted many times during the meeting that there are a myriad of source variables, such as the radioactivity content of the source, the porosity and moisture content of materials, meteorological effects, temporal changes, and air exchange rates. The

participants were asked to explicitly address these source variables from the perspective of whether we know how to characterize the sources of radon in buildings, what is known, what is unknown, and what are the research needs.

The measurement of emanation rates* from various building materials was immediately identified as one area in which further research would be highly useful. It was noted that radon escapes very readily from some materials, but not from others, such as phosphate slag in Butte, Montana which seems be be highly vitrified. One participant indicated that a crucial variable for the emanation rate is the water content of the material. Another participant reported that preliminary results from work (being done under contract for the Mine Safety and Health Administration) to characterize the effects of moisture content on emanation from uranium ore indicates that there is a specific water content that results in maximum emanation. The emanation rate is lower at both very high and very low water concentrations.

A significant point was made by another participant who indicated that if the important parameter is the amount of radon that is released from materials, then an emanation rate measurement standard may be more appropriate than standards for the radioactivity content of the material. He said that the measurement of emanation rates has received very little attention in the past, and suggested that we need to give more consideration to methods for measuring emanation rates, to standardizing the methods, and to establishing mechanisms for measurement intercomparisons between laboratories.

Another participant suggested that in some cases present measurement methods are probably adequate. He reported that, in a twenty-house study in the New York-New Jersey area done by the Environmental Measurements Laboratory (EML),the annual mean radon concentration could be accounted for by considering the radon flux from the cellar floor, radon concentration in water, and an inferred average ventilation rate. Measurement data for these variables were subjected to multiple regression analyses, and the results were then used to obtain calculated values of the average annual working level which were in agreement with directly determined levels. The conclusion is that the results are "perhaps better than we have a right to expect", and that the "measurements were fairly good."

The adequacy of existing measurement methods, with respect to emanation rates, was also addressed. It was reported that the Technical University of Denmark has characterized emanation rates for several materials. This participant indicated that studies show the material should be characterized in terms of the emanation rate per unit surface area in some cases while in other cases it is more relevant to describe the material in terms of the emanation rate per unit mass. To a large extent, it depends on the porosity and permeability of the material. He also suggested that it is completely possible with existing techniques to characterize emanation rates of materials under various conditions (humidity, pressure, etc.). "It's not so much a question of technique, it's more of just doing the work."

The issue was raised whether these measurements, to be of particular use, should be made on building materials when they are in place or as they are actually used (e.g. on wallboards after they are painted). Similarly, the emanation into a room will depend on the amount of thermal insulation and on the presence of a vapor barrier. Some possible problems with these in situ measurements were considered. The results may be confounded by ground-soil radon or by other sources in the building. It was indicated that one would certainly want to characterize the site before initiating such in situ building material measurements. An alternative approach is to characterize the basic building materials, from which you can then usually establish an upper limit on what this material will contribute to a

*In response to a specific question about the use of activated charcoal for the measurement of radon emanation by the charcoal canister method, a participant reported that coconut charcoal is the best choice.

given construction.

The relative importance of the various sources of radon was also considered. It was reported that in buildings on reclaimed phosphate lands in Florida, some radon comes from building materials, but most originates from the soil outside the building. Similarly, Canadian studies indicate that most of the radon originates from soil leakage. These areas in Canada use lake water and do not have the problems associated with high-radon water supplies that might be found in Maine. In the work at Elliot Lake, Ontario [see p. 66], it was found that the major source of radon in buildings was not concrete or other building materials, but rather was soil gas containing radon which entered by discontinuities in the construction, floor cracks, drains with improper traps, etc. In 74 houses in Elliot Lake, radon infiltration was significantly reduced by blocking the routes of entry of soil gas into basements. In the EML study referred to earlier, emanation rates were measured over floor cracks in older houses as well as over intact concrete floors in newer houses. Although the ^{226}Ra concentration in the soil around the houses is fairly uniform at approximately 1 $pCi \cdot g^{-1}$, and all building codes in the New York-New Jersey area require a 4-inch thick concrete floor in the basements, a 10-fold range in the average radon flux from the floors was found. The causes of this variation, part but not all of which can be explained by cracks, are unknown. It was suggested that these wide variations, as well as similar 100-fold ones seen in houses with unvented crawl spaces, indicate that the rate depends on the type of soil. It was also pointed out that soil type is only one of many factors. Depending on conditions above the soil, 100-fold changes in a 12-hour period can be observed. Soil is a major source in many cases, but this is not necessarily universal. Some studies in Denmark, for example, indicated that radon originated primarily from building materials. Indoor radon concentrations could be calculated from exhalation rates of walls and floors. Significantly, no differences in the rates between floors in contact with soils and walls not facing soils were found. In the course of the discussion it became apparent that the source of radon is very situational and site specific, and that characterization will depend on the specific type of source, viz., water, building materials, soil.

Earlier in the discussion, it was implied that we know how to characterize the sources, and that we only need to go out and do the work. This was viewed somewhat skeptically, however, by several participants. One asked, for example, if we know how to predict what the WL in a structure built on reclaimed phosphate lands in Florida will be before it is built. Past efforts have not been very successful, and it was asked if we can now do better by considering additional parameters such as land class [as described in one of the Brief Reports, p. 56]. It was clarified that land class is not an aid in predicting. Land classification is just a manifestation of the soil radium content and, perhaps as a second order effect, the radon emanation rate of the soil. The suggestion was made that we need to focus on soil radium content and perhaps other parameters, including simpler ways of measuring both the lateral and vertical distribution of radium in lands. It was pointed out that we should not completely judge things on the basis of the situation in Florida. Present land reclamation techniques are such that the radium concentration varies greatly both vertically and horizontally within very short distances. Soil radium concentrations can differ by a factor of 10 within a few feet. One of the major problems that must be addressed is finding appropriate techniques for averaging over distance and depth. Measurements of external gamma-radiation exposure rates, which in effect integrate over large areas, may be a better predictor than anything else because of these drastic variations. In Canada, similar gamma-radiation surveys are conducted to detect site anomalies. Obviously, one does not want to build a housing development on a radon anomaly.

The question of prediction appeared to be very important to a number of participants. One of them, referring to the EML study, found it interesting that the WL could be predicted on the basis of emanation rate measurements. He suggested

that it is easier to measure radon concentrations in air than either emanation rates or radon-daughter concentrations in air. He proposed, however, that existing WL monitors [e.g., described by Keefe, et al., p. 54] can be used to obtain average radon-daughter concentrations. Using data collected in an Argonne National Laboratory study [see p. 63], he demonstrated that one could obtain $^{218}Po/^{214}Bi$ and $^{214}Pb/^{214}Bi$ concentration ratios under different conditions with available instrumentation. For example, measurements indicated that when an air conditioner fan was used continuously, the ratios were reduced by half compared to when the fan was off or used only in conjunction with the compressor. He concluded that it is possible, irrespective of the source of radon, to obtain valuable information on the average radon-daughter concentrations and thereby predict the WL if a sufficient number of measurements, under a variety of conditions, are made with these existing instruments.

The discussion shifted to a related, but slightly different aspect when another participant asked if it is the respirable fraction of the radon daughters that is hazardous. If it is, could the measurement problem and the question of prediction be simplified by focusing on known particle-size distributions and measuring the activity on just the respirable fraction? This was viewed as an oversimplification since the daughters, in the decay sequence $^{218}Po \rightarrow {}^{214}Pb \rightarrow {}^{214}Bi \rightarrow$, can attach, unattach, and reattach to any size particles in air. It was also noted that the radon daughters are almost always respirable in the conventional sense of particle-size definitions. For lung dose assessments, the unattached or uncombined fraction of the radon daughters, and not the respirable fraction, is the critical size factor. Unattached fractions, however, are not usually measured. It was further suggested that air filtration and recirculation results in a reduction of the ^{214}Pb and ^{214}Bi daughters because the unattached fraction of their precursor ^{218}Po deposits on filters and fan blades and remains attached to these surfaces. The ^{218}Po is not similarly decreased since it is continually replenished by decay of ^{222}Rn in the air.

* * * * *

Measurement Needs

Identification of specific measurement needs was the major focus of the next topic of discussion. It was suggested that this has to be considered from the perspective of having differing needs, depending on whether one is interested in broad-based surveys or monitoring of buildings, or if one is trying to understand the problem or study the mechanisms and systems involved, or if the measurements are being used to help establish standards or compliance criteria. Survey measurement needs appeared to be the area of most immediate and greatest concern.

It was noted that we are increasingly forced to rely on State radiation control offices to make the necessary measurements. They have primary responsibility, but they are "already pushed to the limit" and do not have adequate resources to make complicated measurements. Florida, for example, surveyed 100 houses over several years and selected one measurement technique--track etch film--mainly because it is a simple, relatively inexpensive, passive method. The number of houses we may be faced to deal with is not encouraging. For example, the TVA phosphate-production facility at Muscle Shoals produced, over many decades, huge quantities of phosphate slag that was incorporated into concrete building blocks. It is estimated that there are 100,000 to 200,000 houses in four states which were constructued with these blocks. The State of Alabama is conducting a small pilot study of these houses, and it appears that there may be a problem requiring remedial action, but we have no idea on how to survey a population of houses of this magnitude. It was emphasized that it certainly can not be accomplished with conventional air-sampling methods. What is needed is a simple means of integrating annual exposure. Another participant referred to the previously reported [see p. 63] chance observation of elevated indoor radon-daughter levels which were not a consequence of "technological enhancement," and

rhetorically asked if it is reasonable to survey all homes in the United States.

The implied need for more inexpensive instruments was questioned by another participant. His view was that labor is expensive, and it contributes to the high cost of measurements. Therefore, automated instruments are needed instead. The initial cost of an automated instrument is admittedly higher, but the final cost of the measurements will be much lower.

It was suggested that we do not yet know how to optimize our measurements. We know that single, short-term measurements are inadequate for characterizing a house. One participant felt reasonably confident in week-long integral measurements taken quarterly or more frequently over a year. The optimum is probably somewhere between these two extremes, but we do not know where it is. Another participant indicated that if a house has very low or high levels,then many measurements are needed because of the inherent statistical difficulties. In addition, another important factor is that occupants become annoyed by the intrusions of frequent measurements. One must reconcile this practical problem when trying to survey an occupied house. It was reported that in Canada a comprise of 13 short-term measurements over a three-week interval is made.

The suitability of the track etch technique was discussed in considerable detail. One participant felt that although the measurement costs are much less than other instrumental methods, his experience was that this method is too imprecise and unreliable. He added that if the technique could be refined it would be very useful for surveying thousands of houses. Another participant indicated that some of the early surveys made with this technique were done during the initial phases of applying it to measurements at environmental levels. He indicated that there have been significant improvements in precision, sensitivity and discriminatory ability of the material. Track-etch materials are simple devices that allow one to make integral measurements in many houses at a cost of approximately $10 per house. Track-etch cups can be employed with a variety of membranes to achieve different hold-up times, and can also be used with a simple filter barrier to exclude the radon daughters. One participant encouraged further development, and hoped that the acceptability of this technique can be demonstrated for it appears to be the only economical mass screening device on the near horizon.

The length of time needed to obtain measurements was also raised as another practical problem. If, for example, a regulation specifies an upper limit of 0.02 WL in a house, does the builder constructing to this specification have to wait a year to obtain the results? Further, if remedial action is needed, does one have to wait a year to learn if the corrections were adequate? It was suggested that in many of the cases construction errors are so gross that they show up very quickly. This is not always the case, however, particularly in the "grey area" where you may find individual measurements in the range of 0.01 to 0.03 WL and where the average may very well be above 0.02 WL. The ability to predict in a short period of time whether a house meets compliance criteria was suggested as an area requiring further research. Another approach may be to characterize the conditions which will allow one to predict the working level. In this way, one could build the house in the right way to satisfy the conditions without making any measurements. It was pointed out, however, that this may be slightly visionary. Based on experiences in Canada, major flaws can occur in houses built under even the most demanding construction specifications. At Elliot Lake, for example, one house built under direct supervision passed inspection while a similar house built by the same builder but without supervision failed. After investigation, to the dismay of the builder, it was found that its failure was partly due to the absence of a caulking strip at the floor-wall joint for a stretch of nearly 5 meters!

* * * * *

Control Technologies

The last topic of discussion focused on the adequacy of existing control technologies, and on

how concern for indoor radon pollution may influence building practices.

Primary emphasis was centered on methods to reduce or control the WL in buildings. One participant asked if the only practical method was increasing or maintaining high air-exchange rates. If so, it has a large economic penalty. It was noted that buildings consume 30% of the energy used in the United States, and that ventilation, heating, cooling and conditioning of ventilation air is 20 to 30% of that. Therefore, ventilation currently comprises 5 to 10% of total U.S. energy use. To reduce these energy-use costs, it may be worthwhile to assume considerable front-end capital investment and construction costs to reduce the WL by other means. Another participant suggested that the role of ventilation may be overemphasized. He reported that in tests at Elliot Lake on both electric and oil heated buildings, measurements of ventilation rates and radon and radon-daughter concentrations indicated that: 1) fluctuations in radon concentrations and working levels are mainly caused by variations in the radon supply rate into the house rather than by variations in the ventilation rate; and (2) equilibrium fractions and radon-daughter concentration ratios are almost independent of ventilation rate and mainly depend on the plate-out rate of ^{218}Po. It was pointed out that this implies that the equilibrium fraction is the same inside and outside the building, and will not be affected by a factor of two or three change in the ventilation rate in the absence of recirculation.

Air cleaning or filtering was considered as another possible remedy. It became apparent, however, that this may not be effective. Electrostatic precipitators or other electronic air cleaners will not work unless the particles can be charged. Furthermore, the first decay product, ^{218}Po, is continually replenished in the air by decay of the radon, and the radon itself cannot be removed from air by filters or by any other practical means. The only known ways are to freeze it (e.g., with liquid air) or to trap it in charcoal. Because of the maintenance problems, there does not currently appear to be any satisfactory mechanism for maintaining charcoal or media filters in a residence.

The suggestion was made that we may be looking too parochially at the control of radon. Certainly efforts should be made to control the sources of radon since we have seen anomalies in some conventional residences, but there are also many other indoor contaminants. For example, formaldehyde originating from "chip board" glues and other building materials has been found in tight trailers at concentrations exceeding occupational standards. The number of potential contaminants is great, and a solution which consists of eliminating the source of only one - radon- and then tightening the house is not adequate. Unless all contaminants are known and controlled by other methods, which is not probable, we must supply adequate ventilation. It was recommended that this could be done by heat exchangers. Another participant agreed that this is a solution, but one that bears an economic penalty. The efficiency of simple regenerators is of the order of 60%, so about one-third of the energy would still be wasted. This is a clear case of the trade-off between energy and equipment costs and ventilation rate. It was suggested that an integral heat exchanger system may be cost effective in American homes that already utilize central forced-air heating systems. One participant thought that any control measure must be permanent since the problem remains with the building over its lifetime. One needs either a passive control measure or one that remains an integral part of the building's services which cannot be turned off or tampered with.

* * * * *

The roundtable discussion clearly demonstrated that much is known about radon in buildings. It also demonstrated, however, that there are many uncertainties and outstanding needs, and that significant questions must still be resolved.

Various risk estimators, primarily derived from data on radiation exposure in uranium mines, are available to quantify the risk of lung cancer due to inhalation of radon-decay products. We do not know, however, if the risk estimators are

valid for low-dose environmental exposures. It is not known, for example, if the extrapolations to lower doses are legitimate, or if the etiology and types of cancer are applicable in non-mine environmental settings.

Many sources of radon can be characterized with known variables using existing methods. In most situations, however, we do not know how to systematically treat the source characterization in ways which will allow us to make predictions. For example, given a specific building type and a known concentration of radon in the building's water supply, or the radium content in the soil surrounding the foundation, we can not predict the average radon-daughter concentrations in the building air, or more importantly, predict the occupants' average radiation dose to the lung. In cases such as these, it is not known if the variables we are presently measuring are appropriate and most significant for the problem.

Suitable measurement methods exist for many applications. Notable exceptions include reliable, inexpensive screening methods to evaluate undeveloped lands bearing relatively high levels of radium and to survey large numbers of existing buildings. The adequacy of methods which have been suggested as showing promise - such as track-etch techniques - needs to be unequivocally demonstrated. In addition, there is a great need for measurement standards and interlaboratory comparison programs that can demonstrate the adequacy and reliability of measurements.

A number of remedial and preventative construction techniques - mainly removal of contaminating soil, installation of subfloor ventilation systems, and sealing of foundations and services which penetrate the foundation - have been successful in reducing and controlling radon and radon-daughter concentrations in buildings. These have for the most part been applied in situations where the major source of radon was from infiltration of soil gas into the building. It is not apparent, however, that these techniques are applicable for other sources of radon such as emanation from building materials or release from water. In cases where control relies exclusively on supplying adequate ventilation, we do not know how to provide efficacious methods which are consistent with the need for reducing energy consumption.

It is hoped that this discussion has in some small way contributed to a better understanding of the problems, and provided a stimulus for further experimental and theoretical work on the subject.

U.S. DEPT. OF COMM. BIBLIOGRAPHIC DATA SHEET	1. PUBLICATION OR REPORT NO. NBS SP-581	2. Gov't. Accession No.	3. Recipient's Accession No.

4. TITLE AND SUBTITLE

RADON IN BUILDINGS: A proceedings of a Roundtable Discussion of Radon in Buildings held at NBS, Gaithersburg, MD, June 15, 1979.

5. Publication Date June 1980

6. Performing Organization Code

7. AUTHOR(S)

R. Collé and P. E. McNall, Jr. (eds.)

8. Performing Organ. Report No.

9. PERFORMING ORGANIZATION NAME AND ADDRESS

NATIONAL BUREAU OF STANDARDS
DEPARTMENT OF COMMERCE
WASHINGTON, DC 20234

10. Project/Task/Work Unit No.

11. Contract/Grant No.

12. SPONSORING ORGANIZATION NAME AND COMPLETE ADDRESS *(Street, City, State, ZIP)*

Same as item 9.

13. Type of Report & Period Covered Final

14. Sponsoring Agency Code

15. SUPPLEMENTARY NOTES

Library of Congress Catalog Card Number: 80-600069

☐ Document describes a computer program; SF-185, FIPS Software Summary, is attached.

16. ABSTRACT *(A 200-word or less factual summary of most significant information. If document includes a significant bibliography or literature survey, mention it here.)*

This is the proceedings of a Roundtable Discussion of Radon in Buildings held June 15, 1979 at the National Bureau of Standards in Gaithersburg, Maryland. The meeting brought together a number of participants with diverse interdisciplinary interest in radiation protection, radiation measurement and building technology, provided a forum to exchange information, and drew attention to some of the problems and research needs associated with radiation exposure due to radon in buildings. Emphasis was placed on (1) the characterization of the sources and pathways of radon in buildings; (2) the biological and health effects; (3) measurement considerations; and (4) strategies and control technologies to minimize indoor radiation exposure.

17. KEY WORDS *(six to twelve entries; alphabetical order; capitalize only the first letter of the first key word unless a proper name; separated by semicolons)*

Buildings; environment; health; measurements; radiation; radon; radon daughters; ventilation.

18. AVAILABILITY ☒ Unlimited

☐ For Official Distribution. Do Not Release to NTIS

☒ Order From Sup. of Doc., U.S. Government Printing Office, Washington, DC 20402

☐ Order From National Technical Information Service (NTIS), Springfield, VA, 22161

19. SECURITY CLASS (THIS REPORT) UNCLASSIFIED

21. NO. OF PRINTED PAGES 84

20. SECURITY CLASS (THIS PAGE) UNCLASSIFIED

22. Price $3.75

☆ U.S. GOVERNMENT PRINTING OFFICE : 1980 O-311-046 (109)

USCOMM-DC

NBS TECHNICAL PUBLICATIONS

PERIODICALS

OURNAL OF RESEARCH—The Journal of Research of the National Bureau of Standards reports NBS research and development in those disciplines of the physical and engineering sciences in which the Bureau is active. These include physics, chemistry, engineering, mathematics, and computer sciences. Papers cover a broad range of subjects, with major emphasis on measurement methodology and the basic technology underlying standardization. Also included from time to time are survey articles on topics closely related to the Bureau's technical and scientific programs. As a special service to subscribers each issue contains complete citations to all recent Bureau publications in both NBS and non-NBS media. Issued six times a year. Annual subscription: domestic $17; foreign $21.25. Single copy, $3 domestic; $3.75 foreign.

NOTE: The Journal was formerly published in two sections: Section A "Physics and Chemistry" and Section B "Mathematical Sciences."

DIMENSIONS/NBS—This monthly magazine is published to inform scientists, engineers, business and industry leaders, teachers, students, and consumers of the latest advances in science and technology, with primary emphasis on work at NBS. The magazine highlights and reviews such issues as energy research, fire protection, building technology, metric conversion, pollution abatement, health and safety, and consumer product performance. In addition, it reports the results of Bureau programs in measurement standards and techniques, properties of matter and materials, engineering standards and services, instrumentation, and automatic data processing. Annual subscription: domestic $11; foreign $13.75.

NONPERIODICALS

Monographs—Major contributions to the technical literature on various subjects related to the Bureau's scientific and technical activities.

Handbooks—Recommended codes of engineering and industrial practice (including safety codes) developed in cooperation with interested industries, professional organizations, and regulatory bodies.

Special Publications—Include proceedings of conferences sponsored by NBS, NBS annual reports, and other special publications appropriate to this grouping such as wall charts, pocket cards, and bibliographies.

Applied Mathematics Series—Mathematical tables, manuals, and studies of special interest to physicists, engineers, chemists, biologists, mathematicians, computer programmers, and others engaged in scientific and technical work.

National Standard Reference Data Series—Provides quantitative data on the physical and chemical properties of materials, compiled from the world's literature and critically evaluated. Developed under a worldwide program coordinated by NBS under the authority of the National Standard Data Act (Public Law 90-396).

NOTE: The principal publication outlet for the foregoing data is the Journal of Physical and Chemical Reference Data (JPCRD) published quarterly for NBS by the American Chemical Society (ACS) and the American Institute of Physics (AIP). Subscriptions, reprints, and supplements available from ACS, 1155 Sixteenth St., NW, Washington, DC 20056.

Building Science Series—Disseminates technical information developed at the Bureau on building materials, components, systems, and whole structures. The series presents research results, test methods, and performance criteria related to the structural and environmental functions and the durability and safety characteristics of building elements and systems.

Technical Notes—Studies or reports which are complete in themselves but restrictive in their treatment of a subject. Analogous to monographs but not so comprehensive in scope or definitive in treatment of the subject area. Often serve as a vehicle for final reports of work performed at NBS under the sponsorship of other government agencies.

Voluntary Product Standards—Developed under procedures published by the Department of Commerce in Part 10, Title 15, of the Code of Federal Regulations. The standards establish nationally recognized requirements for products, and provide all concerned interests with a basis for common understanding of the characteristics of the products. NBS administers this program as a supplement to the activities of the private sector standardizing organizations.

Consumer Information Series—Practical information, based on NBS research and experience, covering areas of interest to the consumer. Easily understandable language and illustrations provide useful background knowledge for shopping in today's technological marketplace.

Order the **above** *NBS publications from: Superintendent of Documents, Government Printing Office, Washington, DC 20402.*

Order the **following** *NBS publications—FIPS and NBSIR's—from the National Technical Information Services, Springfield, VA 22161.*

Federal Information Processing Standards Publications (FIPS PUB)—Publications in this series collectively constitute the Federal Information Processing Standards Register. The Register serves as the official source of information in the Federal Government regarding standards issued by NBS pursuant to the Federal Property and Administrative Services Act of 1949 as amended, Public Law 89-306 (79 Stat. 1127), and as implemented by Executive Order 11717 (38 FR 12315, dated May 11, 1973) and Part 6 of Title 15 CFR (Code of Federal Regulations).

NBS Interagency Reports (NBSIR)—A special series of interim or final reports on work performed by NBS for outside sponsors (both government and non-government). In general, initial distribution is handled by the sponsor; public distribution is by the National Technical Information Services, Springfield, VA 22161, in paper copy or microfiche form.

BIBLIOGRAPHIC SUBSCRIPTION SERVICES

The following current-awareness and literature-survey bibliographies are issued periodically by the Bureau:

Cryogenic Data Center Current Awareness Service. A literature survey issued biweekly. Annual subscription: domestic $25; foreign $30.

Liquefied Natural Gas. A literature survey issued quarterly. Annual subscription: $20.

Superconducting Devices and Materials. A literature survey issued quarterly. Annual subscription: $30. Please send subscription orders and remittances for the preceding bibliographic services to the National Bureau of Standards, Cryogenic Data Center (736) Boulder, CO 80303.

NATIONAL BUREAU OF STANDARDS

The National Bureau of Standards[1] was established by an act of Congress on March 3, 1901. The Bureau's overall goal is to strengthen and advance the Nation's science and technology and facilitate their effective application for public benefit. To this end, the Bureau conducts research and provides: (1) a basis for the Nation's physical measurement system, (2) scientific and technological services for industry and government, (3) a technical basis for equity in trade, and (4) technical services to promote public safety. The Bureau's technical work is performed by the National Measurement Laboratory, the National Engineering Laboratory, and the Institute for Computer Sciences and Technology.

THE NATIONAL MEASUREMENT LABORATORY provides the national system of physical and chemical and materials measurement; coordinates the system with measurement systems of other nations and furnishes essential services leading to accurate and uniform physical and chemical measurement throughout the Nation's scientific community, industry, and commerce; conducts materials research leading to improved methods of measurement, standards, and data on the properties of materials needed by industry, commerce, educational institutions, and Government; provides advisory and research services to other Government agencies; develops, produces, and distributes Standard Reference Materials; and provides calibration services. The Laboratory consists of the following centers:

Absolute Physical Quantities[2] — Radiation Research — Thermodynamics and Molecular Science — Analytical Chemistry — Materials Science.

THE NATIONAL ENGINEERING LABORATORY provides technology and technical services to the public and private sectors to address national needs and to solve national problems; conducts research in engineering and applied science in support of these efforts; builds and maintains competence in the necessary disciplines required to carry out this research and technical service; develops engineering data and measurement capabilities; provides engineering measurement traceability services; develops test methods and proposes engineering standards and code changes; develops and proposes new engineering practices; and develops and improves mechanisms to transfer results of its research to the ultimate user. The Laboratory consists of the following centers:

Applied Mathematics — Electronics and Electrical Engineering[2] — Mechanical Engineering and Process Technology[2] — Building Technology — Fire Research — Consumer Product Technology — Field Methods.

THE INSTITUTE FOR COMPUTER SCIENCES AND TECHNOLOGY conducts research and provides scientific and technical services to aid Federal agencies in the selection, acquisition, application, and use of computer technology to improve effectiveness and economy in Government operations in accordance with Public Law 89-306 (40 U.S.C. 759), relevant Executive Orders, and other directives; carries out this mission by managing the Federal Information Processing Standards Program, developing Federal ADP standards guidelines, and managing Federal participation in ADP voluntary standardization activities; provides scientific and technological advisory services and assistance to Federal agencies; and provides the technical foundation for computer-related policies of the Federal Government. The Institute consists of the following centers:

Programming Science and Technology — Computer Systems Engineering.

[1]Headquarters and Laboratories at Gaithersburg, MD, unless otherwise noted; mailing address Washington, DC 20234.
[2]Some divisions within the center are located at Boulder, CO 80303.

Measurement Technology for Safeguards and Materials Control

Proceedings from American Nuclear Society
Topical Meeting held November 26-30, 1979
Kiawah Island, South Carolina

Edited by

Thomas R. Canada

Los Alamos Scientific Laboratory
Los Alamos, New Mexico 87545

B. Stephen Carpenter

National Measurement Laboratory
National Bureau of Standards
Washington, D.C. 20234

Sponsored by

American Nuclear Society
Isotopes and Radiation Division
Institute of Nuclear Materials Management
and
National Bureau of Standards

U.S. DEPARTMENT OF COMMERCE, Philip M. Klutznick, Secretary

Luther H. Hodges, Jr., Deputy Secretary
Jordan J. Baruch, Assistant Secretary for Productivity, Technology and Innovation

NATIONAL BUREAU OF STANDARDS, Ernest Ambler, Director

Issued June 1980

Library of Congress Catalog Card Number: 80-600072

National Bureau of Standards Special Publication 582
Nat. Bur. Stand. (U.S.), Spec. Publ. 582, 769 pages (June 1980)
CODEN: XNBSAV

U.S. GOVERNMENT PRINTING OFFICE
WASHINGTON: 1980

For sale by the Superintendent of Documents, U.S. Government Printing Office, Washington, D.C. 20402
Price $11.00
(Add 25 percent for other than U.S. mailing)

CONFERENCE OFFICERS

GENERAL CHAIRMAN

T. Canada (LASL)

TECHNICAL PROGRAM COMMITTEE

R. Walton (LASL), Chairman
S. Baloga (DOE)
B. S. Carpenter (NBS)
J. Duguid (Battelle)
L. Dressen (NRC)
R. Hoffman (B&W)
S. Johnson (Rockwell-Hanford)
W. Lyon (ORNL)
E. Schneid (Grumman)
J. Shipley (LASL)
N. Trahey (NBL)

HOUSING AND FINANCE

B. S. Carpenter (NBS)
P. Russo (LASL)

PUBLICITY

R. Ragaini (LLL)

SOCIAL CHAIRMAN

G. Sinclair (Nuclear Data)

REGISTRATION COMMITTEE

D. Gary (NBS), Chairman
K. Eccleston (LASL)
M. Thompson (NBL)

EDITED BY

Thomas R. Canada and B. Stephen Carpenter

ACKNOWLEDGMENT

The conference officers are indebted to Mrs. Donna Stevens for her expert assistance with the meeting preparations and the compilation of these proceedings.

ABSTRACT

This publication contains the proceedings of the American Nuclear Society's Topical Conference entitled, Measurement Technology for Safeguards and Materials Control. The meeting, co-sponsored by the Office of Measurements for Nuclear Technology of the National Bureau of Standards and the Institute of Nuclear Materials Management, was held at Kiawah Island, South Carolina, on November 26-30, 1979. The objective of this conference was to provide a forum for reports of current work and for information exchanges on technical subjects that are relevant to measurement technology for nuclear safeguards and material control.

The presentations were applications oriented and offered a good balance between chemical analysis, nondestructive assay techniques, bulk measurement techniques, inspection techniques, and integrated systems for material measurements and control. Reports discussing preparation and use of reference materials and measurement traceability were included. Examples of measurement requirements and techniques used for both national and international safeguards are given. Approaches to various analysis of materials throughout the fuel cycle from enrichment and fuel fabrication to spent fuel and reprocessing are considered.

Key words: Accountability; accuracy; gamma spectrometry; mass spectrometry; nondestructive assay; nuclear safeguards; precision; reference materials; special nuclear materials; x-ray fluorescence.

CONTENTS

SESSION I - STANDARDS AND ANALYTICAL CHEMISTRY
Chairman: *R. Larsen*
Session Coordinators: *N. Trahey and S. Johnson*

Disclaimer:

Certain trade names and company products are identified in order to adequately specify the experimental procedure. In no case does such identification imply recommendation or endorsement by the National Bureau of Standards, nor does it imply that the products are necessarily the best available for the purpose.

Reference Materials and Measurement Traceability

Fact vs. Fiction

by

CARLETON D. BINGHAM
U. S. Department of Energy, New Brunswick Laboratory, Argonne, Illinois

ABSTRACT

Nuclear materials safeguards within the U.S.A. are accomplished by the integration of activities involving physical protection, material control and material accountability. Material accountability requires both sound measurement technology and well-defined accounting procedures to provide final evidence that physical protection and materials control have achieved their purpose.

The quantities of nuclear materials received, shipped, stored or in process must be verified by accurate and precise physical and/or chemical measurements of the materials themselves and of their bulk properties. Measurements of concentration (both elemental and isotopic) are combined with measurements of bulk properties (mass or volume) to verify the total quantities of materials being protected.

When safeguards measurements are performed, the ability to demonstrate and document the accuracy of the measurement system being utilized is of ultimate importance. This importance is more apparent when the consequences of inaccurate measurements are considered. The inaccuracy of measurements or the incompatibility of measurement systems can contribute to inventory differences (ID) within a material balance area (MBA) or to shipper-receiver (SR) differences between MBAs, between plants, between countries, and/or between a facility and its safeguards authority and could, in reality, mask a diversion.

Private nuclear plant operators in the U.S.A. are required by license conditions to demonstrate through a measurement assurance program that safeguards measurements are compatible with, i.e., traceable to, a nationally accepted reference base. A similar requirement exists for U.S. Government facilities.

Reference materials are one means by which measurement technology may be transferred to users in that measurement methods or measurement systems can be calibrated to produce and reproduce the value assigned to the reference. Reference materials are also a means for relating measurements made at different sites, within or between countries, to each other.

This paper discusses some facts vs. some fallacies regarding the use of reference materials and the establishment of traceability of destructive and nondestructive measurements.

Nuclear materials safeguards within the U.S.A. are accomplished by the integration of activities involving physical protection, material control, and material accountability. Material accountability includes data on quantities of nuclear materials and their locations and those measurements and physical inventory procedures used to verify the data. Material accountability incorporates measurement technology and accounting procedures

to provide final evidence that physical protection and materials control have achieved their purpose.

The quantities of nuclear materials received, shipped, stored or in process must be verified by accurate and precise physical and/or chemical measurements of the materials themselves and of their bulk properties. Measurements of concentration (both elemental and isotopic) are combined with measurements of bulk properties (mass or volume) to arrive at estimates of the total quantities of material being protected.

Whether measurements are performed for safeguards purposes, for process controls, for health or safety considerations or as the basis of fiscal transactions, it is the accuracy of the measurement or of the measurement system that is of ultimate importance. (Accuracy is defined as the degree of agreement between a measured value or the mean of several measured values and the "true" or accepted value - in absolute or in relative terms.) Accurate measurements are those which can be related directly, or through a series of controlled experimental procedures to, or are compatible with nationally or internationally accepted reference bases, i.e., a so-called "national or international measurement system." Such a "system", except for a system of units, does not, in fact, formally exist. A systems approach to measurement accuracy has been described by Cali[1] and further by Uriano and Gravatt.[2]

The demonstration and documentation of the accuracy or compatibility of measurements is frequently called "traceability." Traceability is a subjective concept in that there is no single "cookbook" approach to it. (Figure 1 presents a hierarchical structure of measurement methods and reference materials. The function of each component is to transfer accuracy to the level immediately below it and to help provide traceability to the level above it.) The application of individual measurements or the utilization of a measurement to specify end purposes may require different procedural approaches to achieve traceability. How to achieve or realize traceability is beyond the scope of this paper.

The importance of accurate measurements is more apparent when the consequences of inaccurate measurements are considered. In the safeguards realm, it is the inaccuracy or lack of compatibility of measurements or of the measurement system which contributes to ID within a MBA or to SR differences between MBAs, between plants, between countries, and between a facility and its safeguards authority and could, in reality mask a diversion. "Measurement compatibility means that all measurement stations within a given measurement network obtain identical values within uncertainties that have been agreed upon when measuring a specific property of the same material."[3] It is the accuracy of measurements which determines the ability of an operator to determine and/or to demonstrate that a diversion of material has not occurred. The precision with which measurements can be performed becomes the basis for the uncertainty ascribed to a measurement or a measurement process. Thus, precision defines the sensitivity with which, based upon measurements, one is able to detect that a diversion has occurred or state that a diversion has not occurred.

---

1 J. P. Cali, "The NBS Standard Reference Materials Program: An Update", Analytical Chemistry, Vol. 48, 1976, p. 802A.

2 G. A. Uriano and C. C. Gravatt, "The Role of Reference Materials and Reference Methods in Chemical Analysis", CRC Critical Reviews in Analytical Chemistry, October 1977.

3 G. A. Uriano, "The NBS Standard Reference Materials Program: SRM's Today and Tomorrow", ASTM Standardization News, September 1979, p. 8.

Figure 1

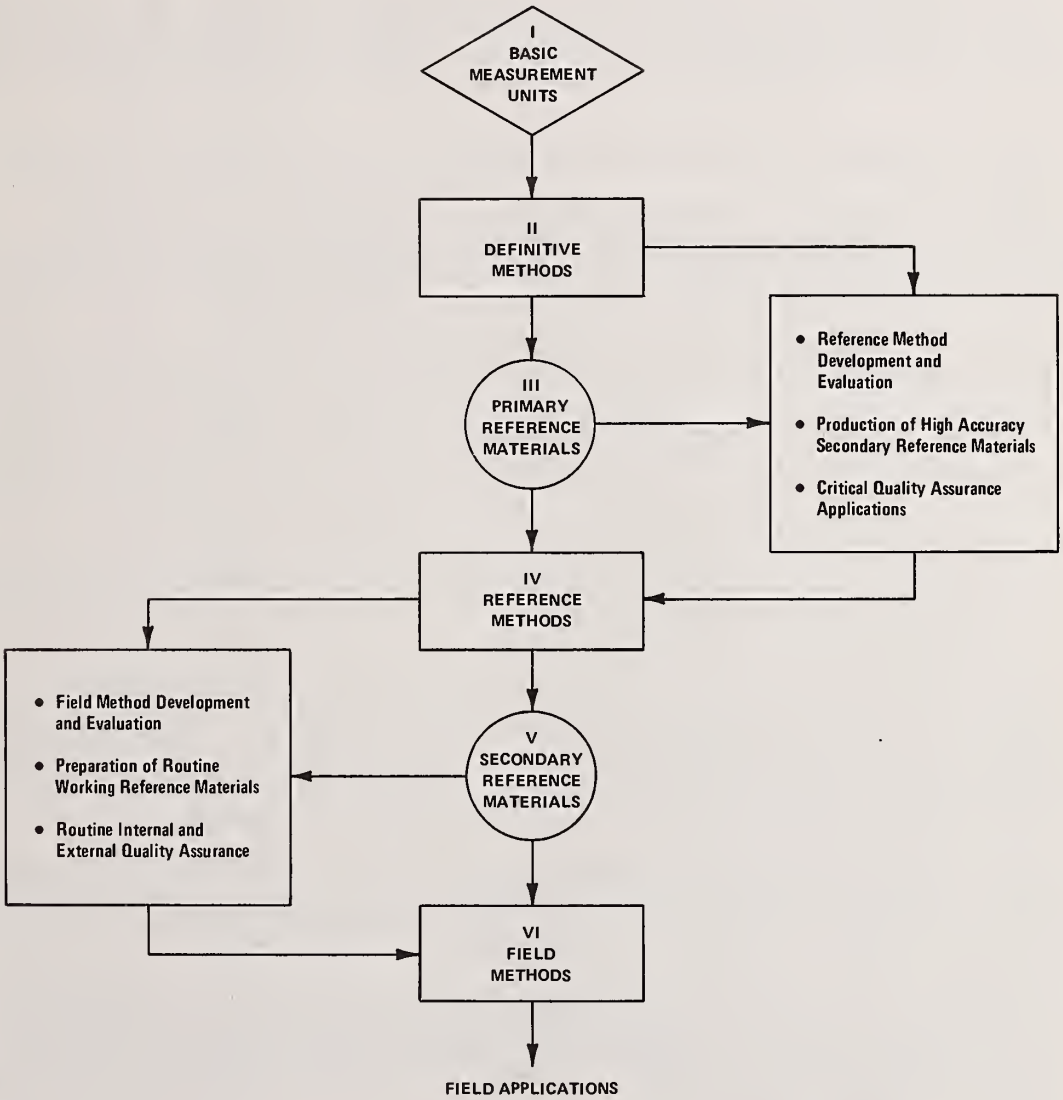
I
BASIC
MEASUREMENT
UNITS
II
DEFINITIVE
METHODS
III
PRIMARY
REFERENCE
MATERIALS
• Reference Method Development and Evaluation
• Production of High Accuracy Secondary Reference Materials
• Critical Quality Assurance Applications
IV
REFERENCE
METHODS
• Field Method Development and Evaluation
• Preparation of Routine Working Reference Materials
• Routine Internal and External Quality Assurance
V
SECONDARY
REFERENCE
MATERIALS
VI
FIELD
METHODS
FIELD APPLICATIONS

Private nuclear plant operators in the U.S.A. are required by license conditions[4] to demonstrate through a measurement assurance program that safeguards measurements are compatible with, i.e., traceable to, a nationally accepted reference base. A similar requirement exists for U.S. Government facilities. The U.S. Department of Commerce, through the National Bureau of Standards (NBS), is charged with the responsibility for establishing and maintaining the reference bases essential for a national measurement system. (NBS, independently or in collaboration with other laboratories, establishes and disseminates measurement technology to users where necessary to fulfill its mandated mission.)

Reference materials are one means by which measurement technology may be transferred to users in that measurement methods or measurement systems can be calibrated to produce and reproduce the value assigned to the reference. Reference materials are also a means for relating measurements made at different sites, within or between countries, to each other.

FACT: Measurement technology may be transferred by use of reference materials.

FICTION: The use of a reference material for calibration per se assures the traceability of subsequent measurements. Improper preparation or handling of the reference material can be a source of measurement bias which is difficult to detect through many internal measurement quality assurance (QA) programs.

Examples of pitfalls which lead to biased calibrations and subsequently to biased measurements are:

1. incomplete transfer or recovery from a reference material "certified to contain" a specified quantity of material or incomplete dissolution of a standard of certified concentration.

2. inaccurately weighed aliquant of a material of certified concentration.

3. failure to correct for temperature coefficients of volume when delivering aliquants of a reference solution by volume.

4. transpiration/evaporation of a prepared reference solution. (See Figure 2.)

5. failure to observe instructions or caveats on the certificate. Some certificates indicate that material should be heated to constant weight at a specified temperature prior to using. Some certificates indicate a quantity of material below which homogeneity is not assured.

6. use of a reference material in a manner not intended or prescribed, e.g., taking a 10-mg aliquant when the certificate indicates that no less than 500 mg should be taken or assuming stoichiometric U_3O_8 in the NBS SRM isotopic uranium series when calibrating a spike for isotope dilution mass spectrometry (IDMS).

7. "certificate values" must be appropriately corrected for decay of radionuclide constituents. When mixing uranium and plutonium isotopic standard solutions, the effect of decay must be considered - e.g., in mixed (U,Pu) solutions, decay of plutonium yields uranium daughters whose presence requires normalization of the stated uranium and isotopic content.[5]

---

4 Code of Federal Regulations, Title 10, Part 70.57.

5 S. F. Marsh, W. D. Spall, R. M. Abernathey, J. E. Rein, "Uranium Daughter Growth Must Not Be Neglected When Adjusting Plutonium Materials for Assay and Isotopic Contents", LA-6444, November 1976.

Figure 2

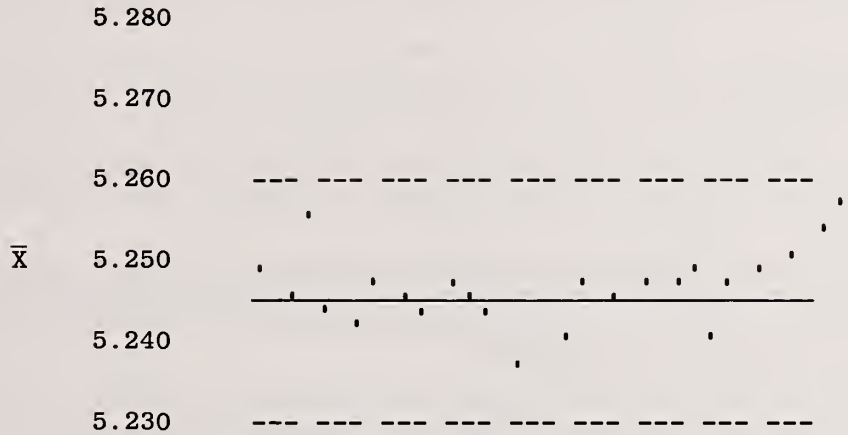

EFFECT OF TRANSPIRATION UPON STANDARD CONCENTRATION

FACT: The use of control charts for measurement results of a reference material is useful in demonstrating that a measurement system is in control.

FICTION: The ability to precisely reproduce assigned values for reference materials within control chart limits assures that accurate measurements will be produced by a measurement system.

1. Merely being within control limits, without concurrently testing for trends or preponderances, does not assure measurement accuracy. (See Figure 3.)

2. An NDA instrument system which properly performs within control limits when measuring a reference material (calibration standard) will yield inaccurate measurements on samples which possess properties to which the system is sensitive that are not contained in the reference material and for which their presence is not compensated.

FACT: The chemical species present in and/or the physical properties of a sample or sample solution as they affect a given measurement system must be considered when performing a measurement.

FICTION: A reference material must be identical in chemical and physical properties to the material to be measured in order that proper transfer of measurement technology can be accomplished.

1. The dissolution, for example, of UO_2, U_3O_8 or uranium metal, can produce the same uranium species in solution. These species in solution are indistinguishable as to their material origin; hence, measurement compatibility for UO_2 may be demonstrated using U_3O_8 or U metal as a reference.

2. The density and effective atomic number of a material influence the observed response of passive gamma-ray and x-ray emission and absorption instrumentation. A proper selection and use of an internal standard in x-ray fluorensence may compensate for density difference between the sample and the reference. The greater the difference between the energy of the line from the internal standard and the element of interest in the sample, the less compensated will be the measurement.

3. The presence of Pu(VI) in solutions of reference material prepared to calibrate controlled-potential coulometry or IDMS may contribute to biased measurements. A proper selection of electrolyte permits reduction of Pu(VI) by controlled-potential coulometry. A suitably vigorous oxidation-reduction treatment will accomplish the isotopic equilibration required for IDMS.

4. The calibration of redox titrimetric measurements for uranium or plutonium can be traced through reference to NBS SRM $K_2Cr_2O_7$, As_2O_3, or $Na_2C_2O_4$.

The overriding consideration here is a thorough knowledge and understanding of the measurement system - its specificity and limitations, its "ruggedness" - i.e., its sensitivity to slight variations in the practiced procedure, and the conditions which contribute to perturbations in the response of the measurement system. A thorough knowledge of the solution chemistry of a sample vis a vis the reference materials is also required.

FACT: A knowledge of the isotopic composition of a material is essential to accurate measurement of the elemental composition of a material.

FICTION: The ability of two or more laboratories to continually reproduce the value assigned to a properly characterized and certified material assures that future measurements of elemental composition are not likely to differ.

1. Redox titrimetry relates the equivalents of species in the titrant to equivalents in the sample solution. Errors in excess of 1% - with excellent precision - (See Figure 4.)

Figure 3

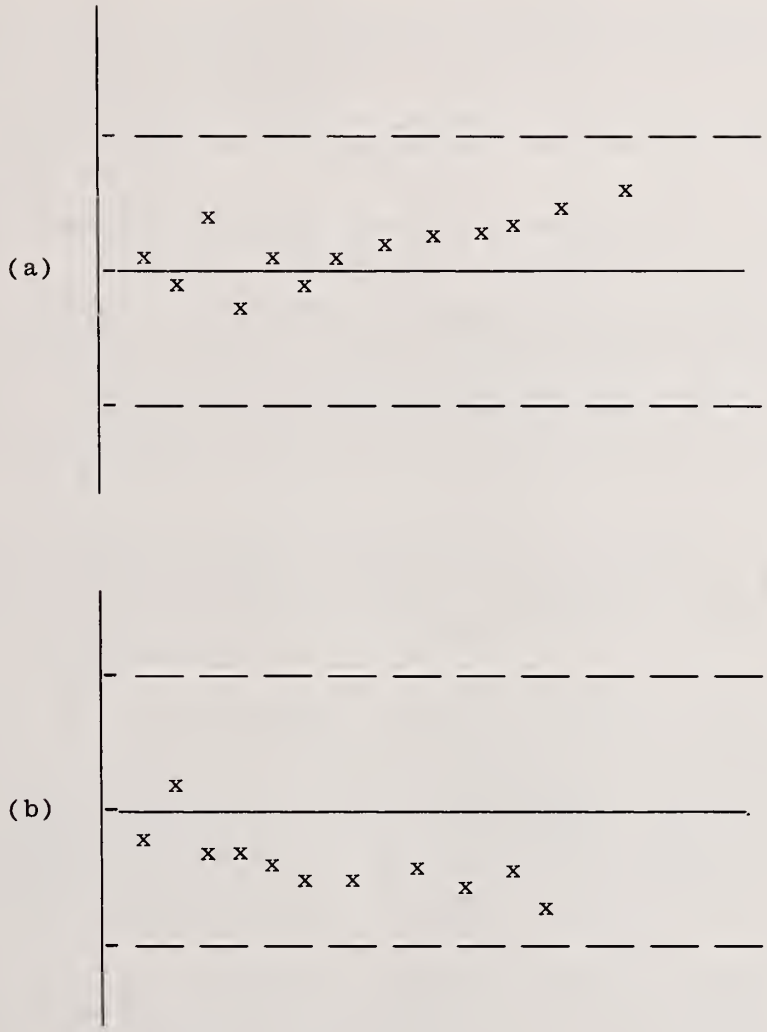

TRENDS (a) OR PREPONDERANCES (b) IN CONTROL CHART DATA

Figure 4

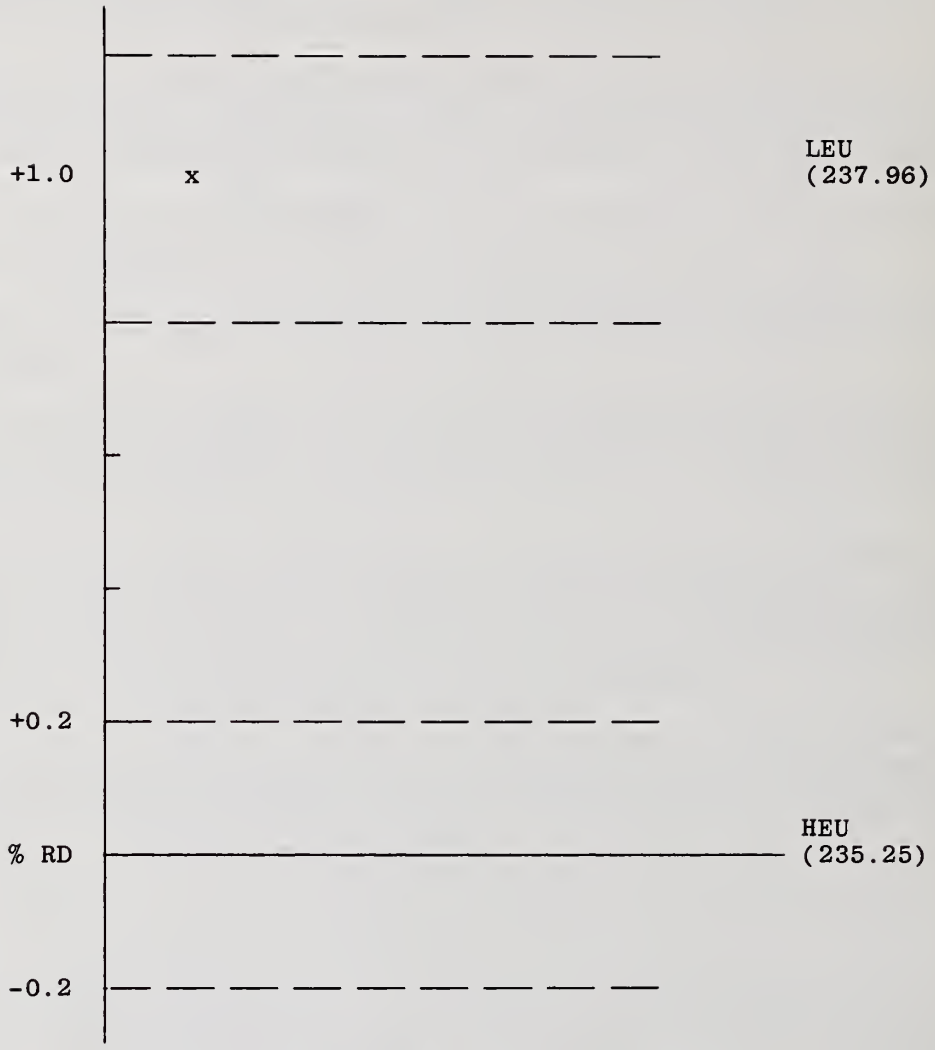

SYSTEMATIC MEASUREMENT ERROR RESULTING FROM INCORRECT ATOMIC WEIGHT

can be introduced by an incorrect (or incorrectly assumed) atomic weight of the element being measured.

2. X- and gamma-ray spectrometric measurements observe the response of a system to numbers of atoms not their masses. Measurement error can result by failing to consider the effect of differing atomic weights (i.e., atomic densities - atoms/gram) between the reference and the sample.

3. Accurate measurements of the heat release of a container of plutonium does not assure accuracy of the assignment of a quantity of plutonium within the container unless the isotopic composition and "age" since purification is specified or otherwise determined by measurement.

FACT: Measurements based upon "first principles" can be used as primary or definitive measurement methods.

FICTION: Measurements calibrated relative to fundamental physical constants are inherently accurate, thus additional traceability is not required.

1. Electrical calibration of controlled-potential coulometric measurements to the Faraday, even after correcting for recently reported anomalies in analog, i.e., capacitive, integrators, results in accurate measurement of the quantity of species electrolyzed not the quantity of species in the sample being electrolyzed. The magnitude of correction factors, for reversible reactions, depends upon the magnitude of the differences between the redox solution potentials and the "formal" potential of the species in the solution being measured. (See Figure 5.)

2. Coulometric measurements calibrated against the Faraday, corrected for the unelectrolyzed fraction, determine gram-equivalents in the sample. Accurate mass determinations require an accurate knowledge of equivalent (atomic) weight. Differences of greater than 0.1% exist between the equivalent weights of so-called "weapons grade" plutonium and that resulting from power reactor fuel burned to $\sim$ 20GWD/T. (See Figure 6.)

3. Values assigned to physical "constants" are not invariant with time. Currently accepted values must be used in calculating or deriving results from "first principles." (See Figure 7.) The Avogadro (atoms/mole) has changed from 6.02252×10^{23} to 6.022045×10^{23} (nearly 0.01%) from 1963 - 1973. Similarly the Faraday (coulombs/equivalent), related to the Avogadro, has changed from 9.6496×10^{4} to 9.648456×10^{4} (or 0.012%) in the same period. Greater deviations exist when compared to the values "accepted" when many of us were studying physics or physical chemistry in college. One still finds in the current literature derivations based upon outdated "constants."

My examples are by no means exhaustive, but merely chosen from some measurement "systems" currently being applied to various portions of the nuclear fuel cycle. I was asked by the Program Chairman to be "controversial" in this keynote in order to stimulate discussion. Earlier in this paper I stated that there is no "cookbook" to traceability. I trust that the pitfalls described herein may provide enlightened awareness that the road to traceability is not smooth nor clearly marked and will serve to stimulate discussion at this meeting.

Measurement science is just that - a science. The fundamental precepts of any scientific discipline must be learned and understood before effective application, effective supervision, or effective regulation can be expected to occur.

Figure 5

$\lvert E-E_0 \rvert$, volts	Correction Factor
0.05	1.333266
0.10	1.041652
0.15	1.005845
0.18	1.001815
0.20	1.000833
0.22	1.000382
0.25	1.000119
0.30	1.000017

SYSTEMATIC MEASUREMENT ERROR BASED UPON ELECTRICAL CALIBRATION OF CONTROLLED-POTENTIAL COULOMETRY

Figure 6

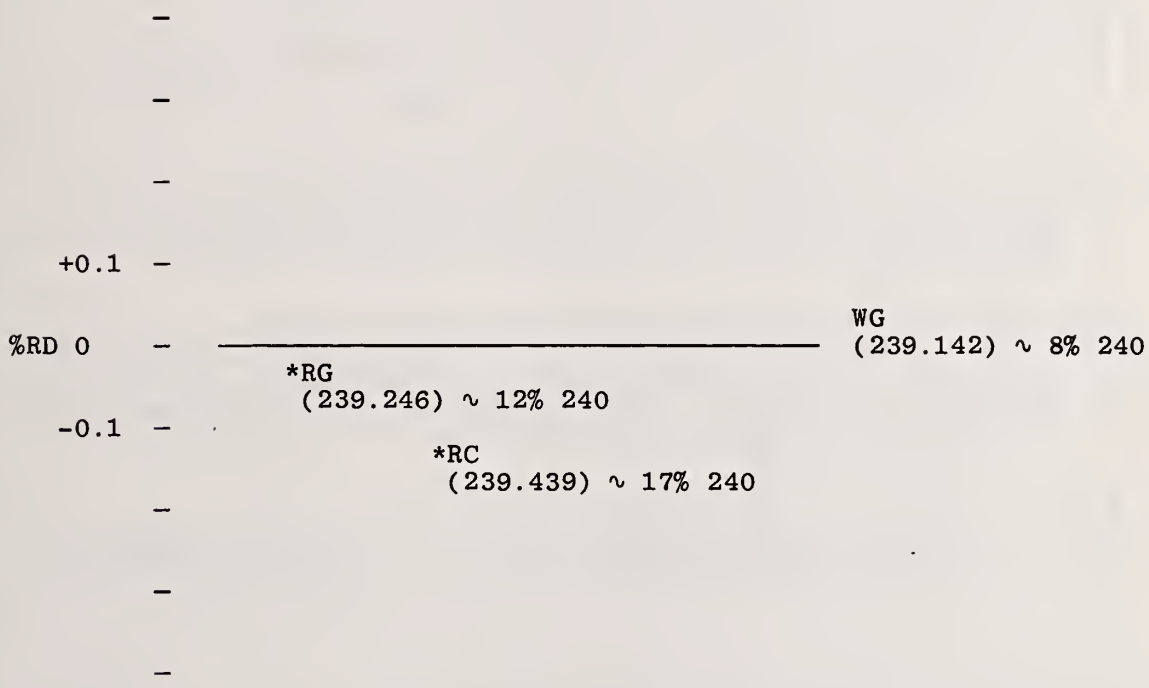

SYSTEMATIC MEASUREMENT ERROR
RESULTING FROM INCORRECT ATOMIC
WEIGHT

Figure 7

CONSTANT	ACCEPTED VALUE 1963	1973
AVOGADRO (ATOMS/MOLE)	6.02252×10^{23}	6.022045×10^{23}
FARADAY (COULOMBS/EQUIVALENT)	9.6496×10^{4}	9.648456×10^{4}

VARIATIONS WITH TIME IN THE VALUE OF PHYSICAL CONSTANTS

Discussion:

Persiani (ANL):
You did imply at the beginning of your talk that you could declare diversion if measurements were outside the precision and accuracy limits, and you also inferred that, if your measurements were within these limits, diversion did not occur. From your discussion on measurement biases, can you ever really make this latter statement? If it's outside limits, I think you are pretty much on sound ground to say that diversion has occurred. If you are within those limits you can only say the measurement does verify proper control of the material but you can never really say diversion has not occurred.

Bingham (NBL):
Thank you, Paul. I think what I stated was, it is the accuracy of the measurements that become the basis for stating that a diversion has or has not occurred (i.e., that an inventory difference does or does not exist). However, it is the precision with which those measurements are performed that defines the sensitivity for making that statement. By example I may say that within an uncertainty of x kg based on an assumed or stated measurement precision (again assuming that my measurements are in control and are accurate) there has not been a diversion. If one were able to analyze the whole inventory with zero uncertainty (obviously not possible), one could state with certainty whether or not material is accounted for.

Persiani:
I was really talking to the words that were used that diversion has not occurred. You can say that the operator has met whatever you have agreed to verify, traceability for example, but I don't think that you can ever say you have not diverted. You can say that the operator has met his responsibilities by staying within a certain measurement range.

Larsen (ANL):
In this situation you are defining a priori what you consider diversion to be in that set of circumstances. If you do not detect it, you say it has not occurred. There may be some smaller fraction of that material that you are trying to maintain control over, then indeed it has been actually diverted, but not detected. Diversion is an operational definition for a particular system in a particular location.

Persiani:
But within your limits a bias might set in, knowingly and/or unknowingly. If a bias has set in, then the operator can stay within the accuracy limits and still be diverting.

Larsen:
Small diversions can never be detected.

Campbell (Exxon):
I wanted to see if I couldn't get a little comment on bias corrections. Isn't this one way of adjusting the very precise measurements that are all gathered at a point distant from the 100% recovery point on your graph?

Bingham:
Bias corrections, when appropriately applied are certainly a way of adjusting the observed response of a measurement system to reproduce or to produce the assigned value. The inappropriately applied bias correction can be the source of an additional bias in measurements. This is a statician's or measurement scientist's nightmare as to what constitutes appropriate and what constitutes inappropriate bias corrections.

Campbell:
You are not going to tell me what is inappropriate?!

Bingham:
I'll refer you to the statisticians and then we can argue.

Campbell:
I don't understand them. (Laughter)

Bingham:

I'll tell you what my definition is, Milt if that will help. When the bias is not statistically different from zero we do not apply a bias correction.

Larsen:

I think this discussion could go on as a very philosophical one. In fact you pointed out the fact on one of your slides with controlled potential coulometry, where you said that the equivalence point and the inflection point of the titration are not the same. You were applying a bias to the analytical method or were correcting for that bias in the analytical method. That is a way of adjusting the results as well as changing the results from the coulometer to what you know to be the true result and that is a standard system that everybody uses. It is inherent in any analytical method for which the equivalence point and the end point are not the same. When you get down to very small amounts then everybody can make that bias correction without cringing but when it gets to a half of one percent then they cringe. But all these adjustments are the same thing, buggering the results. Whether there is honesty or not about what is being done, is the question.

The Role of Standard Reference Materials in Achieving Measurement Traceability

by

WILLIAM P. REED
National Bureau of Standards
Washington, DC 20234

ABSTRACT

This paper will discuss the general concept of a measurement system and the various components of that system as applied to analytical measurements. It will emphasize the relationship of the components of the system including the SI base units, standard reference materials, and reference methods and how these components contribute to making accurate and thus compatible measurements. The concept of compatibility of measurements is a key to understanding traceability requirements and one reason for the use of Standard Reference Materials. In addition, the status of current NBS projects for the preparation and certification of new Standard Reference Materials for nuclear measurement systems is discussed.

KEYWORDS: Standard Reference Materials; measurement compatibility; traceability; SI units; protocol; reference methods; definitive methods.

Traceability is a concept that is of considerable interest in many industries, especially those that are highly regulated such as the nuclear industry. In some instances methods used to achieve traceability are well defined while in other instances traceability is not defined at all. In order to discuss the role of Standard Reference Materials in achieving traceability it is important to discuss the general concept of traceability first. From these concepts, the role of Standard Reference Materials (SRM's) or other Certified Reference Materials (CRM's) will be developed.

The fundamental units of all accuracy based on measurement systems are the International System of Units (SI). Ultimately "Traceability" implies traceability of measurements to these SI units. The SI contains 7 base units and two supplementary units chosen such that all other physical quantities may be realized by an appropriate combination of these units. For example, a measurement of kilometers per hour is simply a combination of the length and time standards. Relating a measurement of kilometers per hour to the SI units is done by using the individual parameters of length - the meter, and time - the second.

In the area of chemical measurements, the most often encountered SI base units are the kilogram, the mole, the ampere and the second. In actual practice (with the exception of the kilogram) it is somewhat difficult to relate these base units to actual measurements of chemical composition in the field. Such work is usually encountered in laboratories that are involved in standardizing activities and then only when highly accurate measurements are required. There are a variety of reasons why this situation exists in the area of analytical measurements. One reason is that many measurements are ratio measurements i.e., μg per gram (ppm) or percent by weight. In this case any self consistent set of units would provide identical numerical values. Another reason why the SI base units are not referenced is that most analytical measurements are influenced by a variety of matrix effects. Generally the uncertainties of measurement due to these effects are much larger than any uncertainties of reference to the SI base units. Lastly the precision of most analytical measurements is a far larger source of uncertainty than the uncertainties of reference to the SI base units. Exceptions to this include measurements involving "Primary" chemical standards where uncertainties of one to two parts in 10,000 are often encountered and reference to an absolute scale is required to insure compatability of these measurements. This compatibility is illustrated by the work of Sappenfield, et.al. (1)

where several "Primary" redox SRM's are intercompared using the coulomb (ampere second) as a basis of measurement.

Most analytical measurements are not directly related to the SI units for the reasons just mentioned. In actual practice they are usually related by means of analytical methods or protocols to Reference Materials (RM's) or Certified Reference Materials (CRM's). These reference materials in turn have been independently measured by some analytical methods or protocols in order to assign a reference or certification value to them. The accuracy of this assigned (or certified) value is an important consideration in the measurement process. It is important here because it leads to compatibility of measurements between laboratories, and it is this compatibility that is one of the major reasons for requiring measurements to be traceable. A more complete examination of accuracy and compatibility as well as the role these components play in an analytical measurement system has been explored by others (2,3) and is the basis for these observations.

Transferring Accuracy (compatibility) Throughout a Measurement Network

Using the SI base units and CRM's as a starting point, a measurement tree or pyramid can be developed for the transfer of accuracy throughout a measurement system via some kind of a hierarchy of methods and transfer standards. A simplified diagram of this hierarchy is shown in figure 1. At the top of this pyramid-shaped structure are the metric, or SI, base units, the heart of the measurement system. Below this are the "primary" standards, which for chemical analysis are usually certified reference materials. They are followed in hierarchial order by secondary standards, working standards, and laboratory samples. Depending on the measurement being made, not all of the steps in the measurement hierarchy are necessary. If a "primary" standard is readily available and inexpensive, it may be used and related directly to laboratory samples. In other cases, three or four steps in the measurement hierarchy may be required to relate the "primary" standards to the laboratory samples. The space between each layer of standards (reference materials) represents the test method, or measurement protocol. This is the measurement process that relates one level of laboratory standard with another and finally with the laboratory samples. In some measurement systems, this process is identified and spelled out in detail with the intent of providing quality assurance and also providing a means to audit or verify laboratory performance and thus the compatibility of the measurements. Other measurement systems do not emphasize measurement protocols but utilize measurement verification schemes to assure measurement compatibility. For purposes of clarity it might be useful to briefly examine a real measurement system or tree as shown in Figure 2. This is the International and National Radioactivity Measurements Traceability Tree (4).

At the top of this hierarchy system is the Bureau of Weights and Measures (BIPM) which is responsible for the developing and maintaining an accurate radioactivity measurement base. Below this are the various national laboratories including NBS and the National Research Council of Canada (NRC). Traceability between these laboratories is maintained by international "round robin" exercises organized by BIPM and also by bilateral intercomparisons between two or more of the national laboratories.

While the national laboratories maintain traceability links with BIPM and each other, they also seek to maintain traceability with radioactivity measurement laboratories within their own countries. In this example, NBS seeks to establish and maintain traceability with key laboratories in the third level such as those of the Environmental Protection Agency (EPA) and the Department of Energy (DOE), and others. As with any large measurement network, it is impossible to directly maintain traceability of measurements between NBS and each laboratory measuring radionuclides. NBS can only maintain traceability with the third level and occasionally the fourth to be sure that measurement traceability exists down to the field measurements.

In this measurement system, traceability is established by interlaboratory comparison of measurements using blind samples for verification of measurement compatibility. Radionuclide Standard Reference Materials, issued by NBS are used to assure adequate internal laboratory quality control and directly for calibration purposes. Measurement protocols are not specified.

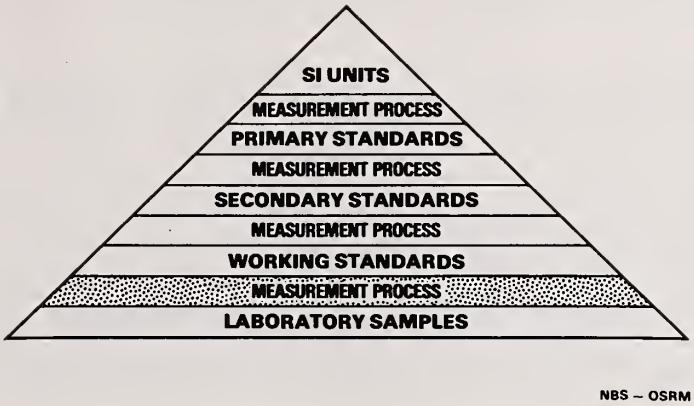

Figure 1

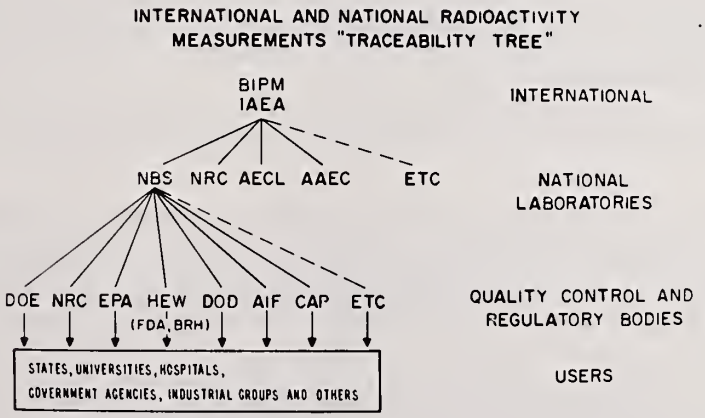

Figure 2

Since in the nuclear industry, blind or audit samples are not used extensively by the Nuclear Regulatory Commission for establishing traceability it might be instructive to examine the measurement system (Figure 3) developed by Uriano and Gravatt (3) as a more appropriate model. This idealized system shows the relationship of the SI base units to the Primary Reference Materials and Secondary Reference Materials using various levels of measurement protocols or test methods. These protocols are titled Definitive Methods, Reference Methods and Field Methods. The definition of each of these methods/protocols is as follows:

> A definitive method is one in which the property in question is either directly evaluated in terms of fundamental units of measurement or indirectly related to the base units via exact mathematical equations. Definitive analytical methods are those that have a valid well-described theoretical foundation, have been experimentally evaluated so that reported results have negligible systematic errors and have a high level of precision. Techniques such as gravimetry or coulometry fall within this definition.
>
> A reference method is a method of proven and demonstrated accuracy. The accuracy of the reference method can be demonstrated by direct comparison with a definitive method or a primary reference material as will be discussed later. Reference methods themselves are key components of a chemical measurement system.
>
> A field method may be defined as any method of chemical analysis used in an application requiring large numbers of individual measurements to be made on a routine basis. Typically, a field method is a highly automated instrumental method operated by a laboratory technician. Many of these methods utilize instrumental techniques and reference materials to correct for systematic biases inherent in the system. An example of this would be a non-destructive assay (NDA) technique used to analyze fissile material in scrap or waste containers.

The role of CRM's (or SRM's) in developing these protocols is discussed in some detail by Cali and coworkers (2,5). While the system is idealized some of the concepts have been used in actual measurement systems, e.g. clinical chemistry. A good example of the development of a reference method is the development of a reference method for calcium in serum (5). While the method is not particularly useful for those working in the nuclear industry the approach used to develop this reference method makes a good case study for this component of a measurement system.

Generally, five major steps are involved in the establishment of a reference method. These are:

1) Establish the accuracy goal of the method, or alternatively, the limit of inaccuracy to be allowed from the true value. Typically this goal should be set at least a factor of three higher than is dictated by end use requirements. Other factors play a role in establishing this criterion and ultimately the accuracy (and precision) of the method will be established through statistical analysis.

2) Choose a candidate method which when demonstrated to produce accurate results become a reference method. If possible the candidate method should be one that has been previously evaluated in terms of both precision and systematic error and should inherently be one of high precision.

3) Determine the "true value" of the property under consideration in a homogeneous stable lot of material similar to the matrix which would normally be analyzed by the reference method. This may be accomplished through comparison with values obtained by a definitive method or, alternatively a series of primary matrix reference materials may be used.

4) Determine the numerical value of the property under study by using the candidate method protocol (i.e. a step-by-step experimental and statistical procedure) together with the samples from 3. If the precision of the method is known or demonstrated to be small relative to any systematic error, the deviation of the mean value from the true value is a measure of the bias of the candidate method. If this bias is less than the reference method accuracy goal then the candidate method becomes the reference method.

5) If the systematic error is greater than required by the reference method goal, further study of the candidate method is required to identify and eliminate (or correct) sources of systematic error until the condition stated in step 4 is reached.

In addition to these steps, there are certain conditions that are necessary for the successful development of a reference method. The method should be developed on an interlaboratory basis and the laboratories participating in this should be recognized for their technical competence in the area. A panel of qualified experts must review and direct all technical phases of the work, including the statistical design and analysis. If possible, a definitive method having a known accuracy of at least a factor of 2 better than the stated accuracy goal of the reference method under test should be available to measure the property of the material under consideration. Finally, recognized CRM's must be available and certified by a laboratory or group of the highest technical competence.

Observations Concerning Development of a Reference Method

The development of the Calcium in Serum Reference method is a good case study. A flame atomic absorption spectrometric (FAAS) method was chosen as the candidate method and a high purity calcium carbonate (SRM 915) was used as the primary standard. The accuracy of the FAAS method was assessed by comparing the results obtained by it on several human serum pools by several selected clinical laboratories against results obtained for the same pools by an Isotope Dilution Mass Spectrometry (IDMS) method.

In carrying out the evaluation five sets of interlaboratory measurements were made before reaching the desired result i.e. an accuracy of $\pm$ 2% of the "true value". The study provided a variety of interesting information. Among the most interesting were that while the precision of the measurement as carried out in many of the laboratories was good, the variability between laboratories and the accuracy was poor. Also the strict adherence to the protocol was absolutely necessary. Small errors such as variation in pipetting contributed significantly to the overall error. Finally the study demonstrated the value of CRM's in transferring technology and measurement accuracy thru a measurement system. The development of this reference method should be studied in some detail, since it could well serve as a model for the development of reference methods in other areas such as the nuclear industry.

The Status of Standard Reference Materials for the Measurement of Nuclear Material

This use of SRM's (CRM's) in a measurement system is one of their more important roles and it is appropriate to report on the current status of SRM's available from NBS and also those planned for issue in the near future. Table I lists Special Nuclear Materials currently available as SRM's. A variety of other materials applicable to the analysis of nuclear material is also available. These include a number of radioactivity and primary chemical SRM's. From this list one can see that the basic standards for making measurements of nuclear material are available. That is, there are assay SRM's for both uranium and plutonium as well as isotopic SRM's for the measurement of isotopic ratios of both of these materials. Thus in theory at least there are sufficient SRM's available to measure the amount of fissile material present in a system. In actual practice this is not completely true due to the accuracy requirements of some measurement methods and also due to the need to accurately relate some SRM's to non-destructive measurement methods. For these reasons it is appropriate to now discuss what is being done to develop new SRM's to meet these needs.

A SYSTEMS APPROACH TO MEASUREMENT COMPATABILITY

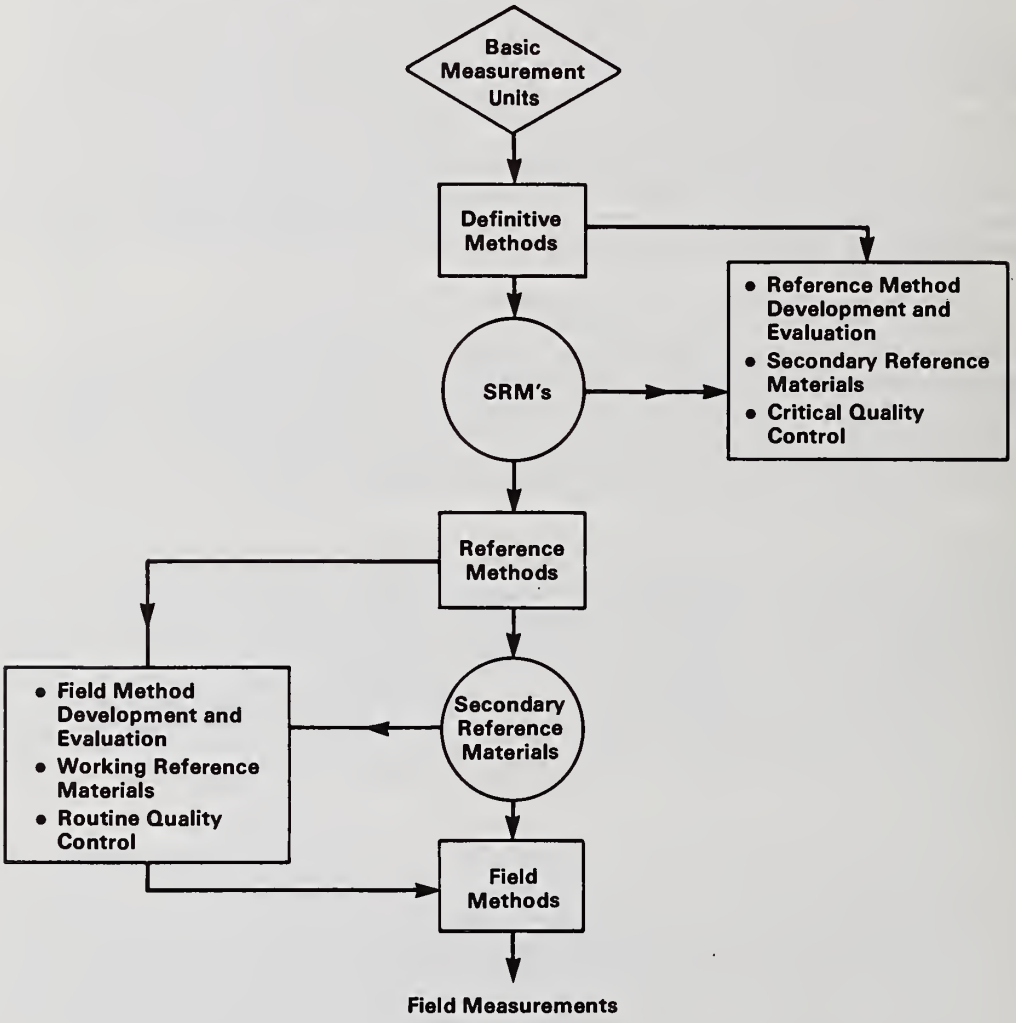

Figure 3

Table I

Currently Available Special Nuclear
Standard Reference Materials

SRM Number	Description	Certification
950b	Uranium Oxide (U_3O_8)	Uranium Content
960	Uranium Metal	Uranium Content
949e	Plutonium Metal	Plutonium Content
944	Plutonium Sulfate Tetrahydrate	Plutonium Content
945	Plutonium Metal	Trace Elements
U-0002 thru U-970 (18)	Uranium Oxide (U_3O_8)	Isotopic Abundance
946		Isotopic Abundance
947	Plutonium Sulfate Tetrahydrate	Isotopic Abundance
948	76% to 92% Pu-239	Isotopic Abundance
993	Uranium Solution (U-235 SPIKE)	Uranium Content and Isotopic Abundance

For the past several years NBS has had a Nuclear Safeguards Program. Much of the work supported by this program has been directed toward the development of facilities and research leading to new SRM's.

Important projects have included the development of two "spike" SRM's useful for the measurement of nuclear material by IDMS techniques. These projects are of overall importance because of the general applicability of the IDMS technique to measurements that are independent of the matrix material.

The first "spike" SRM is a Uranium-233 material. It consists of 5 milligrams of U-233 contained in 10 grams of solution in a glass ampoule. Approximately 400 units have been prepared. The analytical work has been completed and the data has been submitted for statistical evaluation. Certification should be completed within the next few months.

The second "spike" SRM is a Plutonium-244 material. This material has been prepared in individual teflon bottles and dried for shipping purposes by Los Alamos Scientific Laboratory (LASL). It is being characterized in cooperation with New Brunswick Laboratory (NBL) and LASL. Currently the characterization is about 75 percent complete. Certification is expected to take place early in 1980 provided no major problems arise during the statistical analysis of the data. This particular material should be of considerable use in the measurement of plutonium using IDMS techniques.

Besides the preparation and characterization of the two "spike" SRM's, NBS has received support for the development of a plutonium laboratory located at the NBL Laboratory in Argonne, Ill. This laboratory facility is intended specifically for the absolute isotope ratio measurements of plutonium although other work is also planned. With the help of NBL a considerable amount of work has been performed in the establishment of this facility. An NBS mass spectrometer has been installed and the chemistry laboratory is ready to be occupied. Other items of work planned in addition to the absolute ratio measurements include the remeasurement of current plutonium isotopic SRM's and the preparation of a new higher burn-up plutonium isotopic SRM.

In regard to the high burn-up isotopic SRM, a 65% Pu-239 material is planned. NBS is currently looking for a source for this material both in the United States and in Europe through the cooperation of several European laboratories. Current plans call for the processing of this material in FY 81 and certification a year later. It is anticipated that sufficient material will be set aside to also prepare an SRM suitable for the measurement of isotopic ratios by gamma spectrometry. If that SRM proves feasible it is entirely possible that a portion of the currently available plutonium isotopic SRM's will also be certified for measurement of isotopic ratios by gamma spectrometry. This particular set of SRM's appears to be very desirable for NDA measurements especially when used in conjunction with the calorimetric procedure for the determination of plutonium.

NBS has also been involved in the measurement of plutonium heat sources in conjunction with Mound Laboratory. Sources prepared and measured by Mound Laboratory have been intercompared at NBS using an ice calorimeter. Subsequently a heat flow calorimeter was obtained and a series of measurements has been performed on that calorimeter. The results of these measurements, both between calorimeters and between NBS and Mound Laboratory, have been consistent and should lead to the issuance of a reference material. The exact form of the certification has not been established at this point but a mechanism will be developed so that users of these reference materials can satisfy "traceability" requirements for their measurements.

In addition to the NDA reference materials for plutonium, work is also proceeding on the preparation of uranium NDA reference materials. These particular materials will be uranium oxide certified for enrichment measurements by gamma spectrometry. Enrichment levels will range from 0.3% to 4%. The material will be supplied in sealed aluminum containers along with an empty container. These reference materials are being developed in cooperation with an ESSARDA working group and the GEEL Laboratory of Euratom. At the present time, the preliminary set of reference materials has been measured by all laboratories and the material and containers for the final set has been ordered and is being fabricated. The time scale for completion of this work is probably about two years, Certification and

distribution of these materials in Europe will be carried out thru Euratom-Geel while certification and distribution in America will be thru NBS.

Alternative fuel cycles using thorium as their basis have often been discussed. While very little research is currently being done on these fuel cycles, it has often been suggested that NBS should prepare thorium standards. For the past two years NBS has had a small project to develop a thorium reference material. A reasonably pure thorium metal has been obtained and a small amount of funding was made available to develop a new thorium assay procedure. Unfortunately this work is proceeding slowly since it is of lower priority.

One last area that has not been mentioned is the preparation of a series of low enriched UF_6 SRM's certified for enrichment. These SRM's are intended to compliment the current U-series, isotopic SRM's for thermal source mass spectrometers. The levels of accuracy needed for the certification of these materials is quite high and represents a major scientific challenge. A laboratory for the high pressure fluorination of uranium and for the hydrolysis of UF_6 is being prepared. A considerable amount of staff time has gone into this as well as the construction of the actual fluorination apparatus. Once completed a major effort will be required to perform the certification since this work is quite similar to that required for the certification of the U isotopic series. Priority for this work is low since it serves a limited group.

Once the standardization efforts described above are completed, a major portion of the primary reference materials necessary for establishment of traceability will be available. There are still other areas however that require intensive efforts before traceability and compatibility of measurements in the nuclear industry is firmly established. These areas include measurement methods and protocols and verification of traceability thru blind audit samples.

REFERENCES

1. Sappenfield, K. M., Marinenko, G., and Hague, J. L., Comparison of Redox Standards, National Bureau of Standards (U.S.) Special Publication 260-24, U. S. Government Printing Office, Washington, DC.

2. Cali, J. P. and Reed, W. P., "The Role of National Bureau of Standards' Standard Reference Materials in Accurate Trace Analysis", Proc. Symp. on Accurate Trace Analysis, National Bureau of Standards Special Publication No. 422, U. S. Government Printing Office, Washington, DC.

3. Uriano, G. A. and Gravatt, C. C., "The Role of Reference Materials and Reference Methods in Chemical Analysis", CRC Critical Reviews in Analytical Chemistry, Vol. 6, Issue 4, pp 361-412.

4. NCRP (1978). National Committee on Radiation Protection and Measurements. A Handbook of Radioactivity Measurement Procedures, NCRP Report No. 58-305 (National Council on Radiation Protection and Measurements, Washington, DC.)

5. Cali, J. P., Mandel, J., Moore, L. J., and Young, D. S., "A Reference Method for the Determination of Calcium in Serum", National Bureau of Standards (U.S.) Special Publication 260-36, U. S. Government Printing Office, Washington, DC.

Discussion:

Walton (LASL):

Addressing the first two speakers, is there a systematic comparison of the accuracy of chemical measurement of uranium in different materials forms, that is looking, searching for biases between the materials forms - for example, UF_6, U_3O_8, and perhaps uranium from hard to dissolve nuclear fuels. Has any such thing in the standards program been directed to this.

Reed (NBS):

Maybe Bing could answer that better than I, but it would seem to me that your question is more a question of when we speak of systematic biases, you want to talk of methods rather than materials.

Walton:

I think if we go back to the premise of Bingham's, namely, the accuracy for safeguards purposes, my question concerns plants that handle different material forms and have to draw balances based on measurements of the different material forms.

Bingham (NBL):

I might answer your question, Roddy, in two parts - one is that there are in existence a number of measurement comparison programs utilizing different materials - each of which has been characterized, certified, if you please, to know what the "right answer" is. One of these programs is the SALE program and the recently released report for measurements of uranium to which your question was specifically directed have indicated that in the area of measurements on uranyl nitrate and uranium dioxide - virtually 100% of the participating labs are able to measure the uranium content of those materials to within an accuracy of 0.25% irrespective of the destructive method used. Some laboratories, and I think the figure for uranium dioxide is two thirds of the laboratories, have demonstrated an accuracy of measurements to better than .05%. Now, the second part of that question was partially answered by Bill, is that we are looking at the effect of measurement methods as opposed to the effect of materials. In the examples you gave, once those materials are in solution the chemical system is virtually identical between UF_6, UO_2, uranyl nitrate, uranium metal. The measurement, irrespective of the material, should be identical and for most of the well defined methods one cannot distinguish a measurement "bias" based on the material. A measurement bias may be determined based on the handling or the preparation or the analysis procedures used prior to the actual measurement.

Preparation of Prototype NDA Reference Materials: A Progress Report

by

ANNA M. VOEKS and NANCY M. TRAHEY
U. S. Department of Energy, New Brunswick Laboratory, Argonne, Illinois

ABSTRACT

Three prototype NDA reference materials for scrap and waste have been developed at the New Brunswick Laboratory for use in an interlaboratory evaluation program. They are ion exchange resin, cellulose fiber and synthetic calcined ash. A total of 19 reference materials containing varying amounts of enriched uranium were prepared. Details of the preparation, packaging and characterization are described.

KEYWORDS: Nondestructive assay, uranium reference material, interlaboratory evaluation program

INTRODUCTION

Increasing reliance on the use of nondestructive assay (NDA) techniques for nuclear material safeguards and accountability measurements over recent years has encouraged efforts to develop instrumentation systems capable of measuring the SNM content of all types of nuclear materials encountered within the industry. The degree of sophistication already achieved by a number of these systems thus far has made possible the evaluation of such systems by accepted calibration and standardization procedures. However, the physical standards or reference materials required to establish measurement compatibility within the national measurement system are not yet available. Some preliminary work conducted by the U. S. Department of Energy, New Brunswick Laboratory (NBL), on the development of materials specifically for use as NDA physical standards has already been reported in the literature.[1] Three of the materials tested have now been prepared to serve as prototype NDA uranium reference materials for scrap and waste in an interlaboratory evaluation program to be administered by the New Brunswick Laboratory. They are (1) an ion exchange resin, (2) a cellulose fiber, and (3) a synthetic calcined ash.

EXPERIMENTAL

Preparation

Ion Exchange Resin

Two batches (900 g each) of Bio-Rad anion exchange resin, AG1-8X, 50-100 mesh (297-150 μm), chloride form, were placed in 4-L beakers, rinsed in distilled water, then allowed to settle so that as much water as possible could be decanted. Next, 2 L of HCl were added to each batch of resin, the mixtures stirred for five minutes before being allowed to settle and the acid removed by suction. Another 2 L of acid were added to each batch and again the mixing-settling-removing process was repeated. The same process was then followed three more times using 6 N HCl, after which each resin batch was poured into a HCl solution containing 28 g of 93% enriched uranium. The resulting mixtures were stirred

---

[1] A. M. Voeks, N. M. Trahey, and J. M. Scarborough, "Preparation of Test Materials for an Interlaboratory Comparison Program on NDA Physical Standards," Analytical Chemistry for Nuclear Fuel Reprocessing, Science Press, Princeton, NJ, 1978, pp. 338-344.

five minutes and allowed to settle one hour, during which time the uranium, as uranyl chloride, was adsorbed onto the resin. The excess acid in each beaker was removed by suction and the two batches of resin with uranium combined. Next, 2 L of 6 N HCl were added and the mixture stirred five minutes before it was allowed to settle and the acid removed. The 6 N acid wash was repeated twice more before the resin was transferred to a large Pyrex dish with a minimal amount of 6 N HCl. In order to dry the processed resin, the bulk of the liquid was evaporated on a steam table. Further drying was accomplished using a hot plate and finally, after transferring the resin to a porcelain tray, in a vacuum oven at 38-51 cm Hg (51-68 kPa) and approximately 50°C. After cooling, this resin, designated as the master batch, was V-blended and analyzed for uranium content. Based on volumetric titration, the master batch was calculated to contain 54 mg U/g resin. Six dilutions of the master batch were then prepared by V-blending it with uranium-free resin which had also been acid-treated (Table I).

Table I

Master Batch-to-Diluent* Ratio for Preparation of Ion Exchange Resin Reference Material (RM)

RM Container No.	Ratio	% Uranium
R1	all diluent	0
R2	0.23	1
R3	0.59	2
R4	1.25	3
R5	2.27	4
R6	all master batch	5.5

*uranium-free resin

Cellulose Fiber

The technique of preparing a master batch of material and blending it with uranium-free matrix was also used to prepare the six cellulose fiber reference materials. For the master batch, 100 g of Whatman chromatographic grade fibrous cellulose powder was spread on the bottom of a porcelain tray. Then, 200 mL of very dilute HCl containing 56 g of 93% enriched uranium were carefully poured on the cellulose so that the solution was completely absorbed but did not come in contact with the tray. An additional 50 g of cellulose powder were placed over the areas where the uranium solution had been absorbed, and the material was dried in a vacuum oven for two days at 38 cm Hg (51 kPa) and approximately 75°C. The chunks that formed during drying were crushed by ball milling and hand grinding, then the material was returned to the vacuum oven and dried for an additional 24 hours. The material was crushed again, V-blended and analyzed for uranium content. Based on gravimetric analysis, the master batch was calculated to contain 197 mg U/g cellulose. Six dilutions of the master batch were then prepared by V-blending it with untreated cellulose which had been ball milled to approximately the same particle size as the master batch (Table II).

Table II

Master Batch-to-Diluent* Ratio for Preparation of Cellulose Fiber Reference Material (RM)

RM Container No.	Ratio	% Uranium
C1	all diluent	0
C2	0.06	1
C3	0.14	2.5
C4	0.21	3.5
C5	0.28	4
C6	0.40	6

*uranium-free cellulose

Synthetic Calcined Ash

Seven synthetic calcined ash reference materials, containing from 0 to 15% enriched uranium were also prepared by a batch process. Table III lists the starting materials and final oxide concentrations for a given batch.

Table III

Starting Materials and Final Oxide Contrations of Synthetic Calcined Ash

Starting Materials	Oxide Concentrations
kaolin [$Al_4Si_4O_{10}(OH)_8$]	48-52% SiO_2
SiO_2	25-27% Al_2O_3
cellulose,* fibrous powder	-
$FeCl_3 \cdot 6 H_2O$	13-15% Fe_2O_3
$ZrOCl_2 \cdot 8 H_2O$	5-6% ZrO_2
Nb_2O_5	4-5% Nb_2O_5
$CaCl_2$	2-3% CaO
$BaCl_2 \cdot 2 H_2O$	1-2% BaO
UO_2Cl_2 (93% ^{235}U)	0-15% U_3O_8

*Added to facilitate grinding of final product; removed by ignition.

A total of four batches, 400 g each, were prepared to make up each reference material. For a given batch, the cellulose, kaolin and silica were suspended with stirring in 1 L of 0.1 N HCl. The remaining ingredients were mixed separately in 500 mL of 0.1 N HCl then added to the suspension and stirred for five minutes. The combined starting materials were then poured quickly into 3600 mL of 4 N NH_4OH and stirred vigorously for five minutes. The resulting precipitate was allowed to settle on a steam table for two to three hours, then filtered through Whatman 541 filter paper and washed three times with 0.7 N NH_4OH. The filter cake was transferred to three 1-L platinum dishes and dried at 110°-120°C for 18 hours. The dishes were then placed in a cold furnace and the temperature slowly (over six hours) raised to 800°C and held there for 18 hours after which it was raised to 1000°C and held for one hour. After the ash was cooled in a desiccator, four batches were combined, ball milled and hand ground, then sieved through a 325 mesh (425 μm) screen to obtain a reference material of particular uranium concentration (Table IV).

Table IV

Synthetic Calcined Ash Reference Material (RM)

RM Container No.	% Uranium
1	0
2	0.5
3	1
4	2.5
5	5
6	10
7	15

Size Reduction and Classification

The homogeneity of a reference material is, to a great extent, a function of its particle size. Therefore, a uniform particle size for each material prepared was sought in order to reduce the possibility of segregation and a variation of density of the final

products. Thus, size reduction and classification of these reference materials, prior to their final containment, was performed with this in mind.

The ion exchange resin reference material was the most manageable of the three materials. The matrix was reasonably well classified at the start: 50-100 mesh (297-150 μm). The beads did swell considerably during the preparation; however, when examined under a microscope, the dried master batch and diluent resin appeared to be the same size. Thus, V-blending the material resulted in a final product of uniform particle size, as desired.

The cellulose fiber reference material posed a greater challenge. In this case, the matrix was a fibrous powder of non-uniform particle size and shape. However, once the master batch and diluent cellulose were ball milled and V-blended, a sieve analysis showed that 90-94% of the final product passed a 325 mesh (45 μm) screen and that the particle shape was more uniform. Again, a controlled particle size of the final product was achieved.

Classification of the calcined ash reference material required the most effort. A particle size greater than 325 mesh (less than 45 μm) was selected for the final product. This selection was based on the fact that the major constituents, kaolin and silica, are that size (actually 45 μm and 30 μm, respectively). Also, there is evidence that the friable ash would generate fines if a larger particle size was selected. The latter phenomenon could result in widely varying packing densities within a single contained reference material.

Packaging

Two types of primary containers were chosen for the three materials. For the synthetic calcined ash, specially fabricated cylindrical polypropylene containers, 20.3 cm x 8.6 cm, wall thickness, 0.15 cm, were used. Each container was cleaned, then weighed to 0.01 g before and after filling. Nine hundred fifty grams (950 g) of each of the seven reference materials were packed into the containers. Although the material looks striated in the containers, its uniform particle size greatly reduces the possibility that the packing density differs significantly within each container. However, the density does differ from container to container; it increases with increasing uranium content. This can be easily seen by comparing the fill heights of the containers. They vary from 1-3 cm from the top. These sealed containers, labeled 1 through 7, and an empty sealed container, labeled EMPTY, comprise Set I.

Standard tin plate cans, 12.2 cm x 6.6 cm, wall thickness, 0.02 cm, with an oleoresin coating on the inside surface were selected for the cellulose fiber and ion exchange resin reference materials. The cans were cleaned, then weighed to 0.1 mg before and after filling. One hundred seventy-five grams (175 g) per cellulose reference material were sealed in each of six cans and labeled C1 through C6. These six cans and a sealed empty can, labeled EMPTY 2 C, comprise Set IIA. Similarly, 250 g per resin reference material were sealed in each of six cans and labeled R1 through R6. These six cans and a sealed empty can, labeled EMPTY 1 R, comprise Set IIB.

A secondary container for Set IIA and Set IIB was also fabricated. It consists of a five-gallon metal pail with two removable holders with seven slots each (one for each can). This container is intended for use when measuring more than one can at a time. For shipment of the reference materials to program participants, the five-gallon pail and the polypropylene containers are located in a reusable 55-gallon DOT 7A stainless steel drum.

Table V is a summary description of the reference materials and their containers.

Characterization

In order to properly certify each reference material for NDA measurement usage, chemical characterization measurements were performed to determine the total uranium and

Table V

Description of Reference Materials

Parameter	Material I - Set I (1-7)	Material II - Set IIA (C1-C6)	Material II - Set IIB (R1-R6)
Matrix Composition	calcined Si, Al, Fe, Zr, Nb, Ca, Ba	fibrous cellulose powder, chromatographic grade	resin, styrene-divinyl-benzene polymer
Uranium Isotopic/ Chemical Composition	93% $^{235}U/U_xO_x$	93% ^{235}U/uranyl chloride	93% ^{235}U/uranyl chloride
Container Composition	polypropylene	tin plate w/oleoresin coating on inside surface	tin plate w/oleoresin coating on inside surface
Container Dimensions	cylindrical - 20.3 cm x 8.6 cm wall thickness - 0.15 cm	cylindrical - 12.2 cm x 6.6 cm wall thickness - 0.02 cm	cylindrical - 12.2 cm x 6.6 cm wall thickness - 0.02 cm
Total Number of Containers in Set	7 (plus one empty)	6 (plus one empty)	6 (plus one empty)
Quantity of Material per Container	950 g	175 g	250 g
Nominal % Uranium per Container	0, 0.5, 1, 2.5, 5, 10, 15	0, 1, 2.5, 3.5, 4, 6	0, 1, 2, 3, 4, 5.5

uranium-235 contents. For the characterization, well documented analytical methods and nationally certified standard reference materials were used whenever possible.

Ion Exchange Resin

Samples from each resin reference material containing uranium (R2 through R6) were weighed into disposable plastic ion-exchange columns and the adsorbed uranium eluted with 200 mL of 0.1 N HCl into 400-ml beakers. The samples were evaporated to dryness on a steam table and converted from the uranyl chloride to the uranyl nitrate form by fuming to dryness repeatedly with HNO_3 on a hot plate. The residues were then dissolved in 8 N HNO_3, evaporated to incipient dryness, redissolved in 10-12 ml H_2O, and titrated using the NBL titrimetric method for uranium. Uranium reference solution samples prepared from NBS SRM 960 uranium metal were analyzed with the samples. In addition, a set of uranium reference solution samples which had been adsorbed onto the same kind of resin used to prepare the reference material then eluted exactly like the samples, was also analyzed with the samples. The actual sequence of titration was as follows: reference, eluted reference, sample, reference, eluted reference, sample, etc. The 0% uranium resin reference material (R1) was analyzed by spectrophotometric and fluorometric methods to confirm the absence of uranium.

Characterization of the isotopic composition of the material used as the source of uranium in the preparation of these reference materials was performed by thermal ionization mass spectrometry. Appropriate NBS SRM uranium isotopic standards were analyzed with the samples.

Cellulose Fiber

Samples of each cellulose reference material containing uranium (C2 through C6) were weighed into platinum dishes, thoroughly dampened with water, then dried at 115°-120°C for three hours. After slowly charring the samples, they were ignited at 900°C for two hours and cooled. The residues were dissolved in 8 N HNO_3 and fumed to dryness, redissolved in 8 N HNO_3 and HF and fumed to dryness again, dissolved a third time in 8 N HNO_3, quantitatively transferred to 400-ml beakers and evaporated to dryness on a steam table. The samples were subsequently titrated using the NBL titrimetric method for uranium. Uranium reference solution samples prepared from NBS SRM 960 uranium metal were analyzed with the samples. The sequence of titration was as follows: reference, sample, reference, sample, reference, etc. The 0% uranium reference material (C1) was analyzed by spectrophotometric and fluorometric methods to confirm the absence of uranium.

Synthetic Calcined Ash

Samples of each of the six uranium-containing synthetic calcined ash reference materials (2 through 7) were weighed into platinum crucibles and fumed repeatedly with HNO_3 and HF to remove the silica. They were then fused with sodium carbonate for four to six hours. After cooling, the crucibles, including crucible covers, were placed in 400-ml beakers; 50-100 ml of 8 N HNO_3 were added and the beakers covered. After the effervescence subsided, the crucibles and covers were removed and rinsed carefully with 8 N HNO_3. The samples were subsequently evaporated to dryness on a steam table, then fumed on a hot plate with five ml of $HClO_4$ and a small amount of HF to remove any silica still remaining, and redissolved in 10-12 ml of H_2O. (Any samples not completely dissolved at this point were heated on a steam table to promote dissolution.) After each sample was cooled it was titrated using the NBL titrimetric method for uranium. Uranium reference solution samples prepared from NBS SRM 960 were analyzed with the samples. The titration sequence was as follows: reference, sample, reference, sample, etc. The 0% uranium reference material was analyzed fluorometrically to confirm the absence of uranium.

RESULTS AND DISCUSSION

The NDA interlaboratory evaluation program, for which the materials described were prepared and packaged, has now entered into the measurement phase.[2,3] By the time this phase is completed, 14 nuclear facilities in this country and in Europe will have analyzed the same 19 containers of prototype NDA reference materials for uranium-235 and total uranium content. Some of these facilities will have never measured materials like these by NDA techniques. However, lack of measurement experience should not be considered a disadvantage. These are, after all, prototype materials; therefore, all program participants will have an equal opportunity to evaluate them.

It is evident that these prototypes represent only a small fraction of the many types of materials routinely analyzed by NDA techniques. The results of a questionnaire sent to NDA developers and users indicated that many types of reference materials would have to be prepared to satisfy all of the stated needs.[4] Such an undertaking was not possible nor was it clear that such a large number of reference materials were really necessary. Therefore, the decision was made to prepare three "typical" materials which would represent a good cross section of those routinely measured.

The ion exchange resin, a styrene-divinylbenzene polymer, and cellulose fiber, a carbohydrate, represent low density, low Z organic materials. The synthetic calcined ash represents slightly higher density, intermediate Z refractory oxides. As described, all three materials were prepared with 93% enriched uranium. Although most facilities do not routinely measure materials containing uranium with an enrichment this high, 93% was selected so that counting times during analysis would be short. It was felt that this was a necessary trade-off in order to complete the measurement phase of the program in a timely manner.

In summary, every effort was made to provide useful and representative NDA reference materials. These materials were well characterized using reference analytical methods and nationally certified reference materials. Of course, it is the results of the program that will show how well they serve as reference materials and how well NDA techniques can measure them.

ACKNOWLEDGEMENT

The authors thank Glennda J. Orlowicz for her assistance, particularly in the preparation of the synthetic calcined ash reference material.

---

[2]N. M. Trahey, J. M. Scarborough, and C. D. Bingham, "Design of an Interlaboratory Comparison Standard for NDA Measurement of Scrap and Waste" 18th INMM Proceedings, Vol. VI, No. III, Fall 1977, pp. 659-662.

[3]Letter, w/encl., J. M. Scarborough to Program Participants, dated September 21, 1979.

[4]Letter, w/encl., J. M. Scarborough to Colleagues, dated April 11, 1977.

Discussion:

Larsen (ANL):
You used such substrates as ion exchange resin, and the cellulose. Are there actually individuals in the industry going to be measuring uranium-235 on ion exchange resins or was that a material that would typify a low Z matrix?

Voeks: (NBL)
Correct, yes. The three materials were selected to represent all the materials that were out in the field. Obviously they can't represent every possible material, but we have covered a range.

Eccleston (LASL):
A lot of work has been spent on the reference materials but one important item needing more attention is packaging. For example, using polyethylene containers. If we have to do measurements with epithermal neutron techniques then this type of packaging can be detrimental to the measurement and it is very difficult to obtain accurate results, no matter how good the reference standard. Have you addressed that to some extent?

Voeks:
Yes, on that questionnaire, many indicated that they used 2 liter polyethylene containers and the choice was based mostly on that. The choice of the cans was also based on the questionnaire. I imagine that for the polypropylene containers it is possible that those people were using gamma ray spectroscopy rather than neutron.

Campbell (Exxon):
Two questions, first the easy one: What is the uranium-235 content of these standards?

Voeks:
On the cellulose fiber and the resin it ranges from 0 to approximately 6% and on the synthetic calcined ash it ranges from 0 to 15%. That is the uranium content and it is 93% enriched so that gives you a good idea.

Campbell:
That is the point, 93% enriched isn't used by industry.

Voeks:
As I said, if you use low enrichment the counting times for the analyses would be greater.

Campbell:
That is our problem. Your problem is that you are not relating to the total measurement requirement. If you have extremely highly enriched U-235 you have to measure at 5% or less.

Voeks:
We realize that this obviously doesn't cover the whole range, but we had to make some limitations. As it is, we made one set of each and they are going to go around to 14 facilities and it is going to be very time consuming. I think we had to make some sort of time considerations.

Campbell:
Well, only the people that make bombs are interested in that material. The second question is how did you assure homogeneity after you had a master mix and you mixed, I presume, two considerably different density materials? What tests were these that you mentioned that assured homogeneity?

Voeks:
They are analyzed for uranium content and they were sampled such that we would see if there was a difference in homogeneity.

Campbell:
Would this be on a macro basis that would kind of average out or on a micro basis?

Voeks:
I would say macro. We were taking relatively small sample sizes. For each reference material it varies. For example, on the cellulose, the samples are 3-4 gms and replicate samples are done.

Campbell:
There would be no separation then of the uranium loaded resin bead from the total non-uranium loaded resin bead?

Voeks:
These are prototype materials. We don't expect to see any variations or change in the homogeneity with time, but we'll find out.

Trahey (NBL):
If I could just amplify a little bit on what Anna said with regard to the packaging, the actual enrichment, and the types of materials selected for these prototypes. Again I use the word and I stress it, prototype. It is unlike anything in the way of reference materials that anyone has ever done before. There have been some NDA reference materials made but they are strictly for U-235 concentration. They are product material and we are trying to address the problem of scrap and waste measurements when we could. We recognize that polypropylene, for some types of NDA measurement systems, are a problem. 93% enriched cannot be handled by licensees; however, there are other laboratories in the US that can handle 93% enriched. Therefore, we tried to strike some kind of compromise. We are hoping to make some evaluation of the measurement data whereby we can get further direction on where to go next with NDA. It should turn out to be quite an enlightening program for all concerned.

George (UCC):
I would like to say it is not just the bomb people, but also those who make medical radioisotopes are interested in these materials.

Hoffman (B&W):
Do you have any suggestions for calcining waste generated in the manufacture of fuel to get its homogeneity up and to make it like the calcined ash synthetic standard?

Voeks:
I am not very well versed in the real stuff. The method that we used to prepare the synthetic calcined ash was specific so that the material would turn out homogeneous; for example, the constant stirring when ingredients were mixed and the rapid precipitation of all ingredients at one time. I really can't say, but I am sure if we can talk afterwards, I can find someone who can help you out on that.

Bingham:
Further amplification: recognizing that nondestructive measurement technology has sensitivities to a number of physical as well as chemical parameters, the intent in these waste and scrap stream prototypes was to identify many the chemical and physical properties of these materials to the participants of this comparative measurement system. That is, particle size, density, chemical properties, even the enrichment value is being specified, and what is being asked of the participants is, using whatever correction factors that you normally apply for particle size, or for density, for transmission, etc., measure and report to the best of your NDA capability, the quantity of material in that can. The evaluated data will give some sense of direction to whether or not non-facility specific reference materials that typify the scrap and waste streams (which are a number of the real problem areas in this technology) can be prepared for uniform use within the community or whether everyone is going to have to prepare his or her own. That is the bottom line of this comparison program.

Mass Spectrometric Measurements to Determine the Half-Life of ^{241}Pu

by

ERNEST L. GARNER AND LAWRENCE A. MACHLAN
National Bureau of Standards, Center for Analytical Chemistry, Washington, DC 20234

ABSTRACT

The isotopic abundance ratios of a group of plutonium reference samples and Standard Reference Materials were precisely determined by thermal ionization mass spectrometry. The procedure was based upon the well developed methodology for uranium, making appropriate allowances for relative differences in the ionization efficiencies of the elements. The ^{241}Pu half-life results for independent decay curves for the samples involved in the study varied from 14.32 to 14.36 years and were independent of ^{241}Pu atom composition.

KEYWORDS: Half-life, plutonium-241, mass spectrometry, thermal ionization.

INTRODUCTION

The National Bureau of Standards (NBS) needs accurate half-life values of the plutonium isotopes as part of the continuing effort to accurately certify and to keep current the isotopic composition of its plutonium Standard Reference Materials (SRM). Secondly, but equally important, is the commitment to provide essential standardization for nuclear safeguards and related measurements, especially the effort to develop SRMs for non-destructive assay techniques. The availability of accurate and reliable half-life values which are accepted internationally will also make it practical to utilize a common set of values for all inventory adjustments for radioactive decay.

An accurate value for the half-life of ^{241}Pu has been a particularly elusive parameter for more than a decade. Measurements by alpha counting, calorimetry and mass spectrometry have yielded values which range from a low of 13.8 ± 0.3 years to a high of 15.16 ± 0.19 years [1, 2]. With apparent measurement precisions and/or accuracies of approximately one percent and a significantly longer half-life by the more precise mass spectrometry determinations, it appeared for a brief time that the nearly 10% discrepancy in ^{241}Pu half-life values could be explained by an isomeric state of ^{241}Pu [3]. Once the suggestion of an isomeric state was discounted as the probable cause of discrepant half-life values, the focus shifted to measurement error [2].

Since the essence of a half-life determination is the precise and/or accurate measurement of the number of atoms present at two points in time or a series of isotopic ratio measurements as a function of time, the high precision capability of mass spectrometry for atom composition measurements is a particularly attractive approach for accurate half-life measurements. Especially attractive is thermal ionization mass spectrometry where precisions (95% confidence limits) approaching 1 in 10^4 can be achieved utilizing either microgram or nanogram quantities of plutonium. The major disadvantage in the mass spectrometric approach for plutonium is the lack of calibration standards of known isotopic composition which can be utilized to measure isotopic abundance ratios on an absolute basis. A calibration of this nature provides a means of correcting for systematic error, evaluating the random error component and making an allowance for all known sources of possible systematic error. Consequently, all isotopic ratio measurements for plutonium have been made on a relative scale, or corrected to a "pseudo-absolute" scale on the basis of uranium and plutonium exhibiting identical behavior during mass spectrometric analysis. Both the relative and the

"pseudo-absolute" measurement are subject to significant error. For example, two different sets of relative measurements may be highly precise but biased to a different degree with respect to the "true" value. This type of bias can be difficult to detect without the appropriate standards since it is primarily a mass dependent isotopic fractionation effect which may be highly reproducible but different for each set of conditions used [4, 5]. Thus, controlling the isotopic fractionation is a necessary and essential condition for an accurate half-life measurement by thermal ionization mass spectrometry.

The purposes of this paper are two-fold: (1) to give a description of the methodology developed for the measurement of plutonium isotopic ratios and (2) to evaluate the known sources of error in the measurement.

MASS SPECTROMETRY

In practice, mass spectrometry is frequently perceived and utilized as a single analytical discipline, but for best results mass spectrometry must be utilized as a combination of classical wet chemistry and the isotope ratio measurement methodology of the mass spectrometer. A sound approach to precise and/or accurate measurements must include these two basic components. Specific benefits of well developed chemical procedures are high purity samples, solutions of known elemental concentration and reproducible stoichiometry. These outputs from the chemistry are necessary if the isotope ratio measurements are to be made under conditions in which the isotopic fractionation is precisely reproduced for each analysis. The basic analytical approach for plutonium as well as other elements includes the following general steps: (1) preanalysis; (2) chemistry; (3) sample mounting; (4) isotope ratio measurement.

Preanalysis

The purpose of the preanalysis phase of the analytical methodlogy is to take the necessary precautions to maintain throughout the analysis the integrity of high purity solutions produced by chemical separation. For example, impurities, either organic or inorganic, may combine with the analyte element, evaporate as a high molecular weight species and thereby produce a bias because of variable isotopic fractionation. The watchword of preanalysis is cleanliness and includes: (1) selecting and cleaning all storage and preparation containers; (2) production and use of high purity reagents; and (3) cleaning and testing of all filaments for background contributions and interference from the alkali elements.

Chemistry

Chemical separation of ^{241}Pu from ^{241}Am and the production of high purity plutonium is accomplished by anion exchange chromatography. Plutonium, when necessary, is converted to Pu^{+4} and then dissolved in 5M nitric acid and transferred to an anion exchange column where americium and other impurities are eluted with 5M nitric acid. Plutonium is removed from the column using either a dilute nitric acid or a dilute nitric acid-hydrogen peroxide solution. After evaporation of the plutonium fraction to dryness, the plutonium is further purified within 24 hours of the isotope ratio measurement on a second anion exchange column using the same elution procedure.

Sample Mounting

Sample mounting is that part of the thermal ionization mass spectrometry procedure in which a solution containing a known amount of plutonium is dried on a filament and then treated in a manner which will yield either a salt or metal. The form used for analysis is usually not well known but selected empirically on the basis of the precision of the ratio measurement. The procedure for plutonium is based upon the methodology developed for uranium [5] and is as follows: the solution is dried for 10 minutes using 1.0A electrical currents and heat lamps; the current is increased to 1.3A for 3 minutes; the current is increased to 1.5A for 3 minutes; the heat lamp is turned off and the current increased until the filament temperature is approximately 600 °C (barely detectable red-heat); the current is reduced to zero and the filaments prepared for insertion into the mass spectrometer.

Isotope Ratio Measurement

The mass spectrometric procedure for plutonium isotopic ratio measurement is similar to the method developed for precise and accurate measurements of uranium. A solid sample therm-ionization mass spectrometer with a triple filament rhenium ribbon ion source is used [5, 6]. The collector, especially designed for in-depth suppression of secondary electrons, was equipped with a tungsten ribbon (0.025 x 0.76 mm) transmission grid shadowing a series of 0.10 mm suppressor grids [6]. An estimated sample size of 0.5 μg of Pu per filament is used to generate a Pu^{+} ion current of 2-3 x 10^{-11}A. The ionizing filament is maintained at a constant temperature (2120 °C) and the sample filaments adjusted in a stepwise manner according to a strict time schedule to obtain the target intensity. The Pu isotopic ratio measurements were started after an elapsed time of 30 minutes and were measured in the same sequential and symmetrical pattern for each analysis. During the final stages of these measurements, it was discovered that ionizing filament temperatures of 2160 °C is too hot, best results being obtained at a lower temperature of 2120 °C. At the lower temperature a spurious but significant interference at mass 238 was eliminated.

Discussion:

Interference:

The general sources of error recognized in the measurement are interference, isotopic fractionation and analytical blank. The interference can be traced to isobars, background contributions from either organic or inorganic molecules, and ion scatter or signal suppression from intense ion beams other than the analyte element. All of the indicated types of interference as well as the general sources of error are directly effected by both the chemistry and mass spectrometry. For example, interference from intense alkali ion currents occurs if poor quality reagents are utilized and/or if the filament assembly is not properly cleaned. While the effect of this type interference is subtle and cannot be ignored, the major concern is for isobaric interference at masses 238 (uranium) and 241 (americium). The effectiveness of the chcmial separation procedure was established by both gamma spectrometry and mass spectrometry. Analysis of a freshly separated plutonium sample gives an upper limit of 2 ng of ^{241}Am per gram of plutonium. The low level of residual ^{241}Am and strict adherance to analyzing all samples within 24 hours of column separation minimized the contribution from ^{241}Am as a source of bias. Additionally, the $^{241}Pu/^{240}Pu$ ratios were determined (Table 1) under conditions of single, double, triple and quadruple column separations for both the plutonium and americium fractions without any evidence of isobaric contributions exclusive of the first americium fraction. For the ^{238}U isobar, a minimum of two passes through the ion column were required to be certain that contributions were less than the detection limit of the mass spectrometer.

Table 1

$^{241}Pu/^{240}Pu$ Ratio for Multiple Column Separations

	Americium Fraction	Plutonium Fraction
Col. I	∿3.5	0.5039
Col. II	0.5036	0.5037
Col. III	0.5038	0.5041
Col. IV	0.5036	0.5041

Subsequent to completion of the isotopic measurements for plutonium half-life determinations, it was observed that operating a rhenium ionizing filament at 2160 °C was sufficiently hot to yield a detectable background contribution of unknown origin at mass 238. Between analyses this contribution was intermittent and barely detectable but could be reduced to insignificance by operating the ionizing filament at 2120 °C. Exclusive of mass ^{238}U, no other significant background signals from molecular species were detected in the plutonium mass range.

Isotopic Fractionation

With ^{241}Am removed from plutonium, the next most significant source of error is isotopic fractionation. Using uranium as a model, it was demonstrated that the mass dependent isotopic fractionation effect could range from 0.2% to zero per mass unit. Under adverse conditions this range could be as large as 0.3% per mass unit. While it has been well recognized for many years that varying conditions at the mass spectrometer, such as time and filament temperature, can significantly change the isotopic fractionation pattern, it was only recently clearly demonstrated that time and filament temperature are also critical parameters during sample mounting. This sample mounting effect is illustrated in Figures 1 and 2. In figure 1, each point represents a single ratio measurement within an analysis and the only known variable is the length of time maintained at the final drying temperature, estimated to be less than 600 °C. In figure 2, each point represents a different analysis where sample filament temperature during sample mounting was estimated below 700 °C and measured by an optical pyrometer at or above 700 °C. From approximately 700 °C to 780 °C a distant shift in $^{235}U/^{238}U$ value is observed. These values are biased approximately 0.1% from the "true value" of 0.9997 for SRM U500 and are different from the values obtained at the normal sample drying temperatures. This phenomenon is attributed to the formation of different uranium compounds during sample mounting and subsequent evaporation during the ionization process. If isotopic fractionation is mass dependent, then shifts of this nature should occur. Another possible explanation, supported by measurements of other researchers [7, 8], is diffusion into the filament, re-emission and then ionization. Sample mounting studies at NBS for the elements thorium and plutonium, while not as extensive as uranium, support the conclusion that with normal controls, the bias in the actinide mass range due to isotopic fractionation is not likely to exceed 0.2% per mass unit, even if no correction is applied.

The correction for isotopic fractionation was determined by analyzing uranium SRM U500 under equivalent analytical conditions as plutonium. This correction was found to be 0.125% per mass unit. Equivalent rather than identical analytical conditions were utilized because uranium and plutonium have different ionization efficiencies. Since plutonium was determined to be a factor of 3-5 more efficiently ionized, it was necessary to compensate by adjusting either the sample size or ion current intensity relative to uranium. After the initial correction of the isotopic abundance ratios of each sample used in this study at time zero, the $^{239}Pu/^{240}Pu$ ratio was then used as the normalization ratio for isotopic fractionation for all subsequent measurements. Even with the advantage of internal normalization and appropriate adjustments for radioactive decay, all analyses were made according to a strict analytical protocol to precisely reproduce the isotopic fractionation effect.

Analytical Blank

The error due to analytical blank was found to be insignificant for the analysis of 0.5 to 2 μg of plutonium. Even when the sample size was reduced to 100 ng, blank was not a significant factor in the measurement. Primarly sources of blank were reagents, environment, source memory and filament loading procedure.

Results

The analysis of a group of six different plutonium samples, including three SRMs, has yielded reproducible values for the half-life of ^{241}Pu. The proposed half-life value, 14.34 ± 0.04 years, is still subject to a final statistical review. The indicated uncertainty is the sum of the precision of the measurement (95% confidence limit) and allowances for known sources of possible systematic error. Assuming variable and uncontrolled isotopic fractionation during the mass spectrometry, the estimate of the maximum possible systematic error in any of the $^{241}Pu/^{240}Pu$ measurements is 0.3%. Since all analyses were made under strict analytical conditions which are known to precisely reproduce the bias due to isotopic fractionation, this error is believed to be much less than 0.2% per mass unit.

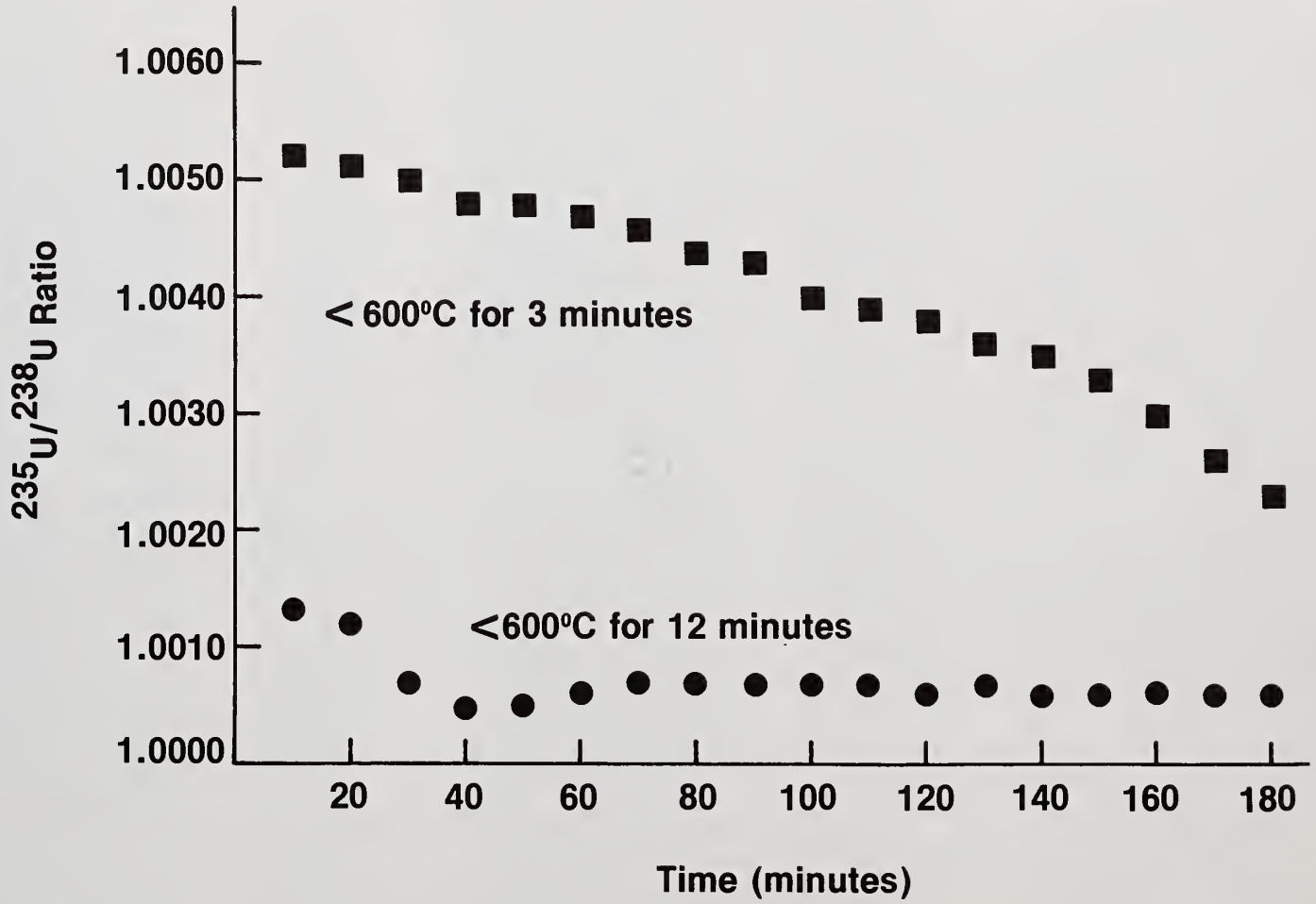

Figure 1. Effect of Sample Mounting at Constant Filament Temperatures and Different Drying Time

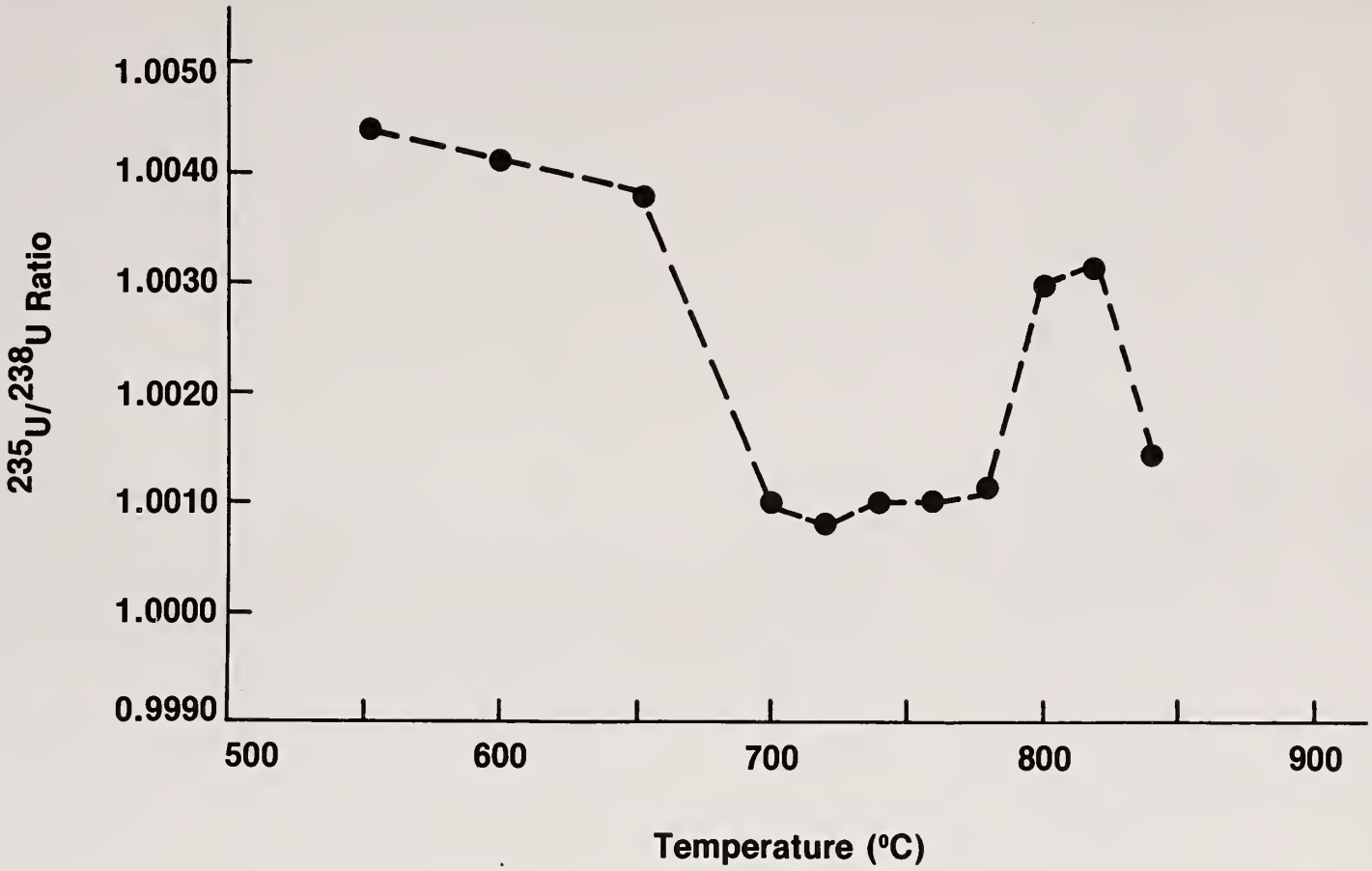

Figure 2. Effect of Sample Mounting at Different Filament Temperatures and Constant Drying Time

Even at the maximum, systematic errors of this magnitude are not sufficient to explain the discrepant values (mass spectrometric) reported in the literature and also observed in the early half-life measurements obtained in this study. With proper allowances for the decay of the other plutonium isotopes and proper standardization of the number of atoms of plutonium, the half-life values for all samples investigated are independent of isotopic composition and consistently between 14.30 and 14.40 years.

REFERENCES

1. Rose, B. and Milsted, J., J. Nucl. Energy, 2, 264 (1956).

2. Cabell, M. J. and Watkins, M., An Isomeric State of ^{241}Pu?, J. Inorg. Nucl. Chem., 33, 903 (1976).

3. Nisle, R. G. and Stepan, I. E., Nucl. Sci. Engng., 39, 257 (1970).

4. Catanzaro, E. J., Murphy, T. J., Garner, E. L., and Shields, W. R., J. Res. Nat. Bur. Stand. (U.S.) 70A (Phys. and Chem.) 453 (1966).

5. Garner, E. L., Machlan, L. A. and Shields, W. R., Nat. Bur. Stand. (U.S.) Spec. Pub. 260-27, (April 1971).

6. Shields, W. R. (ed.), Nat. Bur. Stand. (U.S.), Tech. Note 277, 99 (July 1966).

7. Casar, I., Personal Communication, 1979.

8. Rokop, D. J., Personal Communication, 1979.

Discussion:

Persiani (ANL):

What is the status of the other heavy elements with respect to isotope half-life accuracy? - U-233, U-232, Pu-239, etc.?

Garner (NBS):

There is an organized program, headed by the DOE half-life committee, in which they are making a systematic attempt to determine the half-lives of all of the plutonium isotopes. There has been some effort with uranium, which is not nearly in the sad state that plutonium has been. It is something of an embarrassment to have a highly precise technique and then it is necessary to take five, six, seven years to find out why you didn't make the measurement. The measurements that we are now getting for plutonium should have been achieved six or seven years ago. What we are now seeing is that there is a high degree of consistency among all laboratories -- I didn't mention that -- but, independent of techniques used, the values for the 241 now, between 14.30 and 14.40 -- I believe there will be another paper today by LASL, which will give some additional information on the status of the plutonium.

Analytical Data for Practical Safeguards: Performance and Evaluation of International Intercomparison Programs

by

W. BEYRICH*), G. SPANNAGEL**)
Kernforschungszentrum Karlsruhe, Projekt Spaltstoffflußkontrolle
Karlsruhe, Federal Republic of Germany

ABSTRACT

During the past decade, a number of international analytical intercomparison programs have been organized by the Karlsruhe Nuclear Research Center in order to investigate the capability of measuring methods used in safeguards when applied under routine conditions. A survey is given of the main results of these experiments which have been directed specifically to analyzing materials from reprocessing and enrichment facilities. Based on the experience gained, general design problems of the experiments are discussed. Furthermore, an empirical method of evaluation is described briefly which proved to be effective in handling the data material which, as obtained during such programs, was mostly statistically inhomogeneous. Examples are given for using this evaluation method.

KEYWORDS: Safeguards, intercomparison programs, uranium, plutonium, mass spectrometry, alpha spectrometry, statistical evaluation

INTRODUCTION

The knowledge of measurement accuracies attainable in routine analyses of nuclear material is of basic importance for the development of safeguards concepts as well as in the practical implementation of safeguards measures. In particular, it is a prerequisite of founded judgement of analytical interlaboratory differences observed.

Since intercomparison measurement programs proved to be the most appropriate means of acquiring such data, the Safeguards Project of the Karlsruhe Nuclear Research Center has organized experiments of this kind for 10 years with the participation of an increasing number of scientific and industrial laboratories of many countries, the Commission of the European Communities (CEC, Brussels, Belgium) and the International Atomic Energy Agency (IAEA, Vienna, Austria). It is the specific goal of these programs to explore the capability of the different feasible analytical techniques when applied in routine operation to the analysis of materials originating in the actual production process[a]. The objective is neither to determine the highest accuracies achievable under optimum conditions nor to qualify single laboratories. However, it seems realistic to assume that such excercises improve the overall situation with time, since they offer the possibility for the individual laboratory to compare its own results with those of other laboratories and to detect and correct sources of error.

SURVEY OF RESULTS

The interlaboratory experiments initiated by the Karlsruhe Nuclear Safeguards Project are compiled in Table I including references to the reports published on their performance and results. Because of the particular importance in nuclear fuel cycle control, studies of methods applied to the analysis of materials from reprocessing plants and enrichment facilities preponderate.

---

*) Delegate of the Commission of the European Communities (CEC/EURATOM)

**) Institut für Datenverarbeitung in der Technik

a) Most comparison programs run by other organizations differ somewhat in structure and/or objective.

Table I: Intercomparison programs organized by the Safeguards Project of the Karlsruhe Nuclear Research Center, F.R. Germany

Experiment	Analytical Problem	Sample Origin	Number of Participating Laboratories
JEX-70 /1/	U- and Pu-concentrations by chemical methods; U- and Pu-isotope abundances by thermal ionization mass spectrometry	Reprocessing plant, product	8
IDA-72 /2/	U- and Pu-concentrations by mass spectrometric isotope dilution analysis; U- and Pu-isotope abundances by thermal ionization mass spectrometry	Reprocessing plant, input	22
UF_6 Test*) /3/	U-235 abundance in UF_6 by gas mass spectrometry	Enrichment facility	8
ASET-74 /4/	Evaluation of Pu-alpha spectra	-	10
AS-76 /5,6/	Pu-238 determination by alpha spectrometry	Reprocessing plant, input	26
IDA-80**) in preparation	See IDA-72	Reprocessing plant, input	37 (Participation announced)

*) Organized by Messrs. Dornier-System GmbH, Friedrichshafen, F.R. Germany, on behalf of the Karlsruhe Nuclear Research Center.

**) Formerly planned as "IDA-78". Operated jointly with the Central Bureau for Nuclear Measurements (CBNM/CEC, Geel, Belgium) under the auspices of the European Safeguards Research and Development Association (ESARDA).

General Observations

An important result common to nearly all cases investigated is the observation that the so-called "interlaboratory" or "between laboratory" deviation[a] constitutes the main part of the total measurement uncertainty. By contrast, the error contribution of the reproducibility of determinations within the individual laboratory (precision) is small and often negligible. In Fig. 1(a) this is demonstrated by an example taken from the IDA-72 experiment. It concerns the determination of U-238 concentration in a diluted reprocessing input solution by isotope dilution mass spectrometry. Evaluation of the data set shown by analysis of variances results in estimates of 0.84 % and 0.45 % for the interlaboratory deviation and the precision, respectively. Hence, the interlaboratory deviation constitutes in this case more than 90 % of the total measurement uncertainty if double analysis is assumed[b].

Another general experience regards the occurrence of extreme values as shown in Fig. 1(b). This represents the Pu-239 concentrations determined on the same sample material by the same group of laboratories as in Fig. 1(a). The results of the four laboratories 4, 6, 8, and 21 representing about 1/4 of all determinations are considerably higher than those obtained by

a) The interlaboratory deviation is the variance of the "systematic" error component related to a group of laboratories, usually expressed as relative standard deviation (RSD).

b) If s_a and s_e are estimates of the standard deviation of the error components interlaboratory deviation and precision, respectively, the estimate for the total uncertainty of a double determination is given by $\sqrt{s_a^2 + s_e^2/2}$ /7/.

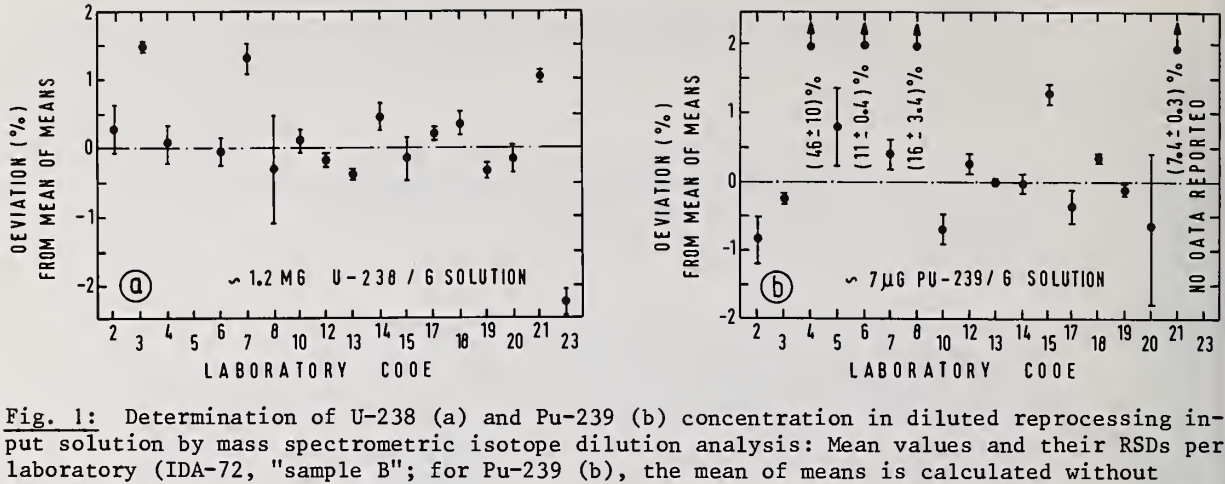

Fig. 1: Determination of U-238 (a) and Pu-239 (b) concentration in diluted reprocessing input solution by mass spectrometric isotope dilution analysis: Mean values and their RSDs per laboratory (IDA-72, "sample B"; for Pu-239 (b), the mean of means is calculated without laboratories 4, 6, 8 and 21).

the other laboratories[a]. When occurring so frequently, such extreme values point to a specific error source of the analytical procedure under investigation. The size and the sign of such data supply valuable information for its identification: In the example given, valenc adjustment of the plutonium was recognized as one of the most critical steps in the isotope dilution procedure.

By appropriate design of the experiments it was possible to identify in almost all cases those steps of the individual chemical or measurement techniques which are the main contributors to the total uncertainty of the analytical methods investigated.

Element Concentration Determinations

The results presented in Fig. 1 for the isotope dilution analysis of a diluted reprocessing input solution reflect no error contribution of the spiking step since the material for all samples was spiked in one common procedure. If, in addition, errors from individual spiking by the laboratories are taken into consideration the IDA-72 data yield approximately the same measurement uncertainty of slightly below 1 % for both the plutonium and uranium determinations, assuming that the chemical sample conditioning mentioned above is properly applied.

Wet chemical analytical methods were investigated only in JEX-70 for the analysis of samples of reprocessing products. Interlaboratory deviations of about 0.2 % were found for the concentration determinations of uranium as well as for plutonium. However, for the latter an additional error component of at least the same magnitude was indicated which was possibly caused by the instability of the sample material[b].

Isotope Abundance Determinations

As far as determinations of uranium and plutonium isotopes by thermal ionization mass spectrometry are concerned, extensive data were obtained in the experiments JEX-70 and IDA-72. For this analytical method the interlaboratory deviation was again found to be the most essential error component and is plotted versus the isotopic ratio in Fig. 2.

For some sets of data extraordinary high values were found indicating in these cases again the influence of specific additional error sources. For the Pu-238/Pu-239 measurements, this is with high probability due to the contribution of U-238 ions. For the higher value related to Pu-242/Pu-239 determinations, sample contamination with Pu-242 spike material

---

a) From the statistical point of view, the four values are outliers according to the Dixon criterion /8/ with a probability of error less than 5 % for laboratory 8 and less than 0.5 % for the three other laboratories.

b) Comprehensive data on wet chemical analyses of other materials were obtained in particular by the SALE program /9/.

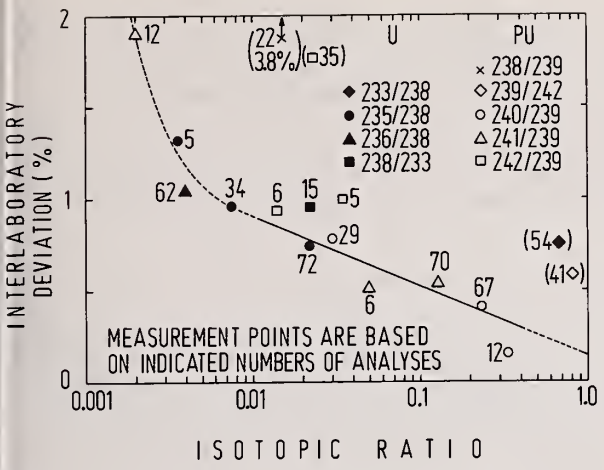

Fig. 2: Isotopic ratio determination by thermal ionization mass spectrometry: Estimates for RSD of the interlaboratory deviation (JEX-70 and IDA-72).

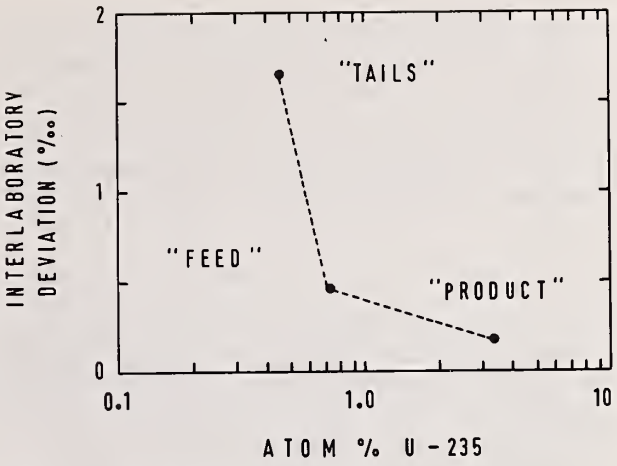

Fig. 3: Determination of U-235 in UF_6 by gas mass spectrometry: Estimates for RSD of the interlaboratory deviation of the ratio of ratios $(U\text{-}235:U\text{-}238)_{test\ material}$ / $(U\text{-}235:U\text{-}238)_{reference\ material}$ versus U-235 abundance (UF_6 Test).

might be an explanation. Special attention should be paid to the increased uncertainty of the U-233/U-238 and Pu-239/Pu-242 ratio measurements on spiked samples, which indicate error contributions from the preceding steps of chemical preparation[a].

For the remaining sets of data a common curve was traced, with the linear part least-squares fitted[b].

From the gas mass-spectrometric measurements of the U-235 isotope in uranium hexafluoride, Fig. 3 shows the interlaboratory deviation of the ratio of ratios $(U\text{-}235:U\text{-}238)_{test\ material}$ / $(U\text{-}235:U\text{-}238)_{reference\ material}$ for the three sample materials analyzed in the UF_6 Test[c]. For this ratio measurement this error component proved again to constitute the main part of the uncertainty. However, for the accuracy achievable for the U-235 abundance it was found that for samples having a natural U-235 content and greater the uncertainty in the isotopic composition of the reference material available was the most serious limitation.

The intercomparison programs ASET-74 and AS-76 provided evidence for the importance of the spectra evaluation method used in alpha spectrometry of plutonium if corrections are required for the contribution of the low-energy tail of the Pu-238 peak to the peak of the Pu-239 and Pu-240 isotopes. Fig. 4 shows

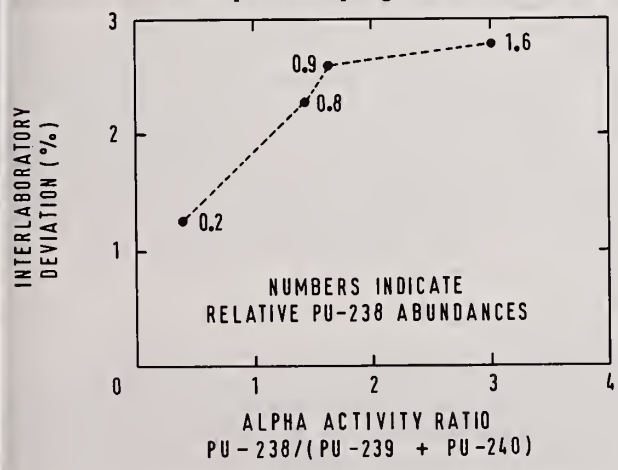

Fig. 4: Determination of Pu-238 by alpha spectrometry: Estimates for RSD of the interlaboratory deviation of the alpha activity ratio Pu-238/(Pu-239 + Pu-240) (AS-76).

a) Although not evident from Fig. 2, increased measurement uncertainty has been observed also for the Pu-241 isotope, probably due to insufficient separation and/or correction of Am-241 /9,10/.

b) The numbers of analyses on which the measurement points are based were used as statistical weights. - The steep increase of the curve at low isotopic ratios is endorsed at even smaller ratios not covered in this figure.

c) All laboratories used the same reference materials with U-235/U-238 ratios deviating about 5 % from those of the test samples.

the interlaboratory deviation calculated for the alpha activity ratio Pu-238/(Pu-239 + Pu-240) of the four sample materials analyzed in AS-76. By applying one common evaluation procedure to the spectra of all participants a significant reduction of this deviation was achieved for the highest investigated alpha activity ratio of about 3; in this case substantial tail corrections had to be applied /11/.

Once more the interlaboratory deviation accounts for about 90 % of the total uncertainty for this ratio measurement in routine analyses. It should be noted, that for the Pu-238 abundance calculation further errors will contribute, such as for example half-life uncertainties.

Testing of Newly Proposed Analytical Methods

Also in the framework of these experiments, newly developed analytical techniques were examined for their efficiency and applicability in practice. In JEX-70 as well as in IDA-72, one laboratory applied X-ray fluorescence analysis in addition /12, 13/ and in the IDA-72 experiment the use of two new methods for non-liquid sample handling was tested with favorable results: the "dried spike technique" /14/, applied for several years by IAEA and the "aluminium capsule technique" /15/.

In the IDA-80 experiment now in preparation it is intended to compare the "in-situ" solid spike technique /16/ with the conventional use of liquid spike solutions for the determination of the uranium and plutonium content in input solutions of reprocessing plants by mass spectrometric isotope dilution analysis. From the safeguards point of view this method is of particular interest because it allows the nuclear material concentration of undiluted reprocessing input material at the time and place of sampling to be fixed.

DESIGN CONSIDERATIONS

Basically, an analytical intercomparison program simply consists of the distribution of identical sample material among the participating laboratories for analyses and the evaluation of their measurement data using, primarily, statistical methods. However, in order to obtain results which - according to the specific objective - reflect the conditions of practical safeguards as closely as possible, some particularities have to be observed with regard to the design and performance.

Sample Material

The sample material has to be taken from actual industrial production lines to be representative in respect of possible impurities. Contrary to the use of purified synthetically blended sample material, its true composition is therefore necessarily unknown and often the possibility of an existing inhomogeneity cannot be excluded. Furthermore, the stability of the sample material over the time of sample preparation and transportation may be doubtful in particular for solutions containing fission products.

Although inhomogeneity and stability of samples are serious problems for practical safeguards, their investigation cannot be the goal of an analytical intercomparison program but requires precise measurements by experienced laboratories having direct access to the production process material in question. If there are any doubts with regard to the homogeneity, appropriate studies have to be carried out before the sample material is distributed in order to ascertain that this is sufficient in relation to the measurement accuracies to be expected in the interlaboratory experiment /17, 18/. Anticipated instability restricted the use of the reprocessing input material to samples which were already spiked before shipment or distributed as exactly weighed aliquots, evaporated to dryness[a] /2/.

Sample Characterization

Determinations of "true values" for the composition of sample material taken from a production process require extensive and expensive measurements by specialized laboratories using different analytical methods, if possible. By close cooperation with such laboratories a sample material characterization has become possible to an increasing extent during recent years /19,20,21/.

---

a) In IDA-80, besides other methods the distribution of liquid diluted reprocessing input solution in sealed glass ampoules is planned.

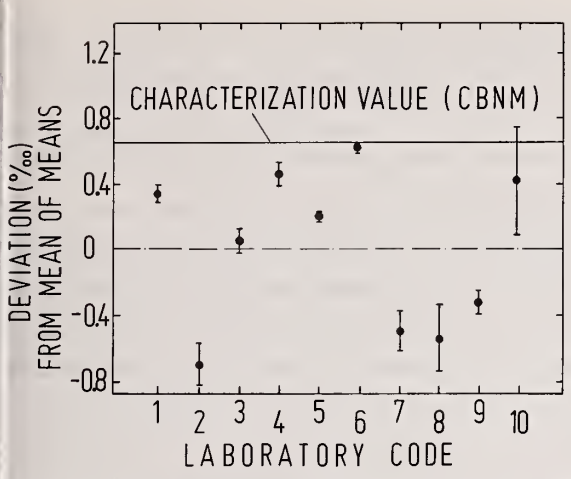

Fig. 5: Determination of U-235 in UF_6 by gas mass spectrometry: Mean values and their RSDs per laboratory of the ratio of ratios $(U\text{-}235:U\text{-}238)_{test\ material} / (U\text{-}235:U\text{-}238)_{reference\ material}$ (UF_6 Test, "Feed sample").

Above all, those determinations are of interest for detecting a possible method-specific bias shifting the results of all laboratories in the same direction. Under these circumstances, it is not meaningful anymore to use a statistical mean value calculated from the results of any group of laboratories as best estimate for the true value of sample composition. As shown in Fig. 5, this was observed in the UF_6 Test /3/: All the data reported by the participants are below the value stated by the characterization laboratory[a]. This indicates an error source causing deviations to occur always in the same direction. In this case, memory effects in the ion source and inlet system of the mass spectrometers are the probable reasons since a single standard measurement technique was used /22/.

Performance

With respect to the performance of the measurements at the participants' laboratory, a distinction must be made between the necessity of clear instructions to be followed about the structural layout of the analytical procedure and the liberty of the laboratory to choose the methods to perform the various analytical steps. For example, when studying the alpha spectrometric analysis of plutonium in the AS-76 experiment /5,6/, it was important to advise the laboratories of the number of alpha sources to be prepared and also whether the preceding chemical step of plutonium purification should be done only once or for each alpha source separately. However, no instruction was given as to the methods of plutonium purification and source preparation.

The careful design of the experimental layout (by the organizer) and the readiness of the participants to follow the specified setup in the various steps with the requested number of repetitions is an important premise for successful evaluation of the experiment. Only in this case are balanced sets of data obtained which permit detailed statistical calculations.

On the other hand, the liberty of the individual laboratory to choose that method in which it is most experienced is a necessity if the measurement program aims at investigating the actual analytical situation.

For the same reason of representativeness the participants are asked to perform the analyses under routine conditions and not to invest extraordinary efforts. The importance of this requirement becomes evident by the observation that characterization measurements carried out with extreme care and effort may lead to uncertainty ranges of an order of magnitude lower than obtained in general by routine operation /6/.

Undoubtedly, it cannot be ensured that this request is always fulfilled. In our experience however, the laboratories are ready to report also the less satisfactory - but not necessarily less realistic - data to the evaluation group and to provide all useful additional information. This is certainly facilitated by the fact that the Karlsruhe Nuclear Research Center has no safeguards control function and since it is guaranteed that the results are published in a codified manner only.

Participation

A further point of interest is the number and qualification of the participating laboratories. Participation of the majority of laboratories concerned with the specific analytical problem under investigation is certainly desirable in order to obtain a representative picture of the prevailing situation. For reasons of statistical evaluation, approximately 8 to 10 participants are considered to be the minimum.

---

a) For the characterization value a maximum uncertainty of ± 0.5 ‰ was communicated. - One of the participants used three mass spectrometers; therefore, the number of measurements reported exceeds the number of participants stated in Tab. I.

No restriction on one side or the other would be meaningful for the qualification requirements for participation. Actually, in practical safeguards, scientifically orientated laboratories are involved as well as industrial laboratories representing a wide scope from the point of view of the analytical workload, the demands on the promptness of producing results and the time during which experience has been gathered. Since results are aimed at which describe the actual analytical situation achievable on an average, all contributions are valuable.

Furthermore, it is difficult to define in an objective manner the qualification of a laboratory so that it can be correlated to the reliability of its results in routine operatic The capability of achieving a high accuracy in a particular test run is only one component in such a measure of qualification another being the laboratory's experience, if it is expressed by the frequency and length of time the type of analysis in question has been performed.

All laboratories contributing to the intercomparison programs discussed here are listed in Table II. Another 11 laboratories, not mentioned in this table, have announced their participation in IDA-80.

EVALUATION OF DATA

Such a layout of an experiment as mentioned above allows the calculation of estimates fo the variances of the different error components involved in the analytical procedure under investigation. However, in many cases problems arise in the application of the usual statistical methods, in particular the analysis of variances, because of insufficient homogeneity of the data sets yielding extreme values which have to be considered as outliers from the statistical point of view as already discussed before /23, 24/.

If the reasons for their occurrence cannot be identified clearly as being untypical of the specific analytical problem studied, their rejection on the basis of purely statistical criteria is unsatisfactory and the justification problematic. This holds in particular if the results of more than one laboratory are concerned. By exclusion of such values, the actual state of the measurement technique may be overestimated which leads to the derivation of reference data unrealistic for practical safeguards.

An Empirical Evaluation Method

All attempts made so far to overcome the difficulty described above were barely satisfactory. As already mentioned, in the IDA-72 experiment /2/ the values were rejected on the basis of the Dixon outlier criterion /8/ and the percentage of values excluded was given as additional information to the estimates of variances calculated from the remaining group of data. Other authors reported both results, those obtained with and without the values identified statistically as outliers /25/, or partly renounced on the derivation of estimates for variances of error components /26/.

This unsatisfactory situation was the reason for an attempt of the Karlsruhe Nuclear Safeguards Project to make a more empirical approach of data treatment. As demonstrated later, for this approach the interlaboratory differences (including those originating from extreme laboratory means) are used as the basic elements of evaluation /27,28/. By plotting the frequency of their occurrence in a cumulative manner versus their moduli, a curve is obtained from which a reasonable estimate for the relative standard deviation of the underlying set of laboratory means can be derived; it corresponds to the value exceeded by approximately 50 % of the differences /29/.

This estimate describes the actual situation in a more satisfactory way than calculation by usual statistical methods, since it is based without exception on all measurement data obtained and is influenced more by the quantity than by the quality of statistical outliers. The latter is meaningful because the occurrence of a relatively high number of outliers is more important for evaluating the capability of a method than an extreme single value.

An example is given in Fig. 6: The left part (a) shows the distribution of laboratory means (without error bars). The laboratories 9 and 11 display extreme values[a)]. Depending on whether or not these two values are excluded the relative standard deviation calculated as usual for the scattering of the laboratory results varies by a factor of about 6. In

---

a) According to Dixon criterion /8/ to be rejected as outliers with a probability of error of less than 1 %.

Table II: List of Participants (A: JEX-70; B: IDA-72; C: UF_6 Test; D: ASET-74; E: AS-76)

Aktiebolaget Atomenergi Studsvik	Nyköping/Sweden	(B)
Alkem GmbH	Hanau/F.R. Germany	(D,E)
Atomic Energy Research Establishment	Harwell/United Kingdom	(B,E)
Atomic Weapon Research Establishment	Aldermaston/United Kingdom	(B)
Bhabha Atomic Research Center	Trombay/India	(B,D,E)
British Nuclear Fuels Limited	Capenhurst/United Kingdom	(C)
Bundesanstalt für Materialprüfung	Berlin/F.R. Germany	(C,E)
Comitato Nazionale per l'Energia Nucleare		
Centro di Studi Nucleari	Casaccia/Italy	(E)
Impiato EUREX	Saluggia/Italy	(E)
Commissariat à l'Energie Atomique		
Centre d'Etudes de Bruyères le Chatel	Montrouge/France	(E)
Centre d'Etudes Nucléaires de Saclay	Gif-sur-Yvette/France	(B)
Centre de la Hague	Cherbourg/France	(B)
Commission of the European Communities		
Central Bureau for Nuclear Measurements	Geel/Belgium	(A,B,C,D,E)
Joint Research Center Ispra	Ispra/Italy	(A,B,D,E)
European Institute for Transuranium Elements	Karlsruhe/F.R. Germany	(A,B,D,E)
Compagnie Générale des Matières Nucléaires	Marcoule/France	(E)
Dornier System GmbH	Friedrichshafen/F.R. Germany	(C)
Dounreay Nuclear Power Development Establishment	Dounreay/United Kingdom	(E)
EUROCHEMIC	Mol/Belgium	(A,B)
Gesellschaft zur Wiederaufarbeitung von Kernbrennstoffen mbH	Leopoldshafen/F.R. Germany	(B,D)
Institut "Jozef Stefan"	Ljubljana/Yugoslavia	(B)
Institut for Atomenergi	Kjeller/Norway	(B)
International Atomic Energy Agency	Seibersdorf/Austria	(A,B)
Japan Atomic Energy Research Institute	Tokai-mura/Japan	(E)
Kernforschungsanlage Jülich GmbH	Jülich/F.R. Germany	
Institut Chemische Technologie		(E)
Zentralabteilung Strahlenschutz		(E)
Kernforschungszentrum	Karlsruhe/F.R. Germany	
Institut für Kernverfahrenstechnik		(C)
Institut für Radiochemie		(A,B,D,E)
Kraftwerk Union AG	Karlstein/F.R. Germany	(B,E)
Los Alamos Scientific Laboratory	Los Alamos/U.S.A.	(B,D,E)
Maschinenfabrik Augsburg-Nürnberg	Munich/F.R. Germany	(C)
National Bureau of Standards	Washington/U.S.A.	(E)
Netherlands Energy Research Foundation	Petten/The Netherlands	(B,E)
New Brunswick Laboratory	Argonne/U.S.A.	(B,D,E)
Oak Ridge National Laboratory	Oak Ridge, Tennessee/U.S.A.	(A,B)
Power Reactor & Nuclear Fuel Development Corp.	Tokyo/Japan	(B,D,E)
Risø National Laboratory	Roskilde/Denmark	(E)
Studiecentrum voor Kernenergie	Mol-Donk/Belgium	(A,B,E)
Universität Kiel, Institut für Physikalische Chemie	Kiel/F.R. Germany	(C)
Urenco Nederland Operations N.V.	Almelo/The Netherlands	(C)

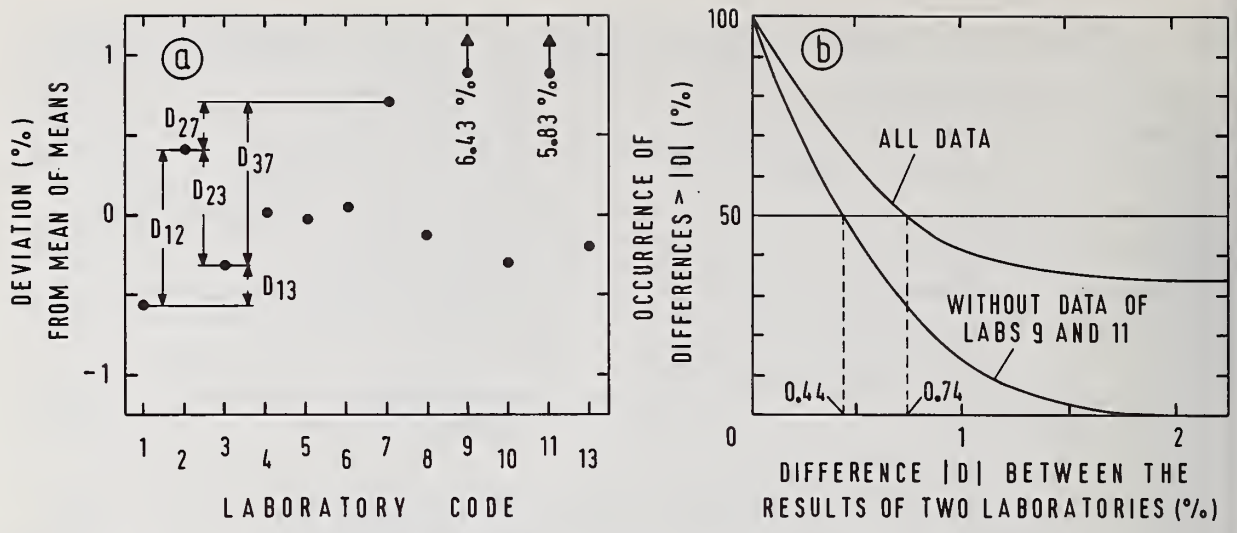

Fig. 6: Empirical evaluation method: Derivation of interlaboratory differences (a) to establish distribution curves (b) (Laboratory means taken from Pafex II /25/, Pu-concentration "spike-2" method. In (a) error bars are suppressed and mean of means is calculated without laboratories 9 and 11).

addition, in this part (a) of the figure it is indicated how all possible interlaboratory differences D_{ik} ($i < k$) are derived to be used as the basic elements for the empirical evaluation method demonstrated in the right part (b) of the figure: It shows the cumulative distribution of these interlaboratory differences for both cases, i.e. with and without the two "outlier" values. The estimates for the relative standard deviations of the underlying sets of data derived as described above and indicated in the figure differ by only a factor of 1.7[a]. Compared to the factor of about 6 obtained by conventional statistical methods this increase seems more adequately to reflect the influence of the two extreme values.

Experience gained so far proves the effectiveness of this empirical evaluation procedure in three fields of application:
- for the evaluation of data sets statistically inhomogeneous as shown above,
- for comparing the performance of different analytical methods,
- for judging deviations between the results of two laboratories, e.g. shipper-receiver or operator-inspector differences.

Comparison of Analytical Methods

The suitability of the evaluation procedure described above for the comparison of different analytical techniques is shown with the two examples given in Figs. 7 and 8.

Fig. 7 again refers to the data obtained in the Pafex II experiment /25/ for the determination of plutonium concentrations in input solutions of a reprocessing plant by isotope dilution mass spectrometry. Two different ways had been used to prepare the samples: With the "spike-1" procedure, weighed aliquots of sample and spike solution were consecutively evaporated to dryness in each vial whereas with the "spike-2" procedure known amounts of sample and spike solution were thoroughly mixed and then (unweighed) aliquots were dropped into the vials and dried.

Whilst the tails of the curves are affected by some extreme values, 0.74 and 1.55 % are found as differences exceeded by about 50 % of the values. According to our experience, this difference of more than a factor 2 points to an additional error contribution for the "spike-1" procedure and suggests incomplete redissolving of the plutonium which, in this case, has to be quantitative[b]. Since it had been camouflaged by the extreme values, it was difficult to

a) The two RSD values obtained by the different evaluation methods after rejection of the suspicious data are in satisfactory agreement (0.40 and 0.44 %).

b) For the uranium contained in this sample material no such effect was indicated.

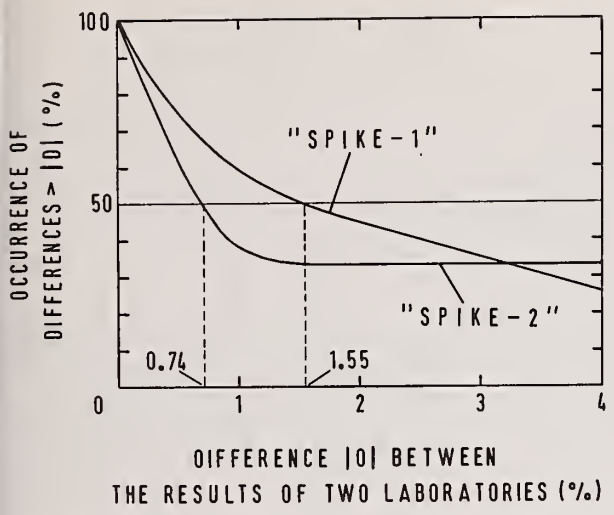

Fig. 7: Comparison of two sample preparing methods by empirical evaluation procedure (Pafex II /25/, Pu-concentration determination according to "spike-1" and "spike-2" methods).

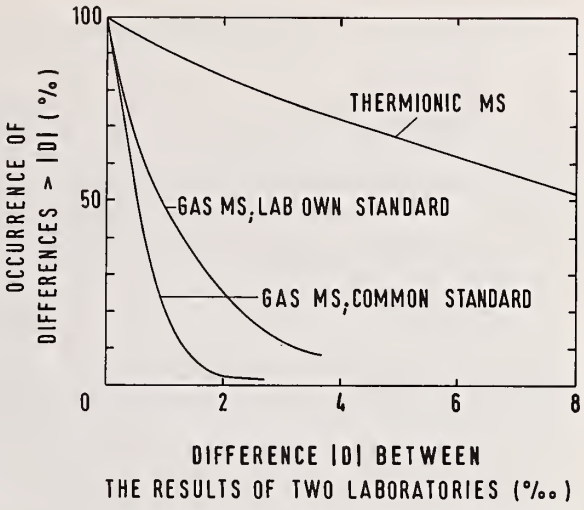

Fig. 8: Comparison of U-235 determination in UF_6 by different analytical procedures using empirical evaluation method (≈ 0.7 % U-235; values taken from UF_6 Test /3/ and GAE program /26/).

make this effect visible by conventional statistical data treatment.

The example given in Fig. 8 concerns the mass-spectrometric determination of the U-235 isotope in uranium hexafluoride samples with about natural abundance. The data obtained with the UF_6 Test /3/ and the GAE program /26/ were evaluated with respect to the three different methods of U-235 determination applied: thermal ionization mass spectrometry and gas mass spectrometry, the latter both with and without a common reference material /30/. The much better agreement of data expected from gas mass spectrometry as compared to thermal ionization mass spectrometry is strongly confirmed. But the improvement which can be obtained by application of a common standard in the gas mass-spectrometric procedure also becomes evident.

Judgement of Interlaboratory Differences

Once such a curve for the distribution of interlaboratory differences has been established for a given analytical problem, it can easily be used by the control authority as a basis for judging differences occurring between declared values and the results of verification analyses. As shown in Fig. 9, two abscissa values D_o and $k \cdot D_o$ ($k > 1$) are chosen for this purpose as threshold values; they generate three ranges for the classification of a discrepancy:

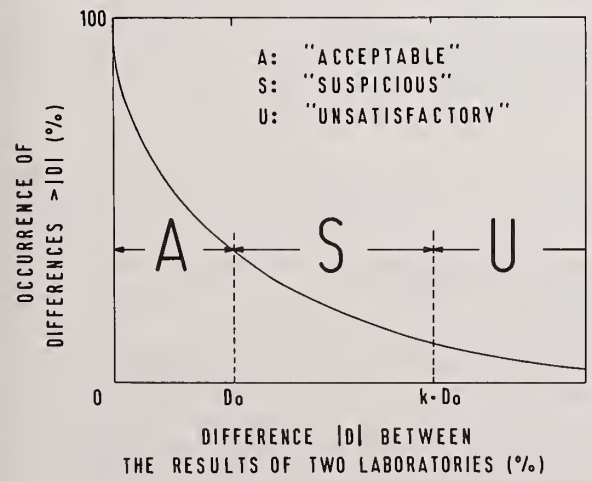

Fig. 9: Classification ranges for judging analytical interlaboratory differences (schematic)

- If the difference observed is smaller than D_o, it is considered as "acceptable" and no further action is required.
- If the difference observed is greater than the second threshold value $k \cdot D_o$, it is considered to be "unsatisfactory" and it would be advisable for the control authority to contact the plant operator immediately in order to clarify the situation.
- The range in-between the two threshold values, called "suspicious", serves to indicate if relatively high differences are occurring frequently which may indicate a systematic deviation between the measurements of the operators and the verification laboratory.

This procedure has been tested since 1977 by the EURATOM Safeguards Directorate, Luxemburg, and the results have been encouraging /10/. Its application guarantees to the plant operator that his data are judged according

to uniform criteria derived directly from experience gathered with the relevant measuring technique.

Furthermore, use of this method may considerably reduce the analytical workload of the verification laboratory: Double analyses usually performed can be avoided if application of this judging procedure after the first verification determination yield "acceptable" differences. Only if "suspicious" or "unsatisfactory" discrepancies have been found, repetition measurements become necessary in order to endorse the reliability of the first analysis.

As well as this, it might be expected that continual application of this judging procedure will result in the smallest scatter of the interlaboratory differences achievable in fiel application of the analytical techniques involved being gradually approached.

A drawback of the method may be seen in the necessity of establishing separately such distribution curves of differences for all analytical problems. However, from interlaboratory comparisons, verification analyses and shipper-receiver measurements, comprehensive data are already available for most of the analytical procedures relevant to safeguards. The main effort required consists in the appropriate classification of this data material and in its computer storage. A joint effort of all institutions interested could certainly solve this problem.

ACKNOWLEDGEMENT

This paper is based on the results obtained by cooperation of the numerous laboratories listed in Tab. II. The authors would like to express their thanks for all contributions. In addition, the interest in and support of these activities by the Project Leader of the Karlsruhe Safeguards Project, Dr. Dipak Gupta, are acknowledged.

REFERENCES

/1/ R. KRAEMER, W. BEYRICH, "Joint Integral Safeguards Experiment (JEX-70) at the EUROCHEMIC Reprocessing Plant, Mol, Belgium", KfK 1100/EUR 4576e (1971)

/2/ W. BEYRICH, E. DROSSELMEYER, "The Interlaboratory Experiment IDA-72 on Mass Spectrometric Isotope Dilution Analysis", KfK 1905/EUR 5203e (1975)

/3/ W. BEYRICH, W. DUERR, W. GROSSGUT, "Determination of the Isotope U-235 in Uranium Hexafluoride by Gas Mass Spectrometry: Results of an Interlaboratory Experiment Performed in 1975", KfK 2340/EUR 5503e (1977)

/4/ W. BEYRICH, A. CRICCHIO, "The ASET-74 Intercomparison Experiment on the Evaluation of Alpha-Spectra of Plutonium", KfK 2265/EUR 5208e (1976)

/5/ W. BEYRICH, G. SPANNAGEL, "Performance and Results of the AS-76 Interlaboratory Experiment on the Alpha Spectrometric Determination of the Pu-238 Isotope", Proceedings of the 1st Annual ESARDA Symposium, Brussels, April 25-27, 1979

/6/ W. BEYRICH, G. SPANNAGEL, "The AS-76 Interlaboratory Experiment on the Alpha Spectrometric Determination of Pu-238", Part I, KfK 2860/EUR 6400e

/7/ R. AVENHAUS, "Analysis of Variances", see /1/, chapt. 7, pp. 130-138

/8/ W.J. DIXON, "Processing Data for Outliers", Biometrics 9 (1953), pp. 74-89

/9/ C.D. BINGHAM, "Safeguards Analytical Laboratory Evaluation (SALE)", 1977 Annual Report, NBL-290, Vol. 1 and 2, New Brunswick Laboratory, U.S. Department of Energy, Argonne, Illinois (1978)

/10/ W. BEYRICH, G. SPANNAGEL, "Practical Approach to a Procedure of Judging the Results of Analytical Verification Measurements", Int. Symp. Nuclear Material Safeguards, International Atomic Energy Agency, Vienna (1978)

/11/ G. SPANNAGEL, W. BEYRICH, G. BORTELS, "The AS-76 Interlaboratory Experiment on the Alpha Spectrometric Determination of Pu-238", Part II, KfK 2861/EUR 6401e

/12/ A. v. BAECKMANN, L. KOCH, J. NEUBER, M. WILHELMI, "Automatic Analysis of Uranium and Plutonium in Solutions", International Atomic Energy Agency, Vienna, Proceedings SM-149/42 (1972)

/13/ L. KOCH, E. MAINKA, "Progress in the Verification of Reprocessing Input Analysis for Nuclear Material Safeguards", American Nuclear Society, Symposium Series (1979, pp. 73-81

/14/ H. FRITTUM, "Sample Preparation for the Dry Spike Technique", see /2/, Vol. II, pp. 49-51

/15/ K. KAMMERICHS, H. LOHNER, "Preparation of Samples for the Aluminium Capsule Experiment in the Framework of the IDA-72 Experiment", see /2/, Vol. II, pp. 52-56

/16/ P. DE BIEVRE, J. BROOTHAERTS, M. GALLET, A. LOOPMANS, E. SATTLER, J. VAN AUDENHOVE, "Performing Accurate Measurements of Fissionable Material for Safeguards Purposes in Reprocessing Plants in Europe", Proceedings of the 17th Annual Meeting, Institute of Nuclear Materials Management (1976)

/17/ H. BERNHARDT, H. DEUTSCH, E. GANTNER, M. HARTMANN, E. MAINKA, H. WERTENBACH, "Homogeneity Test on Reprocessing Input Solutions" (Kernforschungszentrum Karlsruhe; in preparation)

/18/ P. DE BIEVRE, "Accurate and Installation-Independent in situ Assay of Fissile Isotopes in Inputs of Reprocessing Plants", Proceedings of this Conference (1979)

/19/ P. DE BIEVRE, W. DE BOLLE, M. GALLET, G. MUESCHENBORN, E. SATTLER, "The Characterization of Test Materials for the GfK/Dornier Interlab Test on UF_6", see /3/, Annex V

/20/ G. BORTELS, P. DE BIEVRE, L. BARNES, K. GLOVER, "Characterization of the Samples Used in the AS-76 Interlaboratory Experiment on the Determination of Pu-238", Proceedings of the 1st Annual ESARDA Symposium, Brussels, 1979

/21/ G. BORTELS, P. DE BIEVRE, L. BARNES, K. GLOVER, "The AS-76 Interlaboratory Experiment on the Alpha Spectrometric Determination of Pu-238", Part III, KfK 2862/EUR 6402e

/22/ W. BIER, P. BLEY, "Memory Effect in Uranium Isotope Determination", see /3/, Annex VIII

/23/ H. AHRENS, "Varianzanalyse", Akademie-Verlag GmbH, Berlin (1968)

/24/ G. GOTTSCHALK, R.E. KAISER, "Einführung in die Varianzanalyse und Ringversuche", B.I. Hochschultaschenbücher, Bd. 775 (1976)

/25/ E. SZABO, W. BUSH, C. HOUGH, "Results of the IAEA Process Analysis Field Experiment II for Safeguards (Pafex II)", IAEA report STR-71 (1978)

/26/ C.D. BINGHAM, C.T. BRACEY, "Results of the General Analytical Evaluation Program for Uranium Hexafluoride, Phase 1", NBL-274 (1975)

/27/ W. BEYRICH, "The Problem of Analytical Interlaboratory Differences in Practical Safeguards", Symp. on Safeguarding Nuclear Materials, International Atomic Energy Agency, Vienna (1975)

/28/ W. BEYRICH, G. SPANNAGEL, "Distribution of Analytical Interlaboratory Differences", KfK 2888/EUR 6404e (in preparation)

/29/ R. AVENHAUS, R. BEEDGEN, "A New Variance Estimate of Normally Distributed Random Variables" (Kernforschungszentrum Karlsruhe; in preparation)

/30/ W. BEYRICH, G. SPANNAGEL, "The Mass Spectrometric Determination of Uranium-235 in Uranium Hexafluoride", Nucl. Techn., Vol. 42 (1979), pp. 337-42

Discussion:

Larsen (ANL):

A particular question I would be interested in, with reference to your last graph: what criteria do you use to establish what is unsatisfactory? Is this based upon what laboratories have demonstrated they can do or is taking the authoritative position of what someone says you should be able to do - you must be able to do this and therefore we decide this is what is unsatisfactory. It seems to me that there is involved, in much of this analytical chemistry.....an attempt to apply democratic principles where obviously all chemists are not created equal.

Beyrich (NRC - Karlsruhe):

Well, let me sum it up this way. The curve is the result of the intercomparison programs performed by many laboratories. But the threshold values are then chosen arbitrarily by the control authority. It may use very severe threshold values allowing only small deviations. However, this will have the effect that the authority has to contact the operator very often to discuss the reasons. The control authority probably cannot do this in practice. But the threshold values may be chosen in such a way, for instance, that according to the curve 70% acceptable values can be expected and 30% being suspicious or unsatisfactory. This was done in the field testing of the material and indeed, about 30% of the discrepancies were in the unaccepted range. This means that conditions found in practical safeguards were in agreement and confirming what had been found before in the comparison programs. If the discrepancy values, observed with a certain plant laboratory, are extra ordinarily often in the suspicious or unsatisfactory range, the control authority may discuss this with the plant operators. In this way, systematic deviations in the analytical methods or similar reasons may be found. Their improvement will lead, step by step, to an improvement of the slope of the curve and it can be expected that the smallest scatter of inter-laboratory differences achievable in field application will be generally approached.

Larsen:

It seems to me in a meeting like this, there are basically two parts. There are the analytical chemists who are trying to provide or make a series of measurements intented to provide safeguards information, and there is a group of individuals who are saying these are the quality of measurements I have to have in order to provide safeguards. The safeguards criteria set the accuracies that are required. These are not necessarily the accuracies that the analyist can achieve. Hence, you cannot decide what is satisfactory, or unsatisfactory on the basis of what the analyst is capable of doing.

Bingham (NBL):

I think what he is attempting to portray here is the first conscious attempt to scientifically define a basis for making this differentiation as opposed to having a legislated, politicized set of criteria for acceptability of measurements for safeguards. I wholeheartedly support the approach he is taking and there are virtual treasures of data that already exist by virtue of the interlab comparison programs that have been completed that I would like to see used with the technology that have been developed at Karlsruhe. I would like to see more of this data generated to see if there is a scientific basis for defining what this K factor ought to be.

Hakkila (LASL):

Referring to the question of what to do with outliers in interlaboratory exchanges, it seems to me that experiments serve two purposes. One is to determine what some people refer to as the systematic error of a method; the other is to identify where a laboratory is improperly analyzing the sample. When analytical errors are identified as the source of the outliers I think you are unfairly biasing the systematic error for the method by including these data points.

Computer-Aided In-Line and Off-Line Analytical Control System for an Experimental Thorium-Uranium Reprocessing Facility

by

BERT - G. BRODDA
Institute for Chemical Technology, Nuclear Research Centre Juelich GmbH,
Federal Republic of Germany

ABSTRACT

The paper discusses in brief the technological background and specific obstacles of general process control and nuclear material assay in reprocessing facilities. It also describes essential parts of an analytical control system designed to service an experimental reprocessing plant for spent thorium-uranium fuel. The features displayed are the data processing system, sample identification applying bar coded labels, remote pipetter and sample lock systems as well as a remote XRF sample preparation device.

KEYWORDS: Automation; data processing; HTGR spent fuel reprocessing; in-line measurements; off-line measurements; process control; remote pipetters; remote sample preparation; SNM accountancy; X-ray fluorescence

INTRODUCTION

In the past years much labor has been invested in the development of techniques and systems for the control of facilities handling nuclear material in many parts of the world.

This is especially the case for the back-end of the nuclear fuel cycle, although some people or governments have deferred fuel reprocessing and plutonium recycling for an indefinite period of time.

Anyhow, these efforts are motivated by two requirements:
basic process control like for any conventional chemical plant, and nuclear material accountancy for safeguards purposes.

The problems arising from these demands created a series of solutions fitting to the particular tasks, either as a single component or as a systemic approach. A general handicap in nearly every respect was the radiation hazard accompanying the materials under investigation and the thus required operation of analytical tools and measurement devices under remote conditions.

In the field of process control very special solutions have been found for quite common problems such as the various titration techniques, which are mostly performed with potentiometric end point detection and applied to the determination of free acidity, heavy metal and other species' concentrations. In this case remote, in part automatically operating titrators were constructed.

An associated problem is the provision of well defined material aliquots. The solutions are numerous types of volumetric pipetters and, for those who do not trust in such devices, gravimetric systems. It seems typical that nearly every laboratory applies its own specific method.

There exists a variety of spectrophotometric methods for heavy metal determinations. These methods are quite sensitive and thus principally applicable to the specification of waste and scrab solutions. Unfortunately, they are sensitive also against interferences caused by other components normally present in such phases and may require elaborate separation procedures. In some cases remotely operating devices have been developed.

A promising but not yet often used tool is X-ray fluorescence as wavelength- or energy-dispersive system. Interferences are not frequent and can be controlled by calibration and mathematical methods. Sample preparation for off-line measurement needs sophisticated instrumentation if applied to the highly radioactive dissolver or feed solutions. In-line suitability is limited mainly due to the mechanically complex and maintenance-requiring set-up.

The group of conventional nuclear physical methods like γ- and α-spectroscopy, gross-β- and -γ-counting makes use of in part sophisticated marketable instrumentation but shares sampling and sample preparation difficulties with the beforementioned methods.

Polarography seemed to be applicable to the in-line determination of uranium and plutonium for some period and a lot of research and technological effort has been spent with this method. However, systematic interferences and technical complexity will very probably not allow for an acceptable continuous operation period of an in-line device, and due to poor experiences several laboratories have given up in the meantime: so we did.

Process control applies many more in-line and off-line techniques which cannot be mentioned here, part of them being used for the purpose of nuclear material assay too, e.g. the modified Davies & Gray uranium method and other titrimetric procedures, not forgetting gravimetry, which is but restricted to pure or purified samples. It would be of interest to examine the capability of XRF for Special Nuclear Material (SNM) assay. Here calibration and instrument stability problems are handicaps against the advantage of few interferences only.

SNM accountancy differs from process control in one main respect: measurement accuracy must be significantly better. Additional conditions are described under the concepts of tamperproofness, static or dynamic physical inventory taking applying wash-out or dynamic procedures, and interfaces to national and international control authorities.

The methodology consists of a combination of problem-adapted chemical, physical and nuclear-physical techniques such as titrimetry, gravimetry, photometry, α-, γ-, neutron- and mass spectrometry, the latter being a key technique for SNM accountancy and, when applying the resin bead sample preparation technique, especially useful for off-site inspector analysis.

There exists a long list of excellent methods capable of performing SNM accountancy at its best, but it should not be forgotten that another strategic input is necessary to calculate for an inventory figure: that is the mass or volume of the content of containers or tanks located somewhere in a shielded process cell.

In reprocessing plants the pneumatic dip tube method is normally applied for bulk volume measurement. This method is in principle, which means in a clean and well controlled environment, of comparable accuracy as the other analytical tools are. But after some time of hot operation the primarily measured calibration coefficients will have changed considerably. The necessary frequency of recalibration is less inferable from observation but more defined administratively. Recalibration itself of an unaccessable tank is a task, which presumably will never yield in a calibration function of the original quality and reliability. In clear text, one has to calculate for volume errors of one per cent or higher.

This provokes the question for the reasonability of disputing 0.1 % errors (or less) for accountability concentration determinations of any kind if the accuracy of the volume factor necessary to calculate the SNM mass value is worse for about a magnitude.

To my knowledge and from my experience bulk volume measurement is the weakest point in the overall SNM accountancy of relevant facilities. And to my opinion it is rather worthless to fix any MUF value as long as it is not possible to verify those volume figures with the same precision and reliability, and also repeatedly, throughout hot operation.

I must confess that I don't have the key at hand to resolve this problem, but it is obvious that the gap between the achievable precision and accuracy of off-line and accountability-relevant in-line measurement methods is waiting for being closed.

KFA REPROCESSING CONTROL SYSTEM

The facility, for which the analytical control system developed in our laboratory primarily was designed, is an experimental reprocessing pilot plant for spent HTGR fuel of the Juelich pebble bed test reactor AVR.

This facility is intended to reprocess the well-known fuel balls consisting of typically 1 gram high enriched uranium and 5 to 10 grams thorium as BISO coated mixed oxide particles embedded in a 200 grams graphite matrix after a burnup of up to 120000 MWd/MT of heavy metal.

The technological part of the project has suffered a considerable delay from various reasons and is now scheduled to begin cold operation in 1983.

The analytical part of the project was designed in 1974 based on the plant parameters defined at that time and under the conditions of a narrow timetable. It was intended to develop an analytical system being capable of chiefly servicing the chemical process part from dissolver to product solutions for the purposes of process control, but also offering a flexible interface to make relevant data available for safeguards purposes.

Data Processing System

Besides the development of analytical tools the installation of a suitable data acquisition and processing system was required. Due to the special environmental conditions like highly radioactive samples and the high number of samples to be carried through the analytical laboratories a considerable degree of automation of sample handling and measurement devices had to be realized.

Following the philosophy of automating remotely operating devices to a reasonable extent only, as seen from the point of view of maintenance problems, but assuring strict control of data flow by an effective data organization and management system, we are operating the basic level of this system for about a year. The acronym given to it is RADAR (Remote Analytical Data Acquisition and Reduction).

The guidelines of RADAR can be described by the following aims:
- improvement of process transparency by computer-aided tank control,
- improvement of analytical laboratory transparency by direct access to computer managed sample and measurement data,
- reduction of bulk to few relevant data immediately after data acquisition,
- tamperproof correlation of sample and measurement data by computer-internal data organization,
- flexibility in fitting evaluation algorithms to varying composition of samples,
- improvement of the quality of results by application of statistical methods,
- unburden laboratory personnel by computer-aided sample magazining, preparation and data acquisition.

Figure 1 informs about the expected sample flow and throughput during an about 10 days reprocessing campaign. The two input magazines are fed from about 210 sampling stations (50 tanks and 160 mixer settler sections) and distribute the samples to the various experiments.

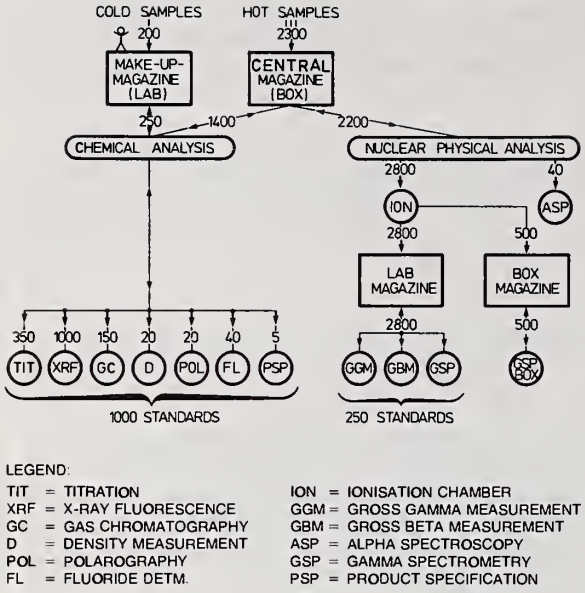

Figure 1: Sample Flow and Throughput per Campaign

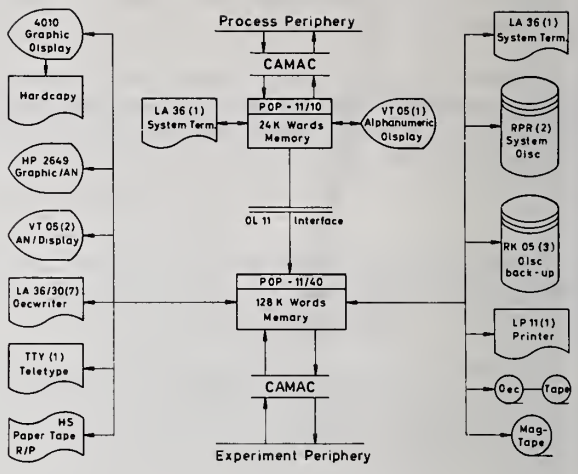

Figure 2: Computer Hardware Configuration

It is obvious already from the numbers of figure 1 that an unresolvable informations pool would be created if the analytical services would not be computerized adequately.

Figure 2 describes the present computer hardware configuration. System software is real-time RSX-11D on the central and RSX-11S on the satellite computer.

Tracking a sample from sample taking to being disposed-of the following paragraphs focus on some characteristic features of our system.

Sample Identification and Storage

A key factor of an analytical process control system, especially under remote conditions, is a reliable sample identification, repeatable at any strategic place throughout the sample's lifetime. Its realization is not trivial within the corrosive and abrasive environment of hot chemical operation. After checking various options we finally have chosen the optical bar code system with, to our judgment, the most positive balance of advantages and disadvantages (figure 3). The advantages are: a simple mechanical setup for the reading device, longlived optics, radiation resistance of labels, labels fixable to samples of different geometry and material, random assignment of number to sample, automatic redundancy check of number when read and additional clear text information. Remaining disadvantages are: labels are not resistant against chemicals like nitric acid but they can be protected by films or foils, and no direct relationship between label number and sampling device. The available experiences are, however, promising.

Sample identification is first performed after sampling, the code is linked within the satellite PDP 11/10 with tank number, charge number, date and time of sampling and in-line data for density, liquid level and temperature and via DECNET shifted to the central PDP 11/40.

In parallel, the 5-ml-vial is shut through a pneumatic rabbit line into a lead shielded box, where after reidentification it is assorted into the computer-controlled 1200-position central magazine. The assigned position is being indicated by a discharge lamp switched on by the computer (figure 4).

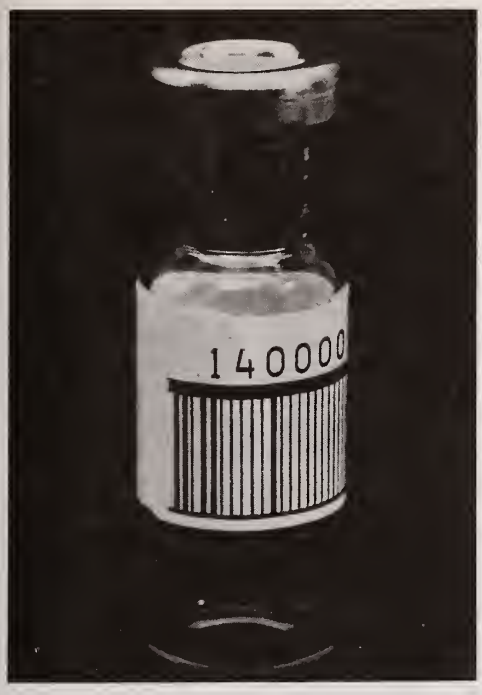

Figure 3: Labeled Sample Vial

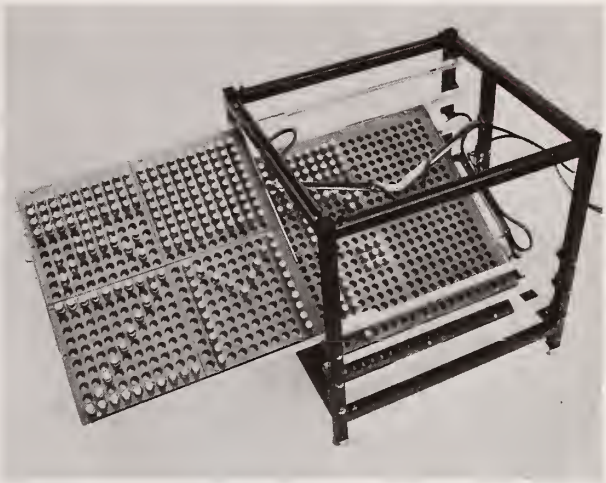

Figure 4: Central Magazine

From this central magazine for hot, and a parallel make-up magazine storing non-radioactive samples, the vials are requested by the individual experiments.

Starting a codeword-dialogue, the experiment operator is being informed on the numbers of existing samples assigned to his experiment. He then orders one or more samples from the respective magazine. The magazine operator, after being informed on the magazine position, checks the sample for correct number and delivers it to the ordering experiment.

After receipt, the sample is reidentified again as being ordered and fed into the sample preparation and/or measurement cycle.

Sample Preparation and Measurement

Besides the few make-up samples, which can be handled on the bench without applying shielding precautions, this area offers its characteristic features in the necessity of performing remote sample preparation for various measurement methods, often including locks for transferring samples from contaminated radiation-shielded boxes to a measurement device which can only be operated in a laboratory. Examples are gamma spectroscopy, gross beta and gross gamma counting, gas chromatography and X-ray fluorescence.

Pipetter Systems

The most important condition in aliquoting liquid samples for fission product radioactivity measurements is to avoid cross-contamination of the aliquots considering a possible range of about 10^{10} in radioactivity concentration between sequential probes. This excludes the application of a reusable pipetter head but presumes exchangeable pipetter tips.

As shown in figure 5, a coupling device takes up a plastic throw-away counterpart of an appropriate size, fitted with syringe needles to enter different kinds of sample vials[1]. The coupler is connected to an ordinary HAMILTON pipetter. The whole system is located in a lead shielded box and interfaced to the laboratory by a special lock (figure 6), which

[1]K. Kroth, private communication.

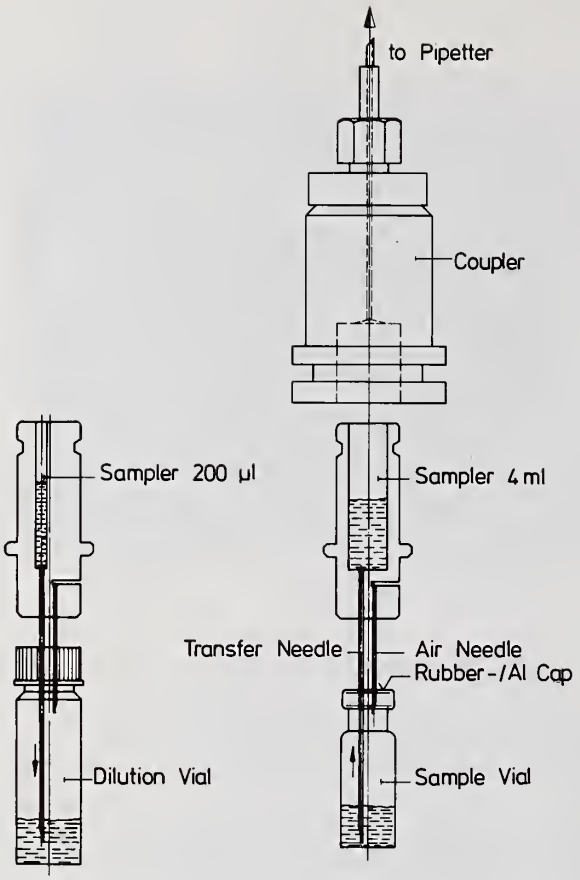

Figure 5: One-Way Pipetter System

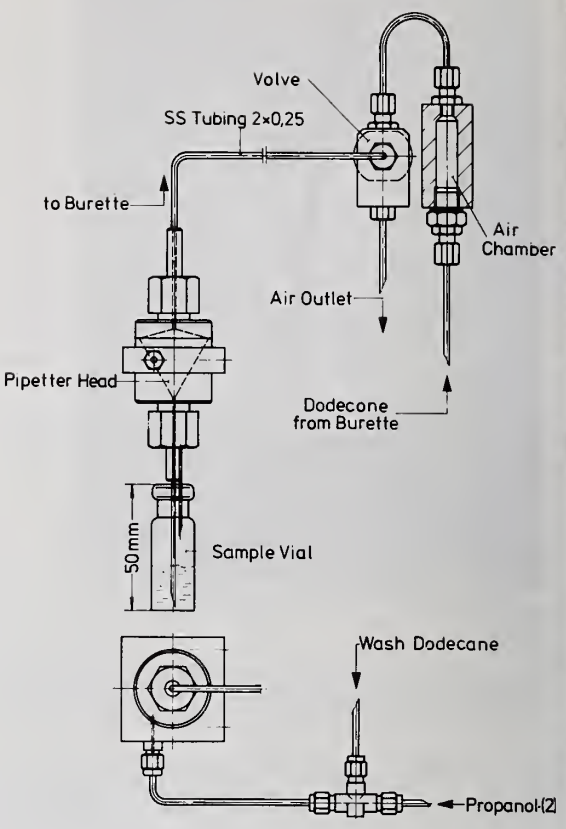

Figure 7: Re-used Pipetter

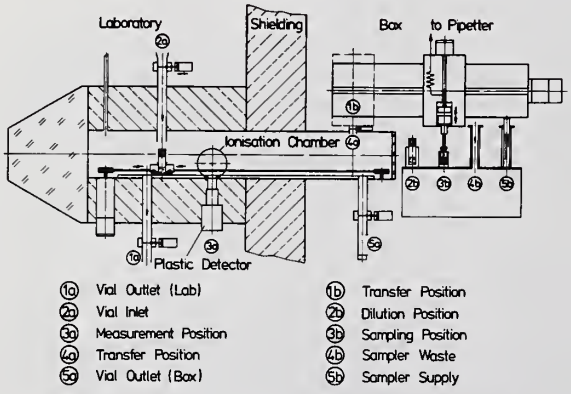

Figure 6: Sampling and Locking Device for Gamma Spectroscopy

allows for a contamination-free sample transport into the laboratory, monitored for an upper radioactivity level, and equipped with an additional ionization chamber for the specification of intermediate dilution steps[2].

A different approach is made for aliquoting samples assigned to titrimetry, X-ray fluorescence or gas chromatography. A minimum of cross-contamination can be accepted here without affecting the results significantly. A reused system is applied (figure 7) which by a dodecane-filled stainless steel tubing is air-free connected to a motor-driven burette in the laboratory and equipped with devices for de-aeration and rinsing of the pipetter head with dodecane and propanol-(2).

[2]P. Filss and H. Kirchner, Analytical Chemistry in Nuclear Fuel Reprocessing (Science Press, Princeton, 1978), p. 258

Since long we have decided on a filter paper sample preparation technique that fits the given demands best[3].

As mentioned before, a sample vial received from the central magazine is checked for being ordered by label code identification. Positive identification yields in the display of sample data and preparation parameters like type of internal standard to be used, aliquot setting and number of parallel samples.

The vial is then located in the receptacle of the preparation device and the mechanism is started. It follows a preprogrammed sequence of dilution with internal standard, aliquoting onto one of the filter papers of the preparation tape, identification of the associated label code and registration in the relevant data block, transportation through the time-controlled drying compartment to the punch position, where rounds containing both filter and label are punched from the tape into a plastic frame which rolls into an intermediate magazine. The complete assembly, as operating in a box, is shown in figure 8.

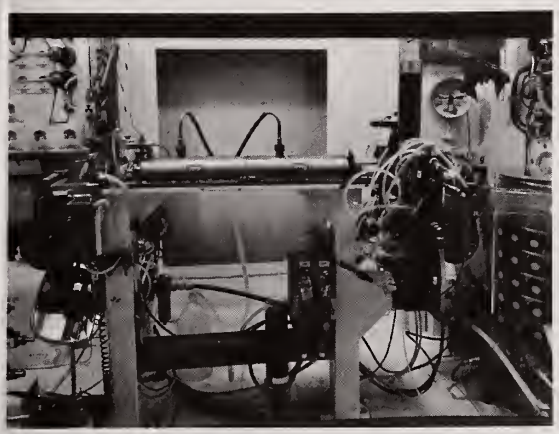

Figure 8: XRF Sample Preparation

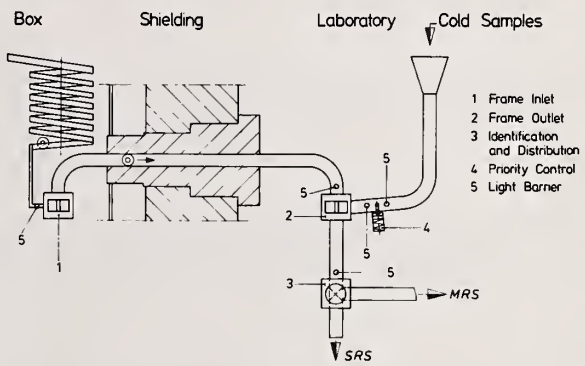

Figure 9: Pneumatic Frame Transport

On request of the spectrometer a frame is pneumatically transferred through the box shielding to another identification station which starts the measurement cycle (figure 9). After termination of the measurement the frame finally is being disposed-of by pneumatic transfer into a waste box. The on-line acquired data are processed according to the correspondent software modules.

CONCLUSION

Results produced from XRF or other types of measurement are generally displayed as hardcopy report at the experiment-specific terminal. There will be no closed-loop feedback of results into the process neither from off-line nor from in-line measurements.

In-line measurements, which are performed applying the dip-tube method for density and liquid level and with thermocouples for temperature, produce a report at the process control board on individual request, in case of a preset tank parameter overflow and with any sample taking.

[3]B.-G. Brodda, H. Lammertz, H. Maselter and J. Vieth, Kerntechnik 19, 433 (1977)

Future intentions for system development are:

- to reduce the interrupt load of the PDP 11/40 CPU by delegation of data acquisition to intelligent periphery, as planned with e.g. a new gamma spectroscopy system running on a PDP 11/34 which could be coupled to the central CPU through DECNET, this is planned also for XRF and may apply to a thermionic mass spectrometer, and
- to realize a data bank system to manage accountability-relevant data and for correlating results obtained during the campaign for purposes of trend analysis and other general process evaluation.

So far, the analytical control system RADAR could only partially be tested under realistic conditions, a final evaluation can only be made after some time of hot operation. In the meanwhile, the system has found some interest by the LWR fuel reprocessing industry in Germany for application in their large scale industrial plant under design.

Discussion:

Hakkila (LASL):
What is the cost of your sample identification system? Have you made any attempt to harden it against operator misuse.?

Brodda (KFA - Julich):
The cost of the sample identification system - well, it differs. The labels themselves are very cheap, but the electronics part, if you buy it completely, will cost about $3,000 per station. But you can make it yourself, and we have made the electronics part in an amount of about 30 stations - then it becomes much cheaper. The hardware you need, motor and brass or steel is quite cheap. It depends on the cost of your mechanical workshop. I would say $1,000 per item. On the second question, we have a random number assignment to the samples, as I already said, so no operator can identify the sample when reading the sample number. We feel that this is an inherent type of information securing.

Larsen (ANL):
Are you saying then that the assignment of the sample number is made in such a way that the operator has no idea of what the result would be? He would have to know something about the nature of the sample.

Brodda:
When he receives the sample at his experiment place, he receives from the computer the recipe of how to handle the sample. This does not include information on the expected result of the sample. This is completely unknown to the operator.

Larsen:
Doesn't the individual still have to have some idea about the magnitude of, let's say, the uranium concentration in the sample? He has to have some idea whether he is measuring a concentration of 1 mg per liter or 100 mg per liter. He has to have some input in order to even choose the method he is going to use.

Brodda:
The operator does not choose the method. The system manager has chosen the method for a certain combination of tank and flow sheet before the campaign has been started, and the operator only receives the methods and some figures and types of reagents or dial settings he has to use. He has no information on the expected result of the measurement. He could possibly deduct that the concentration might be of a certain magnitude, but not more than that.

Johnsen (NBS):
I am interested in the control mechanisms that you are using for your remotely handled equipment.

Brodda:
Each device has a particular control system. This might be a card controller or a combination of microcomputer-controlled driving mechanisms and digital control outputs from the central PDP-11/40.

Suda (BNL):
I'd like to comment on your statement about the measurement error in volume determinations. We have developed a system that involves an electromanometer that is controlled by a desk-top computer that has accuracy on the order of one tenth of one percent This sytem was tested at the Barnwell Nuclear Fuels Plant and installed at the PNC spent fuel reprocessing plant at Tokai-Mura. We are currently analyzing PNC data results and we hope to have the results of that experiment available soon. Automating the bubbler probe measurements so that one collects data over several seconds and averaging the results yields very precise measurements. Working with the averages improves the measurements substantially and in fact, I think the density measurements that we can get off the bubble probes now is probably superior to that achieved in the laboratory. Furthermore, the data are available whenever both bubble probes are covered.

Brodda:
The problem I see is that the primary function will drift during hot operation and I expect it will be difficult to recalibrate the whole system during hot operation.

Suda:
That is true, but the tank does have a certain amount of stability. With the automated electromanometer system, we do look at the probes independently so that there are a number of comparisons of redundant data that can be made. We have a pneumatic scanner that reads data from as many probes as there are, once every two minutes. The measurements are precise enough that one can observe changes as they occur in the tank and then devise and perform several tests to identify the cause. Some of these techniques for tracking the changing conditions in the tank are very promising in terms of tamper indicating applications to international safeguards.

Johnson (Exxon):
We have been working on an extended electromanometer system under Task I of TASTEX for testing at Tokai-Mura. One of the techniques we are looking at is the capability for doing continual calibration checks. This requires precise level and volume measurements in process tanks and verifying transfers among tanks. This may not duplicate the precision of the initial calibration, but will at least provide some ongoing checking capability. We hope to have that technique verified and the results on it by the end of January.

Brodda:
The problem is that any tank has to be seen as an individual and that the bubbler tubes within the individual tank might change their specifications due to precipitation of solids during the campaign, which will lead to a drifting pressure difference with time, thus changing the calibration function.

Johnson:
We have noticed some variations between tanks at the ICPP (the Idaho Chemical Processing Plant) due to off-gas variations and compensations have to be made. At this point we are collecting operational data to evaluate and isolate some of these factors, but you are correct in that there are variations that require compensation.

Larsen:
The critical measurement that is involved here is the tank volume. The point is, as you pointed out, that it is of no value to pursue analytical methods that provide accuracies to a tenth of one percent when you don't know the tank volume to plus or minus one percent. It seems that an apparently significant effort is being directed to the problem of how we improve the method of obtaining tank volumes. Now some few months ago at a meeting at BNL there were some discussions of an analytical technique of spiking the dissolver tank with some other constituent. I think somebody made the decision to use lithium at one time although lithium is a devil to do by mass spec isotope dilution. Well, there are other materials that could be spiked into the dissolver tank and then by doing a double mass spec isotope dilution on the dissolver tank one could recalibrate the dissolver tank. How accurately can those measurements be made? We don't know how much uranium is in the dissolver tank, but we spike in a known amount of some other element and analyze for both of them and then by a ratio method you determine the amount of uranium in the tank.

DeBievre (CBNM - Geel):
I think I can provide some answers to your questions Mr. Chairman - and then I'll have a question for Mr. Suda. Several attempts along the lines you describe have been made over the last ten years. The lithium was tried out and I think that that is a poor choice; I do not know too many spectrometrists who can do lithium measurements to a reasonable degree of accuracy. We have done, at the request of Karlsruhe, hydrogen deuterium ratio measurements. One can indeed spike a light water or a light nitric acid fuel tank with heavy water - a few liters or ten liters or so, very cheaply. However this gets you to the problem of accurate hydrogen deuterium ratio measurements, and although we have been working on that for six to eight years (achieving eventually a 99.7% D_2O Reference Measurement Method), I would not encourage other people to go through the same difficulties. It can be done but it is very difficult. I think that the Indians have done some useful work by spiking total tank with magnesium and with lead. Isotope ratio measurements for both of the elements have been well developed. I have another proposal in my talk this afternoon

-- to tackle the problem of accurate determination of mass (not volume) of total solution by isotope dilution. Solution mass independent of the form of the container tubing or what else, and if it is followed by an accurate isotope ratio measurement, then accuracies, not precisions, of 1/2 percent are within reach. That leads me to the question for Mr. Suda. He made a statement about a .1% accuracy. Can he come up with some proof? This might be a controversial question, but you have asked for something like that this morning and so far, haven't gotten it.

Larsen:

I think that this is a major point, and if we go on beyond the time that is allotted for a particular paper, it is obviously worth doing.

Suda (BNL):

This stated accuracy is based on the calibration data. We have standards that are traceable to NBS. The increment method of calibration involves the introduction of known masses of liquid into the tank. What is of interest here is the accuracy associated with the calibration equation. This is the real problem. In a reprocessing plant, where you may have a tank filled every day, or perhaps twice a day, the random error of two tenths of a percent is negligable at the end of the month. It is the systematic error that one worries about. If the calibration curve is off by some value, this error is perpetuated in every measurement that is made. Periodic checks are needed to assure the continued validities of the calibration equation. NBS has been involved in using an electromanometer in calibration exercises at the Barnwell Nuclear Fuels Plant at the Savannah River Plant and there are other facilities also using this technique. I think they are in agreement that one does get a tenth of one percent accuracy on the calibration equation.

I would also like to comment on the spiking technique. We have been looking at the spiking technique as a way of periodically verifying the bubbler probe calibration curve. One of the problems with the spiking technique is the very high cost. Also the time delay associated with hot sample analyzes is substantial. The spiking technique is very costly and you may wait 7-10 days to learn what the volume of a tank transfer was.

Filby (Exxon Nuclear, Idaho):

We've been working with the spiking technique for some time at the Idaho chemical processing plant. We've considered everything that has been mentioned here plus some others. I have several points. First of all, it is a very expensive technique. Turnaround time is a little better than Sylvester was talking about - we've managed about three days on it, including the chemical processing time. The worst problem we've had with the spiking technique in the operating system is getting the spike reproducably into the tank. Of course, we have an old plant. We've had hangups during that introductory phase. In controlled conditions with a very skilled group of people, we've had very reproducible results. But to make a routine check of your calibration perhaps once a week, a well thought-out system would be needed. You have to have careful control because your spike doesn't always get into your tank the way you want it to.

Skinner (DOE - SROO):

I'd like to reinforce what Mr. Suda was saying. We have had this problem at SRP for all these years. The analytical people were saying why should we try to do better because the volume is bad. We engaged NBS to help us - they were to be our experts - and they did, and we have done it. We have reinstrumented the tanks and we are down in the range of one tenth of one percent. It has been done on several tanks.

Nuclear Materials Analysis Using Plasma Desorption Mass Spectrometry

by

WILLIAM H. ULBRICHT, JR.
U. S. Department of Energy, New Brunswick Laboratory, Argonne, Illinois

ABSTRACT

A unique time-of-flight mass spectrometer has been built to make use of a process referred to as plasma desorption to measure isotope ratios of materials which contain fissionable material. Plasma desorption is the very rapid and energetic process by which a fission fragment may desorb and ionize minute portions of the sample. It is so rapid that fractionation is thought not to occur, and the amount of material removed from the sample is extremely small. The mass spectrometer construction is discussed and a description of the timing electronics is given.

KEYWORDS: Time-of-flight mass spectrometer, plasma desorption, fission fragment desorption, isotope ratio measurement

INTRODUCTION

Properties of Fission Fragments

When a ^{235}U nucleus captures a thermal neutron and fissions, two fission fragments are released along with several neutrons. The two fragments are usually of unequal size. The mass of the lighter fission fragments center around mass 95 and the heavier fragments near mass 140. The lighter particles have approximately 100 MeV of kinetic energy and the heavier particles have approximately 70 MeV. Each fission fragment has a charge of about +20 and a cross sectional area of less than $1Å^2$.

As a fission fragment travels through a condensed medium, it deposits some of its energy through coulomb interaction. An estimate of energy deposition in a hydrocarbon medium is 10 MeV per micron in about 10^{-13} sec.[1] Studies with CsBr have shown that at a radius of 25Å from the fission fragment's trajectory, temperatures reach 66,000°K and at 80Å radius, 10,000°K.[2] Temperatures along the trajectories of fission fragments passing through other substances have been found to be of the same order of magnitude. The time scale for energy deposition is also the same.

Plasma Desorption

When a fission fragment exits the surface of a condensed medium, little material may be expected to be ejected by a head-on-collision since the cross section of a fission fragment is so small.[2] But, the highly energetic condition near the trajectory causes some of the material to be ejected and ionized within the 10^{-13} second time frame.[1]

Although intensely energetic, this process has been demonstrated to be an extremely gentle method of ejecting and ionizing. The energy from the fragment probably becomes translational energy in the desorbed ions rather than coupling into the unstable vibrational modes in the short time of the process.[1]

---

[1] R. D. Macfarlane and D. F. Torgerson, Science 191, 920 (1976).

[2] R. D. Macfarlane and D. F. Torgerson, Phys. Rev. Lett. 36, 486 (1976).

Plasma Desorption Mass Spectrometry

Unlike thermal ionization, plasma desorption is a discrete event which releases a few ions from an extremely energetic, localized, short-lived event. A mass spectrum is a composite of many such events where major peaks represent ions which were given off most often by the sample. Even a very large number of fission fragments would remove only a minute amount of the sample; therefore, the process does not destroy the sample. Since the process is so rapid, intermolecular interactions would not be expected to happen before desorption; therefore, fractionation would not be expected to occur.[3] And, since many molecular ions tend to be released, isotope ratios will probably be taken from the parent ion peaks, a process more complex than interpreting peaks from singly charged uranium ions. This may offer an added bonus, however, in mixtures where different elements of interest with the same mass may be bound in different compounds. Again, since molecular ions are ionized and vaporized, sample analysis of an unknown mixture should consist of locating the major uranium bearing parent ion peaks and extracting the isotope ratio.

INSTRUMENTATION

Introduction

The plasma desorption time-of-flight mass spectrometer constructed by R. D. Macfarlane and D. F. Torgerson used ^{252}Cf to generate the fission fragments for desorption and ionization.[4] One fragment was used to start the timing of the ion's flight while the recoil fragment passed through the sample support material and through the sample, exiting the outer face.

The mass spectrometer systems described in this paper make use of the fission properties of the ^{235}U within the sample. Exposing the sample which is in the mass spectrometer to a neutron flux causes some ^{235}U nuclei within the sample to fission. The fission fragments which pass out of the exposed face of the sample cause desorption and ionization of the material within the sample.

The Neutron Source

The neutron flux emanates from a 240 μg ^{252}Cf source. This neutron source is housed in a shielded well that is designed to accommodate the mass spectrometer. Shielding within the well is 18 inches (46 cm) of borated polyethylene. At the bottom of the well is a cup-shaped container which surrounds the ^{252}Cf source with 4 inches (10 cm) of D_2O to partially reflect and thermalize the neutron flux. In the present configuration, the sample-containing end of the mass spectrometer is brought to within approximately 8 inches (20 cm) of the ^{252}Cf source. In Figure 1 the mass spectrometer has been lowered into position in the shielded well.

The Time-of-Flight Mass Spectrometer

General Description

The time-of-flight mass spectrometer is a long slender stainless steel tube which has been designed to have the source-containing end lowered into the neutron flux of the well described above. Figure 2 shows the full length of the mass spectrometer and the supporting crane. The black unit at the top of the assembly is a 100 liter/second ion pump. The large tubing just below the pump covers the upper grid assembly and electron multiplier. The lower grids, fission fragment detector and sample plate exist as an assembly which slides

---

[3] R. D. Macfarlane, private communication.

[4] R. D. Macfarlane and D. F. Torgerson, Science 191, 920 (1976).

Time-of-Flight Mass Spectrometer in Shielded
Well of Neutron Source

Figure 1

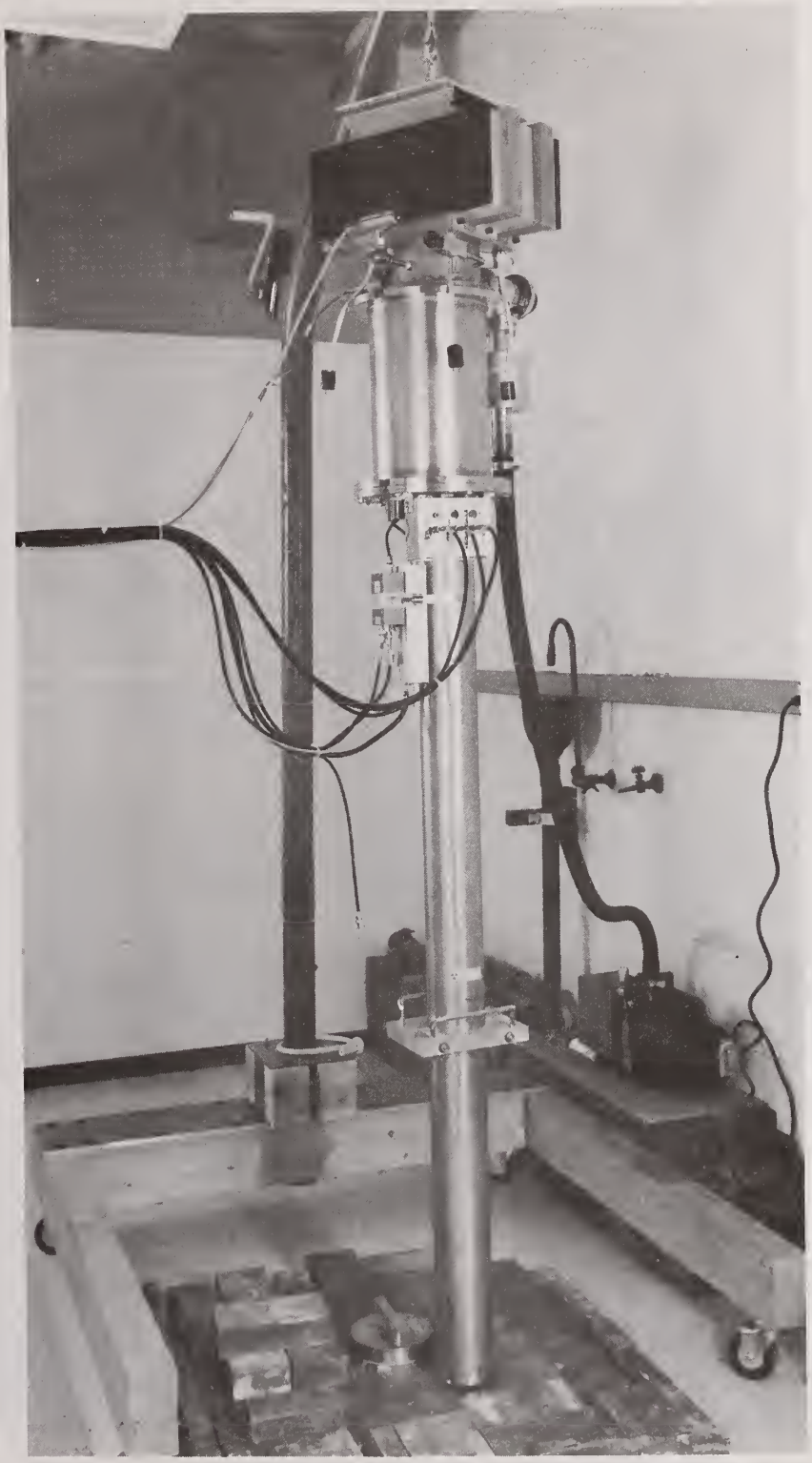

Full View of Time-of-Flight Mass Spectrometer

Figure 2

into the bottom of the unit. The drift tube is contained within the vacuum envelope and is 59.1 inches (150 cm) long. One hundred (100) mesh 82% transmission Ni grids are mounted at both ends. A 1-mil (0.025 mm) stainless steel wire is mounted on the axis and extends the length of the drift tube.

The Detectors

The system contains a surface barrier detector and an electron multiplier. The electron multiplier is mounted above the upper grid and detects desorbed ions from the sample, which travel through the drift tube. The multiplier and upper grid assembly are shown in Figure 3. The surface barrier detector is placed near the sample to detect fission fragments. A fragment marks the start of the ions flight.

The Sample Holders

Two types of sample holders are being used. The first consists of thin aluminized mylar onto which the sample is placed. In this configuration the sample has to be thin enough to allow a fission fragment to pass through the exposed face for desorption while permitting the recoil to pass through the lower portion of the sample and the aluminized mylar to strike the surface barrier detector.

The second holder type consists of a stainless steel plate on which a thick sample is placed. The sample is partially covered by an annular surface barrier detector. The diameter of the sample is about twice the diameter of the hole in the annulus. The fragment that causes ion desorption strikes the detector while the desorbed ions pass through the annular hole into the drift tube. Assembled and partially disassembled views of the lower grid, source holder, and annular surface barrier assembly are shown in Figures 4 and 5, respectively. Figure 5 shows the sample as a black spot in the upper portion of the left subassembly.

The System Potentials

In both configurations described above, the sample holder is held at a potential of 5000 V. The drift tube and grids are held at ground potential. The first grid is 2 mm above the sample. Ions of the same polarity as the sample holder are repelled and accelerated toward the first grid.

The guide wire held at an attractive potential of 200 V causes ions that have a small component of kinetic energy perpendicular to the drift tube axis to orbit the wire.[5] The process allows the collection of ions which would otherwise not strike the electron multiplier and enhances the signal by a factor of up to 1000.

Flight Time

All ions created by the plasma desorption process start at the sample surface, which is on a plane parallel to the first grid. The flight time of the fission fragment to the detector, as well as the desorption time, is considered negligible in comparison to the ion flight time. The flight time of the desorbed ions is then the sum of the time spent in the three main regions of the mass spectrometer.

In the first region, defined by the sample holder and the first grid, and in the third region, defined by the last grid and the electron multiplier face, ions are accelerated due to the applied potentials. At the first grid each ion has 5 keV of kinetic energy from the electric field between the sample holder and grid and approximately 8.5 eV (66,000°K)

---

[5] M. D. Edmiston, "Construction and Use of an On-Line Mass Identification System", Ph.D. Dissertation, Michigan State University (1976).

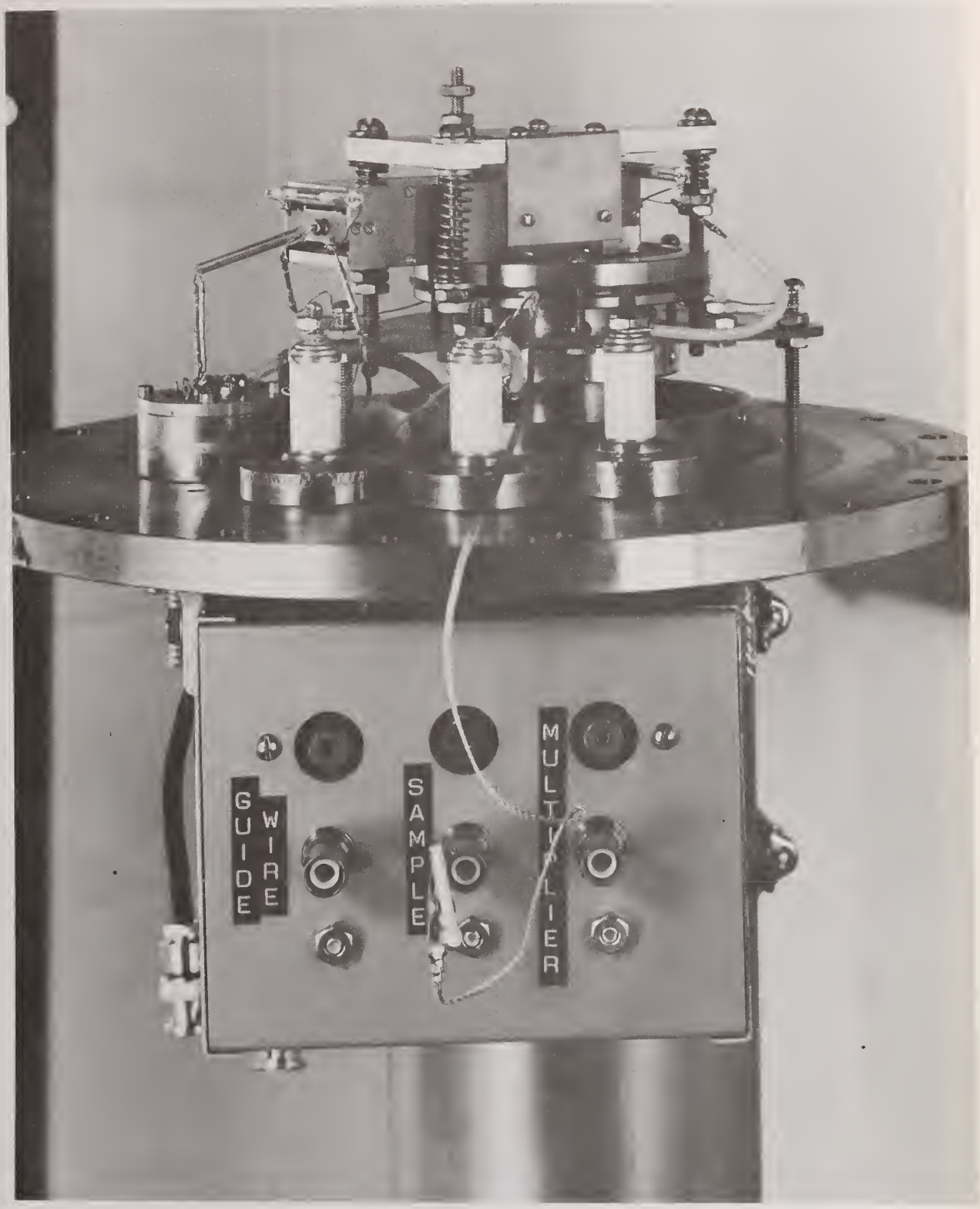

Upper Grid and Electron Multiplier Assembly

Figure 3

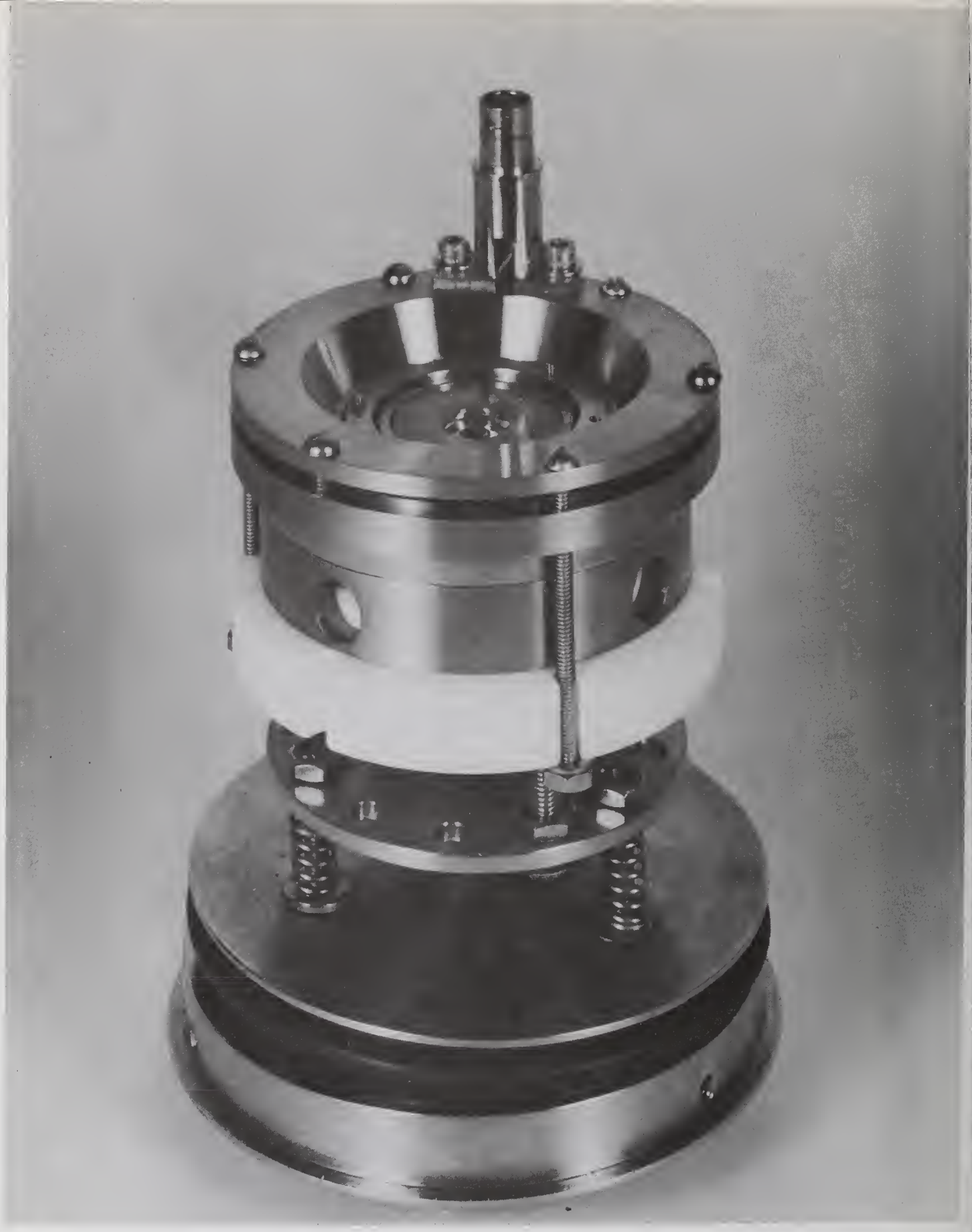

Lower Grid, Surface Barrier Detector
and Sample Plate - Assembled View

Figure 4

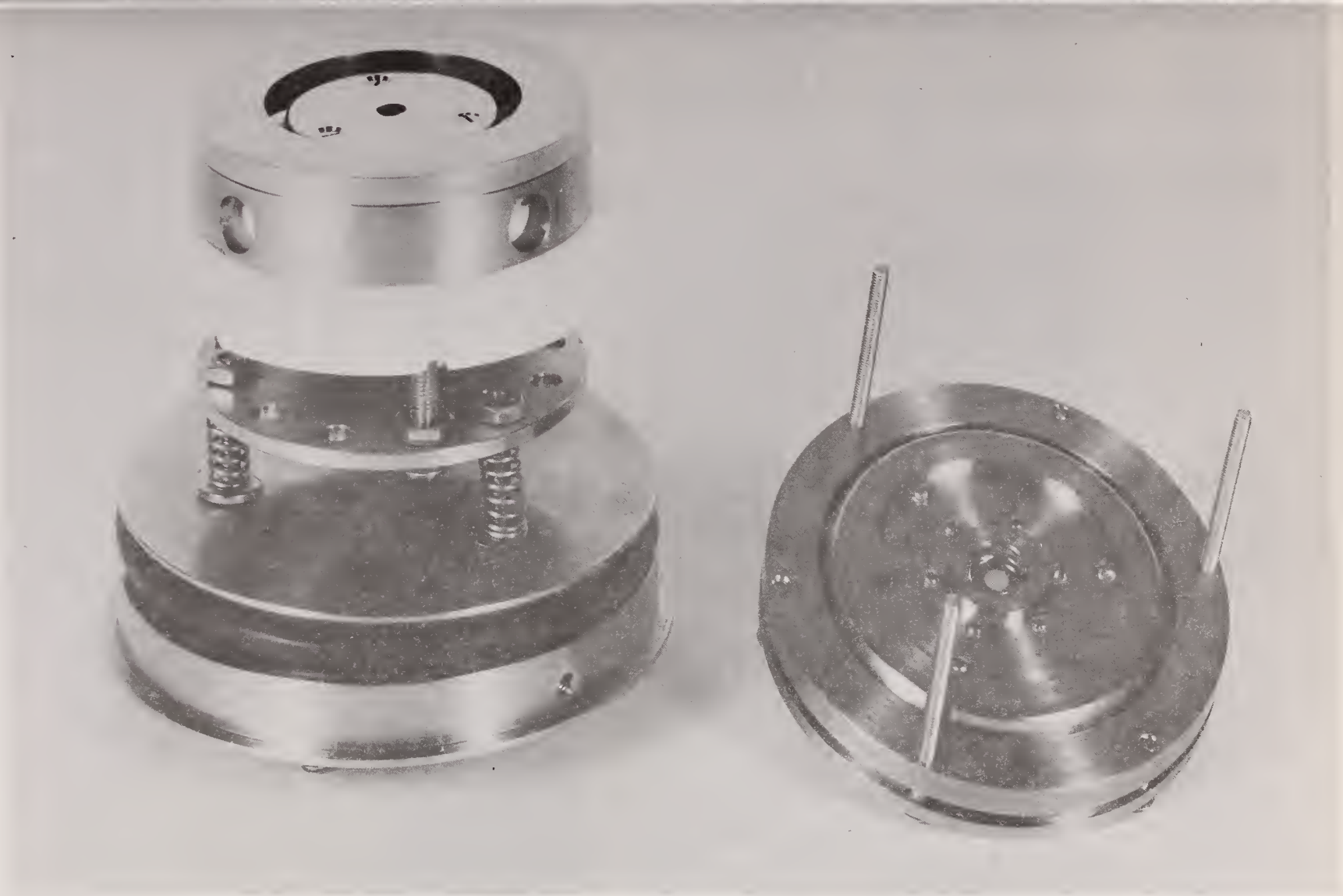

Disassembled View of Lower Grid,
Surface Barrier Detector and Sample Plate

Figure 5

from the desorption process. The multiplier face has a potential of -1500 V, causing further acceleration of the ions. Of the total flight time of the ions, a negligible portion is spent in these two regions. The second region, the drift tube, is field free along the tube axis; therefore, ions drift at a velocity determined by the axial energy component with which they entered from region 1.

The Electronics

The time-of-flight mass spectrometer system detects fission fragments and desorbed ions and collects ion flight times in a multichannel analyzer. A diagram of the electronics is shown in Figure 6. The ion flight times are measured between "start" and "stop" pulses. A "start" pulse is generated when a fission fragment strikes the surface barrier detector. This marks the desorption of ions from the sample surface. When the ions arrive at the other end of the drift tube, having separated in time, and strike the magnetic electron multiplier, a "stop" pulse is generated. The difference in time between a "start" and a "stop" pulse is measured by a time-to-amplitude converter (TAC). The TAC generates an analog pulse precisely proportional in height to the flight time of the ion. This pulse is sent to a multichannel analyzer (MCA). The MCA sorts and stores these pulses within its memory and displays this information as a histogram of pulse height (or time) versus intensity.

Two Tennelec TC444 timing single channel analyzers (TSCAs) are used in the circuit as discriminators and as crossover pickoffs. As discriminators, the units allow the rejection of unwanted signals. Signals from the surface barrier detector caused by α decay within the ^{235}U bearing samples are rejected by raising the TSCA discriminator level to allow only the larger signals caused by fission fragments to pass. Signals from the electron multiplier caused by ions from the ion pump are rejected in the same way. The TSCAs are used to gain timing information from the signals as well. Bipolar pulses from the amplifiers are fed into the TSCAs, which put out fast negative pulses to the TAC when the voltage of the signals of interest reaches zero in crossing from positive to negative.

CONCLUSIONS

The mass spectrometer has been constructed, the electronics assembled and tested, and a number of mass spectra of UO_2 with a ^{235}U enrichment of 93% have been accumulated to demonstrate that the instrument is working in its present form. Both negative and positive ion spectra have been acquired. The ion activity is very low as can be seen from Figures 7 and 8, where the accumulation time in seconds is shown as the number in the center. The mass calibration has not yet been confirmed and peaks on the present spectra are as yet unidentified. Future plans include modifications to increase the number of ions detected as well as the number desorbed. The timing electronics will also be modified to increase the resolution. Then, a series of spectra of samples of different isotope ratios will be acquired.

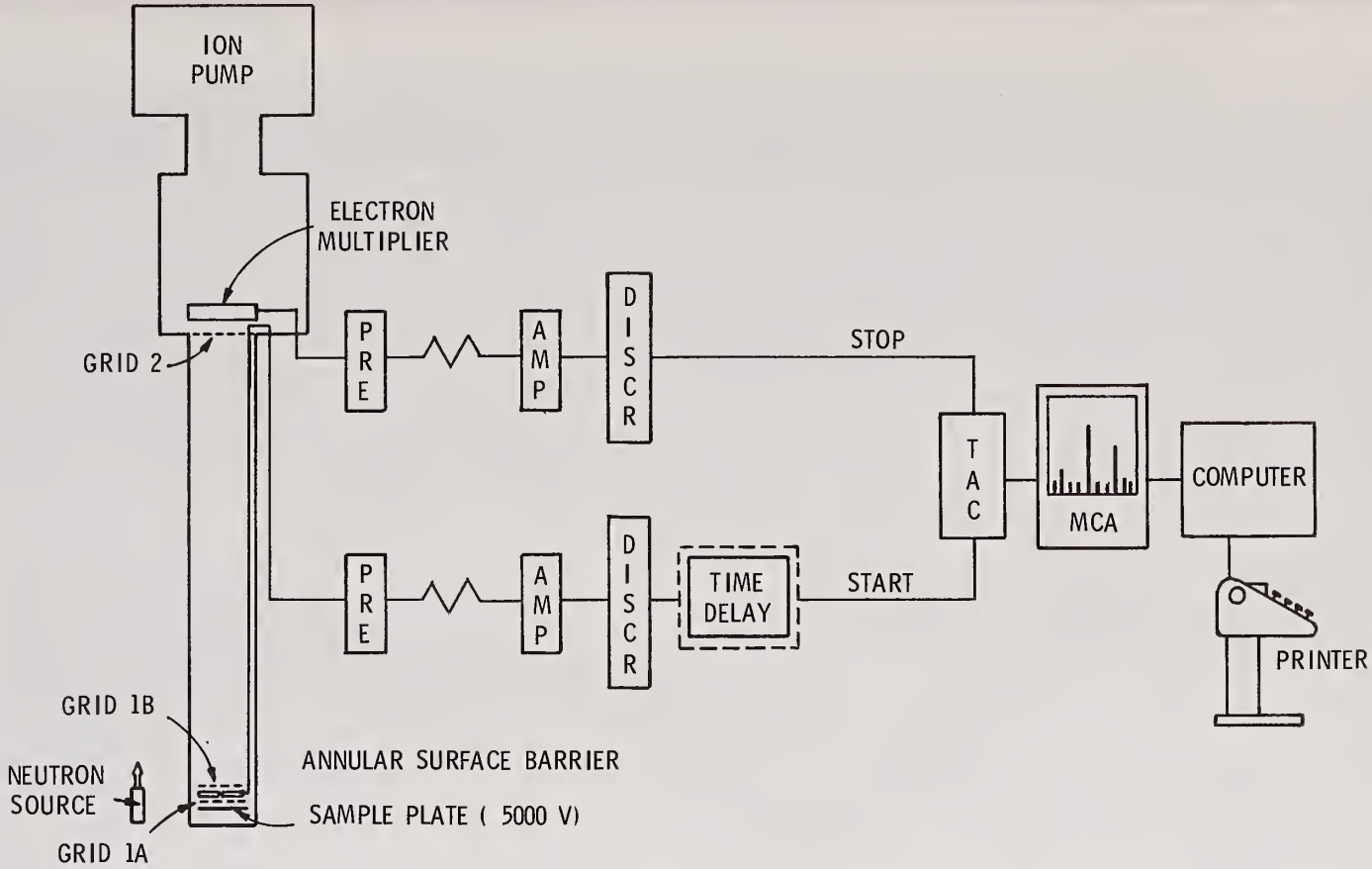

Diagram of Time-of-Flight Mass Spectrometer
Pulse Counting Electronics

Figure 6

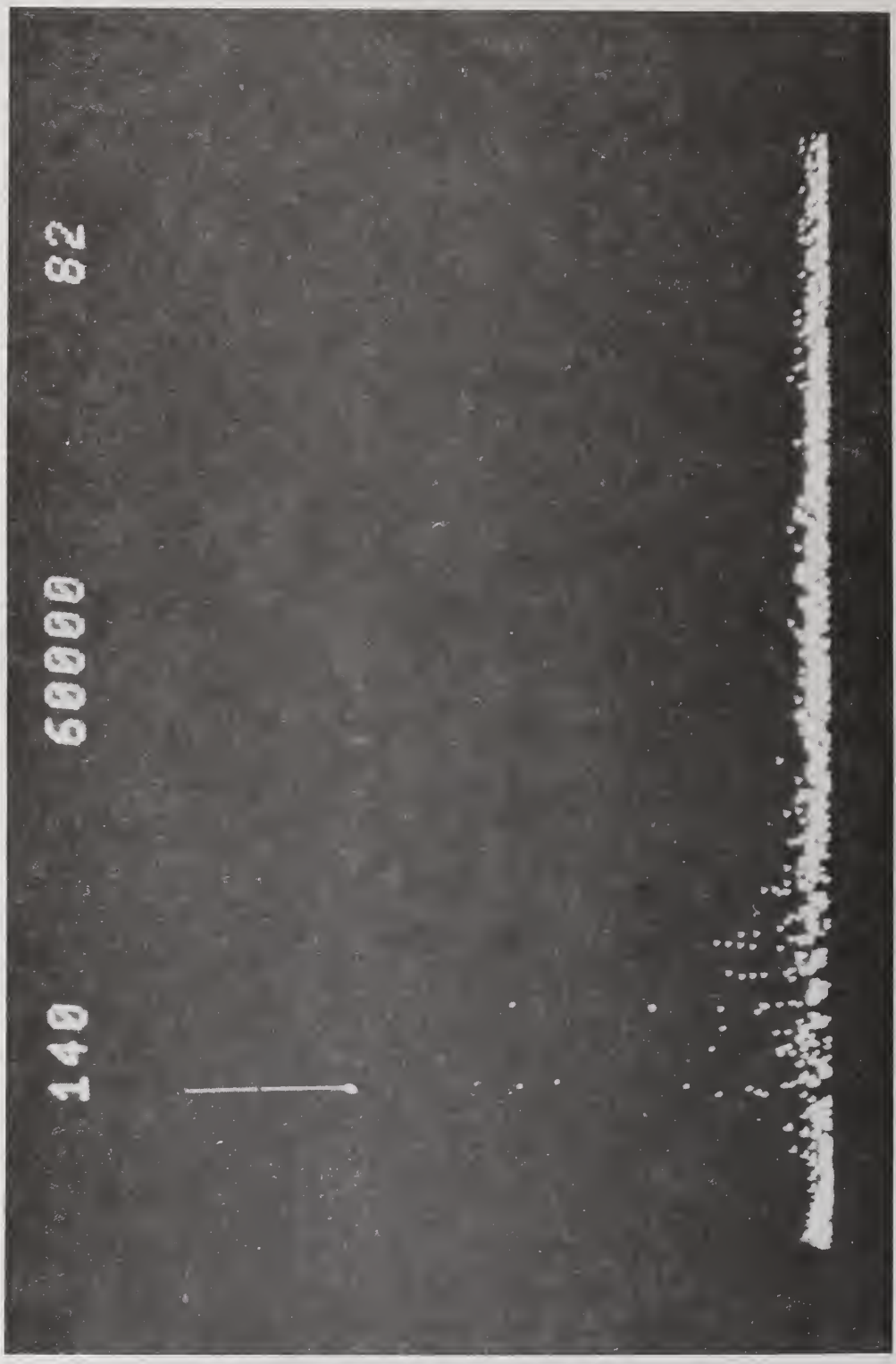

Negative Ion Mass Spectrum

Figure 7

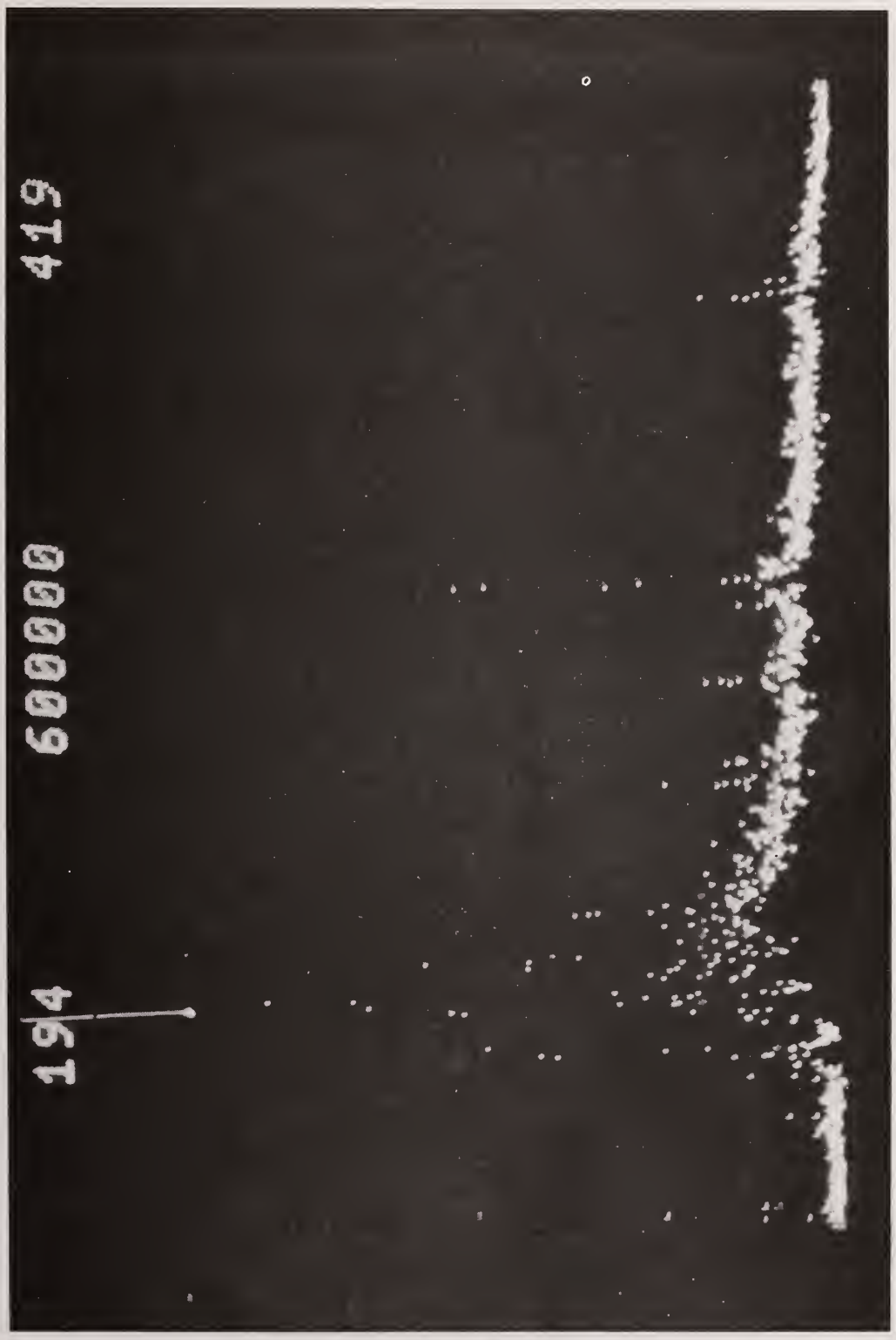

Positive Ion Mass Spectrum

Figure 8

Discussion:

Larsen (ANL):
You are using the fission process to establish some relationship to the 235 - is that right? And how is that related to, let's say, the total amount of uranium in the sample?

Ulbricht (DOE - NBL):
Essentially, I cause fission of a small amount of the U-235 to cause the desorption and the desorbed ions, which contain some U-235, are detected and displayed as the mass spectrum.

Harwell (EG&G, Idaho):
If I understand you correctly, you furnish a start pulse for the time of flight spectrometer from one of two fission fragments while the other fission fragment causes the desorption process. It appears to me that you then have an accidental coincidence problem, do you not? How is this compensated for? It's possible that you generate spurious start pulses and have ions that travel through the time-of-flight spectrometer that do not in fact coincide with any start pulses.

Ulbricht:
That's correct, they lie along the baseline as background.

Charles Roche (ANL):
Are you limited to any particular sample thickness with this method?

Ulbricht:
With the annular surface barrier detector, there is no limit. I actually use the desorbing fragment to trigger my start.

Quadrupole Mass Spectrometry for Isotopic Analysis of Uranium Hexafluoride

by

H. S. KUSAHARA and C. RODRIGUES
Instituto de Pesquisas Energéticas e Nucleares, São Paulo, SP - Brasil

ABSTRACT

This paper describes the procedures for isotopic analysis of uranium in UF_6 using a quadrupole mass spectrometer/computer system in a closed loop mode. The results of a series of measurements on natural uranium samples are discussed. A typical internal precision of about 10^{-4}% for the $^{235}U/^{238}U$ ratio was obtained.

KEYWORDS: Quadrupole mass spectrometer, uranium isotope analysis, uranium hexafluoride, nuclear safeguards, precision

INTRODUCTION

Nuclear materials under safeguards are present in the fuel cycle in various physical states, chemical compositions and isotopic abundances. The ease of access for measurement, containment, surveillance and identification will vary from convenient to extremely difficult, depending upon the particular key measurement point in the nuclear fuel cycle.

From the point of view of nuclear safeguards, uranium enrichment plants for industrial scale production of uranium enriched to about 3% of U-235 play an important role due to the diversion potential at such facilities.

Material accountability is the basic and amost direct means to safeguards a nuclear facility against a misuse. For those concerned with safeguarding instalations for uranium enrichment, one of the major tasks is the establishment of material balances which call for precise and fast methods for the knowledge of the U-235 of the facility.

Besides the nuclear safeguards aspects, the economic operation of an enrichment plant also requires means to monitor the purity and the isotopic abundances of circulating uranium hexafluoride gas at different stages of enrichment and for controlling the final product.

The mass spectrometry, primarily because of its precision and accuracy capacibilities has proved to be the most valuable of the several techniques available for determining the isotopic composition of uranium. Magnetic mass spectrometers have been used for many years and have proved satisfatory for precise isotopic measurement of uranium hexafluoride gas.

For such reasons as compacteness, fast scanning, low expediture, ease of operation and maintenance and reliability over long period the quadrupole mass spectrometers apperars to offer attractive possibilities for routine measurements of U-235 content in uranium hexafluoride. The errors resulting from the fluctuations in the intensities of the ion currents measured sequentially - the double collector technique is precluded in QMS - could be minimized by adequate automatic operation.

The purpose of this paper is to present and discuss the preliminar results obtained for the isotope ratios U235/U238 in uranium hexafluoride samples using a gas quadrupole mass spectrometer/computer system in a closed - loop mode.

The operation of the mass spectrometer in a closed-loop mode enables fully automatic control of the mass spectrometer as well as data acquisition and data processing. Besides the isotopic measurement the system can also be used to investigate and determine the presence of gas impurities in the uranium hexafluoride samples.

URANIUM HEXAFLUORIDE ISOTOPIC MEASUREMENTS

The analytical system for isotope and impurities determination of UF_6 consists of a digitally controlled quadrupole mass spectrometer interfaced to a PDP 11 type computer.

Basically the mass spectrometer consists of a quadrupole mass analyser, a Faraday cup ion detector, a molecular beam inlet integrated in the electron impact ion source and a liquid nitrogen cold trap which involves both the ion source and the molecular beam device acting as an effective cryogenic pump for the uranium hexafluoride gas. A conventional dual sample manifold permits alternate measurements using reference materials.

The closed-loop operation of the mass spectrometer/computer system is performed by acquiring data from the mass spectrometer, evaluating them by the computer and thereafter changing the mass spectrometer settings under computer control, acquiring data again and so forth. Adequate provisions covering both the hardware of the QMS (ion source, rod system, eletronic supply unit and ion current amplifier) and the software (procedure of measurement)permits to minimize the errors resulting from fluctuations of the absolute ion intensities measured sequentially. Memory effects and damage of the ion source parts are reduced since the UF_6 is introduced via a well collimated molecular beam.

The computer control of the quadrupole mass spectrometer allows adequate procedures for sample handling and measurement. To measure 235U/238U ratio the QMS is set to mass 327 for base line measurement, to 330 ($^{235}UF_5^+$) and 333 ($^{238}UF_5^+$). After the measurements of these intensities, the program starts again for the next cycle by scanning the peak top 333 and remeasuring the intensities on the masses 327, 330 and 333. After a preselected number of cycles the program calculates the mean value, the standard deviation of the measured isotope ratios and the correction factor for the contribution of the isotope ^{234}U to the intensity of the peak 330.

The samples of uranium hexafluoride used in this work were prepared from uranium oxide throug the cobaltic fluoride technique. Three ampoules of UF_6 were prepared. Prior to each measurement the ampoules were cooled to $-80^{o}C$ and evacuated for possible impurities, and later heater again to room temperature at which point, the gas is let into the mass spectrometer. For each uranium hexafluoride sample, isotope measurement of twenty groups, each having nine cycles, were measured. The results for these measurements are shown in the Table I. The Table II presents the grand mean of the isotopic ratios and the internal variance determined from the experimental results for each samples. The relative deviations of the group means from the grand mean for each sample have been represented in Figures 1 to 3. The error bars denote the relative standard deviation of the group means.

CONCLUSIONS

The results obtained show that under adequate automatic operation measurements of isotope ratio U235/U238 in uranium hexafluoride can be performed by quadrupole mass spectrometry with satisfatory precision. It therefore seems useful to carry out measurements on reference samples of uranium hexafluoride with diferents degrees of enrichment before arriving at a final conclusion.

Table I : Results of the isotopic uranium ratios for the samples 1 to 3

Number of groups	SAMPLE 1		SAMPLE 2		SAMPLE 3	
	$R_{corr.}$ $\frac{U\text{-}235}{U\text{-}238}$ (%)	$\sigma \times 10^{-3}$	$R_{corr.}$ $\frac{U\text{-}235}{U\text{-}238}$ (%)	$\sigma \times 10^{-3}$	$R_{corr.}$ $\frac{U\text{-}235}{U\text{-}238}$ (%)	$\sigma \times 10^{-3}$
01	0.724485	0.035929	0.722155	0.258404	0.724164	0.059418
02	0.724281	0.106573	0.722457	0.411513	0.723655	0.417085
03	0.724143	0.271601	0.722190	0.787334	0.723827	0.604447
04	0.724148	0.114106	0.722126	0.192250	0.723436	0.207461
05	0.723728	0.307097	0.722215	0.493908	0.723703	0.292302
06	0.722543	0.566302	0.722345	0.804811	0.723388	0.361559
07	0.723500	0.326226	0.722474	1.003480	0.723396	0.445927
08	0.722913	0.370046	0.722295	0.259098	0.723524	0.259995
09	0.722745	0.213172	0.721972	0.360878	0.723315	0.326269
10	0.723202	0.909370	0.721679	0.964711	0.723984	0.236144
11	0.722618	0.114134	0.721230	1.412340	0.723308	0.237291
12	0.722135	0.487419	0.721718	0.552097	0.723782	0.605249
13	0.722125	0.445734	0.721380	0.599467	0.723593	0.513284
14	0.722118	0.163554	0.722338	0.303822	0.723949	0.166370
15	0.724279	1.862570	0.721350	1.003510	0.724153	0.582735
16	0.724152	0.291755	0.721079	0.347259	0.724010	0.473178
17	0.724244	0.583643	0.721846	1.031040	0.723935	0.234230
18	0.723739	0.661111	0.721986	1.551200	0.724128	0.443368
19	0.723667	0.750820	0.722162	1.405380	0.724020	0.186869
20	0.722986	0.753281	0.721547	0.828871	0.724056	0.356765

Table II : Results of the grand means and internal variances for the samples 1 to 3

SAMPLE	R (%)	$Sin^2 \times 10^{-8}$
01	0.723393	3.8130892
02	0.721927	8.7848667
03	0.723766	2.0626709

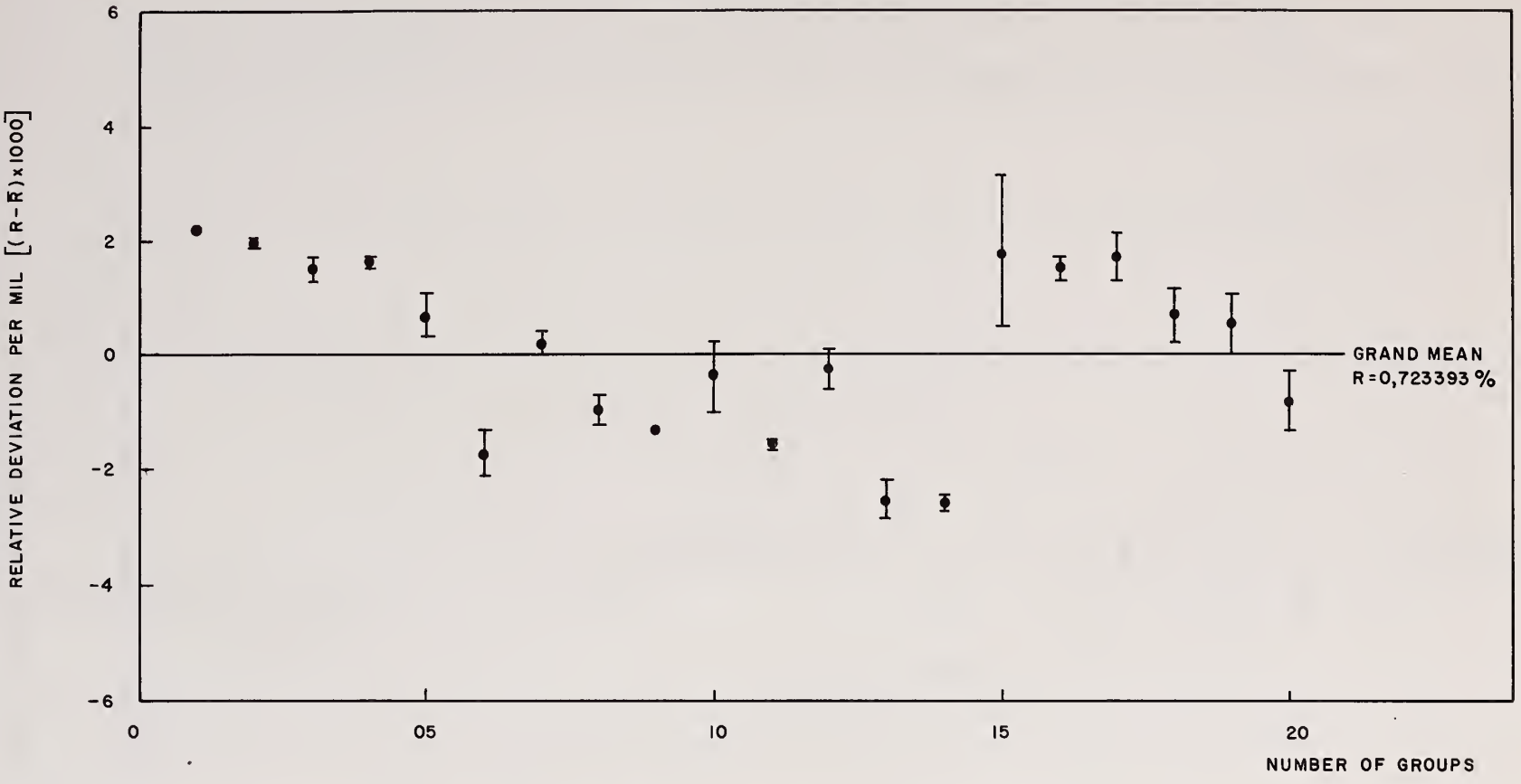

FIGURE I – DEVIATION OF THE GROUP MEANS FROM THE GRAND MEAN (ERRORS BARS INDICATE THE RELATIVE STANDARD DEVIATION OF GROUP MEANS)

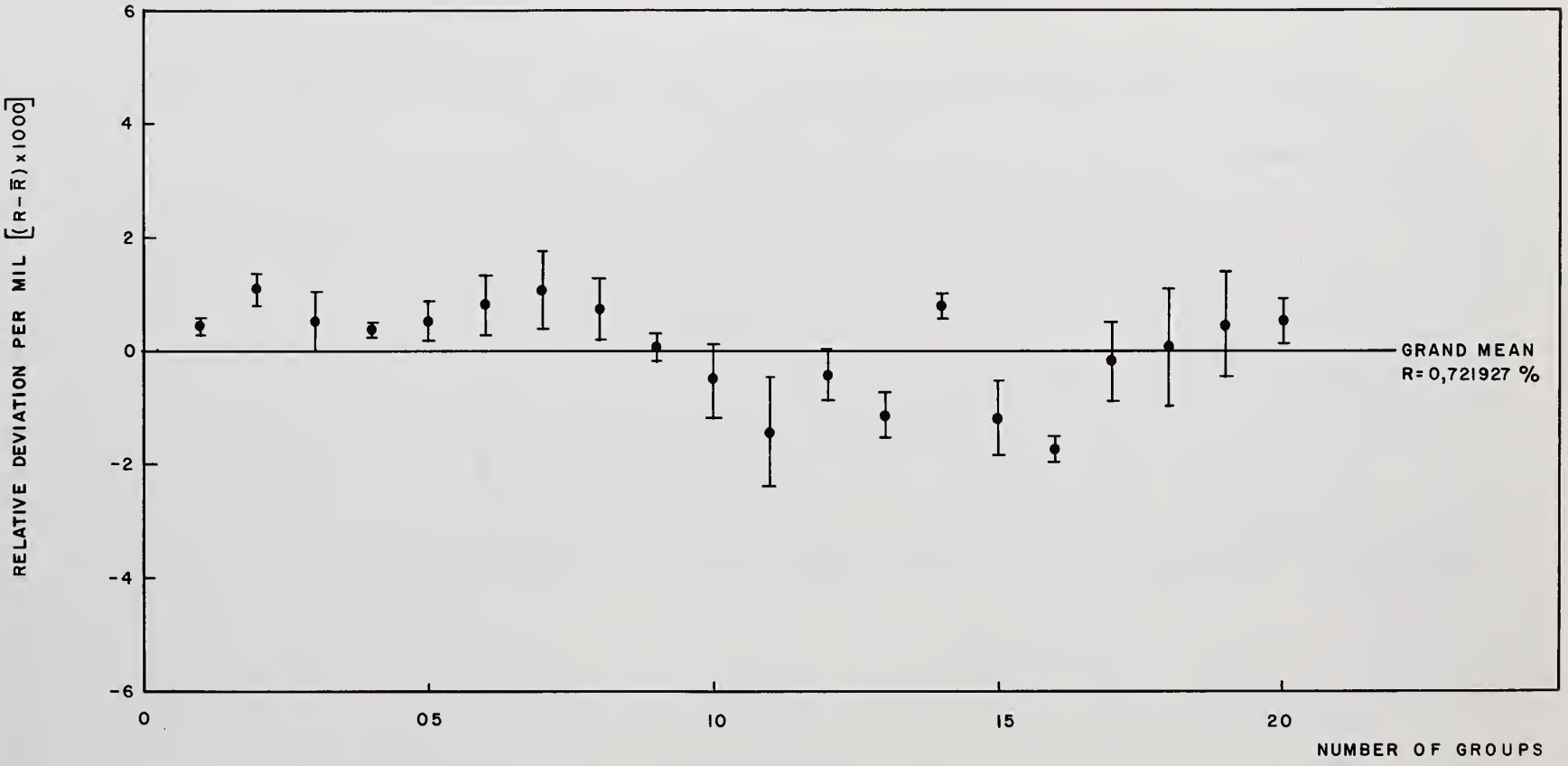

FIGURE 2 – DEVIATION OF THE GROUP MEANS FROM THE GRAND MEAN (ERRORS BARS INDICATIVE THE RELATIVE STANDARD DEVIATION OF GROUP MEANS)

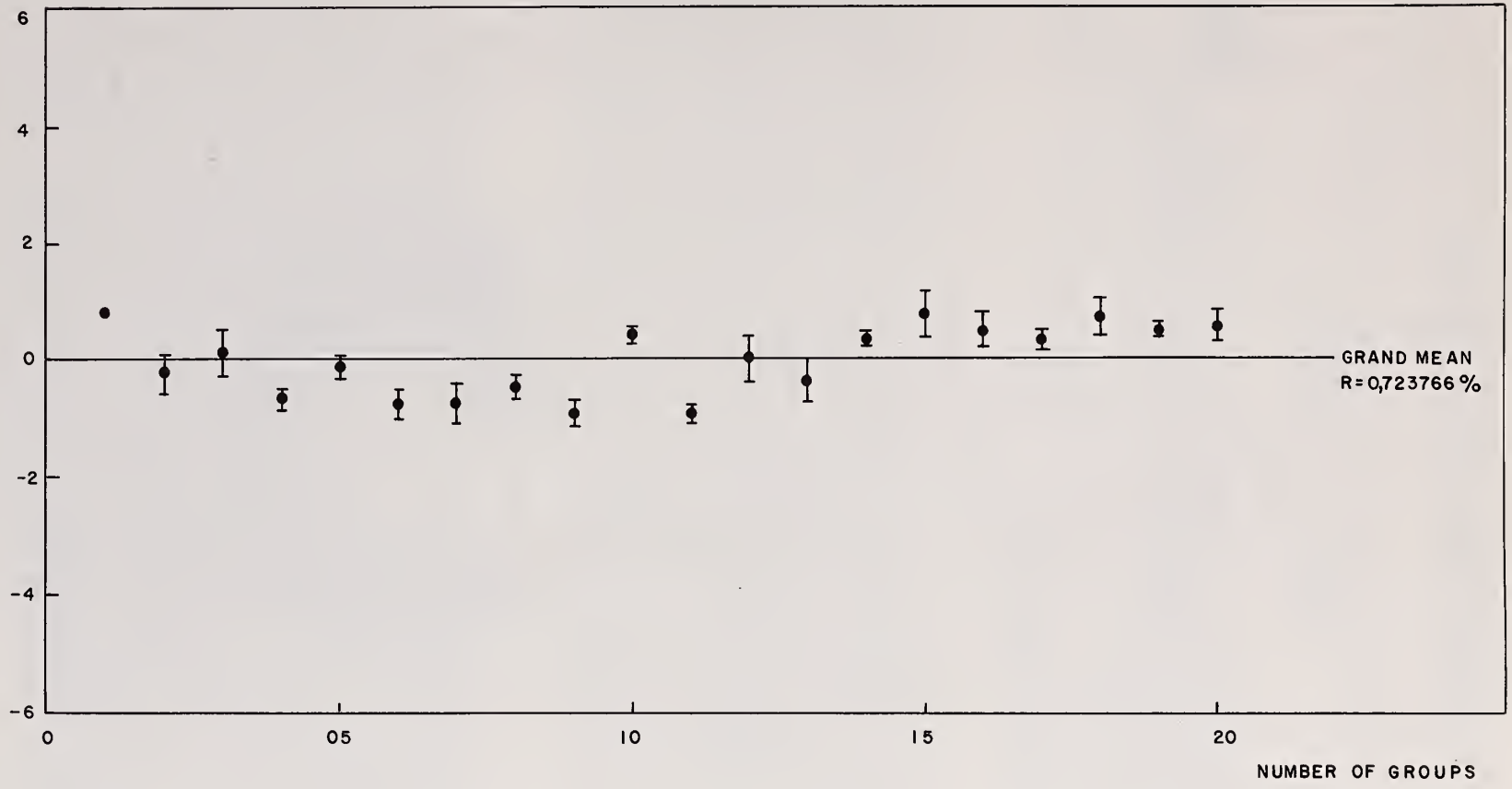

FIGURE 3 – DEVIATION OF THE GROUP MEANS FROM THE GRAND MEAN (ERRORS BARS INDICATE THE RELATIVE STANDARD DEVIATION OF GROUP MEANS)

Safeguards Reference Measurement System Utilizing Resonance Neutron Radiography

by

R. A. Schrack, J. W. Behrens, C. D. Bowman, and A. D. Carlson
National Bureau of Standards
Washington, DC 20234, USA

ABSTRACT

A resonance neutron radiograph system is being developed to provide a reference method for nondestructive assay (NDA) measurements for the safeguards program. Initial tests have produced radiographs of 5 mm and 1 mm resolution and determined the uranium content of commercial reactor fuel pellets.

[Epithermal neutron energy, neutron radiography, nondestructive assay, position-sensitive proportional counter, uranium.]

INTRODUCTION

A resonance neutron radiography system is being developed at the National Bureau of Standards to provide a reference method for nondestructive assay (NDA) measurements for the safeguards program. Although the special properties of the technique recommend its use as a reference system, it may also be attractive in special field measurement systems.

Nondestructive assay techniques are generally dependent to some degree on the matrix of materials contaning the material to be measured. Because of the measurement technique employed in resonance neutron radiography, it is possible to provide an assay of an isotope in a mixture without interference from other materials. The method therefore promises a singificant advantage in terms of isotopic and elemental discrimination over thermal neutron radiography, which is a well-developed analytical method. Resonance neutron radiography probably will fall short of thermal neutron radiography in terms of image quality. Previous work on neutron radiography has been reported which utilized a variety of neutron sources and detector systems, and a review of early work has been published by Berger.[1,2,3,4]

EXPERIMENTAL ARRANGEMENT

The experimental arrangement is shown in Fig. 1. The neutrons are produced in a water-moderated tungsten target by the pulsed electron beam from the NBS linac. The linac is typically operated at 100 MeV with an average current of 30 μA, producing a pulse of electrons 0.5 μs long at a rate of 720 pps. The detector is a position-sensitive proportional counter (PSPC) placed 4.4 meters from the neutron source. The object to be radiographed is placed on a carrier that can be incrementally moved under computer control. The neutron beam is collimated into a narrow fan-shaped beam so as to provide even illumination of the position-sensitive detector. The object is then placed in the beam, and the neutron transmission as a function of energy is determined by time-of-flight for successive increments of the object carrier. The position-sensitive detector has a resolution of about 1% of its length. Data can be stored in the computer memory tagged for energy and position. An image of the object can thus be generated by storing information for each elementary picture element (or pixel). For each pixel we have stored a time-of-flight spectrum for neutron energies ranging from 0.5 eV to 20 eV. By analyzing an energy region of the spectrum containing a large resonance in the neutron total cross section unique to a particular isotope, the number of atoms of that isotope in the pixel area can be determined. From the knowledge of each pixel, the distribution and quantity of the isotope in the sample can thus be determined.

The first test of the concept was carried out with a commercially available PSPC having a sensitive length of about 20 cm and a resolution of about 5 mm.[5] A test object was constructed, shown in Fig. 2, which consisted of brass and stainless steel discs which were brazed together with silver solder.[6]

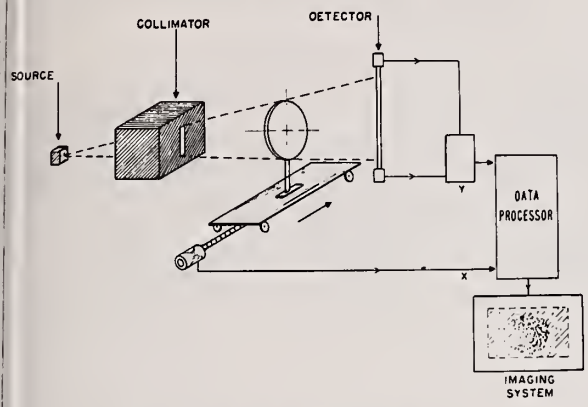

Fig. 1. Resonance Neutron Radiograph System

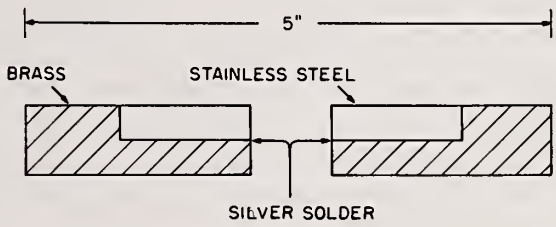

Fig. 2. Cross Section of Silver Solder Test Object

A defect was deliberately introduced in the silver solder. Conventional x-ray analysis of the object did not reveal the defect. Thermal neutron radiography disclosed variations in density but did not indicate clearly the magnitude of the imperfection. A resonance neutron radiograph using the 4 eV resonance of ^{109}Ag clearly shows, in Fig. 3, the density and distribution of the silver with no interference from any of the other elements in the discs. This figure represents 650 pixels (25 x 26). Each pixel measures 3 mm x 3 mm.

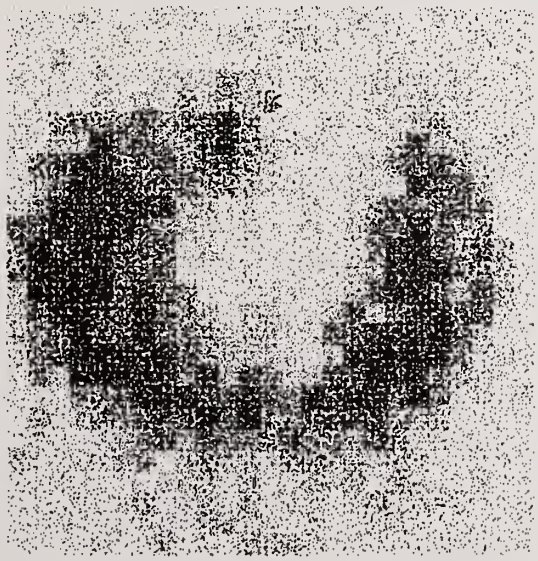

Fig. 3. Resonance neutron radiograph of silver solder joint. The defect in the solder is clearly visible.

While this experiment demonstrated interesting prospects for large objects of interest in the safeguards program, such as waste cans, the application to smaller objects, such as fuel elements, requires higher resolution. In collaboration with ORNL a small high-resolution PSPC was developed having a sensitive length of 5 cm and a resolution of about 1 mm.[7] This PSPC, shown in Fig. 4, operates at a pressure of 3 atm ^{3}He, 8 atm Xe, and 0.5 atm CO_2. Position sensing was obtained with RC-encoding electronics.[8]

This detector has been used to obtain a neutron radiograph of fresh nuclear fuel pellets 1 cm in diameter and 1 cm in length weighing about 9 grams.[9] The results of a single scan are shown in Fig. 5. These data took about 8 hours to collect. The relative transmission for the total neutron spectrum from about 1 eV to about 12 eV is shown as a function of position. The figure has a resolution of about 0.6 mm/channel, about half the intrinsic resolution of the detector. The neutron total cross sections used for the resonance analysis of the ^{235}U and ^{238}U content were obtained from BNL and are shown in Fig. 6. The ^{235}U cross section has a number of isolated resonances that have no interference from other isotopes, but the large ^{238}U resonance at 6.6 eV is straddled by substantial resonances in ^{235}U. This intereference caused no problem with the analysis.

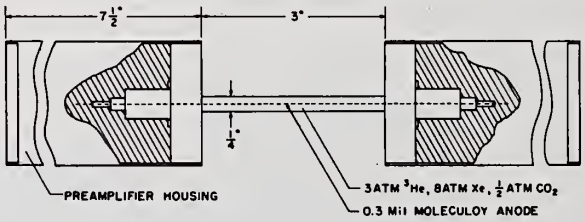

Fig. 4. High resolution position sensitive proportional counter.

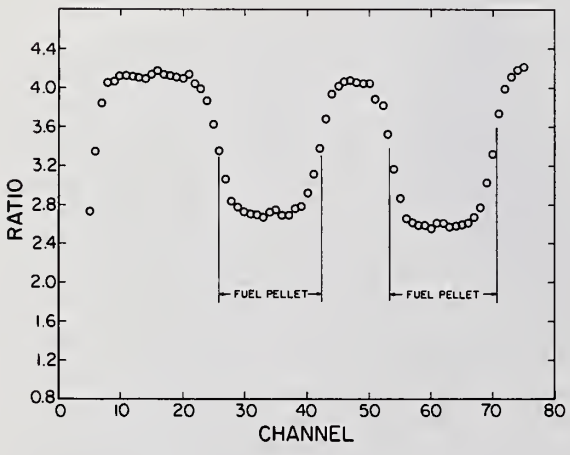

Fig. 5. Resonance neutron radiograph scan of fuel pellets.

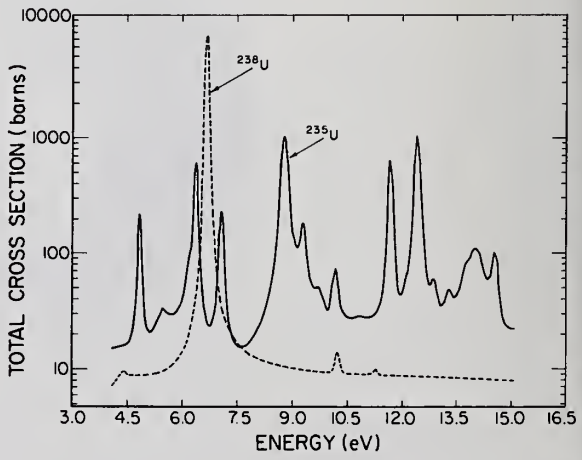

Fig. 6. The neutron total cross sections for ^{235}U and ^{238}U from 4 to 15 eV. These cross sections are Doppler-broadened ENDF/B-IV files as supplied by BNL.

The technique of analysis used was a non-linear fitting program, with initial values determined by a linear least squares fit routine. The linear least squares fit routine cannot give a correct answer because the energy resolution of the experimental system cannot be introduced correctly into the linear least squares fitting algorithm. The effects of resolution in the experiment were taken into account in the following way. The observed neutron transmission is given by:

$$T(E_o) = \int_{-\infty}^{+\infty} R(E_o, E_n) T(E_n) dE_n$$

where E_o is the observed neutron energy

E_n is the actual neutron energy

$R(E_o, E_n)$ is the response function of the experiment

and

$$T(E_n) = \exp\left\{ - \sum_{i=1}^{m} n_i \sigma_i(E_n) \right\}$$

where m is the number of isotopes

n_i is the atoms/barn of the ith isotope

and $\sigma_i(E_n)$ is the neutron total cross section in barns/atom of that isotope.

The response function R of the experiment was determined by fitting the shape of the narrow resonances in ^{235}U at 11.6 eV and 12.4 eV. The response function has a width of about 2.5 channels and a small tail about 10 channels long extending in the direction of higher channels. By taking the logarithm of the observed transmission (and neglecting the response function) one obtains a data set:

$$- \log \left(T(E) \right) = \sum_{i=1}^{m} n_i \sigma_i(E)$$

that can be fit with a linear least squares procedure using the cross sections $\sigma_i(E)$ as basis functions.

This concept was tested with data that were synthesized from the basic cross sections, and counting statistics simulated by the Poisson distribution, and the experimentally determined resolution function.

The linear least squares fit to this synthetic data resulted in values of n_i (atoms/barn for the isotope) within only 30% of the true value used to develop the synthetic data. The results of the linear least squares fit were then used as starting values in a non-linear least squares fitting program that did correctly include the response function of the experimental system. The non-linear fitting procedure did in all cases converge to within a couple of percent of the correct value. When data having an average count of 10,000 per channel were synthesized and then analyzed, the mean value of the isotopic abundance of ^{235}U for 8 tries was 0.994 of the true value, with a standard deviation of the mean of 0.9%. The same procedure with 1,000 counts/channel data yielded a result that was 1.01 times the true value and a standard deviation of the mean of 2%.

Once the analysis procedure was shown to operate effectively, the data from the experiment shown in Fig. 5 were analyzed.

To obtain a better statistical precision, the data of channels 54 through 68 of Fig. 5 were summed to obtain about 1000 counts/channel. The resultant time-of-flight spectrum for the transmission is shown in Fig. 7. The solid curve is the best fit that was obtained to the data.

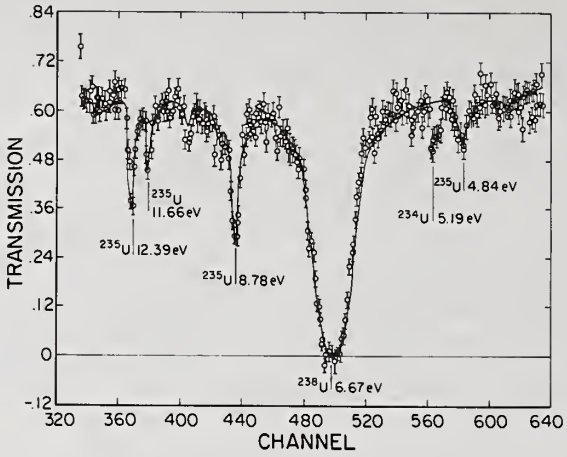

Fig. 7. Transmission data for nuclear fuel pellet.

The values obtained were

$$0.417 \pm .005 \text{ g/cm}^2 \ ^{235}\text{U}$$

$$10.120 \pm .150 \text{ g/cm}^2 \ ^{238}\text{U}$$

$$\text{or } 4.01 \pm .08\% \ ^{235}\text{U}$$

The pellet was analyzed by a scintillation spectroscopy technique by the manufacturer and found to have a relative abundance of

$$3.96 \pm .005\% \ ^{235}\text{U}$$

The mean value obtained by resonance neutron radiography is thus about 1% different from the accepted value, well within the 2% error. This error includes the statistical and systematic errors. The systematic errors are associated with timing, flight path, response function, cross section, background, and normalization uncertainties. The statistical uncertainty can be reduced by increasing the total accumulated counts, and the systematic errors can be eliminated by a calibration run of the system using a known thickness of uranium or some other isotope having a resonance in the same energy region.

There is a small amount of ^{234}U also in the sample as can be seen in Fig. 7 by the small dip at 5.19 eV. This could have been included in the analysis by the addition of the additional basis function of the ^{234}U neutron total cross section. An area analysis of the resonance gave a value within about 6% of the expected value, which is about the uncertainty associated with the statistical precision.

The pellet shown at channels 28 through 39 in Fig. 5 was also analyzed by summing the data together. There is less ^{235}U in this pellet and the analysis is thus much less precise. The relative abundance as determined by resonance neutron radiograph is:

$$^{235}\text{U} = 1.10 \pm 0.06\%$$

The value supplied by the manufacturer is:

$$^{235}\text{U} = 1.19 \pm .005\%.$$

Here the mean value of the result obtained by resonance neutron spectroscopy is about 8% different from the value given by the manufacturer. We attribute this to the poor statistical precision of the experiment.

DISCUSSION

The theory and experimental realization of resonance neutron radiography indicate the ability to determine the amount and distribution of isotopes without interference. Improvement in the statistical precision will allow higher precision in determination of the amount of material and higher resolution in the distribution description. We are now involved in several programs that will allow us to increase greatly the rate of data accumulation. Two-dimensional detector systems are being developed that will allow data to be collected for all the pixels at once and eliminate the need for systems that require multiple scans of an object. In addition, higher speed electronic and computer systems are being acquired that will permit the acquisition of more than one event per linac pulse.

Studies have also been made of methods of neutron production. In a recent paper it has been shown that a small low-energy single-section linac in combination with a low-Z photoneutron source can have as high or higher efficiency of neutron production as a conventional high-energy linac and high-Z photoneutron source.[10] The development of a small, relatively inexpensive, neutron source of this type would allow for the practical and effective use of resonance neutron radiography in installations outside a research laboratory.

We are also investigating the ability to analyze spent fuel to determine the distribution of the uranium and plutonium isotopes for use in isotope correlation studies. In addition, we are investigating the feasibility of in-line analysis of dissolver solution in a reprocessing plant.

ACKNOWLEDGMENTS

We would like to acknowledge the contributions to this paper by many people, especially Rolf Leicht for his non-linear least squares program and Ron Johnson for his image reconstruction program.

The assistance of the NBS Linac operators is also acknowledged. Without their assistance no results would have been possible.

This work is sponsored in part by the U.S. Nuclear Regulatory Commission.

REFERENCES

1. H. Berger, Neutron Radiography Methods, Capabilities, and Applications (Elsevier Publishing Co., New York, 1965).

2. L. Forman, C.U. Benton, D.A. Garrett, and A.D. Schelberg, Rev. Sci. Instrum. 41, 1900 (1970).

3. S. Kaplan, K. Valentine, L. Kaufman, V. Perez-Mendez, "Neutron Radiography with a Multiwire Proportional Chamber-Performance and Projections", Trans. Am. Nucl. Soc. 15, 140 (1972).

4. H.G. Priesmeyer and U. Harz, Atomkernenergie 25, 109 (1975).

5. Reuter-Stokes, Inc., Cleveland, Ohio.

6. J.W. Behrens, R.A. Schrack, C.D. Bowman, Trans. Am. Nucl. Soc. 32, 207 (1979).

7. M.K. Kopp and J.A. Williams, Instrumentation and Controls Division, Oak Ridge National Laboratory, Oak Ridge, Tennessee.

8. C.J. Borkowski and M.K. Kopp, Rev. Sci. Instrum. 46, 951 (1975).

9. General Electric Company, Wilmington, North Carolina.

10. C.D. Bowman, "Efficient Neutron Production Using Low-Energy Electron Beams", Proceedings of the International Conference on Nuclear Cross Sections for Technology, Univ. of Tennessee, USA, Oct. 22-26, 1979.

Accurate in-situ Assay of Total Fissile Isotopes in Inputs of Reprocessing Plants: a Reference Method or a "Definitive" Method?

by

W. LYCKE, M. GALLET, F. PEETERMANS, R. DAMEN, E. BOUWMEESTER,
P. DE BIEVRE, J. VAN AUDENHOVE
Central Bureau for Nuclear Measurements Geel, Joint Research Centre,
Commission of the European Communities

ABSTRACT

The solid spike method previously established and used by this laboratory to assay fissile isotope concentrations in-situ in undiluted input samples from reprocessing plants, has been improved considerably for Pu by replacing previously used $^{235}U/^{239}Pu$ solid spikes by $^{235}U/^{242}Pu$. Results of plant tests are given indicating a same 0.3 % standard deviation on a single determination for both U and Pu. Comparison with the former method is made.

Also presented are the results of the first laboratory tests of an extension of the above-mentioned method to include the determination of the total mass of a solution using again isotope dilution mass spectrometry.

The combination of both methods, concentration and total mass determination, allows the in-situ assay of total U and total Pu in any input batch of a reprocessing plant.

KEYWORDS: Input concentration, total mass, uranium, plutonium, neodymium, spike, blend, isotope dilution, alloys, safeguards,

1. INTRODUCTION

All determinations of U and Pu concentrations in inputs of reprocessing plants use diluted input samples (dilution factor 100-250) to reduce a) radiation b) $^{233}U/^{242}Pu$ spike consumption. The dilution process either by weight or by volume must be performed in a hot cell and carries its uncertainty. Also the risk of contaminating diluted samples in a cell where much more concentrated solutions are present, is not negligible.

In order to know total amount of U and Pu (or fissile isotopes), the volume or mass of the accountability tank solution must also be known. This is done by such methods as volume calibration, dip tube manometer or direct weighing. A density measurement and consequently a temperature determination must be carried out. These methods, however, may not be the most reliable in terms of accuracy on the mass of the solution and they are installation-dependent, i.e. they require active cooperation from the operator through reliable data of tank calibration, assurance that no changes have been made, etc.

The approach taken by this laboratory to the problem of highly reliable assay of total U and Pu in an input accountability tank have been led by the following considerations from the start:

1. the assay should be performed on undiluted samples
2. no high consumption of expensive spike isotopes can be tolerated
3. volume measurements (either when diluting samples or measuring tank volumes) should be avoided as they are not accurate enough and temperature dependent
4. the inspector (and/or his verification laboratory) should be the only person(s) who can calculate final results of verification measurements
5. the verification measurement should contain a mechanism to warn that the verification measurement is reliable or went wrong in some step (all measurements are likely to go wrong at some time).

Earlier work of this laboratory[1,2] was focussed on determination of U and Pu concentrations by isotope dilution mass spectrometry (IDMS) and fulfilled the above-mentioned requirements: homogeneous U/Pu alloys were prepared for use as solid spikes. They were made of ~ 93 % enriched ^{235}U and ~ 97 % ^{239}Pu. They allowed :

1. to spike an undiluted sample because a sufficiently large amount of spike could be used (^{235}U and ^{239}Pu are abundantly available)
2. to avoid consumption of expensive highly enriched ^{233}U and ^{242}Pu spike isotopes
3. to circumvent the dilution of the sample in a hot cell.

This approach led to U and Pu concentration determinations in inputs with an accuracy of 0.3 % and 2 % respectively. It was frequently used in operational reprocessing plants in Europe in the period 1972-1979, but in order to attain 1-2 % accuracy on Pu concentrations, high precision Pu isotope ratio measurements were required to measure the small change induced in a sample with say $^{239}Pu/Pu = 0.70$ by means of a spike with $^{239}Pu/Pu = 0.97$ resulting in a blend say with $^{239}Pu/Pu = 0.85$.

Two problems remained unsolved:

a) the larger uncertainty on Pu determinations
b) the determination of the total mass of the solution.

2. REDUCING THE UNCERTAINTY OF Pu MEASUREMENTS

2.1 Theoretical

^{242}Pu metal was expected to reduce the uncertainty of Pu measurements to the same value as for U i.e. a few ‰. However the large spike consumption per spiking process (~ 1 mg to spike 1 g solution containing ~ 1 mg Pu/g) precludes the use of expensive and rare highly enriched ^{242}Pu. The amounts available to us were anyway too small for conversion into metal needed for preparation of solid spike alloy. Close examination of the isotope dilution proces and its error propagation, showed that assay by isotope dilution is based on the measurement of the change of an isotope ratio $R = {}^{242}Pu/{}^{239}Pu$ in the sample (R_x) by diluting it with the isotope ratio of the spike (R_y) into a blend ratio R_B. For the simplest case, we have $R_x = 0$ (pure 239), $R_y = \infty$ (pure 242) and $R_B = 1$ (when a number N_x of element atoms in the sample are mixed to an equal number N_y of element atoms in the spike). It follows that

$$\frac{N_x}{N_y} = R_B \qquad (2.1)$$

The uncertainty on N_x is equal to the sum of uncertainties on R_B and the spike N_y. Because N_y is known (= spike), N_x can be calculated from a measurement of R_B. When sample and spike are not isotopically pure, the following equation applies [3]

$$\frac{N_x}{N_y} = \frac{R_y - R_B}{R_B - R_x} \cdot \frac{\Sigma R_{ix}}{\Sigma R_{iy}} \qquad (2.2)$$

where ΣR_i is the sum of all isotope ratios (all referred to the same reference isotope, in this case ^{239}Pu).
Now we had relatively large amounts of lower enriched ^{242}Pu available ($^{242}Pu/Pu = 0.87$). Table I gives its isotopic composition next to that of a typical input Pu to be determined for concentration.

So for a 1 to 1 spiking of sample and spike amount

$$\frac{N_x}{N_y} = \frac{162.28 - 1.54}{1.54 - 0.076} \cdot \frac{1.69}{185.19} = 1.00 \qquad (2.3)$$

---

[1] P. De Bièvre, J. Van Audenhove, An accurate procedure to safeguard the fissile material content of input and output solutions of reprocessing plants, IAEA-SM-201/108, Proc. Symp. Safeguarding Nuclear Materials, Wien, October 1975

[2] P. De Bièvre, J. Broothaerts, M. Gallet, A. Loopmans, E. Sattler, J. Van Audenhove, Performing accurate measurements of fissionable material for Safeguard purposes in reprocessing plants in Europe, Proc. 17th Ann. Meeting INMM June 1976, Nucl. Mat. Man. V, 478-484 (1976)

[3] P. De Bièvre, G.H. Debus, Precision mass spectrometric isotope dilution analysis, Nucl. Instr. Meth. 32, 224-228 (1965)

One observes that systematic errors on R_y and ΣR_{iy} are about the same and of the same sign. It therefore cancels out in Equation (2.2) ($R_B \ll R_y$). On the other hand the uncertainty on ΣR_{ix} is very small and is almost negligible in the error propagation of Equation (2.2). Since $R_x \ll R_B$, the uncertainty on R_B determines essentially the uncertainty on N_x/N_y. We conclude that the main uncertainty contribution comes from the measurement of R_B and for reasonable enrichments say > 50 % in sample (^{239}Pu) and spike isotope (^{242}Pu) the limiting accuracy of the isotope dilution assay is the accuracy of the R_B measurement[3].

Pu isotope dilution can be performed with lower ^{242}Pu enrichments[4]. Consequently the $^{242}PuO_2$ ($^{242}Pu/Pu = 0.87$) was converted into metal* for subsequent use in solid spikes.

Table I

Isotopic composition of a typical reactor-grade Pu and of the spike used

	Input Pu x	Spike y
Isotopic composition (atom %)		
^{238}Pu	1.3	1.01
^{239}Pu	59.1	0.54
^{240}Pu	23.7	8.52
^{241}Pu	11.4	2.28
^{242}Pu	4.5	87.63
^{244}Pu	-	0.02
R_x ($^{242}Pu/^{239}Pu$)	0.0760	
R_y (id.)		162.278
238/239	0.0219	1.8704
239/239	1	1
240/239	0.400	15.778
241/239	0.192	4.222
242/239	0.076	162.278
244/239	-	0.04
ΣR_i	1.69	185.188

2.2 Preparation and Characterization of the $^{235}U/^{242}Pu$ alloy

9.964 g U ($^{235}U/U = 0.85$) and 0.516 g ^{242}Pu ($^{242}Pu/Pu = 0.87$) were weighed, brought into the induction coil of a high frequency levitation unit (see Fig. 1), levitated contact-free until a white-hot molten drop was obtained (see Fig. 2). After vigorous stirring of the melt by the induced Faraday currents to homogenize the melt, the alloy was quenched in a water cooled copper crucible and weighed again.

mass before levitation	mass after levitation
9.964 g U	
0.516 g Pu	
10.480 g	10.4771 g

Even if all the loss would have to be ascribed to the minor component (worst case), the relative error on its concentration would still be less than 0.6 %, but this is very unlikely.

The alloy was then divided into small pieces of about 40-60 mg. Each of them were individually weighed to a certified ± 0.01 mg (i.e. to 0.02 %) and thus constituted a "solid spike". A series of 5 solid spikes were then characterized by isotope dilution against NBS 950 a U_3O_8 and NBS 944 Pu sulphate. Results are given in Table II.

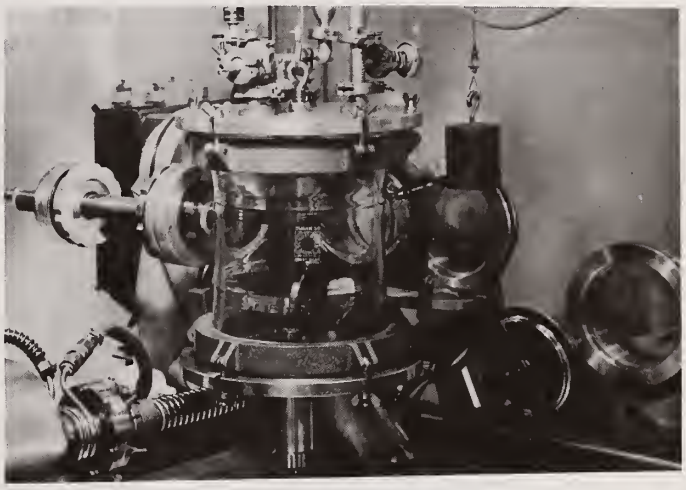

Fig. 1 High Frequency Levitation Unit

Fig. 2 Induction coil with a white-hot molten drop

* at CEA, Fontenay-aux-Roses

[4] P. De Bièvre, Isotope Dilution of the Actinide Elements, Proc. 26th Ann. Meeting Amer. Soc. Mass Spec. (1978)

Table II

Characterization of solid spikes ^{235}U - ^{242}Pu.

Spike number	Pu element concentration (%)	U element concentration (%)
44	0.5560	99.16
53	0.5544	99.08
62	0.5535	99.22
80	0.5531	98.99
85	0.5557	99.19
	0.5545	99.13
	± 0.0013	± 0.10
Leviation synthesis	0.558 ± 0.003	

2.3 Application of $^{235}U/^{242}Pu$ solid spikes to operational reprocessing plants

An undiluted sample of a true reprocessing campaign on typical Power Reactor spent fuel was obtained from the Karlsruhe reprocessing plant (WAK) and transferred to the hot cell of the KFK-IRCh.

6 samples 1 g each were taken (series 130 ... See Table III) and weighed in one day and all of them spiked in one day. The spike was allowed to dissolve at about 60° C. To ensure complete dissolution of input particles and spike, a few drops of HF were added. A fraction of this spiked sample was then transferred to CBNM Geel, valency homogeneized and fission products separated. Careful preparation for mass spectrometric isotope ratio determination was performed incl. U/Pu separation. Results are summarized in Table III.

Table III

Determination of Pu and U concentration in undiluted input samples with the aid of ^{235}U - ^{242}Pu solid spikes.

1st series. Spiking on same day

Sample number	Sample-taking Weighing Ali	Spiking	mg Pu/g solution	mg U/g solution
AS I /130 - 101	25.01.78	30.01.78	1.4800	182.686
AS II /130 - 201	"	"	1.4891	184.034
AS III/130 - 301	"	"	1.4826	183.930
AS IV/130 - 401	"	"	1.4800	182.961
AS V /130 - 501	"	"	1.4833	184.370
AS VI/130 - 601	"	"	1.4733	183.590
			1.4813	183.595
			s = ± 0.35 %	s = ± 0.37 %
			spread: 1.08 %	spread: 0.92 %
			U/Pu = 124.04 ± 0.35 %	

In parallel another 6 samples (series 139... in Table IV) were spiked with $^{235}U/^{239}Pu$ solid spikes and treated the same way. See results in Table IV.

Another series (series 140... in Tables V and VI) of 6 samples were aliquoted and spiked with $^{235}U/^{242}Pu$ spikes on different days and further prepared similarly for measurements. See results in Table V for Plutonium and Table VI for Uranium.

In order to separate weighing accuracies in the hot cell (estimated at 0.1-0.2 %) and possible inhomogeneities from particulate matter (estimated at a possible 0.1 % from other experiences[5], the first 3 samples of each series were divided in 3 parts, each of them

5G. Bortels, P. De Bièvre, I.L. Barnes, K.M. Glover, Characterization of the samples used in the AS-76 Interlaboratory Experiment on the Determination of ^{238}Pu, Proc. 1st Ann. Symp. Safeguards & Nucl. Mat. Man. pp 380-387 (1979)

Table IV

Determination of Pu and U concentration in undiluted input samples with the aid of ^{235}U - ^{239}Pu solid spikes.

Spiking on the same day

Sample number	Sample-taking Weighing Ali	Spiking	mgPu/g solution	mg U/g solution
AS I /139 - 101	25.01.78	26.01.78	1.4859	182 81
AS II /139 - 201	"	"	1.4920	183 61
AS III/139 - 301	"	"	1.4771	183 19
AS IV/139 - 401	"	"	1.4972	182.08
AS V /139 - 501	"	"	1 4937	182.28
AS VI/139 - 601	"	"	1.4666	182.41
			1.4854	182.73
			s = ± 0.78 %	s = ± 0.32 %
			spread: 2.07 %	spread: 0.84 %

valency homogeneized, U/Pu separated and measured. The resulting standard deviation was 0.1 % in all cases (U and Pu). See again Tables V and VI (upper part).
Since the different analysts each with their own mass spectrometer were separately proven to attain routinely 0.1 % external single standard deviation (see definition in [6]), the ~ 0.35 % external standard deviation for single spiked determinations indeed seems attributable to weighing uncertainties and particulate matter inhomogeneities combining to at least a 0.25 % uncertainty.

Table V

Determination of Pu concentration in undiluted input samples with the aid of ^{235}U - ^{242}Pu solid spikes.

2nd series: Spiking on different days

A. Plutonium

Sample number	Sample-taking Weighing Ali	Spiking	mg Pu/g solution 01	02	03	
ASI /140 - 101	26.01.78	30.01.78	1 4839	1 4864	1.4868	s = ± 0.098 % (n = 9)
ASII /140 - 201	"	"	1 4925	1.4917	1.4911	
ASIII/141 - 301	"	08.02.78	1 4832	1.4839	1.4867	
ASIV/141 - 401	"	"	1 4786			
ASV /142 - 501	"	14.03.78	1 4805			
ASVI/142 - 601	"	"	1.4954*			
			1.4856			
			s = ± 0.46 % (± 0.36 % without outlier *)			
			spread: 1.14 %			
			U/Pu = 124.02 ± 0.17 %			

Table VI

Determination of U concentration in undiluted input samples with the aid of ^{235}U - ^{242}Pu solid spikes.

2nd series: Spiking on different days

B Uranium

Sample number	mg U/g solution 01	02	03	
ASI /140 - 101	183 757	184 383	184 202	s = ± 0. 1 % (n = 9)
ASII /140 - 201	184 625	184.573	184.651	
ASIII/141 - 301	184 038	183.952	184.374	
ASIV/141 - 401	183 846			
ASV /142 - 501	183 863			
ASVI/142 - 601	185.224			
	184 235			
	s = ± 0.31 %			
	spread: 0 80 %			

[6] P. De Bièvre, Accurate Isotope Ratio Mass Spectrometry, Proc. 7th Intern. Mass Spec. Conf. Firenze 1976, Adv. Mass Spec. 7A pp. 395-447, Heyden and Son Ltd London (1978)

Table VII

Determination of Pu and U concentration in undiluted input samples with the aid of ^{235}U - ^{242}Pu solid spikes.

3rd series: Spiking and weighing on different days

Sample number	Sample-taking	Spiking Weighing Ali	mg Pu/g solution	mg U/g solution
AS I /150 - 101	01.02.78	01 02.78	1 4865	183 909
AS II /150 - 201	"	"	1 4817	184 223
			[1 4841]	[184 066]
AS III/152 - 301	14.03.78	14.03.78	1 4937	185 614
AS IV/152 - 401	"	"	1 4955	184 934
			[1 4946]	[185 274]
AS V /153 - 501	26.06.78	26.06.78	1 6214	200 411
AS VI/153 - 601	"	"	1 6145	200 286
			[1 6180]	[200 348]

0.71 % 0.66 % 9.0 % 8.8 %

U/Pu = 123.94 ± 0.26 %

Finally 3 pairs of samples (series 150... in Table VII) were aliquoted and immediately spiked at 3 different points in time over more than 4 months. Both U and Pu concentrations increase by the same amount but U/Pu ratios stay constant (s = 0.26 %). See results in Table VII.

The U and Pu concentrations of all series measured are summarized in Table VIII and the external standard deviations observed, in Table IX.

Table VIII

Summary of U and Pu concentrations.

Spike used	U (mg/g)	Pu (mg/g)	U/Pu
$^{235}U/^{239}Pu$ series 139..		1 4854	
$^{235}U/^{242}Pu$ series 130..	183.58	1 4814	123 93
$^{235}U/^{242}Pu$ series 140.	184 23	1 4856	124 01
$^{235}U/^{242}Pu$ series 150..	var.	var.	123.94
Max spread		0 28%	

Table IX

Summary of observed external **S**

Spike used	U	Pu	U/Pu
$^{235}U/^{239}Pu$ series 139...	0 32 %	0 78 %	
$^{235}U/^{242}Pu$ series 130.	0 37 %	0 35 %	0.35 %
$^{235}U/^{242}Pu$ series 140..	0.31 %	0 46 % or 0.36 %*	0.18 %

* after rejection of one outlier

2.4 Conclusions from the results obtained with $^{235}U/^{242}Pu$ spikes

a) the precision of Pu assay has improved and is now of the order of that of U (from 2 % to 0.3 %
b) there is no difference in the Pu assay obtained with ^{239}Pu spike and that obtained with ^{242}Pu on the basis of 6 determinations; so the use of ^{239}Pu spike only results in a larger spread, not in a systematic error;
c) leaving an undiluted input sample in a closed bottle does not generate effects selective for Pu; the U/Pu ratio remains unchanged; the solution becomes more concentrated presumably due to a simple evaporation process;
d) abundantly available ^{235}U at a reasonable enrichment ($^{235}U/U$ = 0.85) is perfectly suited for use as a spike and allows to reach the optimal accuracy in the isotope dilution assay; furthermore the accuracy attained is the same as would have been obtained with highly enriched ^{233}U;

e) abundantly available ^{242}Pu at a reasonable enrichment ($^{242}Pu/Pu = 0.87$) is perfectly suited for use as a spike and allows to reach the optimal accuracy in the isotope dilution assay; furthermore the accuracy attained is the same as would have been obtained with highly enriched ^{242}Pu or ^{244}Pu;

f) the weighings of the undiluted samples in the hot cell (and possibly some slight inhomogeneities caused by particulate matter in the samples) seem to be responsible for the too large standard deviation of 0.3 %; 0.1 % is within reach as repeated treatments and measurements of a same spiked sample show; this is also the precision obtained on Uranium in previous work [2].

3. DETERMINATION OF A TOTAL MASS OF SOLUTION BY ISOTOPE DILUTION

3.1 Principle of total mass determination

Normally isotope dilution leads to an unknown concentration C_x by assaying total isotope or element in a known mass M_x of solution. Now, if we had a known concentration at our disposal, the reverse could be done. Recalling that $N = \frac{C.M}{A}$ the isotope dilution equation becomes

C = weight concentration
M = mass of solution
A = Atomic Weight

$$\frac{A_y}{A_x} \cdot \frac{C_x M_x}{C_y M_y} = \frac{R_y - R_B}{R_B - R_x} \cdot \frac{\Sigma R_{ix}}{\Sigma R_{iy}} \qquad (3.1)$$

If an isotope dilution would consist of changing a measured isotope ratio R_x by adding a known mass M_y of a spike with element concentration C_y and containing an isotope ratio with value R_y, a measurement of the resulting value R_B for the isotope ratio R in the blend, will allow - with knowledge of the concentration C_x - to compute the total mass M_x of the solution.

We have chosen an element concentration existing in a real input: Nd fission product with the ratio $R = \frac{^{142}Nd}{^{143}Nd}$ having a value 0 (in fission products no ^{142}Nd present).

After C_x has been determined in the same way as U and Pu, the total solution is spiked with natural Nd as Nd_2O_3

$$C_y = Nd/Nd_2O_3$$

$$R_y = \frac{^{142}Nd}{^{143}Nd} = 2.230$$

$$M_y = \sim 15\,g$$

and the resulting R_B value for the ratio $^{142}Nd/^{143}Nd$ measured. Also R_x in the fission product Nd is measured. M_x can then be calculated with Equation (3.1).

3.2 Determination of Nd concentration in a simulated (synthetic) input

This determination is performed in an entirely analogous way as the U and Pu concentration under points 2.2 - 2.3 and described earlier [2], except that no Nd solid spike is used but a natural Nd spike solution made from pure Nd_2O_3 (Merck 12276). A ^{142}Nd solution (SS) and a real input solution (RISL) (isotopic compositions different from natural) were used for the tests. Resulting Nd concentrations are 57.93 and 637.17 μg Nd/g.

Table X

Isotopic composition values for test solutions and spike

	^{142}Nd solution SS	Natural Nd used as spike		RISL
Isotopic composition (atom %)	x	y		x
^{142}Nd	98.26	27.157		0.359
^{143}Nd	0.71	12.177		21.098
^{144}Nd	0.58	23.795		31.322
^{145}Nd	0.12	8.293		17.209
^{146}Nd	0.24	17.188		16.624
^{148}Nd	0.05	5.755		9.078
^{150}Nd	0.04	5.635		4.310
$^{142}Nd/^{143}Nd$	138.39	2.230		0.01702
ΣR_i	140.84	8.212		4.740
R_B	26.44			0.09958
M	$M_x = 0.72645$ g	$M_y = 0.11499$ g	$M_y = 0.580$ g	$M_x = 0.1478$ g
C μg/g solution	$C_x = 57.93$	$C_y = 100.267$	$C_y = 10.857$	$C_x = 637.17$
A	141.945	144.233		144.8202

3.3 Determination of mass of solution

We tested the concept out on

a) a laboratory made synthetic solution (SS)

b) a real (but small) input solution (RISL) also in the laboratory, the Nd concentration of which was known from another programme.

We take back to equation (3.1) and note that we now have to spike the solutions "SS" and "RISL-1" which have known U, Pu and Nd concentrations but unknown mass. Isotopic composition data for SS, RISL, spike and results are given in Tables X and XI. Both SS and RISL were spiked with natural Nd as can be used in a real tank.

Table XI

Isotope dilution data of synthetic solution (SS), real input solution (RISL-1), spike and results

	SS	RISL-1
C_x µg/g	57.93	637.17
R_x	138.39	0.01702
R_y (nat. Nd)	2.230	2.230
ΣR_{ix}	140.84	4.740
ΣR_{iy}	8.212	8.212
C_y µg/g	100.267	10.857
M_y	0.34709 g	1.160 g
R_B	22.45	0.1776
M_x (determined)	1.7685 g	0.14641 g
M_x (from make-up values)	1.75465 g	0.14776 g

3.4 Conclusions from results on determination of solution masses

3.4.1 Laboratory tests show that it is possible to determine mass of solutions by spiking a total solution. Achievable accuracy is $\leqslant$ 1 %.

3.4.2 The method should be tested out on a real input tank but Table XII shows that the same result must be expected: a ratio $R_B \cong 0.04$ can be measured to the same accuracy as a ratio 22.45 or 0.177 and we have seen (see 2.1) that the uncertainty on this ratio measurement determines the uncertainty of the total isotope dilution.

Table XII

Comparison of laboratory test and real tank showing which R_B values are achieved

	laboratory test SS	laboratory test RISL	real tank (expected)
C_x µg/g	57.93 *	637.17 *	~ 600
Total Nd ($C_x \cdot M_x$)	101.647 µg	94.148 µg	900 g
C_y	100.267 µg/g	10.857 µg/g	0.857 g/g
Amount M_y of spike	0.34709 g	1.160 g	~ 15 g
R_B	22.45	0.1776	~ 0.04
M_x	1.75465 g	0.14776 g	~ 1500 kg

* comes from assay in Table X

The tank could be spiked with ~ 15g Nd_2O_3 costing $ 2.8 (99.9 % purity).

3.4.3 There is a need for a Nd Isotopic Reference Material (IRM) to calibrate the Nd isotope ratio measurements. Absence of this calibration is estimated to contribute at least 0.5 % of the uncertainty.

3.4.4 Larger samples (say 1 g) for spiking would reduce the uncertainty by several ‰ by making weighing errors negligible.

3.4.5 If a similar operation would be carried out using another element concentration in the tank (Eu, Sr, H, other Fission Products) or even several of them, very strong confirmatory evidence could be gained. Or, alternatively, if the results would not coincide, proof is given that something went wrong in at least one step of the procedure and that a timely warning is given.

3.4.6 The method provides an accurate burn-up determination through the Nd measurement.

4. GENERAL CONCLUSIONS

4.1 It is possible to determine total amount of fissile material (isotopes and element) in an input tank to better than 1 % accuracy, possibly 0.3 %, by determination of

- U concentration
- Pu concentration
- total mass of solution

using isotope dilution mass spectrometry.

4.2 If desired, the verification laboratory delivering the spike is the only one which can calculate end results and, if duplicate measurements are performed, can verify that all steps are performed properly.

4.3 The actual isotope ratio measurements can be performed by any laboratory incl. at the plant itself; passing the results onto the laboratory having delivered the spike, allows the latter - and nobody else - to compute end results.

4.4 Results are valid for time and place of spiking i.e. of inspection and not for - as in the case of classical analytical measurements - time and place of measurements.

4.5 The key elements of the determination are located (or can be located) outside of the installation: amount and isotopic composition of the U-, the Pu- and the Nd-spike.

5. ORIENTATIONS FOR THE FUTURE

5.1 A triple solid spike U-Pu-Nd should be prepared and used for concentration determinations, possibly a quadruple spike U-Pu-Nd-Eu.

5.2 Natural Nd spike capsules in readily dissolvable material should be prepared and used for tank calibration.

5.3 A Nd IRM should be established.

5.4 At least a second element (e.g. Eu) should be tested out for the mass determination (duplicate measurement to provide the built-in detection device for accidental or introduced error).

Discussion:

Larsen (ANL):

Do you contemplate any difference in the oxidation state of the plutonium? The problem is that you dissolve the nuclear fuel and the plutonium has gone through a certain number of chemical processes. The oxidation state of the plutonium that comes from the nuclear fuel may be different from that of the dissolution of the spike.

DeBievre (CBNM):

That indeed is the eternal problem with the plutonium valence state. We did valency homogenize the samples in a number of cases, however we have now sufficient indication that the large excess of the uranium metal acts as a sufficient vigorous reductor for the plutonium not to give us any problems.

Larsen:

Then what you are saying is that, in the dissolution process of the metal spike, all of the plutonium in the solution is being reduced to the trivalent state by the excess of uranium metal that is present during that dissolution operation.

DeBievre:

Exactly, simply following the analytical procedure, of course.

Gamma-Ray Measurements for Uranium Enrichment Standards

by

T. DOUGLAS REILLY
Los Alamos Scientific Laboratory, Los Alamos, New Mexico 87545

ABSTRACT

The gamma-ray spectroscopic measurement of uranium enrichment is one of the most widely used nondestructive analysis techniques. A study has been started of the precision and accuracy achievable with this technique and the physical parameters which affect it. The study was prompted by questions raised during the ongoing ESARDA-NBS experiment to produce uranium oxide reference counting materials for the technique. Results reported here using a high-quality Ge(Li) spectrometer system show reproducibility comparable to that attainable with mass spectrometry (approximately 0.1% for low enrichment uranium).

KEYWORDS: Uranium enrichment measurement, gamma-ray spectroscopy, mass spectroscopy, accuracy, precision

INTRODUCTION

The gamma-ray spectroscopic measurement of uranium enrichment is one of the most widely used and highly developed nondestructive analysis techniques. The measurement is based on the fact that the intensity of the 185.7-keV gamma ray of ^{235}U from an appropriately collimated sample of uranium bearing material is almost directly proportional to the enrichment of the sample ($^{235}U/U$).[1,2] The essential requirement is that the gamma-ray detector view the sample through a collimator chosen such that there is an infinite path length (greater than approximately six mean free paths) within the sample along any path from the detector to the visible part of the sample. If this is met, the measured 185.7-keV activity is exactly proportional to the ^{235}U enrichment, independent of the sample density, and nearly independent of the uranium concentration. The dependence of the activity on uranium concentration is given by the term

$$\left(1 + \frac{\mu_m \rho_m}{\mu_u \rho_u}\right)^{-1}$$

where

μ_u, μ_m = mass attenuation coefficient of uranium, matrix (all nonuranium materials in the sample)
ρ_u, ρ_m = density of uranium, matrix.

While widely used in uranium fuel fabrication and enrichment facilities by operators and nuclear safeguards authorities, this gamma spectrometric measurement is presently considered to be significantly less accurate than the mass spectrometric measurement which is used for most definitive enrichment determinations. There appears to be no intrinsic limit to the accuracy of the gamma-ray spectrometric measurement, so a study has been started of the precision and accuracy achievable with this technique and the physical parameters which affect it. This study was prompted by questions raised during the ongoing experiment of the European Safeguards Research and Development Association (ESARDA) and the National Bureau of Standards (NBS) to produce U_3O_8 reference counting materials for the gamma-ray enrichment measurement technique.[3]

The samples used for the measurements reported here include several cans (11-cm-diam by 12-cm-high by 0.28-mm wall thickness) of uranium oxide with nominal enrichments of 0.7%, 1.9%, 3%, 10%, and 93% ^{235}U. Each can contains approximately 1 kg of uranium.

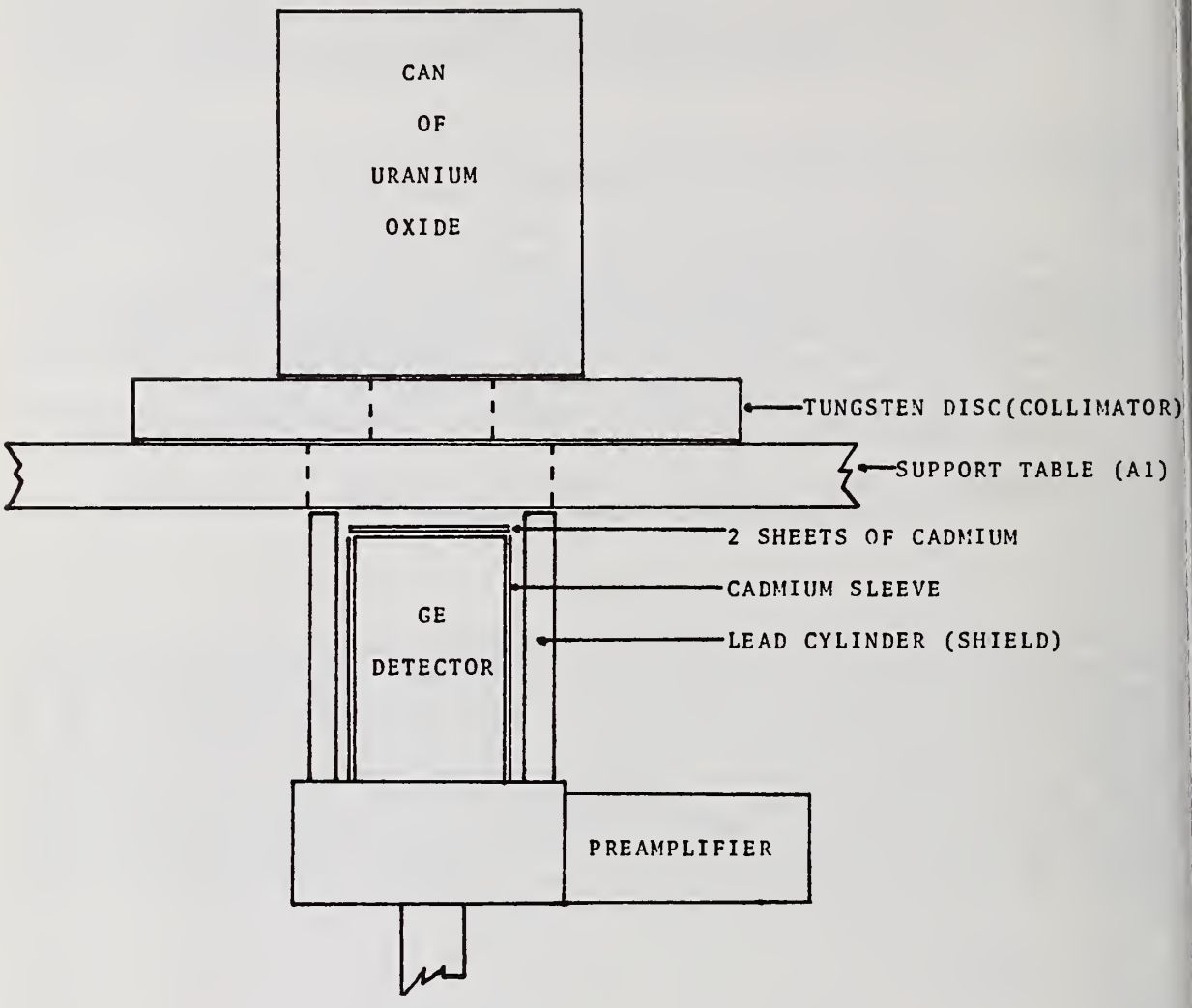

TUNGSTEN COLLIMATOR:

OUTER DIAMETER = 18 cm

INNER DIAMETER = 5 cm

HEIGHT = 4 cm

SUPPORT TABLE THICKNESS = 12 mm

DETECTOR TO SAMPLE = 64 mm

Fig. 1. ENRICHMENT COUNTING GEOMETERY

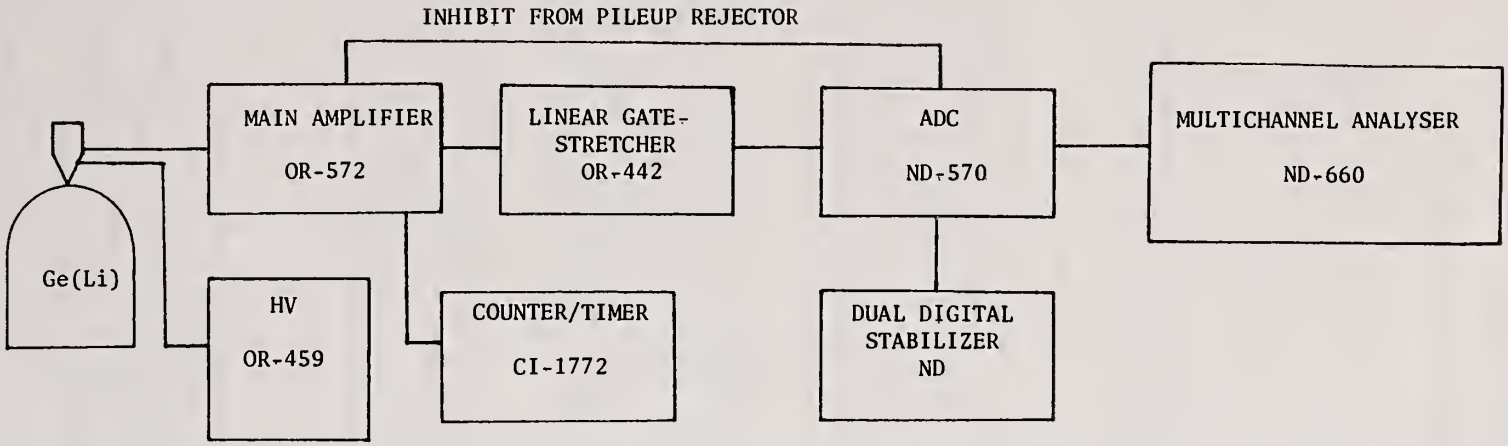

Fig. 2. Block Diagram of Enrichment Counting System

Multiple samples were available for each enrichment except 93%. Each uranium material was carefully characterized by the Analytical Chemistry Group at Los Alamos; they were sampled three times each and analyzed for uranium concentration and isotopic composition. A 93% enriched disc of uranium metal (6-cm-diam by 0.5-cm-thick) was also measured to test the density independence of the enrichment measurement.

MEASUREMENT SYSTEM DESCRIPTION

The counting geometry used for the measurements reported here is shown in Fig. 1. The tungsten collimator defines the required infinite counting geometry; the detector must not be able to view the edges of the can since these do not provide infinitely thick path lengths. The cadmium filter on the face of the detector serves to reduce the intensity of unwanted low-energy gamma rays and x-rays which increase deadtime and pulse pileup losses. The counting electronics is shown as a block diagram in Fig. 2. Electronic pulse pileup rejection is provided by the main amplifier and the use of the linear gate stretcher. In addition a small ^{57}Co ($\sim$10 μCi) source is glued to the cadmium filter to provide a reference peak (122.06 keV) in the measured spectrum which serves as a live time and pulse pileup correction. The measured parameter which should be proportional to ^{235}U enrichment is the ratio of the 185.7-kev activity of ^{235}U to the 122.0-keV activity of the ^{57}Co reference source. The ^{57}Co source activity must be corrected for decay (271.65 day half-life) and a weak interference at 120.9 keV from ^{234}U.

The total count rate from the ^{57}Co reference source alone was approximately 10 000 cps with 5600 cps occurring in the full energy peak at 122 keV. The ^{234}U interference at 120.9 keV from the 93% oxide can is only approximately 10 cps indicating a correction of less than 0.2%. Therefore, the correction for the lower enrichment samples is less than 0.02% and can be ignored. In some cases it may be desirable to maintain a lower total count rate by using a smaller ^{57}Co reference source. If so, careful attention must be paid to the measurement of this correction; essentially the ratio of activity at 120.9 keV to that at 185.7 keV must be measured for each sample in the absence of the reference source.

The detector used for these measurements was a coaxial Ge(Li) with a nominal relative efficiency of 11% and measured resolution in optimum conditions (low count rate, 4 μs time constants) of 1.79-keV FWHM at 1332 keV and 0.68 keV at 122 keV. With the counting geometry shown in Fig. 1 and the reference source described above the total system count rate varied from approximately 12 000 cps for the natural uranium samples to approximately 13 000 cps for the 10% enriched samples and approximately 23 000 cps for the 93% sample. Over this range of count rates the system resolution with 2 μs time constants varied from 0.80 keV to 0.81 keV at 122 keV and from 0.87 kev to 0.89 kev at 186 keV.

The system gain was set to give an energy calibration of 0.05 keV/channel. A double digital stabilizer was used to keep the 122.0-keV peak in channel 2440 and the 185.7-keV peak in channel 3714. The desired peak areas were determined using a three-window channel summation procedure with symmetrically placed background windows.[4] The peak windows were chosen to be three full-widths-half-maximum wide or 49 channels at 122 keV and 53 channels at 186 keV. All background windows were 50 channels wide.

MEASUREMENT RESULTS

A series of measurements were made on each of the various samples over the course of eight days. Each sample was measured several times to compare measurement reproducibity with that predicted by simple Poisson counting statistics. Table I shows sample measurements obtained on the 1.9% and 3.0% enriched oxide cans. Relatively long count times were used so that the counting statistical precision of the average measured response of each sample would be well below 0.1% (one relative standard deviation). The count rate in the full energy peak at 185.7 keV for samples of 1.9%, 3.%, and 10% ^{235}U was approximately 72, 112, and 365 cps, respectively. The measurement result is given in weight percent ^{235}U using a calibration obtained from the average response of three cans containing 1.9%, 3% and 10% uranium oxide. As shown in Table I the measurement reproducibity is very good (of the order of 0.1%) and consistent with that predicted by Poisson counting statistics.

TABLE I

ENRICHMENT MEASUREMENT REPRODUCIBILITY

Sample Enrichment = 3.023 wt % Uranium Concentration = 86.90%				Sample Enrichment = 1.937 wt % Uranium Concentration = 87.75%			
Day	Live Time (s)	wt % ^{235}U (% RSD)*		Day	Live Time (s)	wt % ^{235}U (% RSD)	
1	3200	3.023	(0.18)	1	6381	1.935	(0.16)
2	11001	3.026	(0.10)	2	2459	1.940	(0.26)
2	8836	3.021	(0.11)	2	8199	1.937	(0.14)
4	7703	3.020	(0.12)	5	8202	1.936	(0.14)
	mean =	3.023			mean	1.937	
	sigma =	0.0026	(0.09%)		sigma =	0.0022	(0.11%)

* This is the percent relative standard deviation predicted by Poisson counting statistics.

Table I also shows that the measured enrichment is in good agreement with that determined by mass spectrometry. This is better illustrated in Table II which gives the weighted average for the measured enrichment from all measurements and the mass spectrometrically determined value. The 1.9%, 3%, and 10% samples show excellent agreement, however, the 0.7% sample measures 0.35 $\pm$ .08% ^{235}U higher than the mass spectometrically determined enrichment. The origin of this difference cannot now be explained with any certainty; it may, in fact, lie within the limit of error of the mass spectrometry determination (see later discussion). In looking for possible explanations for this discrepancy there came to light several possible weak interferences which could perturb the gamma-ray measurement of natural or depleted uranium samples. Table III shows three possible interfering gamma rays from daughter products of ^{238}U.[5] These have energies almost identical to the ^{235}U gamma ray and would be included in the measured peak area. Assuming the tabulated intensities to be correct the ^{238}U daughter product contribution to the 185.7-keV peak for natural uranium would be at least 0.14% of the total activity (i.e., this is the sum of ^{234m}Pa and ^{234}Pa. A value is not given for the intensity of the ^{234}Th gamma ray.) For the case of depleted uranium (0.2% ^{235}U) the ^{238}U daughter product contribution would be at least 0.5% of the total activity. It will be interesting to investigate in future experiments if these gamma rays are real and if they represent a slight interference to the enrichment measurement.

As mentioned earlier samples of 93% enriched uranium oxide and 93% uranium metal were available to test the density dependence of the enrichment determination. These were measured with the same counting geometry shown in Fig. 1 but with an additional lead filter to reduce the overall count rate. The corrected response from the oxide sample (density $\approx$ 1.5 g/cm^3) differed from the response of the metal sample by -0.20 $\pm$ 0.24% confirming within the measurement uncertainty the invariability of the 185.7-keV response over wide ranges of bulk density.

TABLE II

COMPARISON OF GAMMA-RAY SPECTROMETRY AND MASS SPECTROMETRY ENRICHMENT VALUES

wt % ^{235}U		
Gamma-Ray Spectrometry	(% RSD)	Mass Spectrometry
10.10	0.09	10.09
3.023	0.05	3.023
1.936	0.05	1.937
0.718	0.09	0.714

TABLE III

POSSIBLE INTERFERING GAMMA RAYS (Ref. 5)

Isotope	Energy (keV)	Intensity (γ/g/s)
^{235}U	185.715	4.31×10^4
^{234}Th	184.8	not given *
^{234m}Pa	184.7	0.149 *
^{234}Pa	185.95	0.281 *

* These are short half-life daughters in equilibrium with the parent ^{238}U. The intensity is stated per gram of ^{238}U.

MEASUREMENT TIMES - CONCLUSIONS

Little has so far been said regarding measurement times, although Table I does show the counting times used for specific measurements. No special effort was made for the measurements reported here to minimize required measurement times. The goal of this study was to see if, under laboratory conditions, the gamma-ray spectroscopy measurement could be performed with a reproducibility approaching 0.1% and to compare these measurements with mass spectrometry.

A limited number of measurements were performed with a thinner collimator disc (12-mm-high) and with no collimator to study the time required to achieve a given counting precision with more efficient counting geometries. A summary of these results is presented in Table IV which gives the time required to reach a precision of 1.0%, 0.2%, or 0.1% for the four enrichments measured here in each of the three geometries. These times should not be understood as representing the ultimate limit of the gamma-ray spectrometric measurement. Table IV does show that a typical LWR fuel material of 3% ^{235}U can be measured to a precision of 0.1% in less than one hour. It also shows that very long count times would be required to achieve similar precision on samples of natural or depleted uranium.

For comparison purposes it is interesting to look at the stated precision of thermal ionization mass spectrometry for measuring uranium enrichment. Table V shows the precision of the ^{235}U determination as a function of enrichment as declared by the New Brunswick Laboratory of the U.S. Department of Energy.[6] Reference 6 states that ten determinations can be performed during a day which implies something less than one hour per measurement; this presumably includes the time necessary for sample preparation and filament loading. Table V shows that for low enriched uranium the precision of the mass spectrometric determination is similar to that achievable with the gamma-ray spectrometric determination.

The measurements discussed in this paper are just the beginning of a study of the accuracy and precision of the gamma-ray spectrometric enrichment measurement technique. Mass spectrometry is a well-studied and qualified technique having certified reference materials and an accepted accuracy and precision demonstrated through intralaboratory measurement control programs and interlaboratory sample exchange programs. If gamma-ray spectrometry is to become an accepted enrichment measurement technique, it must undergo similar development and testing as has occurred for mass spectrometry. This process is now beginning with the planned fabrication of counting reference materials and accompanying interlaboratory comparison measurements.

TABLE IV

TIME REQUIRED TO REACH GIVEN PRECISION (RSD)

With 40-mm-High by 50-mm-Diameter Collimator

% ^{235}U	Count Time for Precision (RSD)		
	1.0%	0.2%	0.1%
10%	31 s	765 s	3060 s
3%	102 s	2550 s	10200 s
2%	167 s	4180 s	16700 s
0.7%	560 s	13900 s	55700 s

With 12-mm-High by 50-mm-Diameter Collimator

% ^{235}U	Count Time for Precision (RSD)		
	1.0%	0.2%	0.1%
10%	17 s	428 s	1710 s
3%	54 s	1340 s	5360 s
2%	86 s	2160 s	8620 s
0.7%	230 s	5760 s	23000 s

Without Collimator

% ^{235}U	Count Time for Precision (RSD)		
	1.0%	0.2%	0.1%
10%	8 s	209 s	840 s
3%	22 s	560 s	2240 s
2%	34 s	840 s	3380 s
0.7%	88 s	2190 s	8760 s

TABLE V

PRECISION OF MASS SPECTROMETRIC DETERMINATION OF URANIUM ENRICHMENT (Ref. 6)

Wt % ^{235}U	RSD %
0.5 - 0.7	0.20
0.7 - 1.0	0.15
1.0 - 1.5	0.125
1.5 - 10	0.10
10 - 15	0.09

REFERENCES

1. T. D. Reilly, R. B. Walton, and J. L. Parker, "The 'Enrichment Meter' - A Simple Method for Measuring Isotopic Enrichment," in Nuclear Safeguards Research Program Status Report, September - December 1970, Los Alamos Scientific Laboratory report LA-4605-MS (1970) pp. 19-21.

2. L. A. Kull and R. D. Ginaven, "Guidelines for Gamma-Ray Spectroscopy Measurements of ^{235}U Enrichment," Brookhaven National Laboratory report BNL-50414 (1974).

3. R.J.S. Harry and H. T. Yolken, "Development of Uranium Oxide Reference Materials for Gamma-Ray Measurements of the Enrichment," Nucl. Mater. Manage. VIII, Proceedings Issue, 54-64 (1979).

4. T. D. Reilly and J. L. Parker, "A Guide to Gamma-Ray Assay for Nuclear Material Accountability," Los Alamos Scientific Laboratory report LA-5794-M (March 1975) pp. 7-9.

5. C. M. Lederer and V. S. Shirley, Table of Isotopes, 7th Edition, (John Wiley and Sons, Inc., New York, 1978).

6. C. E. Pietri, J. S. Paller, and C. D. Bingham, "The Chemical and Isotopic Analysis of Uranium, Plutonium, and Thorium in Nuclear Fuel Materials," in Analytical Methods in Safeguards and Accountability Measurements of Special Nuclear Material, (NBS Special Publication 528, Nat. Bur. Std., 1978) H. T. Yolken and J. E. Bullard, Eds., Proc. ANS Topical Meeting, Williamsburg, Virginia, May 15-17, 1978, pp. 1-18.

Discussion:

Camp (LLL):
Would you comment on the size of detector you use?

Reilly (LASL):
There are several ways of stating it. It is basically 11% efficient, in the normal way, relative to a three-by-three inch NaI(Tl) -- so essentially about 65 cubic centimeters. It is a closed-end coax.

New Advances in Alpha Spectrometry by Liquid Scintillation Methods*

W. J. MCDOWELL AND G. N. CASE
Oak Ridge National Laboratory, Oak Ridge, Tennessee 37830

ABSTRACT

Although the ability to count alpha particles by liquid scintillation methods has been long recognized, limited use has been made of the method because of problems of high background and alpha energy identification. In recent years some new developments in methods of introducing the alpha-emitting nuclide to the scintillator, in detector construction, and in electronics for processing the energy analog and time analog signals from the detector have allowed significant alleviation of the problems of alpha spectrometry by liquid scintillation. Energy resolutions of 200 to 300 keV full peak width at half maximum and background counts of <0.01 counts/min with rejection of >99% of all beta plus gamma interference is now possible.

Alpha liquid scintillation spectrometry is now suitable for a wide range of applications, from the accurate quantitative determination of relatively large amounts of known nuclides in laboratory-generated samples to the detection and identification of very small, subpicocurie amounts of alpha emitters in environmental-type samples. Suitable nuclide separation procedures, sample preparation methods, and instrument configurations are available for a variety of analyses.

KEYWORDS: Alpha particle, spectrometer, liquid scintillation, alpha counting, solvent extraction

BACKGROUND

No alpha assay method that is good both in identification of alpha energy and quantification of the alpha count is currently available. Surface barrier detectors and Frisch grid detectors give excellent energy identification if the sample is properly prepared, but self-absorption and geometry duplication problems prevent consistently accurate quantification of the alpha events. Even with painstaking and time-consuming sample preparation methods, it is difficult to obtain an average reproducibility better than ±10%. Addition of a tracer isotope can improve accuracy but at the expense of an additional operation and additional counting statistics considerations. Proportional counter methods have about the same problems with poorer energy resolution. Zinc sulfide foil methods offer neither energy resolution nor accurate quantification. They, like surface barrier detectors, do offer very low background from beta, gamma, and cosmic radiation.

Liquid scintillation as it is usually practiced for beta assay work can, under certain conditions, give excellent count quantification, but the energy identification capabilities are nearly nonexistent. However, improvements in instrumentation, scintillators, and sample preparation methods have made liquid scintillation an attractive addition to alpha assay methods in that useful nuclide identification and improved quantification can be achieved using relatively simple procedures.

*Research sponsored by the Division of Chemical Sciences, U.S. Department of Energy under contract W-7405-eng-26 with the Union Carbide Corporation.

The fact that liquid scintillation methods can be used for alpha counting has been known for almost as long as the method has been used for beta counting,[1-4] and the ability to obtai a useful degree of alpha energy resolution was demonstrated several years ago.[5,6] However, the application of liquid scintillation to alpha counting and spectrometry has been limited partly because alternative methods such as gas-flow proportional counting, zinc sulfide scintillators, and surface barrier detectors have become established as the conventional methods and partly because of some disadvantages of liquid scintillation as it is ordinarily used and perceived. These disadvantages are primarily related to two areas: (1) determination of background and (2) energy resolution and identification.

Beta or gamma radiation produces more light for the same amount of energy absorbed in a liquid scintillator than does alpha radiation, resulting in a serious overlap of beta-gamma and alpha spectra. Figure 1 illustrates the type of energy (pulse-height) distribution observed for alpha, beta, and gamma emissions. The interfering beta and gamma radiation may arise from the alpha nuclide decay scheme, may be introduced to the scintillator as an impurity along with the sample, or may be of external origin (including the sample container and phototube face). Therefore, the usual method of background counting and subtraction will frequently be inadequate in liquid scintillation counting.

Energy resolution constraints arise from a variety of sources. Beta liquid scintillation equipment usually has limited energy resolution capability for alpha particles because highly refined energy resolution is not needed for the broad zero-to-maximum energy distribution of beta spectra. Further, quenching effects tend to complicate the calibration of an alpha energy scale in liquid scintillation. When a sample for alpha counting is prepared in the manner normally used for beta counting, the addition of water, acids, salts, or other impurities changes the scintillator response and shifts the alpha spectrum up or down scale; thus, although the alpha counting efficiency usually remains at 100%, the ability to identify alpha energies is impaired or lost. These circumstances have made the usual beta liquid scintillation methods unattractive for alpha counting except under special conditions.

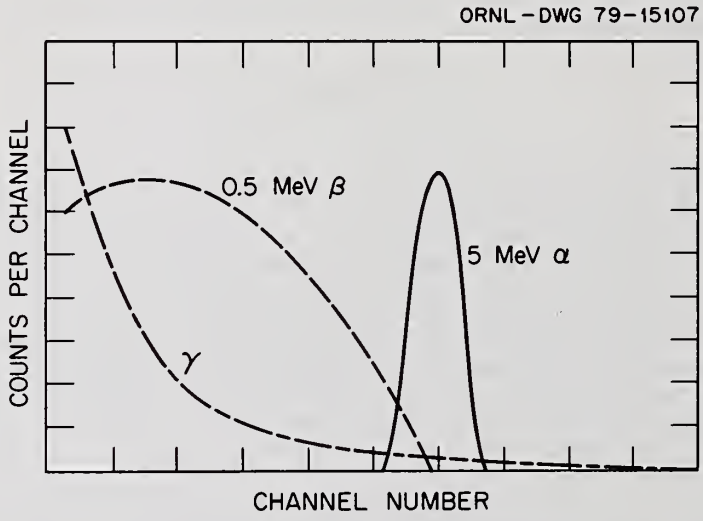

Fig. 1. Typical liquid scintillation spectra of alpha, beta, and gamma radiation.

NEW ADVANCES

Over the past 10 to 12 years substantial improvements have been made in nuclide separation procedures, in methods of preparing liquid scintillation samples, in the optics and electronics of detectors, and in methods of reducing background so that alpha counting and spectrometry by liquid scintillation is now often practical and simple to use.[5,7-14] In the

degree of energy resolution obtained, the new techniques are generally intermediate between alpha counting with a beta liquid scintillation counter and with a surface barrier detector, as they also are in regard to the difficulties of sample preparation. Energy resolution of 200 to 300 keV full peak width at half maximum (FWHM) and background count rates of <0.01 counts/min are easily obtained. Pulse-height response is linear with alpha energy, quenching effects can easily be made negligible, counting efficiencies are 100%, and nuclide quantification is generally superior to other alpha counting methods.

Scintillators

A key factor in the successful application of liquid scintillation to alpha spectrometry is the use of a liquid-liquid extraction reagent in the scintillator. This allows the alpha-emitting nuclide of interest to be extracted into a water-immiscible scintillator without transferring unwanted salts, acids, or other quenching materials. Various extractants are effective for this purpose,[15] and the use of the "extractive scintillator" is usually part of a chemical separation scheme that aids in identification of the nuclide. Appropriate preliminary separation and/or concentration steps are usually included to prepare the sample for final extraction into the scintillator.

The extractive scintillator can be used to prepare samples for the usual commercial beta liquid scintillation counter or for the improved, high-resolution detector. In both cases quenching effects are reduced, and the response of the scintillator is more constant, sample to sample. Aqueous solutions and all agents for incorporating them into the scintillator (e.g., solubilizing, dispersing, gelling agents) are avoided, eliminating their large and variable quench effects. In effect, only the trace nuclide is added to the standardized scintillator. This allows the pulse-height and consequent peak position for a given alpha to be made constant. A few typical extractants and their properties are listed in Table 1. An extractive scintillator composition of 0.1 to 0.2 mole/liter of the extractant, 150 to 200 g/liter of naphthalene, and 4 to 5 g/liter of a single fluor was found to have the best pulse-height and pulse-shape resolution properties. Of the various fluors tested, αNPO [2-(1-naphthyl)-5-phenyloxazole] and PBBO [2-(4'-biphenylyl-6-phenylbenzoxazole)] were found to have the best pulse-height response and energy resolution properties.[16] The extractant used in the scintillator (and the aqueous medium from which the extraction is made) can often be chosen so as to provide a degree of selectivity for the nuclide of interest; thus the extraction into the scintillator becomes the last step in a separation scheme that aids in identification of the nuclide.[12,16-19]

TABLE 1. Extractants for use with extractive scintillators

Extractant	Alpha emitter extracted	Quenching
Di(2-ethylhexyl)phosphoric acid	All cations; trivalent actinides, thorium, and uranyl best	Very slight
Tertiary amine sulfate (trioctyl, triisooctyl, or triisodecyl)	Uranium(VI)	Very slight
Primary amine sulfate (branched 16- to 20-carbon compound)	Uranium(VI), thorium	Very slight
Tertiary amine nitrate	Plutonium(IV), (VI)	Moderate to severe[a]
Tertiary amine chloride	Polonium, uranium(VI)	Moderate to severe[a]
Trioctylphosphine oxide	Uranium(VI), thorium, plutonium(IV)	Depends on anion present;[a] slight for sulfate, moderate to severe for nitrate or chloride
Tributyl phosphate	Uranium(VI), thorium, plutonium(IV)	

[a]May be necessary to strip and reextract into scintillator containing di(2-ethylhexyl)phosphoric acid to obtain good energy and pulse-shape resolution.

A detector with improved optical and electronic properties[7,9-11] has been built to take advantage of the reduced background, controlled quenching, and improved energy response of the aqueous-immiscible extractive scintillator. The basic detector design is shown in Fig. 2. Although detectors of this type are not commercially available, they are simple and can be easily built for less than $1000, including the cost of the phototube. The dual phototube-coincidence arrangement used to reject random noise pulses and lower the energy detection threshold for soft betas is not needed, nor is the refrigeration chamber for the detector that is used for the same purpose.

The optical requirements for good alpha energy resolution appear to be as follows:

1. A scintillation event must appear the same to the phototube irrespective of where it occurs in the sample.

2. Since the photocathode is not homogeneous but varies in sensitivity from place to place, the light from any scintillation anywhere in the sample must be spread evenly over the face of the phototube.

3. Light collection must be efficient because the resolution is a statistical function of the quantity of light collected.

Horrocks and Studier[6] were among the first to seek optimization of sample size, light coupling arrangements, and reflectors to increase energy resolution. Although these innovations were made to lower the counter background and to improve efficiency for soft beta emissions from ^{241}Pu, the presence of alpha-emitting plutonium isotopes in the same sample allowed the investigators to recognize possibilities for improved alpha energy resolution. Subsequent work confirmed that small samples, good optical coupling, and efficient reflectors were necessary to obtain good alpha energy resolution. Although later work by others showed some progress in optimizing sample size and light-collection arrangements,[5,7,10,18] it is not certain that the best conditions have been attained. However, Hanschke,[19] who has made an extensive study of the effects of reflector shape, sample volume and shape, and photocathode variability, concludes that a small-volume

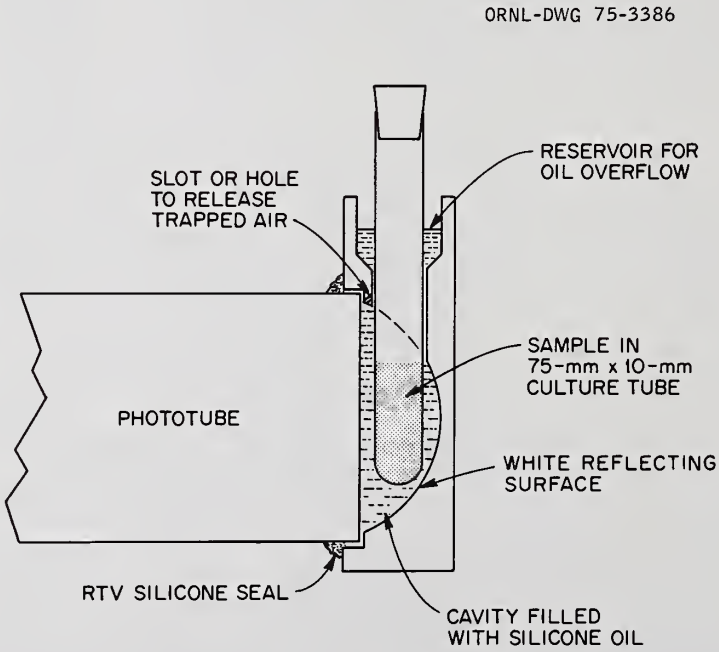

Fig. 2. Detector-sample holder for alpha liquid scintillation spectrometer.

sample and a reflector that is a section of a sphere give the best resolution for a given phototube situation. At ORNL good light-collection and good pulse-height resolution have been obtained using standard 10- by 75-mm culture tubes in the detector as shown in Fig. 2. The space between the reflector and phototube face is filled with silicone oil to minimize reflecting surfaces at refractive index discontinuities. A large number of sample sizes and reflector arrangements were evaluated before arriving at this arrangement. Some of this work has been reported previously.[10]

General improvements in multiplier phototubes have contributed significantly to the ability to develop an alpha liquid scintillation detector with improved energy resolution characteristics. Only limited tests of available phototubes for this application have been made.[12] At ORNL, two flat-faced, 2-in., bialkali phototubes have been found useful: the RCA 4523 and the EMI 9840A. Other tests indicate that the RCA 8575 phototube has favorable characteristics; however, differences between phototubes of the same type are often greater than those observed for different types.

Electronics

Energy Resolution

In order to take advantage of the improved characteristics of the scintillator reflector and phototube, the electronics system for processing the signal must retain the energy information produced by the detector system. Linear amplifiers and preamplifiers of the type generally used for gamma spectrometry with sodium iodide crystal–phototube combinations appear to be quite suitable for this application. Such equipment has been used by several investigators.[5-7,18] Typically, a scintillation preamplifier is followed by a linear amplifier that feeds the signal into a multichannel analyzer. Alpha energy resolution typical of such electronics in conjunction with a single bialkali phototube with reflector and small-volume sample as described previously is shown in Fig. 3. A spectrum of the same pair of nuclides (^{232}Th and ^{239}Pu; 1.15-MeV separation) in the same scintillator recorded from the output of a commercial beta liquid scintillation spectrometer is included for comparison. The higher energy resolution for the alpha scintillation counting is due partly to the more efficient light-collecting arrangement and partly to the improved electronics system.

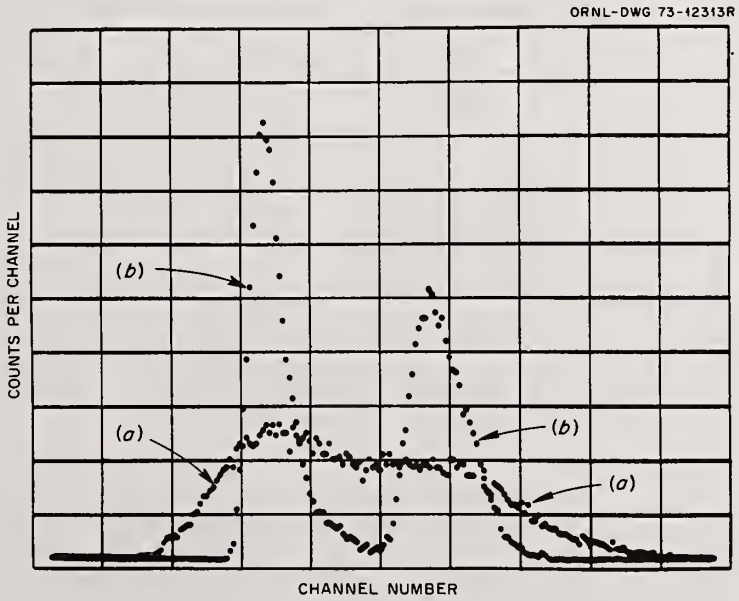

Fig. 3. Comparison of spectra from (*a*) a commercial beta liquid scintillation spectrometer and from (*b*) a high-resolution alpha liquid scintillation spectrometer. The same pair of alpha emitters (^{232}Th, 4.01 MeV; ^{239}Pu, 5.15 MeV) were used in the same scintillator in both cases.

Pulse-Shape Discrimination

One of the most important developments in electronics for alpha liquid scintillation counting is the use of electronic pulse-shape discrimination to separate and reject pulses produced by beta and gamma radiation. The techniques of pulse-shape discrimination are well known and have been extensively applied to the rejection of gamma background in neutron spectrometry[20,21] and to the isolation of fission events in liquid scintillation counting.[22] Only limited application has been made, however, to the separation of beta- and gamma-produced pulses from alpha-produced pulses arising from a liquid scintillator.[9,18,23,24]

Pulse separation in pulse-shape discrimination is achieved by taking advantage of the slower decay of the light pulse produced by alpha particles compared with that produced by beta or gamma radiation. Thus the effectiveness of pulse-shape discrimination, like that of pulse-height resolution, depends on several factors. For example, the scintillator must be high efficiency and free of chemical quenching materials, particularly dissolved oxygen. In addition, the optical coupling between sample and phototube must be optimum. Although reflectors yielding good pulse-shape resolution apparently always give good pulse-height resolution, the reverse is not necessarily true.[10] Finally, the phototube and amplifiers must be able to retain in their output signal the time difference in light pulse produced in the scintillator by the different types of radiation.

Several types of pulse-shape discrimination electronic circuits have been described in the literature.[25] A very efficient and reliable arrangement using commercial components has been used at ORNL.[9] More recently, Thorngate has designed a very simple two-unit-wide pulse-shape analyzer, designed primarily for alpha spectrometry.[26]

Figure 4 shows the results of using pulse-shape discrimination circuitry to resolve the mixed beta, gamma, and alpha pulses from a sample containing ^{232}Th and its daughters (spectrum A). Spectrum B is a time spectrum showing the beta-gamma pulses (left) separated from the alpha pulses. When the alpha pulses are selected by a single-channel analyzer and a logic pulse derived from them is used to gate the multichannel analyzer, spectrum C, devoid of the beta-gamma continuum, is obtained. Backgrounds of 0.01 counts/min are easily obtained with pulse-shape discrimination, and with careful work it has been possible to achieve backgrounds as low as 0.002 counts/min under a typical alpha peak. With samples containing internal beta and gamma radiation, it is possible to remove at least as much as 99.9% of the beta-gamma component and retain a similar percent of the alpha counts.

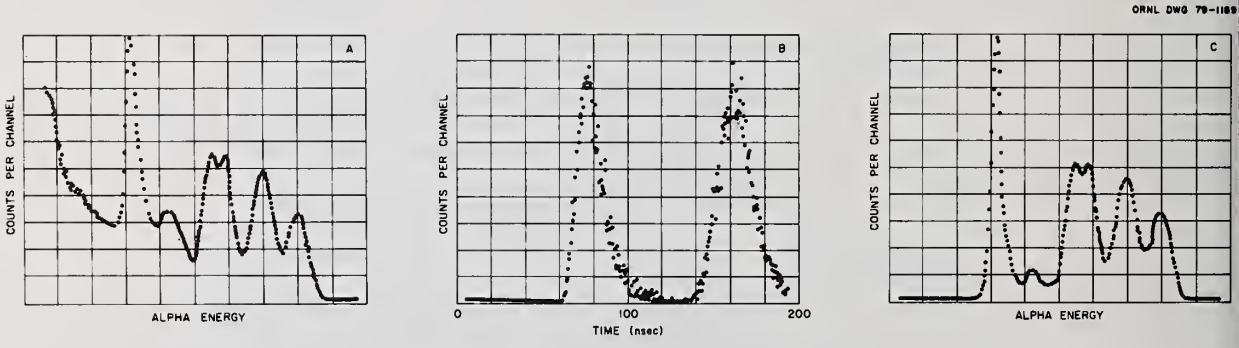

Fig. 4. Spectrum of ^{232}Th and daughters (*a*) including beta-gamma component, (*b*) time spectrum showing beta-gamma component, left, and alpha pulses, right, and (*c*) ^{232}Th and daughters, energy spectrum with beta-gamma component removed by pulse-shape discrimination.

The degree of complexity and sophistication necessary in alpha liquid scintillation is dictated by the properties of the sample (physical and chemical forms, impurities present, type of nuclide to be counted) and the accuracy of the results required. Several of the possible options are listed in Table 2.

If the samples contain only one alpha-emitting nuclide and minimum, or known, amounts of beta and gamma emitters and if the count rate is sufficiently above background, commercial beta liquid scintillation equipment and scintillators are an appropriate and convenient means of alpha counting. Useful background reduction and scintillator-response standardization can be achieved by the use of an extractive scintillator in conjunction with a beta liquid scintillation counter.

The ability to isolate alpha-emitting nuclides chemically and to identify them by a combination of chemical selectivity and alpha spectrometry may be realized by using a combination of standard chemical separations, an extractive scintillator, and high-resolution alpha liquid scintillation spectrometry. For example, plutonium can be extracted selectively from nitric acid digests of a variety of materials and then stripped and reextracted into a scintillator (1.2 to 1.5 ml) for subsequent counting in a high-resolution detector.[16] Uranium and thorium can be extracted together, stripped into an aqueous phase, and reextracted selectively into separate scintillators.[14] The trivalent actinides can be separated by conventional methods and then extracted into a scintillator containing di(2-ethylhexyl)phosphoric acid.[7]

A typical analysis would proceed as follows: A sample is placed in solution in a medium from which it can be separated and/or concentrated by ion exchange, solvent extraction, or some other applicable method. (If the sample is a solid, this could be the most time-consuming step in the analysis.) After the nuclide of interest is concentrated into a suitable volume (2 to 10 ml), it is extracted into the extractive scintillator. Oxygen is removed from the scintillator by bubbling with an inert gas for 1 to 2 min. The sample is corked, and is then placed in the detector and counted for sufficient time to obtain the desired counting accuracy, usually 10 min or less but occasionally as long as 1000 min. The time required to prepare a single sample after it is in solution is about 45 min. Six to eight samples can be prepared in 1.5 hr.

In a recently developed procedure, $^{234-238}U$ and ^{230}Th are extracted together into a solution of trioctylphosphine oxide (TOPO) in toluene and are then stripped into an aqueous phase by sequential contact with 0.5 M ammonium carbonate followed by 0.5 M H_2SO_4. The

TABLE 2. Options for alpha liquid scintillation

Method	Capability	Advantages	Disadvantages
Aqueous sample All-purpose scintillator Beta LS[a] counter	Gross α count of relatively high count rate	Easy sample preparation Available equipment and scintillator	Little energy resolution Variable quench Variable background
Extractive scintillator Beta LS counter	Gross α count of somewhat lower count rate	Less background variation Reproducible quenching	Little energy resolution Still relatively high background
Extractive scintillator Alpha LS spectrometer	α spectra 200- to 300- keV FWHM Lower detection limit	Lower external background Usable energy spectrum	More sample preparation β-γ from nuclide or daughters visible
Extractive scintillator Alpha LS spectrometer Pulse-shape discrimination	α spectra Still lower detection limit	Internal β-γ rejected Low, reproducible background	Additional sample preparation Additional electronics

[a]LS = liquid scintillation.

strip solution is reduced in volume and converted to a sulfate system. The uranium and thorium are then extracted into separate extractive scintillators. Figure 5 shows the extraction coefficients (organic phase concentration divided by aqueous phase concentration) for both systems as a function of pH.

The overall accuracy of the $^{234-238}U$ and ^{230}Th assays, including the dissolution and two extraction steps, is estimated at ±5%. Reproducibilities of ±0.3% (including the two extraction steps and counting) were easily obtained for the uranium at the 100- to 150-ppm level. Detection limits for 1-g samples were found to be 1.1 parts per 10^8 for ^{238}U and 4 parts per 10^{13} for ^{230}Th when pulse-shape discrimination was used. This is competitive with fluorimetric methods for uranium and may be better than most existing methods for ^{230}Th.[14]

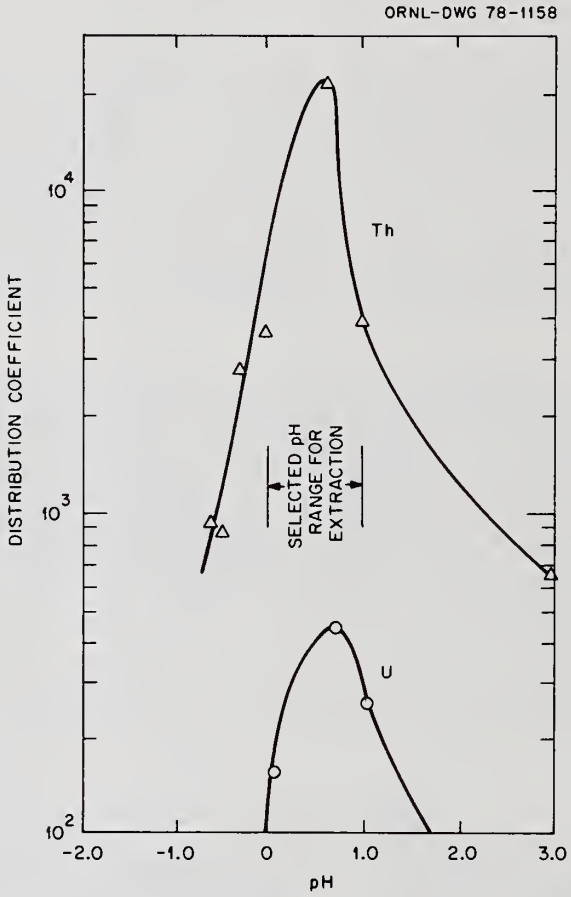

Fig. 5. Thorium distribution to the primary amine sulfate scintillator and uranium distribution to the tertiary amine sulfate scintillator as a function of aqueous-phase pH.

FUTURE UTILIZATION

Widespread use of the more refined forms of alpha liquid scintillation spectrometry described here depends on (1) an increased interest and need for such procedures and (2) promotion of the development of commercial supplies of the necessary reagents, detectors, and special electronic (pulse-shape discrimination) units. Several laboratories are currently using these procedures and devices on a research basis, however, and it is hoped that commercial supplies will become available as was the case with beta liquid scintillation.

Chemical separation steps are required for alpha liquid scintillation spectrometry just as they are for alpha spectrometry by other methods. These steps generally involve much hand labor in either case, and methods of simplifying and automating these time-consuming steps are needed. Some work in this direction has been done at ORNL. Initial separation steps can, of course, be done in multiples. Automatic pipetters and dispensers can simplify reagent measurements. An equilibration vessel for the final extraction into the scintillator has been designed that allows extraction, deoxygenation of the scintillator, and counting in the same vessel.

It is not clear whether the practical limit of energy resolution for alpha liquid scintillation work has been reached. The relevant factors are associated either with the scintillator or with the detector since electronic signal processing is clearly not a limit. Considerable improvements have been made in resolution by choosing the purest and most effective ingredients,[15-17] but these measures have not extended energy resolution capability beyond 200- to 300-keV FWHM. This resolution, which corresponds to 4 to 6%, is somewhat better than can be obtained in gamma spectrometry by optimizing a phototube—sodium iodide crystal combination.

Most detectors now in use for alpha liquid scintillation spectrometry do not incorporate sample changers, partly because of their experimental nature and partly because they are not really needed for low-count-rate samples. Sample changers using the detector and sample configuration described for high-resolution alpha liquid scintillation spectrometry have been constructed;[13] however, like the detector, they are not commercially available.

CONCLUSIONS

There is a great need for a simple, rapid, and accurate method of alpha counting and spectrometry. Unfortunately, the nature of alpha radiation makes the development of such a method difficult. Liquid scintillation methods, however, offer inherent advantages for alpha counting and spectrometry with regard to sample preparation and counting efficiency. Recent improvements in sample preparation, scintillators, and equipment designed to optimize the system for alpha assay indicate that rapid, accurate, and efficient methods of alpha counting and spectrometry are possible with liquid scintillation. Further improvements are needed in sample preparation methods, scintillator efficiency, and detector design to encourage widespread use of alpha liquid scintillation spectrometry.

REFERENCES

1. V. I. Broser and H. Kallmann, *Z. Naturforsch. Teil A* 2(439): 642 (1947).
2. G. T. Reynolds, F. B. Harrison, and G. Salvini, *Phys. Rev.* *78*: 488 (1950).
3. J. K. Basson and J. Steyn, *Proc. Phys. Soc. London Sect. A* *67*: 297 (1954).
4. D. L. Horrocks, *Applications of Scintillation Counting*, Academic Press, New York, 1974, pp. 1-3, 100-102.
5. D. L. Horrocks, *Rev. Sci. Instrum.* *35*: 334 (1964).
6. D. L. Horrocks and M. H. Studier, *Anal. Chem.* *36*: 2077 (1964)
7. W. J. McDowell, pp. 937-50 in *Organic Scintillators and Liquid Scintillation Counting*, ed. by D. L. Horrocks and L. T. Peng, Academic Press, New York, 1971.
8. J. W. McKlveen, Ph.D. thesis, Nuclear Engineering Department, University of Virginia, 1974.
9. J. H. Thorngate, W. J. McDowell, and D. J. Christian, *Health Phys.* *27*: 123-26 (1974).
10. J. W. McKlveen and W. J. McDowell, *Nucl. Technol.* *28*: 159-64 (1976).
11. W. J. McDowell and J. F. Weiss, *Health Phys.* *32*: 73-82 (1977).
12. J. H. Thorngate and D. J. Christian, *Health Phys.* *33*: 443-48 (1977).
13. J. H. Thorngate, *An Alternating Sample Changer and an Automatic Sample Changer for Liquid Scintillation Counting of Alpha Emitting Materials*, ORNL-5307 (August 1977).
14. E. J. Bouwer, J. W. McKlveen, and W. J. McDowell, *Nucl. Technol.* *42*: 102-10 (1979).
15. W. J. McDowell and C. F. Coleman, *Anal. Lett.* *6*: 795-99 (1973).
16. W. J. McDowell, D. T. Farrar, and M. R. Billings, *Talanta* *21*: 1231-45 (1974).

17. W. J. McDowell, *IEEE Trans. Nucl. Sci.* NS-22: 649 (1975).
18. J. W. McKlveen and W. Johnson, *Health Phys.* *28*: 5 (1975).
19. T. Hanschke, *High Resolution Alpha Spectroscopy by Liquid Scintillation Through Optimization of Geometry*, Ph.D. dissertation, Hannover Technical University.
20. D. Horrocks, *Appl. Spectros.* *24*: 397 (1970).
21. R. Winyard, J. Lutkin, and G. M. McBeth, *Nucl. Instrum. Methods* *95*: 141 (1971).
22. D. Horrocks, *Rev. Sci. Instrum.* *34*: 1035 (1963).
23. A. Lindenbaum and C. Judd, *Radiat. Res.* *37*: 131 (1969).
24. K. Darall, G. Hammond, and J. Tyler, *Analyst* *98*: 358 (1973).
25. G. McBeth, R. Weinyard, and J. Lutkin, *Koch-Light Booklet*, Koch Light Laboratories, Ltd., Colnbrook, Bucks, England, 1971.
26. J. Thorngate, *Health Phys.* *34*: 103 (1978).

Discussion:

Larsen (ANL):
What are the possibilities, with the very low backgrounds you are talking about, of applying this system to the determination of ^{241}Pu. That's a reverse situation. You are counting a low energy beta in the presence of lots of alpha. Have you set up your discrimination circuit in such a way that you can discriminate the low energy beta from 241 from the alphas of the ^{239}Pu and ^{240}Pu?

McDowell (ORNL):
You can discriminate either way, so you could do that if you have the plutonium chemically separated. You would need to determine the ^{241}Pu counting efficiency.

Harlan (Rocky Flats):
Is the separation extremely clean between the beta, gamma and the alpha time peaks?

McDowell:
Well, you saw the time spectrum. It is a good deal better than that now. It is very clean, it goes down to the base line. The time separation is about 30 to 40 nanoseconds between peaks. It is better than 99.9%.

Acid-Compensated Multiwavelength Determination of Uranium in Process Streams

D. T. BOSTICK
Oak Ridge National Laboratory, Oak Ridge, Tennessee

ABSTRACT

Uranyl absorbance was measured in the presence of 0.02-5M HNO_3 to determine the effect of nitric acid concentration on the absorbance of uranium in the concentration range of 20-200 g/l. The uranyl absorbance was found to be primarily the result of three uranyl species: UO_2^{2+}, $UO_2NO_3^+$ and a uranyl dimer. The concentration of HNO_3 determines the relative concentration of each of these uranyl cations and, hence, their contribution to the total absorbance. Because UO_2^{2+} and $UO_2NO_3^+$ are the major uranyl species in streams containing excess acid (0.5-5M HNO_3), the absorbance at 416 and 426 nm is used to simultaneously calculate the total uranium and nitrate concentration in a stream to within 5% and 0.5 molar units, respectively. The uranyl absorbance in acid deficient aqueous streams (0.02-0.5M HNO_3) is due primarily to the absorbance of UO_2^{2+} and the uranyl dimer. As a result the absorbance at 416 and 426 nm can be used to simultaneously calculate the total uranium and hydrogen ion concentration in samples to within 3% and 0.2 molar units, respectively.

KEYWORDS: Uranium, nitric acid, spectrophotometric, dual wavelength, determination

INTRODUCTION

Continuous in-line analysis of uranium in process streams can enhance plant operations by allowing continuous process optimization, resulting in a higher quality product with reduced losses. Real time analysis also provides a greater degree of process safety through continuous material balance control and better operator awareness. Instrumentation designed to meet these goals has frequently been based on the direct colorimetric measurement of uranyl ion (UO_2^{2+}) at 416 nm. The in-line detectors incorporate a dual beam optical system to reduce errors resulting from cell window fouling and sample turbidity. Errors in the determination of uranium concentration attributable to these sources generally do not exceed 5% (1-4). However, errors as great as 15-30% are often encountered with these single wavelength instruments, due to variations in nitric acid concentration and temperature (2).

Several adaptations of the photometric method have been suggested to minimize the effect of nitric acid on the determination of uranium, and thereby improve the accuracy of the continuous monitors. Prohaska noted the fact that U-HNO_3 solutions contain both UO_2^{2+} and $UO_2NO_3^+$ (1). He therefore proposed the use of a second order calibration equation, after Betts and Michels (5), in which the absorption at 416 nm was corrected for the presence of UO_2NO_3. Prior knowledge of the nitrate concentration in the stream was required before this correction could be made. Bhargava et. al. (6) found that the absorption due to the total uranium concentration in the sample is linearly proportional to acid concentrations above 0.5M HNO_3. If either the HNO_3 or total uranium concentration is known, one can calculate the concentration of the other component from the solution absorbance at 416 nm. Erickson and Slansky also noted this linear relationship and suggested that uranium and HNO_3 concentrations might be simultaneously determined by using a multi-wavelength approach (7). However, this proposal was not incorporated into their prototype uranium monitor.

This report further defines the influence of 0.02-5M HNO_3 on the uranium absorption spectrum. These results, together with the above recommendations, have led to the development of a dual wavelength technique for the determination of total uranium concentration,

which requires little prior knowledge of stream conditions. The modified photometric method improves the accuracy of existing in-line uranium monitors by compensating for fluctuations in HNO_3 concentration. The improved accuracy is demonstrated over a wide HNO_3 concentration range.

EXPERIMENTAL

Uranium standards were prepared from serial dilutions of 520.1 g/l depleted uranium stock solution containing 0.001M HNO_3. The uranium concentration of the stock was determined coulometrically (8) and the acid concentration was determined titrimetrically after the uranium was complexed with fluoride (9). Reagent grade nitric or perchloric acid and sodium nitrate were used to adjust the concentrations of free acid and nitrate ion, respectively, in the diluted uranyl nitrate standards.

A Cary 14 recording spectrophotometer was used to scan uranyl solutions contained in a 0.1 cm path length quartz cell. Further experimental details are described elsewhere (10)

RESULTS AND DISCUSSION

Typical aqueous streams in the Purex fuel recycling process contain from 20-200 g/l U and up to 1M free nitrate ion. These streams may either contain excess acid (0.5-4M HNO_3) or be acid deficient (0.02-0.5M HNO_3). The concentration of all stream components will vary by at least 10%. The visible spectra of uranium solutions containing varying concentrations of acid and free nitrate were examined in order to develop a uranium monitor that could accurately operate under any of these variable process stream conditions.

The visible uranium spectrum contains several absorption maxima at 426, 416, 403 and 359 nm. Calibration curves obtained at constant HNO_3 and nitrate concentrations are linear with uranium concentration at each of these wavelengths. If, however, the HNO_3 concentration of the solution varies, the absorption at a given concentration of uranium will change considerably. Figures 1 and 2 demonstrate the extent to which the uranium spectra shifts with fluctuations in HNO_3 concentration under both acid-deficient and -excess conditions, respectively. The uranyl spectrum is transformed from the typical UO_2^{2+} triplet to a single broad absorption envelope, having a maximum absorption coefficient which increases significantly as the HNO_3 concentration decreases from 0.2 to .02M HNO_3. Under excess acid conditions, the uranium spectrum is also modified, but to a lesser extent. The absorption coefficients in this case increase with acid concentration from 2-6M HNO_3.

A composite of uranium behavior for both acid conditions is shown in Figure 3. Each curve represents the effect of HNO_3 on the absorption at a given total uranium concentration. A similar set of curves was also generated for the 426 nm absorption maxima. The minimum absorbance for each uranium concentration occurs at a U/HNO_3 molar ratio of approximately 2.

It becomes obvious from the previous figures that uranium analysis based on the absorption at any single wavelength will be considerably influenced by fluctuations in HNO_3 concentration, such as commonly encountered in reprocessing streams. An expression must be derived which will adequately describe the effect of HNO_3 over the 0.02-5M range, as presente in Figure 3. For present purposes, acid-deficient solutions will more accurately be defined as solutions in which the U/H^+ molar ratio exceeds 2 and excess acid solutions will be those with a U/H^+ molar ratio of less than 2. The analysis of each type of solution will be treate separately in the following sections.

Uranium Analysis in Excess Acid Solutions

The absorbance of uranyl solutions is linearly proportional to HNO_3 concentration under excess acid conditions. To define the exact nature of this behavior, the uranium spectra were observed in the presence of increasing hydrogen ion concentration, added as $HClO_4$, and increasing nitrate ion concentration, added as $NaNO_3$. At constant uranium and nitrate concentration, uranyl absorption is only slightly affected by hydrogen ion concentrations greate than 5M $HClO_4$. At constant uranium and hydrogen ion concentration, uranium absorption increases linearly with nitrate (Fig. 4). The slopes of the curves obtained with varying

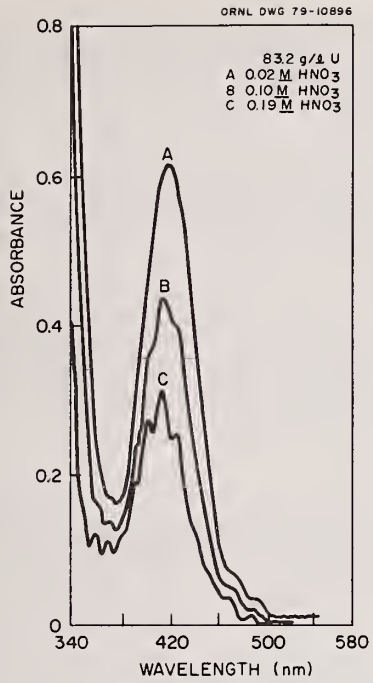

Fig. 1. Uranium Visible Spectra in Acid Deficient Solutions

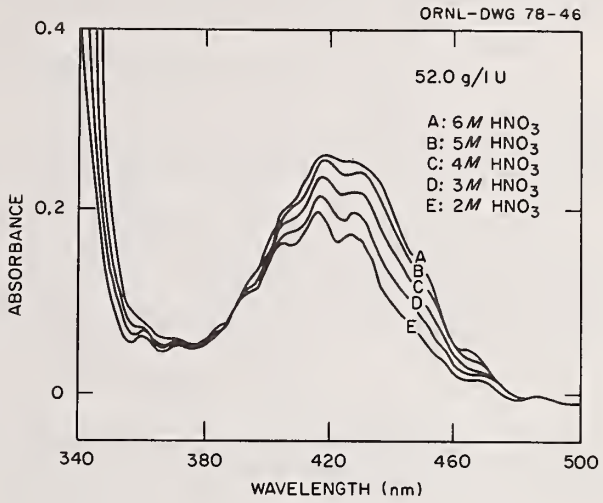

Fig. 2. Uranium Visible Spectra in Excess Acid Solutions

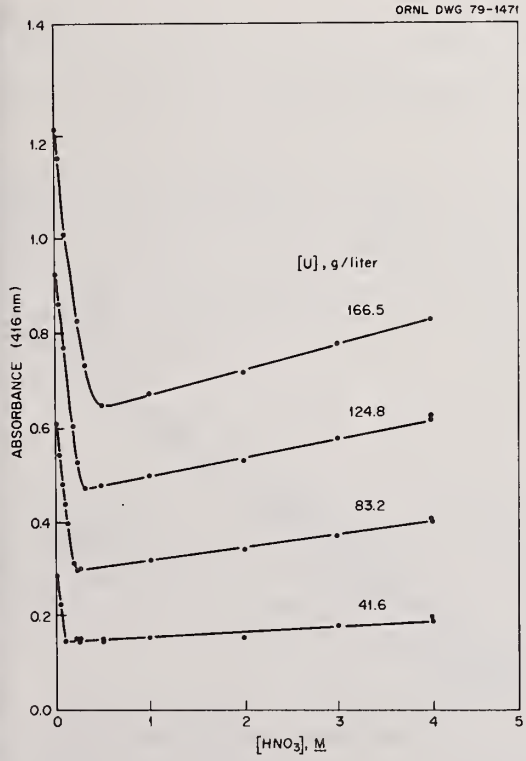

Fig. 3. Effect of Nitric Acid at Various Uranium Concentrations

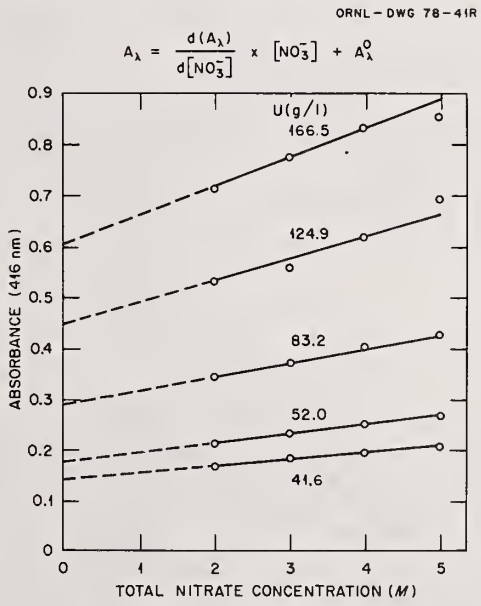

Fig. 4. Effect of Nitrate at Various Uranium Concentrations

nitrate ion were found to be identical to those obtained by varying HNO_3 concentration, indicating that the elevation in uranyl absorption with HNO_3 concentration is proportional to the total nitrate, rather than hydrogen ion or HNO_3, concentration. From Figure 4, the absorbance (A_{416}) at a given uranium concentration is equivalent to:

$$A_{416} = d(A_{416})/d[NO_3^-] \times [NO_3^-] + A^o_{416} \quad , \tag{1}$$

where $d(A_{416})/d[NO_3^-]$ is the slope of a given line and A^o_{416} is the extrapolated intercept. A similar relationship can be written for solutions in which the U/H^+ molar ratio is less than 2 at each of the remaining uranyl absorption maxima.

The uranium concentration appears to influence the magnitude of both $d(A_{416})/d[NO_3^-]$ and A^o_{416}. The exact proportionality can be evaluated by plotting both $d(A_{416})/d[NO_3^-]$ and A^o_{416} versus uranium concentration. Similar effects were observed for all four absorption maxima. As indicated in Figure 5, the slope of 416 nm data can be represented by a proportionality constant, M_{416}, in the following equation:

$$d(A_{416})/d[NO_3^-] = M_{416}[U] + b_{416} \quad . \tag{2}$$

The value, b_{416}, is the intercept of 416 nm data and is essentially equal to zero. A plot of A^o_{416} versus uranium concentration (Fig. 6) permits the calculation of the proportionality constant N_{416} such that:

$$A^o_{416} = N_{416}[U] + c_{416} \quad . \tag{3}$$

Again, c_{416} represents the small negative intercept of the 416 nm data line.

Combining equations 1-3 thus completely describes the effect of nitrate ion on uranium absorption at 416 nm under excess acid conditions:

$$A_{416} = M_{416}[U][NO_3^-] + N_{416}[U] + C_{416} \quad . \tag{4}$$

This behavior is exactly that described by Prohaska (1) in which total uranyl absorption is due both to the absorbance of UO_2^{2+}, calculated by the product $N_{416}[U]$, and $UO_2NO_3^+$, calculate by the product $M_{416}[U][NO_3^-]$.

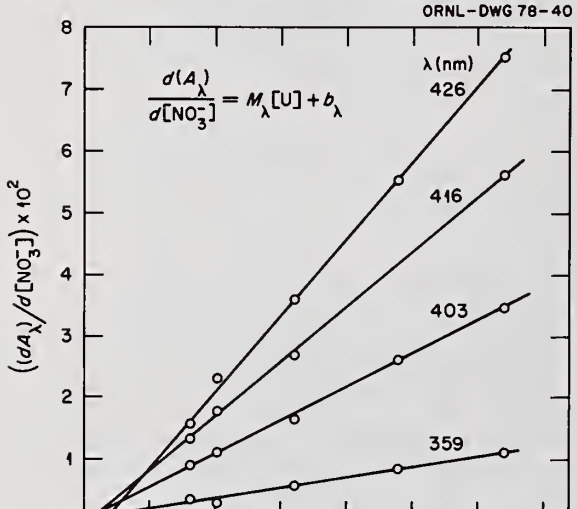

Fig. 5. $d(A_\lambda)/d[NO_3^-]$ versus Uranium Concentration

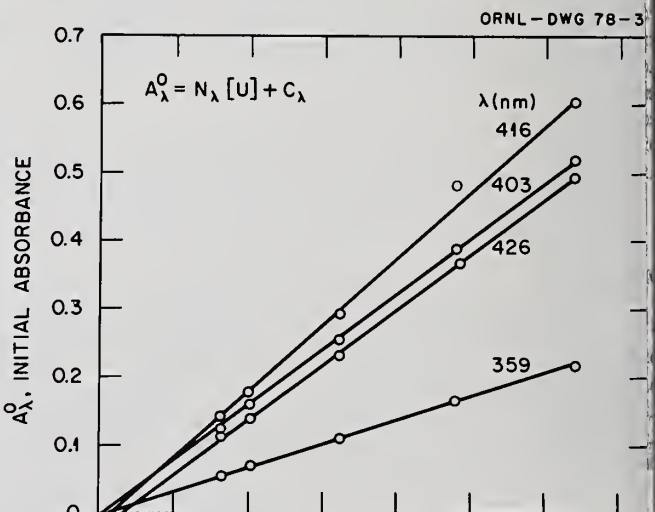

Fig. 6. Extrapolated Absorbance (A^o_λ) versus Uranium Concentration

Both UO_2^{2+} and $UO_2NO_3^+$ similarly contribute to the absorption at the remaining uranyl wavelengths, and therefore relationships analogous to equation 4 can also be written for each of these absorption maxima. By combining equations from any two of the uranyl absorption wavelengths, it is possible to simultaneously calculate the total uranium and nitrate concentrations of a given sample. Because 416 and 426 nm data exhibit the greatest sensitivity toward uranium and nitrate, these two wavelengths were selected for use in the uranium monitor. The simultaneous equations for uranium and nitrate analysis, respectively, in excess acid solutions are given below:

$$[U] = \frac{M_{426}\ (A_{416}-c_{416}) - M_{416}\ (A_{426}-c_{426})}{M_{426}N_{416} - M_{416}N_{426}} \qquad (5)$$

and

$$[NO_3^-] = \frac{N_{426}\ (A_{416}-c_{416}) - N_{416}\ (A_{426}-c_{426})}{M_{416}\ (A_{426}-c_{426}) - M_{426}\ (A_{416}-c_{416})} \ . \qquad (6)$$

For a 0.1 cm path length optical cell, these calibration equations numerically reduce to:

$$[U] = 6.83X10^2\ A_{416} - 5.00X10^2\ A_{426} - 0.973 \qquad (7)$$

and

$$[NO_3^-] = \frac{3.10X10^{-3}(A_{416}+0.0114) - 3.74X10^{-3}(A_{426}-0.0175)}{3.10X10^{-4}(A_{426}+0.0175) - 4.23X10^{-4}(A_{416}+0.0114)} \ . \qquad (8)$$

The estimated relative standard deviations using the above equations are 5% and 15% for 20-200 g/l uranium and 0.5-5M nitrate, respectively.

Uranium Analysis in Acid Deficient Solutions

Above a U/H^+ molar ratio of 2, the uranyl absorbance is no longer proportional to the total nitrate concentration. Instead, the absorbance sharply increases as the acid concentration of the solution decreases. Uranyl absorbance in acid deficient solutions was found to be proportional to the square of uranium concentration and the inverse of hydrogen ion concentration in the sample. Because the absorbance is dependent on the square of uranium concentration, the uranyl species formed in the 0.02-0.5M HNO_3 range is assumed to be a dimer of uranium, although its exact identity is unknown. The complete equation which describes uranyl absorbance at 416 nm in the 0.02-5M HNO_3 can be written as:

$$A_{416} = K_{416}\ [U]^2/[H^+] + M_{416}\ [U]\ [NO_3^-] + N_{416}[U] + c_{416} \ , \qquad (9)$$

where the term $K_{416}[U]^2/[H^+]$ represents the absorbance due to the uranyl dimer.

In excess acid streams the hydrogen ion concentration is so high that the contribution of the dimer to the total absorbance of the sample becomes negligible. The calculation of A_{416} then reduces to that described in equation 4. Conversely, the nitrate concentration in acid deficient streams is generally so low as to make the product $M[U][NO_3^-]$ negligible in comparison to the absorbance produced by UO_2^{2+} and the uranyl dimer. Equation 9 can then be simplified for acid deficient streams to:

$$A_{416} = K_{416}[U]^2/[H^+] + N_{416}[U] + c_{416} \ . \qquad (10)$$

The 426 nm data also exhibit the same response to HNO_3 so that a simultaneous equation can be derived for the calculation of uranium concentration in acid deficient samples based on 416 and 426 nm absorbance:

$$[U] = \frac{K_{416}\ (A_{426}-c_{426}) - K_{426}\ (A_{416}-c_{416})}{K_{416}\ N_{426} - K_{426}\ N_{416}} \ . \qquad (11)$$

Because the simultaneous solution for hydrogen ion concentration is mathematically too comple to be useful, acid concentration is determined subsequently, based on the calculated uranium concentration:

$$[H^+] = \frac{K_{416}[U]^2}{(A_{416}-c_{416}) - N_{416}[U]} \quad . \tag{12}$$

A computer routine was used to determine the optimum values, based on a least squares criterion, for the constants in equations 11 and 12. The numerical values of the constants are given below, assuming a 0.1 cm optical path length:

$$[U] = \frac{1.165X10^{-6}(A_{426}+0.0194) - 1.294X10^{-6}(A_{416}+0.0128)}{(1.165X10^{-6})(3.25X10^{-3}) - (1.294X10^{-6})(3.83X10^{-3})} , \tag{13}$$

which reduces to

$$[U] = 1.106X10^{3}\ A_{416} - 9.959X10^{2}\ A_{426} - 5.16 , \tag{14}$$

and

$$[H^+] = \frac{1.165X10^{-6}[U]^2}{(A_{416}+0.0128) - 3.83X10^{-3}[U]} \quad . \tag{15}$$

The estimated relative standard deviations using the above equations are 3% and 0.2 molar units for 20-200 g/l uranium and 0.02-0.5M HNO_3, respectively.

SUMMARY

The above derived equations demonstrate that by monitoring the 416 and 426 nm absorbance of a uranyl process stream, uranium concentration can be accurately determined in the presenc of varying concentrations of HNO_3 and free nitrate ion. Prior knowledge of exact concentrations of these constituents is not required for the analysis. Once the operating range of the hydrogen ion concentration has been established for a given process stream, the appropriate simultaneous equation can be applied to the absorbance data. In streams for which the U/H^+ molar ratio will be greater than 2, the acid deficient form (eq.11 and 12) can be used to determine uranium and estimate hydrogen ion concentration. The excess acid form (eq. 5 and 6) can be used to calculate uranium and free nitrate concentration in streams where the value of the U/H^+ molar ratio will be less than 2. If the molar ratio is anticipated to vary about the value of 2, equation 11 rather than equation 5 should be used to calculate uranium concentration. As indicated in Table 1, the acid deficient form of the simultaneous equation results in less error in predicting uranium concentration for streams operating near the intermediate U/H^+ molar ratio of 2.

Use of the descriptive expressions derived above will significantly decrease the analytical error in the estimation of total uranium concentration in actual process streams and also provide estimates of other important components (hydrogen or total nitrate ion) in the same stream.

Table I. Accuracy in the Simultaneous Determination of Uranium Concentration

Exp. [U] (g/l)	Exp. [HNO_3] (M)	U/H Molar Ratio	Calc. [U] Equation 5	% Diff.*	Calc. [U] Equation 11	% Diff.*
124.8	0.048	10.9	174.0	39.0	124.4	0.3
83.2	0.048	7.28	111.2	34.0	80.7	3.0
83.2	0.080	4.37	104.3	25.0	81.9	1.5
166.5	0.320	2.19	179.3	7.7	166.4	0.1
124.8	0.256	2.05	134.3	7.6	129.5	3.8
114.4	0.256	1.89	118.5	3.5	118.7	3.7
124.8	0.320	1.64	125.0	0.2	125.3	0.4
166.5	0.512	1.37	166.8	0.2	163.8	1.3
83.2	1.02	0.341	82.1	1.3	78.7	5.4
83.2	3.06	0.117	81.3	2.3	65.4	21.0

*Represents the absolute value of 100·(Experimental [U] - Calculated [U])/Experimental [U].

REFERENCES

1. C. A. Prohaska, "A Flow Colorimeter for Measuring Uranium Concentrations in Process Streams", DP-229 (1957).

2. D. W. Colvin, "A Colorimeter for the In-Line Analysis of Uranium and Plutonium", DP-461 (1960).

3. J. W. Landry, "In-Line Instrumentation Gamma Monitor, Uranium Colorimeter", ORNL-2978 (1960).

4. F. A. Scott and R. D. Dirks, "Photometer for Continuous Determination of Uranium in Radioactive Process Streams", Anal. Chem., 32, 268-72 (1960).

5. R. H. Bëtts and R. K. Michels, "Ionic Association in Aqueous Solutions of Uranyl Sulphate and Uranyl Nitrate", J. Chem. Soc. (London) 1949: S286.

6. V. K. Bhargava, E. S. Chandrasekharan, R. H. Iyer, V. K. Ras, M. V. Ramaniah and N. Srinivason, "In-Line Analytical Methods for Fuel Reprocessing Streams. Part I. Direct Colorimetry for Uranium and Free Acid", BARC-510 (1970).

7. E. E. Erickson and C. M. Slansky, "A Continuous Photometer for Low Concentrations of Uranium in Aluminum Nitrate-Nitric Acid Solutions", IRE Trans on Nuclear Science, 8, 83 (1961).

8. G. L. Booman, W. B. Holbrook and J. E. Rein, "Coulometric Determination of Uranium (VI) at Controlled Potential", Anal. Chem., 29, 219 (1957).

9. O. Menis, D. L. Manning and G. Goldstein, "Detection of Free Acid in Solutions of Uranyl Sulfate", ORNL-2178 (1956).

10. D. T. Bostick, "The Simultaneous Analysis of Uranium and Nitrate", ORNL TM-6292 (1978).

Acknowledgement

Research sponsored by the Nuclear Power Development Division, U.S. Department of Energy under contract W-6405-eng-26 with Union Carbide Corporation.

Discussion:

Persiani (ANL):

Can a similar system be applied to the plutonium stream and to a mixture of plutonium and uranium?

Bostick (ORNL):

That's what we are working on right now. We are mainly looking at plutonium (III) and (IV) in aqueous streams. The plutonium (III) absorbance doesn't seem to vary much with acid concentration, but the plutonium (IV) absorbance is quite dependent on acid concentration. We are investigating whether we can use a similar dual wavelength approach for plutonium. Our final goal is to be able to determine plutonium (III) and (IV) and uranium all in a single stream with about a 5% accuracy.

Questioner:

Basically, when you get into a situation where there is a hundred times as much uranium as there is plutonium you're in trouble. The absorbancies for the plutonium species are not significantly different from those for the uranium species.

Bostick:

We are looking at the visible plutonium (IV) spectra and mainly the 476 wavelength line. The 565 and 603 nm lines are being monitored for plutonium (III). Typically uranium concentrations will vary between 2 and 200 g/L. The plutonium concentrations will vary between about 1 and 20 gms per liter. Plutonium can be easily analyzed under these experimental and process stream conditions.

Questioner:

Can your in-line monitor system be adapted to handle low uranium concentrations at the waste station and second, can your system be calibrated in-line?

Bostick:

Let me answer your second question first. The design and maintenance of the in-line instrument is too complex to build in a self-calibrating system. Instead, samples will be drawn and analyzed for safeguard requirements every place the instruments occur and we will use those for calibration. The first question: we have been thinking about looking at trace levels of uranium by using a long path-length cell. We thought that fluorescence might be a better way of looking at trace levels of uranium.

Hakkila (LASL):

What is the advantage for high uranium concentrations of using the spectrophotometric method over the densities methods?

Bostick:

Well, actually we have made that study. We have had a mini-process going where we have had a densitometer and the photometer side-by-side in the stream. The dual wave length procedure was much more accurate than the density measurement. Using a densitometer you have to assume a concentration for nitric acid and nitrate. Our levels of uranium concentration are going to be about 80 gms per liter and lower. There was too much inaccuracy because of the stream composition variability, particularly in the assumed nitrate and HNO_3 concentration. You need the dual wave length approach to get the 5% accuracy that is wanted in process control.

LASL Analytical Chemistry Program for Fissionable Materials Safeguards

by

D. D. JACKSON and S. F. MARSH
Los Alamos Scientific Laboratory, Los Alamos, New Mexico

ABSTRACT

Major tasks in this program are (1) development of dissolution techniques for refractory nuclear materials, (2) development of methods and automated analyzers for determining plutonium, uranium, and thorium, (3) preparation of plutonium reference materials distributed as certified reference materials by the National Bureau of Standards, used in the Safeguards Analytical Laboratory Evaluation (SALE) program administered by the New Brunswick Laboratory, and used to calibrate nondestructive analysis apparatus at LASL, and (4) preparation and characterization of plutonium isotope materials and participation in an intralaboratory program to measure longer-lived plutonium isotope half lives. More recent and significant achievements are reported. Gas-solid reactions at elevated temperature, used previously to convert uranium in refractory forms to species readily soluble in acid, are being applied to thorium materials. A microgram-sensitive spectrophotometric method was developed for determining uranium and the LASL Automated Spectrophotometer has been modified to use it. The instrument now is functional for determining milligram amounts of plutonium, and milligram and microgram amounts of uranium. Construction of an automated controlled-potential-coulometric analyzer has just been completed. It is giving design performance of 0.1% relative standard deviation for the determination of plutonium using a method developed especially for the instrument. A method has been developed for the microcomplexometric titration of uranium in its stable (VI) oxidation state. A color probe analyzer assembled for this titration also has been used for microcomplexometric titration of thorium. The present status of reference materials prepared for NBS and for the SALE program, as well as examples of working reference materials prepared for use with nondestructive analyzers, is given. The interlaboratory measured value of the ^{239}Pu half-life is 24,119 yr. Our just completed measurement of the half life of ^{241}Pu is 14.38 yr. Measurement of the ^{240}Pu half life is in progress.

KEYWORDS: Assay of uranium, plutonium, and thorium, automated spectrophotometer, automated controlled-potential analyzer, complexometric titration of uranium and thorium, dissolution of nuclear fuel-cycle materials, plutonium reference materials, half lives plutonium isotopes.

INTRODUCTION

The primary purpose of characterizing nuclear fuel cycle materials for safeguards application is measurement of their uranium, plutonium, and thorium contents. All measurements must be accurate, with precision requirements ranging from < 0.1% standard deviation for product materials to several percent for scrap materials containing low quantities of these three elements. Many fuel-cycle materials, including scrap materials produced in calcination processes, contain highly refractory components and have multiphase, heterogeneous composition. At present, a particularly time-consuming operation in the chemical assay of such materials is their dissolution to effect solubilization of the uranium, plutonium, and thorium. In addition to fast, effective dissolution technique, automated analyzers for assaying the three elements will provide economy. The accuracy of assay measurements,

whether by chemical analysis or by use of nondestructive (NDA) techniques, depends on calibration, best attained by use of proper reference materials. Accurate plutonium isotope half life values are essential to NDA methods based on radioactive calorimetry and decay measurement, as well as for adjusting reference materials and accountable material inventories for their changing plutonium content with time.

DISSOLUTION OF NUCLEAR FUEL CYCLE MATERIALS

Techniques currently being investigated to attain rapid and effective solubilization of uranium, plutonium and thorium in refractory materials are mineral acid reactions at elevated temperatures in pressurized containers and reactions with reactive gases at elevated temperatures.

We previously developed a dissolution apparatus of a Teflon container in pressure-supporting stainless steel and nickel shells which permit reactions with various mineral acids at temperatures up to 260°C and pressures to 320 atm (5000 psi). The apparatus design was made available to industry and was adopted by the Parr Instrument Company. A stainless steel shell is used with HNO_3, H_2SO_4, and HNO_3-H_2SO_4 mixtures. A nickel container is used for HCl, HF, and their mixtures. The dissolution apparatus has been applied successfully to a variety of materials including Nb-U alloy, UO_2ZrO_2 in Zr matrix, U-Zr-Hf carbide, 1600°C-sintered $(U\text{-}Pu)O_2$, and a variety of scrap-type materials supplied by the New Brunswick Laboratory (NBL).

We verified NBL findings that the Parr Teflon containers frequently failed when used at 270°C with HNO_3-low molarity HF mixtures for the dissolution of materials such as high-fired PuO_2 and calcined mixed oxide. The Parr Company supplied Teflon containers made from new Teflon stock and we fabricated new containers. Both failed even when heated at only 250°C with a HNO_3-low molarity HF mixture and without samples.

The du Pont Company, in response to our request, recommended two Teflon grades, molded 7A and Type 1 Premium per ASTM D-3294. Containers fabricated from both grades withstand repeated use with the HNO_3-HF mixture at 260°C. The Parr Instrument Company has changed its production to use only the molded 7A grade.

Gas-solid reactions at elevated temperatures are being investigated for converting refractory materials to soluble compounds or for forming volatile uranium and thorium compounds that condense as compounds readily soluble in mineral acids. Materials in a quartz boat are reacted in a quartz tube heated by a resistance furnace. The tube is designed to provide a controllable atmosphere and effective recovery of the volatilized compounds.

Reactions with chlorine gas and carbonyl chloride, especially the latter, are effective for volatilizing uranium. For example, 0.1 g of U_3O_8 (as well as UO_2, UO_3, and UC_2) volatilizes completely when reacted with chlorine at 1000°C for 12 h or 1200°C for 5 h. With carbonyl chloride, using the same reaction conditions for chlorine, 0.1 g U_3O_8 volatilizes completely in < 0.5 h at 1000°C and in < 1 h at 700°C. The system has been applied successfully to a variety of uranium-containing materials produced in a LASL waste-recovery calcination facility and supplied for testing by NBL. The method is effective for materials containing zirconium and niobium which, like uranium, volatilize as chlorides.

The technique now is being evaluated for thorium materials. As predicted by the relative boiling points of UCl_4 and $ThCl_4$, thorium is proving more difficult to volatilize. For example, $< 1\%$ of ThO_2, previously calcined at 1200°C in air, volatilizes during a 1-h reaction with chlorine, contrasted to about 40% for U_3O_8. Under the same conditions using carbonyl chloride instead of chlorine, uranium was completely volatilized, but volatilization of thorium increased only to 36%. The formation of volatile UCl_4 and $ThBr_4$ by reaction of the oxides with chlorine and bromine in the presence of carbon[1] prompted an evaluation of various forms of carbon. Charcoal is proving the most effective. With

[1]G. T. Seaborg and J. J. Katz, The Actinide Elements (McGraw-Hill, New York, 1954), pp. 84, 153.

mixtures of the 1200°C calcined ThO_2 and various charcoals, at a C/ThO_2 mole ratio > 3, the thorium volatilization is > 99% in 1 h at 1000°C. The condensed thorium compound dissolves readily in mineral acids.

ANALYTICAL METHODS AND AUTOMATED INSTRUMENTS FOR URANIUM, PLUTONIUM, AND THORIUM DETERMINATIONS

Automated Spectrophotometer

The LASL Automated Spectrophotometer is designed primarily for determining uranium and plutonium in scrap materials. The method used in the original instrument[2] provides high tolerance for the many impurity elements present in scrap materials. Measurement precision is about 1% standard deviation for a range of about 1 to 14 mg of either element determined in sample portions up to 0.5 ml.

Because many scrap materials have very low uranium and plutonium contents, measurements of microgram quantities of the two elements often are required. A method, designed for use in the automated spectrophotometer, was developed.[3] It features measurement of 2.5- to 100-µg amounts of uranium and high tolerance for impurity elements present in scrap materials. The method consists of extracting the U(VI)-benzoyltrifluoroacetone complex into butyl propionate from a solution that contains Mg(II)-cyclohexanediaminetetraacetic acid masking agent to provide high selectivity and hexamethylenetetramine and triethanolamine to provide high buffering capacity.

The automated spectrophotometer, shown in Fig. 1, was modified to use this microgram-level uranium method as well as the original methods for determining low milligram levels both of plutonium and uranium. Modifications include (1) a separate reagent dispensing system for the microgram-level method, (2) a mechanism to switch the pneumatic-hydraulic system automatically between the two sets of dispensers, (3) removal of the cam-actuated switches that had controlled mechanical operations and expansion of the microcomputer system to provide complete control of all mechanical and electrical operations, (4) installation of a pair of interference filters for absorbance measurements for the microgram-level method, and (5) replacement of the $3\frac{1}{2}$-digit, analog-to-digital converter with a $4\frac{1}{2}$-digit converter to cover a larger dynamic range.

Output response for the microgram-level method is linear over the range of 2.5 to 100 µg of uranium. The precision ranges from 0.5% standard deviation at 90 µg to 3% at 5 µg of uranium. Under instrument operation conditions, tolerances of 48 metal ions and 17 nonmetal anions have been established.[4]

Automated Controlled-Potential Coulometer

We previously have described[5] a controlled-potential-coulometric method for plutonium developed for use in an automated analyzer. Construction of the analyzer has been completed recently. The method features high tolerance for impurities, a precision of 0.1%

[2] D. D. Jackson, D. J. Hodgkins, R. M. Hollen, and J. E. Rein, "Automated Spectrophotometer for Plutonium and Uranium Determination," Los Alamos Scientific Laboratory report LA-6091 (February 1976).
[3] S. F. Marsh, "Extraction-Spectrophotometric Determination of Microgram Quantities of Uranium with Benzoyltrifluoroacetone," Anal. Chim, Acta 105, 439-443 (1979).
[4] G. R. Waterbury, Compiler, "Analytical Methods for Fissionable Materials in the Nuclear Fuel Cycle, October 1, 1978-September 30, 1979," Los Alamos Scientific Laboratory report, in press.
[5] D. D. Jackson, R. M. Hollen, F. R. Roensch, and J. E. Rein, "Highly Selective Coulometric Method and Equipment for the Automated Determination of Plutonium," in Analytical Chemistry in Nuclear Fuel Reprocessing, W. S. Lyon, Ed., Proc. 21st Conf. Anal. Chem. Energy Technol., Gatlinburg, Tennessee, October 4-6, 1977 (Science Press, Princeton, 1978), p. 51.

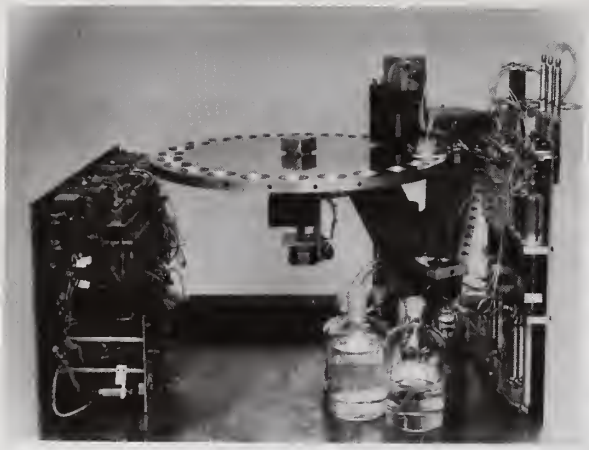

Fig. 1. Automated Spectrophotometer

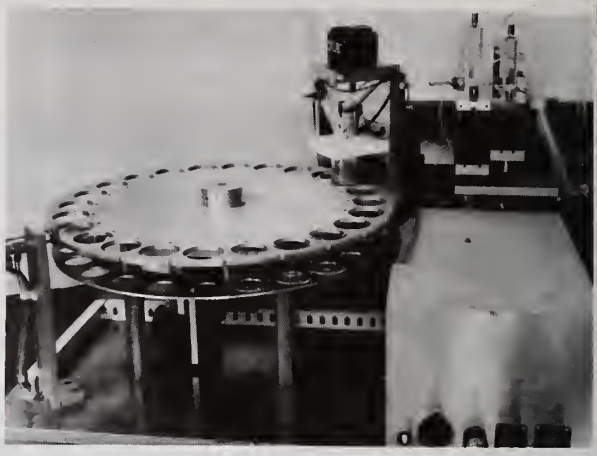

Fig. 2. Automated Controlled-Potential-Coulometric Analyzer

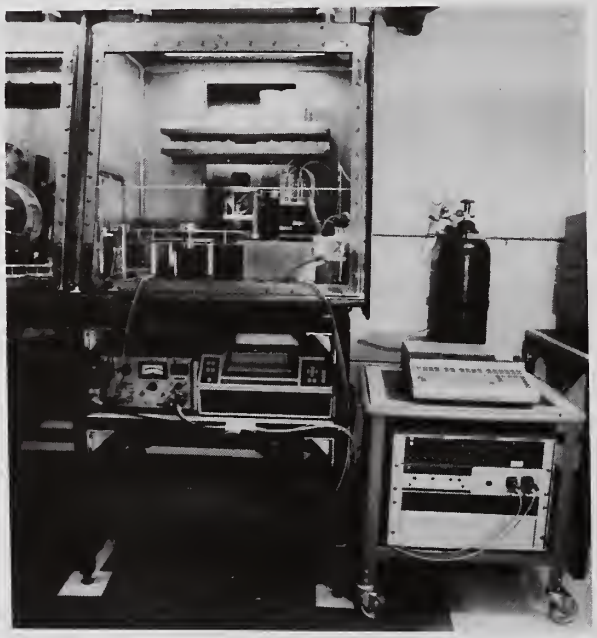

Fig. 3. Automated Controlled-Potential-Coulometric Analyzer in Box

standard deviation for the determination of 5 mg plutonium, and operational simplicity. Plutonium is reduced at 0.25 V (vs SCE) to Pu(III) in 5.5M HCl - 0.015M sulfamic acid electrolyte. Diverse ions are oxidized at 0.57 V at which Pu(III) is not significantly oxidized. Phosphate (as NaH_2PO_4) is added to lower the Pu(III)-Pu(IV) potential and Pu(III) is titrimetrically oxidized to Pu(IV) at 0.68 V. Results of a detailed investigation of diverse ion tolerances for more than 75 metal ions and nonmetal anions have been reported.[5] Metallic elements normally present in nuclear fuel cycle materials do not interfere at equal-mole ratio relative to plutonium. Most interfering nonmetal anions are separated by fuming with perchloric acid prior to analysis.

An overall view of the instrument components is shown in Fig. 2 and its installation in a containment box is shown in Fig. 3. The mechanical portion is installed in the sloping, open-front box that is 0.91 m wide, 0.79 m deep, and 0.84 m high and the electronic components are mounted outside the box.

The major electronic components of the instrument, shown in Fig. 4, are commercial which simplifies maintenance. A Hewlett-Packard 9825 Programmable calculator controls all mechanical and electrical operations, processes titration data, and outputs results on paper tape. A Princeton Applied Research Corporation 173 Potentiostat-Galvanostat and 179D Digital Coulometer, modified for calculator control, do the electrolysis. Also interfaced and under calculator control are a D to A converter, a digital multimeter, a scanner, a real time clock and a digital plotter. The D to A converter provides calculator capability to select electrode potentials. The digital multimeter measures electrolysis conditions of interest and serves as an A to D converter to input data to the calculator. The digital multimeter also monitors interlocks designed to protect the instrument in case of a malfunction. The scanner switches the digital multimeter to the point to be measured. The mechanical operations are controlled through the scanner by contact closure of relays. The real-time clock monitors electrolysis times and by means of an interrupt system terminates analyses in which the times exceed those found to affect the determination adversely. The plot of log current vs. time provided by the on-line digital plotter allows a trained analyst to spot deviations indicative of a faulty analysis.

The mechanical assembly is designed for long-term, trouble-free operation. A turntable holding up to 24 electrolysis cells rotates them into position under a fixed Teflon support. Smooth and accurate rotation is provided by a Geneva-drive, intermittent motion assembly. Positional accuracy is further insured by a cylindrical rod, driven by a pneumatic cylinder, that engages slots in the edge of the turntable at each of the 24 positions.

The electrolysis cells are simply fabricated from 4.8-cm-diam glass tubing by flame sealing a flat bottom and grinding the top flat. The electrodes, stirring mechanism, reagent-delivery tubes, inert-gas inlet, and rinsing system are mounted in a rigid Teflon support. The cells are raised by a hydraulic-cylinder-driven assembly to form a gas-tight seal against the Teflon support and to position the various components reproducibly. The reagent dispensers for the HCl-sulfamic acid electrolyte and the phosphate complexant are similar to those used in the automated spectrophotometer.[2] Only glass, Teflon, and Kel-F contact the highly corrosive reagents.

The analyzed sample and rinse solution are withdrawn by suction through a Teflon tube. The aspiration tube is driven by a pneumatic-cylinder mechanism to an exact position at the bottom of the cell near the platinum-gauze electrode for efficient removal of the liquid. Two consecutive rinses, each with ~ 25 ml of 5.5M HCl, leave less than 0.01% of the previous sample.

Complexometric Titration of Uranium and Thorium

Methods are being developed for the determination of microgram and milligram levels of uranium and thorium applicable to materials produced in various stages of fuel production and ultimately for irradiated fuel analysis. A versatile, automated apparatus, shown in Fig. 5, has been assembled for this purpose. In the instrument, titrant is delivered by a micrometer pipet driven by a stepping motor to provide precise increments. A probe colorimeter immersed in the solution monitors the continuously changing color. Light is transmitted to the probe tip through a flexible fiber-optic light guide. The light passes through the solution and is reflected by a mirror at the end of the probe tip back

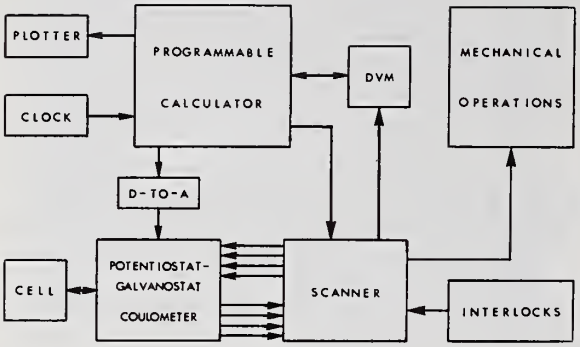

Fig. 4. Control System for Controlled-Potential-Coulometric Analyzer

Fig. 5. Complexometric Titration Apparatus

through another portion of the fiber-optic light guide to the photodiode detector. A programmable calculator controls the titrant addition, senses the approximate inflection point, processes the data, and calculates the quantity of titrant at the endpoint as the intercept of least squares fitted lines before and after the inflection point. A digital voltmeter serves as an analog-to-digital converter to transfer the measured absorbance values into the calculator. A stripchart recorder also monitors the absorbance output from the colorimeter and provides a plot of absorbance vs delivered titrant volume.

Thorium is determined by titrating the thorium-xylenol orange complex with diethylenetriaminepentaacetic acid. Over the range of 20 to 140 μg thorium, the precision is < 1 μg standard deviation. Because this method is not selective, a chemical separation procedure is being developed.

A selective, complexometric titration method has been developed for determining uranium. The U(VI)-arsenazo I complex is titrated with dipicolinic acid (pyridine-2,6-dicarboxylic acid) at a pH of 4.9 attained with hexamethylenetetramine buffering. Selectivity is gained by use of cyclohexanediaminetetraacetic acid and diethylenetriaminepentaacetic acid as masking agents. Measurement precision for 30 to 180 μg of uranium is about 0.6% standard deviation. Tolerances of diverse impurities are being established.

PREPARATION OF REFERENCE MATERIALS

Reference materials, mainly containing plutonium with lesser numbers containing uranium, are prepared for distribution as NBS standard reference materials, for use in the NBL-administered Safeguards Analytical Laboratory Evaluation (SALE) program, and as working calibration materials for various nondestructive analyzers in operation at the new LASL plutonium processing facility and elsewhere. Table I summarizes the status of LASL-prepared materials prepared for NBS. The status of materials prepared for the SALE program is given in Table II. Examples of working calibration materials for nondestructive analyzers are given in Table III.

Table I. Plutonium Reference Materials Prepared by LASL as NBS Certified Reference Materials

Composition	Designation	Certified for	Status
Pu metal	SRM 945	purity 99.9%, impurity blend matrix	present lot in ample supply
Pu metal	SRM 949	assay g Pu/g	eighth lot to be prepared in 1980
Pu-244	not assigned	atoms Pu-244 per container	prepared. characterization in progress

Table II. Reference Materials Prepared by LASL for NBL SALE Program

Composition	Certified for	Status
Pu nitrate solution	g Pu/container, isotopic	one series used in the past. Not planned for future use.
PuO_2	g Pu/g	second series of 3 lots scheduled for 1980.
$(U-Pu)O_2$ powder	g Pu/g, g U/g Pu and U isotopic	previous series of 3 lots prepared. Not planned for future use.
$(U-Pu)O_2$ pellets	as above	second series of 3 lots prepared. Characterization in progress.

Table III. Typical Reference Materials Prepared by LASL Analytical Chemistry Group for Calibration of NDA Instruments

Material	Characterization	Various Configurations
PuO_2	Pu assay, particle size, impurities	solutions
		solids
$PuCl_3$	Pu assay, isotopic	
		solids on specific
$Pu(NO_3)_4$	Pu assay, isotopic	substrates
$UO_2(NO_3)_2$	U assay	geometric containers
$(U-Pu)Cl_4$	U, Pu assay	

PLUTONIUM ISOTOPE HALF-LIFE MEASUREMENTS

Accurate half-life values of longer-lived plutonium isotopes are essential to non-destructive methods of analysis that measure a nuclear property associated with a disintegration rate, including calorimetry and various radioactive particle measurements, and to adjust the plutonium content and isotopic distribution values of reference materials and accountable material inventories. In an interlaboratory effort sponsored by the DOE Office of Safeguards and Security, LASL prepares and characterizes pure, enriched-isotope plutonium materials for distribution to participating laboratories, and participates in the half-life measurements.

As shown in Table IV, the intralaboratory effort has produced a precise measurement of the half-life of ^{239}Pu.[6] Our recently completed measurement of the ^{241}Pu half-life, based on mass spectrometric determinations of the decreasing $^{241}Pu/^{242}Pu$ ratio over a 3.6-yr time period, is 14.38 yr with a 95% confidence limit of 0.06 yr. At present, an interlaboratory effort is in progress for the measurement of the ^{240}Pu half-life.

[6]L. L. Lucas and W. B. Mann, Editor, Int. J. Appl. Radiat. Isotopes, 29 (No. 8), 479-524 (1978).

Table IV. Plutonium Isotope Half-Life Measurements Status

Isotope	Measurement Technique	Laboratory*	Status
238	not done	-	recommended average of 87.74 yr measured by ANL and ML
239	α-particle calorimetry mass spectrometry of U-235 daughter	ANL, LLL, NBS LLL, ML ANL, LASL, LLL	complete: 24, 119 ± 26 y
240	α-particle calorimetry mass spectrometry of U-236 daughter	LASL, NBS LLL, ML LASL	$^{240}PuO_2$ prepared. Characterization and half-life measurements in process
241	mass spectrometry of changing 241/242 ratio	LASL	complete: 14.38 ± 0.06 y

*ANL- Argonne National Laboratory
LLL- Lawrence Livermore Laboratory
NBS- National Bureau of Standards
ML- Mound Laboratory
LASL - Los Alamos Scientific Laboratory

Discussion:

Larsen (ANL):
Why does zirconium interfere?

Jackson (LASL):
Because I am using phosphate to lower the plutonium (III)-plutonium (IV) potential. Zirconium interferes by forming a precipitate and flocculating plutonium which results in a low value.

Larsen:
Then you said that oxidation of the electrolyte makes it necessary to lower the plutonium (III)-plutonium (IV) potential. Are you saying that you would start generating hydrogen as readily as you start generating plutonium (IV)?

Jackson:
What I am saying is the oxidiation of plutonium (III) to plutonium (IV) in 5.5 M HCl requires a sufficiently high potential that oxidation of the electrolyte would take place during a high background current. So we add a complexing to lower the plutonium (III)-plutonium (IV) potential before carrying out the oxidation.

Larsen:
Have you considered the possibility of doing low-levels of uranium, plutonium, and thorium, in the of 5, 10 or 25 micrograms range, by x-ray spectrometry?

Jackson:
We have not worked on that. There is certainly a lot of that type of research in progress, but not by us.

Larsen:
I wonder what the relative merits of spectrophotometric methods are in terms of specificity. Xylenol orange is a notoriously bad reagent. It seems to me that energy dispersive x-ray spectrometry would be particularly advantageous. Put a microgram of thorium in an energy dispersive instrument and the peak pops out at you. It is a matter of the specificity. In x-ray analysis there is no interference whatsoever, and you have sensitivity.

Brodda (NRC - Julich):
In the thorium titration you used diethylene-triaminepentaacetic acid instead of EDTA. Why?

Jackson:
It offers no particular advantage. We had standardized solutions of it available, so we used it.

Strohm (Mound):
Concerning the dissolution work, I am wondering where that stands. I have two concerns: one is plutonium NDA. We want to consider a measurement control program and verification measurements. Dissolution for traceability for chemistry is very important and is very difficult in scrap. The second thing is a verification measurement of a gamma-ray isotopic measurement of plutonium, which includes americium. With a simple dissolution we find that we get preferential dissolution of americium over plutonium. Is this program being actively pursued and where do we stand as far as being able to have a verification of those two measurements?

Jackson:
The method we have used for plutonium-containing materials is the Teflon-container apparatus. We have applied this to a variety of plutonium-containing materials. It is very effective. The gas-solid reaction we have not. We intend to investigate this gas-solid technique for plutonium, but have not done so yet. It is hard to make general statements about dissolution, because every type of scrap material tends to be unique. New

Brunswick helps us by supplying a variety of difficult-to-dissolve materials. We have looked at these and have been fairly successful. However, the next one we get might give us problems.

Bingham (NBL):

One of the situations that has been mutually discussed here is the sample size liquidation of the Teflon bomb. The heterogeneity that is inherent in the scrap materials doesn't lend them to representative sampling. If you have a kilogram of junk and can only dissolve a gram at a time, that takes 10 hours. Traceability of the measurement becomes a problem.

Jackson:

Agreed. Sampling is a real problem, particularly in scrap material, regardless of technique.

Larsen:

A paper should be written on the dissolution of samples. I wrote one a long time ago on the dissolution of uranium and its allies. There was very little original work in it. I collected a bunch of information through the years and a bunch of in-house experience from chemical engineering at Argonne and published a paper. I got more requests for reprints on that paper than any other paper I have written and I have written much better papers -- I think - (laughter). I think there are some people in this business who should jointly put together a compendium of procedures for the dissolution of these devilish samples. I can remember particularly the people at Gulf General Atomic having a problem years ago with carbide-coated thorium oxide pellets. We got some of those samples and Ralph Bine at ANL knew of a dissolution procedure. He popped them in just like that. Another individual, who was working on the problem, used to fume them in perchloric acid for 48 hours, and then hoped they were in. And yet, somebody knew of a trick that popped the stuff into solution just like that. I wonder just how many people who are dissolving plutonium oxide know that plutonium oxide dissolves like a charm in concentrated hydrobromic acid, even the high-fired stuff. These kinds of things ought to be put together.

Low Level Uranium Determination by Constant Current Coulometry

by

WANDA G. MITCHELL and KENNETH LEWIS
U. S. Department of Energy, New Brunswick Laboratory, Argonne, Illinois

ABSTRACT

A scaled-down version of the titration of uranium by electrogenerated V(V) has been studied at the New Brunswick Laboratory. The full-scale method, automated by the Lawrence Livermore Laboratory, was based on a modification by Goldbeck and Lerner of the titrimetric method for uranium by Davies and Gray. A 1/4 scale-down of the coulometric method has resulted in precise and accurate titrations of 5-40 mg levels of uranium. Modifications were made in the approach to the end point of the titration and in the treatment of the indicator electrodes.

KEYWORDS: Uranium titration, low level titration, constant current coulometry, vanadium (V) titrant

INTRODUCTION

A titrimetric method for the determination of uranium, originally developed by Davies and Gray,[1] was evaluated by the New Brunswick Laboratory (NBL) and found to be relatively selective and simple. Extensive investigation of the procedure at NBL led to modifications resulting in a precise and accurate titration for uranium which was relatively rapid and specific.[2] Automated procedures offer the advantages of increased sample output with decreased manpower per sample. Initial investigations of automation resulted in systems using volumetric and gravimetric delivery of potassium dichromate titrant. The development of a constant current coulometric titration by Goldbeck and Lerner,[3] using generation of vanadium (V), offered the added advantages of elimination of the preparation and storage of a standard titrant and of traceability to the coulomb.

The Lawrence Livermore Laboratory (LLL) built a totally automated titrator for NBL based on the constant current coulometric titration. The automated instrument which is completely computer monitored and controlled was evaluated by NBL.[4] The initial evaluation was carried out, using quantities of uranium from 20 to 140 mg at 20-mg intervals, with quantities of reagents similar to the manual NBL titration (final solution volume of about 250 ml). Results obtained at the 20 mg level were variable; thus, the final evaluation was carried out over the range of 40 to 140 mg. The precision obtained over the entire range was 0.05% (RSD) or better. Accurate results were obtained at the 40 mg level. Although results were consistent and reproducible at all levels, an increasingly negative bias was found with increasing quantities of uranium titrated above 40 mg.

---

[1] W. Davies and W. Gray, Talanta 11, 1203 (1964).

[2] A. R. Eberle, M. W. Lerner, C. G. Goldbeck, and C. J. Rodden, NBL-252 (1970).

[3] C. G. Goldbeck and M. W. Lerner, Anal. Chem. 44, 594 (1972).

[4] K. Lewis, D. L. Colwell, C. G. Goldbeck, and J. E. Harrar, "Analytical Chemistry in Nuclear Fuel Reprocessing," W. S. Lyon, Ed. (Science Press, Princeton, NJ, 1978), pp. 134-141.

The present investigation was carried out primarily to determine if a scaled-down version of the coulometric titration could be applied to the determination of uranium in the 5-40 mg ranges. Other workers [5,6] have successfully scaled down the volumetric titration; this indicated that smaller quantities of the reagents should be adequate. It was also felt that information derived from the titration of smaller quantities of uranium might lead to an explanation of the bias found in the automated titrator evaluation study.

EXPERIMENTAL

Reagents

The reagents were the same as those used in the automated titrator[7] except that the Fe(II) solution and the concentrated H_3PO_4 were not mixed prior to addition to the sample. The volume of all reagents was scaled down by a factor of four compared to those used in the automated titrator system.

Apparatus

Cell Assembly

The cell consisted of a 70-ml weighing bottle, 40 mm in diameter, with a Vikem stopper as a cell head. The stopper was drilled to hold the indicator and generator electrodes and two glass tubes (the reference and the counter electrode compartments) with porous Vycor plugs force-fitted with Tygon tubing into the ends of the glass tubes. The glass tubes were filled with electrolyte (0.14 M H_2SO_4, 2.5 M H_3PO_4, and 0.35 M HNO_3).

Electrodes

The reference electrode was a Radiometer mercurous sulfate electrode.

The cathode was a coil of #16 gauge Pt wire 8 cm long suspended in the counter electrode compartment.

The anode was one of three cylinders of gold mesh attached to a gold wire. The cylinders were about 3.5 cm in diameter by 2.0 cm in height. The three electrodes had estimated total areas of 20, 50, and 80 cm^2, respectively.

The indicator electrodes were 10-cm coils of #16 gauge Pt wire.

Coulometer

Two systems were used. An MT Model 3 Coulometer, in the constant current mode with a precision resistor, supplied currents up to 50 mA for initial work. A stable current source was assembled by the instrumentation section using a CEA, Berkleonics Inc. constant current supply with a General Resistance Inc. 1 ohm $\pm$ 0.01% resistor. An HP 3455A Digital Voltmeter accurate to 0.005% was used to monitor the voltage across the precision resistor. Timing was done with an Electronic Research Co. Series 2600 Digital Stop Watch in the remote control mode reading to 0.001 sec.

---

[5] J. Slanina, F. Bakkar, A. J. P. Groen, and W. A. Lingerak, Fresenius Z. Anal. Chem. 289, 102 (1978).

[6] S. D. Reeder and J. R. Delmastro, NBS Special Publication 528, 247 (1978).

[7] J. E. Harrar, W. G. Boyle, J. D. Breshears, C. L. Pomernacki, H. R. Brand, A. M. Kray, R. J. Sherry, and J. A. Pastrone, UCRL-52351 (1977).

Voltammeter

Current-voltage curves were obtained with a PAR 170 Electrochemistry System.

Procedure

Weigh a sample, containing 5-40 mg of uranium in a volume of 3 ml or less, into the cell. Add to the sample with stirring the following pre-titration reagents: 1.25 ml of sulfamic acid solution; 10 ml of concentrated H_3PO_4 (treated with 2% $K_2Cr_2O_7$); 1.25 ml of Fe(II) solution; wait 30 seconds, and add 2.5 ml of the oxidizing solution. Three minutes after the black color disappears, add 40 ml of diluent. Stir rapidly, and insert the cell-head containing the electrodes. Titrate at the selected generating current (50-200 mA) to the vicinity of the end point. Complete the titration using current pulses. Use the second derivative method[8] to calculate the total generation time (t) to the end point using the following equation:

$$t = t_A + \left[\frac{B-A}{(B-C) + (B-A)}\right] (t_B - t_A)$$

where B = the maximum change in the potential per current pulse,
A = the change in potential for the preceding pulse,
C = the change in potential for the following pulse,
t_A = the total generation time up to the pulse which gave the maximum change in the potential, and
t_B = the total generation time through the pulse which gave the maximum change in potential.

RESULTS AND DISCUSSION

Basic Method

The method of analysis consisted of the reduction of U(VI) to U(IV) by Fe(II) in strong H_3PO_4. Excess Fe(II) was oxidized by HNO_3 with a Mo(VI) catalyst. A V(IV) solution (0.025 M) in dilute H_2SO_4 (0.3 M) was added as diluent, and V(V) was coulometrically generated at a gold electrode. The titration of U(IV) was followed potentiometrically using a platinum indicator electrode and a mercurous sulfate reference electrode. The end point was taken as the inflection point of the potentiometric curve. The general reaction scheme is outlined in Figure 1.

(1) $U(VI) + 2\ Fe(II) \xrightarrow{H_3PO_4} U(IV) + 2\ Fe(III)$

(2) $2 \cdot Fe(II) + HNO_3 + 2\ H^+ \xrightarrow{Mo(VI)} 2\ Fe(III) + HNO_2 + H_2O$

$HNO_2 + NH_2SO_3H \longrightarrow N_2\uparrow + H_2SO_4 + H_2O$

(3) $U(IV) + 2\ V(V) \longrightarrow U(VI) + 2\ V(IV)$

General Reaction Scheme for Titration of Uranium by Electrogenerated Vanadium

Figure 1

---

[8] G. C. Goode, J. Herrington, and W. T. Jones, Anal. Chim. Acta 37, 445 (1967).

Initial Investigation

A manual, coulometric titration system was assembled for the present work, because the automated titrator cell head was designed for the full-scale titration and would have required extensive revision to accommodate a scaled-down procedure. Since the volume of all of the reagents was scaled down by a factor of four from those used in the automated titrator, resulting in a final solution volume of 60-65 ml, a 70-ml weighing bottle was used as a cell.

Initial evaluation of the scaled-down procedure was carried out using 10-mg quantities of uranium. The coulometric system assembled supplied a maximum current of 50 mA, and the initial gold generator electrode had an area of 20 cm^2. Preliminary results obtained with this system on 10-mg quantities of uranium gave a precision of 0.05% RSD and an accuracy of better than 0.05%. Although these results were sufficient to encourage further investigation, problem areas in the titration method also became evident.

The approach to the end point was found to be critical in achieving accurate and precise results. The generation of V(V) was carried out rapidly and continuously while monitoring the generator potential. It had been previously established that high generator electrode potentials (>710 mV for the present system) would lead to a black deposit on the generator electrode and decreased current efficiency for generation of V(V). The indicator electrode potential was also monitored, and the continuous generation of V(V) was stopped when the indicator potential reached a value of -10 mV *vs* the mercurous sulfate reference. The titration was continued from this point using current pulses of approximately 0.5 sec. Apparently, in the pre-end point region at the foot of the titration curve from -5 mV to +5 mV, either the titration reaction or the platinum indicator electrode response is slow. Therefore, it is essential to allow a wait time after the addition of each increment of titrant for accurate indicator readings to be obtained. The current pulse in this region causes a rise in the indicator potential to about +5 mV, followed by a potential decay back to -5 mV. The rate of decay is rapid initially but becomes slower with subsequent pulses until stable potentials are obtained in the vicinity of +5 mV. The titration can then be completed with short wait times between pulses. The total titration time varies from 6 to 10 minutes, and it takes 2 to 3 minutes to go through the pre-end point region. It has been found that low results are obtained if the rate of titration is too fast through the region at the foot of the titration curve. This observation indicates that the negative bias in the LLL automated titrator may be related to the rate or mode of approach to the end point. It is planned to examine this possibility further.

A second problem was encountered which appeared to agree with the observations of Reeder and Delmastro.[9] Maintaining the stability of response of the platinum indicator electrode in titrations of small amounts of uranium was difficult. The indicator electrodes had to be treated by flaming, quenching in HNO_3, water washing, and storing in a previously titrated solution after about ten titrations to attain the desired accuracy and precision of 0.05% at the 10 mg uranium level.

Additional Studies

Accumulated Results

The initial interest was to obtain a titration procedure for the range of 5-40 mg of uranium. Having established the basic procedure for 10 mg quantities, attempts were made to titrate larger and smaller amounts of uranium. Some problems involved with the extension to lower and higher quantities of uranium then became apparent. When the initial coulometric system was used to titrate 20 mg and 40 mg, the precisions attained were the same as for the 10 mg quantities of uranium, but the recoveries were about 0.1%

---

[9]Reeder, *loc. cit.*

low at the 20 mg level and about 0.2% low at the 40 mg level. It has been established for the volumetric titration[10] that low results are obtained with prolonged titration times. The relatively low current (50 mA) in the initial coulometric system resulted in prolonged titrations which caused the low results. The analytical instrumentation section assembled a more suitable instrument providing generation currents, stable within 0.01% over a range of 50-200 mA. Table I shows the results achieved with this coulometric system over a period of time during which the electrode conditions were studied in more detail, as described below. The range of 5-40 mg of uranium was of primary interest, but some results were obtained at the 1 mg level. The precision and accuracy obtained at all levels, with the revised instrumentation, was quite satisfactory.

Table I

Accumulated Titration Results for Uranium with Electrogenerated Vanadium (V)

~ mg U	n	% RSD	% Diff
1	5	0.081	+0.090
5	16	0.037	+0.057
10	48	0.046	-0.001
20	50	0.036	-0.008
40	48	0.018	-0.039

Current and Titration Efficiencies

The higher generating currents, used for the larger quantities of uranium on the initial gold generator electrode (20 cm^2), caused polarization of the electrode to excessively high potentials. The high potentials caused a deposit to form on the generator electrode and led to low current efficiency and high results. It was apparent that the current density was too high. Thus, two more generator electrodes were constructed with respective areas of 50 cm^2 and 80 cm^2. An examination of the current efficiency for the three electrodes was carried out using current-voltage curves to evaluate the electrodes under the titration conditions. These curves were obtained by two controlled-potential techniques, a slow scan method and a steady state method. Typical curves using the slow scan method are shown in Figure 2.

Goldbeck and Lerner[11] determined current efficiencies directly for a large gold generator electrode by generating V(V) and titrating the generated material with standardized Fe(II). They obtained efficiencies of 99.97% for current densities in the range of 0.1 to 3 mA/cm^2. Harrar and Boyle,[12] using current-voltage curves in the presence and absence of uranium, showed that uranium as well as vanadium was oxidized directly at the generating electrode and that the resulting generator potential was lowered by the presence of uranium. The current-voltage curves obtained in the present study with smaller electrode areas show current efficiencies between 99.9 and 100.0%. The titration results in Table I indicate titration efficiencies of 99.95% or better. A current density of 2.5 mA/cm^2 was found from these results to allow reasonable currents to be utilized without polarization problems.

Indicator Electrode Sensitivity

Although the titration range has been extended to 5 mg and some 1-mg quantities were titrated, the indicator electrode problems previously noted became very pronounced at these

---

[10]Eberle, loc. cit.

[11]Goldbeck, loc. cit.

[12]J. E. Harrar and W. G. Boyle, UCRL-52060 (1976).

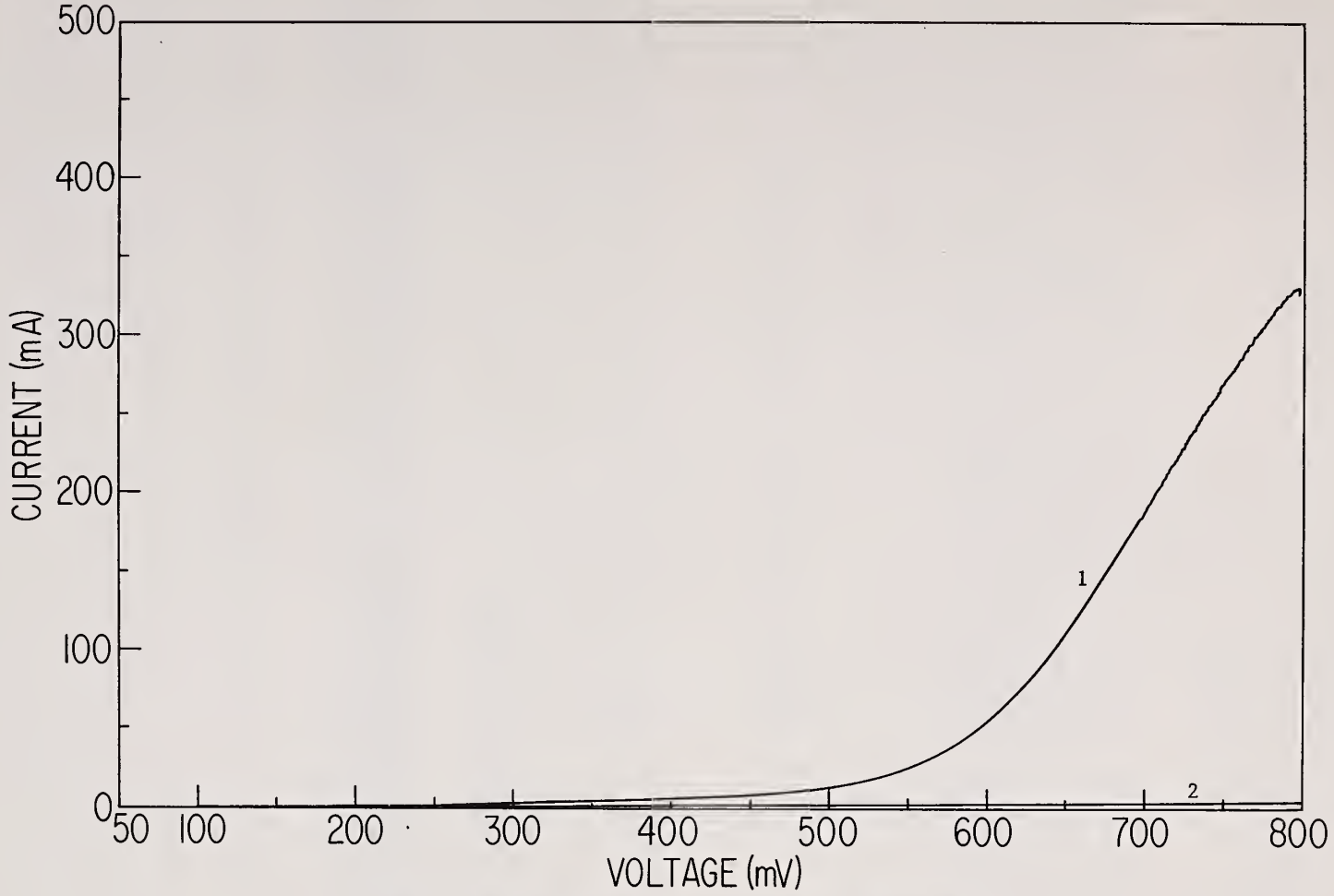

Current Potential Curve for Oxidation of Vanadium (V)

(1) Pre-titration reagents + 0.025 M V(IV), 0.3 M H_2SO_4 Diluent
(2) Pre-titration reagents + 0.3 M H_2SO_4 Diluent

Figure 2

low levels. The indicator electrodes were treated after only five titrations at the 5 mg level and after each titration at the 1 mg level. This increased sensitivity of the indicator electrode with smaller quantities of uranium titrated has not been reported in some scaled-down volumetric[13] and gravimetric procedures with $K_2Cr_2O_7$ titrant. Since this indicator electrode sensitivity would be a problem for 1-5 mg level determinations on an automated instrument, other modes of electrode treatment and possible alternative end point procedures are being investigated.

CONCLUSIONS

It is concluded that results with an accuracy and a precision of 0.05% can be obtained by coulometric titration of uranium using electrogenerated vanadium (V) over the range of 5-40 mg. The present work shows that titrations of 10-40 mg uranium can be accomplished without major problems. Titrations of 5 mg or less require frequent treatment of the indicator electrode to maintain the desired precision. Automation of the scaled-down procedure will require further examination of the stability of the indicator electrodes and also a careful choice of the mode of approach to the end point which the present study has shown is critical to attaining accurate and precise results.

---

[13]Slanina, loc. cit.

Discussion:

Larsen (ANL):
What about interference problems?

Mitchell (DOE-NBL):
When Goldbeck and Lerner set up the original method, they studied the interference problem. I think they found that manganese is among the interfering ions. We're doing a scale-down of their original method and we don't expect to find any additional problems.

Application of a Direct Method for the Determination of Trace Uranium in Safeguards Samples by Pulsed Laser Fluorometry

by

A. Creig Zook and Linda H. Collins
U.S. Department of Energy, New Brunswick Laboratory, Argonne, Illinois

ABSTRACT

A direct method for the fluorometric determination of trace amounts of uranium in solution has been developed. Precision and accuracy are better than 5% with a sensitivity of 0.005 ng U. The method employs a pulsed nitrogen laser to excite uranium atoms in solution containing a pyrophosphate fluorescence reagent. The resulting fluorescence is filtered, electronically gated, and integrated. A standard addition technique is used to overcome sample matrix effects.

KEYWORDS: Uranium determination: fluorometry; laser-induced fluorescence; trace levels; low-level analysis; waste solution analysis; nuclear safeguards; analyses

INTRODUCTION

Fluorometric methods for the determination of uranium have been recognized since 1935 for their sensitivity and selectivity and have been used extensively for the quantitative determination of trace amounts of uranium since the early 1950's. The basic method has been improved little since then. It is a lengthy procedure involving separations, extractions, and a fusion or sintering of a solid sodium fluoride or sodium carbonate-fluoride pellet containing the purified uranium. The pellet is placed into a fluorometer, irradiated with ultraviolet light, and the resultant emitted light is measured. The identification and control of some of the many variables of the procedure have allowed some laboratories to obtain precisions of 10-12%.[1,2]

In 1976, a commercially-available laser fluorometer was introduced by Scintrex, Ltd. for the direct determination of trace amounts of uranium in natural waters.[3] This instrument seemed to provide significant potential for laboratory application where rapid, accurate, and precise analyses of uranium in solutions of various materials are required.[4]

[1] J. E. Strain, "The Fluorophotometric Determination of Uranium: An Automated Sintering Furnace and Factors Affecting Precision", ORNL/TM-6431.

[2] Savannah River, Analytical Procedure (unpublished), 2SP40.3a, Uranium, Fluorophotometric Hexone Extraction, (January 1978).

[3] J. C. Robbins, "Field Technique for the Measurement of Uranium in Natural Waters", CIM Bulletin 793, (May 1978), pp. 61-67.

[4] Private communication, T. M. Florence, AAEC, to C. E. Pietri, NBL, (July 1978).

In its continuing effort to upgrade and improve measurement technology, the U.S. Department of Energy's New Brunswick Laboratory (NBL) undertook the task of evaluating the instrument and its performance and to develop an analytical method for a more precise, accurate, and rapid fluorometric method for the analysis of uranium solutions including safeguards inventory verification samples.

THEORY OF OPERATION

A small nitrogen laser supplies monochromatic ultraviolet light (337 nm wavelength) to the sample cell. Uranium atoms absorbing this energy emit a green luminescence which is read by a photomultiplier tube (PMT). Since organic matter fluoresces mainly in the blue region of the spectrum, a green filter is placed between the sample cell and the PMT. Longer wavelengths will still be transmitted however. Taking advantage of the longer fluorescence "lifetime" of uranium, the instrument pulses the laser about 16 times per second, each pulse lasting 3-4 nanoseconds. Since the organic component of the fluorescence decays away in a shorter period of time than the uranium component, an electronic gating system is employed to wait a specified time before actually "reading" the fluorescence. The fluorescence signals from 64 pulses are amplified and integrated, and the result is displayed on a meter.

As in other fluorometric techniques, several interfering species exist which either enhance or quench the fluorescence. Any long-lived green fluorescence from samples high in organic content is compensated for with a "balance" control while reading the "residual" or background fluorescence of the sample before the addition of a proprietary buffered pyrophosphate reagent, "Fluran", which causes the uranium to fluoresce. Interfering species which decrease the fluorescence either by absorbing the excitation light or the fluorescence emission are compensated for by a standard addition technique.

EVALUATION

The New Brunswick Laboratory for many years has used the conventional fused pellet fluorometric method for the determination of trace amounts of uranium. In order to determine the potential of this new instrument, an initial evaluation of the laser fluorometric method versus the fused pellet fluorometric method was designed to cover a wide range of uranium concentrations and impurities commonly encountered at NBL. Four uranium standards were prepared: 0.05, 0.5, 5 and 50 µgU/g. Ten additional standards (5 µgU/g) were spiked with one or more groups of impurities (Ce, V and Th; Fe, Cr, Cu, Ni and Zr; Mn, Zn and Ti; Ca, Si and Al) at two levels, 50 µg impurity/g and 1000 µg/g. Also, fourteen actual field samples of various types were included for comparison. The samples and standards were then analyzed in triplicate by both methods.

The mean percent recovery of standards for three or more determinations for the laser fluorometer method ranged from 92.8% to 106.5% with a mean of 101.9% $\pm$ 2.3% (95% confidence interval, 13 degrees of freedom), as compared to the fused pellet method which ranged from 62.1% to 104.4% with a mean of 90.2% $\pm$ 6.4% (95% confidence interval, 12 degrees of freedom). The bias was statistically significant for the fused pellet method, but not for the laser fluorometer method. The standard deviation of the relative differences for the uranium standards analyzed by the laser fluorometer method was 5.3%, as compared to 11.3% by the fused pellet method.

Figure 1 indicates that the laser method consistently exhibited a small positive bias ($\sim$ 2%), discussed later. Only the fused pellet method was affected by impurity group A (Ce, V, Th) at the 1000 µg impurity/g level, and to a smaller degree at the 50 µg/g level. These elements are known to be fluorescence quenchers, and extract into the ethyl acetate used for the uranium separation. The fused pellet method was not capable of analyzing standards below 1 µgU/g accurately.

The analysis of the actual field samples, Figure 2, also gave statistically significantly lower results (-17.0% $\pm$ 6.1%, 95% confidence interval, 12 degrees of freedom) for the fused pellet method when compared to the laser method for all levels of uranium from 0.02 µgU/g to 42 µgU/g; differences were even greater below 1 µgU/g. The laser method gave good precision (4.7% mean RSD) over the whole range.

Figure I. Evaluation of Standards

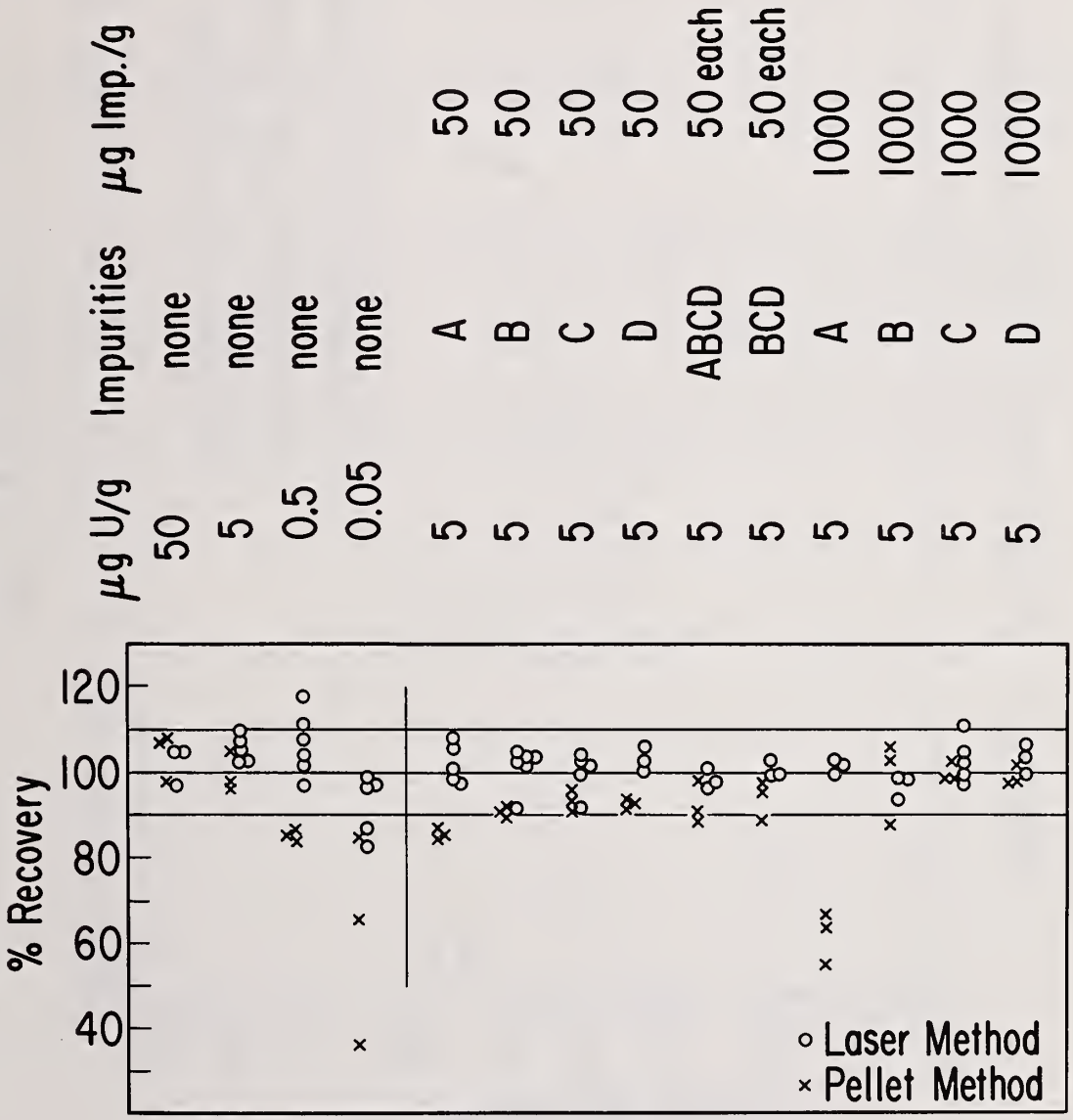

Figure 2. Evaluation of Field Samples

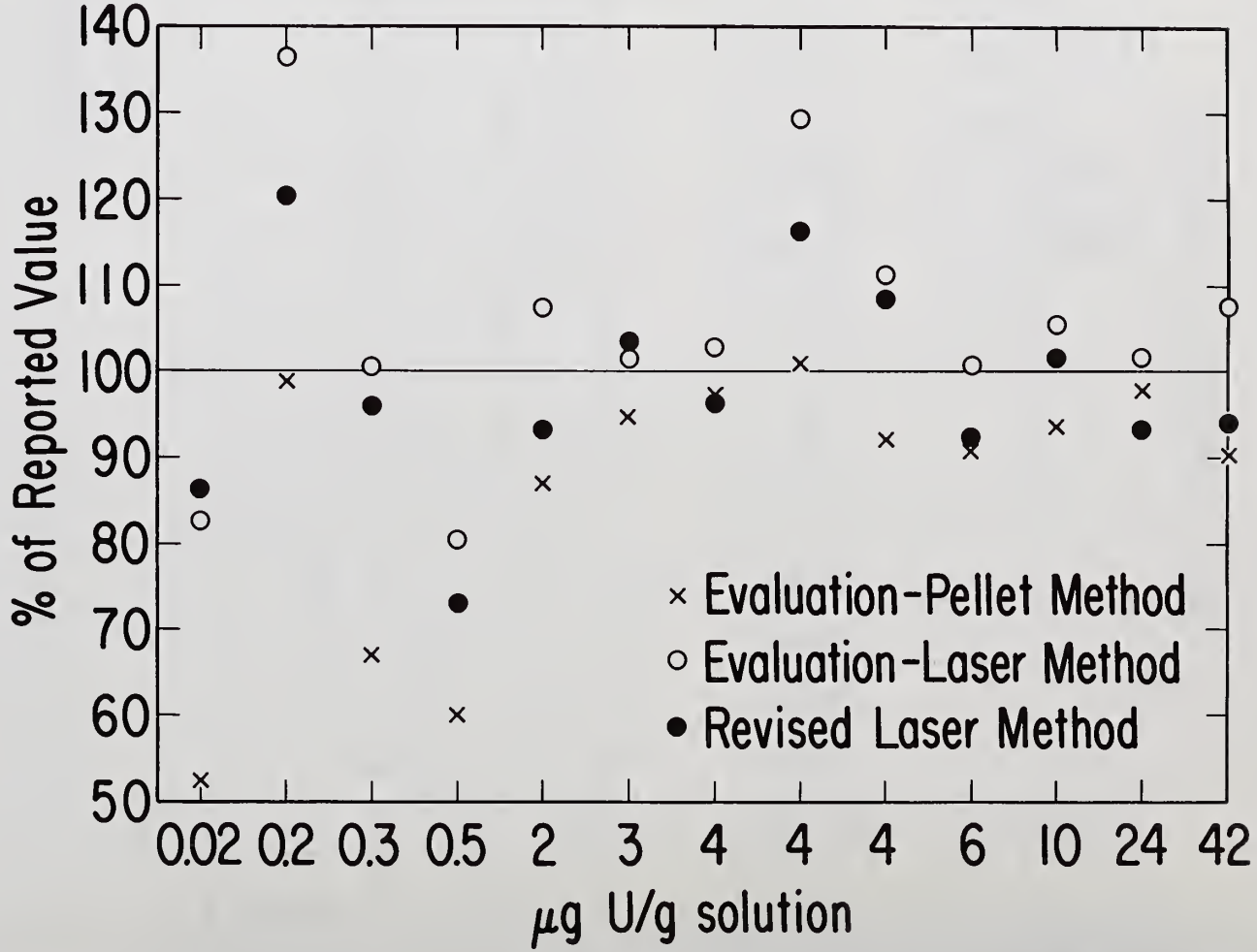

METHOD

The initial evaluation had proven the new instrument's potential. Further evaluation led to several improvements in the method which improved both its precision and accuracy. The present method is described here.

Sample solutions must be relatively free of suspended matter, should not be excessively acidic or basic for compatibility with the buffering action of the fluorescence reagent, nor should they contain large amounts of organic materials. If the uranium concentration is too high for analysis, a simple weight dilution of the sample can be made.

For the samples normally encountered at NBL, dilution is almost always necessary and is accomplished simply by adding a small amount of sample (0.02 to 1.0 ml) to the sample cuvet which already contains 5.0 ml of water. The cuvet is placed on a self-taring balance readable to 0.0001 g, the sample is added using a variable volume pipettor with disposable tip, and the resultant weight gain is recorded.

The cuvet, which contains a stirring bar, is placed on a magnetic stirrer for about 15 seconds before insertion into the fluorometer, and the fluorescence is adjusted to zero with the "balance" control to compensate for any residual fluorescence not due to uranium. The cuvet is placed on the stirrer again, 0.7 ml of the fluorescence reagent is added, and the solution is stirred for 15 seconds. The cuvet is placed in the fluorometer and the resultant fluorescence recorded. The cuvet is placed on the balance, the balance is tared, a standard uranium solution is added, and the weight is recorded. After stirring the solution for 15 seconds, the fluorescence is read and recorded. It is important that the fluorescence reading of the standard be taken under the same matrix conditions as the sample fluorescence. The standard addition volume must be small enough so as not to dilute the solution significantly, and it must not contain large amounts of acids or impurities which would alter the solution matrix.

The concentration of uranium in the sample is calculated by the following equation:

$$\mu gU/g \text{ sample} = \frac{WF_1S_1}{Z(F_2S_2 - F_1S_1)}$$

where:

W = grams of uranium added in the standard addition.

F_1 = the fluorescence of the solution, S_1.

S_1 = grams of total solution in the cuvet at F_1: water + fluorescence reagent + sample.

F_2 = the fluorescence of the solution, S_2.

S_2 = grams of total solution in the cuvet at F_2: water + fluorescence reagent + sample + standard addition.

Z = grams of sample added to the cuvet.

DISCUSSION

Accuracy and Precision

In the initial testing of the laser fluorometer method, accuracies of $\pm$ 5% were accepted as being at least as good as the fused pellet method for small numbers of analyses. It was concluded that the laser method performed well within these limits for all types of samples tested and in the presence of all impurities tested. Upon further evaluation of the method and subsequent results, a small consistent positive bias (2-4%) was noted. It was suspected that there was a correlation between this bias and the

fluorescence temperature dependency: a sample left in the fluorometer would steadily decline in fluorescence over a period of several seconds. Temperature measurements made on cuvet solutions at each step of the analysis revealed that the solution temperature was rising noticeably during the procedure. This was due to a cuvet compartment temperature of 32°C in comparison to normal room temperature of 23-25°C. A one-degree increase in the solution temperature gave fluorescence readings several percent lower. Since in the standard addition technique, two fluorescence readings are compared, these two readings must be made at the same temperature. It was empirically found that the temperature at which no change would take place was about 27.5-28°C. This temperature varies with the analyst, depending on the residence time of the cuvet in the fluorometer and the time between the two fluorescence readings, since cooling occurs between readings. To achieve the optimum operating temperature, the cuvet containing 5 ml water is heated on a hotplate at low temperature for about 5 seconds. A simpler method might be to store the water dispenser in a water bath of the appropriate temperature. For the most part, this procedure has eliminated any bias in the method.

Another parameter effecting accuracy involves the rinsing of the cuvet between analyses. Negatively biased results were noted to occur with samples which had more "residual" fluorescence than normal. This residual fluorescence was zeroed out with the "balance" control to bring the meter back to zero before beginning the analysis. It was determined that if the cuvet was rinsed more thoroughly, the residual fluorescence of the second aliquot would be lower. Evidently a carry-over of a very small amount of the fluorescence reagent from the previous analysis causes a small portion of the uranium to fluoresce during the balancing procedure. This falsely high residual fluorescence, when zeroed out, causes the subsequent sample uranium fluorescence to be measured low. Experience coupled with careful rinsing generally has eliminated this problem. Interestingly, the problem has been most prevalent on standard material, and not on field samples. Constituents in actual sample solutions apparently react with the reagent sufficiently to prevent adherence to the cuvet walls while high purity standards do not.

The initial evaluation indicated a precision of 5.3% on standards spiked with impurities. Further refinement of the method, as previously noted, gave a precision of 2-3% on field samples. At the present time, duplicate results exceeding a 5% relative difference are not accepted. Quality control standards which are run daily along with field samples have produced standard deviations of the relative differences between prepared values and assayed values of 1.6%, 1.7%, and 1.2% for three analysts for 10 determinations with mean relative differences of less than $\pm$ 0.5%. These improvements are attributed to: 1) weighing the sample and standard aliquots when they are added to the cuvet, 2) controlling the initial solution temperature, 3) careful technique including precise timing between sample and standard fluorescence readings and adequate rinsing of the cuvet between analyses.

Current modifications are being made to improve the readability of the fluorometer's meter by substituting either an analog, large-scale meter or a digital voltmeter to the meter circuit. Unfortunately, noise interference from the high voltage circuits of the laser adversely affects the performance of the meters tested to date. A special shielded cable is being tested to resolve the problem.

Analysis Time

One of the major drawbacks to the fused pellet method was the length of time required to obtain a result. At NBL, one 8-hour workday was the minimum elapsed time required. Groups of 15 samples took three days including preparation and cleanup time. The laser fluorometer method, because it is a direct method requiring no separations, extractions, or fusions, is very rapid. A single determination requires about five minutes. Although it could be completed in about three minutes with less precise results. Routinely, four samples are completed in duplicate per hour, including preparation and cleanup time. This throughput makes reruns practical without significant delay.

Sensitivity

The manufacturer claims a sensitivity of better than 0.05 ng U/g solution, which is about 0.3 ng U in the cuvet. In actual practice, 0.005 ng U has been determined to be the detection limit. An important feature of the instrument and the method presented is the ability to measure any uranium solution concentration easily from 0.05 ng/g to 50,000 ng/g by the turn of a "sensitivity" control, or the adjustment of sample and standard volumes chosen for analysis. Furthermore, weight dilutions may be used to bring samples into a more convenient concentration range.

SUMMARY

A direct method for the determination of trace amounts of uranium has been needed for some time, which is accurate, precise, sensitive, rapid, and free from interferences. A pulsed laser fluorometric method has been introduced which, when used with a standard addition technique and a pyrophosphate fluorescence reagent, fulfills these needs extremely well.

A precision and accuracy of 2-3% are not difficult to attain. The method is sensitive to 0.005 ng U. Analysis times are on the order of a few minutes. No separations, extractions, or fusions are required, and no interfering species, which effect the precision or accuracy of the analysis, are known.

Discussion:

Larsen (ANL):
We did fluorometric measurements with an accuracy of 4%. You have a detection factor of 1,000 higher. Are you sure you know the difference between picograms and nanograms?

Zook (NBL):
In the normal operation of the instrument, full scale deflection is two nanograms per gram with the sensitivity set midway. If you turn the sensitivity up you can get a lot more.

Larsen:
What's in the magic potion? They won't tell you?

Zook:
I'm not sure of the exact ingredients, although I do know you can obtain it. I think it is about 4% sodium pyrophosphate, in 1.5 molar phosphate.

Larsen:
That isn't too magic. I was just curious if somebody had found some minor constituent which gave you this increase.

Zook:
I suppose the laser is one answer to that question, and another is the pyrophosphate reagent. You can't do the analysis without either one. The laser, by itself, will not cause the uranium to fluoresce -- and of course the fluorescence reagent will not work alone in a conventional fluorometer without the intense, pulsed laser.

Larsen:
May I say to anyone who goes ahead and starts to use this method for determining uranium concentrations that he is going to find uranium in everything -- the nitric acid for instance. I've seen nitric acid at about 10 nanograms per milliliter, so you add 1 ml of nitric acid and you are 1,000 times the detection limit. You'll have to turn down the sensitivity. Clean reagents are the problem.

Zook:
Most of the time we have to dilute the sample, and therefore the impurities, to be able to analyze it. NBL seldom receives samples in the "normal" operating range of the instrument.

Larsen:
How do you keep the reagents clean? Is your water that clean?

Zook:
Yes. In the concentration range of our sample work, the water that we use has no detectable amount of uranium. I might make a comment about one of the last things I said. I said that there are no interfering species known to affect the precision and accuracy. I did not mean there is no fluorescence quenching effects. I meant that the results are not affected because of the standard addition technique used.

Larsen:
The regular pellet uranium fluoremetric method, in comparison with all analytical methods, provided a combination of high sensitivity and high specificity. Here you are saying that the senstivity is remarkably improved. There is the same specificity and the technique of standard addition can be used. Now it seems to me that your next step is to increase the accuracy of the determination by a factor of 10 and you can run a number of your other methods out of existence.

Persiani (ANL):
I could understand the selection of some of the impurities you added. However, I don't understand thorium being one. Why did you not include plutonium, and would that interfere?

Zook:

I don't know -- we are going to be doing some plutonium in the very near future. I have been told that plutonium will fluoresce, but I don't know if it will in this particular reagent.

Larsen:

It would be an interesting thing to examine. In this solution you should examine the fluoresence of that situation as a function of plutonium oxidation state. Is that fluorescence related to the electron structure of the plutonium? The possibility exists that you might develop a method for doing plutonium, if you could oxidize the plutonium in the solution to the VI state. It may fluoresce like uranium.

Zook:

In the analysis of uranium, of course, plutonium would not be a problem as far as quenching, because of the standard addition technique.

Armento (ORNL):

Could you tell us how they selected this particular wavelength for fluorescense excitation? Did they look at the excitation spectrum and pick this wavelength out as a maximum?

Zook:

Although I'm not really versed in this, I assume that the uranium has a fairly broad wavelength excitation band. The nitrogen laser supplies 337 nm, and Scintrex used it because it's convenient.

An Automated Ion-Exchange System for the Rapid Separation of Plutonium from Impurities in Safeguards Analyses

by

Brian P. Freeman, Jon R. Weiss and Charles E. Pietri
U.S. Department of Energy, New Brunswick Laboratory, Argonne, Illinois

ABSTRACT

Many plutonium samples cannot be analyzed directly after dissolution because of their high impurity content. Even when relatively interference-free methods such as controlled-potential coulometry are used, dissolved organic matter and high salt content from sample dissolution fusion treatments may require separation for highly reliable results. The anion-exchange separation of these interferences from plutonium (IV) in the Dowex-1 8N HNO_3 system has been successfully used at the New Brunswick Laboratory (NBL) for many years. However, the demand to increase sample analysis output, to decrease sample turnaround time, and to reduce operating costs, has prompted the development of an automated system, AUTOSEP, based on the manual ion-exchange method. Application of this automated system to the analysis of safeguards inventory verification samples should have significant positive impact on those goals.

The AUTOSEP system is designed as a batch-type operation in which ten sample aliquots are simultaneously passed through mini ion-exchange columns in a pattern nearly imitating NBL's manual procedure for this same process. Weighed aliquots of dissolved sample, each containing 5-10 mg of plutonium, are added to each of ten reservoirs in the mini anion-exchange separator. The volume of liquid in each reservoir is adjusted uniformly by reagent addition, and all subsequent steps in the separation are performed automatically. The system incorporates a means of programming reagent delivery, adjustment of the sample to the plutonium (IV) oxidation state via Fe(II) reduction/HNO_3 oxidation, plutonium sorption on the resin in 8N HNO_3, washing of the resin bed with 8N HNO_3 to remove impurities, elution of the purified plutonium with 0.36N HCl-0.01N HF, and waste effluent disposal. The reagents are delivered by gravity from a module whose only moving parts are rotary valves. The eluted plutonium solutions are collected in glass coulometer cells in stainless steel holders for subsequent automated coulometric analysis.

KEYWORDS: Automated ion-exchange; plutonium; ion-exchange separation; automated plutonium separation; impurity separation; AUTOSEP.

INTRODUCTION

The AUTOSEP system, previously described,[1] was designed to automate a mini ion-exchange procedure for separating plutonium from interfering impurities prior to analysis by con-

[1] J. R. Weiss, C. E. Pietri, A. W. Wenzel, and L. C. Nelson, Jr., U.S. Atomic Energy Commission Report, NBL-267, p. 101 (September 1973).

trolled potential coulometry.[2-4]

Description

The AUTOSEP system, Figure 1, consists of five modules. The modules, identified as a mini ion-exchange separator, a reagent delivery system, a programmer, a controller, and a waste handling system, are described below.

Mini Ion-Exchange Separator

The mini ion-exchange separator module, Figure 2, designed for gloved box operation, is used for separating plutonium from impure samples. The module incorporates ten commercially available disposable polyethylene ion-exchange columns mounted in a rack. Each column has a removable graduated reservoir at the top for sample loading, reagent addition, and mixing. Mixing is accomplished by means of a motor-driven stirrer positioned above each reservoir. The flow of column effluents is controlled by a three-positioned motorized stopcock at the bottom of each column. The stopcock position either shuts off all flow, diverts the wash solution to a waste container, or directs the plutonium eluate to a coulometer cell for analysis. The structural parts of the module are made of stainless steel for corrosion resistance. All components which come in contact with samples and reagents are fabricated from plastic and glass.

Reagent Delivery Module

The reagent delivery module frame mounted above the gloved box provides for the aliquotting and delivery of reagents to each of the ten ion-exchange columns inside the box. A gravity flow system is used for liquid transfers. The module simultaneously delivers to each of the ten columns an aliquot of 10.0 $\pm$ 0.1 ml concentrated HNO_3 (for acidity and oxidation state adjustment) or 32 ml of 8$\underline{M}$ HNO_3 (wash solution), or 32 ml of 0.36$\underline{M}$ HCl-0.01$\underline{M}$ HF (eluting solution) upon signal from the programmer. The reagent volumes are measured by ten self-filling pipets. Commercial tetrafluoroethylene-fluorothene rotary valves driven by a motorized gear box, Figure 3, provide the proper dispensary of reagents to these pipets, and subsequently, the columns.

Programmer Module

A 24-step Agastat Programmer is used to select and switch reagent flow and to time the various flow steps for ten ion-exchange columns operating simultaneously.[1] The programmer shuts off the system at the end of the operating cycle and its start switch must be activated before the cycle can be repeated.

Control Module

The control module contains the wiring interfaces for the other three modules. Each function that is controlled by the programmer may be deactivated by a switch. This feature

[1] J. R. Weiss, C. E. Pietri, A. W. Wenzel, and L. C. Nelson, Jr., U.S. Atomic Energy Commission Report, NBL-265, p. 101 (September 1973).

[2] C. E. Pietri and A. W. Wenzel, U.S. Atomic Energy Commission Report, NBL-159, p. 73 (May 1960).

[3] J. R. Weiss, C. E. Pietri, A. W. Wenzel, and L. C. Nelson, Jr., U.S. Atomic Energy Commission Report, NBL-265, p. 94 (October 1972).

[4] M. K. Holland, J. R. Weiss and C. E. Pietri, Anal. Chem. 50, 36 (1978).

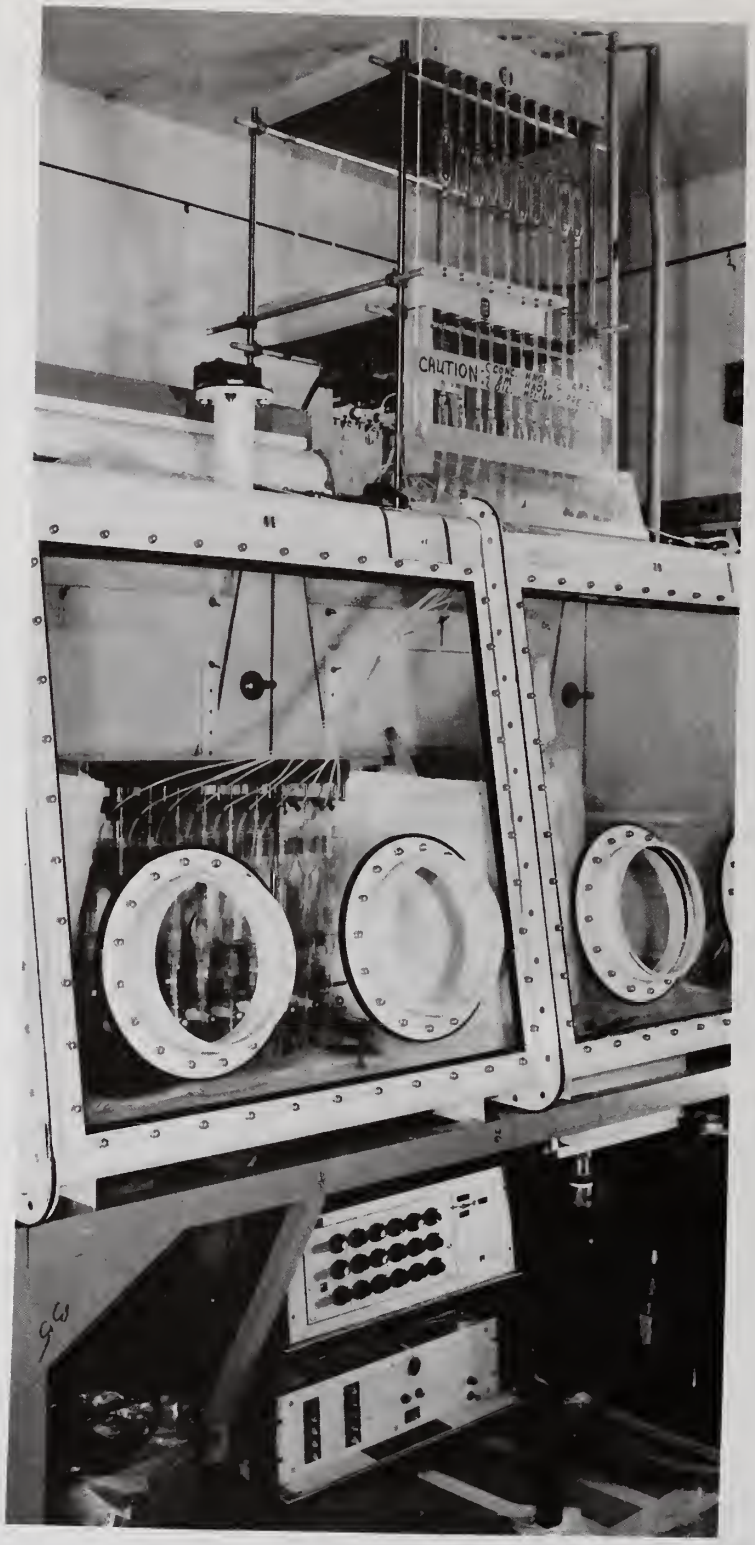

Figure 1. AUTOSEP System.

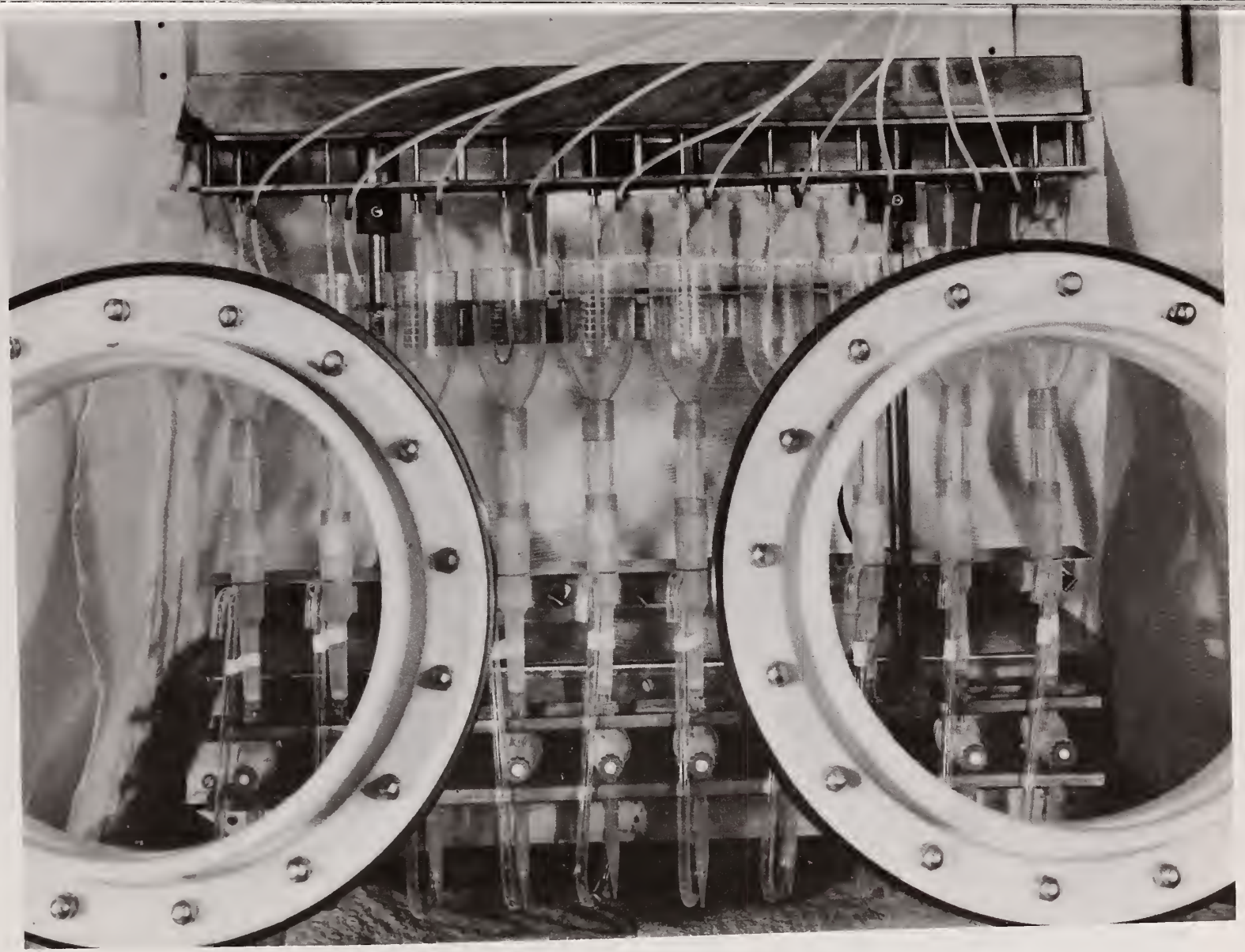

Figure 2. The Mini Ion-Exchange Separator Module.

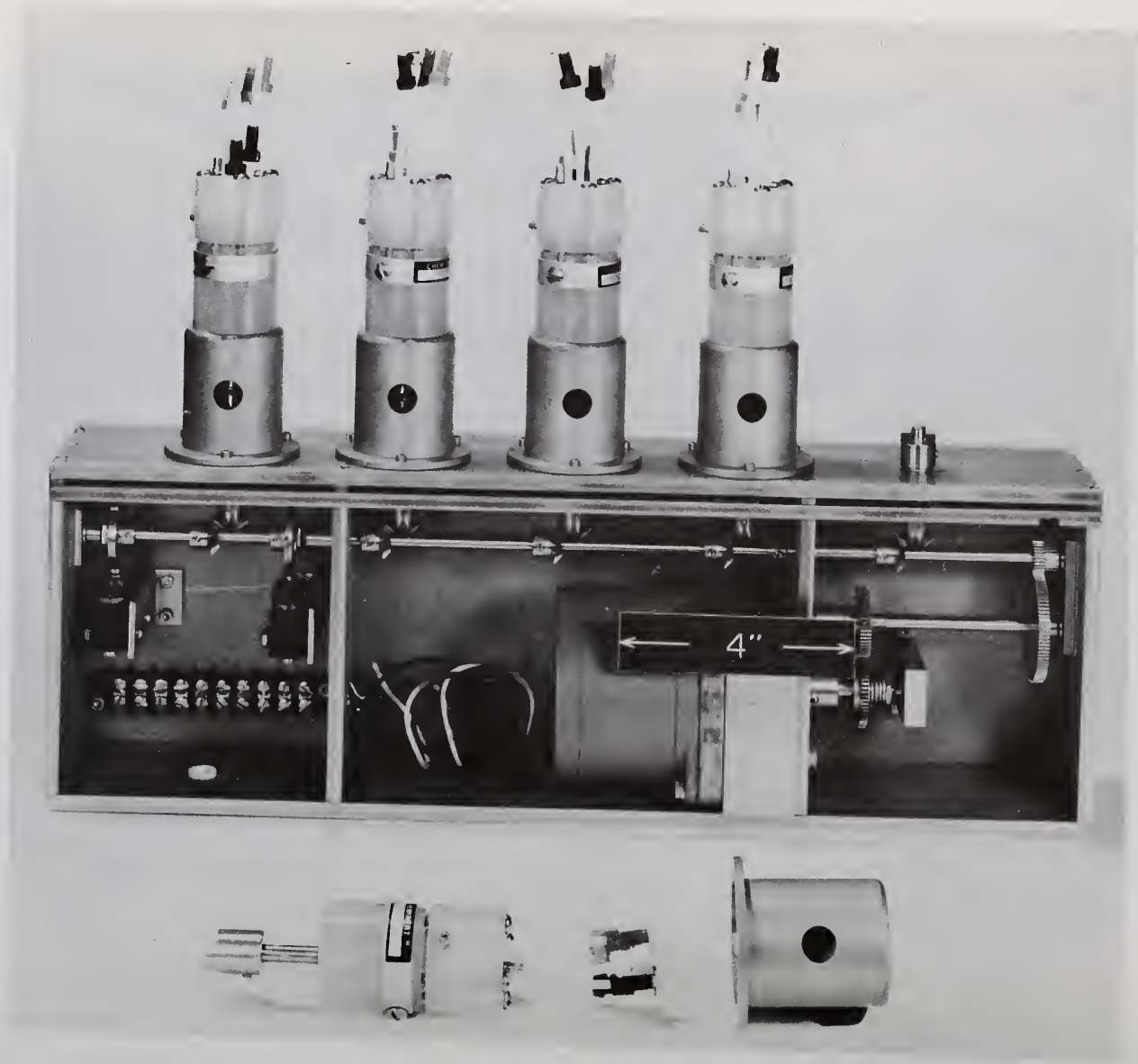

Figure 3. Rotary Valves Driven By Motorized-Gear Box.

allows for complete control of each function when manual operation is desired. The "on-off" power switch, the programmer "start" switch, and protective fuses are mounted in this module.

Waste Handling System

The waste handling system, mounted in front of the mini ion-exchange separator module, is used to evacuate the wash solution to a waste container. This system was designed to decrease head pressure and increase the flow rate of the ion-exchange waste to its container. This system consists of ten glass "S"-shaped tubes connected by vinyl tubing to each stopcock waste vent in the separator module. These "S" tubes direct the wash waste to five polyethylene reservoirs (two "S" tubes per reservoir), which subsequently lead to a 1" I.D.-angled polyethylene tube. This tube is joined to a 0.5" O.D. vinyl tube. The flexible vinyl tube then leads to a waste container in the sink. The large internal diameter of each component in the waste handling system facilities the flow of wash waste, eliminating possible backwash and waste buildup which was evident in a previous prototype waste handling module.

PROCEDURE

A simplistic operating cycle has been developed[5] which parallels the manual ion-exchange procedure used at NBL. The automated procedure is given in Table I.

Table I. AUTOSEP Operating Cycle

Dwell Time, Sec.	Step	Stopcock Position	Description of Operation
Manual			Dissolve sample in 10 ml 1.0N HNO_3
Manual			Reduce sample with 1.0 ml (1.0M $FeSO_4$)
Manual			Load reduced sample into reservoir
180	1	Off	Stir, fill pipets with conc. HNO_3
60	2	Off	Conc. HNO_3 flows to reservoir
80	3	Off	Stir
800	4	Wash	Load columns
180	5	Wash	Fill pipets with 8N HNO_3
800	6	Wash	Wash columns with 8N HNO_3
180	7	Wash	Fill pipets with 0.36M HCl-0.01M HF
800	8	Elute	Elute columns
180	9	Elute	Fill pipets with conc. HNO_3
10	10	Off	Alarm - separation completed
---	11	Off	System hold

RESULTS AND DISCUSSION

Several improvements in the system have been made to eliminate operating deficiencies. The most notable changes are described below. Faster reagent measuring steps were obtained by modifying the delivery module to increase head pressures in the gravity-feed system. Three-way solenoid switching valves formerly used for controlling reagent flow[5] were replaced by tetrafluoroethylene-fluorothene rotary valves operated by a newly-designed motorized gear box. (The solenoid valves proved unreliable due to electrical shorts and component failures.) Improved waste handling was obtained with the design of the waste

[5] B. P. Freeman, J. R. Weiss, and C. E. Pietri, U.S. Department of Energy Report, NBL-289, p. 84 (January 1979).

handling module, mentioned previously. Operator safety was enhanced with the addition of structurally-sound stainless steel reagent delivery module supports, a methyl methacrylate splash shield, and acid reservoir containers consisting of flat polyethylene pans.

Operational testing was performed after each modification, which included system evaluation with inert reagents, selected reagents, and samples not containing plutonium. For example, uranium and iron samples were used to evaluate separation efficiency for a typical cycle. Uranium, since it is very difficult to elute completely from the resin, was used to test the efficiency of the washing step. Results obtained using 32 ml of 8N HNO_3 wash solution indicated that from 99.0 to 99.9% of the uranium was eluted. Plutonium, if present, would remain on the column. Iron is the most serious interference in the determination of plutonium by controlled-potential coulometry in nitric acid media. The feasibility of using an anion-exchange method to separate iron from plutonium has been demonstrated previously.[3] To test the effectiveness of the AUTOSEP system in iron removal from the resin column, 10 mg amounts of iron were processed through the separation procedure, and the eluates which would normally contain plutonium were analyzed for iron. (The relatively large amounts of iron used in this test and in the subsequent study were necessary to simulate the quantity ordinarily employed for oxidation state adjustment in the manual ion-exchange method.) Tests with a resin bed height of 4.7 cm showed that up to 24 µg of iron would accompany the plutonium. This quantity of iron is sufficient to cause a positive error of about 2% in the amount of plutonium determined in a typical sample. Further tests using up to 20 mg of iron showed that by reducing the resin bed height of 3.8 cm and by limiting the height of the liquid above the resin bed to less than 1 cm, the iron content of the eluate was reduced to about 0.5 µg. The error introduced by this residual quantity of iron is thereby reduced to an acceptable level. Additional studies were performed with a quantity of iron ($\sim$ 3 mg) more appropriate to AUTOSEP operations. In these tests, the liquid level above the resin was further reduced to 1 mm. Results showed insignificant quantities of iron, < 0.04 µg, remaining after separation.[6]

Several separations using plutonium sulfate tetrahydrate standard material (NBS SRM 944) have been satisfactorily performed to date. Recoveries of plutonium standard aliquots using the NBL manual controlled-potential coulometric method[4] are shown in Table II.

Table II. Plutonium Recoveries of Aliquots of Plutonium Standards

SET A		SET B		SET C	
Aliquot	Wt. Recovery, %	Aliquot	Wt. Recovery, %	Aliquot	Wt. Recovery, %
1	99.99	1	99.92	1	100.05
2	100.06	2	99.90	2	100.07
3	100.00	3	100.11	3	100.04
4	100.10	4	100.09	4	99.90
5	100.12	5	100.00	5	100.11
6	100.12	6	100.07	6	100.13
7	99.89	7	100.04		
8	100.11	8	99.90		
Mean	100.05_0		100.02_6		100.05_0
RSD, %	0.07_9		0.08_4		0.07_4

[3] J. R. Weiss, C. E. Pietri, A. W. Wenzel, and L. C. Nelson, Jr., U.S. Atomic Energy Commission Report, NBL-265, p. 94 (October 1972).

[4] M. K. Holland, J. R. Weiss, and C. E. Pietri, Anal. Chem 50, 36 (1978).

[6] M. K. Holland and J. R. Weiss, U.S. Department of Energy Report, NBL-292, p.28 (October 1979).

Minor refinements in reagent delivery and waste handling are currently being performed to enhance the precision and reliability of AUTOSEP. Shortly, evaluation using plutonium standard material will be completed and separations of actual sample material will be initiated.

The following studies are being made currently to further enhance the efficiency and productivity of AUTOSEP: automated sample loading, sample reduction Pu(IV) → Pu(III), and pressurized ion-exchange column effluent flow.

Discussion:

Larsen (ANL):

A question which should be borne in mind by everybody who has anything to do with plutonium analytical chemistry is that of oxidation state. Do you have any problems or have you run into any problems with the samples, in the dissolution of the samples, in the storage of the samples -- the kind of thing where you couldn't subsequently get quantitative reduction of all the plutonium to the trivalent state with the ferrous sulfate, and followed by the quantitative oxidation to the tetravalent state? Those are good steps as far as I know -- providing that there is no polymeric material present.

Freeman (NBL):

I think there was one occasion where we did have some minor problem with that. We were performing some work on the SALE characterization of the Lots 105 and 106 mixed oxide and plutonium dioxide. We were using some mixed uranium plutonium standard material which was several months old at the time. During this time, uranium, as you know, picks up water. The standard materials are dry 10 mg plutonium aliquots in the sulfate form, and they are bone dry.

Larsen:

You've got plutonium and you've got sulfate in there to start. As soon as you have sulfate in there you're forstalling the probability, quite significantly, of forming a polymer of plutonium.

Freeman:

Right. The samples did pick up water at the time, and it appeared that some of the plutonium was polymerized, at least to the extent of anywhere from 0.06 to 0.1 percent. This introduced a negative bias. This is the only example that I know of where we have had difficulty.

Larsen:

I was just curious, because I think one of the things to warn about is what people can and cannot do with solutions that are freshly prepared. If you are going to store them for a long time, what precautions do you take?

Pietri:

What we do, Bob, is when we get a solution in, or we make a solution, we aliquot it immediately and dry it down in a sulfate form. Plutonium in a sulfate form is usually very readily redissolved. So we avoid that problem, because we recognize that there is really no good way to store solutions. In fact I think Bingham had a slide this morning that shows what happens to plutonium nitrate solutions over a period of time -- you get radiolyis, you get evaporation, you get polymerization, and precipitation.

Computer-Assisted Controlled-Potential Coulometric Determination of Plutonium for Safeguards Measurements

by

Michael K. Holland, Thomas L. Frazzini, Jon R. Weiss, and Charles E. Pietri
U.S. Department of Energy, New Brunswick Laboratory, Argonne, Illinois

ABSTRACT

A computer-assisted coulometric system, based on the New Brunswick Laboratory (NBL) manual controlled-potential coulometric method for plutonium determination has been developed. This system reduces the costs and operating time for plutonium measurements without loss in reliability in the analysis nuclear safeguards materials.

The computer-assisted system employs the same features as the manual method: 1) electrical calibration of the integration system is used to relate the coulombs produced during sample electrolysis to the quantity of plutonium electrolyzed, 2) corrections for the nonelectrolyzed fraction of the sample and for the coulombs resulting from background current (faradaic, charging, and constant currents) are applied, and 3) the control-potential adjustment technique developed at NBL is used for endpoint location.

KEYWORDS: Computer-assisted coulometry; plutonium; electrical calibration; control-potential adjustment; controlled-potential coulometry; plutonium determination.

INTRODUCTION

Controlled-potential coulometry is recognized as a reliable analytical technique for the determination of plutonium. Automated controlled-potential coulometers for plutonium determination with reliabilities ranging from 0.1% to 0.25% relative standard deviation (RSD) have been reported.[1,2]

In this paper we describe an automated coulometer, based on the New Brunswick Laboratory manual controlled-potential coulometric method for plutonium determination, with a reliability of 0.02% RSD with no statistical bias. The development of the computer-assisted controlled-potential coulometry system is a part of an overall plan at NBL for automating the plutonium assay measurement. The completed system will include an automated

[1]G. Phillips, D. A. Newton, and J. D. Wilson, J. Electroanl. Chem., 75, 77 (1977).

[2]P. D. Jackson, R. M. Hollen, F. R. Rocnsch, and J. E. Rein in (Gatlinburg, p. 151).

weight aliquoting system (AUTOALIQUOTOR), an automated anion exchange purification system (AUTOSEP), and a computer-assisted controlled-potential coulometry system with an automated sample handler (AUTOCOULOMETER).[3-8]

ROUTINE SAMPLE PREPARATION

Aliquots containing 5-10 mg of plutonium were taken by weight from sample and standard solutions and fumed to dryness in sulfuric acid. The plutonium aliquots were adjusted to the plutonium (IV) oxidation state and purified by anion exchange separation. The aliquots were fumed to dryness twice in sulfuric acid, then cooled, covered with Parafilm, and stored dry until analyzed.

COMPUTER-ASSISTED COULOMETRY SYSTEM

The first prototype of the computer-assisted coulometry system with controlled-potential adjustment capability consisted of the following components: a programmable calculator, a controlled-potential coulometer, a 6½-place digital voltmeter, two dual potential sources, a series of relays, and interfacing circuitry. The programmable calculator was used for control of the commercial state-of-the-art controlled-potential coulometer consisting of a potentiostat with an analog integration system. The 6½-place digital voltmeter was used for monitoring the output of the analog integrator. This system required complex mathematical and procedural corrections for the nonideal responses of the analog integrator.[9] The potentiostat and the two custom-made dual potential sources are interconnected and permit remote selection of one of four predetermined control-potential output signals by the potentiostat. They were used for switching from oxidation to reduction mode and for adjustment of the control-potential. Computerized prediction of the solution redox potential was used in order to automate the control-potential adjustment technique. The first dual potential source was set at 0.40 V and 0.48 V vs. SCE, and the second dual potential source was set at 0.91 V and 0.85 V vs. SCE. Sample reduction was initiated at 0.40 V vs. SCE.

[3] J. R. Weiss, A. W. Wenzel, and C. E. Pietri, U.S. Atomic Energy Commission Report, NBL-267, p. 101 (1973).

[4] J. R. Weiss, A. W. Wenzel, and C. E. Pietri, U.S. Atomic Energy Commission Report, NBL-272, p. 74 (1974).

[5] J. R. Weiss, A. W. Wenzel, and C. E. Pietri, U.S. Atomic Energy Commission Report, NBL-272, p. 78 (1974).

[6] G. E. Peoples, S. A. Malone, J. R. Weiss, A. W. Wenzel, and C. E. Pietri, U.S. Energy Research & Development Administration Report, NBL-277, p. 80 (1975).

[7] B. P. Freeman, J. R. Weiss, and C. E. Pietri, U.S. Department of Energy Report, NBL-289, p. 84 (1979).

[8] M. K. Holland, J. R. Weiss, C. E. Pietri, and B. P. Freeman, U.S. Department of Energy Report, NBL-289, p. 86 (1979).

[9] T. L. Frazzini, M. K. Holland, J. R. Weiss, and C. E. Pietri, submitted to Analytical Chemistry for publication.

The control-potential adjustment technique was accomplished by using exponential decay equation ($i_t = i_o e^{-t/\tau}$) and the Nernst equation to predict when the solution redox potential would reach 0.48 V vs. SCE at which time the control-potential was switched to 0.48 V. Sample oxidation was initiated at 0.91 V vs. SCE, and when the solution redox potential reached 0.85 V vs. SCE, control-potential adjustment was accomplished by switching the control-potential to 0.85 V. The series of relays and the interfacing circuitry were used to interconnect the modules into a working system. This prototype was evaluated using NBS SRM 949e and the results showed an uncertainty of 0.1% RSD with no statistical bias. While the system generally provided reliable results, some difficulties in automated control, electrical calibration, temperature sensitivity, and maintenance indicated the need for upgrading.

An updated system has been designed, fabricated, assembled, fully bench-tested, and programmed for plutonium analysis. This system consists of the following components: an improved programmable calculator, two potentiostat modules, an NBL-designed digital integrator, a calculator-controlled variable power supply, two 6½-place digital voltmeters, a timing generator, a series of relays, and interfacing circuitry. The improved programmable calculator with external interrupt and increased instrument control capability is used for control and data manipulation. Two potentiostat modules are used, one for prereduction steps and one for oxidation steps. The use of the two potentiostat modules provides the system with an extremely desirable feature: virtually continuous system calibration. Three electrical calibrations are performed concurrently with the sample analysis. The first potentiostat, which is not connected to the digital integrator, is used to reduce the supporting electrolyte before background current determination and to reduce the plutonium before sample determination. During each of these reduction steps, the second potentiostat, which is connected to the digital integrator, is used to perform an electrical calibration. The second potentiostat is then used for the measurement steps, which are the oxidation of the supporting electrolyte and the oxidation of the plutonium sample. A third electrical calibration is done after completion of the analysis while the coulometry cell is being prepared for the next sample (see Figure 1). This virtually continuous calibration capability insures proper instrument operation throughout the multiple blank and sample measurement sequences without loss of time and provides the automated system with a built-in capability to self-monitor performance. The NBL digital integrator was designed to optimize the linearity of voltage-to-frequency converters and to minimize the temperature sensitivity of the circuit.[10] Compensation for the $\sim 0.001\%/^{\circ}C$ change in the instrument calibration due to laboratory temperature fluctuations is achieved by the computer-controlled continuous calibration feature.

The additional potentiostat and the variable power supply replace the two dual potential sources of the previous system. The variable power supply permits remote adjustment of the control-potentials of both potentiostats allowing the use of the control-potential adjustment technique to locate the solution redox potential without use of any predictive coulometry techniques. The two digital voltmeters are used to monitor the electrolysis current during the control-potential adjustment. The output of the variable power supply is changed in increments of 1 mV until the electrolysis current is at approximately zero (background current <3 μA) which closely resembles the manual application of the control-potential adjustment technique. Automation of the control-potential adjustment technique permits the same decrease in the electrolysis time as is obtained manually. In addition, the two digital voltmeters are used in determining the solution redox potential at the completion of an electrolysis and in determining the constant current used in electrical calibration. The timing generator is used to improve time measurement steps previously done by the programmable calculator. Finally, the series of relays and interfacing circuitry are used to interconnect the modules into a working system.

[10] T. L. Frazzini, M. K. Holland, J. R. Weiss, and C. E. Pietri, manuscript in preparation.

FIGURE I. Flow Chart of the Sequence of Operations in Plutonium Analysis.

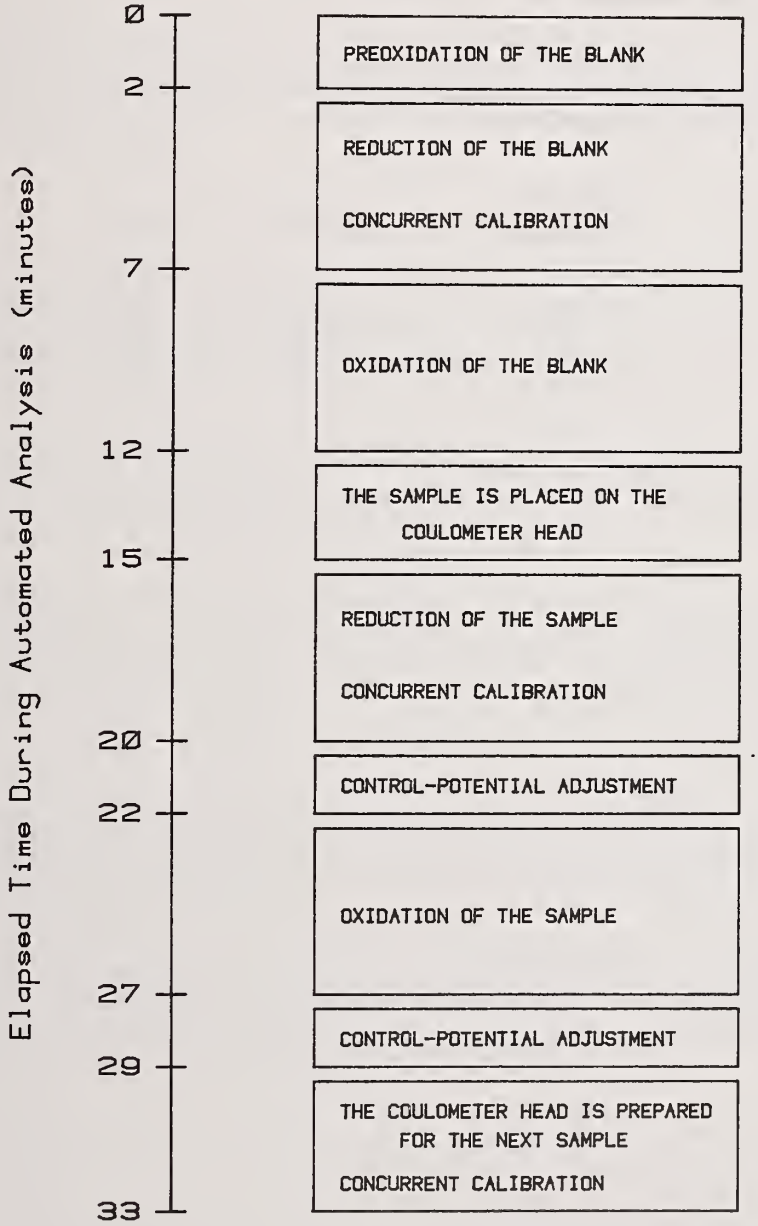

Evaluation of the system with NBS SRM 949e plutonium metal gave unbiased results with an RSD of 0.02% as compared to previous unbiased data with 0.05% RSD obtained from the manual coulometric method (see Table I). Addition of an automatic sample changer, presently nearing completion, will fully automate this system. The improvement in precision, the ruggedness of the system, and the relative simplicity of the automated analysis make the computer-assisted coulometry method for plutonium superior to the manual technique.

Selected standards used in this evaluation were prepared and analyzed in conjunction with safeguard samples. The precision obtained from routine safeguard samples was comparable to the data from standards.

Table I. Determination of Plutonium Using the Computer-Assisted Coulometry System

Standard Preparation	Number of Replicates	Pu Recovery, %	RSD, %
A	3	100.05	0.02
B	3	99.98	0.01
C	6	99.97	0.02
D	2	99.96	0.01
E	13	100.00	0.01

MEASUREMENT REQUIREMENTS AND EXPERIENCE IN INTERNATIONAL SAFEGUARDS

by

A.J.G.Ramalho and L.W.Thorne
Department of Safeguards, International Atomic Energy Agency

ABSTRACT

This report describes IAEA experience in the application of NDA techniques in international safeguards. It refers to the main pieces of equipment and their use, placing emphasis on high resolution gamma spectrometry and neutron coincidence counting. Some recent experience, problems found and improvements needed are also touched upon.

INTRODUCTION

Measurements of SNM materials are an important part of IAEA inspection activities and are routinely performed by the inspectorate. The items assayed are randomly selected from "frozen" populations in accordance to sampling plans prepared in advance and adjusted at the time of the inspections. Assurance that a population is static is reached either with the inspector's presence of through containment and surveillance measures.

The measurements have to be fully independent, therefore they are generally performed with IAEA owned and calibrated equipment. In the cases where facility owned equipment is used, either it has been calibrated or the calibrations verified by the Agency. In the course of time the calibrations are checked or re-established and to prevent the equipment from being tampered with, sealing is applied when possible.

The sample sizes are calculated on the basis of a zero-acceptance number [5] which means that a stratum under verification is accepted if no defects are found amongst the items sampled. This approach results in the minimum inspection effort for a given probability of failing to detect a given discrepancy. This therefore also gives the minimal interference with the operator. The sampling plans are constructed to take into consideration diversion strategies involving total and partial item removal.

The measurements themselves need, therefore, to be performed at different levels, namely to be capable of detecting large, medium and small removals [5]. The first type is covered by an attributes measurement while the last two involve the variables type of measurement. Although the same instrumentation may, in due course, be used for both purposes, the verification of most of SNM materials requires more than one type of instrument.

In field measurements are performed using NDA techniques but concomitant with them samples for destructive analysis are also taken particularly from fuel fabrication and reprocessing plants. Such samples are part of a variables type of measurement but their taking is usually limited to the cases where NDA methods have not yet been implemented or further calibration or checking of the equipment is required.

TYPES OF MEASUREMENTS

In field measurements are performed aimed at qualitative or quantitative verification of the amount of SNM material present.

(a) Qualitative tests are conducted mainly with single channel analysers. These have their windows set at particular energies to identify the types of material as well as to assure the presence of nuclear material. They cannot, in general, be used to determine the amount of SNM present but combined with other information available to the inspector might generate confidence in the correctness of a declaration. Furthermore in the absence of adequate quantitativ verification methods or in other circumstances, such as time availability, accessibility of the materials or failure of more sophisticated pieces of equipment, they often are the only feasible measurements.

In addition to single channel analysers, ionization chambers or other radiation sensitive devices have also been used. The quality of the information collected with these categories of instruments can and needs to be improved, for example through the use of high resolution gamma detectors which are capable of quick and unique identification of the nuclear materials. A device of this type to be used in the circumstances described above needs however to be highly portable and to have a visual display.

Simple pieces of equipment such as single channel analysers can in some cases be used to generate quantitive information. This can, for example, be the case of measuring the active length of a fuel rod. In this situation the instrument is required to define boundaries of the nculear material in a "yes or no" type of application and can do the job almost as well as any sophisticated piece of equipment.

(b) Comparison between identical items (consistency checks) is a common practice which has its most significant applications when adequate standards to calibrate the equipment are not available or when proper techniques for quantitive measurements do not exist.

If the type of response function of the equipment to the amount of material is known, then measurements of non-identical items can be performed and comparisons among them established. Depending on the range of the materials to be assayed, it may be possible to establis in this way a kind of calibration curve. The inspector who does not have calibrated equipment would be able in this case to derive from his measurements a further degree of verification.

(c) Quantitive measurements are the most important since they are the only ones that can provide the basis for full objective conclusions on verification. They are conducted with various types of instruments which are of the portable or in plant type. So far in most of the inspections portable IAEA owned equipment has been used but, when available, plant owned instrumentation has also been employed after the Agency has assured itself of its adequacy for an independent verification. A trend also exists to have IAEA equipment localized at facilities and to the introduction of larger units (sometimes more transportable than portable) specially at facilities demanding a large inspection effort. Clearly in these cases the question of portability becomes less stringent but the equipment must be capable of long periods of reliable operation.

MAIN TYPES OF EQUIPMENT AND ITS USE

To perform the types of measurement described, the inspectorate is using different instrumentation comprising among others single and multi-channel analysers and total and coincidence neutron counters.

Eberline Assay Meter

The single channel analyser mostly used has been the Eberline SAM 2 assay meter employed in quantitive mode, namely in:

- The verification of the uranium enrichment in metal or in oxides be it in cans of powder, pellets or fuel rods;
- The verification of MTR fuel assemblies and plates;
- Plutonium measurements both as mixed oxide fuel pins and metal plates.

The enrichment type of applications which constitutes the bulk of the instrument use are well documented, therefore reference will be made here only to the last two cases.

Regarding the verification of MTR fuel assemblies and plates [8] the materials are measured in fixed geometric conditions using as signal the net count rate under the U-235, 186 KeV peak. Once the signal is corrected for self absorption and source dimensions the response depends only on the amount of material present. The corrections are determined theoretically beforehand using a point source model and information contained in the design data (plate dimensions, amount of material per plate, cladding thickness, meat thickness, uranium fraction in the meat and number of plates per assembly). A source-detector distance equal to 1.2 m which is equal to twice the largest active dimension of a standard MTR type assembly has been adopted. In this way the assembly or plates can be considered as point sources, located in the detector axis and having the same intensities as the samples themselves. It is easy to show that, for a uniform narrow plate source of length x, placed centered with the axis of a detector and at a distance $2x$ from it, the maximum difference in the detector response to radiation originated in any two of its points is 6.3%. The technique used as described gives only the fissile content of the item; in order to obtain the amount of the element an absorption measurement is also required.

Concerning the plutonium measurements the system has been used both as a neutron and a gamma ray counter. In the first case the standard SNAP [9] system and a specifically developed [10] measuring head applicable to the assay of plutonium platelets in storage containers have been used. The measuring head consists of one array of four He-3 detectors embeded in a moderator block which is placed surrounding the container. The system can be assembled in two different ways, one applicable to the containers, the other to individual platelets. In any one of these situations the system is responding to the total neutrons, originated mainly in the spontaneous fissions of the even isotopes, therefore an independent characterization of the Pu is also necessary in order to be able to derive the total amount of material.

Regarding the gamma measurements, a two detector system has also been used in the case of mixed oxide fuel pins of the FBR type. This technique which was applied by Beets et al [7] to the measurement of uranium fuel pins aims at examining each portion of an extended source with the same detector efficiency. To achieve this objective the distances between the detectors and between the detectors and the radiation source are determined so that for any point of the source the sum of the signals induced in the two detectors remains constant.

Despite the wide application to which it has been put the Eberline assay meter has some well known drawbacks therefore another unit the B-SAM [1] developed under the US support program is being field tested and it is expected to be fully operational in the near future.

Multi-Channel Analysers

The multi-channel analysers - Silena B-27* one thousand channels - are practically used only as part of high resolution gamma spectrometry systems based on intrinsic germanium de - tectors. The volume of the Ge detectors ranges from a few to about 80 cc. Viewing the intermittent use of the equipment as well as transportation and servicing conditions, it is essential for the Agency to use intrinsic Ge detectors.

The most frequent use of the HRG systems include the determination of plutonium isotopic characteristics and amounts, uranium enrichment and spent fuel measurements.

Concerning the plutonium isotopic characteristics, the applications range from pure identification to full isotopic analysis. They include therefore some significant ratios like the Pu-241/Pu-239 or direct comparison between spectra of items of the same batch.

Enrichment measurements using HRG are only performed when a clear advantage over simpler systems exists. This is, for example, the situation in the case of low enriched UF_6 cylinders, and materials irradiated in zero power reactors.

* This multichannel analyser was first used in field by the Agency in the summer of 1976 in replacement for the LP-4840 NOKIA System.

Spent fuel measurements using HRG systems are currently being done[3][4][11]. In most of the cases the aim is the determination of burn-up and cooling time but in some instances only identification is performed. Identification meaning, in this case, an attributes type of verification to assure that the material contain fission products. In the quantitative mode of operation it has been found that more precise results can be obtained in cooling time than in burn up determination. It is not uncommon to have results with errors below 2% in the first case while several percent are found for the Cs-134/Cs-137 ratio.

As indicated the HRG systems are used in a variety of circumstances. Being able to unequivocally identify the nuclear materials by their characteristic gamma rays they are among the most interesting pieces of equipment from the inspector's point of view. The present cost, size and weight of such equipment prevents its substitution for units which are smaller and therefore much handier, even if they are not as good.

The HRG measurements can be lengthy, an aspect that needs to be improved in order to reduce the inspection time. Such aim can be achieved by the use of large detectors and multichannel analysers capable of handling high count rates. The Silena system has proved to be somewhat insufficient in this aspect as well as in the number of channels. Both this features are particularly desirable in order to improve the quality of the data on both spent fuel and plutonium analysis measurements.

Neutron Counters

The most widely used neutron counter by the Agency is the high level neutron coincidence counter [2][6](HLNCC) developed under the US support program. This detector initially intended for the measurement of large amounts of Pu, like cans of feed material, has been also applied to metal plates and mixed oxides contained in cans, fuel pins and fuel assemblies. Although some results of the use of this equipment have already been published [12] and inference on the expected results can be extracted from the user's manual, reports on field experience are still lacking. It seems therefore appropriate to give here some more information, even if, due to its origin, only in a relative form. The attached table summarises results of measurements of fast critical type plutonium coupons, assembled in fuel drawers and of mixed oxide fuel clusters. All measurements were done at different occasions on randomly selected items from given populations and not necessarily with the same instrument. Statistical analysis of the results can show whether the different means are the same or not, a question that has to be asked even if the maximum difference between them does not exceed 2%. These small differences are of the type that inspections are aiming to detect, therefore extreme care needs to be used both in calibrating and setting the measurement conditions each time. For example, in the case of metal plates, due to the short length of the active dimensions of the counter, each result is a double measurement so that each point of the item is observed once with high and once with low efficiency. This procedure allows for uniform assaying of the item but requires two adjustments of the position which can introduce systematic differences particularly if proper adjustment of the reference marks was not achieved during the equipment setting. Since this measurement can have errors in the percent range (see table) such adjustments become difficult to check during inspections because such checking would require lengthy tests. In the present case 3 mm misadjustment can originate a change in response up to 1%. To avoid that situation new measuring heads with larger sensitive regions are being developed and built at LASL. They are expected to be ready for use soon.

The present measuring head of the HLNCC [2][6] is formed by the He-3 detectors and the surrounding moderator material (there are 18 detectors embeded in 6 polythylene slabs). The remaining components of the system are the preamplifiers, electronic package and calculator. In some of the new heads which will have different number of detectors the sensitive region will be close to one meter in length, therefore the units themselves become difficult to transport. On the other hand they would also be usable to assay fast breeder type fuel pins in a single measurement.

In the assay of mixed oxide clusters a concentration concept coupled with active length measurement is used. The results presented in the table are ordered by decreasing Pu concentration per unit length and this is the reason for the increase in the standard deviation as one goes down through the table. In this case the count rates are relatively small and the

effect of large totals rate background can also be seen. This is the case of the second series of measurements - all of them performed in a storage room - where larger amounts of material were present in the vicinity of the equipment.

The HLNCC has also been used in the measurement of fuel pins and scraps. In this last case the measurements which generally become less precise can be also difficult to interpret. In measuring Pu one is frequently faced with multiplication type of effects which being shape dependent are, in general, difficult to account for. Standardization of the containers would be a large step forward in solving this difficulty. It has been found that the multiplication correction technique as developed by Ensslin et al (2)(6)(13) is in several cases extremely useful. Certainly spurious values can be generated due, for example, to the application of the technique to insufficient or improperly characterized samples. Analysing the results using different approaches may help in removing those anomalies

Table

MEASUREMENTS OF IDENTICAL ITEMS ON DIFFERENT OCCASIONS

ITEM DESCRIPTION	NUMBER MEASURED	MEAN VALUE OF MEASURED CONTENT ($\bar{x}$)	STANDARD DEVIATION POPULATION as % of $\bar{x}$	TYPICAL STANDARD DEVIATION (COUNTING ONLY) as % of $\bar{x}$	COUNTING TIME (SEC)
Metal Plates	33	x	1.26	1.40	2 x 200
+ Various Matrix	19	x 1.020	1.44	1.40	2 x 200
Materials	16	x 1.011	1.05	1.40	2 x 200
Mixed Oxide	7	x	2.24	1.60	400 *
Fuel Clusters	7	x 0.984	2.35	2.22	300 +
3 # Loadings	3	x	0.93	2.30	400 *
	7	x 1.014	2.87	3.20	300 +
	7	x	1.75	2.75	400 *
	6	x 1.014	5.26	4.15	300 +

* Some measurements were done with longer counting times.

\+ Larger totals background.

If the samples are not strong (α,n) neutron emiters our experience seems to indicate that a large variety of samples can be assayed using the same calibration curve which becomes linearized by the multiplication correction technique. This would obviously be of great consequences in reducing the number of standards required for the calibration of the equipment.

Since the neutron counters respond to the non-fissile components of the plutonium, information on the isotopic composition is required to derive the total amount of material present in a sample. It is for this reason that now in practically all Pu determinations done by IAEA, both HRG and neutron coincidence oounting are used. Since there is always the problem of the amount of time consumed in the measurement, they are performed simultaneously whenever possible and for this purpose holes have been drilled in HLNCC measuring heads, through which the samples are viewed by the Ge detectors.

Use of the HLNCC in an active mode for the determination of U-235 is also being introduced. In this case the interrogating neutrons are originated in Am-Li neutron sources which are localized in the axis of the end plugs which where redesigned (14) to create an optimal cavity about 10 cm in height. The system due to its low sensitivity is intended principally to probe relatively large pieces of uranium metal which can also be assayed by other methods like weighing. With this apparatus 3% counting precision can be obtained in a 1000 seconds counting time of a 2 kg highly enriched uranium button (14). An active well coincidence

counter (AWCC)[15][16], an instrument one order of magnitude more sensitive than the one just referred to, is also being introduced for the uranium assay.

As mentioned above the HLNCC system is being widely employed by the Agency but its application can still be further improved through the use of objective specific measuring heads. Other than the cases of the fast critical assembly drawers and FBR type pins that were mentioned above measurements of Plutonium metal platelets contained in storage canisters and of FBR assemblies may also be mentioned.

In all the applications referred above only the detecting part of the system is being adapted to the different situations. Keeping the same electronics for a variety of measurements is a key factor for the reliability of the measurements and therefore for the effectiveness of the international safeguards due to the reduction in inspector's training.

EQUIPMENT CALIBRATION AND STANDARDS

As previously mentioned some of the measurements performed aim at qualitative information, but the objective of the really significant ones is the quantitative determination of the amount of SNM present in the items assayed. Such determination implies equipment calibration which in turn means standards. It has long been recognized and repetitively mentioned that one serious difficulty in implementing field measurements by the Agency is the absence of adequate standards.

To circumvent this difficulty use has been made of materials characterized and made available to the IAEA by member states. In many cases the materials are not standards as such but are sufficiently well characterized for the purpose. In other cases actions have or are being taken in co-operation with national safeguarding authorities and the operators to select materials from facilities which will be characterized by the parts involved. On other occasions the equipment has been calibrated in member states and used in other member states where agreement has also been obtained to keep some of the materials measured with those systems as a reference for subsequent use.

It is clear that frequently the materials used as standards do not fully match the ones to be assayed. This is not surprizing since in some cases these may have been pre - pared or developed as part of specific projects that are not duplicable. Calculation methods which would for example be used to reduce the number of required standards need to be applied in order to adequately analyze measurement results.

It has sometimes been possible to construct a set of calibration curves for different values of some parameter and interpolate between them if the value of that parameter in the assayed material is different. The measurement of mixed oxide fuel clusters included in the table falls into this category. In this case it has also been found that by applying a multiplication correction technique [13] to the measurement of different types of clusters (different in Pu type and concentration and number of fuel rods) all the results could be described by the same linear relation.

Multiplication correction techniques like calculational methods can be most valuable in reducing the number of standards required for the calibration of the equipment. However, some of the equipment now in use is capable of furnishing, in routine inspection, results identical or better than the ones included in the table and the application of alternative methods to circumvent proper standards might not be an adequate procedure. Somewhat connected with this subject, mention can be made of plutonium measurements using the HLNCC and the Pu-240 effective concept. It has been found that in some cases better results are obtained when the Plutonium non-fissile fraction is used instead of the Pu-240 effective. This seems to result from the fact that the Pu-240 effective value places heavier weight on the Pu-238 and Pu-242 content whose itotopic fractions are frequently not known or obtained with sufficient accuracy.

In some cases it is possible for the inspectors to have at the facilities either IAEA owned standards, sent from HQ for that purpose, or reference materials made accessible under some agreements such as the ones indicated above. However, in several instances that is not the case and alternative approaches to calibrate the equipment or assure of its correct working conditions have to be applied. It is possible, for example, to use as a reference,

operator's material which is sampled for destructive analysis. This procedure has been used for example for the enrichment of uranium powders but the values obtained with this in the field calibration have to be checked and, eventually, corrected a posteriori once the DA results are obtained. Such an approach has the drawback that if the values furnished by the operator are found to be incorrect, then defects on the samples assayed can reveal themselves later therefore at a time where immediate action can no longer be taken.

When the calibration of the equipment is done outside the facilities only the proper functioning of the equipment might need to be verified. To fulfill this objective, normalization sources can be used; such sources are measured at the times of calibration and assay and the normalization factors so determined are applied to correct the data. In the case of the HLNCC Cf-252 neutron sources with activities of the order of 9 μCi are used, and for the SAM-2 Ho-166m gamma sources with activity of the order of 0.2 μCi. This last source is also convenient for the energy calibration of the multi-channel analysers.

RESULTS OF THE NDA MEASUREMENTS

A safeguards inspection aims at the verification of the amounts of SNM with minimal intrusion. This implies sampling plans drawn on the basis of zero deffects and also measurement systems capable of giving, in field, the content of the items assayed so that at least their classification as good or defective is obtained. That this classification is essential can easily be seen because if a deffect is found all the plan of the inspection has to be modified since no deffects are allowed by the sampling plan. The measurement result might eventually be such that no further treatment is necessary but frequently more elaborated calculations are unavoidable. The achieve in field data reduction and treatment capacity HP-97 programable calculators are being used concomitantly with the measuring equipment and in some cases interfaced with it. In some situations such as most of the HLNCC measurements the calculator has the capacity to deal with one type of measurement, collecting the data and via calibration curves calculate the final result. In other cases such as the HRG systems the calculators are not interfaced with the equipment but programs are being used to obtain a result. Those calculators are insufficient to handle more complicated situations therefore final treatment of inspection data is being done at Headquarters. Although this type of situation is bound to continue because the additional calculational capacity is probably not compatible with the transportability of the equipment, improvements are required both in interfacing and expanding the capacity of the presently employed calculators. As an example both in the case of the HRG and the HLNCC a slightly more powerful calculator could permit the unification of the programs now in use - presently each type of measurement requires a different program but most of them have large portions in common - which would greatly simplify the procedures.

Simplification of the procedures and equipment manipulations during data taking are fundamental steps towards safeguards effectiveness. This statement may sound strange until it is realized that international safeguards are conducted by inspectors hired on a fixed term contract. The average duration of this is such that if the equipment and procedures are complicated, the inspector can hardly become familiar with them. Even in the case of inspectors staying with the Agency for longer periods since they are not constantly using the equipment specific details on its use at certain places may easily be forgotten.

OTHER IMPLEMENTATION ASPECTS

Successful NDA measurements in the international safeguards depend on various factors of which some are inspector specific, others are equipment related and finally others that are not associated with any of the previous causes.

(a) Perhaps the most important requirement is the inspector being familiar with the measurement technique that he is applying. This is achieved through basic training involving equipment and methods (the inspectors are attending training courses either in the Agency or outside like for example at LASL under the US support program) as well as by refreshing at least before the inspections.

(b) The equipment is frequently used in non optimal conditions; for example the temperature and humidity may cover a very wide range as well as electrical noise or vibrations caused by

different machinery. Obviously the equipment needs to be reliable, even in the most adverse working conditions, and its operation needs to be as simple as possible. Even if highly reliable, the equipment is bound to fail and in some cases would be impossible to obtain substitution in time therefore trouble shooting should be easy so that simple repair could eventually be done during the inspection. Kits of spare parts should be available as well as adequate auxiliary equipment like pulse generators, osciloscopes and volt-meters. Again all these pieces should be reliable and small in size.

(c) The equipment might have to be transported for large distances both internationally and within the countries; during this process the handling is, in general, not adequate. Ruggadizing is recommended for all pieces and if they are also light and easy to pack, i.e. regular and simple shapes with no protruding sensitive parts, handling would become a much less serious problem. In field repacking is normally done by inspectors after the equipment has been used; such operation normally takes place at the end of the day and frequently in rush. Small reference sources are normally required and for some of these such as the Am-Li and Cf-252 neutron sources the transportation and use are heavily regulated introducing exceedingly high delays for the nature of the problem at hand. Difficulties are also found regarding transportation of standards particularly of the Pu ones.

REFERENCES

1. Zucker, M.S. et al -"The Development of a New Survey Meter in Fulfillment of IAEA and US DOE Requirements",International Symposium on Nuclear Materials Safeguards, Vienna, October 1978.

2. Krick, M.S. et al -"A Portable Neutron Coincidence Counter for Assaying Large Plutonium Samples",Internationa Symposium on Nuclear Materials Safeguards, Vienna, October 1978.

3. Beyer,N. et al -"IAEA NDA Measurements as Applied to Irradiated Fuel Assemblies", International Symposium on Nuclear Materials Safeguards, Vienna, October 1978.

4. Ramalho,A. and Payne, E. -"Spent Fuel Measurements Using High Resolution Gamma Systems",Nuclear Materials Management Vol. VIII No.3 (1979)

5. IAEA - 174 - IAEA Safeguards Technical Manual Part F - Statistical Concepts and Techniques.

6. Krick, M.S. and Manlove, H.O. -"The High-Level Neutron Coincidence Counter (HLNCC) - User's Manual",Los Alamos Scientific Laboratory, LA - 7779 - M, June 1979.

7. Beets, C. et al -"Aspects du Controle d'Installations Representatives de l'Industrie",4th International Conference - P.U.A.E. Volume 9, 449 (1972).

8. Ramalho, A. -"Measurement of MTR Fuel Assemblies and Plates Using SAM-2" (1976) - unpublished.

9. Augustson, R.H. and Reilly, T.D. -"Fundamentals of Passive Non-Destructive Assay of Fissionable Material",Los Alamos Scientific Laboratory, L.A. 5651-M (September 1974).

10. Taylor, W.H. et al -"Assay of Pu content of Birdcage Storage Containers by Measurement of Natural Radiations (from the Pu) Made External to the Container",IAEA Technical Contracts No.1403/TC April 1974.

11. Kupryashkin, V. et al -"Gamma Spectrometric Measurements of LWR Power Reactor Spent Fuel",This Conference.

12. De Carolis, M. et al -"Non-destructive Assay of Large Quantities of Plutonium", International Symposium on Nuclear Materials Safeguards, Vienna, October 1978.

13. Ensslin, N. et al -"Self Multiplication Correction Factors for Neutron Coincidence Counting", Nuclear Materials Management Vol VIII No. 2 (1979)

14. Foley, J.E. -"Measurement of Highly Enriched Uranium Metal Buttons with the HLNCC Operating in the Active Mode", February 1979 - unpublished.

15. Menlove, H.O. -"Description and Operation Manual for the Active Well Coincidence Counter", Los Alamos Scientific Laboratory, LA 7823-M, May 1979

16. Menlove, H.O. et al -"Experimental Comparison of the Active Well Coincidence Counter with the Random Driver", Los Alamos Scientific Laboratory, LA 7882-MS, June 1979.

Discussion:

Bowman (NBS):
Could you describe what means you have for calibrating fuel rod scanners for the International Community?

Ramalho (IAEA):
We have not been using rod scanners so far. We, in fact, intend to use the rod scanner -- if we had it available. The Agency doesn't have it, but may make use of it in some facilities. What we are planning to do is make arrangements with the operator, whereby we would select some of their rods to be used as standards. We would have to establish beforehand that those rods are good by comparison with the IAEA standards. So we have to go in a chain process in order to achieve the use of the rod scanner at this stage.

Schleicher (EURATOM):
In the European Community, we use, in certain cases, the rod scanner of the operator. For this we are really controlling the preparation of some rods, which we select as standards, supervising the whole fabrication process, taking samples of the pellets which are put into rods, etc., thus obtaining comparison standards for future use.

Inventory Verification Methods In DOE Safeguards Inspections

by

Craig S. Smith and Rush O. Inlow
Safeguards & Security Division
U.S. DOE, Albuquerque Operations Office
Albuquerque, New Mexico 87115

ABSTRACT

The most difficult and complex activity of a nuclear materials safeguards survey involves measurements review and inventory testing. At the Albuquerque Operations Office, we have relied on remeasurements as the key to inventory verification. Measurement of inventory items is accomplished by weighing, non-destructive assay (using contractor instruments and our assay meter), sampling/chemistry, and the use of off-site laboratories. The emphasis on each of these methods shifts from one contractor facility to another depending on processing history during the survey period and measurement capabilities required for proper safeguards accountability. ALO surveys five major facilities and we use five completely different approaches to measurement verification.

The goal of inventory verification is to assure that the contractor has all the nuclear materials reported to be in his possession. Verification is complete when it has been demonstrated that items purported to be in the inventory are present and easy to locate, that SNM items in the inventory are on the inventory listing, and that items contain the purported amounts of SNM. Ideally, an independent verification of inventory holdings would require a 100% remeasurement. This is not possible for facilities with large inventories. An alternate method is to remeasure items randomly selected through an attribute sampling plan. In our experience, this is unworkable for large, throughput-dominated facilities. By subdividing the inventory holdings into categories depending on the nature of the material, process characteristics, and measurement methods, the inspector can logically design a remeasurement campaign. This method is the most efficient means for examination of measurement performance during the entire accountability period.

Inspector remeasurement activities may be categorized under bulk properties determination, sampling and chemical assay, or NDA measurements. When possible, measurements are performed by the inspector or done under direct observation of the inspector. Samples are selected for each measurement method and material category such that the entire calibrated range of an instrument is tested. These measurements provide verification of random errors only. Off-site independent assays are provided by reference laboratories such as NBL or Mound Facility. This facet of our program has been very successful in improving contractor measurement systems and identifying or reducing significant biases. Samples returned after calorimetry at Mound are especially valuable in that they may be used as working standards for calibration of NDA instruments with actual process materials. When a facility possesses NDA and calorimetry capabilities, a dynamic calibration program may be established with process stream samples, reducing the need for extensive stocks of prepared standards.

ALO plans to field test a transportable calorimeter being designed and built by Mound for the Office of Safeguards and Security, DOE. This instrument has potential to be a valuable addition to our measurement capabilities by providing a rapid, inspector-operated assay system.

INTRODUCTION

The most difficult and complex activities of a nuclear materials safeguards survey are inventory testing and appraising the measurement systems. At the Albuquerque Operations Office we consider remeasurement as the key to assuring both the quality of the inventory and the reliability of the measurements. Our remeasurement efforts include the use of contractor instruments, our own portable and transportable equipment, and reference laboratories. Each of these methods is employed in varying degrees at our five major contractor facilities according to their processing history for the survey period as well as their measurement capabilities.

Ideally, an independent verification of inventory holdings would require a 100% remeasurement. Since this is not possible for facilities with large or throughput-dominated inventories, we custom tailor our remeasurement plan to fit our objectives at each facility. Furthermore, each facility under the Albuquerque Operations Office has different materials and material forms, different process characteristics, and different measurement systems. This paper will present some of the activities that have been developed to improve our verification of measurements and measurement systems. The topics covered in this paper are conveniently divided into Onsite Verification, Offsite Verification, and some examples. Our onsite activities comprise the bulk of the inventory certification and will be the first subject discussed.

I. ONSITE VERIFICATION

Onsite verification data are gathered during a survey and are largely responsible for our conclusions regarding the status of the nuclear materials physical inventory. Our statement about the status of the inventory includes the presence of all identifiable items, and the accuracy of the accountability weight values. Indirectly this is also a statement about the operability of the measurement systems since it was the values derived from these systems that provided our confidence in the inventory. Our onsite verification program, then, is designed to concentrate on the special nuclear material, certain measurement methods, and specific categories of material that are unique to each facility. Consequently the following discussion will include several examples of our rationale in fitting an onsite verification program to the five major contractors.

Measurements at Contractors

1. Los Alamos Scientific Laboratory - University of California. First we'll analyze the program at our most diverse and complex contractor, Los Alamos Scientific Laboratory (LASL). LASL has two facilities which are the focal point of our survey, namely, TA-55 and TA-21. TA-55 is the newly constructed plutonium processing facility housing CMB-11 and featuring Dynamic Materials Control, (DYMAC) and TA-21 is the location of the enriched uranium recovery group, CMB-8. They present similar problems, but the measurement systems are different, the categories of material are different, and processing histories for the survey period must be considered.

Group CMB-8. A normal inventory for CMB-8 will consist of uranyl nitrate solutions in 55 L transparent pencil tanks, 2 gal. Volrath cans containing enriched uranium in a dense matrix with a gross weight of 8-12 kgs, enriched uranium product oxide, and metal buttons. The majority of the material is either as solutions or as scrap in the 2 gal. Volrath cans. Both categories are measured by nondestructive analysis (NDA) instrumentation designed by LASL. The solution samples are assayed by the Uranium Solutions Assay Device (USAD), and the volume is taken from a calibrated, transparent pencil tank. The cans of scrap are measured by the Random Driver (RD) which is a neutron-activated coincidence counter using three calibration curves according to the type of scrap.

Random Driver. In order to judge the reproducibility of the RD and the reasonableness of the enriched uranium scrap inventory, we select a number of inventory items from the scrap categories to be recounted. So as not to impact production inordinately, we limit the recounts to the number that can be accomplished in two days. Items are selected that span the range of inventory values and that utilize more than one calibration curve. Unfortunately, there are no practical methods of cross-checking the accuracy of the RD during our survey or at a reference lab. The subject scrap categories have already been through various leaching steps and would be difficult to destructively analyze, are too inhomogeneous to sample for weight X factor analysis, and are not amenable to any other current NDA technique. We can also request that the RD be recalibrated before the recounts begin. However, the recalibration reduces the number of recounts, and we normally resort to counting the standards required by the programmed diagnostics.

Uranium Solutions Assay Device. In contrast to the restrictions on the scrap items, the uranyl nitrate solutions can be verified in a number of ways. Instead of relying on an offsite laboratory, we have turned to LASL's own analytical laboratory, Group CMB-1, for assistance in verifying the accuracy of USAD. Until recently our resamples of inventory solutions had to be prepared by CMB-8 personnel for submission to the analytical labs. This time-consuming operation was inefficient and burdensome. Therefore, we reversed the procedure and requested CMB-1 to furnish three blind samples at concentrations selected to test each of three separate ranges programmed into the USAD. The speed of the USAD allowed replicates on each blind and also allowed the measurment of the tanks resampled in our presence. In some cases the observed sampling and measuring establishes the inventory values, and in others, it verifies the inventory value. Either process serves to certify the inventory.

TA-55 (Group CMB-11). Four distinct plutonium operations are carried out in TA-55, namely, plutonium recovery, plutonium fabrication, Pu-238 processing, and advanced carbide fuel production. With nearly 5000 items of every imaginable description, inventory verification at TA-55 is a sizable challenge. The challenge is made manageable by the full utilization of DYMAC information and instrumentation. The instrumentation includes a segmented gamma-scan unit, a neutron coincidence counter, an in-line thermal-neutron coincidence counter, and a solution assay system. The information file includes date of last measurement, material description, instrument used, and area of origin.

In the time allotted for verification, it is impossible to select samples from all the scrap, intermediate product, and product categories. Thus, we reduce the total population to a few categories by choosing processing and counting characteristics representative of many. With this approach, we are able to verify the random errors throughout the calibrated range of the instruments. We are not, however, able to estimate the systematic errors.

The verification is partitioned into testing the stored or inactive inventory with the segmented gamma-scan unit and the neutron coincidence counter while the active items in the glovebox lines are remeasured in the thermal-neutron coincidence counters and solution assay system. Normally, the inventory at the time of survey is principally stored items, and we spend most of our time remeasuring those. We include standards as much as practicable and, on those items which are amenable to either neutron or gamma assay, we recount in both instruments. This gives us an indication of the packaging and correct categorization by scrap codes. At LASL this is a very important exercise because the recovery operations handle atypical scrap that could easily be miscategorized.

The foregoing remeasurement activities are the highlights of our program at LASL. Not included are our normal reweighing and other measurements which supplement our remeasurements.

2. Mound Facility - Monsanto Research Corporation. The Mound Facility is noted for its expertise in calorimetry. This was a logical measurement development because Mound's inventory consists primarily of Pu-238 and tritium items. Calorimetry is easily the most accurate method for measuring these materials and is therefore the basis of our verification program.

At Mound the calorimeters are sized to accommodate routinely used sample containers in a particular building. We stratify the inventory by the building and the secondary container size so as to identify which items will fit the various calorimeters. Time-wise we are restricted to the number of samples which Mound can run in a workweek. This means that the samples must be selected during the physical inventory without the benefit of a statistically generated random sampling.

To make the verification as independent as practical, we observe the sample as it is placed in the calorimeter, observe the last two or three readings at the end of the equilibrium period and make sure the same sample is removed from the calorimeter.

For measuring their low-level Pu-238 solid scrap and waste Mound employs an in-line gamma-ray assay system which measures the intensity of the 743 keV and 766 keV gammas using a Ge(Li) detector. The scrap/waste is packaged in paper "ice cream" cartons and can vary from a lightweight combustible matrix to a dense, metal matrix. Because of the matrix variability, Mound has established a calorimeter cross-check program which routinely compares gamma-scan values with calorimetry. Our verification uses the same program for this level of material. The first phase is to observe remeasurement of between twenty and thirty inventory items in the gamma assay system. These remeasurement values are assigned from manual calculations which are also verified. Normally, a good portion of the low-level inventory is certified in this manner, but the system's accuracy is still in question. To give us information on the accuracy we also observe two or three low-level cartons being calorimetered. This is one of the few situations which allows us to compare in-plant measurement capabilities.

There is only one way to verify Mound's Pu-238 solutions; we observe the resampling, labelling, sample preparation, and alpha pulse height counting as well as check calculations. What makes this possible is the small number of accountability tanks in the process and the individual attention the analytical labs can afford us.

3. Rocky Flats Plant - Rockwell International. The Rocky Flats Plant is a Pu-239 production facility which is fully supported by storage, recovery, and R&D operations. Translated, that means the facility is throughput dominated with a large backlog of unprocessed scrap and a substantial holding of feed material. The scrap is of every imaginable description and is stored on the plant site awaiting recovery. It comprises a sizable portion of the inventory and is most subject to errors in measurement. Feed material is also stored in large quantities and is not amenable to direct verification such as sampling/chemical analysis or weighing. These are the major problems at Rocky Flats and, over the years, we have employed some verification techniques which provide us with a high degree of confidence. For the scrap, we have developed an offsite sample verification program with the Mound Facility, and for the feed material, we rely upon the capabilities of portable NDA instrumentation. These methods will, however, be discussed in other portions of this paper while methods to verify the active inventory are covered here.

The recovery operations group performs a total shutdown, cleanup, and physical inventory annually to coincide with our survey. For the purpose of saving time and effort, a large proportion of their inventory is plutonium nitrate solutions in calibrated, Raschig-ring-filled tanks. Accountability values are derived from the typical volume X assay. Since the dominant error in this value is due to the error in the volume calibration, our emphasis is placed on verifying the accuracy of the sight gauges. The sight gauges are fabricated and mounted according to the correlation between the calibrated volumes introduced into the tank and the height of the liquid level. Each tank is calibrated by adding known amounts of water and measuring the height of the water in the sight glass from a permanent reference point. A computer performs a least squares fit, scribes the sight gauge, and prints a calibration certificate. It is our task to verify how well the gauge is mounted in accordance with the certificate. We consider that the gauge is properly mounted if three points on the full range of the gauge measure within the standard error, two sigma, of the certified height. Every one of the 70 + tanks is physically verified in this fashion.

A very unsettling aspect of observing a physical inventory is certifying that a metal button is present when all you see is a metal can with the correct serial identification. At Rocky Flats we are not limited to a simple verification of the presence of a metal can in the button vault. An instrument known as a button counter is available for qualitative measurement of plutonium. It measures the 384 keV gamma as well as the neutrons from the Pu-240. Empirical limits which bracket the average gamma and neutron counts for Savannah River buttons have been established as part of the verification procedures on external receipts. These limits are used as a guideline in verifying any button. Due to concerns for personnel exposure, we have informally limited our efforts to the number of buttons that can be counted in two hours. At 20 seconds per button that number can vary from 50 to 100 according to the accessibility of the containers. Another limiting factor is the tier of holders we select. For instead of making a truly random selection, we indicate by tier which samples to count. This greatly reduces the time wasted hunting samples. Although the sampling method is not statistically sound, the number of samples verified is large and the exposure time is reduced.

In one area called the XY Retriever we perform a random verification of the book inventory. This is preferable to a complete physical inventory because the mechanical retrieval system combined with weighing each of the 200 + items would expend greater than 17 hours. Again, our sample size is related to time; it is the number of ingots that can be verified in one day. These 45 or so samples are checked for serial identification, weighed, and scanned by our portable gamma and neutron instrumentation. The portable instruments are set up above and below the glovebox with the two detectors directed at the pan of a 10-kg balance. A significant count above background registered on both rate meters is considered a positive indication of Pu-239 (a significant count = 5 times background). We consider this a variables test of the inventory with 0 rejects allowed; one reject and we perform a 100% inventory.

We perform a similar verification of the metal parts stored in carriers on the chainveyor lines inside of gloveboxes. By setting up the detectors on top of the gloveboxes, the parts can be verified as the chainveyor is operating. A person can observe the ratemeter and parts simultaneously or connect the single channel analyzer output to a strip chart recorder. Presently, we only have this capability for one instrument. It works best with the gamma detector because the background and chainveyor speed are too high for significant count rates with the neutron detector. Of course this is not the extent of our activities at Rocky Flats, but the foregoing examples are unique to the facility.

4. Pantex Plant-Mason & Hanger - Silas Mason Co., Inc. The Pantex Plant is a nuclear weapons assembly installation which handles only finished parts; it performs no chemical processing or physical transformations. Consequently, it relies solely upon radiometric verification of the SNM by means of portable, gamma/neutron instruments. This facilitates our verification program by allowing us to concentrate on the use of our own portable gamma/neutron equipment. With this equipment our objective is to obtain a signature for the presence of SNM in shipping containers or completed weapons.

In order to optimize the verification we take all readings *in situ*. For instance, we'll walk into a vault with our heavily shielded gamma detector and place it directly on top of the shipping container for our count. The background is simply the count with the probe inverted. In this way, we can verify the entire content of the vault without removing each container to a low background area for a timed count. It's a two-person operation; one person handles the probe while the other watches the ratemeter. The count can be influenced by so many variables that we allow 3-5 times background as a significant indication of SNM. This is especially true for enriched uranium gammas which are easily attenuated. In less crowded conditions, we use the neutron probe in tandem with the gamma detector for Pu-239 items. Under cramped conditions, however, the neutron counter is swamped and cannot be used. Additionally, we monitor the response for a series of identical items and question any atypical reading. Such things as the age of the item, the radioactivity of adjacent items, and the position in the storage area will cause fluctuations in the expected response.

The method we use to distinguish the difference between depleted and enriched uranium items is by varying the energy window examined. First, we look for a significant count above background in the window calibrated to bracket the 186 keV gamma from U-235. With a positive indication of nuclear material, we then adjust the threshold above and below the 186 keV setting looking for a well-defined peak. If the count doesn't drop off to near background on either side of the peak the material is depleted uranium, and the 186 keV window is counting Compton scatter.

Using these above expendiencies we are able to verify 50 to 100% of Pantex's nuclear materials inventories during a survey. We consider the portable radiometric equipment as an invaluable tool of our trade.

5. Sandia Laboratories, Albuquerque - Western Electric. Sandia is a design and testing facility with a wide range of enterprises. Their inventory consists primarily of irradiated special nuclear material either as fuel in reactors or as stored samples in the cool-down stage. Of course, the material in the reactors cannot be verified except by gross counting and the reactivity as indicated by flux meters. The material of concern to us is the low-level, irradiated samples and fuel plates which are in storage.

The most effective verification technique available is weighing and simultaneous radiometric scanning with our portable gamma/neutron instruments. Although the induced radioactivity of most samples overwhelms the peaks of interest, we are still interested in checking whether the response is due to natural or induced radioactivity.

Since most of the material is enriched uranium, we use the 186 keV settings and vary the energy range of the instrument. Occasionally, the material is sufficiently cooled to distinguish the enriched uranium. Usually, however, the count rate is uniform throughout the range of energies. For this case, the only difference is the intensity of the response. If the ratemeter pegs at the highest range setting the material is too irradiated to verify. Otherwise, the material is considered to be depleted uranium.

There is no requirement to verify the irradiated material, but we still consider much of the low-level, irradiated material attractive for diversion.

II. OFFSITE VERIFICATION

Mound Exchange

As mentioned earlier under Onsite Verification, Rocky Flats has an extensive backlog of unprocessed scrap which defies normal verification techniques. A collateral concern is the accuracy of the NDA systems which establish the inventory values for the bulk of the scrap categories. Previously, the available onsite techniques for verifying the backlog could not satisfy our criteria of independence, accuracy, and timely results. The overriding factor was independence, and this led us to consider an impartial reference laboratory. Because of the advantages of calorimetry, the Mound Laboratory was funded to perform our offsite verification project, which soon became known as the Mound Exchange. Needless to say, the exchange program has experienced some growing pains and lessons learned the hard way, but overall it has provided gratifying results.

In describing the Mound Exchange we'll skip all the mistakes and comment on the final product. Over the years, the Mound Exchange has evolved into a twofold experiment. The first part remains as always, verification that the inventory is accurately stated. As the potential of dynamic calibration was realized, the second part has become an opportunity for the facility to perform a calibration of their NDA equipment for specific categories. With this duality in mind, the statistical sample is selected to represent a large portion of the backlog, represent routinely-generated material, and provide a spread of points which will optimize calibration. Unfortunately, the Department of Transportation (DOT) has packaging and transportation regulations restricting the categories of material and amount of SNM per package which can be shipped. Difficulties in this exchange are further compounded by the lack of uniform containers and the size of packages that the calorimeters can accommodate. Though we've learned to live with the restrictions, some of the effects on the ground rules of the exchange are: 1) the variety of scrap categories we can sample have been seriously limited; 2) all samples must be calcined in order to eliminate moisture and

oxidize any metal; 3) every sample must be quantitatively transferred and repackaged; in some instances one package is divided in two; and 4) samples exceeding a plutonium content of 10% by weight or 400g cannot be shipped.

At the outset of an exchange, the scrap categories are mutually agreed upon, and the samples are selected during our survey. We participate in the selection, obtaining the sample identification and the inventory value. From this point on the contractor prepares and ships the samples to the Mound Facility. The contractor also supplies subsamples according to Mound specifications.

Upon receipt of samples and subsamples, Mound performs mass spectrometry or gamma spectroscopy of the subsamples and the samples, and calorimeters all samples. Mound personnel have been able to furnish results with limits of error within six weeks for sample sizes no larger than fifty.

The results from the exchange are compared to the original inventory values and statistically evaluated for significant biases. If significant biases do exist, the inventory values are adjusted, and instrument calibration is realigned. Some categories have required adjustment and recalibration; these, however, are not considered deficiencies, but, rather, benefits derived from the program. Some of these benefits will be discussed later.

Chemistry

Although we have not relied on offsite verification for solution chemistry nearly as much as calorimetry, some situations have called for engaging a reference or umpire laboratory to analyze solution samples. An example of this was the need for an umpire laboratory to resolve a significant shipper/receiver difference between Rocky Flats and Rockwell Hanford. In this case, separate samples had been set aside just for such an eventuality. At our request, LASL agreed to act as the umpire laboratory for all the solution shipments between the two parties. The wisdom of this planning became evident when LASL released the results. LASL found undissolved precipitates which required special treatment. Failure to correct for the particulates would bias the results. Due to the condition of the samples and to LASL's thorough analysis, the umpire results were accepted by both parties.

Another situation which required reference laboratory expertise was the verification of the isotopic makeup and total uranium in high level uranyl nitrate solutions at LASL. Before the advent of the Uranium Solution Assay Device, the analytical labs group, CMB-1, performed all of the solution analyses. In order to examine and evaluate the analytical chemistry errors, we contracted the New Brunswick Laboratory to perform the independent verification. We observed all the sampling, sample preparation, and packaging by LASL personnel. NBL's results supported LASL's published random and systematic errors.

III. EXAMPLES

The practicality of our overall verification program can best be measured by the numerous improvements in measurement and verification techniques. Some examples of these improvements and how they came about will illustrate our program.

Benefits of Offsite Verification

1. In terms of grams, the offsite verification of Rocky Flats scrap categories has been the most beneficial. Results from the Mound Exchange have identified significant measurement biases. The most recently identified bias was in the ash heel category. Estimates of the biases from four separate exchanges were pooled to arrive at the final estimate. This pooled bias was used to adjust the entire ash heel inventory backlog by 12.9 kg. As you can see, this is a significant adjustment and reflects the importance of verification. Earlier in the program a similar adjustment was made to the virgin ash category. As the ash was processed through recovery it became evident that the ash portion of the backlog had indeed been "fine tuned", because the inventory differences attributed to ash recovery shrank to the random error level after the correction.

2. For many years Rocky Flats was obliged to bear the cost and impact of their end of the Mound Exchange. The increasing cost of the exchange has compelled Rocky Flats to develop an alternative.

Consequently, they developed a calorimetry capability comparable to the Mound Facility. To prove this comparability, they proposed that the 1978 Mound Exchange include the comparison of wattages on all samples. The proposal further stated that if the wattages agreed, Rocky Flats would perform the verification in place of Mound and would endeavor to satisfy whatever degree of independence we would require.

Rocky Flats proved their competence and have already performed an onsite verification of four scrap categories during our recent survey. They used the same guidelines for independence as are followed at Mound. The most meaningful outcome, however, was not the shift of sites from Mound to Rocky Flats, but the fact that Rocky Flats now performs their own dynamic calibration every month.

3. LASL's plutonium recovery group, CMB-11, is responsible for receiving, measuring and storing for recovery some difficult-to-measure scrap. CMB-11 does not have the gamma spectroscopy and calorimetry instruments to measure these categories. Therefore, we designed a Mound Exchange which would accomplish two goals: namely, verify portions of the inventory and provide standards for specific scrap categories. These were the beginnings of dynamic calibration.

Benefits of Onsite Veriication

1. During two days of NDA remeasurement activities at one of our contractors, we observed variations between the original value and recount that were as large as 100g. This was quite unexpected, and it prompted an immediate investigation into the possible causes. A check of the window energies revealed a drastic shift in the instrument gain. When no evidence of electronics malfunctions wa s found, it was postulated that the unseasonably warm weather had raised the room temperature above the critical operating temperature of the electronics. Further testing confirmed this suspicion and corrective steps were taken. A thermostat was installed to give temperature control year-round, and all the items measured during the hot weather were remeasured.

2. At another contractor our onsite verification program called for recalorimetering a number of Pu-238 items. An analysis of the results revealed relative differences larger than the published precisions for each calorimeter. Moreover, there was an apparent bias in the data; eleven of the seventeen items had remeasurements which were less than the inventory value. We suspected that decay had not been properly accounted for when the contractor converted from a manual to an automated accounting system. The contractor traced histories, remeasured numerous items, and finally tracked the problem to an error in the decay program. Now, realizing the benefits of a remeasurement program, the contractor has implemented a formal program of its own.

3. One of our contractors formerly used a weight-times-a-factor method in accounting for a special material. The factor was based on the calorimetric value of a sample from a large batch. The large batch as well as any cuts from it were weighed and factored. As a crosscheck of this method we calorimetered representative samples which were on the inventory at weight X factor. The disparity between calorimetry and the factor method convinced the contractor to change over to calorimetering all items of this type.

4. In some circumstances we have employed our portable gamma detection instruments linked to a strip chart recorder to verify material on a chainveyor inside of a glovebox while it is in operation. This exercise does not have to be attended and it provides a permanent record. Rocky Flats was so impressed with the idea that they now have a similar setup used to certify that no one has diverted material from the chainveyor during off-shift hours. The chart taken at the end of the day shift is compared with the chart taken the following morning. This procedure is a valuable part of the safeguards requirements for daily inventories.

The Mound Facility has attempted to predict the trend of safeguards verification activities. They were aware of the increasing costs of offsite verification in addition to the increasingly stringent regulations covering the shipment of radioactive material. With this motiviation, Mound began developing a transportable calorimeter which will be supported by reliable gamma spectrometry measurements. This combined instrumentation package will be field tested in 1980 at both LASL and Rocky Flats. Ultimately, ALO inspectors will be trained to use both instruments.

Fig. 1. Transportable Calorimeter Developed at the Mound Facility.

Discussion:

Cullington (EURATOM):
In your first slide you said that one of the things you did was to check that all identifiable items were accounted for. Does this mean that some items are not identified and therefore are not checked by the inspector?

Smith (DOE-ALO):
All items at our contractors must be identified. Therefore, the statement says that we have observed every identifiable item and are assured that it is present at the facility

Cullington:
A second question, please. You said that the weight values derived were checked. Does this mean that you calibrate their weighing scales or is this a check of the actual weights of the items?

Smith:
We make that statement as a result of our on-site and off-site verification programs. There are many parts to our program that I have not discussed today and, as you mentioned, verifying the accuracy of the field is one of them.

Bingham (NBL):
I'm a little concerned with statements relating to accuracy of measurements solely based on calorimetry, no disrespect to our calorimetry colleagues, and based on stream averages. Granted, that the measurement of heat can be performed very precisely and very accurately, but referencing my pitfall talk yesterday, the transfer of heat measurement to plutonium content must be based, and has to be based, on a very accurate knowledge of the isotopic content, the age, and the americium content of what you've got in the can.

Smith:
What I meant by that statement was that Mound and Rocky Flats were selected because they do have stream averaging, but Rocky Flats also has a very good quality assurance program and very good records on their scrap. We are not relying strictly on stream averaging, but that was one of the considerations in choosing Rocky Flats over, let's say LASL.

Bingham:
I am not disputing that part of the program. I am just pointing out that to extrapolate from this program to other plutonium facilities and use calorimetry without the benefit of the stream average assurance that you feel you apparently have, is a dangerous extrapolation for measurement accuracy.

Strohm (Mound Laboratory):
We at Mound do not blindly use the stream average from Rocky Flats in the calorimetry assay of plutonium. We do measurements - nondestructive gamma-ray isotopic measurements of cans, and we do take aliquots from a selected number of the cans for confirming isotopic measurements by mass spectrometry and alpha counting. We then, sometimes, establish a steam average for a given category, and, based on our independent isotopic measurement, apply an uncertainty to that stream average. That error is folded into the assay value that we report back to the ALO. The gamma-ray isotopic measurements have advanced far enough that now we are more and more often determining an independent set of isotopics for each can, and have less reliance on stream averages.

Persiani (ANL):
I am going to ask a generic question that relates to the first paper as well as this current paper. It has to do with item accountability and sampling methods. I'd like to use an example of the spent fuel measurements mentioned in the previous paper. I assume by spent fuel measurements, that this is done on a single rod so that the basic item unit becomes the rod. However, the spent fuel assemblies are an assemblage of rods. Now when you compromise that package to make a measurement on the single rod, does this not impact on your sampling techniques? How do you handle this in the field, both in EURATOM or IAEA, or as in your case, when you have to break a package into smaller sub-units? What is the unit of item accountability?

Smith:

I'm really not involved in spent fuel, but I'll address it as it applies to me. The only thing we can do with our verification program is remeasure or verify what is in the unit container, and, normally, we try to restrict our contractors to have one unit in one identifiable container. Now this isn't true in all cases, but this is what we try to do and, as you point out, it is very difficult to say that one item out of fifty is in there, if all we can see is the outside container and take measurements of that outside container.

Schleicher (EURATOM):

Certainly, you measure sometimes rods, sometimes bundles. If the operator accounts first for rods and later on for bundles he has to declare a rebatching operation, giving all necessary data. A priori this does not influence the sampling plan.

Safeguards Independent Measurements Program

by

Walter G. Martin
Chief, Safeguards Branch
Nuclear Regulatory Commission, Region I
Office of Inspection and Enforcement
631 Park Avenue
King of Prussia, PA 19406

ABSTRACT

The special nuclear material (SNM) control and accountability inspection program of the U.S. Nuclear Regulatory Commission (NRC) stresses independent verification of their inventories of SNM. In addition, independent assessments of the licensee's measurement systems are also performed by NRC Safeguards inspectors. The independent measurements program consists of two major areas; one being nondestructive assay and the other being destructive analyses. Both areas employ the use of NRC and NBL prepared standards to independently assess a licensee's capability in performing NDA and DA measurements.

In the area of nondestructive assay, the inspectors perform gamma spectroscopy and neutron counting measurements for both variables and attribute testing of the licensee's SNM. Regional inspectors have performed NDA measurements of licensee's special nuclear material in forms such as oxides, solutions, fuel elements and rods, residues, sludge, scrap, ash, and waste. In addition, NDA measurements of SNM holdup in piping, ducts, process equipment, and floors have been performed. The NRC has also performed NDA measurements to independently verify the SNM contained in licensee's ponds or lagoons - both the ponds' contents and the ponds themselves.

Due to the fact that generally recognized standards are not available for many of the above-mentioned items, NRC inspectors prepare field standards of different forms and matrices. Asphalt has been spiked with uranium solutions to obtain pond liner standards. Planar standards have been developed for different quantities of SNM to construct standards for piping, ductwork, and process equipment. Standards have been developed for waste drums, filters, and sludges. One of the major problems existing today in the field of nondestructive assay is the lack of adequate standards. Matrix problems and geometry problems must also be resolved. The NRC has instituted a measurements committee to investigate possible solutions for these problems. One area we are looking into is standardizing container sizes for various types of materials. Another area of concern is material segregation; i.e., removing certain types of extraneous materials from sludge produced by machining or sawing fuel elements.

NRC inspection modules require NDA measurements of licensee special nuclear material on inventory by attribute testing (qualitative) and of material measured by the licensee, using NDA techniques, by variable testing (quantitative). The NRC has prepared programmable calculator programs to determine sample size of a population, calibration using standards, differences (Licensee-NRC), and statistical evaluation of the differences may be performed and reported to the licensee prior to conclusion of the inspection.

The NDA equipment currently used by Region I consists of the following:

1. Hewlett Packard, 1024 Channel, multichannel analyzer
2. Tracor-Northern portable multichannel analyzer
3. Survey Assay Meter (SAM II)
4. Isotopic Source Adjustable Fissometer (ISAF)
5. Neutron Well Correlation Counter
6. Neutron Rod Correlation Counter.

We are purchasing a nuclear data quantitative isotope measuring system to measure uranium and plutonium isotopes. This system will also be used as a backup system for radioisotopic measurements in the environmental area.

In the area of destructive analysis, independent verification is performed by two distinct techniques. Destructive analyses of split samples of licensee special nuclear material by the New Brunswick Laboratory and the licensee's laboratory enable the inspectors to compare the analytical results. Also, NBL prepares and certifies, for the NRC, standards that are closely representative of the licensee's material being analyzed by a specific measurement system.

The licensee is requested, by our inspectors, to perform analyses on these standards. The inspectors are then able to compare the licensees' analytical results to the known values of the standards. A statistical evaluation of the differences is then performed to ascertain that the licensees' performance is adequate. This technique has been used by Region I to identify errors in analytical procedures that have an impact on inventory differences and shipper-receiver differences.

Discussion:

Belew (DOE-SR):
I would like to know what type of sampling plan you use to determine how many samples you are going to need?

Martin (USNRC):
Normally, we use MIL standard 105D. Frequently, we throw out the sampling plan depending on how we want to treat a certain inventory. Depending on the material, we do 100%, sometimes we will decide to do 50%. We work out the statistics after the fact in many instances but, for the most part, it is based on the 105D standard.

Suwala (B&W):
One of the observations I have made at a NRC auditor inspection is that the auditors have so many modules and paperwork to fill out that he can easily spend most of his time filling out paperwork instead of being on the floor observing what is going on. What is your comment on this?

Martin:
First of all, which B&W (Apollo). The people who are in the office are the auditors. They are meant to be in the office filling out paperwork. We get out on the floor; in fact, the picture you saw here was actually taken at Apollo. I think we have probably been out in the plant at Apollo more than any other facility. That plant has been walked through, looked at, and crawled over, including the piping. It appears that the only people you see are the auditors or that you have not been out in the plant while we are inspecting.

Green (BNL):
In anticipation of IAEA inspection of some U.S. facilities, and also understanding the necessity for independent verification on the part of the IAEA, you mentioned two activities: one is verification of the inventory and the other is the incorporation of working field standards. Would you care to comment on the compatibility of the NRC procedures with the IAEA inspection - perhaps they can take advantage of the kind of work you are doing.

Martin:
We have had the IAEA inspectors accompany us on our inspections. I'm not sure if they are trying to determine the quality of our inspections or whether they are trying to learn. They are coming with us again in January, and this will be about the third or fourth time they have accompanied the Region I inspection personnel. So far as I can tell, what we are doing would be compatible with what the IAEA would expect to do. My current understanding is that they would not duplicate our effort when they inspect a U.S. facility, but they would go with our inspectors and, again, determine what the quality of our inspections were and make statements with regard to that. I do not think that they, at least at the present time, intended to duplicate our effort. Did I answer your question?

Green:
Partially.

Martin:
My understanding is that they will make use of the same program. Theirs may require a little less work than ours, but they would make use of the same techniques.

Schleicher (EURATOM):
I think you are a little optimistic. (Laughter.) There should be an understanding with the Agency on sampling plans, which is perhaps not as difficult, but major questions will probably be standards. The standards must be accepted by the Agency if you don't want them to double your work. This sometimes can be troublesome because the Agency wants to be fully involved in the preparation of the standards in order to be assured that they are correct.

Martin:
This was one of the reasons why I spent two weeks in Vienna in 1977 and one week there in 1978. I was working on the problem of NDA standards. It is my understanding that they will be able to calibrate, or check the calibration of, our equipment by bringing some of their standards or having some here. We could then work back to accepting our working standards.

Bingham (NBL):
I'd like to make a comment, if I may, on the subject of standards and the compatibility of various systems nationally vs. internationally. We are rapidly approaching a point where, if we don't have a better degree of international cooperation in ease of transport and interchange of materials between national measurement systems, we are going to end up with a set of standards in this country and a set of standards in that country and no way of verifying the compatibility of these various measurement systems. For international safeguards, which relies on the compatibility of measurements internationally, I think we are getting to a place where the technical people are going to have to stand up and say we must do some things, and we have got to do away with some of the bureaucratic impediments that are preventing us from assuring that the EURATOM, the U.S., Japan, etc., are all self-consistent in their measurement systems.

Martin:
I think the main problem is one of transporting the standards. The various laws in the countries create a problem. I know that the IAEA, for instance, has trouble getting even their equipment from one country to another.

Instrumentation Development for the Enhanced Utilization of Calorimetry for Nuclear Material Assay

by

Curtis L. Fellers, Walter W. Rodenburg, John H. Birden
M. Fred Duff, and Jerry R. Wetzel
Monsanto Research Corporation, Mound Facility*, Miamisburg, Ohio

ABSTRACT

Calorimetric assay is an accurate and reliable technique for safeguards measurements. It is used extensively in DOE laboratories for SNM accountability and quality assurance measurements. To enhance the usefulness of calorimetric assay, an instrumentation and operating method development program is conducted at Mound. Recent development efforts have been directed at reducing analysis time, providing transportable instrumentation and relating calorimetric assay to chemistry.

KEYWORDS: Plutonium assay; calorimetry; calorimetric assay; plutonium safeguards

INTRODUCTION

Due to the accuracy, reliability, and simplicity of operation, calorimetry is used extensively in DOE facilities for special nuclear material (SNM) accountability and quality assurance measurements. In addition, calorimeters are used to verify previous SNM measurements [1], identify measurement biases, and calibrate other NDA measurements [2].

At the present time ten DOE facilities regularly use calorimetry for SNM accountability and quality assurance measurements. Three of these laboratories, Los Alamos Scientific Laboratory, Rockwell-Hanford Operation, and the Savannah River Plant, are expanding their usage by ordering new multi-calorimeter systems including 15 new calorimeters. As calorimeter usage is expanded, new applications of the technique are recognized, operating requirements are changed, and additional needs are identified.

In order to satisfy these current and future measurement needs, a continuing development effort is being conducted at Mound aimed at enhancing the usefulness of calorimetry. Instrumentation and operating methods are being developed and tested to provide solutions to specific measurement problems and to satisfy new and changing measurement requirements. Current development programs include a mathematical technique for predicting calorimeter equilibrium aimed at reducing analysis time, a transportable calorimeter which will allow SNM inspectors to perform in-field measurements, and an analytical calorimeter which will relate calorimetric assay to the chemical laboratory.

Prediction of Equilibrium

The equilibrium prediction technique has been developed to reduce calorimeter assay time and thereby increase sample throughput. This is a mathematical technique and does not require hardware modifications or additions to the calorimeter [3]. The technique makes use of the fact that the calorimeter equilibrium response function is dominated by a single time dependent exponential of the form $Y = A + Be^{-\lambda t}$ where t is the time, λ is the decay constant characteristic of the sample, and B is a scaling constant. By monitoring the

---

*Mound Facility is operated by Monsanto Research Corporation for the U.S. Department of Energy under Contract No. DE-AC04-76DP00053.

output of the calorimeter, Y, at equally spaced time intervals, the equilibrium value. A, can be predicted.

The mathematical prediction is accomplished by evaluating the calorimeter response curve in real time and subsequently estimating the final value based on this evaluation. Actually, the calorimeter itself never achieves equilibrium since the analysis is terminated when the final value is predicted. This particular mathematical algorithm is applicable only when the equilibrium process can be described by a single exponential equation, but is valid for either exponential growth or decay.

The equilibrium value, A, can be determined by solving the simultaneous equations generated from three data points separated by equal time intervals, ε.

$$Y_1 = A(1 + Be^{-\lambda t})$$

$$Y_1 = A(1 + Be^{-\lambda(t + \varepsilon)})$$

$$Y_3 = A(1 + Be^{-\lambda(t + 2\varepsilon)})$$

$$A = \frac{Y_2 - Y_1\left(\frac{Y_3 - Y_2}{Y_2 - Y_1}\right)}{1 - \left(\frac{Y_3 - Y_2}{Y_2 - Y_1}\right)}$$

Figure 1 shows a typical response curve from a calorimeter approaching equilibrium. With the addition of each data point, another equilibrium value can be predicted. These predicted data points are also plotted in Figure 1. When the calorimeter response data can be described by a single exponential, the predicted values lie on a straight line parallel to the time axis and are reliable estimates of the true equilibrium value. This fact is used to decide when the best value has been predicted and, therefore, when the analysis can be terminated. The slope and precision of the ten most recent predicted values are monitored and compared to pre-set values. When these parameters meet the predetermined criteria, the average of those ten predicted values is accepted as the best equilibrium value and the data collection is stopped. The same calorimeter response data is used to evaluate the random uncertainty in the predicted equilibrium value.

The equilibrium prediction technique has been tested on a variety of calorimeters and power levels at Mound. Twenty-five independent tests have been conducted using five different calorimeters and sample powers ranging from 0.1 to 8.0 watts. For these tests, the calorimeters were allowed to equilibrate so that comparisons of predicted and observed values could be made. A time savings of 55% was realized with the technique and the standard deviation of the unbiased difference between the predicted and observed equilibrium values was 436 microwatts.

An independent test and evaluation of this technique was conducted at Rockwell Hanford under the direction of Dr. Richard A. Hamilton [4]. One calorimeter was used to make 36 independent tests on samples between 0.06 and 5.3 watts. A comparison of the predicted and observed equilibrium values yields a standard deviation of the difference of 639 microwatts with no significant bias. The average time savings for these tests was 43%.

The equilibrium prediction technique has been demonstrated to be a reliable method for reducing calorimeter assay time without sacrificing accuracy. This technique is available for use on existing calorimeters as well as new instrumentation and is currently being incorporated into a bulk sample assay calorimeter which will be used by IAEA inspectors.

Transportable Calorimeter

For calorimetry to be a viable technique for field inspectors use, instrumentation must meet the special needs of the inspector. For example, the system must be light weight, rugged, and easy to set up and operate. At the same time, the design should not jeopardize the accuracy and reliability which make calorimetry such an important tool.

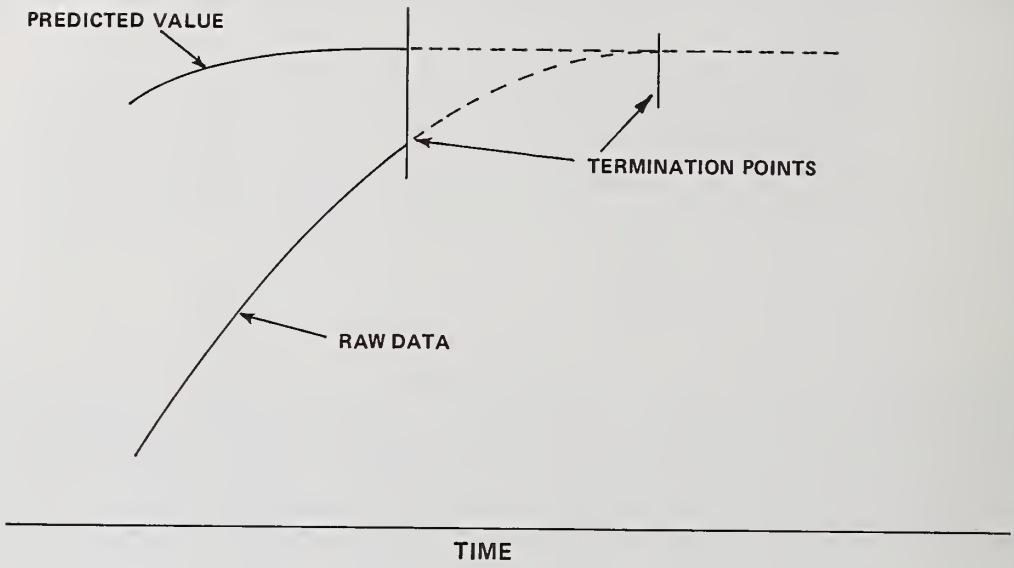

FIGURE 1

PREDICTION OF EQUILIBRIUM SIGNIFICANTLY
REDUCES ANALYSIS TIME

To accomplish these goals, the conventional environmental water bath (200-400 liters) in which the calorimeter is immersed was replaced by a heat exchanger surrounding the calorimeter jacket (Figure 2). Water from a small (15 liters) recirculating bath is pumped through the heat exchanger to provide the constant temperature environment required by the calorimeter. For compactness, the standard twin bridge calorimeter was oriented so that the sample and reference units were end to end.

Feasibility tests were first conducted on a prototype instrument [5] which measured samples 5 cm diameter X 15 cm high samples. Water was circulated around the calorimeter from an external temperature control led reservoir. The reservoir was a commercially available eight-liter tank with heating and cooling capabilities. Test results indicated that the calorimeter precision was not affected by the use of the heat exchanger and external reservoir.

The calorimeter shown in Figure 3 was designed and constructed specifically for the use of DOE/ALO auditors. The instrument will be used to verify stated SNM values in ALO contractor facilities. This will provide rapid feedback of results and minimize the need to ship SNM to other sites for independent verification.

The instrument shown in Figure 3 is capable of measuring samples 13 cm in diameter and 28 cm high. The calorimeter and heat exchanger form a cylindrical unit 28 cm in diameter by 84 cm high. The total system including calorimeter, external constant temperature bath, and computer based data acquisition system is mounted on a single cart for ease of movement.

In addition to meeting the inspectors need for portable instrumentation, the calorimeter requires minimal operating space. The reduced water requirements of the environmental chamber permits usage where large quantities of water may provide a criticality hazard.

The second transportable calorimeter is now under test at Mound. It will be field tested by ALO auditors in February and June of 1980.

Analytical Calorimeter

The conversion factor relating watts to grams Pu, known as the effective specific power (P_{eff}), can be determined by two methods. The computational method, which is most often used, involves determining the relative abundance of the americium-241 and plutonium isotopes and computing P_{eff}. The second method, known as the empirical method, involves calorimetry and destructive assay of a small quantity of Pu. The empirical method is directly traceable to the national measurement system through chemical assay calibrated against NBS certified elemental Pu standards. However, this method has received little attention due to the unavailability of suitable instrumentation.

The analytical calorimeter shown in Figure 4 measures small samples (1-5 grams of Pu) which are similar to the sample size required for chemical analysis. In addition, the primary sample container is a standard two dram glass vial of the type used in many analytical laboratories.

The calorimeter includes an automated sample loader which allows for analysis of up to 16 samples without operator intervention. The samples pass through a temperature controlled zone before entering the calorimeter. Thus, while one sample is coming to equilibrium, a second sample is being temperature equilibrated to reduce assay time.

The calorimeter is designed to fit inside a standard three foot glovebox. Water is pumped from an external circulating bath to provide the temperature controlled environment for the calorimeter. If desired, the calorimeter can be used in an open hood or on the bench top.

Test results on ten-milliwatt samples indicate a precision of $\pm$0.05% with biases <0.05%. Assay time is approximately 30 minutes per sample.

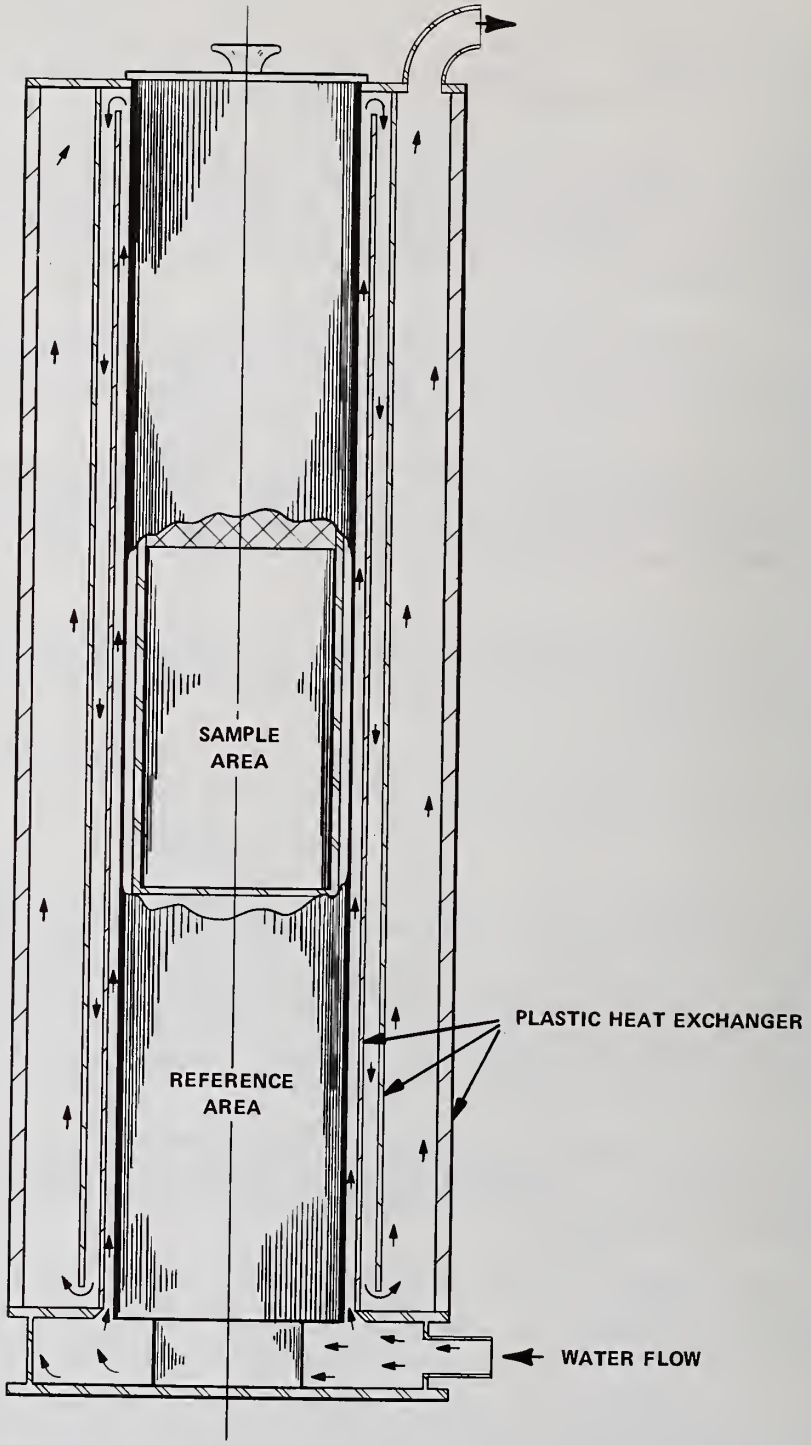

FIGURE 2. CROSS SECTION OF TRANSPORTABLE CALORIMETER DESIGN

FIGURE 3. TECHNICIAN LOADING TRANSPORTABLE CALORIMETER

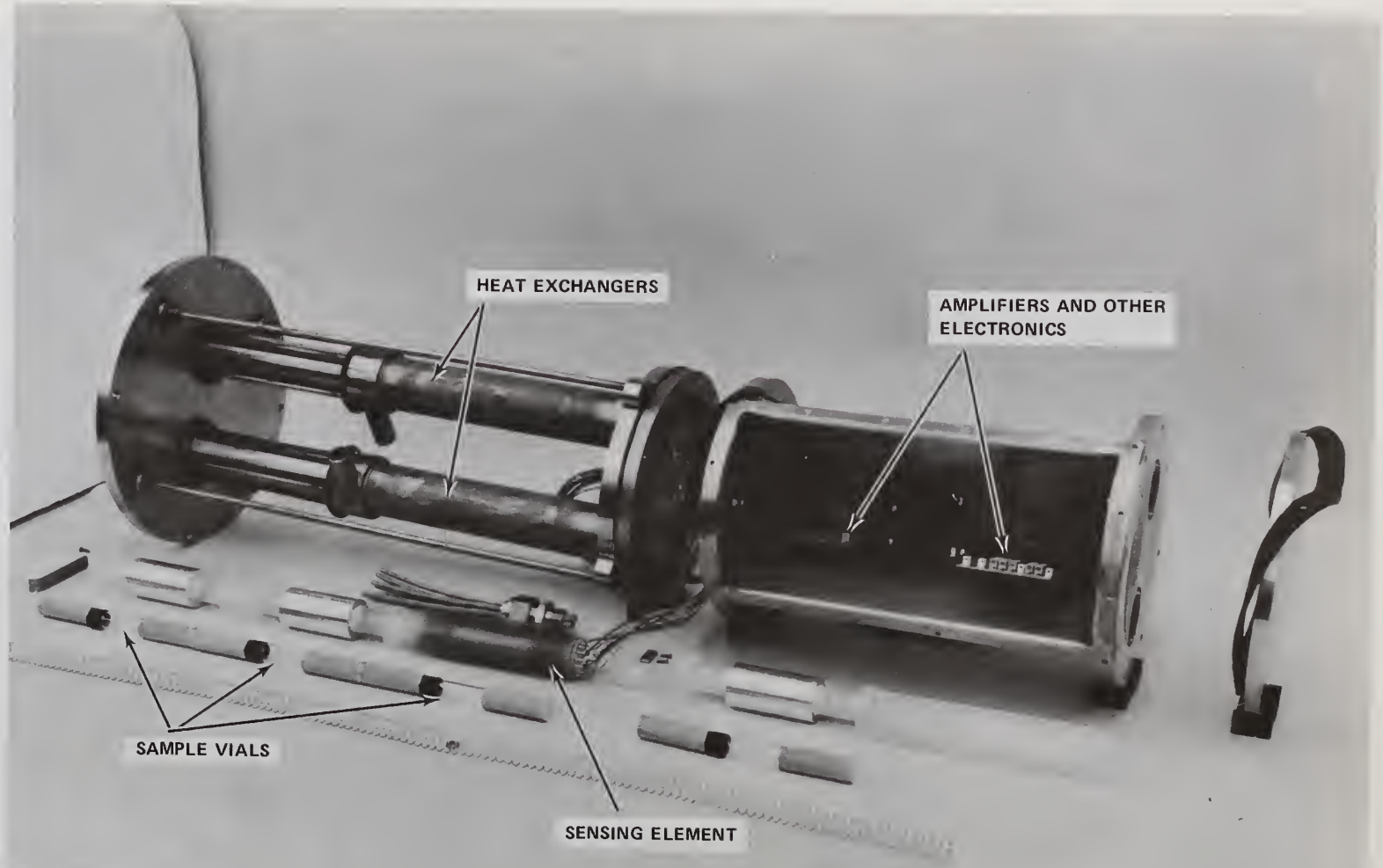

FIGURE 4. THE ANALYTICAL CALORIMETER IS DESIGNED AROUND A STANDARD TWO DRAM GLASS VIAL. (DISASSEMBLED VIEW)

In addition to the Peff determination, the calorimeter can be used to test for sample homogeneity. Since the wattage of a sample is directly proportional to the grams of Pu, the watts/g of sample is a direct indication of the g of pu/g of sample. By combining the calorimetry measurement and sample weight the analytical chemist can nondestructively test for sampling errors which are frequently the largest errors encountered. Furthermore, the analytical calorimeter can be used to nondestructively verify historical sample contents based on stated isotopic data or on gamma-ray isotopic analysis [6].

SUMMARY

Calorimetric assay provides an accurate, reliable, and timely technique for SNM accountability and quality assurance measurements. As its use expands, new applications and measurement requirements are being identified. As a result a continued development effort is being conducted to provide calorimetry instrumentation and operating methods responsive to the needs of the users. Current development programs are providing solutions to identified measurement requirements.

A mathematical technique has been developed to predict equilibrium values and significantly reduce calorimeter analysis time. Tests conducted at Mound and at an independent laboratory indicate that time savings approaching a factor of two can be realized using this technique.

The need for portable instrumentation is being met by the development of a transportable calorimeter. By minimizing the controlled environment surrounding the calorimeter, the instrument size and weight are reduced. This instrument can be easily moved between sites and requires little operating space.

Calorimeter measurements on isotopically homogeneous bulk samples can be linked to the chemistry laboratory only by destructively analyzing a known fraction of the total sample. An analytical calorimeter has been developed for in-line operation which is capable of accurately measuring one to five gram aliquots of plutonium. This instrument will provide the relationship between nondestructive calorimetric assay and chemical analysis.

REFERENCES

1. R. S. George and R. B. Crouch, "Inspector Measurement Verification Activities," Nucl. Mater. Manage., Vol. IV, III 327-336 (1975).

2. W. W. Strohm, W. W. Rodenburg, J. F. Lemming, D. R. Rogers, and C. L. Fellers, "The calibration of Plutonium NDA by Calorimetric Assay," presented at the IAEA International Symposium on Nuclear Material Safeguards, Vienna, Austria, October 2-6, 1978.

3. C. L. Fellers and P. W. Seabaugh, "Real-Time Prediction of Calorimeter Equilibrium" Nucl. Inst. and Methods, 163 499-505 (1979).

4. R. A. Hamilton, "Evaluation of the Mound Facility Calorimeter Equilibrium Prediction Program" RHO-SA-114, Rockwell Hanford, in publication.

5. M. F. Duff and C. L. Fellers, "Feasibility of a Mound Designed Transportable Calorimeter," MLM-2603, Mound Facility (April 16, 1979).

6. J. G. Fleissner, J. F. Lemming, and J. Y. Jarvis, "A Study of a Two-Detector Method for Measuring Pu Isotopics," paper presented at ANS topical conference, Kiawah Island, S.C., November 26-30, 1979.

Discussion:

Roche (ANL):

Curt, could you give a little more data on the portable instrument you're developing, such as the sample size, the assay time, and expected precision?

Fellers (Monsanto-Mound):

The prototype calorimeter that I showed in the picture measures samples that are 13 centimeters in diameter and 28 centimeters tall. The test that we are running now indicates that we will be able to get the assay time down to about four hours on this particular instrument, and I believe that will be accomplished by using the prediction technique that I spoke of. The test that we are running, using the Pu-238 standards, for the accuracy test indicates that in the 1-watt range, the accuracy is 0.1 to 0.3%. We believe that this is due primarily to the poor temperature control that we are getting on our commercially available water baths. We are purchasing a new instrument that will provide (manufacturer says) improvements in temperature control by an order of magnitude. We believe this will bring the performance of the calorimeter back in line with the conventional instruments.

EXPERIMENTAL COMPARISON OF THE ACTIVE WELL COINCIDENCE COUNTER WITH THE RANDOM DRIVER

by

Howard O. Menlove, Norbert Ensslin, and Thomas E. Sampson
Los Alamos, New Mexico 87545

ABSTRACT

A direct comparison has been made between the IAEA Active Well Coincidence Counter (AWCC) and the LASL Random Driver at CMB-8. The comparison included an experimental evaluation of precision, counting rate, accuracy, penetrability, stability, and the effect of sample inhomogeneity.

Samples used in the evaluation included highly enriched U_3O_8, U_3O_8 mixed with graphite, highly enriched uranium metal discs, and depleted uranium metal. These materials are typical of the samples of interest to the IAEA inspectors.

We concluded from these investigations that the two instruments had very similar performance characteristics with the Random Driver giving better penetrability and the AWCC giving better stability.

KEYWORDS: Nondestructive assay, uranium, random driver, neutron, coincidence counter, stability, precision, calibration

INTRODUCTION

In recent years, random driver (RD) type instruments have been widely used for the nondestructive assay (NDA) of ^{235}U. There have been several versions of random drivers;[1] some designed and built by LASL and some by commercial instrumentation vendors. The paper by Paul Goris in Session IV of this symposium described the application of a commercial random driver to the NDA of ^{233}U. The different RD units have generally improved over the years with better detectors, electronics, and data analysis techniques. However, this type of system is not readily adaptable to portable applications for field inspections because of its weight and complexity.

The Active Well Coincidence Counter[2] uses a combination of a small AmLi neutron interrogation source and a ^3He thermal-neutron well coincidence counter. This Active counter can be used for uranium samples, including high gamma-ray background materials such as ^{233}U-Th fuels. The present AWCC was developed to be more lightweight and portable than the conventional fast random driver assay system.

The purpose of the present paper is to make a direct experimental comparison of the RD and the AWCC. The performance parameters of interest in the comparison are:

1. counting rates,
2. precision,
3. stability,
4. response linearity, penetrability,
5. geometric effects,
6. sample inhomogeneities and matrix effects.

Samples that were available for the comparison included highly enriched U_3O_8 in recovery cans, U_3O_8 mixed with graphite, and uranium metal discs (93.15% ^{235}U) similar in size to the "buttons" and ingots used for fuel fabrication. The mass of the samples ranged from 250 to 4000 g U.

RANDOM DRIVER DESCRIPTION

The Random Driver is typically used to determine the enriched uranium content of oxide, metal, or residue samples.[3] Typical container sizes are 5 to 10 liters capacity. AmLi random neutron sources are used to induce fisson reactions in the ^{235}U present in the material. Relatively few fissions occur in the ^{238}U because the neutron energy spectrum of the AmLi sources (0.3 MeV average) is below the fission threshold for ^{238}U. Also, the spontaneous fission rate of ^{238}U is very low. The fissions induced in ^{235}U are observed by coincidence counting the time-correlated fission neutrons with two 5 x 25 x 50 cm Pilot F fast plastic scintillators, located on opposite sides of the assay chamber as shown in Fig. 1. By requiring the detection of neutrons in both scintillators within 45 nanoseconds, it is possible to distinguish fission events from randomly produced AmLi source neutrons. The coincidence counting rate is proportional to the quantity of ^{235}U in the material being assayed, and thus provides a measure of the uranium content.

A number of features are incorporated in the design of the RD to reduce potential sources of assay bias. The interrogating neutrons are not thermalized, and the assay chamber is lined with boral to absorb low-energy neutrons, thus ensuring good neutron penetrability through the sample. The detectors are also shielded with 5 cm of lead, because the fast plastic scintillators are sensitive to energetic gamma rays as well as neutrons. This lead eliminates the gamma rays from the AmLi source and some of the induced fission gamma-rays from ^{235}U. The attenuation of gammas in most large samples is greater than the attenuation of neutrons. To make assays less dependent on sample density and composition, the RD discriminates against gamma rays by the use of lead and by time-of-flight. Gamma ray signals are detected in the scintillators in the first 2-3 ns, whereas neutron flight times are typically 20-40 ns. A time window of 5-45 ns is used to accept most (n,n) coincidences and reject most (γ,γ) coincidences. For typical energy thresholds of 650 keV for neutrons and 220 keV for gammas, the RD response consists of 78% (n,n) coincidences and 22% (n,γ) coincidences.[4]

Two techniques are used to reduce the effects of loading differences between samples. The sample is rotated during assay to minimize the effect of asymmetric loading of material within the container, and the AmLi sources are positioned to produce a nearly uniform vertical response profile over the typical range of container fill heights (2-20 cm). There is a 3-5% variation in RD response as a function of height, as determined by moving a small sample along the central axis of the sample chamber. For large samples the total integrated response is constant to 1% or less over the range of fill heights.

The effect of introducing moderating material into the assay chamber is to reduce the energy of the interrogating spectrum, which increases the rate of induced fission in ^{235}U. Light element moderating material can appear either as matrix or in polyethylene containers and bags. Because the type of container (i.e., metal or polyethylene) used for most material being assayed is dictated by the process stage in which the material occurs, assay data should normally be corrected for perturbations caused by moderating material in the sample chamber. This correction is based on the response of two ^{3}He proportional counters, located adjacent to the sample assay position, which monitor the interrogating neutron flux.

Elimination of some sources of assay bias by the instrument design features and corrections described above has reduced the number of physical standards required for calibration of the RD. However, experience with a wide variety of sample types has shown that widely different materials require different calibration curves to obtain good accuracy. The RD described in this report has separate calibration curves for pure uranium oxide, oxide mixed with graphite, uranium in hydrofluoric slag, and reduction metal residues.

ACTIVE WELL COINCIDENCE COUNTER

The basic principle of the AWCC is the same as the RD. That is, fast-neutron interrogation using a random neutron source (e.g., AmLi) and counting the induced fission reactions using coincidence techniques to suppress the signal from the random interrogation source. The primary difference is that the AWCC uses ^{3}He detectors which are sensitive to neutrons after they have slowed. This necessitates the use of relatively long (32-64 μs) coincidence time gates resulting in a large fraction of accidental coincidence events

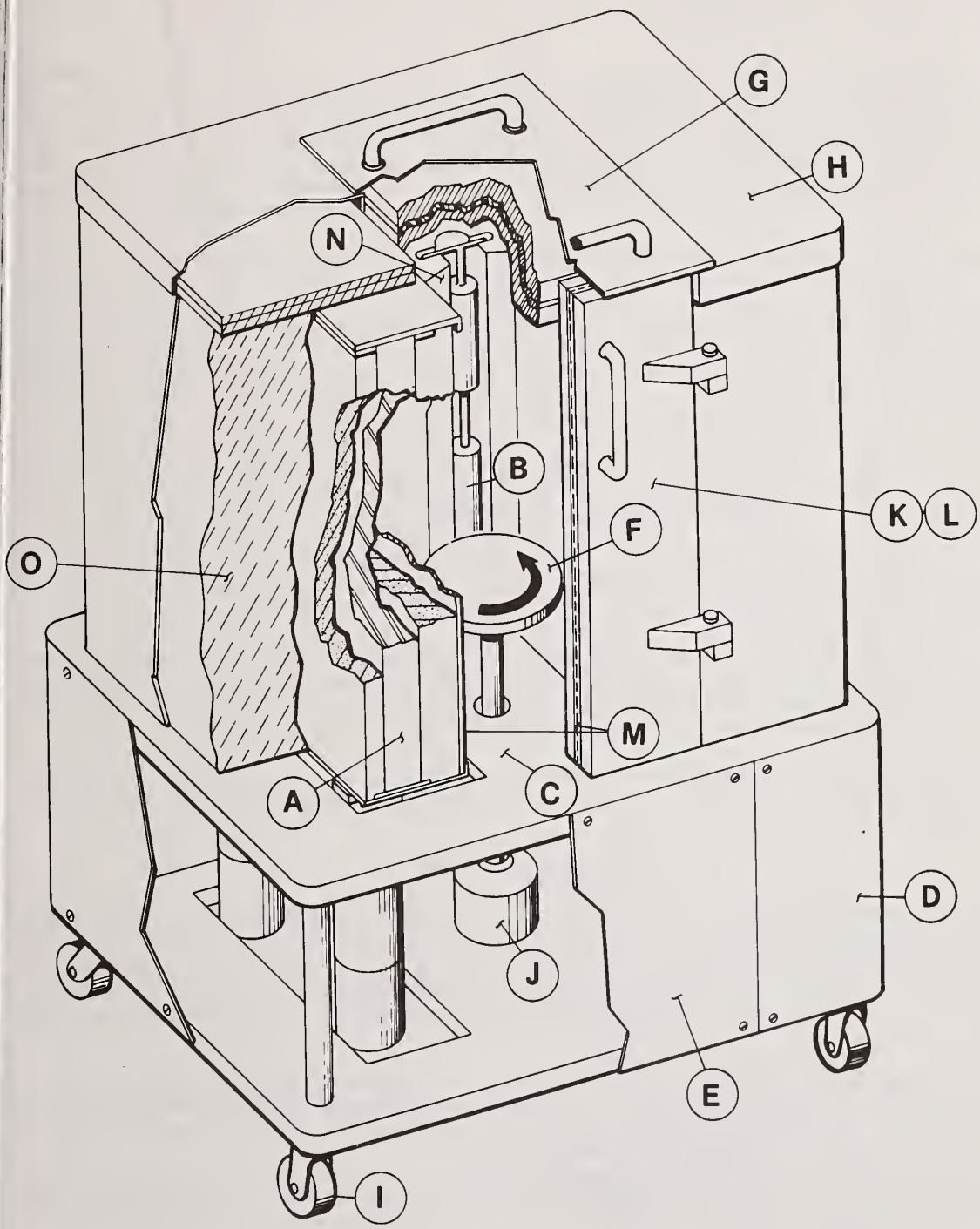

Figure 1
Random Driver (RD) counting chamber - legend: A. scintillator assembly, B. source, C. base, D. base skirting, E. front maintenance panel, F. sample platen, G. lid, H. top cover, I. casters, J. weighing mechanism, K. door, L. steel shielding, M. boral shielding, N. source tailoring container.

for high counting rates. To help alleviate this problem, we have positioned the AmLi source inside CH_2 shielding (the end plugs) as shown in Fig. 2 to reduce the accidental pileup rate. With this technique, the induced signal-to-interrogation neutron background ratio is improved by a factor of ten.

The AWCC has been designed to take advantage of the portable electronics package[5] that was developed for the HLNCC. To keep this initial model as simple as possible and to take direct advantage of the previously developed electronics package, no neutron flux monitor has been incorporated into the present AWCC. Flux monitors are often used with active neutron assay units to make corrections for neutron self-shielding or for neutron moderation in hydrogeneous matrix materials. Operational experience with the present model will be used to evaluate the need for a flux monitor in more advanced models.

Normally the sample cavity wall of the AWCC is lined with a 2.54-cm-thick nickel reflector to give a more penetrating neutron interrogation. However, the sample cans for the U_3O_8 plus graphite were so large (20-cm diam) that it was necessary to remove the nickel liner and the top and bottom CH_2 discs (7.6-cm-thick) to accomodate the cans. The removal of the nickel results in some loss of penetrability. The counter was returned to the configuration shown in Fig. 2 for the measurements on the HEU metal discs. There is a sleeve of Cd in the detector sample well to remove thermal neutrons from the interrogation flux and to improve the shielding between the ^3He detectors and the AmLi source.

To obtain a more uniform spatial interrogation, two neutron sources of similar yield are used. One is in the lid and one is in the bottom plug as shown in Fig. 2. The use of two sources results in a rather uniform vertical response.

The unit uses 42-^3He gas (4 atm pressure) tubes that are 2.54 cm diameter and 50.8 cm long (active length). This detector configuration gives an absolute efficiency of approximately 30% for counting fission spectrum neutrons.

The electronics unit is directly interfaced to the HP-97 programmable calculator shown in Fig. 3. A microprocessor in the unit reads out the run time, total counts, reals plus accidental counts, and accidental counts to the HP-97. The HP-97 is then used to reduce the data using the software package selected by the operator.

Table I gives the specifications for both the RD and the AWCC showing the major physical differences in the two systems. The weight and size of the AWCC is considerably less than for the RD.

EXPERIMENTAL PROCEDURES

For the comparison, the AWCC was taken to the uranium recovery plant at LASL, where the CMB-8 Random Driver shown in Fig. 4 is in routine use. Thus, both systems were operating side-by-side to obtain the same environmental factors. The samples were alternatively counted in the RD and the AWCC for the same time intervals - typically 1000 s. Repeat runs were performed on the lower mass samples to improve the counting statistics.

The samples selected for the measurement were those normally used for the calibration of the RD (U_3O_8) plus the HEU metal discs that were prepared for IAEA detector calibration. Also, depleted uranium metal discs of the same size as the HEU discs were mixed with HEU discs to create inhomogeneities in the sample.

To check the stability of the systems, cyclic runs were performed over two nights and over a three day weekend. High mass samples were used for these runs to give good counting statistics to better check the precision.

The primary evaluation considered the RD coincidence response directly without making corrections for the flux monitor or temperature sensor. This was to permit a direct comparison with the AWCC coincidence response which has no correction sensors in the present model. The data shown in the graphs and tables corresponds to the uncorrected response from both systems. The magnitude of the correction factors for the RD were observed to be small and rather uniform over each of the sample categories.

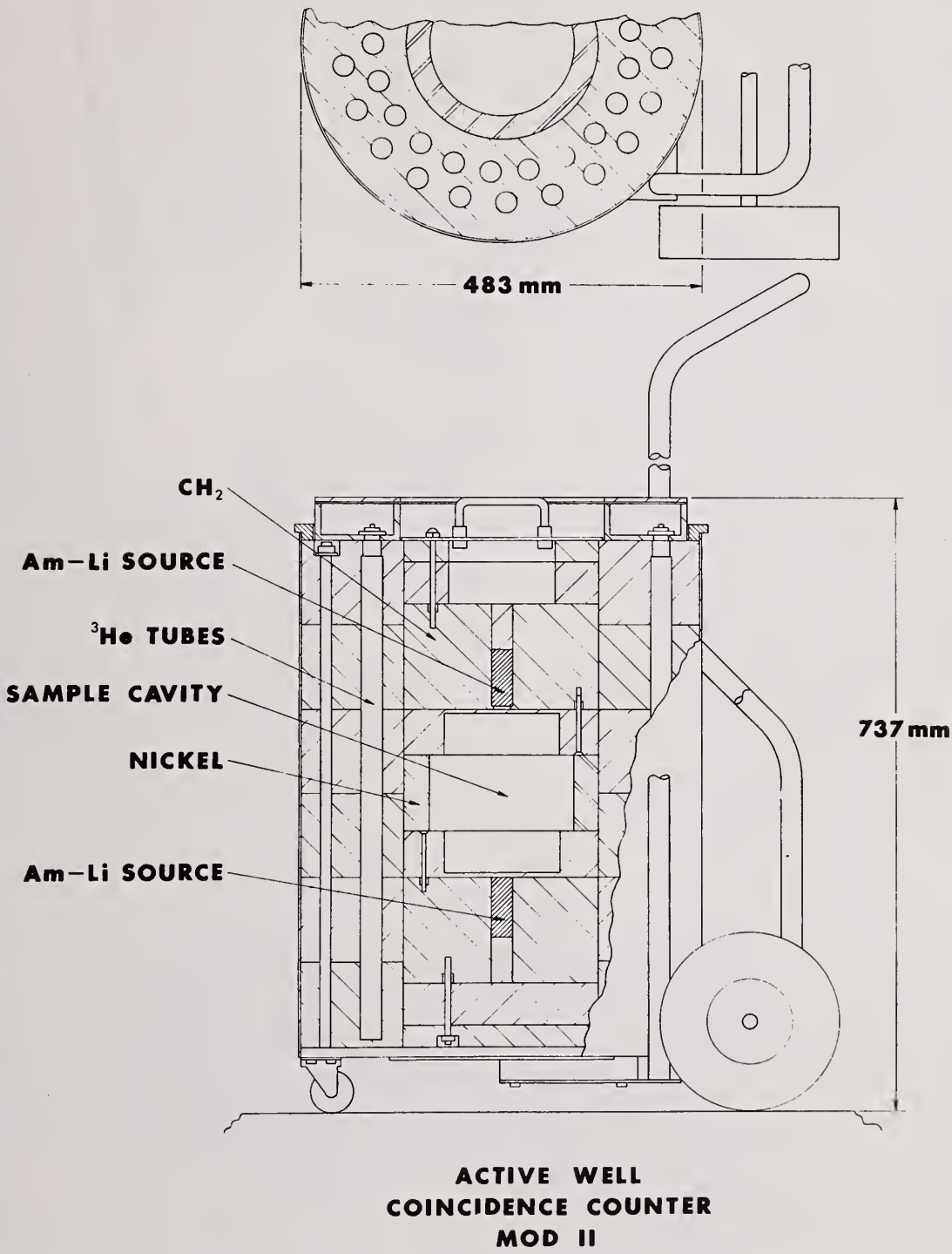

Figure 2
Schematic diagram of Active Well Coincidence Counter (AWCC) in its normal configuration for counting small samples.

Figure 3
Photograph of AWCC system complete with detector body and cart, electronics package and HP-97 calculator for automated data readout and analysis.

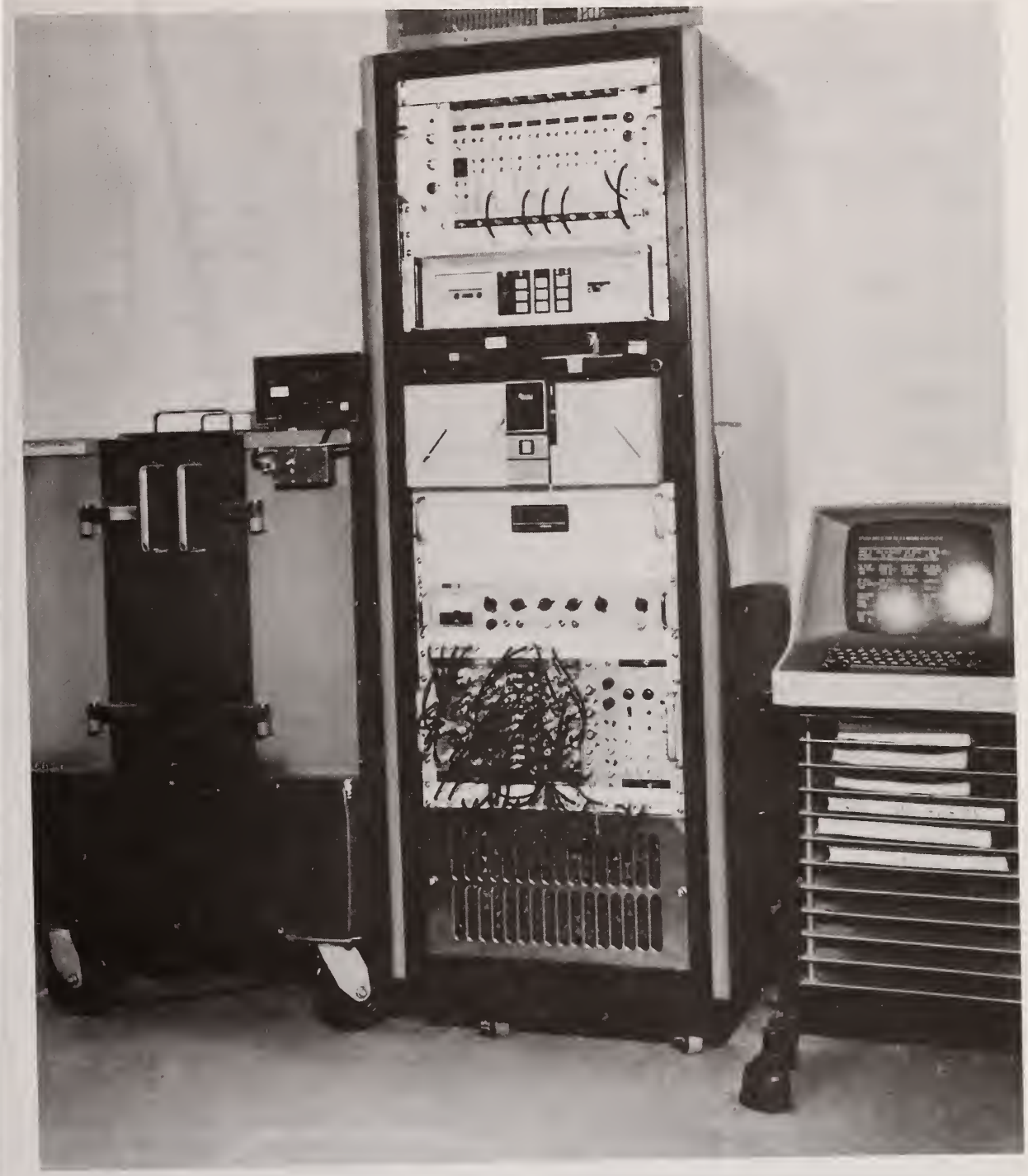

Figure 4
Photograph of RD system at CMB-8 including detector body, minicomputer, electronics rack and TSI terminal.

TABLE I

RD AND AWCC SYSTEM SPECIFICATIONS

	RD	AWCC
Number of AmLi sources	2	2
Total source strength	10^6 n/s	10^5 n/s
Interrogation energy	Fast neutron	Fast neutron
Detector type	Plastic scintillators	^{3}He tubes
Counting	Fast neutrons and gamma rays	Thermalized neutrons
Response signal	Fast coincidence	Slow coincidence (auto-correlation)
Coincidence gate	∿ 45 ns	∿ 64 μs
Body weight	1150 kg	125 kg
Electronics	2 NIM BINS plus minicomputer	HLNCC package plus HP-97

RESULTS

U_3O_8-Large Containers

The RD located at the LASL uranium recovery facility is normally used to measure the ^{235}U content of U_3O_8 in stainless steel cans that are ∿ 20-cm-diam x 25 cm tall. This material is in two sample categories - each having its own set of standards. The first is pure U_3O_8 ranging in mass from 250 to 4000 g uranium (∿93% enriched in ^{235}U). The standards of this type material that were used for the comparison are listed in Table II. The uranium is very concentrated and fills only the bottom few centimeters of the can resulting in a "pancake" shaped sample. The U_3O_8 had a density of approximately 2.38 g/cm^3 resulting in a ^{235}U density of 1.96 g/cm^3. This density was basically the same for all of the U_3O_8 standards with only the fill height changing as the sample mass increased.

The set of U_3O_8 standards mixed with graphite are listed in the bottom section of Table II. In this case the graphite fills most of the volume resulting in a low ^{235}U density. The mass of the uranium ranged from 234 to 4000 g. The ^{235}U densities were 3 to 30 times lower than for the pure U_3O_8 material. Also, the densities and fill heights had large variations as given in Table II. The large quantities of graphite in these containers had a significant effect on the observed signal for both assay systems.

Random Driver Results

The net coincidence response of the RD as a function of uranium content is shown in Fig. 5. All of the data points lie on a smooth curve which has the functional form aU/1+bU for uranium values less than 2000 g. For the 4000 g sample, the multiplication gives a slight increase in the coincidence response.

The curve for the U_3O_8 plus graphite falls below the curve for pure U_3O_8 for the RD. This result is somewhat surprising because the graphite will increase the interrogation flux density and increase the number of slow neutrons which have a high fission cross section for ^{235}U. However for the RD, the graphite has the opposite effect on the

Figure 5
Random Driver response vs g U for highly enriched U_3O_8 powder and U_3O_8 mixed with a graphite matrix.

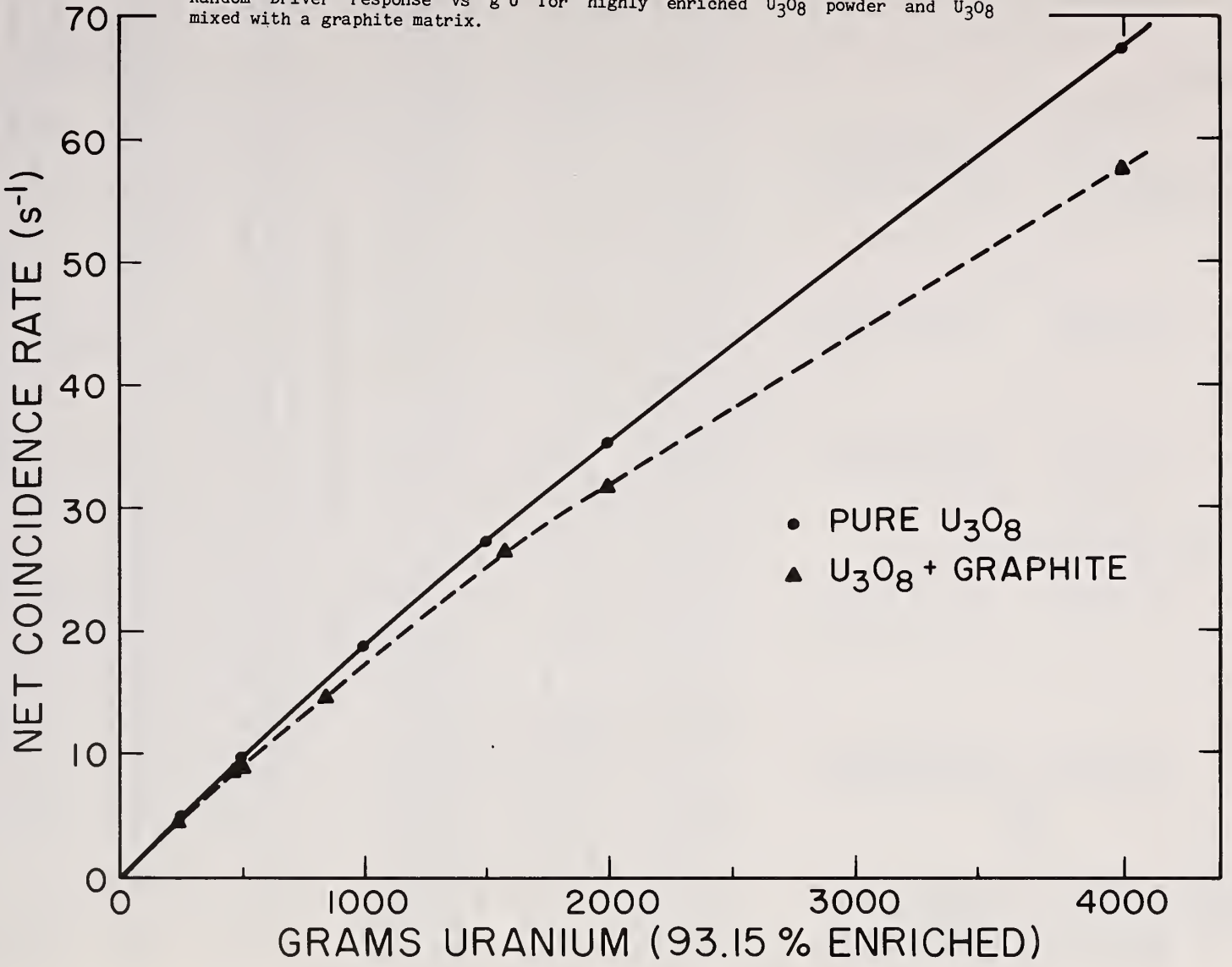

TABLE II

STANDARD SAMPLE CHARACTERISTICS

Sample ID	Net Wt. (g)	Fill Ht. (cm)	Diam (cm)	gU	Enrichment (%)	$\rho^{235}U$ (g/cm^3)
Pure U_3O_8						
TRN-250	296	0.46	18.2	250	93.14	1.94
TRN-500	591	0.91	18.2	500	93.14	1.96
TRN-1000	1183	1.82	18.2	1000	93.14	1.96
TRN-1500	1774	2.73	18.2	1500	93.14	1.96
TRN-2000	2366	3.64	18.2	2000	93.14	1.96
U_3O_8 Plus Graphite						
STD-234	4678	13.5	20.0	234	92.83	.0512
STD-468	4678	12.0	20.0	468	92.83	.115
STD-500	7005	19.3	20.0	500	92.88	.0765
STD-846	4230	10.0	20.0	846	92.83	.250
STD-100	7335	18.6	20.0	1000	92.88	.159
STD-1591	4679	12.5	20.0	1591	92.83	.376
STD-2000	7640	19.0	20.0	2000	92.88	.311
STD-4000	9691	18.0	20.3	4000	92.88	.657

counting channel. That is, the induced fission neutrons and gamma rays have a more difficult time being counted by the plastic scintillators. The cans contain 4-6 kg of graphite which both absorbs fission gamma rays in transit to the scintillators and slows down the fast neutrons so that they are below the counting energy-threshold. This graphite has the opposite effect on the response for the AWCC which will be discussed in the next section.

The net coincidence response for the U_3O_8 samples are listed in Table III. The error corresponds to the calculated standard deviation for a 1000 s run. For the low mass samples, several measurements were performed to obtain better precision than the value listed in the table.

The last column in Table III gives the coincidence rate per gram sample. This is an indication of the penetrability of the interrogation flux. A linear calibration curve would correspond to a constant value for the response per gram. The pure U_3O_8 curve is more linear than the graphite curve because the graphite moderates the interrogation neutrons resulting in more low-energy neutrons and thus more self-shielding in the ^{235}U.

Active Well Coincidence Counter Results

The results for the same set of standards measured with the AWCC are shown in Fig. 6. These curves are more nonlinear than the corresponding curves for the RD. This indicates a softer interrogation neutron spectrum for the AWCC. The reason for this is the large amount of hydrogen in the CH_2 end plugs and detector walls.

The curve for the U_3O_8 plus graphite is above the U_3O_8 curve. We expect this to be the case because the large quantity of graphite increases the low energy neutron flux. As opposed to the RD, the graphite has little or no effect on the efficiency of the AWCC for counting the induced fission neutrons.

The data point at 1591 g U falls significantly below the curve through the other data points. A likely reason for the low response is that this can contains less graphite than the other cans with similar amounts of uranium resulting in less neutron moderation. Also, the graphite acts as a diluting agent for the U_3O_8 and less graphite means a higher concentration of U_3O_8 and thus more self-shielding. The AWCC is more sensitive to this type problem than the RD. The large sample cans made it necessary to remove the nickel liner from the AWCC and this increased the self-shielding problems.

Figure 6
AWCC response vs g U for highly enriched U_3O_8 powder and U_3O_8 mixed with graphite.

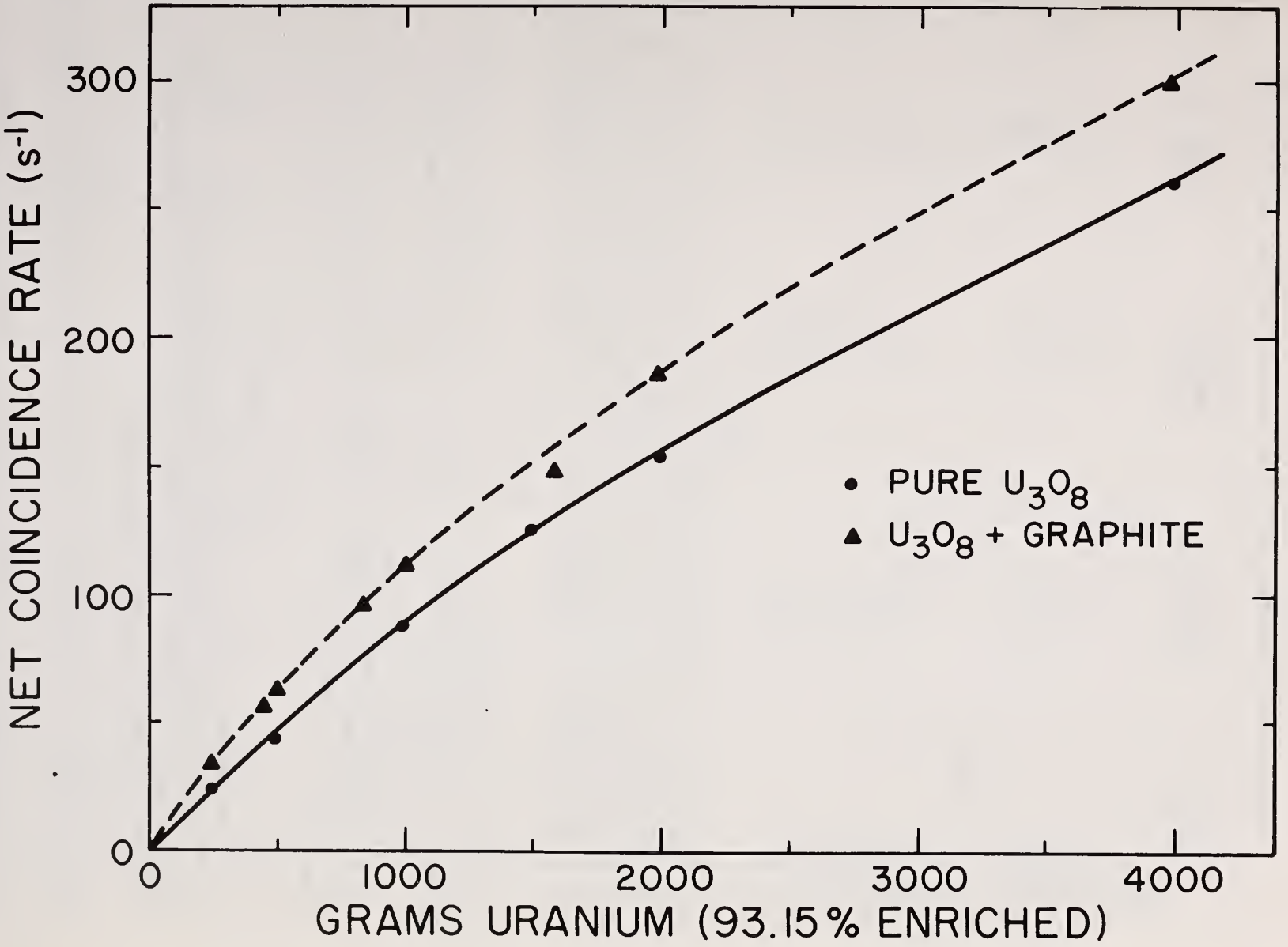

TABLE III

RANDOM DRIVER MEASUREMENT RESULTS FOR U_3O_8 AND U_3O_8 PLUS GRAPHITE STANDARDS

Sample I.D.-g U	Coincidence Rate (s^{-1})	Standard Deviation (1000 s)	Counts / s·gU x 1000
U_3O_8			
TRN-250	4.90	5.2%	19.6
TRN-500	9.75	2.0%	19.5
TRN-1000	18.7	1.5%	18.8
TRN-1500	27.3	1.1%	18.2
TRN-2000	35.3	0.88%	17.6
U_3O_8 plus Graphite			
STD-234	4.27	5.8%	18.3
STD-468	8.56	3.0%	18.3
STD-500	8.84	2.9%	17.7
STD-846	14.7	1.8%	17.4
STD-1000	16.8	1.6%	16.8
STD-1591	26.3	1.1%	16.5
STD-2000	31.5	0.98%	15.8
STD-4000	57.8	0.62%	14.5

The results of the AWCC measurements are listed in Table IV, and we see that the net coincidence rate for the AWCC is approximately 6 times higher than for the RD even though the AmLi source strength is a factor of ten smaller. The reason for this is the higher detector efficiency and the softer interrogation flux. It should be noted that the standard deviations for both the AWCC and RD are about the same in spite of this higher count rate. This is because of the high accidental coincidence rate in the AWCC contributing to the statistical error. The coincidence time gate in the AWCC is 64 μs compared with about 45 ns for the RD.

HEU Metal Discs

The high enrichment metal discs used in the present experiment are similar to metal buttons of interest in inventory inspections. The two diameters (6- and 7-cm) for the discs were used to check the effect of diameter variations in the measurements.

To obtain the mass range from approximately 500-4000 g U, the discs were stacked on top of each other to form a cylinder with heights varying from 1-cm to 7-cm. The uranium metal had a density of 18.7 g/cm^3 resulting in a ^{235}U density of 17.5 g/cm^3. To avoid oxidation and contamination by the uranium, the discs were coated with a thin nickel plate.

Random Driver Results

The samples were counted in the RD with no change in the detector configuration used for the large U_3O_8 cans. The results of the measurements are given in Table V. The response per g U of a single disc (17.2) is somewhat less than the response per g U for the U_3O_8 samples (19.5 for TRN-500). This reduction is likely caused by neutron or gamma self-shielding in the higher density metal.

As the sample mass increases from 1 disc to 7 discs, the response per gram increases from 17.2 to 20.7 or a 20% increase. This is caused by the multiplication of the induced fission neutrons.

Figure 7 gives a plot of the net coincidence rate as a function of uranium mass. The curve is fit through the data for the 6-cm-diam discs. The larger 7-cm discs had an average response per gram that was only 1.6% higher than the smaller diameter discs.

Figure 7
Random Driver response vs g U for HEU metal buttons.

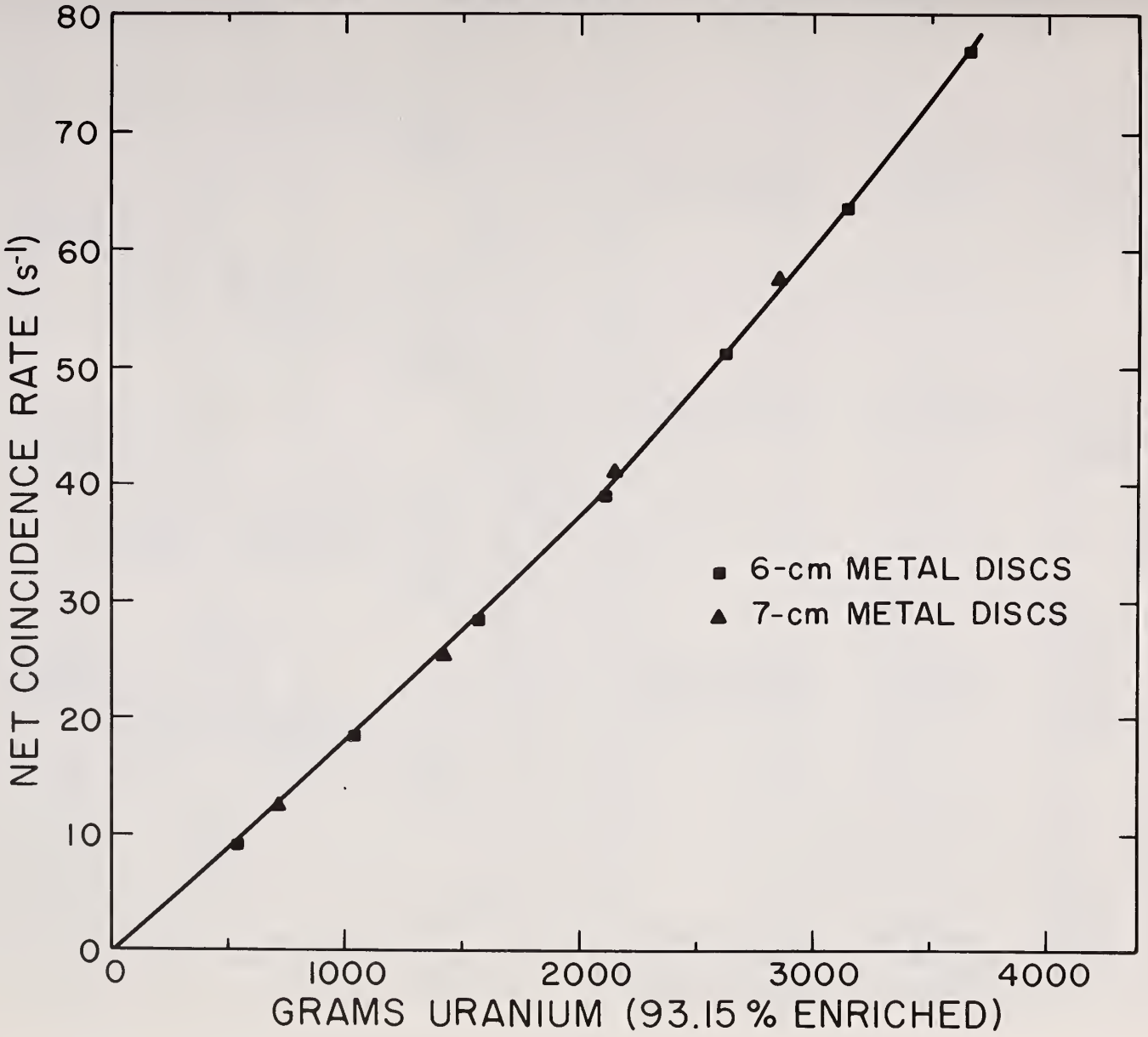

TABLE IV

AWCC MEASUREMENT RESULTS FOR U_3O_8 AND U_3O_8 PLUS GRAPHITE STANDARDS

Sample I.D.-g U	Coincidence Rate (s^{-1})	Standard Deviation (1000 s)	Counts / s·gU x 1000
U_3O_8			
TRN-250	24.2	6.4%	96.8
TRN-500	42.9	3.8%	85.9
TRN-1000	88.0	1.9%	88.0
TRN-1500	124.9	1.4%	83.3
TRN-2000	153.3	1.2%	76.6
U_3O_8 Plus Graphite			
STD-234	33.4	5.1%	142.6
STD-468	56.0	3.1%	119.7
STD-500	61.9	2.8%	123.8
STD-846	96.6	1.9%	114.2
STD-1000	109.6	1.6%	109.6
STD-1591	147.3	1.2%	92.6
STD-2000	185.5	1.0%	92.7
STD-4000	300.2	0.61%	75.0

TABLE V

HEU METAL BUTTONS MEASURED WITH THE RANDOM DRIVER

Sample Size diam x ht. (cm)	Sample Mass[a] (g U)	Coincidence Rate (s^{-1})	Standard Deviation (1000 s run)	Counts / s·g U x 1000
6 x 1	528	9.10	4.2%	17.2
6 x 2	1055	18.16	1.6%	17.2
6 x 3	1583	28.44	1.1%	18.0
6 x 4	2112	39.04	0.80%	18.5
6 x 5	2640	51.30	0.65%	19.4
6 x 6	3168	63.81	0.54%	20.1
6 x 7	3692	76.43	0.46%	20.7
7 x 1	718	12.36	2.16%	17.2
7 x 2	1434	25.36	1.15%	17.7
7 x 3	2152	40.94	0.78%	19.0
7 x 4	2870	57.69	0.60%	20.1

a) Uranium metal samples 93.14% enriched in ^{235}U.

b) Corresponds to relative error in net coincidence rate considering only counting statistics.

The upward curvature of the response from multiplication is evident. Techniques are under development to make automatic corrections in the data for multiplication.

Active Well Coincidence Counter Results

For the HEU disc measurements, the AWCC was returned to its normal configuration as shown in Fig. 2. This smaller sample cavity increases the irradiation efficiency and the nickel liner improves the penetrability of the neutron flux.

Table VI gives the results for the different sample masses. The coincidence response per gram for a disc (87.2) is very close to the response for the U_3O_8 samples (85.9 for TRN-500); however, this is only a "coincidence" because the detector and end plug configuration was different for the two cases.

The response per gram changes by only 8% in going from 1 disc to 7 discs. There is a cancellation of self-shielding and multiplication effects. For the lower mass region (<1500 g U) the self-shielding dominates resulting in a decline of the response per g U, but for the higher mass values (>2000 g U) the multiplication dominates resulting in an increase in the response per g U. The average difference in response per g U from the mean was only 2.7%.

A plot of the coincidence rate versus the response is shown in Fig. 8. The curve is fit through the data points for the 6-cm- diam discs. The 7-cm discs fall slightly above the curve. The average rate per gram for the 7-cm discs is 2.2% higher than for the 6-cm discs.

Inhomogeneities

A pair of 6-cm-diam x 1-cm-thick depleted uranium metal discs were used to check the sensitivity of the assay systems to inhomogenous samples. Two HEU metal discs were measured in the following configurations: a) two HEU discs with no depleted uranium (DU) discs, b) two HEU discs inside the DU discs, and c) two HEU discs outside the DU discs.

We observed that the DU disc inhomogeneities change the results by only approximately 2% for the AWCC, but the change is approximately 5% for the RD. The RD has the larger perturbation because gamma rays contribute to its signal and the DU absorbs some of the gamma rays before they reach the scintillators.

TABLE VI

HEU METAL BUTTONS MEASURED IN AWCC WITH Ni LINER IN WELL

Sample Size diam x ht. (cm)	Sample Mass[a] (g U)	Coincidence Rate (s^{-1})	Standard[b] Deviation (1000 s run)	Counts / s·g U x 1000
6 x 1	524	45.72	3.2%	87.2
6 x 2	1055	86.289	1.55	81.8
6 x 3	1583	127.55	1.2%	80.6
6 x 4	2111	170.30	0.85%	80.7
6 x 5	2636	218.73	0.74%	83.0
6 x 6	3164	268.33	0.64%	84.8
6 x 7	3692	318.33	0.55%	86.2
7 x 1	718	66.22	2.3%	92.2
7 x 2	1434	116.19	1.4%	81.0
7 x 3	2152	179.11	0.92%	83.2
7 x 4	2870	246.65	0.69%	85.9

a) Uranium metal samples 93.17% enriched in ^{235}U.

b) Corresponds to relative error in net coincidence rate considering only counting statistics.

Figure 8
AWCC response vs g U for HEU metal buttons.

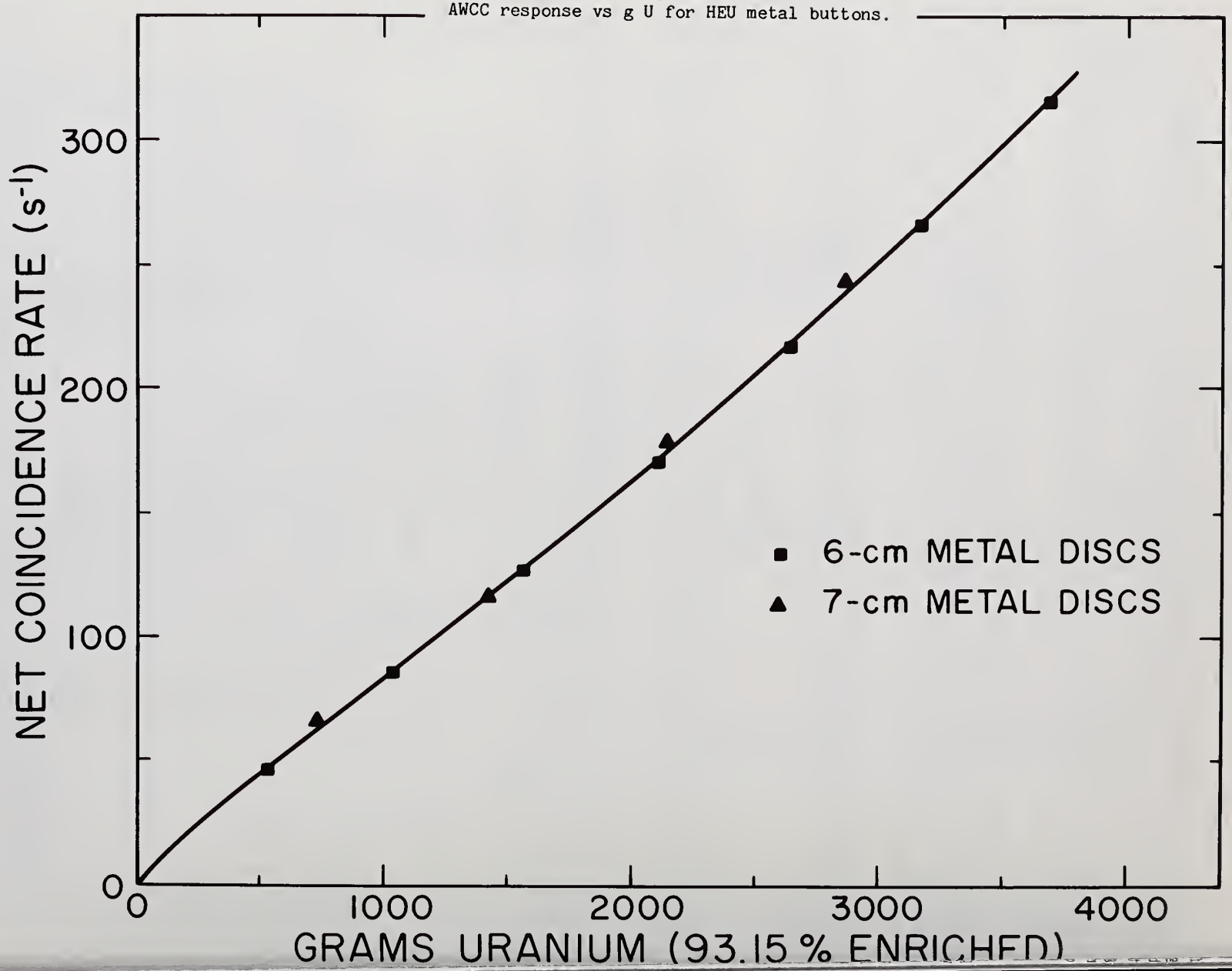

Additional tests were performed where the U_3O_8 contents of sample TRN-2000 were forced to one side of the can. The measured rate was compared with the normal sample geometry. In this case the RD had less of a perturbation than the AWCC. This is partly because the RD has a more penetrating interrogation flux than the AWCC and partly because there is less radial geometric variation in the RD. The sample rotates past the interrogation sources which averages out radial variations in the RD; whereas, there is no sample rotation in the AWCC, and the interrogation flux decreases with radial distance from the central axis of the well.

Measurement Precision and Stability

A series of measurements were performed overnight and over the weekend to check the precision and stability of the two systems. Normally the 1500 g U or 2000 g U samples were used in the counters to give the coincidence response.

The results of the measurements are given in Table VII. The observed standard deviations are very close to the standard deviations predicted by counting statistics for the AWCC. The standard deviation in parentheses for the RD corresponds to the measured value after making corrections with the temperature sensor and the minicomputer. For cases with better statistical precision (e.g., the 10,000 s runs), the observed RD deviations are larger than would be expected from counting statistics alone. The cause of the instability is likely to be the scintillator-photo tube system. The stability of the ^3He detector system in the AWCC is very good.

CONCLUSIONS

There are many characteristics and parameters to be considered in the comparison of the RD and AWCC systems. The relative importance of these parameters depends on the application and constraints on the user. A brief summary follows for the major parameters of interest.

Counting Rates

The net coincidence counting rate is approximately 18 x 10^{-3} counts/s·gU for the RD and approximately 84 x 10^{-3} counts/s·gU for the AWCC. However, this difference in rate is not important because the statistical error is dominated by the accidental coincidence rate which is considerably higher for the AWCC.

TABLE VII

STABILITY RESULTS FOR AWCC AND RD

	Net Coincidence Counts	
	AWCC	RD [a]
Wednesday Overnight (4000 s runs - 15 h period)		
1σ predicted	0.55%	0.42%
1σ observed	0.59%	0.82%(0.54%)
Thursday Overnight (4000 s runs - 15 h period)		
1σ predicted	0.58%	0.42%
1σ observed	0.59%	0.45%(0.40%)
Friday - Monday (10000 s runs - 60 h period)		
1σ predicted	0.26%	0.26%
1σ observed	0.28%	1.04%(0.96%)

a) The 1σ value in parenthesis for the RD corresponds to the standard deviation of the coincidence count after making the temperature correction with the temperature sensor and minicomputer.

The fact that the AWCC uses AmLi sources that are an order of magnitude smaller than the RD is important for portable applications.

Precision

The precision is linked to the net coincidence counting rate but it also includes the background rates and the electronic stabilities. The observed precision of the RD and the AWCC were essentially the same (approximately 4-0.5%) for the counting intervals (approximately 1000 s) and mass range (500-4000 g U) of the present comparison. For higher masses or longer counting times, the statistical precision would drop below approximately 0.5% and the AWCC would have some advantage because of its better stability.

Other versions of random drivers that do not have the Pb shielding and gamma-ray time gate rejection, have a higher counting rate and better statistical precision. However, the penetrability/linearity is then worse and RD stability limits the observed precision in any case.

Penetrability and Linearity

Because of the large quantities of iron and lead close to the AmLi source and sample chamber, the RD has a harder neutron interrogation flux than the AWCC. This is demonstrated by the calibration curves for U_3O_8 where the linearity is better for the RD than the AWCC. The better penetrability of the RD makes it possible to tolerate a larger variation in certain types of sample inhomogeneities.

Geometric Effects

Changes in coincidence rates because of sample position variations or geometric effects were only briefly studied in the present work. The two source approach to flatten the spatial response is used in both instruments. The response variation as a function of fill height or vertical position is very small and essentially the same for both systems. The RD incorporates a rotating sample holder and side mounted neutron sources to reduce the effects of radial sample variations. The AWCC does not have this feature for two reasons. One is to keep the system simple from a mechanical standpoint, and the other is that the AmLi sources are mounted on the center axis of the AWCC to take advantage of the end plug shielding of the AmLi background neutrons.

Because of the above reasons and the larger sample cavity of the RD, that system is somewhat less subject to sample geometric effects.

Stability

One of the reasons for selecting ^3He tubes for the AWCC was their excellent stability and their insensitivity to gamma rays. For high precision counting ($1\sigma \leqslant 0.5$-1%) or applications with long periods between calibrations, the AWCC has better performance than the RD. The RD system uses plastic scintillator-phototube detectors which are subject to temperature variations and radiation fatigue. A temperature sensor is incorporated into the system and computer based corrections are made for these effects.

Matrix Effects and Flux Monitors

The effects of matrix materials in the sample and the role of the flux monitor were only lightly studied in the present comparison. This was because of the limited sample categories and the lack of a flux monitor in the AWCC.

The primary function of the ^3He flux monitor in the RD is to make corrections for hydrogen that might be present in the sample. Because there was no significant amount of hydrogen in the standards used in this comparison, the flux monitor correction was not large. However, if assay samples have moisture content or a large amount of plastic bagging material, a flux monitor might be required to indicate the problem and make appropriate corrections.

The harder neutron interrogation spectrum of the RD makes it less sensitive to inhomogeneities that effect the interrogation neutrons such as self-shielding in lumps of fissile material. However, the AWCC is less sensitive to matrix materials that effect the counting of the induced fission reactions. Examples of this are density variations in the matrix materials which change the gamma-ray absorption and/or the fission neutron moderation.

In summary there is not a consistent advantage of one system over the other with respect to matrix effects. If the samples contain a significant amount of moisture, a flux monitor should be used, or if the fissile density is low, thermal-neutron interrogation can be used to override the hydrogen effect.

Portability

The relative portability of the two systems was only indirectly checked in the present work. That is, the AWCC was carried to the site of the RD rather than the other way around.

In all factors which pertain to portability, the AWCC is better. The key parameter is the weight and the AWCC is roughly a factor of ten lighter. The size of the AWCC electronics is about an order of magnitude smaller than for the RD. However, the RD electronics could be reduced with sufficient effort. The AWCC is more rugged, stable, less complex, and less sensitive to temperature variations than the RD. Also, when the AWCC is turned on at a new location, the warmup time for the electronics is only a few minutes compared with several hours for the RD. The factor-of-ten smaller Am-Li source strength is another advantage of the AWCC with respect to transportation logistics.

In summary, the performance characteristics of the RD at CMB-8 and the AWCC are quite similar with respect to precision and sensitivity. The AWCC has many obvious advantages for portable applications as detailed above. For in-plant or fixed-site applications the RD has the advantage of better neutron penetrability. Also the minicomputer based data analysis system can be used for measurement control functions that are not possible with the smaller portable electronics. For samples with high gamma-ray backgrounds such as irradiated fast critical assembly plates and ^{233}U-Th fuel materials, the AWCC has the advantage of being insensitive to the gamma-ray backgrounds.

IAEA inspector applications normally require equipment that can be easily moved from one site to another, and thus the AWCC more closely meets their need.

ACKNOWLEDGEMENTS

The authors would like to thank John Foley and Merlyn Krick for their help in the design of the instrumentation and H. R. Baxman for his assistance in the preparation of the standards and use of the CMB-8 facility.

REFERENCES

1. T. L. Atwell, J. E. Foley, and L. V. East, "NDA of HTGR Fuel Using the Random Driver," Journal of the Institute of Nuclear Materials Management, Vol. III, No. III, pp. 171-188 (1974).

2. Howard O. Menlove, "Description and Operation Manual for the Active Well Coincidence Counter," Los Alamos Scientific Laboratory report LA-7823-M (1979).

3. D. Langner, T. L. Atwell, T. R. Canada, N. Ensslin, L. Cowder, T. Van Lyssel, and H. R. Baxman, "The CMB-8 Material Balance System Measurement Control Program," Los Alamos Scientific Laboratory report (1979).

4. D. M. Lee, N. Ensslin, C. Shonrock, and T. Van Lyssel, "Random Driver Studies," Los Alamos Scientific Laboratory report LA-7211-PR, Sept.-Dec. 1977, p. 14.

5. Merlyn Stewart Krick and Howard O. Menlove, "The High-Level Neutron Coincidence Counter (HLNCC): Users' Manual," Los Alamos Scientific Laboratory report LA-7779-M (1978).

Discussion:

Hopwood (Union Carbide):

I noticed you showed the effects of graphite in depleted uranium. What other major matrices have given problems or had a pronounced effect on the measurement?

Menlove (LASL):

In this examination, we didn't study other matrices. From other works, as a general statement, hydrogeneous matrices are the ones that can give trouble with the active neutron systems. Most metal matrices, or any high atomic number material, will not make any difference with the measurement with the active well counter. It will make some difference with random driver, because of the gamma-ray absorption. The key thing in these is the hydrogeneous materials that have to be watched.

Green (BNL):

I hope you will forgive me, Howard, but I think I have another comment for LASL. I don't know exactly where the seed of this idea originated, but it was encouraged and it was understood as a need by the fact that a number of LASL experts have been serving on the IAEA staff. This particular device was recognized as an important IAEA need by John Foley, and I think all the people at LASL are to be congratulated for working so well with the Agency and helping satisfy their needs.

Menlove:

Thank you, Leon. This particular instrument was developed under support from the ISPO office, so we are appreciative of that.

A Rapid Inventory Taking System

P. S. S. F. MARSDEN
Nuclear Materials Accounting Control Team (NMACT)
Harwell, England

ABSTRACT

A data processing system designed to facilitate inventory taking is described. The process depends upon the earliest possible application of computer techniques and the elimination of manual operations. Data is recorded in optical character recognition (OCR) 'A' form and read by a hand held wand reader. Limited validation checks are applied before recording on mini-tape cassettes. The data is read from the cassette directly into a computer system. A software package has been developed to validate the data, collate it with verification data, compare the physical and book inventories, and output the data in the form required to satisfy Regulation 3227/76. The system depends critically on label security and aspects of this problem are considered.

1. INTRODUCTION

Much of the nuclear material held by the United Kingdom Atomic Energy Authority (UKAEA) at its research and development establishments is static or slow moving and is held in storage locations between periods of use. Physical inventory taking in these stores can be a time consuming manual operation, which has the undesirable consequence of exposing those workers involved to low levels of radiation. In some cases, they may possibly accumulate a substantial fraction of their permissible annual exposure.

It is believed that a major source of error at physical inventory taking time stems from the necessity to transcribe data from the labels on nuclear material containers to working papers and the subsequent manual manipulation of this data.

At all UKAEA establishments comparison of the results of physical inventory taking with the book inventory is a manual and time consuming process. The discovery of discrepancies and consequent investigations tends to be slow and results in delays in final preparation of the physical inventory listing (P.I.L.).

With these three situations in mind NMACT have been investigating ways in which these problems can be solved. By replacing manual operations by machine operations, and removing the potential source of transcription errors by using a form of machine readable data, NMACT believe that the accuracy and speed of the whole process can be improved. Our work, which is about to be field tested, suggests that our expectations will be realised.

At the same time we have had the essential features of the physical inventory taking process in mind from the point of view of accountancy. Namely that physical inventory taking is a process of searching a locality for nuclear materials with the objective of ensuring that all nuclear materials are brought into the accounts.

We have therefore designed the system so that the operator can move through the area reading each label as he comes to it without stratifying or ordering the contents of the area in any way. If items are discovered which do not bear appropriately encoded labels the data derived from either an ordinary label or as determined, by weighing, analysis, and/or non destructive methods, at the time or subsequently, can be input into the system. The minimum requirement at the stage of discovery is the recording of a batch number with all other fields entered as zero. The system is capable of enlargement so that as it develops data on the integrity of the container, mass, analysis, or isotopic composition of the sample can be handled directly as and when they are determined.

At an early stage in our development we were faced with a choice between the use of "bar coded" labels and labels written in OCR characters. We selected the latter and our decision was influenced by a number of factors, which were:

i) Labels in OCR characters can be read by the human eye without difficulty, "bar coded" labels must have a translation printed beside the pattern of bars.

ii) The machine needed to print "bar coded" labels is specialised and costly when compared with a standard IBM 'golfball' typewriter with interchangeable typesphere. The relationship of cost is 10 to 1 respectively.

iii) The number of digits to be coded results in lengthy 'bar coded' labels which become difficult to 'read.'

iv) Commercially available 'bar code' reading equipment is not user programmable and is therefore not as versatile or adaptable as the OCR Wand Reader.

v) Neither equipment could read a complete range of alphabetic characters, so the coding of alphabetic characters to numeric form proved unavoidable, however, the OCR Wand Reader could read a limited range of alphabetic characters. Developments in OCR readers suggests that all alphabetic characters are likely to be readable in the near future.

2. DATA FLOW IN THE SYSTEM

2.1 Summary

The rapid inventory taking system is essentially a four step process. The four steps, which will be amplified in more detail later in this section of the paper, are:

i) Data creation--the translation of the data to be recorded on the label affixed to the nuclear materials container into machine readable OCR 'A' code, which can be read, incidentally, by the human eye.

ii) Data gathering--the reading by machine of labels on all nuclear materials containers in an MBA and the storage of the data in machine readable form on mini-tape cassettes. Limited data validation is carried out at this stage.

iii) Data transmission--the reading of the data from mini-tape cassettes into a data file on a computer system.

iv) Data processing--the validation and checking of the data transmitted to the computer system, translation of codes, collation and comparison with verification data obtained independently, comparison with the book inventory, followed by the printing of the physical inventory listing.

2.2 The Data Creation Step

There seems to be no alternative to the manual recording of data at some stage in any inventory taking system. Accepting this to be the case there are advantages to be gained from arranging for this manual process to take place at a period when time can be made available for adequate checking of the data, rather than at a period when time is short and the time consuming process of data checking may have to be rushed.

In this inventory taking scheme manuscript lists are prepared containing all the data required for the label. This includes such information as batch number, mass, elemental analysis, isotopic abundance, number of items, and the codes for material description, container, state (i.e. fresh, irradiated, etc.) element, isotope, measurement regime, obligation and use. The reading wand has limited alphabetic capability and most alphabetic codes must be translated into a numeric form. All fields are controlled by check digit verification[5] against transmission errors, and these check digits must be calculated and added to the data fields. A computer program has been written to calculate check digits in accordance with the standard regime adopted by us for our field trials.

The data when set out on the label consists of seven fixed length fields each identified by a leading alphabetic character. Where numeric data does not fill a field the left most columns of that field are filled by a predefined filler character. The data fields are as follows:

Field Identifier: (first character) C
Field Length: 18
Description: Batch code, either 8 numeric characters or 8 alphabetic characters coded to 16 digits or a combination of alphabetic and numeric characters all in digital form.
Last Digit: CDV (check digit verification)

Field Identifier: N
Field Length: 6
Description: Number of items in batch 4 numeric characters
Last Digit: CDV

Field Identifier: M
Field Length: 11
Description: Mass of nuclear material in grams--9 numeric characters
Last Digit: CDV

Field Identifier: A
Field Length: 7
Description: Isotopic Abundance--5 numeric characters
Last Digit: CDV

Field Identifier: P
Field Length: 7
Description: Percent accountable element--5 numeric characters
Last Digit: CDV

Field Identifier: D
Field Length: 14
Description: Description field--6 alphabetic characters coded as 12 numeric characters
Last Digit: CDV

Field Identifier: X
Field Length: 14
Description: Further descriptive matter--6 alphabetic characters coded as 12 numeric characters
Last Digit: CDV

The code used to convert alphabetic characters to numeric form is A, B, C....Z = 01, 02, 03....26 with "blank" coded as 00. A Modulus 10 check digit verification gives a 90% assurance of the validity of any digit string. Thus since three of the fields (M, A and P) contain quantitative data there would be a 73% assurance that all three data fields are simultaneously correct; and there would be a 48% assurance that all seven fields are simultaneously correct.

Two different processes have been used for printing the labels. The first procedure is appropriate where small numbers of labels are to be prepared. It is not a procedure to be recommended where large numbers of labels are required, because of the precision and accuracy which is required and because of the tedium of the task.

In this first procedure the manuscript list is typed by a copy typist onto the self adhesive labels using an electric typewriter fitted with an OCR 'A' type.

The second procedure involves taking a manuscript list of the necessary data (which in this case can consist of the data in its uncoded form and without check digits) and keying it into a computer file. This data set is then processed by a computer programme which translates alphabetic characters to numeric code, and calculates the check digit, at the same time reformatting the data to the form required for the labels and outputting a data

set which can be printed on a printing terminal fitted with an OCR 'A' type under the control of a computer.

The latter procedure is that recommended where large numbers of labels are required. A significant advantage of this procedure is that the initial data set created from the keyboard of a terminal can be printed, checked for errors and edited to correct these errors before it is processed by the computer. The labels produced in this way, given an error free input data set, are produced with a high degree of precision and free from errors.

2.3 Label Security

Label security is a matter of concern wherever nuclear materials are stored for any significant period and NMACT have been giving this matter some attention. Whilst the precise features to be incorporated in a secure form of label are classified and cannot, therefore, be discussed, it is possible to detail the threats against which protection is sought. These are:

1) The counterfeiting of a blank label on which spurious data can be recorded.

2) The alteration of data already recorded on a genuine label.

3) The removal of a genuine label and its reuse either with or without alteration.

4) Theft of genuine blank labels and their subversive use.

It is generally true that any document can be counterfeited, given the will, the time, and the resources. It is thus very difficult to design a label which cannot be counterfeited. The best chance of achieving this is the incorporation of some subtle feature in the label design that is not readily apparent. The use of check digit verification is a feature of this kind, and if the fact of the use of CDV is not widely known and the particular regine in use is kept secret, this can be used to detect counterfeiting. The use of CDV in a serial number is an example. There are a number of other features which would come into this category and which I must leave to your imagination and ingenuity.

Data can be altered by two methods, i) erasure of the original data and the re-entry of spurious data and ii) the obliteration of the original data followed by the entry of spurious data. This is the problem encountered commonly with cheques and bonds and can be solved in the same ways by the use of moire patterns and similar features.

For labels to be of real utility in the application we have in mind they must be self adhesive. To prevent the removal of a label the adhesive used must be very tenacious, so that removal cannot be effected except by the destruction of the label or the use of a solvent to destroy the adhesive properties of the gum. Supermarkets have this problem and have introduced cuts in their labels so that it is not possible to remove the price tag without the possibility of its being torn. The use of solvent sensitive inks in the printing of the label consistutes another obvious form of protection.

In order to prevent the subversive use of genuine labels it must be possible to uniquely identify each label and the issue and use of labels must be strictly controlled. This implies the use of serial numbers, a label accounting system, the handling of labels only by trustworthy staff and the return to control of damaged or unused labels and their subsequent destruction by burning.

Labels incorporating security features of the kind envisaged above are expensive and may cost in the region of £0.10 (or $0.20) each.

2.4 Data Gathering Step

The portable OCR Wand Reader consists of a hand held reading head (Wand) incorporating a keyboard and a display panel. This arrangement allows data input eithr by reading OCR character coded labels, or by keyboard entry or partially by reading OCR character fields and partially by keyboard entry.

The hand held unit is connected to an electronic module powered by a rechargeable battery module, which is attached and forms the base of the assembled unit. At one end of the electronics module are the control switches and the shuttered recess which takes the mini-tape cassette upon which data is recorded. On top of the electronics module is a display which indicates the stage which has been reached in the reading sequence and the status of the electronics module.

The electronics module of the Wand Reader is user programmable. The user can specify the identify, sequence order, and length of fields to be read. These three parameters provide a part of the data checking facilities, since fields can be recognized and read only in the permitted sequence. Fields are also checked to ensure that a longer field length than that defined in the program cannot be read. The user may also specify that certain fields are to be subjected to check digit verification and a variety of check digit schemes can be specified. The electronics module can also be programmed to accumulate (a) a count of items read and (b) the total of a specific field. Both the count and the total are decremented when items wrongly recorded are subsequently deleted. The fact that an item is deleted is recorded on the mini-tape cassette which provides an auditable record of what has been done.

An audible signal indicates that a field has been read correctly and a different signal indicates failure or fault conditions. The entire system is protected against battery power failure, the user's attention is drawn to this condition as it approaches, in time to save the data on the mini-tape cassette and close the tape cassette file. The program within the electronics module is protected at all times against interference during use of the Wand Reader and against power failure. It is written on a read only memory (ROM) controlled by a physical key.

For further details of the equipment and its capabilities and the method of programming the equipment, reference should be made to the manufacturer's manuals.[1,2]

In practice, labels are read by passing the Wand Reader in either direction over the data fields in the specified order. When the field has been read a short bleep indicates successful data transfer. No bleep indicates that the data field has not been read. A long bleep indicates that the field has been read but rejected because of some fault condition, for example, check digit verification has failed, too many characters in the field, or incorrect field sequence.

In application a header record is first entered on the tape.
Field Identifier: F1
Output Identifier: T
Field Length: 7
Description: Date or time--6 numeric digits representing DD (day) MM (month) YY (year)

Field Identifier: F2
Output Identifier: L
Field Length: 9
Description: MBA or location--4 alphabetic characters coded as 8 numeric characters

Field Identifier: F3
Output Identifier: K
Field Length: 3
Description: KMP an alphabetic character coded as two numeric characters

The header is entered via the key-board as the first record of any data gathering session and consists of data common to all following labels read.

The sequence of fields which the Wand Reader expects to receive is thus:

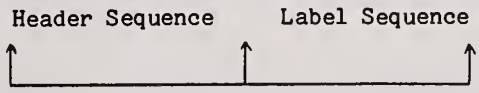

When the label sequence has been completed, the Wand Reader expects to read either the start of a new label sequence field, or the start of a new header sequence; no other field

identifiers will be accepted. Similarly only the specified sequences within the header and label fields will be accepted.

2.5 Data Transmission

The mini-tape cassette is removed from the body of the electronic module and transferred to a cassette playback module (Model 3431) connected to a PDP 11/45 computer via a visual display unit (VDU). See section 3.7 for technical details and reference[3] for a full description. Output from the cassette playback module in its standard configuration is in 7-bit ASCII 128 character code which is compatible with the PDP 11/45 system. However, output can be obtained in EBCDIC code which is compatible with an IBM 370 or ICL 2980 computer. Systems of all three kinds are used by the UKAEA for processing nuclear materials data.

2.6 Data Processing

A suite of computer programs has been developed for handling the data once it has been transferred to the computer system. It is at this stage that data from two other sources is brought together with the physical inventory data namely:

a) verification data, and

b) the book inventory.

The programs perform the following function:

i) Data Validation

This program checks the structure of the physical inventory data file to ensure that it consists of a header record followed by a number of detail records. Each field of a header or detail record is checked for valid identifier and correct field length. Then specific checks are applied to all fields for example the data field is checked to ensure that the day of the month is compatible with the month (i.e. no more than 28 or 29 days in February). All data fields which are controlled by check digit verification are checked to ensure that the verification test is passed. Certain fields cannot have values in excess of a certain figure and cannot have zero or negative values, and these are checked. Other fields must be filled with numerically coded alphabetic characters which may assume only certain values or combinations of values and these are validated.

Errors detected by the validation procedure are reported and provision is made for their correction. After correction, the physical inventory data file is updated.

ii) Collation of Verification Data with Physical Inventory Data

The next program compares the verification data for all those items where verification data has been obtained. If the verification data differs from that recorded on the label of the item and captured at the data capture stage, then the verification data is substituted for the label data, and this fact is recorded and reported.

iii) Comparison between Physical Inventory and Book Inventory

This program compares the physical inventory with the book inventory. When discrepancies are found these are recorded and reported. There is no presumption as to which is correct, so the report consists of a line showing the physical inventory record, a line showing the book inventory record and a line in which asterisks indicate where the two records differ. This highlights the discrepancy and provides the data from which an investigation can be mounted with the object of resolving the discrepancy. When resolution is achieved provision is made for the amendment of either set of records.

iv) Printing the P.I.L.

The final programs in the suite at present print the physical inventory listing in accordance with the form required by Regulation 3227/76, and carry out 'housekeeping'

operations such as the deletion of unwanted data and work files. A minor modification to the printing program would enable this program to produce punched cards or to write the data to magnetic tape in a form suitable for onward transmission to Euratom.

The suite of programs was written in such a way that it could be implemented on any or all of the three computer systems currently used within the UKAEA for nuclear materials accountancy.

3. MATERIALS AND EQUIPMENT

3.1 Labels

The stock on which the labels are printed must conform to certain criteria if the labels are to be read satisfactorily.

These criteria are:

Media reflectance (PCS) 79%

Media opacity 85% (recommended 90%)

Background "see through" opacity PCS change 10% or less.

Media gloss $\leqslant$ 60%--TAPPI T-480 (non-glossy stock recommended).

The stock used experimentally was provided by Avery Label Systems as samples. The labels were 74 x 102 mm and self adhesive, in continuous fan-fold sheets 3 labels wide x 4 labels deep. The sheet size was 305 x 337 mm with edge perforation for computer printer sprocket wheels. The sheets were perforated horizontally at the sheet junction and twice vertically between the rows of labels. The labels had an imprint on reverse of the designation 'P4'.

The labels described above are not security labels and would not be used in any practical application. Preliminary work on a security label has been undertaken in collaboration with Metal Box Limited, Security and General Printing Divsion, London, England.

3.2 Character Font

The OCR font used in our trials was OCR-A (NRMA) and the following 23 characters could be used:

0123456789ACDMNPRUXY/"$

The specification of this font is available from Recognition Equipment Inc.[4]

3.3 Label Printing Equipment

Labels were typed on an electric typewriter fitted with an OCR 'A' typesphere, or were printed on a printing terminal fitted with an OCR 'A' type under the control of a computer.

3.4 Label Reading Equipment

Labels are read with the portable OCR Wand Reader Model 3440 made by Recognition Equipment Incorporated, Dallas, U.S.A.

3.5 Mini-Tape Cassettes for Data Recording

Suitable mini-tape cassettes are supplied by Recognition Equipment, Dallas, U.S.A. namely "Recognition" brand ref. 3471 in boxes of 5. An alternative is "Verbatim" brand (ref. 0968 5785). Both are double sided.

3.6 Accessories for Use with the Wand Reader

Battery packs (REI) ref 3470
Shoulder strap (REI)
Waist strap (REI) ref 3472
Carrying case (REI) ref 3473
Sustainer (REI) ref 3421
Battery charger (REI) ref 3411
Model LG150. The input is 250 volts at 50 Hertz, the output is 0.45 amp. at 1.2 to 12 volts.

3.7 Data Transfer Equipment

The mini-tape cassettes are read on a mini-cassette Playback Console (Model 3431) manufactured by Recognition Equipment Inc. This is an asynchronous RS-232-C compatible unit which is mains powered (220-240 VAC, 50 Hz, 100 W). Output from the device is in 7-bit ASCII 128 character code or optionally in EBCDIC at a variable baud rate from 110 to 9600.

The device has internal switch controls which determine the configuration and protocol of systems with which the device can communicate.

3.8 Software

The software has been written in American National Standards Institute (ANSI) 1966 FORTRAN IV so as to be as transportable as possible, and was written in modular form.

3.9 Computers

Data processing was done on two computer systems:

i) An IBM 370/168 computer running under the MVS operating system with FORTRAN H extended compiler. Direct access peripheral storage devices are used throughout.

ii) A DEC PDP 11/45 computer running under the RSX 11 M operating system with the FORTRAN IV PLUS compiler supporting 4 byte integers. Direct access peripheral storage devices are used throughout.

4. RESULTS

4.1 Test Data Trials

Various types of error were presented to the system incorporated in packages of test data. The following types of error were introduced at the data creation stage:

i) incorrect field identifiers

ii) incorrect field length

iii) transposition of digits within a data field

iv) missing digits in a data field

v) incorrectly calculated check digit

At the data gathering stage all the above errors were detected and in addition attempts to read data fields out of sequence was found impossible. There was one exception to this latter condition. In the original data sequencing plan two fields were defined by the identifiers D and U and they were both specified as 13 characters long. It was found in practice that the Wand Reader could not differentiate between these fields. The difficulty was overcome by identifying the second field as X but stipulating in the programming of the electronics module that X was to be output as U.

Occasionally, it was found that a correct data field could not be read by the Wand Reader (about 2% of labels read or .3% of fields read). This was found to be due to two causes. Extraneous ink marks adjacent to the characters in the field seem to be responsible, or alternatively, some bold characters on a stratum below the label were transmitted through the stock of the label, because it was not sufficiently opaque, thus causing confusion.

At the data processing stage all the following errors were successfully detected:

i) incorrect field identifiers

ii) incorrect field length or data outside permitted range

iii) transposition of digits within a data field

iv) missing digits in a data field

v) incorrectly calculated check digit

vi) date not agreeing with month of year

vii) KMP not in permitted range

viii) %age accountable element or isotopic abundance greater than 100%

ix) measurement, material description, element, unit, isotope, obligation, and use codes not in permitted lists.

There were no exceptions. The purpose of this data validation stage is to detect the corruption of data which may occur during data transmission and to apply more extensive validity checks than can be applied at the data gathering stage.

The collation of physical inventory label data and verification data draws attention to discrepancies between recorded and measured parameters. Whilst in theory it would be possible to measure the parameters on all items physically present, in practice time precludes this and it is only possible to measure the parameters of a sample of items. The software, whilst designed to accommodate the latter situation, will also handle the former. When the comparison takes place correspondence is deemed to have been achieved if the discrepancy is less than 0.5%. The parameters compared are mass, factor (%age accountable element) and isotopic abundance. The results of test runs using test data designed to test this part of the system proved entirely satisfactory.

The comparison between physical inventory data, updated by verification data and the book inventory is designed to detect discrepancies between these two sets of records. The kinds of discrepancy of interest are:

i) items found during physical inventory and not on the book inventory

ii) items not found during physical inventory and yet on the book inventory

iii) items on both inventories where the recorded parameters do not correspond.

These cases have been thoroughly explored using test data and the program and methods for correcting the appropriate records have worked satisfactorily.

4.2 Field Trials

The entire system is now ready for field trials which we hope to commence shortly.

5. CONCLUSION

A rapid physical inventory taking system has been developed making use of commercially available equipment at the forefront of technological development and using computerised

data handling techniques. The entire system has been tested extensively and found to work as designed. The system is now ready for field trials and is confidently expected to improve the speed and accuracy of physical inventory taking in storage areas. Wider applications of the system are being consdered. An important implication of the system is that the integrity of labels must be guaranteed.

6. REFERENCES

1. Recognition Equipment, "Portable OCR Wand Reader--3440--Users Guide." 1977. Recognition Equipment Incorporated, Dallas, USA.

2. Recognition Equipment, "Portable OCR Wand READER--3440--System Manual." 1977. Recognition Equipment Incorporated, Dallas, USA.

3. Recognition Equipment, "Cassette Playback Module--3430--System Manual." 1978. Recognition Equipment Incorporated, Dallas, USA.

4. Recognition Equipment, "Recognition Products--OCR A/OCR B Wand Media Specifications," Recognition Equipment Incorporated, Dallas, USA.

5. Wild, W. G., "The Theory of Modulus N Check Digit Systems," Computer Bull. 12 309-311, December 1968.

Discussion:

Questioner:
Have you thought about doing this in real-time?

Marsden (UKAEA-Harwell):
It is real-time in the sense that you collect the data while you are carrying out your physical inventory. Almost all of the systems that are referred to as real-time, in the accountancy field are not, in fact, real-time at all. They are what are referred to, in data processing, as transactional real-time systems.

Questioner:
So if there are any errors in the inventory they will not be detected right away?

Marsden:
They will be detected as soon as the data, which has been recorded on the labels, has been transferred to the computer system, which could be in a matter of minutes. The aim being, to process the data contained on a mini-cassette as soon as the cassette has been filled.

Questioner:
Have you evaluated the readability or reading error rate for bar code labels?

Marsden:
We have not evaluated the readability of bar-coded labels vs. OCR labels for the simple reason that bar code labels would not satisfy our requirements. The field length that is normally available for bar coded labels is something like a maximum of 17 characters. We are handling a great many more than 17 characters. The reason for this is that we wish to eliminate the need for any human intervention after the data gathering stage, with the exception of error correction procedures which involve the manual editing of computer data files via a terminal.

Wagner (LASL):
We considered using the bar code reader in the early stages of the DYMAC system. We have not implemented it for the simple reason that it requires doing a physical inventory and the actual contact of the reader with the can. As was mentioned this morning, because of the large number of items in our inventory, exposure to personnel becomes a problem when taking a physical inventory. My question is, is it possible to read the can label from a distance?

Marsden:
It is possible to obtain OCR readers which will read labels at a distance of about 18 inches. The reading accuracy is improved if the sensing head is stationary and the item to be scanned is held and presented to it mechanically. One of the big problems with OCR technology at the moment is that hand-held readers are rather sensitive to the way in which they are used. A very considerable improvement in accuracy is achieved in ticket or document readers where the medium containing the data is moved mechanically past the reading head.

Wagner:
Has anyone looked into the compatability of the labels in the hostile atmosphere present in a processing line?

Marsden:
No, we have not looked at this aspect in any great detail. We have considered ways of protecting labels from dirt and we know that this can be achieved by cladding the label with some easily cleanable plastic cover. Such a covering is acceptable, provided that the optical properties of the clad conform to the requirements of the OCR reading system. I had meant to mention the question of label security during my talk, however, I ran out of time. It must be appreciated that the label is used as a primary source of data in this system and, therefore, label integrity becomes a very important aspect. We have been discussing this problem with a firm of security printers.

Questioner:
Do you have any feel of about how long it would take to do about 10,000 items?

Marsden:
I did not make reference to the speed of label reading in my paper as we have yet to carry out field trials. Reading labels with the OCR reader is very quick, it is quicker than reading the label by eye and transcribing the information to paper. So I would imagine one would probably achieve a three or fourfold improvement in recording speed. We anticipate that a 'learning curve' effect is likely to be realised, as the reading process is a manual skill.

Questioner:
You mentioned information on the label. What kind of information are you reading off the label?

Marsden:
The information that we are reading off the label is batch number, mass, conversion factor, isotopic abundance, number of items in the batch and other descriptive material which is required by the regulations.

Questioner:
Do you have any unique numbers assigned to the labels?

Marsden:
The system is not yet established as a routine procedure within the Authority. However, in any final implemented version, we anticipate that a form of security label would be used. An essential feature of any such security label would be a serial number. The whole question of label security is mentioned in the published paper, and the need for a serial number to implement any label control system is discussed.

Heinberg (LASL):
Could you give me some indication of what kind of error rate you expect with this reader?

Marsden:
Yes. In our proving trials, which of course are not field trials, we found that about 2% of the labels could not be read. This could be narrowed down to about 0.3% of the characters on the labels. These were usually not readable because of extraneous matter adjacent to the character which interfered with the reading process.

Heinberg:
Then you would get an indication that it is not readable, but I am talking about reading incorrectly as well. Could you give me an indication of that kind of error rate?

Marsden:
That is a very difficult question to answer, because until, at some later stage, one compares the data that one has gathered with the original label or the book inventory, one doesn't know whether the data has been read correctly or not. The use of check digit verification is extensive in our system and this gives a 90% assurance that each field has been read correctly or at least has been transcribed to the label. Obviously, one combines these probabilities to arrive at something rather less than 50% assurance that the total data from the seven fields has been read correctly.

Schleicher (EURATOM):
Normally an inventory is verified by the inspectors. How does the inspector's activity fit into your described scheme? You indicate, for instance, that you might make corrections if there are differences found with the book inventory. Should such corrections not be reported to the control authority, e.g., as "new measurements"? Furthermore, if you proceed in the proposed way verifying the whole inventory, you risk that the inspectors have to repeat the whole operation. Could they participate at the preparation of the inventory?

Marsden:

As regards the inspectors, we would obviously afford all the facilities to the inspectors during the inventory taking. As far as corrections to the inventory are concerned, at each stage where corrections are necessary, a computer printout is produced to show what errors have been found and therefore what corrective action is necessary. The mini-casette itself forms an auditable document and could be made available to the inspectors. However, we do not envisage that the inventory-taking process would give rise to ICR corrections which would reach EURATOM or the Agency, because until the inventory was considered to be correct it would not have been transmitted to EURATOM. Any new measurements which had been incorporated from the verification data file would, of course, give rise to ICRs.

Chanda (Rocky Flats):

Judging by the number of questions here I think we have hit a very senstive subject. I know at Rocky Flats, as you heard earlier, we have a very sizable inventory and therefore radiation exposure problems, thus speed of taking the inventory is a vital topic. I would urge those of you in the R&D field to work on this and I am sure that other technical program committees, such as the INMM meeting in June, would look favorably upon some definitive input for papers. It is a very good topic.

Gottschalk (Westinghouse-Hanford):

I just wanted to make a point that HEDL is working on a system for new fuel facility that incorporates what you've been talking about. We are going to briefly describe this system this afternoon.

Evaluation of Reactor Track-Etch Power Monitor

by

B. S. CARPENTER, I. G. SCHRODER
National Bureau of Standards, Washington, DC 20234

and

L. J. PILIONE
The Pennsylvania State University, University Park, PA 16802

and

J. W. ROE
Nuclear Regulatory Commission, Washington, DC 20555

and

S. SANATANI
International Atomic Energy Agency, Vienna, Austria A-1011

INTRODUCTION

The National Bureau of Standards was requested by the International Atomic Energy Agency through ISPO to evaluate the capability of the track-etch power monitor [1, 2] for providing an independent record of reactor power by conducting field tests under very well defined experimental conditions. The track-etch power monitor was designed by G. E. Vallecitos Nuclear Center to operate unattended in a neutron field to provide an independent permanent record of the periods of reactor operation and shut-down, in addition, to provide information concerning the neutron energy spectrum.

GENERAL DESCRIPTION OF THE TRACK-ETCH POWER MONITOR

The track-etch power monitor is an externally-powered device designed to record the neutron flux from operating reactors and other sources for extended periods of time. A strip of 35 mm wide polyethylene terephthalate plastic film is driven past a group of six fissionable deposits (Table I) which are exposed to the local neutron flux. A given fraction of the fission fragments generated penetrate the film producing radiation damaged tracks that are subsequently etched and counted to permit a reconstruction of the temporal flux history to which the monitor was exposed. The monitor is equipped with enough film to cover a years operation. Under these conditions the monitor is designed to operate at a neutron flux of 10^6n $cm^{-2}s^{-1}$.

Table I

The fissionable nuclides contained in the source plate are:

Material	Enrichment	Source Diameter(cm)	Source Collimator	Quantities Per Foil(mg)	Activity(Curies)
^{235}U	99.83wt%	0.32	3	0.74	4.89×10^{-3}
^{237}Np	--	0.32	1	0.079	6.25×10^{-3}
^{238}U	6ppm ^{235}U	0.32	1	0.70	--
^{252}Cf	--	0.32	1	0.006µg	3.192×10^{-1}

The monitor was designed to fit within the ion chamber thimbles normally used by power reactors for detector monitors. It is contained within a sealed aluminum can of two different sizes, 8.4 cm in diameter and 26 cm long or 10.2 cm in diameter and 26 cm long. The total weight is approximately 1.2 kg and 1.5 kg, respectively. There is an eye-bolt located at the end opposite the fission sources for insertion and retrieval. Power is supplied to the monitor from an external source through a sealed electrical connector. The synchromous motor within the monitor uses either 115V or 240 V AC for operation and drives the take-up reel for the 35 mm film at speed of 4.75 cm per day. In addition a micro-switch is placed on the drive sprocket of the feed reel to allow remote indication of proper film transport operation.

INVESTIGATIVE STUDIES

In order to test the monitor under a controlled and known neutron environment a monitor was installed in the Nuclear Detector Well #2 of the 10MV NBS Research Reactor. At this position the monitor was exposed to a neutron flux of 1 x 10^6n $cm^{-2}sec^{-1}$ and a gamma dose of 500 R/hr. The monitor remained in this position for 56 days and during this time the NBS Reactor cycled through six start-ups and shut-downs. Following the removal of the monitor from the reactor, the exposed film, 2.69 m in length, was processed (etched) to optically reveal the latent track density. The film was etched in a 6.5 N NaOH solution at 50 °C for 50 minutes, rinsed in distilled water and air dried. The film contained a 12 μm gelatin layer on one surface and required a second etch in a 1:1 mixture by volume of ethanol and 6.5 N NaOH at 55 °C for 5 minutes to remove the gelatin. Next, the track densities were counted manually using an optical transmission microscope and the optical densities were measured with the aid of an image analyzing microscope. The variation in both track density and optical density show an exact correlation with the reactor power out put as determined by the monitors in the NBS Reactor control room and log (Figure 1).

Additional tests and evaluation of the monitors in known neutron fields have been made in order to determine the monitor's response to field changes. Some of these tests have been conducted with a highly thermal neutron beam from one of the NBS Reactor beam tubes. The monitor was placed in the beam and the intensity of the beam recorded with a fission chamber. The beam intensity was then changed by means of lead attenuators for fixed periods of time. The film was removed from the monitor and etched. The track densities in the three ^{235}U channels and ^{252}Cf channel was counted along the length of the tape and the variations in track densities matched exactly the changes in neutron measured with the fission chamber (Figure 2). A similar study is underway using a ^{252}Cf neutron source, to relate the track density of the ^{238}U and ^{237}Np channels to changes in neutron intensity.

FIELD TESTING OF THE MONITOR

The final phase of evaluating the monitor was actual field testing in operating nuclear power facilities. For this test, two Pressurized Water Reactors (PWR) were chosen on with a net power output of 790 MWe and the other with 535 MWe. In each case, the monitors were installed in a location above the head of the reactor instead of in a neutron detector well. The monitors in both cases were positioned to receive a neutron flux of $1x10^6$n $cm^{-2}s^{-1}$ and a gamma dose of 500 Rhr^{-1}.

References

[1] Fleischer, R. L., Price, P. B. and Walker, R. M., Nuclear Tracks in Solids: Principles and Applications, University of California Press, Berkeley (1975).

[2] Weidenbaum, R., Lovett, D. B. and Kosanke, H. D., American Nuclear Society Transactions, 13 pp. 524-526, (1970).

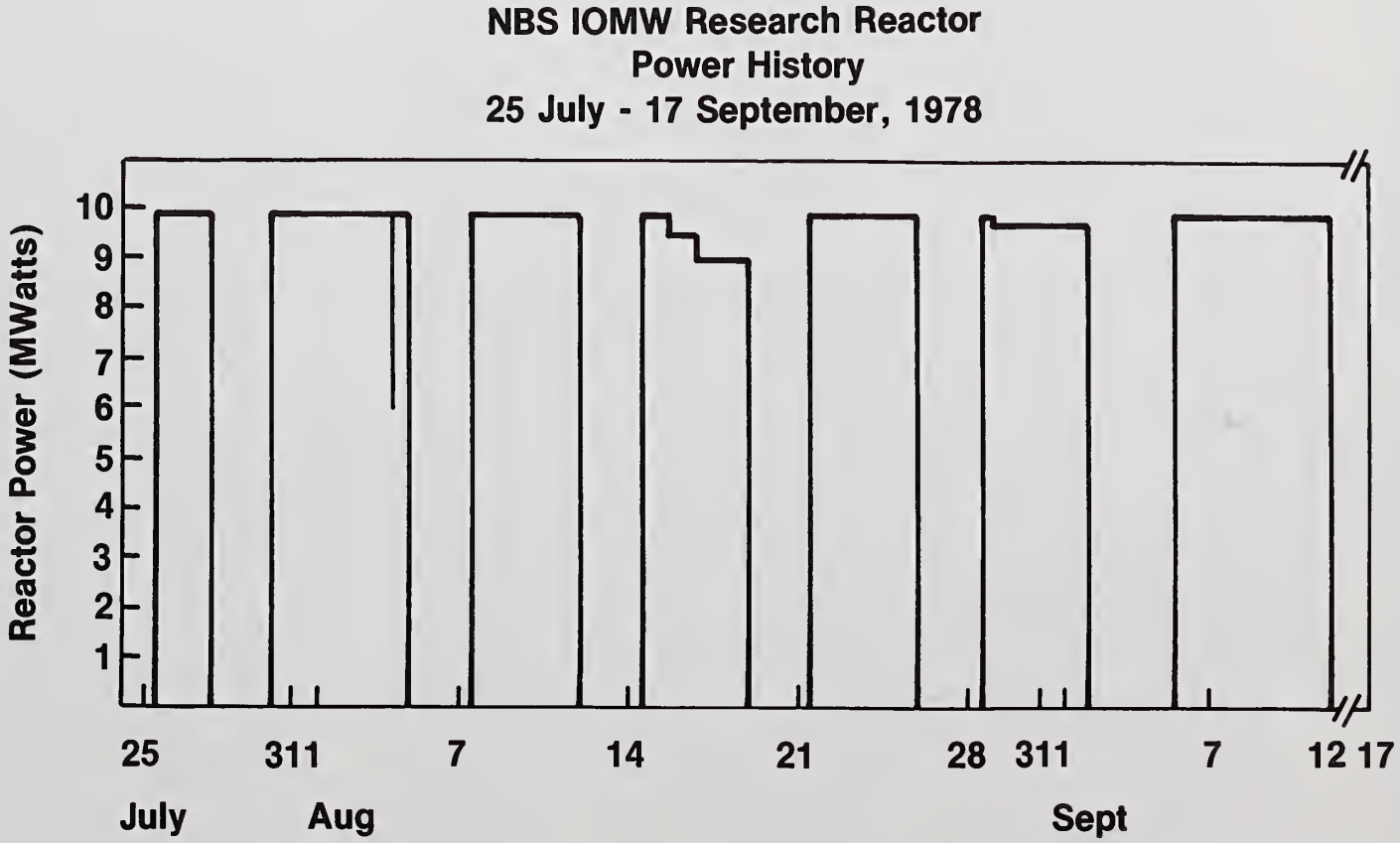

Figure 1. The Power History of the NBS Research Reactor from 25 July - 17 September, 1978 obtained with the Track-Etch Monitor

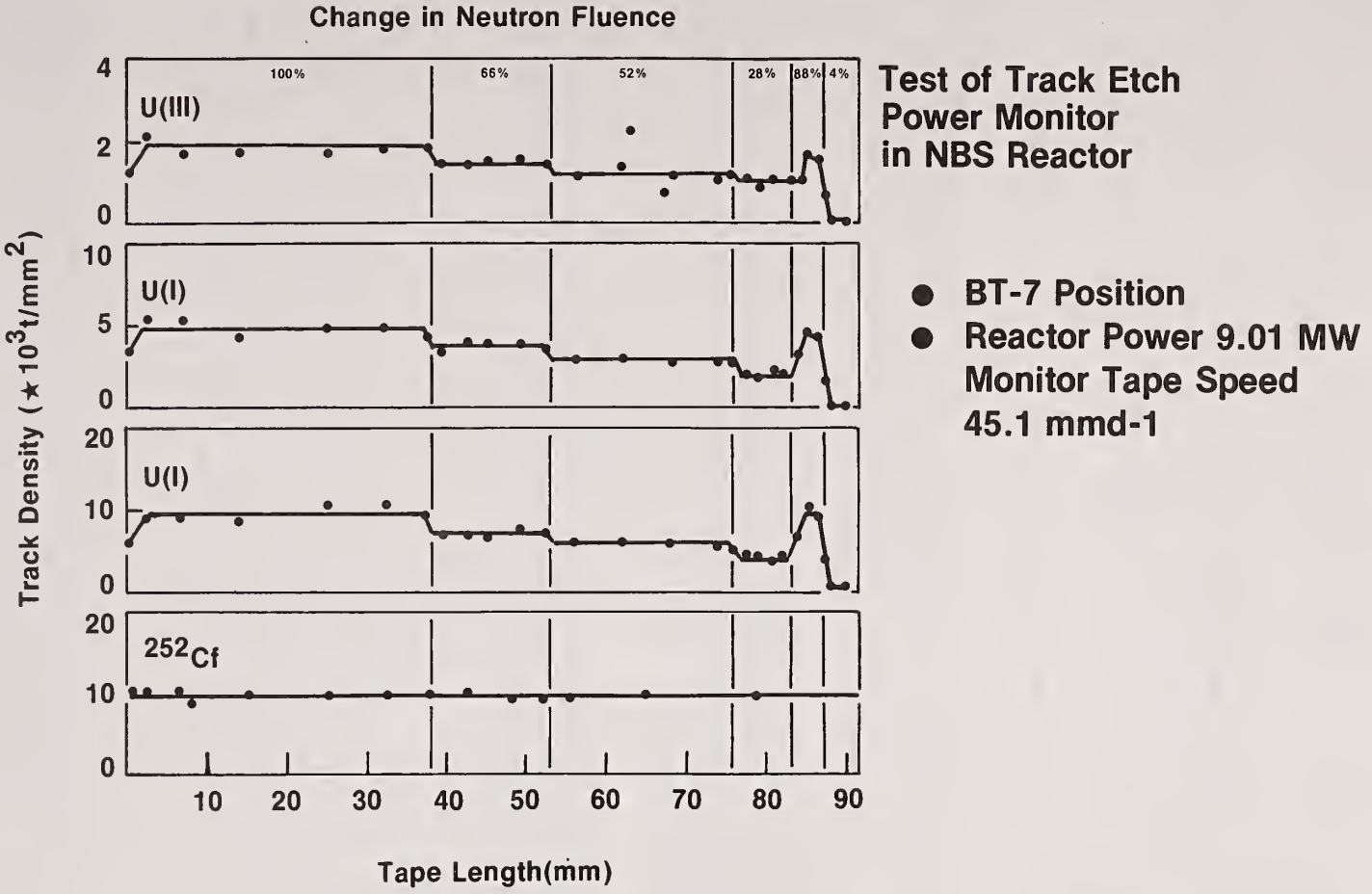

Figure 2. The Change in Track Density of the Three ^{235}U Foils as the Neutron Flux is Varied

Discussion:

Stirling (AEC):
If the reactor has to be shut down to remove the monitor, how can it be a timely warning of a diversion strategy? It will be at least 18 months after that point.

Carpenter (NBS):
That is true for the US power reactors that were used in this evaluation. However, this particular monitor was also placed in a CANDU facility. In this case, they were placed in a neutron detector well where one could retrieve it without having to shut the reactor down.

Stirling:
That's the point. You've really got to have it in a place where it can be removed without having to shut it down so late.

Carpenter:
That's correct

Schleicher (EURATOM):
How long does it take to evaluate the films in order to draw conclusions?

Carpenter:
At present, the processing time is short. That is, about 45 minutes to etch the films and about two to three hours to read a 50 foot tape, using an optical densitometer.

Menlove (LASL):
If there is a power outage during operation of the monitor, what is the result?

Carpenter:
The Cf source will continue to spontaneously fission and you will get a dense track area in that channel. If the monitor is still in a neutron field, the other channels will also be producing high trace densities. You then have to worry about interpreting the length of time the monitor was out from the track density. It is line time, so that does give it some disadvantages.

Green (BNL):
Just so that people won't be misled by a previous statement, this device has been under development by the IAEA in cooperation with, initially, ACDA, and now through the U.S. support program. The IAEA has had a long-standing interest in using this device for independent verification and, therefore, they have requested a field test of the device. That is the work that Dr. Carpenter is assisting them with.

IRRADIATED FUEL MONITORING BY CERENKOV GLOW INTENSITY MEASUREMENTS

by

E. J. Dowdy, N. Nicholson, and J. T. Caldwell

ABSTRACT

Attribute measurement techniques for confirmation of declared irradiated fuel inventories at nuclear installations under safeguards surveillance are being investigated. High-gain measurements of the intensity of the Cerenkov glow from exposed assemblies in water-filled storage ponds are promising for this purpose. Such measurements have been made of Materials Testing Reactor plate-type fuel assemblies and Pressurized Water Reactor pin-type fuel assemblies. The measured intensities depend on cooling times as calculations predict.

INTRODUCTION

Confirmation of declared irradiated fuel inventories in storage ponds of nuclear installations under safeguards surveillance and consistency checks of repeated inspections are responsibilities of both domestic and international safeguards inspectors. Currently, no fieldable hardware exists for carrying out such inspections, but inventory verification techniques are being investigated vigorously. Under the US program for technical assistance to international safeguards, we are investigating several approaches to spent fuel attribute measurements that were identified as promising in our earlier work.[1] The criteria used for selecting promising techniques included ease of implementing the technique, simple interpretation of the measurement data, and minimal impact on the facility operator's routine schedule. Strict adherence to these criteria precludes any movement of the fuel assemblies. In addition, simple interpretation of the measurement data precludes sampling of nuclear radiation fields above the assemblies, as such data interpretation requires unfolding algorithms.*

The most promising technique satisfying our criteria is based on measuring the intensity of the Cerenkov glow resulting from the interaction of the radiation from fission products in the assemblies with the cooling water in the storage ponds. Currently, International Atomic Energy Agency inspectors visually confirm the movement and storage of freshly exposed fuel assemblies during refueling operations, when the Cerenkov glow from such intensely radioactive assemblies is visible. Although shortly thereafter the glow is not visible to the unaided eye, electronic light amplification renders the low light levels measurable. Because water has a very small attenuation coefficient for visible and near-ultraviolet (uv) light,[2] the measurements can be made from above the storage pond surface, obviating the introduction of equipment into the pond. For the standard vertical assembly storage, the penetrations in the upper mechanical structure of the assembly serve as Cerenkov light channels, allowing sampling of the nuclear radiation intensity to be much deeper than the top of the fuel assembly. The Cerenkov light intensity measurement is thus much less susceptible to crosstalk among adjacent assemblies than are nuclear radiation intensity measurements made at the tops of the assemblies.

---

* Such was our experience in interpreting results of thermoluminescent dosimeters (TLD) measurements of the Omega West Reactor fuel elements made at the same time as the Cerenkov measurements. TLD results will be included in a separate report.

The problem of crosstalk among assemblies has made insitu measurement results suspect in the past; it sometimes has been handled by moving an assembly from the normal storage rack to a location in the spent fuel storage pool where the assembly is isolated from the remainder of the spent fuel. Fuel movement is usually possible in the storage ponds at reactor sites, but the Away From Reactor (AFR) storage facilities, like the General Electric Morris facility,[3] probably will not accommodate such movement because the cover water is not deep enough to allow extraction of an assembly for passage over the remaining assemblies.

Cerenkov light intensities can be measured in several ways. We have concluded preliminary tests of the technique using imaging instruments that included a silicon-intensified target (SIT) video camera, an intensified silicon-intensified target (ISIT) video camera, a prototype hard-film camera that incorporates a microchannel plate image intensifier, and a standard hard-film camera with uv-transmitting lenses. Images of both Materials Testing Reactor (MTR) plate-type fuel elements from the Los Alamos Scientific Laboratory (LASL) Omega West Reactor (OWR) and commercial Pressurized Water Reactor (PWR) pin-type assemblies from the Zion Nuclear Station have been made. The Cerenkov intensity was quantified by photometric measurements of selected bright spots on the recorded images corresponding to the water-filled interstices of the assemblies. For this report, only measurements made with the SIT video camera are included. Results of earlier measurements using the ISIT camera, the microchannel plate image intensified film camera, and the standard camera with uv lenses are contained in a separate report.[4]

THEORETICAL BACKGROUND

Electromagnetic Cerenkov radiation is emitted whenever a charged particle passes through a medium with a velocity exceeding the phase velocity of light in that medium. In water, the phase velocity of light is about 75% of the value in vacuum. Any electron passing through water and having a $\geq$0.26-MeV kinetic energy is thus a source of Cerenkov radiation. Irradiated fuel assemblies are a prolific source of beta and gamma rays and neutrons. All three types of emissions can produce Cerenkov light.

Considering the normal fuel rod cladding, we assume that few beta rays escape directly into the pond water and thus that beta rays are not a significant direct source of Cerenkov light. It is possible that electron bremsstrahlung from energetic beta rays interacting in the fuel rods could be a significant source of gamma radiation escaping into the pond water. In the water, energetic gamma rays undergo pair production or Compton scattering to produce $\geq$0.26-MeV electrons. Neutrons may undergo H(n,γ) reactions in the water and produce Cerenkov light through interactions in the water with the 2.23-MeV capture gamma rays.

The most significant production of Cerenkov light is from high energy fission fragment-decay gamma rays that penetrate the cladding. The number of Cerenkov photons generated from gamma rays of any energy passing through water can be calculated. Such calculations have been made and the results have been verified by experimental measurements with several radioactive gamma-ray sources. One calculation result is shown in Fig. 1. In this calculation, we assumed that the gamma rays must penetrate the equivalent of 5 mm of uranium before entering the water, thereby accounting for typical self-attenuation of the fuel and attenuation of the cladding.

Only Cerenkov photons in the visible range of 4000-6000 Å were considered. The calculations indicate that Cerenkov light production is negligible for gamma rays with $E \leq 0.6$ MeV and rises steeply with greater gamma-ray energy, reaching values of 50 or more Cerenkov photons per gamma ray for $E \geq 2$ MeV.

We have calculated Cerenkov light intensity as a function of exposure and cooling time. We used ^{235}U thermal fission data and included all significant fission fragment gamma activities giving rise to gamma rays with $E \geq 0.6$ MeV. Using 1 MWD (megawatt-day) = 2.85×10^{21} fission events and assuming that a total exposure time for 30 000 MWD/MTU

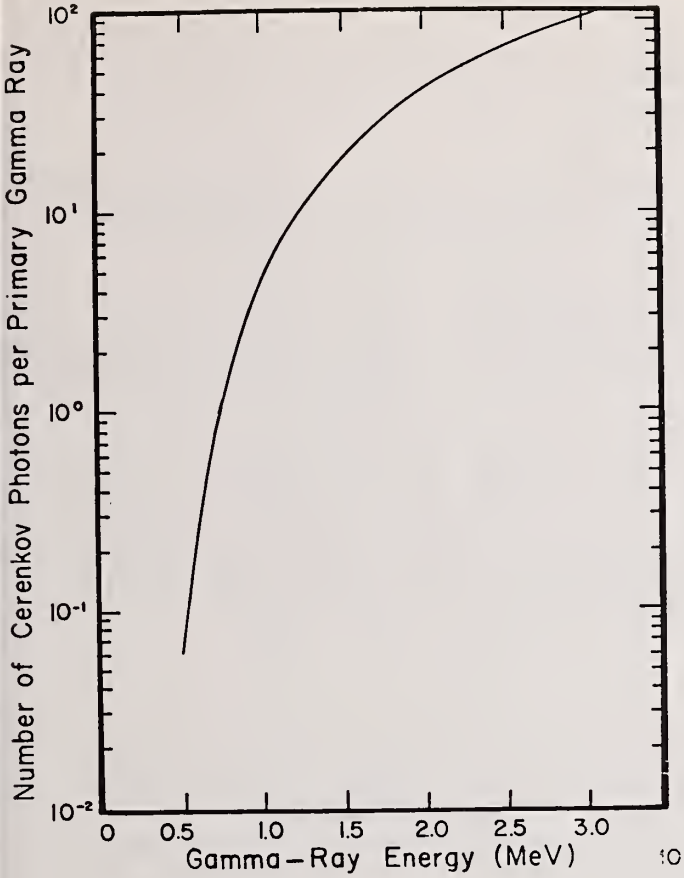

Fig. 1. Cerenkov photon production in water as a function of gamma-ray energy (photon wavelengths are 4000-6000 Å). Gamma rays are emitted behind 5-mm uranium-equivalent shielding.

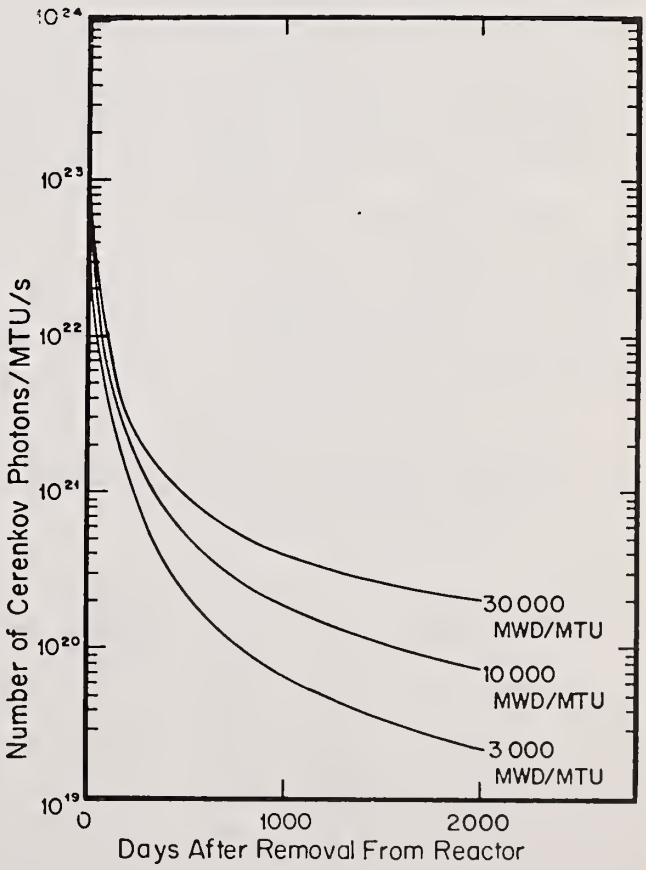

Fig. 2. Cerenkov photon production in water between 4000 and 6000 Å as a function of the exposure and cooling time of irradiated fuel.

(megawatt days per metric ton of uranium) is 10^3 days and that no beta emissions contribute to the Cerenkov production, the results for the calculated Cerenkov light intensities are shown in Fig. 2. Immediately after withdrawal from the core there appears to be little difference between high- and low-exposure material. However, at long times after withdrawal there is a nearly linear dependence on burnup.

From 10 000 to 30 00 MWD/MTU exposure material, we expect neutron emission rates of $\sim 10^7$ to 10^9 n/s/MTU. These rates generate Cerenkov light $\sim 10^9$ to 10^{11} photons/s/MTU by the $^1H(n,\gamma)$ reaction, which is negligible compared with the fission fragment gamma-ray induced source.

The information obtained from a Cerenkov measurment is burnup-related in that the absolute Cerenkov light level and its decay with time are related to burnup. Successful diversion either by substitution of dummy fuel assemblies or by incorrectly stating burnup would be difficult as long as the Cerenkov light intensity was measured accurately.

The spatial extent of the Cerenkov glow surrounding an isolated irradiated assembly in water probably will be determined by the gamma radiation from the assembly's outer pins. The 10th-value-layer thickness of water for 1.0-MeV gamma rays is ~36 cm, which is a reasonable estimate of the Cerenkov "halo" around an isolated point source. Fission product radiation from an irradiated fuel assembly's inner pins, however, must penetrate a much denser composite of fuel, cladding, and interstitial water, which greatly reduces crosstalk among assemblies in either regular or high-density storage racks.

EXPERIMENTAL PROCEDURES

Because deep sampling (for minimizing crosstalk among assemblies) of the fission product radiation is accomplished by detecting the Cerenkov radiation coming from deep within the assembly, the optical axis of the Cerenkov measuring instruments should be aligned with each assembly axis. The SIT video camera was aligned this way for the spent fuel measurements at the LASL OWR. The SIT video camera was clamped to the spent fuel storage pond bridge railing for the measurements of the Zion Station PWR assemblies; the bridge was used to transport the camera above the storage racks. Because each storage location has a larger cross-sectional area than that of an assembly, assembly alignment was nonuniform. As shown in the results section, the lack of perfect alighnment does not obviate the attribute measurements, but it leads to a presumed decrease in precision.

The experimental configuration of the five fuel elements used in the OWR measurements are shown in Fig. 3. The same calculational procedures used to generate the curves in Fig. 2 were used to estimate the inventory of fission products that give rise to Cerenkov photons. The fuel elements used in this test included three that were reinserted in the reactor for a second exposure after having been removed following an initial burnup. This two-step burnup program adds some complexity to both Cerenkov intensity calculations and the subsequent interpretations. The results of the calculations are given in Table I.

TABLE I

EXPOSURE HISTORY AND CERENKOV INTENSITIES FOR OWR SPENT FUEL ELEMENTS ON 9/18/78

	#1			#2			
Element Number	In	Out	Exposure (MWD/MTU)	In	Out	Exposure (MWD/MTU)	Cerenkov Intensity (photons/s/MTU)
0-355	?	10/73	38 728	--	---	-----	2.9×10^{20}
0-380	08/73	07/76	35 200	11/77	02/78	4 800	2.5×10^{21}
0-381	08/73	07/76	35 200	11/77	02/78	4 300	2.5×10^{21}
0-382	08/73	08/76	35 400	11/77	02/78	4 053	2.3×10^{21}
0-396	01/75	04/78	39 754	--	---	-----	5.4×10^{21}

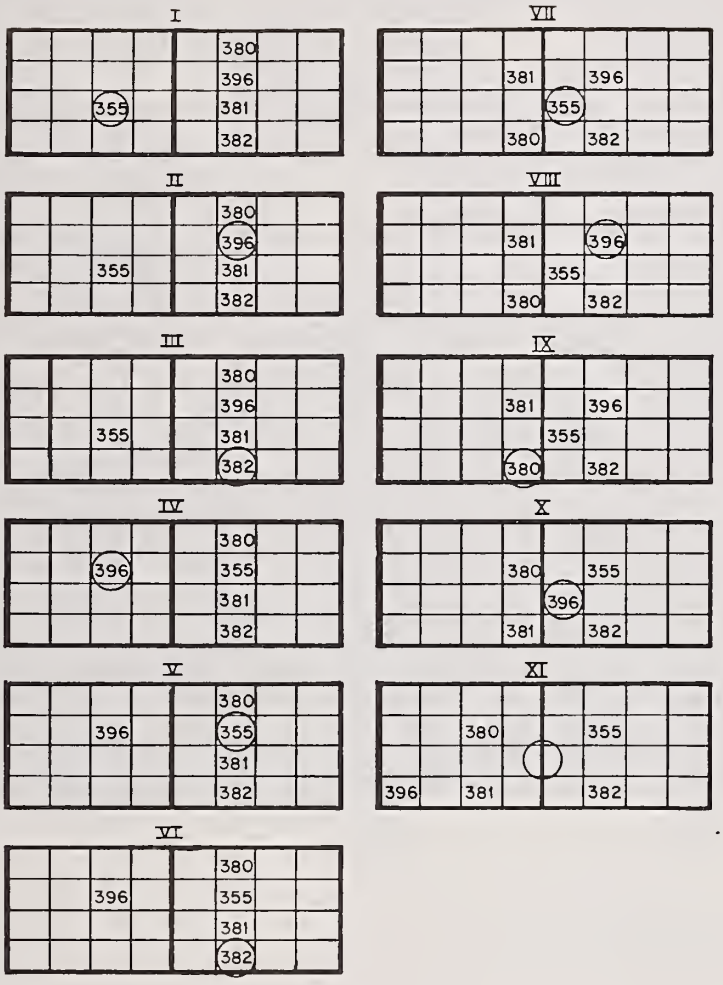

Fig. 3. Configuration of the MTR-type fuel elements used in the measurements at the OWR. Circle indicates the camera axis orientation.

At the Zion station, two complete rows of the storage pond were imaged through about 8 m of water. These rows contained 28 fuel assemblies, 15 of which contained the standard PWR burnable poison pin cluster. The exposure and discharge dates of each are given in Table II. After assemblies in the storage racks were imaged, one recently discharged assembly was extracted vertically and the entire assembly was imaged from the edge of the storage pond. This was done to confirm that radiation profiles also can be obtained using the Cerenkov intensity measurement technique. Radiation profiles have been used[5] with point measurements of fission product isotopic ratios to estimate assembly burnup.

TABLE II

IMAGED ZION IRRADIATED FUEL

Assembly Number	Discharge Date	Exposure (MWD/MTU)
A 06 P[a]	03/76	19 102
A 18 P[a]	03/76	19 290
A 30 P[a]	03/76	19 224
A 54 P[a]	03/76	18 821
B 01 R[a]	09/77	30 885
B 13 R[a]	09/77	31 228
B 25 R[a]	09/77	31 009
B 37 R	09/77	27 923
B 49 R[a]	09/77	29 875
B 61 R[a]	09/77	30 551
A 09 R	02/78	27 163
A 21 R[a]	01/77	20 539
A 33 R[a]	01/77	18 974
A 45 R[a]	01/77	19 728
A 57 R[a]	01/77	19 723
B 04 P	02/78	30 439
B 16 P	02/78	28 969
B 28 P	02/78	28 978
B 40 P	02/78	30 221
B 52 P[a]	02/78	30 174
B 64 P[a]	02/78	31 491
C 12 R	09/78	33 482
C 24 R	09/78	38 484
C 36 R	09/78	33 976
C 48 R	09/78	35 536
C 60 R	09/78	33 530
C 63 P	09/78	38 565
C 64 P	09/78	38 636

[a]Contains poison pin cluster

Images of the fuel assemblies were recorded on video tape as a convenience for subsequent off-line analysis. On-line digital analysis of the analog video signals is possible with commercially available hardware. The video tapes were replayed, and individual frames were grabbed and stored on a video disk. Each selected single frame on the disk was displayed in conventional 512-line US television format on a cathode ray tube (CRT) with raster address using xy crosshairs. The raster address size was a single pixel. An associated electrometer indicated the electron current forming the intersection pixel that is directly proportional to the pixel brightness. The brightness of pixels representing the Cerenkov glow in the interstitial water was determined in this way. To obtain a relative real-image brightness from the measured pixel brightness, the SIT camera lens aperture size variable was removed by normalizing all brightness to a common f/stop value.

RESULTS

Figure 4 shows the video monitor display of a typical single video frame (1/30 s) of OWR fuel elements. Figures 5 and 6 are the comparable displays for PWR assemblies with the

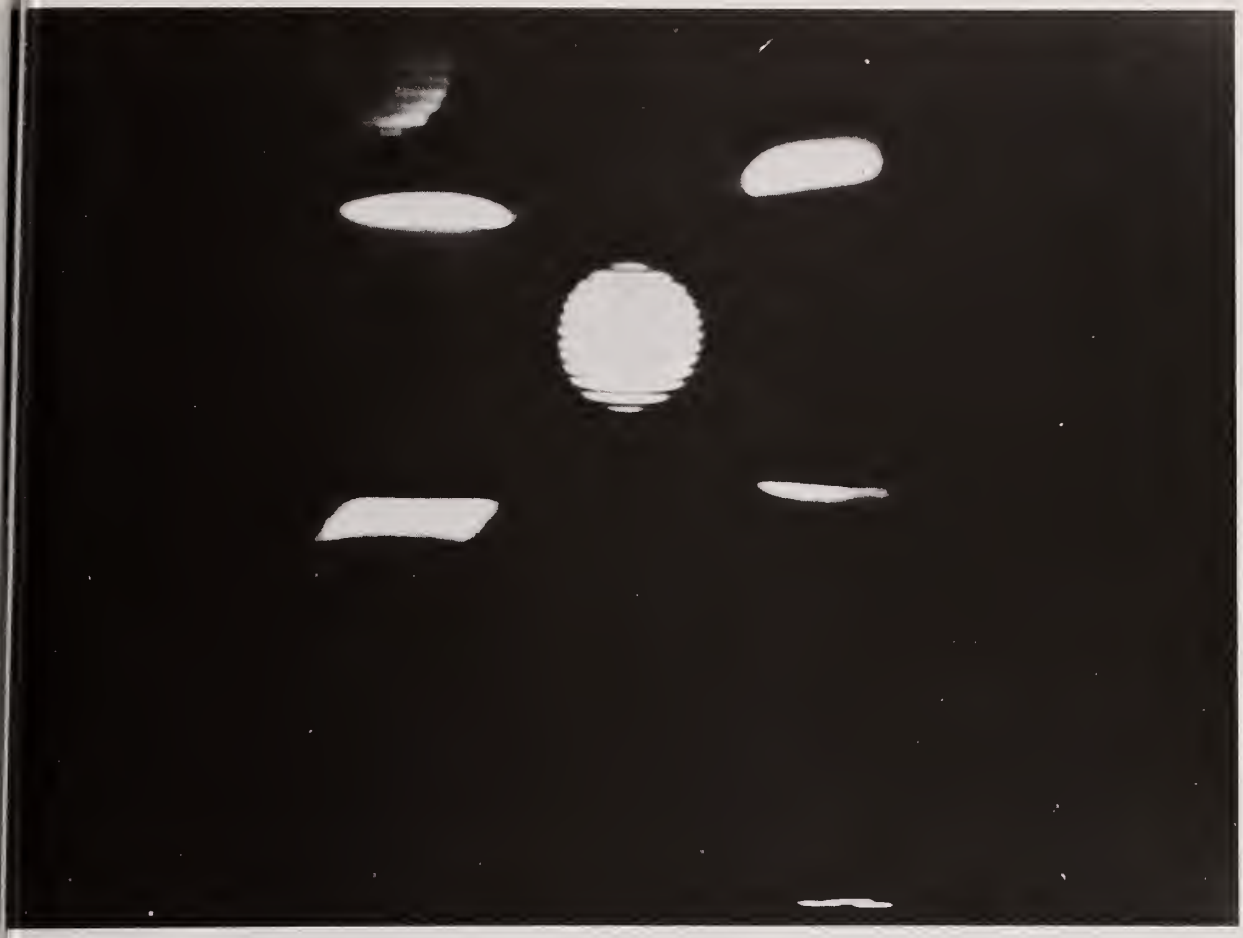

Fig. 4. Cerenkov image of OWR elements. Individual plates of each element are discernible.

central assembly in Fig. 5 containing a poison pin cluster and that in Fig. 6 being an unpoisoned PWR assembly. The images resulting from the last two cases are obviously different, precluding confusion between the two.

The OWR and PWR data were handled in different but equivalent ways. For the OWR data, we compared each element's relative measured Cerenkov intensity with its calculated value for the fuel element configurations in which the element of interest was relatively isolated. These intensity values were all normalized to unity for the least radioactive element, No. O-355. The results are given in Table III. A comparison of the calculated intensity values and the measured intensity values supports our claim that the Cerenkov intensity variation with exposure and cooling time is calculable.

TABLE III

CERENKOV INTENSITIES OF OWR FUEL ELEMENTS

Configuration Number[a]	Element Number	Calculated Normalized Intensity	Measured Normalized Intensity
I	O-355	1.0	1.0
V	O-355	---	1.1
VII	O-355	---	1.9
IX	O-382	7.9	5.4
III	O-380	8.6	7.6
V	O-396	18.6	20.6

[a]Refers to Roman numeral designation of configuration shown in Fig. 3.

The last column in Table III contains three entries for element No. O-355. The first entry is the normalized intensity for the isolated element. The second entry is the measured normalized intensity of the element #O-355 when two adjacent storage bins were occupied by elements with intensities approximately eight times greater than that of element No. O-355. The crosstalk amounts to about 10% in this case and corresponds to placing elements with comparable exposure, but with cooling times of 2 and 5 years, in adjacent storage locations. The third entry is the measured normalized intensity of element No. O-355 when four diagonal storage locations were occupied by elements with average intensities more than 10 times greater than that of element No. O-355. In this case, the crosstalk amounts to 90% of the measured intensity of the weakest element. However, this case corresponds to placing elements with comparable exposures, but with cooling times of 5 months and over 5 years, in such proximity.

The results of relative Cerenkov intensity measurements of the Zion PWR irradiated assemblies are shown in Fig. 7. The solid curve in the figure is the calculated intensity versus cooling time for an exposure of 30 000 MWD/MTU. We took no account of the fact that these assemblies had exposures different from 30 000 MWD/MTU because we did not expect the measurement precision in this particular test to be sufficient to distinguish among assemblies with different exposures. The Cerenkov photon intensities from these assemblies depend on cooling time, as the calculations predicted.

An additional capability of the Cerenkov photon intensity measuring technique is the rapid profiling of the radiation intensity. At the Zion station, we requested that a single assembly, No. C-63P, be extracted from the storage rack. The SIT video camera was set up on a tripod at one end of the pond, and video images of the extracted element were recorded on video tape. A typical frame of the video image was video-disk recorded and is

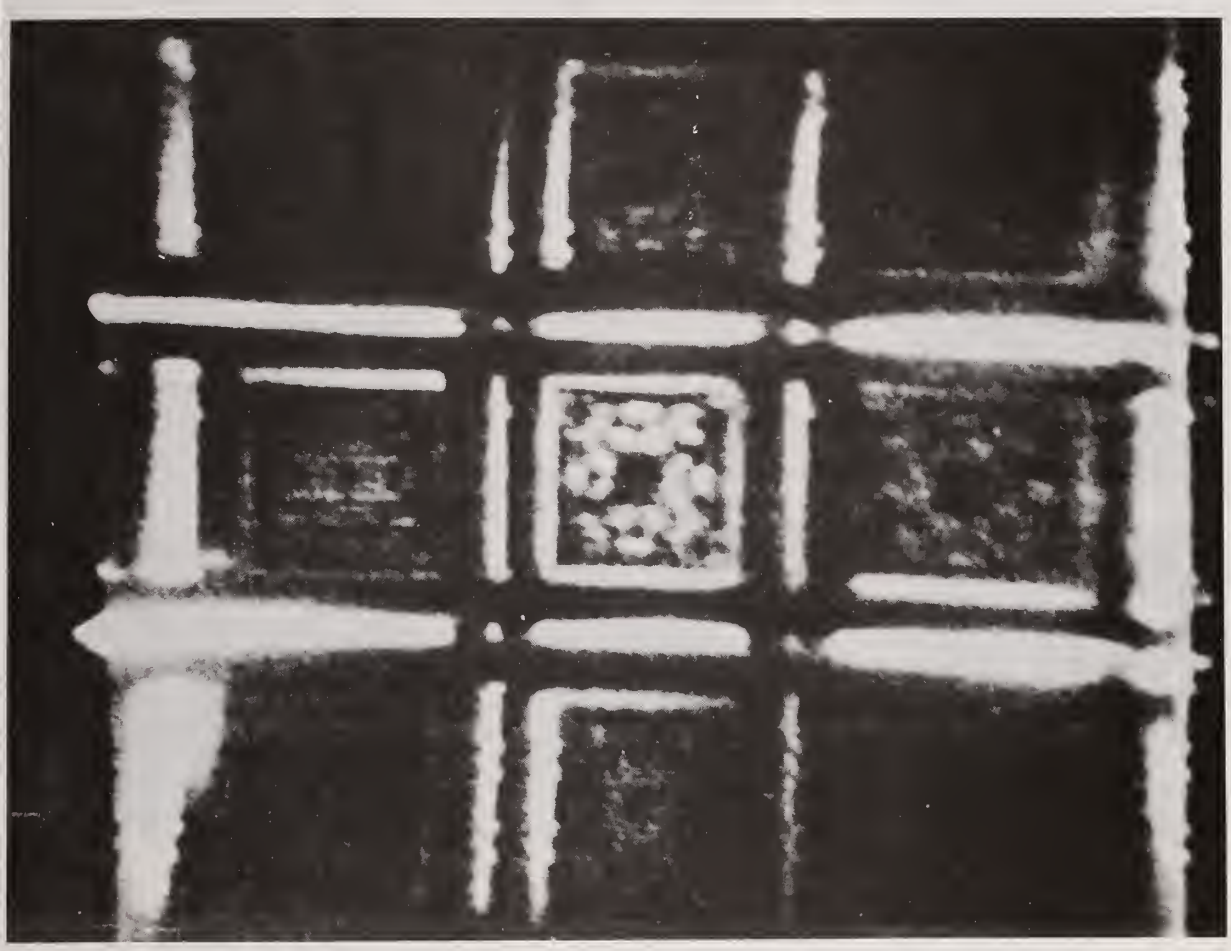

Fig. 5. Cerenkov image of a PWR assembly containing a burnable poison pin cluster. A typical "rosette" light pattern results.

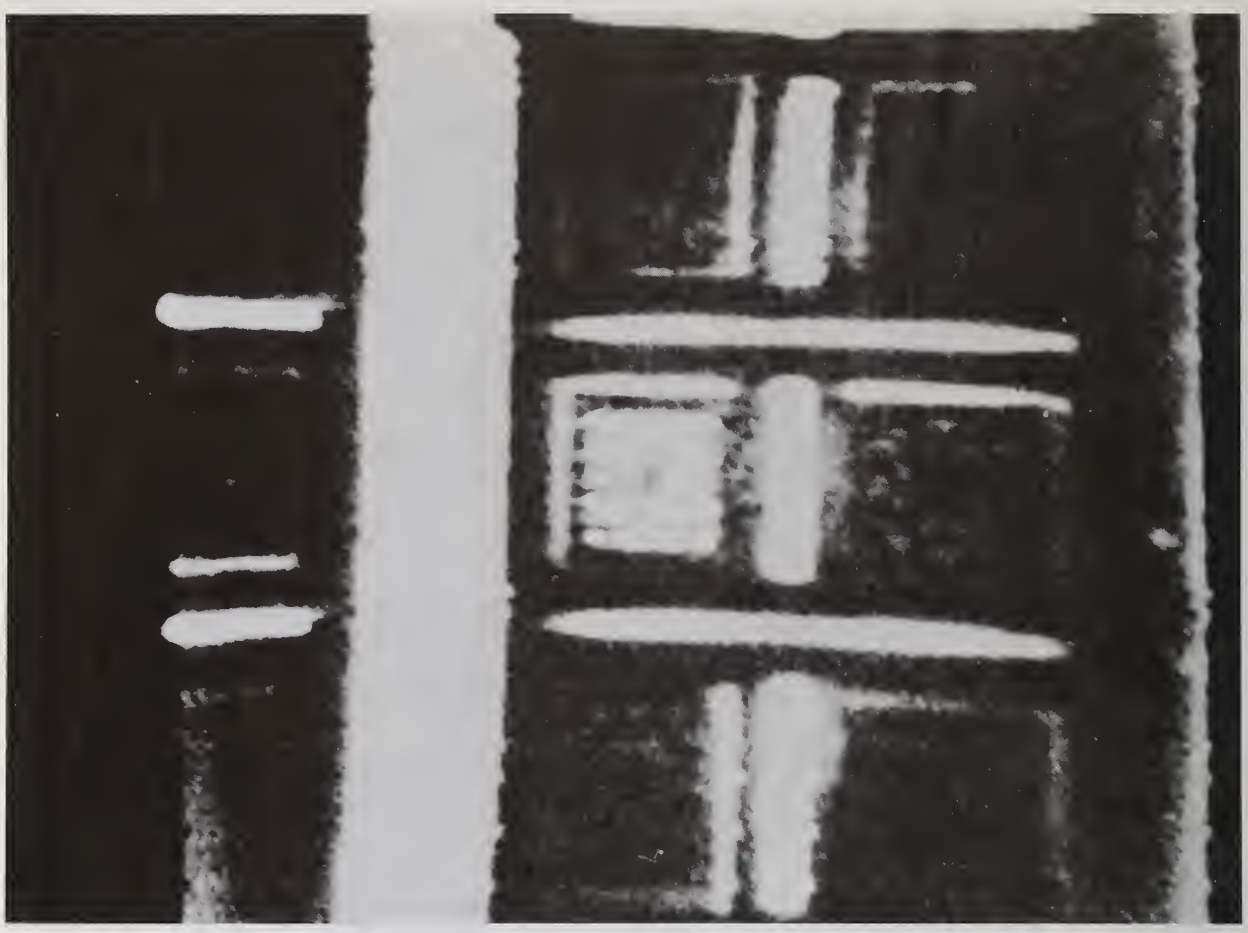

Fig. 6. Cerenkov image of an unpoisoned PWR assembly. The bright light from the poison pin holes is clearly discernible.

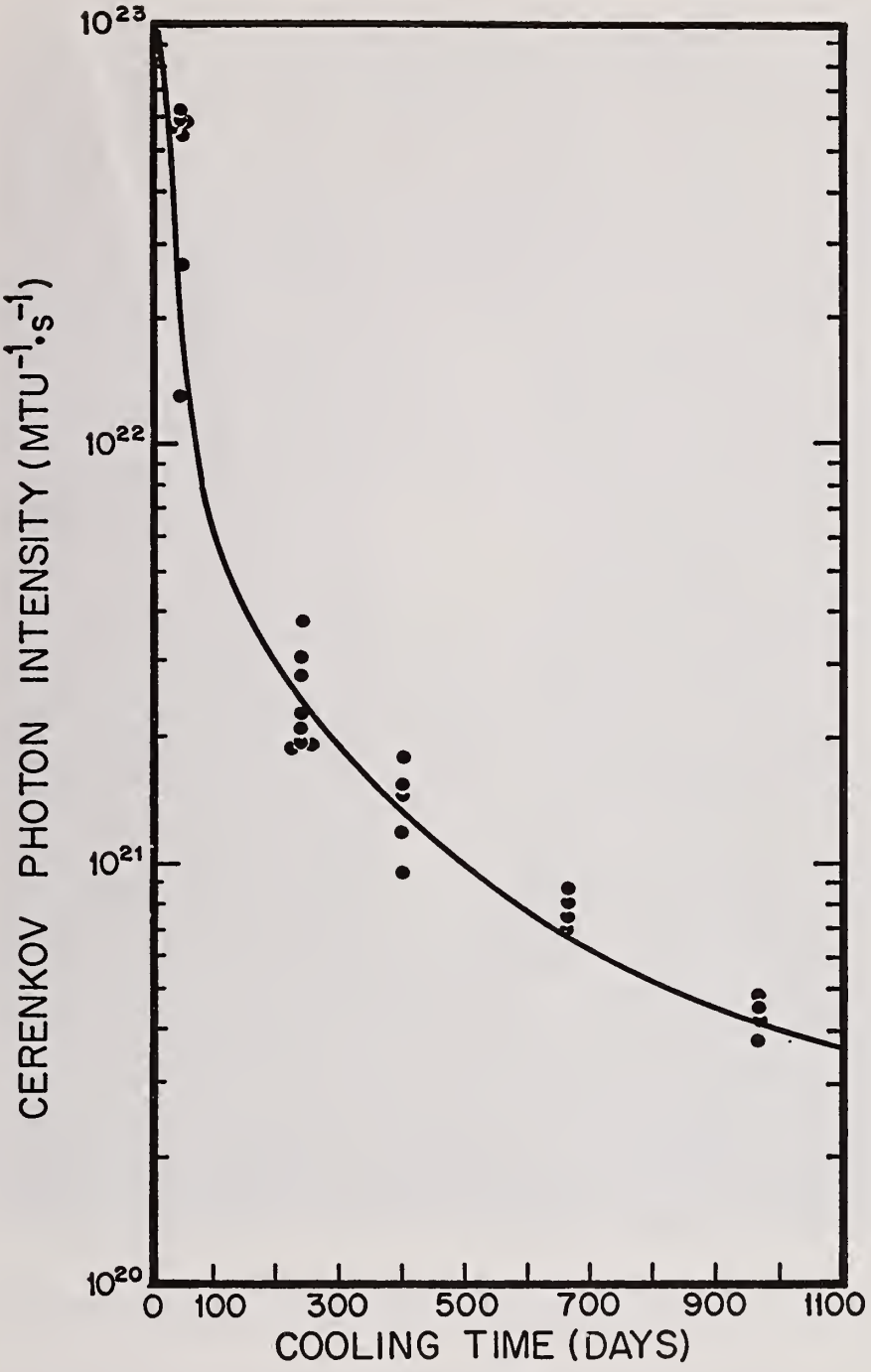

Fig. 7. Cerenkov intensity measurements of the Zion assemblies normalized to the calculated value

shown in Fig. 8. The video-disk-recorded image was displayed on the CRT with the xy crosshair raster address. With the x-axis crosshair disabled, the y-axis crosshair provides the axial Cerenkov intensity profile. This automatic trace is shown in Fig. 9. Although no detailed comparisons have been made with other measurements, this profile is typical of such PWR assemblies.[5]

The video editor used for the Cerenkov intensity determinations and the profile display also can provide three-dimensional (x,y,brightness) isometric displays of single video frames from a video disk. Isometric displays of OWR element arrays and PWR assembly arrays are shown in Figs. 10 and 11, respectively. This isometric feature was used to rotate the PWR assembly image shown in Fig. 8. The result is shown in Fig. 12 with the assembly structure distinctly noted in the center portion and the radial "halo" of the Cerenkov glow displayed as the monotonically decreasing intensity on either side of the isolated assembly. Measurement of the falloff reveals that the 10th-value-layer thickness is about 25 cm, somewhat less than the 36 cm estimated earlier for 1-MeV gamma rays. Such radial profiling may provide information about cooling time because the fission product gamma-ray spectrum changes with a known dependence on time and the Cerenkov profile is expected to change accordingly.

CONCLUSIONS

We have completed a set of Cerenkov light intensity measurements from two types of spent-fuel assemblies in water-filled storage ponds. We have compared observed light intensity as a function of burnup and cooling time with a simple computational model of the Cerenkov light production process and find reasonable agreement over a dynamic range of three decades. These intensities were measured without moving the stored assemblies from their resident locations. The precision, reproducibility, rapidity, and nonintrusiveness of these measurements make the Cerenkov light technique ideal for systematic attribute measurements on large fractions of (or entire) storage pond inventories.

The present measurements, made using a SIT video camera with off-line video tape analysis, are considered to be proof of the Cerenkov light technique principle. The full capability of the technique will be determined using a high-sensitivity wide dynamic-range photometer with variable field of view coupled to an ISIT video camera. Direct quantification of the Cerenkov intensity will be possible using this equipment. Comparable results are expected from fieldable instruments now under construction. This equipment will consist of telephoto optical lenses, microchannel plate image intensifiers, and 35-mm camera backs with incorporated light meters.

We have demonstrated an additional capability of the Cerenkov light measurement technique: that of obtaining radiation profile maps of the irradiated assemblies rapidly and nonintrusively.

REFERENCES

1. E. J. Dowdy and J. T. Caldwell, Eds., "Irradiated Fuel Monitors: Preliminary Feasiblity Study," Los Alamos Scientific Laboratory report LA-7699, ISPO No. 51 (May 1979).

2. Thomas Woodlief, Ed., SPSE Handbook of Photographic Science and Engineering, Wiley-Interscience, New York, 1973, p. 283.

3. E. A. Grimm, "Design and Operational Characteristics of High-Density Fuel Storage Facilities," Nucl. Tech. 43, 146 (1979).

4. E. J. Dowdy, "Interim Report on Irradiated Fuel Monitors: Cerenkov Detectors," Los Alamos Scientific Laboratory unpublished data, 1978.

5. D. M. Lee, J. R. Phillips, S. T. Hsue, K. Kaieda, J. K. Halbig, E. G. Medina, and C. R. Hatcher, "A New Approach to the Examination of LWR Irradiated Fuel Assemblies Using Simple Gas Chamber Techniques," Los Alamos Scientific Laboratory report LA-7655-MS (March 1979).

Fig. 8. Cerenkov image of a single PWR assembly extracted from the storage rack.

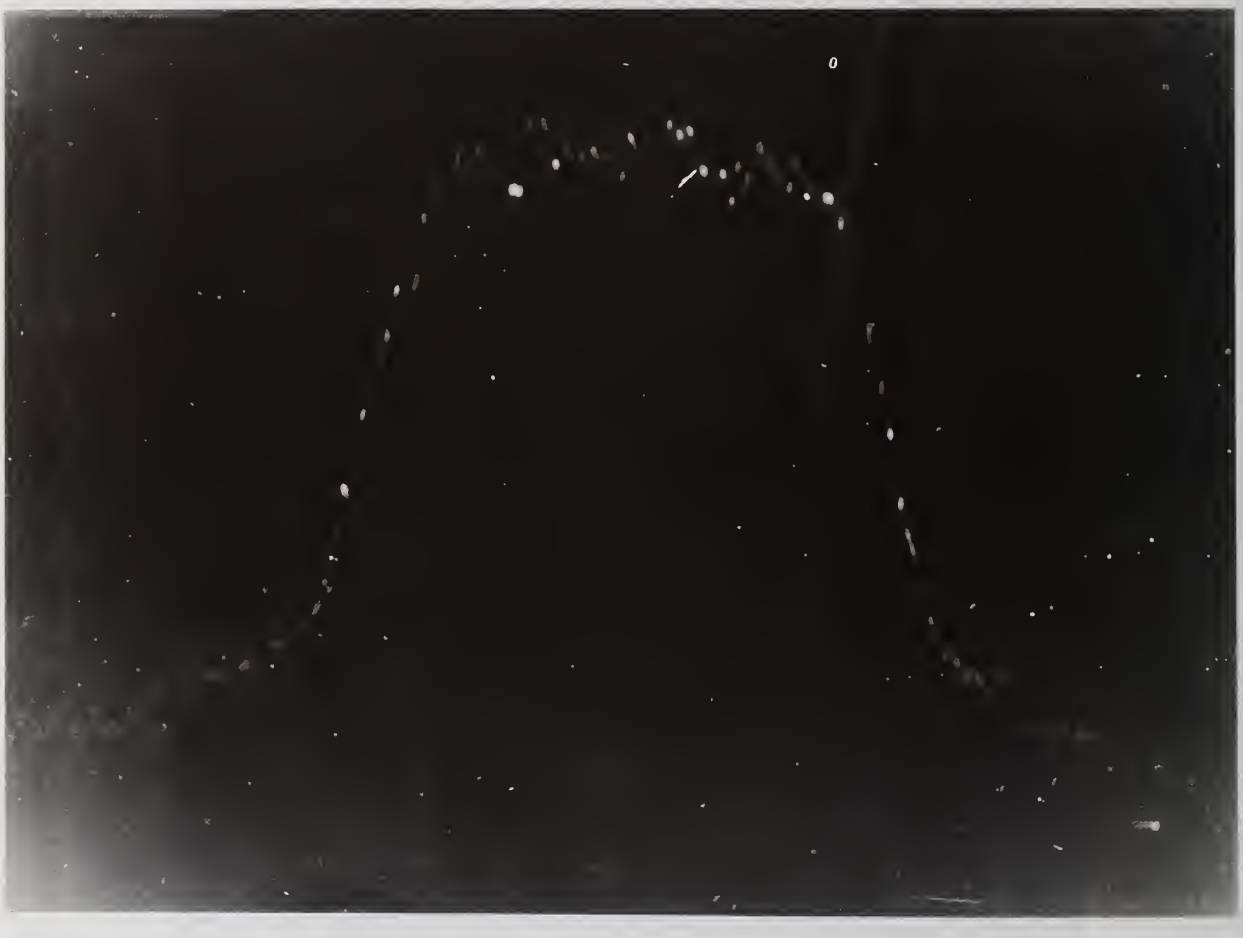

Fig. 9. Axial profile of the Cerenkov intensity of a single PWR assembly. Obtained by analysis of a single video frame (1/30 s).

Fig. 10. Isometric display of the Cerenkov intensity of OWR elements. Light from individual coolant channels of the element with greatest intensity are distinguishable. Light from two adjacent assemblies are also visible.

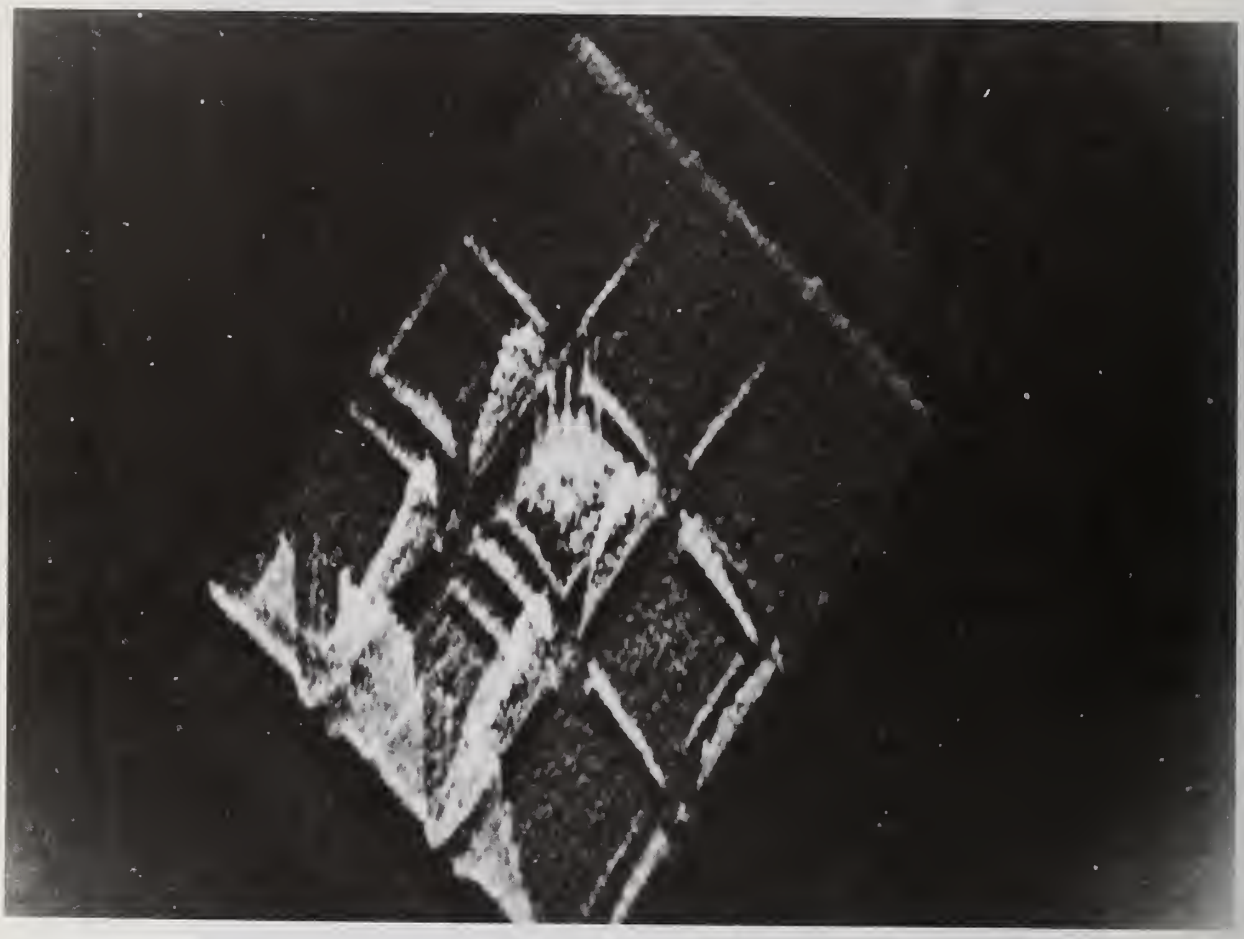

Fig. 11. Isometric display of the Cerenkov intensity of PWR assemblies. Light from the individual coolant holes of the aligned assembly appear as distinct spikes. Interference from adjacent assemblies appears to be negligible.

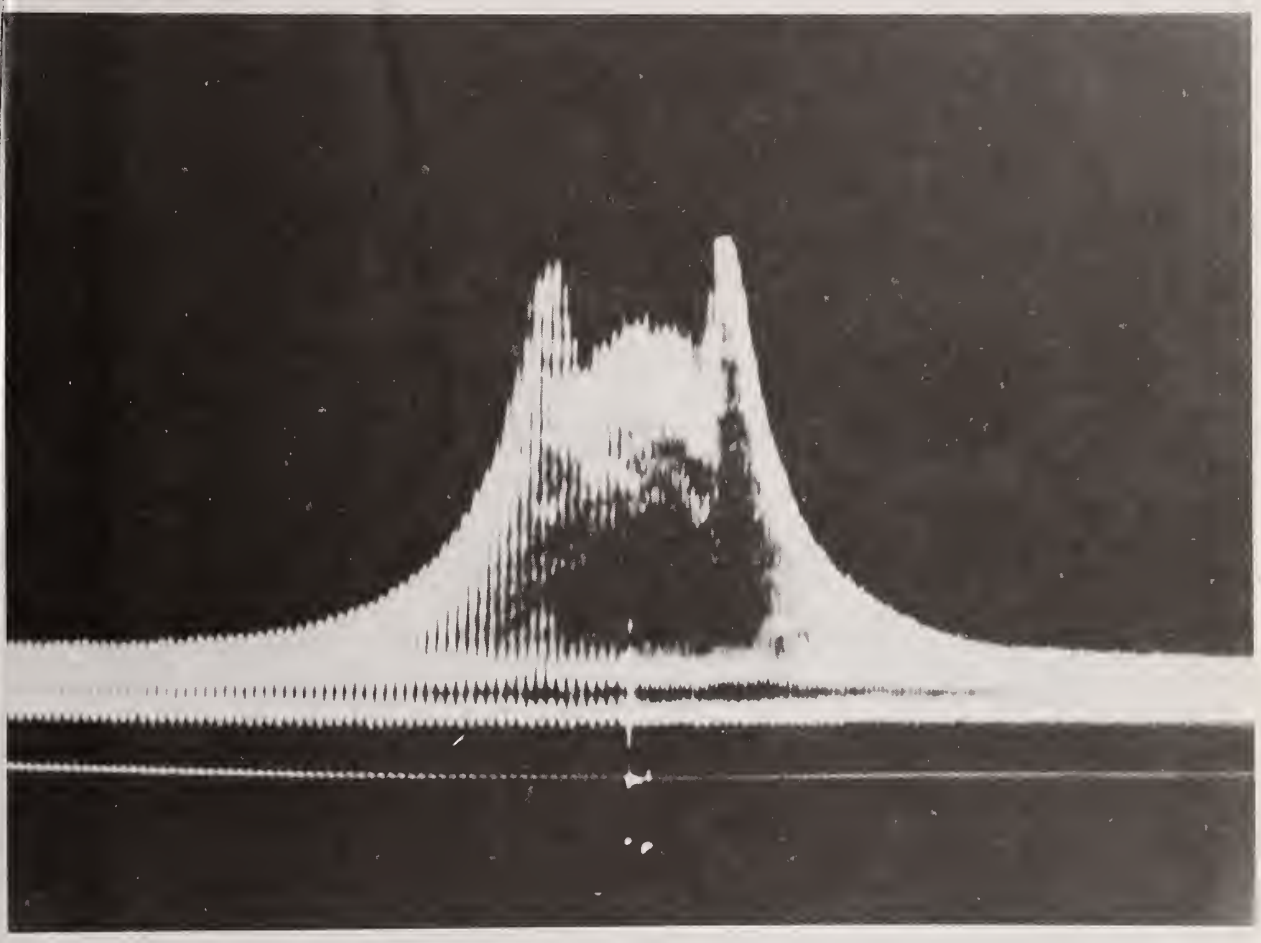

Fig. 12. Radial profile of the Cerenkov intensity of a single isolated PWR assembly. The less intense light in the center portion is the assembly structure.

Discussion:

Persiani (ANL):
Do you see the need to redesign fuel assemblies in order to exploit this technique more effectively? You did say the possibility does exist that you can detect the removal of a few elements within an assembly.

Dowdy (LASL):
From the pictures I showed you of the Zion PWR assemblies, one with the poison pin clusters still in place and one without, one concludes that it would be better if the poison pin clusters could be removed and stored elsewhere. It would also help if there wasn't so much mechanical structure on top. For the PWR assembly there is a problem in determining if a single or a few pins have been removed, because you can't see them all. In BWR assemblies you can see each one of them. I don't know if redesign would be warrented.

Schleicher (EURATOM):
There is a very nice correspondence between the calculated curve you have shown here and the measured data; however, the scatter of the measured data is very different. Is this an indication of unknown error sources, e.g., the water was not clear or not completely even on the surface?

Dowdy:
I suspect that the scatter of the points in the figure is due to the fact that the camera was not aligned over each assembly. Even though the storage racks are dense storage racks, there is still the possibility of canting of assemblies in the storage position. So when you don't align the camera, scatter of results would be expected, and I think the scatter is from non-alignment.

Fainberg (BNL):
Do you think you will be able to say anything about cooling time or intensity, or is it just a very qualitative thing, and not quantitative at all?

Dowdy:
We are anticipating delivering an instrument that will measure the Cerenkov photon intensity. We will recommend that it be used for consistency checks, from inspection visit to inspection visit, or as a relative measurement within a storage pond.

Fainberg:
I understand that you only look right at the top of the pellet.

Dowdy:
You look down from the storage pond surface, but the optical path goes all the way through the assembly, if you are aligned well.

Fainberg:
Isn't the attenuation length for the water somewhere between 1 and 10 meters down at 3,000 angstroms?

Dowdy:
The attenuation coefficient of the water is very high from 3,067 angstroms down to shorter wave lengths. There is obviously a relaxation length problem for any wave length, so the sampling is not uniform along the axis of the assembly.

A Tamper Recorder for Unattended Safeguards Instruments*

by

DOUGLAS C. SMATHERS
Sandia Laboratories, Albuquerque, NM 87185

ABSTRACT

The Secure Counter Panel is an electro-mechanical module which records attempts to tamper with instruments of an unattended safeguards system in a way which cannot be sabotaged or bypassed without leaving obvious evidence of tampering. A number of novel tamper-safing techniques are included in the design, some of which are widely applicable to other safeguards instruments.

KEYWORDS: tamper, unattended safeguards system, safeguards instrument, seal.

INTRODUCTION

Important elements of safeguards systems are the steps taken to meet the threat of tampering with safeguards equipment. While tamper-safing can be important for national safeguards, it is crucial to the success of international safeguards because the threat at the international level is much more severe.

The goal of tampering with a safeguards instrument is to prevent its normal functioning by disabling or bypassing the instrument or by compromising the validity of the data produced by the instrument. Tampering may be overt or covert. During an overt tamper attempt the perpetrator disables the instrument or its alarm reporting elements but makes no effort to conceal observable evidence of tampering. Covert tampering leaves no easily observable evidence that the system has been compromised thereby increasing the time interval between tampering and the discovery of the tampering. The Secure Counter Panel (SCP) is designed to make covert tampering extremely difficult.

In a typical safeguards application, when a tamper attempt is discovered a detailed investigation is begun. The investigation may involve disrupting site operations for costly and time consuming inventory procedures. A tamper recorder should record as much information about safeguards instrument operation and tamper attempts as practical. This information could be used to guide the investigation. The information would help an inspector distinguish between intentional tamper attempts and inadvertent actions.

The SCP is intended to be located within a locked equipment enclosure with the safeguards instruments to be protected. The present design is part of an unattended personnel portal.[1] It records tamper attempts and other selected operating data that cannot be erased without leaving obvious physical evidence of tampering. The SCP includes backup power and continues to monitor tamper attempts and instrument activities during a power outage. The data recorded in the SCP are recovered by visually inspecting or photographing the front panel during periodic visits by an inspector.

---

*This work supported by the U. S. Department of Energy.

[1] D. L. Mangan, "A Personnel Portal for International Research Facilities Safeguards", Nuclear Materials Management, VIII, 674 (1979).

DESIGN FEATURES

The SCP is sealed in a deep-drawn and welded aluminum box with a color anodized finish (Figure 1). Data are recorded on 14 five-digit electro-mechanical impulse counters. Since they register data mechanically, the counters do not lose their data during a power outage. Low-power integrated logic circuits buffer count signals from tamper switches, door sensors, voltage monitor circuits and other instrument control circuits. The logic circuits filter out transient noise pulses and minimize power consumption by forming high power count pulses when control signal transitions or switch closures occur. The logic circuits also limit the count rate for some counters to once every 10 seconds so the counters cannot be reset by counting 99999 times between inspector visits. While this count limit may cause some rapidly occurring events to be miscounted, it is only applied to events like EMERGENCY EXIT where a single count will trigger an investigation. Optical isolators, used on all incoming signal lines, prevent application of voltages to alter functions or damage the circuitry. Current limiting is provided on circuits which sense external switch closures to prevent rapidly discharging the internal battery.

Figure 1. The Secure Counter Panel records tamper events and other operating data.

Events which are almost certainly tamper attempts are recorded separately from events which are abnormal but may not be tamper attempts. Clearly abnormal events are grouped at the top of the panel as SAFEGUARDS ALERTS. A magnetically latched flag indicator, ALERT FLAG, is set whenever one of these conditions occurs. This flag alerts

an inspector that a serious event has occurred since the last inspection. The ALERT FLAG is manually reset with a magnetic switch. Seven counters are grouped as OPERATING WARNINGS. These events are probably not tamper attempts but can be analyzed for suspicious trends. NORMAL PASSAGE and ABORTED PASSAGE events are recorded to indicate if expected normal operations are occurring.

Three LED indicators display the status of the input signals. If an ALERT or WARNING signal is active, a red indicator is illuminated. If none except the equipment door switch is active, the green NORMAL indicator is lit. The indicators are turned off to conserve power except when manually activated with a magnetic switch.

At each inspection, the current number on each counter is compared with the count at the last inspection. While an inspector could write down the counter readings each time, this is an error-prone procedure. Photographing the front panel is a simpler way to make a permanent record of the count data. An identification plate on the front panel uniquely identifies the unit in a photograph.

A power supply and battery within the SCP insure normal functioning for seven days should external power be interrupted. A battery charger maintains a 5 Ampere-hour sealed lead-acid battery on floating charge until power is interrupted. A voltage sensing circuit detects loss of external power and counts the occurrence. Another circuit senses low battery voltage and disconnects the battery before it can be damaged by excessive discharge. The BATTERY DISCHARGED condition is also recorded because after it occurs no tamper monitoring takes place. A power-up reset circuit prevents spurious counts when power is restored.

Several design features minimize the possibility of tampering with the SCP without leaving obvious physical evidence. The color anodized finish makes it very difficult to repair a penetration without leaving an obvious flaw. A stressed glass window covers the counters and will shatter if it is scratched or cut.[2] The glass can only be replaced by removing the cover. A sheet of unstressed glass protects the stressed glass from inadvertent scratches.

Figure 2. Inspecting the integrity of a fiber-optic seal.

The cover is sealed with a fiber-optic seal[3] installed through the cover mounting bolts and holes in the cover and box. The integrity of the fiber-optic seal is inspected with a hand-held illuminator/microscope shown in Figure 2. In addition, tamper switches inside the box sense when the cover is removed. A tilt switch inside the box senses when the box is tipped from its normal attitude.

The signal cable connectors on the rear panel are secured with locknuts inside the box. To avoid additional holes in the box, the STATUS and RESET switches are operated by a magnet through the stressed glass window.

The design features of the SCP working together make a tamper recorder that is difficult to defeat.

---

[2]Chemcor, Corning Glass Works, Corning NY 14830.
[3]Mark I Fiber Optic Seal, Fiber-Lock Corporation, P.O. Box 263, Kensington, MD 20795.

Discussion:

Stirling (AEC):

What made you choose seven days as the internal power capability? Was it a size limitation of the battery, or the time between the inspections?

Smathers (Sandia):

Primarily the time between the inspections. The people who have studied an international inspection system for a site which would have something as complicated as a personal portal indicate that an inspector would probably make a daily round, or at least every two days. The seven-day power supply would give them an opportunity to miss a flight, or go through a hurricane, and still get back in a week. We can easily double or triple the time by putting in a larger battery.

International Safeguards at the Feed and Withdrawal Area of a Gas Centrifuge Uranium Enrichment Plant*

by

DAVID M. GORDON AND JONATHAN B. SANBORN
Brookhaven National Laboratory, Upton, New York 11973

ABSTRACT

This paper discusses the application of International Atomic Energy Agency (IAEA) safeguards at a model gas centrifuge uranium enrichment plant designed for the production of low-enriched uranium; particular emphasis is placed upon the verification by the IAEA of the facility material balance accounting. After reviewing the IAEA safeguards objectives and concerns at such a plant, the paper describes the material accountancy performed by the facility operator, and discusses strategies by which the operator might attempt to divert a portion of the declared nuclear materials. Finally, the paper discusses the verification of the declared material balance, including sampling strategies, attributes and variables measurements, and nondestructive measurements to improve the efficiency of the inspection measures.

KEYWORDS: gas centrifuges; IAEA safeguards; isotope separation; material balance; material unaccounted for; nondestructive analysis; safeguards; uranium; uranium hexafluoride; uranium 235.

A number of enrichment facilities will come under international safeguards for the first time in the near future. The nature of international safeguards concerns for an enrichment plant depends heavily on the enrichment technology involved. In this paper we discuss these problems for a large gas centrifuge facility in the context of the structure and techniques currently accepted by the International Atomic Energy Agency (IAEA).

THE OBJECTIVE OF IAEA SAFEGUARDS

The IAEA implements its safeguards based on the IAEA Statute[1], in accordance with two main types of Agreements. As described in documents INFCIRC/153[2] and INFCIRC/66/Rev. 2[3], these Agreements are concluded with States (nations) party to the Non-Proliferation Treaty (NPT) and non-NPT-States, respectively[4]. This paper shall consider the application of IAEA safeguards at a model gas centrifuge uranium enrichment facility in the context of an Agreement based on INFCIRC/153.

The objective of IAEA safeguards is given in paragraphs 28-30 of INFCIRC/153 as follows:

> 28. The Agreement should provide that the objective of safeguards is the timely detection of diversion of significant quantities of nuclear material from peaceful nuclear activities to the manufacture of nuclear weapons or of other nuclear explosive devices or for purposes unknown, and deterrence of such diversion by the risk of early detection.
> 29. To this end the Agreement should provide for the use of material accountancy as a safeguards measure of fundamental importance, with containment and surveillance as important complementary measures.

* The views expressed herein are those of the authors, and do not necessarily reflect those of Brookhaven National Laboratory or the United States Department of Energy.

30. The Agreement should provide that the technical conclusion of the Agency's verification activities shall be a statement, in respect of each material balance area, of the amount of material unaccounted for over a specific period, giving the limits of accuracy of the amounts stated.

At a uranium enrichment facility, the fulfillment of this objective must take into account the unique capability of such facilities to increase the U-235 concentration of the uranium to levels suitable for nuclear explosives. For the purpose of planning safeguards activities, the IAEA has adopted the following as the quantities of safeguards significance: 75 kg of U-235 contained in low-enriched uranium (U-235 < 20%, including natural and depleted uranium) and 25 kg U-235 in highly-enriched uranium (U-235 $\geq$ 20%)[4].

IAEA Safeguards Concerns at Declared Uranium Enrichment Facilities

There are three principal safeguards concerns at uranium enrichment facilities subject to IAEA safeguards and which have been declared for the production of low-enriched uranium (LEU). These are the following, carried out either in an abrupt or protracted manner[5]:

i) the production and diversion of a significant quantity of uranium at an enrichment greater than declared (in particular, highly-enriched uranium), using either declared or undeclared feed.
ii) the production and diversion of a significant quantity of undeclared low-enriched uranium, using undeclared feed.
iii) the diversion of a significant quantity of declared uranium from the facility (particularly in the form of low-enriched uranium product).

The first concern above is of the greatest importance because of the possibility that the operator would produce highly-enriched uranium usable in nuclear explosives. For the gas centrifuge enrichment process, production of uranium with greater-than-declared enrichments can be accomplished via off-design cascade operation, batch recycle of product through the cascade, or rearrangement of a portion of the isotope separation equipment. The second and third concerns above are also of importance since the diverted low-enriched uranium could be used as feed for clandestine enrichment elsewhere or used in a nuclear reactor to produce plutonium.

As this paper is directed primarily at issues concerning material accountancy, we will not address the problems of detecting the clandestine introduction of undeclared feed materials (whether stored in a special non-access material balance area before the initiation of safeguards activities or introduced clandestinely into the facility after the initiation of safeguards). Since in many instances the production of low- or high-enriched product from undeclared feed can be carried out so as to not affect the declared material balance (for example, by storage of tails and wastes from such production in a non-access MBA, should one exist), this detection is necessarily the function of a containment/surveillance system and inspections to verify and reverify the design information regarding the facility. These subjects are beyond the scope of this work, and our concern here is limited to detection of diversion from the declared nuclear material inventories and flows. In general, however, material accountancy, containment, and surveillance measures must be employed together in order to provide the IAEA with completeness and continuity of knowledge concerning the nuclear material flows and inventories at the facility.

REFERENCE GAS CENTRIFUGE URANIUM ENRICHMENT PLANT

For the purposes of material balance verification by the IAEA, accountancy data are partitioned in space and time into material balance areas (MBAs) and physical inventory periods. After each physical inventory period, the facility is required to report to the IAEA a material balance for each MBA. This must include a statement of material unaccounted for (MUF) for U-235 and all the components of that MUF: beginning inventory

(BI), ending inventory (EI), additions to inventory (A), and removals from inventory (R). Mathematically:

$$MUF = BI - EI + A - R. \quad (1)$$

The facility also has the responsibility of informing the IAEA of the nature of and uncertainties in its measurements so that the IAEA can calculate an uncertainty for the reported MUF.

In this paper we will assume a material balance interval of six months. Below we describe the MBA structure, the components of the material balance, and the measurement methods and uncertainties related to the calculation by the facility of MUF and its uncertainty.

Suggested MBA Structure

A suggested MBA structure for IAEA safeguards at the reference gas centrifuge plant is illustrated in Figure 1. In this arrangement, there are three MBAs; a Shipper/Receiver MBA, a UF_6 Handling MBA, and a Cascade MBA.

Shipper/Receiver MBA

The Shipper/Receiver MBA would provide a mechanism for the determination and isolation of shipper-receiver (S/R) differences between facilities; by IAEA convention, the S/R differences are evaluated at the receiver facility. Thus, the MUFs for the MBAs of the facility in question would not include S/R differences. For the reference centrifuge plant, the Shipper/Receiver MBA would be used to keep track of the cumulative shipper/receiver difference for feed cylinders. Feed cylinders received from customers would be held on inventory at shipper's values in the Shipper/Receiver MBA until they were weighed and sampled; they would then be transferred to the UF_6 Handling MBA.

UF_6 Handling MBA

The UF_6 Handling MBA would contain the major inventories of uranium and U-235 present at the reference plant. This MBA would include all product and tails cylinders in storage, all feed cylinders in storage (exclusive of feed cylinders held at shipper's values in the Shipper/Receiver MBA), all cylinders undergoing sampling, and all cylinders (feed, product, and tails) attached to the cascades. In addition, this MBA would include chemical traps in the Feed/Withdrawal Building.

Cascade MBA

The Cascade MBA would include the centrifuge cascades, maintenance areas, and centrifuge testing areas. It would include the gas-phase portion of the feed system beyond the feed cylinder valve, and the product and tails withdrawal systems up to their respective cylinder valves. At the time of the physical inventory for IAEA purposes (assumed to occur once every 6 months), flow cutoff procedures could be followed such that the contents of the product and tails desublimers or other process vessels would be emptied into their respective cylinders. The IAEA would verify the inventories of these desublimers or process vessels at zero values. If the cascade area were a non-access area (special material balance area) or a limited access area, the IAEA might not be able to verify the inventory for the remainder of the Cascade MBA; these inventories would include the in-process gas phase and holdup inventories. However, this inability may be of little import, since for a number of cases, such non-verifiable inventory would be small (compared with both the semi-annual U-235 feed and the quantity of safeguards significance) and nearly constant when the plant was operating at full design capacity. In this instance, the material balance around the Cascade MBA would consist of a flow balance; the nuclear materials flows to and from the Cascade MBA (the only location in the plant where the strategic value of the nuclear material changes) would be verifiable by the IAEA with high accuracy and precision.

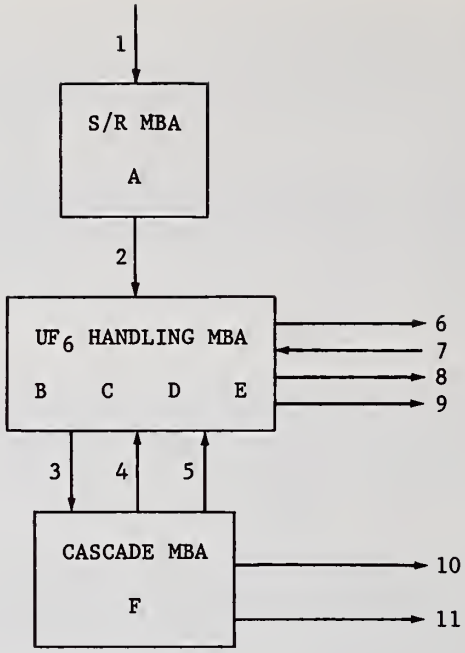

Flow Key Measurement Points

1 Full UF_6 feed cylinders received at shipper's values.
2 Full UF_6 feed cylinders at receiver's values.
3 Feed UF_6 gas.
4 Product UF_6 liquid.
5 Tails UF_6 liquid.
6 Empty feed cylinders returned.
7 Empty product cylinders received.
8 Full product cylinders shipped.
9 Miscellaneous wastes shipped.
10 Spent chemical trap material shipped.
11 Decontamination solutions shipped.

Inventory Key Measurement Points

A Full UF_6 feed cylinders stored at shipper's values.
B Cylinders in short-term storage.
C Tails cylinders in long-term storage.
D Cylinders undergoing sampling.
E Cylinders attached to the cascades.
F Verifiable portion of Cascade MBA inventory (desublimers and process vessels).

Figure 1: Suggested MBA Structure for the Reference Gas Centrifuge Enrichment Plant, with Inventory and Flow Key Measurement Points as Indicated.

Nuclear Material Flows at the Reference Plant

At a gas centrifuge uranium enrichment plant, the beginning and ending inventories are composed primarily of UF_6 in cylinders located in storage yards or attached to the cascades, UF_6 in desublimers or buffer vessels, and relatively small quantities of UF_6 as in-process gas-phase inventory in the cascades. In addition, uranium is contained in the form of various waste materials awaiting processing, in laboratory samples, in chemical traps, and as solid deposits on the internal surfaces of the isotope separation equipment; unlike the other components of inventory, this last inventory quantity is very difficult for the operator to measure.

As regards the flows of uranium, the additions to material in process consist of UF_6 feed, which is ultimately vaporized from the shipping cylinders and fed as gas-phase UF_6 to the cascades. The removals from material in process are composed primarily of shipments of enriched (product) and depleted (tails) UF_6 in cylinders. In addition, various waste materials containing uranium, such as spent chemical trap media, are routinely shipped from the enrichment facility and/or processed on site for recovery of uranium. These waste streams are commonly quite small compared to the other flows of uranium at the plant, comprising on the order of 0.1% of the uranium contained in the feed. In summary, the nuclear material flows at a gas centrifuge plant are feed UF_6, product UF_6, tails UF_6, and a variety of small waste streams.

The characteristics of the reference gas centrifuge enrichment plant considered in this paper are given as follows:

Separative Capacity	
MTSWU/yr[a]	3000
Feed Rate (0.71 wt % U-235)	
MTU/yr	3817
MTU-235/yr	27
No. of 10-ton cylinders/yr, Model 48X[b]	592
Product Rate (3.00 wt % U-235)	
MTU/yr	697
MTU-235/yr	21
No. of 10-ton cylinders/yr, Model 48X	108
Tails Rate (0.20 wt % U-235)	
MTU/yr	3120
MTU-235/yr	6
No. of 14-ton cylinders/yr, Model 48G	363
Waste Rate (trap material)	
kg U/yr	2700
kg U-235/yr	27
No. of containers/yr	400

a) MTSWU = 1000 kg of separative work.
b) Specifications for cylinders are given in Ref. 6.

It has been assumed in this paper that the product UF_6 would be withdrawn from the cascades into 10-ton cylinders. In many facilities, this product material is transferred to 2.5-ton cylinders prior to shipment to the customers. For the purposes of a material balance drawn around the Cascade MBA, this subsequent transfer is not important; it adds a relatively minor complication to the verification of the material balance for the UF_6 Handling MBA.

Material Balance Accounting by the Facility Operator

In order to close a material balance around an MBA, the facility operator must measure the flows and inventories for that MBA, as noted in eqn. (1). The following practices for material balance measurements are typical of U.S. enrichment facilities.

Facilities in other States may use different sampling procedures, follow different inventory measurement procedures, or quote different measurement uncertainties, depending upon the specifics of the facilities and instrumentation.

Measurements of Feed, Product, and Tails UF_6 Flows

The quantities to be measured for each cylinder of UF_6 fed to or withdrawn from the cascades are the net mass, the weight fraction uranium, and the weight fraction U-235 of the material transferred. From these the operator determines the quantities of uranium and U-235 transferred via these major flows.

Measurements of mass of UF_6 transferred. The net mass of UF_6 transferred to or from the cascades is determined by weighing the cylinder before and after the transfer, preferably on the same scale in order to minimize weighing bias.

In the U.S., 10- and 14-ton cylinders are weighed on platform scales with $\pm$ 2.0 lbs. rated precision at maximum load. The relative random limit of error (95% confidence level) for the net weight of UF_6 in these cylinders is approximately $2\sigma = 0.01\%$. The relative systematic uncertainty in the net weight of UF_6 transferred is negligible in comparison with the relative systematic uncertainties in the chemical and isotopic measurements of weight fraction U and weight fraction U-235.

Bulk sampling. An acceptable sample of UF_6 must represent both the chemical and isotopic content of the cylinder of UF_6. U.S. experience has shown that the most representative sample of the UF_6 in a cylinder is one withdrawn in the liquid phase after complete homogenization. A 10-ton or 14-ton cylinder is heated in a steam autoclave in order to liquefy the contents and obtain complete chemical and isotopic homogenization of the UF_6. Two independent samples are removed from each large cylinder. One of the samples is analyzed immediately; the second sample is retained for potential umpire use. The contribution to the relative uncertainty in the uranium content of a 10-ton or 14-ton cylinder due to sampling is believed to be about $\pm$ 0.02 - 0.04% (95% confidence level).

Measurement of weight fraction uranium in UF_6. Very precise and accurate analytical chemical techniques are available for the determination of the uranium concentration in UF_6; that is, the number of grams of uranium per gram of sample. At U.S. enrichment facilities, a widely-used technique for the determination of uranium in UF_6 samples is the gravimetric (ignition and impurity correction) method[7].

This method is generally recognized to be exceedingly accurate and precise. For very pure UF_6, the relative precision of the analysis, at the 95% confidence level, is $2\sigma = 0.04\%$ per determination[7]. When impurity levels rise to 0.2%, the relative precision becomes approximately $\pm$ 0.1%. The accuracy achievable with the above method is very high; the relative systematic uncertainty (for very pure UF_6) is believed to be about 0.04%.

Measurement of weight fraction U-235 in UF_6. Mass spectroscopic techniques are available for the measurement of the weight fraction U-235 with high precision and accuracy for a UF_6 sample. In particular, samples of UF_6 withdrawn from the cylinders are analyzed mass spectroscopically for weight fraction U-235, using instruments in which the UF_6 gas is introduced directly and ionized by electron bombardment.

The most precise technique in common use for isotopic analysis of UF_6 is the double-standard mass-spectrometer method[7]. In this technique, the unknown sample and two standards whose U-235 contents bracket that of the unknown are introduced in sequence into the mass spectrometer, and measurements are made which are a function of the mole ratio of U-235 to the total of the other isotopes of uranium. These measurements together with the known composition of the standards permit calculation of the U-235 composition of the sample by linear interpolation.

At the Oak Ridge Gaseous Diffusion Plant, fifteen gas-phase mass spectrometers are automated via a computer system; each instrument is dedicated to a very specific range of isotopic assays. Measurement control tests have shown measurement precisions of $\pm$ 0.1% (relative, 95% confidence level) over the range of interest; sampling errors were found to be neglibible. Measurements are made relative to a series of reference standards (traceable to the U.S. National Bureau of Standards) which bracket the samples within 5% relative; bias introduced by uncertainty in these standards is believed to be less than

0.1% (relative). It is assumed here that these random and systematic relative uncertainties apply to the measurements of U-235 concentrations for feed, product, and tails UF_6.

The uncertainties in measurements of uranium isotopic composition appear to be the major contributor to the uncertainty for the U-235 material balance for a gas centrifuge enrichment plant.

Measurements of Waste Streams

The measurements of the U and U-235 content of the waste streams, such as spent chemical trap media or decontamination solutions, can be carried out via chemical analysis. A sample of measured weight or volume can be analyzed for uranium content (gm U/gm sample or gm U/liter) and for weight fraction U-235. The total amounts of U and U-235 in the measured discards can be deduced from the above measurements and from the total mass (for solid waste) or volume (for liquid waste) of the discarded material.

Measurement of Inventory Quantities

Cylinders in storage yards. The U and U-235 contents of feed, product, and tails UF_6 cylinders on inventory in storage yards would be based upon previously measured full and empty cylinder weights, and upon previously measured values for weight fraction U and weight fraction U-235.

Cylinders attached to cascades. The weight of UF_6 remaining in a feed cylinder attached to the cascades would be determined from the initial full weight of the cylinder minus the quantity of UF_6 that had been removed from the cylinder, after allowance had been made for the cylinder tare weight. The amount of UF_6 removed would be determined from flow data integrated over time for that cylinder. The weight fraction U and weight fraction U-235 would be known from previous measurements.

Product and tails cylinders would be weighed for process control as they were being filled. At inventory time, the weight of UF_6 in a product or tails cylinder would be determined from the partially full weight minus the previously measured empty weight. The weight fraction U-235 would be determined from on-line mass spectrometers installed for process control.

Cascade gas-phase inventory. The cascade gas-phase inventory would be calculated from physical measurements of process parameters (such as pressures, temperatures, and flow rates) and from single-machine characteristics. Because this information would be considered by the facility operator to be sensitive for commercial or non-proliferation reasons, it is unlikely that such source data or the inventory would be made available to the IAEA.

Expected Uncertainty in the Flow Components of the Operator's Material Balance

For material balances drawn every six months, the uncertainty in the facility U-235 material balance contributed by uncertainties in the flows of nuclear material is dominated by the systematic uncertainties in the measurements of weight fraction U and weight fraction U-235 for the feed, product, and tails UF_6 flows. Propagation of the random and systematic uncertainties for the feed, product and tails UF_6 streams indicates that the contribution of the flow components of the material balance to the semi-annual uncertainty in the reference facility U-235 material balance is σ_{MUF} (flow) = 9.4 kg U-235.

IAEA VERIFICATION OF THE OPERATOR'S MATERIAL BALANCE ACCOUNTING

The facility operator will report his material balance measurements and his MUF for each MBA to the IAEA in accordance with the safeguards agreement for that facility. The IAEA verifies the material balance declared for each MBA by the operator. Because the IAEA in general does not have the resources to make enough measurements to determine completely its own material balance, such verification involves the independent measurement of a statistically sampled subset of the reported items comprising the material balance,

the observation (and verification) of facility operator measurements of other items, and the auditing of facility material balance records and reports for completeness, formal correctness, and consistency. Efficient measurement verification strategies are available which conserve IAEA measurement resources and which permit verification without repetition of more than a small fraction of the operator's measurements. The purpose of the IAEA verification of the material balance accounting carried out by the facility is to detect, and thereby deter, the abrupt or protracted diversion of declared nuclear materials at the facility; for the Cascade MBA, this includes the detection of the abrupt or protracted introduction of undeclared feed materials through the Feed/Withdrawal facilities.

This structure of facility reporting and IAEA verification defines two general strategies for an operator who wishes to divert material undetected from the material balance. He can report an unfalsified material balance (accurately reporting his own measurements) and divert an amount which will result in a reported MUF which is within the range of the uncertainty in his material balance, implying that this MUF arose through measurement uncertainties. This strategy is called "diversion into MUF". Alternatively, he may falsify his reported measurements so as to reduce his reported MUF. The concealment of diversion via falsification of records or measurements can take any or all of the following forms:

- understatement of receipts of feed UF_6
- overstatement of shipments of product UF_6
- overstatement of shipments of tails UF_6
- overstatement of measured discards (wastes)
- overstatement of accidental losses
- overstatement of cascade gas-phase inventory and solid holdup (if declared)
- overstatement of uranium held on inventory in process vessels or UF_6 cylinders.

It is convenient to define two levels of falsification: a defect and a bias. A "defected item" is an item whose reported content (of U-235) differs from its actual value by an amount which is significantly greater than the combined uncertainties of the operator's measurement and the inspector's most accurate measurement for that item. This means that a falsification will be very clearly indicated if the inspector decides to measure accurately a defected item. A "bias" is a falsification by an amount smaller than a defect.

The countermeasures used against the diversion strategies discussed above are of three types: (1) "attributes" sampling, (2) the MUF-D statistic, and (3) a set of chi-square statistics.

The purpose of attributes sampling is the detection of falsification via defects. Attributes measurements usually take two forms: (1) a "gross" attributes measurement which can be done quickly but has poor sensitivity, performed on a large fraction (possibly unity) of all items in order to detect large defects; (2) a "fine" attributes measurement (sometimes called a variables measurement in the attributes mode), performed on a smaller sample with better accuracy, in order to detect small defects.

Falsifications below the defect level (i.e., biases) cannot be detected with a single measurement by the inspector. It is therefore useful to calculate a statistic which covers the whole material balance for an MBA. The MUF-D statistic is an estimate of the MUF corrected for biases introduced by the operator; its variance is unaffected by operator systematic error. This means that the inspector can verify the material balance for an MBA with a sensitivity which is largely determined by his own systematic errors.

The MUF statistic is simply the operator's U-235 MUF, calculated over the material balance period. The D statistic is an extrapolated difference between inspector and operator measurements. It estimates the total amount by which the operator has falsified MUF (either intentionally via biasing, or unintentionally through systematic errors tending to reduce MUF; the two are indistinguishable). In the absence of diversion, MUF, D and MUF-D should all be zero to within the uncertainties caused by measurement error. The strategy of diversion into MUF by the operator will cause a positive MUF; the strategy of falsification by biasing will cause a negative expected value for D. Either strategy will cause an increase in the MUF-D statistic, which, if statistically significant, is indicative of diversion.

The sensitivity of the MUF-D statistic depends on its variance. This in turn, of course, depends on the variances of the individual measurements which go into the

statistic. In some cases it may be to the advantage of the diverter to increase those variances artificially, thereby increasing the variance of MUF-D and decreasing the probability of detection. For this reason, another type of statistical test (involving a chi-square statistic) is used by the inspector to estimate the operator's random error variance in each of the major strata (feed, product, and tails). This statistic is designed to detect large increases in the operator's random error variance over those stated in the design information.

The statistical tests discussed above are consistent with IAEA publications and supporting studies[8,9].

The present paper focuses on the application of the above concepts to the verification of the material balance for the Cascade MBA; this is clearly of major importance since it is at this area that the strategic value of the nuclear material is changed. Only a few comments will be made concerning verification for the UF_6 Handling MBA.

Verification of the Cascade MBA Material Balance

Ordinarily, the IAEA verification procedures include a "physical inventory taking", in which the inventory for an MBA is sampled and verified. Since it may not be possible for the IAEA to verify the in-process and holdup inventories for the Cascade MBA, we assume that a "flow material balance" will be computed every six months for this MBA. In a flow material balance, the difference between material input to the MBA and material output from the MBA is regarded as material unaccounted for (MUF). As noted above, such a balance is meaningful as an indicator of diversion only if the fluctuations of the unavailable in-process inventory and the holdup are small compared with other material uncertainties and with the quantity of material regarded as being "significant". We shall assume this to be the case for the Cascade MBA of the reference gas centrifuge enrichment plant.

Verification of the Feed, Product, and Tails UF_6 Flows

The data supplied by the operator would include the U and U-235 weight for each batch (assumed to be one cylinder); the inspector should be able to randomly verify these quantities for any item whose content has been reported by the operator.

The major flows of uranium to and from the plant will be in the form of feed, product and tails UF_6 in 10- and 14-ton cylinders. In order to verify these flows of uranium and U-235, the IAEA should obtain UF_6 samples for analysis, and should verify the following quantities: the mass of the UF_6 transferred via cylinder to and from the cascades, the weight fraction U in the UF_6 (gravimetric factor), and the weight fraction U-235 in the uranium. It is assumed here that the random and systematic relative uncertainties for the measurements of weight fraction U and U-235 as carried out by the IAEA analytical laboratory would have the same magnitude as those of the facility operator (as noted above). Because the reference plant would operate on a continuous basis, IAEA inspectors would have to be present at the facility Feed and Withdrawal area on a continuous basis in order to carry out the verification program suggested below.

Suggested sampling strategy. It is assumed that the facility operator would homogenize and liquid sample all feed cylinders, all product cylinders, and some fraction of the tails cylinders for his nuclear material accountability program. It is suggested here that the IAEA inspectorate obtain a liquid UF_6 sample (in a Model 1S sample cylinder) for each of these cylinders; that is, the facility operator would withdraw three liquid samples instead of the usual two samples. An IAEA inspector should observe the withdrawal of the sample intended for use by the Agency. In addition, it is assumed that, at the request of the IAEA inspectorate and at a reasonable and mutually-agreed upon frequency (up to a limit of one liquid sample per cylinder), the facility operator would withdraw liquid UF_6 samples for IAEA use from the piping used in filling the remainder of the tails cylinders.

While only a fraction of the above samples would actually be analyzed for weight percent uranium and weight percent U-235 by the IAEA at its own analytical laboratory, a complete set of samples should be obtained by the IAEA so that it could make a random selection of the samples to be analyzed without the facility operator having knowledge of which samples were so selected. Otherwise, the operator could simply divert material

from a cylinder which he knew had not been verified by the IAEA. The on-site inspector would need storage facilities for the UF_6 sample cylinders. At some reasonable time following the end of a given material balance period and after the resolution of any material balance quantity discrepancies, the IAEA would return the unused samples to the facility operator. The Model 1S sample cylinder[6], which can contain a maximum of 450 grams of UF_6, is recommended so as to minimize the quantity of UF_6 stored by the IAEA inspectorate.

Verification of mass of UF_6 transferred. We shall assume that the facility operator would measure the full and empty weight of every cylinder of UF_6 fed to and withdrawn from the cascades. The IAEA inspector would observe the full and empty weighing by the facility operator of each of these cylinders. For feed cylinders arriving under IAEA seal, the verification of the full cylinder weight would be performed on a test basis. In addition, the IAEA should observe the facility operator calibrate the accountability scales. If feasible, the IAEA should obtain a calibrated set of full and empty 14-ton cylinder replicas; from time to time, the IAEA inspector would request the operator to weigh these IAEA-owned replicas under observation of the inspector.

Verification of weight fraction uranium. The UF_6 purity for feed, product, and tails UF_6 transferred to and from the cascades can be expected to be greater than 99.5%; that is, the uranium weight fraction would be within 0.5% (relative) of the nominal value. $g = 0.676$ for this UF_6. Hence, reported values of UF_6 purity less than 99.5% would be, a priori, not credible, and the IAEA would need to check for falsifications and biases smaller than 0.5% (relative).

For the variables measurements, the IAEA inspectorate would send a randomly selected sample of the sample cylinders (Model 1S) to the IAEA analytical laboratory for very precise and accurate measurement ($2\sigma = 0.1\%$ relative) to check for such bias or falsification. The sample size for each stratum (feed, product, tails) is given in Table I. The IAEA would use the above data in generating a MUF-D statistic, and would be able to determine whether the reported random error variances had been inflated and whether a bias had been introduced.

Verification of weight fraction U-235. The verification of weight fraction U-235 would be accomplished using a combination of attributes and variables measurements; the attributes measurements contribute substantially to the efficiency (as regards IAEA resource utilization) of the safeguards measures applied. In this context, the U.S. government is developing in-line enrichment monitors for the continuous attributes measurement of the feed, product, and tails assays (weight fraction U-235) of the UF_6 transferred to or from cylinders; these measurements are expected to have precisions of $2\sigma = 2\%$ (relative) or better[10-13]. Such a 100% sampling and measurement program at the 2% precision level would detect defects greater than about 4% (relative) with a high probability.

The feed, product, and tails in-line enrichment monitors are all based upon the passive detection of the 186-keV gamma rays from U-235 in either liquid or gas-phase UF_6. A product monitor would be installed at each liquid product transfer line connecting a product desublimer or buffer vessel to the 10-ton cylinder. These monitors would use a NaI-phototube combination to detect the 186-keV gamma rays. A device of this type has already been developed and installed at the Portsmouth Gaseous Diffusion Plant; it has routinely achieved a measurement accuracy of $2\sigma = 0.5\%$ (relative) during 10-minute assays[10,11]. Similarly, a tails enrichment monitor would be installed at each liquid tails transfer line connecting a tails desublimer or buffer vessel to the 14-ton cylinder. A monitor for this purpose would utilize either a NaI-phototube combination or a germanium solid-state detector for gamma-ray detection; the expected accuracy of the enrichment measurement is about $2\sigma = 1$-2% (relative) for a 10-minute assay, depending on whether the germanium or the NaI detector is used, respectively[12,13]. A feed monitor could be placed at the outlet of each feed autoclave; however, an alternative which is nearly as effective would be to place a single feed monitor at the main feed line to the cascades. A monitor for this purpose would measure the number of gamma rays from a well-defined volume of gas; a correction for the absorption and scattering of the gamma rays by the gas and by the measurement cell wall would be determined via a simultaneous transmission measurement for an external gamma-ray source. A monitor of this type

utilizing a NaI-phototube combination is expected to have an accuracy of 2σ = 2% (relative) for a 10-minute assay[12,13].

Variables measurements would be made to detect small defects and biases. The IAEA inspector would send a randomly selected sample of the Model 1S sample cylinders to the IAEA analytical laboratory for very precise and accurate measurement (2σ = 0.1% relative). The necessary sample size for each stratum is given in Table I. The IAEA would use the above data in generating a MUF-D statistic for the U-235 material balance, as well as estimates of the operator's random error; it would thus be able to determine whether the reported random error variances had been inflated and whether a bias had been introduced.

Verification of the Waste Streams

As noted above, the total amounts of uranium and U-235 removed via the waste streams (such as spent chemical trap media and decontamination solutions) could comprise on the order of 0.1% of the plant feed. Nevertheless, for large capacity enrichment plants, the quantities of U-235 discarded could comprise a substantial fraction of a significant quantity of nuclear material, and the overstatement of the uranium in these wastes could thus present an attractive falsification path for the operator. Thus, the IAEA should verify these quantities of U-235, in order to detect and deter gross overstatements. Such verification would be carried out on a random sampling basis using non-destructive assay methods. It appears that in many instances, the IAEA need only make a crude measurement of these quantities; for example, a measurement having a relative standard deviation of $\pm$ 20% might suffice for some waste streams while merely placing an upper limit on the quantities might suffice for others.

The IAEA could use, for example, a thermal neutron well coincidence counter to measure the amounts of U-235 and U-238 being removed with the spent chemical trap media. The coincident (spontaneous fission) neutron rate is determined primarily by the quantity of U-238 present while the total neutron rate is determined primarily by the quantities of U-234 and U-238 present. If the uranium to be assayed contained no U-232 or U-236, and if the U-234 to U-235 ratio were assumed to be approximately constant (1/125), and further, if small (few percent) contributions to the neutron yield were ignored, then the total neutron rate could be related to the mass of U-235 present, while the coincident (spontaneous fission) neutron rate could be related to the mass of U-238 present. Such an instrument is at present being developed by the U.S. government[12,13]. For the purposes of this paper, we shall assume that spent chemical trap material comprises the only waste stream and that an NDA instrument (such as the above) is used by the IAEA to measure the U-235 content of the waste. In addition, we shall assume that the resultant NDA measurement has a relative random limit of error (2σ) of 20% and a relative systematic limit of error of 10%. The number of containers to be measured on a random sampling basis for a six-month material balance interval is given in Table I.

Numerical Results

The sample sizes given in Table I are determined from a calculation similar to that outlined in Ref. 8 and 9. These documents are somewhat general in nature, however, and necessarily tend to be overly conservative with regard to sample sizes in specific instances. Sample sizes must be large enough to (1) enable the detection of the diversion of 75 kgs of U-235 through defects with the desired probability, (2) enable the detection of a strategy in which the operator artificially inflates his random measurement errors by large amounts, and (3) minimize the contribution of random errors to the variance of the MUF-D statistic when these errors are not falsified by large amounts.

In the present case, considerations (2) and (3) are dominant. Sample sizes were chosen to minimize the total number of samples required subject to the constraints that (1) random error not contribute more than 15% to the total standard deviation of MUF-D, and (2) a given detection probability be achieved if the diverter artificially inflated his random error variance so as to increase the standard deviation of MUF-D by more than 15%.

The results of these calculations are shown below for three levels of desired detection probability for a single six-month material balance. The standard deviations of the MUF-D statistic are given for the cases in which (a) the operator does not inflate his random errors, and (b) the operator inflates his random errors in such a way that the

contribution of random error to the overall standard deviation is 15%; if he exceeds this limit he will be detected by other statistical tests with the desired detection probability. "Sensitivity, bias" is the amount (kg U-235) which, when diverted into MUF or falsified by biasing, can be detected with the stated probability. The total false alarm probability, including both the chi-square and MUF-D tests, is 10^{-3}. "Sensitivity, defects" is the amount (kg U-235) which, when diverted as defects, can be detected with the stated probability. This corresponds to a strategy in which the operator falsifies the enrichment of a number of product cylinders by about 2-3% (relative). Falsifications greater than about 3% (relative) are detected by the in-line enrichment monitors. As these sensitivities to defects are quite conservative, and as they are much smaller in any case than the bias sensitivities, falsification by defects does not appear to be an attractive diversion strategy for the operator.

Table I

The number of samples to be measured for each flow stratum, the standard deviation of MUF-D, and the sensitivities to diversion via biases and defects as a function of the desired detection probability, for a false alarm probability of 10^{-3}

	Desired Detection Probability		
	0.8	0.9	0.95
Sample Sizes (semi-annual)			
Feed	21	24	27
Product	17	20	22
Tails	9	10	11
Waste	10	10	10
Sigma MUF-D (kgs U-235)			
No inflation	9.9	9.8	9.7
15% inflation	10.8	10.8	10.8
Sensitivity, bias (kg U-235)	42.1	46.6	50.1
Sensitivity, defects (kg U-235)	19	25	32

We note that for a 95% probability of detection, high accuracy (variables) measurements would be performed for samples from about 9%, 41%, and 6% of the feed, product, and tails cylinders, respectively.

Verification of the UF_6 Handling MBA Material Balance

The major inventories in the UF_6 Handling MBA would consist of cylinders in storage yards, cylinders being sampled, and cylinders attached to the cascades for feed/withdrawal of UF_6. For cylinders in storage, verification would consist primarily of cylinder identification and seal integrity verification, carried out on a random sampling basis.

We next consider cylinders undergoing homogenization and sampling in the autoclaves. The facility operator would have weighed (under IAEA observation) the full feed, product, and tails cylinders prior to loading the cylinders into the autoclaves for sampling. A preliminary value of the weight fraction U for these cylinders could be assumed by the IAEA to be g = 0.676. A preliminary value for the U-235 assay of product and tails cylinders would be obtained by the IAEA from the in-line enrichment monitor record for these cylinders; the U-235 assay of normal feed would be assumed to be 0.71% U-235. These preliminary values would be replaced by the more precise and accurate values obtained by analysis (at the IAEA laboratory) of liquid samples obtained from these cylinders.

We finally consider the verification of cylinders attached to the cascades. The initial full weight of a feed cylinder, and the initial empty weights of product and tails

cylinders would have been verified by the IAEA (via observation of weighings by the facility operator). At the time of the physical inventory, the cylinder weights would be observed by the IAEA; it is assumed that these cylinders would be located on load cells or scales so that they could be continuously weighed for process control. Load cell calibration would be checked from time to time by the weighing of cylinder replicas by the facility operator (observed by the IAEA). It would be desirable if the load cell electrical connections and instrumentation were accessible to the IAEA so that it could assure itself that the load cell readings had not been subjected to tampering by the operator. From the verified empty weights for product and tails cylinders, the nominal tare weights for feed cylinders, and the observed partially full weights for all the cylinders, the IAEA could determine the amounts of UF_6 therein.

Prior to attachment to the cascades, a feed cylinder would have been homogenized and sampled, and a liquid sample would have been obtained by the IAEA. Therefore, the IAEA would verify the gravimetric factor, via IAEA laboratory analysis of randomly selected samples, for feed cylinders attached to the cascades. Similarly, the IAEA would verify the weight fraction U-235 in the feed UF_6. For product and tails cylinders, the initial value of weight fraction U could be taken to be $g = 0.676$ and the initial value of weight fraction U-235 would be obtained from the in-line enrichment monitor. These approximate values would be replaced by the more precise and accurate values obtained after the product and tails cylinders had been homogenized, sampled, and the samples analyzed at the IAEA analytical laboratory.

SUMMARY

This paper has discussed the material balance accounting carried out by the operator of a reference 3000 MTSWU/yr gas centrifuge uranium enrichment plant, including measurements for feed, product, and tails UF_6 flows. After discussing two operator strategies for undetected diversion of uranium from the declared nuclear material balance ("diversion to MUF" and falsification), the paper discussed the IAEA material balance verification strategies intended to detect, and thereby deter, the above diversion strategies. For material balances drawn every six months for the Cascade MBA of the reference gas centrifuge plant, the verification strategy permits the IAEA to detect the diversion of 50 kg of U-235 with a probability of 0.95 and a false alarm probability of 10^{-3}.

References

1. Statute (as amended up to 1 June 1973), International Atomic Energy Agency, Vienna, Austria.

2. The Structure and Content of Agreements Between the Agency and States Required in Connection with the Treaty on the Non-Proliferation of Nuclear Weapons, IAEA Document INFCIRC/153 (Corrected), International Atomic Energy Agency, Vienna, Austria, June 1972.

3. The Agency's Safeguards System (1965, as Provisionally Extended in 1966 and 1968), IAEA Document INFCIRC/66/Rev.2, International Atomic Energy Agency, Vienna, Austria, 16 September 1968.

4. G. Hough, T. Shea, and D. Tolchenkov, "Technical Criteria for the Application of IAEA Safeguards", paper IAEA-SM-231/112, IAEA International Symposium on Nuclear Material Safeguards, Vienna, Austria, 2-6 October 1978.

5. Safeguards Considerations for Uranium Enrichment Facilities, As Applied to Gas Centrifuge and Gaseous Diffusion Facilities, U.S. Contribution to the International Nuclear Fuel Cycle Evaluation, Working Group 2, 1 March 1979.

6. Uranium Hexafluoride: Handling Procedures and Container Criteria, U.S. Atomic Energy Commission, Report ORO-651 (Revision 4), April 1977.

7. Procedures for Handling and Analysis of Uranium Hexafluoride, Vol. 2, Analysis, Oak Ridge Operations Office, United States Atomic Energy Commission, Oak Ridge, Tennessee, Report ORO-671-2, April 1972.

8. IAEA Safeguards Technical Manual, Part F, Document IAEA-174, International Atomic Energy Agency, Vienna, Austria, 1976.

9. C.G. Hough, R.A. Schneider, K.B. Stewart, J.L. Jaech, and C.A. Bennett, "Example of Verification and Acceptance of Operator Data - Low-Enriched Uranium Fabrication", Battelle Pacific Northwest Laboratories, Richland, Washington, Report BNWL-1852, August 1974.

10. T.D. Reilly, E.R. Martin, J.L. Parker, L.G. Speir, and R.B. Walton (Los Alamos Scientific Laboratory), "A Continuous In-Line Monitor for UF_6 Enrichment", Nucl. Technology 23, 318 (1974).

11. R.B. Walton, "The Feasibility of Nondestructive Assay Measurements in Uranium Enrichment Plants", Los Alamos Scientific Laboratory, Los Alamos, New Mexico, Report LA-7212-MS, April 1978.

12. J.W. Tape, M.P. Baker, and R.B. Walton, Los Alamos Scientific Laboratory, Los Alamos, New Mexico, Report LA-7439-PR, p. 46-51, December 1978.

13. J.W. Tape, M.P. Baker, R. Strittmatter, M. Jain, and M.L. Evans, "Selected Nondestructive Assay Instrumentation for an International Safeguards System at Uranium Enrichment Plants", Proceedings of the 20th Annual Meeting of the Inst. of Nuclear Materials Management, Nucl. Material Management VIII, 791 (1979).

Discussion:

Bingham (NBL):
Dave, what was the basis for the values on the random and systematic errors that were stated for the measurements of uranium fraction, the .04% two sigma values, from whence came those data?

Gordon (BNL):
The relative random uncertainty is taken from the USAEC report ORO-671-2, which includes data for the determination of uranium in UF_6 by the ignition and impurity correction (gravimetric) method. The relative random limit of error quoted in that report is .04% per single determination. The relative systematic uncertainty was derived from consideration of the General Analytical Evaluation for UF_6 carried out by the New Brunswick Laboratory (NBL-274, by Bingham and Bracey), looking at only those laboratories which performed gravimetric measurements. Of the 20 or so laboratories, only about 9 performed gravimetric measurements similar to the U.S. enrichment plant method; that is the ignition and impurity correction method. I calculated the standard deviation of the relative differences from the reference value, for those laboratories which performed gravimetric analyses.

Nilson (Exxon Nuclear):
I think that you've shown that this system is capable of detecting the types of diversions in Category III. Those concerns are not unique to an enrichment plant, any bulk facility has those same types of concerns. To me the real concern, in your facility, is the recycle concern, which you didn't touch on. Are you trying to do some work in that area, because this is where the threat is in enrichment plants?

Gordon:
The least controversial subject in the area of safeguards for a gas centrifuge enrichment plant is the verification of the declared nuclear material balance. The questions of undeclared feed and the production of highly enriched uranium within the facility are more controversial subjects. The IAEA is considering such questions, as well as inspector access to the cascades; these issues are not at all resolved by the IAEA and the Member States. The United States is attempting to develop a technique to directly detect production of highly enriched uranium in the cascades, via detection of neutrons with detectors located on the process building roof. That project is underway at LASL, and is still in a relatively early stage of development.

Persiani (ANL):
In the last table you had listed numbers of samples, e.g., 27 for the 95% confidence level. I am trying to relate the number of samples to throughput for 6 months or the number of feed or product cylinders.

Gordon:
Those numbers of samples were for a 6 month materials balance. For the case of 95% probability of detection, those numbers correspond to 9% of the feed cylinders, 41% of the product cylinders, and 6% of the tail cylinders. Thus, the IAEA would place most of its effort on the product cylinders, on a relative basis.

NDA for the SRP Fuel Fabrication Process

by

R. V. STUDLEY
E. I. du Pont de Nemours, Savannah River Plant

ABSTRACT

The Savannah River Plant fuel fabrication process is described to illustrate requirements for a variety of assay techniques. Criteria and design of some NDA systems for this process are discussed. Initial performance of a neutron activation analysis system (californium shuffler) as an assay method for several varieties of material is reported.

KEYWORDS: Nondestructive assay (NDA), safeguards, accountability in fabrication of reactor fuel, active neutron interrogation, neutron activation analysis, material control

INTRODUCTION

The Savannah River Plant (SRP) was built and has been operated by the Du Pont Company since 1951 for AEC, now DOE. The plantsite is located (figure 1) in South Carolina adjacent to the Savannah River, and roughly equidistant from Aiken, S.C., and Augusta, Ga. The 300-square-mile plantsite includes a central administration area, the reactor charge component fabrication area where fuel assemblies and targets are manufactured, a heavy water refining area producing moderator for our reactors, three operating materials production nuclear reactors, two similar nuclear materials chemical separations areas primarily used to refine products from our own reactors, plus waste storage tank farms and burial grounds as well as a variety of supportive facilities.

The reactor component fabrication facility (figure 2), designated the Raw Materials Area, includes several buildings where nonfissile reactor target elements or other core and assembly components are manufactured. Also, in this area is Building 321-M where reactor fuel assemblies containing highly enriched ^{235}U are fabricated.

DISCUSSION

Reactor Fuel Fabrication

Building 321-M (figure 3) consists of seven main process areas plus offices, miscellaneous facilities, and storage areas. Process areas are: receiving for enriched uranium (EU), casting, machining, assembly, extrusion, finishing, and shipping. Layout of the building, constructed in the early 1950's, was designed for efficient manufacturing in an earlier form of the process, long before accountability was important for more than production economy and health protection.

Receiving. In this part of the process, chemically pure, solid uranium metal packed in sealed-steel cans is received from Oak Ridge. This uranium may be virgin or may be uranium recovered from our reactors which has been recycled for re-enrichment through the Oak Ridge Y-12 process. This recycled uranium may contain up to 40% of the ^{236}U isotope which is not practical to remove. Uranium metal is accurately weighed on receipt, sampled for isotopic determination in the laboratory, and stored in a vault.

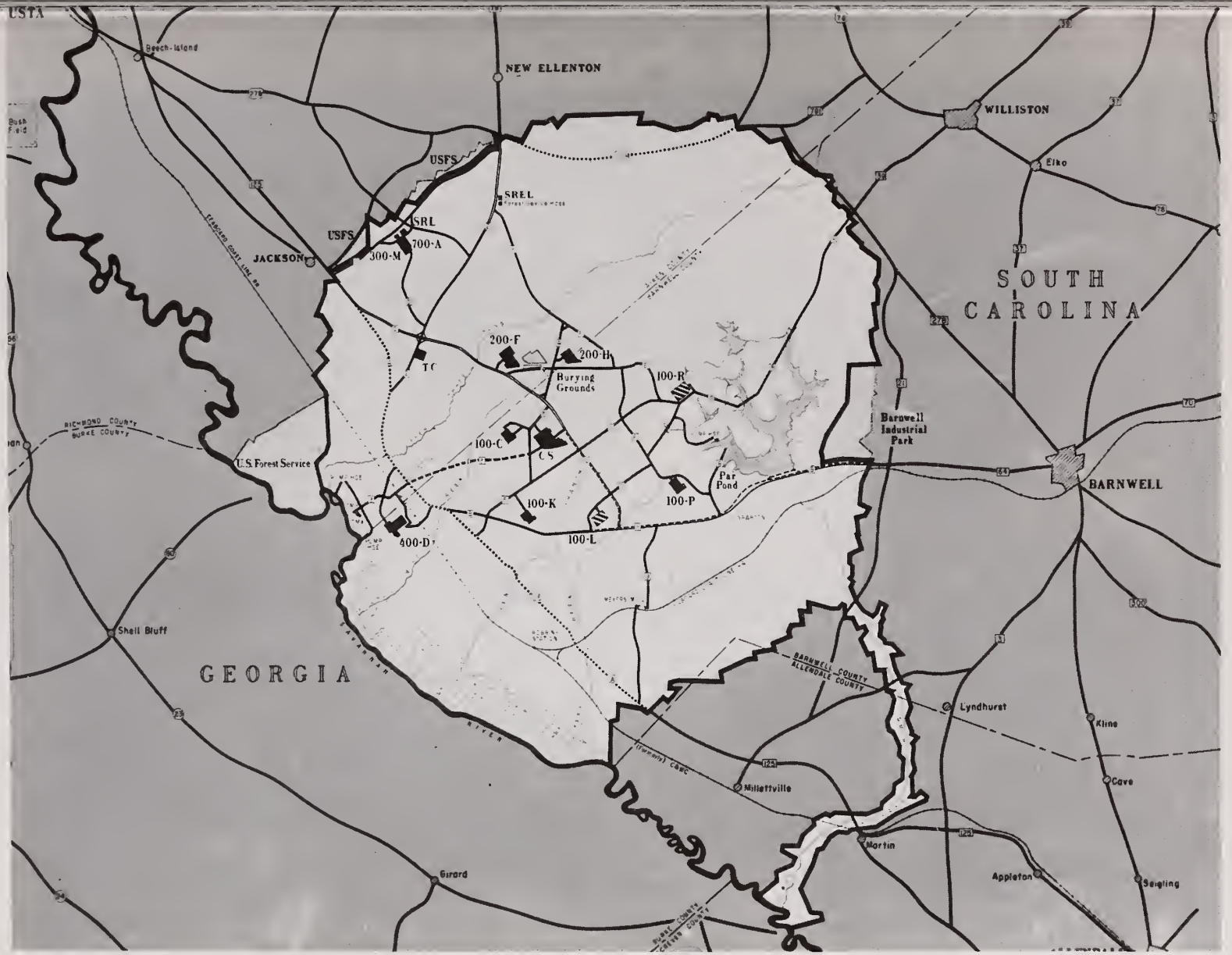

Fig. 1. Savannah River Plant Location and Site.

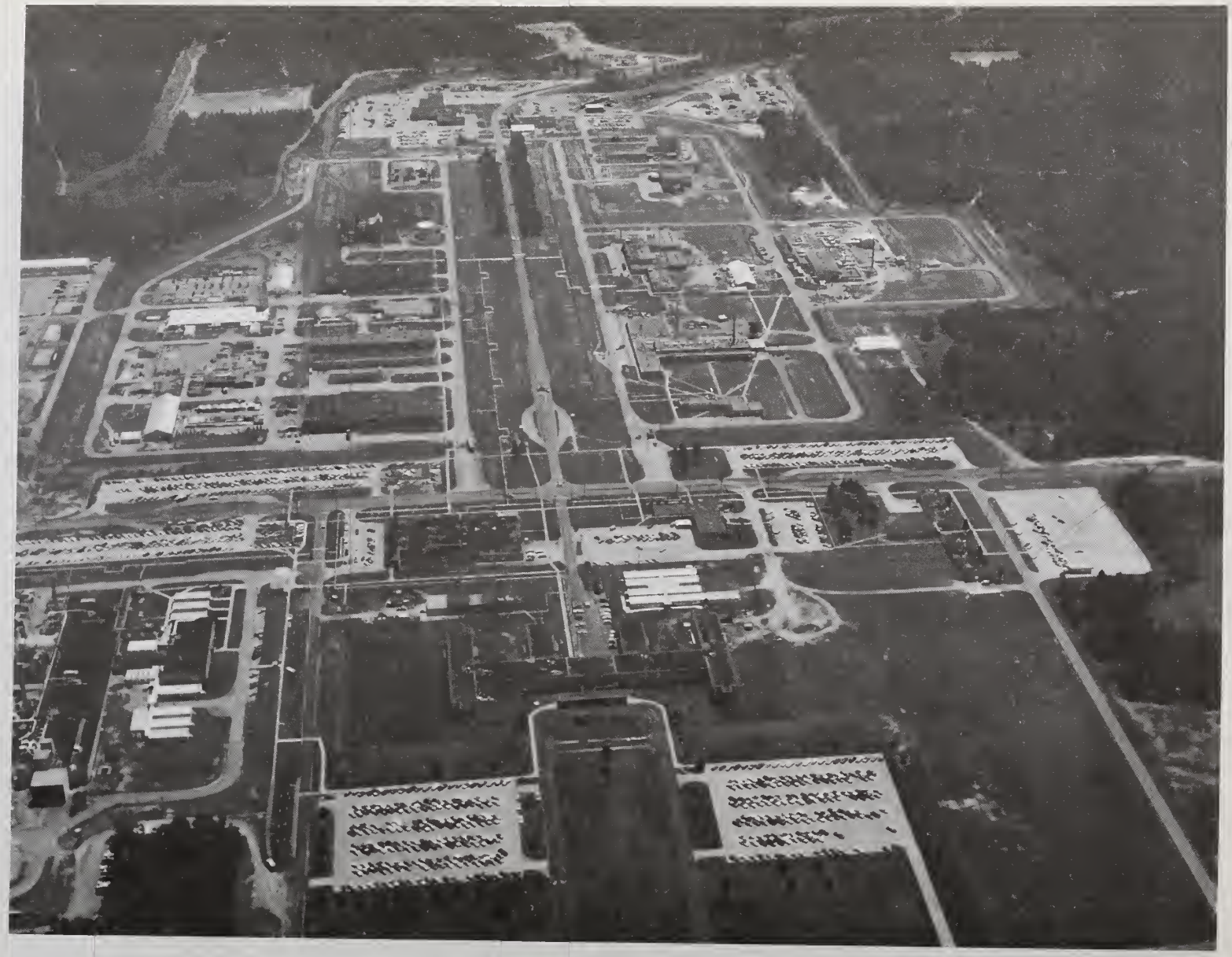

Fig. 2. Raw Materials Area Layout.

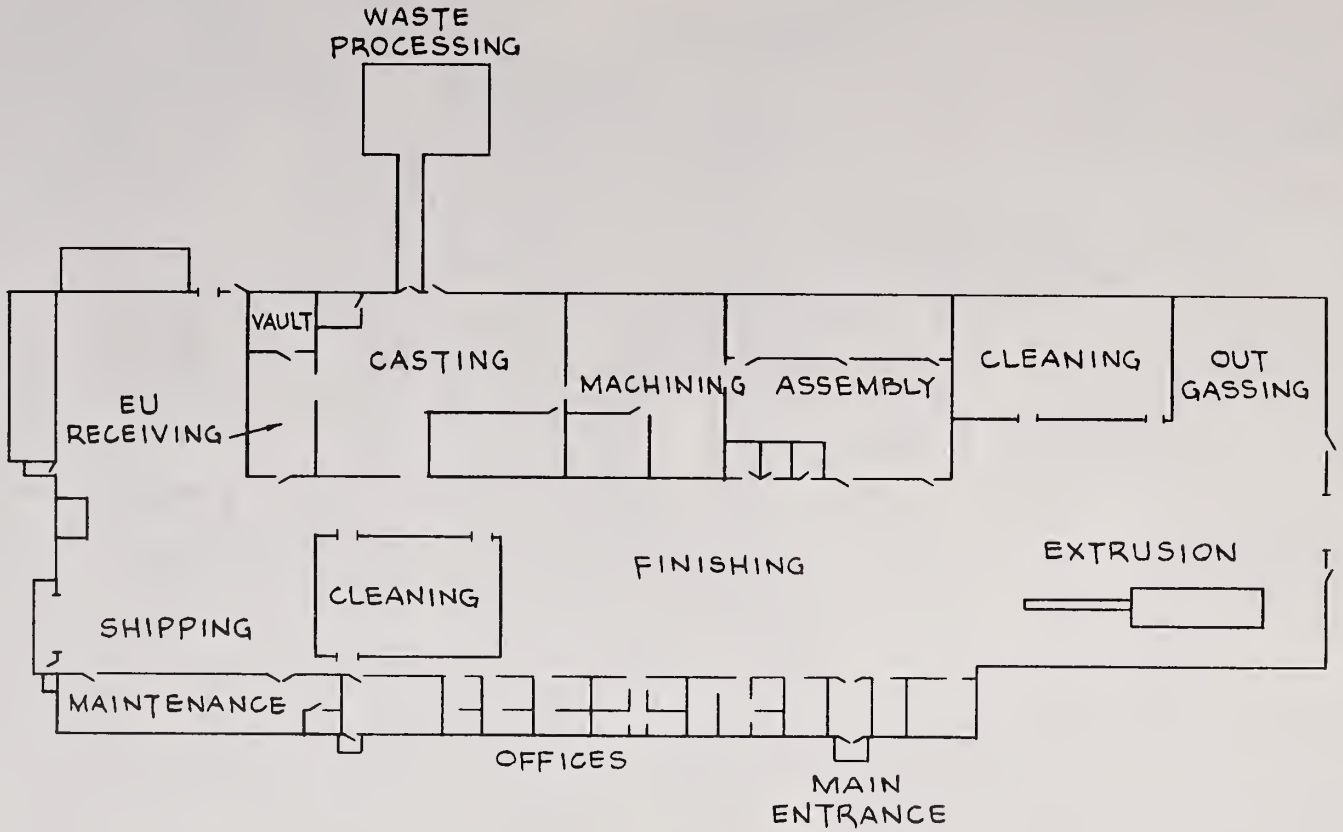

Fig. 3. Fuel Fabrication Building 321-M Layout.

Casting. Batches of about 2 kg of uranium metal are usually blended from several receipt lots. In the casting process, each batch is melted with pure aluminum (figure 4) in graphite crucibles using inductive heating and stirring. The melted mixture is poured slowly into graphite molds to prevent separation of the metals. Molds consist of a cylindrical sheath with bottom and a center spire to form a hollow cylindrical casting (figure 5). Castings of several diameters are produced, depending on requirements for the final product (figure 6).

Machining. Castings removed from molds are mounted in a lathe and the rough, porous upper ends are removed (figure 7). Inner and outer surfaces are also trued but relatively little metal is removed. The upper section which is removed, termed a riser, plus chips from the cutting constitute the bulk of all scrap which is reprocessed in this building. The scrap is clean since no oil is used in machining.

Assembly. Several machined castings with differing diameters are stacked concentrically and placed in an aluminum housing (figure 8) fully enclosing the core. This assembly, called a pre-extrusion billet (figure 9), is welded closed after being baked under vacuum to eliminate trapped air.

Extrusion. The outgassed billet is then heated and placed in a high pressure hydraulic press to be extruded into a log (figure 10). The 250-lb hollow center log is then returned to machining where it is cut into about nine billet cores (figure 11). These cores are then returned to assembly and again housed in aluminum jackets which are also welded closed after outgassing (figures 12, 13). Billets are then preheated and extruded (figure 14), using the same press, into tubes about 20 ft long and from 1-1/2 to 3 in. in diameter.

Finishing and shipping. Extruded tubes are straightened, stretched, cleaned, cut to length, and tested (figure 15). Tubes are then assembled in groups or with targets using aluminum components. The finished fuel tube assemblies (figure 16) are shipped to one of our three reactors for charging into the core.

Safeguards

Physical security. The entire Building 321-M plus a small amount of surrounding territory constitutes the material balance area (MBA). Primary physical security protection is provided by barrier fences, various alarms internal and external to the building, plus our security force. Secondary protection is provided by the M-Area perimeter fences and tertiary protection by plant perimeter fences and limited access permitted to this area.

A centralized, computer-based alarm and data collection system is being implemented. This system will be connected to alarms in all plant areas to provide local assessment of all physical security alarms to security force personnel and will collect all data in a centrally located alarm assessment facility as a backup. Such physical security features are typical of those developed and described by Sandia and others.

Accountability. A high frequency accounting system (HIFACS) is being developed at SRP. This computer-based, centralized data acquisition system will be connected eventually to all SRP production sites to collect and analyze material balance data. Inputs to this system will include data from assay equipment such as that discussed below, many process control instruments, and new operator communications stations at all primary process control locations. Design of this system is similar to other computerized management information systems for accountability data such as DYMAC, DYMCAS, CNMCAS systems which have been widely discussed. HIFACS will utilize the Digital Equipment Corporation's (DEC) Distributed Plant Management (DPM) system including a central PDP 11/70 supervisory computer, PDP 11/34 peripheral data collection computers in each major plant operating area, and LSI 11 series microcomputers and RT805 operator input terminals within production facilities. Programming of a prototype system is in progress.

Safeguards requirements analysis. Both formal and informal analyses of needs for fissile material protection are being completed for all SRP processes. The Diversion Path Analysis (DPA) developed by NBS, various forms of risk and threat analyses (as well as an assessment of facility and production requirements) were completed to assess physical security, material control, and nondestructive analysis requirements for the Building 321-M facility.

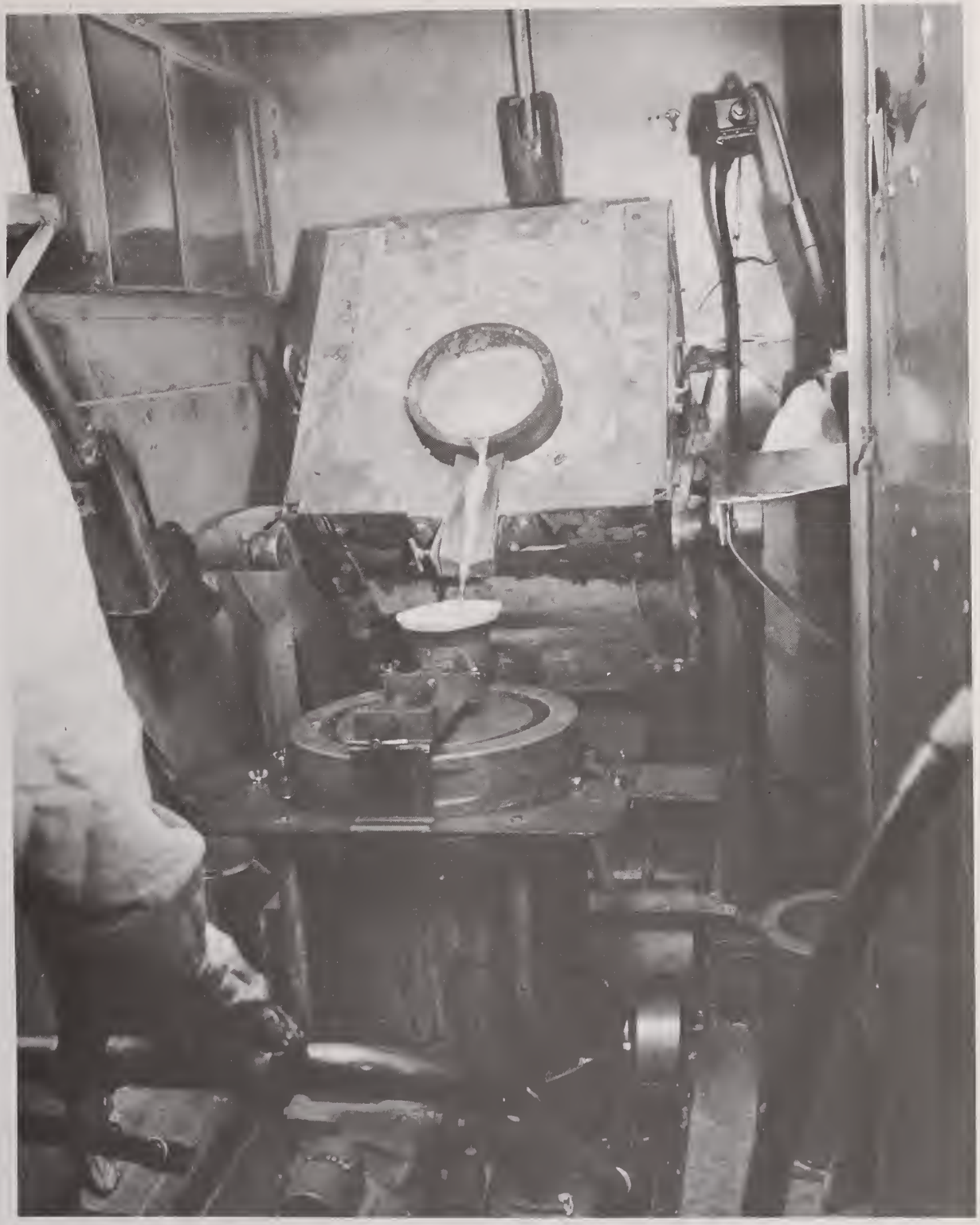

Fig. 4. Pouring a Uranium-Aluminum Casting.

Fig. 5. Uranium-Aluminum Casting Being Removed from a Mold.

Fig. 6. Uranium-Aluminum Castings of Various Sizes.

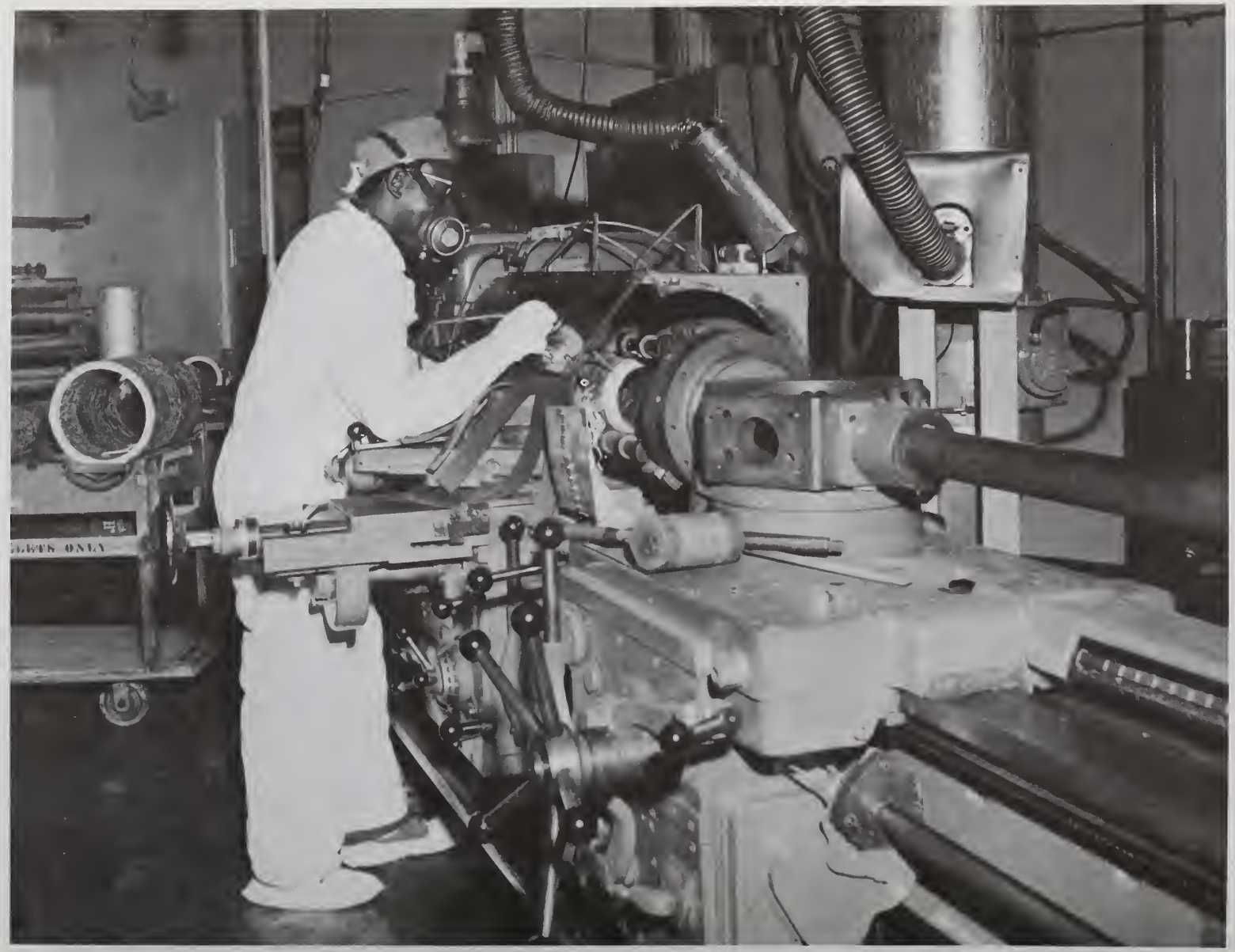

Fig. 7. Machining Uranium-Aluminum Casting.

Fig. 7. Machining Uranium-Aluminum Casting.

Fig. 8. Pre-extrusion (PX) Billet Components.

Fig. 9. Welding Pre-extrusion Billet.

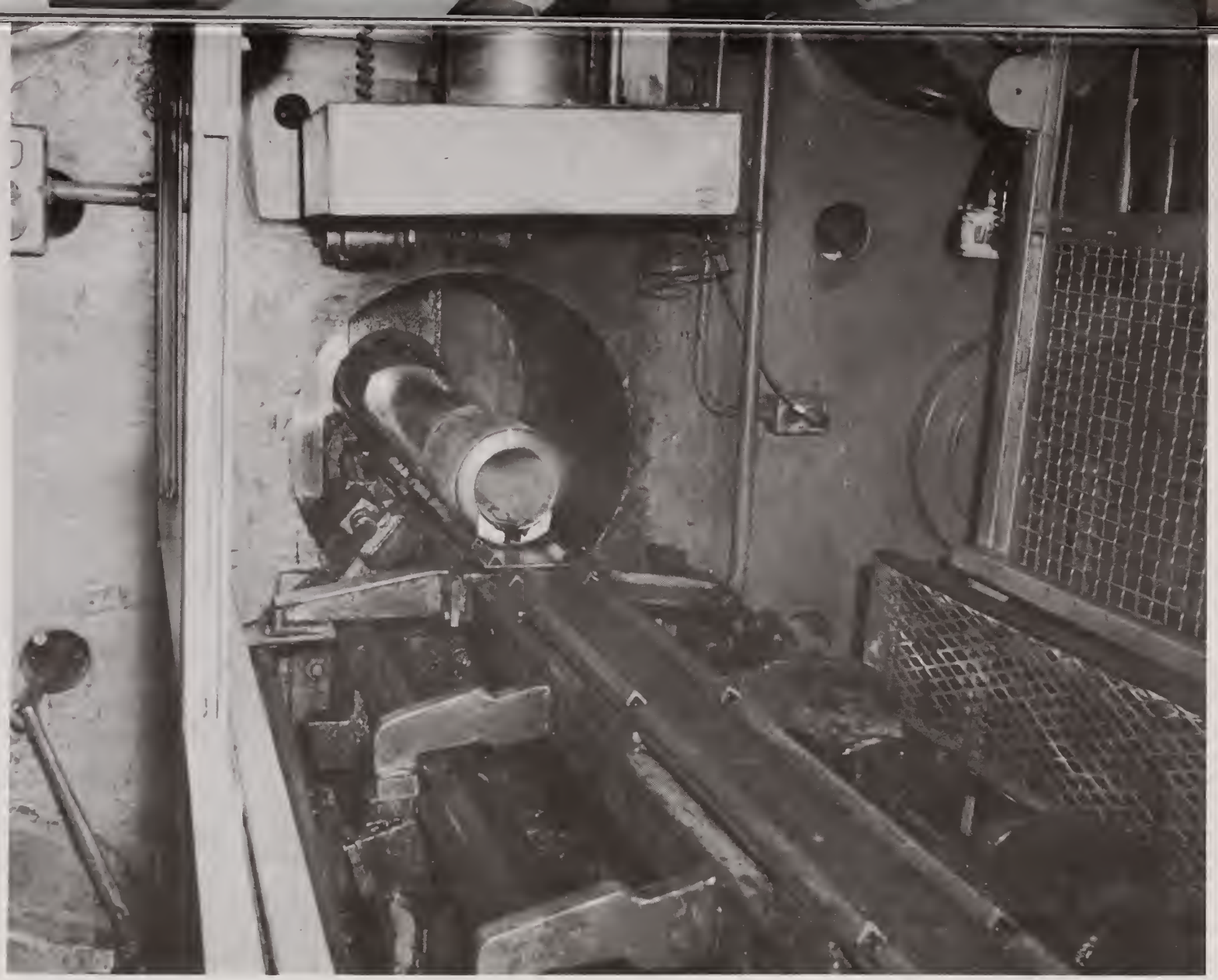

Fig. 10. Log Extrusion.

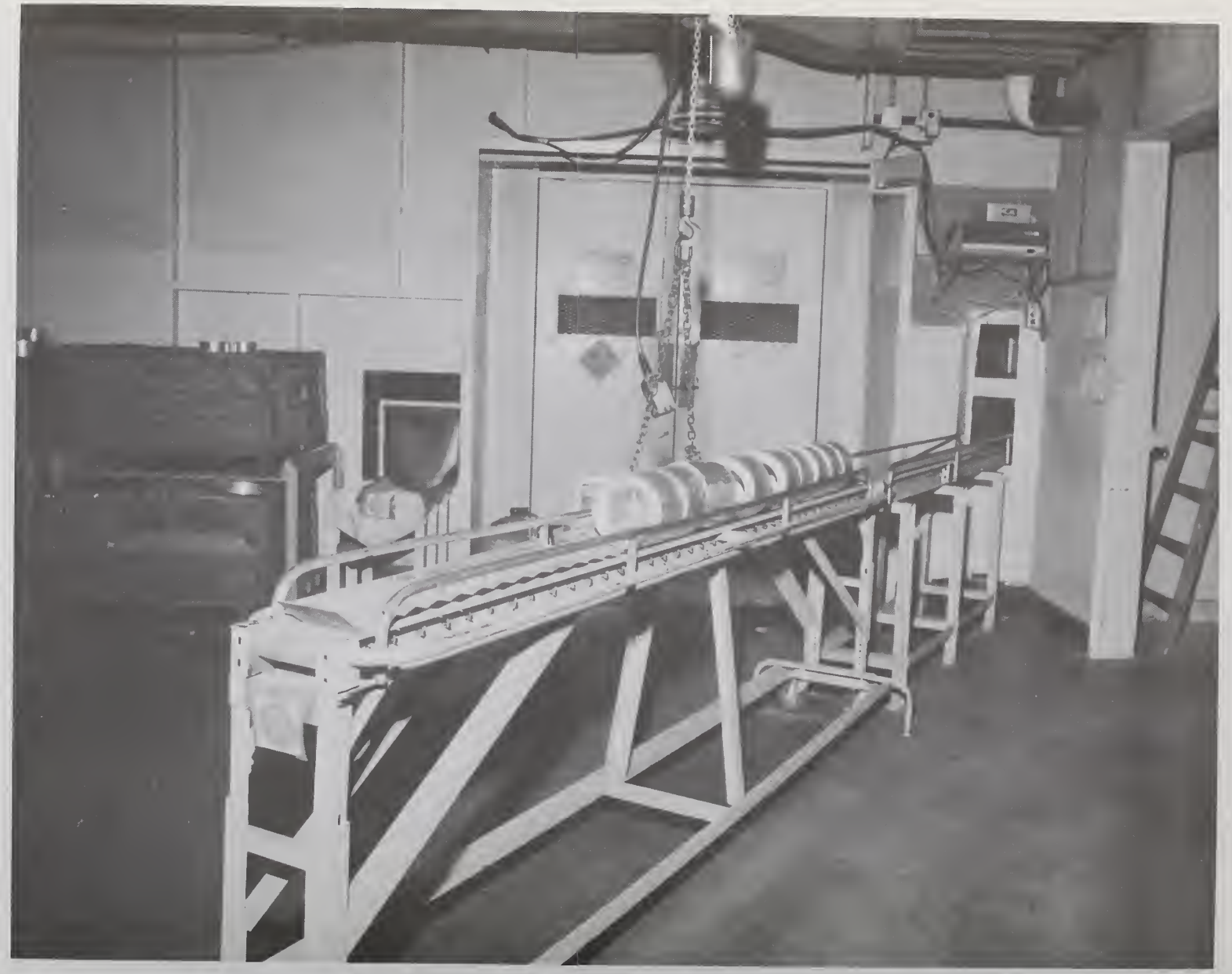

Fig. 11. Coextrusion (CX) Billet Cores.

Fig. 11. Coextrusion (CX) Billet Cores.

Fig. 12. Coextrusion Billet Assembly.

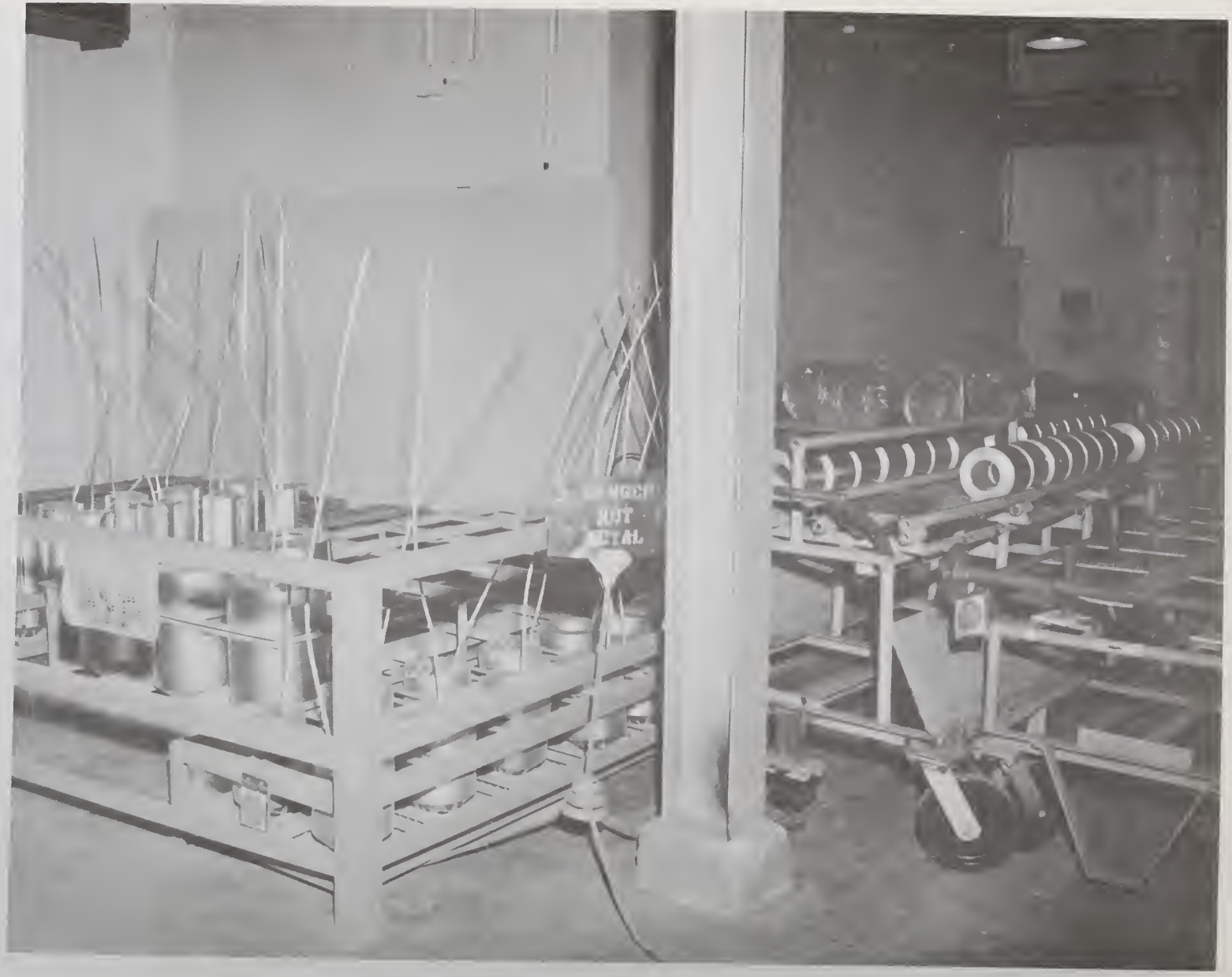

Fig. 13. Billets Ready for Outgassing and Extrusion.

Fig. 13. Billets Ready for Outgassing and Extrusion.

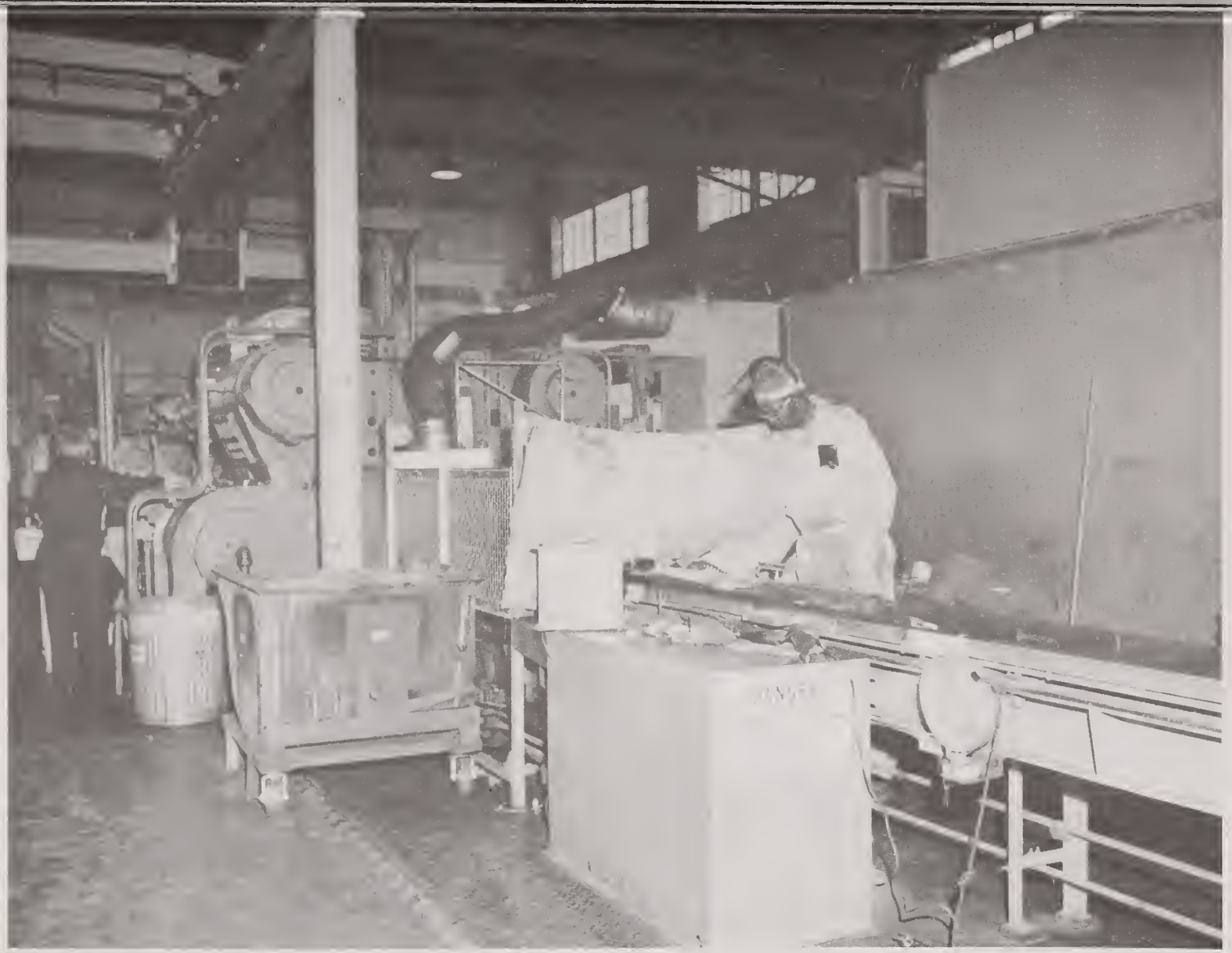

Fig. 14. Fuel Tube Extrusion.

Fig. 15. Fuel Tube Finishing.

Fig. 15. Fuel Tube Finishing.

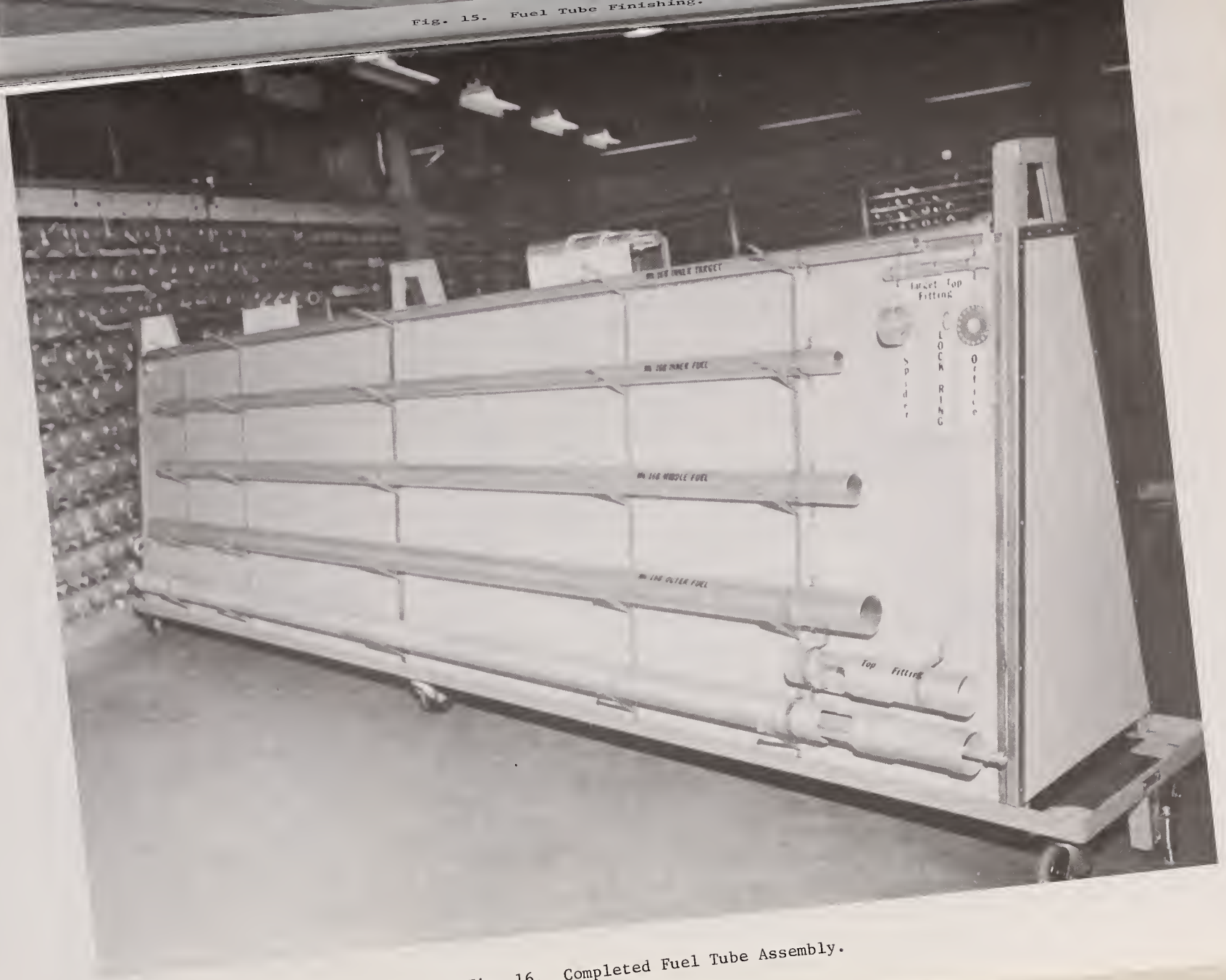

Fig. 16. Completed Fuel Tube Assembly.

Assessment of criteria for nondestructive assay (NDA) and material control systems determined that equipment should be installed in-line with the process in a manner to minimize the possibility of being avoided, bypassed, or having material recirculated around the measurement. The equipment should be inviolate, self-sufficient, operator independent, and provide unambiguous measurements with high confidence so that data reflect an accurate evaluation of materials of interest. This equipment must also communicate with operating personnel (on a limited, guidance basis) and security forces as well as the accountability data collection system. However, all communications should be guarded against defeat of the intended function.

Material Control Systems

High sensitivity of detection and speed of response may be employed in many safeguards measurements instead of high precision. Most systems in this category are breakthrough sensing devices to detect nuclear materials where none should be. Examples of this class of instruments are doorway monitors used to assist establishment of impenetrable physical security barriers, detectors for drainlines and filter effluents, plus screening devices for supposedly clean waste and scrap. Another group of devices fitting this category are surveillance systems used to protect stored materials.

An example of a material control system designed for the Building 321-M process is the boxed clean waste SNM detector (figure 17). This instrument checks 30 × 30 × 30-in. (0.75 m) cardboard boxes filled with up to 50 lb (23 kg) of waste from offices. The system is designed to require less than 1 minute to detect 10 g of ^{235}U (worst-case conditions). Operator requirements for the system are limited to loading boxes and acknowledging the fact with a start pushbutton or resetting the system after a box causing an excessive count (any gamma) is removed. Clean boxes are automatically ejected from the exit which would not be accessible by the operator, except through a doorway monitor (also sensitive to 10 g of ^{235}U). System conditions, such as door positions, internal weight, metal content of boxes, background internally before a test as well as externally during tests of boxes, standards and general system operation, are frequently checked by a microprocessor in the system to obtain high confidence that performance continues to meet requirements. The system is also designed to fail "softly" and recover automatically whenever possible to minimize false alarms and maintain confidence in the system by production personnel.

A second material control system has been designed to monitor enriched uranium metal stored in the vault (figure 18) between time received and use in casting. A weight detector located inside each storage container is scanned by a microprocessor-based monitor. Unauthorized weight changes of 10 g in any container will generate alarms. Operators making normal additions or deletions of materials are prompted by the system. Operators are also assisted in recovering from common mistakes but repeated errors or tampering with the system causes alarms.

Nondestructive Assay Systems

Prime measurements. The most significant assay measurements are receipts (metallic-enriched uranium in chunk form) and shipments (reactor fuel tube assemblies). The best methods to make these assays are currently being studied. A receipts monitor would typically employ a fully penetrating, definitive measurement (such as active neutron interrogation) plus confirmatory measurements such as weight (higher precision) and gamma analysis (isotopic content and enrichment) with data correlated and checked against shipper's claims.

Process scrap. The next most valuable measurement for accountability in our fuel fabrication facility is scrap assay. In the fuel tube fabrication process (figure 19), a variety of ^{235}U bearing scrap which is produced is recycled into castings. Over a period, ^{235}U returned to castings is about equal to the amount charged from raw material receipts. Short-term accountability balances, therefore, depend greatly on knowledge of the ^{235}U content of this scrap. ^{235}U assay accuracy should, therefore, be equal to or better than measurements of receipts or shipments.

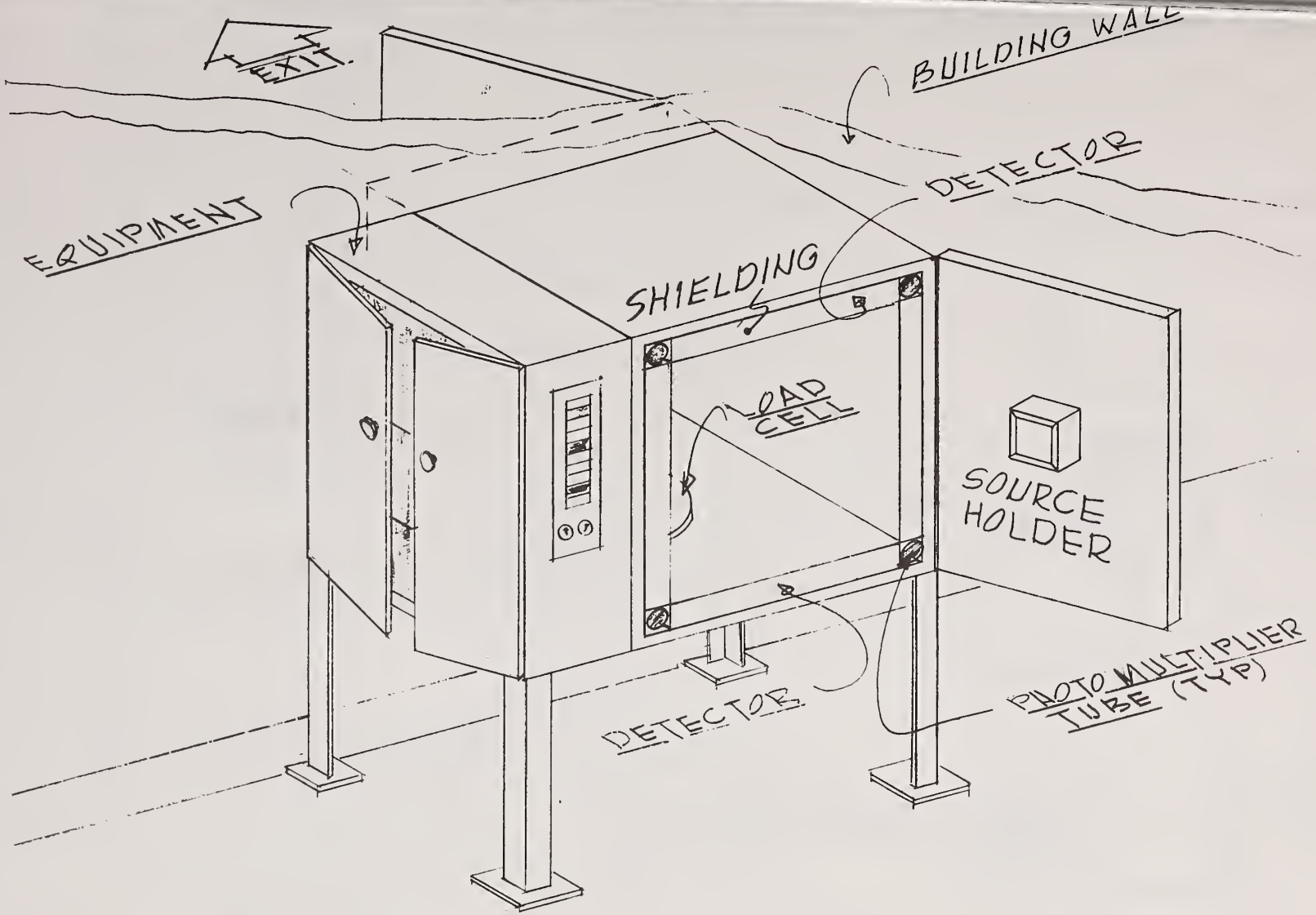

Fig. 17. Boxed Clean Waste SNM Detector.

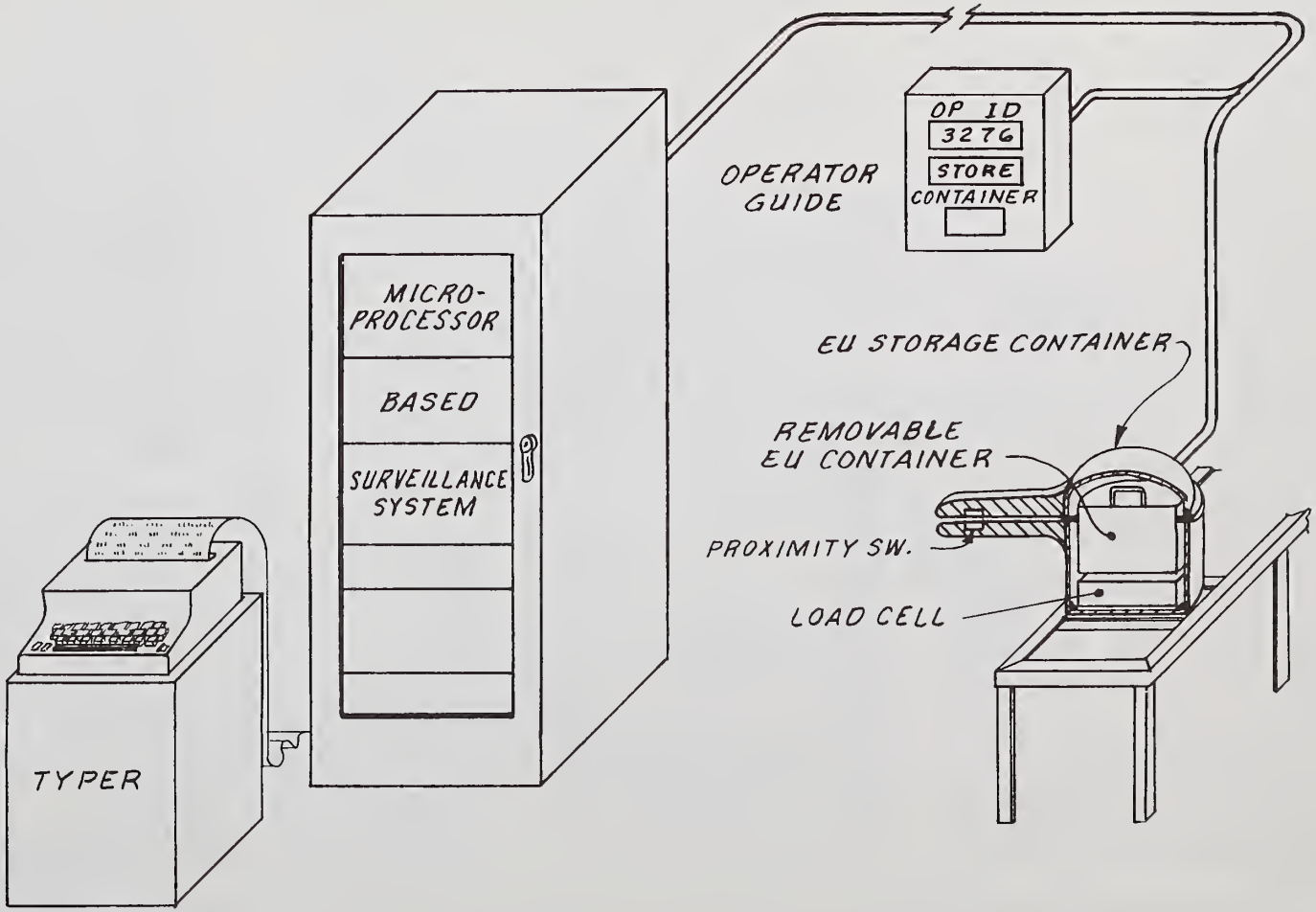

Fig. 18. Enriched Uranium Vault Surveillance System.

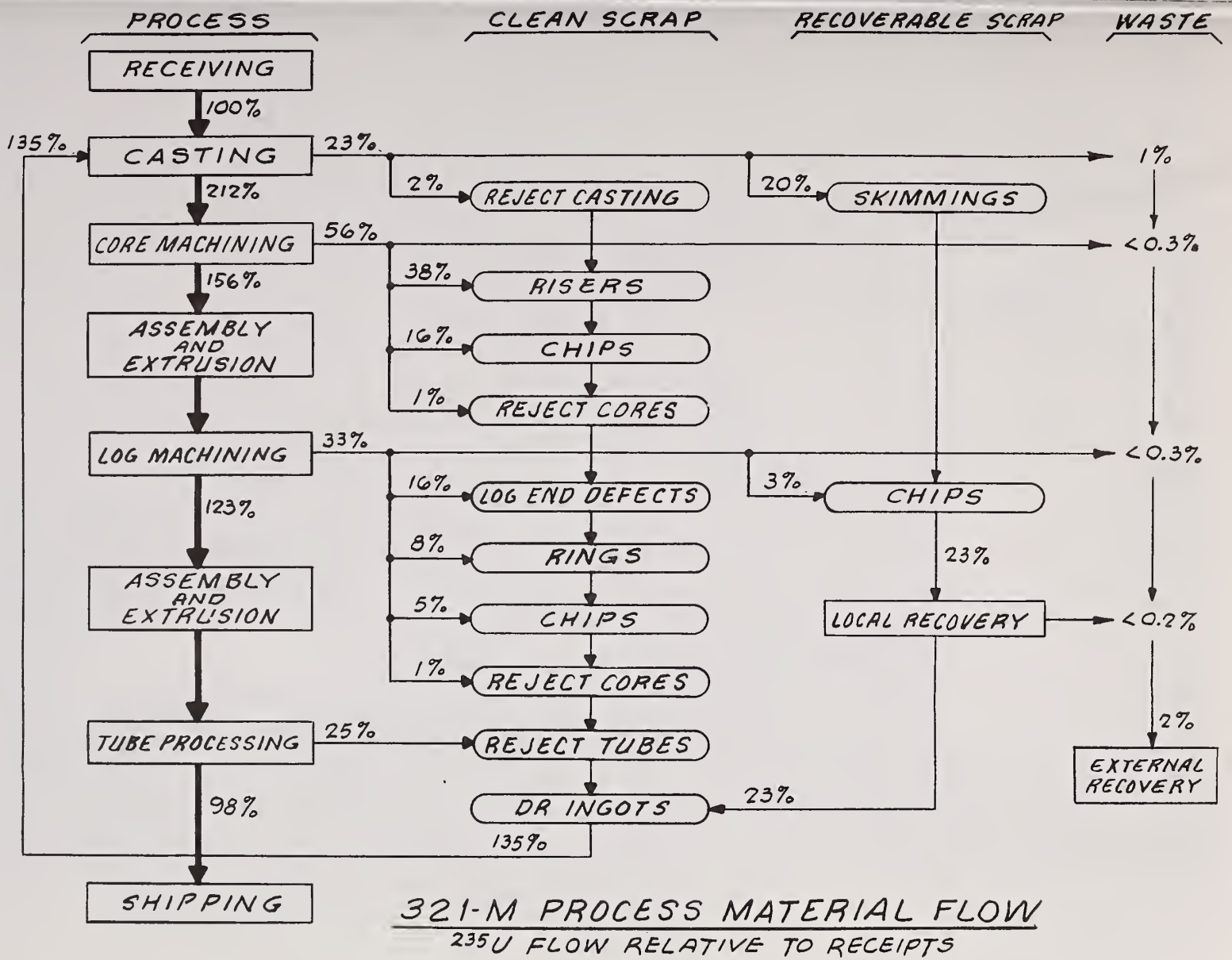

Fig. 19. Process Material Flow.

Scrap characteristics. Assay of scrap to high precision and confidence is complexed by the many possible forms having widely differing geometries, matrices, and densities. Risers, the porous tops cut from castings, and the lathe chips from cutting and facing the castings are major contributors to the scrap. Log end defects, which are mostly aluminum, are the ends with irregular uranium-aluminum concentrations remaining after an extruded log is cut into billets. Rings are small sections of these logs too short for a billet. DR ingots are a product of a local scrap recovery process where heavily oxidized froth skimmed from the top of a crucible in casting plus any other material with suspect purity is reclaimed. The 6 × 6-in. (15 cm) solid cylindrical DR ingot is poured rapidly, unlike a casting, and the slow solidification permits the uranium-aluminum mixture to separate, the heavier uranium settling to the bottom. Uranium concentration ratios of three to one from bottom to top are common.

Scrap containers. Loose scrap such as chips or the casting froth skimmings is placed in 7-in.-dia × 12-in.-high (18 × 30 cm) stainless steel, thin wall, capped scrap cans. Parts of larger pieces, broken before being recharged into casting crucibles, are also placed in scrap cans. Materials of differing types or from different batches are not mixed in these cans.

Scrap Assay

Current method. ^{235}U content of scrap is now accounted for by tracing materials from the source and is confirmed later with laboratory analysis of samples. Some inaccuracies result in this method, however, for the more inhomogenous forms of scrap. Additional errors result where scrap such as heavily oxidized skimmings from the casting process must be purified in the local recovery process.

NDA methods. Nondestructive assay methods available for measurement of this scrap are limited due to the variability and high density of some forms. Gamma measurements of natural 185 keV photons respond only to surface materials due to the 0.24 mm half thickness of uranium at this energy. Large assay errors would result wherever surfaces were not fully representative of the scrap (such as in casting risers, DR ingots, etc.). Many other NDA techniques, such as weight, are not sufficiently definitive to provide adequate assurance that material substitutions had not been made. Neutron measurements are sufficiently penetrating and are definitive. Natural productivity of neutrons from spontaneous fission of ^{235}U is too low to obtain a reasonable measurement period. However, active interrogation where an external neutron source is used to induce some of the ^{235}U to fission produces adequate number of neutrons for satisfactory counting statistics in a reasonable period from well under 1 g of ^{235}U.

Variables in process scrap can cause significant measurement errors due to neutron absorption and moderation. Neutron absorption by ^{236}U content of recycled EU increases rapidly as neutron energies decrease into the thermal energy region. Neutron energies are reduced by moderators such as aluminum content of the scrap. Reduction in neutron energy increases the probability of capture by ^{235}U and the detectors as well as increasing absorption, all of which change response per gram of ^{235}U for differing variables in the scrap. These errors may all be reduced by maintaining neutron energies at a high level where response to variations is fairly constant or linear.

Californium shuffler. An NDA system was developed by Los Alamos Scientific Laboratory to assay scrap in the SRP fuel fabrication process (figure 20). This system utilizes neutron activation analysis (active neutron interrogation) and weight measurements to assay ^{235}U content of all forms of scrap in this process. A high energy, high strength (1 Ci, 1 mg) ^{252}Cf source is used to irradiate samples (generates about 1.5×10^9 neutrons/sec). Neutrons generated by fissions of the ^{235}U in samples are counted by ^{3}He detectors. To eliminate the requirement to differentiate between source and sample generated neutrons, the source is oscillated between the irradiation position and a shielded, storage position. Detectors count about 3,000 neutrons/sec from 3 kg of ^{235}U. The system cycles through eight irradiation and counting cycles of 12 seconds each for a total test time, including background and weighing, of about 8 minutes.

Fig. 20. ^{252}Cf Shuffler.

In service, a loaded scrap can containing up to 25 kg of scrap is inserted in an aluminum canister. The canister is connected to a hoist provided with the system and is lowered into the measuring chamber (well) onto a turntable support. The hoist is disconnected from the canister and is used to lower an 85-lb shield plug into the chamber top above the canister to protect personnel from the intense (approximately 1 rem) radiation field produced by the californium interrogation source. An operator enters the sample ID through the typer and prompts the microprocessor to start the assay. The canister is then lowered by an internal elevator (figure 21) onto three load cells three times and the average weight is calculated. The canister is then raised and rotated for the remainder of the assay. The californium source is moved (shuffled) about 4 ft from the storage position to the irradiation position in 0.5 second. The sample is irradiated for 12 seconds during which two small ^{3}He flux counters measure irradiation field strength. The source is then withdrawn to the storage position and delayed neutrons produced by fissions of ^{235}U are counted for 12 seconds by 22 large ^{3}He neutron detector tubes. The alternate irradiation and counting cycle is repeated five to 30 times to accumulate about 300-k delayed neutron counts, enough, depending on ^{235}U content for satisfactory (0.3%, 2σ) counting statistics.

Calibration performance. In laboratory tests, reference source disks specially manufactured and analyzed for this system were used to evaluate performance of the shuffler. Precisions of about 0.1% were achieved in tests with measuring times extended to 30 cycles, repeated 30 times to calibrate the system using these sources. Precisions better than 0.4% are achieved for normal assays of materials containing more than 600 g of ^{235}U. System stability was better than 1% per month.

Vertical linearity of the sample chamber was measured by elevating a single 1-in. disk in 1-in. increments. Calculated ^{235}U content increases 4% near the center of the well and then drops to -20% at the top due to nonuniformity of the irradiation field and sensor arrangement. Actual scrap measurement errors due to nonlinearity are much less (about 1%) since scrap is loaded relatively uniformly from the bottom of the can, rarely filling most cans. Additionally, measurement corrections are made by fitting data to a curve determined during system calibration.

Sensitivity of measurements to aluminum content (moderator) was measured by surrounding reference source disks with pure aluminum disks of the same size. Worst-case error with one uranium-aluminum disk placed among 10 aluminum disks was +20%. This error is attributed primarily to increased capture by ^{235}U of interrogation neutrons reduced in energy by aluminum moderation. Data from these tests are currently being evaluated to determine if corrections, such as by sample weight, can be calculated.

Assay performance. Experience with the shuffler in Building 321-M has been good. Operating reliability has been excellent during the 6 months since installation with no significant problems. System stability over this period, checked daily using six source disks, showed changes typically less than 0.05% per day without any measurable long-term accumulation. Assays of various forms of scrap indicate that results are very consistent (well within 1% of expected values) for single types of scrap. However, results between types of scrap differ from expected (traced) values and the reference source, particularly for lowest density materials. This indicates the need for corrections for type of material possible by weight and a height (density) measurement or by identifying the type material being tested. Response data are currently being analyzed to evaluate possible corrections and to identify the number of types which must be accomodated to achieve a specified level of accuracy. Additional standards with accurately known ^{235}U content and with other parameters closely matched to a particular type of scrap (DR ingots, chips, etc.) have been designed and are being fabricated to evaluate corrections.

To assess potential applicability of neutron activation analysis for other materials in this process, billet cores cut from logs were also assayed in the shuffler. Performance is good with excellent self-consistency. However, indicated ^{235}U content per gram exceeds that for chips since these billets are relatively thin wall and have a low overall density.

Reference sources. To determine response of the californium shuffler, a set of solid uranium-aluminum disks was specially manufactured. The constituents of the metal closely correspond to current production alloys and density is equivalent to the most dense scrap which would be measured. Each disk is 1 in. (2.5 cm) thick × 6-in. diameter (15 cm) and weighs about 1.7 kg of which about 300 g is ^{235}U, 200 g other uranium isotopes, and the remainder fairly pure aluminum. Disks are encapsulated in a welded aluminum can (figure 22) making the finished source disk 1.1 in. (2.8 cm) × 6.75-in. diameter (17 cm). Eleven of these disks will fit into a standard scrap can.

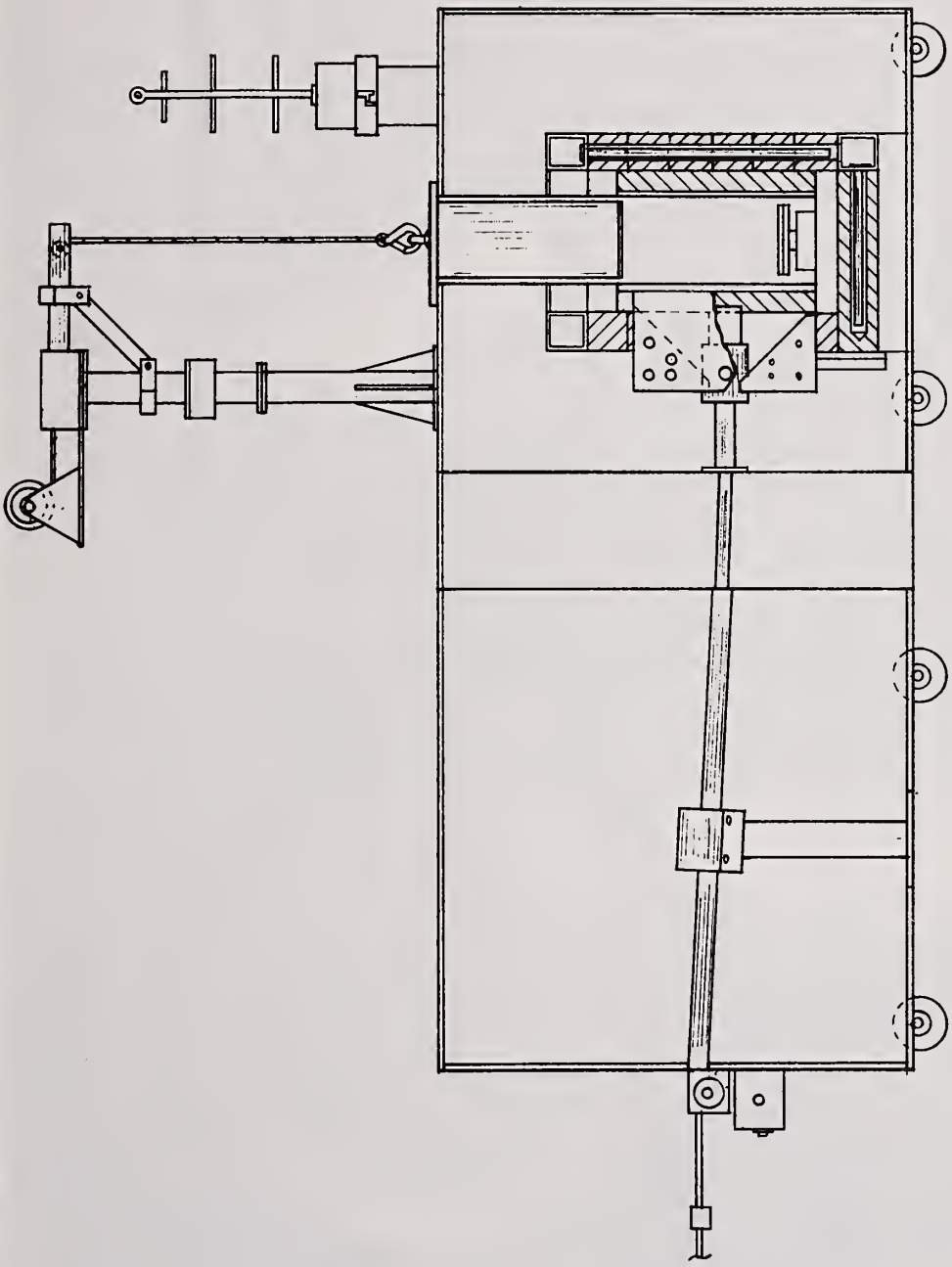

Fig. 21. ^{252}Cf Shuffler Layout.

Fig. 22. Encapsulated Source Disks and Scrap Can.

Manufacture of these disks was carefully controlled to achieve maximum material uniformity and to permit the highest accuracy calibration of ^{235}U content currently available. All new materials were used (virgin ^{235}U and recycled uranium blended to match current production alloys and all virgin aluminum) and traced. A special-collapsed center, solid log (figure 23), was manufactured using carefully controlled standard production techniques. Source disks were then cut from the log, with original orientation of each disk documented. A 1/4-in.-thick (0.6 cm) disk was also cut between each 1-in. disk to provide representative laboratory samples. These sample disks were sectioned in quadrants and four sets of laboratory samples were assembled by selecting quadrants rotated 90° for each successive sample disk throughout the log. This reduces effect of linear or circumferential concentration of materials in the log. One of the four sets of samples was then destructively analyzed by laboratories at SRP and at LASL using several analytical techniques (figure 24). Analysis of laboratory data and maximum precision measurements with the shuffler (figure 25) provides ^{235}U content of each disk with an uncertainty of 0.91 g (±0.3%). One-inch source disks were also examined using gamma analysis of many small surface areas and by fluoroscopy to confirm that no significant segregations of uranium were present.

Fig. 22. Encapsulated Source Disks and Scrap Can.

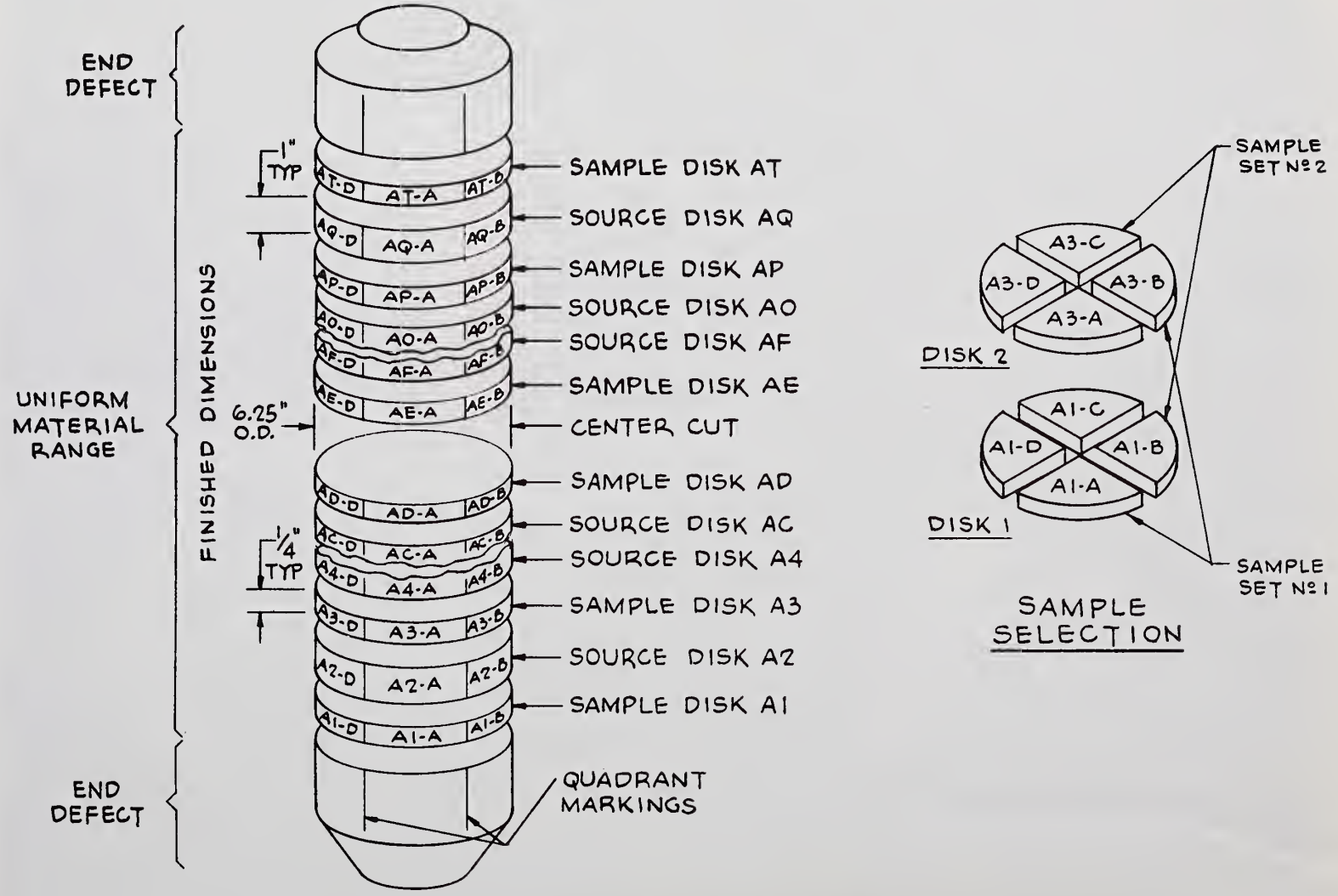

Fig. 23. Reference Source Log Arrangement.

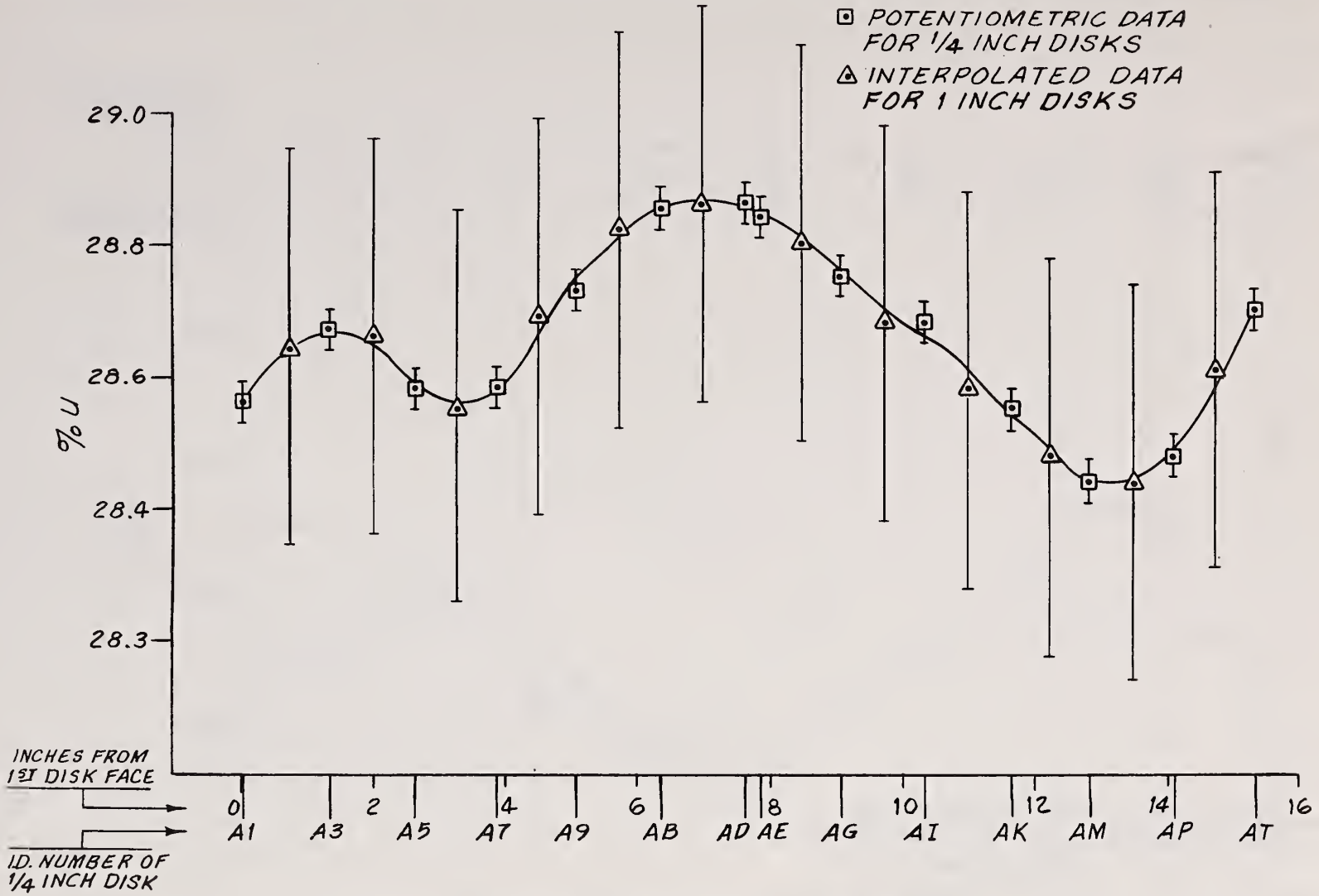

Fig. 24. Laboratory Analysis of Reference Source Disks.

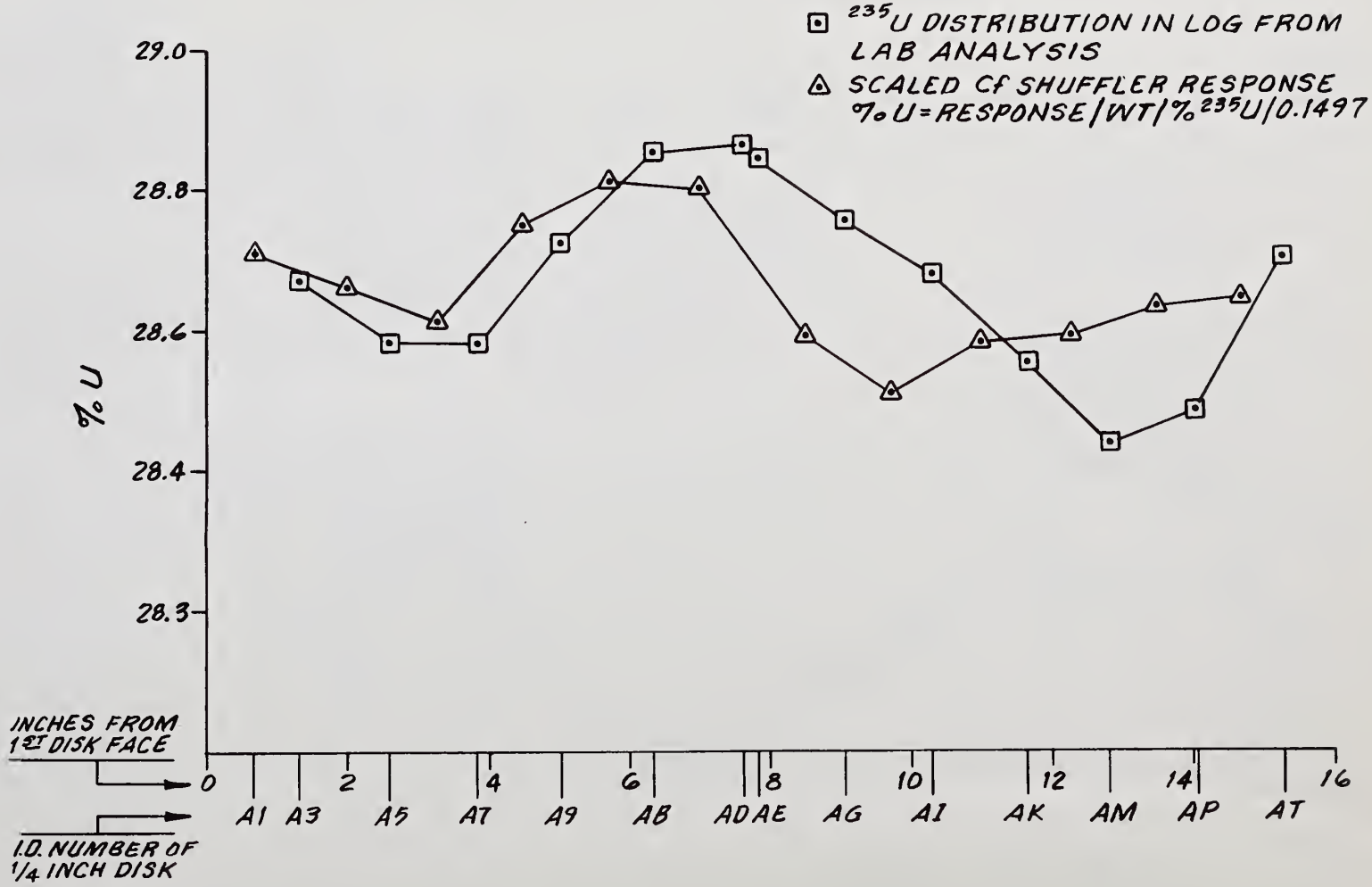

Fig. 25. Californium Shuffler Response to Source Disks.

Discussion:

Nilson (Exxon Nuclear):
You have a very complicated fuel fabrication process and it is interesting to see how you have been able to instrument it in a nondestructive way. I wonder how you made your material balance before this?

Studley (SRP):
Primarily by tracing the original material from the uranium put into the casking. Of course as material recycles through the scrap process problems increased in maintaining accuracy.

Nilson:
And this is all highly enriched uranium too, it is very sensitive to safeguards.

An In-Line Monitor of Plutonium Holdup in Glovebox Filters

T. K. LI and R. S. MARSHALL
University of California, Los Alamos Scientific Laboratory,
Los Alamos, NM 87545

ABSTRACT

An in-line filter holdup monitoring system has been designed and installed in the Los Alamos Scientific Laboratory (LASL) Plutonium Processing Facility to detect plutonium buildup in a glovebox exhaust filter. The filter is located on top of a glovebox in which PuO_2, UO_2, and carbon are blended, milled, and prepared for making advanced fast breeder reactor (FBR) fuel. The system uses a 5- by 5-cm NaI detector for the gamma-ray nondestructive assay of plutonium in the filter. The system is simple and inexpensive, and is able to automatically and continuously collect data on plutonium buildup. The system is capable of measuring less than 0.1 g of plutonium in the filter.

KEYWORDS: In-line holdup monitor; glovebox filter; NaI detector; nondestructive assay; real-time accountability.

INTRODUCTION

Plutonium holdup in glovebox exhaust filters can be a significant fraction of plutonium holdup in process gloveboxes. This situation frustrates real-time accountability and nuclear material control because the filters are typically changed and measured for plutonium holdup only at several-month intervals. From the safeguards point of view, it is important to determine the rate of plutonium buildup on filters as a function of the amount of plutonium processed.

An in-line filter holdup monitoring system has been designed and installed in the new Plutonium Processing Facility at the Los Alamos Scientific Laboratory (LASL) to determine the rate of plutonium buildup in a glovebox exhaust filter. The monitored filter is located on top of a glovebox in which PuO_2, UO_2, and carbon are blended, milled, and prepared for making advanced fast breeder reactor (FBR) fuel. The monitoring system uses a NaI detector for the gamma-ray nondestructive assay of plutonium in the filter. Advantages of the NaI detector are its high efficiency, low cost, compact size, and its ability to operate at room temperature. The only disadvantage of the NaI detector is that the resolution is not good enough to separate the major gamma rays of ^{239}Pu from other interfacing peaks. However, all the PuO_2 used for fabricating the FBR fuel is aged enough so that the daughter products and parent isotopes are in equilibrium. Furthermore, since the isotopic composition in the process is consistent, gamma-ray intensity ratios from different isotopes remain unchanged. Gamma rays over the range of 320 to 470 keV emitted by ^{239}Pu, ^{241}Pu-^{237}U, and ^{241}Am are measured for determining the plutonium buildup in this study.

This paper describes the measurement method, including calibration, and reports the results of a study of the rate of plutonium buildup in a typical glovebox exhaust filter.

MEASUREMENT METHOD

The Glovebox Exhaust Filter and the Holdup Monitor

Glovebox air is exhausted through at least three stages of filtration to remove airborne contamination. A high-efficiency particulate air (HEPA) filter, located in a filter housing on top of the glovebox (Fig. 1), removes most of the particulate matter.

Additional filtration in the building glovebox exhaust system traps any airborne radioactive particles that pass through the glovebox filter.

The 20.3-cm-diam by 14-cm-long HEPA filter (Fig. 2) is rated at 99.97% efficiency for 0.3-micron particles. A perforated spacer located above the active HEPA filter allows the exhaust air flowing through the filter to pass out into the exhaust duct. Above the spacer is a replacement HEPA filter that blocks upward contamination in the filter housing. When the active HEPA filter needs to be replaced, the replacement filter is pushed downward until the active filter drops into the glovebox.

The in-line filter holdup monitor, a 5- by 5-cm NaI gamma-ray detector, is installed on the top of the glovebox at a distance of 18 cm from the active HEPA filter. The detector is well shielded and collimated by lead. The design of the collimation and shielding allows the detector to view the entire active HEPA filter only, and sufficiently eliminates the gamma-ray signal coming from large quantities of plutonium in the glovebox beneath the detector. The cylindrical column that houses the filter is also well shielded to prevent gamma rays emitted by radioactive materials in adjacent gloveboxes, conveyors, or equipment from reaching the detector. Absorbers of lead (approximately 1.5-mm-thick) and cadmium (approximately 0.8-mm-thick) are placed in front of the detector to attenuate the intense low-energy gamma rays and x rays.

Electronics

A block diagram of the monitoring system electronics is shown in Fig. 3. Gamma rays emitted from the filter are detected by the NaI detector and analyzed by single-channel analyzers (SCAs). Three SCAs are used for determining the plutonium gamma-ray peak area and adjacent backgrounds. Because all the plutonium processed in this particular glovebox is aged and of consistent isotopic composition, the assay window is set at 320 to 470 keV for the ^{239}Pu and ^{241}Pu gamma-ray complex. An automatic gain-control (AGC) amplifier minimizes shift from counting-rate variation and photomultiplier-tube aging. The system is stabilized by setting the SCA discriminators in the AGC amplifier at the 662-keV gamma-ray peak emitted from a 1-μCi ^{137}Cs source. The SCA outputs, including output from the AGC amplifier, are fed to counters that are interfaced to a printing unit. The printer is a digital printing accessory and program-control center for the data acquisition system. The data from each counter in the system is printed in sequence, with an automatic paper-tape

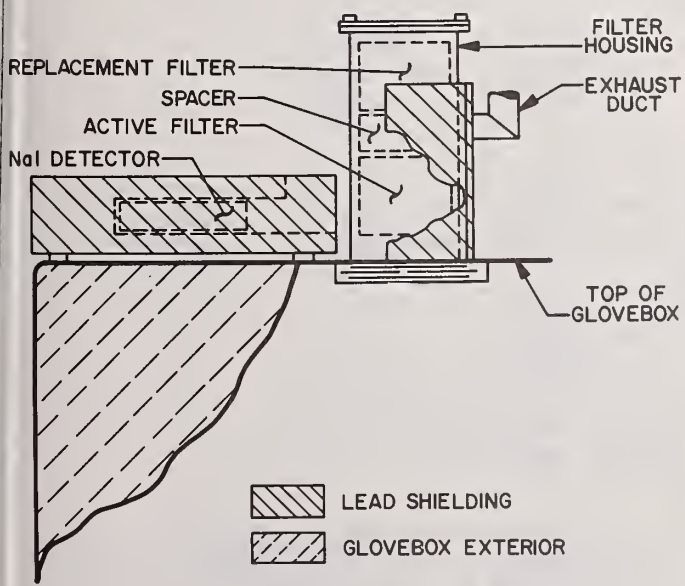

Fig. 1. Arrangement of the glovebox, filters, and detector, including shielding and collimation.

Fig. 2. The HEPA filter for the holdup monitoring system.

advance for each new data word. By presetting the printer to recycle, and the counter/timer to a specific counting time interval, the system will continuously collect and print the data. This automatic system minimizes operator intervention once the system has been calibrated and set up for measurements. The multichannel analyzer (a Tracor-Northern NS-710) is used only during the initial set-up.

CALIBRATION

The system was calibrated with three plutonium filter standards. The LASL Analytical Chemistry Laboratory prepared the standards by adding known quantities of PuO_2 to filters of the same type used in the glovebox exhaust system. Each standard was prepared by sprinkling PuO_2 powder evenly over the surface of the filter while drawing air through it, thus simulating the type of filter loading that might be observed in a glovebox exhaust filter. The individual filter standards were then sealed with aluminum foil covers, packaged in double plastic bags, and centered in plastic boxes having 6-mm-thick walls. The calibration system set up, including detector shielding and collimation, was the same as the in-plant set up at the LASL plutonium facility.

The idea for preparing the plutonium filter standards in the manner just described was gained from a previous experiment in which we investigated whether plutonium distribution in the filter would affect the response of the NaI detector. In this study, a 10-g plutonium source was moved horizontally and vertically across the area of the filter and the response of the detector was noted for every source position. The detector proved to be insensitive to the distribution of a given amount of plutonium in the filter.

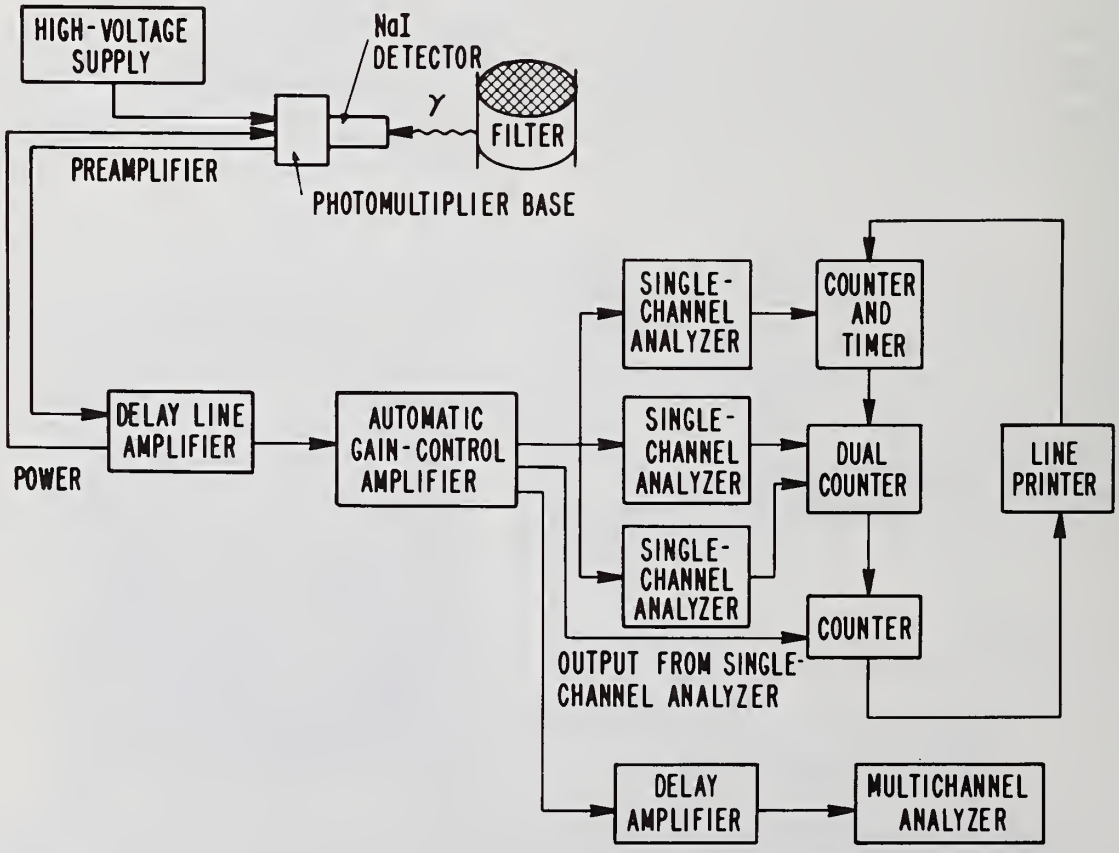

Fig. 3. Block diagram of the monitoring system electronics.

The calibration results are plotted as closed circles in Fig. 4. Each calibration point is an average of four independent measurements derived from four sides of the boxes that housed the filter standards. The response decreases slightly as the plutonium in the filter increases, due to self-attenuation and to rate-related counting losses in the electronics, including pile-up and deadtime losses. To determine whether the monitoring system and the filter standards were properly designed, we measured the magnitudes of the correction factors attributable to attenuation and rate-loss. The 662-keV gamma-ray peak from a 1-μCi ^{137}Cs source was used to determine pile-up and deadtime corrections of the system. A 10-g reactor-grade plutonium source was used as a transmission source for measuring sample self-attenuation. The calibration results with attenuation and rate-loss corrections (shown as open circles in Fig. 4) demonstrate the expected linear behavior for measured response vs plutonium in the filter. Attenuation correction for the filter standard containing 1 g of plutonium was 32%; attenuation correction for the filter standard containing 20 g of plutonium was 39%, with a rate loss of about 5%.

RESULTS

The monitoring system successfully detected plutonium in the glovebox active exhaust filter. The plutonium buildup in the active HEPA filter was measured during the preparation of 16 batches of advanced carbide fuel. The data were taken right after each batch of PuO_2, UO_2, and carbon had been weighed, mixed, blended, milled, and unloaded from ball-mill jars. The results are plotted as a function of batch in Fig. 5(a). The buildup is essentially linear. The error bars represent both statistical counting uncertainties

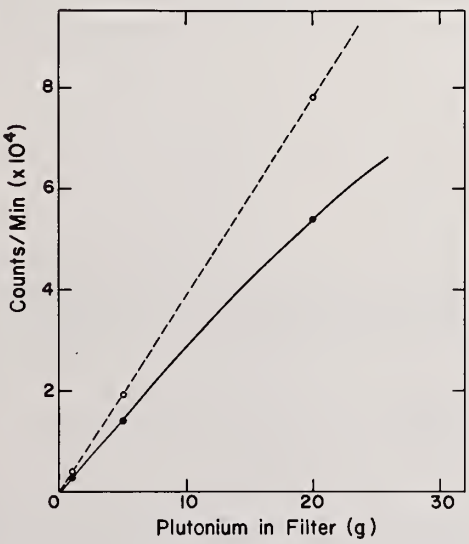

Fig. 4. Calibration results for three plutonium filter standards. The open circles show the calibration points with attenuation and rate-loss corrections; the closed circles show the calibration points without correction.

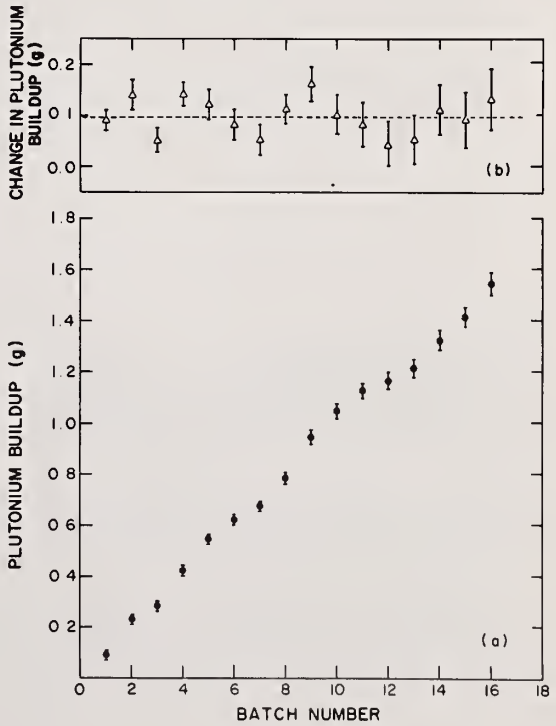

Fig. 5. Plutonium buildup in the glovebox exhaust filter as a function of the batch.

and uncertainties associated with calibration. A counting time of approximately 100 min is required to obtain a statistical uncertainty of less than 1%. Figure 5(b) shows the amount of plutonium buildup per processed batch. The average detected accumulation of plutonium per batch, as indicated by a dashed line, is 0.096 $\pm$ 0.037 g.

CONCLUSION

In summary, we have demonstrated an in-line monitoring system for measuring the plutonium buildup rate in a filter as a function of the amount of plutonium processed. The system is simple, inexpensive, automated, and easy to operate, and is sensitive to less than 0.1 g of plutonium buildup in a glovebox filter. This system could be moved from filter to filter to establish the plutonium buildup rate in filters throughout the plant. Once the rate of plutonium buildup is known for each filter, safeguards personnel can estimate the amount of plutonium buildup in the filters at any time. Subtracting the estimated filter-holdup values from the material-unaccounted-for (MUF) value for each glovebox should substantially increase the credibility of estimates of nuclear material holdup in process gloveboxes. The rate of plutonium buildup in the glovebox filter observed in this study is relatively low. The plutonium-buildup-per-kilogram-of-plutonium-processed varies widely in high-throughput gloveboxes and might be expected to be ten times higher than that observed in this study.

ACKNOWLEDGEMENTS

The authors wish to thank Don Shirk for technical help in the early stage of this project, and personnel of the LASL Advanced Fuel Laboratory for their cooperation.

Discussion:

Nilson (Exxon Nuclear):
I have a question, T.K. Your calibration standards were of a given isotopic ratio. Have you looked at how the standards vary with different plutonium types?

Li (LASL):
We used a reactor grade plutonium of about 12% ^{240}Pu. We didn't measure the calibration constant's dependence upon isotopic abundance. This should, however, be approximately linear versus the ^{239}Pu abundance.

Suwala (B&W):
We have done some work in trying to measure the filters in our plutonium line in place with a gamma counter and we have found that we couldn't do it because of the high background in the area. Have you encountered problems such as this?

Li:
No, with our design, we don't have a background problem. The design of the shielding and collimation cuts off the background.

Integrated Quality Status And Inventory Tracking System For FFTF Driver Fuel Pins

by

G. P. GOTTSCHALK
Westinghouse Hanford Company, Richland, Washington

ABSTRACT

An integrated system for quality status and inventory tracking of Fast Flux Test Facility (FFTF) driver fuel pins has been developed. Automated fuel pin identification systems, a distributed computer network, and a data base are used to implement the tracking system.

KEYWORDS: Fuel pins, quality status tracking system, inventory tracking system, fuel pin identification system, manufacturing information system.

INTRODUCTION

Rigid manufacturing, quality assurance, and safeguards requirements support the need for an integrated system for management of breeder reactor fuel pin and assembly manufacturing data. Reliability must be maximized by compiling all required data in one central store and by minimizing manual data entry.

This paper describes a system at the Hanford Engineering Development Laboratory (HEDL) for demonstration in the FFTF driver fuel assembly manufacturing process. The system design and concepts provide a basis for use in other processes as well as the one described herein.

PRINCIPLE OF OPERATION

The quality status system concept is based upon the elimination of manual record systems at individual process and inspection stations and establishing one central, on-line set of process, inspection, and inventory data. This concept allows real-time maintenance of all data enabling background status checks to prevent further processing of defective materials, or materials being held for nonconformance processing.

Automated data acquisition techniques are employed to minimize the need for operator entry of data. A distributed microcomputer system is integrated with the existing process equipment to allow acquisition of the process data from the various fuel pin and assembly stations. A combination of hardware and software is used to implement the on-line system and maintain the quality status and inventory data. The hardware and software meets the design goals to provide:

- Data protection and data access controls
- Real-time response to process and inspection data
- User oriented work station operation

PROCESS DESCRIPTION

Commercially manufactured FFTF nuclear fuel pins are received, inspected, and processed into 217-pin bundles. Addition of a duct over the bundle completes the assembly process. The assembly is then inspected and characterized prior to certification for use in the FFTF reactor. The FFTF fuel pin and assembly designs are shown in Figures 1 and 2.

Each individual fuel pin is uniquely identified by a six-digit code indicating the manufacturer, fuel enrichment, and sequence number. As received, the identification is roll-stamped around the circumference of the top end cap. The first process operation is to laser-engrave this identification on the end surface of the top end cap. In addition to being more amenable to machine reading, the laser-engraved characters provide a means of identifying fuel pins once they are fixed into the 217-pin bundle. The identification systems and work station used for laser-engraving the end characters are shown in Figure 3.

The fuel pin receiving inspection and fuel assembly manufacturing processes are well established and have been operating routinely for approximately six years. The process and the integration with the quality status and inventory tracking system are outlined in Figure 4.

The first step in the process involves adding a pre-shipment data set to the on-line data base. This information, furnished by the fuel pin manufacturer, consists of fuel pin manufacturing and component lot data. Each fuel pin is checked against this data base to assure the pin was accepted and certified by the vendor as part of the receiving operation. A series of 100-percent and sampling inspections are performed prior to releasing the fuel pins for assembly operations.

Processing at each station is preceded by a background check to assure that no hazardous conditions are created by further processing the fuel pin. For the bundle assembly operation, the quality status of the pins is also checked to assure that only accepted pins are included in the finished assembly.

Following final assembly inspections all data are again reviewed as part of the assembly certification process.

SYSTEM DESCRIPTION

The project described herein is implemented as a collection of individual subsystems, carefully integrated to form the system required to maintain continuously current information.

The major components described in the following sections include:

- Information Management Center (IMC)
- Remote Process Stations

At the end of the section, a specific application is described:

- Fuel Pin Fissile Assay--an example remote station

Each individual component contributes to the performance of the system and is described with reference to its relationship in the system.

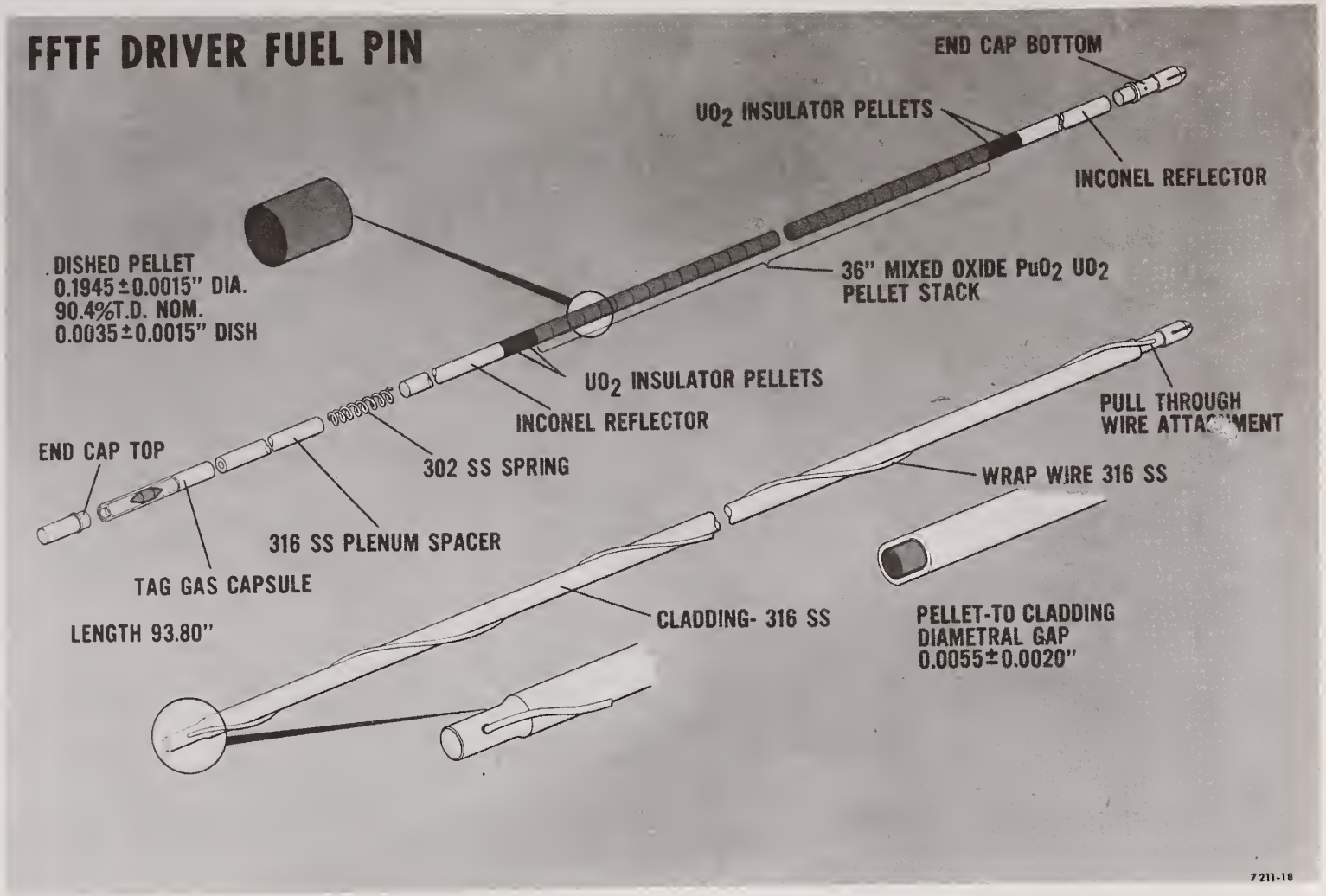

FIGURE 1. FFTF DRIVER FUEL PIN

FIGURE 2. FFTF DRIVER FUEL ASSEMBLY

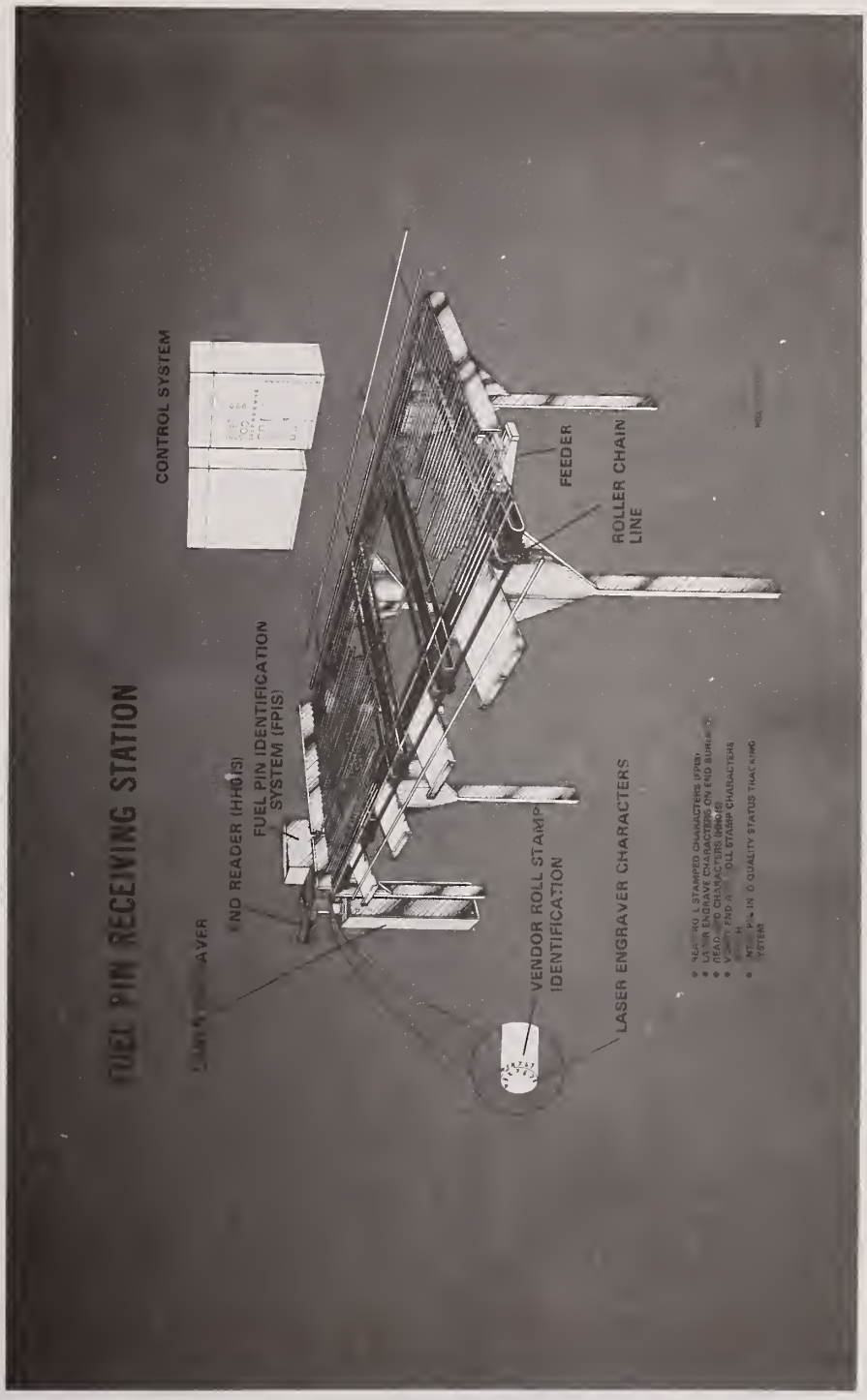

FIGURE 3. FUEL PIN RECEIVING STATION

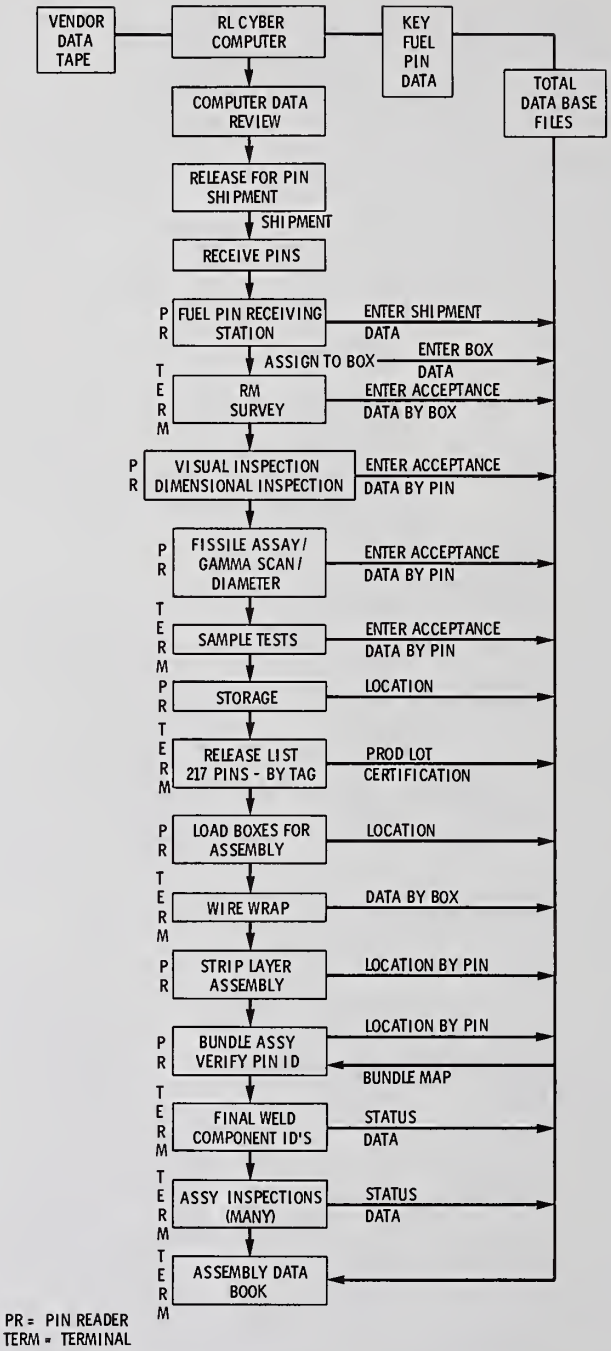

FIGURE 4. FLOW CHART OF DATA ACQUISITION IMPLEMENTATION

Information Management Center

The primary function of the Information Management Center (IMC) is to provide a central store for all process, inspection, and inventory data. This data consists of actual transactions received from the remote stations and additional summary items calculated in a real-time fashion. Additionally, the IMC acts as the communications and access control manager for the integrated system. Combining these features with the real-time data handling capabilities, the system allows constant monitoring of fuel pin and assembly status as well as current inventory and item location data. These features are provided by the use of a PDP-11 minicomputer operating under the RSX-11M operating system. The TOTAL data base system is combined with application specific software to manage the quality status and inventory data.

During on-line operations, data are pre-processed by the remote process stations and submitted as transactions to the IMC. Following additional validity checks by the IMC, the transactions are processed and the transaction status returned to the remote station.

A central access control file is maintained by the IMC. Access to each mode of operation is allowed only if associated access flags are set for both the requesting operator and the requesting station. The remote station submits a logon transaction to the IMC and the IMC returns a transaction to the remote station indicating the allowed operating modes for display and menu selection at the remote station.

The following are allowed operating modes:

Logon-Menu	- As described above
Move	- Update fuel pin locations
Process	- Add process/inspection data to the data base
Certify	- Complete fuel/assembly certification reviews
Trans	- Privileged access to host

Each mode involves a cooperative effort between the IMC and remote station. By allowing only pre-tested programs for normal operation, the system reliability is greatly improved. The trans mode allows privileged users direct access to specific tasks residing in the host. Such tasks include BASIC, QUERY, and REPORT-WRITER. Normal users are allowed access only to the functions required by their particular job description.

Remote Process Station

The remote station concept evolved from the need for local automated data acquisition at selected work stations, to provide stand-alone systems for easy interface to the existing process equipment, and to allow for expansion to meet future unforseen requirements.

The primary function of the remote station is to act as a pre-processor for the IMC. In operation, the remote stations acquire all real-time process data and perform the time consuming validation and verification checks in all transactions for the IMC. One of the major advantages of the remote station concept is in providing an additional access control level between the user and the host. Each remote station is configured to run only specific programs. This concept, in conjunction with the central host control of access rights, makes inadvertant or intentional tampering with the data base exceedingly difficult.

The remote stations, by performing many of the tedious and resource consuming check functions, free up valuable resources on the host while giving the user nearly instantaneous response at his operator terminal. Figure 5 shows a typical remote station consisting of the fuel pin reader system, dedicated operator CRT, and microprocessor controller. The pin reader consists of the large electronics cabinet, the actual camera, and a small CRT for display of the raw video data and processed pin identification characters. The microprocessor provides for control of the pin reader, communication with the operator and the IMC, and for the acquisition of process data as required for each station.

FIGURE 5.

In operation, the pin identification is read by the automated reader system and verified from the operator keyboard. Key process data and the pin identification are screened and transmitted to the IMC for processing.

Additional verification is performed by the IMC prior to updating the data base. The IMC always returns a transaction status to the remote station providing feedback on the success of the transaction.

Fuel Pin Fissile Assay--An Example Remote Station

One of the primary process operations in the receiving inspection process is the fuel pin fissile assay system. The ^{252}Cf fuel pin assay system developed by the Los Alamos Scientific Laboratory (Reference 1) has been upgraded (Reference 2) and integrated into the quality status system. This equipment is used to inspect the commercially produced FFTF driver fuel pins. Total fissile content, fuel column fissile uniformity and fuel pin diameter are measured, and the pin identification is automatically determined at the assay station (Figure 6). In operation, the fissile assay, gamma scan, and pin diameter data are accumulated. Calibration data obtained at four-hour intervals provide the basis to calculate actual pin mass, pellet deviations, and pin diameter from the raw data acquired during the assay cycle. The raw data, pin identification, and calculated acceptance information are logged to magnetic media for permanent storage. Key process information is transmitted to the IMC to update the quality status and location records. Once this information and the other process status data are stored in the central data base, it is available for further calculation, various process reports, and for generating the final inspection records package for each fuel pin.

SUMMARY

The quality status tracking system provides the capability for real-time monitoring of the HEDL FFTF fuel pin inspection and assembly processes. The use of a distributed computer network allows for increased reliability, automated acquisition, and multi-level protection of the process, inspection, and inventory data. The hardware and software design incorporates the capability for distributed control of processing operations by the remote stations. The implementation of the system described is progressing and a rapid pace. The target goal for complete implementation of the components described in this paper is mid-1980.

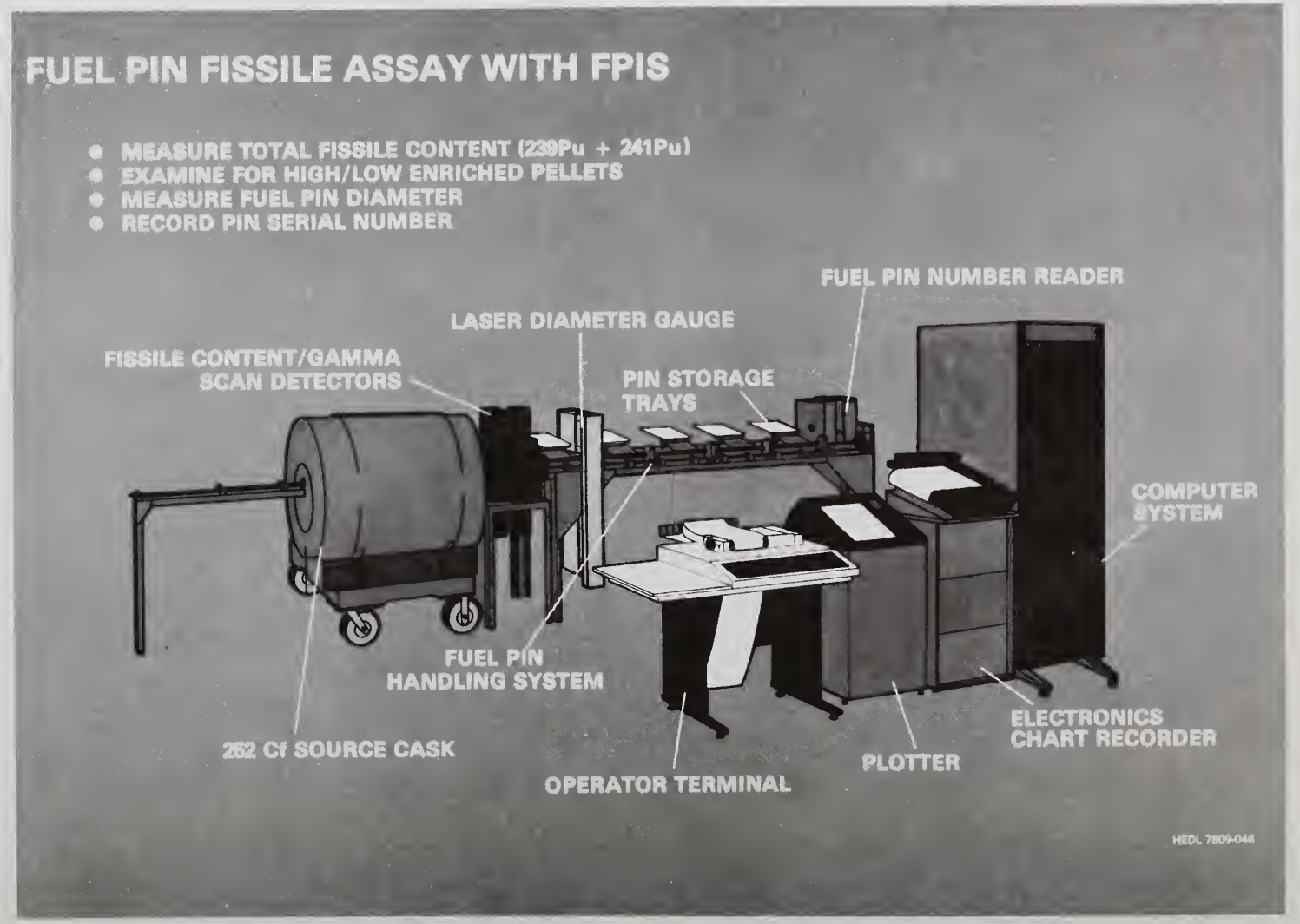

FIGURE 6. FUEL PIN FISSILE ASSAY

REFERENCES

1. H. G. Menlove, et al, ^{252}Cf Assay System for FBR Fuel Pins: Description and Operating Procedures Manual, LA-5071-M.

2. G. P. Gottschalk, Real-Time Analysis of FFTF Fuel Pin Inspection Data at the ^{252}Cf Assay Station, HEDL-TME-79-1.

Discussion:

Persiani (ANL):
What do you have in the way of plans for item identification of the fuel assembly per se, through the fuel handling system, loading and unloading of the reactor, etc?

Gottschalk (Westinghouse-Hanford):
The FFTF fuel assemblies themselves are identified with a unique assembly number which identifies the zone of the reactor they are going in, and also a sequence number for the assembly. Once the pins are all assembled into the assembly, the assembly becomes the item we trace. On the assembly itself, the identification is binary coded on a notch on the handling socket. The fuel handling equipment can identify this assembly by a mechanical mechanism. We would hope that eventually this quality status and inventory tracking system concept will be extended from where we've started with the pin and assembly processing, on back through from the feed materials and on out through the assembly use in the reactor--basically close the loop completely. The project is funded by DOE just for demonstration in the fuel assembly area, in order to determine the economic feasibility for doing that in an existing plant.

Nilson (Exxon Nuclear):
Can these assemblies be easily disassembled?

Gottschalk:
The disassembly process is similar to that for an LWR assembly and, in fact HEDL has developed a disassembly machine for FFTF assemblies.

Nilson:
How do you protect the integrity of the fuel assembly from somebody substituting a rod?

Gottschalk:
It takes quite a bit of special gear to cut the assembly apart. Also, one of the reasons we wanted to etch the fuel pins on the top of the end cap was so that a person or machine can look in on the top of a bundle and verify by pin number that items are still there. In addition, for assembly verification, we have proposed programs for complete assembly assay in conjunction with LASL. Right now there is only one place that makes breeder assemblies in the U.S., and they only go a short distance from the fuel fab plant to the reactor. We would expect that some type of fissile assay device for a completed assembly would be required should the breeder industry expand and become commercially viable.

The In-Plant Evaluation of a Uranium NDA System

by

JAMES K. SPRINKLE, JR., HORACE R. BAXMAN, DIANA G. LANGNER,
THOMAS R. CANADA, and THOMAS E. SAMPSON
Los Alamos Scientific Laboratory, Los Alamos, New Mexico

ABSTRACT

The Los Alamos Scientific Laboratory has an unirradiated enriched uranium reprocessing facility.

Various types of solutions are generated in this facility, including distillates and raffinates containing ppm of uranium and concentrated solutions with up to 400 grams U/ℓ. In addition to uranyl nitrate and HNO_3, the solutions may also contain zirconium, niobium, fluoride, and small amounts of many metals.

A uranium solution assay system (USAS) has been installed to allow accurate and more timely process control, accountability, and criticality data to be obtained. The USAS assays are made by a variety of techniques that depend upon state-of-the-art high-resolution Ge(Li) gamma-ray spectroscopy integrated with an interactive, user-oriented computer software package.

Tight control of the system's performance is maintained by constantly monitoring the USAS status. Daily measurement control sequences are required, and the user is forced by the software to perform these sequences.

Routine assays require 400 or 1000 seconds for a precision of 0.5% over the concentration range of 5-400 g/ℓ.

A comparison of the USAS precision and accuracy with that obtained by traditional destructive analytical chemistry techniques (colorimetric and volumetric) is presented.

KEYWORDS: Uranium Assay, Densitometry

INTRODUCTION

The Los Alamos Scientific Laboratory (LASL) has operated an unirradiated enriched uranium reprocessing facility for 25 years. This facility generates solutions with uranium concentrations varying from 0.001-400 grams/liter. Until January of 1976 chemical analysis was used for accountability and a simple NaI-based single-channel analyzer was used for process control/criticality safety. Despite its accuracy, the chemical analysis was not timely enough for practical use, and despite its timeliness, the NaI-based system was not sufficiently accurate for practical use.

In December of 1975, the LASL safeguards technology group, Q-1, installed a Uranium Solution Assay System (USAS). After an initial calibration period the USAS went into routine operation in January of 1976. This instrument incorporated both the process control/criticality function and the accountability function into one device, which can measure the U solution concentrations to $\pm$ 1.0% (2-400 g/ℓ) or better.

The following sections will describe the plant and its measurement points, the instrument and its operation, and an evaluation of the instrument's accuracy and precision.

THE URANIUM RECOVERY FACILITY[2]

The enriched uranium recovery is carried out by the physical chemistry and metallurgy group, CMB-8. A section of this group operates two plants, a Concentration Plant that is primarily for head-end processing and solvent extraction and concentration and a Final Recovery and Purification Plant that is primarily for intermediate processing and final purification.

Virtually every solution generated in the chemical and physical manipulation during processing and purification is measured in the USAS as well as solutions obtained from other groups. Some of these solutions contain many materials besides uranyl nitrate and HNO_3, such as zirconium, niobium, aluminum, iron, sodium, phosphates, sulfates, and trace amounts of various metals. Some of these ions, iron, zirconium, and niobium in particular, interfere with the chemical analysis of uranium by the colorimetric method and must be removed prior to analysis by solvent extraction and electrolysis.

Graphitic materials (fuel rods and casting residues) are crushed, milled to a powder, and burned to remove essentially all the carbon. The ash is leached with hot 60% (13N) HNO_3 and the slurry is filtered. The filtrate is assayed for accountability and for process control/criticality. The uranium is typically in the 5-15 g U/ℓ range. This filtrate is combined with filtrates from the H_2O_2 precipitation mentioned below, concentrated to about 20-25 g U/ℓ (assays are done during the concentration for process control, and a final assay is done for accountability) and run through solvent extraction. The raffinate is measured for accountability and to determine if it can be discarded. Typical assays give 0.005-0.015 g U/ℓ. The aqueous product is concentrated to about 200 g U/ℓ and is analyzed for both accountability and process control. The distillate from this concentration step as well as others is also assayed for accountability and to determine if it can be discarded. Assays are typically in the range of 0.005-0.010 g U/ℓ.

The concentrated aqueous product is filtered and the filtrate assayed for accountability and process control. The U is then precipitated with H_2O_2 and the resultant slurry is filtered. The precipitate is calcined to our final product, pure U_3O_8, and the filtrate is assayed (5-10 g U/ℓ), combined with other filtrates, and recycled through solvent extraction.

Nongraphitic materials (rags, gloves, towels, etc.) are burned and the ash is leached successively with hot HNO_3 and a mixture of 10 M HF-1.7 M HNO_3 at 90-100°C. After cooling, the excess fluoride is complexed with $Al(NO_3)_3$ and the slurry is filtered and assayed for process control. U assays will range from 1-15 g U/ℓ. The filtrate, which is relatively unstable, is run through solvent extraction and the aqueous product is treated as described above.

All other residual solids that have been previously leached with HNO_3 are treated the same as the ash from burning nongraphitic combustibles except that the leach with hot HNO_3 is left out.

THE URANIUM SOLUTION ASSAY SYSTEM[3,4]

The USAS assays are made by a variety of techniques that depend upon state-of-the-art high-resolution gamma-ray spectroscopy integrated with an interactive, user-oriented computer software package. The USAS is shown in Fig. 1. The hardware cost of such a system is approximately $60K.

The design of the measurement station, Fig. 2, was determined by the wide range of uranium concentrations present in the process and the accuracies to which these must be measured. The concentration range, 0.001-400 g/ℓ uranium, is divided into three material categories described below. Each category has a corresponding turntable measurement port into which is placed a plastic bottle containing the sample. The sample is rotated into the measurement position above the Ge(Li) detector for the assay.

The Ge(Li) detector is a closed-end crystal with a diameter of 42 mm and a length of 30 mm. The relative efficiency and resolution at 1.33 MeV are 7% and 1.75 keV, respectively. The resolution at 122 keV is 0.8 keV.

Fig. 3, a cutaway drawing of the station top, shows a sample in the measurement position. The Index Lock positions and holds the sample accurately above the collimated detector. The position indicator is interfaced to the computer and checks that the assayist has placed the sample in the measurement port corresponding to the material category for which he is requesting an assay. The ^{169}Yb transmission source is mounted above the sample and may be isolated from it by an automated computer-controlled shutter. A ^{109}Cd

1. The Uranium Solution Assay System

2. The USAS measurement station

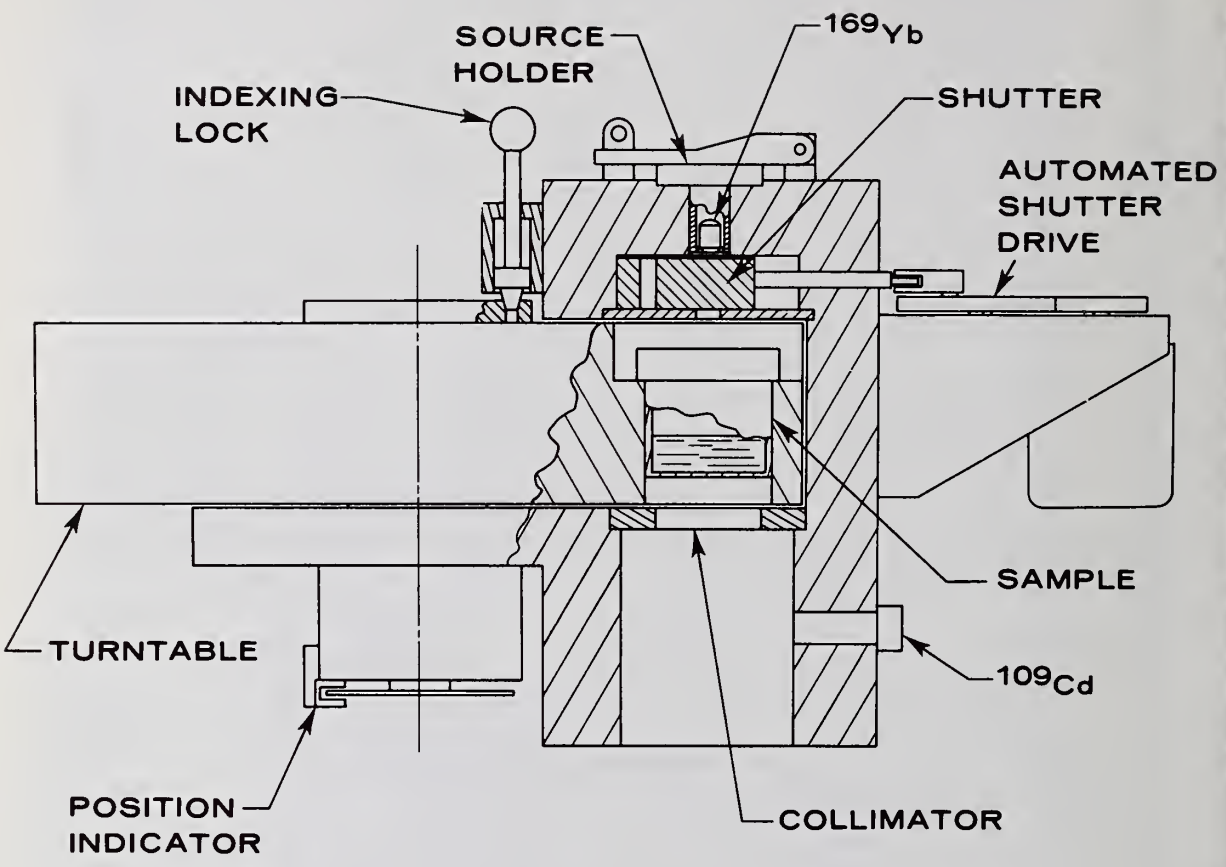

3. A cutaway view of the measurement station

source is placed on the end of the indicated plug nearest the detector. The ^{109}Cd 88-keV gamma ray is used as the gain-stabilizing signal for the system electronics.

Standard high-resolution electronics are used to process the USAS detector signals. The system is controlled by the minicomputer via a program written in BASIC. The program and the final results of each assay are stored on floppy diskettes. There are two CRT terminals for operator interaction and a hard-copy printer for the results.

During normal operation the user pushes the "request assay" button and then is prompted to enter a line of information on the CRT. This line consists of operator ID, sample ID, sample type, volume of material sample was drawn from, count time, and sample enrichment. When this information is sent to the computer, the assay begins.

Three gamma-ray assay techniques are used, each corresponding to a material category. The material category is determined by where the solution originates within the plant's process, which to a large degree also determines the uranium concentration range within a given category.

Material Type 1 (uranium concentrations of 0.001 to 0.5 g/ℓ): These by-products normally contain a very small fraction of the total uranium processed, and therefore highly accurate assays are not required. However, data must be available at a 10% one-sigma level for a uranium concentration of 0.01 g/ℓ in order to determine which solutions meet the disposal criterion.

The assay is made by pipetting 50 cc of the type 1 solution into an 80-cc sample bottle and positioning it above the detector. A spectrum is accumulated for 2000 s with the transmission shutter closed.

The concentration of uranium ρ_u is determined from these data by

$$\rho_u = \frac{I(186)/I(pulser)}{K}$$

where I(186) and I(Pulser) are the number of counts in the 186-keV and pulser peaks respectively, and K is a calibration constant determined from standards.

The results of a series of raffinate standard measurements are summarized in Fig. 4 where K is plotted versus log ρ_u. The distillate K value was found to be approximately 10% larger than for the raffinate. The computer software requires the assayist to identify the sample as a distillate or raffinate and uses the corresponding K value in the data analysis.

Material type 2 (uranium concentrations of 1 to 50 g/ℓ): As with material type 1, the assay depends on the measurement of the ^{235}U 186-keV gamma-ray intensity. In addition, a transmission measurement, which corrects for the absorption of the 186-keV gamma ray in the sample, is required.

T, the transmission of a gamma ray at 186 keV, is determined by measuring the transmissions, T_1 and T_2, of the ^{169}Yb 177-keV and 198-keV gamma rays and linearly interpolating. The transmission T is then given by

$$T = T_1 \exp^{-[9/21(\, n\, T_1/T_2)]}.$$

The assay is made by pipetting 20 cc of the type 2 solution into a 50-ml bottle, positioning the sample above the detector, and simultaneously counting the 186-keV and the transmission gamma rays for 400 seconds. The uranium concentration is obtained from these data by

$$\rho_u = \frac{I(186)/I(Pulser)}{K(T)}$$

K(T) was determined using a set of standards with $2 \leq \rho_u \leq 50$ g/ℓ. The transmissions were measured relative to an identical water sample. Typical results are shown in Fig. 5

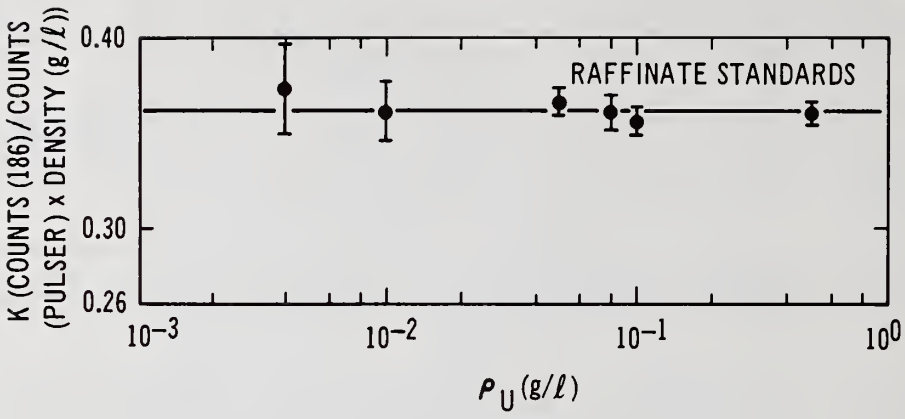

4. A type 1 calibration

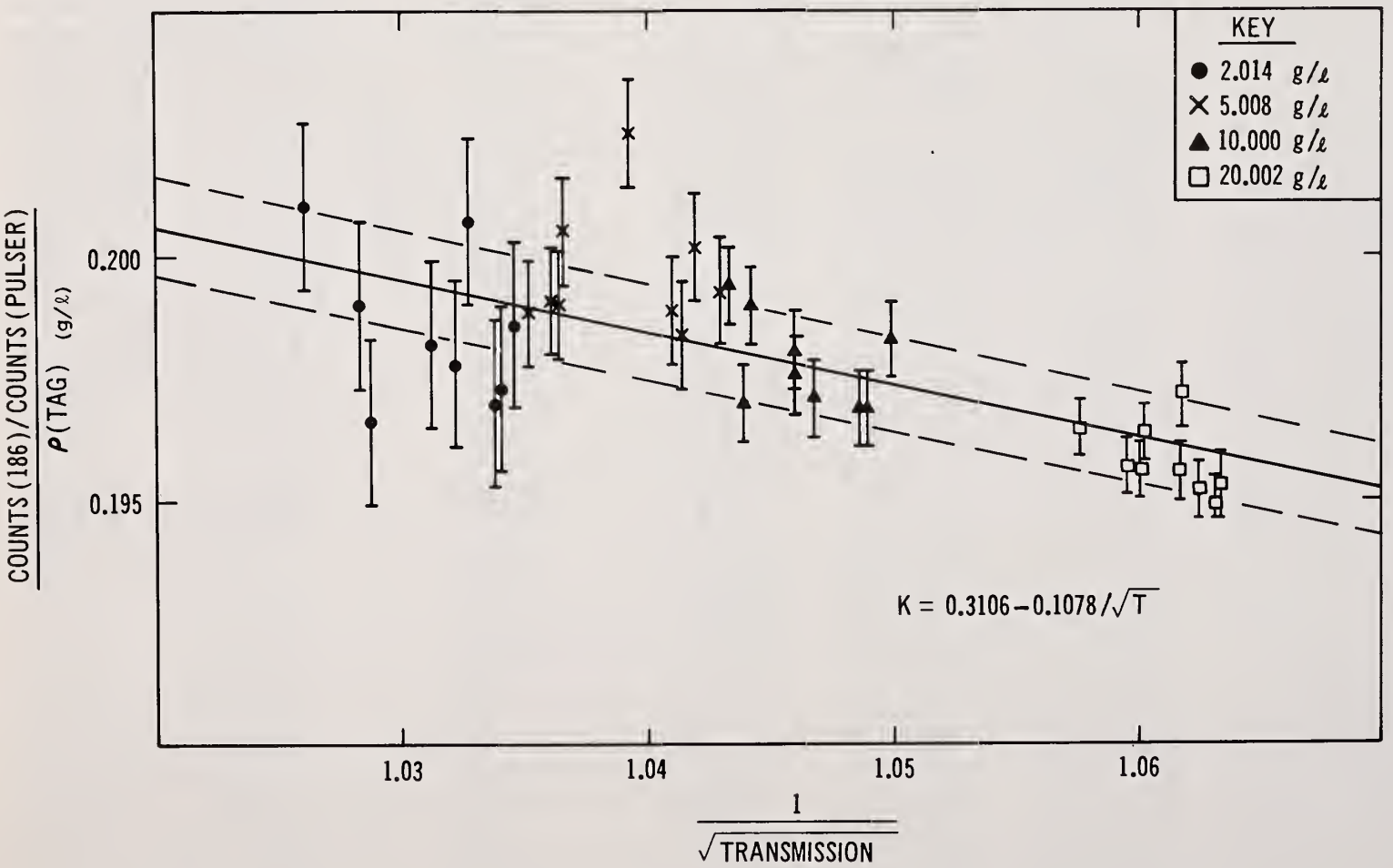

5. A type 2 calibration

where K is plotted versus $1/\sqrt{T}$. The solid line is a linear least squares fit to the data and gives K(T) for the T range of interest. The calibration function should not be extrapolated beyond this range as the linearity assumption will not hold for smaller T. The two dashed lines represent a $\pm$ 0.5% variation in K(T). The low concentrations ($\sim$2 g/ℓ) demonstrate a $\pm$ 0.7% precision, while the higher concentrations ($\sim$20 g/ℓ) demonstrate a $\pm$ 0.35% precision for the 400-s count times.

Material Type 3 (uranium concentrations of 100-400 g/ℓ): Twenty-cc samples, placed in the 50-ml bottles, are assayed by an absorption-edge densitometry technique.[1] The nominal count time is 1000 seconds. The ratio of transmissions of two gamma rays from ^{169}Yb(110-keV and 130-keV gamma ray) with energies on either side of the uranium K-absorption edge (115.6 keV) is measured, relative to a water standard. The ratio of transmissions, R, is then given by

$$R = \frac{I(130)}{I(110)} \frac{I_w(110)}{I_w(130)} ,$$

where I(130)/I(110) is the ratio of the peak intensities transmitted through the sample and $I_w(110)/I_w(130)$ is the inverse of that ratio measured through the water standard. The latter is a constant for a given transmission source and needs to be measured only once. The total uranium concentration, ρ_u(g/ℓ), is then given by

$$\rho_u = \frac{-\ell n\ R}{K} .$$

The calibration constant K is determined using a set of standards that are representative of the type 3 samples. The results of a USAS material type 3 calibration is shown in Fig. 6. Each point corresponds to an average of nine assays. The standard deviation in each of the four averages is 0.55% or less. The solid line is a fit to the four data points of the function $\ell nR = -K\rho_u$ and yields a K value of $4.146 \cdot 10^{-3}$ ℓ/g, with a standard deviation of 0.57%.

Although the USAS is extremely stable, its performance is checked daily to ensure accurate assay results. The standards used for this purpose consist of a reference plastic standard for type 2 measurements, a 0.0025-cm-thick 93.15% enriched uranium foil (FOIL-2) to check type 1 and type 2 performance, and a 0.0025-cm-thick depleted uranium foil (FOIL-3) to monitor type 3 performance. Both foils are encased in plastic. Secondary standards are used rather than solution standards because experience has shown that the plastic sample containers are inadequate for long-term storage of the solutions.

The daily performance check routine consists of measuring these three standards and monitoring certain parameters. The intensity of the ^{169}Yb source is verified so sufficiently accurate assays can be obtained with the normal count times, the transmissions through the foils must fall within predefined limits, and the FOIL-2 186-keV peak area is checked against predefined limits. If these tests are passed, assays are allowed for the remainder of the day and if any test is failed, an appropriate alarm message is printed at the terminals.

Figure 7 shows a recent 45-day series of FOIL-2 results. The normalized 186-keV peak area is plotted as a function of time. The standard deviation in these data is 0.45%, a typical value for a monthly average. Figure 8 shows the performance check results from FOIL-3 in the form of the equivalent concentration as a function of time. The standard deviation in the FOIL-3 data is 0.55%. The performance checks should be source independent and the ^{169}Yb source change indicated on July 3, 1979 (the 18th day in Figs. 7 and 8) had no effect on the performance check parameters. These two figures demonstrate the short-term stability of the USAS. The long-term performance check results show a similar pattern and are also verified with primary solution standards. In its current mode of operation, the USAS calibration is checked against fresh primary solution standards every six months. Calibration shifts as large as 0.5% have been discovered. Typically they are approximately 0.2%.

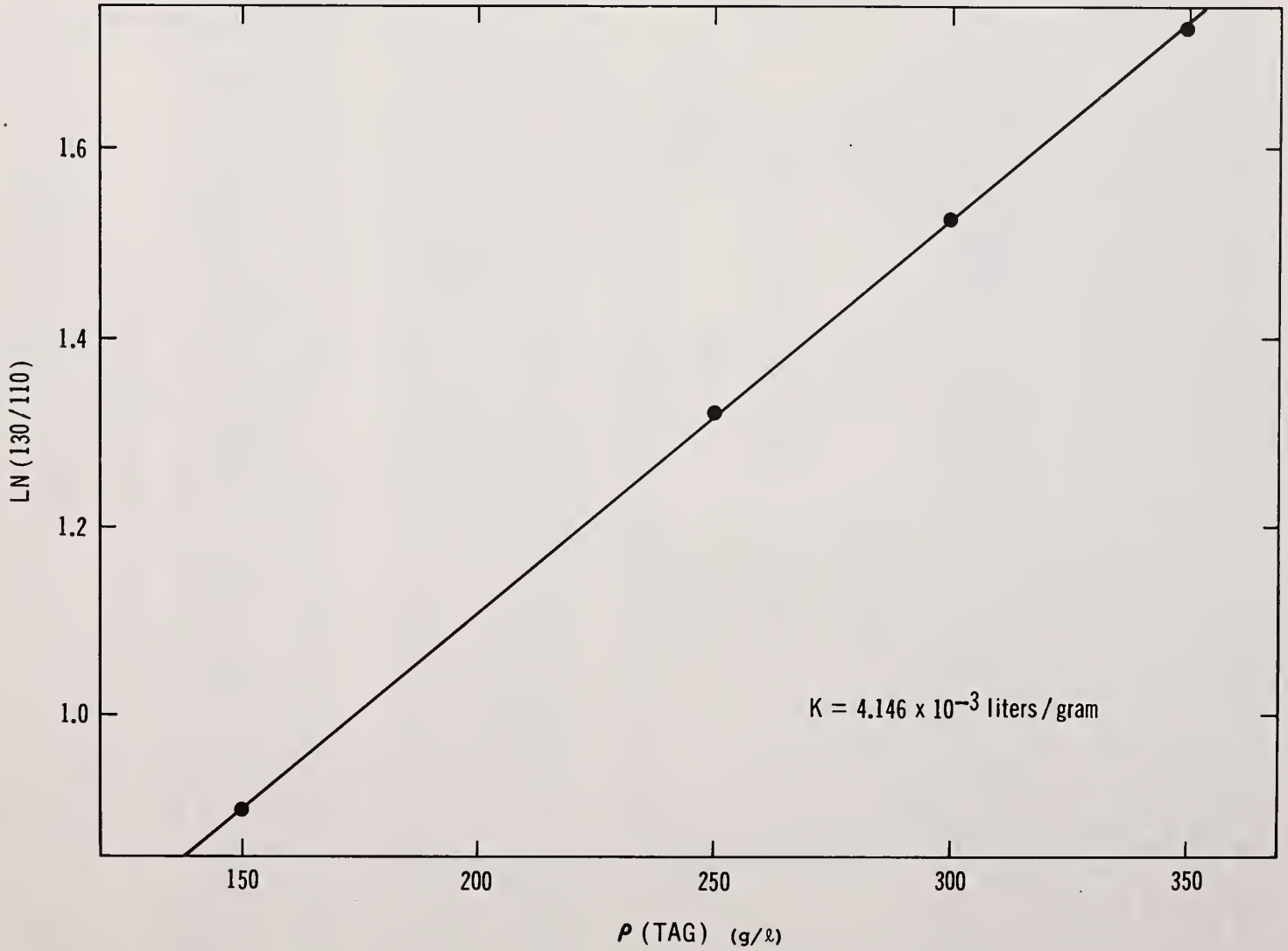

6. A type 3 calibration

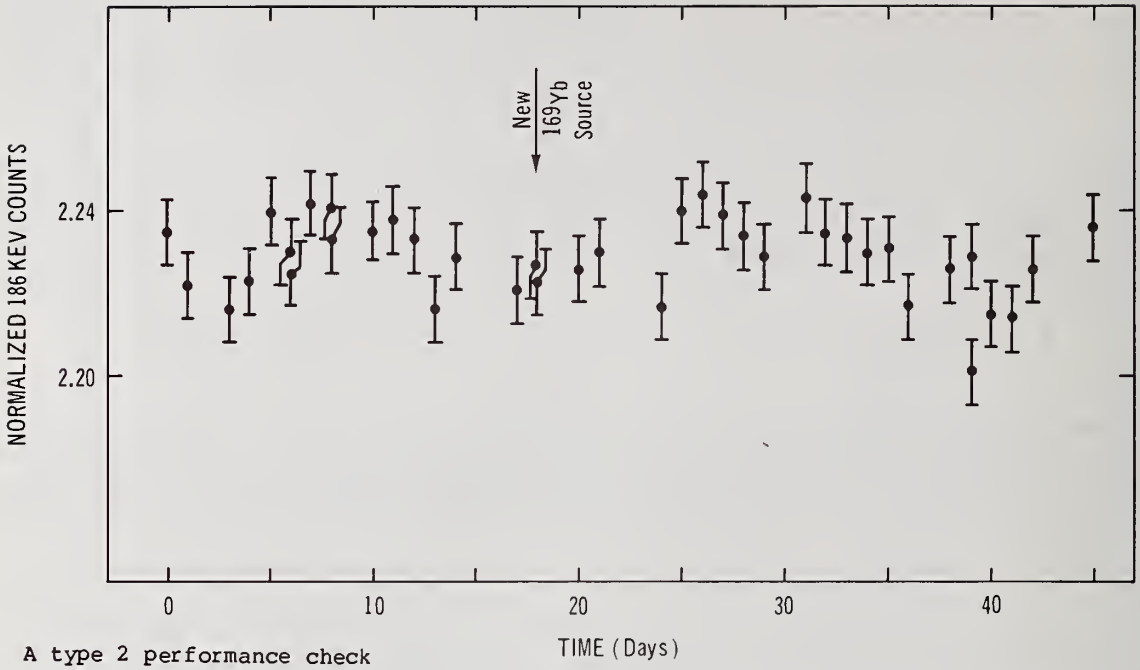

7. A type 2 performance check

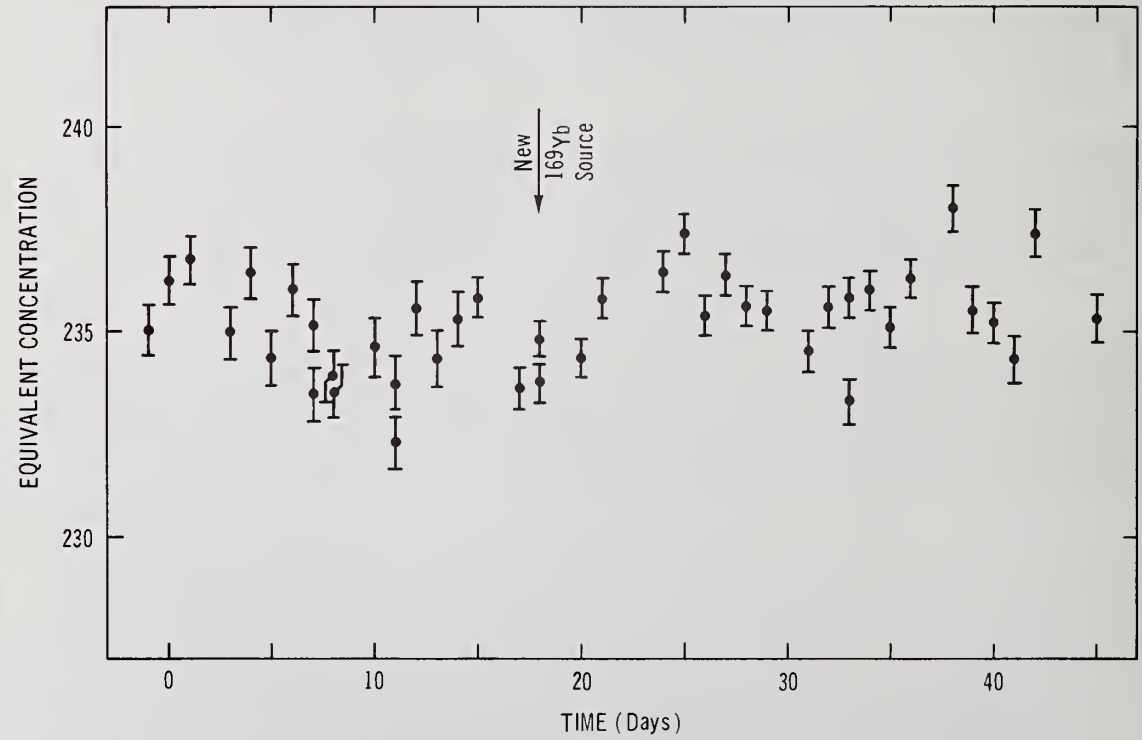

8. A type 3 performance check

The ^{169}Yb source has a 32-day half-life and consequently it must be replaced about three times a year. It can be irradiated and reused but only after a four to six-week cooling time to allow the intensity of the shorter half-life contaminants to die away. The only other maintenance the system requires is that required by standard computer and commercial nuclear instrumentation.

MEASUREMENT ACCURACY AND PRECISION

The type 1 measurements are the basis for determining whether or not a distillate, raffinate, or other solutions can be discarded. High accuracy is not required for these particular measurements. These solutions are nearly always 0.010 g/ℓ ^{235}U and it is extremely difficult to chemically analyze solutions that are this dilute. Consequently a comparison with chemistry was not repeated during this analysis. The type 2 comparison verified the system's capability to measure the 186-keV gamma ray from ^{235}U, and the type 1 measurement merely needs to determine whether the 186-keV radiation emitted from the sample is negligibly low.

Figure 9 shows the results of chemical analyses on type 2 solution standards. The ordinate is the fractional difference between the tag value and the chemical analysis. The abscissa is the tag value for the uranium concentration. Two types of chemistry were used, colorimetric and volumetric. Table I lists the biases and standard deviations for the data in Figs. 9 and 10. A large negative bias and a large standard deviation for volumetric chemistry on type 2 standards would arise from the one outlier data point obtained for a 20 g/ℓ standard. This poor result could arise from one of two sources, a pipetting error, discussed below, or a misapplication of the chemical technique. The type 2 standards are made to resemble

TABLE I. ANALYTICAL CHEMISTRY RESULTS ON SOLUTION STANDARDS

Material Type	Chemistry Technique	Bias	Standard Deviation
2	Colorimetric	-0.53%	±0.80%
	Volumetric	Insufficient data	
	Both	-0.72%	±1.11%
3	Colorimetric	-1.51%	±0.51%
	Volumetric	-0.26%	±0.30%
	Both	-0.84%	±0.76%

the plant solutions; consequently, they contain some amounts of interfering ions. The USAS is insensitive to these contaminants but the the chemical techniques are not. Figure 10 shows the chemical analysis results for the type 3 standards. The large negative bias displayed for the colorimetric analysis is probably not due to pipetting errors but more likely to an incorrect calibration in the chemical technique. Five of the six colorimetric values were obtained with the same chemical setup.

There is a certain amount of pipetting involved in drawing the samples and in the chemical analysis. Therefore, an independent analysis of the reproducibility of the pipetting was carried out.[5] Three operators using two uncalibrated pipettes drew a total of nine samples. The standard deviation of the nine values was 0.5%, and there were no significant differences between the averages of the values obtained by the different operators or the values obtained with the two pipettes. In another test, one operator drew eight samples with one pipette and obtained a standard deviation of 0.3%. This was not statistically different from the 0.5% obtained in the three-operator test.

Figures 11 and 12 show the results of a comparison between analytical chemistry and the USAS assays of several unknowns. The type 2 and type 3 assays were 400 and 1000 seconds respectively and had a calculated uncertainty of 0.7% to 0.4%. In both figures, the ordinate is the fractional difference between the chemistry and the USAS results, while the abscissa is the USAS value for the concentration. Table II lists the biases and standard deviations for these comparisons.

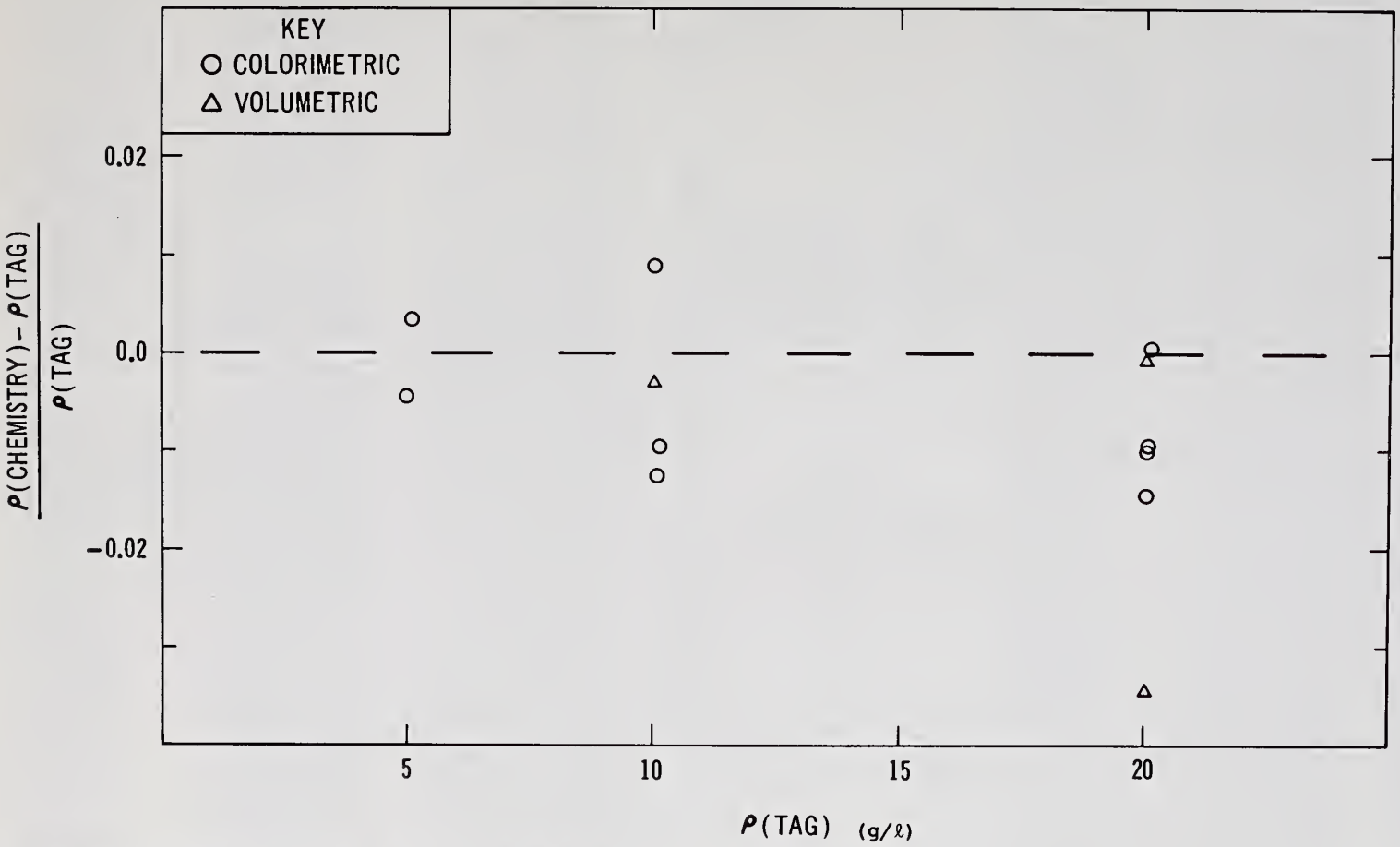

9. Chemical analyses of type 2 solution standards

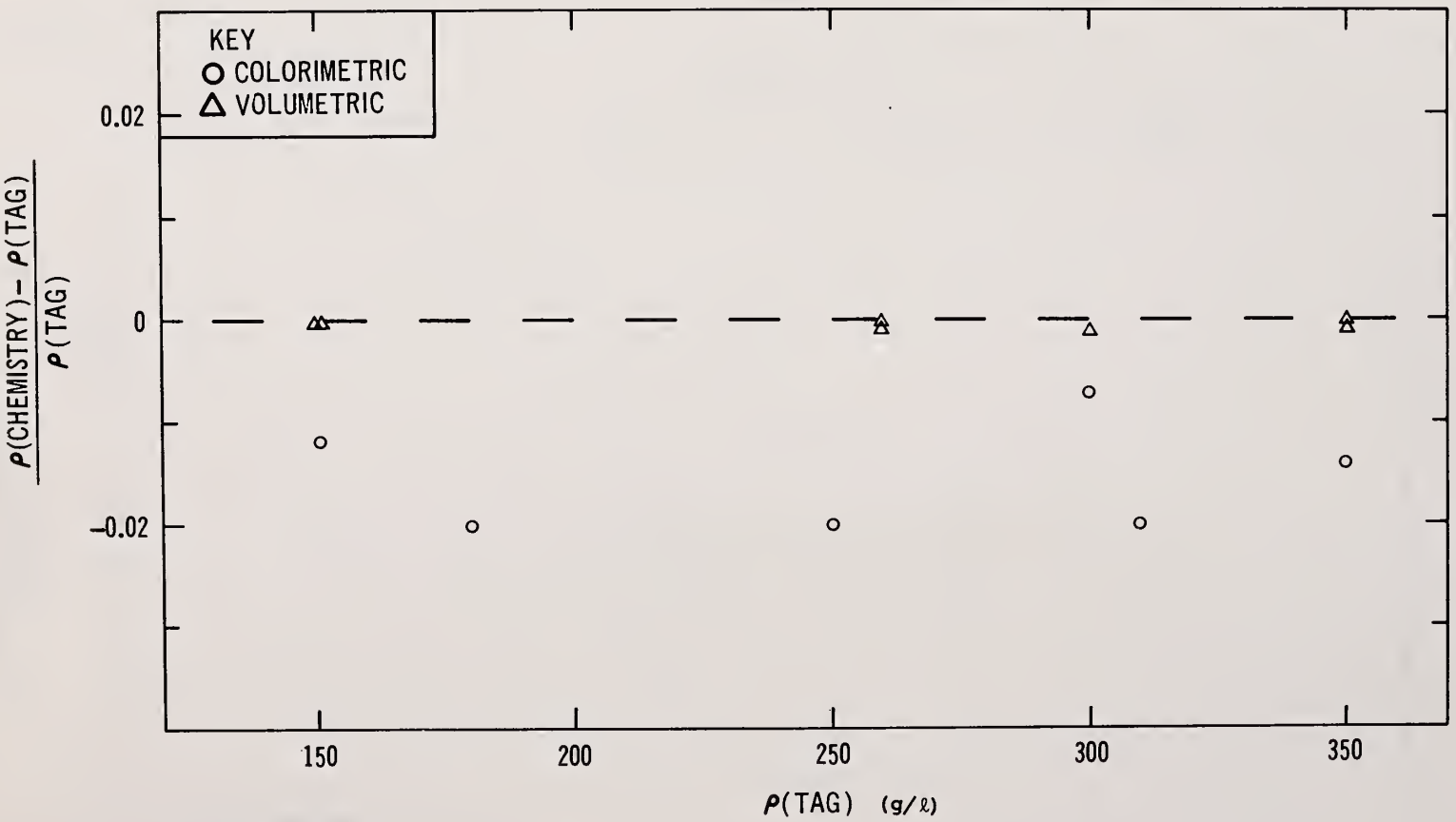

10. Chemical analyses of type 3 solution standards

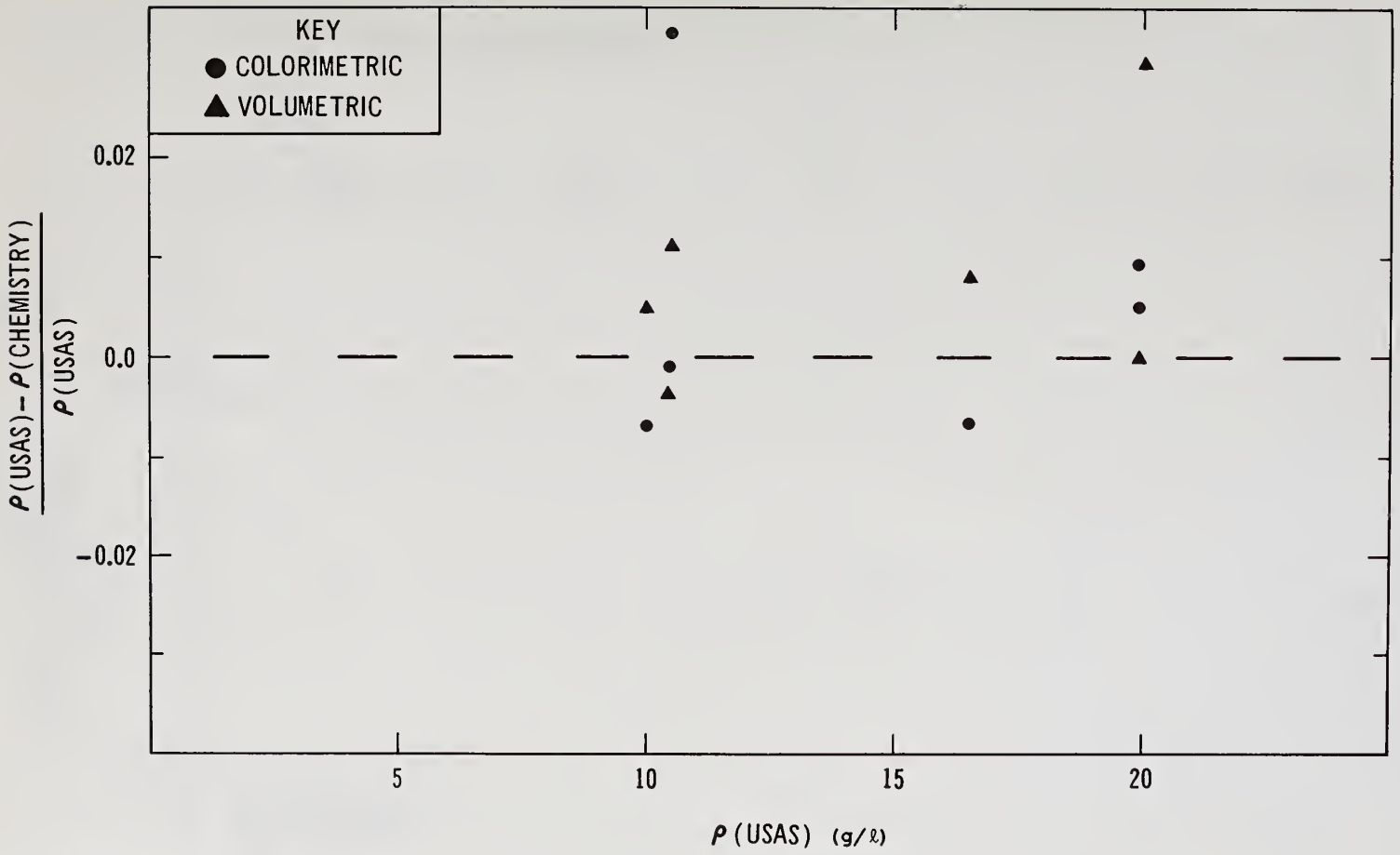

11. Chemical analyses of type 2 unknowns

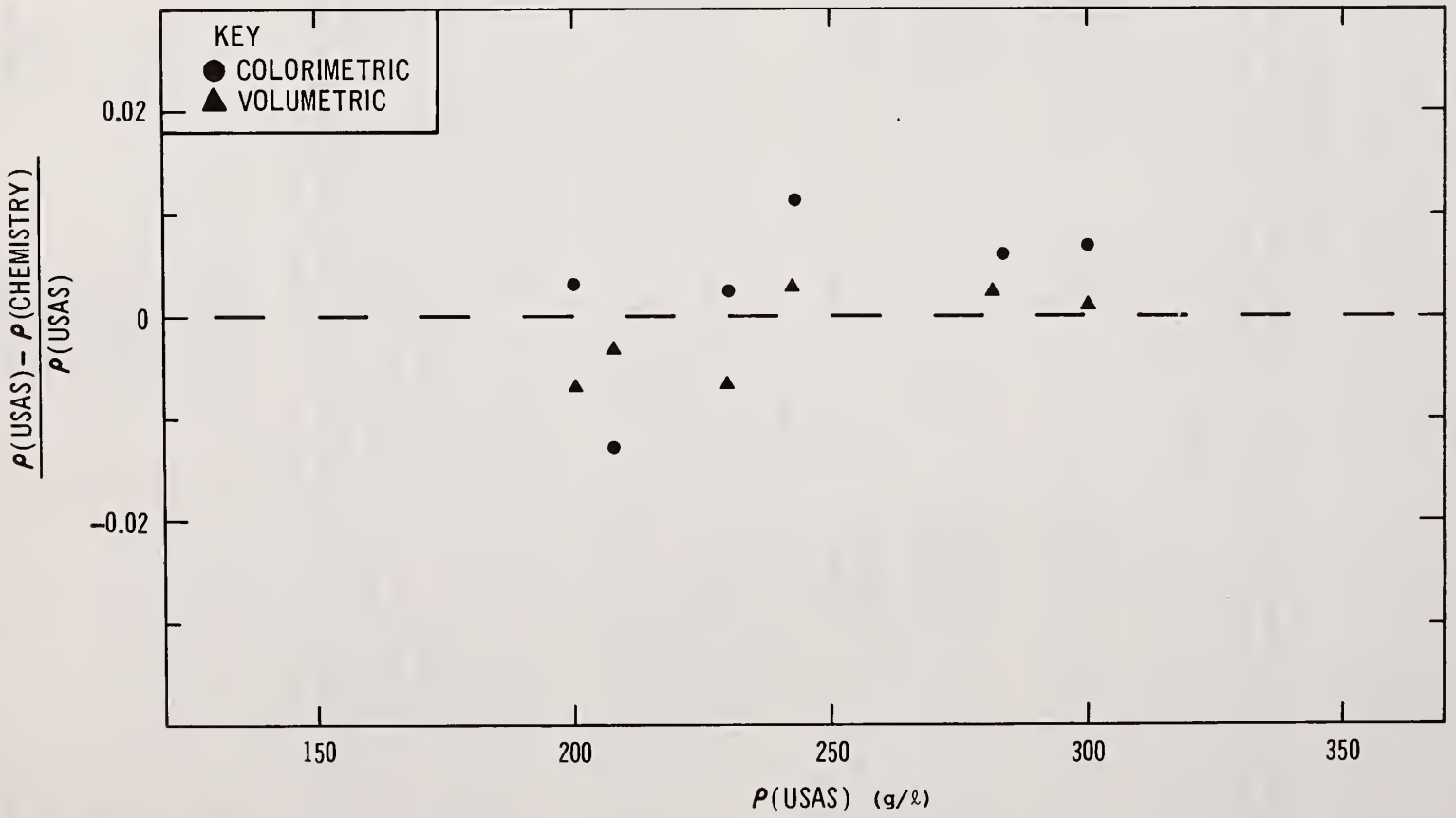

12. Chemical analyses of type 3 unknowns

TABLE II. ANALYTICAL CHEMISTRY RESULTS COMPARED TO USAS ASSAYS

Material Type	Chemistry Technique	Bias	Standard Deviation
2	Colorimetric	-0.51%	+1.40%
	Volumetric	-0.96%	+1.05%
	Both	-0.74%	±1.21%
3	Colorimetric	-0.29%	+0.84%
	Volumetric	+0.17%	±0.45%
	Both	-0.06%	±0.68%

For the type 2 unknowns comparison, the chemistry results showed the same negative bias that was obtained with solution standards. For both the colorimetric and the combined results, the standard deviation is larger than that obtained with standard solutions, but this is expected since two additional sources of fluctuations are included in this comparison. These are the ∿0.5% caused by the USAS precision and the ∿0.5% caused by pipetting the USAS sample. When the three errors are combined in quadrature, the result is consistent with the value in Table II. The standard deviation exceeds the bias in all three cases, as it did for the chemistry results on the solution standards. In the comparison of the type 3 unknowns, the bias is less than that obtained with the standards. Once again the three precisions are consistent with the combined uncertainties. These data indicate that the USAS is performing as well as the two chemical techniques.

A measure of the USAS's long-term accuracy can be obtained from the semiannual verification with solution standards. Using the six-month-old calibration, the results in Table III were obtained with eight freshly made standards. The USAS average in each case is the average of 20 assays made over a period of six days. These data show that the USAS bias is less than 0.96% for the range 5-350 g/ℓ. They also support the conclusion that the USAS can do as well as the chemical techniques for the range 10-350 g/ℓ.

TABLE III. USAS ACCURACY COMPARISON

Tag Value	USAS Average	USAS Precision	USAS-Tag / Tag
2.002 g/ℓ	2.036 g/ℓ	+0.018 g/ℓ	+1.70%
5.003	5.051	+0.034	+0.96%
10.000	10.085	±0.054	+0.85%
20.000	20.079	±0.071	+0.40%
150.001	151.253	±1.16	+0.83%
249.996	250.348	±1.66	+0.14%
299.994	298.506	±1.72	-0.50%
350.006	350.028	±1.77	+0.01%

CONCLUSION

The USAS was designed around this recovery plant's requirements. The three assay techniques span five orders of magnitude in concentration. They are optimized to achieve the best results on these process solutions, which clump around three concentrations in the middle of each assay technique.

The USAS has been in operation for almost four years in this process plant environment. During this time it has reliably provided approximately six assays daily, five days a week. It supplies at least two assays every workday and has supplied as many as twenty. It provides the process control/criticality function and the final numbers for accountability purposes. It is considerably more accurate than the previous NaI system was, largely through its ability to distinguish U from various other radionuclides, and it is just as timely. It is at least as accurate as the colorimetric chemical analyses used previously,

and it has considerably faster response times. In terms of actual process plant man hours, it requires one to two orders of magnitude less time to prepare the samples than the chemical analysis requires. In addition, an answer is returned in 400-2000 seconds compared to an average two-week turnaround time for the chemistry.

REFERENCES

1. T. R. Canada, D. G. Langner, J. W. Tape, "Nuclear Safeguards Applications of Energy-Dispersive Absorption Edge Densitometry," Amer. Chem. Soc. Symp. Series No. 79, Nuclear Safeguards Analysis (1978).
2. R. J. Bard, "Nuclear Criticality Safety in Enriched Uranium Recovery Operations at LASL," presented at Nuclear Criticality Safety Short Course (University of N. M.'s D. H. Lawrence Ranch, Taos, NM, May 1977.
3. D. G. Langner, T. Canada, N. Ensslin, T. Atwell, H. Baxman, L. Cowder, L. Speir, and T. VanLyssel, "The CMB-8 Material Balance System Manual," Los Alamos Scientific Laboratory report, to be published.
4. T. R. Canada, J. L. Parker, and P. A. Russo, "Computer Based Inplant Nondestructive Assay Instrumentation for the Measurement of Special Nuclar Materials," ANS Topical Conf. on Computers in Activation Analysis and Gamma-Ray Spectroscopy, proc. to be published.
5. G. Tietjen, private communication.

Discussion:

Mallett (GE-Wilmington):

On your low-level solutions, do you know what the minimum detectable limit is that you can go down to? You mentioned 10 mg per liter.

Baxman (LASL):

We can go down lower than that. Actually, at 10 mg per liter, the precision is approximately 10%. We can go down to about 1/2 mg per liter, but there you are talking about a precision of 50%.

Hawkins (NUSAC):

You said there was a difference in the calibration constant between the raffinate and distillate. What is the reason for that difference?

Baxman:

The reason is that the distillate contains just a small amount of uranium and nitric acid. The raffinate will contain that plus the zirconium ions, niobium ions, iron, a lot of nitrate, aluminum, magnesium, and a lot of other ions. You don't get as much transmission of the 186 keV gamma because of the other ions present. More of the gamma-rays are absorbed in the sample.

Automated In-Line Measurement of Nuclear Fuel Pellets

by

David R. McLemore and David H. Nyman
Hanford Engineering Development Laboratory, Richland, Washington

ABSTRACT

The Hanford Engineering Development Laboratory (HEDL) operated by the Westinghouse Hanford Company for the United States Department of Energy is currently developing, fabricating, and evaluating automated fuel fabrication equipment. This program has as its major goals: reduced personnel exposure, improved safeguards/accountability and improved fuel performance.

One of the automated equipment items which has been fabricated is a fuel pellet inspection system. This system inspects fuel pellets for surface flaws and measures pellets for length, diameter, and weight at a rate of one pellet per second. The inspected pellets are sorted automatically and the results of the inspection are transmitted to a central computer for trend analysis and verification of accountability data.

INTRODUCTION

The development and evaluation of automated equipment for the fabrication and inspection of nuclear fuel is being performed as part of the Breeder Fuel Fabrication Development Program conducted by the Hanford Engineering Development Laboratory (HEDL) for the United States Department of Energy (DOE).

A major operation in the process is the inspection of fuel pellets for dimensions (length and diameter), surface flaws, and weight. The current process utilizes a sample plan to inspect fuel pellets due to economics and personnel exposure considerations. To minimize these limitations and to provide enhanced quality assurance information and improved Special Nuclear Material (SNM) accountability, an automated gaging system has been designed and fabricated that measures these attributes on fuel pellets at a rate of one pellet per second.

The pellet gaging system is divided into two parts: (1) mechanical and (2) electronic. The mechanical portion consists of a pellet handling system; inspection stations for measuring length, diameter, weight, and surface flaws; a glovebox-like containment which isolates SNM and associated hardware from the surrounding environment. The length, diameter, and surface flaw inspections utilize laser optical systems with solid-state detection devices. Both the diameter and length measurement stations use linear self-scanning

MECHANIZED FUEL PELLET INSPECTION SYSTEM

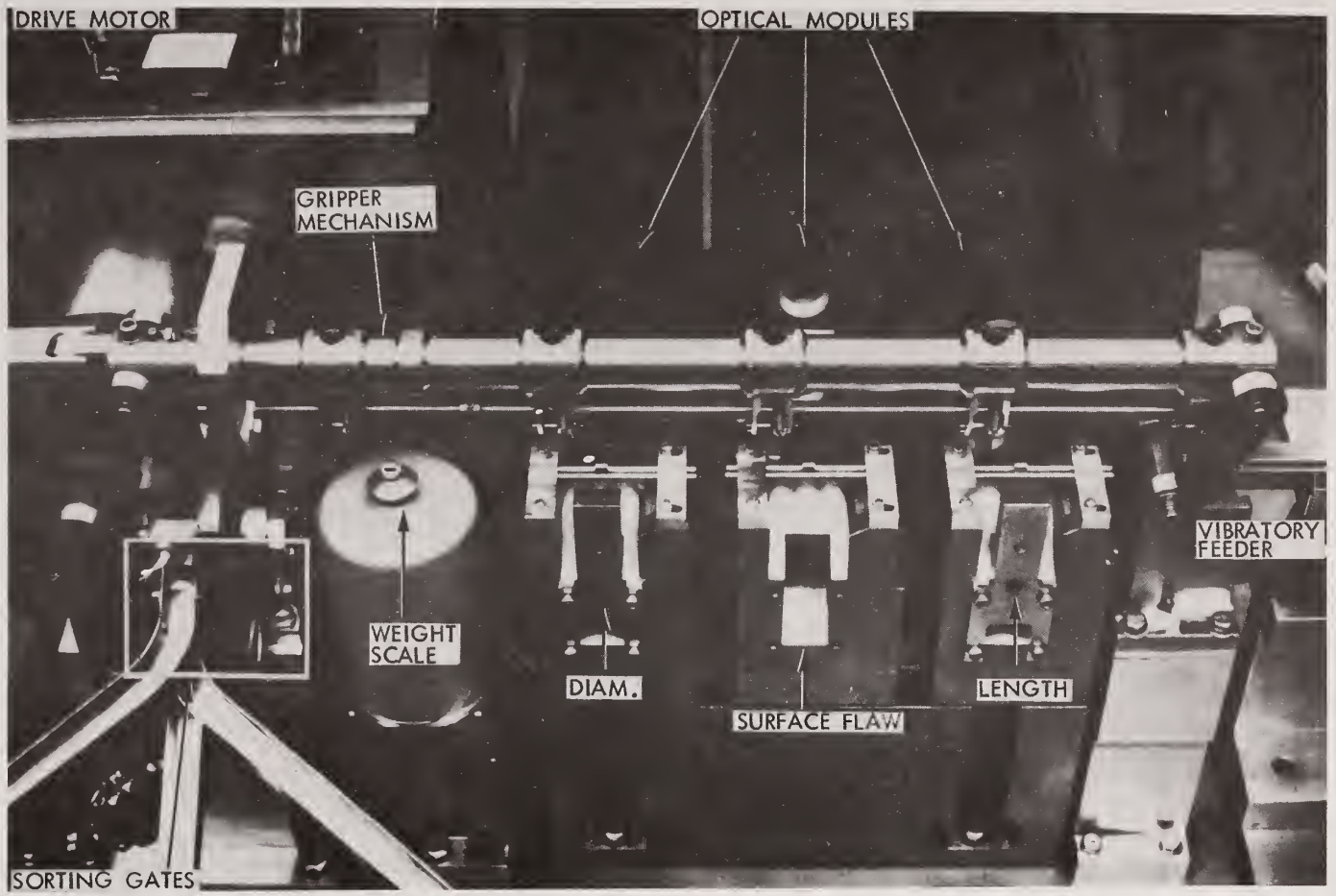

FIGURE 1: Mechanized Fuel Pellet Inspection System (Pellet Gage)

diode arrays, while the surface flaw station[1] uses a single element detector to distinguish between flawed and unflawed areas. A standard, commercially available weight scale statistically samples pellets to determine pellet densities.

Figure 1 shows the pellet gaging system. Fuel pellets are placed in a vibratory feed system for orientation and delivery to the handling system. Pellets are transported through the various inspection stations with a reciprocating overhead gripper mechanism. The transport system utilizes a pick-and-place operating principle[2] (zero velocity at each end of the handling cycle) to minimize wear of the gaging components and damage to the pellets.

A removable tray is supplied which is designed to catch or redirect mishandled pellets so that they will not fall into the apparatus from where they would be difficult to retrieve. The tray elevation is at the same level as the top of the pellet inspection stations.

The electronic portion of the gaging system consists of a process control system, a small dedicated minicomputer, and a supervisory computer system which will be located in a centralized control center.[3]

The gaging system can be operated either through a local teletype or via the supervisory computer in the centralized process control room. The dedicated computer system is used to control the operation of the mechanical handling system, synchronize data inputs and outputs with the handling cycle, process data, and sort the fuel pellets into one of three categories: acceptable, rejectable, and hold (oversize diameter for centerless grinding).

Variables data are transmitted to the supervisory computer for trend analysis and process control information.

Mechanical System

Bulk Feed Hopper and Vibratory Bowl Feeder

The point of entry for pellets into the pellet gaging system is the bulk feed hopper. It is designed to hold six kilograms of mixed oxide fuel pellets in bulk. Its purpose is to dispense pellets to the vibratory bowl feeder so that the mass load on the bowl feeder and its feeding characteristics remain relatively constant. The bowl feeder longitudinally orients and feeds pellets to the pellet escapement.

Pellet Handling

Handling is a key technological element in any production system that performs varied tasks at high speeds. Specifically, the pellet inspection system handling tasks to be performed are:

- Accept pellets from feed hopper
- Present pellets to length gage
- Present pellets to diameter gage
- Present pellets to weight scale
- Present pellets to flaw detection system
- Deliver acceptable pellets to holding area
- Deliver reject pellets off line
- Deliver oversize diameter pellets (acceptable to all other requirements to a separate holding area
- Perform the above functions at a throughput rate of one pellet per second

---

(1) D. R. McLemore, D. H. Nyman, and R. S. Wilks, "Automatic Surface Flow Inspection of Nuclear Fuel Pellets," The Society of Photo-Optical Instrumentation Engineers Proceedings, Volume 143 (1978).

(2) D. H. Nyman, D. R. McLemore and R. H. Sturges, "A Handling System for Nuclear Fuel Pellet Inspection," Transactions of the American Nuclear Society, Volume 28, (June 1978).

(3) R. L. Fritz and J. A. Hubbard, "Fuel Fabrication Instrumentation and Control System for Remote Operation," Transactions of the American Nuclear Society, Volume 32 (June 1979).

The constraints imposed on these operations are:

- Minimize shock to avoid damage to the pellets
- Minimize sliding of pellets to avoid generation of dust and to minimize wear of machine parts
- Minimize anomalous behavior of system due to presence of off-size pellets, partial pellets, loose chips and dust
- Present pellets to gage sensors in such a manner as to avoid interference with the measurement
- Design for easy and rapid replacement of components

A pick-and-place handling system was selected as the best alternative for this application. Sliding of parts is eliminated, therefore, dust generation and machine wear are minimized. Five sets of grippers are used joined together on a common overhead bar. Drive motion is provided by a reciprocating cam that provides for $\pm$ 90° rotation on the output shaft with continuous (360°) rotation of the input shaft.

Figure 2 shows the relationship between the input and output shafts on the drive mechanism. The cam is designed to move fastest when transferring pellets between stations and then returns at a slower speed. This allows most of the handling cycle to be used for measurements and analysis.

The only surfaces to come in contact with the pellet are those associated with the measurement devices and the grippers. The grippers grasp the pellet by the sides, and the shape of the grippers allows for process variances in pellet diameters. End squareness and pellet length are not factors for efficient operation. The pair of grippers, illustrated in Figure 3, move symmetrically to grasp and release a pellet; thus, a minimum amount of motion is required. The only wearing is on the inner surfaces of the jaws as they pick up or set down the pellets.

Ideally, the pellet should be placed precisely on the measurement stand with no displacement error. This means that the pellet is presented to the stand with zero momentum. This can be accomplished by releasing the pellet above the measurement stand a minimum distance equal to half the difference between the largest and smallest expected diameters. Practically, this distance has been increased by the vertical error in grip positioning.

Another source of pellet momentum arises from relative pellet motion during release and grasp. To prevent this, the path from station to station features a dwell at each end.

Figure 4 is a temporal description of the handling cycle. Station time is 60% of the total cycle time. Thus, a pellet "rests" in the station for 200 ms and is move in 300 ms of a 1000 ms cycle. This yields reasonable accelerations for the handling device since the spacing between stations is four inches.

Sorting Gates and Receiving Bins

As each inspected pellet emerges from the pellet transfer mechanism, it is directed through the sorting gates to one of three receiving bins by a computer-originated signal. This signal indicates whether to accept, to reject for oversized diameter (but acceptable for all other attributes), or to reject for any other reason. The receiving bins are easily removable to permit dumping. These bins each hold a minimum of 6 kg of mixed oxide pellets.

Length Inspection

The length of the fuel pellets measured at the length station is defined as the distance along the pellet axis between planes held flush with the ends. It measures pellets 6.160 $\pm$ 0.97 mm (0.2425 $\pm$ 0.038 in.) long with a $\pm$ 0.05 mm ($\pm$ 0.002 in.) precision. The length station can be modified to inspect pellets to 9.14 mm (0.360 in.) nominal length with minor adjustments to the optical system. Pellets longer than 9.14 mm (0.360 in.) would require lens changes. The accept/reject limits are teletype-adjustable in 0.03 mm (0.001 in.) increments within the $\pm$ 0.97 mm (0.038 in.) range.

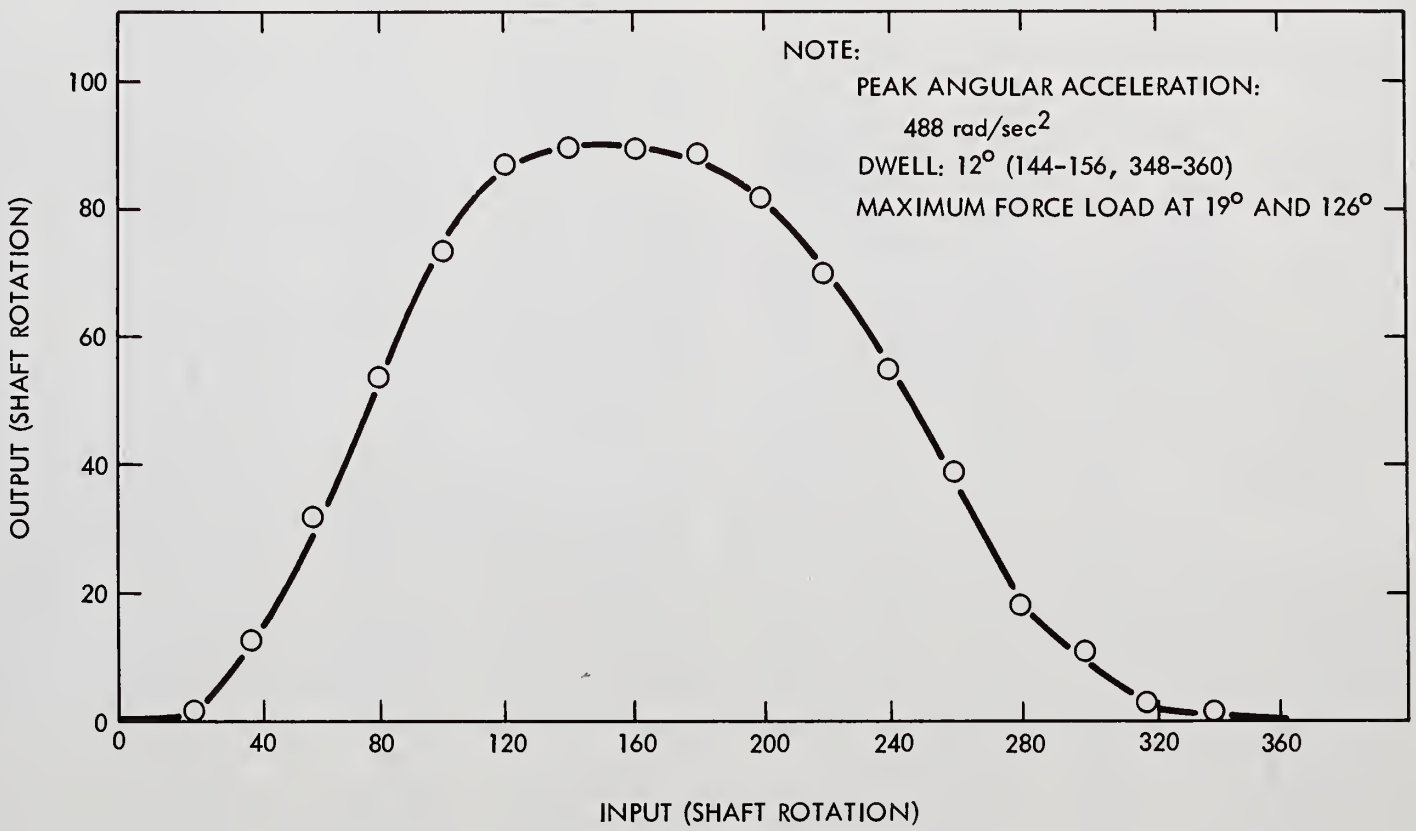

HEDL 7911-032.2

FIGURE 2: Drive Mechanism Analysis

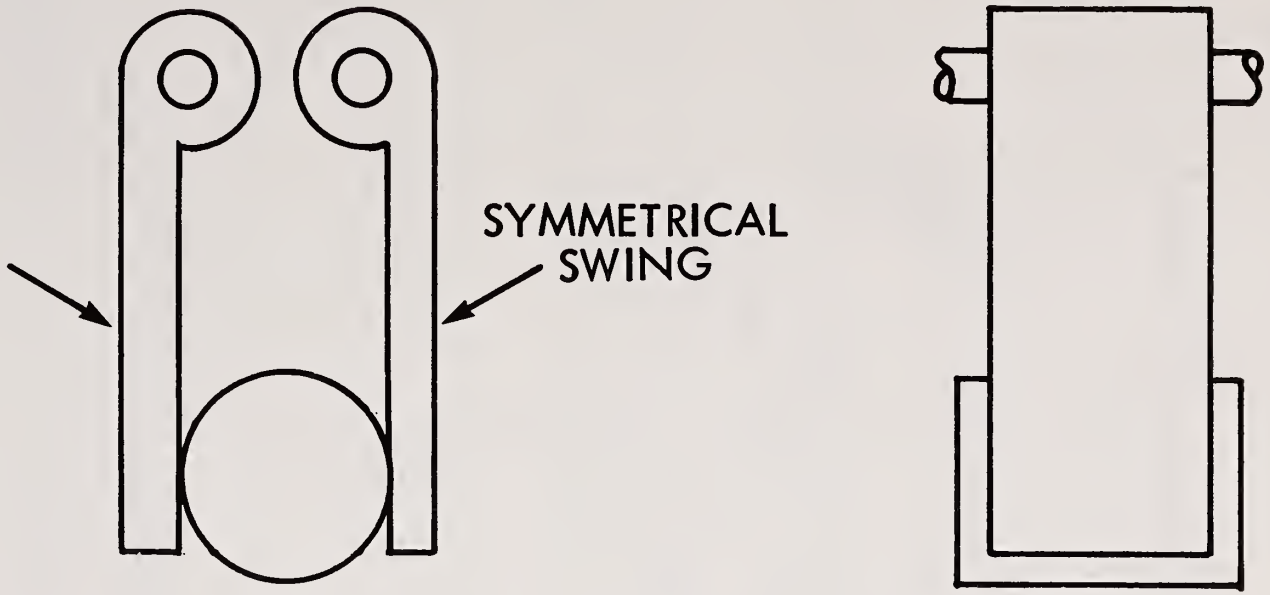

HEDL 7911-032.1

FIGURE 3: Preferred Method of Holding a Pellet

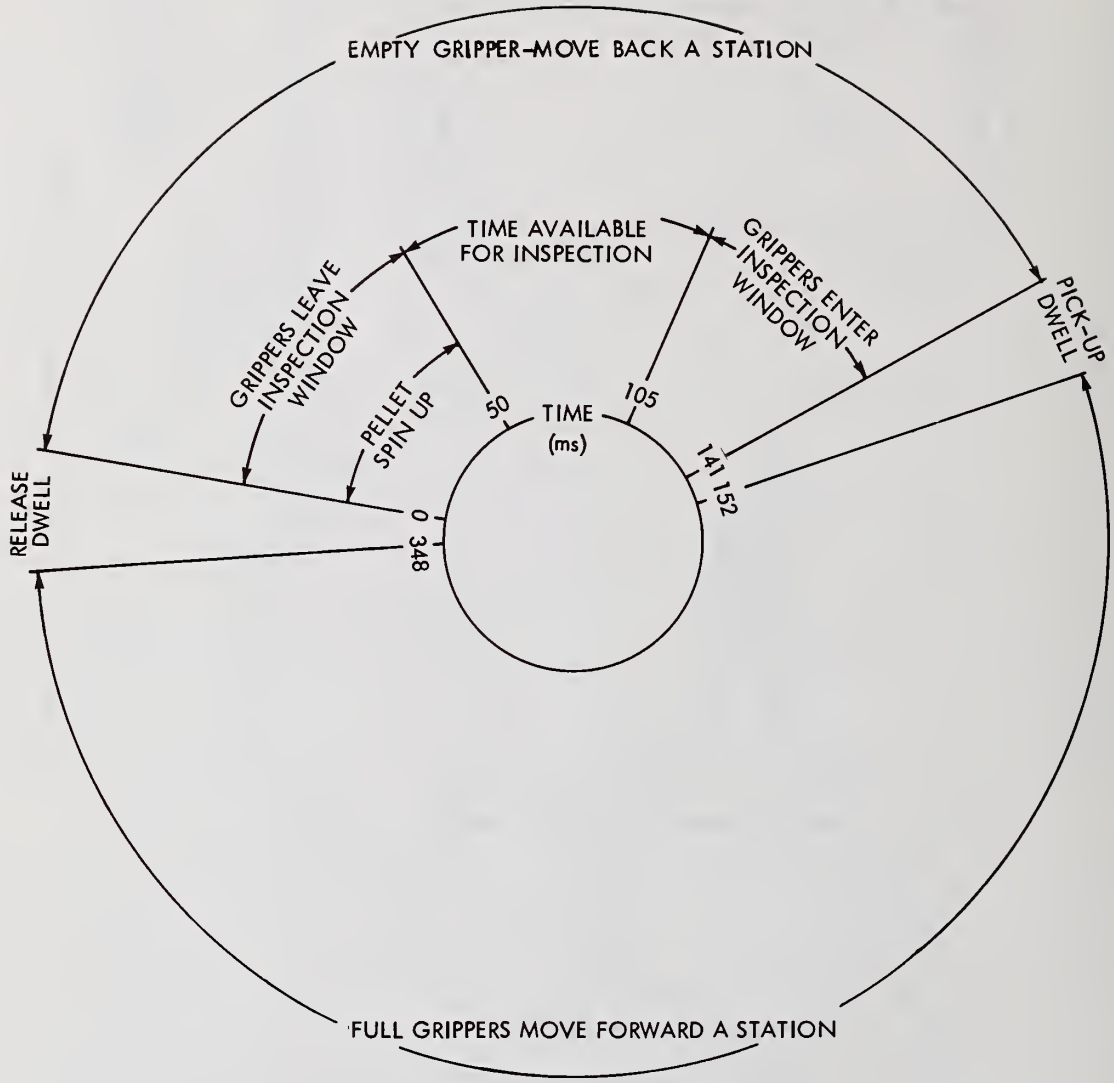

FIGURE 4: Fuel Pellet Handling Cycle

The length measurements concept is shown in Figure 5. The laser beam is expanded along one direction so as to form a rectangular beam of collimated light longer than the pellets to be inspected. The pellet is cradled upon precisely parallel cylindrical and horizontal rollers positioned such that the beam passes over the pellet ends and orthogonally intersects the extended pellet axis. The pellet's shadow is then brought to focus upon a linear photosensor array. The motor driven rollers continuously spin the pellet during the length inspection so that all possible shadows of the pellet length are sampled.

This technique determines the mean length of the spinning pellet's shadow. Figure 6 illustrates how this mean length is determined. A fuel pellet with an exaggerated non-square end is shown. The front view shows the rectangularly collimated laser beam intersecting with and passing the pellet. As the pellet is rotated, its shadow, cast upon the linear photosensor array, will change according to the angularity of the ends. Figure 6 shows how the illumination varies as the pellet rotates. The light-dark boundary resembles a rectified sinusoid. This occurs because the greatest extensions of the pellet's length block the beam twice per revolution. The mean length of the pellet is then taken as the length detected between line segments k and 1.

At the end of the measurement cycle, one 16-bit word representing the desired pellet length is transferred to the dedicated inspection minicomputer.

The pellet length information is then evaluated to determine if the length is within the specified limits. A software subroutine performs this operation permitting changes in the maximum and minimum limits if manufacturing tolerances change.

Diameter Measurement

The diameter station measures the 4.940 $\pm$ 0.25 mm (0.1945 $\pm$ 0.010 in.) diameter by 6.160 $\pm$ 0.97 mm (0.2425 $\pm$ 0.038 in.) long pellets to a precision of $\pm$ 0.008 mm ($\pm$ 0.0003 in.) over the diameter range. Diameter is reported as the maximum of approximately 50 readings spaced along the length of the pellet. The diameter station has been designed so that it can be modified to inspect pellets to 8.89 mm (0.350 in.) nominal diameter without changing the optics. The accept/reject limits are teletype-adjustable in 0.003 mm (0.0001 in.) increments anywhere within the $\pm$ 0.25 mm ($\pm$ 0.010 in.) range.

The concept used is shown in Figure 7. A collimated ribbon-like beam of light is scanned across one side profile of the pellet by the rotating prism. That portion of the ribbon-like beam, not obscured by the pellet, is focussed onto the narrow photosensor array. The instantaneous pellet diameter is indicated by the length of the shadow projected onto the array. Beam position in the gaging field is determined by counting an oscillator that is set to a multiple frequency of the scanning frequency. Count is initiated by the first light to strike the photodiode array during each scan.

Approximately 50 diameter measurements are preprocessed to determine the maximum pellet diameter. One 16-bit digital word of pellet diameter information is then transmitted to the dedicated minicomputer for analysis.

Each pellet is evaluated against diameter limits. The pellet is accepted if no diameter exceeds the maximum limit and if a designated number of diameters are above minimum limits. The designated number of diameters will be a presettable parameter.

The diameter measuring system is similar to the length measuring concept described previously. The needed maintenance and repair skills are also very similar with both systems using many of the same repair parts.

Mass and Mass/Length Measurement

A commercial weigh scale with automatic tare is used. The unmodified balance has an accuracy of 1 mg + 0.02% of weight and a weighing speed of two seconds. This is the fastest scale available on the market and since it cannot operate at the required throughput rate of one pellet per second, sampling inspection is used.

LENGTH INSPECTION

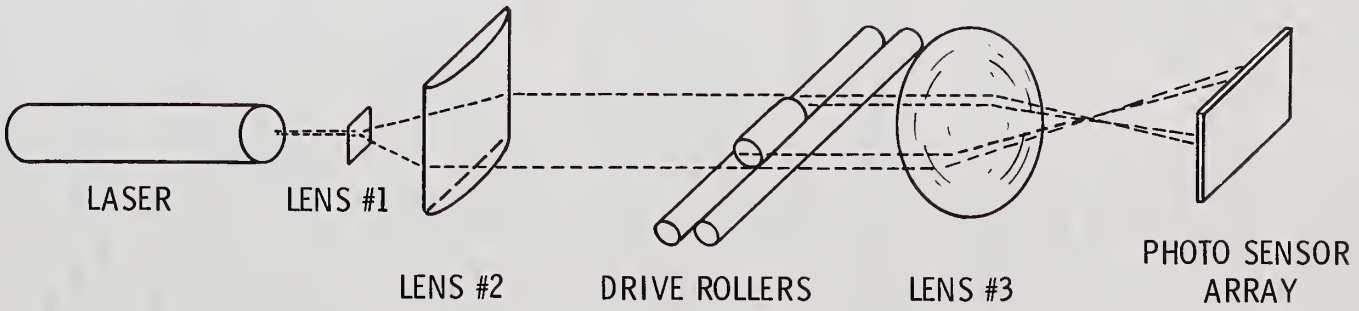

FIGURE 5: Schematic Diagram of Fuel Pellet Length Inspection Station

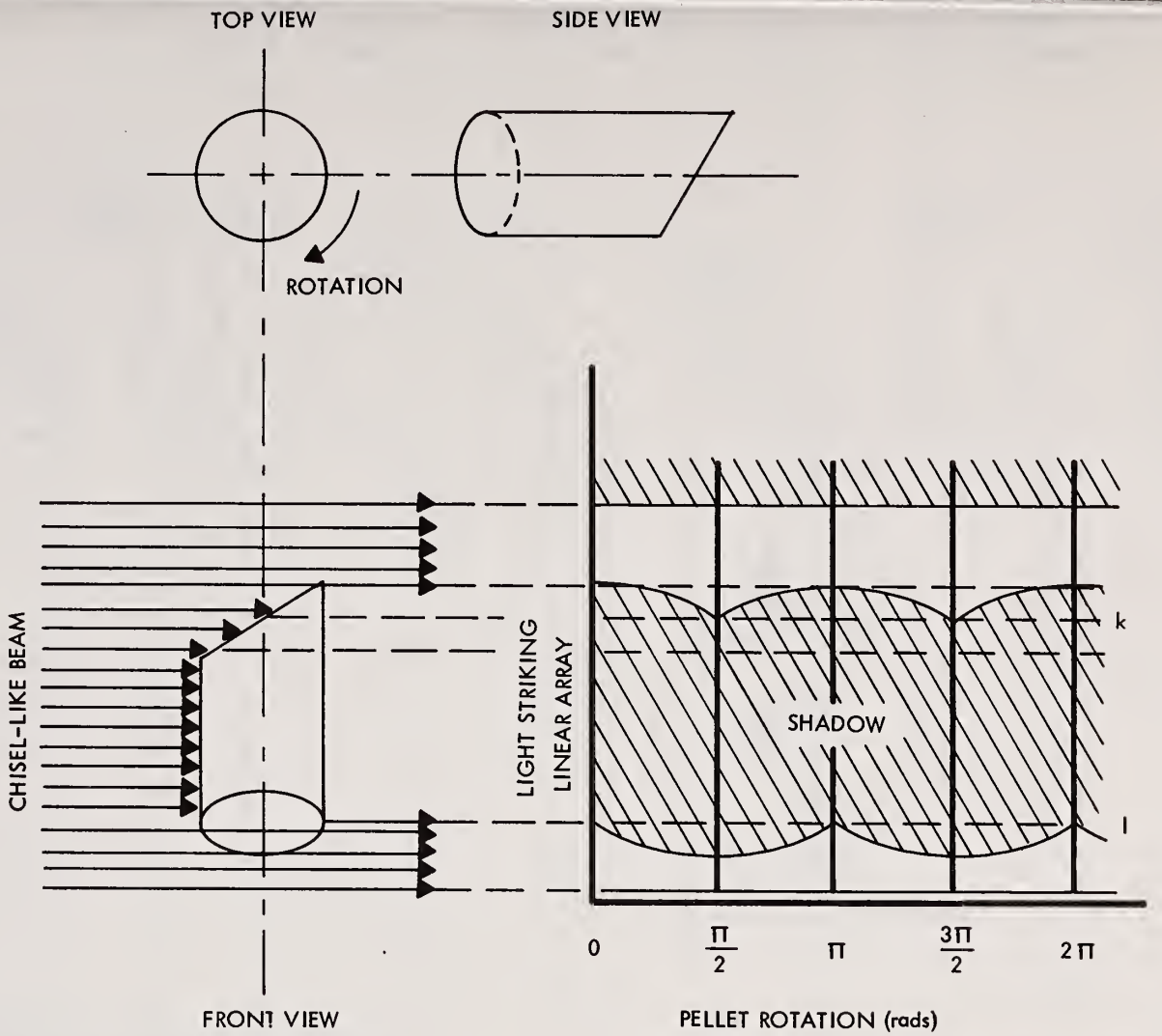

HEDL 7911-032.4

FIGURE 6: Technique for Determining Mean Length

DIAMETER INSPECTION

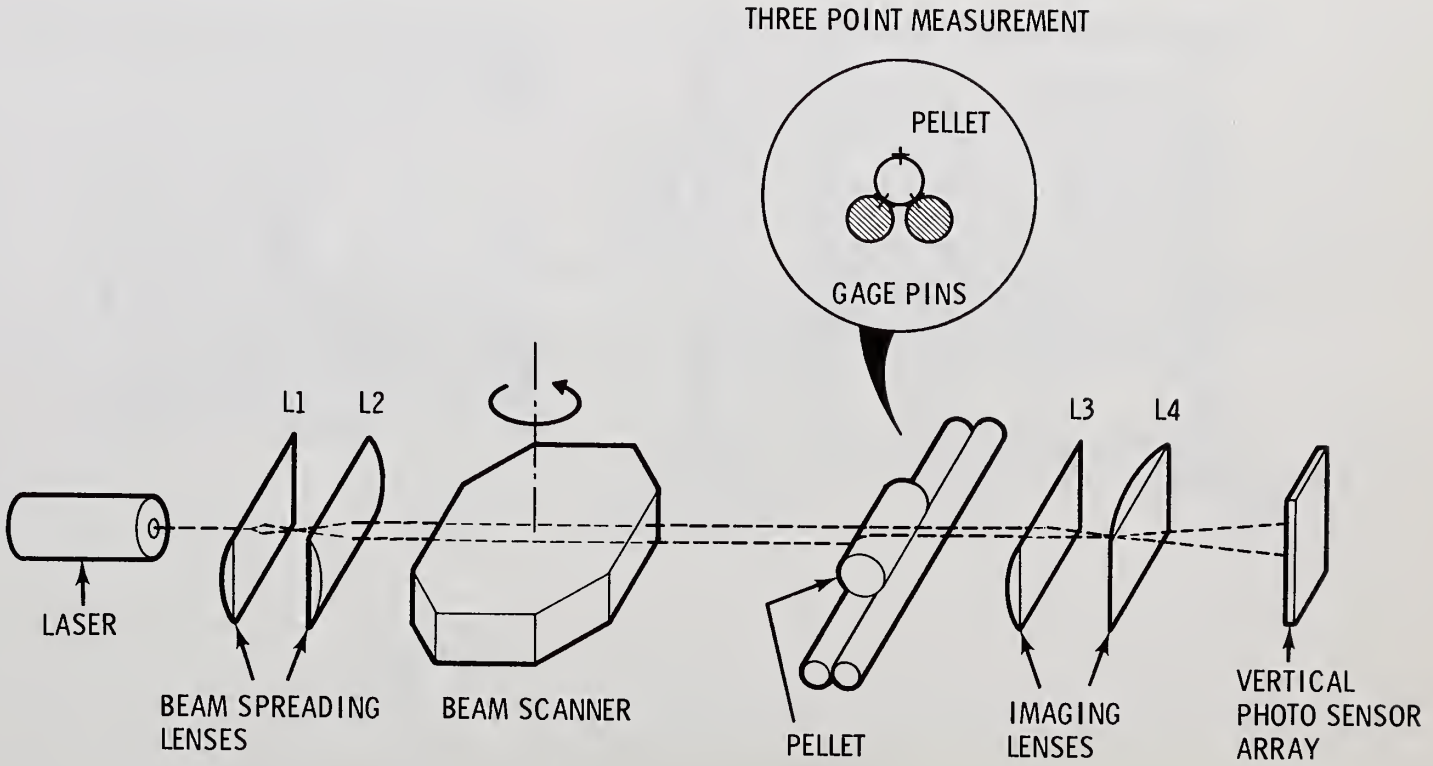

FIGURE 7: Schematic Diagram of Fuel Pellet Diameter Inspection Station

During the time that pellets are not being weighed, the handling system functions in the normal mode-pellets advancing one inspection station on each cycle. When a weight sample is to be taken, the gripper fingers are held open two cycles (two seconds) to allow time for the balance to settle and be read. Then the gripper fingers are returned to the normal operating mode. In the normal mode, pellets are passed through the scale, but no weight readings are taken.

The frequency of weight sampling and the number of empty transfer cycles that elapse during a weighing period are software adjustable.

If a pellet is outside the sorting limits because of a deviation in mass or mass divided by length, the system reverts to a mode where every pellet is inspected for mass until a software preset number of successive pellets (say 100) have been inspected and judged acceptable.

Mass per unit length will incorporate the measurement made at the length station. The aglebraic division is accurate to $\pm$ 0.001 grams per inch.

Surface Flaws

The system will detect chips and cracks with depths exceeding 0.08 mm (0.003 in.) and minor dimensions greater than 0.08 mm (0.003 in.) {probability of detection would be about 50% at 0.038 mm (0.0015 in.)}.

The system is designed to measure the combined flaw area of two round random chips of 1.27 mm (0.050 in.) diameter to an accuracy of 1% of nominal pellet area on pellets with nominal dimensions.

The method used to detect surface flaws is based on changes in the reflected light level of a moving spot of light. The reflected beam exhibits a strong specular component even though the surface appears relatively nonreflective. Many mixed oxide pellets have been examined in design testing, and although the overall light level varies between pellets, the specular component remains a prominent feature.

Microscopic features of the pellet surface affect the amount of specular reflection. A flat spot tends to reflect the beam away from the "nominal" path the light would follow from a rounded surface; a small pit may reflect the beam internally, while larger defects reflect the beam in various directions, all contributing to significant loss of light.

The method used for scanning the pellet surface is shown schematically in Figure 8. The incoming beam of light is focused to a small spot and is deflected through a small angle by a multifaceted mirror. During inspection, the rollers rotate the pellet with the light beam sweeps across the pellet's surface.

The beam size is adjusted to the required instrument resolution for a minimally rejectable feature. Light from the pellet surface is then imaged onto a photodetector by means of another lens.

The received illumination signal is processed by setting a "dark level" below which any signal is considered to represent a defect area. The dark level coupled with the aperture determines the sensitivity of the signal to surface depressions (flaws).

To extract the area and size of a defect from the signal, the light level must be synchronized with beam position on the pellet surface. This is accomplished using a synchronous motor drive for the pellet rollers and a reference grid to locate the moving light beam. The use a reference grid was dictated by the need for a stable, linear, high-speed position sensor. Other techniques, such as a shaft encoder or resolver coupled to a rotating scanning mirror, would require a resolution on the order of one part in 7000. A resonant vibrating mirror-type scanner would be unusable without some external means of accurately determining beam position.

SURFACE FLAW INSPECTION

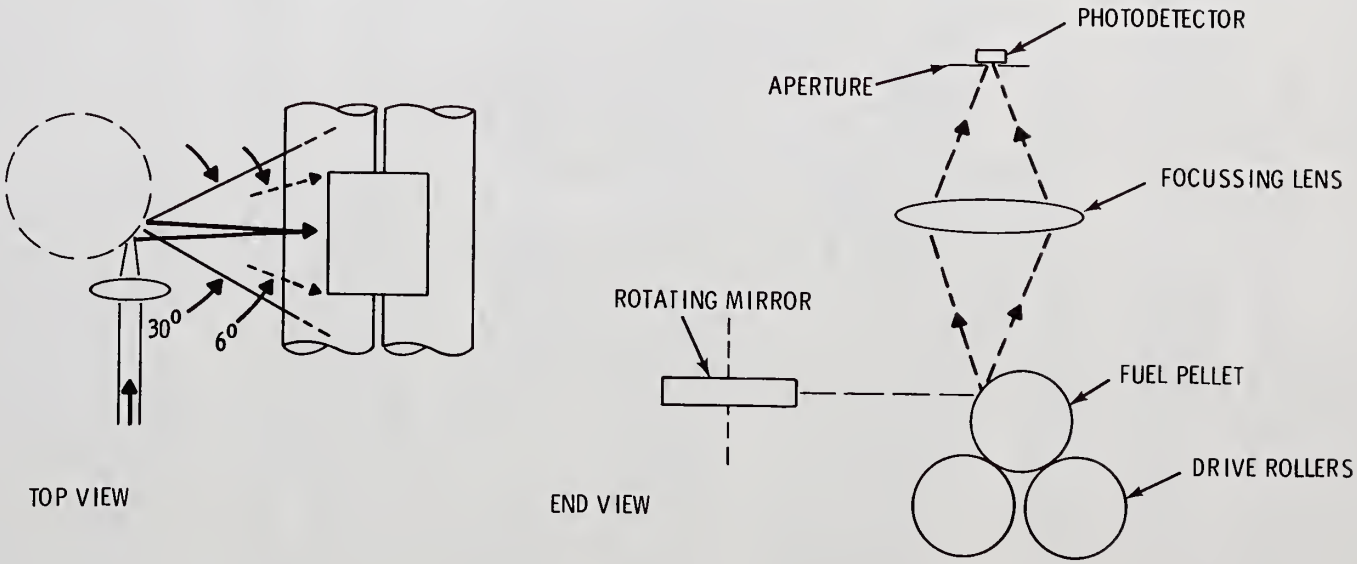

FIGURE 8: Surface Flaw Inspection Method

Given sufficient information to determine beam position and the light level of the reflected beam, one can construct a surface map of a pellet in the memory of a digital data processor. Decisions to accept or reject pellets are based on a combination of flaw area, flaw perimeter and flaw location.

Commercial optical inspection systems that detect surface discontinuities are available, but these systems do not directly measure defect size and are not capable of distinguishing between defect types. Determining defect size and type (crack, pit, chip, etc.) becomes very important when one considers the reasons for performing surface flaw inspections. Flaw inspections are needed: (1) to assure efficient heat transferability from fuel pellets to cladding and (2) to assure that no pellet is likely to fall apart due to flaws during fuel pin loading.

Geometry factors that affect in-core pellet heat transfer are pellet-to-cladding clearance and the distribution of clearance volume between pellet and cladding. The importance of pellet chips when considering heat transfer can be better understood in an example. Suppose a pellet contains a hemispherical surface chip. In-core, heat generated behind the chip must either traverse a greater air gap to reach the cladding or must travel around the chip to reach the nominal pellet surface and then cross the air gap to the cladding. Either way, the local heat flow path is longer and a pellet hot spot develops. If, instead of a concentrated hemispherical chip, the pellet had lost the same material uniformly over its entire cylindrical surface, then the pellet would run slightly warmer but no local hot spot would develop. Therefore, a hemispherical chip is more serious than a long cylindrical chip of equal volume. Thus, chip sizes, shapes and their relative proximities are important to heat transfer efficiency.

Processing Algorithm

The data processing proceeds as follows: light levels from the photodetector are amplified, digitized and presented serially to the processor for storage. Synchronizing signals control the digitizing process and deposit the data bit by bit, row by row, into the memory to form an image.

Total "dark" area can be accumulated in a counter as the data are loaded in real time. This area becomes equal to defect area when combined with the length measurement from another section of the gage:

Defect area = dark area + length x diameter x ¶ - total field area.

The diameter measurement controls the number of scans made across the pellet surface and is thus inherently reflected in the total number of bits stored.

Defect area serves as the first stage of a two-stage sort and is used to speed subsequent detailed processing: a pellet with less defect area than the minimum rejectable single surface flaw cannot fail in subsequent examination of surface features.

Detection of individual surface features requires a scan of the stored image and an accumulation of related properties. The scan begins with a test for end chips. A pointer moves from left to right until it encounters a light area, thus marking the edge of the pellet. A second pointer performs the same operation but from right to left in parallel. A simple algorithm then moves the pointer downwards along the edge. At each row, the address of the pointer is added to a counter. The sum at the end of the downward scan gives the left and right areas of darkness. Combining the left and right areas with known parameters gives end chip area:

Each chip area = left area + right area = (length x diameter x ¶) - total area

Also collected by the algorithm are the differences between consecutive addresses during the downward scan. This yields the perimeter of the pellet's edge.

$$\text{Perimeter} = \sqrt{1 + (\Delta \text{ edge location})^2}$$

To save processing time, the square is not actually calculated, but a table of values is used instead. The table is indirectly addressed by the differences in consecutive pointer locations:

Δ Location	Δ Perimeter
0	1
1	1.41
2	2.23
3	3.16

To isolate interior defects, a pointer first scans the field from left to right until it encounters a dark area. (The end areas have been "erased" at this point in the processing). If no dark area is encountered, the pointer skips several lines down and tries again. Every line need not be scanned, since resolution need only be sufficient to trap minimally rejectable defect lengths. Once a defect area has been found, pointers are set at the "top" of the area (Figure 9) and move down together, following the edges of the defect until they meet.

The area is found by taking the accumulated differences in pointer locations; perimeter information is gathered as in the edge-defect case. Also, as the pointers move along, the area becomes "erased" to avoid interferring with subsequent scanning. Having isolated area and perimeter, an empirical function is employed to determine acceptability (Figure 10), similar to the edge-defect case. During downward pointer travel, a check may be made of defect size in one dimension. This alone may flag a pellet as defective and save processing time.

This processing algorithm allows accept/reject decisions to be based on flaw type (geometry) as well as area. Because of the flexibility of this detection scheme, a tiered acceptance criterion can be developed. For each pellet scanned, the first criterion checked would be the total defect area found. Assuming this area to be less than the maximum defect area allowable, individual defects could be analyzed in terms of an area-to-perimeter ratio to determine if the defect were circular or elongated in shape. Each type of defect would have its own maximum allowable dimension to establish acceptance.

Controls and Data Processing

The control system is designed to monitor and control the pellet handling system, obtain data from each of the inspection stations, process all collected data, determine the pellet accept/reject disposition and format data to be transferred to the supervisory computer.[4]

The design requirements for the control and data processing subsystem were as follows:

(1) Monitor the handling system to determine if pellets are entering and leaving the gaging system. This function will account for all pellets within the inspection boundaries.

---

(4) E. Sternheim, "Computer System for Automatic Inspection of Fuel Pellets", Transactions of the American Nuclear Society, Volume 34, (November 1979).

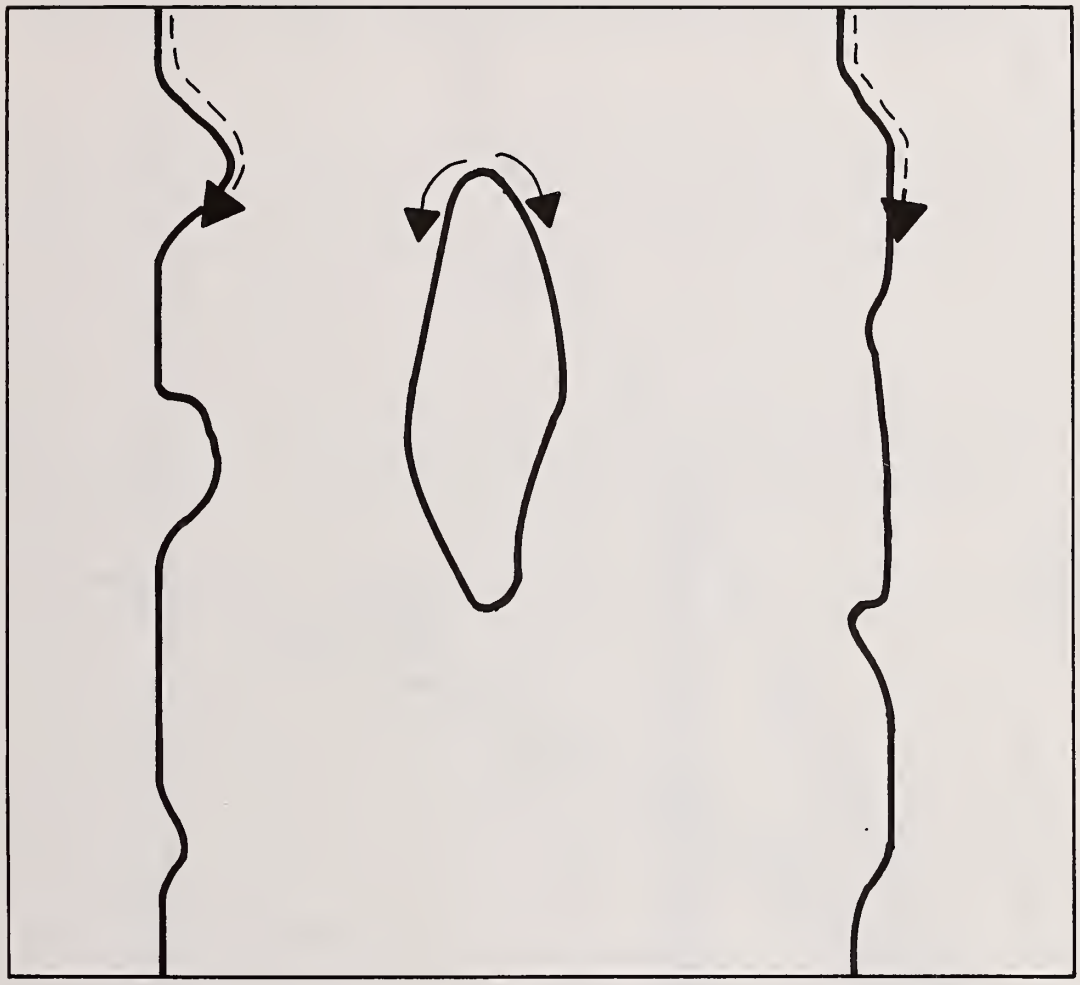

HEDL 7911-032.5

FIGURE 9: Pointers Tracing the Edges of Defects for Area and Perimeter Values

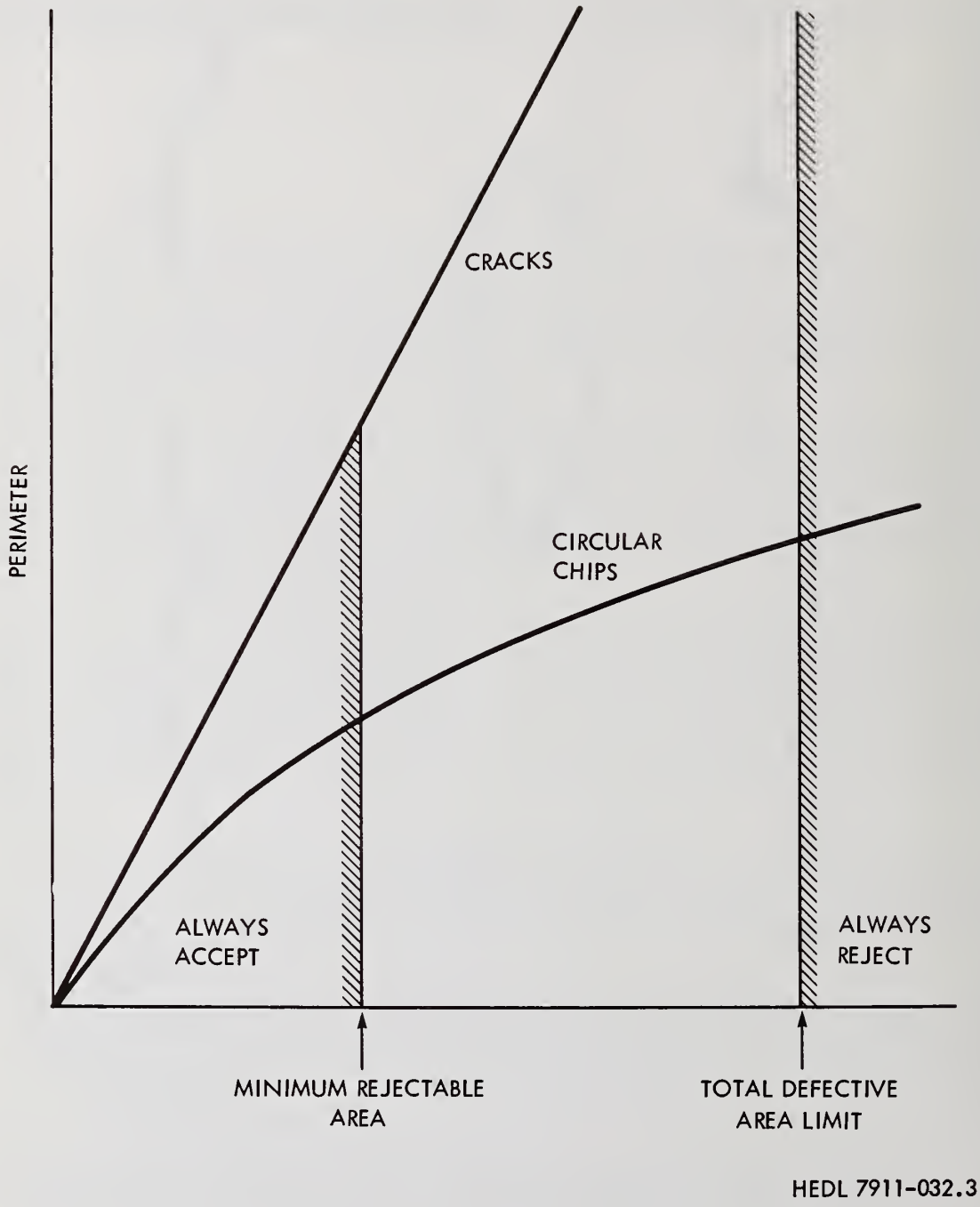

FIGURE 10: Function for Determination of Defect Severity Based on Empirical Data

(2) Synchronize the mechanical and electronic systems.

(3) Determine pellet quality and control the disposition gating.

(4) Provide a system control and operation panel.

(5) Collect and process pellet inspection data from each inspection station. Approximately 50 diameter and 40 length samples will be taken for determining the pellet diameter and length.

(6) Calculate mass per unit length and the surface quality index.

(7) Format and transmit data between the inspection computer and supervisory computer system. Supervisory computer processing, data storage and display software are not included. Software to accept and analyze station data, compare the data with standard tolerances (specified in proceeding sections), perform accept/reject decisions, control the accept/reject hardware and control operation functions are included.

The basic control system configuration is shown in Figure 11.

The pellet transfer mechanism positions individual pellets at each station. The data acquisition electronics then gathers the inspection data from each station and preprocesses the data into a specified transmission format. A dedicated minicomputer is used to process the collected data, make calculations and determine the inspection disposition of each pellet. A serial data link provides communication between the dedicated inspection minicomputer and the supervisory computer.

System operation is synchronized to the handling hardware by the timing and control logic. This section of the control system performs the following:

(1) Synchronizes the mechanical and electronic functions.

(2) Starts the data acquisition process.

(3) Controls data collection and preprocessing.

(4) Formats inspection data for transfer to the dedicated inspection minicomputer.

(5) Establishes all data transfers.

(6) Controls the sorting gates.

(7) Monitors pellet detections devices.

Data transmission between the inspection minicomputer and the flaw station electronics is over a dedicated DMA channel. The flaw station establishes the data transfer requirements in that each transition point will be a 16-bit word and transition points could occur on adjacent data matrix points. Therefore, data rates will be high as specified times requiring a DMA channel controlled by the measurement system control logic.

Measured length, diameter and weight data words (16 bits each) are included in the block data transfer to the supervisory computer. The computer processing time is structured so a period is reserved for length, diameter and weight calculations and limit checking. The minicomputer also establishes a transfer medium between the fuel pellet inspection system and the supervisory control computer.

The Control System and Data Processing configuration permits software operational program down loading from the supervisory computer mass storage device. Supervisory and inspection computer control and monitoring functions include the following:

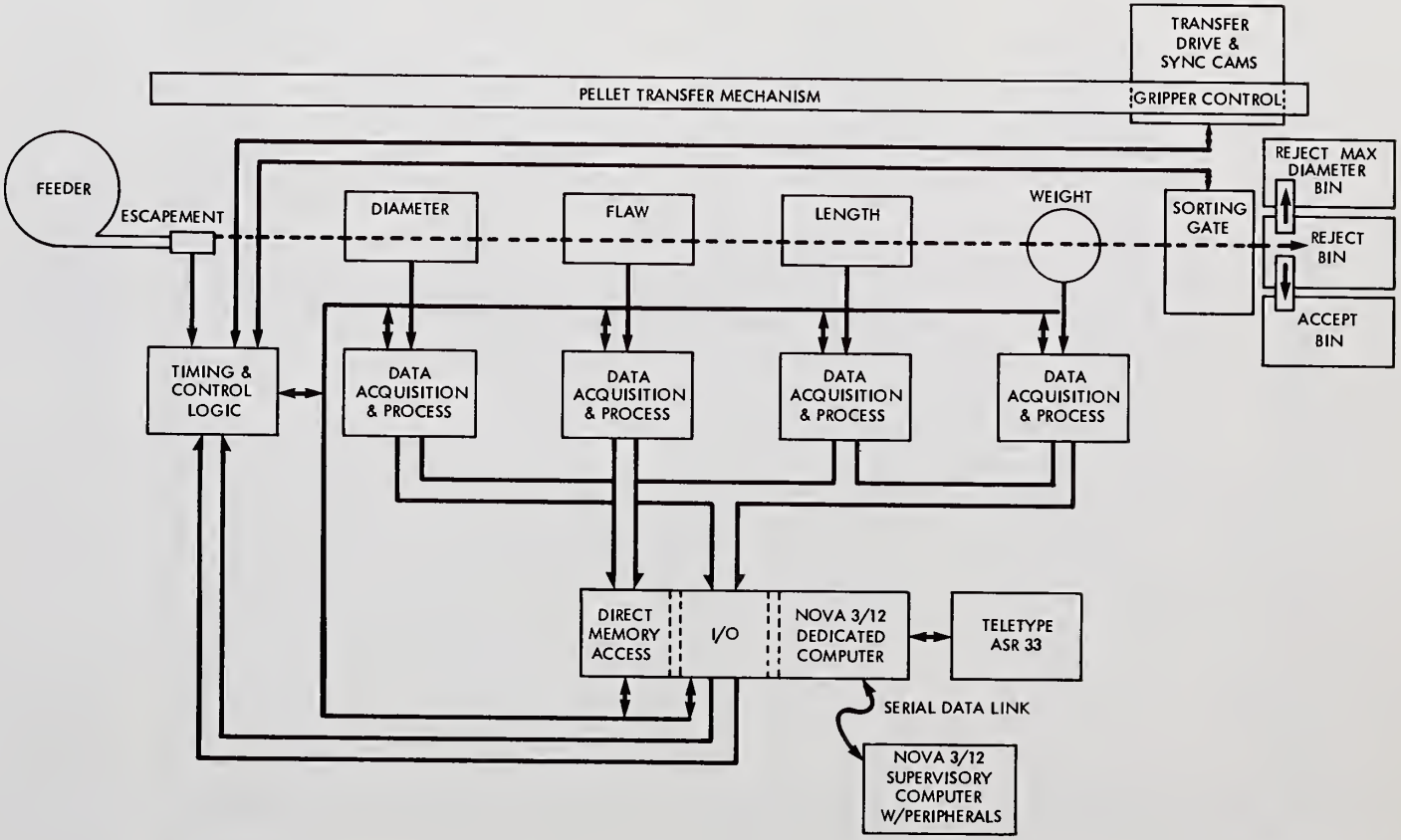

FIGURE 11: Fuel Pellet Gauge Signal Paths

Supervisory Computer Functions

- pellet escapement control
- inspection system start (activate grippers)
- inspection system stop (open grippers)
- misplaced pellet alarm
- inspection station parameter limit changes

Inspection Computer Functions

- accept/reject decisions
- start (activate grippers)
- stop (open grippers)
- inspection station parameter limit changes
- misplaced pellet alarm
- weighing cycle frequency modifications

The prototype gaging system is being performance tested at this time. HEDL personnel are verifying measurement precision under simulated operating conditions. Preliminary results indicate that the basic measurement algorithms are sound and that the system meets the design objectives for throughput and precision. The system has been operated for over 500,000 cycles at this time.

Table I is a copy of a printout of typical data that are stored in the supervisory computer. In addition to the accept code, pellets are classified into eleven reject categories that are used for quality assurance analysis. Pellet weight and density calculation are supplied to the accountability computer for comparison with final fuel pin and scrap weights and reconciliation of SNM received.

Table II is a copy of the printout from a typical system calibration. Length, weight, and diameter are calibrated simultaneously using ten simulated pellets with known physical attributes.

HEDL plans to continue performance testing of the system to determine long-term operating characteristics and estimate system reliability.

DIAMETER (inch)	LENGTH (inch)	WEIGHT (gms)	WEIGHT/ LENGTH (gms/inch)	SQI	STATUS CODE*
0.1941	0.244	1.204	4.940	0	1
0.1931	0.243	1.192	4.900	0	1
0.1940	0.245	1.186	4.847	0	1
0.1931	0.246	1.178	4.786	0	1
0.1934	0.245	1.188	4.855	0	1
0.1942	0.223	1.211	5.421	0	8
0.1937	0.251	1.189	4.746	0	1
0.1937	0.246	1.202	4.883	0	1
0.1938	0.244	1.184	4.858	0	1
0.1939	0.243	1.186	4.876	0	1
0.1932	0.243	1.193	4.904	0	1
0.1937	0.247	1.205	4.885	0	1
0.1938	0.245	1.187	4.851	0	1
0.1936	0.244	1.193	4.885	0	1
0.1937	0.243	1.192	4.910	0	1
0.1937	0.241	1.196	4.956	0	1
0.1931	0.246	1.186	4.818	0	1
0.1938	0.247	1.185	4.795	0	1
0.1938	0.244	1.187	4.870	0	1
0.1939	0.243	1.201	4.937	0	1

*STATUS CODE:

1 = ACCEPT
2 = REJECT OVER LENGTH TOLERANCE
3 = REJECT UNDER LENGTH TOLERANCE
4 = REJECT OVER MAXIMUM DIAMETER
5 = REJECT UNDER MINIMUM DIAMETER
6 = REJECT FOR MAXIMUM SURFACE QUALITY INDEX (SQI)
7 = REJECT FLAW PROCESSING TIME EXCEEDED
8 = REJECT FOR OVER WEIGHT/LENGTH TOLERANCE
9 = REJECT FOR UNDER WEIGHT/LENGTH TOLERANCE
10 = SORT FOR OVER WEIGHT
11 = SORT FOR UNDER WEIGHT

HEDL 7911-032.11

TABLE I: Pellet Inspection Information

CALIBRATION RESULTS

	BIG PELLETS			SMALL PELLETS		
	DIA	LNG	WGT	DIA	LNG	WGT
1	0.2025	0.2794	1.4901			
2	0.2024	0.2799	1.4941			
3	0.2025	0.2804	1.4961			
4	0.2025	0.2794	1.4926			
5	0.2023	0.2794	1.4926			
6				0.1861	0.2061	0.9133
7				0.1861	0.2070	0.9133
8				0.1861	0.2084	0.9151
9				0.1861	0.2065	0.9151
10				0.1860	0.2065	0.9254
AVERAGE						
	0.2025	0.2797	1.4937	0.1860	0.2069	0.9164
STANDARD DEVIATION						
	0.0000	0.0004	0.0022	0.0000	0.0008	0.0051

TABLE II Calibration Data

Discussion:

Wagner (LASL):
Do you have any need to inspect the top and bottom of the pellet, or has that need gone away since the specification was changed from planar smear density to fissile weight per length?

Gottschalk (Westinghouse-Hanford):
There is really no need to inspect the top or bottom of pellets since the specification is in weight per length now, rather than in planar smear square density.

Wagner:
Can you tell whether a pellet is barrel shaped or hourglass shaped from the diameter data?

Gottschalk:
The diameter processing looks to assure that there are no points that exceed a maximum diameter, to assure the pellet can be loaded in the rod. The second step in that analysis is to make sure that a given number of the points exceed a minimum diameter. If so many of readings exceed the minimum diameter, we will accept it, otherwise we will just throw it out. The capability is there to dump that data to the host computer for a detailed pellet analysis if it wants to perform additional analysis. Normally it is not worth it. If the pellet does not meet those requirements, generally it would be sent to the recycle line.

Nilson (Exxon Nuclear):
You measure the length to get the density. Do you reject on length?

Gottschalk:
No, the length is useful for process control applications in that it is a good feedback to the people doing the pressing. Generally, the length will follow the weight to length and if you have length problems it is indicative of future problems in the density area.

Nilson:
What are the grippers made out of?

Gottschalk:
The grippers are made of stainless steel.

Nilson:
You say you need some experience. Have you considered using your equipment in one of the commercial fuel plants?

Gottschalk:
Yes. In fact, one of our people is working with GE to develop a second version of this to be used in their plants. The people from Exxon have also observed the equipment. I think all of the fuel vendors - maybe not from every plant - but at least from every vendor have been in to look at the technology.

Armento (ORNL):
Is this technique applicable to hot cell operations for fuel cycles like U-233/thorium?

Gottschalk:
Yes. In fact, this gauge was designed to be operated automatically with no operator intervention. In addition, all the components in the gauge are modularly replaceable. For example, in a hot cell if you lost the length system for some reason you just take that whole system out and set a new one in. HEDL did additional work and built another prototype gauge specifically for remote operations which could actually be maintained by a robot.

Armento:
Does it require manipulator intervention?

Gottschalk:
Only for maintenance. Normally the gauges run completely self-standing, but they were designed so they could be maintained remotely.

Passive Nuclear Material Detection in a Personnel Portal

by

PAUL E. FEHLAU
Los Alamos Scientific Laboratory, Los Alamos, New Mexico

and

MICHAEL J. EATON
Sandia Laboratories, Albuquerque, New Mexico

ABSTRACT

The concepts employed in the development of gamma-ray and neutron detection systems for a special nuclear materials booth portal monitor are described. The portal is designed for unattended use in detecting diversion by a technically sophisticated adversary and has possible application to International Atomic Energy Agency safeguards of a fast critical assembly facility. Preliminary evaluation results are given and plans for further parameter studies are noted.

KEYWORDS: Portal monitors, SNM monitors, radiation detectors, neutron detectors, IAEA safeguards, ZPPR

INTRODUCTION

The work described here is part of a joint Sandia Laboratories-Los Alamos Scientific Laboratory (LASL) effort to examine techniques for possible IAEA safeguards use at fast critical assembly (FCA) facilities and to develop and demonstrate components of an advanced containment and surveillance system. A study that examined methods for safeguarding fast critical facilities[1] identified containment of nuclear material by an unattended special nuclear material (SNM) portal monitor as a key element of the safeguards system. To meet that requirement, the monitor described here was developed by Sandia in consultation with LASL and has been described by Mangan.[2] Here, we intend to examine in depth the concepts used in the design of the neutron and gamma-ray detection system, and to indicate the results of the first steps in evaluation of the detection system performance, and to mention plans for further evaluation.

FIRST CONSIDERATIONS

The SNM inventory at a FCA facility includes plutonium of various isotopic contents and highly enriched uranium (HEU). The useful radiation characteristics of these two materials in an SNM monitor are quite different because plutonium fuel constituents emit both strong gamma-ray radiation and neutrons while uranium emits only rather soft gamma-ray radiation at a much lower specific activity. Further, examination of the unreflected

---

[1] D. O. Gunderson and J. L. Todd, "International Safeguards for Fast Critical Facilities," Sandia Laboratories report, SAND 78-0168 (1978).

[2] D. L. Mangan, "A Personnel Portal for International Research Facility Safeguards," Nuclear Materials Management VIII, Proceedings Issue, 674 (1979).

critical masses[3] indicates that the critical mass of HEU is more than three times that of plutonium. Thus, more material must be diverted to achieve the same effect with uranium. Table I shows the specific intensity of penetrating radiation emitted by the major components of FCA fuel that are useful in detecting the presence of the fuel in a monitor. The first isotope, ^{235}U, is the principal component of the uranium fuel (93%) and the rest of the table entries are found in the plutonium fuel.

TABLE I

MAJOR GAMMA-RAY AND NEUTRON SIGNATURES[4] OF FCA FUEL COMPONENTS

Isotope	Energy (KeV)	Intensity gammas/g/s	Comment
^{235}U	185.7	4.3×10^4	Only intense gamma ray easily attenuated.
^{238}U	1001.1	1.0×10^2	Arise from ^{234m}Pa daughter of ^{238}U.
	766.4	3.9×10^1	
^{239}Pu	413.69	3.4×10^4	
	129.28	1.4×10^5	
^{240}Pu	SF neutrons	1.0×10^3	
^{241}Am	59.5	4.6×10^{10}	Strong, but easily attenuated.

Table II shows the characteristics of some plutonium fuel at the Zero Power Plutonium Reactor (ZPPR), Argonne-West, Idaho, which is being used as a model facility for design purposes in development of the portal described here. The ZPPR fuel is all in the form of a plutonium-aluminum or plutonium-uranium alloy, an advantage for detecting diversion. In one case aluminum dilutes the plutonium, decreasing the self absorption of gamma-ray radiation in the fuel and augmenting the spontaneous fission (SF) neutrons with (alpha,n) reaction neutrons while, in the other case, ^{238}U adds some amount of penetrating gamma-ray radiation to the fuel. The trend shown in the final column of Table II results from the ^{241}Pu that decays to ^{241}Am. The amount of the latter closely follows the ^{240}Pu content listed, but there is an additional variation with the age of the fuel because the amount of ^{241}Am builds up with time. Other sources of possibly useful radiation that have been considered for detection of SNM, such as fission products[5] or ^{232}Th daughters in enriched uranium,[6] have not been found in large quantity in samples of fuel examined as part of this investigation[7], but could still be of importance for heavily shielded fuel because they emit more penetrating radiation.

---

[3]W. R. Stratton, "Criticality Data and Factors Affecting Criticality of Single Homogenous Units," Los Alamos Scientific Laboratory report, LA-3612 (1967).

[4]R. H. Augustson and T. D. Reilly, "Fundamentals of Passive Nondestructive Assay of Fissionable Material," Los Alamos Scientific Laboratory report, LA-5651-M (1974).

[5]Tsahi Gozani, "Evaluation of Portal Monitors for the Detection of Nuclear Materials," Nuclear Materials Management VIII, Proceedings issue, 128 (1979).

[6]P. E. Fehlau and W. H. Chambers, "Perimeter Safeguards Techniques for Uranium Enrichment Plants," to be published.

[7]Hsiao-Hua Hsu, Los Alamos Scientific Laboratory, unpublished data, 1979.

TABLE II

ZPPR MAJOR FUEL TYPE CHARACTERISTICS

Manufacturer's Type	Components	Mass % Pu-U	Atom % ^{240}Pu	n/s/in[8]	Relative[8] Emission of ^{239}Pu γ/in	Relative[8] Emission of ^{241}Am γ/in
PANI	Pu-Al	95	4.50	2,630	1.26	0.42
PUMS	Pu-U-Mo	20-78	8.66	1,730	0.67	0.49
PUMD & PUMN	Pu-U-Mo	28-69	11.6	3,000	1.0	1.0
PAHN	Pu-Al	97	22.3	11,600	0.96	3.44
PUMH	Pu-U-Mo	34-63	26.4	10,000	0.95	4.47

The nature of the plutonium fuel with its intense penetrating gamma-ray emitters is readily detected with conventional gamma-ray detectors when it is bare--i.e., not shielded--or when it is lightly shielded. Heavy gamma-ray shielding could hide the plutonium from a conventional gamma-ray detection so there is good reason to try to use the more difficult-to-shield neutron emission. Of course, it also makes sense to try to detect the presence of shielding material and Lopez[9] has described the system used in this portal. We pursued the neutron detection approach in addition to the detection of shielding in order to prevent passage of material that may be shielded with a more sophisticated gamma-ray attenuator made of a material such as lead dispersed in polyethylene. Dispersed small particle shielding is difficult to detect with metal detectors, but is a standard commercial item[10] and readily available. So, for plutonium there are good reasons for monitoring for both gamma-ray and neutron radiation in the context of safeguards where the adversary is technically competent and the monitor is unattended.

The uranium fuel is more difficult to safeguard because the intensity of the emmited gamma-ray radiation is lower than in the plutonium fuel and also, the gamma-ray radiation is all relatively soft and easily shielded. There is no useful neutron signature so the only alternate means to detect diversion is to detect shielding material.. Our approach includes metal detection, as mentioned, and the use of the optimum detector for the detection of shielded uranium,[11] a plastic scintillator. Additional measures involving the detection of a decrease in gamma-ray and neutron backgrounds may be useful for detecting shielding and we intend to examine this concept during an upcoming evaluation period. A

---

[8]J. T. Caldwell, Los Alamos Scientific Laboratory, unpublished data, 1978. The unusual unit of length used here, the inch, has become the unit of length in fuel plate sizes and they are found in sizes 1 through 8 inches. The inch is 2.54 cm long. The source strength for a particular fuel plate is obtained from the product of the tabulated numbers and the fuel plate length in inches.

[9]A. A. Lopez, "Shielding (Metal) Detector Development Program," Sandia Laboratories report, SAND 78-1969 (1979).

[10]Reactor Experiments, Inc., "General Catalog," 963 Terminal Way, San Carlos, CA 94070 is one supplier, but there are certainly others.

[11]P. E. Fehlau and E. R. Shunk, "UF_6 Gamma-Ray Measurements for SNM Portal Monitor Application," to be published.

[12]C. N. Henry and J. C. Pratt, "A New Containment and Surveillance Portal Monitor Data Analysis Method," 1st Annual ESARDA Symposium on Safeguards and Nuclear Materials Management, Proceedings, ESARDA 10, p. 126 (1979).

data analysis technique, described by Henry and Pratt,[12] may extend the effectiveness of the booth for detecting a protracted diversion. This approach saves a net count for each occupancy and summation of data from many passages can achieve increased sensitivity.

DESIGN CONSTRAINTS

Instrumentation for containment and surveillance in international safeguards must function unattended, supported only by occasional visits from an inspector. Unattended operation translates directly to the requirement that a portal monitor, by its design and without human intervention, successfully deter diversion of nuclear material by any subterfuge available to an adversary short of physical destruction of the portal. Our choice of the booth configuration over the simpler walk-through designs commonly used in domestic safeguards was necessary to prevent several postulated defeat thechniques, including the simple expedient of throwing material through the detectors too rapidly for detection. The most basic of design features--the use of separate detectors for metal, gamma-rays, and neutrons--resulted directly from the knowledge that an adversary can use large amounts of shielding to attempt to conceal material. Likewise, the arrangement of the gamma-ray detectors to eliminate regions of low sensitivity was dictated by the fact that an unobserved portal user is free to place or suspend material in any position in the portal volume where detection is least likely.

Integrating the three detector systems and the tamper-resistant features, with the often conflicting requirements of each, also imposed constraints on the design. For example, limited space available within the portal volume resulted in the combination of the lead background shielding and part of the polyethylene neutron moderator/reflector into one layer of lead-loaded polyethylene. The portal interior is another case. For the metal detector to function properly, the user had to be isolated by nonmetallic interior surfaces. These surfaces also had to be transparent to gamma-ray and neutron radiation, as well as have some tamper-indicating qualities. Walls, ceiling and floor fabricated of special boron-free fiberglass/epoxy with an overlay of Kevlar were used to simultaneously meet all these needs.

To minimize processing time per user, the gamma-ray, neutron, and metal detectors must operate simultaneously, but experiences with earlier versions of the portal indicated that cross-talk would be a problem. Electromagnetic shielding, careful routing of cables and wiring, and avoidance of current carrying loops partially solved these difficulties. However, to completely eliminate interference between the neutron and metal detector systems, we found it necessary in addition to actually interrupt both time and pulse counts in the neutron detector at the times when the metal detector shifts power from one transmit coil to the next.

Only occasionally did superposition of the three detector subsystems compromise the needs of one over another. Inclusion of background shielding in the doors could have caused sufficient flexure or position change to disrupt the metal detector, but omission of shielding from doors raises the background level inside the portal, which commensurately reduces gamma-ray detection sensitivity. Because the possible effect on the metal detector was worse, shielding was omitted from the doors.

THE GAMMA-RAY MONITOR

In order to avoid unnecessary development work, we chose to adapt commercially available SNM monitor components to our needs. Working together with a commercial manufacturer in a design study, we developed the system based on six large plastic slab scintillation detectors each of which is 3.8 cm thick and 160 cm by 20.8 cm in area. A second set of thicker detectors is also available for use in parameter studies. Placememt of the detectors in the booth is illustrated in Fig. 1. Background is reduced by the 2.5-cm-thick lead-loaded polyethylene covering the wall behind the detectors and the interior booth surfaces are designed to minimize attenuation of gamma-ray radiation. Detector signals are ganged and processed in a single signal-conditioning amplifier and single channel analyzer in our initial configuration. We anticipate possible advantages in grouping detectors into perhaps three separate groups and will examine this concept later.

The single channel analyzer (SCA) is used to define an energy window that we plan to set for optimum detection of shielded material. The basic approach used to optimize an energy window utilizes as a figure of merit the ratio S^2/B. Here, S is the net signal count in a convenient time interval and B is the experienced background count in the same interval. The ratio of S^2/B is used because we are searching for a signal S among statistical fluctuations that are sized proportionally to $\sqrt{B}$. Thus S^2/B clearly shows us when we have changed the detection sensitivity of a system. Examples of the utility of this approach are given by Fehlau.[13] In setting up the portal for initial operation, we have made measurements using a bare uranium source to determine appropriate system gain and SCA energy window.

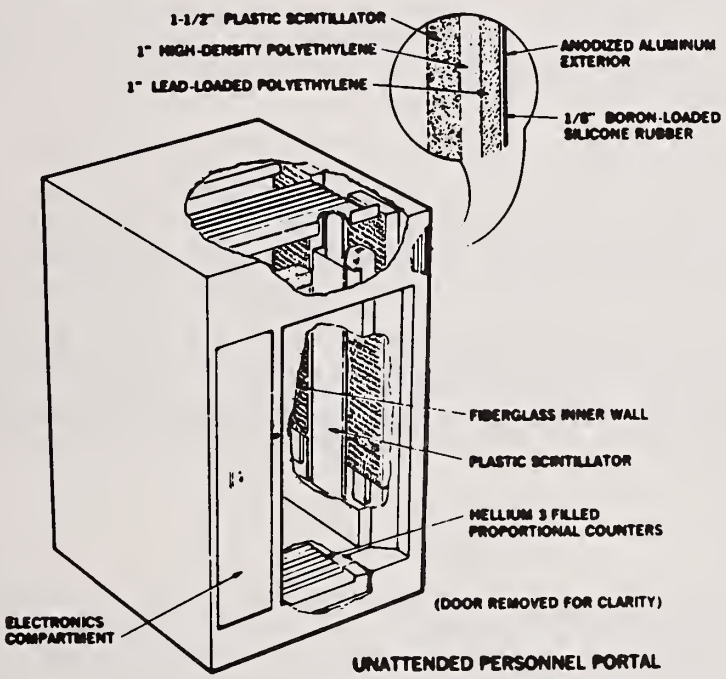

Fig. 1

The logic function for the gamma-ray system is based on a digital logic unit developed by a commercial manufacturer for possible application to domestic safeguards. The necessary logic unit modifications for this application were designed by Sandia who also carried out an extended debugging-development exercise on the software modifications to provide a workable unit. The basic logic approach is background following with a sliding interval signal algorithm[14] used to test against an alarm level derived from the background plus multiples of the standard deviation of the background. Many parameters of

---

[13] P. E. Fehlau, et al., "On-Site Inspection Procedures for SNM Doorway Monitors, U. S. Nuclear Regulatory Commission report, NUREG/CR-0598 or Los Alamos Scientific Laboratory report, LA-7646 (1979).

[14] W. H. Chambers, et al., "Portal Monitor For Diversion Safeguards, Los Alamos Scientific Laboratory report, LA-5681 (1974).

the logic module are variable and final values await completion of the evaluation. Initially we use an alarm level of 4 standard deviations above the background and a 5 second count time. Other features of the logic module include the usual high limit alarm that prevents subversion by artificially raising background intensity and a low limit alarm to detect subversion or equipment failure. Command controlled LED's self-test the gamma-ray system by producing a pulse of light in each scintillator slab and an associated signal in the electronics.

Our preliminary testing of the gamma-ray system using the energy window for unshielded uranium consisted of static measurements rather than actual pass-through tests. We measured the response of the gamma-ray system to bare uranium samples and found that in the worst position in the booth, we should easily detect a compact 1 g sample of HEU in 2 seconds. This compares very well with domestic walk-through systems that use a 10 g sample for their procurement specification. Our initial measurements on shielded uranium fuel plates were done at the geometrical center of the booth, which is neither the highest nor the lowest sensitivity position. We found we could easily detect the smallest (72 g) HEU plate inside of a 5 cm thickness of lead loaded polyethylene that is equivalent to 1 cm of solid lead on a mass basis.

Preliminary testing with plutonium used a 1 inch size PANI fuel plate. This is the only fuel that has plates less than 2 inches long and, from the data of Table II, has the minimum gamma-ray and neutron intensity. At the central position we found that the 1 inch plate was easily detectable in 2 seconds inside of 5 cm of lead shielding that had a mass of 11 kg. An additional borated polyethylene shield with a mass of 32 kg for neutron shielding further reduced the gamma-ray signal, but it could be detected using a 3 second count.

For reference, these results were obtained in a gamma-ray background of 17 microR/h measured outside the portal. Inside, we measured 7 microR/h. We expect these reported sensitivities to change with background intensity as well as other variables such as shielding thickness and position of the source in the portal. We plan to publish more detailed results later.

THE NEUTRON MONITOR

The approach taken for neutron monitoring is novel and arises out of the development of a monitor for very large vehicles by Caldwell.[15] The unique feature is that the volume to be monitored is located inside a 4π solid angle neutron detector. This is achieved by including in the booth walls an almost continuous surface of polyethylene material that serves as neutron moderator and reflector. Neutrons born in the booth enter the moderator and some fraction of the neutrons are returned to the booth interior as thermal neutrons. These thermal neutrons may undergo several reflections before being lost by capture in polyethylene or in one of two arrays of ^{3}He proportional counters within the polyethylene cavity. Detector placement is not critical in the design and Fig. 1 shows our arrangement where twelve 5-cm-diameter by 90-cm-long ^{3}He tubes are in the floor and twelve in the ceiling. The total efficiency of this neutron detector has been calculated by Atwater.[16] We have verified his calculations by using PANI and PUMH ZPPR fuel plates in the otherwise empty booth and we measured a total efficiency value of 0.048. We used standard NIM proportional counter electronics and a logic system similar to the gamma-ray system.

Our initial evaluation was conducted at an altitude of 1676 m, so our natural background, from cosmic ray events, is near the maximum that will be experienced. We found that a background suppression of about 4% was caused by occupancy and our 43 kg

---

[15] J. T. Caldwell, et al., "A Large Vehicle Portal Monitor for Perimeter Safeguards Application, 1st Annual ESARDA Symposium on Safeguards and Nuclear Material Management, Proceedings, ESARDA 10, p. 122 (1979).

[16] H. F. Atwater, Los Alamos Scientific Laboratory, unpublished data, 1978.

gamma-neutron shield caused an 8% reduction. The 32.5 g PANI plate in this shield was easily detectable and, in fact, we estimate that the total number of ^{3}He tubes may be reduced to perhaps as few as 4 from the present 24.

SUMMARY

To put this monitor in perspective, we point out that present practice in domestic safeguards utilizes rather inexpensive walk-through[14] or hand-held[17] monitors that detect gamma-ray radiation. Great reliance is placed on the inspector in attendance to properly operate the monitors and prevent unusual behavior by those being monitored. In contrast, the booth monitor we have described is a stand alone instrument capable of detecting gamma-ray radiation, neutron radiation, and shielding in a manner that is difficult to subvert. It employs novel techniques for neutron detection and its gamma-ray system represents what we believe is an optimal detector for monitoring a booth size volume. The effort spent in development of the booth monitor by many individuals at Sandia and LASL has benificial effects in developing expertise in the basic problems pertinent to SNM monitoring.

ACKNOWLEDGMENTS

The authors appreciate the efforts of the many individuals who participated in the design, construction, and testing of the SNM monitor described here. P. E. Fehlau would like to specifically thank two individuals at Sandia Laboratories who have been involved in bringing the passive detection system into being; Anthony E. Sill, who was responsible for the system logic and Donald J. Gould, who was responsible for the radiation detectors.

The work reported here was performed under the auspices of the U. S. Department of Energy.

---

[14] W. H. Chambers, (1974).

[17] W. E. Kunz, "Portable Monitor for SNM," Los Alamos Scientific Laboratory informal report, LASL-77-18 (1977).

An Active Neutron Technique for Detecting Attempted Special Nuclear Material Diversion*

by

G. W. SMITH and L. G. RICE, III
Sandia Laboratories, Albuquerque, New Mexico

ABSTRACT

The identification of special nuclear material (SNM) diversion is necessary if SNM inventory control is to be maintained at nuclear facilities. (Special nuclear materials are defined for this purpose as either ^{235}U or ^{239}Pu.) Direct SNM identification by the detection of natural decay or fission radiation is inadequate if the SNM is concealed by appropriate shielding. The active neutron interrogation technique described combines direct SNM identification by delayed fission neutron (DFN) detection with implied SNM detection by the identification of materials capable of shielding SNM from direct detection.

This technique is being developed for application in an unattended material/equipment portal through which items such as electronic instruments, packages, tool boxes, etc., will pass. The volume of this portal will be 41-cm wide, 53-cm high and 76-cm deep. The objective of this technique is to identify an attempted diversion of at least 20 grams of SNM with a measurement time of 30 seconds.

INTRODUCTION

Control of a special nuclear material (SNM) inventory implies the capability to identify attempted SNM diversion. (SNM is defined for this purpose as ^{235}U and ^{239}Pu, fissile isotopes of Uranium and Plutonium.) This control is presently based on the detection of radiation from either natural radioactive decay or fission. The threat of SNM concealment by radiation shielding materials seriously limits all methods currently used for this purpose. For this reason, efforts, under the auspices of DOE, are underway to develop a method to detect sophisticated attempts to conceal and divert SNM.

The development of an unattended material or equipment pass-through is directed at the inventory control requirements envisioned for fast-critical-reactor facilities. The pass-through or portal is designed to accommodate electronic instruments, tool boxes, packages, etc., and will be nominally 41-cm wide, 53-cm high and 76-cm deep. A threshold sensitivity of 20 grams of SNM, which is expected to be the smallest individual quantity, has been selected as the design goal. A measurement time of approximately 30 seconds has been chosen as consistent with personnel monitoring in progress concurrently with the instrument pass-through measurement.

*This work is supported by the U. S. Department of Energy.

BACKGROUND

Several considerations must be made about the problem of identifying an attempt to divert SNM by concealment. The first deals with the methods of identification.

Radioactive decay of SNM results in relatively soft gamma radiation that is easily attenuated by several centimeters of high Z material such as iron or lead. Fission produces energetic, penetrating (neutron and gamma ray), prompt radiation that is difficult to attenuate. Delayed, penetrating radiation from fission products is both less abundant and less energetic, increasing the attenuation effect of shielding material. Fission can be induced in SNM by neutrons, with a probability that varies as a function of the energy of the neutron, and the unique property of fissile material is its affinity for slow neutron fission.

Fission occurs spontaneously at significant rates in a few non-fissile isotopes, one of which (^{240}Pu) is found in concentrations of at least a few percent with ^{239}Pu. This substantial radiation forms the basis for some passive methods of assaying and/or detecting fissile plutonium (^{239}Pu). Unfortunately, no such spontaneously fissioning uranium isotope is found with ^{235}U. For detection or assay purposes using fission radiation, ^{235}U must be induced by external means to fission and produce radiation that will lead to its identification. Some existing assay and detection methods for ^{235}U are based on active neutron interrogation.

Of the two radiations, gamma rays from radioactive decay or gamma rays and neutrons from fission, the more energetic radiations from fission provides the greater possibility of SNM detection in the presence of shielding. Several techniques have been developed for non-destructive assay of SNM based on identifying fission radiation. Four such assay methods were selected for evaluation as techniques for direct detection of concealed SNM. Of these four techniques, coincidence detection[1] and correlation counting[2] both imply the occurrence of a fission event based on timing and multiplicity of prompt fission radiation detection. Two gross count methods identify fission neutrons by time discrimination (DFN[3]-Delayed Fission Neutron) or time and energy discrimination (PFN[4]-Prompt Fission Neutron).

All of these methods were examined either theoretically or experimentally or both and in each case found to be prohibitively vulnerable to shielding.[5] Given the internal volume of the instrument portal and the shield material volume that can be accommodated, each of the direct detection methods examined must be disqualified as a stand alone method of identifying SNM if the SNM is substantially shielded.

---

[1] T. J. Atwell, J. E. Foley, and L. V. East, "NDA of HTGR Fuel Using the Random Driver", Nuclear Materials Management, Fall 1974, pg. 171.

[2] Edward J. Dowdy, Carl N. Henry, Arnold A. Robba, John C. Pratt, "New Neutron Correlation Measurement Techniques for Special Nuclear Material Assay and Accountability", Los Alamos Scientific Laboratory-Report LA-UR-78-690, Submitted to: IAEA (IAEA-SM-231/69).

[3] Howard O. Menlove and Thomas W. Crane, "A ^{252}Cf Based Nondestructive Assay System for Fissile Material", Nuclear Instruments and Methods 152 (1978), pg. 549.

[4] Gerald W. Smith, "Status Report on the Development of a Prompt Fission Neutron Uranium Borehole Logging Technique", Sandia Laboratory - Report SAND77-0336, 1977.

[5] Gerald W. Smith and Lucien G. Rice, "Status Report on the Development of an Active Neutron Technique for Detecting Special Nuclear Material Diversion", Sandia Laboratory - Report SAND79-0897, 1979.

PROPOSED METHOD

The prospect of a single detection technique directly identifying SNM is not practical given the large volume of the portal available for shielding. However, a direct SNM detection measurement for unshielded or lightly shielded SNM combined with a measurement to identify shielding material capable of shielding SNM from direct detection will be described The direct SNM measurement is intended to force the use of shield material that can be identified and distinguished from legitimate materials.

Gamma rays are effectively attenuated by dense material such as iron and lead, which for the most part must be considered legitimate material and passed. Neutrons are best attenuated by a shielding material with a large concentration of hydrogen for moderation and a neutron absorber such as boron, cadmium, lithium, etc., for absorbing the moderated neutrons. A hydrogenous material such as polyethylene, paraffin, or water containing a small amount of neutron absorber could constitute effective shielding for concealing SNM against neutron interrogation and fission neutron detection. This is a material that could be administratively prohibited from routine passages through the portal, if it can be uniquely identified. In order to insure the exclusion of such material, a measurement of the perturbing effect that a thermal neutron absorber will have on a thermal neutron population can be used to identify its presence.

As seen in Figure 1, the effectiveness of a neutron absorber (increased absorption) increases as the energy of the neutron decreases. Through moderation, a neutron will reach equilibrium with its surroundings, and by convention this equilibrium condition has been established at 300°K with the resulting energy of equilibrium neutrons being 0.025 eV.

The most sensitive measurement for the perturbing effect produced by the presence of a neutron absorber would be made with a population of neutrons most affected, neutrons at equilibrium (thermal) energy.

In a steady state neutron environment, neutrons from an isotopic source, energies ranging from thermal equilibrium to generation energy would coexist. In a pulsed neutron environment, pulse timing and rate can be selected such that all energetic neutrons will be moderated to thermal equilibrium energy and survive exclusively as thermal neutrons for a time governed by the absorption and diffusion properties of the materials defining the portal test volume. By selecting materials that minimize absorption and diffusion, the mean lifetime of thermal neutrons will be maximized, increasing sensitivity to the presence of a neutron absorber.

Thermal Die-Away Perturbation

A pulsed neutron source creates mono-energetic neutrons that are moderated by the scattering properties of the materials they encounter. The time histories of fast, intermediate, and thermal neutron groups are shown in Figure 2.

The die-away of thermal neutrons is described by the exponential expression

$$n(t) = n(o)e^{-\alpha t}$$

where $n(t)$ is the instantaneous thermal neutron rate and $n(o)$ is the initial rate. The decay constant α is a function of absorption and diffusion as follows

$$\alpha = \nu\Sigma_a + \nu DB^2$$

where ν is the thermal neutron velocity, Σ_a is the macroscopic absorptiion coefficient, D is the diffusion coefficient and B^2 is the geometric buckling. The thermal neutron mean lifetime is

$$T = \frac{1}{\alpha} = \frac{1}{\nu\Sigma_a + \nu DB^2}$$

which illustrates the mean lifetime dependence on the two loss mechanisms of absorption and diffusion. If the materials and geometry are such that the geometric buckling is zero, the only thermal neutron losses would be to absorption and the mean lifetime would be maximized.

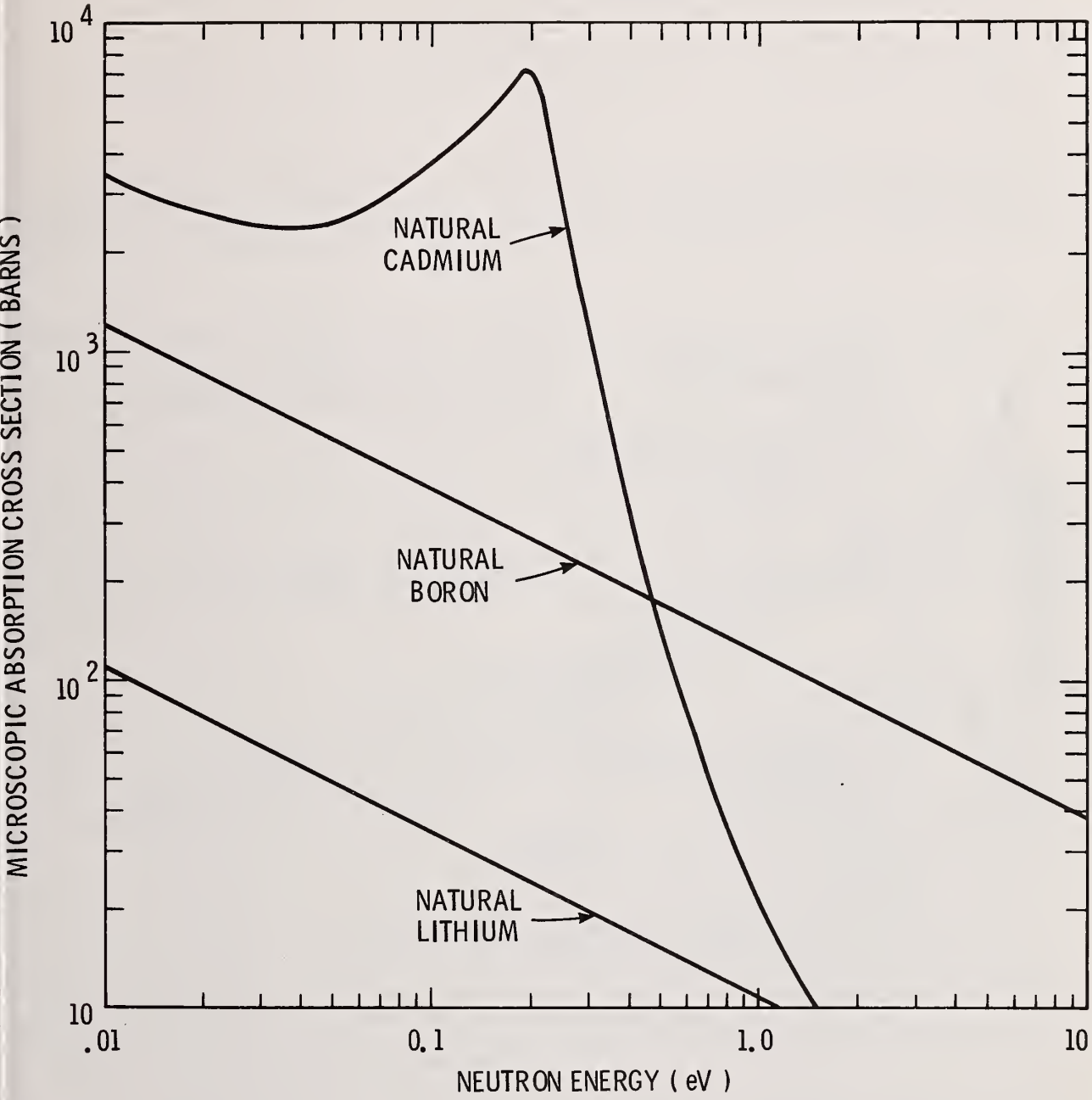

FIGURE 1. NEUTRON ABSORBER CROSS SECTIONS

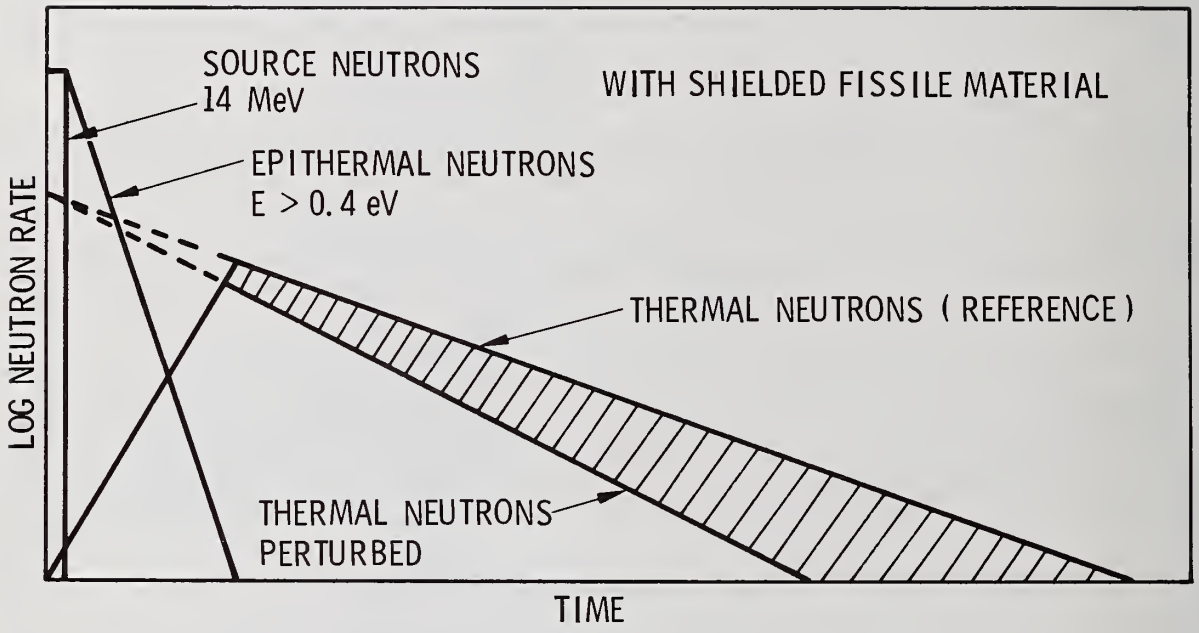

FIGURE 2. NEUTRON TIME HISTORIES

However, in most finite systems diffusion losses to buckling will be a factor depending on materials. For analysis, those losses can be expressed as absorption by an effective macroscopic absorption cross section for the portal which is defined as

$$\Sigma_{eff} = \Sigma_a + DB^2$$

and the thermal neutron mean lifetime of the portal will be

$$T = \frac{1}{\nu\Sigma_{eff}} .$$

Material that will best define the portal test cavity and reveal the presence of absorbing material in a neutron shield will be material that effectively moderates fast neutrons and, of those thermalized neutrons created, captures very few. A figure of merit for materials suitable to this application is the moderation ratio

$$MR = \xi\bar{\Sigma}_s/\Sigma_a$$

where ξ = average logarithmic energy decrement per collision
$\bar{\Sigma}_s$ = average macroscopic scattering cross section (0.025 eV $\leq$ energy $\leq$ 0.1 MeV
Σ_a = macroscopic absorption cross section for thermal neutrons.

The product $\xi\bar{\Sigma}_s$ is called the slowing down power. While large moderation ratio is a good indication of properties desirable for this application, a small absorption cross section must be considered most important. Table 1 is a list of these properties for good neutron moderating materials. Deuterated materials are by far superior because they combine very small absorption with large slowing down power. Unfortunately, they are very expensive and will not be considered at this point in the system development. Carbon has a very small absorption cross section (most desirable) but poor slowing down power. Beryllium is possibly suitable but also expensive. Polyethylene has very large slowing down power but its absorption cross section is large.

No single material, other than deuterated materials, has all of the desired properties for this application, but a reasonable set of properties can be developed by a combination of carbon and polyethylene. With carbon slabs backed by polyethylene lining the portal cavity, the high energy neutrons will be efficiently slowed by the bulk polyethylene and the thermal neutrons that find their way into the cavity will have a long die-away time due to the very small absorption cross section of carbon.

Another factor to be considered is the effective reflection coefficient (albedo) which is an indication of diffusion losses. Albedos of the carbon and polyethylene as a function of thickness are shown in Figure 3. Thermal neutrons that diffuse through the carbon are likely to be absorbed, with an undesirable increase in the effective absorption of the cavity. This diffusion loss can be reduced by a carbon slab that is sufficiently thick to maintain a large albedo within the carbon (perhaps 10 to 15 cm). A further increase in carbon slab thickness will tend to decrease the net thermal neutron population in the cavity because fast neutrons are being moderated further away from the volume and an increase in carbon albedo will tend to reflect these neutrons away from the cavity. A 15 cm thickness of carbon was selected for testing. Figure 4 shows an experimental portal designed for evaluation of this measurement technique.

The neutron source is a DT generator (14 MeV) that produces greater than 10^6 neutrons per pulse and can be operated at pulse rates up to 100 pulses per second. The thermal neutron detector is a single ^{3}He proportional counting tube, 1-cm in diameter and 25-cm active length with a ^{3}He gas pressure of 10 ATM. The delayed fission neutron detector consists of 30 ^{3}He proportional counting (PC) tubes in an array outside the carbon cavity liner on three of the side walls. Each PC tube is 5-cm in diameter and 61-cm active length with a gas pressure of 4 ATM. Figure 5, measured time histories for different portal contents, shows the thermal neutron die-away change resulting from absorption losses to two shield material blocks of 32% borated polyethylene at 7.5-cm and 12.5-cm thickness. These changes are based on thermal neutron mean lifetime change. Either of these shields would be readily distinguished from the empty cavity reference.

TABLE 1

NEUTRON MODERATION PROPERTIES OF VARIOUS MATERIALS

MODERATOR	SLOWING DOWN POWER (CM^{-1}) $0.025eV \leq$ ENERGY ≤ 0.1 MeV	ABSORPTION CROSS SECTION Σ_a (CM^{-1}) E = 0.025 eV	MODERATION RATIO
HEAVY WATER * D_2O	0.18	0.000031	5670
DEUTERATED POLYETHYLENE ' CD_2	.21	0.00018	1130
CARBON* C	0.060	0.00031	192
BERYLLIUM * Be	0.158	0.0011	143
WATER * H_2O	1.35	0.019	71
POLYETHYLENE ' CH_2	1.65	0.026	64

* "NEUTRON PHYSICS ", K. H. BECKURTS, KWIRTZ

' CALCULATED VALUES

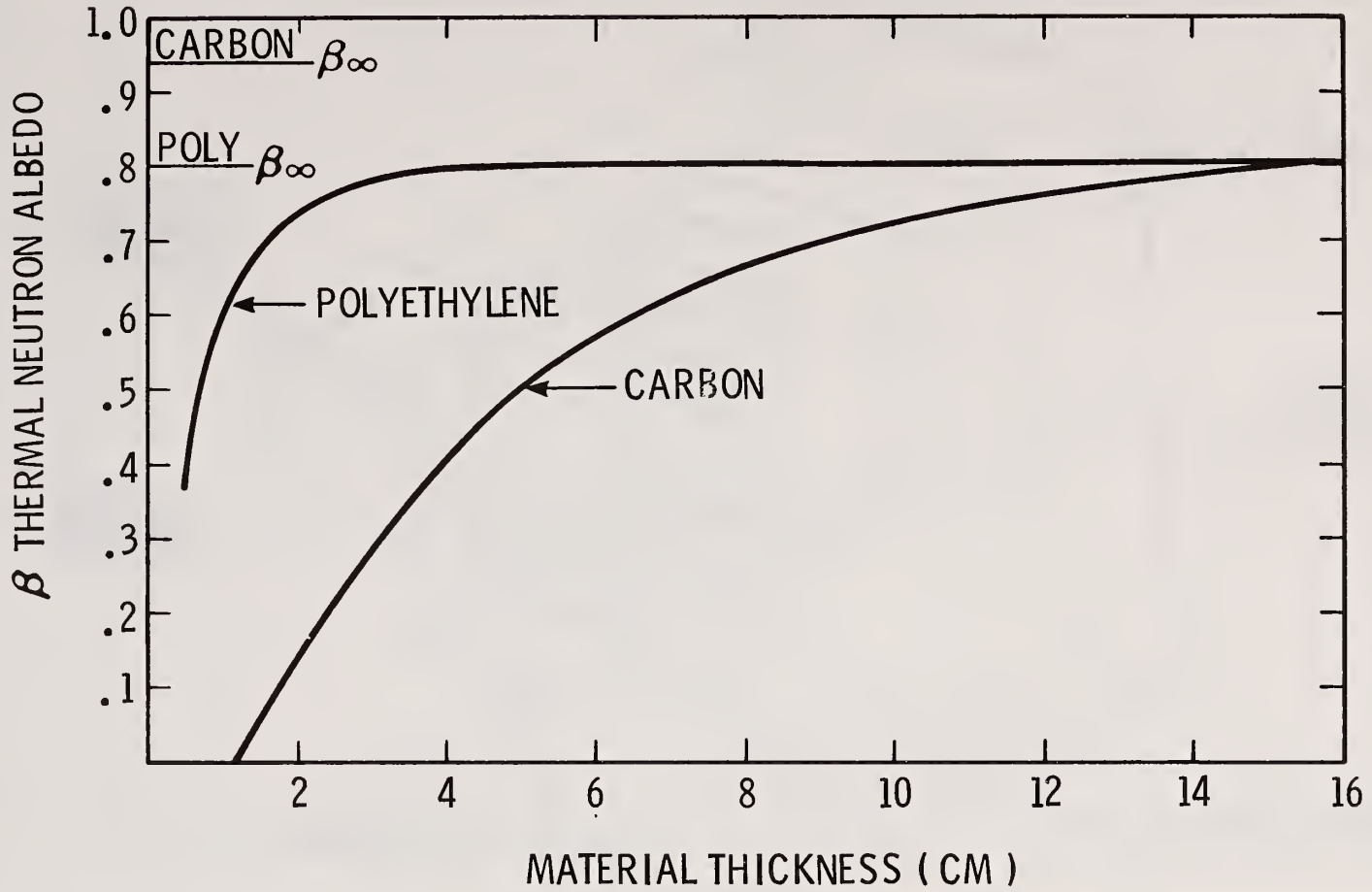

FIGURE 3. THERMAL NEUTRON ALBEDOS

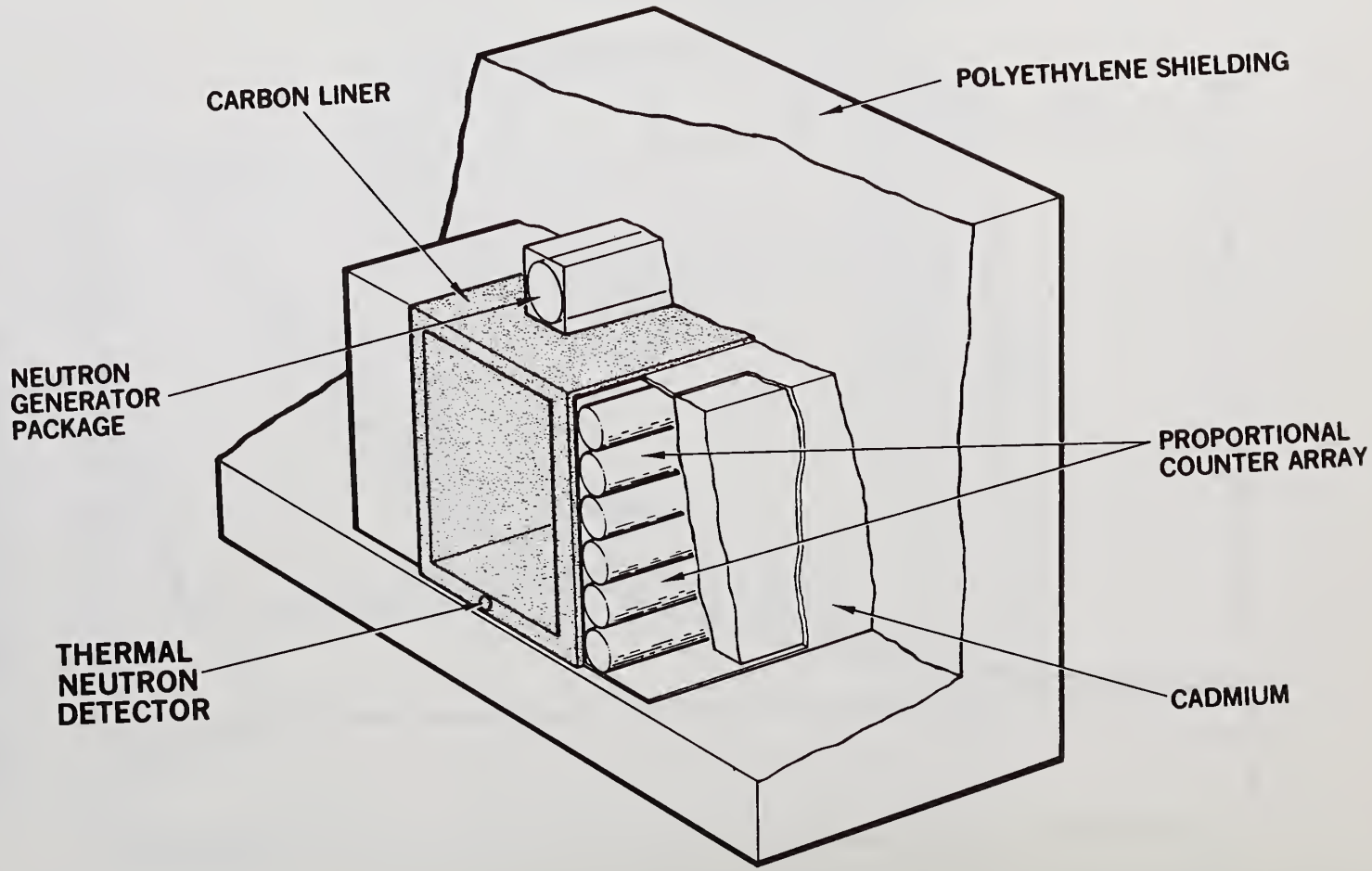

FIGURE 4. INSTRUMENT PORTAL TEST FACILITY

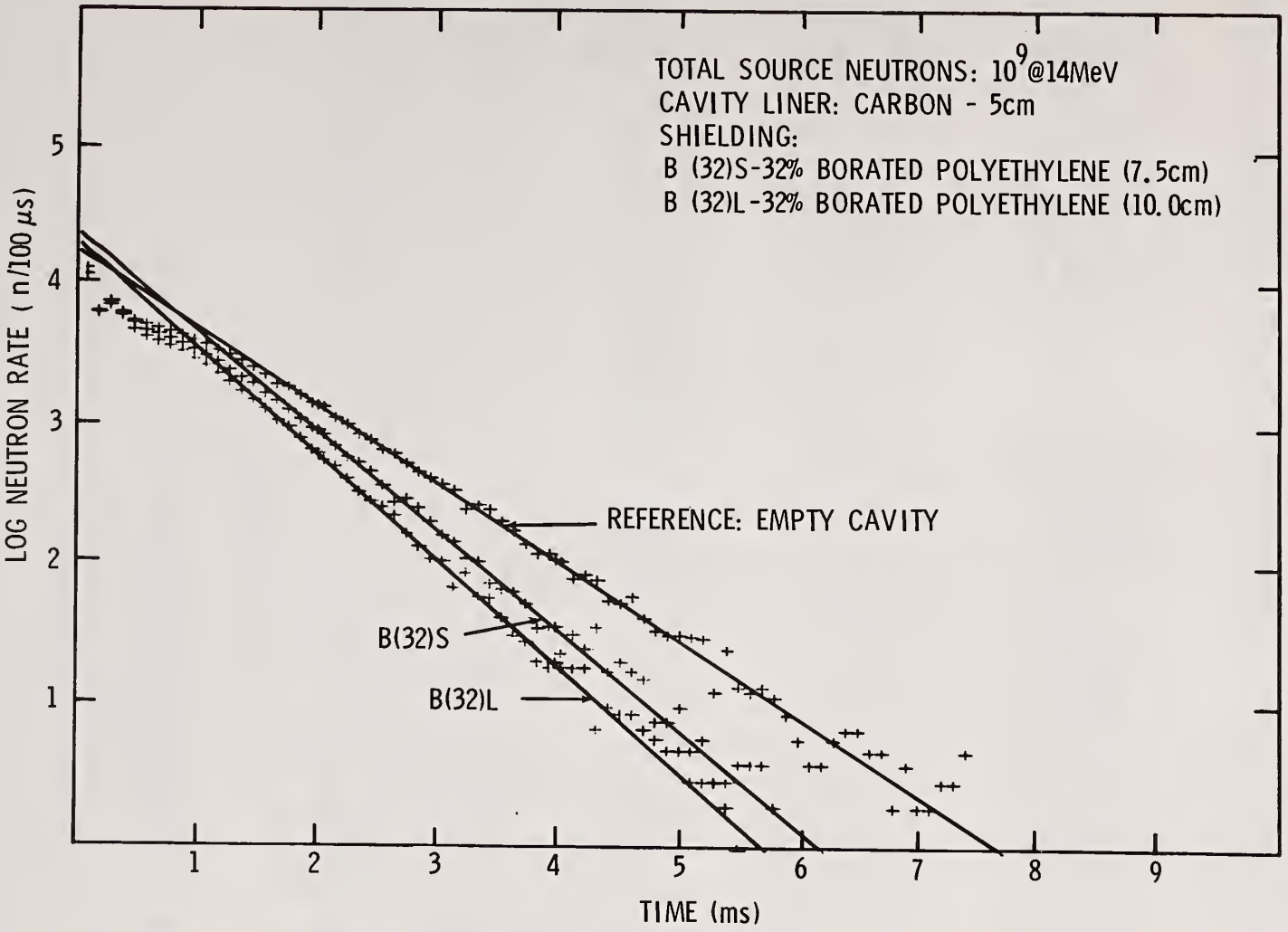

FIGURE 5. TIME HISTORIES

Direct SNM Detection

For unshielded or lightly shielded SNM, direct identification of the SNM is accomplish by detecting delayed fission neutrons resulting from fissions produced by the source neutron Prompt fission neutron (PFN) detection as described in reference 5 was initially considered for direct SNM detection but found to be less suitable than DFN because of shielding vulnerability. The total number of delayed neutrons (N_T) from a ^{235}U sample under interrogatio is the product of the number of fissions produced (F) and the total number of delayed neutrons per fission ($\frac{N}{F}$).

$$N_T = F \times \frac{N}{F}$$

For the portal configuration described in Figure 4, the fission production efficiency (f), fissions per gram of SNM and per source neutron as a function of shielding is given in Figure 6. The fission production efficiency is derived from Monte Carlo analysis of the portal. The Monte Carlo code (MORSE) is a three dimension, time dependent, neutron transport code. The total number of fissions produced is

$$F = f \times m \times N_s$$

where (m) is the mass of ^{235}U and (N_s) is the total source neutrons. The number of delayed neutrons that are detected by the neutron detector is directly proportional to the delayed neutron fraction transmitted through the shield (ε_s) shown in Figure 7. The absolute efficiency of the delayed neutron detector array is (ε_{PC}). The number of delayed neutrons detected also depends on the time window available for counting (T), the time available for counting normalized to the total time required to sample all delayed neutrons. The number of delayed neutrons counted is

$$N_D = \varepsilon_{PC} \times \varepsilon_s \times T \times N_T .$$

If all source neutrons were generated in a single pulse and sufficient time after the pulse was used for counting, essentially all delayed neutrons generated are available for detection and counting and the time fraction (T) approaches unity. However, for the case of a rapid pulse generator, the optimum time window for sampling delayed neutrons is a function of the pulse rate.

The time required for a population of source neutrons to moderate and be captured or diffuse from the system is approximately 10 milliseconds. Therefore, the generator cannot be operated at a pulse rate greater than 100 pulses per second. Based on estimates of the total source neutron requirement, not less than 10^3 pulses of the neutron source will be required for each measurement which must be made in 30 seconds or less. The minimum rate at which the source can operate and generate 10^3 pulses in 30 seconds is 33 pulses per second. Figure 8 shows the dependence of the time fraction (T) on neutron source pulse rate. From Figure 8, the optimum source rate for maximum sampling interval is 40 pulses per second which permits the detector to look for 45% of the delayed neutrons generated.

The final expression for the number of delayed neutrons detected is

$$N_D = \varepsilon_{PC} \times T \times \frac{N}{F} \times \varepsilon_s \times f \times N_s \times m$$

where ε = 0.036 (absolute delayed neutron efficiency)
T = 0.45 DFN measurement time fraction
$\frac{N}{F}$ = 0.0165 $\frac{\text{delayed neutrons}}{\text{fission}}$ (^{235}U)
ε_s = delayed neutron fraction transmitted through shielding
f = fission production efficiency
m = ^{235}U mass
N_s = Total source neutrons.

From this model, threshold mass for direct detection of ^{235}U are shown in Figure 9 as a function of background for various shielding conditions.

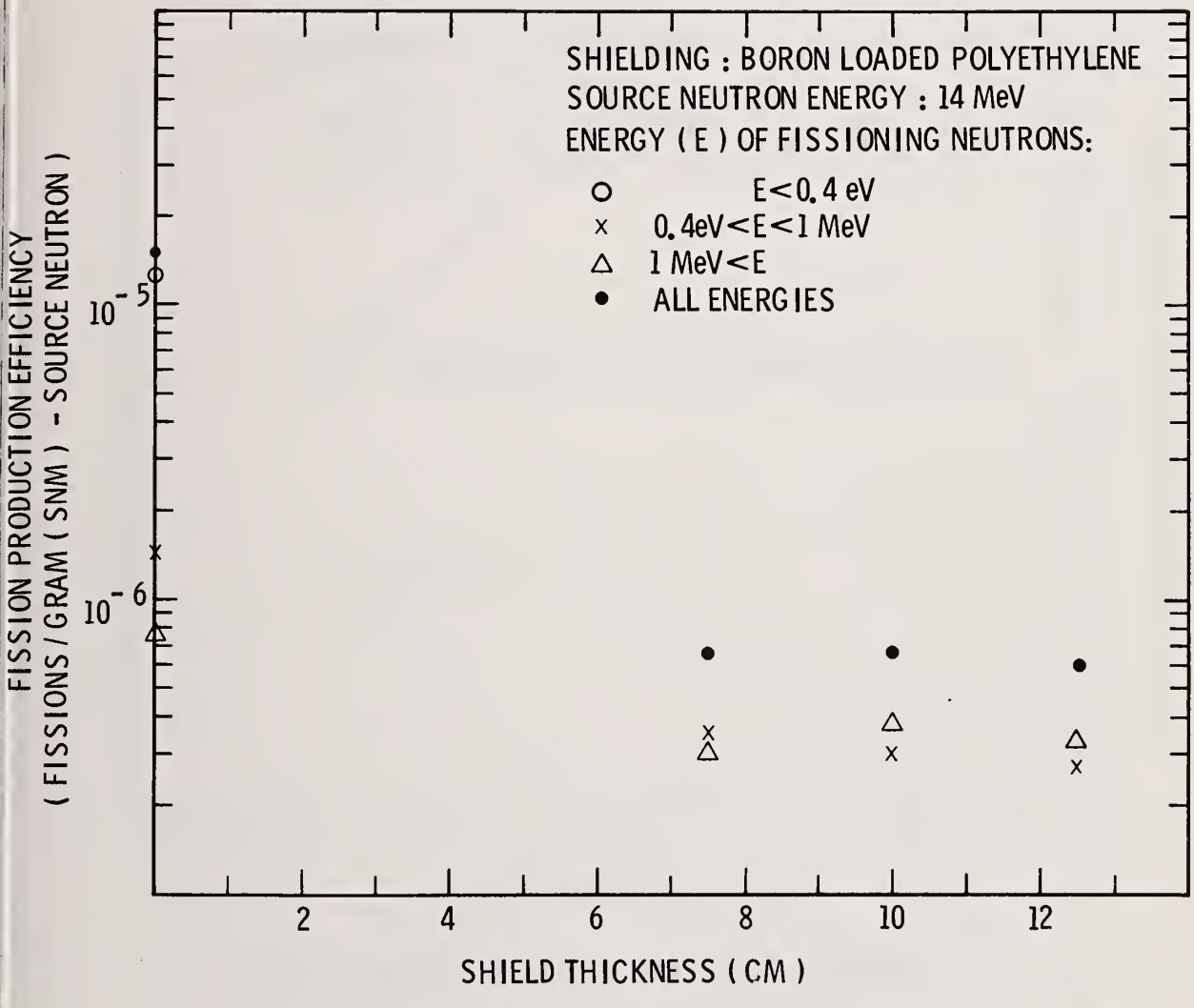

FIGURE 6. INDUCED FISSIONS IN SNM

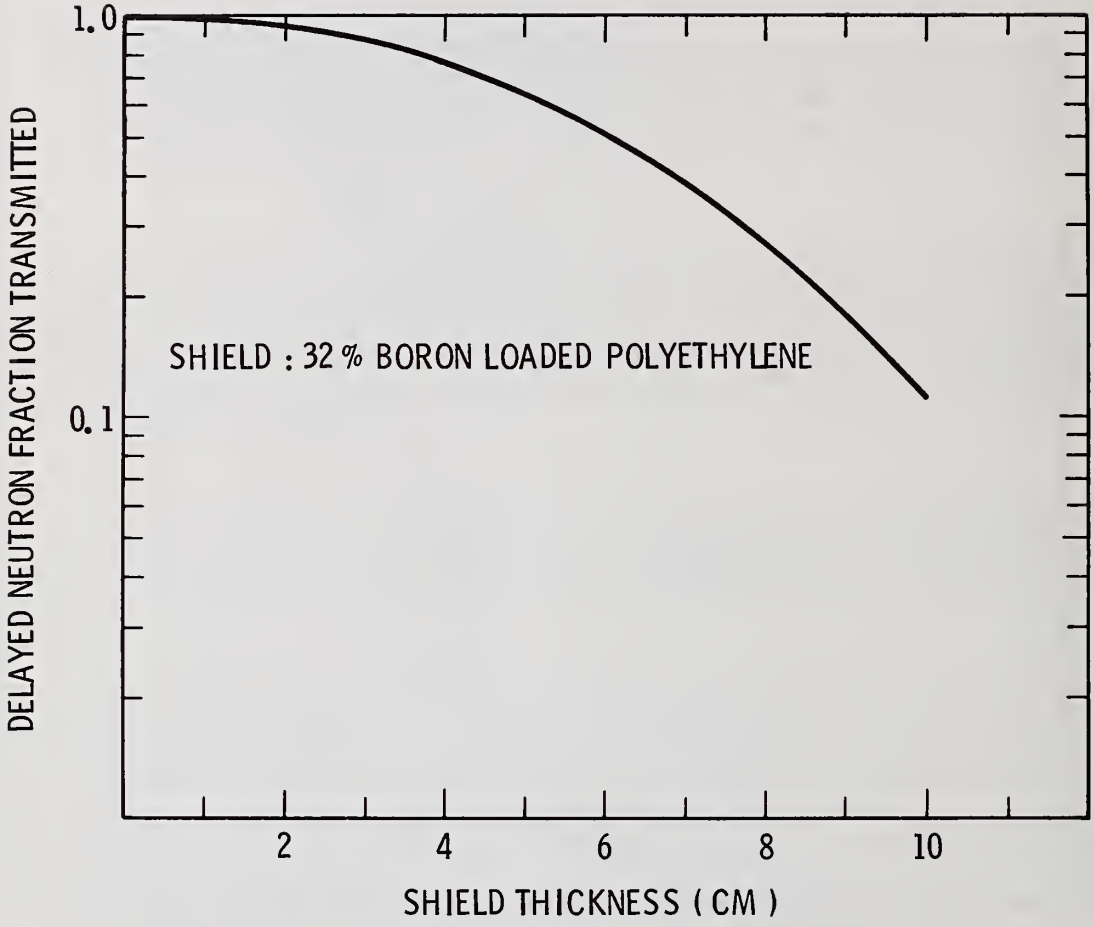

FIGURE 7. DELAYED NEUTRON SHIELD LOSSES

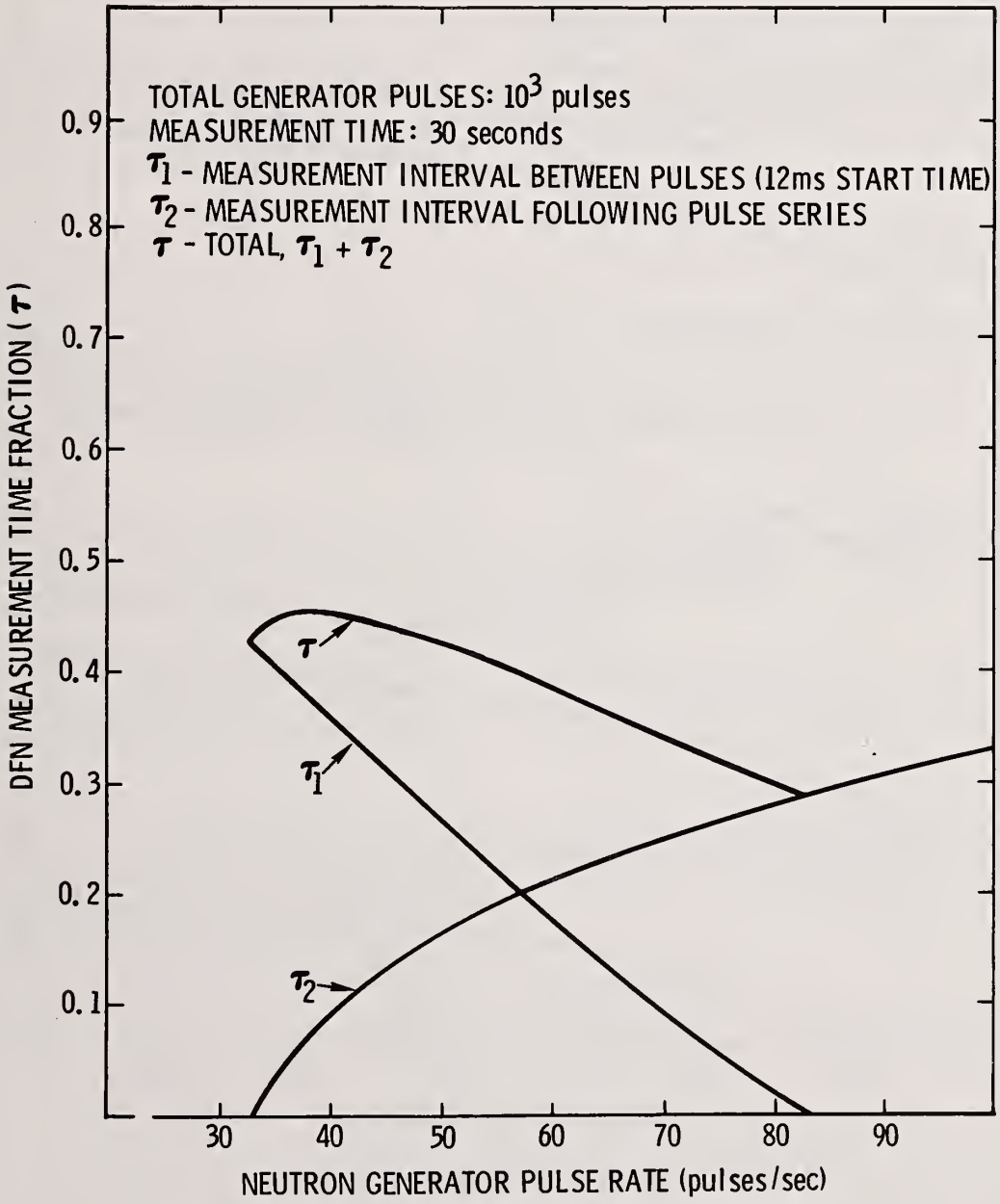

FIGURE 8. DFN MEASUREMENT TIME FRACTION

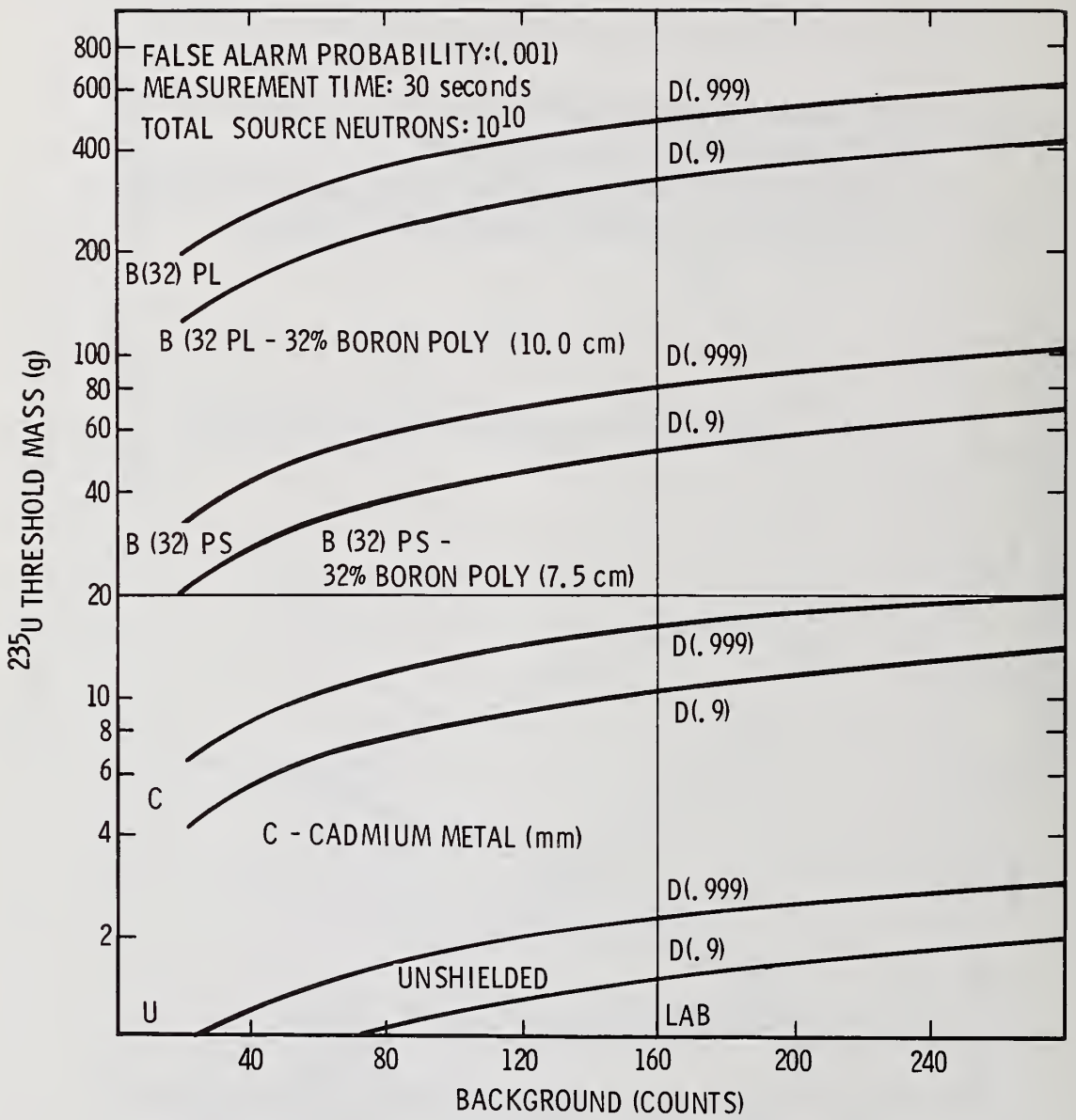

FIGURE 9. DFN DETECTION THRESHOLDS

A critical parameter for threshold estimates is the background and the acceptable false alarm criteria. Laboratory background for these measurements was 160 counts. For unattended applications such as this portal is intended, a very low false alarm rate is desirable. For the purpose of this evaluation, the false alarm probability has been chosen to be 0.001, one false alarm every 1000 measurements. Each shielding configuration in Figure 9 shows two detection thresholds, one representing a detection probability of 0.999 and the other a detection probability of 0.9.

The SNM thresholds shown in Figures 9 and 10 indicate how good the thermal neutron die-away perturbation measurements for shielding must be in order to prevent 20 grams of ^{235}U from being successfully concealed. For the laboratory background of 160 counts unshielded ^{235}U in quantities of a few grams could be reliably detected. If the SNM were concealed in a thin cadmium envelope essentially all thermal fissions are eliminated and the threshold is degraded nearly an order of magnitude. However, even with a cadmium shield 20 grams is detectable.

For more substantial shielding in the form of borated polyethylene, Figure 9, the detection threshold is seriously compromised. Borated polyethylene in the amounts shown must be identified by thermal neutron die-away perturbation if detection is to succeed.

Figure 10 shows effects on detection threshold produced by pure polyethylene. The pure polyethylene shields moderate neutrons sufficiently so that penetration of the carbon cavity liner is effectively reduced and fewer neutrons reach the neutron detector array. The fact that pure polyethylene contains no significant thermal neutron absorber severely limits the effectiveness that can be expected of the thermal die-away perturbation measurement.

Measured mean lifetimes of the thermal neutron die-away for these various shields are shown in Figure 11 on the left of the time axis. On the right are die-away times for the empty cavity and legitimate items for passage through the portal.

CONCLUSION

From Figures 9, 10 and 11, it is clear that the direct DFN detection of 20 grams of ^{235}U is not possible for some shielding conditions. Furthermore, not all of the successful shield configurations are distinguishable by thermal neutron die-away perturbation from legitimate items requiring passage.

A number of options that will improve the detection threshold are available for consideration. Generate more source neutrons, reduce measurement background, and improve DFN detector efficiency, are possibilities obvious in the delayed neutron production equation. For shield identification, there is the possibility of further material identification by spectral signatures of thermal neutron capture gamma radiation. This possibility is currently being examined.

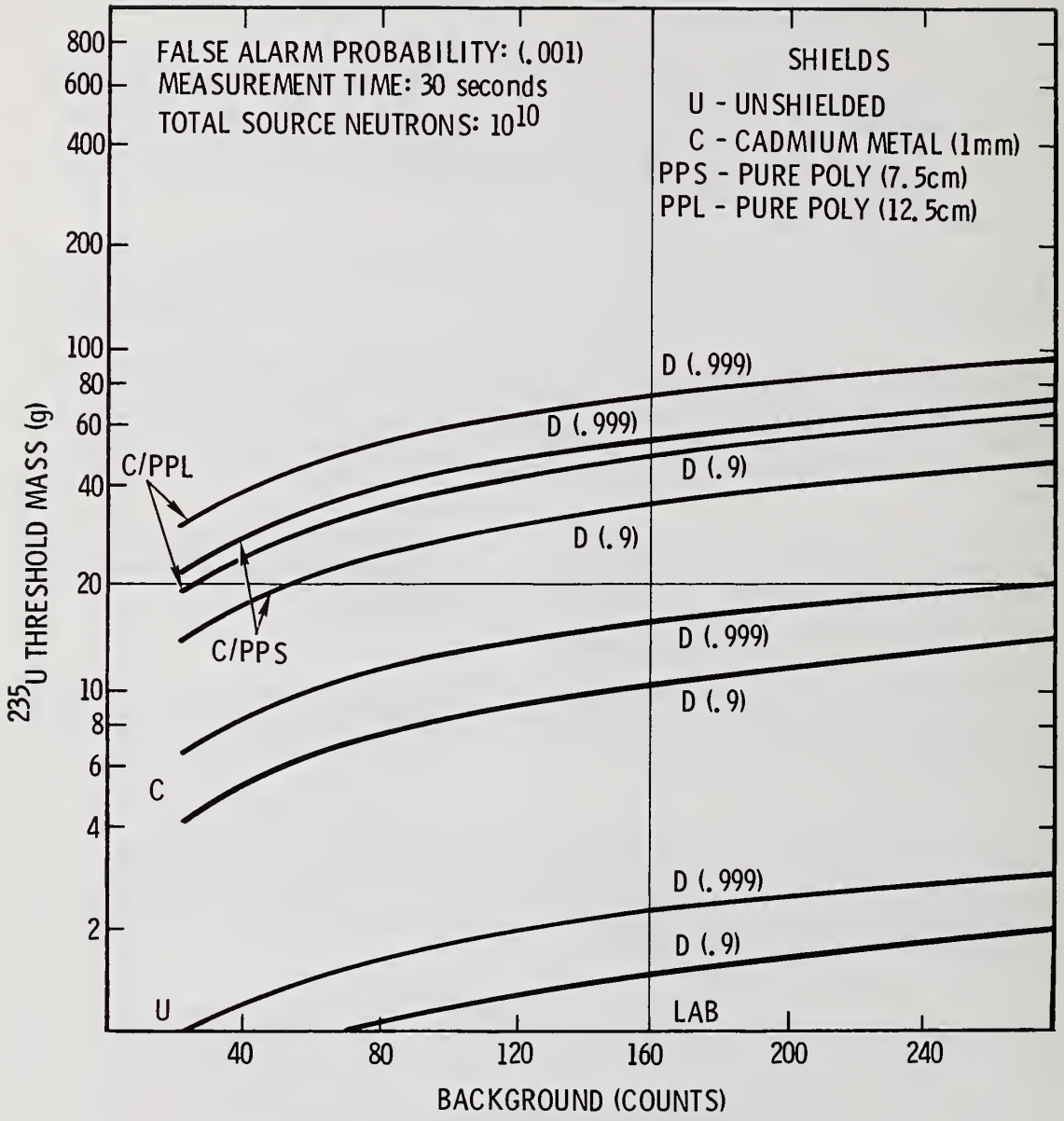

FIGURE 10. DFN DETECTION THRESHOLDS

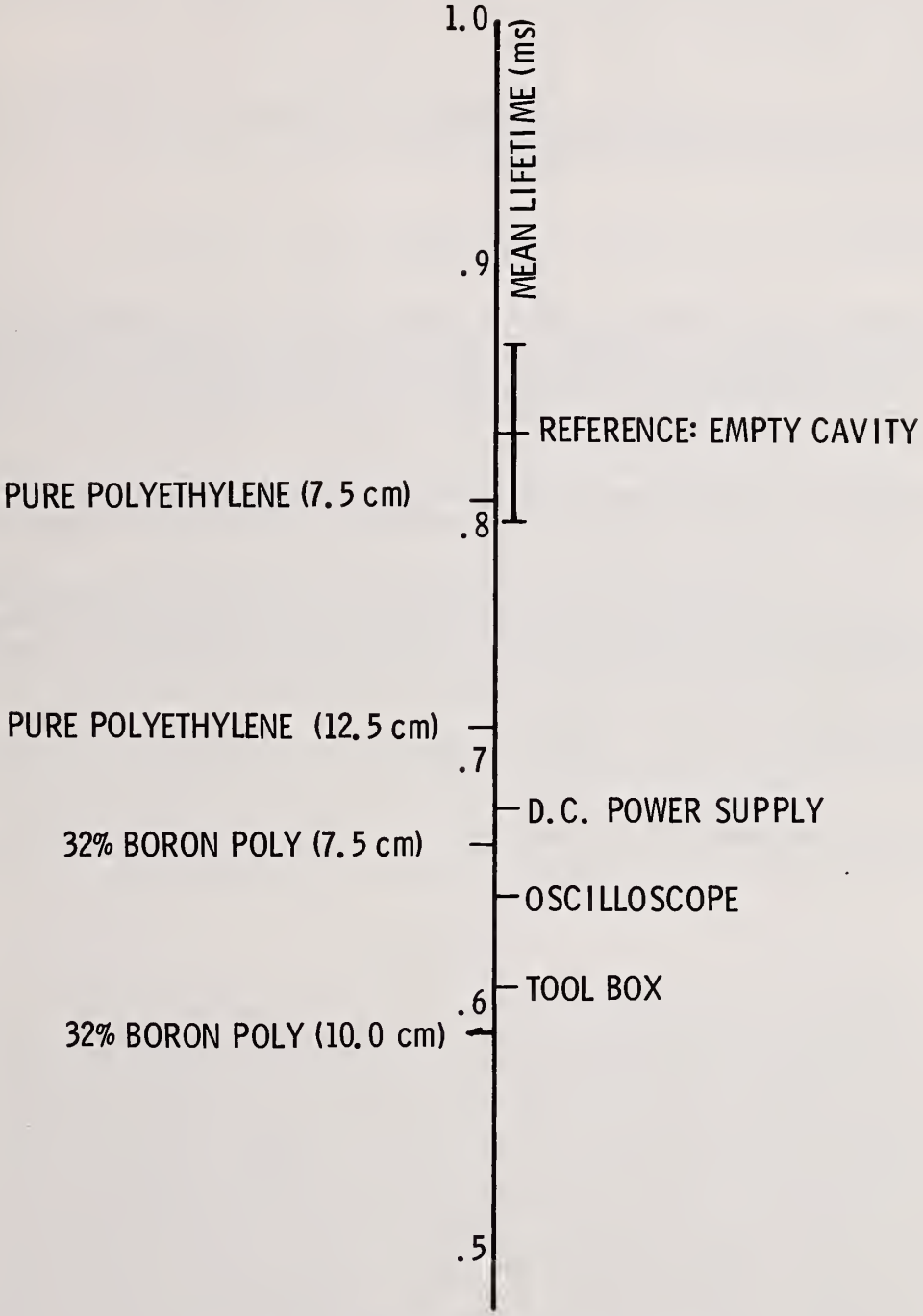

FIGURE 11. MEAN THERMAL LIFETIMES

Discussion:

Weinstock (BNL):
Couldn't you use a transmission method to measure the presence of shielding with a thermal or a fast neutron beam through the cavity? It would, I think, be a lot simplier than a die-away measurement.

Smith (Sandia):
We have considered the possibility of making shadow graphs. I can say at this point that we have not pursued that possibility, but considering the difficulties we have encountered, we may very well look at other options.

Nilson (Exxon Nuclear):
Is it necessary to have an accelerator, or could you use a CF source?

Smith:
This technique could be easily used with an isotopic source. The reason we went to a neutron generator was twofold: it can be turned off and we don't have the continuous shielding problem associated with an isotopic source. Plus, we can generate neutrons so that we have, at a measurement time, only a thermal neutron population. We don't have a combination of all energy neutrons from generated energy down to thermal.

Nilson:
I am thinking about the problems of having an accelerator in a commercial fuel facility. Do you think that a plant like that could service and maintain an accelerator?

Smith:
That's true. It's certainly not as reliable as an isotopic source. At this point we are trying to determine the characteristics of this kind of source option and we have chosen the path with the accelerator because of the reasons I've mentioned. It may very well turn out that there are more suitable options.

Persiani (ANL):
Aren't you talking of a Kayman type of DT source?

Smith:
Right, it is a DT generator and accelerator.

In-situ Verification Techniques for Fast Critical Assembly Cores

by

S.B. Brumbach and P.I. Amundson
Argonne National Laboratory, Idaho Falls, Idaho

C.T. Roche
Argonne National Laboratory, Argonne, Ilinois

ABSTRACT

Active and passive autoradiographic techniques were used to obtain piece counts of fuel plates in fast critical assembly drawers and to verify the assembly loading pattern. Active autoradiography using prompt-fission and fission-product radiation was more successful with uranium fuel while passive autoradiography was more successful with plutonium fuel. A source multiplication technique was used to measure changes in reactivity when small quantities (2-2.5 kg) of fissile material were removed from a subcritical reference core of the Zero Power Plutonium Reactor. Efforts to compensate for the loss of reactivity by substituting polyethylene for fuel were largely unsuccessful. Some compensation was achieved by replacing U-238 with polyethylene. The sensitivity for detection of partially compensated fuel removed from minimum worth regions was approximately 2.5 kg (fissile) for a core containing 2600 kg (fissile). Substitution of polyethylene was detected with a spectral index which was the ratio of the rate of the In-115 (n,γ) reaction to the rate of the In-115 (n,n') reaction. This spectral index was sensitive to the presence of an 0.64-cm-thick, 5.08-cm-high polyethylene column 10-15 cm away from the indium foil. The reactivity worth of Pu-239 was also obtained as a function of location in the reactor core with the use of an inverse kinetics technique. Reactivity worths for Pu-239 varied from a maximum of 58.67 Ih/kg near the core center to a minimum of 14.86 Ih/kg at the core edge.

KEYWORDS: Nondestructive assay, plutonium, uranium, reactivity, autoradiography, spectral index, fast critical assemblies.

INTRODUCTION

Fast critical assemblies such as the Zero Power Plutonium Reactor (ZPPR) facility require large inventories of plutonium and enriched-uranium fuels. The ZPPR fuel is primarily in the form of thin metal or alloy plates (0.066-0.64-cm-thick, 5.08-cm high, and from 2.54 cm to 20.3 cm long) and small metal-oxide-containing rods (0.95 cm diam by 7.62-15.24 cm long). Uranium enrichments vary between 16% and 93% U-235, and plutonium concentrations vary from 15% to 99%. Fissile materials in these sizes and purities present an attractive target to a potential diverter. Because of this diversion potential, it is important that effective safeguards be implemented at fast critical assembly facilities. The subject of critical facility safeguards has been recently reviewed.[1,2] Fuel elements at ZPPR are normally located in the reactor itself or are stored in canisters in a vault. Most of the time, a large majority of the fuel is in the reactor. The reactor has two halves, each of which consists of a square array of matrix tubes. The fuel is contained in drawers, 5.08 cm square by up to 91.4-cm long. The drawers also contain structural, coolant, and fertile materials. A typical drawer includes a core segment containing either one or two columns of fuel plates (~ 0.5 kg or 1.0 kg of fissile material) and a second segment containing typical axial blanket materials. The drawers are inserted into the matrix tubes, and the halves are brought together to form the final reactor configuration.

Because of the large number of fuel plates, and because the plates are normally located in the reactor, verification of the fissile material inventory of the facility is time-consuming. If individual plates, or even whole drawers are removed from the reactor for

verification, the efficiency of the experimental program will be adversely affected. A complete physical inventory at ZPPR, including visual inspection of each fuel element and nondestructive assay (NDA) measurements on 5% of the inventory, requires about 30 eight-hour shifts. Because of accumulated radiation exposure, individual participation is limited to 5 shifts. As a result, 36 persons are required to perform the inventory.

In order to reduce the impact of inventory verification, it is desirable to assay the fuel in the reactor core in the largest possible units. This is especially important during the long periods between major loading changes when fuel is not accessible to assay in small units. The most efficient inventory verification method would be able to examine the entire reactor core in a single measurement or combination of measurements. Ideally, the validity of the whole-core measurements should be verifiable by inspectors not normally part of the fast critical facility. This is especially important in international safeguards where institutional diversion is considered. Two potentially powerful assay methods, when used in combination, are autoradiography and the measurement of integral (whole core) reactivity.

EXPERIMENTAL METHODS

Autoradiography

When x-ray sensitive film is placed against the edge of a fast critical assembly fuel plate, the radiation emitted by the isotopes in that fuel plate form a clear image (autoradiograph) of the edge of the fuel plate. Two types of autoradiography can be used to obtain piece counts of fuel elements in reactor drawers. The first type is passive autoradiography in which spontaneously-emitted beta and gamma radiation form the fuel-plate image. The passive autoradiographic method was previously applied to plutonium-containing fast critical assembly fuels[3] and to low-enriched uranium fuel in LWR assemblies[4]. The second type of autoradiography is active, in which prompt fission gamma radiation and fission-product beta and gamma radiation produced during and immediately after critical reactor operation form the fuel-plate image.

Passive autoradiographs of fuel plates in reactor drawers can be obtained by sliding a packet of x-ray film between the top of the contents of a drawer and the matrix element above that drawer. The clearance between the top of a fuel element and the matrix tube is 0.152 cm in the ANL fast critical assemblies. The film used in previous applications to plutonium fuel was Kodak Ready-Pack Type-M X-ray film. The film packet was 3.81 cm wide and was 0.089 cm thick where the ends of the packet were sealed with black tape. Typical exposure times were 15 min. The passive autoradiographic method allowed a fuel-plate piece count to be made in a large number of drawers in a short time. For plutonium fuels, passive autoradiographic images are predominantly formed by the 60 keV gamma ray from Am-241.

The passive autoradiography of uranium fuel in reactor drawers is less satisfactory than for plutonium fuels. One difficulty is that exposure times of many hours are required if ordinary x-ray film is used for uranium fuel. This problem is caused by the low gamma-ray emission rate for U-235 compared to the gamma-ray emission rates for the isotopes present in plutonium fuels. Intensifying screens cannot be used in reactor drawers because of their thickness. A second problem with the passive autoradiography of uranium is the large contribution from U-238 to the image density of a fuel plate. The U-238 daughter Pa-234 emits 2.29 MeV beta radiation which efficiently exposes film. The image densities from unclad depleted uranium plates and from unclad 93%-enriched plates are nearly equal. Uranium fuel plates used at ANL are not clad. Additional filtration is needed to reduce the contribution to image density from U-238, but additional filtration increases the thickness of the film packet. Further work is required to investigate possible methods for applying passive autoradiography to uranium fuel in reactor drawers.

The need to distinguish between U-235 plates and U-238 plates in an assembly core led to the development of active autoradiographic methods. In active autoradiography the prompt-fission gamma radiation and/or the short-lived fission-product beta and gamma radiation produces the fuel plate image. The formation of an image is the direct result of the critical operation of the assembly. Because the spontaneous radiation emission from uranium is small, two types of active autoradiography are applicable to uranium fuel. In the first type, the fuel plate images are formed by both prompt-fission and fission-product radiation. Operationally, there are three steps: (1) film is inserted into drawers, (2) the reactor

is brought to a critical configuration and operated at an appropriate power, and (3) film is removed and processed after shutdown and cooling. Relatively insensitive film is used in this first type of active autoradiography. In the second active autoradiographic method the fuel plate images are produced only by fission-product radiation. The steps are: (1) the reactor is operated at high power without film, (2) the reactor is shut down and allowed to cool over night, (3) the following day film is inserted into drawers and exposed for a few hours, and (4) the film is removed and processed. In this second method, more sensitive film is used. Active autoradiography is somewhat more complicated for plutonium than uranium because of the large spontaneous radiation component from plutonium fuel. Only at-critical active autoradiography is practical for plutonium.

Integral Reactivity Measurements

Reactivity Measurement Methods

A variety of reactivity measurement methods has been developed which are applicable to fast critical assemblies.[5,6,7] The two basic types of methods are static (equilibrium) and dynamic (kinetic). Equilibrium methods are conceptually simple because details of the delayed-neutron behavior or the prompt-neutron lifetimes are not needed. One equilibrium technique in common use with subcritical systems is the source-multiplication method.[6,8] For a plutonium-fueled reactor, the spontaneous-fission neutrons from the even plutonium isotopes provide a neutron source of known strength. The reactivity of the assembly can be deduced from the extent to which the fissile isotopes in the assembly multiply the spontaneous-neutron flux. The neutron flux can be monitored by detectors within the core or outside the core.

Dynamic techniques are also available which infer reactivity or changes in reactivity from the time-dependent changes in neutron flux. Knowledge is required of the delayed-neutron parameters and the prompt-neutron lifetime. Dynamic measurements are often made by measuring the change in neutron flux during and after the movement of a control rod or of other material within the reactor. Perhaps the conceptually simplest dynamic technique is the determination of reactivity from the measurement of the reactor period.[5] For a supercritical reactor, the reactivity can be inferred from just the period and the prompt-neutron lifetime. Period measurements, however, suffer from many of the uncertainties and long measurement times encountered in the equilibrium methods. At ZPPR the more commonly used dynamic method involves perturbation techniques in which inverse reactor kinetics equations are used to derive values of time-dependent reactivity from measured time-dependent neutron fluxes.

Reference Configuration

The core configuration of a fast critical assembly may be designed to model a postulated reactor design or to address a generic reactor physics issue. For either type of experiment, it is useful to establish a reference core configuration for which various reactor physics parameters, including reactivity, are well characterized. As experiments progress, many modifications are made to this configuration. These modifications are very frequent, but often involve only a small fraction of the total number of drawers in the core. One way to verify the fissile content of the core is to periodically return to the reference configuration and experimentally verify that the reactivity is the same (within uncertainty limits) as it was when the reference core was initially established. When possible, such a reactivity verification could be scheduled to coincide with a time during the experimental program when the core was close to the reference configuration. The use of reference reactivity values from a reference configuration assumes that the initial reference core loading was independently verified. This initial verification can be accomplished by making NDA measurements on fuel elements or drawers as they are being loaded, by verifying the loading pattern with autoradiography, or by calculation of the reactivity expected for a particular core configuration and composition.

Reactivity Worth

The effectiveness of reactivity measurements as a diversion detection technique will depend upon the sensitivity with which these measurements can detect missing material. The factors influencing the diversion sensitivity are the uncertainty of the reactivity measurement and the reactivity worth of the fuel in the assembly. The reactivity worth of a

material is that reactivity effect, per unit mass (e.g., Ih/kg), produced by the addition of that material to the core. Reactivity worth can be either positive or negative, and both the magnitude and the sign of reactivity worth can vary as a function of position within the core.

Reactivity Compensation

The agreement between two measured reactivity values for a core in a reference configuration still does not necessarily mean that the fissile content has not changed in the time between measurements. The loss of reactivity by removal of fissile material can, in principle, be compensated for by addition of materials which also have a positive reactivity worth. Similarly, compensation might be accomplished by removing materials, such as absorbers, which have negative reactivity worth. A third compensation scheme could involve removal of fissile material from a region of relatively low worth with a simultaneous transfer of fissile material from a region of relatively low worth to a region of relatively high worth. This third scheme would, of course, constitute a deviation from the reference configuration.

EXPERIMENTAL RESULTS

Autoradiography

The ZPR-9 fast critical assembly was used to test the applicability of active autoradiography to uranium-fueled cores. The fuel drawers of the assembly contained a single column of 93%-enriched fuel plates. Each plate was 5.08 cm wide, 0.16 cm thick, and from 2.54 to 7.62 cm long. On either side of the uranium plate was a thin steel plate, and the remaining drawer volume was occupied by thick steel plates. The drawers contained only steel and uranium.

An example of an active autoradiograph produced by fission product radiation is shown in Fig. 1A. This autoradiograph was obtained approximately 18 hours after reactor shutdown. The reactor had been operated at a power of 255 watts for 66 min. Film exposure time was 66 min. The film used was the relatively sensitive Kodak AA Industrex X-ray film. The fuel column was readily visible. The individual fuel plates could not be distinguished because they were unclad and were fit tightly together in the column. Figure 1B shows a passive autoradiograph of an identical fuel column obtained with Kodak AA Industrex film and a 75-min exposure. The uranium plates in Fig. 1B had not been irradiated in the reactor for several weeks.

An example of an active autoradiograph obtained during a critical operation of the reactor is shown in Fig. 2. The film used was the relatively insensitive 3M QA-V graphic-arts-type film. Sheets of film were cut into strips approximately 3.81 cm wide and were contained in Kodak Ready-Pack film holders. The autoradiograph of the fuel column segment in Fig. 2 was obtained during a 15-min reactor operation at a power of 85 watts followed by a three-hour cooling period. The film was in the reactor for a total of approximately four hours. The contribution to image density from spontaneous radiation during the four-hour period was very small. The 0.16-cm-thick fuel column can be clearly seen as the darkest part of the line in the center of Fig. 2.

The sensitivity of the active, at-critical autoradiographic technique to some simple drawer-loading defects was tested. Figure 3A shows an active autoradiograph of part of a fuel column from which a 7.62-cm-long, 93%-enriched uranium plate was removed. Figure 3B shows an active autoradiograph of part of a fuel column in which a 7.62-cm-long, 93%-enriched fuel plate was replaced by a 20%-enriched fuel plate. Both defects in Fig. 3 were easily detectable. In another case, a 0.080-cm-thick fuel plate was substituted for a 0.61-cm-thick plate. The presence of the thin plate was detectable, but only upon careful inspection of the autoradioagraph. Smaller differences in plate thickness would probably not be detectable.

The film base and film packaging materials are hydrogenous, and in the ZPR-9 core described here, the film had a positive reactivity effect. A reactivity worth of 103 Ih/kg was measured for Kodak 35 mm Ready Pack X-ray film randomly distributed through a quadrant of one-half of the ZPR-9 assembly. This reactivity worth meant that only approximately 30 pieces of film, each 102-cm long, could be placed in the 800-drawer assembly without violating safety regulations. More pieces of film could be added, but the assembly reactivity

Fig. 1. A: Post-irradiation Active Autoradiograph of a Highly-enriched-uranium fuel column
B: Passive Autoradiograph of Highly-enriched-uranium Fuel Column

Fig. 2. At-critical Active Autoradiograph of a Highly-enriched-uranium Fuel Column

Fig. 3. At-critical Active Autoradiographs of 93%-enriched Uranium Fuel Columns With Defects
A: Missing Plate
B: 20% Enriched Plate

would have to be decreased by removing fuel drawers. In order to insure safe reactor operation, the reactivity effect of the film must always be considered when doing an at-critical autoradiographic verification.

The success of the active autoradiographic technique for uranium fuel in an assembly core led to a test of the applicability of the active technique to a plutonium-fueled assembly core. An example of an active autoradiograph obtained in the 6100-liter ZPPR assembly 10D is shown in Fig. 4A. The autoradiograph was produced during a 100 watt-hour operation of the reactor. The film was in the reactor core for 5.5 hours. This active autoradiograph shows portions of the edges of two 0.64-cm-thick plates in the center. The image at the right edge of the autoradiograph and parallel to the fuel plates corresponds to a column of U-238 plates. The space between the U-238 column and the fuel-plate column was occupied by a can containing sodium. Figure 4B shows a passive autoradiograph produced in a 5.5-hour exposure when the assembly halves were separated. Both autoradiographs were obtained with 3M QA-V film. The film was processed by hand at room temperature in Kodak X-Omat chemicals.

The 5.5 hours the film spent in the assembly core was greater than the minimum time necessary for autoradiography because other experiments were also conducted. The minimum time for an active autoradiographic irradition is approximately 2.5 hours, which includes reactor startup, irradiation, and reactor cooling.

The fuel-column image is more dense in the active autoradiograph (Fig. 4A; 1.2 optical density units) than in the passive autoradiograph (Fig. 4B; 0.6 optical density units). However, the background density is also higher in the active autoradiograph. The density difference between active and passive fuel plate images may have been greater if the total time the film was in the core had been the minimum 2.5 hours, instead of the actual 5.5 hours.

The plutonium fuel-plate images in the active autoradioagraphs obtained in the assembly drawers had only very small contributions from the fuel columns in adjacent drawers. Active autoradiographs were obtained in drawers which contained a single fuel column and which also had drawers above containing a single fuel column. The two fuel columns were separated by 0.28 cm of steel in the two matrix tubes and in the bottom of one drawer. Active autoradiographs were also obtained in drawers which contained a single fuel column, but which had no fuel-containing drawer above. The density of the fuel column images were nearly identical in both cases. From this observation of nearly equal image densities, it was concluded that the 0.28-cm-thick steel separating the two fuel columns absorbed most of the radiation which produced the fuel column images. This, in turn, led to the conclusion that low-energy radiation produced the images. This final conclusion is not surprising, because low-energy photons dominate both the prompt-fission gamma ray spectrum[9] and the fission-product spectrum[10] even though some very high energy photons are produced. In addition, the beta radiation from fission products will be highly absorbed by the 0.28-cm-thick steel, but will still be able to expose film within the drawer.

Active autoradiographs were also obtained for blanket drawers which contained no fuel, but which had fuel-containing drawers above them. The fuel column in the drawer above was not visible on the blanket drawer autoradiographs. Images of the U-238 plates in the blanket drawers were visible. An active autoradiograph of a blanket drawer is shown in Fig. 4C. It was obtained simultaneously with the autoradiograph in Fig. 4A. In Fig. 4C, the light, center portion of the autoradiograph corresponds to an 1.27-cm-wide sodium can, and the darker regions correspond to U-238 plates.

In Fig. 4A, the density of the image of the plutonium-containing fuel plates is approximately equal to the density of the image of the U-238 plates. This equality of density may be surprising at first because the fission rate in the U-238 in the assembly was only 15% of the total fission rate. However, the plutonium fuel plates were clad in 0.03-cm-thick stainless steel, while the U-238 plates were unclad. It was earlier concluded that the fuel-plate images were produced primarily by low-energy photons and beta radiation. If this conclusion is correct, then it can be expected that the image density of the U-238 plates will be enhanced because these plates have no cladding to absorb low-energy photons or beta radiation. While the images of the clad fuel plates and of the unclad U-238 plates do not look the same, their equal image densities for unequal fission rates presents a potential complication for interpreting active autoradiographs of drawers containing both clad plutonium

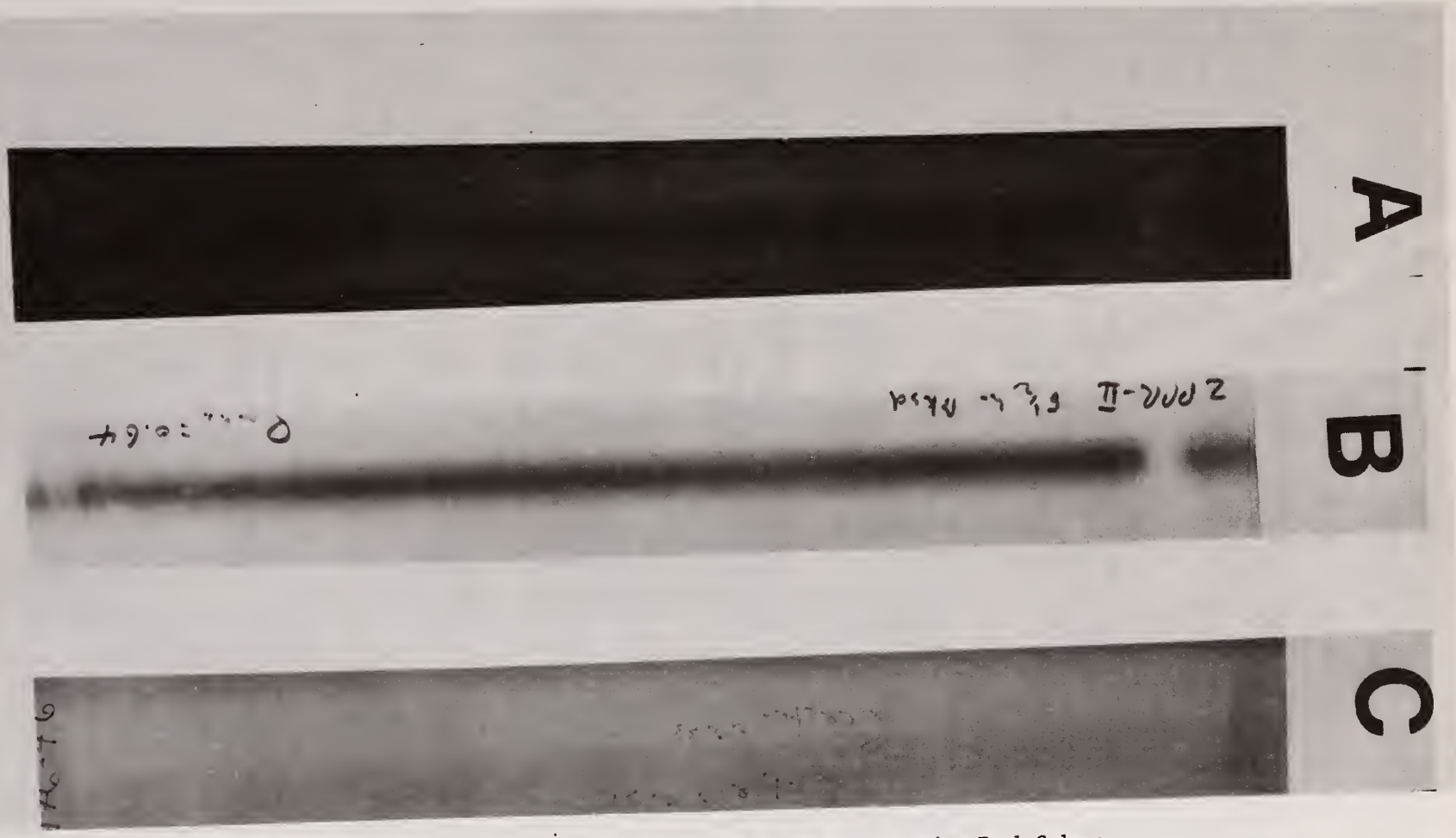

Fig. 4. A: At-critical Active Autoradiograph of Plutonium Fuel Column
B: Passive Autoradiograph of a Plutonium Fuel Column
C: At-critical Active Autoradiograph of a Blanket Drawer

plates and unclad U-238 plates. The density of the images of the U-238 plates in Fig. 4C is low compared to the density of the images of U-238 plates in Fig. 4A because the fission rates are much lower in the blanket region than in the core region.

Reactivity Worths

As a first step in assessing the sensitivity of reactivity measurements to diversion detection, reactivity worths were measured for Pu-239 as a function of position within the ZPPR core. These measurements were made on ZPPR assembly 10-A whose reference configuration is shown in Fig. 5. The assembly was a hexagonal 4590-liter mockup of an LMFBR which contained 19 mockup control-rod positions. The core had an axial length of 101.6 cm and was divided into two fuel-enrichment zones. The inner core, with the mockup control-rod positions, contained, primarily, drawers with a single column of Pu-alloy fuel. The outer core was loaded with single-column drawers and double-column drawers in alternate positions. The 5.08 cm by 5.08 cm cross section of the core zones of a single-column drawer and a double-column drawer are shown in Fig. 6. Outside the outer core was a blanket zone whose drawers contained fertile material and coolant. The outermost zone contained a steel reflector. The ZPPR-10A reference configuration was critical, with a total fissile mass of approximately 2100 kg.

Reactivity worths were obtained with the use of inverse kinetics techniques. The neutron flux was measured as a function of time for a fissile sample which was moved across the center of the axial midplane of the core. The sample was moved in steps by remote control so that an entire traverse was performed during a single reactor run. A traverse was made with an empty sample holder to correct for the reactivity effect of the holder. Neutron flux measurements were made with BF_3 detectors located outside the core.

In addition to the experimental results, first-order perturbation reactivity worths for the isotopes Pu-239, Pu-240, and U-238 were obtained from a 28-neutron-energy-group diffusion calculation in two-dimensional geometry. Isotopic worths were combined in the proper weight fractions so that results could be compared to the experimental samples. A sample size (self-shielding) correction was also made.

The experimental and computational results for Pu-239 reactivity worths as a function of radial position at the centerline of the core axial midplane are presented in Table I. The uncertainties in the measured worths are 1σ statistical variations. Graphical results are displayed in Fig. 7. The squares in Fig. 7 are the experimental data, while the solid line was obtained by applying a normalization factor to the calculated data over the fuel-bearing regions. The normalization factor was derived from a comparison of calculation and experiment.

The second factor required to determine the sensitivity of reactivity measurements to fissile material removal is the uncertainty of such measurements. One obvious contribution to this uncertainty is the simple experimental uncertainty in making any single reactivity measurement. However, because reactivity verification measurements will be compared to previously measured reference reactivities, the long-term reproducibility of reactivity measurements is also important.

In a fast critical assembly such as ZPPR, differences between reference reactivity measurements may arise from temperature variations, irreproducibility of table closure and control-rod positions, and unavoidable changes in the core composition, particularly the decay of Pu-241. The temperature of the ZPPR cell can be held constant to within $\pm$ 0.14°C. Therefore, if the approach to critical is always the same, uncertainties associated with temperature variations during reference measurements are small. Experience at ZPPR indicates that overall reproducibility of reactivity measurements on the same assembly over a short period (< 1 week) should be approximately $\pm$ 1 Ih. However, over a longer time period, the decay of the Pu-241 (14.4-year half-life) present in small quantities in the ZPPR fuel alloy, produces consistent and observable reactivity loss with time. Corrections can be made for the Pu-241 decay, but the decay still makes a contribution to the overall uncertainty. Assessment of these factors (for a range of critical assemblies containing 1.5% Pu-241 in Pu fuel) leads to a long-range (several month) uncertainty of $\pm$ 3 Ih.

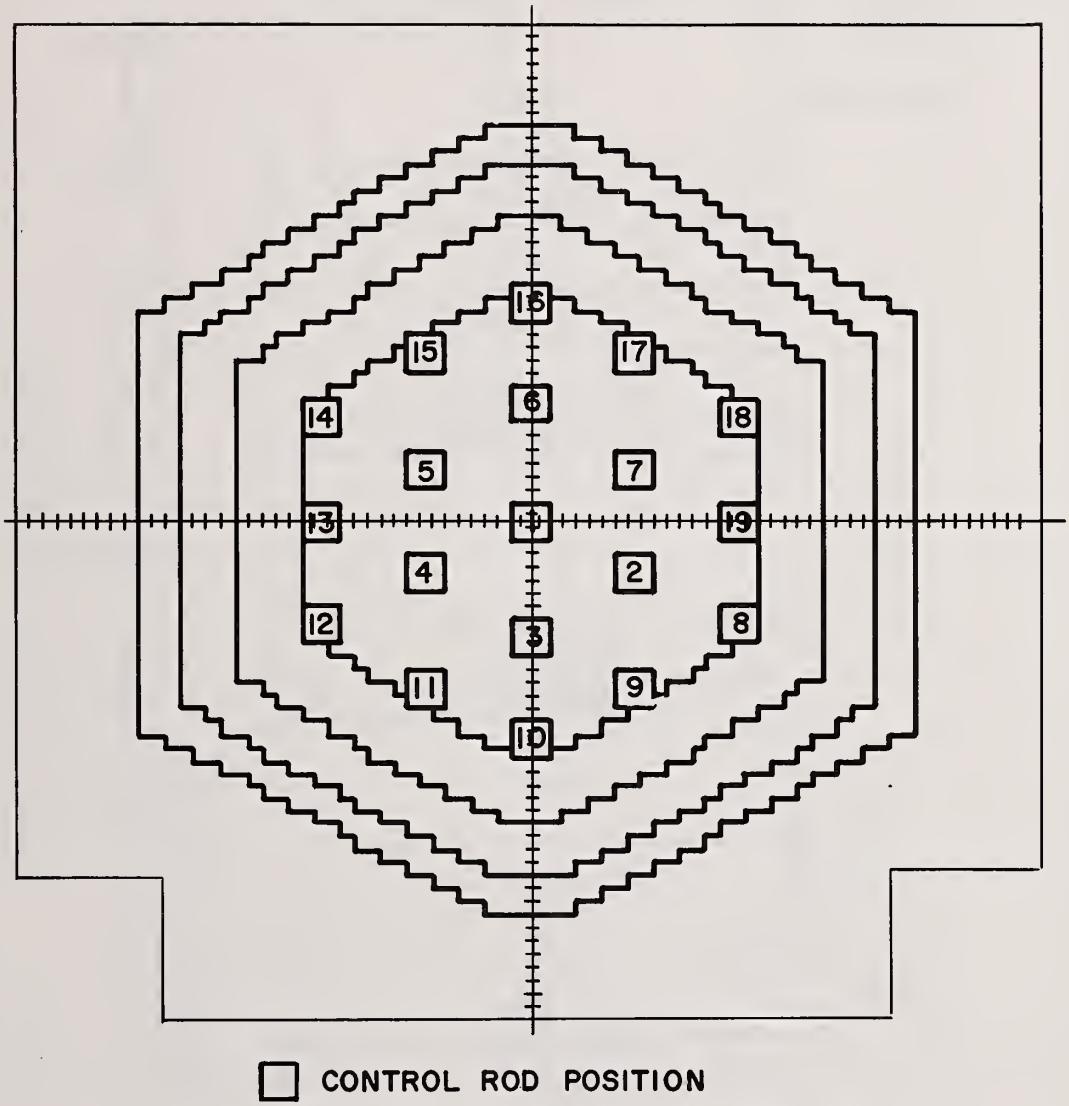

Fig. 5. Core Configuration for ZPPR Assembly 10A

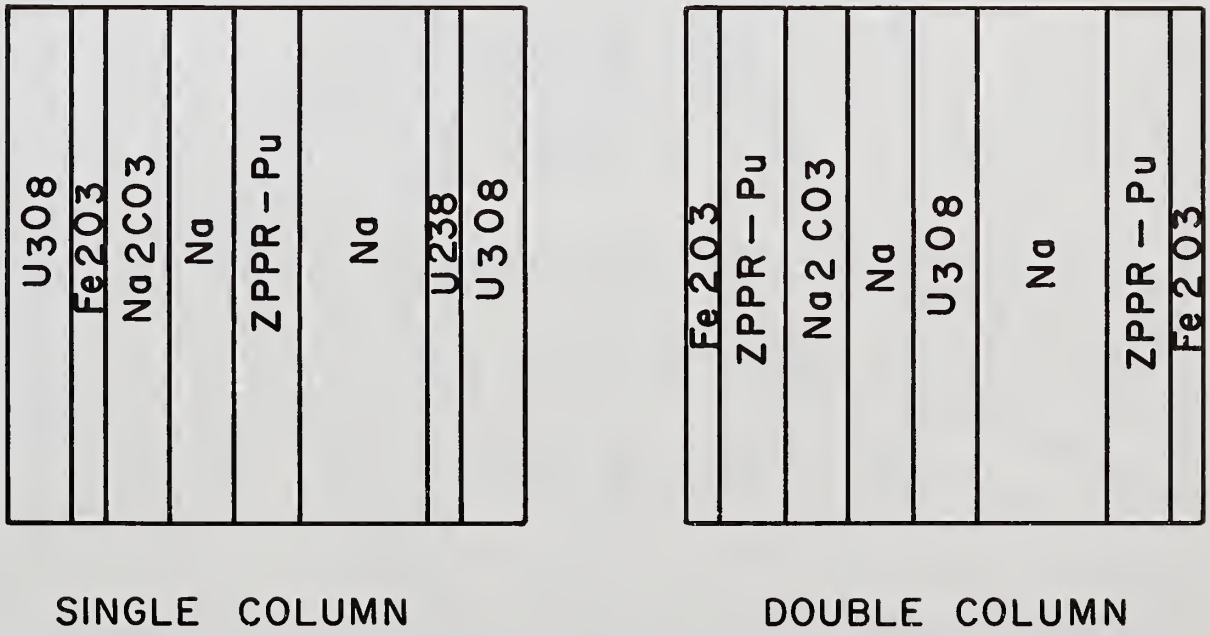

Fig. 6. Cross Section Views of Single- and Double-column Fuel Drawers

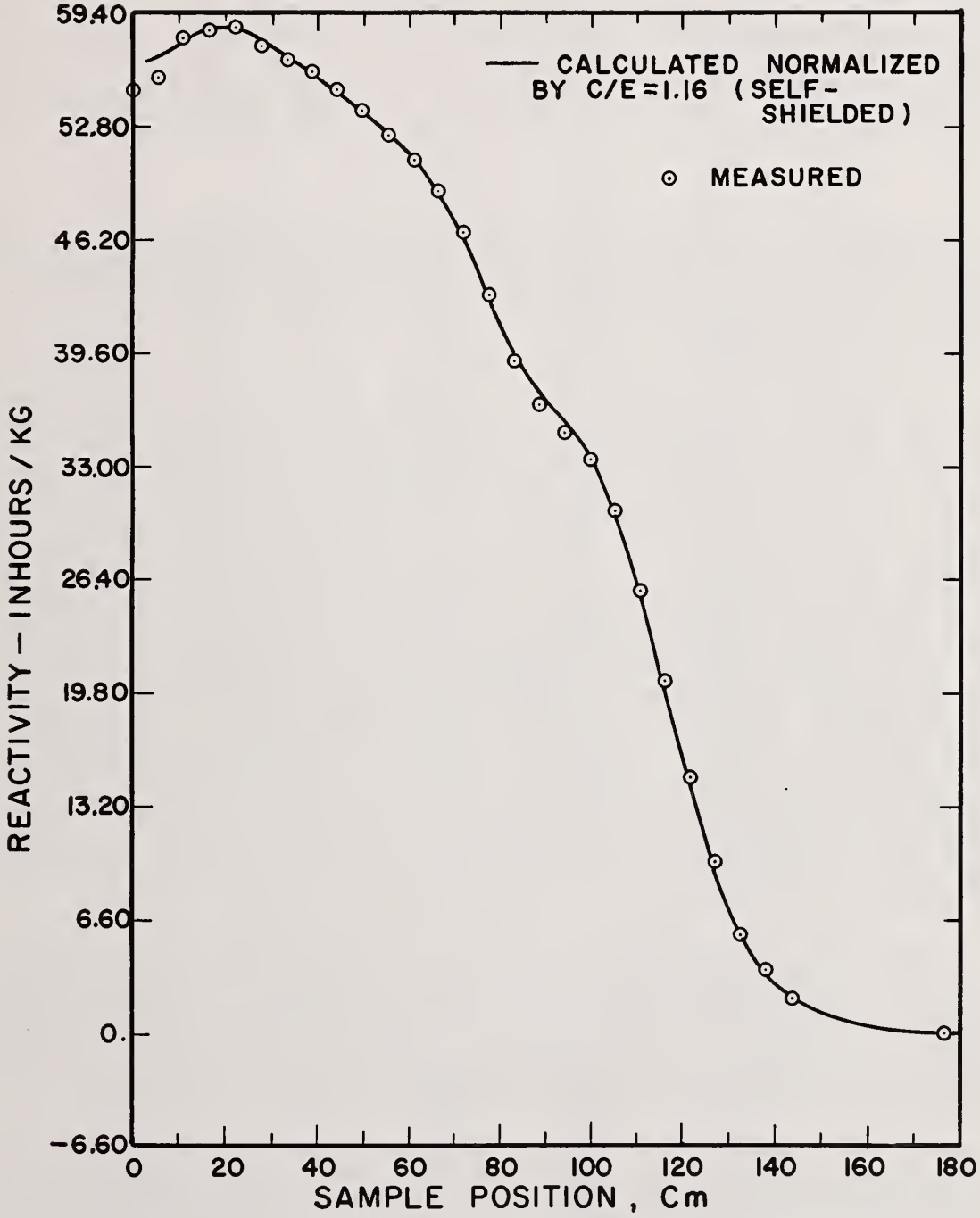

Fig. 7. Pu-239 Reactivity Worth as a Function of Position in Core

These short- and long-term uncertainties can be combined with the reactivity worth results in Table I to obtain estimates of the fissile removal sensitivities. These sensitivities are presented in Table II for three core positions: the core center (0,0), the core edge at the axial midplane (124,0), and the minimum reactivity position at the radial and axial core edge (124,50). These sensitivities are only estimates and will later be compared with observed changes in reactivity when fuel was removed. Also, these sensitivities represent removals of almost pure fissile fuel material. Actual fuel plates which contain mixtures of fissile and fertile material will have reduced detection sensitivities at the core center and probably slight enhancement at the core edge due to the presence of the fertile material. This is expected because of the fertile material's negative reactivity effect at the core center and small positive reactivity effect at the core edge.

Effects of Fuel Removal

The next step in assessing the sensitivity of reactivity measurements to diversion was the measurement of reactivity change when fuel was removed from a reference core. These measurements were made on ZPPR assembly 10D. This assembly was a hexagonal 6100 liter mockup of an LMFBR which contained 31 control-rod positions. Though larger than the core in assembly 10A, the loading pattern was similar. Reference core 10D contained a fissile mass of roughly 2600 kg.

The reactivity of the subcritical 10D reference core was determined by the source-multiplication method. This reference reactivity was -0.29$. In the source-multiplication measurement, the neutron flux was measured by 64 in-core fission counters. Each fission counter consisted of a thin U-235 foil inside an ionization chamber filled with an argon-methane mixture. The fission counter was enclosed in a stainless steel chamber, 5.08 cm by 0.64 cm by 15.2 cm. The fission counters took the place of the fuel plate nearest the axial mid-plane in 32 different single-column fuel drawers in each reactor half. Reference assembly 10D is shown in Fig. 8. The x's indicate the location of fission counters in Half 1, while the o's indicate the location of fission counters in Half 2. One advantage in using the source-multiplication method to determine reactivity for diversion detection purposes is that one can simultaneously obtain both an integral reactivity for the entire core and a relative fission-rate distribution map from the 64 individual fission counters. The value of the integral reactivity is obtained from the weighted absolute fission rates of all 64 counters. This integral reactivity is then compared to the previous result for the reference core. In addition, the relative fission rate for each detector (fraction of the total fission rate in the core seen by one detector) in the verification measurement can be compared to the relative fission-rate obtained in the reference measurement. If a local diversion has occurred, the absolute fission-rate measurements will detect the reduced integral reactivity, and the fission-rate distribution map may be able to indicate the location of the diversion. If a diversion is made uniformly throughout the core, the integral reactivity will still decrease, but the fission-rate distribution could essentially be unchanged.

Operationally, fuel was removed from selected drawers of the reference configuration, and then the reactor halves were brought together and the control rods set to their reference positions. After a wait of a few minutes to assure equilibrium, the fission-counter outputs were read and stored by a digital computer. The computer then calculated the integral reactivity, the relative fission rates for each detector, and the ratio of these relative fission rates to the relative fission rates for the reference. The relative fission-rate ratios were displayed on a core map so that local variations could be seen.

The first simulated fuel diversion was a simple removal of all fuel plates from four single-column drawers near the center of the inner core. Approximately 2 kg of fissile material was removed. The fuel plates were not replaced with any other material. The results for this simulated diversion are shown in Fig. 9. The drawers with an "x" are those from which fuel was removed. This fuel removal resulted in a decrease in the integral reactivity of 0.16$. The numbers in Fig. 9 represent the changes in relative fission rates from the reference values. Each number appears at the approximate core location of its respective fission counter. The numbers, which we will call "Q", were computed from the expression

TABLE I. Calculated and Corrected Measured Radial Traverse for Pu-30, Sample in ZPPR Assembly 10A

Position, cm	Sample Worth, Ih/kg				
	Experiment	Calculated	Self-Shielding	Corrected Calculated	C/E
0.023	55.04 ± 0.09				
5.522	55.67 ± 0.12	63.66	1.04	65.97	1.19
11.052	57.95 ± 0.10	64.39	1.04	67.06	1.16
16.576	58.48 ± 0.12	65.00	1.05	67.94	1.16
22.095	58.67 ± 0.09	64.96	1.05	68.00	1.16
27.625	57.49 ± 0.09	64.26	1.05	67.29	1.17
33.147	56.68 ± 0.11	63.12	1.05	66.11	1.17
38.671	56.01 ± 0.11	61.82	1.05	64.82	1.16
44.201	54.94 ± 0.12	60.52	1.05	63.54	1.16
49.720	53.71 ± 0.10	59.33	1.05	62.22	1.16
55.245	52.33 ± 0.10	58.03	1.05	60.83	1.16
60.772	50.77 ± 0.07	56.42	1.05	59.22	1.17
66.294	49.01 ± 0.12	54.14	1.05	56.97	1.16
71.818	46.55 ± 0.11	51.28	1.05	53.76	1.15
77.346	42.91 ± 0.09	47.53	1.04	49.63	1.16
82.867	39.05 ± 0.11	44.11	1.04	45.90	1.18
88.389	36.57 ± 0.11	41.70	1.04	43.42	1.19
93.914	34.95 ± 0.09	39.59	1.05	41.39	1.18
99.444	33.37 ± 0.09	37.08	1.05	39.09	1.17
104.965	30.32 ± 0.14	33.24	1.06	35.14	1.16
110.490	25.65 ± 0.13	28.02	1.06	29.66	1.16
116.017	20.46 ± 0.11	21.88	1.06	23.09	1.13
121.539	14.86 ± 0.13	15.82	1.05	16.57	1.12
					core edge
127.066	9.90 ± 0.12	10.87	1.01	11.04	1.12
132.588	5.66 ± 0.13	6.90	0.97	6.73	1.19
138.115	3.71 ± 0.08	4.25	0.93	3.95	1.07
143.634	2.04 ± 0.13	2.73	0.87	2.38	1.18
176.789	0.00 ± 0.06	0.00	0.67	0.00	

TABLE II. Fissile Removal Detection Sensitivity - ZPPR-10A (Using 1 Ih short-term and 3 Ih long-term Reactivity Sensitivity)

Radial Position, cm	Axial Position, cm	Isotope	Sensitivity, kg Short Term	Long Term
0	0	^{239}Pu	0.017	0.05
124	0	^{239}Pu	0.067	0.2
124	50	^{239}Pu	0.267	0.8
0	0	^{235}U	0.023	0.07
124	0	^{235}U	0.09	0.27
124	50	^{235}U	0.36	1.09
0	0	^{233}U	0.012	0.036
124	0	^{233}U	0.05	0.15
124	50	^{233}U	0.20	0.60

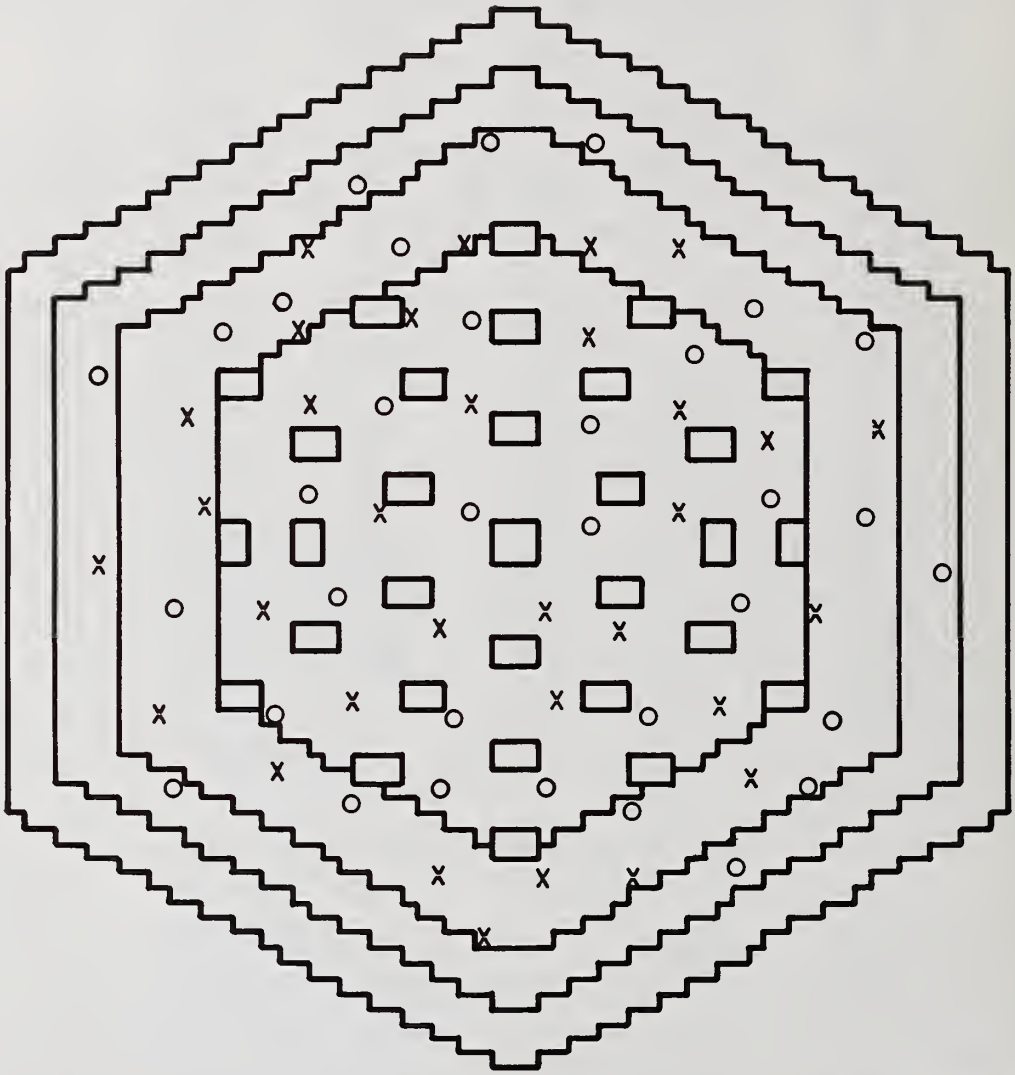

Fig. 8. ZPPR-10D Core Configuration Showing Locations of Fission Counters

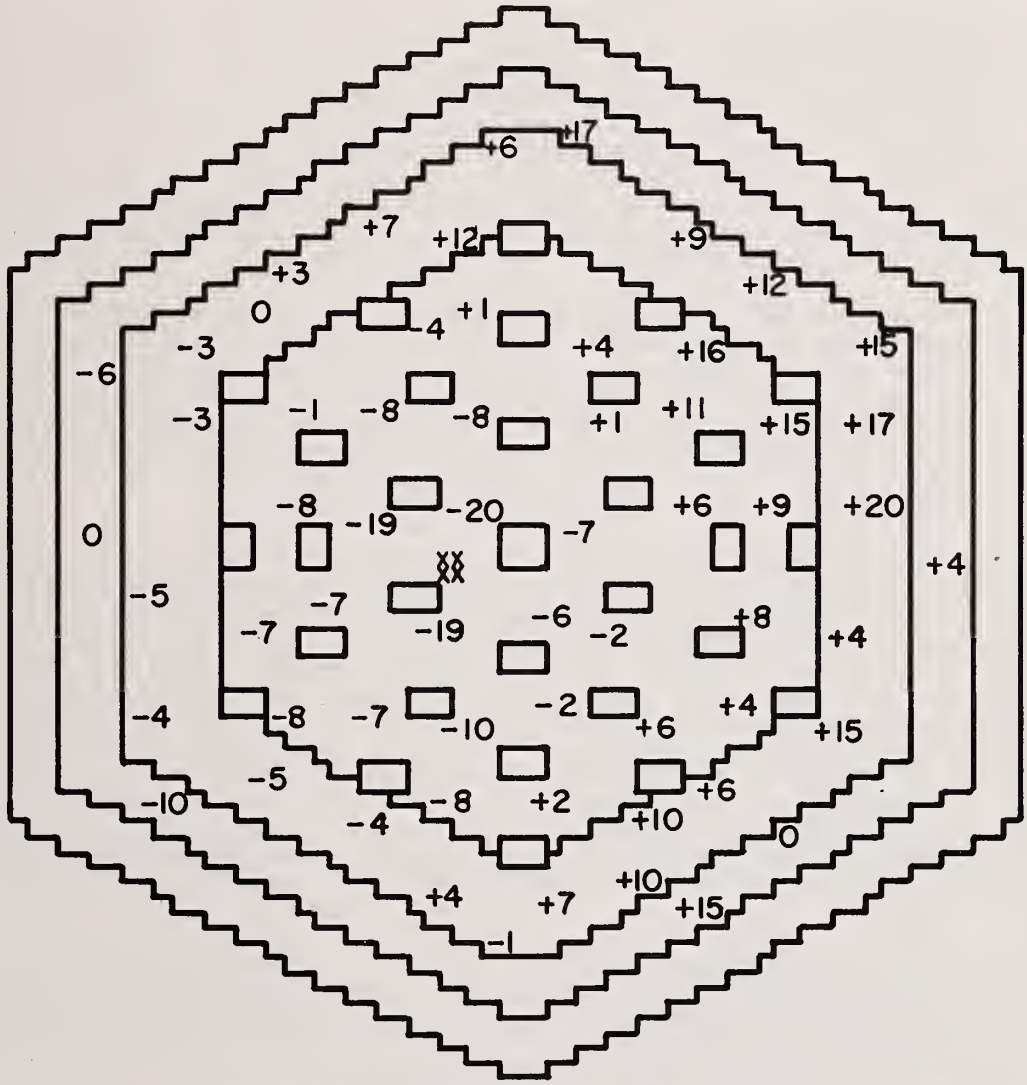

Fig. 9. Fission Rate Distribution Map for the First Simulated Diversion

$$Q = 1000 \left[\frac{\frac{a_i R_i}{\sum_i a_i R_i}}{\left(\frac{a_i R_i}{\sum_i a_i R_i} \right)_{ref}} - 1 \right]$$

where R_i is the fission-counter count rate and a_i is a weighting factor for that counter. The subscript "ref" indicates values for the reference configuration. Thus, a Q of -20 indicates a 2% decrease in the relative fission rate for that detector compared to the relative fission rate for that detector in the reference measurement. As indicated by the Q values in Fig. 9, there is a definite decrease in relative fission rates in the vicinity of the 2-kg localized fuel removal. The statistical uncertainties of the Q's (1σ) were ± 3 for the inner core, ± 4 for the outer core, and ± 6 for the blanket. The uncertainty in the integral reactivity measurement was approximately 0.003$ (1σ), although, when long-term instabilities are included (comparisons with reference reactivities made months previously), this uncertainty is likely to be 0.01$.

Table I gives a plutonium reactivity worth near the core center of ZPPR-10A of approximately 56 Ih/kg. Using a conversion factor of 333 Ih/$, one would predict that a removal of 2 kg of Pu from the core center would reduce the reactivity by about 0.33$. The observed reactivity reduction in the larger but similar ZPPR-10D was 0.16$. This smaller reactivity decrease is expected because fuel was removed from the entire 50.8-cm fuel column, and because the reactivity worth of fuel decreases with increasing distance from the axial midplane. Axial worths at 50.8-cm from the midplane can be as much as a factor of four lower than at the midplane, so an 0.16$ change in reactivity is reasonable.

One postulated method of compensating for a reactivity loss due to fissile removal is the substitution (or addition) of moderator material which may have a positive reactivity worth in a fast critical assembly. A very simple moderator substitution was made in the second simulated diversion. The voids created in the drawer by the fuel removal of the first simulated diversion were filled with polyethylene plates having the same dimensions as the fuel plates. Except for the presence of the polyethylene, the reactor core configuration was the same in the second simulated diversion as it was in the first. The source-multiplication measurement results for this second diversion are shown in Fig. 10. The integral reactivity was 0.18$ less than the reference core, which was 0.02$ less than the uncompensated diversion. Obviously, this effort to compensate for the reactivity loss was not successful. A possible explanation for this apparent negative reactivity worth for the polyethylene may be that the local shift of the neutron spectrum resulted in increased absorption in local fertile material (U-238), reducing the neutron flux available to more distant fissile material.

As in the first diversion, the map of Q values shows a marked reduction in relative fission rates in the vicinity of the diversion. These maps can be generated with any set of fission counter readings as a reference. When the first simulated diversion was used as the reference, there was no statistically significant difference betwen the relative fission rate distributions in the second and in the first diversions.

A more rigorous test of the integral reactivity method for detecting diversion (and the relative-fission-rate ratio method for locating diversion) is a distributed diversion in a low-worth region. In the third simulated diversion, fuel was removed from each of four single-column drawers along the core-blanket interface. The fuel plates were replaced with polyethylene plates. The location of the fuel removal and results for this third diversion are shown in Fig. 11. The integral reactivity was 0.02$ less than the reference. This reactivity reduction is in reasonable agreement with the results of Table I when the low-worth locations of the fuel removals are considered. The total fissile material removed was again approximatley 2 kg.

The most notable feature in the Q-value map is the very high reading for the fission counter directly adjacent to the drawer containing polyethylene near the bottom of the reactor. This is due to the counters' high sensitivity to low energy neutrons and the lack of intervening absorber. In the second diversion, the nearest fission detector was four

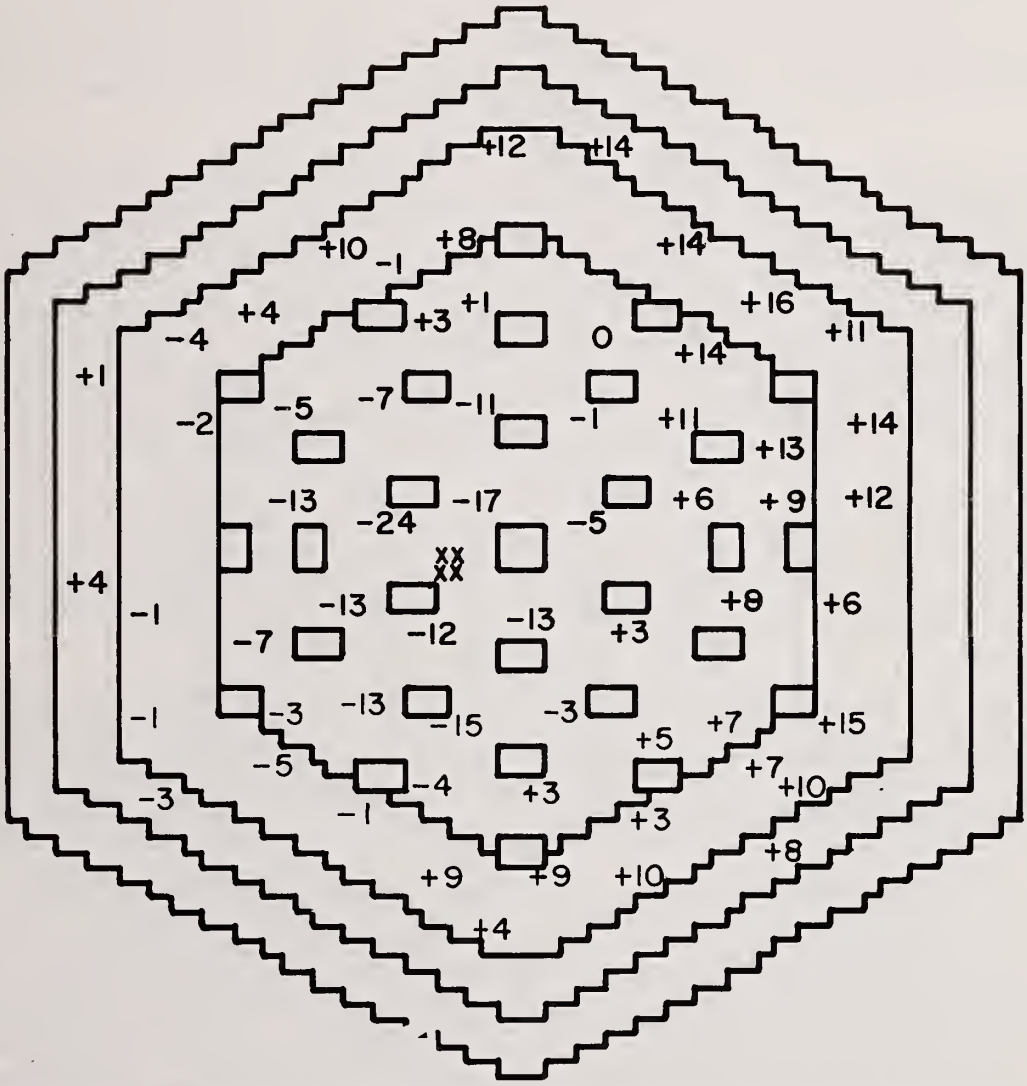

Fig. 10. Fission Rate Distribution Map for the Second Simulated Diversion

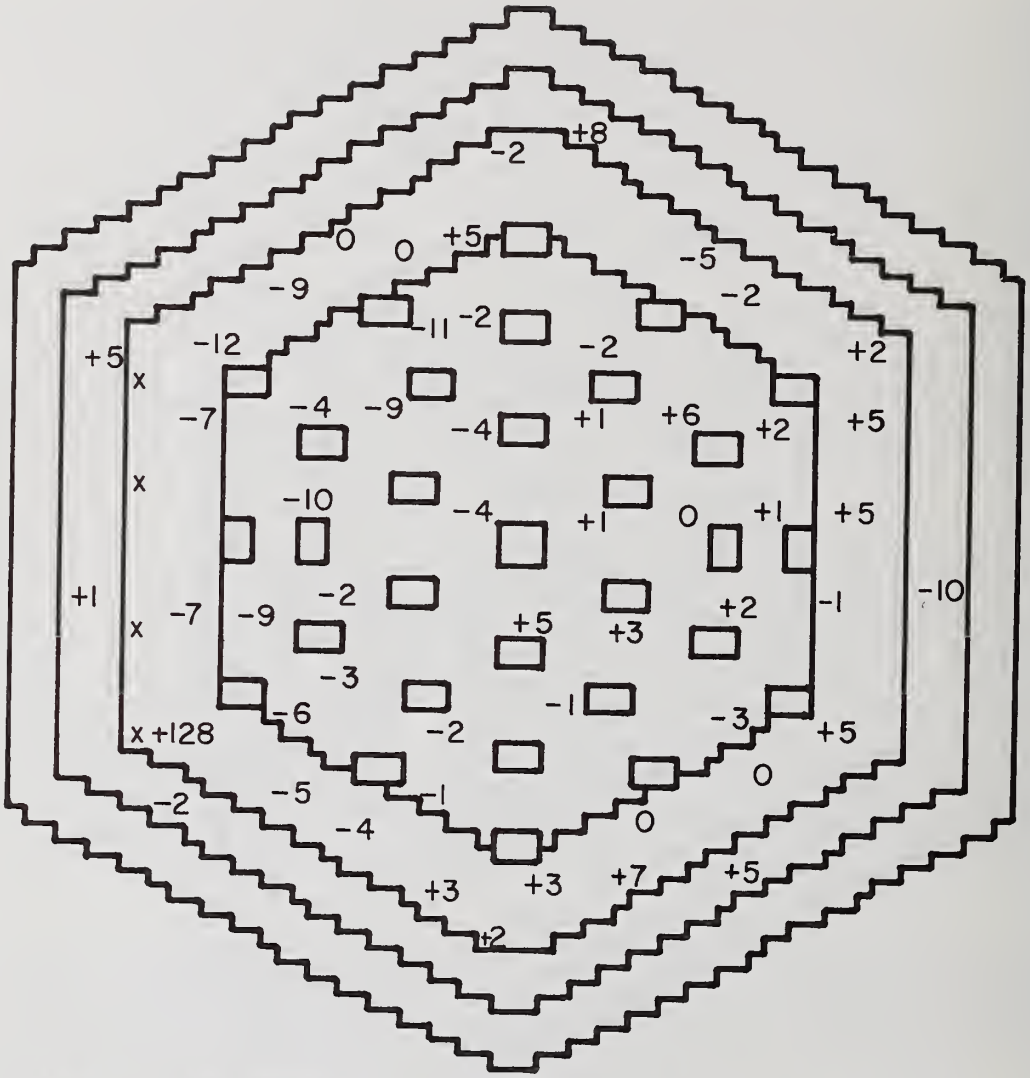

Fig. 11. Fission Rate Distribution Map for the Third Simulated Diversion

drawers away from the polyethylene. The other fission counters show a negative tilt toward the side where the fuel was removed, but these Q-values are not much greater than the statistical uncertainties.

A fourth simulated diversion was made which was localized in a minimum-worth region at a corner of the core. The fuel plates were removed from three single-column drawers and one double-column drawer, and polyethylene plates were substituted for the fuel. Total fissile material removed was 2.5 kg. Figure 12 shows the location of fuel removal and the Q-value map. The integral reactivity was only 0.01$ less than the reference, a value which is close to the expected value for the uncertainty of long-term comparisons to reference measurements. The Q-value map successfully located the region of the diversion. The reason for the rather large positive reading from the fission counter in the blanket near the diversion is not obvious.

In order to test a slightly different reactivity compensation scheme, the configuration of the second simulated diversion was reproduced with the addition that polyethylene was substituted for fertile material (U-238) in two drawers in the outer core. Polyethylene once again replaced fuel removed from the inner core. This fifth simulated diversion is shown in Fig. 13. The x's indicate a drawer in which polyethylene replaced fuel, and the o's indicate a drawer in which polyethylene replaced U-238. The integral reactivity for this configuration was 0.14$ less than the reference, which was 0.02$ more than the case of fuel removal with no polyethylene (first diversion), and was 0.04$ more than the case when polyethylene was substituted only for fuel (second diversion). It appears that replacing U-238 with polyethylene was a more successful reactivity compensation method than was replacing fuel with polyethylene. The Q-value map clearly located the missing fuel.

Figure 14 shows a Q-value map in which the configuration of the fifth simulated diversion was compared to the second simulated diversion. The only difference between these configurations is the polyethylene which replaced the U-238 in the outer core. This change is apparent from the map which shows a positive tilt to the side of the core with the extra polyethylene and the highest Q-values closest to the polyethylene.

Foil-Irradiation Experiments

Because the reactivity of a particular assembly-core configuration depends on the neutron-energy spectrum, it might be necessary to verify the spectrum as part of a reactivity verification. The addition of moderator to a fast reactor core can increase reactivity by increasing the relative neutron flux at low energies where the fission cross sections are relatively large. A typical neutron-energy spectrum for a ZPPR LMFBR mockup is shown in Fig. 15. As indicated, the relative flux is very small below a few hundred eV.

A verification of the neutron-energy spectrum of a fast critical assembly core can be obtained from experimentally determined rates of neutron-energy-dependent reactions. The types of measured data that are sensitive to neutron spectra are called spectral indices. One spectral index which has been used for many years in reactor experiments is the ratio of the fission rates in U-235 and U-238. The fission rate for U-235 generally decreases or is relatively flat with increasing neutron energy, while the fission rate for U-238 increases with increasing neutron energy, with a threshold near 1 MeV. Thus, the ratio of fission-product concentrations in U-238 and U-235 foils can be used as an index of the neutron energy distribution. The use of reaction-rate ratios in metal foils for safeguards purposes has been investigated in the highly enriched uranium-fueled SPECTR assembly in the USSR.[11] The foils should contain a material sensitive to low-energy neutrons in one reaction, and should contain a material sensitive to high-energy neutrons in another reaction. For low-energy sensitivity, (n,γ) reactions are useful, while (n,n'), (n,2n), (n,p) and threshold fission reactions have good high-energy sensitivity.

The spectral index chosen for this study was the ratio of the rate of the In-115 (n,γ) reaction to the rate of the In-115 (n,n') reaction. This index has the advantage of requiring only a single foil of nonradioactive material. Natural indium contains about 96% In-115. The product of the (n,γ) reaction, $In\text{-}116m_1$, has a 54-minute half life and emits several gamma rays, including one at 417 keV. The product of the (n,n') reactions, In-115m, has a 4.5-hour half life and emits a single gamma ray of 335 keV. The ratio of the intensities

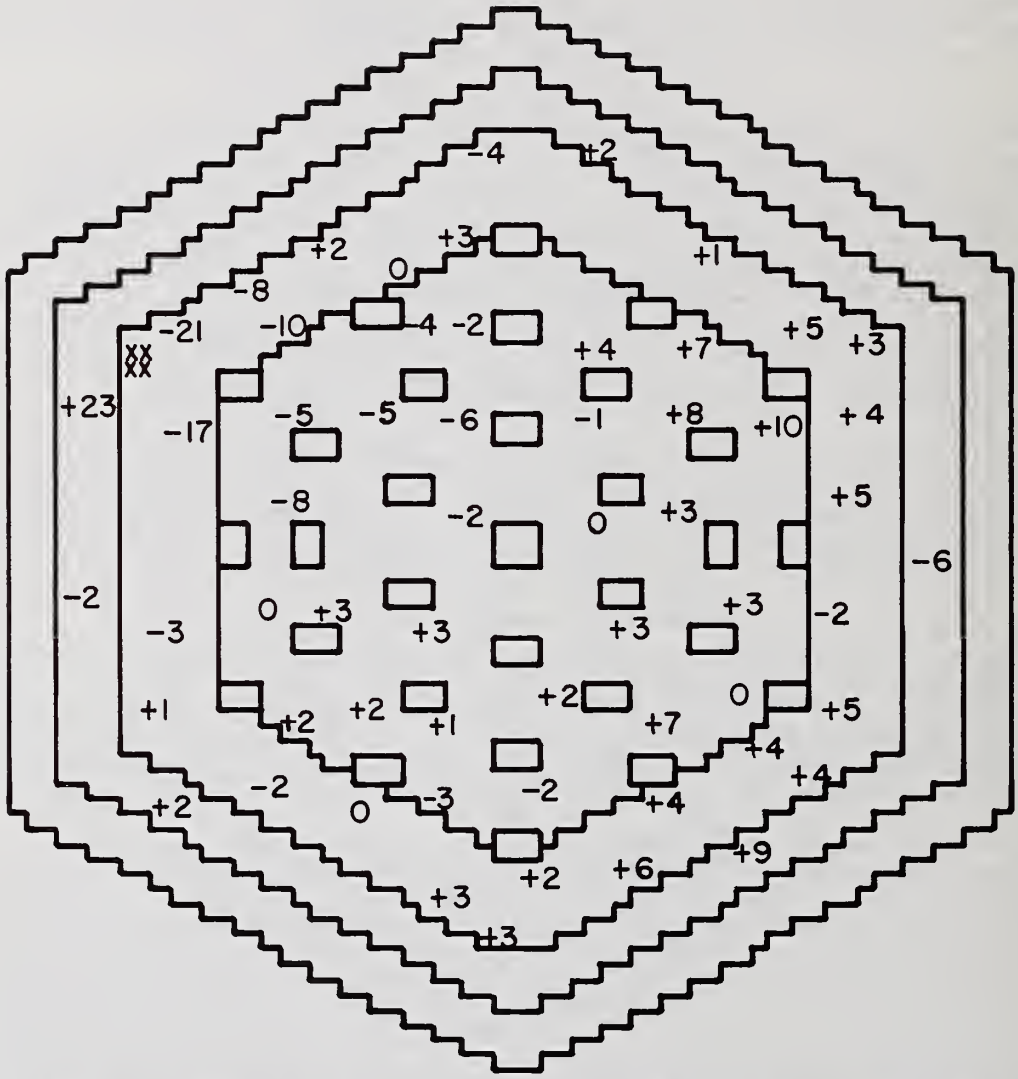

Fig. 12. Fission Rate Distribution Map for the Fourth Simulated Diversion

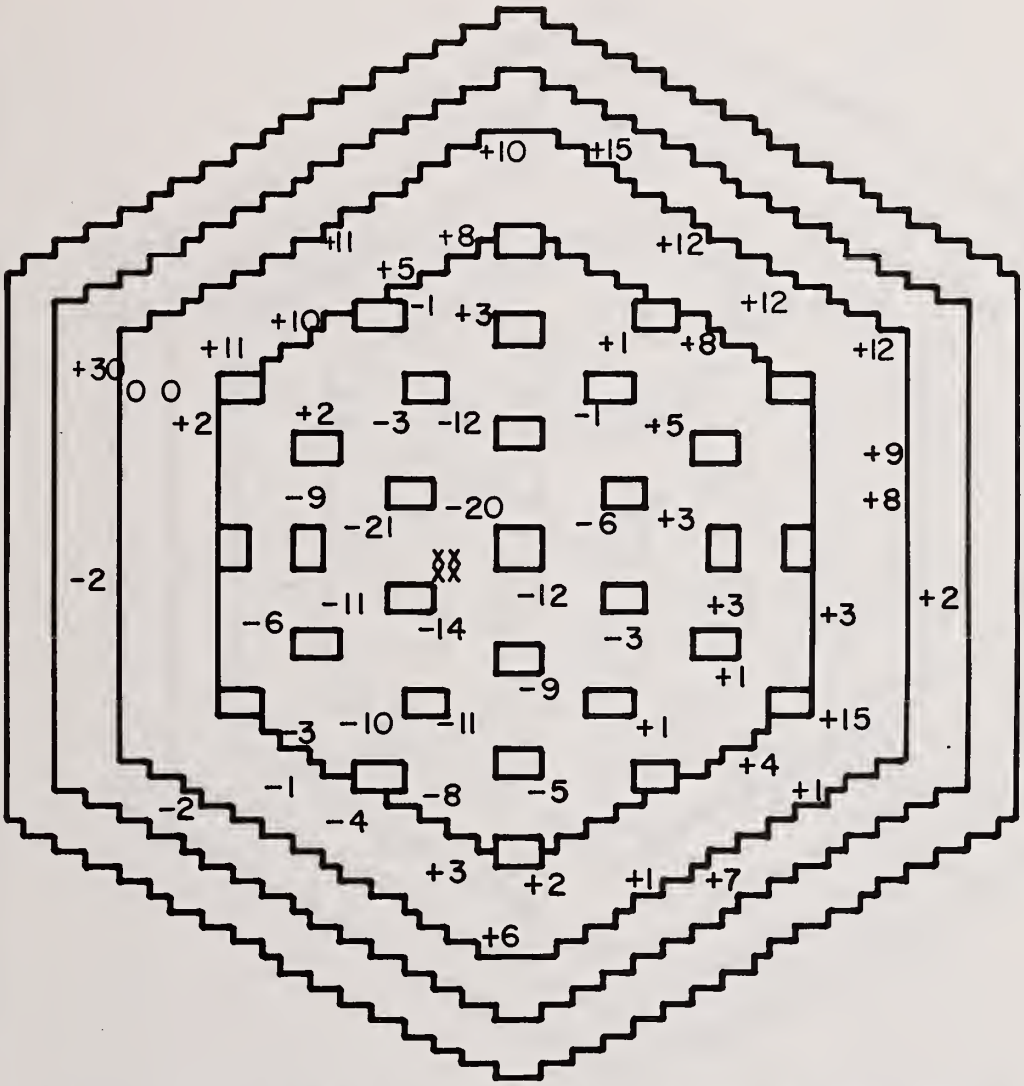

Fig. 13. Fission Rate Distribution Map for the Fifth Simulated Diversion

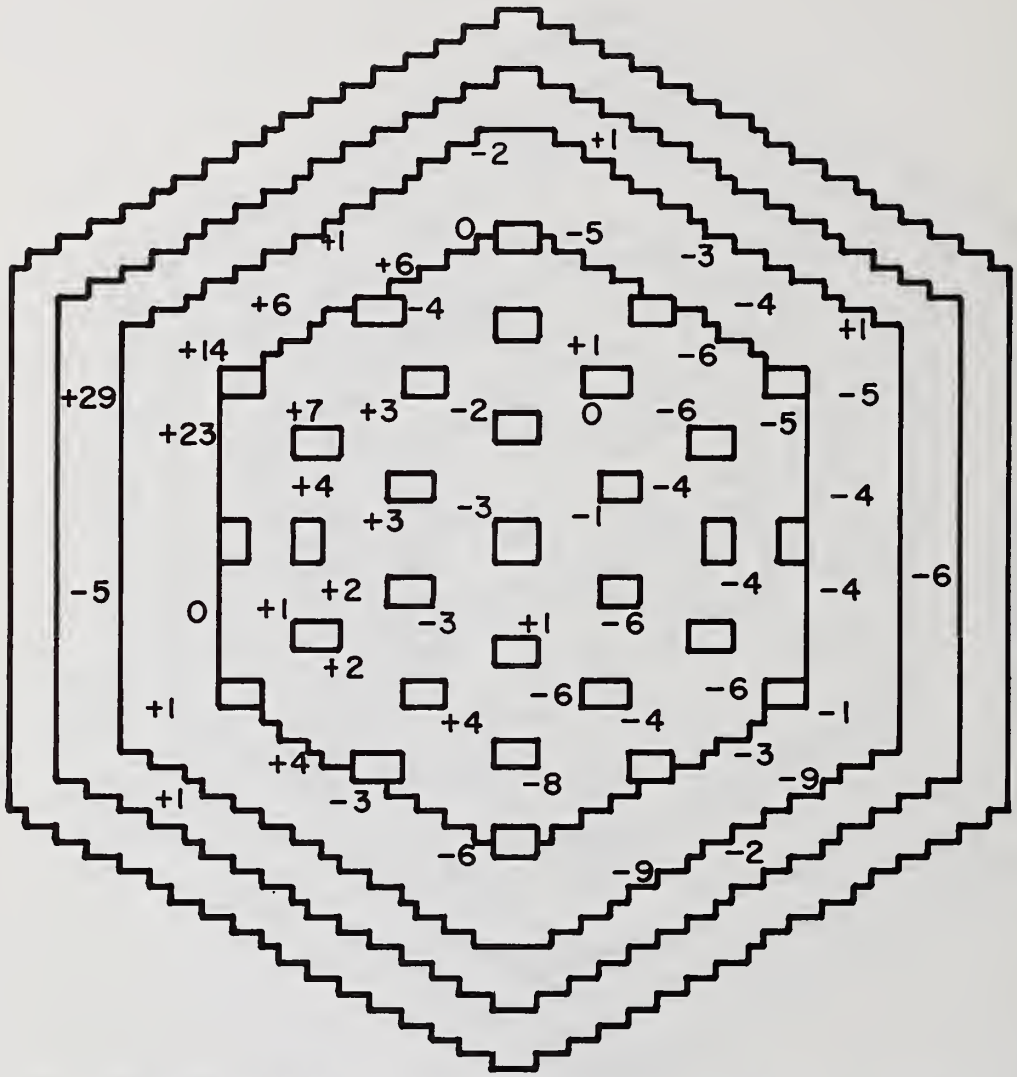

Fig. 14. Fission Rate Distribution Map Showing the Difference Between the Fifth and Second Simulated Diversions

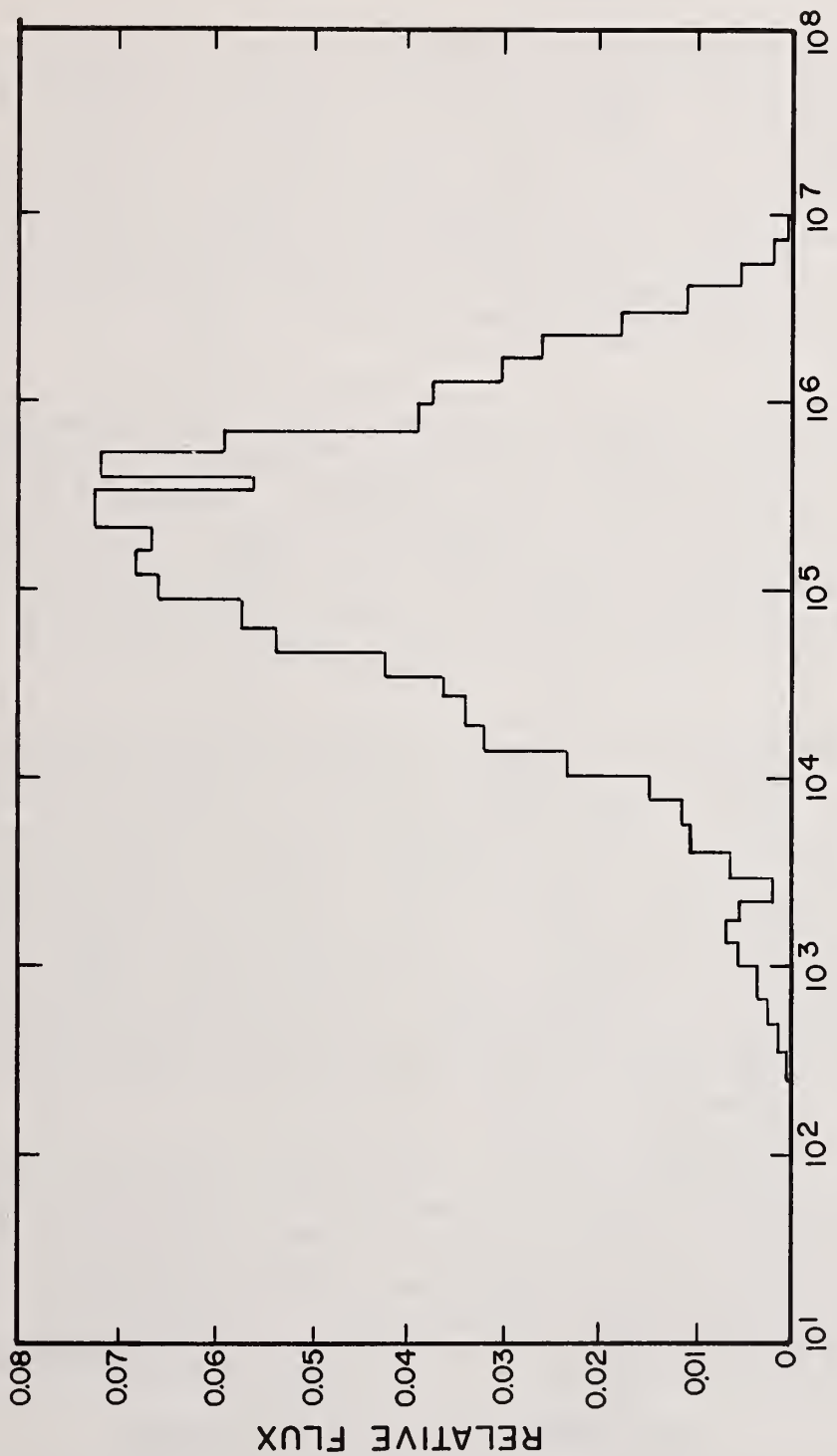

Fig. 15. Typical ZPPR Neutron Energy Spectrum

of the 417-keV and the 335-keV gamma rays was used as the spectral index. The neutron-energy dependence of the In-115 (n,γ) and In-115 (n,n') reactions is shown in Fig. 16.

The ability of the indium-foil spectral index to detect local spectral changes due to moderator substitution was tested by placing indium foils in several locations around the sites where polyethylene had been substituted for fuel. The foil-irradiation test was conducted with the reactor in a configuration which contained both the second and fourth diversion types. That is, polyethylene had been substituted for fuel in four drawers near the core center and in four drawers of a corner of the outer core. Foils were placed in and near the drawers containing polyethylene, and also in symmetrically equivalent drawers away from the diversion locations. These foils away from the diversion points provided reference spectral-index data points for essentially unperturbed regions of the core. Figure 17 gives the core-loading pattern for the foil-irradiation experiment. The x's indicate drawers in which polyethylene was substituted for fuel, and the o's indicate drawers which contain an indium foil.

The indium foils were 1.27 cm in diameter and 0.0127 cm thick. The foils were held in 0.051-cm-thick stainless steel holders. The holders were placed in the drawers parallel to the fuel or coolant plates. Each foil was placed adjacent to the central plate of the drawer, and each foil was 7.62 cm from the axial midplane. The foils were irradiated at a power of approximately 800 watts for 15 minutes. The reactor control rods were withdrawn from their positions during the reactivity measurements to permit the higher power operation. At 800 watts, the total neutron flux near the core center was approximately 8×10^9 neutrons cm^{-2} sec^{-1}. After about a two-hour cooling period, the foils were removed from the core. The foils were then placed in other holders for counting. Two Ge(Li) detectors with automatic sample changers were used to count the 41 foils. Total count time for the 41 spectra was approximately 20 hours. Several spectra were obtained for each sample.

The results for the simulated diversion near the core center are shown in Fig. 18. The horizontal cross-hatch marks indicate a drawer in which polyethylene was substituted for fuel. The numbers at the drawer locations are the ratios of the intensities of the (n,γ)-product gamma rays to the (n,n')-product gamma rays. The intensities were corrected for decay from the time of reactor shutdown. The larger the value of the spectral index, the greater the (n,γ) contribution, and hence, the softer the spectrum. The average value of the spectral index (s.i.) for the 13 foils in drawers in the relatively unperturbed region was 62.3, with a standard deviaton (1σ) of 3.0. The s.i. values of the foils located in the drawers with polyethylene were quite high. The third drawer removed (both horizontally and vertically) from the diversion site had an s.i. which was more than 2σ higher than the s.i.'s in the unperturbed region. The s.i. in the fourth drawer was not significantly higher than the average for the unperturbed region. One of the foils in the unperturbed region also had an s.i. value of 70, which was more than 2σ higher than the average for the region. This value may have been high due to its proximity to the diversion site and to the rather large amount of intervening sodium with its low absorption cross section.

The results for the simulated diversion at the edge of the outer core are shown in Fig. 19. The diagonal cross hatch marks indicate a drawer in which polyethylene was substituted for fuel. The average value of the s.i.'s for the unperturbed region was 49.7 with a standard deviation (1σ) of 3.6. Again, the foil in a drawer containing polyethylene had a very large value of the s.i. The value of the s.i. is significantly higher than the unperturbed average value for only the two drawers adjacent to the diversion site, with the possible exception of the third drawer below the diversion. It appears that the foils are slightly less sensitive to the presence of the polyethylene at the core edge than at the core center, although that conclusion may not be justifiable from this small amount of evidence.

DISCUSSION

Autoradiography can provide a piece count of fuel elements in fast critical assembly drawers, and can also provide a simultaneous verification of the loading pattern in the reactor core. Autoradiography is an in-situ technique which requires no handling of fuel elements or reactor drawers, and a large number of drawers can be examined in a short time. Passive autoradiography, presently applicable only to plutonium fuels, can be used to examine any desired fraction of the reactor drawers. Because the passive autoradiographic images are produced mainly by radiation from Am-241, the verification of the fissile content of

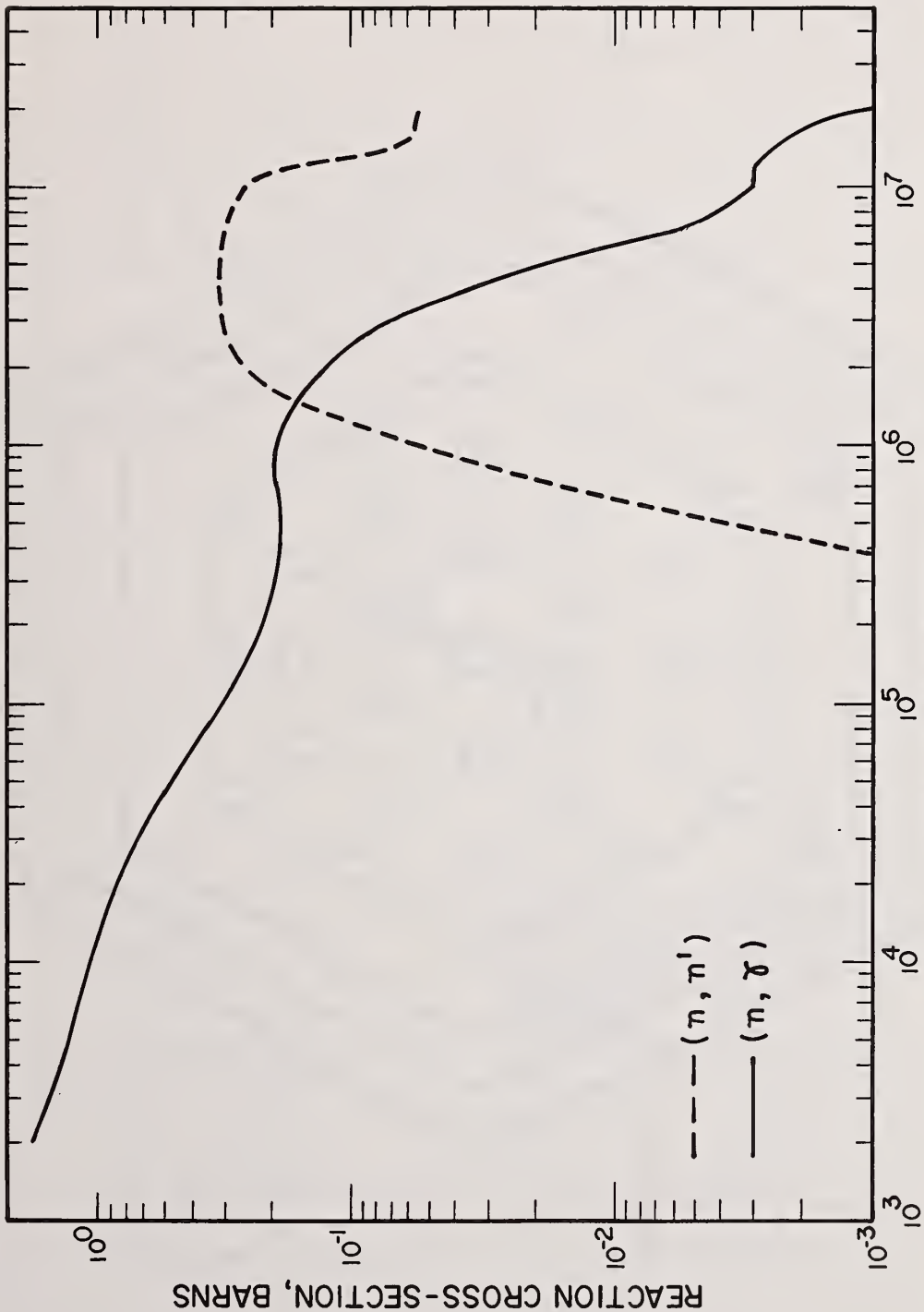

Fig. 16. Cross Sections of the In-115 (n,γ) and In-115 (n,n') Reactions as a Function of Neutron Energy

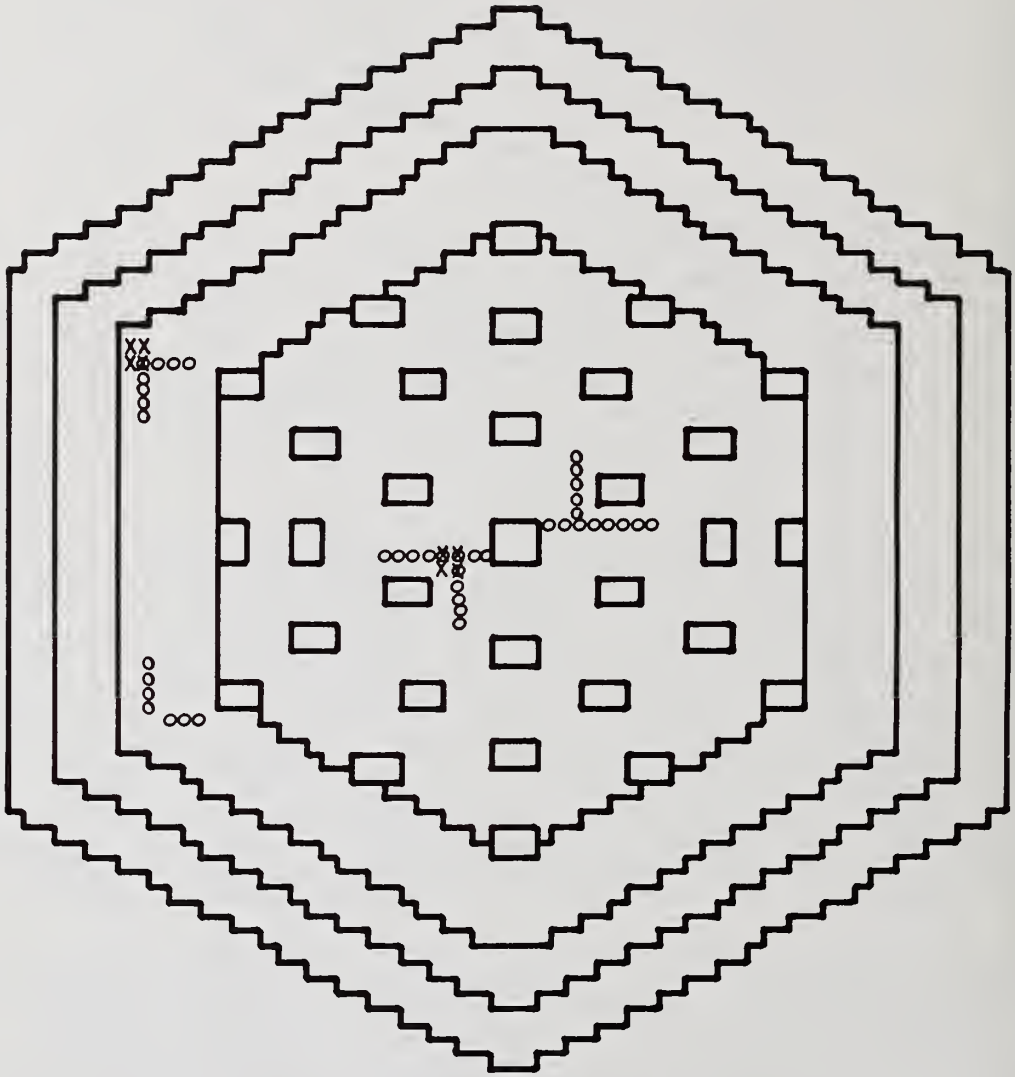

Fig. 17. Indium Foil Loading Pattern

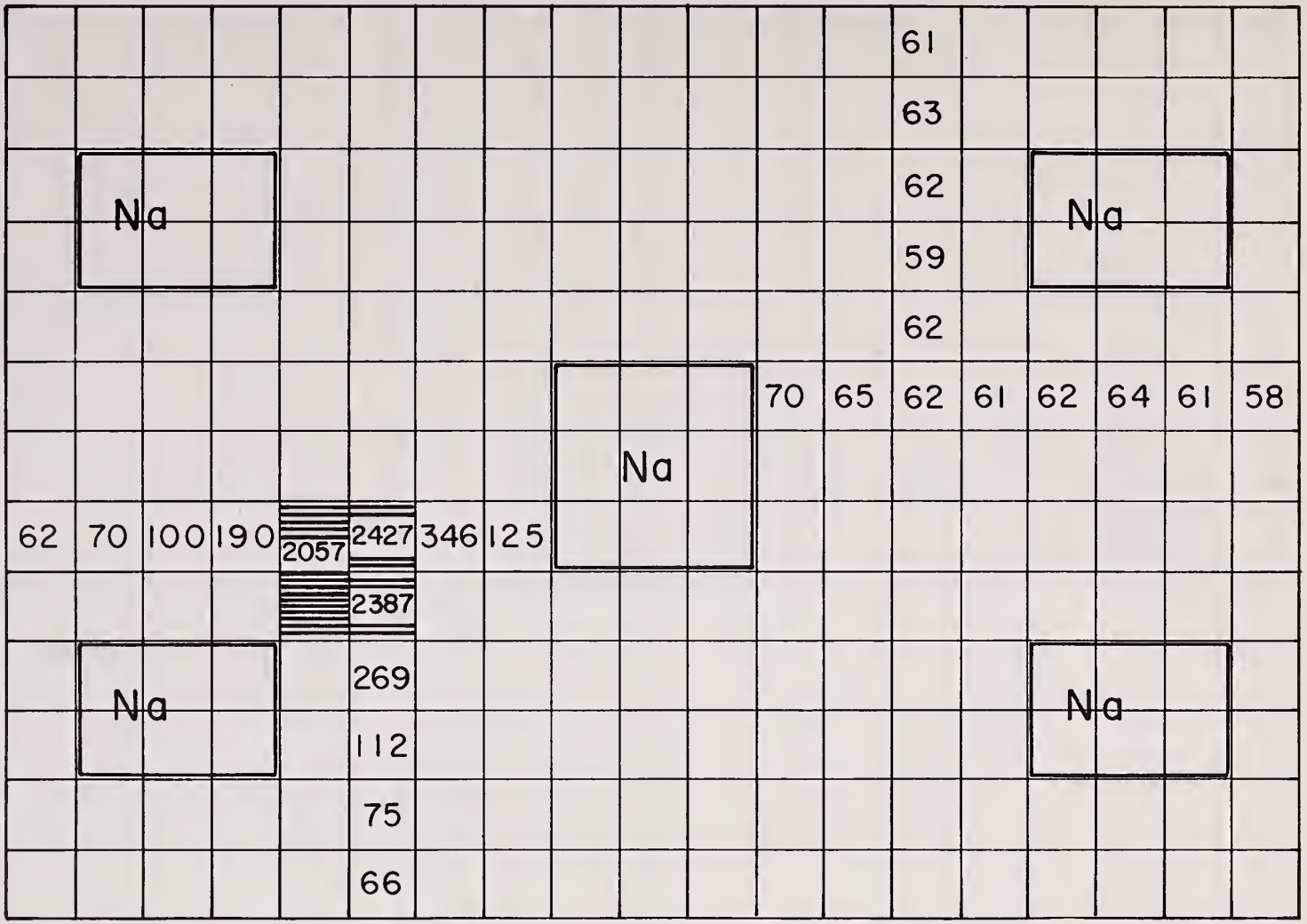

Fig. 18. Spectral Index Values Near the Core Center

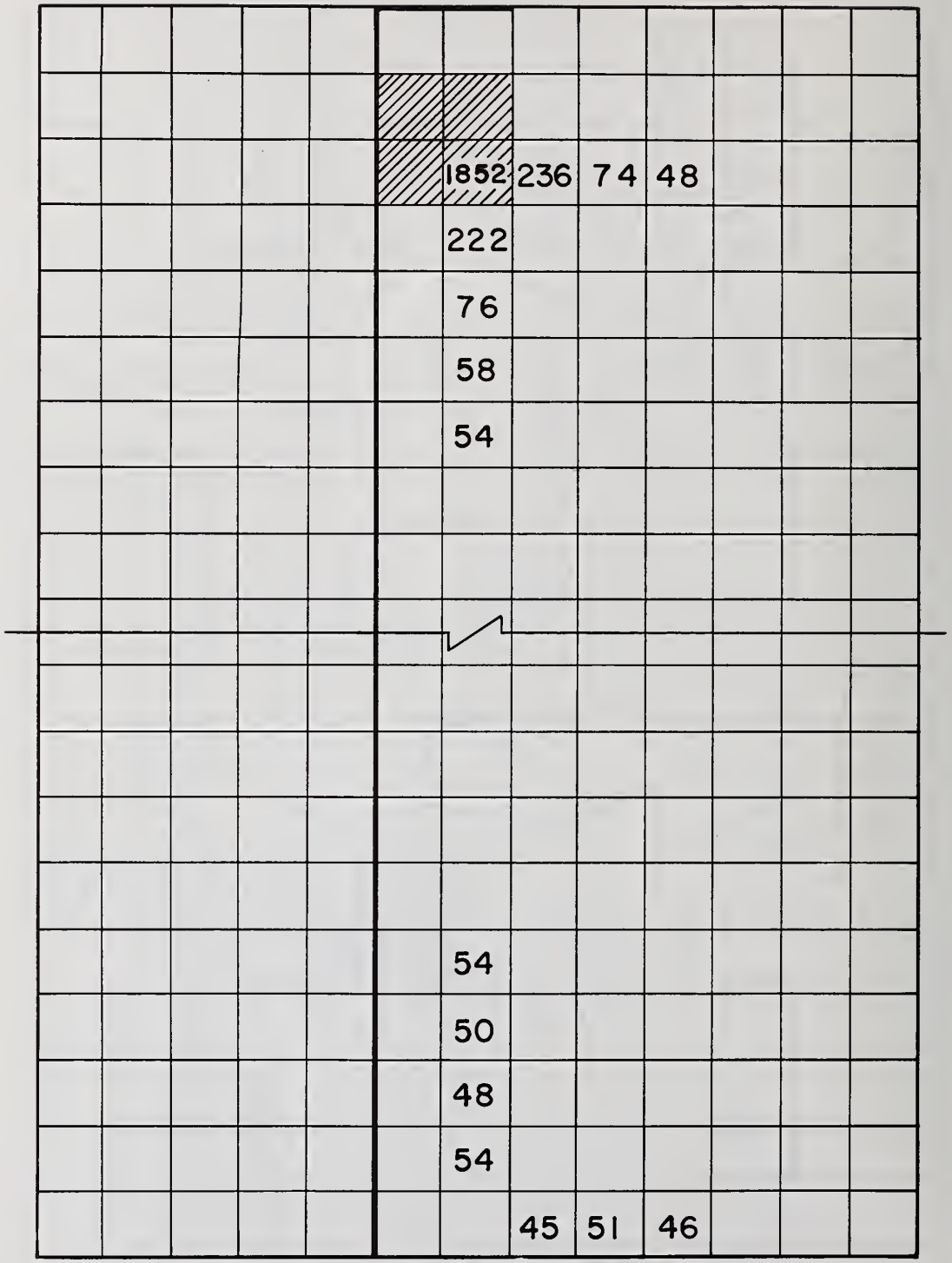

Fig. 19. Spectral Index Values Near the Core Edge

fuel elements is indirect. However, for the active technique, the fuel element images are the direct result of the fissile content of the fuel elements and of the presence of a critical mass in the reactor. The film itself may have a positive reactivity effect that must be considered when planning an active autoradiographic inventory verification. Any reactivity effect must also be considered when interpreting the results of an active autoradiographic inventory.

Passive autoradiography is not presently practical for in-core uranium application. Further work is needed to explore the possibility of adapting existing passive autoradiographic techniques to the in-core uranium problem. The availability of a passive technique is important for verifications when the assembly cannot easily be brought into a critical configuration.

The application of active autoradiography to plutonium-fueled cores is more complicated than it is for uranium-fueled cores because of the approximately equal image densities for the clad plutonium plates and the unclad U-238 plates and because of the large contribution to fuel-plate images from spontaneous radiation. More data is needed to better evaluate the active autoradiographic technique for plutonium-fueled cores. However, the present passive technique is quite adequate as a companion technique to reactivity measurements and foil irradiations.

The reactor power required for film exposure in an active autoradiographic verification is sufficient to activate indium foils. Both the products of the (n,γ) and (n,n') reactions are produced in sufficient concentration with approximately a 100-watt-hour irradiation of the 6100-liter ZPPR. The 100-watt-hour irradiation is recommended for active autoradiography in a core with a volume of 6100 liters. The simultaneous foil irradiation and film exposure is expected to be applicable to uranium-fueled cores.

The results of the integral reactivity measurements have indicated that these measurements are indeed sensitive to the removal of small quantities of fissile material from fast critical assembly cores. The great attractiveness of the integral reactivity measurement lies in its ability to provide a quantitative estimate of the fissile content of an entire core in a single measurement requiring approximately two hours. This measurement time assumes that the reactor is already in its reference configuration. Depending on the degree of deviation from a reference configuration, the time required for a reactivity verification could be significantly longer than a few hours. The use of reference reactivity measurements requires an independent verification of the core contents upon initial reactor loading. The detection sensitivity to the 2.0 - 2.5 kg (fissile) simulated diversion was well outside measurement uncertainties for all but the fourth simulated diversion which was made in a zone of minimum fissile worth. These results were particularly encouraging in view of the IAEA detection-sensitivity goal of 8 kg (fissile).

The attempt to compensate for reactivity loss from fuel removal by substitution of polyethylene was not successful. In the only case where both a compensated and an uncompensated diversion was made (diversions 1 and 2), the compensated diversion actually resulted in a lower reactivity than did the uncompensated case. All other diversions were made with polyethylene substituted for fuel. This reactivity decrease with the addition of moderator was attributed to increased neutron capture in nearby absorbing materials (e.g., U-238). This increased absorption resulted in a reduction in the total neutron flux and consequently in a reduction in the fission rate in fuel several drawers away from the substitution where the nearest fission counters were located. In the third simulated diversion, a fission counter was in a drawer adjacent to a drawer containing polyethylene, and this fission counter showed a much higher relative fission rate than it did in the reference case. This high fission rate was attributed to the high counter sensitivity to low-energy neutrons and to the presence of a relatively large number of low-energy neutrons close to the polyethylene. These low-energy neutrons were not absorbed because of the relatively small amount of absorber material between the polyethylene and the fission counter. Fission counters four drawers removed from polyethylene substituted for fuel showed reduced relative fission rates. These observations with fission counters were supported by the foil-irradiation experiments which indicated that the effects of the polyethylene had a short range. The polyethylene-induced effect on flux was not detectable four drawers away in the inner core, and was not detectable three drawers away at the core edge. In both regions, the effect was readily detected in the adjacent drawer.

In the fifth simulated diversion, polyethylene was substituted for U-238 in fuel-containing drawers. The reactivity effect for this substitution was positive and the effect was observed by fission counters more than four drawers away. The reactivity effect resulted from the removal of U-238 absorber and addition of moderator. No measurements were made to evaluate the effects of U-238 removal alone.

The combined results of the reactivity measurements and the foil-irradiation measurements do seem to suggest that the most effective way to conduct a reactivity-measurement-based verification is to place the indium foils in drawers directly adjacent to the fission counters. This tactic appears to have the best chance of detecting the substitution, or the addition, of moderator to compensate for the removal of fissile material. If a diverter wants to substitute moderator for fuel to cover up the removal of fuel, he must do so close to the fission counter. However, if this substitution is close enough to the fission counter to compensate for the fuel removal, it is likely to be close enough to the indium foil to have a detectable effect on the spectral index.

One other conclusion which can be drawn at this point is that it is not a trivial problem for a diverter to devise a reactivity-compensation scheme. An extensive series of test diversions and compensations would be needed to cover up for any significant fuel removal, especially if 64 fission counters with 64 accompanying spectral-index-measuring foils were used in a verification measurement. Such a diversion and cover-up may be possible for an entire facility working together, but would be exceedingly difficult for an individual, or even a few individuals in collusion.

The applicability of reactivity measurements and other reactor operating parameters to safeguards purposes was studied previously by Gryazev[12,13] at the small, highly enriched uranium-fueled fast critical assembly SPEKTR. In their experiments, Gryazev, et al., made simulated diversions by removing uranium fuel and compensated for the reactivity loss by adding moderator in various parts of the core. They found that they could completely compensate for fuel removal by replacing uranium-containing elements with polyethylene elements. In these experiments, Gryazev measured the fundamental harmonic decay constant for a subcritical configuration whose reactivity was held constant by additions of moderator. Deviations of this decay constant from reference values were due to changes in the prompt neutron lifetime. Compensated diversions as small as 1.5 kg U-235 were detected.

The evaluation presented here of the reactivity measurement as a safeguards technique for fast critical assemblies has been limited to strictly technical considerations, such as detection sensitivities and measurement uncertainties. Another type of evaluation should be mentioned, at least in passing, when considering the application of reactivity measurements to international safeguards. This second type of evaluation concerns the practical application of the method by inspectors who are outsiders at a fast critical assembly, and it also concerns the degree to which reactivity measurements can be made truly independent of the facility and, hence, credible to an outsider. The experiments described here relied on in-core fission counters to obtain reactivity data. Fission-counter output was fed into scalers which were then read by a digital computer which, in turn, calculated reactivities. It would be extremely difficult for an international inspector to assure that all aspects of the fission-counter data-collection and -processing system were working properly and had not been subject to tampering. The practicability of inspectors' supplying their own instrumentation in the form of in-core or outside-core detectors should be considered, but is likely to be a difficult problem.

The foil irradiation techniques used to obtain spectral indices are relatively independent of the facility. The inspector can supply his own foils, can insert them into and remove them from the assembly drawers himself, and can use his own gamma-ray spectrometer to obtain the reaction-rate ratios. It is necessary to make reference spectral-index measurements throughout the reference core when it is first established because spectral indices will vary with location within the core. Foil-irradiation measurements require that the core be capable of producing relatively high fluxes (10^9 - 10^{10} neutrons cm^{-2} sec^{-1}).

The indium reaction products used in these experiments had half-lives of 54 minutes and of 4.5 hours. Because of the gamma-detectors and automatic sample-changing equipment, the 41 foils could be counted quickly enough to make the 54-minute half-life isotope useful.

Inspectors may find it difficult to utilize this isotope because of its short half-life. Several other (n,γ) reactions can be substituted for the In-115 (n,γ) reaction.

Gryazev[11] also studied the application of spectral-index measurements to the detection of moderator-compensated diversions. His spectral index was the ratio of the Au-197 (n,γ) reaction rate to the In-115 (n,n') reaction rate. He found that he could detect polyehtylene-compensated diversions 10 cm away from the point of diversion. This detection range of 10 cm was similar to that observed in the experiments reported here (diversion detectable at least two drawers away -- each drawer ~ 5 cm wide). Gryazev also used foil activation as a neutron flux measuring technique. A flux measuring technique using foils would probably require a prohibitively large number of foils in the large ZPPR cores.

The methods described here for measuring reactivity and for verifying the neutron-energy spectra are only examples of many methods available. Reactivities can be determined by measuring reactor period, or by such perturbation techniques as rod drop or rod oscillation. If external neutron sources are used, reactivities can be determined by a source-jerk technique or by fundamental-mode decay-constant measurements. The source-multiplication technique used in these experiments is applicable as described only for plutonium-fueled cores because the neutron source is the spontaneous fission in the even Pu isotopes. A similar technique could be applied to uranium-fueled cores by introducing some other neutron sources.

Several techniques are available for neutron-energy spectrum verification in addition to the foil-irradiation methods described here. Reactivity worths can also serve as spectral indices, and Gryazev[12] has successfully applied U-238 and boron worth measurements to the detection of compensated diversion in the SPEKTR fast critical assembly. The prompt neutron lifetime is also sensitive to changes in the neutron-energy spectrum. Estimates of prompt neutron lifetimes can be obtained from reactor-power noise measurements or from fundamental-mode decay-constant measurements at constant reactivity.

Each of the three techniques described here -- autoradiography, foil irradiation, and reactivity measurement -- have individual strengths which make them useful as inventory verification techniques, and have individual weaknesses which make them vulnerable to defeat by specific diversion scenarios. The roles of the various inventory verification techniques will be determined, in part, by the credibility of various postulated diversion strategies. For example, passive autoradiography of plutonium fuel in reactor drawers may possibly be vulnerable to defeat by radioactive "dummy" fuel elements which do not contain fissile material. A diversion scenario involving the fabrication of "dummy" fuel elements may be credible in international safeguards problems, and passive autoradiography would be combined with foil irradiation and/or reactivity measurements. However, fabrication of "dummy" fuel elements is much less credible when considering diversion by individuals or groups of individuals so that passive autoradiography may require less support in domestic safeguards applications.

Reactivity measurements have the advantage of great sensitivity to changes in the fissile content of a reactor. The entire core can be examined in a single measurement. However, because of the possibility of reactivity compensation by changes in core geometry, or by the substitution of non-fissile materials with positive reactivity worth, reactivity measurements must be supported by other techniques. If changes in core configuration or core composition are considered credible diversion scenarios, the autoradiography can verify the core loading pattern while foil irradiation measurements can, with some limitations, verify the core composition. Similarly, the foil irradition technique is not very sensitive to core geometry and thus needs to be supported by autoradiography.

The potentially greatest assurance of diversion detection lies in a combination of all three inventory verification techniques. If the reactivity measurements are considered too facility dependent to be credible, then the relatively facility-independent autoradiographic and foil irradiation technqiues should be used in combination. Only autoradiography can be applied to cores which are substantially subcritical.

REFERENCES

1. D.D. Cobb, J.L. Sapir, E.A. Kern, and R.J. Dietz, "Concepts for Inventory Verification in Critical Facilities", LA-7315 (1978).

2. D.O. Gunderson and J.L. Todd, "International Safeguards for Fast Critical Facilities", SAND 78-0168 (1978).

3. S.B. Brumbach and R.B. Perry, "Autoradiography as a Safeguards Technique for Plutonium Fuels", ANL-NDA-2, ISPO-49, (1979).

4. S.B. Brumbach and R.B. Perry, "Autoradiography as a Safeguards Inspection Technique for Unirradiated LWR Fuel Assemblies", ANL-78-27, ISPO-12 (1978).

5. G. Robert Keepin, Physics of Nuclear Kinetics, (Addison-Wesley, Reading, Mass., 1965).

6. W.G. Davey and W.C. Redman, Techniques in Fast Reactor Experiments, (Gordon and Breach, New York, 1970).

7. J.J. Duderstadt and L.J. Hamilton, Nuclear Reactor Analysis, (Wiley, New York, 1976).

8. S.G. Carpenter, H.F. McFarlane, M.J. Lineberry and C.L. Beck, "Conclusions Drawn from Subcritical Multiplication Results in ZPPR", Adv. Reac. Phys; Proceedings of ANS Topical Meeting, Gatlinburg, Tenn., April 10-12, 1978.

9. R.W. Peele and F.C. Maienschein, "Spectrum of Photons Emitted in Coincidence with Fission of U-235 by Thermal Neutrons", Phys. Rev. C, Vol. 3, p. 373 (1971).

10. R.L. Heath, "Gamma-ray Spectrum Catalogue", ANCR-1000-2.

11. V.M. Gryazev, "The Development of Methods and Procedures for Monitoring the Amount of Nuclear Materials in the Core of the SPEKTR Critical Assembly on the Basis of the Spectral Characteristics of the Neutron Flux", translated from Russian, IAEA unpublished data (1978).

12. V.M. Gryazev, "Development of Procedures and Techniques for Verifying the Quantity and Composition of Nuclear Materials at the SPEKTR Fast and Thermal Neutron Critical Facility", translated from Russian, IAEA unpublished data (1974).

13. V.M. Gryazev, "Experiments with a Nuclear Materials Accounting and Control System on the SPEKTR Fast-Thermal Critical Assembly", translated from Russian, IAEA unpublished data (1976).

Discussion:

Fainberg (BNL):
Were you more or less sensitive to the drawers in the central region?

Brumbach (ANL):
That was a region of greatest senstivity. We removed fuel also from regions of lower sensitivity and, in fact, we removed the fuel from four drawers at the core blanket interface, the same amount of fissile material. There the reactivity decrease was 2%, rather than 16%. So, we saw a reduction by a factor of 8 in sensitivity by removing from the core blanket interface rather than the core center. When we went to the corner of the core it dropped by another factor of two, which is about what you'd expect looking at that plot of reactivity worth as a function of position.

Fainberg:
So when it comes to the least sensitive region, the 2-kg are barely detectable.

Brumbach:
Two kilograms were at two sigma at the core blanket interface.

Green (BNL):
Steve, do you see combining these techniques into a procedure for independent IAEA verification?

Brumbach:
I see considerable promise for the foil irradiation method combined with film. I suspect that the IAEA will not have much enthusiam for measuring reactivity, if for no other reason than the fact that it is very facility-dependent. If one were to work at it, one might be able to come up with something that would be facility independent, but you would have to work at it pretty hard.

Persiani (ANL):
I would like to make a comment on that. You are not going to have very many critical facilities. The IAEA could certainly do a determined study of those facilities that are available, and these would be finite in number.

Brumbach:
Well, it would be three or possibly four. I still think it would be hard -- not impossible, but I think it would be difficult.

Nilson (Exxon Nuclear):
There is a related subject here which is the light water reactor systems. It is possible to detect a defect in the loading of 75-kg, ^{235}U, in low-enriched uranium by the reactivity in the reactor. This same technique could thus be used for power reactors. It is very sensitive, and might be something that the Agency could do. The operator always measures reactivity of the reactor after refueling to make sure they get the right loading. It is very sensitive to diversions of this size.

New Developments in Nondestructive Measurement and Verification of Irradiated LWR Fuels

by

DAVID M. LEE, JOHN R. PHILLIPS, JAMES K. HALBIG, SIN-TAO HSUE,
LLOYD O. LINDQUIST, EVITA MEDINA ORTEGA, JAMES C. CAINE, AND JAMES SWANSEN
Los Alamos Scientific Laboratory, Los Alamos, New Mexico 87545

and

KEISUKE KAIEDA
Japan Atomic Energy Research Institute, Tokyo, Japan

and

ELMIR DERMENDJIEV
International Atomic Energy Agency, Vienna, Austria

ABSTRACT

Nondestructive techniques for characterizing irradiated LWR fuel assemblies are discussed. This includes detection systems that measure the axial activity profile, neutron yield and gamma yield. A multi-element profile monitor has been developed that offers a significant improvement in speed and complexity over existing mechanical scanning systems. New portable detectors and electronics, applicable to safeguard inspection, are presented and results of gamma-ray and neutron measurements at commercial reactor facilities are given.

KEYWORDS: Nondestructive assay, ion chamber, fission chamber, axial profiles, irradiated (spent) fuel, instrumentation

INTRODUCTION

Nondestructive assay (NDA) methods for the determination of the fissile content of irradiated nuclear fuels are needed to detect diversions of fissile materials to weapons use. At the present time an applicable nondestructive technique does not exist for directly measuring the fissile content of irradiated fuel assemblies. Instead, the fissile content is normally inferred from indirect measurements of the burnup by using gamma-ray or neutron signatures.

Gamma-ray spectrometry has been investigated as a measurement technique for determining the burnup of irradiated fuels.[1-4] This method requires a high-resolution germanium detector, a multichannel analyzer system and a mechanical scanning system and collimator assembly. Through these investigations the fission products, ^{137}Cs, ^{144}Ce-Pr, and ^{106}Ru-Rh and fission product ratios $^{134}Cs/^{137}Cs$ and $^{154}Eu/^{137}Cs$ have been identified as possible burnup monitors. One limitation of this technique is that the intensities of gamma rays from the interior of the assemblies are substantially attenuated by the relatively dense fuel rods.

Gross-gamma measurements are an alternative to gamma spectrometry. Although the measurement is not able to differentiate the presence of specific fission products, it does sense the high radiation field that must be present in a spent fuel assembly. The measurement is also relatively insensitive to the interior rods because of attenuation.

Passive neutron assay has been identified as a potentially useful inspection assay method of spent fuel in a recent review[2,3] and in the IAEA Advisory Group Meeting.[4] Two aspects make the passive neutron measurement technique particularly attractive for the measurement of spent fuel assemblies. First, neutrons are less subject to self-absorption in the fuel assembly than are gamma rays. Monte Carlo calculations have shown the interior rods of PWR assemblies contribute nearly the same amount to the total neutron emission rate as the exterior rods.[5] Therefore the neutron measurement is more sensitive to all the interior pins in the fuel assembly than is the gamma-ray spectrometry measurement. Secondly, the passive neutron measurement requires very simple electronics and a neutron detector and this simplicity can be a distinct advantage in the hostile environment of a spent fuel storage facility.

In many instances when safeguards inspections are performed,the preferred NDA techniques should be simple to use; portable, easily carried from site to site; and provide rapid and reasonably accurate assays. In other cases, more detailed information is required. This can occur at away from reactor storage facilities (AFRs) and reprocessing plants where NDA methods can be used for criticality control and shipper-receiver verification. Such in-plant instrumentation must be unobtrusive and the measurements rapid enough to not interfere with normal operating routine of the facility.

As part of its on-going investigations into NDA techniques, the Los Alamos Scientific Laboratory International Safeguards Group has been actively investigating NDA methods for the characterization of spent fuel. We have performed investigations into high-resolution gamma-ray spectrometry, passive neutron assay, and gross-gamma measurements. These investigations included burnup correlations, new detector developments, and electronic development.[5-9]

This paper will address some of the more recent developments in this program. We will discuss various methods for the measurement of activity profiles, new detection systems, and portable electronics for safeguards inspections and in-plant assay. Results of experiments at BWR and PWR facilities will be given.

AXIAL ACTIVITY PROFILE

Since the axial burnup of LWR fuel assemblies depends on many factors such as axial power levels, burnable poison rods, control rods, and core locations, the axial burnup will not necessarily be the same from one fuel assembly to another. It is therefore necessary to determine the axial burnup profile of each fuel assembly if an accurate measure of the integral burnup is desired. In addition, if a rapid technique for accurately measuring the axial burnup profile of a fuel assembly can be developed, then a detailed measurement can be performed at one position and related to the entire assembly by using the profile as an integrating function.

We have measured the axial activity profile of both BWR and PWR fuel assemblies with a high-resolution gamma-ray system, a Be(γ,n) detector and an ion chamber. The typical experimental configuration for a reactor spent fuel storage facility is shown in Fig. 1. Complete gamma-ray spectra (500-2300 keV) were collected at specified axial positions on the fuel assemblies and analyzed for comparison to the other profile monitor systems. Also, the gamma-ray data was correlated with the operator-declared burnup values.

The Be(γ,n) detector (Fig. 2) is sensitive to gamma rays with energies greater than the 1660 keV threshold for photoneutron production in beryllium. Neutrons produced in the Be are thermalized by the polyethylene and are counted in the fission chamber. This particular detector is relatively insensitive to high gamma-ray fluxes. In a fission product spectra, the principal gamma ray with an energy above the 1660 keV threshold is the 2186 keV gamma ray of ^{144}Pr. The ^{144}Pr isotope has a very short half-life ($t_{\frac{1}{2}}$ = 17.3 min) and is in secular equilibrium with its parent ^{144}Ce ($t_{\frac{1}{2}}$ = 284.5 day). Therefore, the measured Be(γ,n) profile is essentially the profile of the ^{144}Ce axial distribution.

The ^{137}Cs activity from the germanium detector measurements correlated well with the declared burnup values and was used as the burnup monitor for the burnup profile. The ^{137}Cs burnup correlation is shown in Fig. 3 where the 95% confidence bounds are included. The average percent difference from the regression line is 5.1%. Similar results were obtained for the BWR fuel assemblies.

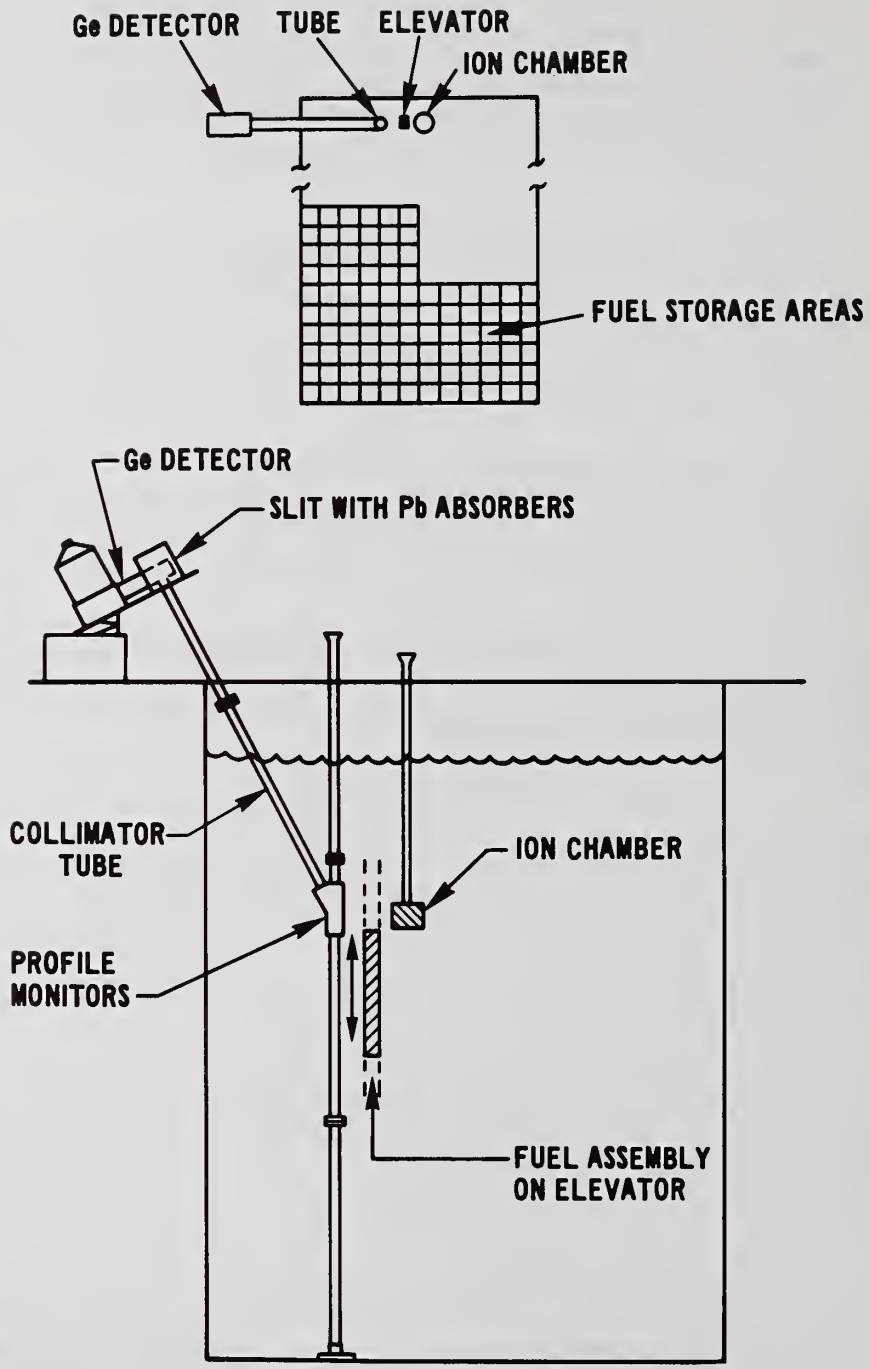

Figure 1
Schematic of experimental apparatus used to examine the LWR fuel assemblies.

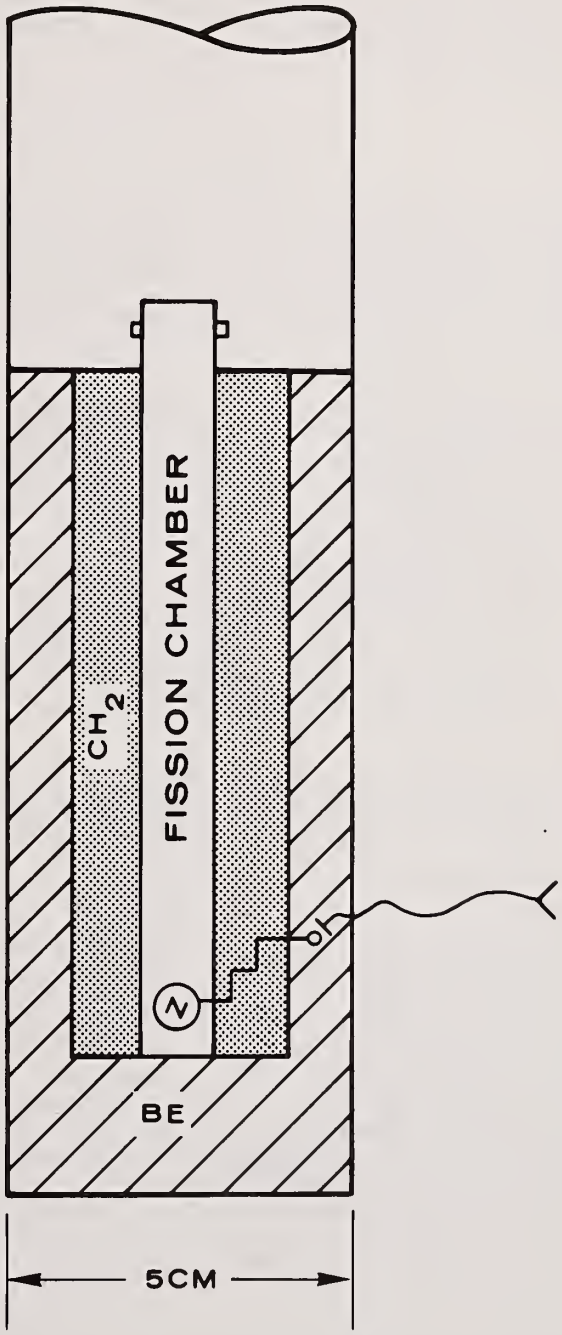

Figure 2
Be(γ,n) detector for measuring the high-energy (> 1660 keV) gamma activity profile.

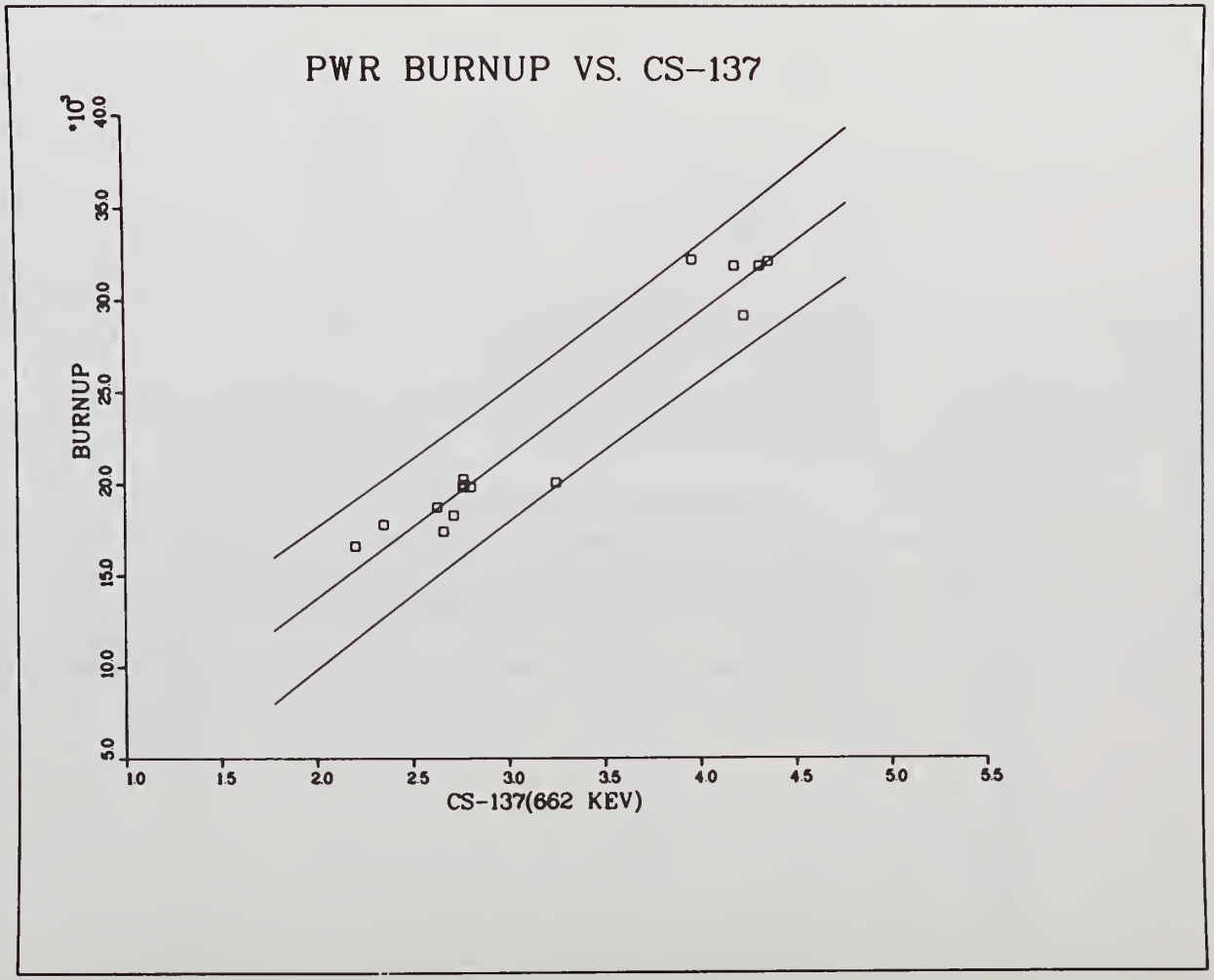

Figure 3
Correlation of the measured ^{137}Cs activities with the declared burnup values.

Typical PWR and BWR axial activity profiles are shown in Figs 4-7. The peak values in Figs. 4-7 were normalized to unity and since the detectors were not all at the same axial position, the profiles have been shifted so that the peak positions coincide. The agreement of the shapes of the ion chamber profiles with both the ^{137}Cs and the Be(γ,n) profiles are within the statistical uncertainties of the measurements. Typical measurement times for each point was approximately 5 min for the Be(γ,n) and germanium detector and approximately 10 s for the ion chamber. The speed of measurement of the ion chamber and the apparently good agreement with the ^{137}Cs profile (and therefore burnup) convinced us that a system could be designed that would eliminate the need for mechanical scanning yet maintain measurement times of approximately 10 s.

MULTIELEMENT DETECTOR

A prototype multielement detector has been designed for measuring the profile of fuel elements from a Materials Test Reactor (MTR) and is shown in Fig. 8. This detector contains fifteen identically constructed ion chamber elements equally spaced along its length (90 cm). The dose from fission product gamma rays is sensed as a current in each ion chamber element and multiplexed by portable instrumentation. The offset current of each element has been measured to be 5×10^{-12} amps.

A block diagram of the microprocessor-based portable electronics for the multielement detector is shown in Fig. 9. The current from each of the ion chamber elements is amplified by the current-to-voltage amplifier with as transfer gain of 10^{-8} A/V. These signals are multiplexed to an instrumentation amplifier whose gain is controlled by the microprocessor and digitized by the 256 channel A/D converter. The microprocessor performs numerous functions all initiated via the keyboard. It can collect and clear data, average data, provide signals for the display of the profile, calibrate the system, output data to a serial output, integrate the data between two cursor settings, monitor and change the high voltage, change the amplifier gain, and perform a programmable set of key functions. A photograph of the prototype electronics is shown in Fig. 10. The total volume of the electronics is approximately .027 m^3. It is possible by a change in software to redefine the functions of the keypad and, in addition, to permit the electronics to be operated under remote computer control.

The application of the multielement detector to BWR and PWR spent fuel is straightforward. Such a system is in the design phase for an AFR spent fuel storage facility, and will incorporate remote computer control features, neutron detector, and Be(γ,n) detectors.

APPLICATION OF GROSS GAMMA AND NEUTRON DETECTORS TO INSPECTION

Generally, large complicated systems such as high resolution gamma spectrometry (HGRS) and multielement profile monitors are not easily applied to routine safeguards inspection. HRGS normally requires that the spent fuel assembly to be examined be isolated from adjacent fuel assemblies. Such isolation is not only time consuming, but not always acceptable to the facility operators. In addition, the collimator assembly, scanning system (either mechanical or multielement), and locating system are expensive, cumbersome and not easily and quickly assembled at each reactor site. To circumvent these drawbacks, a detector system that requires minimum fuel motion and no collimation has been developed. We have constructed an annular (ring) detector that incorporates both a gross gamma measurement and a neutron measurement. This detector is shown in Fig. 11. It is divided into quadrants with a neutron detector and an ion chamber in each quadrant. This detector is designed so that the fuel assembly is positioned inside the annulus. The annular design is intended to minimize variations in signal response due to change in the fuel assembly to detector separation.

We have tested the ring detector on 36 spent fuel assemblies at a commercial PWR reactor storage facility. In this test, two different types of neutron detectors were examined, a B-10 lined and a fission chamber. Each type was placed in opposite quadrants. Both detectors were 2.54 cm diameter x 12.5 cm long. During the examinations the B-10 lined neutron detectors lost sensitivity, presumably because of the high-radiation fields present (10^3-10^5 R/h). Therefore, the neutron results are limited to the data from fission chambers. The results for this test are shown in Fig. 12 for the neutron measurements and Fig. 13 for the gross-gamma measurements. We have plotted the sum of the 2 neutron detectors in Fig. 12 and the sum of the 4 ion chambers in Fig. 13.

Figure 3
Correlation of the measured ^{137}Cs activities with the declared burnup values.

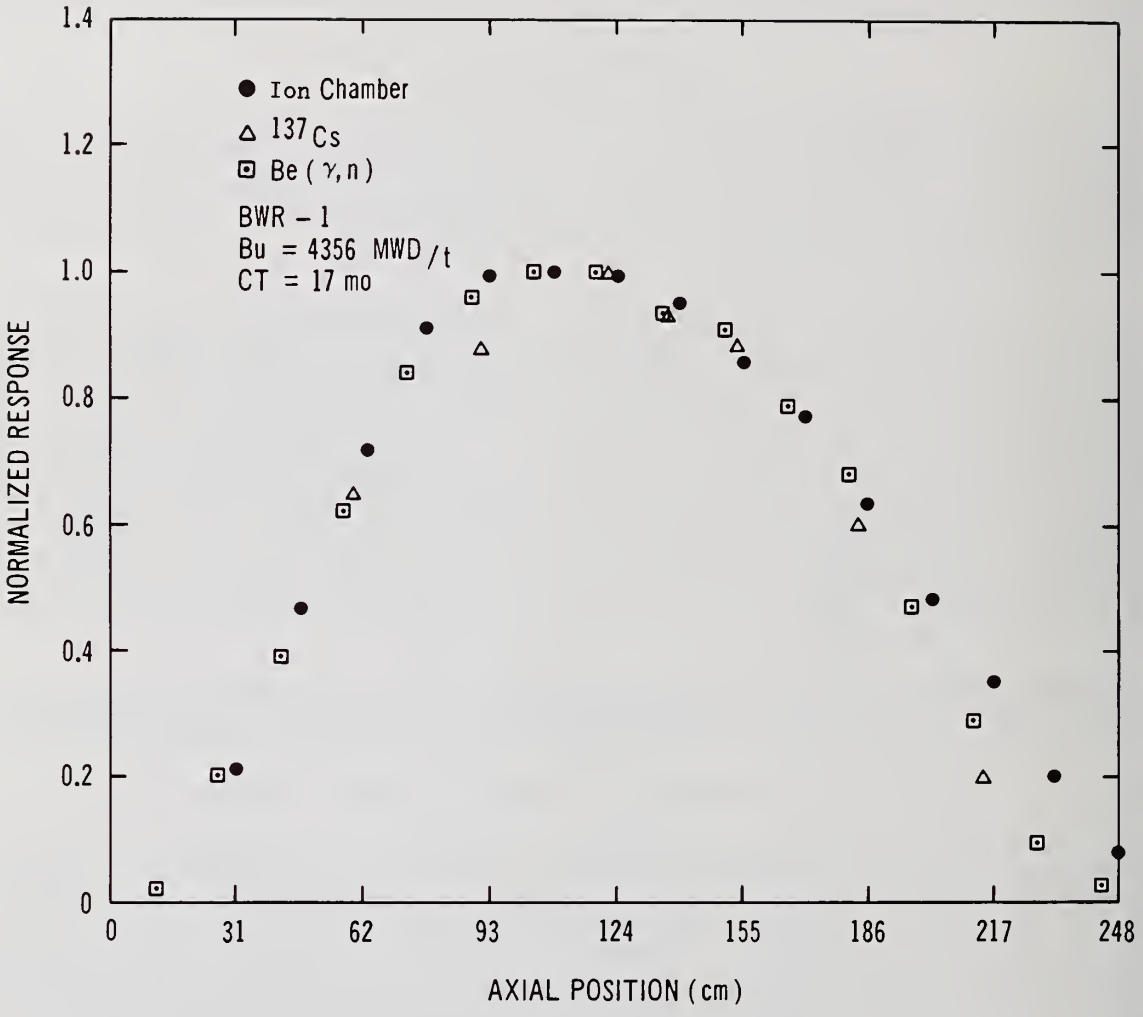

Figure 4
Typical BWR irradiated fuel assembly profile. Burnup is 4356 MWD/t and cooling time is 17 months.

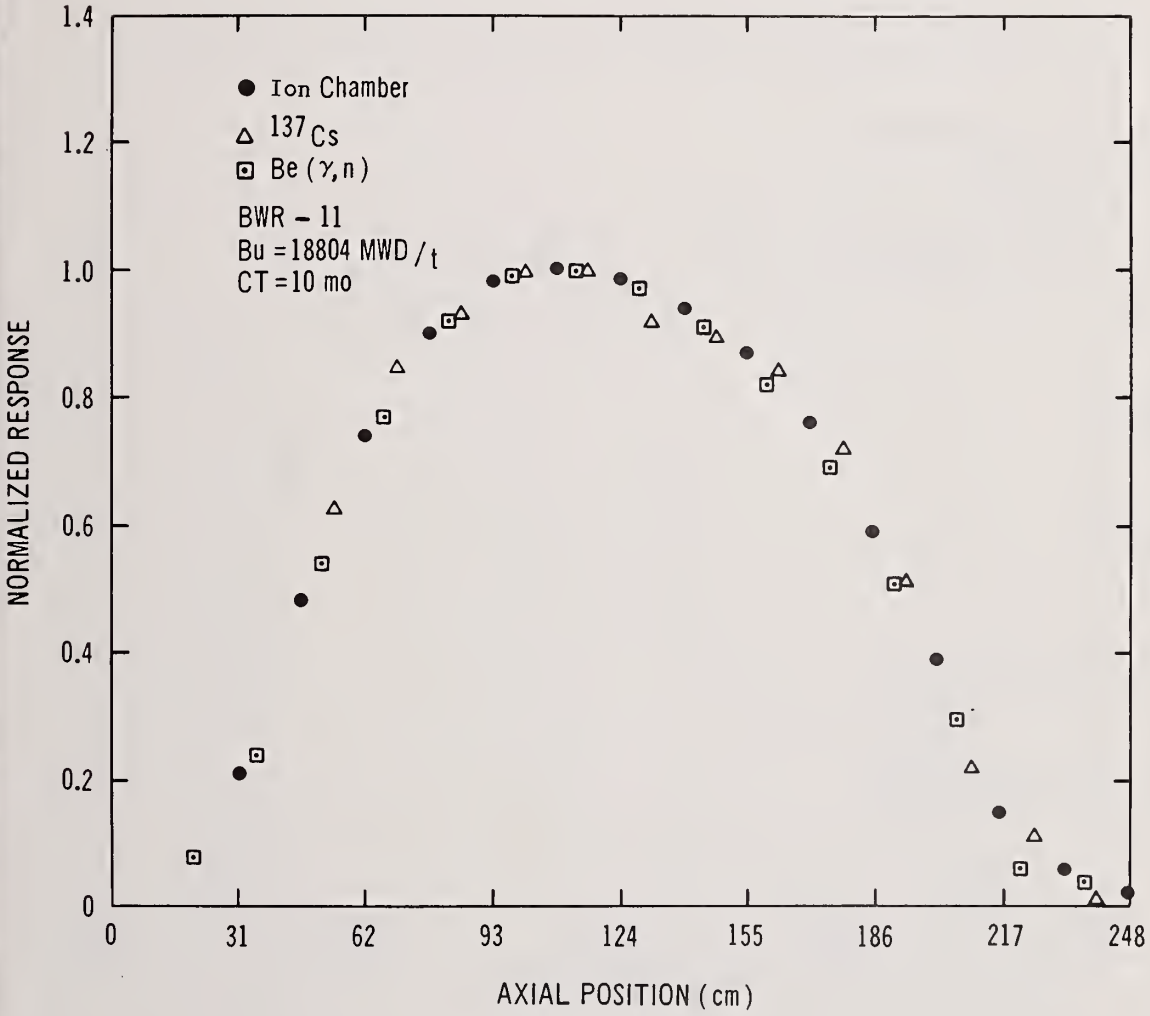

Figure 5
Typical BWR irradiated fuel assembly profile. Burnup is 18804 MWD/t and cooling time is 10 months.

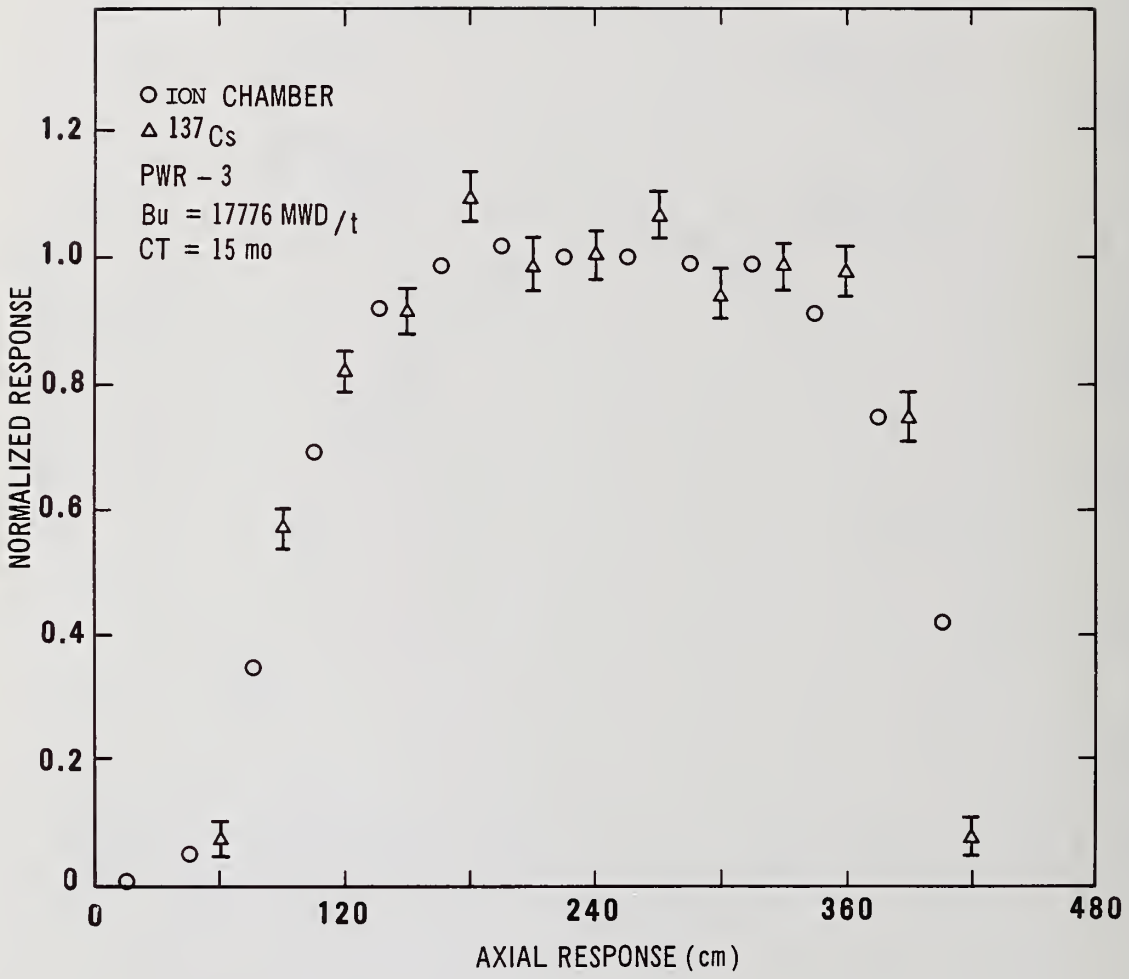

Figure 6
Typical PWR irradiated fuel assembly profile. Burnup is 17776 MWD/t and cooling time is 15 months.

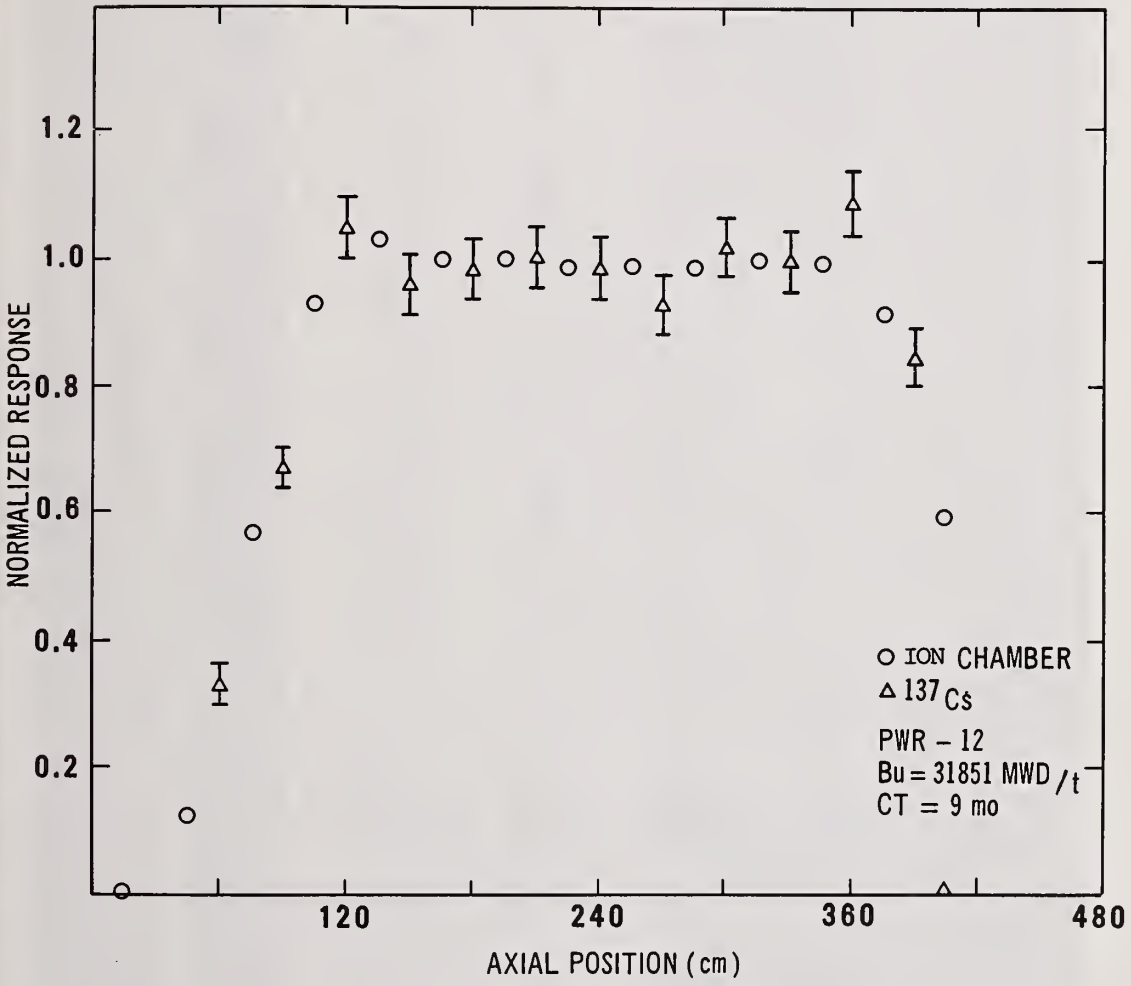

Figure 7
Typical PWR irradiated fuel assembly profile. Burnup is 31851 MWD/t and cooling time is 9 months.

Figure 8
Photograph of a multielement ion chamber for obtaining the axial gross-gamma profiles of irradiated MTR fuel elements.

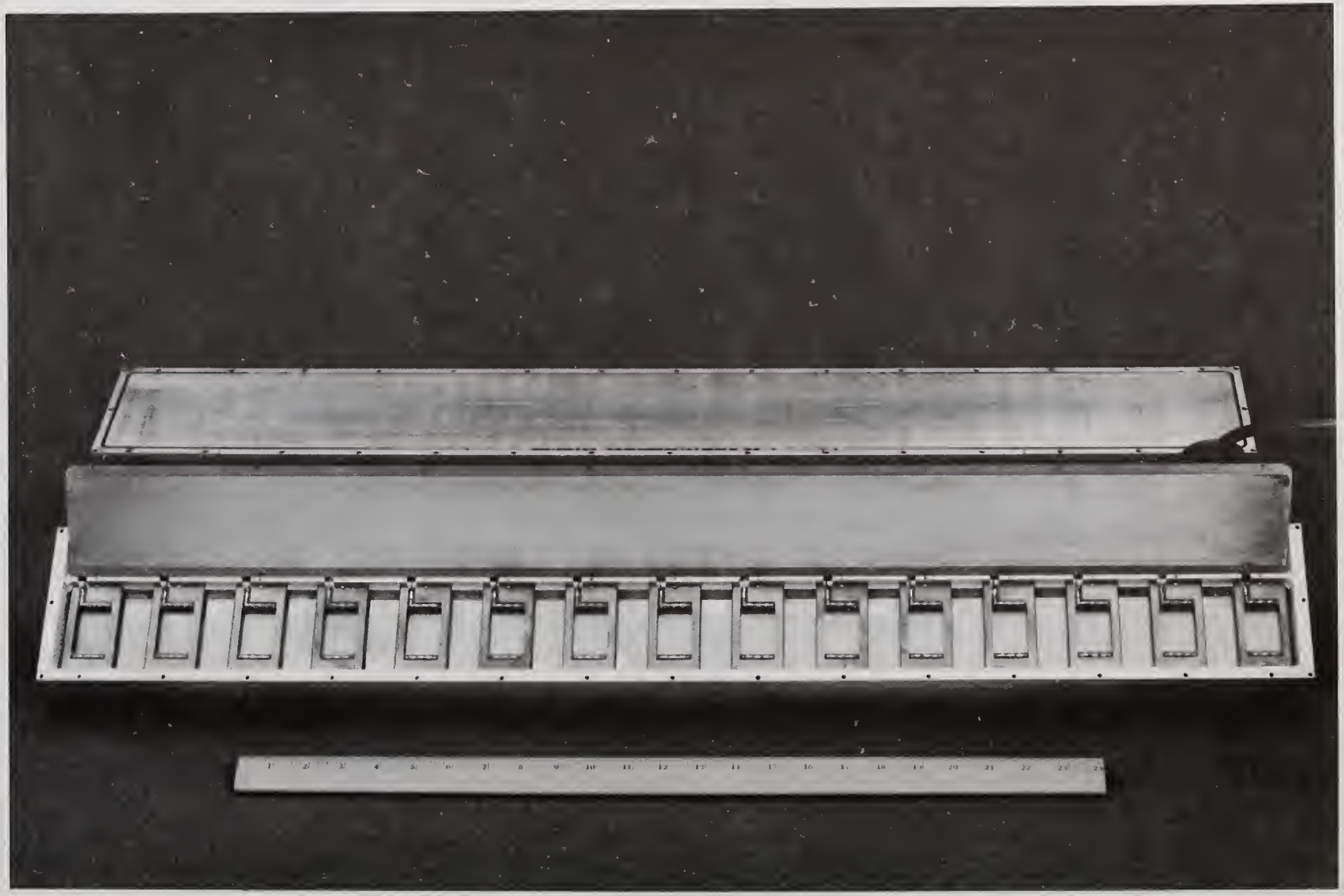

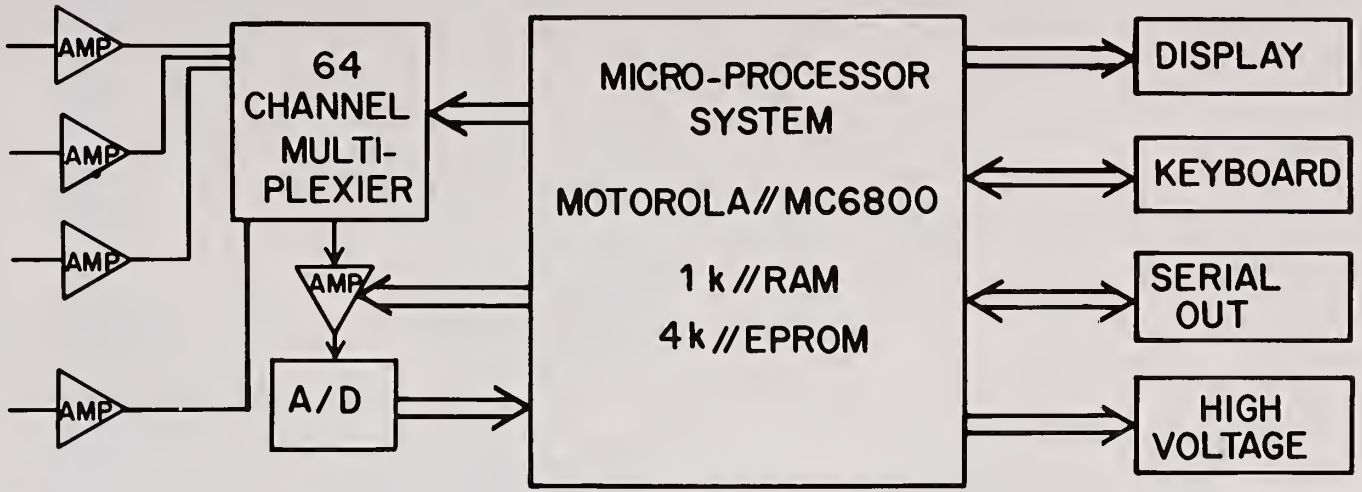

Figure 9
Block diagram of the microprocessor-based portable electronics for the multi-element profile monitor.

Figure 10
Photograph of the multielement profile monitor electronics.

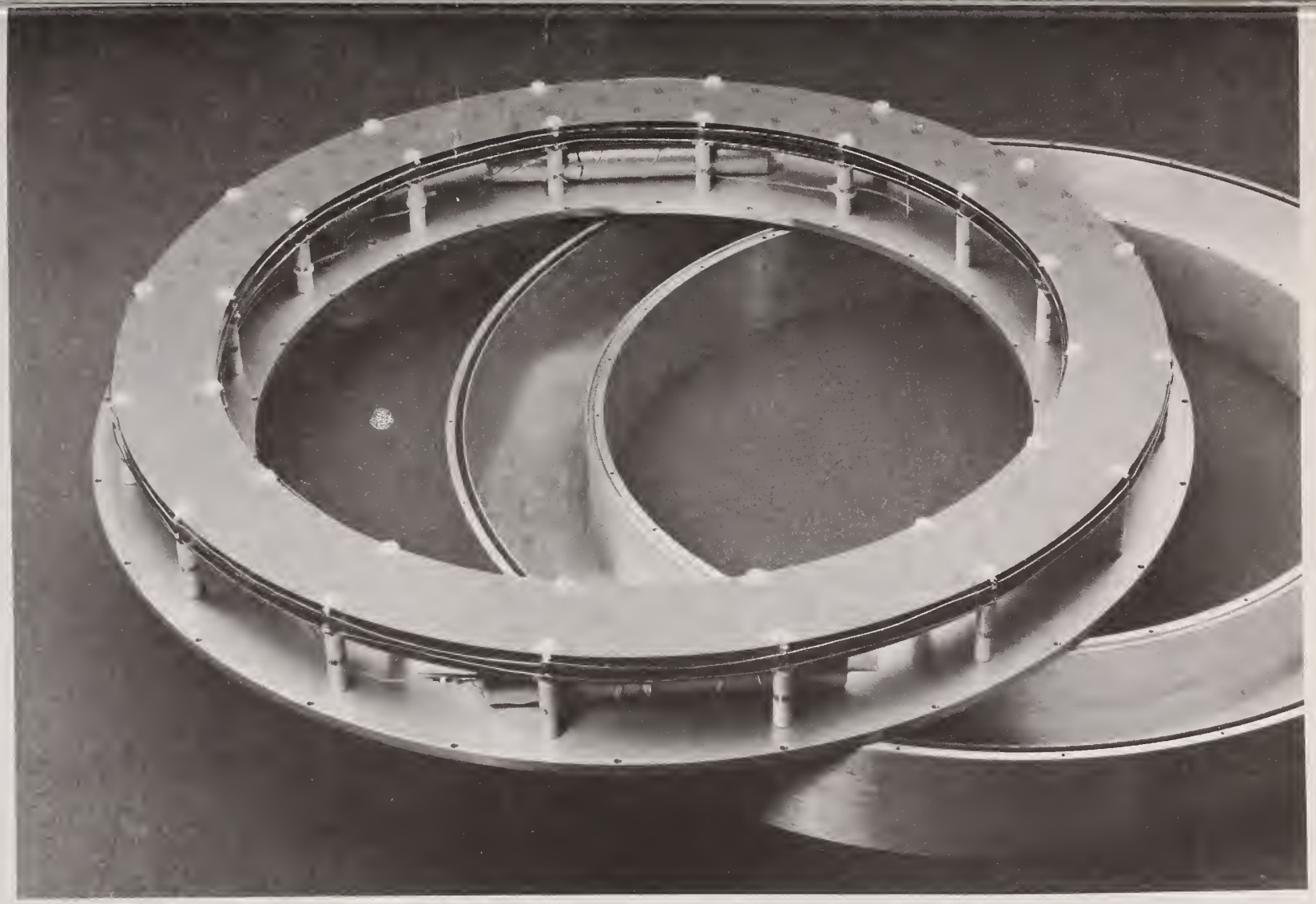

Figure 11
The 'ring' detector. The active elements are shown outside of the waterproof enclosure.

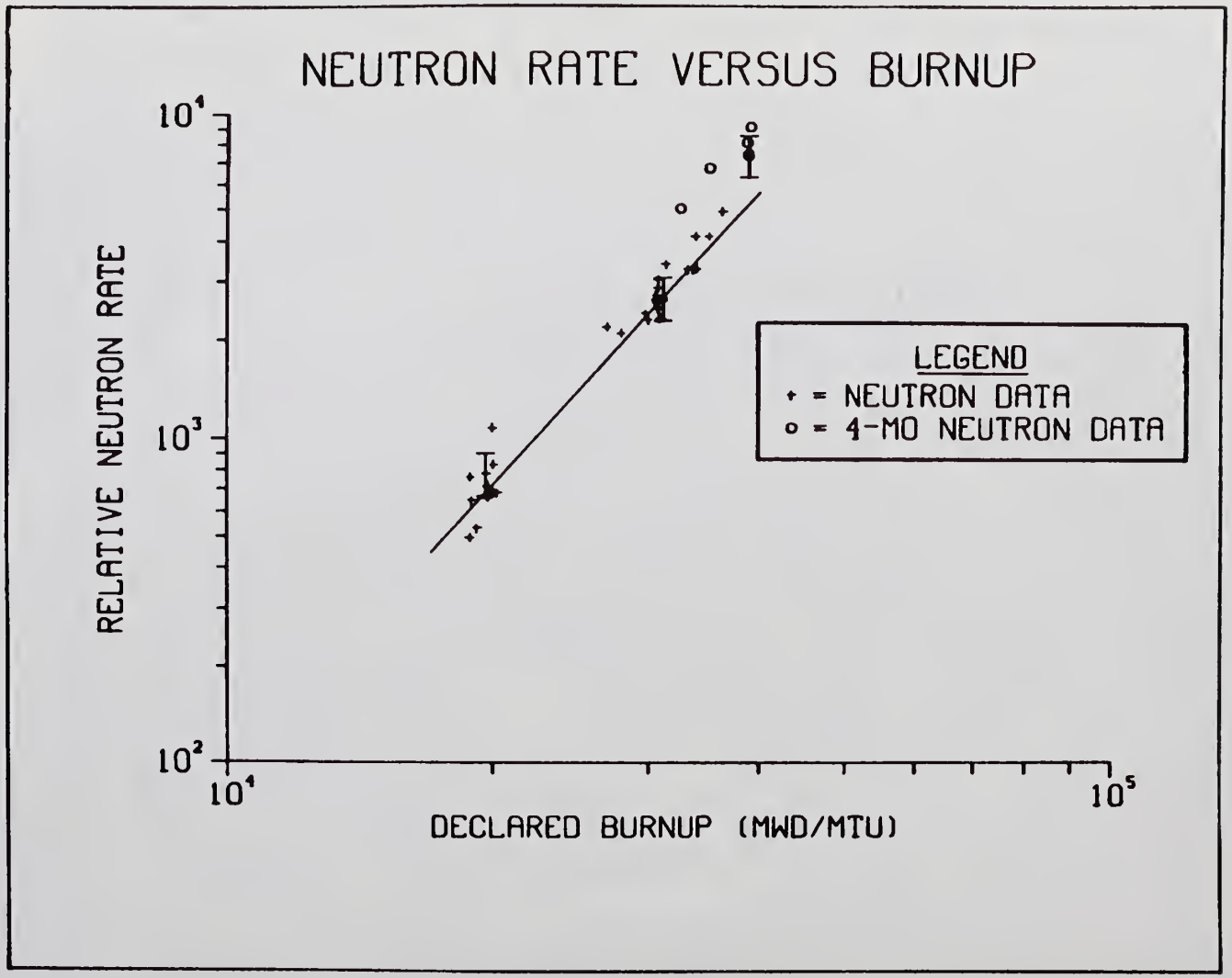

Figure 12
Plot of neutron count rate vs declared burnup.

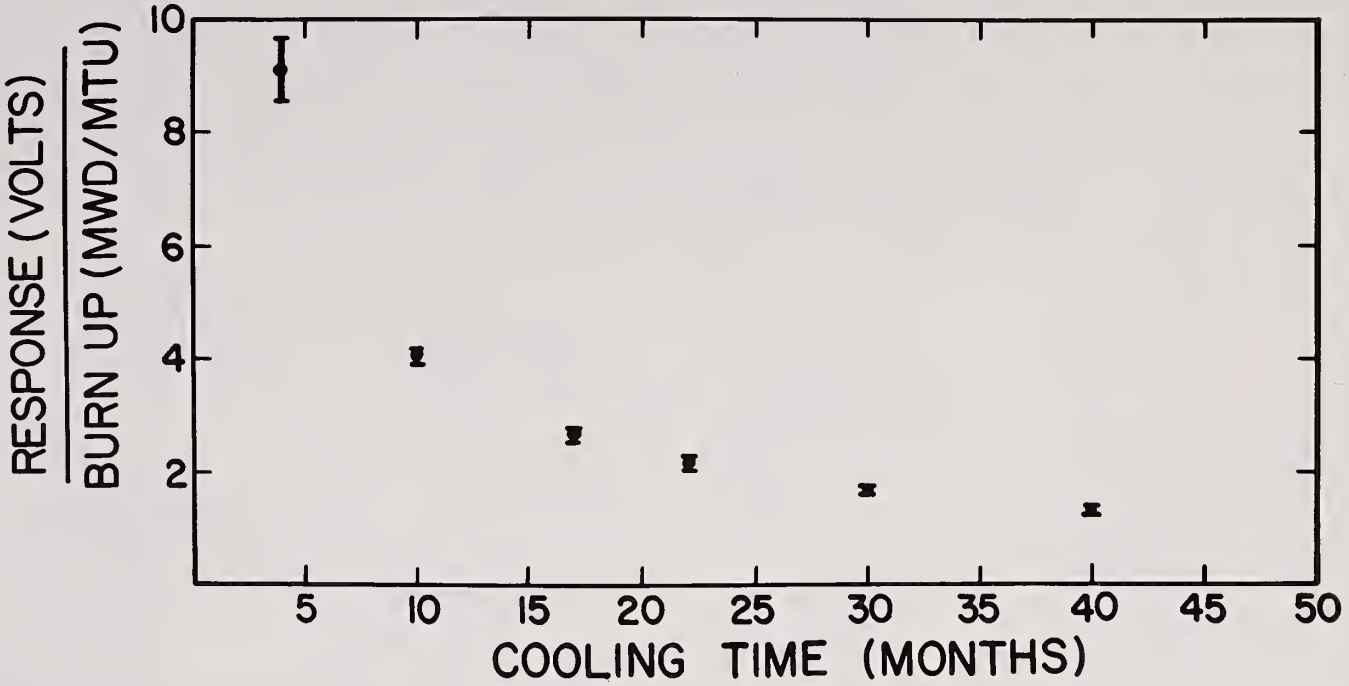

Figure 13
Plot of gamma response/burnup vs cooling time.

The neutron data fall into basically six groups according to cooling times ranging from 4 months to 40 months. The burnup values within each group are similar with the values for the different groups ranging from 18000-38000 MWD/MTU. The uncertainties in the measurements (15-20%) were greater than the statistical uncertainty and is probably due to the difficulty in accurately positioning the detector with respect to the fuel assembly. In a water media a 1-cm positioning error can translate into an error of 10% in the relative neutron counting rate. The errors would be reduced by having a neutron detector in each quadrant.

It is interesting to note that the data plotted in Fig. 13 appear (with the exception of the 4 month cooling time data) to follow the following empirical relationship:

$$\text{Count rate} = \alpha * (\text{Burnup})^{\beta} \quad .$$

The data have not been corrected for cooling time. The fact that the short cooling time data do not follow this relationship can be explained by noting that the ^{242}Cm isotope has a short half-life (163 days) and is an important neutron emitter for short cooling but decreases in importances for cooling times ≥ 1 year. A functional relationship similar to the above has been observed several times before.[5,10]

The gross-gamma ion chamber results also fall into 6 groups. We have plotted the average for each group with the error bars indicating the standard deviation for that group average. The results exhibit a smooth functional relationship similar to that found for the decay power of irradiated fuel after discharge.[11]

The data from the ring detector was recorded using a microprocessor-based data acquisition system. It contained 4 independent ion chamber channels and 4 independent neutron detector channels. In addition to taking the individual data, it averaged the data over several runs and recorded the results along with the time and date on an output terminal.

In general, the portability of the electronics is a desirable feature of safeguards inspection equipment. Therefore, a small (29 x 13 x 33 cm) battery-operated electronics package that can be used with a neutron chamber and an ion chamber was developed. The package is shown in Fig. 14 and a block diagram is shown in Fig. 15. While this package has been used for single detector measurements of neutron and gamma fields, it can also be used with the ring detector when all four neutron channels and four I.C. channels are added. The ion chamber section converts the low level current signal to a voltage level which is amplified, digitized and displayed on the LCD display above the gain switch seen in Fig. 14. The neutron signal requires a preamplifier which can be powered from the box. The preamplified signal is amplified by a shaping amplifier in the electronics package. Those neutron pulses greater than a preset level are counted and displayed. The count time is selected (0-9999 s) using thumbwheel switches on the front panel and the count time remaining is shown by the display above the thumbwheel switches. This package weighs approximately 5 kg and operates for approximately 24 h with a set of 8 alkaline D-cell batteries.

SUMMARY

Nondestructive assay techniques are indispensible in the measurement of spent fuel both for safeguards verification and in-plant control. The characteristics of irradiated fuel that can be measured nondestructively are, among others:

1) the gamma activity from the fission products,
2) the neutron activity from the transuranics, and
3) the burnup profile or activity profile.

Any safeguards verification system for spent fuel assemblies should include both gamma-ray and neutron measurements. HGRS and neutron measurements coupled with axial scanning, either mechanically or through the multielement profile monitor, would give the most detailed information regarding the characteristics of spent fuel. For a simpler and faster safeguards system, a device similar to the ring counter might be able to provide sufficient detail to satisfy lower level verification requirements.

The application of nondestructive techniques for the verification of accountancy by national and international safeguards organizations is of primary importance, but it is

Figure 14
Photograph of battery-powered neutron and gamma-ray electronics.

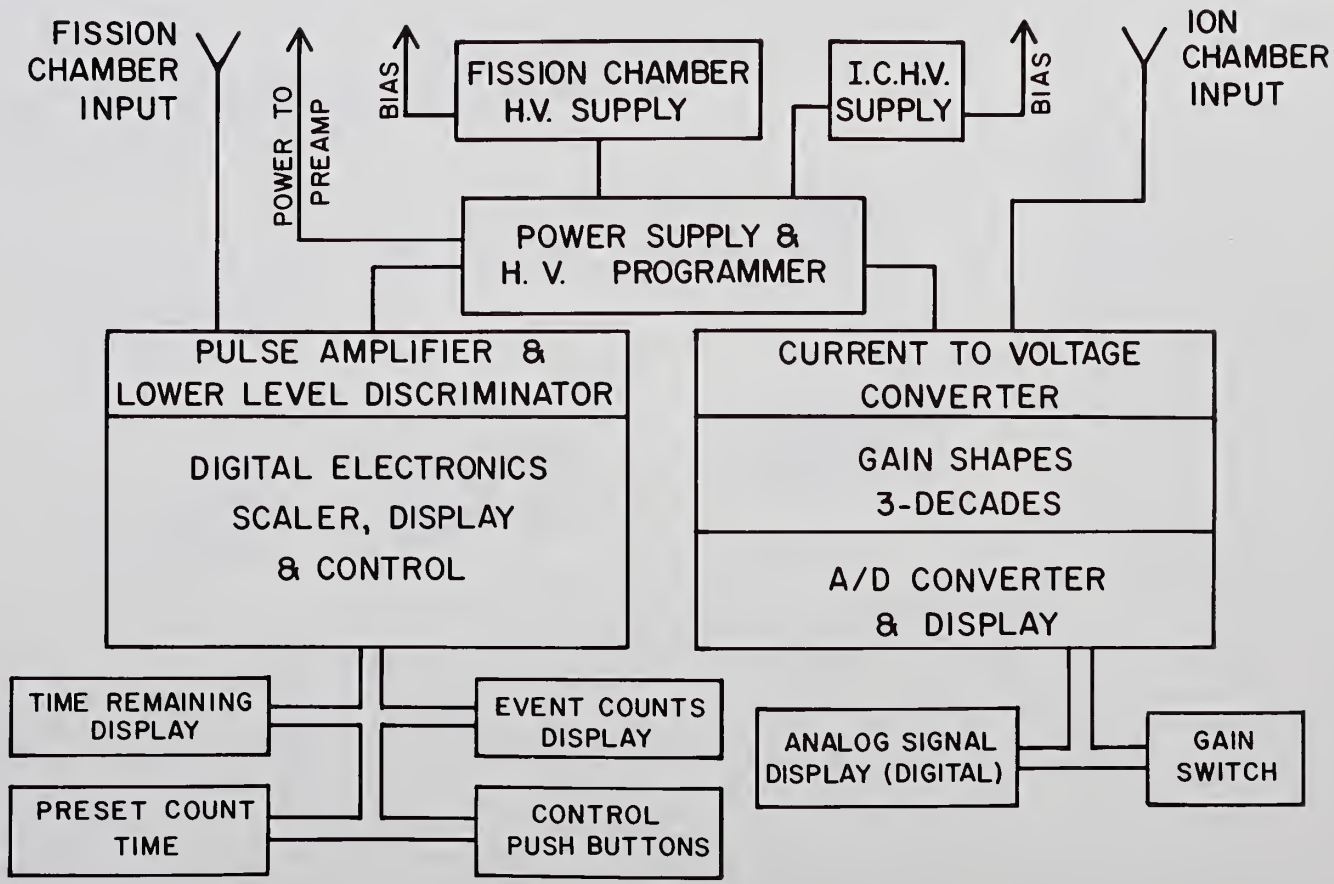

Figure 15
Functional schematic of the battery-powered electronics.

also of importance to the operator of the reprocessing facility to ensure the efficient and economic operation of the facility. In circumstances in which ownership of the fissile material is to be transferred from the reactor operator to the reprocessing facility, shipper-receiver differences could be resolved upon receipt of the material instead of waiting until analysis of the dissolver solution. This would also permit the facility operator the option of mixing fuels from different utilities to obtain specific plutonium and uranium isotopic compositions in the product materials.

Information supplied by nondestructive measurements can also be used to augment in-plant instrumentation for criticality control. The reprocessing facility operator would benefit from the nondestructive assay of fuel assemblies as they are received in the storage area, as well as a rapid verification of the assemblies prior to the transfer to the mechanical shearing cell.

REFERENCES

1. T. N. Dragnev, "Experimental Techniques for Measuring Burnup Nondestructive Techniques: Gamma Spectroscopy," International Atomic Energy Agency report IAEA/STR-48 (October 1974).

2. S. T. Hsue, T. W. Crane, W. L. Talbert, and J. C. Lee, "Nondestructive Assay Methods for Irradiated Fuels," Los Alamos Scientific Laboratory report LA-6923 (January 1978).

3. S. T. Hsue, "Methods for the Nondestructive Assay of Irradiated Fuels for Safeguards," Atomic Energy Review 16, No. 1, 89-128 (1978).

4. "Advisory Group Meeting on the Nondestructive Analysis of Irradiated Power Reactor Fuel," International Atomic Energy Agency report AG-11 (April 1977).

5. S. T. Hsue, J. E. Stewart, K. Kaieda, J. K. Halbig, J. R. Phillips, D. M. Lee, and C. R. Hatcher, "Passive Neutron Assay of Irradiated Nuclear Fuels," Los Alamos Scientific Laboratory report LA-7645-MS (ISPO 43) (February 1979).

6. D. M. Lee, J. R. Phillips, S. T. Hsue, K. Kaieda, J. K. Halbig, E. G. Medina, and C. R. Hatcher, "A New Approach to the Examination of LWR Irradiated Fuel Assemblies Using Simple Gas Chamber Techniques," Los Alamos Scientific Laboratory report LA-7655-MS (ISPO 48) (March 1979).

7. J. R. Phillips, D. M. Lee, T. R. Bement, J. K. Halbig, S. T. Hsue, and K. Kaieda, "Nondestructive Examination of Irradiated LWR Fuel Assemblies," Proc. INMM 20th Annual Meeting, Albuquerque, New Mexico, July 16-19, 1979.

8. D. M. Lee, J. R. Phillips, S. T. Hsue, K. Kaieda, J. K. Halbig, E. G. Medina, and C. R. Hatcher, "A Quick and Accurate Profile Monitor for Irradiated Fuel," Proc. 1st ESARDA Symp. on Safeguards and Nucl. Mat. Management, pp. 265-269, Mol, Belgium, April 25 and 26, 1978.

9. J. R. Phillips, S. T. Hsue, K. Kaieda, D. M. Lee, J. K. Halbig, E. G. Medina, C. R. Hatcher, and T. R. Bement, "Nondestructive Determination of Burnup and Cooling Times of Irradiated Fuel Assemblies," Proc. 1st ESARDA Symp. of Safeguards and Nucl. Mat. Management, pp. 270-276, Mol, Belgium, April 25 and 26, 1978.

10. E. Dermendjiev, private communication, International Atomic Energy Agency (1978).

11. S. Glasstone and A. Sesonske, Nuclear Reactor Engineering, D. Van Nostrand Company, Inc., Princeton, New Jersey (1963).

Discussion:

George (Union Carbide):

Can you recommend any one of these systems for high enriched MTR type fuels?

Lee (LASL):

With MTR fuel you have very little neutron emission. Most of the neutron production, which is small, arises from the curium isotopes. The multi-element system is designed for MTR fuel. I don't like to make recommendations, especially when we are in the prototype stage. We will have some results on correlations and profile measurements with MTR fuel and that will be available hopefully in another month. Other than that, the high resolution or an active neutron interrogation technique would be the only other option.

System for Nondestructive Assay of Spent Fuel Subassemblies—Comparison of Calculations and Measurements*

G. L. Ragan[a] D. T. Ingersoll[b]
C. W. Ricker[a] G. G. Slaughter[c]
M. M. Chiles[a] L. R. Williams[b]
Consolidated Fuel Reprocessing Program
Oak Ridge National Laboratory
Oak Ridge, Tennessee 37830

ABSTRACT

A nondestructive assay system was developed for determining the total fissile content of spent fuel subassemblies at the head end of a reprocessing plant. The system can perform an assay in 20 min with an uncertainty of <5%. Antimony-beryllium neutrons (23 keV) interrogate the subassemblies, and proton recoil counters detect the resulting fission neutrons. Pulse-height discrimination differentiates between the low-energy interrogation neutrons and the higher-energy fission neutrons.

To optimize the performance of the system, 51-energy-group neutron-transport calculations were made, first with a one-dimensional (1-D) computer model, followed by a 2-D computer model. The performance of the as-built system was calculated using a 2-D model. The cross-sections were from the ENDF/B-IV data file and were processed for use in liquid-metal-cooled fast breeder reactor (LMFBR) calculations.

Calculated and measured results were compared for (1) interrogation-neutron penetrability, (2) fission-neutron detectability, (3) radial variation of assay sensitivity, (4) axial variation of assay sensitivity, and (5) the variation of detector count rate as a function of the number of fuel rods in a special 61-rod, LMFBR-type subassembly.

The calculational procedures were validated by comparison with experimental measurements, thus permitting further exploration of system performance by means of additional calculations. In this manner, the following system characteristics were investigated: the relative assay sensitivities of various fissile nuclides; the applicability of the system to a wide variety of fuels, either fresh or spent; the effect on assay accuracy of uncertainties in the isotopic abundances in the fuel; and the efficacy of possible methods of determining isotopic abundances in the sample.

Keywords: Nondestructive assay; neutron interrogation; spent nuclear fuel; nuclear fuel subassembly; calculations; measurements; nuclear safeguards; material accountability; process control; criticality control; assay accuracy.

---

*Research sponsored by Nuclear Power Development Division, U.S. Department of Energy under contract W-7405-eng-26 with the Union Carbide Corporation.

[a]Instrumentation and Controls Division.

[b]Engineering Physics Division.

[c]Physics Division.

INTRODUCTION

A system was developed (Fig. 1) to perform a nondestructive assay (NDA) of the fissile content, either Pu or U, of a spent fuel subassembly as it enters a fuel reprocessing plant and still retains its identity. The assay results can be applied to materials accountability, process control, criticality control, and safeguards. The design objectives of the system are to assay the total fissile content of a subassembly of spent fuel in 20 min with an uncertainty of <5%. Experiments have shown that this NDA system can meet these design objectives.[1]

To achieve uniformity of assay sensitivity over the large cross-sectional area (∿120 cm^2) of a subassembly, the subassembly is actively interrogated by 23-keV neutrons from an ^{124}Sb-Be source. A neutron filter (3-mm-thick boron enriched to 92% ^{10}B) surrounding the subassembly attenuates those source neutrons that would not penetrate far into the subassembly because they have lost energy through moderation. To obtain a signal larger than that from the intense neutron background from spent fuel (∿10^8 neutrons/s), (a) the total number of fission neutrons is measured instead of only the far fewer delayed neutrons, and (b) four intense interrogating sources are required (each with ∿200 Ci ^{124}Sb, producing ∿8 × 10^8 neutrons/s). The high-energy fission neutrons are differentiated from the lower-energy interrogating neutrons by pulse-height discrimination applied to the detectors (methane-filled proton-recoil counters). The counters are shielded against the gamma radiation from the ^{124}Sb sources and the spent fuel by >20-cm-thick lead shields.

The assay-system parameters were optimized on the basis of 51-energy-group neutron-transport calculations (P3-S8 discrete ordinates), first with a one-dimensional (1-D) model (ANISN code[2]), followed by a 2-D model (DOT code[3]). Finally, calculations were made, using the 2-D model of the as-built system, to obtain values for comparison with those measured in various experimental situations. Cross sections were from the ENDF/ B-IV data file and were processed for use in LMFBR calculations.[4]

COMPARISON OF CALCULATIONS AND MEASUREMENTS

Comparative calculated and measured results for the variation of assay sensitivity with radius are given in Table I. The test fuel was unirradiated UO_2, enriched to 7.1% in ^{235}U. The detectors were biased to record only those neutrons that imparted an energy of 450-650 keV to the recoil protons. All values are for the indicated ring relative to the first (innermost) ring of six fuel rods surrounding the central rod of a 61-rod subassembly. The four rings contained 6, 12, 18, and 24 rods. For part A (for the plane perpendicular to the axis at its center), *sensitivity* is taken as the product of two components: the interrogating neutron *penetrability* times the *detectability* of the induced fission neutrons. Calculated and measured penetrabilities are defined, respectively, as the calculated local fission density and as the local fission-product gamma activity measured by a NaI detector following several days of activation by the interrogating sources. Calculated and measured detectabilities are defined, respectively, as the calculated local adjoint flux (which gives the local contribution to the detector signal in a detector-based adjoint calculation) and as the measured detector signal from a ^{252}Cf neutron source placed at the given locality in the subassembly.

---

[1]G. L. Ragan, C. W. Ricker, M. M. Chiles, and G. C. Guerrant, "Experimental Evaluation of a System for Assay of Spent-Fuel Subassemblies," *Trans. Amer. Nucl. Soc.* 28, 128 (1978).

[2]"ANISN-ORNL, Multigroup One Dimensional Discrete Ordinates Transport Code with Anisotropic Scattering," RSIC Computer Code Collection, CCC-254, February 1977.

[3]W. A. Rhoades et al., "The DOT-IV Two-Dimensional Discrete Ordinates Transport Code with Space-Dependent Mesh and Quadrature," ORNL/TM-6529, January 1979.

[4]C. R. Weisbin, R. W. Roussin, J. E. White, and R. Q. Wright, "Specifications for Pseudo-Composition-Independent Fine-Group and Composition-Dependent Fine- and Broad-Group LMFBR Neutron-Gamma Libraries at ORNL," ORNL/TM-5142 (ENDF-224), December 1975.

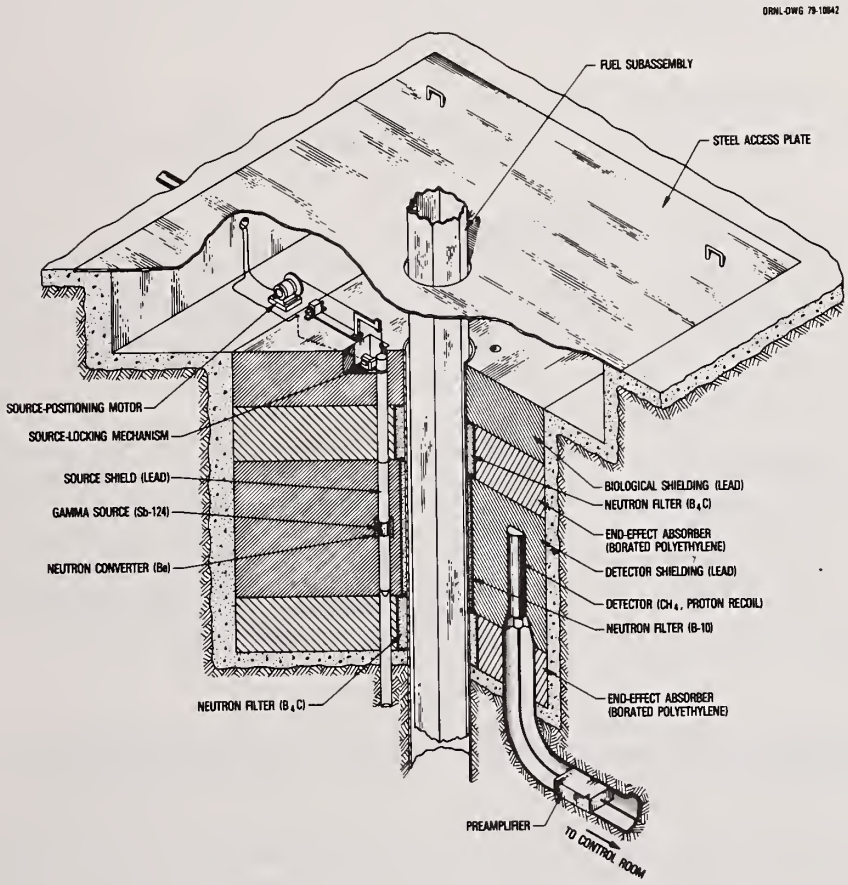

Fig. 1. Experimental system modified for in-the-floor installation. Source and detector locations (four each) alternate every 45°.

Table I. Radial variation of assay sensitivity and of its components (fuel was 7.1% enriched and 450- to 650-keV pulses were detected)

	Values Relative to Ring 1[a]		
	Ring 2	Ring 3	Ring 4
A. In Axial-Center Plane			
Penetrability[b] (P_o)			
Measured	1.005	1.042	1.064
Calculated	1.013	1.033	1.054
Detectability[c] (D_o)			
Measured	1.009	1.027	1.042
Calculated	1.009	1.022	1.038
Sensitivity ($S_o = P_o \times D_o$)			
Measured	1.014	1.070	1.108
Calculated	1.022	1.055	1.094
B. Over Entire Length			
Sensitivity[d] (S)			
Measured	1.031	1.077	1.153
Calculated	1.032	1.074	1.127

[a] In the 61-rod subassembly, one center rod was surrounded by four hexagonal rings of rods.

[b] The fission-neutron density produced in a given ring by the interrogating-neutron source. Standard deviation of the measurements is ∿0.5%.

[c] The detector signal produced by a ^{252}Cf source placed in a given ring. Standard deviation of the measurements is ∿0.4%.

[d] The increase in the count rate when the enrichment was raised from 7.1 to 19.8% in six rods in a given ring. Standard deviation of the measurements is ∿2.3%

For part B (for the entire length), sensitivity is defined as the increase in count rate when six normal (7.1% enriched) fuel rods in a given ring were replaced by six higher-enrichment (19.8%) rods. Part B thus involved an axial average over the assay region. The calculations simulated the experimental conditions: each ring of rods constituted a zone of the appropriate composition, with corresponding detector activities determined in forward calculations--no adjoint calculations were needed.

The calculated and measured axial variation of assay sensitivity can be compared by reference to Fig. 2. The penetrability, detectability, and sensitivity for both calculated and measured cases are defined as in Part A of Table I. The axial variations of the components (penetrability and detectability) of the sensitivity also showed comparable agreement between calculations and measurements.

The shape of the axial sensitivity curve is not important, because the assay procedure will be to program the scan so that each axial element of the subassembly traverses the entire sensitive region of the assay equipment. These scan results will be compared with those from a nearly identical standard subassembly to determine the total fissile content of a subassembly by integrating the axial scan data.

The variations of calculated and measured count rates with the number of 7.1%-enriched fuel rods can be compared by examining Fig. 3. There is a slight nonlinearity of both measured and calculated points, but there is less nonlinearity when the enrichment (with a constant number of rods) is varied.

The foregoing results enable quantitative comparisons of the calculated and measured spatial variations of assay sensitivity, in both radial and axial directions. These results are for ^{235}U-enriched UO_2 fuel, using cross sections from the ENDF/B-IV file processed into a 51-group set for LMFBR calculations.[4] The quantitative aspects of the observed agreement between calculations and measurements indicate the degree to which the 2-D model and the cross-section set may be considered adequate for an expanded calculational program.

This validation of the calculational procedure permits extension of measured results by additional calculations. Among the characteristics that can be explored are: the relative sensitivities of various fissile nuclides; the applicability of the NDA system to a variety of fuels, either fresh or spent;[5] the effect on assay accuracy of uncertainties in the isotopic abundances in the fuel; and the efficacy of possible methods of determining isotopic abundances in the sample. The calculations related to these characteristics are discussed in the next section.

CALCULATIONAL RESULTS

A 2-D calculation was made for a spent LMFBR core subassembly in the normal assay configuration. The isotopic sensitivities (fission neutrons produced per atom of the given nuclide) relative to ^{239}Pu are given in the second column of Table II. Although ^{233}U is not normally present in this fuel, a trace amount was included to obtain its relative sensitivity. The sensitivity range (1.73) is far better than it would be ($\sim$3.4) if only delayed neutrons had been counted in this same system. We believe that the sensitivity range of 1.73 also is better than that for other systems designed specifically to detect only delayed neutrons.

The 1.73 range of relative isotopic sensitivities means that the results of these experiments, based on ^{235}U-enriched fuel, are qualitatively correct (and not far off quantitatively) for other fuels based on different fissile isotopes. Performance estimates have been given elsewhere for the assay, in this NDA system, of four other fuel subassemblies.[5] The four fuels include three LMFBR fuels (containing spent Pu, fresh Pu, or fresh ^{233}U) and one light-water-cooled reactor (LWR) fuel (requiring an enlarged center cavity in the NDA system).

---

[5]G. L. Ragan, C. W. Ricker, M. M. Chiles, D. T. Ingersoll, and G. G. Slaughter, "Nondestructive Assay of Subassemblies of Various Spent or Fresh Fuels by Active Neutron Interrogation," *J. Inst. Nucl. Materials Mgt. Vol. VIII, Proc. Issue* (1979).

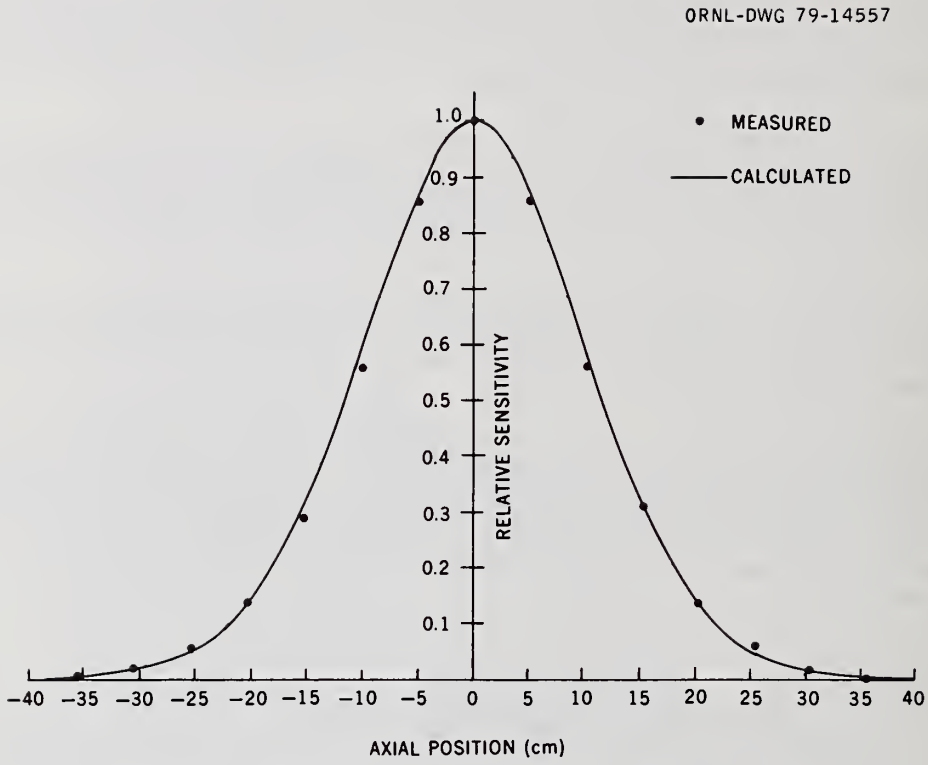

Fig. 2. Comparison of calculated and measured axial sensitivities for 7.1% enriched fuel and 450- to 650-keV pulse detection. Calculated and measured values are normalized to 1.0 at axial position 0.

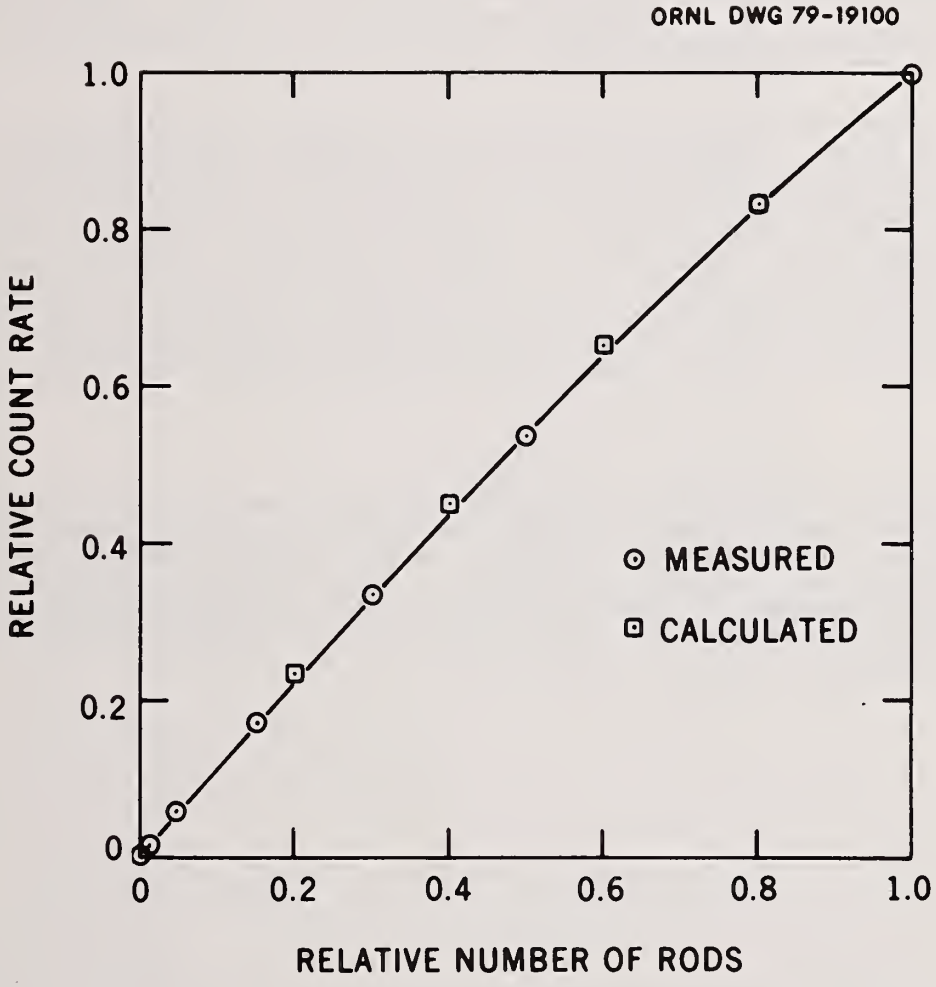

Fig. 3. Variation of count rate with relative number of 7.1%-enriched fuel rods, counting all pulses above 450 keV. Calculated and measured count rates are normalized to 1.0 at an abscissa of 1.0.

In the third column of Table II, relative sensitivities are given for our NDA system with the ^{10}B neutron filter removed. Because of the presence of a greater number of low-energy neutrons, the relative sensitivities changed as shown. Not shown, but indicative of the value of the filter, is that the edge-to-center neutron production density increased from the normal-system value of ∿1.15 to ∿1.30 when the ^{10}B filter was removed.

The last column of Table II shows the factor by which the observed signal would increase, for each isotope, if the ^{10}B filter were removed. A measurement of this ratio during an assay would provide information relative to isotopic composition. Different filters (e.g., filters containing appropriate moderating and resonance-absorbing materials) might give better isotopic discrimination, and by making four different measurements, one might determine the relative abundances of the four fissile isotopes. More-refined calculations with cross sections processed to account for various isotopic dilutions are being made to explore these possibilities.

The estimated accuracy of assay achievable in a 20-min measurement with this system is given in Table III. With careful control of the individual contributing parameters (favorable conditions), a standard deviation of ∿0.2% should be realizable. The most important unfavorable condition would be poor knowledge of the relative isotopic composition. The indicated 3% corresponds to the following improbable scenario: the transfer documents state that the fissile content of a given spent LMFBR subassembly is 93% ^{239}Pu and 7% ^{241}Pu, and we use the corresponding assay sensitivity factors. If, instead, the subassembly contains either 0% or 14% ^{241}Pu, the assay error would be +3% or -3%, respectively. If the ^{241}Pu content is known more accurately than this, as it most probably will be, this component of the assay error will be correspondingly less.

CONCLUSIONS

Experiments have shown that the NDA system can meet the design objectives. The calculational model and cross-section set were validated by comparing calculated and measured results. Calculations have been used to extend the experimental results to determine the following: relative sensitivities of various fissile nuclides; the applicability of the system to a variety of fuels; the effect on assay accuracy of uncertainties in the isotopic abundances in the fuel; and the efficacy of possible methods of determining isotopic abundances in the sample.

Table II. Calculated isotopic sensitivities and effect of ^{10}B filter

Nuclide	Sensitivities Relative To Pu-239: With B-10 Filter	Sensitivities Relative To Pu-239: Without B-10 Filter	Signal W/O Filter / Signal W/Filter
U-233	1.73	1.51	3.62
U-235	1.12	0.89	3.31
Pu-239	1.00	1.00	4.16
Pu-241	1.45	1.26	3.62

Table III. Accuracy Estimates

	Standard Deviation(%)	
	Favorable Conditions	Unfavorable Conditions
Count Statistics	0.1	0.2
Accuracy of Standard	0.1	0.2
Isotopic Composition	0.1	3.0
Detector Temperature	0.1	0.2
Detector High Voltage	0.1	0.2
Combined	0.2	3.0

Discussion:

Cuypers (ISPRA):

Is this system applicable to the initial calibration of all types of tanks? Have you encountered the fact that it would be very difficult to have access to the tubing of various tanks for recalibration, after they have been in hot operation? Is it necessary that the tank be completely empty to be recalibrated or, at least, must have only residual pure water?

Ragan (ORNL):

The answer to the first statement is yes. It is to be used on tanks that are any place in the plant. The answer to the second question is yes. You must have tubes that lead to the tank or you cannot do the calibration. The answer to the third question is that if you want to know the total volume you must drain the tank completely dry. If you are not interested in the heel volume of the tank, i.e., that volume below the end of the bubbler tube, you can use this system even if there is still water in the tank.

Cuypers:

If the residual solution in the tank has a different density, it will influence the calibration by mixing with the water.

Ragan:

That is correct. It would be necessary to have only water in the tank. We have not tested the system in-plant. That will be done in the future, by other people. The system has been tested only as I described by using the initial 30-gallon tank used for initial calibration.

A Study of Gamma-ray Spectroscopy For Spent Fuel Verification at the Bruce CANDU Reactors

by

J.J. LIPSETT, J.C. IRVINE and W.J. WILLIAMS
Atomic Energy of Canada Limited, Chalk River, Ontario

ABSTRACT

A test program was undertaken to establish whether gamma-ray spectroscopy could be used to verify that fuel bundles from the Bruce NGS reactors have been irradiated before they are placed in long-term bonded storage. The verification would be done while the fuel bundles are in transit, and in motion. The fuel-transfer conditions were simulated in the storage bay of the NRU reactor at the Chalk River Nuclear Laboratories, with irradiated test fuel bundles, and the results, as reported in the paper, demonstrated feasibility of this concept.

KEYWORDS: Bruce reactors, nuclear safeguards, spent fuel, verification, bonded storage, γ-ray spectroscopy

INTRODUCTION

As part of the support program for the development of a nuclear safeguards system for the Bruce Nuclear Generating Station (NGS), it was proposed by the IAEA that gamma-ray spectroscopy be used to verify that fuel bundles have been irradiated before they are placed in bonded long-term storage. In the route from reactor discharge to storage, the bundles are held for about eight months in interim storage bays then transferred through a narrow trench to the long-term storage bay. During transit through this trench, and while in motion at ∿1 cm/s, the gamma-ray spectrum from each fuel bundle would be measured and assessed to establish the required verification. Chalk River Nuclear Laboratories (CRNL) undertook as a task in the Canadian Safeguards Support Program to carry out a series of tests

- to determine whether gamma-ray spectroscopy could be used to remotely measure the intensity and isotopic mix of the radioactivity in spent fuel, and
- to provide data for any future equipment design.

An experiment was mounted in the fuel storage bay of the NRU reactor at CRNL, and measurements were carried out that demonstrated feasibility of the concept.

BRUCE NGS FUEL TRANSFER AND STORAGE

The fuel management system at the Bruce NGS involves the on-power fuelling of four reactors where approximately 60 fuel bundles are unloaded per day. These bundles are discharged at burnups in the range of 165 to 250 Mwh/kgU, with an average of 196 Mwh/kgU. Occasionally unusual conditions, such as the unloading of a failed fuel bundle, will result in bundles of lower burnup being discharged, but these occurrences are rare. After discharge, the irradiated bundles are stored for an interim period of 8 to 10 months in the main underwater storage bays prior to transfer to long-term storage in a separate, large underwater storage facility.

The transfer of bundles from interim to long-term storage is made through an interconnecting trench under approximately 10 metres of water. Twenty-four bundles are loaded onto a transfer tray in two rows, as shown in Figure 1, and two such trays, coupled end to end, are moved through the trench, to constitute a transfer. At the long-term storage bay, the trays of fuel bundles are stacked in columns which later would be sealed by the IAEA inspector. Spent fuel verification would be done at the end of the transfer trench, by measuring and assessing the gamma-ray spectrum from each fuel bundle

while in motion at ∿1 cm/s.

In the proposed concept, also shown in Figure 1, air-filled collimators would be used create rectangular beams of gamma rays to the surface of the trench. Each beam would be oriented parallel to the axis of the bundle, and the variation of the intensity of the beam, or spectral components of the beam, would be measured as the bundles moved under the collimators.

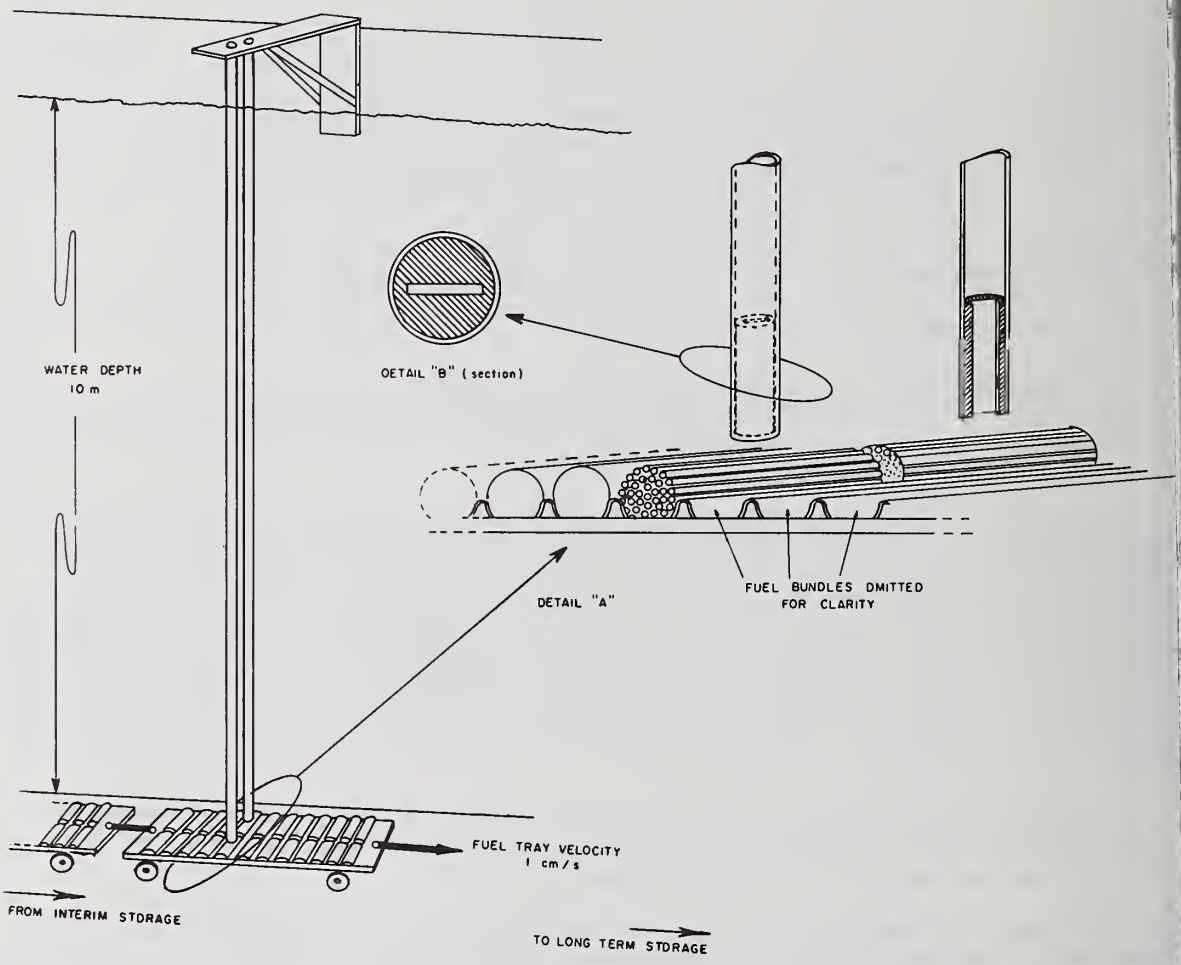

FIGURE 1 SCHEMATIC ARRANGEMENT OF FUEL TRANSFER TRAYS AND PROPOSED COLLIMATORS

Thus the inspector would have the means to determine that

- the bundles being transferred are radio-active,
- the beam intensity changes significantly at the separating gap between bundles, to give a bundle count, and
- if measured, the gamma-ray components of the beam, associated with specific fission products, give an indication of the irradiation history of the bundle.

The latter point becomes a possibility because (i) the on-power fuelling scheme and (ii) the method of fuel management of the Bruce reactors, to produce a flattened flux, result in a relatively narrow band of discharge burnups and post-discharge decay periods for the majority of the irradiated fuel bundles.

These particular circumstances permit several important and useful fission products to become prominent in the gamma-ray spectrum. In principle, the source strength "S" of a fission product will vary approximately as

$$S \propto \frac{1}{\lambda} \left\{ p_1(1-e^{-\lambda t_1})e^{-\lambda(t_2+t_3)} + p_2(1-e^{-\lambda t_2})e^{-\lambda t_3} \right\} \qquad (1)$$

where p_1 and p_2 are the average powers of the fuel during the first and second irradiation steps*,

t_1 and t_2 are the irradiation times for the first and second steps,

t_3 is the decay time between bundle discharge and transfer to long-term bonded storage, and

λ is the decay constant.

Now, for a long-lived fission product whose half-life is greater than 2t, the following approximations hold

$$1-e^{-\lambda t} \simeq \lambda t$$

and $$e^{-\lambda(t_2+t_3)} \simeq e^{-\lambda t_3} \simeq 1$$

Hence $$S \propto \frac{p_1\lambda t_1 + p_2\lambda t_2}{\lambda} = p_1t_1 + p_2t_2 = B \qquad (2)$$

where B is the burnup of the fuel. A fission product that fits these requirements is ^{137}Cs with a 30.2-yr half-life.

At the other end of the scale are fission products whose half-life is less than t/3, in which case $1-e^{-\lambda t} \approx 1$ and $e^{-\lambda(t_2+t_3)}$ approaches zero, so that

$$S \propto \frac{P_2}{\lambda} e^{-\lambda t_3} \qquad (3)$$

and the principal parameter is the final power of the fuel. A fission product that fits these requirements is ^{95}Zr with a 64-day half-life.

In the middle, i.e. where the half-life is equivalent to t_1, t_2 and t_3 (which as a generalization are close to being equal), equation (1) cannot be simplified, and S will vary with p_1, p_2, t_1, t_2 and t_3. A fission product that fits these requirements is ^{144}Ce with a half-life of 284 days. This isotope is particularly important because its equilibrium daughter, ^{144}Pr, decays with an isolated 2.186 MeV gamma ray. This gamma ray should be relatively easy to measure and yet be difficult to duplicate, if fuel diversion was being attempted.

Therefore, if gamma-ray spectrum regions, associated with specific fission products, could be measured dynamically, confirmation could be obtained that fission products are the source of the activity. Furthermore, the magnitudes of the measured spectra should be consistent, to a first approximation, with the recorded irradiation history of the fuel.

Although these principles are simple to express, there are many potential complications in attempting to put this into practice, some of which are

- uneven distribution of fission products in each fuel element,

---

*Of the bundles discharged in the Bruce fuel cycle, 3/8 are irradiated to full burnup in one fuel channel position while 5/8 are irradiated in an "inlet" and "outlet" channel position, in a two-step irradiation, to achieve full burnup.

- self-shielding effects of the fuel and its disruption by "shine" through the cracks always present in the uranium dioxide pellets,
- flux gradients across the fuel bundle, and
- interruptions to the even, normal irradiation of the fuel.

Therefore, no attempt was made to predict the signals that would be obtained, rather, these tests were an empirical evaluation of the principles for this one specific application.

EXPERIMENTAL RESULTS

The conceptual arrangement of the Bruce fuel verification was simulated in the NRU reactor storage bay at CRNL. An 8.8 m long, air-filled aluminum tube, 10.2 cm inside diameter, was used to create a simple collimated beam. The tube contained slotted lead attenuators 29.2 cm long at the bottom and at mid-height, and an annular lead attenuator and instrument shield at the top completed the assembly. The slots in the bottom and mid-height attenuators were 0.87 cm by 8.26 cm and 2.0 cm by 8.26 cm, respectively. The annular attenuator at the top was 10.0 cm outside diameter, 7.0 cm inside diameter and 35.6 cm long. The instrument shield was 16.5 cm outside diameter, 11.4 cm inside diameter and 30.3 cm long of which 16 cm was above the water surface. The top of the annular attenuator overlapped the bottom of the shield by 6.4 cm. A number of lead filter disks, 10.2 cm diameter by 2 cm thick, were available.

Six natural uranium fuel bundles, with a variety of irradiation histories, total burnups, and decay periods (see Table I), were obtained from the Bruce NGS fuel development program for these tests. They were identical to the Bruce bundle shown in Figure 2, except that the central element was removed, to permit their assembly on a tie rod, for experiments in the vertical NRU reactor test loops. These bundles were placed side by side, in two group of three, in a holding tray on the floor of the bay, under the collimator, and with a clearance of 2.5 cm between the top of the bundles and the collimator.

The separation between the outside diameters of the bundles was set at values of 0.09 cm, 1.18 cm, and 2.45 cm, compared to 0.22 cm for the Bruce transfer tray. The aim was to determine whether a significant difference in signal would be obtained as these separating gaps passed under the collimator. However, when the contribution to the bundle diameter by the bearing pads is removed, the gap between the fuel of the test bundles becomes 0.23 cm, 1.5 cm, and 2.77 cm, compared to 0.54 cm for the Bruce bundles.

TABLE I

IRRADIATION DATA FOR TEST FUEL BUNDLES

Bundle Identity	Discharge Burnup Mwh/kg	Final Power Kw/m	Decay Period days
ZM	209.5	31.6	316
ZL	205.5	30.8	316
ZT	152.1	18.0	183
ZK	181.1	26.5	316
AAJ	82.2	35.5	183
XX	172.8	28	183

For these tests, rather than moving the bundles, the collimator was pivoted at the water surface and the bottom swung into position as required. Figure 3 is a photograph of the experimental assembly in use during the tests. The working platform was supported on a

tower made of ABS plastic pipe, water filled, and the bottom of the collimator was driven by a chain and sprocket arrangement directly coupled to the hand wheel, shown on the front-right corner of the platform. Positioning of the collimator bottom to ±1 mm, including backlash, was achieved. In the photograph, the test bundles can be seen under the collimator.

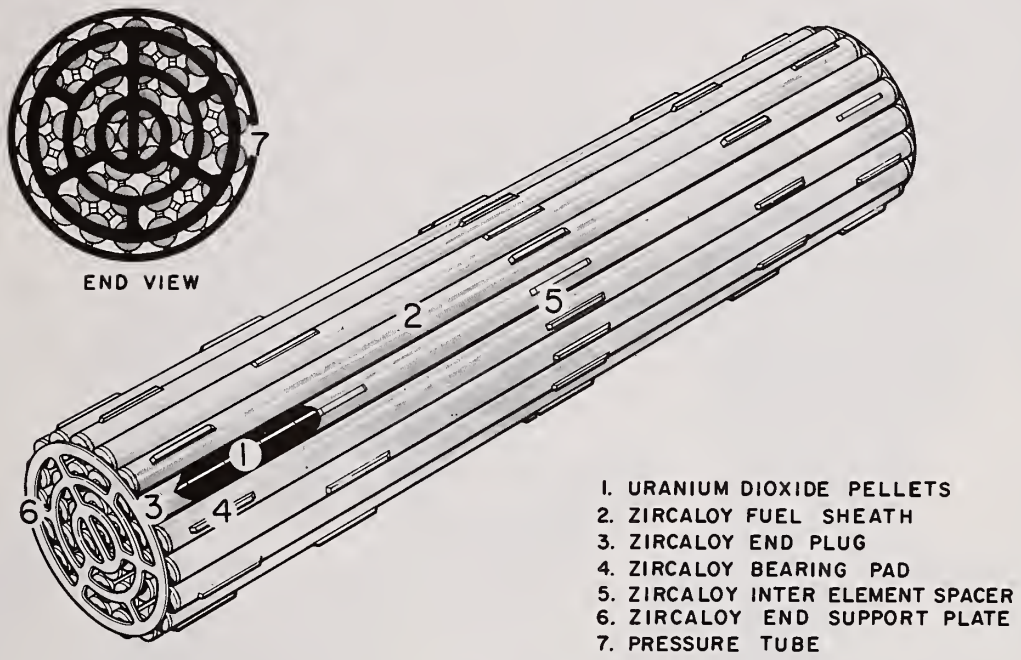

FIGURE 2
BRUCE 37-ELEMENT FUEL BUNDLE

The electronics cabinet contained conventional counting equipment that allowed the acquisition of full spectral data or analog data from spectral regions, for presentation on strip-chart recorders. Figure 4 gives a block diagram of the equipment used.

The intensity of a 0.87 cm by 8.26 cm gamma-ray beam from the fuel bundles, and its spectral components, were measured as functions of position across a number of different combinations of bundles and separation gaps. Three instruments were used for the measurements,

- a γ-radiation survey meter,
- a germanium spectrometer, and
- a NaI(Tl) spectrometer.

To emphasize the high-energy end of the spectrum, and thus take advantage of the ^{144}Pr isotope, the collimator slot was oversized for the NaI spectrometer. Also, the count rate was brought back into the useful range by attenuating the low-energy spectrum, using 4 cm of lead filtering.

The majority of the measurements of the beam intensity profile were made by stepping the collimator across the bundle and stopping to make each measurement. For the germanium and NaI(Tl) detectors, full-energy spectra were obtained for each point using the multichannel analyzer. Subsequently, regions of interest or isotope concentration profiles could be generated using off-line computer analysis.

FIGURE 3 GENERAL VIEW OF THE EXPERIMENT

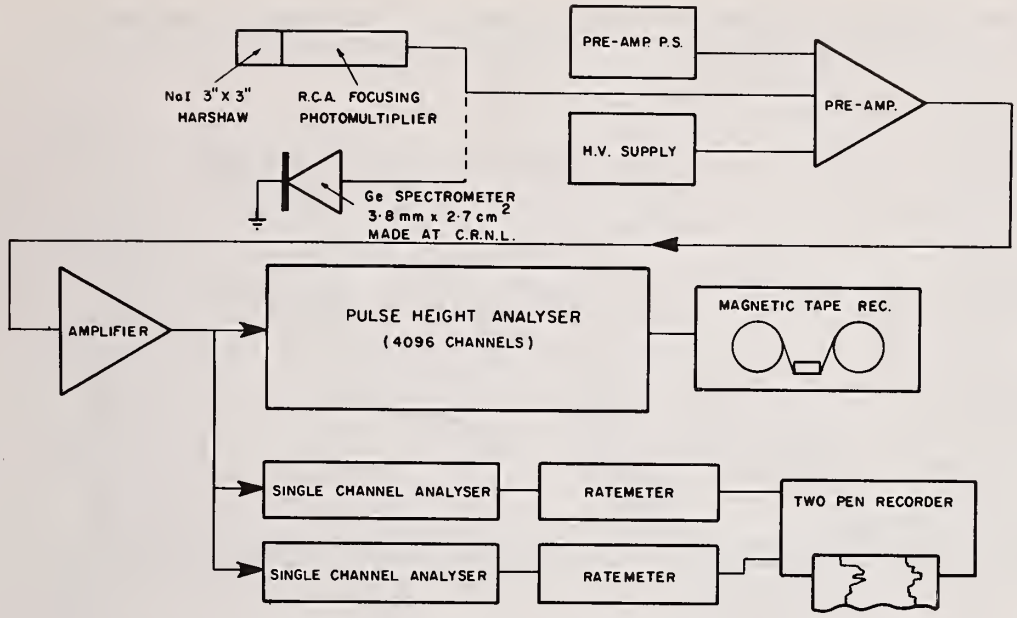

FIGURE 4 BLOCK DIAGRAM, ELECTRONIC EQUIPMENT.

Figure 5 shows such a scan of three bundles, using a γ-ray survey meter. (This set of bundles has been called Group A and consisted of three bundles, code-named ZM, ZL and ZT. The two gaps between the bundles were 0.23 and 2.77 cm, respectively.) As would be expected, because of their similar irradiation histories, bundles ZM and ZL had virtually identical radiation fields in the beam, with a definable drop of 30% at the 0.23 cm separating gap. Bundle ZT, with only 60% of the decay time of the other two, gave 1.8 times the field strength, i.e. ∿50 mR/h. At the 2.77 cm gap, the field dropped to ∿13 mR/h. There was also some irregularity in the fields across the bundles.

Subsequent measurements, using germanium spectroscopy, showed that there was a significant low-energy scattered background due to very low concentrations of the fission product ^{137}Cs dissolved in the storage bay water. Figure 6 gives another view of bundle group A, using a NaI(Tl) spectrometer with 4 cm of lead attenuators, to filter the low-energy segment of the γ-ray beam and thus emphasize the high-energy segment, specifically for the 2.184 MeV gamma-ray of ^{144}Pr. Three spectrum regions are shown, with the top one, Figure 6A, giving the full spectrum results. The spectrum region of 600 keV to 960 keV, Figure 6B, has virtually the same shape as that of the full spectrum, Figure 6A, except that the base line of the latter is 4000 counts/s, not zero. This illustrates the presence of a constant background not associated with the radiation from the bundles. Also, the general conclusions, based on the previous radiation field measurements, hold for the full spectrum results of Figure 6A.

The shape of these curves is important in that the slope at the edge of each bundle is very steep, indicating that the collimator was providing good spatial resolution. For example, at the outside edges of bundles ZM and ZT, the field strength drops to background in less than 2 cm. If the collimator slot was perfectly attenuating and had no width, then the shape would show the fine structure of the γ-ray beam and drop sharply to background at each boundary. Because the collimator slot had a real width of 0.87 cm and was made of "gray", rather than "black", material some of the fine structure was lost. Also the boundaries can be expected to have slopes corresponding to the collimator slot width rather than sharp edges.

The boundaries of the bundles and the collimator slot width at these boundaries have been included on Figures 6B and C. Note how closely the boundary slopes match the collimators thus indicating that the collimator edges were "sharp", i.e. attenuation was

strong, and that the γ-ray beam had a steep boundary at the edge of the fuel bundle.

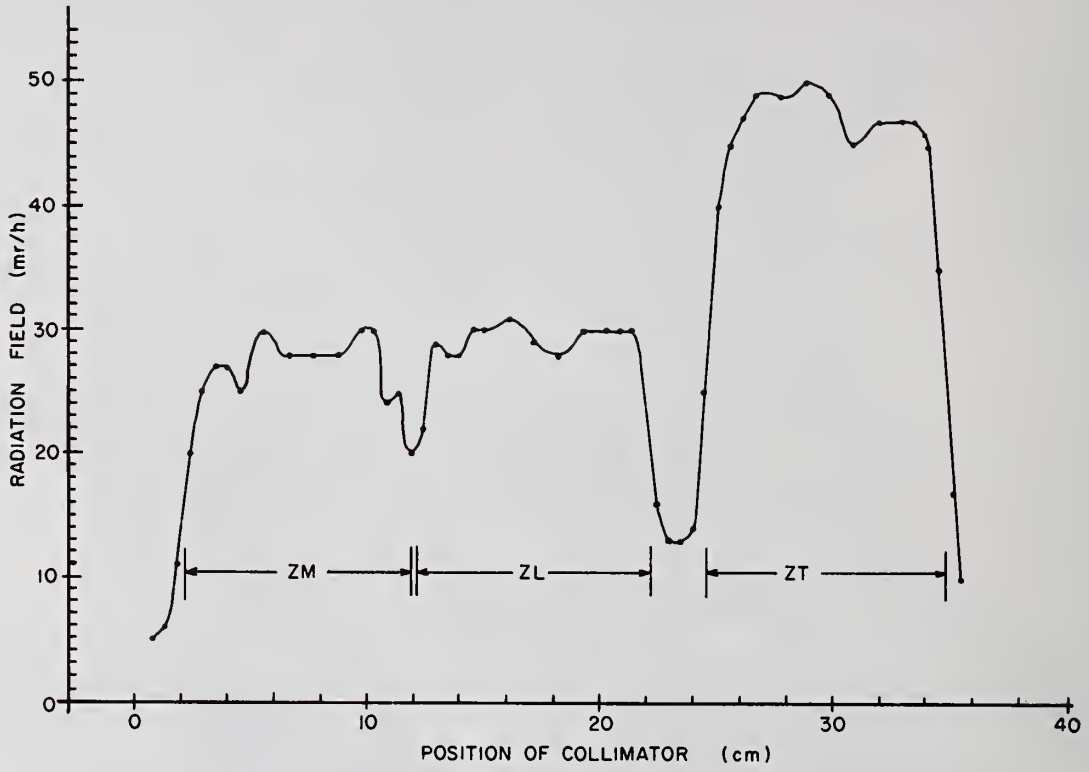

FIGURE 5 RADIATION FIELD SCAN FOR BUNDLE GROUP A

A collimator of slot width W cm, centered over a gap of width w cm between bundles that have count rates K_1 and K_2 at their edges, will produce a count rate K_g (for the zero general background case), given by

$$K_g = K_1\left(\frac{W-w}{2}\right) + K_2\left(\frac{W-w}{2}\right) \quad (4)$$

or

$$\frac{K_g}{K_1} = \frac{W-w}{2}\left(1 + \frac{K_2}{K_1}\right) \quad (5)$$

Now, for the narrow gap between bundles ZM and ZL, $(W-w)/2 = 0.32$ so, if the γ-ray beam was perfectly flat across the bundles and square at the boundaries, then K_g/K_1 should equal 0.64, since $K_1 \approx K_2$. Table II gives the count rates in various energy regions, observed for this group of bundles, and values of K_g/K_1 parenthetically in column 4. For the total spectrum and the low-energy region, K_g/K_1 is high, showing the effects of scattered background. For ^{137}Cs and ^{95}Zr, the values measured for K_g/K_1 approach the derived values above, however, if a background correction is made, these measured values decrease to 0.52 which can be attributed to some decrease in source strength at the bundle edges. This decrease at the bundle edges appears to be even stronger for ^{144}Pr which gives a low value for K_g/K_1.

Careful germanium-spectrometry measurements were made progressively into a bundle from the edge, and it was found that γ-rays from ^{95}Nb, ^{95}Zr, ^{137}Cs, ^{134}Cs appear before those from ^{144}Ce, ^{144}Pr or the uranium X-rays. The ^{95}Nb and ^{95}Zr fission products were undoubtedly supplemented by the activation products of the cladding. The fission products ^{137}Cs and ^{134}Cs are known from other work to migrate to and concentrate at the fuel/cladding interface. It is presumed that these two effects have occurred in this fuel to cause the observed distribution of activity. The net effect is to cause an apparent gap

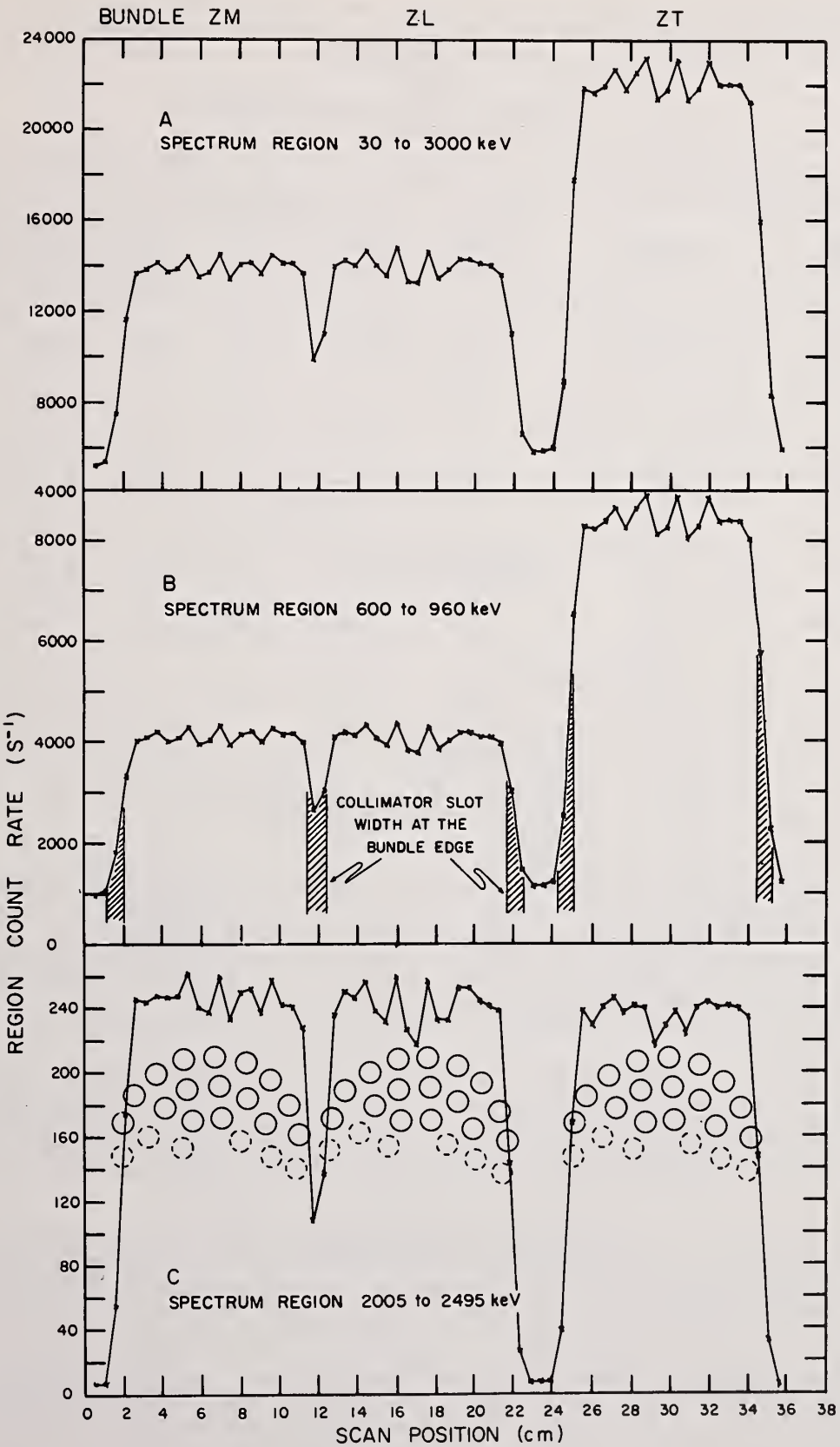

FIGURE 6 NaI SCAN OF BUNDLE GROUP A

between bundles that is larger for ^{144}Pr than for the Cs and Zr(Nb) isotopes.

TABLE II

SUMMARY OF NaI SPECTRUM RESULTS

Window in keV	Comment	Count Rates (s^{-1})					
		Typical ZM	Small Gap	Typical ZL	Large Gap	Typical ZT	Bay Water
0→3000	Total Spectrum	14 000	10 000 (0.71)*	14 000	6000	22 000	5200
0→600	General Low Energy	7 300	5 700 (0.78)	7 300	4000	11 400	3700
600→960	^{137}Cs plus ^{95}Zr	4 100	2 600 (0.63)	4 100	1200	8 400	1000
725→960	Principally ^{95}Zr	2 200	1 350 (0.61)	2 200	500	5 200	400
1660→2495	Wide ^{144}Pr	530	240 (0.45)	530	30	500	20
2095→2495	Narrow ^{144}Pr	245	110 (0.45)	245	5	240	5

*The value in parenthesis represents $\frac{\text{Small Gap Count Rate}}{\text{ZM Count rate}} = \frac{K_g}{K_1}$

From equation (5), it can also be seen that, when $w \to W$, $(W-w/2)$ tends to zero and K_g then goes to background, as can be seen in the gap between bundles ZM and ZT in Figure 6 and Table II. Also, from equation (5), when $1/(1 + K_2/K_1) \leq (W-w)/2$ then $(K_g/K_1) \geq 1$, so there will be no decrease in signal due to the gap. Thus, as long as $(W-w)/2$ is kept small, as in our case, there will be either large steps in activity or characteristic decreases at the gaps to identify when bundle edges pass under the collimators. Both of these conditions were observed in the various combinations of bundles used during these tests.

All three parts of Figure 6 show a consistent fine structure or profile of activity across the bundles that can be characterized by the orientation of the bundle on the holding tray, as shown diagrammatically in Figure 6C. This variable profile of approximately 10% can be a useful additional means of verifying that a bundle is being transferred. However, it also sets some limits on the minimum width of the collimator slot that can be used before confusion occurs between inter-element gaps and inter-bundle gaps.

The objective of the concept is to measure suitable spectrum regions of the gamma-ray beam while the fuel is in motion at about 1 cm/s. To simulate these measurements, the end of the collimator was swung across the bundles while signals were recorded via the SCA and Ratemeter channels shown in Figure 4. The results of such a scan of bundle group A are shown in Figure 7 and curves (a) and (b) can be compared to Figures 6B and C.

The response of such ratemeters to a step change in count rate from K_1 to K_2 is given by

$$\frac{K}{K_1} = 1 + \left(\frac{K_2}{K_1} - 1\right)\left(1-e^{-t/T}\right) \qquad (6)$$

where T is the time-constant setting and t is time. For the case of the gaps between bundles, the time available to sense the signal decrease, as the collimator crosses the gap, is

$$t = (\text{gap width} + \text{collimator slot width})/\text{drive speed}$$

For the case shown in Figure 7, the small gap has $t = (0.23 + 0.87)/0.9 = 1.22$ s. With the time constant $T = 0.3$ s, the recorded trace of the signal at the gap should be within 2% of K_g/K_1.

The percent scatter of the recorder trace, e, due to statistical fluctuation, is given as twice the percent standard error,

$$e = \frac{200}{\sqrt{KT}} \tag{7}$$

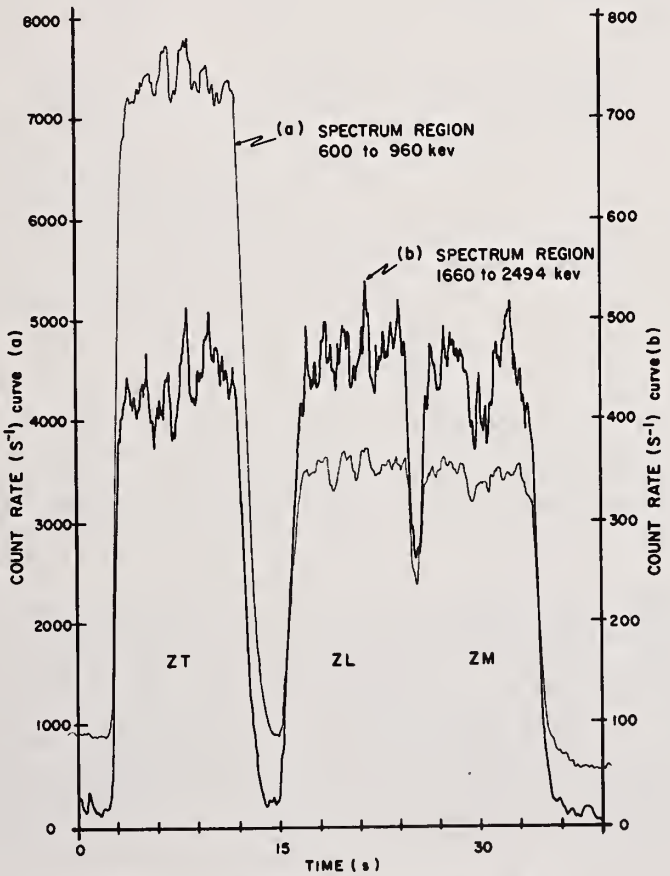

FIGURE 7 RECORDER TRACE OF SIGNALS FROM BUNDLE GROUP A, WITH SIMULATED TRANSFER SPEED OF 0·9 cm/s

To obtain optimum response for fuel verification, it is necessary to obtain a count rate of sufficient magnitude that, in combination with an appropriate time constant, prevents data scatter from obscuring the signal changes that provide the required signature of bundles. For the count rates obtained from these tests and for a speed of about 1 cm/s, a time constant of 0.3 s gave the best performance. The scatter for the spectrum region of 600 to 960 keV, shown on curve (a) of Figure 7, should add 6% to the 10% fluctuations due to the fine structure of the ZM and ZL elements. The measured fluctuations are 14%. For curve (b),

the spectrum region from 1660 to 2495 keV, the scatter would add 17% to the fine structure (i.e. total of 26%), compared to the measured 31%.

The small-gap values of K_g/K for curves (a) and (b) were 0.69 and 0.58, compared to 0.63 and 0.45 obtained previously. These agree within the systematic error (2%) of introducing the time constant plus the statistical errors.

This agreement between the two methods of scanning bundle groups was good throughout the tests, for a wide variety of drive speeds and time constants. (One systematic error caused a 15% difference between the count rates of the two data sets due to a small error in adjustment of the ratemeter output range.) As would be expected, we found that, when drive speeds increased significantly, some corresponding increase in counting rates was required or performance suffered.

The other experimental data obtained were high-resolution spectra of the highest activity points of each bundle. These measurements were carried out with a small planar germanium spectrometer. Corrections for geometry, detector efficiency and gamma-ray intensity were made, and self-shielding effects were estimated, so that the relative source strengths of the fission products could be obtained. The results are listed in Table III.

TABLE III

RESULTS OF GERMANIUM SPECTROMETRY OF THE FUEL BUNDLES

Bundle Identity	Burnup Outer Element Mwh/kg	Decay Days	Relative Source Strength								
			^{144}Ce	^{144}Pr	^{95}Nb	^{95}Zr	^{137}Cs	^{134}Cs	^{103}Ru	^{106}Rh	Uranium X-rays
ZM	209.5	316	62.9	46.7	10.4	5.2	11.8	4.19	0.66	37.0	52.3
ZL	205.5	316	82.9	54.7	12.1	6.7	13.9	5.12	0.66	44.0	75.8
ZT	152.1	183	72.3	56.8	56.1	36.4	7.9	1.87	9.45	27.4	100.5
ZK	181.1	316	60.4	46.7	12.2	5.9	11.1	3.53	1.11	33.2	63.4
AAJ	82.2	183	96.5	74.4	115.3	61.6	5.5	0.73	16.13	24.9	160.6
XX	172.8	183	89.9	73.7	88.3	47.1	11.2	3.98	15.50	46.4	153.0

The isotopes that dominate the spectrum are ^{137}Cs, ^{95}Zr, ^{95}Nb and ^{144}Pr, with ^{134}Cs adding a secondary long-lived component. To determine how well these isotopes could be defined as composing the regions of the NaI spectrum, the empirical relationships given by equations (a), (b) and (c) of Table IV were derived. Equation (a) gives a value for the count rate K_a, in the 2005 to 2495 keV region of a NaI spectrum, from the relative source strength of ^{144}Pr found by germanium spectrometry. A single-term equation is used because this is the highest energy region and thus has no Compton background component. The comparison between the measured value K_p and the calculated value K_a, given in Table IV, shows that the empirical coefficient is consistent. This is expected because the coefficient is an expression of the counting efficiency of the system.

The region of interest (725 to 960 keV), represented by the two-component equation (b), has a signal component due to ^{95}Zr and ^{95}Nb and a background that has been totally attributed to ^{144}Pr. The ratio K_z/K_b in Table IV shows that the empiricism of equation (b) works reasonably well, considering that the ^{134}Cs background was ignored and that the empiricism was derived from statistically fluctuating data.

The third region of interest (600 to 960 keV), given by equation (c), extends the argument to include a third isotope and still remain reasonably consistent.

It therefore appears to be possible to predict, at least approximately, either the count rates of these regions, if the source strengths from the fuel are known, or vice versa

TABLE IV

COMPARISON OF MEASURED NaI SPECTRUM REGIONS TO
RELATIVE SOURCE STRENGTHS OF THE FISSION PRODUCTS

Bundle Identity	^{144}Pr 2005 to 2495 keV		$^{95}Zr + ^{95}Nb$ 725 to 960 keV			$^{137}Cs + ^{95}Zr + ^{95}Nb$ 600 to 960 keV		
	Count Rate K_p (s^{-1})	$\frac{K_p}{K_a}$	Count Rate K_z (s^{-1})	K_b	$\frac{K_z}{K_b}$	Count Rate K_{c+z} (s^{-1})	K_c	$\frac{K_{c+z}}{K_c}$
ZM	262	1.17	2 400	2 200	1.09	4 300	3 740	1.15
ZL	260	0.99	2 400	2 600	0.92	4 400	4 430	0.99
ZT	245	0.90	6 600	6 860	0.96	8 900	10 250	1.15
ZK	230	1.03	2 800	2 340	1.20	4 900	3 920	0.80
AAJ	340	0.95	11 000	12 170	0.90	17 250	17 760	1.03
XX	350	0.99	9 000	9 750	0.92	14 500	14 550	1.00

Equation (a) $K_a = 4.8\ Pr$

(b) $K_b = 28\ Pr + 57\ Zr$

(c) $K_c = 43\ Pr + 81\ Zr + 40\ Cs$

Pr = relative source strength of ^{144}Pr from Table 3

Zr = sum of relative source strengths of ^{95}Zr and ^{95}Nb from Table 3

Cs = relative source strength of ^{137}Cs from Table 3

DISCUSSION OF RESULTS

It has, first of all, been determined that a gamma-ray beam can be created, to allow the activity of a fuel bundle to be measured with reasonable accuracy while in motion during transfer from the interim to the long-term storage ponds. With the proper selection of parameters such as collimator slot dimensions, gamma-ray filtering (to set up appropriate counting rates), and with suitable electronic equipment and settings, a good trace of the profile of a spectrum region from a fuel bundle can be recorded.

As discussed, the relationships between the bundle irradiation history and the magnitude of these records can be developed, to a first approximation, from the data obtained during these tests. The reason for the approximation lies in the irradiation histories of the fuel bundles available for these tests. They were obtained from the CRNL Fuel Engineering Branch and were part of a set of bundles being irradiated to high burnup in the test loops. They were not, however, given a continuous irradiation, in fact quite the reverse was true, since they were frequently exchanged, and irradiations of short and long durations were mixed over a number of years. As a generalization, the irradiations could be lumped into two stages, with a rest period between them. For calculation purposes, the effective power during irradiation was obtained from

$$\text{Effective Power} = \frac{\text{Effective Full Power days}}{\text{Irradiation time}} \times \text{Operating Power}$$

Beginning with ^{137}Cs, equation (2) can be altered by the addition of a coefficient ε_{Cs} to give

$$S = \varepsilon_{Cs} B \qquad (8)$$

For each bundle, the coefficient was obtained from the measured value of S, from the germanium spectrum results, and the burnup data of Table III. The results of the calculations for ^{137}Cs are listed in Table V, along with irradiation data and similar calculations of

coefficients for ^{144}Pr and ^{95}Zr. For ^{137}Cs, the agreement with the principle set out by equation (2) is demonstrated by the agreement between the values for ε_{Cs}.

The same approach was taken for ^{95}Zr, using equation (3) to obtain values of the coefficient ε_{Zr}, and for ^{144}Pr, using equation (1) to obtain the coefficient ε_{Pr}. The agreement among values for these coefficients does not match that of ^{137}Cs, but considering the uncertainties in the calculation, due to the checkered irradiation history of these bundles, the scatter in the results is quite acceptable. For fuel bundles irradiated under the conditions of a power station, predictions of source terms should be much more reliable, so to a first approximation, correlation of spectrum data to fuelling history should be possible.

All of this work has been reported on a relative basis, to establish feasibility, so that any equipment designed for use in the power station would have to be calibrated to obtain the appropriate coefficients for that particular equipment.

TABLE V

COMPARISON OF MEASURED AND CALCULATED SOURCE TERMS

Bundle Identity	Final Irradiation		^{137}Cs		$^{95}Zr + {}^{95}Nb$		
	Effective Power (Kw/m)	Irradiation Time (days)	Measured Source	COEFF ε_{Cs}	Calculated Source	Measured Source (Zr)	COEFF ε_{Zr}
ZM	12.8	283	11.8	0.056	0.42	15.6	37
ZL	12.4	283	13.9	0.068	0.41	18.8	46
ZT	14.5	90	7.9	0.052	1.24	92.5	75
ZK	10.7	283	11.1	0.061	0.35	18.1	52
AAJ	21.7	128	5.5	0.067	2.25	177	79
XX	13.6	199	11.2	0.065	1.67	135	81
MEAN				0.062 +10% -16%			62 +30% -40%

Bundle Identity	First Irradiation		Rest	^{144}Pr		
	Effective Power (Kw/m)	Irradiation Time (days)	Period (days)	Calculated Source	Measured Source (Pr)	COEFF ε_{Pr}
ZM	7.7	630	52	4.2	46.7	11
ZL	6.8	620	82	3.9	54.7	14
ZT	5.2	624	438	2.6	56.8	22
ZK	9.6	365	282	3.1	46.7	15
AAJ	22.9	28	195	4.2	74.4	18
XX	13.0	399	420	4.5	73.7	16
MEAN						16 +40% -30%

CONCLUSIONS

This experimental work has demonstrated the feasibility of a γ-ray spectrometry verification method for Bruce NGS fuel during its transfer to long-term storage. NaI spectrometry, in conjunction with lead filtering and properly selected instrumentation, appears to be the most suitable choice, although germanium spectrometry could also be adapted to the purpose. We found that

(i) Radiation from the fuel can easily be detected, and thus unirradiated or dummy fuel would be discovered.

(ii) Characteristic signal variations due to the fuel elements in the bundle as well as signal steps or depressions at bundle edges can be used to separate bundles and allow them to be tallied.

(iii) The best signal characteristics were associated with the isolated high-energy gamma ray from ^{144}Pr.

(iv) The magnitude of signals from ^{95}Zr and ^{137}Cs, in combination with those from ^{144}Pr, can be used for an approximate assay of the fuel for comparison to the irradiation records.

The practicality and usefulness of the γ-ray spectrometry method should be determined by actual operating experience at the Bruce NGS A in 1980.

Monte Carlo Calculational Design of an NDA Instrument for the Assay of Waste Products from High Enriched Uranium Spent Fuels

by

G. W. ECCLESTON, R. G. SCHRANDT, J. L. MACDONALD & F. H. CVERNA
Los Alamos Scientific Laboratory, Los Alamos, New Mexico

ABSTRACT

The Monte Carlo design of the waste assay region of a dual assay system, to be installed at the Fluorinel and Storage Facility, is described. The instrument will be used by the facility operator to assay high-enriched spent fuel packages and waste solids produced from dissolution of the fuels. The fissile content discharged in the waste is expected to vary between 0 and 400 g of ^{235}U. Material accountability measurements of the waste must be obtained in the presence of large neutron (0.5×10^6 n/s) and gamma (50 000 R/hr) backgrounds. The assay system employs fast-neutron irradiation of the sample, using a 5 mg ^{252}Cf source, followed by delayed neutron counting after the source is transferred to storage. Calculations indicate a $\pm$4-g (2σ) assay for a waste canister containing 300 g of ^{235}U is achievable with an end-of-life (1 mg) ^{252}Cf source and a background rate of 0.5×10^6 n/s.

KEYWORDS: Monte Carlo, delayed neutrons, assay, spent fuel, contaminated waste

An automated delayed neutron interrogation assay system has been designed for the new Fluorinel and Storage (FAST) Facility.[1] This instrument will nondestructively measure the ^{235}U content in high-enriched uranium spent fuels and in waste solids produced from dissolution of these fuels.[2] This paper discusses enhancements to the Los Alamos Scientific Laboratory (LASL) Monte Carlo code that enabled a calculational approach to be used to design the instrument. Calculated data obtained from parameter variations that were used to select design values for the waste assay region are presented. Results of the calculated instrument performance are given for a design basis waste canister assay.

Measurement specifications for the waste solids require a precision of $\pm$30 g (2σ) over the range 0 to 400 g of ^{235}U. The stainless steel waste canister was recently modified to have a 5212-cc volume, 11.43-cm inside diameter, and 50.8-cm length and will be assayed in a scanning mode by lowering it with a crane at a nominal rate of 12 cm per minute through the interrogation region. Assays will be complicated by a background of (α,n) neutrons in addition to prompt neutrons from spontaneous fission of the curium isotopes. The design basis maximum neutron background, based on measurements of representative spent fuels[3], is 0.5×10^6 n/s. The gamma-ray background was specified to be 50 000 R/hr at 30 cm. The amount of curium isotopes is expected to track, because of the chemistry, the amount of ^{235}U placed in the waste canisters. This should result in a significantly lower background than the design basis value with an associated increase in the signal/background ratio providing an improved assay precision. Materials used to specify the solids for the design basis calculations are listed in Table I and represent nominal values expected for the waste.

The assay method selected for this application was based on fast-neutron irradiation of the waste canisters, using a californium source, followed by delayed neutron counting using helium-3 detectors imbedded in polyethylene. The detectors have 2.54-cm diameters and are charcoal lined and filled to 4 atm of helium-3 with 5% CO_2 as a quench gas. The active length was chosen to be short, 30.5 cm, to aid in reducing detection of background neutrons. The background is uniformly distributed throughout the waste but delayed neutrons from fission induced by the californium source exist largely in the region near the source. Limiting the detector lengths and centering them on the source plane produces an enhancement in the number of signal/background events that reach the detectors. The intense gamma radiation from the waste requires a total of 15 cm of lead shielding be placed between the detectors and the assay tube to reduce the gamma flux to below 1R/hr.

TABLE I

DESIGN BASIS WASTE CANISTER MATERIALS

DENSITY OF WASTE SOLIDS = 5 gm/cc
WASTE CANISTER VOLUME = 5213 cc

MATERIAL	DESIGN VALUE QUANTITY (GM)
^{235}U	300
^{238}U	15
Zirconium	18000
Oxygen	6560
Cadmium	125
Carbon	55
Fluorine	260
Boron	200
Iron	520
Hydrogen	30*
TOTAL	26,065 gm

*Corresponds to 1% H_2O by weight in the waste solids.

At this level the detectors will operate without gamma-induced bias effects. Figure 1 is a three-dimensional view of the assay system.

An enhanced version of the LASL Monte Carlo Code (MCNP)[4] was used to obtain the design and performance calculations for the waste assay region. The code permits detailed modeling of a geometry in all three dimensions. Simulation of actual physical processes are accomplished in the code by predetermined probabilities based on randomly selected events. The probablistic description required to simulate a particle history includes specifications of the geometrical boundaries of regions, material compositions within each region, and a description of the cross sections for each isotope.[4,5] The cross sections include energy- and angle-transfer frequency functions for all relevant scattering events. Generation of a sufficient number of independent particle histories, based on random walk, provides separate solutions to the problem whose mean approaches the true value.

Information needed for design decisions required four enhancements be made to the MCNP code.[6] First, a program was written to produce delayed neutrons with the proper yield, energy, and time distribution from the isotopes ^{232}Th, ^{233}U, ^{235}U, ^{238}U and ^{239}Pu. The delayed neutrons were characterized by the measured six-group half-life data from fast fission.[7] The energy distribution was sampled from the measured near-equilibrium ^{235}U delayed neutron spectrum produced in fast fission.[8] Second, neutrons were flagged and then separately tracked and tallied according to whether they were from the californium source, prompt neutrons from fission, or delayed neutrons. Third, a tally was added to permit fissions by isotope and region to be obtained. Fourth, the $^{3}He(n,p)$ reaction was separately tallied to produce detector counts for source, prompt, and delayed neutrons using the track length estimator. The track length per unit volume calculation is a flux that, when multiplied by the appropriate reaction cross section, produces the number of reactions, in this case, the detector counts. This gives better statistics than counting the actual number of ^{3}He captures based on the real random walk. Various Monte Carlo biasing schemes were used to enhance the statistics of collisions producing both fissions and delayed neutrons. This was done by assigning a neutron weight, nominally one, which could be adjusted so that, while one might bias the number of neutrons undergoing an event, the total weight of all neutrons has the correct expected value.

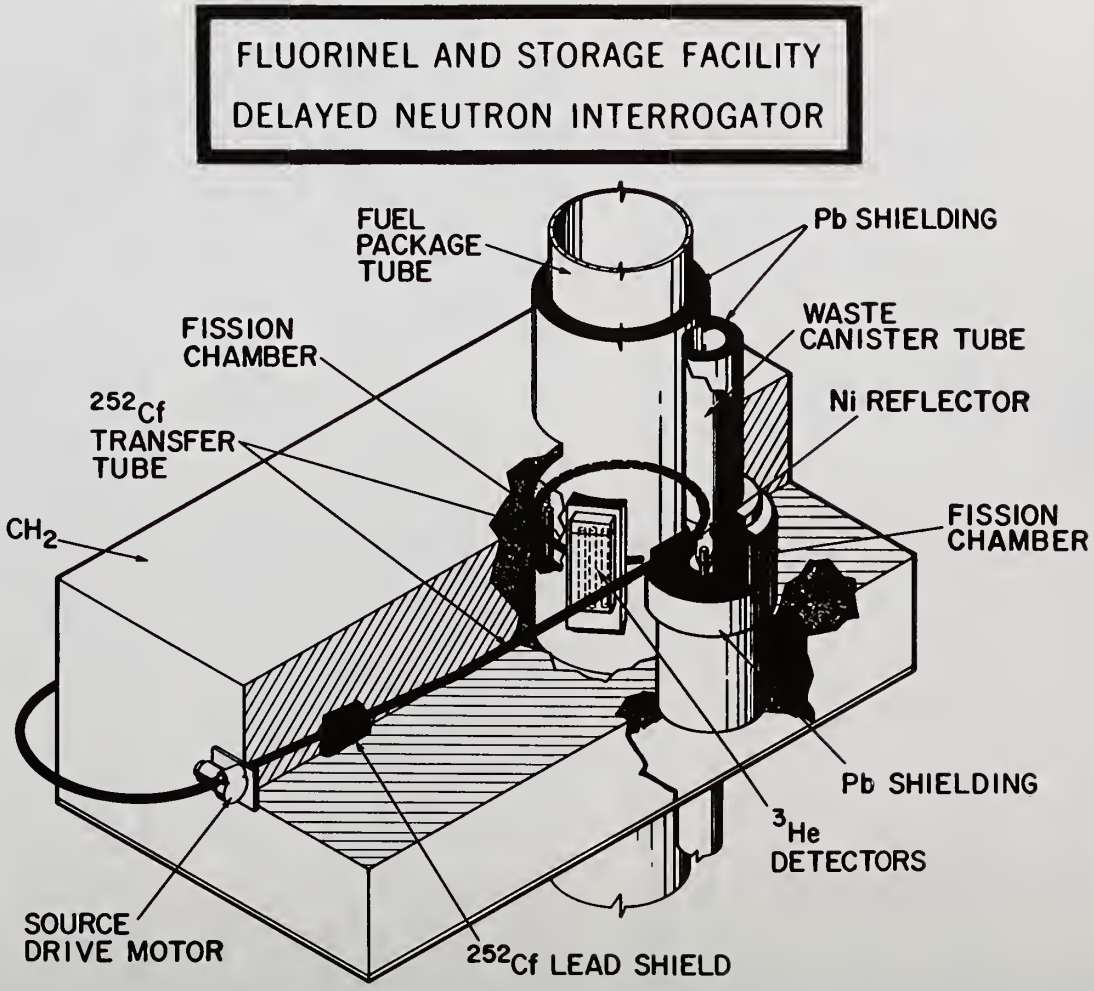

Fig. 1. Fluorinel and Storage Facility Delayed Neutron Interrogator.

For example, suppose a neutron of weight one has a probability P_1 of having a fission. One might sample for fission with probability P_2, $P_2 > P_1$, and assign to the neutron having fission a weight equal to P_1/P_2. Thus, for N neutrons, the total weight having fission is N $(P_1/P_2)P_2$ or $N(P_1)$. In this manner, the number of fission collisions was biased, as well as the delayed neutron production in each of the six groups. Since more delayed neutrons were produced, but with smaller weights, the statistics of the ^{3}He counting rate were improved.

Delayed neutron analysis has generally been performed with two independent calculations.[9] The first calculation provided fission densities in volume elements and the second calculation created delayed neutrons, based on the volume-averaged fission densities, and transported them. The delayed neutron enhancement now combines the above two-step problem into a single calculation. Delayed neutrons are sampled directly producing events at the actual coordinate position, rather than over a volume-averaged region, which provides more accurate results for the delayed neutron tallies. In addition, direct comparisons between fission rates and ^{3}He(n,p) count rates for source, prompt, and delayed neutrons are available with the proper relative errors from one computer run.

Initial design calculations for the waste assay region consisted of varying the number of helium-3 detectors in the polyethylene ring, Fig. 2, which was located at the outside surface of the 15-cm-thick lead shield. A cadmium layer was positioned between the lead and the polyethylene. A 0.635-cm boral sheet was placed on the back surface of the detector ring and followed by an additional 10 cm of polyethylene. The ring was restricted to 230 degrees, and the number of detectors was varied from 21 to 33, the maximum number that would fit. For each configuration the total ^{3}He(n,p) detection efficiency was calculated for a prompt fission neutron point source[10] located at the center of the assay region. The waste canister was void of material for these calculations. The total efficiency increased slowly with the number of detectors from a low of 2.7% to a high of 3.2%, a change of only 0.5%. The slow rise in efficiency resulted, as the number of detectors was increased, because the detectors were placed closer together, decreasing the amount of polyethylene between them. This resulted in less moderation and an increase in detector cross-interaction effects that reduced the efficiency per detector. Since the detector efficiency was not a strong function of number, a total of 24 were selected, to reduce the cost and to allow a range of possible connections (i.e. two banks of 12 each or four banks of 6 each) to permit more channels of data processing to be added if the background rate proved excessive. The detectors were located at a 29-cm radius from the center of the waste tube and separated by 2 cm of polyethylene on a spacing of 9 degrees between detector centers.

Detection of delayed neutrons in the presence of a prompt neutron background can be assisted by judicious specification of the amount of polyethylene surrounding the helium-3 counters. Differences in spectral shapes combined with the optimum amount of polyethylene can increase the relative counting efficiency of the delayed to the prompt neutrons. A series of calculations was completed for varying polyethylene thicknesses. A point source of delayed and then prompt neutrons was positioned at the center of the waste region, which contained the design basis matrix material, Table I, but was void of uranium. A plot of the calculated detector efficiencies and the delayed/prompt efficiency ratio is shown in Fig. 3. The efficiency for detecting the lower energy delayed neutrons is enhanced over the higher energy prompt neutrons when thin polyethlene thicknesses are used to cover the front surface of the detectors.

Selection of the polyethylene dimensions is dependent primarily on decreasing the variance of an assay. Under conditions of no background the amount of polyethylene should be increased to provide the maximum detection efficiency and therefore the most counts in a given measurement time. When a background is imposed the polyethylene thickness should be altered to emphasize differences in detection efficiencies between signal and background events that can aid in reducing the variance of a measurement. Signal (S) and background (B) counts from a measurement (M=S+B) can be used to obtain the relative error (σ_r) as a function of detection efficiencies, according to

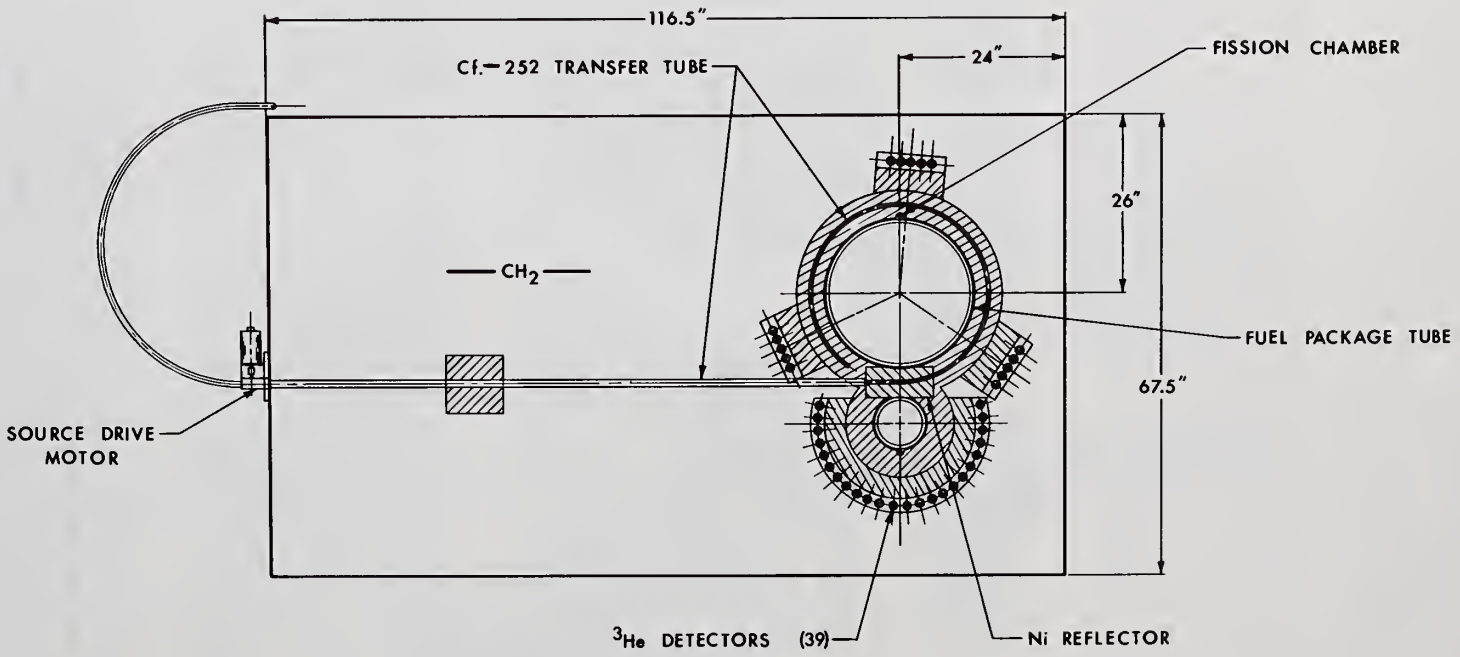

Fig. 2. Delayed Neutron Interrogator plan view.

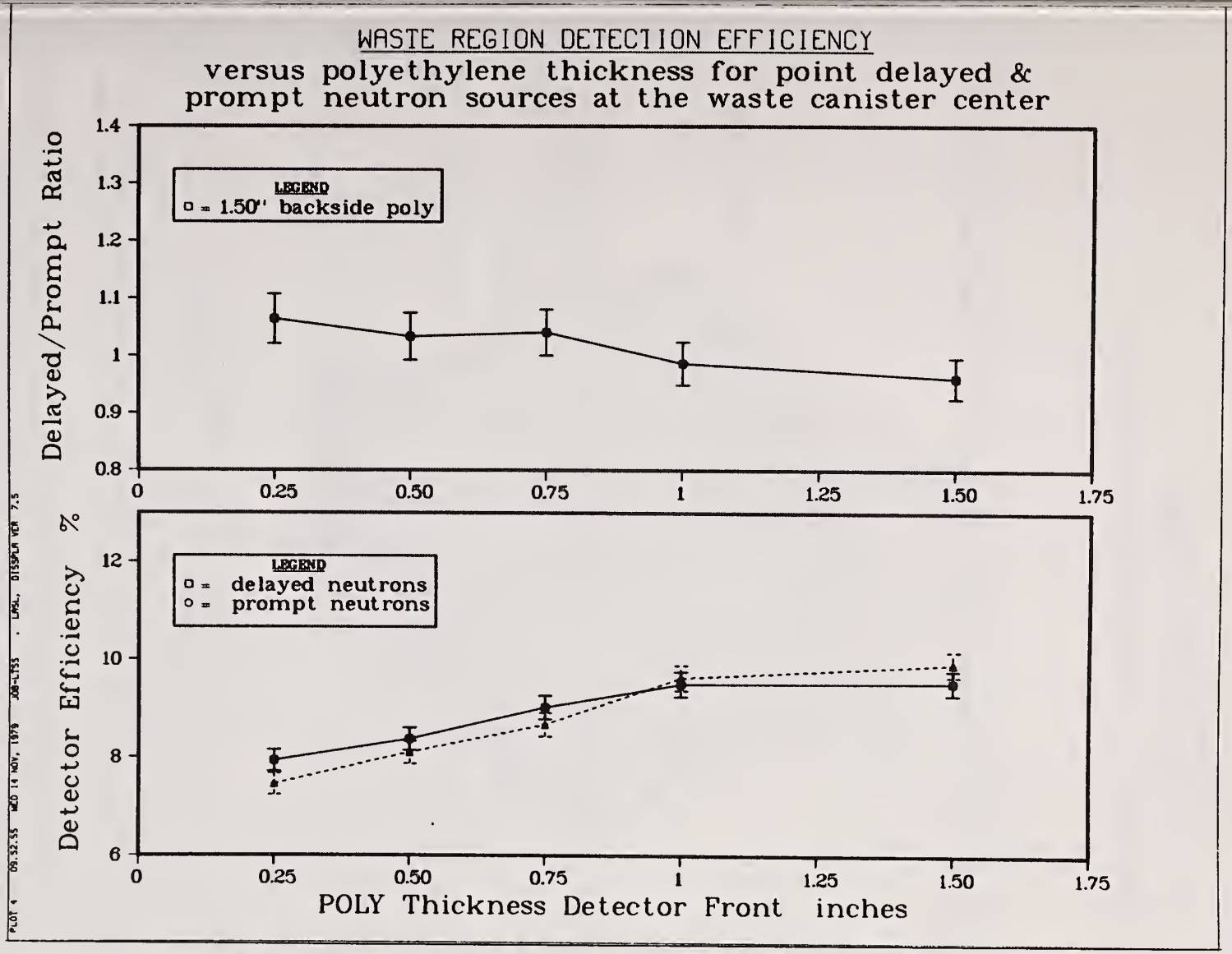

Fig. 3. Waste region detection efficiency for prompt and delayed neutron point sources versus the amount of polyethylene around the detector.

$$S = M - B$$

$$\sigma_S = \sqrt{\sigma_M^2 + \sigma_B^2} = \sqrt{M+B} = \sqrt{S+2B}$$

The signal and background terms can be expressed analytically as

$$S = k_S \varepsilon_S$$

$$B = k_B \varepsilon_B$$

where k_S, k_B are constants representing a specific type of sample matrix and measurement system with detection efficiencies ε_S and ε_B. The relative standard deviation (σ_r) in the measured signal is

$$\sigma_r = \frac{\sigma_S}{S} = \sqrt{\frac{M+B}{S^2}}$$

$$= \sqrt{\frac{(k_S \varepsilon_S + k_B \varepsilon_B) + k_B \varepsilon_B}{k_S^2 \varepsilon_S^2}}$$

When the background dominates the signal ($k_S \varepsilon_S << k_B \varepsilon_B$) then σ_r can be approximated to

$$\sigma_r \sim \sqrt{\frac{2 k_B \varepsilon_B}{k_S^2 \varepsilon_S^2}} = k \sqrt{\frac{\varepsilon_B}{\varepsilon_S^2}}$$

The selected polyethylene thickness should produce efficiencies, ε_S and ε_B, for detecting signal and background events that reduce the relative standard deviation. Figure 4 is a three-dimensional plot showing the variation in σ_r as the polyethylene thickness on the front and backside of the helium-3 detectors was altered. The detector ring for the waste assay geometry was selected, based on the data of Fig. 4, to have 1.91 cm and 5.08 cm of polyethylene on the front and backsides, respectively.

Calculations for various materials surrounding the source were evaluated in terms of tailoring the energy spectrum. The objective was to find a material combination that would limit fissions from the fertile isotope, ^{238}U, to a negligible contribution, to increase the ^{235}U fission rate per californium source neutron, and to provide a uniform sample interrogation. The source was positioned in a 11.43-cm-wide block that is located between the waste and spent fuel tubes, termed the "Ni REFLECTOR" in Figs. 1 and 2, during irradiation of the waste canister. For the material evaluations, the source was positioned at the center of the tailoring region, which corresponds to a distance of 15.24 cm from the center of the waste tube.

Materials placed in the tailoring block for the calculations consisted of a void, nickel, lead, and geometrical combinations of all three. Table II contains the calculated fission rates per source neutron, the fissile/fertile fission ratio, and the inner/outer waste region fission ratio for each of the material combinations. The inner/outer ratio is used to determine the penetration of source neutrons into the sample. This ratio is discussed in detail in a later section of the report. The waste matrix used in the calculations is listed in Table I with the exception that the ^{235}U loading was reduced to 100 g.

The material combination producing the highest fission rate consisted of lead on the front region, between the source and waste tube, and nickel on the back region (lead/nickel) of the source. Other material combinations, such as void/lead and lead-void-lead/nickel, which produced high fission rates, generally had much lower fissile/fertile fission ratios (700 to 800) compared to the lead/nickel value of 1179. One exception was the all-nickel case, which had the largest fissile/fertile ratio, 1713, in addition to a high fission rate. The uranium to be assayed in the waste will be high

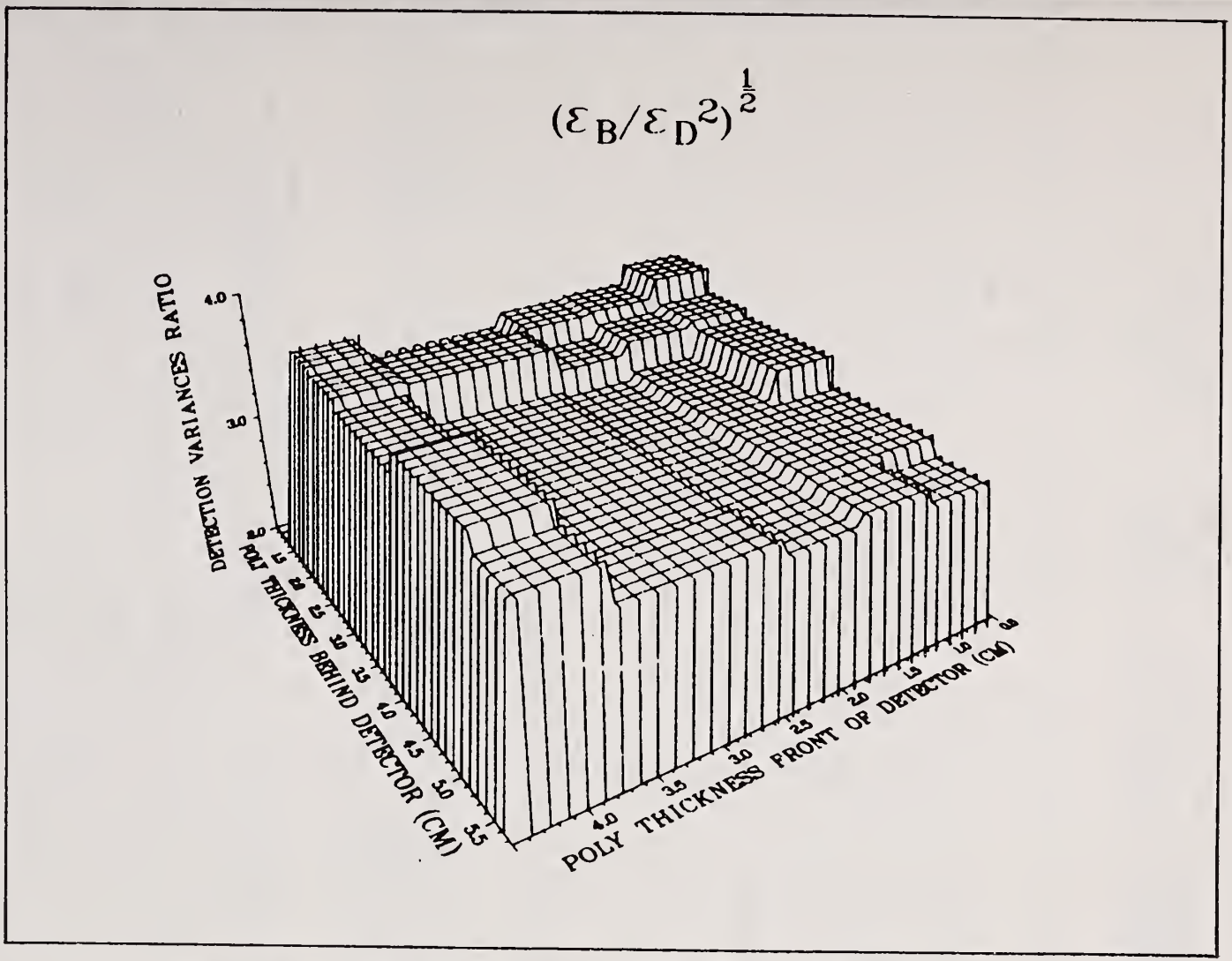

Fig. 4. Relative standard deviation of signal counts versus polyethylene thickness as a function of signal and background detection efficiencies.

TABLE II

	MATERIAL SURROUNDING SOURCE	^{235}U FISSIONS PER SOURCE NEUTRON x 10^{-4}	$^{235}U/^{238}U$ FISSION RATIO	INNER/OUTER WASTE REGION FISSION RATIO
1	VOID	6.07 ± 0.36	652 ± 45	1.25 ± 0.08
2	NICKEL	8.44 ± 0.39	1713 ± 119	1.31 ± 0.07
3	LEAD	7.89 ± 0.41	939 ± 61	1.11 ± 0.07
4	VOID/NICKEL*	8.65 ± 0.44	827 ± 52	1.22 ± 0.06
5	VOID/LEAD	8.67 ± 0.46	750 ± 47	1.24 ± 0.08
6	LEAD/NICKEL	8.93 ± 0.44	1179 ± 76	1.25 ± 0.08
7	NICKEL/LEAD	7.45 ± 0.37	1373 ± 96	1.29 ± 0.07
8	PB-V-PB/NI**	8.68 ± 0.39	705 ± 38	1.25 ± 0.07
9	NI-V-NI/PB	8.01 ± 0.37	641 ± 36	1.28 ± 0.07

*Void on the front region of the source and nickel on the back region of the source.

**Lead with a notched groove on the front region of the source and nickel on the back region.

enriched ($\geq$ 95%) and low in content (0-400 g). Therefore, the selection criteria for a material combination requires first a high fission rate and second a large fissile/fertile fission ratio. Material combination number 6, consisting of lead on the front region of the source and nickel on the back region, satisfied the criteria of high fission rate and large fissile/fertile ratio the best of all materials studied.

A uniform sample interrogation implies that an assay will be independent of the location of the fissile material in the sample matrix. This is obtained when the fission rate-detection efficiency product is constant for all positions in the sample, assuming self-shielding and other matrix effects caused by inhomogeneous material lumps are not significant. A plan view of the waste assay geometry, Fig. 2, contains the californium interrogation source on one side of the through tube and the neutron counters on the other side. The waste canister will be lowered by crane and cannot be rotated during the scanning assay. The fission rate of waste segments close to the source will therefore be higher than for those segments close to the detectors. In contrast, the detection efficiency will be the opposite of the fission rate distribution. Those waste segments near the source will have a lower detection efficiency than those segments close to the detectors. The waste region in the material evaluation studies was divided into two equal volumes called inner and outer; the inner region was adjacent to the source and the outer region was adjacent to the detectors. The inner/outer region fission ratio, Table II, provides a measure of the penetration of source neutrons into the sample. A uniform sample interrogation for this particular assay geometry requires the inner/outer fission ratio must be larger than unity, to balance the differing detection efficiency as a function of position of the fission in the waste. With the source located at the 12.54-cm position in the lead/nickel tailoring block an inner/outer ratio of 1.25 was calculated.

The fission rate and detection efficiency distributions were studied as a function of position in the waste by dividing the canister into four equal volume segments, labeled A, B, C, and D. Segment A was adjacent to the source, B and C occupied the central waste region, and D was nearest the detectors. The neutron detection efficiency for each segment was determined by generating a uniform delayed neutron source independently in each waste region for the full length and central (1/3) length of the canister and calculating the $^{3}He(n,p)$ reaction rate in the counters. A plot of efficiency versus waste segment, Fig. 5, shows a smaller efficiency for those segments farther from the detector ring.

Segment fission rates, Fig. 6, were computed for a homogeneous 300-g ^{235}U loading in the waste at four separate source positions, 10.16 cm, 12.70 cm, 15.24 cm, and 17.78 cm, specified relative to the center of the waste assay tube.

The product of fission-rate and detection efficiency for the central region of the waste canister and at each of the four source positions is plotted in Fig. 7 versus waste segment. The values between each segment A, B, C, and D at each source position agree within the standard deviations of the calculations, which were between 5 and 8%. Table III lists the difference of the fission rate-detection efficiency product of each segment from the average value at the four source positions. The largest deviation from the average, 7.4%, occurred at the 15.24-cm position for segment A, which is adjacent to the source. The highest fission rate was obtained at the 10.16-cm source position, and the largest deviation from its mean was -3.6%, which was within the uncertainty of the calculations. The low uranium content in the waste in addition to the large specified background rate requires a high sample fission rate to obtain a favorable signal/background ratio. Source positions closer to the waste produce an increased fission rate per source neutron and are more desirable. The 10.16-cm source position was selected because the fission rate-detection efficiency product was constant within 5%, the standard deviation of the calculations, permitting a uniform sample interrogation while allowing the largest fission rate per source neutron to be achieved.

Measurements of the waste canister will be obtained in a scanning mode as the canister is lowered and raised by a crane through the interrogation tube. The measured response is a function of the position of the canister in the tube for each irradiation-counting cycle. Response data were obtained from a set of calculations with the canister located at various positions displaced from the central region along the source-detector plane. The fission rate, relative delayed neutron detection efficiency, and relative background detection efficiency normalized to the center position of the interrogator are plotted in Figs. 8, 9, and 10, respectively, versus vertical displacement of the canister. The fission rate

TABLE III

PERCENT DIFFERENCE IN THE SEGMENT FISSION-RATE DETECTION EFFICIENCY PRODUCT FROM THE AVERAGE

SEGMENT	SOURCE POSITION (cm)			
	10.16	12.70	15.24	17.78
A	+1.6	+2.0	+7.4	0.0
B	-3.6	-5.1	-2.5	+0.6
C	+0.7	+0.4	-2.9	-2.2
D	+1.3	+2.8	-1.9	+1.6

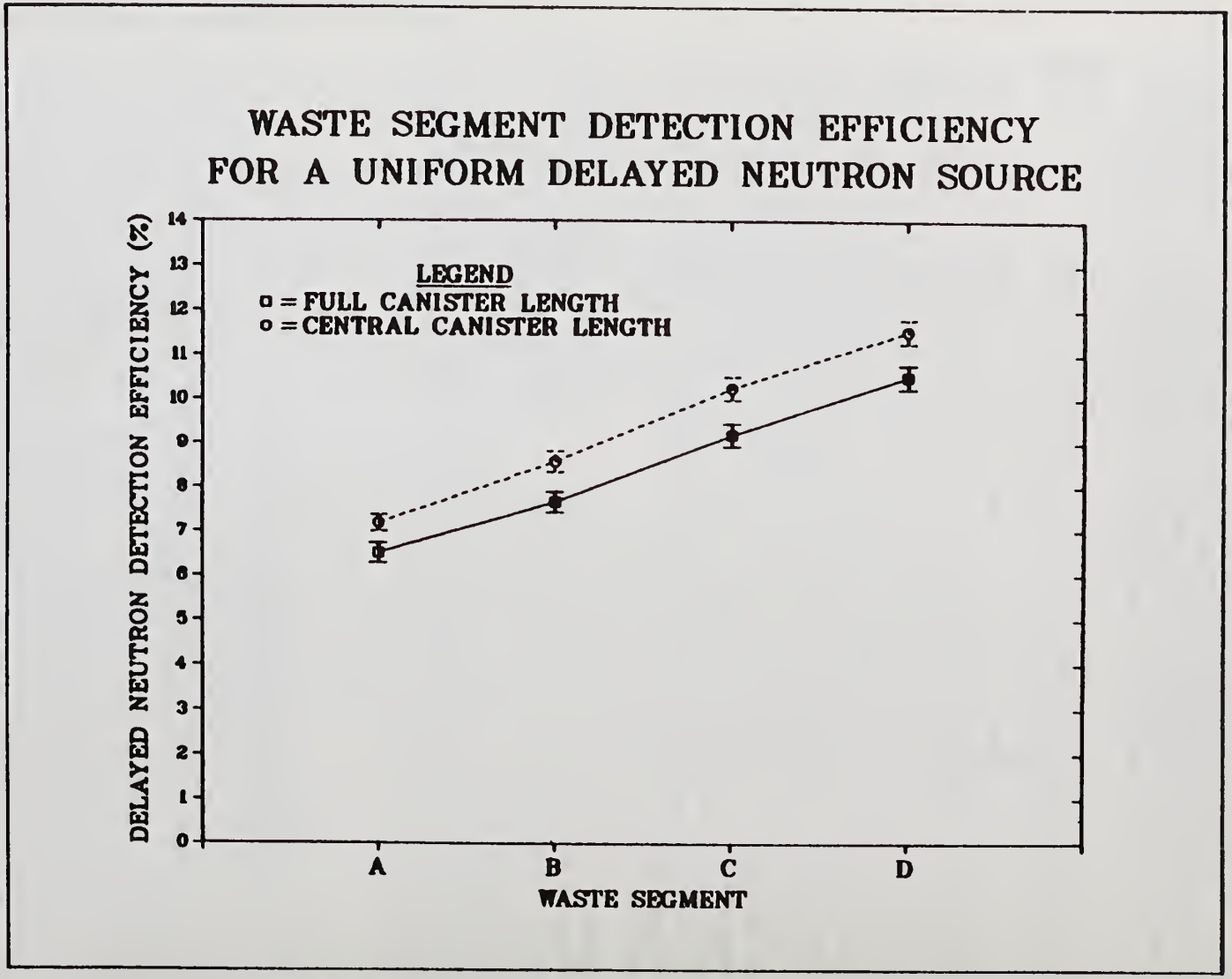

Fig. 5. Waste segment detection efficiency for a uniform delayed neutron source.

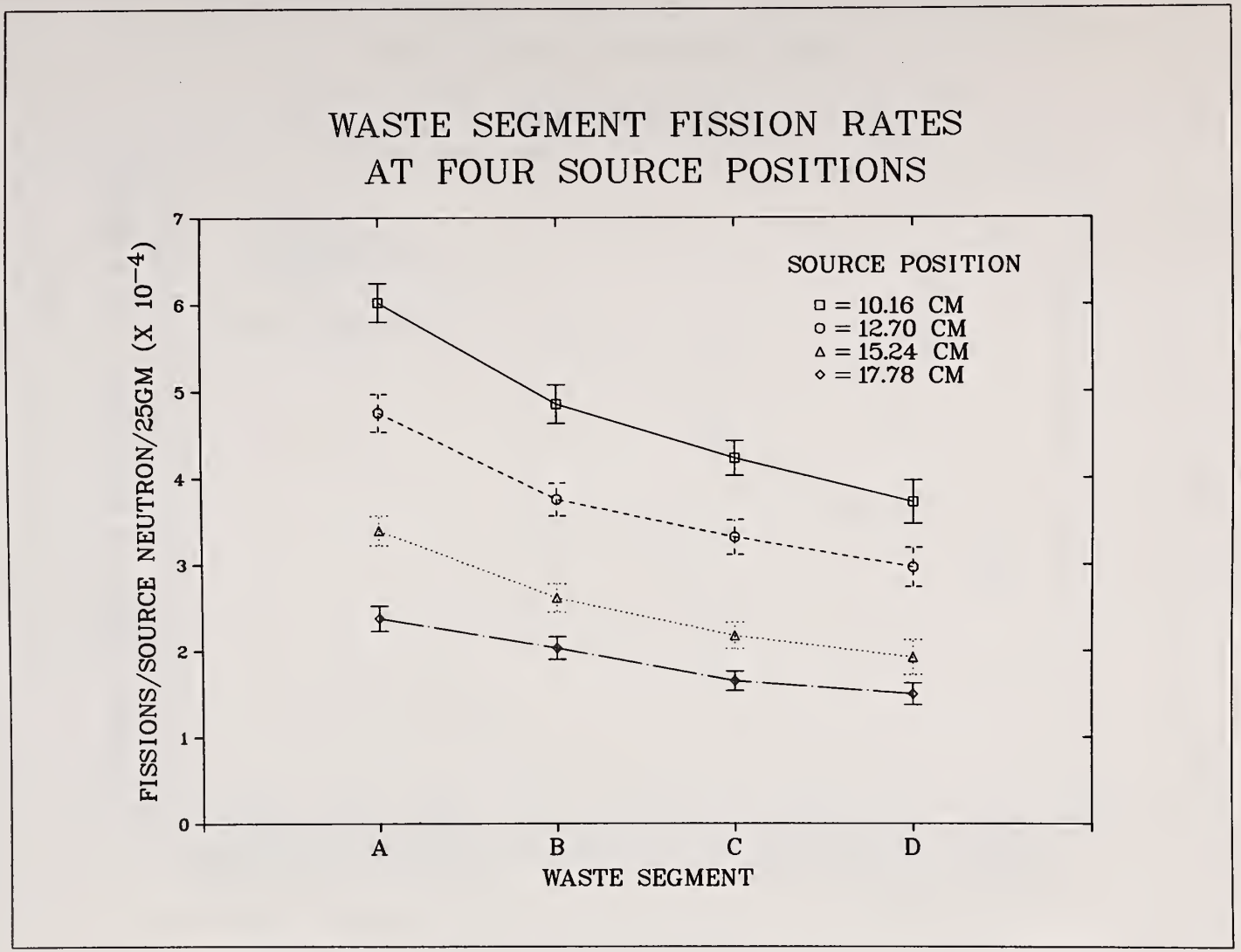

Fig. 6. Waste segment fission rate at four source positions.

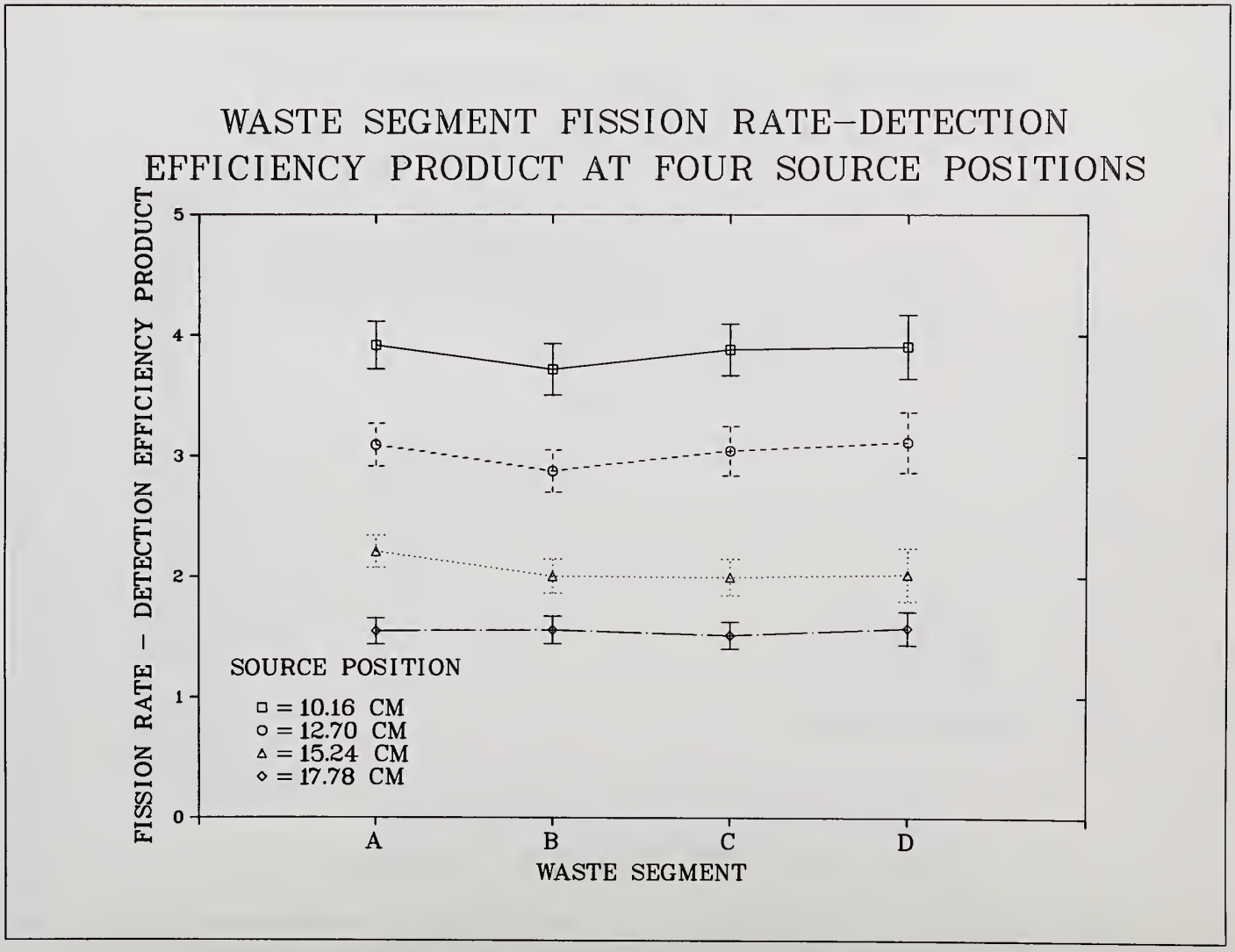

Fig. 7. Detection efficiency—fission rate product at four source positions for each waste segment.

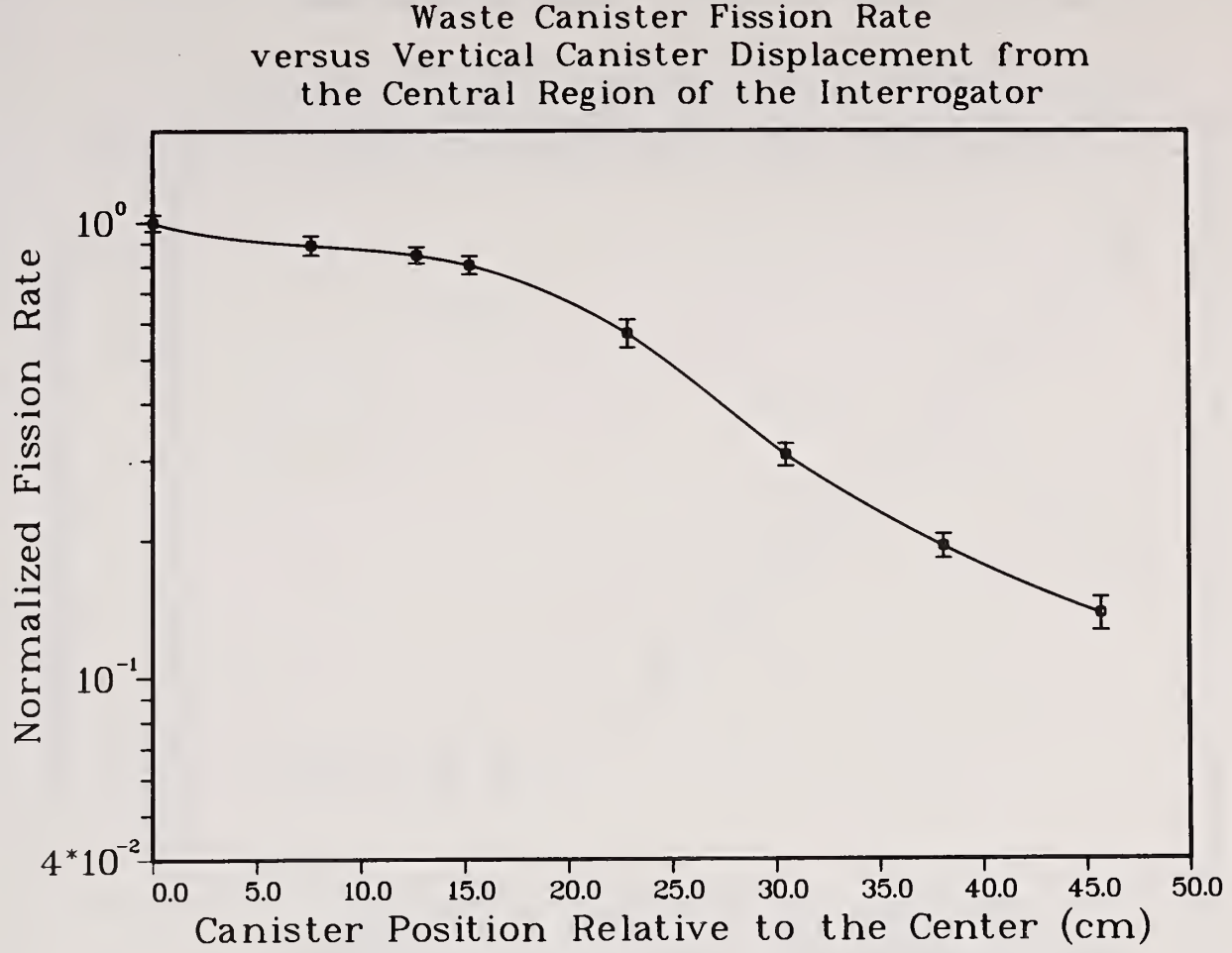

Fig. 8. Waste canister fission rate as a function of vertical displacement from the central region of the interrogator.

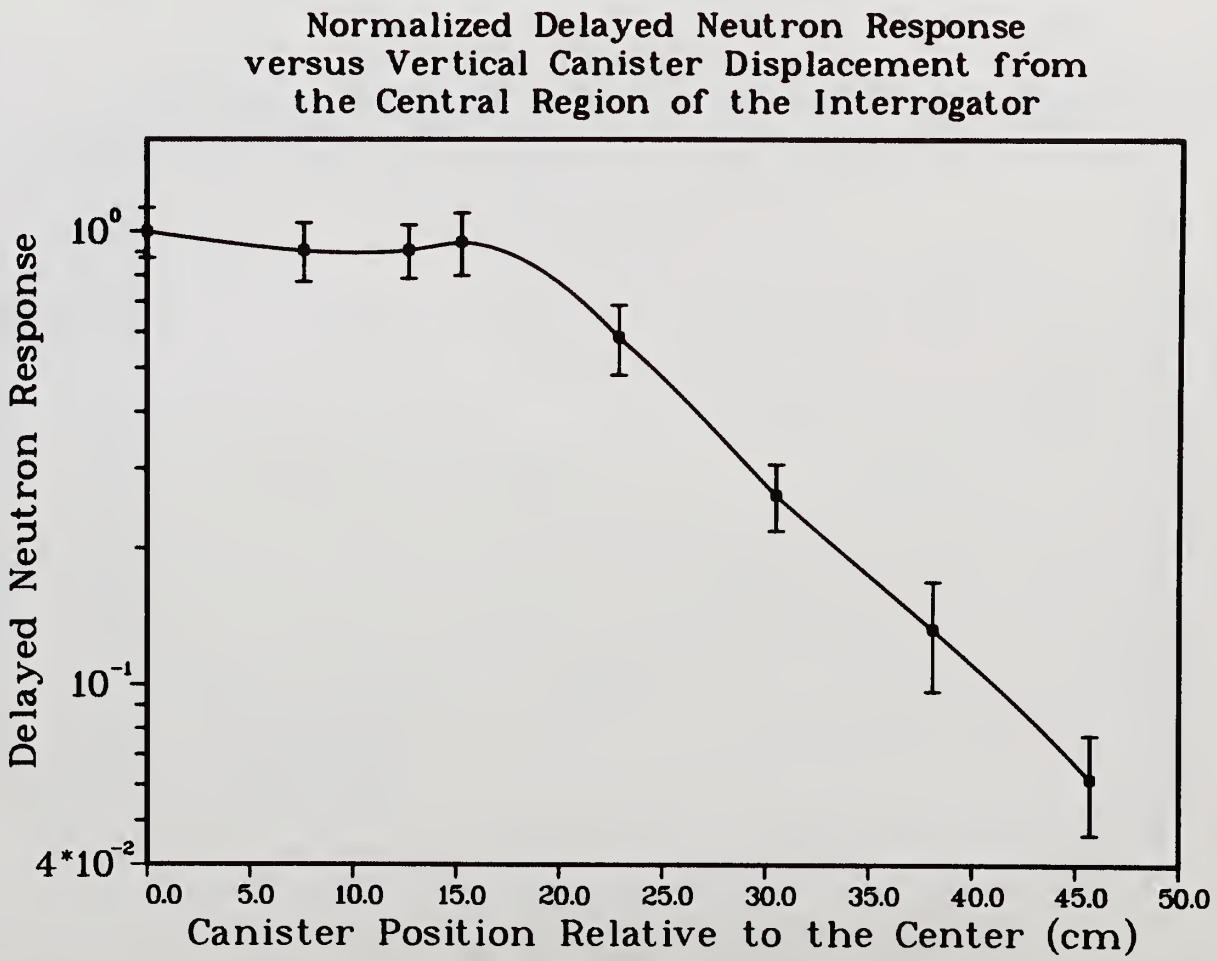

Fig. 9. Normalized delayed neutron response as a function of vertical canister displacement from the central region of the interrogator.

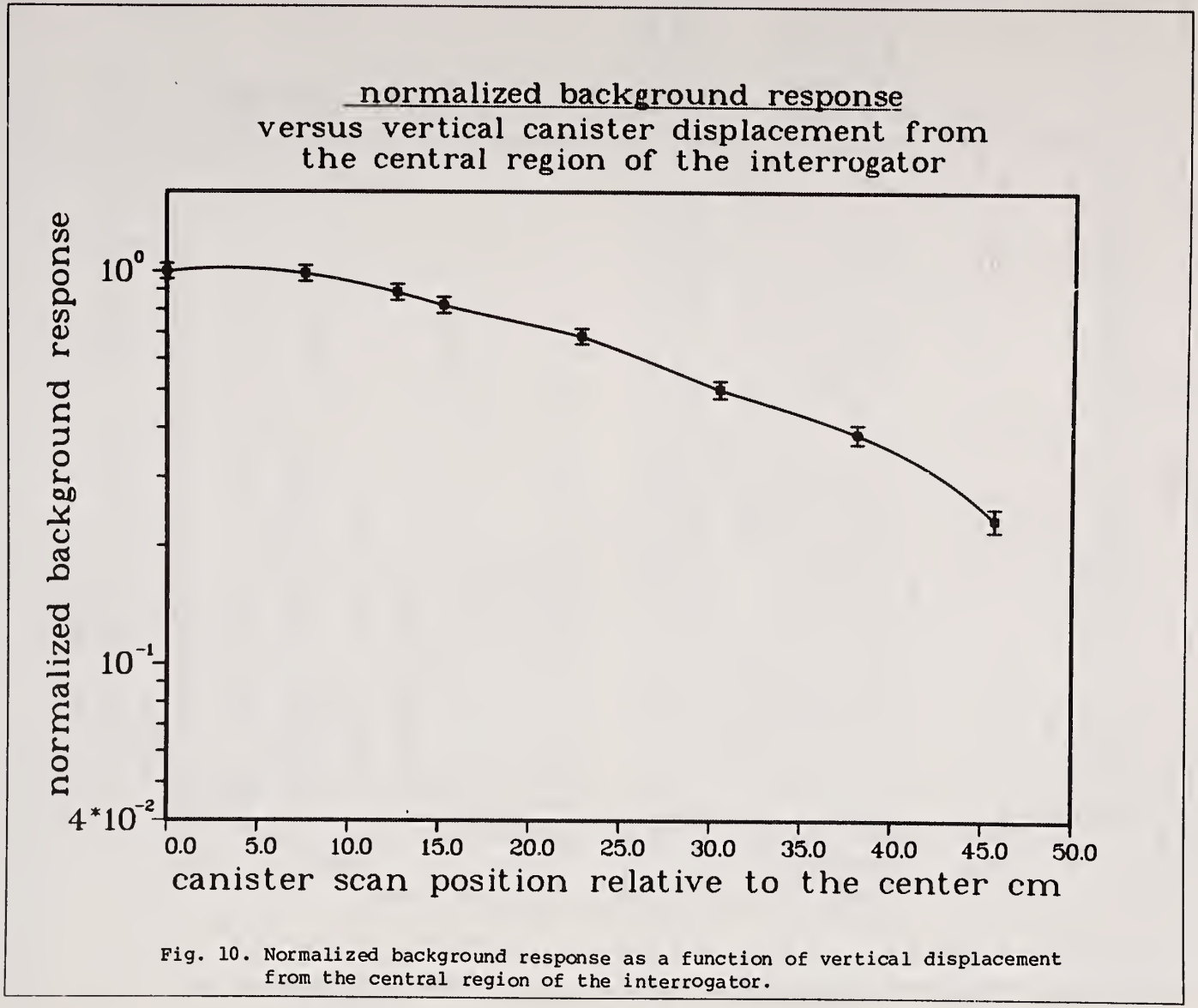

Fig. 10. Normalized background response as a function of vertical displacement from the central region of the interrogator.

slowly decreases with canister displacement. The delayed neutron response remains essentially constant to a 15-cm displacement of the canister and then rapidly falls off. The ends of the waste canister produce a small fraction of the total fissions from source neutrons when the canister is centered in the interrogator. The efficiency for detecting delayed neutrons from fissions in the end regions is also small in comparison to the central region of the waste. The effect is a negligible contribution of the ends of the waste canister to delayed neutron counting and the response remains essentially constant until the canister is sufficiently displaced to where one end contributes a significant fraction of the measured events. The background response was calculated from a uniform distribution of prompt neutrons in the waste canister.

The waste canister fission rate per source neutron (F_o) at the center of the interrogator is plotted in Fig. 11. The response is linear within the uncertainity of the calculation.

The accuracy of an assay is dependent on the number of delayed neutron counts collected and the magnitude of the background. Delayed neutrons will be detected in a cyclical mode consisting of sample irradiation followed by counting as the canister is moved through the tube. Several cycles should be completed on a given waste segment as it moves through the detection region. The canister will be moved at a nominal rate of 12.7 cm per minute. The interrogator has a detection region, Fig. 9, that is roughly 30 cm in length. If a cycle is completed every 12 seconds, corresponding to a movement of 2.5 cm, a sufficient number of scans of each vertical segment of waste should be achieved.

Data collected from a waste canister assay scan can be simulated using the information of Figs. 8, 9, 10, and 11 with the appropriate equations. The delayed neutron counts (D_T) collected from an assay scan is expressed as the sum of the signals (D_n) from each assay cycle, where

$$D_T = \sum_{n=1}^{N} D_n = ST_I F_o \sum_{n=1}^{N} \varepsilon_{D_n} \sum_{j=1}^{n} R_{n-j+1} Y_j$$

where the terms are defined to be

N = Number of cycles completed in the assay scan

S = ^{252}Cf source strength (n/s)

T_I = Irradiation time per cycle (s)

F_o = Fission rate per source neutron per fissile quantity for the sample at the center of the interrogator

ε_{D_n} = Delayed neutron detection efficiency per fission with the canister offset to position n

R_{n-j+1} = Canister fission rate at position n-j+1 relative to the central position

Y_j = Relative delayed neutron yield in the $j^{\underline{th}}$ counting window from the irradiation period.

The relative delayed neutron yields can be calculated using the six-group fast-fission delayed neutron parameters (λ_k, β_k) and a set of cycle times with the expression

$$Y_j = \frac{1}{\beta T_I} \sum_{k=1}^{6} \frac{\beta_k}{\lambda_k} \left(1-e^{-\lambda_k T_I}\right) \left(1-e^{-\lambda_k T_C}\right) e^{-\lambda_k T_D} e^{-\lambda_k (j-1) T_P}$$

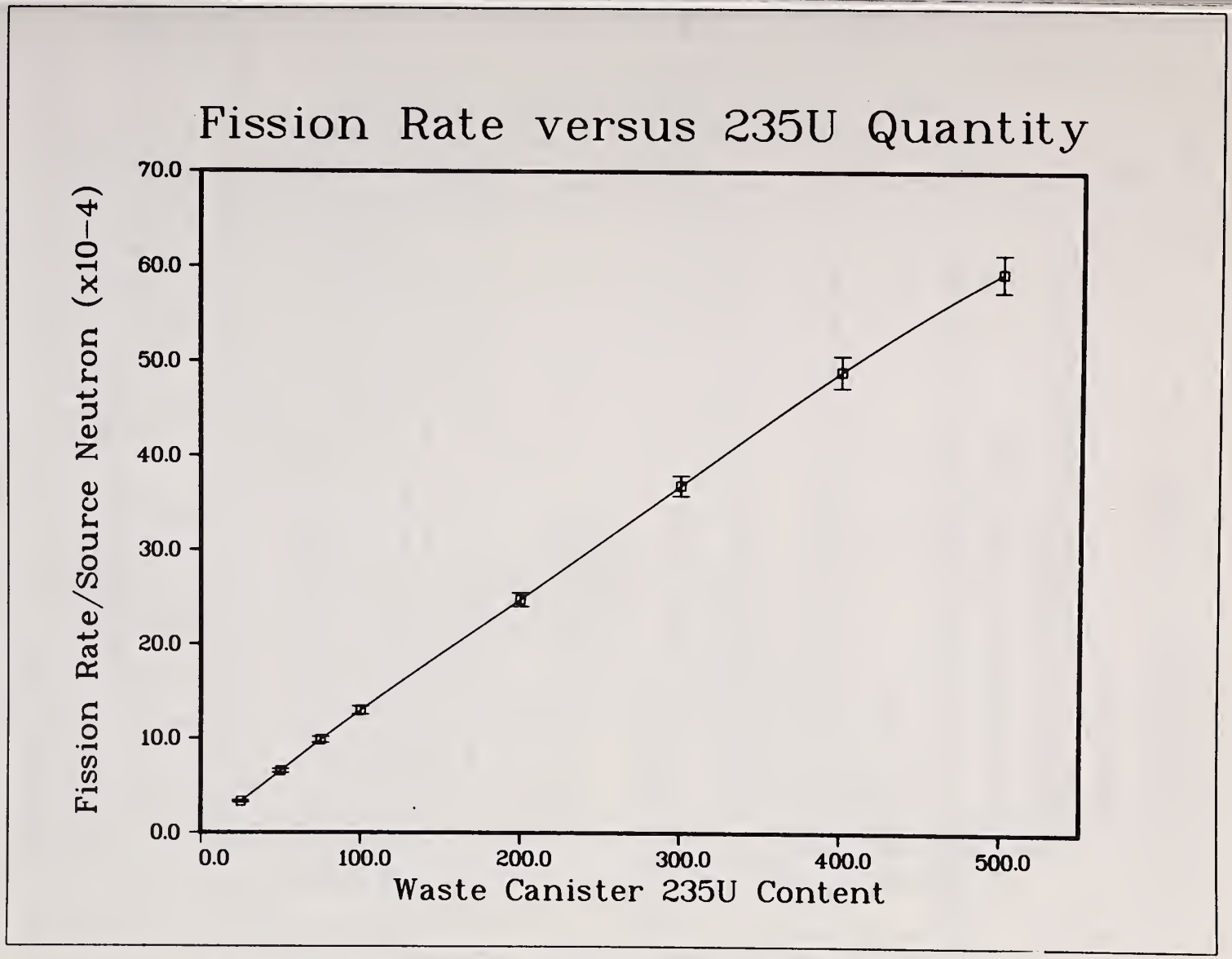

Fig. 11. Fission rate per source neutron versus the quantity of ^{235}U in the canister.

where T_I = Irradiation Time, s

T_D = Delay time from end of irradiation to the start of counting

T_C = Counting Time

T_W = Wait time from end of counting to the start of the next cycle/irradiation

T_P = Total Cycle Time ($T_I + T_D + T_C + T_W$)

The background counts (B_1) obtained during the assay are given by

$$B_1 = \sum_{n=1}^{N} B_R T_C \varepsilon_{B_n}$$

where B_R = Uniform background rate throughout the canister (n/s)

T_C = Counting Time Cycle

ε_{B_n} = Background counting efficiency with the canister at position n relative to the center, Fig. 9

The relative error (σr) in the number of counts collected in an assay is expressed in terms of the previous equations as:

$$\sigma_r = \frac{\sigma_{D_T}}{D_T} = \sqrt{\frac{D_T + B_1 + \left(\frac{NT_C}{T_o}\right)^2 B_o}{D_T^2}}$$

where B_o represents a background measurement for a time T_o prior to the assay.

Relative errors expected from a waste canister assay under various conditions were determined using the above equations and the data contained in Figs. 8, 9, 10, and 11. The irradiation (T_I) and counting (T_C) times to use in an assay were determined from a plot of relative waste assay error versus T_I/T_C at the design background level of 0.5 x 10^6 n/s, Fig. 12. The total cycle time was restricted to 12.0 s and the source transfer time between irradiation and storage (T_D,T_W) was set to 0.5 s. The waste was loaded to 300 g of ^{235}U and the source was set equal to 1 mg (2.34 X 10^9 n/s) of californium.
The relative error for this assay consisting of 29 cycles reached a minimum for a T_I/T_C value of 2.67. This corresponds to an 8-s irradiation time and a 3-s counting time. This cycle time was used in all subsequent calculations.

The effect of source strength and background rate on the waste canister assay error is shown in Fig. 13. The 5-mg curve represents the initial source strength and the 1-mg level is at the end of source life prior to replacement. The design basis background level, 0.5 X 10^6 n/s, indicates that a 0.6% (1σ) assay of the 300 g of uranium in the waste container is obtained at the end of source life. These values represent uncertainties because of counting statistics and do not account for bias affects or matrix affects that will exist in actual waste solids.

The relative assay error as a function of ^{235}U at various background rates is plotted in Fig. 14. The end-of-life source strength (1 mg) was used in the calculation. The dotted line in Fig. 14 represents the required $\pm$15 g (1σ) accuracy level specified for waste assay. The calculations indicate the instrument is well within the accuracy range required, even for backgrounds in excess of the 0.5 X 10^6 n/s design basis value. At the tentative waste canister recycle limit of 300 gm ^{235}U the assay error, with an

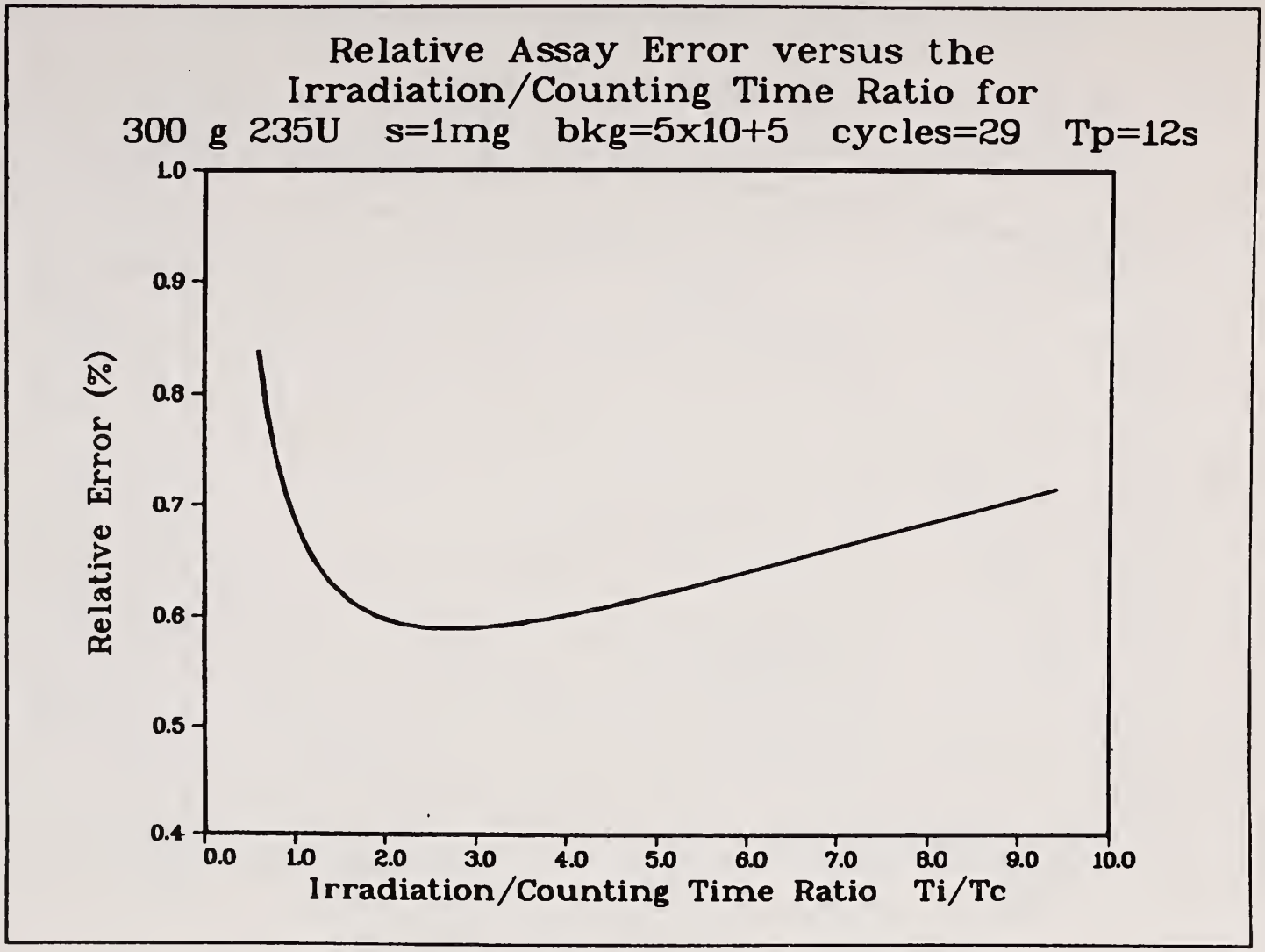

Fig. 12. Relative assay error versus the irradiation/counting time ratio for a source strength of 1 mg ^{252}Cf and 300 g of ^{235}U in the waste.

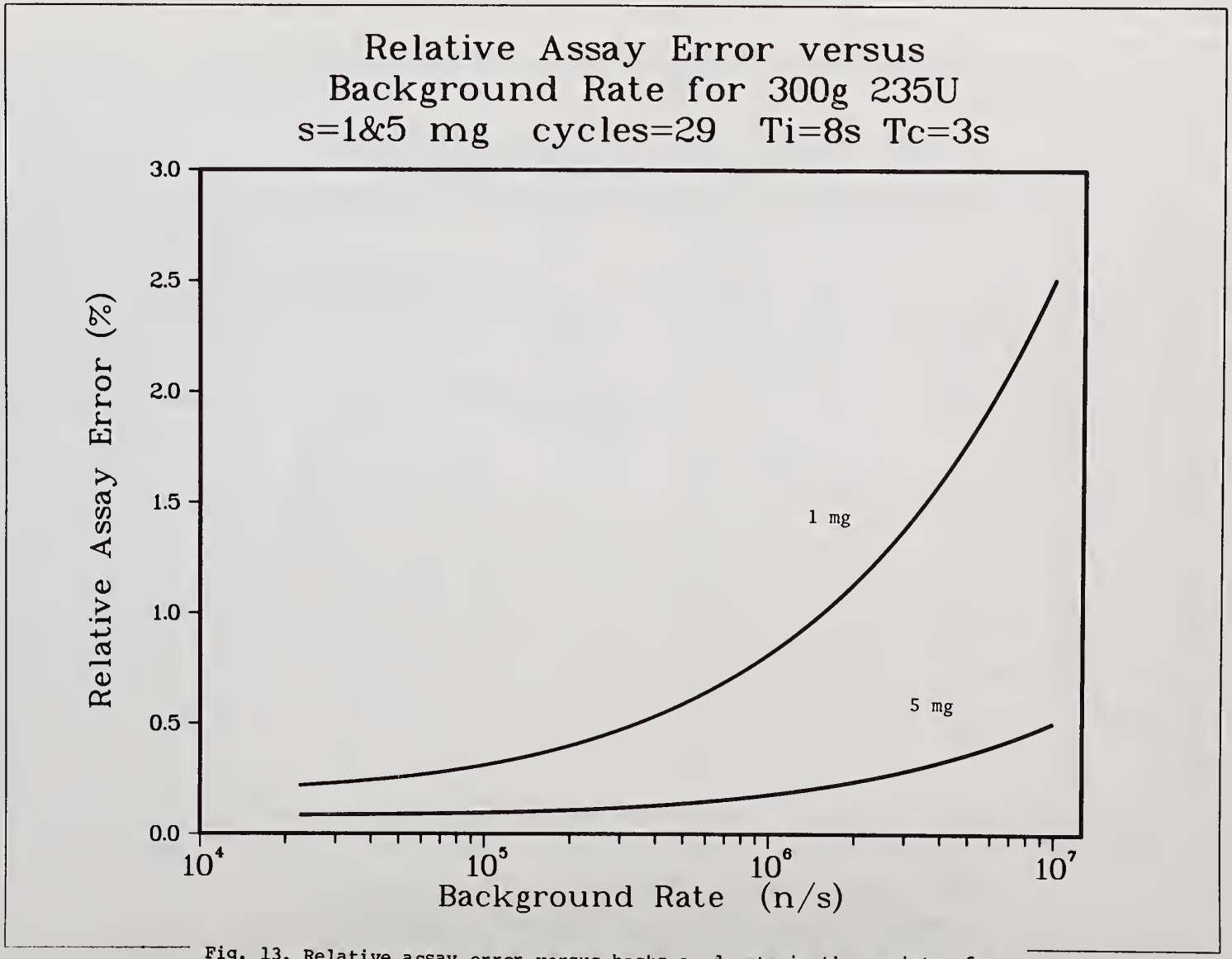

Fig. 13. Relative assay error versus background rate in the canister for T_I/T_C = 2.67 at source strengths of 1 and 5 mg ^{252}Cf with 300 g of ^{235}U in the waste.

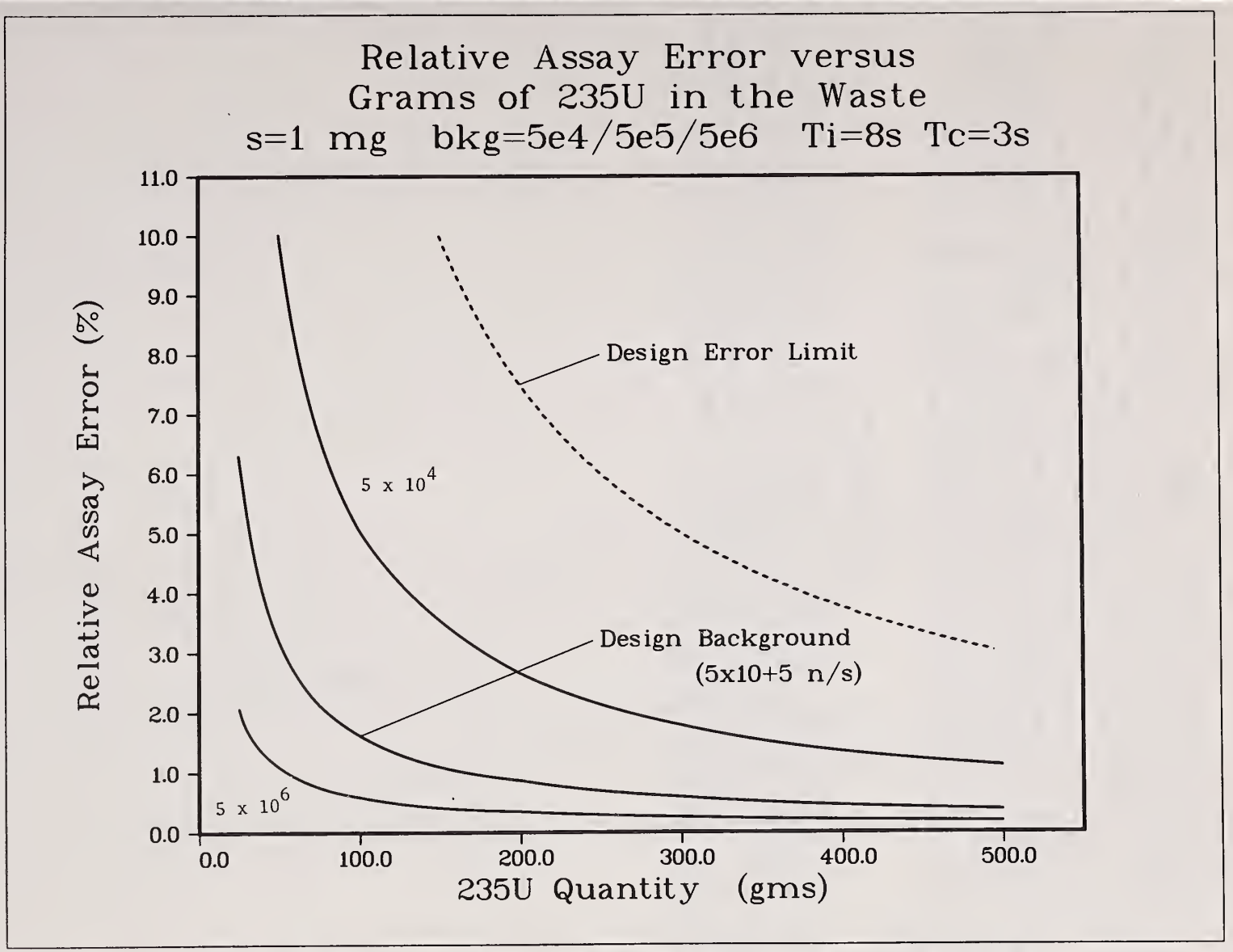

Fig. 14. Relative assay error versus grams of ^{235}U in the waste for a 1-mg ^{252}Cf source.

end-of-life source, has a $\pm$0.6% g (1σ) uncertainty corresponding to $\pm$2 g for the design basis background.

The sensitivity limit for detection of ^{235}U in the waste is plotted in Fig. 15 as a function of the neutron background for the end-of-life source strength. The sensitivity limit is defined to be a delayed neutron signal from the ^{235}U that equals three standard deviations of the background signal. At the design basis background level a detection limit of 4.4 g of ^{235}U exists using an end-of-life source.

Modifications to the LASL Monte Carlo Code (MCNP) enabled a delayed neutron interrogator to be designed for the quantitative measurements of ^{235}U in waste solids produced from dissolution of high-enriched spent fuels. Assessment of the instrument indicates a detection sensitivity for ^{235}U of 4.4 g is possible with an end-of-life 1-mg californium source. The assay uncertainty, based only on counting statistics, for a waste canister with 300 g of ^{235}U is roughly $\pm$4 g (2σ) at the design basis background level of 5 x 10^5 n/s. This uncertainty is within the $\pm$30 g (2σ) design specifications of the instrument.

ACKNOWLEDGEMENTS

The authors would like to thank L. Decker and M. Echo of Exxon Nuclear for their assistance in defining the requirements for the interrogator and providing the contents of the waste material. We are especially indebted to H. Menlove who was responsible for the initial phases of this project. We thank L. Carter and E. Cashwell for their help in developing the delayed neutron biasing scheme. We also express our gratitude to M. Baker and T. Crane for discussions related to this work. Special thanks is given to E. Sandford for providing several of the figures in this report. We also thank J. Hassenzahl and C. Oldenberg for typing this manuscript.

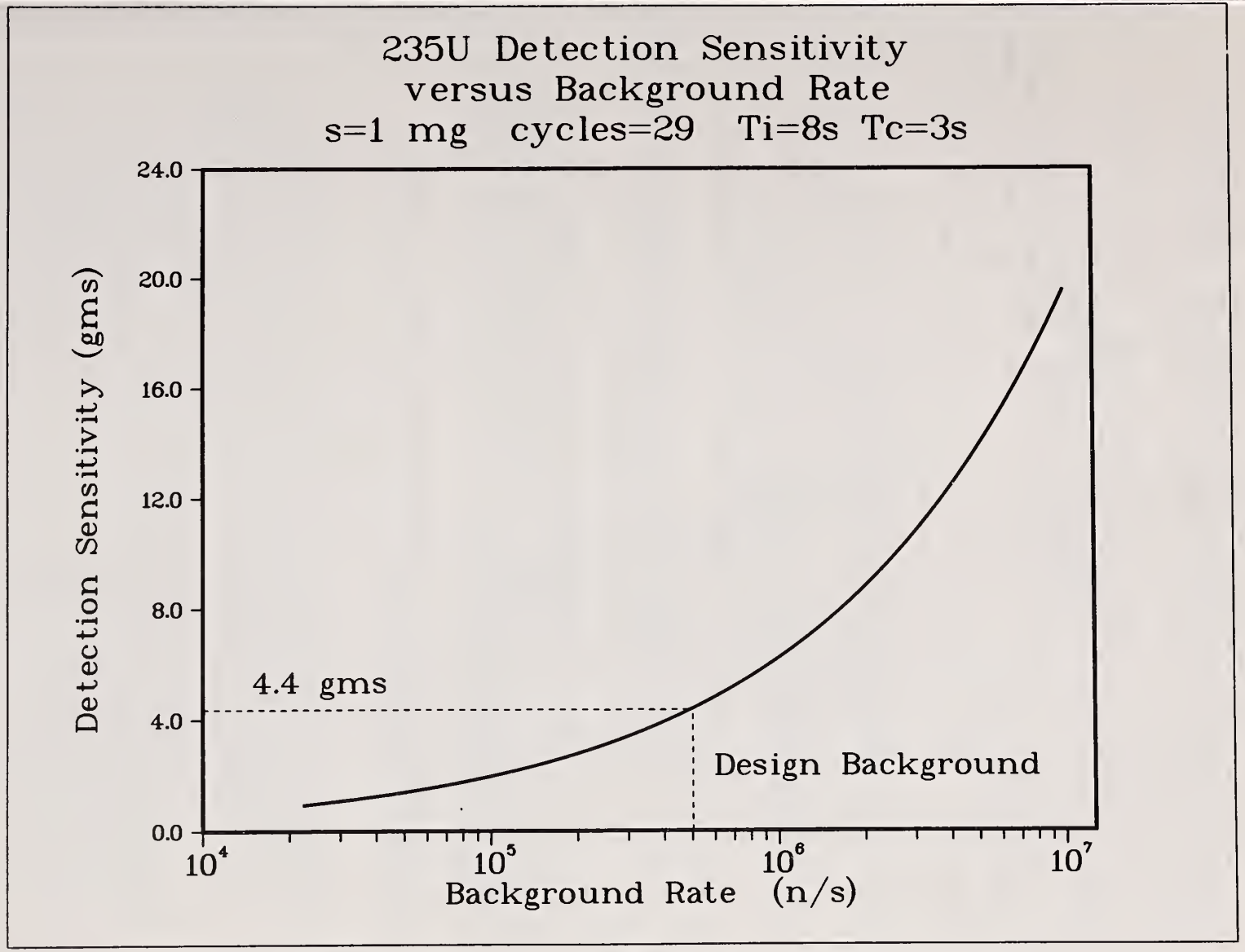

Fig. 15. Detection sensitivity of ^{235}U versus background rate for a 1-mg ^{252}Cf source.

REFERENCES

1. H. O. Menlove, G. Eccleston, D. A. Close, L. G. Speir, "Neutron Interrogator Assay System for the Idaho Chemical Processing Plant Waste Canisters and Spent Fuel - Preliminary Description and Operating Procedures," Los Alamos Scientific Laboratory Report LA-7250-M (May 1978).

2. G. W. Eccleston and H. O. Menlove, "A Measurement System for High Enriched Spent Fuel Assemblies and Waste Solids," 20th Proceedings, Institute of Nuclear Materials Management, Inc., July 16-18, 1979 (Albuquerque, New Mexico).

3. G. W. Eccleston, H. O. Menlove, and E. Medina, "Neutron and Gamma Dose Measurements for High Enrichment Spent Fuel Assemblies," Los Alamos Scientific Laboratory Report LA-7439-PR (December 1978).

4. LASL Group X-6, "MCNP - A General Monte Carlo Code for Neutron and Photon Transport," Los Alamos Scientific Laboratory Report LA-7396-M (July 1978).

5. L. L. Carter and E. D. Cashwell, Particle-Transport Simulation with the Monte Carlo Method," ERDA Critical Review Series, TID-26607, 1975

6. G. W. Eccleston, R. G. Schrandt, J. L. MacDonald, "MCNP Modified to Provide Fission Rates by Isotope, Delayed Neutron Production and ^{3}He Captures," Los Alamos Scientific Laboratory memorandum Q-1-79-357.

7. G. R. Keepin, Physics of Nuclear Kinetics (Addision-Wesley Publishing Company, Inc., Reading, Massachusetts, 1965), pp. 86-87.

8. G. W. Eccleston and G. L. Woodruff, "Measured Near-Equilibrium Delayed Neutron Spectra Produced by Fast-Neutron Induced Fission of ^{232}Th, ^{233}U, ^{235}U, ^{238}U and ^{239}Pu," Nucl. Science and Engineering 62, 636-651 (1977).

9. T. W. Crane, S. Bourret, G. W. Eccleston, H. O. Menlove, L. G. Speir and R. V. Studley, "Design of a ^{252}Cf Neutron Assay System for Evaluation at the Savannah River Plant Fuel Fabrication Facility," in Analytical Methods for Safeguards and Accountability Measurements of Special Nuclear Materials, NBS Special Publication 528, H. Thomas Yolken and John E. Bollard, Ed., Proc. Amer. Nuclear Soc. Topical Meeting, Williamsburg, Virginia, May 15-17, 1978.

10. E. K. Hyde, Nuclear Properties of the Heavy Elements III Fission Phenomena (Prentice-Hall, Inc., 1964), p. 240.

Spectrophotometric Determination of Plutonium in Irradiated Fuels Solutions Procedures and Shielding Facilities

by

M.C. BOUZOU and A.A. BRUTUS
Marcoule Laboratory, Cogema-France

ABSTRACT

The Cogema Laboratory of Marcoule has developed and widely used a spectrophotometric determination of plutonium in the industrial solutions of the Purex process.

This determination based upon the plutonium VI specific absorption is made according to two variants : direct method and internal standard method (with neodymium nitrate as internal standard).

The two methods are routinly employed throughout the irradiated fuel reprocessing control, whatever the solution's activity, the amount of plutonium and the nature of analysed phase may be.

The performances obtained are given and a description of the "hot equipment" used is made.

INTRODUCTION

Plutonium analysis is the principal part of irradiated fuel reprocessing control. This analysis is made using various methods according to the quantity of plutonium or the composition of the sample. The use of these well known analytical techniques (gravimetry, α counting electrochemical methods...) presents the following inconveniences in the control of an industrial plant :

-- Difficulties in application leading to delay in results.

-- Multiplication of analytical methods detrimental to the simplification and rationalizing of analytical control done by operators working in shifts.

-- High automation cost owing to the number of methods used.

To avoid these problems the Cogema Laboratory of Marcoule has looked for a rapid, easy to use and easy to automate method which covers almost all the concentrations met in the control of plutonium solutions of the Purex process.

Thus we improved a spectrophotometric technique based upon the Pu VI specific absorption in the near infrared spectrum.

METHOD USED

We use the direct spectrophotometry of plutonium (VI) according to two variants

-- Direct method

-- Internal standard method

Direct Method

This method suitable for nitric or perchloric plutonium solutions has been widely described in litterature. Thus we shall briefly recall its principle, then we shall describe the range of utilisation and the performances normally achieved.

Principle

-- Oxidation, at room temperature, of plutonium, by silver oxide, to the hexavalent state.

-- Destruction of the excess oxidant by sulfamic acid.

-- Adjusting of nitrate concentration to 3 moles.

-- Measuring the absorbance peak at 831 nm.

Range of Utilisation

The method is employed throughout the irradiated fuel reprocessing control, whatever the solution's beta gamma activity, the amount of plutonium and the nature of analysed phase, may be.

In aqueous solutions we distinguish :

-- The traces assays (from 0,5 to a few mg/l) with a radioactivity as high as 1000 Ci/l and numerous cations such as uranium and fission products which accompany the plutonium. Thus it is not necessary to have a chemical separation before the analysis.
A typical spectrum of plutonium VI in these conditions is shown in figure 1.

-- The assay of higher concentrations (from 0,3 to several g/l) is usually done in the same conditions as in traces assays.

In organic solutions we extended this method to the plutonium determination in the TBP dodecane mixture, using the following procedure :

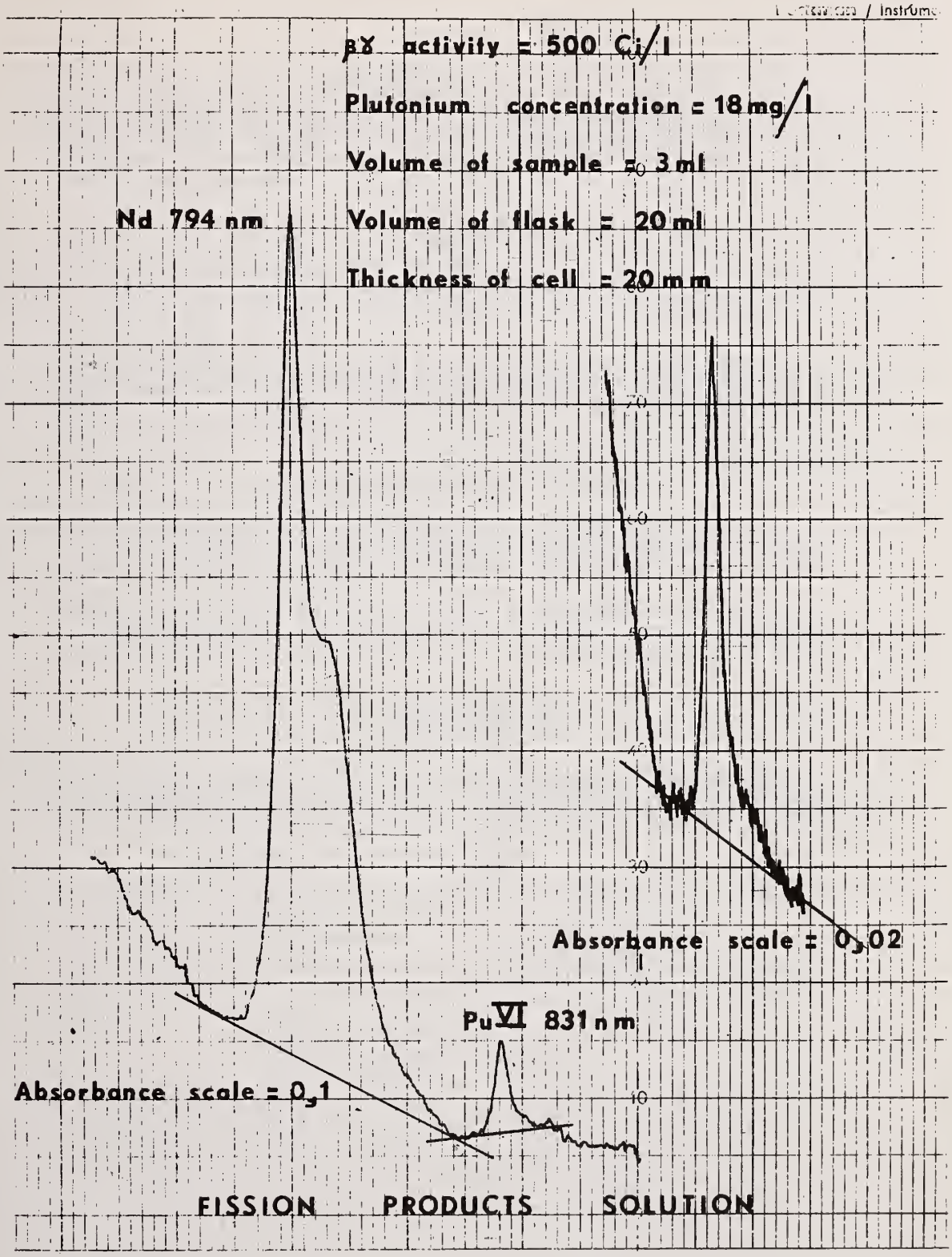
βγ activity = 500 Ci/l
Plutonium concentration = 18 mg/l
Volume of sample = 3 ml
Nd 794 nm
Volume of flask = 20 ml
Thickness of cell = 20 mm
Absorbance scale = 0,02
Pu VI 831 nm
Absorbance scale = 0,1
FISSION PRODUCTS SOLUTION

Figure 1

The organic phase containing plutonium is contacted with uranium IV nitrate solution that strips it from the organic phase. We can determine as little as 10 mg/l of plutonium in the initial organic phase with good accuracy.

Performances

The performances depend on the concentration level. Thus they vary for a spectrophotometer given with the absorbance scale employed.

During traces assays we use a 0,02 expanded absorbance scale while for the determinations of higher concentrations we use a 0,5 or 1 absorbance scale, the accuracy is very different in the two cases.

Sensibility - Detectability

In our working conditions : 20 ml flasks, 2 cm of optic path for the cell and high radioactivity in samples, a concentration of 0,2 mg/l of plutonium in the sample cell produces an absorbance of 10^{-3}.

In the same conditions we reach 3.10^{-3} mg of plutonium in the sample, or 0,15 mg/l in the sample cell which produces an absorbance of 8.10^{-4} which is our detectability.

Reproductibility

We have summarized in table 1 the plutonium uncertainty versus plutonium concentrations in the sample cell (in mg/l). These data are the result of several hundred determinations.

TABLE I

Pu concentration in the cell mg/l	Δ Pu concentration mg/l	
0,15 - 1	± 0,04	± 0,20
1 - 5	± 0,20	± 0,40
5 - 50	± 0,40	± 1,50
50 - 250	± 1,50	± 1,25

Interferences

Anions often interfere more than cations and sometimes require a special treatment of the sample prior to analysis : precipitation, complexing, evaporating to dryness...

The nitrate ion has a special importance because the molar extinction coefficient value falls about 1 % when the nitrate concentration rises to within 0,1 M of 4 M (in nitric solutions).

Nevertheless the Pu VI peak is very specific and few accompanying elements interfere.

The daily use of this method showed us that its usage requires a recording spectrophotometer with precise settings, of the spectral bandwidth, of the resolution, of the scanning speed and of the damping of the pen. In addition the photomultiplier used must have a high signal to noise ratio in the near infrared. Lastly, in very accurate determinations it is necessary to take temperature into account because its influence on the molar extinction coefficient is far from negligible.

When all these parameters are well selected, the method is accurate repeatable and the relation between absorbance and plutonium concentration is linear to two of absorbance.

Nevertheless in some cases the spectrophotometric method has some inconveniences. For instance :

-- When the spectrophotometer is inadequate, the linearity between absorbance and plutonium concentration quickly dissapears and this makes the method less advantageous.

-- When the solutions to be analysed are full of precipitate and a large background absorption appears, the plotting of the base line of the plutonium peak becomes very problematical ant the height of the peak cannot be measured with accuracy.

-- When the nitrate concentration is not well known, it is easy to make a big error in the result.

In order to avoid most of these problems we use a second variant of the method.

Internal Standard Method

This method, suitable for the same samples as the previous has been developed by the COGEMA Laboratory of LA HAGUE. Its principle is the following :

-- Addition to the sample of an internal standard

-- Oxidation, at room temperature, of plutonium, by silver oxide, to the hexavalen state

-- Destruction of the excess silver oxide, by sulfamic acid

-- Adjusting of nitrate concentration to 3 moles.

-- Measuring the ratio of the sizes of plutonium and internal standard peaks. This ratio is called R.

-- Calculation of plutonium concentration in comparison with this ratio R and those obtained with a plutonium standard solution containing exactly the same amount of internal standard as the sample, and treated in the same manner.

The internal standard used is the neodymium nitrate whose principal features are :

-- Spectrum in the near infrared which gives a peak at each side of the plutonium one, one at 793 nm and one at 864 nm (Fig. 2 and 3).

-- Absorbance at 831 nm nearly non existent (even for great neodymium concentrations).

-- Chemical inertia with respect to, plutonium, silver oxide and sulfamic acid.

The addition of neodymium nitrate as standard in the spectrophotometry of plutonium (VI) has the following advantages.

-- Strict plotting of the base line which, being interference free, suppresses inaccuracy in the size of mesured peaks.

-- Suppression of rigorous adjusting of the flasks. In fact the result is not obtained by the comparison of two peak heights which depend on flask adjusting, but by the comparison of two ratio Rs' independant of the adjusting of the flasks. This is interesting in view of automation.

-- The ratio R (plutonium VI, absorbance to neodymium absorbance) fluctuates less, with the nitrate concentrations than does the plutonium (VI) absorbance (figure 4).

On the contrary, the principal disadvantages of the method are the following :

-- Neccesity to introduce exactly the same amount of neodymium in the aliquot of standard solution and in the sample. But if we can weigh the aliquots, this constraint disappears.

-- Necessity to work with a ratio R between 0,7 and 1,3 in order to avoid reciprocal interferences of the plutonium and neodymium peaks.

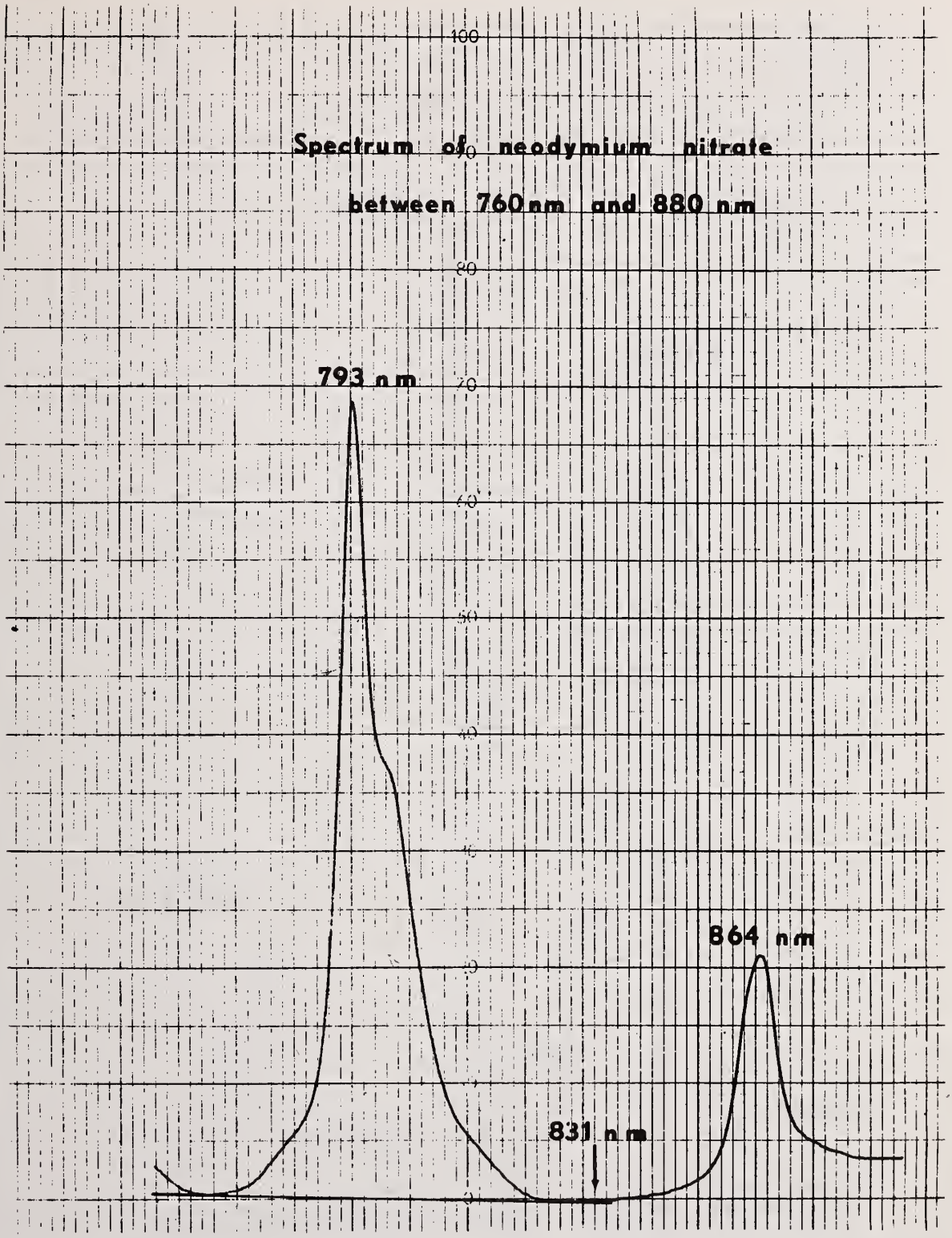
Spectrum of neodymium nitrate
between 760nm and 880 nm
100
80
60
40
20
0
793 nm
864 nm
831 nm

Figure 2

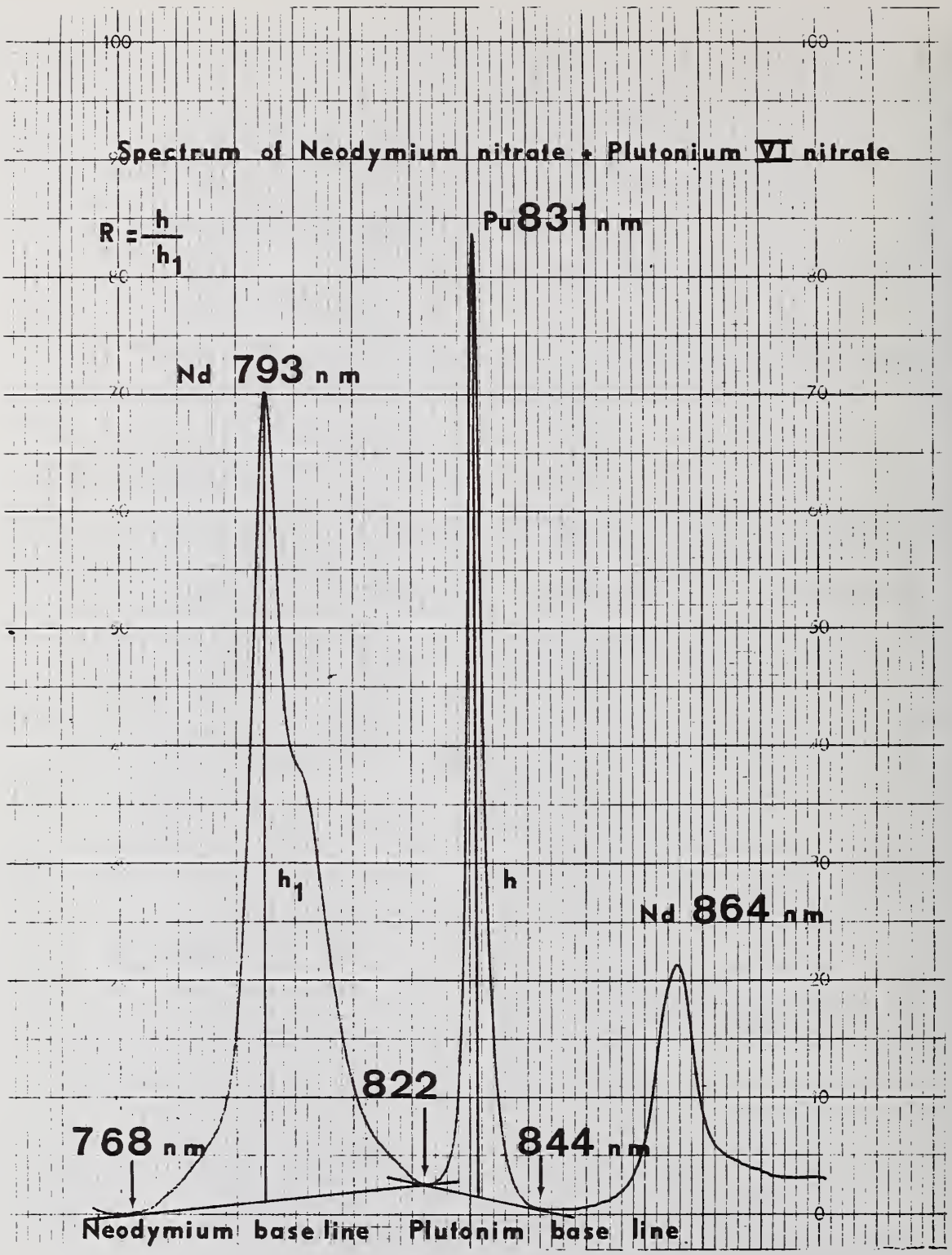
Spectrum of Neodymium nitrate + Plutonium VI nitrate
R = h / h1
Pu 831 n m
Nd 793 n m
h1
h
Nd 864 nm
822
768 n m
844 n m
Neodymium base line
Plutonim base line

Figure 3

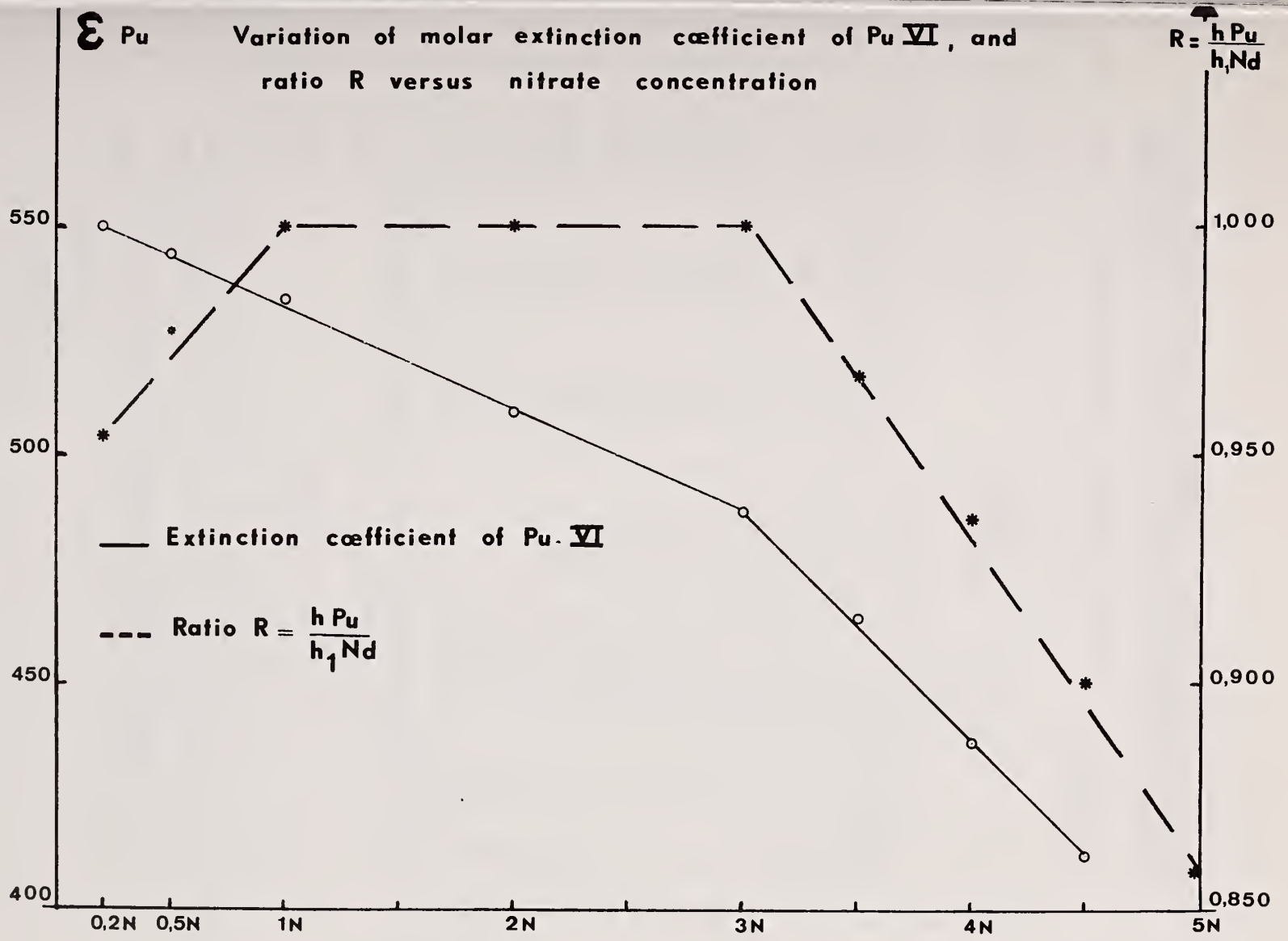
ε Pu
Variation of molar extinction cœfficient of Pu VI, and ratio R versus nitrate concentration
R = h Pu / h1 Nd
550
500
450
400
1,000
0,950
0,900
0,850
Extinction cœfficient of Pu. VI
Ratio R = h Pu / h1 Nd
0,2N
0,5N
1N
2N
3N
4N
5N

Figure 4
505

In our Laboratory, this method is widely used. The fact that it gives a result in less than one hour with a precision of $\pm$ 1,5 % on a lot of industrial solutions, makes it by far the best routine control method.

Moreover this method is excellent for accurate analysis as we can see in table two.

TABLE II

STANDARD SOLUTION				UNKNOWN SOLUTION (Input solution)		
h (Pu) mm	h_1 (Nd) mm	$R = \frac{h}{h_1}$	Assay n°	h (Pu) mm	h_1 (Nd) mm	$R = \frac{h}{h_1}$
160	171,5	1,078	1	160	175	1,093
160	171,5	1,078		160	175	1,093
159	170	1,069	2	160	175	1,090
160	171	1,068		161	175,5	1,093
159,5	171	1,072	3	160	175	1,093
160	171,5	1,071		159	174	1,094
157	169	1,076	4	160	175	1,093
158	170	1,075		160	174	1,087
		$1,073_9$	$\overline{R}$			$1,092_5$
		$0,004_0$	S = Standard deviation			$0,002_4$
		0,37 %	$\frac{S}{R}$ %			0,22 %

Example of results obtained on input solution

A great number of comparisons with isotopic dilution and mass spectrometry on input solutions has produced similar results as we can see in table III.

TABLE III

Mass Spectrometry Pu mg/l	Pu VI Spectrophotometry Pu mg/l	Δ %	Mass Spectrometry Pu mg/l	Pu VI Spectrophotometry Pu mg/l	Δ %
287	286	0,35	1 134	1 126	0,70
921	928	0,76	1 170	1 163	0,60
934	937	0,32	1 170	1 177	0,60
981	989	0,81	1 045	1 052	0,67
990	1 003	1,31	2 160	2 190	1,39
1 003	1 009	0,59	2 160	2 130	1,39
1 009	1 004	0,49	2 610	2 590	0,77
1 020	1 030	0,98	2 840	2 840	0,00
1 056	1 056	0,00	3 180	3 200	0,63
1 057	1 064	0,66	3 210	3 200	0,31
1 067	1 075	0,75	3 700	3 700	0,00
1 107	1 120	1,17	2 931	2 905	0,89

Comparisons of isotopic dilution and spectrophotometry of Pu VI on input solutions

EQUIPMENT

We are using the two methods in glove - boxes as well as in hot cells. The equipment is the same in both cases, the only difference being that the "hot" appartus is used with a biological shielding in lead.

We shall describe the equipment that we have used for making the method suitable for highly radioactive solutions. It consists of :

-- a hot cell

-- a spectrophotometer

-- the joining between the hot cell and the spectrophotometer.

The hot cell consists of an air tight stainless steel box connected with two master slave manipulators and surrounded by a biological shielding of 100 mm of lead. It is used for chemical preparations and contains the laboratory equipment required for the method (Flasks, pipettes...) and a solution transference system from the hot cell to the spectrophotometer. This system consists of a glass container in which the vacuum is made by means of an air pump and which is connected to the analysis flask and the ciculation cell contained in the sample compartment of the spectrophotometer.

The joining between the hot cell and the spectrophotometer consists of a very thick stainless steel tube shielded with 5 cms of lead. In this tube are the P.V.C. tubes through which the radioactive solution flows.

The spectrophotometer is a Beckman U.V. 5240, the sample compartment of which is divided in two parts.

-- an unshielded part which contains the reference cell

-- a shielded part which contains the sample cell. This is enclosed in an α tight box provided with two quartz windows and connected with the steel tube by a supple lip seal, which permits a slight free motion between the spectrophotometer and the steel tube. This α tight box (whose cover can be unscrewed, in case of intervention on the cell) is shielded by a lead box provided with a removable cover. The system lies on a lead plate in the bottom of the sample compartment of the spectrophotometer, but owing to the flexible lip seal, the optical alignment is never disturbed.

To evacuate the sample cell, we draw it from the hot cell by one of the P.V.C. tubes. The part contains the cell (in the bottom of the α tight box) turns and places the cell in the steel tube which connects the hot cell to the spectrophotometer. The contaminated cell is evacuated into the hot cell. After removal of the shielded cover from the α tight box, a new cell can be installed from the outside.

For five years, using this device, we have determined plutonium in highly radioactive solutions (several hundred curies per liter) with a negligible radioactivity level for the operator.

We are now studying a new equipment whose principle will be the same but whose performances will be bettered thanks to :

-- the weighing of the aliquots

-- the automation of chemical analysis directed by computer

-- the thermostating of the sample compartment of spectrophotometer

-- the data processing, and the calculation of the results by computer.

Gamma Spectrometric Measurements of Pressurized Water Power Reactor Spent Fuel

by

V. KUPRYASHKIN, T. HAGINOYA, V. POROYKOV[1/]
International Atomic Energy Agency, Vienna

T. DRAGNEV, B. DAMJANOV
Institute of Nuclear Research and Nuclear Energy, Sofia

ABSTRACT

This report presents the results of gamma spectrometric measurements on spent fuel bundles carried out during a routine inspection at Kozlodui Nuclear Power Station in Bulgaria (PWR - Novovoronezh type) by using portable IAEA equipment. A Ge spectrometer was used to measure gamma spectra in the energy region from 500 to 900 keV. The cooling time was determined from the Zr-95/Cs-137 ratio, and the average burn-up and Pu/U fraction was calculated from Cs-134/Cs-137 ratio.

KEYWORDS: Spent fuel, cooling time, burn-up; Pu/U, Zr-95/Cs-137, Cs-134/Cs-137 ratios.

I. INTRODUCTION

A year's operation of a light water reactor adds about 120 irradiated assemblies to the spent fuel storage. An increase of spent fuel is projected for the future since reprocessing has not yet become a routine procedure. The task of international safeguards is to verify the operators' statements regarding the irradiation history of the individual spent fuel assemblies and the quantity of nuclear material contained in the irradiated assemblies. Although the general approach for safeguarding spent fuel is the application of containment and surveillance systems, in case such systems fail, direct NDA measurements should be applied to re-establish the inventory.

Among the available NDA methods for determining spent fuel characteristics, the gamma spectrometric method is most advanced [1]. In this method, absolute gamma activity measurements and activity ratio measurements on selected fission products are used. These measurements do not yield the fissile content directly, but it is possible to calculate it from isotopic correlation techniques.

Compared with NDA techniques, destructive analysis gives better accuracy for the measurement of small samples and it is relatively easy to obtain absolute values of burn-up. Such techniques are particularly applicable in fuel reprocessing plants where the fuel is dissolved and where a high accuracy is required. But destructive techniques cannot be

---

1/ Former Staff Member of the IAEA

[1] S. T. Hsue, T. W. Crane, W. L. Talbert, Jr., John C. Lee, Non-destructive Assay Methods for Irradiated Nuclear Fuels, LA-6923 (January 1978)

applied for verification of fuel assemblies in a spent fuel storage pond.

Many questions arise as to the accuracy of gamma-ray assay concerning different fission yields for fissioning nuclides, migration in the fuel, radiation history, etc. However, the gamma spectrometric method can give good accuracy in combination with results of destructive measurements in reprocessing plants.

The purpose of this work was to further improve and adjust gamma spectrometric spent fuel measurements for PWRs to IAEA Safeguards conditions and to supply inspectors with more specific instructions for

1. determining the cooling time,
2. evaluating the burn-up,
3. evaluating the Pu/U ratio.

II. MEASUREMENTS

The experimental arrangement used in these measurements has been previously described [2].

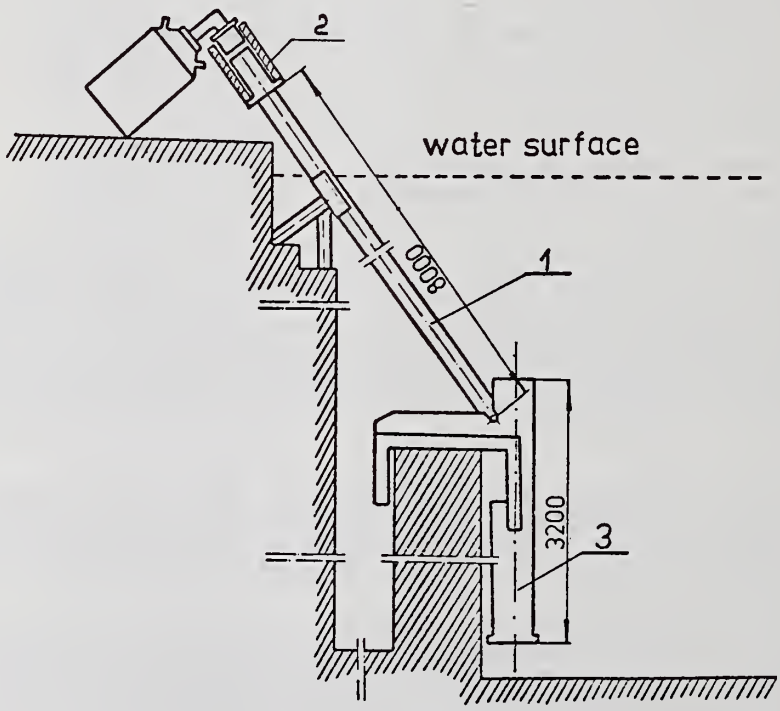

Fig. I Arrangement for spent fuel measurements

1, 2 - gamma collimating arrangements
3 - fuel assembly support

[2] Z. Zhelev, T. Apostolov, V. Christov, T. Dragnev, D. Kharalampiev, I. Marinov, I. Penev, A. Trifonov, I. Uzunov, "Development and application of safeguards instrumental techniques to LWR power stations", Final Report on Research Contract No. 1547/RI/RB, Sofia, 1977.

A long air filled pipe was used to collimate and prevent absorption of gamma-rays coming from fuel assembly to the detector. The isolated assembly was moved vertically for scanning or for measurements at given points along the assembly.

An intrinsic high resolution germanium detector with a sensitive volume of 10 cc and a portable 1024 channel "Silena" analyzer with magnetic tape storage were used for recording spectra. Special attention was paid to the choice of the energy region to be used, background, and collimation. The energy region between 500 - 900 keV was selected for several reasons:

1) The energy of gamma rays is high enough so that attenuation is not too great.

2) The gamma lines should have enough points in the peak to accurately determine peak areas. All gamma lines used for the calculation of cooling time, burn-up and Pu/U mass ratio, including the five gamma lines used for the efficiency determination (563, 569, 605, 796 and 802 keV) are situated in a narrow energy range. Some investigators [3] use the energy region between 500 - 1500 keV, which has certain advantages, particularly for obtaining the relative efficiency system, but for a wider energy range a 2048 channel analyzer is needed.

Background from spent fuel in the pool and from materials dissolved in the water could influence the gamma spectrum, and it was important to reduce undesirable effects and retain only the gamma rays from the measured assembly. The allignment of the collimator through which gamma rays can reach the Ge detector was checked using a light source. Thick collimator walls of about 8 cm also reduced background. To regulate the amount of gamma rays and to reduce the amount of electrons which reach the detector, a beam absorber of Pb, Cd and Cu-plates were used.

Data about assemblies selected for study are in Table 1.

Table 1 The basic data of selected assemblies

No.	Enrichment (%)	Burn-up (MWD/TU)	Cooling time (days)	Working time (years)
2-25	1.6	17470	414	2
2-23	1.6	17110	414	2
2-36	2.4	19860	414	2
2-41	2.4	20260	414	2
2-37	2.4	20180	414	2
2-112	2.4	19790	414	2
2-296	3.6	9600	30	1

It was impossible, under the existing circumstances, to carry out gamma spectrometric measurements for the last assembly 2-296, due to strong radioactivity and high background radiation. The gamma spectra for assembly 2-25 was measured three times to facilitate the selection of the optimal conditions for NDA of spent fuel when measurement time is limited. At the onset of the measurements the gamma spectra were registered point by point (10 points) after every 25 cm and recorded on magnetic tape. Measurement time was 400 s on every point. The spectra were subsequently summed channel by channel in the computer and

[3] N. Beyer, M. De Carolis, E. Dermendjiev, A. Keddar, R. Rundquist, "IAEA NDA measurements as applied to irradiated fuel assemblies", Nuclear Safeguards Technology 1978, V.1, P. 443, IAEA Vienna, 1979.

on further processing the summed spectrum was used. Then the gamma ray measurements were conducted for the same assembly during its up-and-down movement. The results of these three measurements were in good agreement. That is the reason why the remaining assemblies were measured only by scanning as they were vertically moved in the front of the collimator tube. The measurement time was 10 minutes.

III. DATA PROCESSING

The data processing of the measured spectra was carried out using the "Silena" analyzer, programmable calculators [4] and the IAEA Nuclear Data 6620 computer.

Intrinsic calibration was used for the determination of overall relative efficiency of the used spectrometric system [4].

The Cs-134 gamma rays 563, 569, 605, 796 and 802 kev were used for this purpose. The results show that overall relative efficiency in region from 605 kev to 796 kev is close to linear. So in the cases when gamma lines 563, 569 and 802 kev Cs-134 were weak in gamma spectrum we used only lines 605 and 796 kev for determination relative efficiency. Corrected peak areas were calculated using obtained values of relative efficiency.

IV. DETERMINATION OF COOLING TIME

The cooling time was calculated using the following equations from ref. [5]:

$$T(1) = \frac{1}{\lambda_1 - \lambda_2} \ln \left(\frac{\gamma_1}{\gamma_2} \frac{S(1)}{S(2)} \frac{A_2}{A_1} \Delta_1 \right) \quad (1)$$

$$T(2) = \frac{1}{\lambda_1 - \lambda_2} \ln \left(\frac{\gamma_1}{\gamma_2} \frac{S(1)}{S(2)} \frac{A_2}{A_3} \Delta_2 \right) \quad (2)$$

In these equations γ_1, γ_2 are the fission yields of the mass 95 and 137 chains. A_1, A_2, A_3 are the corrected peak areas of the 756 keV Zr-95, 662 keV Cs-137, 724 keV Zr-95 peaks, and Δ_1, Δ_2 are the true ratios of the intensities of the 756 keV Zr-95 to 662 keV Cs-137, 724 kev Zr-95 to 662 keV Cs-137; λ_1, λ_2 are the decay constants for Zr-95 and Cs-137; and parameters S(1) and S(2) are calculated using the following equations:

$$S(1) = \sum_{i=1}^{n} \phi_i \, (1-e^{-\lambda_1 t_i}) \, e^{-\lambda_1 \Theta_i} \quad (3)$$

$$S(2) = \sum_{i=1}^{n} \phi_i \, (1-e^{-\lambda_2 t_i}) \, e^{-\lambda_2 \Theta_i} \quad (4)$$

In the above equations, "S" is summed over all irradiated cycles for which the assembly was in the reactor; t_i is the length of radiation cycle i; Θ_i is the length of the time between the end of cycle i and the beginning of the cooling period; and ϕ is the thermal flux.

---

[4] T. N. Dragnev, "Intrinsic self-calibration of non-destructive gamma spectrometric measurements", IAEA-STR-60, 1976

[5] J. W. Mandler, R. G. Helmer, E. W. Killian, R. A. Morneau, "Programme for technical assistance to IAEA Safeguards", ISPO Report No. 42, TREE-1313 (October 1978)

Two different calculations of cooling time were done:

A. It was assumed that the reactor operated on constant power.

B. The real irradiation history was considered.

The cooling time for both cases was calculated as the average of T(1) and T(2). The results of the calculations are shown in Table 2 together with the operator's data. Assembly 2-25 was measured three times and the results are given in Table 2 separately.

Table 2 Comparative Data for Cooling Time

No. of assembly	Initial enrichment (%)	Method of measurements	Irradiation time (years)	Cooling time (years)		
				Operator's data	Experiment A	Experiment B
2-25	1.6	point by point	2	414	415	419
2-25	1.6	moving up	2	414	416	420
2-25	1.6	moving down	2	414	415	419
2-23	1.6	moving up	2	414	418	422
2-36	2.4	moving up	2	414	421	425
2-41	2.4	moving up	2	414	424	428
2-37	2.4	moving up	2	414	422	426
2-112	2.4	moving up	2	414	425	429

As we can see from Table 2, the results of the cooling time calculations in assumptions A and B are in good agreement with the operator's data. If we compare the average experimental results for all assemblies which have the same cooling time, the difference is only 1.3%, when we suppose that the reactor operated on constant power, and 2.3% when the irradiation history was taken into account. That means, that for cooling time calculations, it is enough to know that the reactor operated on more or less constant power.

Our results are in good agreement with Hatcher's results [6] who analysed statistical errors for spent fuel cooling time measurements and obtained the following equation:

$$\sigma_T = \frac{1}{(\lambda_1-\lambda_2)} \left[\left(\frac{\Delta A_1}{A_1}\right)^2 + \left(\frac{\Delta A_2}{A_2}\right)^2\right]^{1/2} \qquad (5)$$

In this equation,

σ_T = one sigma error in cooling time due to counting statistics.

A_1 = corrected peak area of Zr-95 gamma.

A_2 = corrected peak area of Cs-137 gamma.

λ_1, λ_2 = decay rate of Zr-95 and Cs-137, respectively.

Analyses of the equation have shown that it is not unusual to obtain a $\Delta T/T$ of 1% or 2% with $\Delta A/A$ of 5%.

[6] C. R. Hatcher, IAEA, Personal communication, July 1979.

V. CALCULATIONS OF BURN-UP AND Pu/U RATIO

In our work we used the activity ratio Cs-134/Cs-137 as a burn-up monitor. The possibility of using this ratio was first shown in ref. [7] and later in many other investigations [2, 8, 9, 10]. Activity ratio measurements are less sensitive to the geometrical arrangement than absolute activity measurements and require only the relative detector efficiency to be known. Thus the activity ratio is more convenient for use in field inspection. Correlations have been established between the Cs-134/Cs-137 activity ratio and both the burn-up or Pu/U mass ratio. Empirical equations relating to these parameters have been obtained for several types of reactors [8, 9, 10].

For calculation of burn-up an empirical equation obtained for the Novovoronezh type of reactor was applied which is valid for burn-ups from 5 to 26 kg/TU [10]:

$$B = (16.6 \pm 0.9)\ \eta_o \qquad (6)$$

B = burn-up in kg/TU

η_o = the Cs-134/Cs-137 activity ratio corrected for cooling time.

The activity ratio η_o was calculated from the activity ratio at the moment of measurement η on the basis of the equation

$$\eta = \eta_o e^{-(\lambda_3 - \lambda_2)T} \qquad (7)$$

where η = the Cs-134/Cs-137 activity ratio in the moment of measurement

λ_2, λ_3 = decay rate of Cs-137 and Cs-134, respectively

T = cooling time.

Using $T_{1/2}$ = 30.12 years for Cs-137 and $T_{1/2}$ = 2.06 years for Cs-134, equation (7) becomes:

$$\eta = \eta_o\ e^{0.000859\ T} \qquad (8)$$

where T = cooling time in days, which we used for the calculation of η_o.

Activity ratios η were calculated from known peak areas of gamma lines of Cs-134 and Cs-137.

---

[7] R. L. Heath, "The potential of high-resolution gamma-ray spectrometry for the assay of irradiated reactor fuel", Safeguards Res. Devel., Proc. Symp. Argonne National Laboratory, June 26, 1967, report WASH-1076, pp. 115-129 (1967).

[8] A. M. Bresesti, M. Bresesti, S. Facchetti, F. Mannone, P. Barbero, C. Cerutti, F. Marell, A. Peil, R. Pietra, R. Klersy, A. Schürenkämper, A. Frigo, E. Ghezzi, J. P. Meerschman, A. Pollicini, K. H. Schrader, J. Biteau, A. Cricchio, L. Koch, "Post-irradiation analysis of Trino Vercellese reactor fuel elements", EUR 4909e, 1972

[9] J. Valovi, V. Petenyi, S. B. Rana, D. Mikusova and J. Kmosena, "The application of gamma and isotopic correlation techniques for safeguards identification and verification purposes", Final Report, IAEA research contract 1443, Bohunice Nuclear Power Plant, Bohunice, Czechoslovakia (1975).

[10] L. Golybev, L. Gorobcov, B. Simonov, M. Sunchugashev, "Two methods of gamma spectrometry burn-up determination", Atomnaja Energia, 41, 197 (1976).

Since the gamma spectrum for assembly 2-25 was measured quite accurately, we used a cooling time of 415 days for burn-up calculations for all assemblies.

The Pu/U mass ratio was determined by substituting B into regression equations taken from ref. [9] for the Trino-reactor, which is a presssurized water reactor of nearly the same type of Novovoronezh.

$$Pu/U = 0.6318 \times 10^{-2}\ \eta + 0.9301 \times 10^{-3} \quad (9)$$

$$B = 0.1828 \times 10^{5}\ \eta - 0.1697 \times 10^{4} \quad (10)$$

η = the activity ratio Cs-134 to Cs-137.

Solving equations (9) and (10) jointly, we obtain,

$$Pu/U = 3.45 \times 10^{-7}\ (B + 0.1697 \times 10^{4}) + 0.9301 \times 10^{-3} \quad (11)$$

which was used for the calculation of Pu/U mass ratio.

All results for burn-up and Pu/U mass ratio are presented in Table 3. The burn-up determinations are in agreement with the operator's data to within 10%, except in one case. The Pu/U mass ratio agreement is within 4.2%.

Table 3 Results of Gamma Spectrometric Measurements of Spent Fuel

No. of assembly	Initial enrichment (%)	Method of measurements	Irradiation time (years)	Cooling time (days)	Burn-up (kg/TU)		Pu/U (kg/TU)	
					Exper.	Operator's data	Exper.	Operator's data
2-25	1.6	point by point	2	415	18.60	18.41	7.61	7.66
2-25	1.6	moving up	2	415	18.44	18.41	7.55	7.66
2-25	1.6	moving down	2	415	18.76	18.41	7.66	7.66
2-23	1.6	moving up	2	415	19.14	18.03	7.78	7.61
2-36	2.4	moving up	2	415	18.86	20.93	7.69	7.59
2-41	2.4	moving up	2	415	19.49	21.35	7.90	7.79
2-37	2.4	moving up	2	415	18.93	21.27	7.71	7.89
2-112	2.4	moving up	2	415	19.49	20.86	7.90	7.91

VI. CONCLUSIONS

Spent fuel characteristics (cooling time, burn-up and Pu/U mass ratio) were determined on the basis of gamma spectrometric measurement. The agreement with operator's data is better than 3% for cooling time, 5% for Pu/U mass ratio and 10% for burn-up. All measurements including the preparation of equipment were done during one working day, thereby demonstrating that it is possible to carry out such measurements during a routine inspection if the pipe and collimators have been prepared in advance.

It is also noteworthy that spent fuel assembly characteristics were determined using inspector's measurements and published correlation data without any information from the operator. Therefore, even if the accuracy of the individual parameters obtained is not specially high, the confirmation of the three different parameters within an expected

range of values (cooling time, burn-up and Pu/U mass ratio) results in a high degree of confidence that operator's data are indeed correct and that no diversion of nuclear material has occured.

In some cases it is possible to use empirical correlations established for a given type of reactor and apply these to another similar reactor. Our conclusions are similar to those obtained in reference [3].

As a result of this work the following recommendations have been developed to assist inspectors in the conduct of spent fuel measurements.

It would be useful to have some standard devices in the cooling ponds (it is even better to include them into design criteria of cooling ponds) in order to facilitate measurements. They could also prove useful for operators. In order to aid inspectors in the evaluation of the data, correlations between measured parameters (Cs-134/Cs-137, Zr-95/Cs-137, Ce-144/Cs-137 activity ratios) and burn-up, cooling time and Pu/U ratio should be determined on the basis of destructive measurements for principal types of reactors. This would help improve the accuracy of these measurements and increase the efficiency and effectiveness of inspections at reactors.

Automated Tank Calibrator

G. P. Baumgarten, V. Brame, D. G. Cooper, and B. Robertson
Fluid Engineering Division, National Bureau of Standards, Washington, D. C. 20234

An automated system for remotely calibrating nuclear fuel accountability tanks is described. It uses two turbine meters to measure a quantity of water introduced at up to 40 liters/minute into the tank to be calibrated and records the quantity and the resulting pressure in the tank. A diverter valve, controlled by the computer, directs the flow either into the tank or down a drain. The method of calibrating the turbine meters and determining the correction for the error introduced by the diverter valve is described, and representative data are presented. The turbine and diverter calibration data are referenced by the computer when the system is used to calibrate a tank. The short-term uncertainty in the water volume is ± .02 percent, which is almost entirely due to the nonrepeatability of the turbine meters. Confidence in the uncertainty figure is retained by measuring the ratio of the two turbine meter frequencies. If the ratio changes by more than .02 percent, the turbine meters can be recalibrated in one day.

KEYWORDS: Volume calibration; accountability tanks; turbine meters; automated system; diverter correction

1. INTRODUCTION

An automated system has been developed for calibrating nuclear material accountability tanks in nuclear fuel plants. The calibrator is easily transportable and is intended to be located in an area accessible to personnel even though the tank may be in a canyon or other remote area of intense radiation. The calibrator is designed to be connected to the tank using existing plant tubing for filling the tank and for measuring the liquid level in the tank. The measurements performed by the calibrator will give the tank cross sectional area as a function of height. The system is intended to replace the laborious method of calibrating tanks by filling them manually in increments using a volumetric test measure. The advantages of automating these measurements are 1) human error is minimized, 2) smaller volume increments can be used, and 3) the calibration can easily be repeated. The calibrator thus makes it possible to obtain easily a precise and reliable accountability tank calibration.

A block diagram of the calibrating system, the plant tubing, and the accountability tank to be calibrated is in Figure 1. Filtered plant water flows continuously through two turbine meters and, depending on the position of a diverter valve, either into the tank or into a drain. Initially the tank to be calibrated is empty, the hose leading to the tubing to the tank is full, and the water flow is bypassed down the drain. The needle valve downstream of the turbine meters is adjusted to obtain the desired flowrate up to 40 liters/minute. When the flow is air free and steady, the measurement is started by pressing a key on the computer. The computer actuates the diverter valve to fill the tank and begins recording the data.

The computer keeps account of the volume of water contained in the tank by periodically reading the turbine meter count and multiplying it by the appropriate calibration coefficient C. Since C for a given turbine meter depends on the turbine frequency f divided by the viscosity ν of the water, the computer measures the frequency and determines the viscosity from the water temperature at the turbine meters. It then

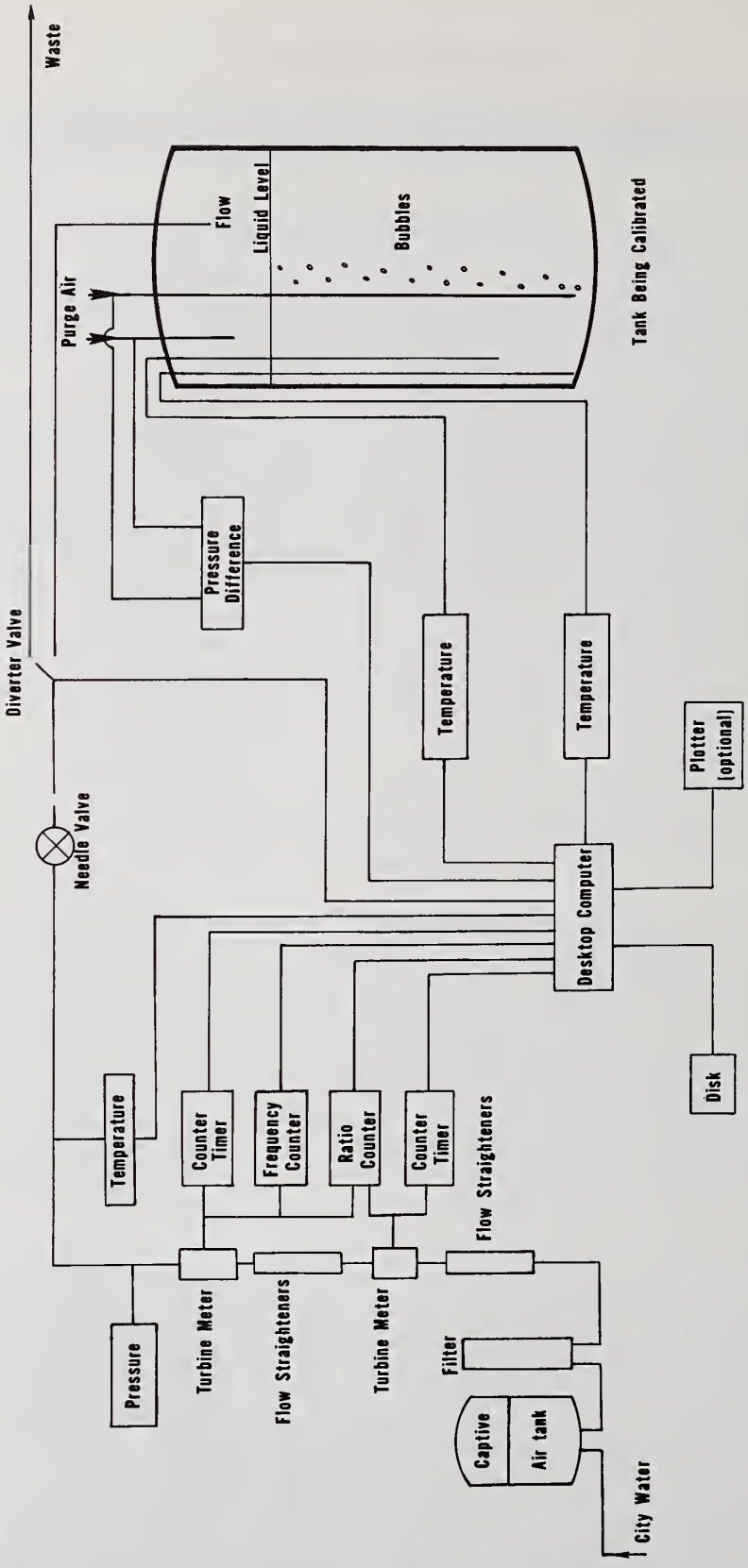

Fig. 1. Schematic diagram of the automated tank calibrator.

goes to a table stored in memory to obtain the calibration coefficient corresponding to the value of f/ν and multiplies the measured count by that coefficient to obtain the volume of water. In order to minimize error due to flowrate (and hence frequency) changes caused by fluctuations in the water supply pressure, the volume increments are measured as frequently as possible. The measurements and multiplication can be done in four turbine propeller revolutions, which at maximum flowrate takes about 15 milliseconds. The captive air tank prevents flowrate changes on a shorter time scale.

Two turbine meters are used in series in order to provide a continuous check of turbine meter long-term repeatability.[1,2,3] The ratio of the upstream turbine frequency to the downstream turbine frequency is a reliable measure of turbine meter repeatability. Since the piping and flowmeter installation is fixed, it is extremely unlikely that both turbine meters could lose accuracy simultaneously in such a way that the ratio remains unchanged. After an initial run-in for 300 hours, the ratio for the turbine meters in the calibrator has been constant within ± .02 percent for at least 300 hours of continuous operation. The ratio is expected to remain within ± .05 percent for at least 20,000 hours of operation and hopefully much more than that.

Since the calibration coefficients for the two turbine meters are slightly different functions of f/ν, the ratio will also depend on f/ν. The computer has a table of this function stored in memory and refers to it periodically to see if the measured ratio has changed from the value in the table. If the difference is too large, the computer will abort the tank calibration.

The computer records the total mass of water introduced into the tank and also records the resulting pressure at the bottom of the tank. Figure 1 illustrates the bubbler tube method for measuring the pressure.[4,5] The tank cross sectional area as a function of height can be obtained from this data.

2. APPARATUS

The photograph, Figure 2, shows the tank calibrator set up in the NBS Fluid Mechanics Building for the initial calibration of the two turbine meters and determination of the diverter correction. The tank calibrator is entirely contained in the electronics rack on the left. The pressure gauge at the top of the rack is used to check that the pressure downstream of the turbine meters is high enough to prevent cavitation in them. The handle of the flow adjusting needle valve (Marsh N1356) is to the right of it. Just below are the three temperature indicators (Doric 410A with BCD interface) and a universal counter/timer (Fluke 1953A with IEEE-488 interface).[6]

Behind the blank panel is a specially designed continuously readable counter and period timer. This had to be constructed at NBS because no combination of commercially available counters or timers could perform the necessary measurements. It is not possible to read the current subtotal count from a conventional electronic counter/timer without making the counter lose counts each time it is read. However, the NBS counter can do it. In addition it can be programmed by the computer to divide the incoming pulses by an integer up to 256 before measuring the period. Division by a multiple of six is used here since the turbines have six blades and since this division aver-

---

[1] G. E. Mattingly, P. E. Pontius, H. H. Allion, and E. F. Moore, "A Laboratory Study of Turbine Meter Uncertainty," U. S. NBS Special Publ. 484, Proc. Symp. on Flow in Open Channels and Closed Conduits, Feb. 1977.

[2] G. E. Mattingly, W. C. Pursley, R. Paton, and E. A. Spencer, "Steps Toward an Ideal Transfer Standard for Flow Measurement," FLOMEKO Symp. on Flow, Groningen, The Netherlands, Nov. 1978.

[3] G. E. Mattingly, "Dynamic Traceability of Flow Measurements," IMEKO Symp. on Flow Measurement and Control in Industry, Tokyo, Japan, Nov. 1979.

[4] R. M. Schoonover and J. F. Houser, "Pressure Type Liquid Level Gages," U. S. NBS Report 10396.

[5] R. M. Schoonover, H. H. Ku, J. R. Whetstone, and J. F. Houser, "Liquid Level Instrumentation in Volume Calibration," U. S. NBSIR 75-900 (1975).

[6] Manufacturer's names and model numbers are cited for reference only. Their reference is not to be construed as an endorsement or recommendation.

Fig. 2. The automated tank calibrator standing to the left of a volumetric test measure used for the initial calibration.

ages out the loping due to unequal spacing of the blades. The computer can read the average period of each of these 6n counts, the total number of the 6n counts, and the current partial count for each of the two turbine meters.

Below the second universal counter timer is the pressure transducer and its display (Ruska DDR-6000), the flexible disk drive (HP 9885M), and the computer (HP 9825A) on a pull-out shelf at desk height. Below the shelf is an I/O expander (HP 9878A). The six gallon captive air tank (Sears 390.29111) and water filter (AMF AP-10) are on the bottom behind a panel. The 10 micron water filter upstream of the turbine meters is essential for maintaining long-term repeatability of the turbine meters. The bladder in the captive air tank is charged with 25 psi (170 kPa) air pressure. Although the city water supply will not be shut off during normal in-plant use of the tank calibrator, the water pressure may quickly change substantially as it does often in the NBS Fluid Mechanics Building. The captive air tank limits the resulting rate of change of flow to 3.4 percent (of maximum flowrate) per second even when the water supply is quickly shut off altogether. This is sufficiently slow that the computer is able to determine the flowrate accurately as described in the Introduction.

The two turbines are in a vertical run at the back of the rack with water flowing upward through them to the diverter valve and through hoses out the back of the rack at the top. One of three platinum RTD temperature sensors is in the vertical run. The diverter valve is a three-way pilot valve (Skinner XL4DM5140) with its pilot pressure inlet connected to the water line between the captive air tank and the filter. The diverter valve was used rather than a shutoff valve in order not to water hammer the turbine meters and hasten their failure. Turbine meters are used for the flow measurement because of their high resolution and high repeatability. The turbines are 5/8 inch diameter (1.5875 cm) (Flow Technology 10M12.5-LB) with RF pickoffs and sleeve bearings. The sleeves are made of carbide with a nickel binder. Sleeves made of carbide with a cobalt binder gave a ten times larger nonrepeatability in flow measurement and failed within 300 hours of operation. Nine sets of ball bearings of two kinds were also tried, and all failed within 250 hours of operation with water; ball bearings do not appear to be sufficiently reliable for use in 5/8 inch turbine meters to measure water flow.

The volumetric test measure (Seraphin S/N 17749) used as a volume transfer standard for the initial calibration of the turbine meters is shown in the center of the photograph, Figure 2. It has a sight tube and a scale on the neck calibrated to read 30 gallons in the center with 1 cubic inch increments, twelve per inch (2.54 cm) up and down from the center. The temperature corrected volume of the test measure has been determined by the mass and Volume Group of the Fluid Engineering Division at NBS to be 29.9937 gallons (113.539 liters) ± .0043 gallon (.016 liter)[7] at 60°F (15.6 °C). A second platinum RTD surface temperature sensor is taped to the bottom (outside) of the test measure and is covered with thermal insulation; it is used for correcting the test measure volume for thermal expansion.

The test measure stands on long legs in order to make the outlet end of the hose higher than the top of the rack. This ensures that the hose remains full after the flow is shut off. The hose is connected to a glass tube used for visual inspection of the flow and of the final water level inside the tube. The tube curves into the tank where it is connected to a vertical thin-walled stainless steel tube. This fill tube goes to the bottom of the test measure in order to prevent air entrainment in the flowing water and subsequent air bubbles inside the tank. The bubbles initially occupy at least several cubic inches and take longer than 15 minutes to rise out of the water and so must be eliminated in order to avoid an error of unknown magnitude. The stopcock at the top of the glass tube is opened after the test measure is full to permit air to enter the fill tube. Then the water in the part of the tube inside the tank drains into the tank from the curved part of the glass down to the water level in the tank neck. The water in the left part of the glass of course stays with its free surface quite repeatably at the bottom of the curve in the glass tube. As a result of the draining of the water from the tube, only the volume of the submerged metal wall of the fill tube needs to be subtracted from the tank reading. This submerged volume is less than two cubic inches (30 cm^3) and is accurately known as a function

[7] R. M. Schoonover, "The Equivalence of Gravimetric and Volumetric Test Measure Calibration," U. S. NBS Overlap #5 (Feb. 1974).

of water level, and so can be used to correct the tank reading. The overall uncertainty in the volume determination is .014 percent.

A corner of the test bench whose pump supplies the flow used in the initial calibration is shown on the right of the photograph Figure 2. This pump maintains a nearly constant 53 psi (360 kPa) water pressure for use in calibrating the turbine meters. The temperature controller (set to 70°F) on the bench holds the temperature of the flowing water constant to 21.1 °C ± .1 °C. After the test measure is filled, the ball valve in front of the tank is opened to drain the water to the right (just below the temperature controller) back to the reserve tank in the test bench. The clear glass section in the 2-inch pipe is used visually to determine when the tank is mostly empty during the wetting procedure described in the next section.

After the turbine meters have been calibrated, only the rack on the left is to be used in a nuclear fuel processing or reprocessing plant for calibration of a large tank in the plant.

3. TURBINE AND DIVERTER CALIBRATION

The procedure for using the apparatus of Figure 2 to calibrate the two turbine meters and the diverter is as follows. With the drain valve open, the filling flowrate is adjusted using the needle valve so that the (dimensionless) frequency number

$$N = D^2 f/\nu$$

of the upstream turbine meter has the desired value in the range $200{,}000 < N < 400{,}000$. Here D is the (1.5875 cm) diameter of the turbine meter, f is the blade frequency, and ν is the kinematic viscosity. The temperature is controlled to 21.1 °C so the value used for the viscosity[8] is $\nu = .0097797\ cm^2/sec$. Thus the frequency will be in the range $776\ Hz < f < 1552\ Hz$.

In order to minimize the diverter correction and to control it so that it is predictable, the bypassing flowrate is adjusted to equal the filling flowrate as nearly as possible. With one fixed adjustment, the ratio of filling flowrate to bypassing flowrate increases from .9995 at N = 200,000 to only 1.0079 at N = 400,000. Since the diverter valve moves in less than about 600 ms and it takes more than three minutes to fill the tank, this ratio is sufficiently close to one that the one fixed adjustment causes an uncertainty much smaller than .01 percent over the range $200{,}000 < N < 400{,}000$.

Before each calibration measurement the volumetric test measure is wetted by filling it at the given flowrate, bypassing the water flow to the drain, draining the test measure, and then shutting off the test measure drain valve 30 sec ± 1/2 sec after the flow through it suddenly decreases to near zero. This precise wetting of the test measure walls is necessary to eliminate an error of about two cubic inches (30 cm^3), which is about .03 percent of the total volume of the test measure.

The test measure is then filled again and the (dimensionless) turbine calibration coefficient

$$C = Q/D^3 f$$

is determined, where Q is the volume flowrate. Here Q/f is just the volume of the test measure divided by the number of turbine pulses during the time voltage is applied to the diverter valve to hold it in the filling position. The volume of the test measure is corrected for thermal expansion[7] using the expansion coefficient $3\alpha = .0000477/°C$, and the result is recorded. Also, the average value of N is recorded, where the frequency f used to compute N is the number of pulses during the time the voltage is applied divided by that time. This frequency is quite accurate but the coefficient C must be corrected for the slowness of the diverter valve, which is done in the next section.

---

[8]CRC Handbook of Chemistry and Physics (CRC Press, Cleveland, 1977), 58th ed., p. F51 and p. F5.

Dimensionless variables F and C are used because, by dimensional reasoning, all effects of changes in the four variables f, ν, D, and Q can be accounted for in terms of just N and C. This simplifies the calibration of the turbine meters enormously since the data at only one temperature (and hence only one viscosity ν) need be taken in order to determine the calibration for all temperatures. This assumes that any effect of temperature on the turbine bearing friction is negligible.[9]

All of the above operations are done by the computer except setting the flowrate with the needle valve, opening and closing the drain valve, and reading the volume; the computer does give explicit instructions to the operator to perform these operations at the correct time so that the chance for error is minimized.

Typical long run-time performance of the turbine meters is shown in Figures 3 and 4. Each data point in these graphs is the average of five calibration coefficients at frequency number N equal to 400,000. After a run-in time of about 300 hours, the average calibration coefficients are constant within $\pm$ .005 percent except that after a total of 880 hours the upstream coefficient has decreased .035 percent from the previous average.

A set of data consisting of five calibration runs at each of eleven different values of the frequency number N can be taken in one day starting with N = 400,000, decreasing N by 20,000 after each five runs, and ending after the five runs at N = 200,000. Six such sets of calibration coefficients are given in Figure 5. Each point on this graph corresponds to a single run. All data were taken after 300 hours of running time. The upper curve is a fit to the first five data sets as described in the next section. The lower curve is a fit to the last data set taken after 880 hours of running. The two data sets cluster around their respective curves within $\pm$ .02 percent. The change in the upstream turbine can be seen to have shifted the calibration coefficient down by about .02 to .035 percent over the range $200{,}000 < N < 400{,}000$. Since the calibration coefficient C is nearly constant, the volume flowrate Q is close to being proportional to the frequency number N, with Q = 39.4 liters/sec at N = 400,000.

The data of Figure 5 was obtained with the volumetric test measure being filled with only one diversion. The data of Figure 6 is similar except that it was obtained with the volumetric test measure being filled with ten diversions; i.e., the water flow was bypassed for five seconds after each three gallons (11 liters) went into the test measure. This magnifies the diverter error by ten and so permits calculation of the diverter correction. Just five data sets were obtained for Figure 6 over the interval of 305 hours to 555 hours of running time. It was not necessary to take a set after 880 hours since the previous data is sufficient to calculate the diverter correction.

The usefulness of the ratio of turbine meter frequencies is illustrated in Figure 7. The data taken after 880 hours of running time is well outside the data taken over the 305 hour to 555 hour interval. This indicates a significant change in the bearings of at least one of the turbine meters. The ratio can be measured at any time in the field without using a volumetric test measure. When a change this large occurs, the user may want to recalibrate the turbine meters. Just one data set with one-diversion filling is necessary, and this can be done in one day using the volumetric test measure.

4. CURVE FITTING AND DIVERTER CORRECTION

The diverter valve takes about .2 sec to move from the bypass position to the fill position, and it takes about .5 to .6 sec to move back. This leads to a systematic error in the measured time to fill the test measure and hence in the calibration coefficient. The procedure for correcting this error while fitting smooth curves to the data is described in this section.

The smooth curves used are

$$C_K = \sum_{j=0}^{4} a_j N^j + K \sum_{j=0}^{2} b_j N^j \quad ,$$

[9] H. M. Hochreiter, "Dimensionless Correlation Coefficients of Turbine-Type Flowmeters," Trans. ASME, 80, 1363-8 (1958).

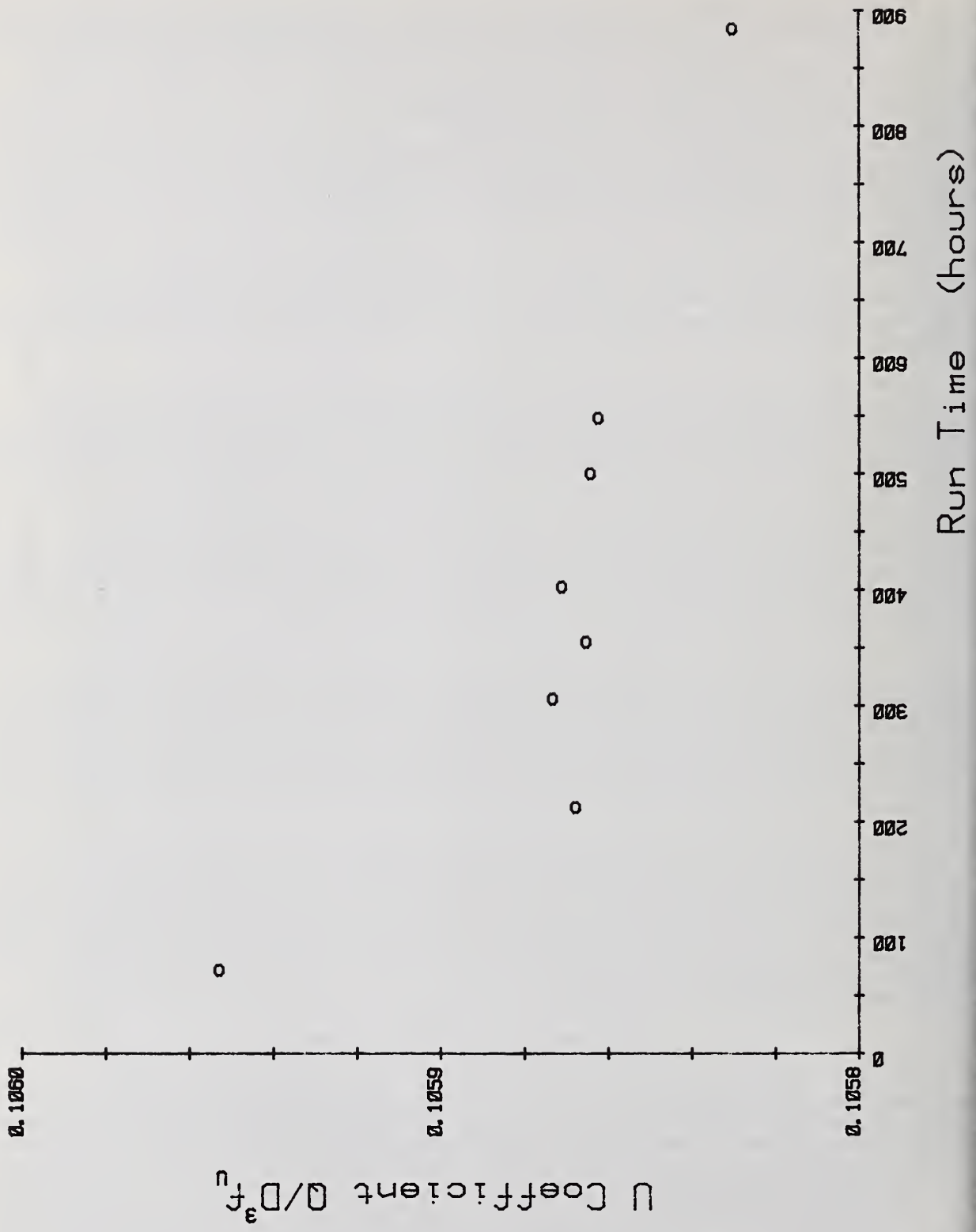

Fig. 3. Upstream turbine calibration coefficient versus running time for N = 400,000.

Fig. 4. Downstream turbine calibration coefficient versus running time for N = 400,000.

Fig. 5. Upstream turbine calibration coefficient versus frequency number with just one diversion during filling.

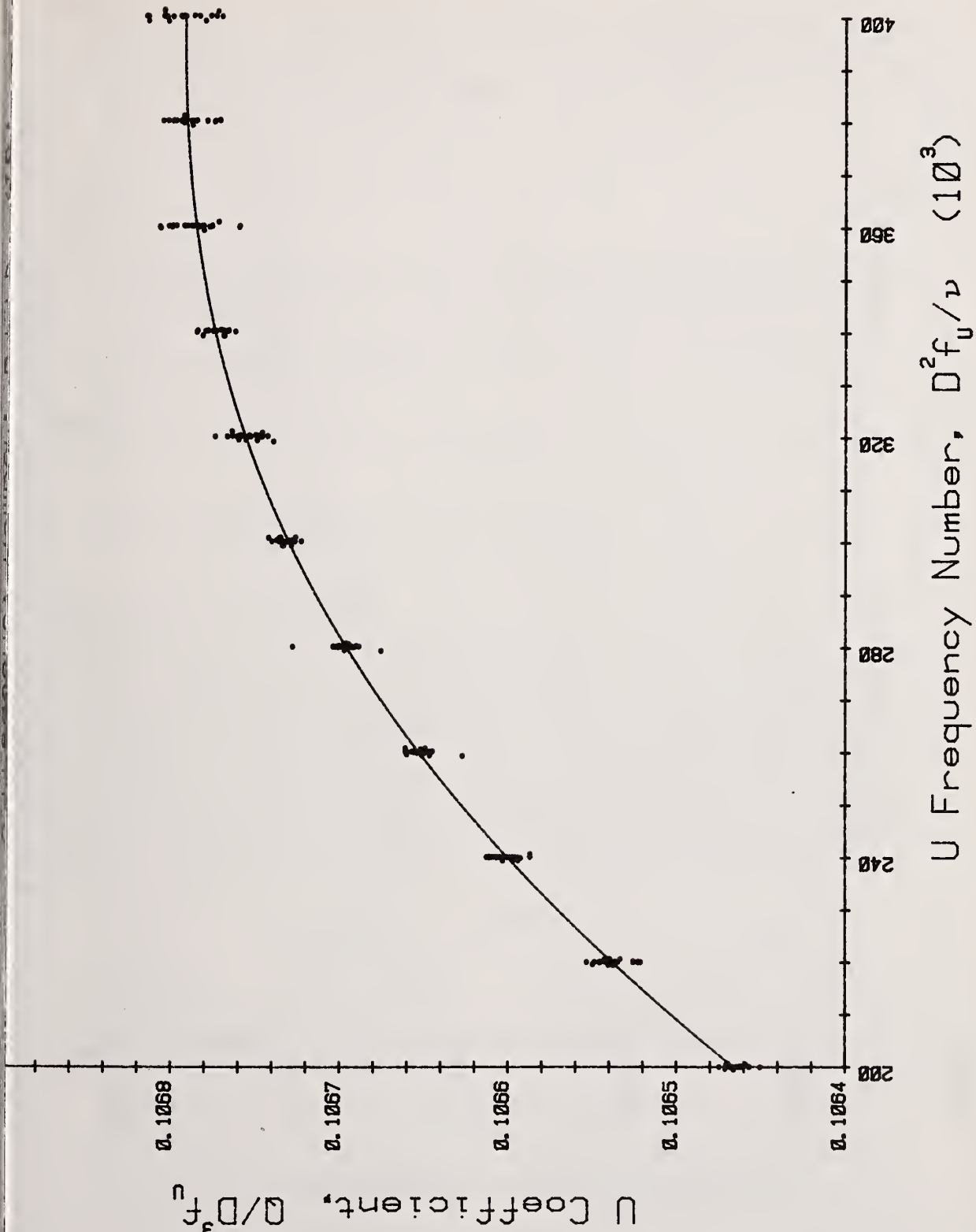

Fig. 6. Upstream turbine calibration coefficient versus frequency number with ten diversions during filling.

Fig. 7. Ratio of turbine meter frequencies versus frequency number.

where C is the calibration coefficient, N^j is the frequency number raised to the power j, a_j and b_j are coefficients to be determined, and K is the number of diversions, 1 or 10. This expression is used because the diverter, to a good approximation, causes an additive error in C. Thus the first sum is the turbine calibration curve with the diverter error removed, and the second term is K times the diverter correction curve.

The a_j and b_j are determined by minimizing the sum of squares

$$\sum_{i=1}^{m} \frac{1}{2}(c_i - C_1)^2 + \sum_{i=m+1}^{n} \frac{1}{2}(c_i - C_{10})^2 ,$$

where the c_i are the measured values of the calibration coefficients with one diversion for $1 < i \leqslant m$ and with ten diversions for $m < i \leqslant n$. Here, the corresponding measured values N_i of the frequency number are to be used in C_1 and C_{10} in place of N.

The result of carrying out the indicated algebra is that a_j and b_j are the solutions to the eight simultaneous equations

$$\sum_{j=0}^{4} \sum_{i=1}^{n} N_i^{k+j} a_j + \sum_{j=0}^{2} \sum_{i=1}^{n} K_i N_i^{k+j} b_j = \sum_{i=1}^{n} N_i^{k} c_i , \qquad k = 0,1,2,3,4,$$

$$\sum_{j=0}^{4} \sum_{i=1}^{n} K_i N_i^{k+j} a_j + \sum_{j=0}^{2} \sum_{i=1}^{n} K_i^2 N_i^{k+j} b_j = \sum_{i=1}^{n} K_i N_i^{k} c_i , \qquad k = 0,1,2,$$

where $K_i = 1$ for $0 < i \leqslant m$ and $K_i = 10$ for $m < i \leqslant n$. The solution to these equations is easily obtained with the computer.

The resulting curves for the upstream turbine meter are plotted in Figures 5, 6, 8, and 9. The diverter corrections in Figure 9 are of the order of .08 to .1 percent of the calibration coefficient. The upper curve in Figure 9 is the diverter correction to the upstream turbine calibration coefficient and is obtained using the upstream turbine data only. The lower curve in Figure 9 is the corresponding thing for the downstream turbine. It is satisfying that the two curves agree within about one percent of the diverter correction, which itself is about .1 percent of the calibration coefficient. Nearly the same diverter calibration curve is obtained when any one, two, or three of the five data sets are used. This agreement adds confidence to the results. The upper curve in Figure 5 is the sum of the curve in Figure 8 and the upper curve in Figure 9. The curve in Figure 6 is the sum of the curve in Figure 8 and ten times the upper curve in Figure 9.

Table I. Coefficients

	U Turbine First 5 Sets	D Turbine First 5 Sets	U Turbine Last Set	U Turbine Values Used
a_0	1.054013 -01	1.034618 -01	1.050603 -01	1.050697 -01
a_1	1.207742 -09	1.660426 -08	6.818746 -09	6.249895 -09
a_2	7.688811 -15	-6.438992 -14	-2.280493 -14	-2.208147 -14
a_3	-3.864874 -20	1.078526 -19	3.660987 -20	3.660987 -20
a_4	4.397430 -26	-6.545040 -26	-2.542219 -26	-2.542219 -26
b_0	-9.389381 -06	-9.514425 -06	-3.152129 -10	-9.389381 -06
b_1	5.688510 -10	5.619277 -10	2.183002 -15	5.688510 -10
b_2	-7.234625 -16	-7.076685 -16	-3.611760 -21	-7.234625 -16

Fig. 8. Upstream turbine calibration coefficient with the diverter correction subtracted out.

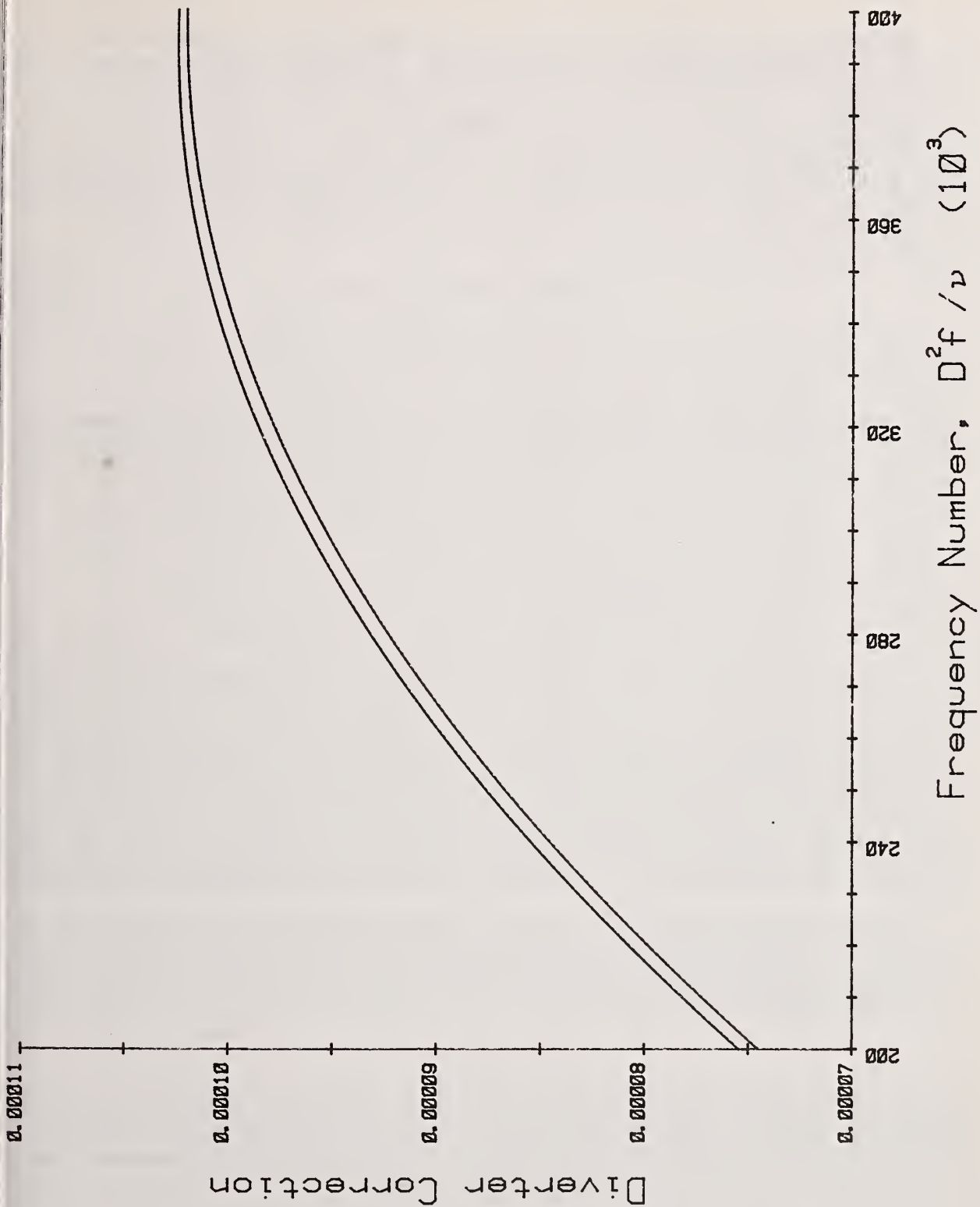

Fig. 9. Diverter corrections to the turbine calibration coefficients. The upper curve is for the upstream turbine, the lower one for the downstream one.

The coefficients are given in Table I. As suggested by Figure 9, the diverter correction coefficients b_j are seen to be almost the same for both the upstream and the downstream turbine meters for the five data sets taken over the 305 hour to 555 hour interval. The coefficients for the upstream turbine meter for the last data set (taken after 880 hours) were obtained by using the one-diversion data twice, once as one-diversion data and again as if it were ten-diversion data. The resulting diverter correction coefficients b_j should be zero. It is satisfying that they are within round-off error. The rightmost column is obtained by using the proven b_j from the leftmost column and using the a_j from the last set with the b_j subtracted. This subtraction accomplishes the diverter correction for the last (one-diversion) data set without having to take ten-diversion data.

5. OPERATION OF TANK CALIBRATOR

Two modes of operation of the calibrator are possible: the incremental mode and the continuous mode. In the incremental mode the computer diverts the flow from the tank to the drain as soon as an increment of say 100 liters has gone into the tank. The computer reads the pressure difference of the bubbler-tube liquid level gauge repeatedly until the pressure becomes constant indicating that most of the water film wetting the tank walls has settled below the main liquid level. This may take more than fifteen minutes. Then the computer stores the pressure measurement, the volume increment, the ratio, and the turbine and tank temperatures on the disk and diverts the flow to the tank again. It repeats this process until the pressure measurement or the total water volume measurement indicates that the tank is full. The incremental mode has the disadvantage that the random part of the diverter error will increase the scatter in the tank calibration results. Much worse, the uncertainty in the correction for the systematic diverter error will accumulate as the number of diversions increases. This uncertainty depends on the water supply pressure and on whether the diverted and bypass flowrates are the same and hence may not be negligible.

In the continuous mode, the diverter valve is actuated only at the start of the measurements and again after all measurements are complete. The uncertainty in the initial diverter correction can be absorbed into the heel volume uncertainty. The final diversion need not be considered. The computer measures the bubbler tube pressure difference periodically while the water is entering the tank. A correction must be made for the effect of the initial momentum of the water jet on the pressure measurement. This correction may be small compared with errors associated with wetting of the tank walls. The uncertainty in correcting for the water required to fill the inaccessible tubing to the tank is a negligible addition to the uncertainty in the measurement of the tank heel volume and does not contribute to the uncertainty in incremental volume measurements. As in the other mode, the computer periodically stores the volume, pressure, and other measurements on the disk.

The diverter correction volume required for the incremental mode is obtained from the (dimensionless) diverter correction to the turbine meter calibration as follows. Since the curve ΔC in Figure 9 is added to the curve C_0 in Figure 8 to get the total volume V of the test measure divided by the number of pulses and by D^3 and since $\Delta C \ll C_0$, the volume correction ΔV per diversion is

$$\Delta V = V \, \Delta C/C_0 \ .$$

So the curve in Figure 9 should be multiplied by $V/C_0 \simeq 65526$ cubic inches (1074 liters) to obtain the volume correction ΔV per diversion. The result increases from about 4.9 cubic inches (80.5 cm^3) at N = 200,000 to about 6.7 cubic inches (109.5 cm^3) at N = 400,000. Alternatively the time correction Δt per diversion can be seen by similar reasoning to be

$$\Delta T = t \, \Delta C/C_0 \ ,$$

where t is the time required to fill the test measure. Now $t = V/CD\nu N$ decreases from about 346 sec at N = 200,000 to 173 sec at N = 400,000. Hence Δt decreases from about .23 sec at N = 200,000 to about .17 sec at N = 400,000. This is roughly similar to the difference in the directly observed valve motion times reported in Section 4.

Both the incremental and continuous modes of operation require the computer to refer

to a table of the turbine meter calibration coefficient as mentioned in the Introduction. The calculation is set up as follows. The turbine meter calibration coefficient C is a function of the frequency number N, say F(N), thus

$$Q/D^3f = F(D^2f/\nu) \quad .$$

If the time for n (= 24) turbine meter pulses to occur is τ, then $f = n/\tau$, and the volume δV transferred in that time is

$$\delta V = Q\tau = nD^3F(D^2n/\nu\tau) \equiv F_n(\nu'\tau) \quad ,$$

where $\nu' = \nu/D^2$ and where F_n is a new function defined (for n pulses) as shown. The total volume of an increment consisting of m groups of n pulses is

$$dV = \sum_{k=1}^{m} F_n(\nu'\tau_k) \quad .$$

Hence only one multiplication, one table look-up, and one addition is required for each n (= 24) pulses. This can be done (with time to spare) using two 100 number data buffers serviced by alternate interrupt routines.

The viscosity ν here is obtained (in cm^2/sec) from

$$\nu = \sum_{j=0}^{4} \nu_j T^j \quad ,$$

where T^j is the temperature (in °C) raised to the power j, ν_0 = 1.7841 -02, ν_1 = -5.946 -04, ν_2 = 1.3685 -05, ν_3 = -1.9998 -07, and ν_4 = 1.3387 -09. This is the result of a least squares fit to the data of Reference 8. This computation is also performed in an interrupt service routine.

So far the operation of the tank calibrator has been tested only by filling the volumetric test measure with water flowing from the city supply. As before, the computer is programmed to make sure the test measure is precisely wetted before each filling. During the filling it uses the above technique to correct for changes in temperature and flowrate and at the end of the filling adds the volume correction for one diversion to obtain a prediction for the volume of water in the test measure. After the operator has read the water level in the neck of the test measure and entered it into the computer, the computer prints its prediction, the percent difference, and other variables.

The test measure was filled eight times with city water having a temperature that varied from 13.7 °C to 14.3 °C. The first five were at a nominally constant frequency number of about 300,000. During each of the last three, the water spigot was shut off altogether for 10 seconds and then turned on again three times, so the average N was about 265,000. The resulting predicted volume did not differ from the measured volume by more than .012 percent.

6. CONCLUSION

On the basis of our work, one can, with care, in general expect to achieve an overall uncertainty (in the volume of water passing through the calibrator) no larger than about ± .02 percent provided the turbine meter frequency ratio stays within ± .02 percent of the value it had during the last turbine meter calibration using a reliable volumetric test measure. If the ratio changes by more than that, the turbine meters can be recalibrated in one day using the volumetric test measure.

In-Tank Measurement of Solution Density

by

FRANK E. JONES, RANDALL M. SCHOONOVER and JOHN F. HOUSER
National Bureau of Standards, Gaithersburg, Maryland

ABSTRACT

This paper presents the results of an experiment which established the feasibility of in-tank determination of the density of nuclear process solutions in the field with an accuracy competitive with the precision claimed for laboratory determinations. The work also provided a calibration factor, with a precision (estimate of the relative standard deviation of the mean) of 2.2 parts in 10,000, which can be used to infer density from differential pressure measurements in the particular accountability tank. The technique eliminates one error in the laboratory determination of density and minimizes another. It also can be used to indicate the homogeneity of the tank solution and thus determine when a sample should be taken for determination of the concentra- of nuclear material in the solution.

KEYWORDS: Accountability tanks, differential pressure, in-tank density determination, nuclear process solutions, solution density

INTRODUCTION

The density of a solution in a nuclear process tank is usually determined by laboratory measurement on a sample taken from the tank. If the laboratory measurement is made at a temperature different from the temperature of the solution in the tank, a significant error is introduced if the relationship between the density of the particular solution and the temperature is not well known. Also, there is an error associated with the sampling. It is possible to eliminate the first of these errors and to minimize the second by making the density measurement in the tank. This is done by inferring the density from the differential pressure measured between two probes immersed at different heights in the solution. This is the conventional method for determining "specific gravity" in the process; however, the availability of electromanometers of excellent precision makes it possible to make in-tank density measurements accurate to several parts in 10,000. This accuracy is comparable to the precision claimed for laboratory measurements and, as mentioned above, two sources of systematic error are either eliminated or minimized.

The relationship between the differential pressure, ΔP, between two points separated in height by a distance, h, measured downward from the higher point, is

$$\Delta P = \rho g h, \tag{1}$$

where ρ is the density of the fluid and g is the acceleration due to gravity. The ratio of ΔP to ρ is a measure of the product (gh). Therefore, a series of measurements of ΔP in a liquid of known density provides a determination of (gh) with an estimate of precision from the multiple measurements. The (gh) so determined then becomes a calibration factor relating ρ to ΔP.

Since the relationship between density and temperature is very well known for water, it is the ideal liquid for making the determination of (gh). The determination involves ΔP measured using an electromanometer of high precision, and the measurement of temperature from which the density of water is inferred. The (gh) determined using water can then be used in a rearrangement of Eq. (1) to infer ρ of a process solution from measurements of ΔP in the solution:

$$\rho = \frac{\Delta P}{(gh)}. \qquad (2)$$

The determination of (gh) can made in the course of volume calibration of a tank with little or no additional effort. Alternatively, an experimental determination can be made in preparation for a volume calibration by connecting an electromanometer across two probes (the "specific gravity" probe and a probe near the bottom of the tank). Calibration run data can then provide confirmation of the (gh) value and its precision.

EXPERIMENTAL

An in-tank density experiment was performed in a dissolver hold tank for enriched uranium reprocessing at the duPont/DOE Savannah River Plant at Aiken, S.C., the site of a previous very successful tank volume calibration (1). The tank is essentially a right circular cylinder 3.35 m (11 ft) high and 3.05 m (10 ft) in diameter. The vertical separation of the probes was approximately 25.4 cm (10 in).

A null-operated quartz bourdon-type differential pressure electromanometer was connected between the two probes and a flow of 8 mL/s (1 cubic foot per hour) of dried instrument air was maintained through each of the two lines communicating the differential pressure from the probes to the electromanometer. The temperature of the calibrating fluid, water, was measured using the nickel resistance thermometer used in the operation of the tank. The output of the electromanometer was displayed on a digital voltmeter (DVM) with 5 decimal place capability and a variable time span.

A quantity of water sufficient to fill the tank to a level approximately 25 cm above the upper probe was introduced into the tank. Prior to each of three sets of measurements of the electromanometer output, the water was stirred using the agitator in the tank and the water temperature was measured. The sample period for the DVM was set at 1 s and the sampling "rate" was set at 2 s; the DVM was read visually. The three sets of measurements provided 33, 42 and 40 consecutive measurements of the differential pressure. The DVM readings were converted to pascals and the water temperature, 28.7°C, was used to infer the density of water from a table (2). The resulting set of 115 (ΔP, ρ) pairs was used to determine (gh) and to assign a measure of precision to the determination.

RESULTS

The mean value of (gh) is 2.48525 $m^2\ s^{-2}$ with an estimate of the standard deviation of the mean of 0.00055 $m^2\ s^{-2}$, which corresponds to a precision of 2.2 parts in 10,000. Using a value of g of 9.79558 m s^{-2}, the vertical separation of the probes is calculated to be 0.253711 m (9.98860 in). It is, of course, unnecessary to know either g or h since the product (gh) is determined from the experimental calibration of the probes and is used subsequently to infer the density of the process solution from measurements of the differential pressure. In the application of (gh) for a solution temperature, t_s, different from the calibration temperature, t, (gh) is multiplied by $[1 + \alpha(t_s - t)]$, where α is the coefficient of linear expansion of the probe material.

After the data for the field experiment were analyzed, data from NBS laboratory work of Schoonover et al (3) in a right-circular cylindrical tank 1.22 m (4 ft) in diameter with a vertical separation of probes of approximately 20 cm were similarly analyzed. The differential pressure measurements were made by connecting an electromanometer, different from the one used in the field experiment, alternately between each of the probes and the atmosphere. The temperature of the water in the tank was measured using a quartz crystal thermometer. A set of 78 (ΔP, ρ) pairs taken from 6 runs was used to determine (gh) and to assign a measure of precision to the determination. The mean value of (gh) is 2.03231 $m^2\ s^{-2}$ with an estimate of the standard deviation of the mean of 0.00021 $m^2\ s^{-2}$, which corresponds to a precision of 1.0 part in 10,000.

DISCUSSION AND CONCLUSIONS

The experimental work at the Savannah River Plant established the feasibility of deter-

mining the density of a nuclear process solution in a tank in the field with an accuracy competitive with the precision claimed for laboratory determinations. The work also provided a calibration factor which could be used to infer solution density from differential pressure measurements in the particular tank. The precision of the calibration factor confirms the feasibility of making accurate in-tank solution density determinations and is within a factor of 2.6 of the precision attained in NBS laboratory in-tank measurements, although the two results are not directly comparable. The precision of the field measurement would be improved by using a DVM with a longer integration time.

The calibration factor, (gh), could in practice be determined during the volume calibration of a tank by recording the outputs of electromanometers connected to the two probes (and taking the differences); the density of the fluid, water, is used in the volume calibration and does not therefore represent additional effort.

The 25.4 cm vertical separation of the probes in the tank delineates a section of the tank containing about 6% of the full volume of the tank and a larger percentage of the liquid if the tank were not completely full above the probes. The in-tank density determination, therefore, involves a sample which is very much larger than is conventionally taken for laboratory density measurements--approximately 1600 liters compared to 0.015 liter.

In the operation of a tank, the differential pressure between the probes could be monitored to determine the adequacy of stirring, as indicated by the constancy of ΔP for successive stirrings, and to determine when the solution was sufficiently homogeneous that a sample might be taken for the measurement of the concentration of nuclear material in the solution.

ACKNOWLEDGMENTS

The authors gratefully acknowledge the financial support of the U.S. Nuclear Regulatory Commission, and the cooperation of members of the staffs of the U.S. Department of Energy and the E.I. DuPont de Nemours and Co., Inc. at the Savannah River Plant.

REFERENCES

(1) F.E. Jones, "The Application of an Improved Volume Calibration System to the Calibration of Accountability Tanks", International Atomic Energy Agency International Symposium on Nuclear Materials Safeguards, Vienna, Austria, 2-6 October, 1978.

(2) H. Wagenbreth and W. Blanke, PTB-Mitt. 81, S. 412-415 (1971).

(3) R.M. Schoonover, H.H. Ku, J.R. Whetstone and J.F. Houser, "Liquid Level Instrumentation in Volume Calibration", NBSIR 75-900, National Bureau of Standards, Washington, D.C., (1975).

Discussion:

Rogers (Monsanto-Mound):
Did you vary the temperature and vary gh?

Jones (NBS):
No. The gh measured here should be called gh sub zero, the zero referring to the temperature at which the calibration was made. Then a simple correction for the linear expansion of the bubbler tube material should be made.

Rogers:
How constant would you expect this gh zero to remain with the use of the tank over the operational period?

Jones:
A gentleman at the Savannah River Plant looked at the stiffness of the mounting of the lower probe and concluded that there would be an insignificant change in its height due to lateral movement. I think that the same would apply to the other probe. The big differences might be due to an accumulation of material in the probe tips and above.

Rogers:
Would it be possible then to remeasure gh at some frequency, and what frequency would you suggest that it be remeasured?

Jones:
If one knew the density of the real solution in the tank, one could use that to recalibrate the gh. If one didn't know it, one would have to go back to using water to recalibrate the gh. I do not know at what frequency, because that depends on what happens to the bubbler probes with time due to an accumulation of material.

Suda (BNL):
Let me address your second question first, i.e., the remeasurement of the gh for a plant like Barnwell when in operation. There is a routine cleanout of the head end of the system and the input tank between process lots. The flush solution is dilute nitric acid whose density is well known. A recalibration value for gh can be obtained based on the nitric acid measurement that has perhaps twice the original uncertainty. Although this is not as precise as the original value, any changes in the bubbler probes or tank conditions would be observed. With regard to the temperature effects in a process tank, I have run two field experiments. The first one was at the Barnwell Nuclear Fuel Plant in Feburary of this year with the assistance of the AGNS people. The equipment used was the automated electromanometer system and the solution was heated UNH that was measured as it cooled. We recorded data every two minutes or so and watched the change in the two bubbler probes as the solution cooled from 55°C to 25°C. After looking at that data and analyzing it, we realized there is probably no need to ever do that again with UNH. The experiment was repeated at the Tokai plant using hot water. The tank was heated to 55°C. What we originally saw happening at Barnwell was confirmed at Tokai. We are now in the process of analyzing these data and hope to report the results soon.

Analysis of Plutonium and Uranium by the Resin Bead-Mass Spectrometric Method

R. L. WALKER and D. H. SMITH
Oak Ridge National Laboratory, Oak Ridge, Tennessee

ABSTRACT

The development of the resin bead method and the techniques employed in its application to isotopic analysis of Pu and U in in highly radioactive solutions of spent reactor fuel will be described. The method, developed primarily for safeguards analyses, may also be applied to isotopic measurements for assessing nuclear fuel cycle technology. Satisfactory analyses of both elements can be obtained from a single resin bead when the initial dissolver solution has a U/Pu ratio in the range of 50 to 300. Optimum bead loadings are 1-3 ng Pu and U; these loadings are obtained if the concentration of the solution is adjusted to about 1 μg U per bead before the beads are introduced. Isotopic composition measurements of NBS standards using this technique indicate a precision of ±0.5% for minor isotopes in the 1% concentration range and ±0.1% for major isotopes in the 50% range. Analyses of a synthetic dissolver solution give an accuracy for the isotope dilution measurement of Pu and U of $\leq$0.5% with an internal precision of 0.9% and 0.6% for Pu and U, respectively.

KEYWORDS: Resin bead, mass spectrometry, plutonium, uranium, isotope dilution, safeguards

INTRODUCTION

Limitations on the amounts of radionuclides that can be readily shipped make it desirable to perform the analytical measurements required by safeguards on as small samples as possible. This is particularly true for Pu, an element of major safeguards concern.

The use of anion exchange resins to achieve chemical separations is well known.[1,2] We have extended this idea to use individual resin beads as vehicles for introducing samples into mass spectrometers. The sequential isotopic analysis of Pu and U in spent fuels by the anion resin bead method was first demonstrated at ORNL in 1974.[3] Some years earlier, a similar approach had been investigated for isotopic uranium analysis utilizing fully-loaded cation resin beads.[4] Our procedure involves adsorbing U and Pu from solutions of suitable concentration onto enough resin beads to supply a sufficient number for analyses; one resin bead serves as one sample for the mass spectrometer and contains 1-3 ng each of U and Pu.

The method shows great promise for analyzing Pu and U from highly radioactive spent fuel solutions for process control and for safeguards accountability. The beads can be packaged and shipped or mailed without requiring shielding or other precautionary measures to protect people handling them from radioactivity. Mass spectrometric analysis, which requires instruments equipped with pulse counting detection systems, yields results comparable to those obtainable using conventional chemical separation and mass spectrometry.

---

[1] R. F. Buchanan, J. P. Faris, K. A. Orlandini, and J. T. Hughes, USAEC Report, TID-7560 (1958)
[2] I. K. Kressin and G. R. Waterbury, Anal. Chem. 34, 1598 (1962).
[3] R. L. Walker, R. E. Eby, C. A. Pritchard, and J. A. Carter, Anal. Lett. 7(8&9), 563 (1974).
[4] D. H. Freeman, L. A. Currie, E. D.Kulhner, and H. D. Dixon, Anal. Chem. 42, 203 (1970).

RESIN BEAD METHODOLOGY

The method is outlined in Fig. 1 and involves the use of anion resin in a dilute solution of the sample adjusted to ∿8 M HNO_3 to selectively adsorb nanogram quantities of Pu and U. The original work done here with the method was designed for an in-house problem with the hope of reducing time, complexity, and cost of the chemical separation and reducing the alpha radioactivity in the mass spectrometry laboratory and in the source region of the mass spectrometer. Under the conditions specified, Pu and U have distribution coefficients of 10^4 and 10^2, respectively. This favors the adsorption of Pu over U, which results in a Pu/U ratio on the beads of about 1:1 for dissolver solutions whose original Pu/U ratio is 10^{-2}. For the chemical isolation step, an aliquot of diluted dissolver sample is taken so that there will be 1-2 μg of U per resin bead in the adsorption apparatus. The amount of Pu may be predicted from burn-up and reactor characteristics, but usually the quantity accompanying uranium is adequate.

Aliquots for spiking are taken which contain ∿1 mg U and ∿10 μg Pu, where possible. Highly enriched spikes of ^{233}U and ^{242}Pu are added and isotopic equilibration is carried out. We are using $HClO_4$ and HF to achieve Pu valence adjustment. We have had good results with this technique but are looking at other techniques to eliminate the use of $HClO_4$.

Actinide elements that adsorb in 8 M HNO_3 are Th, U, Pu, and Np; rare earths, Am and Cm do not adsorb. Np is not an interferent in the mass analysis since there are no Np isotopes with long enough half lives to interfere at Pu or U mass positions. Although Np gives no significant mass interference, its presence must be considered in terms of the over-all radioactivity that is on a bead since ^{237}Np ($T_{1/2}$ = 2.1 x 10^6 a) will be present in spent fuel dissolver samples. Decontamination factors from Am have been measured at >10^3. Although some ^{241}Am will be present on the bead from the original solution, most that is there will grow in from the β decay of ^{241}Pu. This small amount can be eliminated after loading into the mass spectrometer before taking Pu data. A discussion of this will be given in a later section on the procedure for analysis of resin beads.

The optimum concentration of HNO_3 is near 8 M, but a range of ±5-10% around this value is all right for the adsorption. Usually 10 resin beads are used for each adsorption; only two are needed for duplicate analyses, but if beads are lost or if rechecks are needed, a reserve supply is convenient to have for this purpose.

MASS SPECTROMETRY

The mass spectrometers in our laboratory have been previously described.[5,6] Development of the resin bead technique was done primarily on multi-stage instruments, but a single-stage mass spectrometer has also been successfully used.[7] The instruments have 90° sector magnets with 30 cm radii of curvature and are equipped with pulse counting detection systems to allow isotopic analysis of U and Pu samples of less than 1 ng.

Scanning the mass spectrum is accomplished by a locally designed sweep control unit interfaced to a DEC PDP-11/34 computer. Any peak in the spectrum can be scanned any pre-determined number of times for each single traversal of the entire mass range. This allows us to optimize our scanning scheme for the requirements of the sample in question. Multiple scans of minor isotopes yield better precision on measurements of their abundances.

We use a "ferris wheel" sample changer,[8] which allows us to mount six samples in the mass spectrometer simultaneously. Each filament is rotated in turn into position for analysis, which takes 20-30 minutes per element.

---

[5] D. H. Smith, ed., USDOE Report ORNL/TM-6485, Nov., 1978.
[6] D. H. Smith, W. H. Christie, H. S. McKown, R. L. Walker, and G. R. Hertel, Int. J. Mass Spectrom. Ion Phys. 10, 343 (1972).
[7] D. H. Smith, R. L. Walker, L. K. Bertram, J. A. Carter, and J. A. Goleb, Anal. Lett. 12, 831 (1979).
[8] W. H. Christie and A. E. Cameron, Rev. Sci. Instrum. 37, 336 (1966).

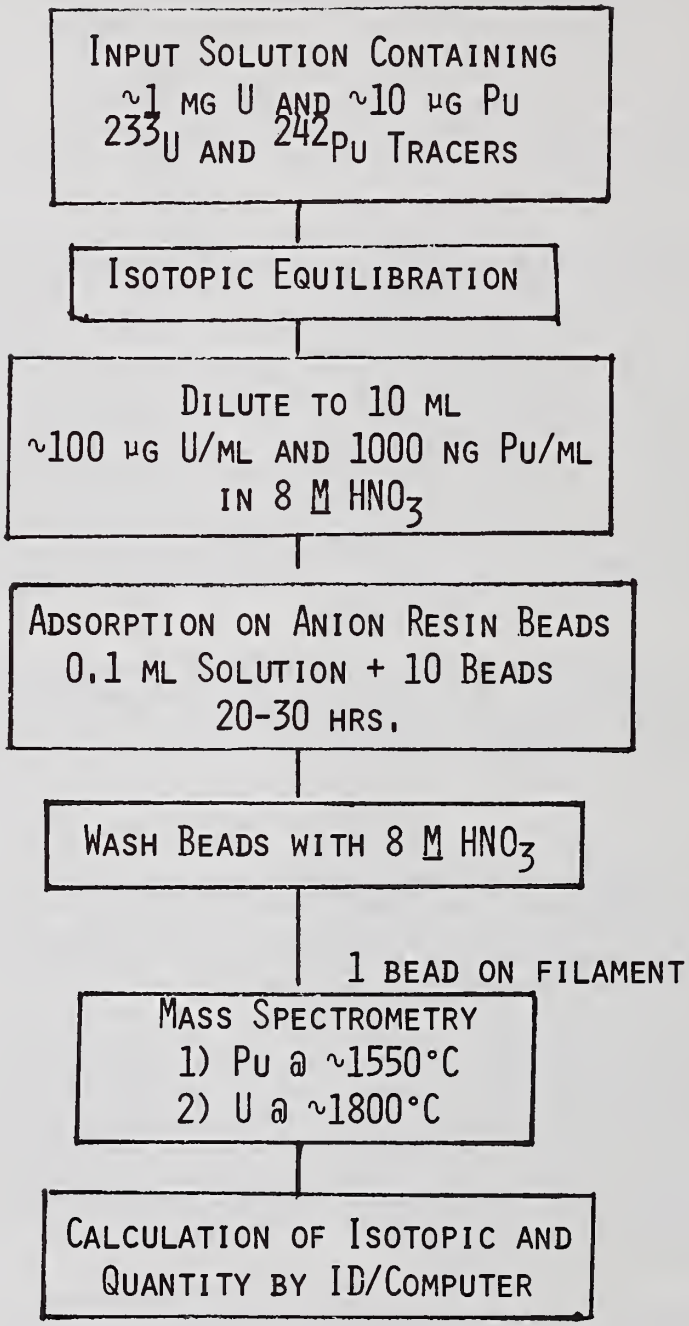

Fig. 1. Sequential Analysis of Pu and U (Resin Bead Method)

We analyze Pu and U sequentially from a single resin bead. Pu, because of its lower ionization potential, ionizes at temperatures below those required for U and is thus analyzed first. After evacuating the system to 5×10^{-8} torr or less, the temperature of the filament is slowly increased. A pressure burst is observed upon disintegration of the resin bead. The Pu^+ signal is found and brought into optimum focus. If ^{241}Am is present, it will be apparent as a shifting 241/242 ratio. The operator observes this ratio until it stabilizes before proceeding further. The temperature is increased to adjust the count rate on the most abundant Pu isotope (usually 239) to 100,000 counts per second; on no account is 1500°C exceeded because $^{238}U^+$ becomes too large at temperatures greater than this to be reliably corrected for. Pu data are collected, which takes about 20 minutes. Peak shapes and count rates are monitored continuously during the analysis to make sure it is proceeding smoothly.

After Pu analysis is complete, the temperature is again raised to burn off excess Pu. The ratio of $^{238}U^+/^{239}Pu^+$ is monitored; when it is greater than 1, the temperature is raised to give a count rate on the most abundant U isotope of 300-350,000 counts per second. The temperature will usually be 1700-1800°C for U analysis, which now proceeds in a manner similar to Pu. It is undesirable to spend too much time burning off excess Pu; U is, of course, evaporating at the same time, and if too long is spent in this step, fractionation of U becomes a problem. We try not to spend more than 10-15 minutes burning off Pu.

We have been analyzing resin bead samples in our laboratory for more than 4 years and have come to prefer this method to loading solutions directly on the filaments. The resin bead serves as a good approximation to a point source for the ion optics, and spectra obtained from resin bead samples are generally cleaner than those obtained from solutions. The result is approximately an order of magnitude improvement in our ion collection efficiency.

QUANTITATIVE ANALYSIS

Mass spectrometric determination of quantities of U and Pu is accomplished through the technique of isotope dilution. In this technique, a known amount of an isotopically enriched spike of known composition is added to the sample solution. The sample and spike are equilibrated, after which it is not necessary to obtain complete recovery of the sample since isotopic ratios are unaffected. Knowledge of the isotopic compositions of spike, sample, and mixture of spike and sample is obtained by mass spectrometric analysis. These data, along with knowledge of sample and spike weights and the dilution factor allow calculation of the concentration of the element in question in the original sample.

ADSORPTION APPARATUS

Figure 2 is a photograph showing an apparatus we have designed to facilitate collecting and shipping samples on resin beads. It consists of a commercially available funnel-shaped liquid chromatographic column tip, a porous filter, a plug, and a cap; the individual pieces are made of polyethylene. The plug and cap are made to our design and may be ordered from Kontes of Illinois, P. O. Box 30, Evanston, IL 60204, by specifying UCND-Y-12 Dwg. T2B-29681; the tip and filter may be purchased from Kontes Glass Co., Vineland, NJ 08360. The entire assembly costs about $2.00.

In use, an inspector will assemble the funnel, filter, and plug, and introduce a small volume of the solution to be sampled into the unit. The only chemical treatment required is adjusting the solution in pH and U concentration unless it is spiked, where isotopic equilibration of Pu requires adjustment of its oxidation state. Sufficient resin beads are added to provide the required number of replicate analyses; the usual number is ten.

After standing for the appropriate length of time, the plug is removed with the help of an especially designed vial with an insert to grip it and a holder to grip the funnel. The solution drains out, the beads are washed, and the plug and cap inserted. The apparatus, with the sample on the resin beads, is now ready for shipment.

The amount of radioactivity on samples prepared in this way is an order of magnitude below the daily exposure allowed to office workers. Since the bulk of the activity is due to

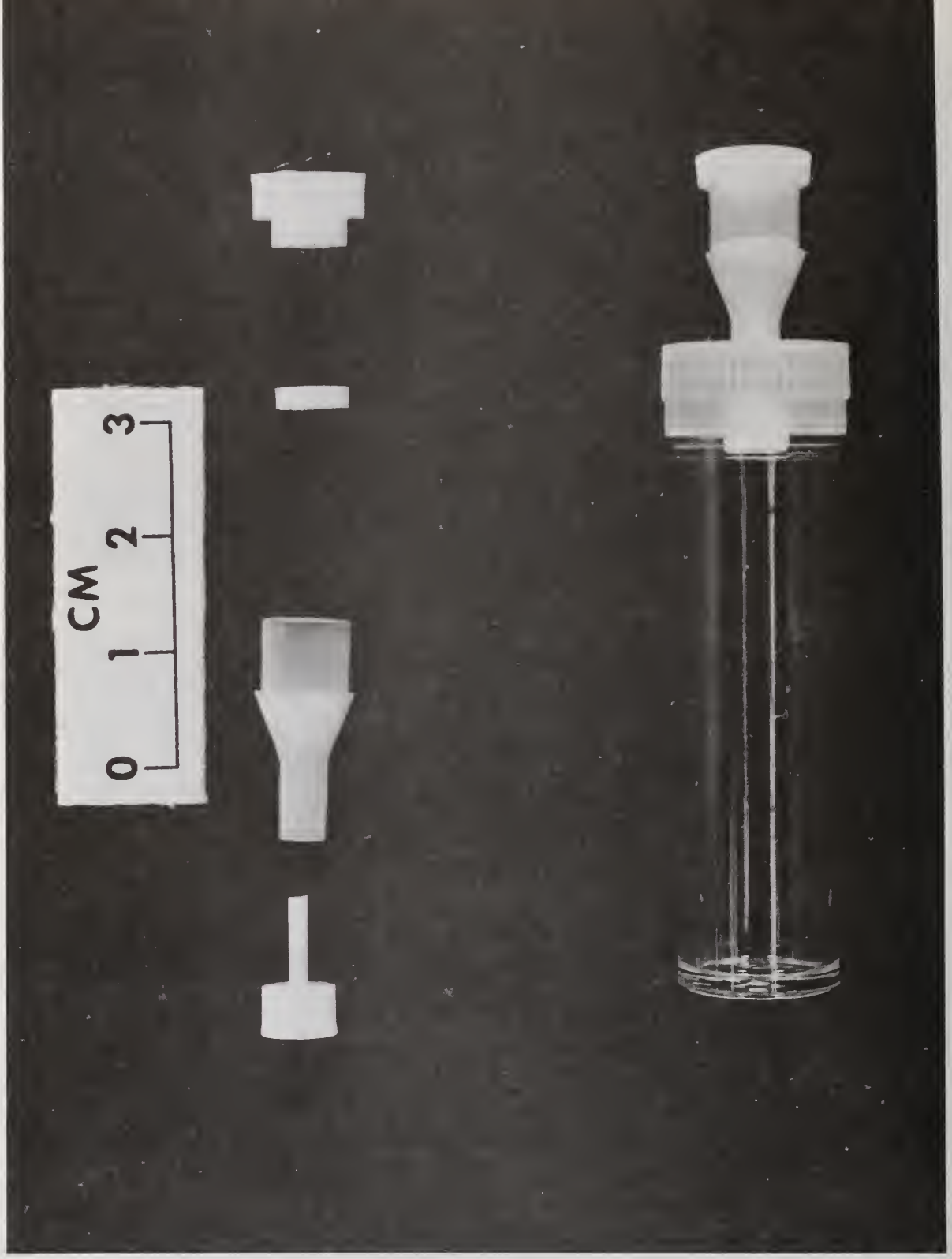

Fig. 2. Combination Adsorption and Shipping Apparatus.

α emission, the shielding provided by the funnel and its packaging reduces this low level even further. We feel that samples prepared in this way can be shipped through the mail with complete safety.

RESULTS AND DISCUSSION

Early experiments using the resin bead method were designed to elucidate the method's reliability and precision, and to compare resin bead results with results from the conventional, solution-loading technique in normal use.

Time studies were conducted to determine the amount of Pu and U that would adsorb on anion beads from a solution under static conditions. The time required to achieve near maximum adsorption is between 20-30 hrs. Very similar adsorption vs. time curves are obtained from a solution having a Pu/U ratio of 10^{-2} and in which ∿10 ng of Pu and 1 μg U per bead are present. One to three ng of each element will adsorb under these conditions. We are now recommending a 24-hr. adsorption time.

Other tests have been made to determine precision of isotopic analysis at various Pu loadings. A set of graded ^{239}Pu standard solutions in 8 M HNO_3 were prepared which contained 10-0.01 ng per resin bead. After 40 hrs., we removed a bead from each concentration. Alpha counting was used to estimate the quantity on each bead. Isotopic analyses of duplicate beads were made to determine the minimum amount required for precise results, and to compare with results obtained from conventional filament loadings. Table I contains the results of these measurements. The minimum amount of Pu required on a bead to give sufficient signals is shown to be ∿0.5 ng; below this the ^{238}U contamination and background adversely affect the minor isotopes due to poor signal-to-noise ratio.

Table I. Plutonium Isotopic Analysis at Various Concentrations

	Atom Percent				
Pu, ng/bead	238	239	240	241	242
0.003	(0.023)	94.0	5.64	(0.31)	(0.027)
0.05	0.0124	94.135	5.572	0.262	0.0184
0.6	0.0095	94.136	5.579	0.259	0.0175
3.0	0.0095	94.132	5.581	0.260	0.0181
10 ng Pu Solution Load	0.0096	94.136	5.572	0.265	0.0175

One of the steps in the data processing program corrects each element for the isobaric contribution of the other to the mass 238 position. This is accomplished by monitoring ^{235}U during Pu analysis and ^{239}Pu during U analysis. This correction is quite small for U, but can be fairly substantial for Pu. The effectiveness of this correction for Pu was tested by measuring Pu-238/239 ratios of a typical dissolver solution after chemically separating the Pu using the thenalytrifluoroacetone (TTA) method. A ratio of 0.01156 compares quite well with the resin bead value of 0.01158. Results of these tests are given in Table II.

The correction and the determination can only be made accurately on high burn-up fuel where the Pu-238/239 ratio is ∿0.01 and the U-238/235 is ≤100. Thus, if the best possible mass spectrometric result for ^{238}Pu is required, U is stripped off the bead with 1-3 M HNO_3 and the two elements are analyzed separately.

Table II. Pu-238 Analysis from Single Bead-Corrected for U-238

Sample	Uncorrected for ^{238}U 238/239 Pu	Corrected for ^{238}U 238/239 Pu
1	0.01302	0.01146
2	0.02157	0.01167
3	0.01523	0.01170
4	0.01163	0.01158
5	0.01176	0.01160
6	0.01215	0.01146
		Avg. = 0.01158 = 0.9%

Pu-238/239 value after TTA extraction, 0.01156
Single element solution filament loading.

Additional tests were made by analyzing NBS plutonium and uranium standards. The isotopic data for U (SRM-015) and Pu (SRM-947) are summarized in Tables III and IV, respectively No mass discrimination for either element is observed, and results obtained are comparable in precision to our measurements made from solution filament loading.

Table III. Isotopic Analysis of SRM-015 Std. by Resin Bead Method

Sample	Atom Percent 234	235	236	238
1	0.00846	1.537	0.0163	98.438
2	0.00856	1.548	0.0165	98.428
3	0.00851	1.540	0.0165	98.435
4	0.00865	1.526	0.0164	98.449
Resin Bead Avg.	0.00854	1.538	0.0164	98.437
Std. Dev.	0.00008	0.009	0.0001	0.009
NBS Value	0.00850	1.532	0.0164	98.443

Table IV. Isotopic Analysis of SRM-947 Std. by Resin Bead Method

Sample	Atom Percent 238	239	240	241	242
1	0.291	76.235	18.451	3.828	1.195
2	0.293	76.213	18.460	3.843	1.191
3	0.290	76.243	18.477	3.803	1.187
4	0.292	76.209	18.464	3.838	1.197
Avg.	0.292	76.225	18.463	3.828	1.192
Std. Dev.	0.001	0.017	0.011	0.018	0.004
Corr. to 10/13/71	0.297	75.647	18.328	4.544	1.184

Table IV - Continued

	Atom Percent				
	238	239	240	241	242
NBS Certified Value 10/13/71	0.296	75.696	18.288	4.540	1.180
95% C.L.	0.006	0.022	0.022	0.006	0.004

Table V presents data we obtained from mixed Pu and U NBS standards by the technique over a two-month period; all data presented were obtained from sequential analyses from single resin beads. Agreement between our results and NBS certified values is excellent.

Table V. Mixed Pu and U Standards on Resin Beads

	NBS-947 Pu			
	238/239	240/239	241/239	242/239
NBS	0.00370	0.24147	0.04309	0.01559
ORNL	0.00371	0.24156	0.04281	0.01559
S.D.	±0.00002	±0.00057	±0.00025	±0.00008

	NBS-500 U		
	234/235	235/238	236/235
NBS	0.01042	0.99971	0.001519
ORNL	0.01034	0.99851	0.001522
S.D.	±0.00005	±0.00209	±0.000005

N = 9 analyses run over a two-month period.

Another, and probably more significant, series of measurements defined the precision and accuracy of the method. Table VI shows the results obtained on synthetic dissolver solutions in which all operations, i.e., weighing, aliquoting, spiking, and isotopic equilibration, were carried out using procedures identical to those for actual radioactive samples. These results indicate an accuracy well within 0.5% from the standard value, with internal precisions of 0.9% and 0.6% for Pu and U, respectively.

Table VI. Results of Synthetic Spent Fuel Dissolver Solution

Element	Std. Value mg/g	Measured mg/g	Percent Bias
Pu	2.356	2.361 ± 0.021	+0.21
U	231.5	232.5 ± 1.4	+0.43

N = 12 analyses for each element.

Further work is currently underway or planned which will hopefully reduce the imprecision by using ^{236}U as the spike for U and ^{240}Pu for Pu. Much of the fractionation effects from small samples using the sequential analysis procedure may be eliminated using these

isotopes, which are nearer in mass to the major isotope in the sample. Preliminary measurements for U concentration have been carried out, and results look very encouraging. Also, an isotopic equilibration test for Pu is underway in which reduced ^{239}Pu and oxidized ^{242}Pu have been mixed and valence adjustment made using $KMnO_4$ for oxidation. This is being compared with the $HClO_4 \cdot HF$ method that we are currently using.

SUMMARY

The principal advantages over conventional techniques offered by the resin bead method are the simplicity and ease of chemical separation and the reduction in the amount of sample required for shipment. Secondary benefits include more efficient ion collection and cleaner spectra. Disadvantages include the necessity of learning new technology (resin bead handling is much easier under a microscope) and the need to have mass spectrometers equipped with pulse-counting detection systems. However, manipulating the beads is much less formidable than it appears, and the techniques and equipment needed for ion counting are well known. By following the procedure outlined, no sacrifice in quality of results in comparison to those obtained by conventional techniques is observed. We thus feel that the resin bead technique can make useful contributions to both domestic and international safeguards programs in areas that are otherwise difficult to attack. In addition, it is a very useful technique for isotopic and concentration measurements in radioactive samples used in process control and development.

Discussion:

Casabona (Teledyne Isotopes):
You make reference to the resin-bead pressure burst. Do I interpret that as being a complete volatilization of the resin off the filament in the ion source?

Walker (ORNL):
Yes.

Casabona:
Do you have any residual organics or hydrocarbons in the spectrum?

Walker:
We do up until 1200 degrees, but sometimes that is confusing because we also get hydrocarbons in the thermal instrument even if you don't load organics. So, I don't necessarily attribute that to the resin bead itself. We have organic residuals that are present in all analysis, whether it is by resin-bead loading or not.

Casabona:
Do you have any feel for what the chemical composition of both the uranium and plutonium are during ionization?

Walker:
We only see metal line-emission. I would assume it goes through a carbide reductive step, with the carbon deposited from the resin-bead onto the filament, and then you carbonized the filament. It goes from an oxide to a carbide, I believe.

DEMONSTRATION OF TOTALLY SAMPLED WAVELENGTH DISPERSIVE XRF FOR USE IN THE ASSAY OF THE SNM CONTENT OF DISSOLVER SOLUTIONS

C. R. Hudgens and B. D. Craft
Mound Facility, Miamisburg, Ohio*

ABSTRACT

X-Ray fluorescence analysis of simulated SNM in solution was demonstrated, using totally sampled, continuously recirculated solutions, some of which contained slurried analyt and dense matrix. The total sampling system contributed no identifiable variation to the data, and the slurried matter, at particle sizes of 20 micrometers or less, contributed no systematic error. Continuous recirculation also removes photolytically produced gas, and maintains homogeneity of the solution or slurry.

KEYWORDS: X-Ray fluorescence analysis, total sampling, solution analysis, slurry analysis, SNM assay, dissolver solution.

INTRODUCTION

At the Williamsburg meeting we discussed the feasibility of the assay of SNM in dissolver solution.[1] The assay problem was shown to be two problems: 1) the analytical method, and 2) the sampling method: the best of analytical methods will give poor results if the sampling is poor.

We also discussed the results of a theoretical study of design parameters and expected performance of an on-line advanced wavelength dispersive XRF system for analysis of dissolver solutions. The precision of data from an XRF system, independent of sampling, was shown to depend on constancy of excitation, the proper matching of x-ray optical components, and stability and precision of the x-ray optical components, including thermal effects.

Some sampling factors deleterious to precision were identified: concentration inhomogeneity of solutions, suspended particulate material, suspended gas bubbles, and density variations from transient thermal effects.

"Total sampling" was proposed as a method of realizing the ultimate sample by using an entire batch of solution as sample. Total sampling includes, as inseparable parts of the concept, the use of an internal standard, and continuous recirculation of the sample through the sample cell and a holding tank. The use of an internal standard yields an assay of the batch with no need for volume and density measurements, or the taking of aliquots and transfer of samples. Continuous recirculation, besides effectively sampling the entire batch, is beneficial because it promotes, and allows monitoring of, the homogeneity of the sample; maintains homogeneity of slurried material; removes photolytically produced gas; and smooths thermal variations.

*Operated by Monsanto Research Corporation for the U.S. Department of Energy under Contract No. DE-AC04-76-DP00053

Total sampling is not limited to XRF; Mathews et al (Bombay) have used the tactic of adding standard to an entire batch of solution for assay of SNM in an accountability tank at a reprocessing plant by mass spectrographic analysis.[2] Total sampling for XRF analysis fits, however, naturally into an automated, on-line analytical system, which automatically includes all of the above enumerated advantages.

OBJECTIVE OF THIS WORK

The objective of the current work is the experimental verification of the validity of the total sampling concept, with demonstration of the advantages of using continuously recirculated samples.

EXPERIMENTAL METHOD

The sampling cell is a stainless steel block into which is machined a 4 mm deep cavity, with the other dimensions (6 x 25 mm) matching the angular aperture of the analyzing crystal. The cavity was covered with a composite window of 0.001" muscovite mica, for acid protection, backed by a 0.010" beryllium plate for mechanical strength. Supply and exhaust tubing of 1/16" i.d. connected the cell into a loop with a pump and a holding tank. During analysis the solution was continuously recirculated through this sampling loop.

The holding tank was of stainless steel, 1" i.d., and of about 175 cc capacity. An o-ring-sealed cover suppressed drift in count rate caused by evaporation. It was soon found that thermal expansion, caused by heat from the pump and Joule heating, caused drift in the counting rate. Water cooled coils wrapped around the tank effectively removed this source of error.

For large tanks, stream-splitting schemes would be used (Fig. 1), for practicality. Careful design and thorough stirring would preserve total sampling.

The x-ray spectrometer was an ARL "XSQ", a Johannsen type (Fig. 2), equipped with an LiF(200) analyzing crystal. Excitation was provided by a Machlett OEG-50 Mo target tube powered by a GE XRD-5 power supply. An NaI(Tl) scintillation detector, with conventional counting electronics, comprised the detector system.

Thorium and uranium were used as both analyts and matrixes, with strontium as internal standard. Each standard solution set was prepared by making successive additions of weighed analyt (Th or U as nitrates) to 3N HNO_3 in which was dissolved accurately weighed $Sr(NO_3)_2$ internal standard. Data was accumulated by alternately counting Th or U L-alpha and Sr K-alpha x-ray emissions. Backgrounds were measured by moving off-peak. After measuring a data point, the next addition of weighed analyt was made. As mixing of the solution proceeded, homogeneity of the solution was verified by monitoring the analyt count rate, after which the analytical data was again taken.

FIGURE 1
LARGE TANK SAMPLING

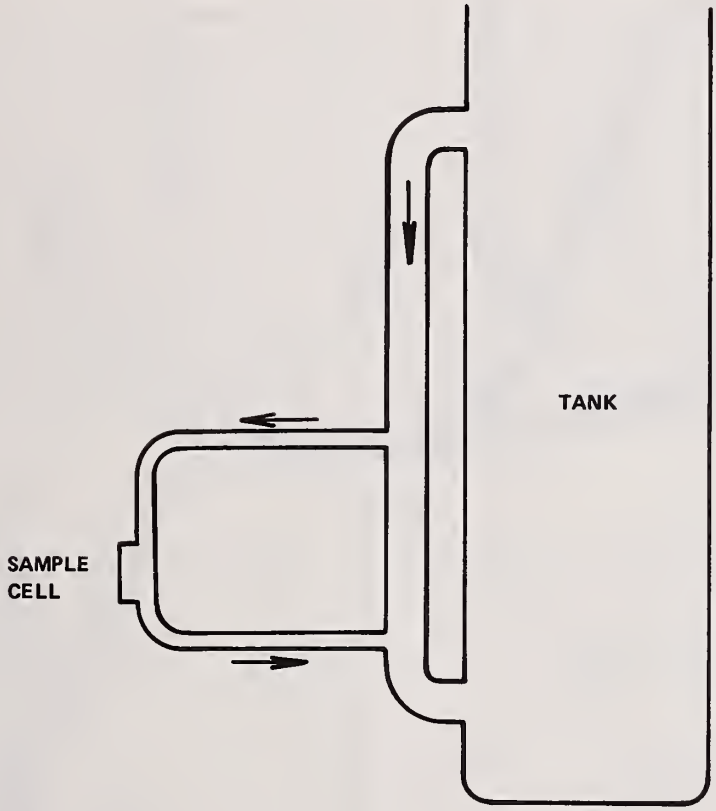

FIGURE 2
SCHEMATIC OF XRF SPECTROMETER WITH SAMPLING SYSTEM

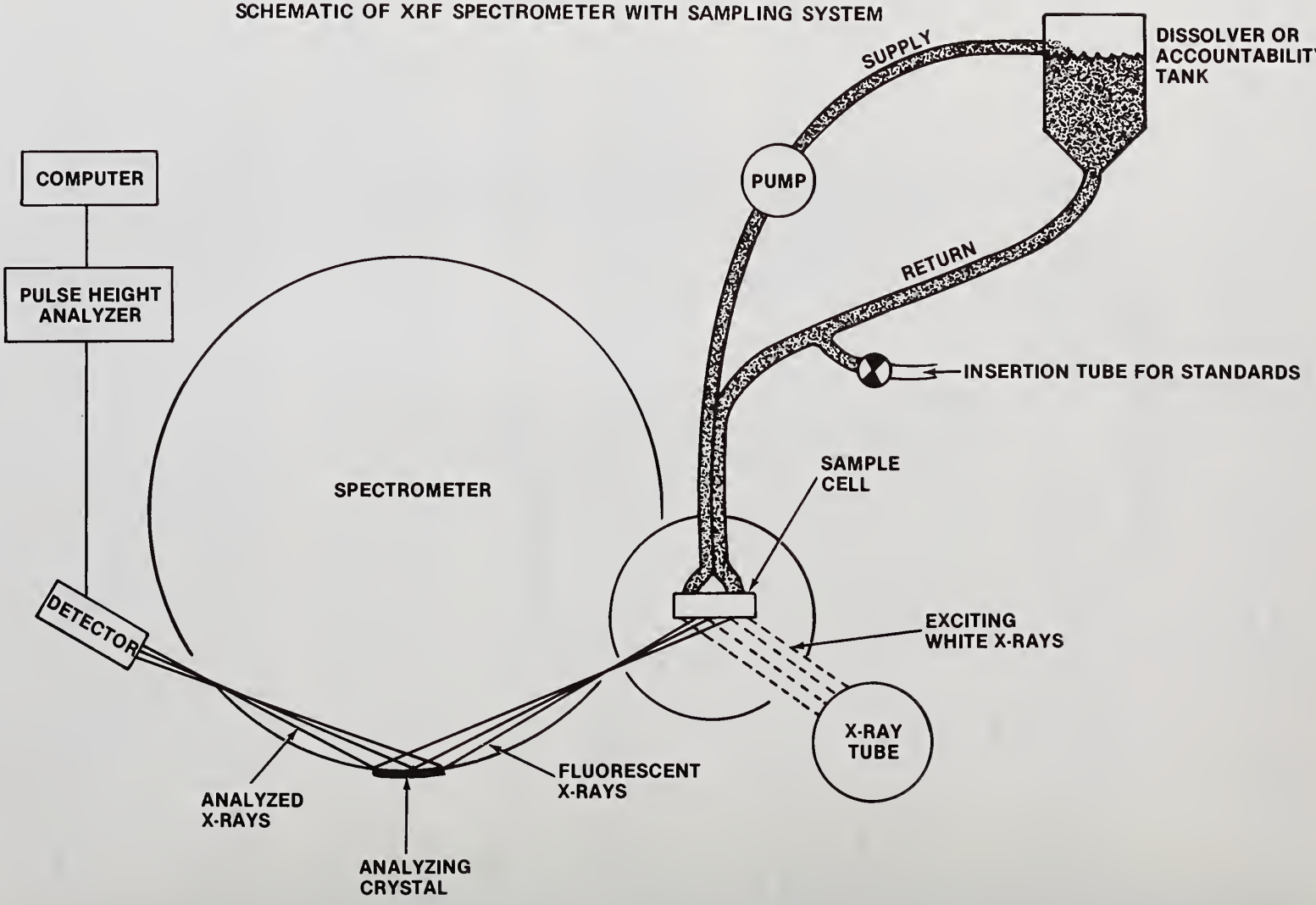

The ratios of intensities of analyt and standard were plotted vs. the concentration of analyt. Solutions were prepared to cover both low and high ranges, with and without a highly absorbing matrix, and with and without slurried analyt as a solid phase. ThO_2, used as slurried analyt, was prepared by sieving fired oxalate to produce powder with particle sizes less than 20 micrometer. This was the maximum size that could be suspended homogeneously by our sampling system.

DISCUSSION OF RESULTS

Individual plots of intensity ratios vs. weight ratios are illustrated in Fig. 3, and are summarized in Table I. The data sets fit straight lines within their precision, which range from 0.5 to 1% (1-sigma). This 1-sigma variation was determined to be the best obtainable with the spectrometer and x-ray generator used. The linear correlation coefficients indicate probabilities all less than 1/1000 that the data sets are uncorrelated with straight line fits. These correlation coefficients include data due to solid analyt (ThO_2) as well as solution. The set whose correlation coefficient has the largest deviation from unity also has the largest number of points due to solid additions. This is probably not coincidental; the liquid, on entering the sample cell, undergoes decrease in velocity, which could allow some settling to develop in the slurry. Reducing the cell volume, increasing the feed line cross-section, or addition of an internal mechanical stirrer should reduce or eliminate this problem.

TABLE I

ANALYTICAL SUMMARY OF X-RAY INTENSITY - MASS RATIO RELATIONSHIPS

Analyt	Weight Range 0 - g/L	Matrix g/L	Internal Std. Wt. g/L	Slope	Correlation Coefficient	Remarks
Th	10	--	1.0	0.2837	0.9999	1 oxide add'n
Th	250	U 400	5.0	0.0755	0.9965	
Th	20	U 300	1.0	0.0436	0.9989	
Th	10	--	1.0	0.2131	0.9956	3 oxide add'ns
U	200	--	5.0	0.0582	0.9993	
U	6	Zr 82	0.25	1.414	0.9998	
		Sn 1.25				

Non-analyt-containing solid should affect an assay negligibly as long as homogeneity is maintained, and this tolerance should extend to larger particle sizes than with analyt-containing solids.

FIGURE 3 X-RAY INTENSITY AND MASS-RATIO RELATIONSHIPS: Th AND U ANALYTS, Sr INTERNAL STANDARDS

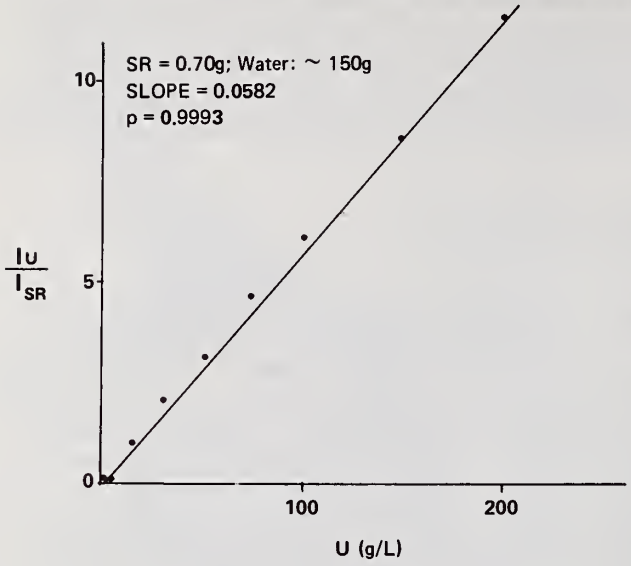

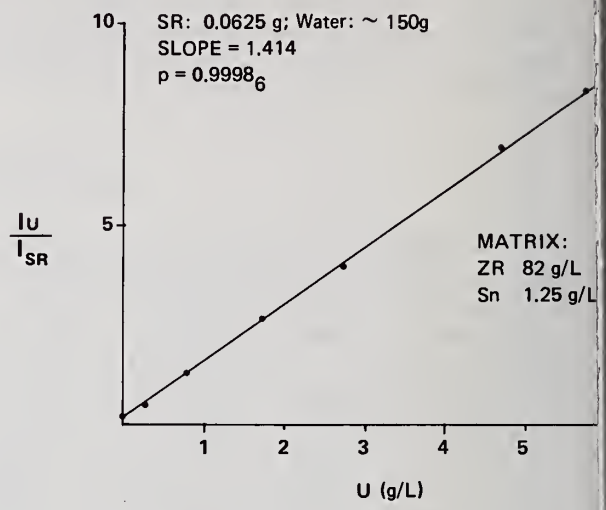

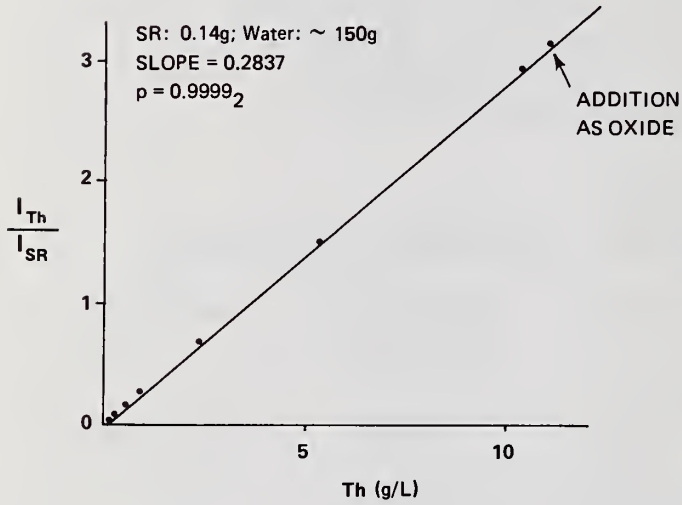

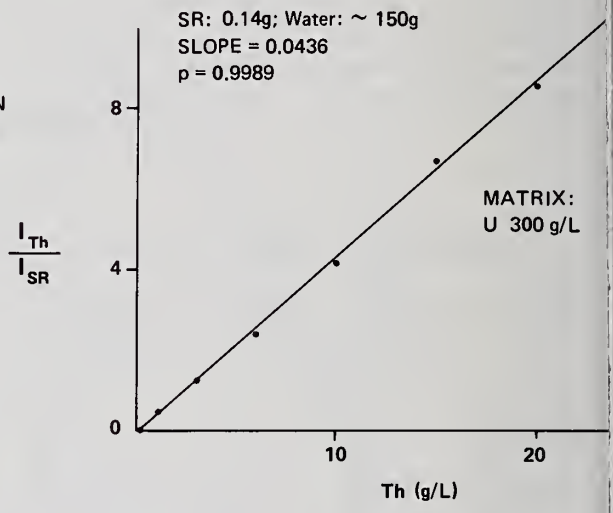

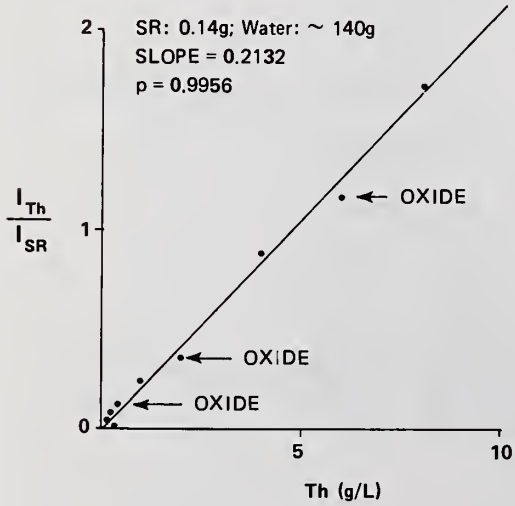

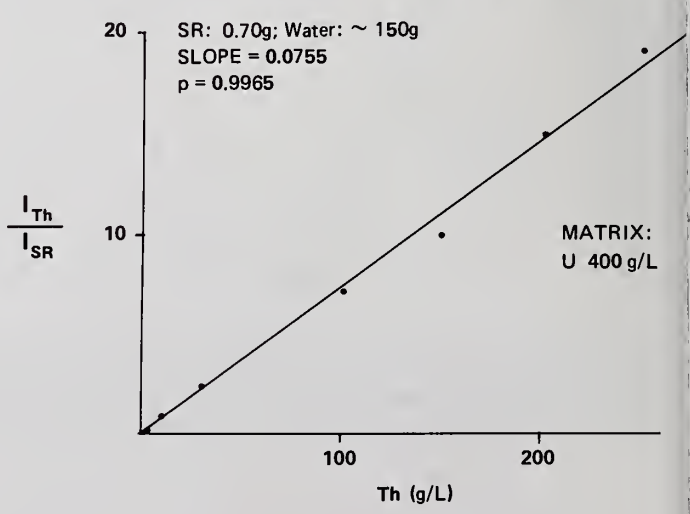

The continuous high speed recirculation of the solution through the sample loop serves to mix and homogenize the solution, to sample the entire batch, and is also completely effective in preventing the agglutination of microbubbles of photolytically produced gas into larger bubbles which could become an analytical interference. The production of these bubbles is rapid under the approximately 20,000 r/sq.cm/min bombardment of the exciting x-ray beam. Within three minutes of the start of irradiation, the solution becomes turbid from the suspended bubbles. In early experiments, using static solutions, bubbles of 1 mm^3, an interfering size, and larger had been observed adhering to the sample cell window.

The U-Th-Sr combination is particularly well behaved in XRF because of a fortuitous interplay of absorption and enhancement factors. Since the spectral relationships which would exist on adding Pu to the Th-U-Sr set or replacing U or Th by Pu would be little changed, the assay of Pu by XRF would be qualitatively the same, and quantitatively little different, than the assay of Th and U.

CONCLUSIONS

1) The total sampling system contributed no identifiable variation to the data, which fell into the 0.5 to 1% range expected of the XRF equipment used in this study.

2) The slurried particulate matter, at particle sizes of 20 micrometers or less, also contributed no systematic error.

3) Removal of photolytic gas by continuous recirculation is effective.

4) Homogeneity is established by continuous circulation, and its condition observable by XRF monitoring.

The analysis of SNM in dissolver solutions should be expected, therefore, to present no unusual problems to either the XRF method or the total sampling method.

BIBLIOGRAPHY

1) C. R. Hudgens and B. D. Craft, "Feasibility Study of a High-Precision XRF System for Analysis of Solutions and Slurries"; ANS Topical Meeting: Analytical Methods for Safeguards and Accountability Measurement of Special Nuclear Materials; Williamsburg, Virginia, May 15-17, 1978.

2) C. K. Mathews, H. C. Jain, V. D. Kavimandan, and S. K. Aggarwal, "Tracer Techniques for the Input Accountability of Plutonium in Reprocessing Plants: Magtrap and Leadtrap"; Nuclear Technology, Vol. 42, 297-303, 1979.

Discussion:

Brodda (NRC-Juelich):
How do you control the influence of direct gamma-ray impact, from fission products, onto the detector? Do you correct for the additional background induced by this effect?

Hudgens (Monsanto-Mound):
This question was not addressed in this paper; an overview can be found in the first reference.

Brodda:
What accuracy and precision do you achieve for uranium and thorium determination in dissolver solutions?

Hudgens:
Precision in the experiments for this paper was about 0.5% (one sigma), and was limited by the equipment. This problem was also addressed in the first paper, and the Mound Laboratory report, MLM-2533.

Brodda:
What is the expected lifetime of the window material? Did you observe any memory effects?

Hudgens:
For the materials used in this paper, lifetimes of the window would be very long. No memory effects were observed. For dissolver solutions, exprimentation will be necessary to resolve this question.

Study of a Two-Detector Method for Measuring Plutonium Isotopics

by

John G. Fleissner, John F. Lemming and Jack Y. Jarvis
Monsanto Research Corporation, Mound Facility, Miamisburg, Ohio

ABSTRACT

A technique to improve the timeliness and accuracy of Pu isotopic measurements for bulk samples has been studied. The technique utilizes two Ge detectors to simultaneously assay different energy regions of the Pu gamma-ray spectrum. Isotopic ratios are determined from the areas of close lying peak pairs. Factors determining the choice of these peak pairs for the total isotopic measurement are discussed. The technique has been tested on samples of varying mass, burnup, isotopic content, age, and chemical composition.

KEYWORDS: Plutonium safeguards, gamma-ray spectrometry, nondestructive isotopic analysis

INTRODUCTION

When nondestructive assay is used for the accountability and safeguarding of plutonium, it is often necessary to determine the amounts of the individual plutonium isotopes from 238 to 242 which are present. For calorimetric assay, the concentration of ^{241}Am is also important. All of these isotopes with the exception of ^{242}Pu can be determined by gamma-ray spectroscopy.

Traditionally, the gamma-ray techniques employed for bulk sample assay use either a small volume, high resolution Ge detector to measure the low energy spectral region (~120-208 keV) or a large-volume Ge detector to obtain spectra from 120 to 400 keV or higher[1-5]. With both of these approaches the isotopics for ^{238}Pu, ^{239}Pu and the ^{241}Pu can be obtained easily. However, the measurements for ^{240}Pu and ^{241}Am are more difficult due to the spectral complexity.

Both the low energy region and high energy region (~300-700 keV) contain peaks which can be used for the analysis of ^{240}Pu and ^{241}Am. In general, the analysis of the high energy region is less complex because the peaks are more widely separated in energy. When a single detector is used for total isotopic measurements, the low branching intensities of the higher energy gamma-rays require longer counting times to obtain counting statistics comparable to those obtained in the lower energy region.

This study describes a technique to improve the timeliness and accuracy of isotopic measurements without loss in precision. The technique employs two detectors to simultaneously assay different energy regions of the Pu gamma-ray spectrum. Isotopic ratios are determined from the areas of close lying peak pairs. Those ratios yielding the best precision, or ease of analysis with no loss in precision, are used to obtain the total isotopic measurement.

PROCEDURE

The two-detector spectrometer system employs high resolution germanium detectors. The type of detector chosen for each energy region is dependent upon the spectroscopic needs of that particular energy region. For the low energy region (120-300 keV), where high resolution is important, a small intrinsic germanium detector (LEPS) was used (resolution = 520 ev at 122 keV). A 70 cc Ge(Li) detector having an efficiency of 14% and a resolution

of 1.78 keV at 1330 keV was used to obtain the high energy spectra (300-700 keV). Identical pulse shaping and amplification modules were used for each detector.

Absorbers were chosen to tailor the spectrum shape such that the count rate in the energy region of interest was enhanced. For the low energy detector it was necessary to use 1 mm of cadmium and 0.25 mm of lead to reduce the count rate contributions from the 59.5 keV transition of ^{241}Am and the x-rays. Without the proper absorbers sum peaks can occur in the 160 keV region which interfere with the ^{240}Pu measurement. The low energy detector absorber selection and its effects on the ^{240}Pu and ^{241}Am measurements will be discussed below.

For the large volume detector 3 mm of lead and 0.5 mm of cadmium were used. These absorbers reduced the count rate at 200 keV by two orders of magnitude while the count rate at 600 keV was reduced only 30%. With the absorbers in place, collimators and source-to-detector distances were varied to achieve identical counting rates for each detector. The maximum count rate was limited to 10 khz so that no degradation in resolution occurred.

Spectra from both detectors were obtained simultaneously using two 4k channel ADC's and a 14k channel MCA. The spectra were stored on disk and analyzed using an automated version of the peak fitting program GRPNL2 of R. Gunnink (LLL). The spectral parameters (e.g., peak energy, background channels, etc.) and nuclear data are stored on disk files such that only the spectral file name is required from the operator for the data analysis. The half-lives used are those recommended in ANSI N15.22[6]. The branching intensities are those of Gunnink, et al[7]. The program occupies less than 25k words of storage on a PDP 11/34 minicomputer.

An intrinsic self-calibration technique is used to obtain the relative efficiency corrections due to the detector response, the absorbers used (including the containment package), and the self-absorption of the sample. A relative efficiency curve is generated from each spectrum measured. Areas for ^{239}Pu, ^{241}Pu, and ^{241}Am peaks are corrected for the gamma-ray branching intensities and are fit using a weighted least-squares technique to the functional form:

$$\ln\varepsilon_i = a_0 + \sum_{j=1}^{2} (a_j E_i^{-j}) + \sum_{j=1}^{3} (a_{j+2} (\ln E_i)^j) + a_6\delta_6 + a_7\delta_7$$

The coefficients a_6 and a_7 are used to normalize the ^{241}Pu and the ^{241}Am data points to the ^{239}Pu data points. These normalization coefficients can be used to obtain the isotopic concentrations for ^{241}Pu and ^{241}Am. Figure 1 shows a relative efficiency curve obtained from the LEPS detector data for a 910 g mixed oxide powder sample. This curve is typical of those observed for all samples.

Twelve samples with differing isotopic concentrations and chemical compositions were measured including the National Bureau of Standards (NBS) SRM-946, SRM-947, and SRM-948. Isotopic abundances of ^{239}Pu ranged from 70% to 94% and sample weights from 0.25 g to 1000 g. Table I lists the sample weights, ^{239}Pu isotopic abundances and chemical compositions for the sample set. Ingrowth of americium in these samples varied from slightly less than 2 years to greater than 16 years. The isotopic composition of the samples as determined by destructive analysis is listed in Table II. All samples were counted for 50k seconds. Those samples with masses greater than 20 g were also counted again at a higher count rate for 2k seconds in order to measure the accuracy obtainable in a shorter counting time. In all, 54 spectra were obtained and analyzed.

RESULTS AND DISCUSSION

^{240}Pu Measurements

The ^{240}Pu concentration from the low energy spectrum was obtained by analyzing the multiplet at 160 keV. This multiplet consists of a peak at 159.96 keV from ^{241}Pu, a peak at 160.19 keV from ^{239}Pu (usually a minor component) and the ^{240}Pu peak at 160.28 keV. The components are shown in Figure 2. The ^{240}Pu contribution to the 160 keV multiplet ranged from 36% to 76% of the multiplet for the samples studied. The energy separation between the ^{241}Pu and ^{240}Pu peaks is 0.32 keV while the energy resolution of the detector at this

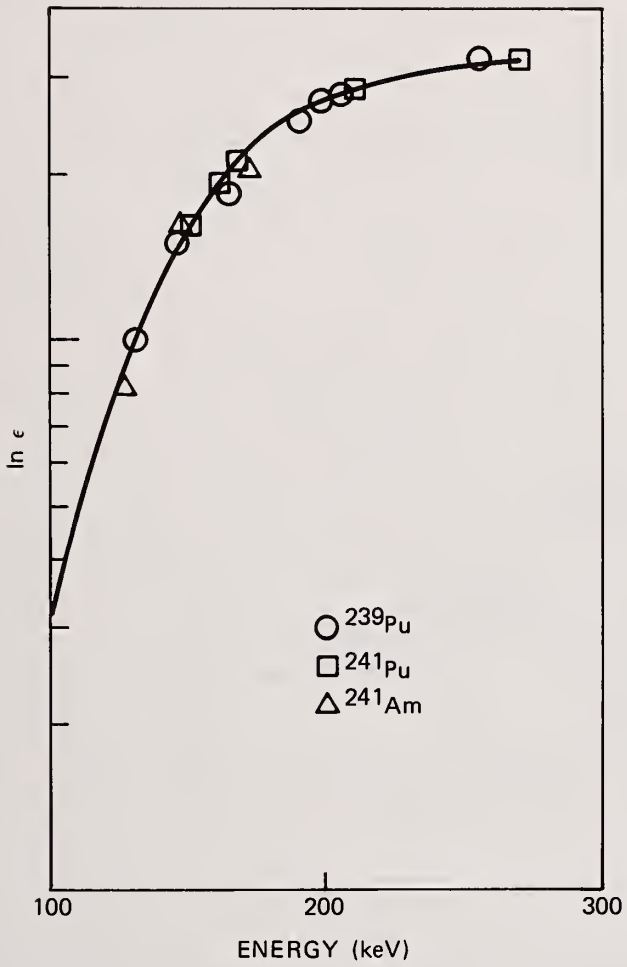

FIGURE 1 Relative efficiency curve obtained from LEPS detector data using 910 g sample (CAN 4). Data points for ^{239}Pu are shown as circles. ^{241}Pu as squares and ^{241}Am as triangles. Curve is typical of those obtained from low energy region using LEPS detector.

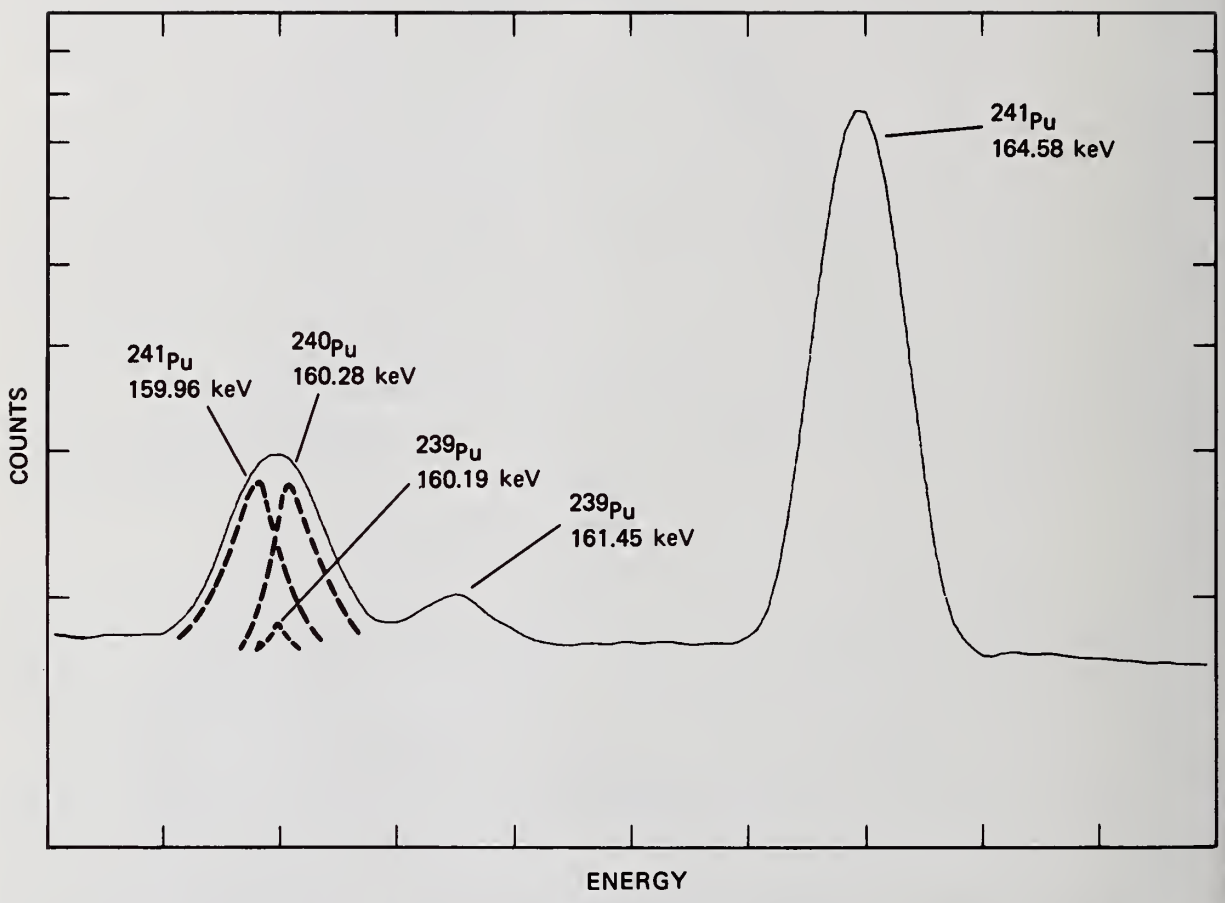

FIGURE 2 Gamma-ray spectrum of 160 keV region obtained with LEPS detector. Spectral components of 160 keV multiplet are shown as dashed lines.

energy is 0.62 keV. In order to unfold such a complex multiplet the option of ratioing the energies and peak heights (areas) in GRPNL2 is used. The spectral peaks from 159.96 keV to 164.58 keV are fit as a five component peak grouping. In the fitting process the FWHM, the height (area), and the centroid of each peak can be varied giving eleven free parameters for the grouping. However, by fixing the energy separations of the multiplet components to the 164.58 keV peak and the height ratios for the two ^{239}Pu peaks, the original eleven free parameters were reduced to six.

The ^{240}Pu concentration is obtained from the high energy region by analyzing the multiplet at 640 keV. For unirradiated samples peaks due to ^{239}Pu at 637.84 and 640.08 are the main contaminants; the Am peak at 641.42 keV is usually a minor constituent. The ^{240}Pu gamma ray energy is 642.48 keV. When the samples have been irradiated, this region may become unsuitable for Pu isotopic analyses due to gamma-ray interferences from fission products.

A reliable background for the 640 keV multiplet could be obtained only by fitting the spectral peaks in the energy range from 633.15 to 664.59 keV due to the energy spacing of the peaks in this region. This peak grouping, shown in Figure 3, contains fourteen gamma-ray components. Again the GRPNL2 option to ratio peak heights and energies was used to reduce the original 29 free parameters to 9.

The use of the 160 keV region presents several spectroscopic problems not encountered in the 600 keV region. First, absorbers for the low energy region detector must be carefully chosen to eliminate count-rate sum peaks. Summing of the 59.5 keV transition and the Np $K\alpha_1$ x-ray occurs at 160.60 keV while the ^{240}Pu peak is at 160.28 keV. This sum peak will produce a bias in the ^{240}Pu concentration measurement. Sum peaks that fall just below the 160 keV triplet in energy also affect the background determination in this region. The use of absorbers to reduce sum peak contributions to the 160 keV region is shown in Figure 4. The amounts of absorbers necessary to eliminate the sum peaks depend on the ^{241}Am concentration in the sample. For the samples measured in this study it was necessary to use a 1 mm cadmium absorber and a 1/4 mm lead absorber. Second, backscatter peaks from the relatively intense 300-400 keV region complicate the 160 keV region. Finally, the relative efficiency corrections are smaller for the 600 keV region. The efficiency correction for the 160.28-164.45 keV peak pair averaged about 5% while the correction for the 642.48-645.97 keV peak pair was always less than 0.5%.

Table III presents a comparison of the gamma-ray isotopic measurements to destructive isotopic measurements for ^{240}Pu. The results from the low energy region are obtained from the 160.28-164.45 keV and the 160.28-148.57 keV peak pairs. For the high energy region the 642.48-645.97 keV peak pair results are given. Small biases exist between the gamma-ray results and destructive analysis for the 160.28-164.45 keV peak pair and the 642.48-645.97 keV peak pair . These biases in part may be due to the branching ratios used to convert the areas to isotopic concentrations. The 160.28-148.57 keV peak pair measurements are not biased. The observation of biases in the 160 keV region is supported by the results of an interlaboratory comparison study organized by ESARDA[8,9].

From the table it can be seen that no loss in accuracy or precision results from using the 600 keV region. It should be noted that the reported accuracy and precision from the 160 keV region can only be obtained when care is exercised to eliminate biases due to count-rate sum peaks.

^{241}Am Measurements

The ^{241}Am isotopic concentration is derived from the low energy spectrum using the 125.29-129.29 keV peak pair. The 125.29 keV peak is a member of a triplet whose contaminants are the ^{239}Pu peaks at 124.51 and 125.21 keV (see Figure 5). Am concentration measurements are obtained from the high energy spectrum by using the 662.42-645.97 keV peak pair. Table IV presents the results of the ^{241}Am isotopic measurements for these peak pairs. For Am concentrations of 4000 ppm or less, the precision of the Am measurement using the 600 keV region is a factor of 2-4 times better than that derived from the 125 keV region. In addition, biases as large as 24% are observed when using the 125.29-129.29 keV peak pair. These biases are apparent at concentration levels of less than 4000 ppm where

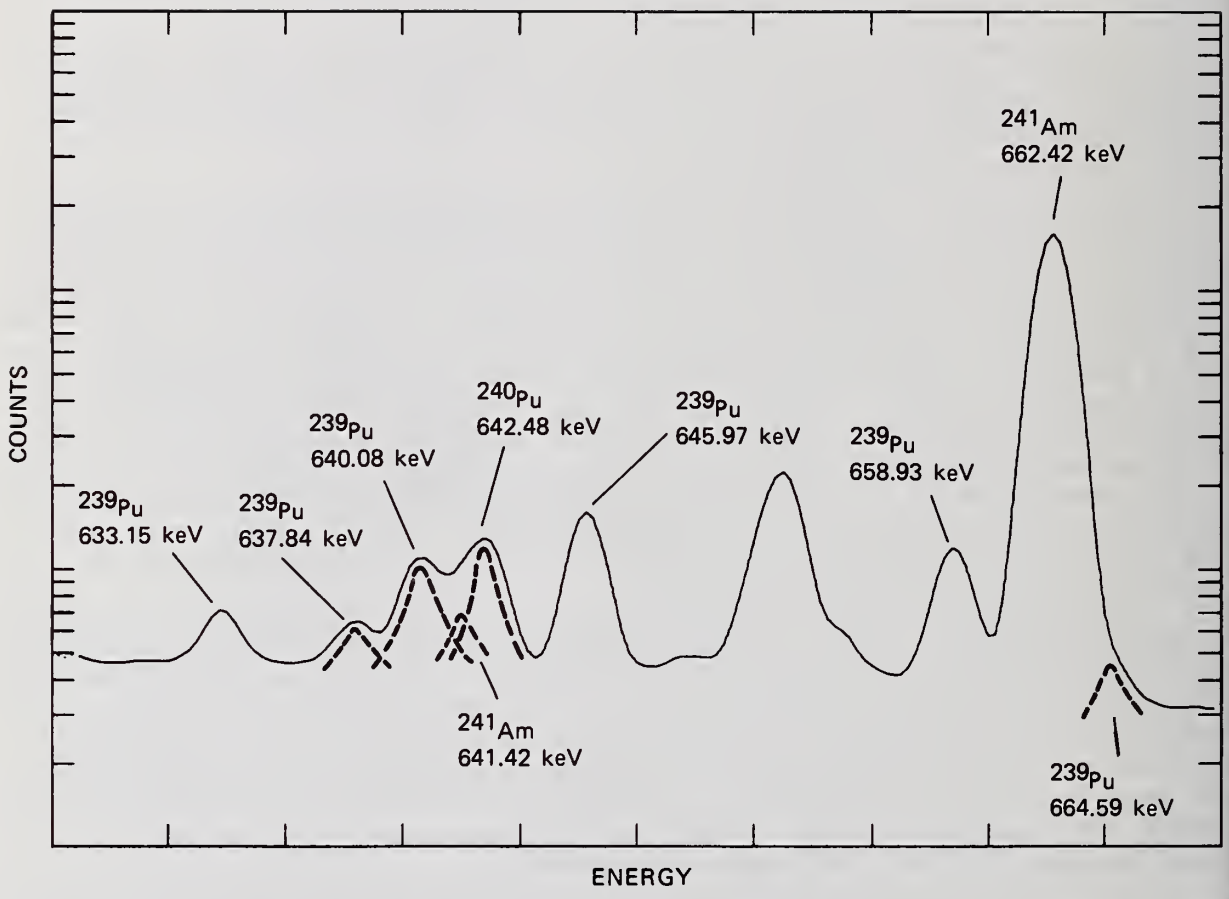

FIGURE 3 Gamma-ray spectrum of 630-670 keV region obtained with 70 cc Ge(Li) detector. Selected spectral components are shown as dashed lines.

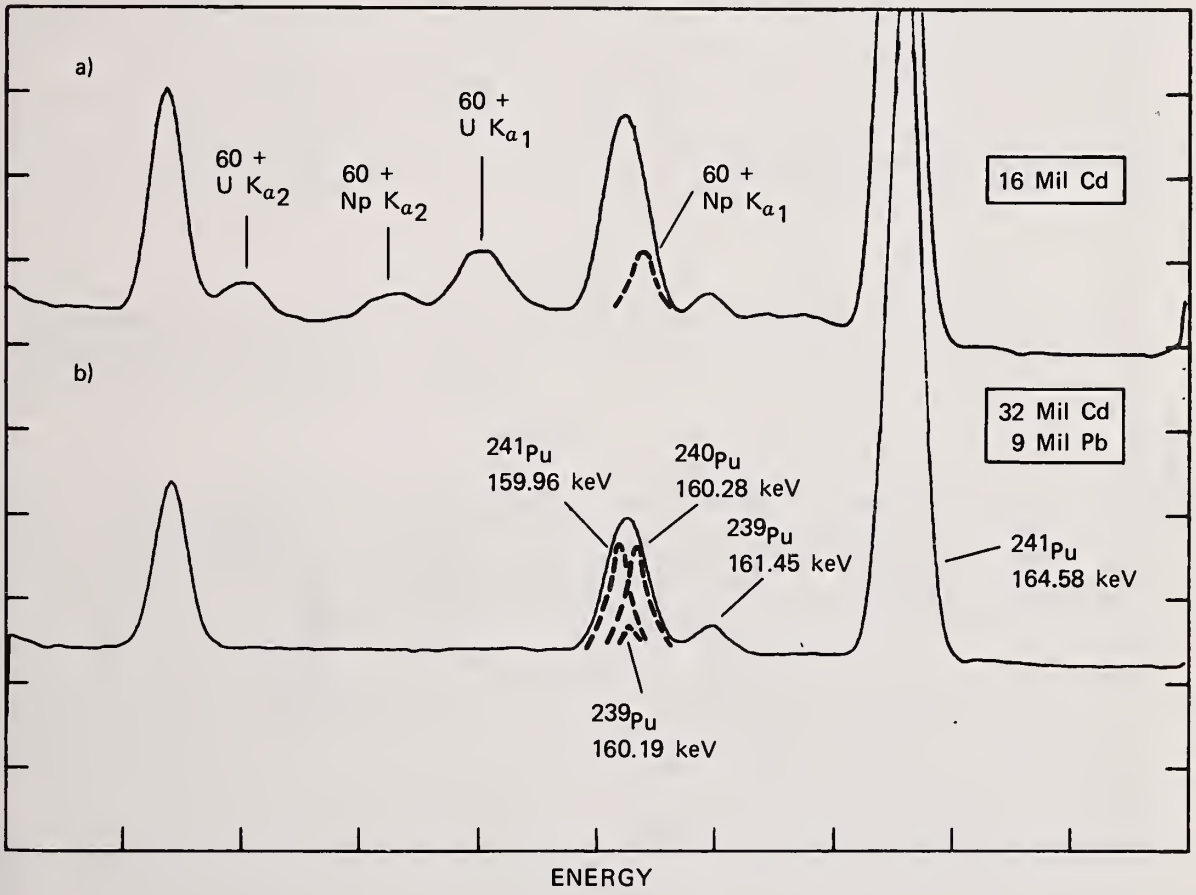

FIGURE 4 LEPS detector spectra of 160 keV region. Upper spectrum (a) obtained using a 16 mil cadmium absorber, shows presence of summing peaks (59.5 keV + x-rays). Lower spectrum (b) shows same sample but with use of 32 mil cadmium and 9 mil lead absorbers.

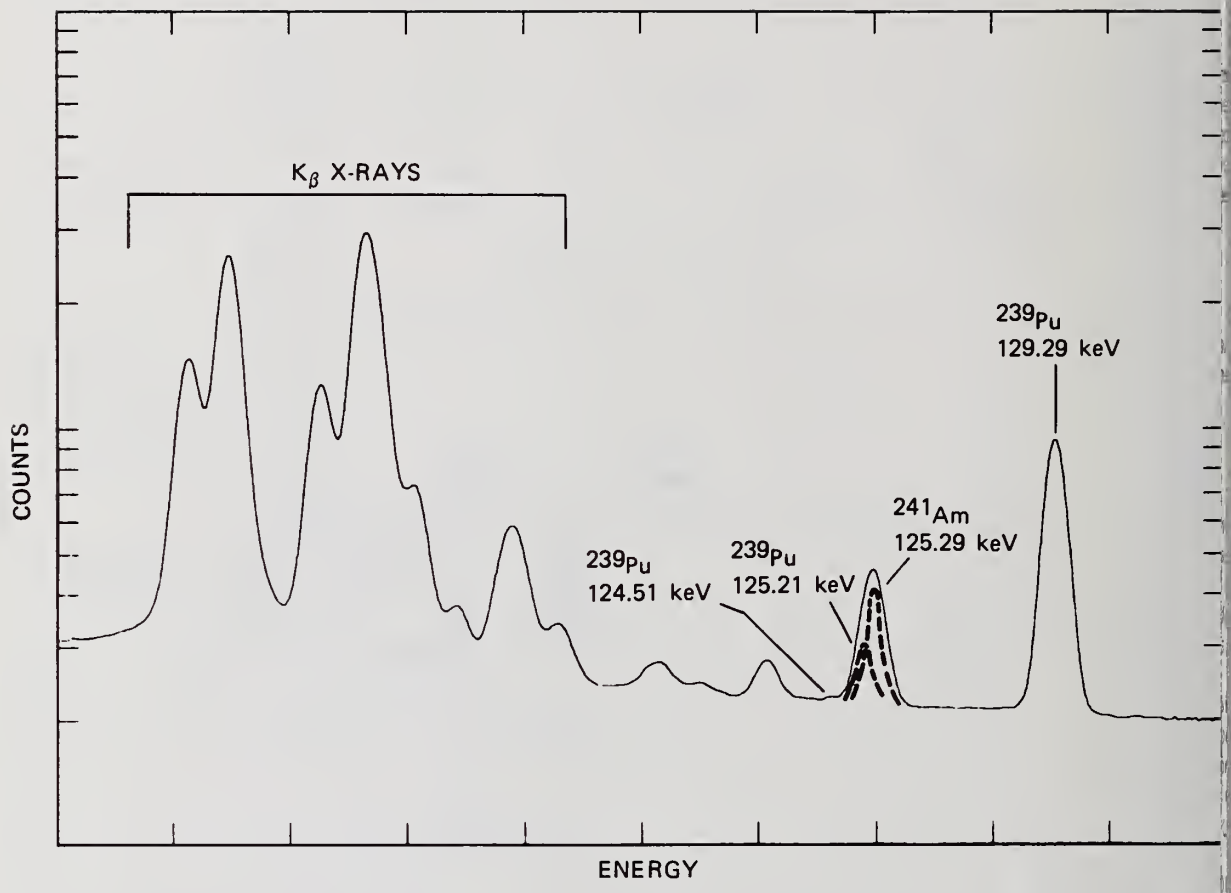

FIGURE 5 LEPS detector spectrum of 125 keV region showing proximity of K β x-rays to 125 keV multiplet. Spectral components of 125 keV multiplet are shown as dashed lines.

the contaminant peaks in the 125 keV multiplet are comparable in intensity to the Am component. These biases may be due to errors in the gamma-ray branching intensities for the 124.51 and 125.21 keV transitions of ^{239}Pu and/or difficulties in background determination for the multiplet due to the presence of K x-ray tails. The precision of the Am measurement in the 125 keV region is affected both by the loss in intensity due to the absorbers needed to eliminate the sum peaks in the 160 keV region and the large Compton background from higher energy gamma-rays.

^{238}Pu Measurements

The ^{238}Pu concentration is obtained from the low energy region using the 152.68 keV gamma-ray. Table V presents the results for the 152.68-144.21 keV and the 152.68-148.57 keV peak pairs. Both peak pairs show a bias of approximately 2.5%. This bias is also observed in the ESARDA study[8,9]. If it is assumed that the recommended half-lives for the relevant Pu isotopes are correct then the branching ratio for the 152.68 keV gamma-ray needs to be reduced by 2.5%.

^{241}Pu Measurements

Concentration measurements for the ^{241}Pu are obtained from the 208.00-203.54 keV and the 148.57-144.21 keV peak pairs. The results are shown in Table VI and excellent agreement with destructive analysis is obtained.

SUMMARY

This study indicates that improved isotopic measurements are obtained using two detectors to simultaneously assay different energy regions of the Pu gamma-ray spectrum. The peak pairs found to yield the best overall isotopic measurements are listed in Table VII. In the cases where a bias was observed with respect to destructive analysis, the results in Table VII have been corrected for the bias. The results of this study suggest that these biases may be due to errors in the gamma-ray branching intensities.

The use of two detectors requires no sacrifice of energy resolution or counting efficiency for a particular energy region. The method is "timely" since the samples are counted by both detectors at the same time. Concentration measurements for ^{238}Pu, ^{239}Pu, and ^{241}Pu are easily obtained from the low energy (120-208 keV) region using a small volume, high resolution intrinsic Ge detector. The ^{240}Pu and ^{241}Am measurements, however, may be interfered with by sample dependent spectroscopic problems. Isotopic measurements of ^{240}Pu and ^{241}Am can be more easily obtained using a large volume Ge detector from the 600 keV region. The precision and accuracy obtained for these isotopes is equal to or better than that obtained from the low energy region.

REFERENCES

1. J. E. Fager, F. P. Brauer, "Rapid Nondestructive Plutonium Isotopic Analysis," in Analytical Methods for Safeguards and Accountability Measurements of Special Nuclear Materials, NBS 528, November 1978.
2. T. D. Reilly, D. D'Adarno, I. Nessler, M. Cuypers, "The Gamma-ray Spectrometric Determination of Plutonium Isotopic Composition," presented at International Symposium on Nuclear Materials Safeguards, Vienna, October 1978, IAEA-SM-231/121.
3. H. Eberle, P. Matussek, H. Ottmar, I. Michel-Piper, M. R. Iyer, P. P. Chakraborty, "Nondestructive Elemental and Isotopic Assay of Plutonium and Uranium in Nuclear Materials," presented at International Symposium on Nuclear Materials Safeguards, Vienna, October 1978, IAEA-SM-231/12.
4. T. N. Dragnev, B. P. Damjanov, "Methods for Precise Absolute Gamma Spectrometric Measurements of U and Pu Isotopic Ratios," presented at International Symposium on Nuclear Materials Safeguards, Vienna, October 1978, IAEA-SM-231/130.

5. T. N. Dragnev, "Intrinsic Self-Calibration of Nondestructive Gamma Spectrometric Measurements Determination of U, Pu, and ^{241}Am Isotopic Ratios," J. Radioanal. Chem. 36 (1977).
6. "Calibration Techniques for the Calorimetric Assay of Plutonium Bearing Solids," ANSI N15.22-1975.
7. R. Gunnink, J. E. Evans, A. L. Prindle, "A Reevaluation of the Gamma-Ray Energies and Absolute Branching Intensities of ^{237}U, ^{238}, ^{239}, ^{240}, ^{241}Pu, and ^{241}Am," UCRL-52139 (1976).
8. H. Ottmar, H. Eberle, "Determination of Plutonium Isotopic Composition by Gamma Spectrometry: Results From Interlaboratory Comparison Measurements Organized by ESARDA," 1st Annual ESARDA Symposium on Safeguards and Nuclear Materials Management, ESARDA 10, April 1979.
9. H. Ottmar, "Results From An Interlaboratory Exercise on the Determination of Plutonium Isotopic Composition by Gamma Spectrometry," INMM Vol. VIII, July 1979.

ACKNOWLEDGEMENT

This work was supported by the Department of Energy under Contract No. DE-AC04-76DP00053.

TABLE I

Sample Weight, Pu-239 Isotopic Abundances and Chemical Compositions for Sample Set

Sample ID	Sample Weight (g)	Isotopic Abundance (%)	Chemical Composition
NBS 946	1/4	84	Sulfate
NBS 947	1/4	77	Sulfate
NBS 948	1/4	91	Sulfate
ROD-7	40	93	Metal
DZO	654	72	PuO_2
YEC	499	71	PuO_2
Can 4	910	79	UO_2-PuO_2
Can 17	1000	87	UO_2-PuO_2
100	15	87	PuO_2
200	15	73	PuO_2
300	15	70	PuO_2
LL-CALOR	600	94	Metal

TABLE II

Sample Set Isotopic Compositions in Weight Percent

Sample ID	^{238}Pu	^{239}Pu	^{240}Pu	^{241}Pu	^{241}Am
NBS946	0.235	84.071	12.248	2.868	1.522
NBS947	0.108	77.705	18.838	3.326	1.611
NBS948	0.010	91.664	7.950	0.349	0.402
ROD-7	0.009	93.737	5.967	0.259	0.255
DZO	0.418	75.590	20.131	3.838	0.686
YEC	0.093	72.323	24.499	3.063	1.309
Can 4	0.243	79.937	16.996	2.800	0.811
Can 17	0.054	86.936	11.743	1.241	0.248
100	0.057	86.917	11.695	1.305	0.179
200	0.247	74.193	22.861	2.676	0.363
300	1.144	71.414	24.385	3.035	0.288
LL-CALOR	0.010	93.688	5.914	0.359	0.084

TABLE III

Nondestructive Gamma-ray Measurements of Pu-240 Abundance Compared to Chemical Analysis
(R = gamma-ray assay ÷ chemical assay)

Peak Pair:		160/164		160/148		642/646	
Sample ID	ΔT(sec)	R	Prec. (1σ)(%)	R	Prec. (1σ)(%)	R	Prec. (1σ)(%)
NBS946	50 K	0.916	2.48	0.917	2.47	1.045	3.18
NBS947	50 K	0.969	2.70	0.956	2.68	1.060	3.23
NBS948	50 K	0.985	1.99	0.988	1.88	1.007	2.53
ROD-7	50 K	0.991	3.02	1.045	2.88	1.026	2.21
	2 K	0.987	10.7	1.098	10.2	0.918	5.66
DZO	50 K	0.979	1.98	1.004	1.98	1.024	1.98
	2 K	0.976	3.94	0.984	3.92	1.021	3.93
YEC	50 K	0.998	1.44	1.027	1.43	1.039	1.59
	2 K	1.005	3.14	0.995	3.09	1.032	4.51
Can 4	50 K	0.944	2.49	0.976	2.48	1.004	1.74
	2 K	1.021	4.25	1.046	4.22	1.043	3.48
Can 17	50 K	0.958	1.99	0.988	1.97	1.016	1.82
	2 K	0.973	5.64	0.951	5.55	1.022	3.49
100	50 K	0.949	1.68	0.958	1.66	1.016	1.83
200	50 K	0.959	1.29	1.007	1.28	1.024	1.49
300	50 K	0.992	1.79	0.962	1.76	1.032	1.45
LL-CALOR	50 K	0.990	2.93	1.032	2.83	0.984	2.60
	2 K	0.958	1.81	0.980	1.76	0.996	1.21
Weighted Average		0.971 ±0.005		0.991 ±0.005		1.018 ±0.005	

TABLE IV

Nondestructive Gamma-ray Measurements of Am-241
(R = Gamma-ray assay ÷ chemical assay)

Peak Pair:			125/129		662/646	
Sample ID	Am-241(PPM)	ΔT(sec)	R	Prec. (1σ)(%)	R	Prec (1σ)(%)
NBS946	17935	50 K	1.003	0.69	1.020	1.54
NBS947	20553	50 K	0.990	0.66	1.017	2.03
NBS948	4344	50 K	0.983	0.62	1.021	1.07
YEC	17952	50 K	1.033	0.63	1.011	1.14
		2 K	1.006	1.13	1.033	3.23
Can 4	10065	50 K	0.991	1.43	0.993	1.05
		2 K	0.994	1.73	1.020	2.11
Can 17	2833	50 K	0.925	2.09	0.997	1.01
		2 K	0.770	5.35	1.003	1.93
100	2046	50 K	0.822	2.47	0.953	1.13
200	4852	50 K	0.936	2.08	0.995	1.12
300	4000	50 K	0.895	2.29	1.000	1.14
LL-CALOR	887	50 K	0.764	4.55	0.999	1.24
		2 K	0.750	3.86	0.998	0.57
Weighted					0.999	
Average					±0.003	

TABLE V

Nondestructive Gamma-ray Measurements of Pu-238
(R = Gamma-ray assay ÷ chemical assay)

Peak Pair:		153/148		153/144	
Sample ID	ΔT(sec)	R	Prec. (1σ)(%)	R	Prec. (1σ)(%)
NBS946	50 K	0.969	0.78	0.983	2.42
NBS947	50 K	0.973	0.77	0.973	3.13
ROD-7	50 K	0.981	7.11	0.983	7.16
	2 K	1.341	23.3	1.345	23.5
DZO	50 K	0.991	0.50	0.983	7.16
	2 K	0.954	1.49	0.992	6.51
YEC	50 K	0.953	1.67	0.880	3.62
	2 K	0.836	5.21	0.795	7.40
Can 4	50 K	0.974	0.80	0.924	3.55
	2 K	0.947	1.68	0.860	5.02
Can 17	50 K	0.979	1.33	0.989	2.14
	2 K	0.964	6.55	1.088	7.65
100	50 K	0.992	1.41	0.983	2.42
200	50 K	0.972	0.52	0.962	2.35
300	50 K	0.969	0.78	0.986	2.80
Weighted		0.975		0.968	
Average		±0.002		±0.009	

TABLE VI

Nondestructive Gamma-ray Measurements of Pu-241
(R = Gamma-ray assay ÷ chemical assay)

Peak Pair:		208/203		148/144	
Sample ID	ΔT(sec)	R	Prec. (1σ)(%)	R	Prec. (1σ)(%)
NBS946	50 K	0.963	0.90	1.016	2.12
NBS947	50 K	0.965	1.56	1.001	3.06
NBS948	50 K	0.991	0.40	0.996	0.96
ROD-7	50 K	1.010	0.49	1.003	0.97
	2 K	1.014	1.19	1.004	3.62
DZO	50 K	0.971	1.63	0.952	3.79
	2 K	0.982	4.17	1.041	6.36
YEC	50 K	0.976	1.72	0.925	3.23
	2 K	0.991	3.91	0.951	5.28
Can 4	50 K	0.979	2.10	0.950	3.48
	2 K	1.027	3.17	0.938	4.77
Can 17	50 K	0.983	0.67	1.011	1.72
	2 K	0.977	1.14	1.129	4.03
100	50 K	0.987	0.66	0.989	1.57
200	50 K	0.987	1.20	0.992	2.31
300	50 K	1.004	1.49	1.016	2.12
Weighted		0.991		0.998	
Average		±0.002		±0.004	

TABLE VII

Isotopic Results for Recommend Peak Pairs

Isotopic Ratio	Peak Pair	<R>*	Standard Deviation (%)
238/241	153/148[a]	1.006[c]	2.4
240/239	642/646[b]	1.003[c]	2.0
241/239	208/203[a]	0.986	1.3
Am/239	662/646[b]	1.007	1.2

[a]Low energy region - 1 cc detector
[b]High energy region - 70 cc detector
[c]Correct for bias with respect to destructive analysis (see text)
*<R> = Average of gamma-ray/destructive analysis ratios for 50K second counts

Discussion:

Walton (LASL):
What about the interference from fission products in the 600 kilovolt range relative to the specifications of those for plutonium?

Fleissner (Monsanto-Mound):
I haven't looked at any samples containing fission fragments. When you have appreciable amounts of fission fragements in your plutonium sample, they will tend to wash out the 600 keV region, and in that case, this method could not be used.

Gamma Ray NDA Assay System for Total Plutonium and Isotopics in Plutonium Product Solutions

by

L. R. COWDER, S.-T. HSUE, S. S. JOHNSON,
J. L. PARKER, P. A. RUSSO, and J. K. SPRINKLE
Los Alamos Scientific Laboratory, Los Alamos, New Mexico
and
Y. ASAKURA, T. FUKUDA and I. KONDO
Power Reactor and Nuclear Fuel Development Corporation, Tokai-Mura, Japan

ABSTRACT

A LASL-designed gamma-ray NDA instrument for assay of total plutonium and isotopics of product solutions at Tokai-Mura is currently installed and operating. The instrument is, optimally, a densitometer that uses radioisotopic sources for total plutonium measurements at the K absorption edge. The measured transmissions of additional gamma-ray lines from the same radioisotopic sources are used to correct for self-attenuation of passive gamma rays from plutonium. The corrected passive data give the plutonium isotopic content of freshly separated to moderately aged solutions. This off-line instrument is fully automated under computer control, with the exception of sample positioning, and operates routinely in a mode designed for measurement control. A one-half percent precision in total plutonium concentration is achieved with a 15-minute measurement.

KEYWORDS: Reprocessing, product solutions, gamma-ray NDA, densitometry, transmission-corrected gamma-ray assay

I. INTRODUCTION

The Los Alamos Scientific Laboratory (LASL)-designed K-edge densitometer for plutonium product solutions accounting at the Power Reactor and Nuclear Fuel Development Corporation (PNC) fuel reprocessing facility in Tokai-Mura, Japan, was shipped to Tokai in summer of 1979 and installed and calibrated during September and October, 1979. The densitometer will continue to operate initially in a schedule that allows for testing and evaluation throughout the late fall and early spring reprocessing campaigns at Tokai. The instrument is intended to be used cooperatively by the PNC and the International Atomic Energy Agency (IAEA) for rapid, off-line assay. It will provide a means to bypass the time-consuming and costly destructive analytical methods for total plutonium measurement.

The densitometer is discussed below in sections describing II) measurement principles and experimental design, III) hardware design, IV) software design, V) concepts of analysis, and VI) preliminary results.

II. MEASUREMENT PRINCIPLES AND EXPERIMENTAL DESIGN

Solution assay performed by K-edge densitometry provides the total concentration of an individual element in a sample of well-defined geometry. The measured transmission of gamma radiation through special nuclear material (SNM) displays a discontinuity at the discrete energy corresponding to the binding energy of the K electrons.

The transmissions, T_1 and T_2, just below and above the K edge, respectively, are related to the total concentration, ρ, of the element by the relation

$$T_i = T_m e^{-\mu_i \rho x}$$

where μ_i is the mass attenuation coefficient of the element for a given photon energy i, x is the sample thickness and T_m is the transmission through the matrix. Thus, the ratio (R) of transmissions is logarithmically related to the elemental concentration, ρ, independent of matrix by

$$\rho = \frac{-\ell n\ T_2/T_1}{\Delta\mu x} = \frac{-\ell n\ R}{k}$$

where $\Delta\mu = \mu_2 - \mu_1$.

Discrete gamma-ray transmission sources can be used for K-edge measurements if the gamma-ray lines closely bracket the absorption edge of interest. For the plutonium case, the 121.1 and 122.1 keV lines of ^{75}Se and ^{57}Co, respectively, are well located with respect to the 121.76 keV K electron binding energy. The measured transmissions of these two gamma-ray lines have previously been used with success to assay plutonium in solution.[1,2] This technique is applied in the Tokai densitometer.

The densitometer design was optimized to measure plutonium solutions, freshly separated, with a total concentration of approximately 225 g Pu per liter. Even with less-than-ideal passive counting geometry, the measurement situation is well suited to transmission-corrected passive assays for isotopics determination. This type of assay has been applied in existing instrumentation[3] to an extremely wide range of plutonium solution concentrations (0.5 to 500 g Pu per liter) where self-attenuation corrections are based on transmission measurements performed with an external plutonium transmission source.

The Tokai densitometer uses measured transmissions of the gamma-ray lines of ^{75}Se and ^{57}Co obtained during the densitometry measurement, in place of those from an external plutonium source, to correct for self-attenuation in the passive assay. The ^{241}Pu and ^{238}Pu isotopes are determined relative to ^{239}Pu in this way using assay gamma rays at 149, 153, and 129 keV, respectively. The measurement for ^{240}Pu and an independent determination of ^{238}Pu are made by obtaining ratios of the respective peak areas (at 45.2 and 43.5 keV) to that of the ^{239}Pu isotope at 51.6 keV. The latter technique is not effective for excessively aged solutions.

The solution assays are performed in two steps. The first is a transmission measurement of the ^{75}Se and ^{57}Co gamma rays utilizing strong sources and tight sample collimation. The second measurement is performed without sources, and the sample collimation is opened to maximize the passive counting geometry. The mechanical details of the measurements are discussed below.

Measurement control is an essential feature of the experimental design. This is a procedure, performed daily, to insure that the calibration for total plutonium, based on previous measurements of solution standards, remains valid. A secondary standard is used in this exercise. The Tokai densitometer is designed to assay, on a daily basis, a plutonium foil of known characteristics for total plutonium. Agreement between this assay and the known result is required before routine assays can proceed. Measurement control on the isotopics analysis consists of a relative efficiency measurement performed with the ^{75}Se transmission source. Since all isotopics data are analyzed relative to ^{239}Pu, it is the relative detector efficiency and not the absolute efficiency that is the critical factor.

III. HARDWARE DESIGN

The two-step (transmission and passive) assay performed in order to obtain results for total plutonium and isotopics is accomplished by rotation of the transmission sources in and out of the measurement position. The process is illustrated schematically in Fig. 1. Two motor-driven wheels containing collimators and sources are positioned synchronously by a Geneva mechanism such that the germanium detector counts, primarily, either transmission gamma rays from one of two (^{75}Se or ^{57}Co) sources with tight sample collimation or the passive gamma rays from the sample with collimation open.

The mechanical system is mounted beneath a glovebox that is modified so that a measurement well extends down from the base of the box between the source and collimator wheels. Solution samples in plastic, disposable sample vials of well-defined dimensions

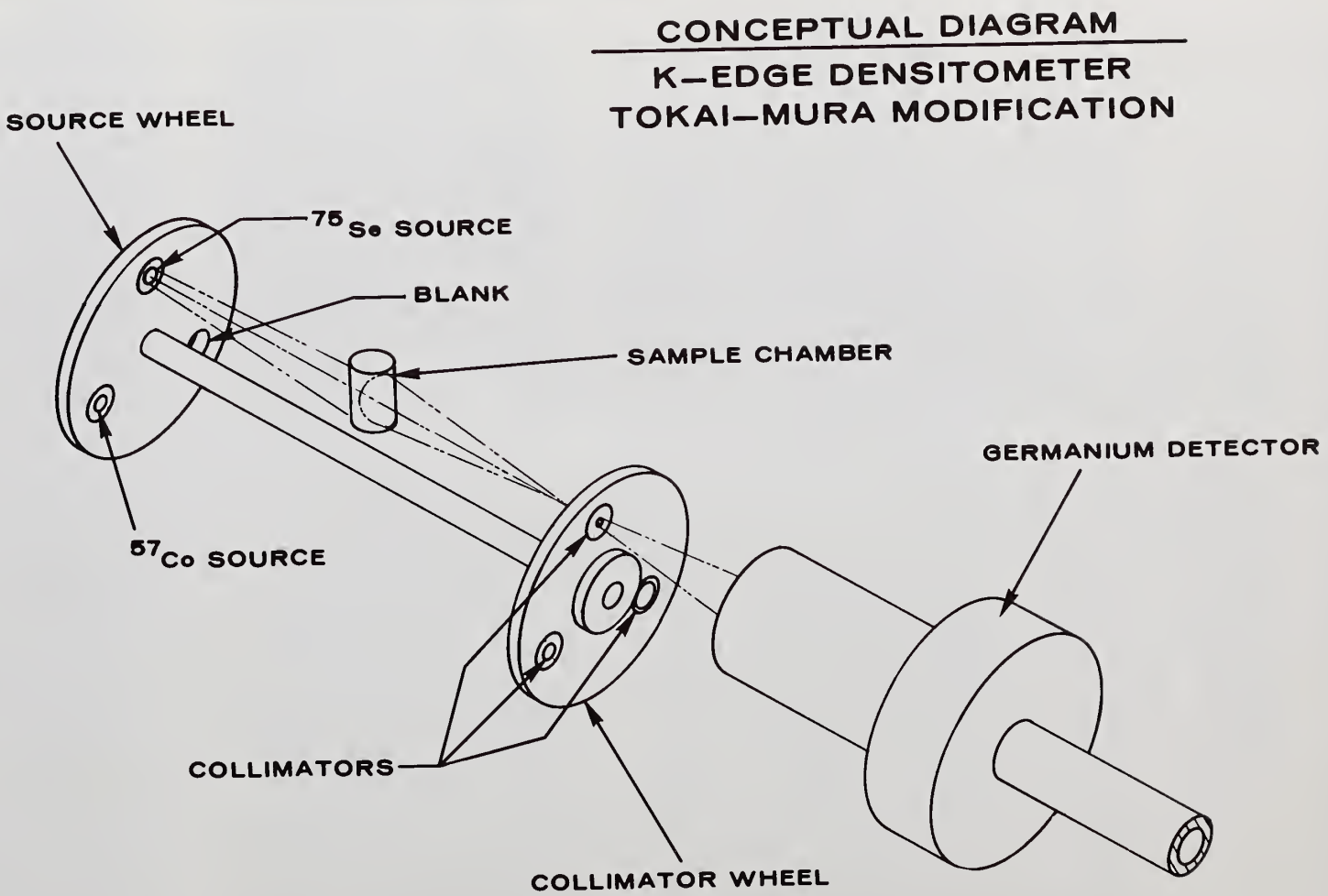

Fig. 1. Conceptual view of measurement configuration. The sample is shown between the source (^{75}Se, in this case) and the collimator in the detector line of sight. Sources and collimators are mounted on separate wheels driven synchronously.

are inserted into the well. The well fixes the position of the sample vial. Secondary standards are also positioned for measurement in this way.

The germanium detector sits beneath the glovebox, facing the sample and transmission sources, in a position downstream from the sample. The configuration at the measurement station is shown in Fig. 2. Figure 3 is a photograph of the measurement station before installation beneath the glove box. Figure 4 shows details of the measurement well and associated hardware approximately to scale.

The optimum ^{75}Se and ^{57}Co source activities are approximately 50 and 25 m Ci, respectively. Gamma rays from the sources are collimated to a diameter of 3 mm at the collimator wheel.

The sample well is a thin stainless steel canister which supports a thick tungsten shield. The tungsten shield is lined with a polyethylene boot into which the sample container fits securely. The stainless steel canister is the containment canister for the glovebox modification. The photon windows on this container are 0.5 mm thick at the entrance (transmission source) side and 0.25 mm thick at the exit side.

Solution sample volumes are a minimum of 10 ml. The photon transmission path length through the sample is approximately 2 cm. The sample cross sectional area viewed by the detector during passive measurements is 3 cm^2.

The germanium detector is a planar intrinsic which is chosen to be relatively thin (7 mm) to limit backgrounds due to Compton scattering of high energy photons. The crystal is located approximately 10 cm from the center of the sample. A 100 μCi ^{109}Cd source is mounted just above the cryostat. This source is used for normalization to correct for losses due to differing count rates.

Pulses from the detector are amplified by a pulsed optical feedback preamplifier and further amplified and shaped with 3 μs time constants. Pile-up rejection is employed to permit higher count rates. The optimized data throughput rate to the computer occurs at detector counting rates of approximately 20 kHz. At this rate, the resolution at 122 keV is approximately 550 eV, full width at half maximum (fw½m).

The amplified pulses are digitized by a digitally stabilized analog-to-digital converter (ADC). The converted data is stored and processed by an LSI-11 microcomputer, part of the Nuclear Data 660 data acquisition system utilized in this instrument.

The computer control of the data acquisition system includes all hardware mechanical operation (except sample positioning) and some electronics adjustment (such as selection of gain stabilization channels), measurement control, and data acquisition and analysis. The control software uses the DEC RT-11 version 3B foreground-background operating system, the Nuclear Data foreground program, ND660, which controls acquisition and display, and FORTRAN-callable subroutines provided by Nuclear Data for communication between foreground and the background control programs. The background code is overlaid in segments that are accessed from floppy diskette. Spectral data are stored on floppy diskette along with measurement parameters, constants, and file identification information. The code is also capable of reanalyzing data stored previously on disk.

Special interfaces to the LSI-11 that are accessed by the code are those for the ADC, the source-collimator wheel drive mechanism and position sensing mechanism, three thermocouples for equipment temperature monitoring, and the gain stabilizer.

Figure 5 is a photograph showing the measurement well (extreme right), control hardcopy terminal (middle), and the rack-mounted electronics. The electronics are (top to bottom), a dual floppy diskette unit, an oscilloscope, the control electronics for the Geneva mechanism and temperature sensors, the computer display terminal, the LSI-11 microcomputer, and the NIM electronics for processing the signals from the detector preamplifier.

IV. SOFTWARE DESIGN

The computer program for automatic data acquisition and analysis and measurement control is written in overlaid form so that the executive routine, any one of three major control routines, and any one of twenty utility routines are resident in core at once. As much as 11.4 K of core is available for the control program. The remainder of the LSI memory is used by the ND foreground program, the 4 K spectrum, and the RT-11 operating system.

This program requires a minimum of operator interaction since the program itself performs diagnostic tests and executes the assay providing the outcome of these tests is positive. Other modes of program operation give the user more flexibility to exercise

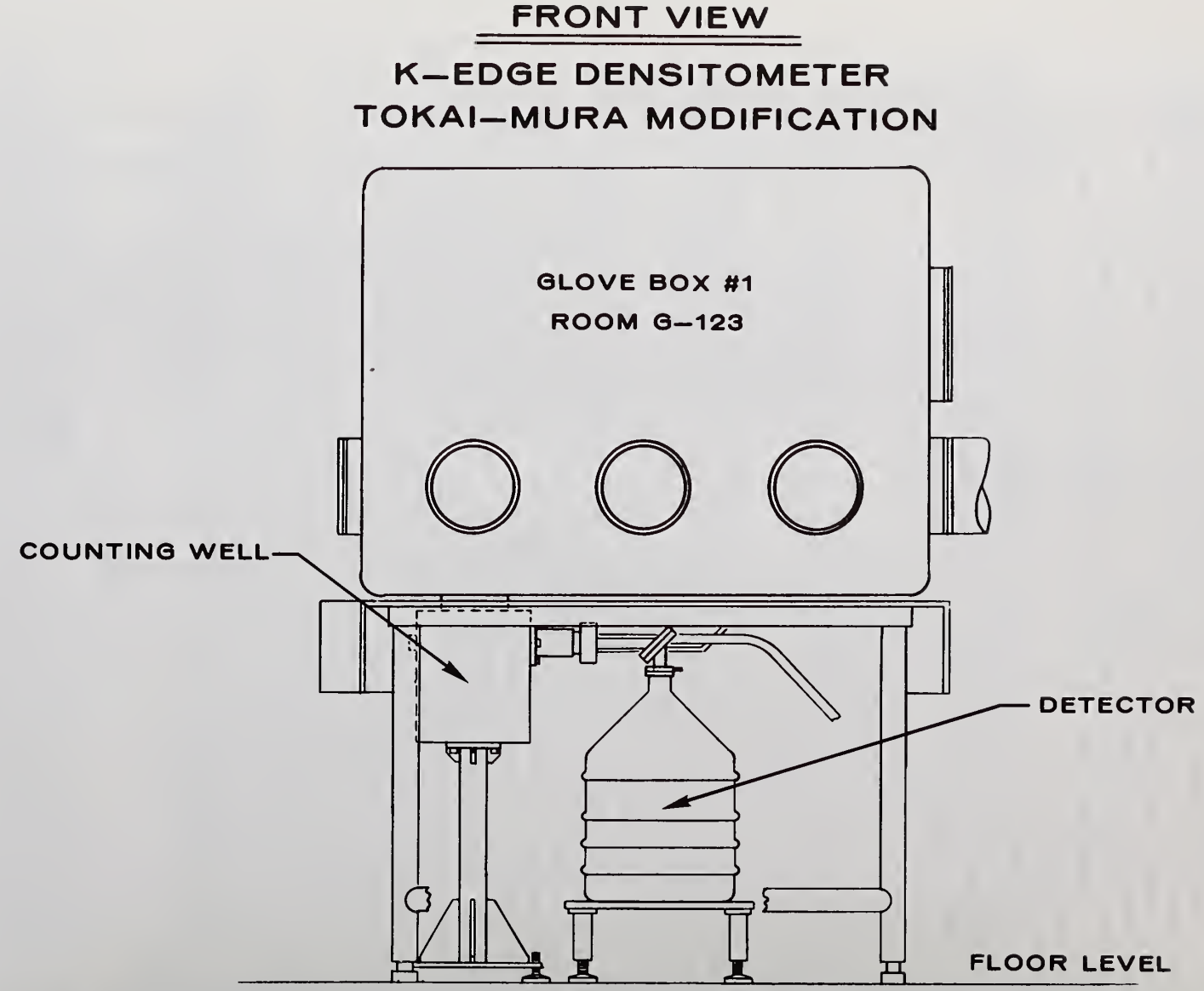

Fig. 2. Schematic view of measurement station extending below and positioned beneath glovebox.

Fig. 3. A close-up view of the measurement well and intrinsic germanium detector.

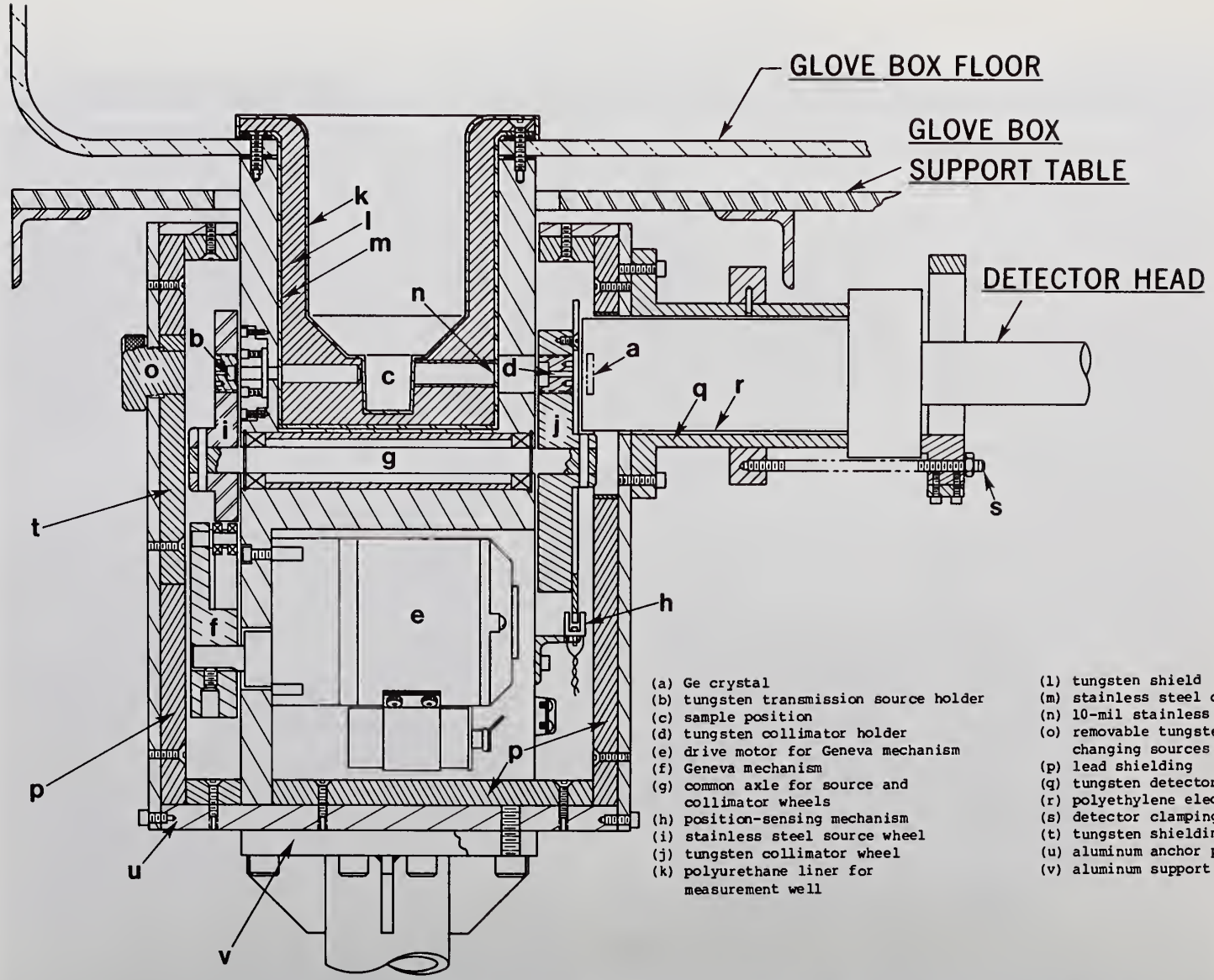

(a) Ge crystal
(b) tungsten transmission source holder
(c) sample position
(d) tungsten collimator holder
(e) drive motor for Geneva mechanism
(f) Geneva mechanism
(g) common axle for source and collimator wheels
(h) position-sensing mechanism
(i) stainless steel source wheel
(j) tungsten collimator wheel
(k) polyurethane liner for measurement well
(l) tungsten shield
(m) stainless steel containment can
(n) 10-mil stainless steel window
(o) removable tungsten plug for changing sources
(p) lead shielding
(q) tungsten detector shield
(r) polyethylene electrical shield
(s) detector clamping device
(t) tungsten shielding
(u) aluminum anchor plate
(v) aluminum support base

Fig. 4. Cross-sectional view of the measurement well extension from the glovebox base.

Fig. 5. Complete K-edge densitometer including computer, MCA, terminal, and measurement well.

diagnostic procedures, but these modes are designed for setup, calibration, testing, and other nonroutine measurements, and are not intended for regular use with the instrument package.

Routine use of the program requires the daily execution of a measurement control sequence. Measurement control establishes the unattenuated gamma-ray intensities used for compiling fractional transmissions, it checks for changes in relative detector efficiencies, and it verifies that the source strengths are sufficient to obtain the statistics required. These ^{75}Se and ^{57}Co spectra are also used to verify the energy resolution and gain of the spectrometer, which must agree with the original values that are stored. Furthermore, the known thickness of a secondary standard plutonium foil must be reproduced by a densitometry measurement to satisfy measurement control requirements.

A successful completion of measurement control allows the user the option to assay a sample. The assay proceeds automatically with the accumulation and storage (on floppy disk) of ^{75}Se and ^{57}Co spectra, calculation of total plutonium concentration and of transmission values that apply to the passive assay, accumulation and storage of the passive spectrum and calculation of the isotopic weight fractions.

V. CONCEPTS OF ANALYSIS

Techniques for extraction of peak areas using straight line background subtraction have been described previously.[4] The reduction of raw data before analysis is accomplished using these techniques both for the active and passive spectra. No peak fitting is employed.

For all analysis which requires the absolute area of a peak in a given spectrum, normalization is accomplished by dividing by the area of the 88 keV ^{109}Cd peak. This normalization is applied to peak areas used for the transmission measurements, both for densitometry and for attenuation corrections.

All peak areas used for transmission measurements are corrected for the decay of the source since the time of measurement of the unattenuated intensities.

Analysis of the transmission data for the densitometry assay is straightforward and has been discussed in sufficient detail in Sec. II. The predicted fractional uncertainty in the measured plutonium concentration is

$$\frac{d\rho}{\rho} = \frac{dR}{R\ell nR}$$

where R is the transmission ratio as defined in Sec. II. The results of the densitometry analysis on standard plutonium solutions appear in the next section.

Analysis of the passive data for isotopics is more complex in that different analysis techniques are used in the two energy regions discussed previously. The two techniques are discussed separately below.

The concentration of a given isotope, ρ_I, measured by gamma-ray spectroscopy can be expressed as

$$\rho_I \propto A \cdot CF \qquad (1)$$

where A is the normalized peak area corresponding to a gamma ray emitted by the isotope of interest. The correction factor, CF, takes into account the energy- and concentration-dependent sample attenuation effects on the gamma ray of interest. The proportionality constant is dependent upon quantities such as branching ratios, half lives, counting efficiencies, the atomic mass, and a calibration factor that disappears if relative peak area results are analyzed as is the case here.

The calculation of CF is performed in order to measure the isotopic contents of ^{238}Pu, ^{239}Pu and ^{241}Pu using the assay gamma-ray peaks at 153, 129 and 149 keV, respectively. Measured transmissions at 122 keV (from ^{57}Co), 136 keV and 279 keV (from ^{75}Se) are linearly interpolated or extrapolated based on both the 122-136 pair and on the 136-279 pair. Therefore, two transmission values are determined for each of the three plutonium gamma-ray energies. The average of the two is the value used in the calculation

of CF, since this has been shown to give a more realistic result than a quadratic fit to three measured transmissions, two of which are closely spaced in energy.

A slab sample with finite thickness, D, which remains small compared to the sample-to-detector distance, x_0, has a correction factor that can be expressed[3] as an integral over the sample thickness

$$CF = \frac{K_0 \int^D dx}{0 \int^D T_x dx}$$

where

$$T_x = e^{-\mu x}$$

and μ is the linear attenuation coefficient. In this case, the integral has an exact solution. However, if D is not negligible compared to x_0, geometry effects due to sample thickness must be included in the integration over sample thickness

$$CF = \frac{K_0 \int^D \frac{dx}{(x + x_0)^2}}{\int_0^D \frac{T_x dx}{(x + x_0)^2}} = \frac{K \frac{D}{x_0 (x_0 + D)}}{\int_0^D \frac{T_x dx}{(x + x_0)^2}}$$

This integral has no exact solution, and thus a numerical evaluation is appropriate. The known (measured) transmission values ($e^{-\mu D}$) are used to empirically evaluate the quantity μ at each energy for each sample. The slab assumption proves to be a valid approximation in this case.

The fractional error in the average extrapolated transmission propagates to one half that in ρ_I.

The approach to isotopic analysis in the low-energy region is less cumbersome, primarily because there is no need to determine the correction factor for sample attenuation. The relative counting efficiencies, R_{eff}, for the ^{239}Pu gamma rays at 39 and 51 keV are determined from the respective measured peak areas, A, and the branching ratios (BR) known for these gamma-ray lines. Thus

$$R_{eff} = A \cdot BR$$

The dependence in $\ell n\ R_{eff}$ versus $\ell n\ (\ell n\ E)$ is interpolated linearly between 39 and 51 keV to obtain R_{eff} at 43 and 45 keV, the energies of the two gamma rays due to ^{238}Pu and ^{240}Pu respectively. The ratios of the weight fractions, f_I, of each of these two isotopes to that of the ^{239}Pu, f_{239}, are then given by

$$\frac{f_I}{f_{239}} = \frac{A\ (43 \text{ or } 45)}{R_{eff}\ (43 \text{ or } 45)} \cdot \frac{R_{eff}\ (51)}{A\ (51)} \cdot K_L\ (43 \text{ or } 45) \qquad (2)$$

where K_L accounts for the ratios of half-lives and branching ratios and atomic masses associated with the ^{239}Pu (51 keV line) and each of the other two.

VI. RESULTS

A. Calibration at LASL

Primary standard solutions of reactor grade plutonium have been used for preliminary calibration of the Tokai densitometer at LASL for total plutonium. Total plutonium concentrations range between 150 and 300 g per liter. The ^{240}Pu isotopic content of the solutions was 15% although the calibration was also verified with solutions of low burnup material.

A summary of the results of the densitometry measurements on the solution standards is shown in Fig. 6. Count times for each transmission measurement were 1000 seconds. Since the data were obtained with solutions of known concentration, the $\Delta\mu\chi$ calibration factor was derived from each measurement. Plotted is the percent deviation from the mean value for each run. The error bars reflect the statistical precision ($\pm 1\sigma$) in the densitometry measurement. The precision of ± 0.1 percent (1σ) in the reference concentrations is not included but has very little effect on these error bars. The scatter in the data is consistent with the statistical prediction shown by the $\pm 1\sigma$ statistical error bars. The data show no evidence of a concentration effect on the calibration factor. It should be noted that the ^{109}Cd source rate was sufficiently low for these measurements (because of positioning) to increase the statistical uncertainty by 60 percent compared to measurements performed with optimized count rates.

Calibration with solution standards was carried out along with routine assays of the plutonium foil. The foil is equivalent to approximately 235 g Pu per liter. The statistical precision on the foil assay for a 1000-s count time is $\pm 0.29\%$. The experimental precision agrees with this as is shown in Fig. 7. These data were obtained in a four-week period after measurement of the solution standards as a demonstration of the stability of the calibration for total plutonium.

Isotopics results have been obtained from passive measurements of the reactor-grade plutonium standard solutions. The results are all based on measurements of peak areas relative to the ^{239}Pu peak area, as described in Secs. II and V. Relative peak area measurements appear to be immune to shifts in gain, resolution, or detector efficiency, since these measurements use ratios of areas of peaks closely spaced in energy.

Thus the data analysis involves obtaining the ratio of each isotopic fraction, f_I, to that for ^{239}Pu, f_{239}. This ratio, f_I/f_{239} is defined by Eq. (2) for the low energy data, and is identical to the ratio, ρ_I/ρ_{239} obtained using Eq. (1) and the high energy data. The experimental ratios can be combined with a result for ^{242}Pu obtained by isotopic correlations using the experimental value for f_{240}/f_{239}(5). The fraction of ^{239}Pu is derived from the equation

$$f_{239} = (1 + R_{238} + R_{240} + R_{241} + R_{242})^{-1} \quad (3)$$

where

$$R_I = f_I/f_{239}.$$

This result for f_{239} is used to obtain the other isotopic fractions:

$$f_I = R_I \cdot f_{239}. \quad (4)$$

The solution standards were used first to determine the relative counting efficiencies for assay peaks in the high-energy region. They were also used to verify (and correct if necessary) the literature values that make up the constants $K_L(43)$ and $K_L(45)$ (see Eq. (2)) for the low-energy analysis. Once the relative efficiencies and constants were established, the isotopic fractions, f_{239} and f_I, were determined for thirteen passive measurements performed on the four solutions listed previously (refer to Fig. 6), all with the same isotopic content (namely 0.349%, 79.85%, 14.30%, 4.56%, and 0.933% for the 238, 239, 240, 241, and 242 isotopes, respectively). The reference values for isotopic content were obtained from mass spectrometric measurements. These initial measurements were performed within several days of the Am separation so the ^{241}Am content was approximately 100 ppm. All passive count times were 2000 seconds.

The results for the early measurements are shown in Columns 2 and 3 of Table I. Column 2 compares the average calculated measurement precision with the experimental

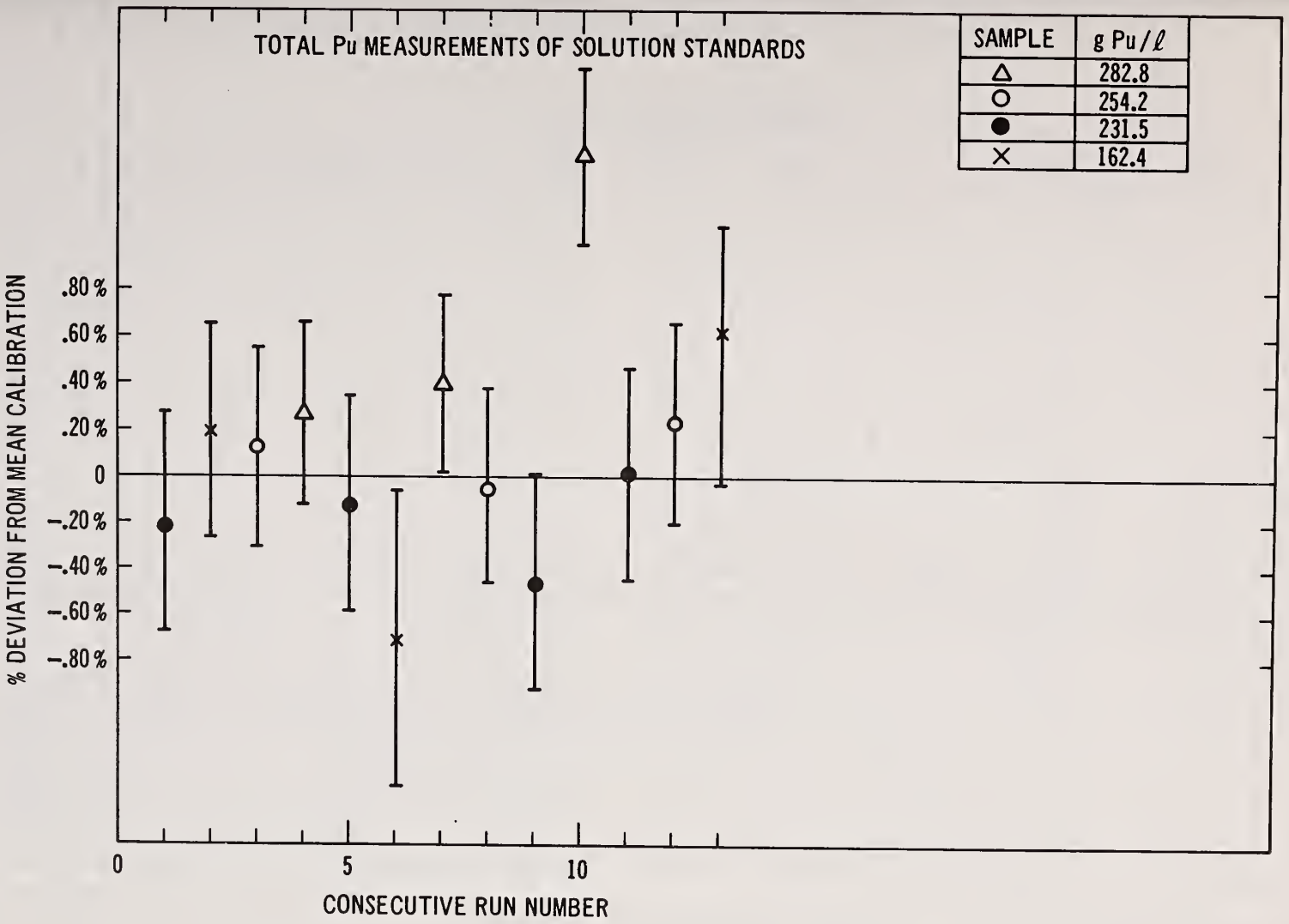

Fig. 6. Total Pu measurements of solution standards at LASL.

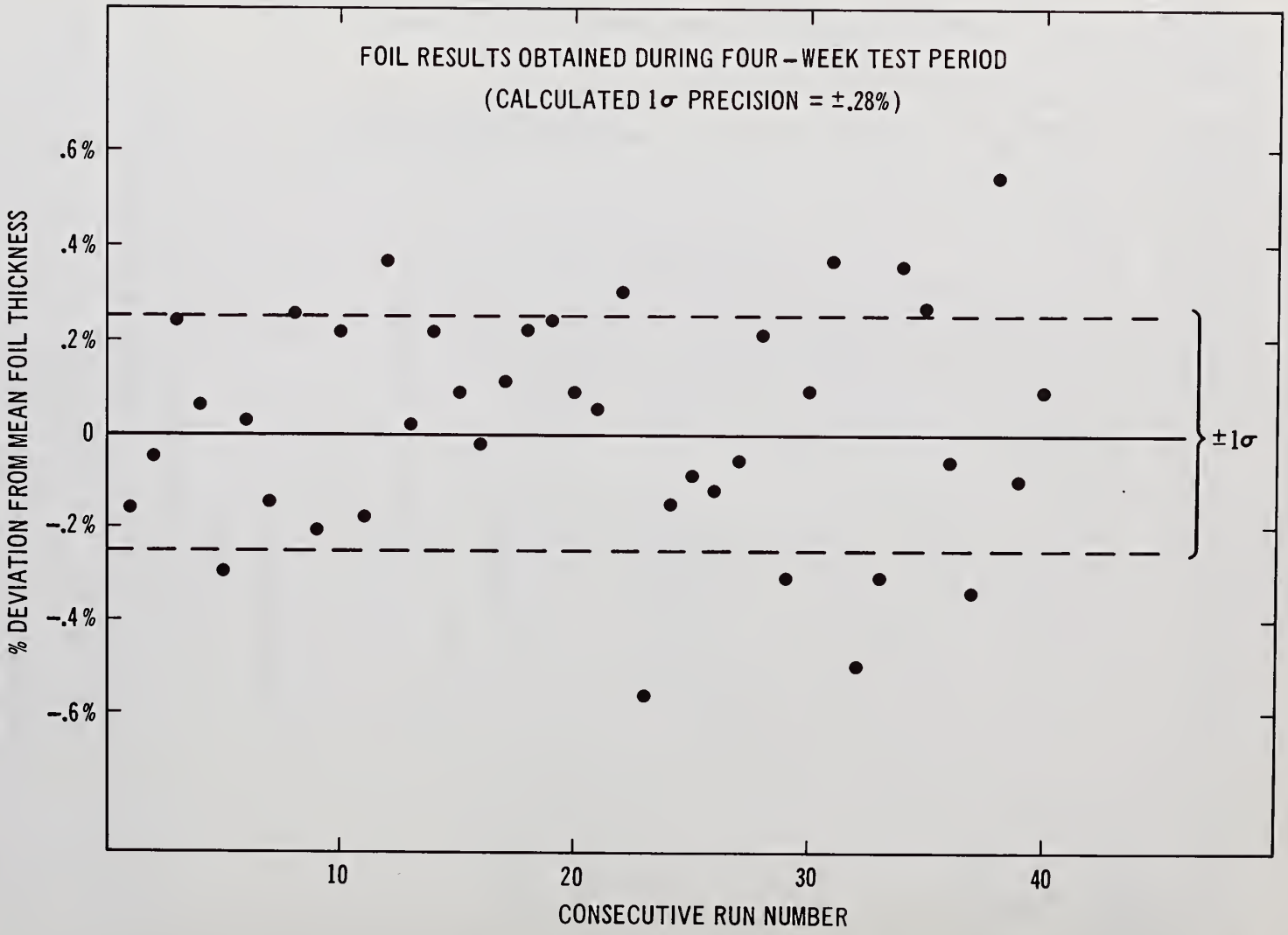

Fig. 7. Foil results obtained during four-week test period.

TABLE I
SUMMARY OF ISOTOPIC FRACTION RESULTS
FOR REACTOR-GRADE Pu SOLUTIONS

ppm americium	100	100		1000		3000	
	$\frac{1\sigma \text{ calc.}}{1\sigma \text{ expt.}}$	CALCULATED 1σ					
		Isotopic	Total Pu	Isotopic	Total Pu	Isotopic	Total Pu
^{238}Pu	1.2	0.9%	0.003%	1.2%	0.004%	1.3%	0.005%
^{239}Pu	1.0	0.45%	0.36%	0.45%	0.36%	0.45%	0.36%
^{240}Pu	1.2	1.0%	0.14%	1.3%	0.19%	1.5%	0.21%
^{241}Pu	0.7	0.9%	0.04%	0.9%	0.04%	0.9%	0.04%
^{242}Pu		40%	0.37%	40%	0.37%	40%	0.37%
$\frac{\text{FISSILE}}{\text{FERTILE}}$		2.6%		2.7%		3.0%	

scatter in the weight fraction for each isotope. The results are close to unity indicating no observable contributions to the measurement precision beyond the statistical contributions. (This result is not shown for ^{242}Pu, since the calculated error in this case is derived from the correlation data rather than counting statistics.)

Column 3 of Table I gives the calculated values of the 1σ precisions in the isotopic fractions for the same data. These are shown as percentages of the isotopic weight fraction ("isotopic") and percentages of the total plutonium concentration ("total Pu").

As the solutions age and ^{241}Am grows in, the statistical uncertainty on the low-energy data increases because of increased Compton background from the 60-keV gamma ray. Data from the more aged solutions were obtained and analyzed as described for Column 3 of Table I. These are shown in Columns 4 and 5, the latter corresponding to the two-month-old LASL solutions. Clearly, the ^{241}Am growth has affected the measurement precision of the even isotopes.

Since the ^{241}Pu content of spent fuel varies with fuel burnup, the level of americium grown in will vary with burnup for a given aging time. A passive measurement on samples with 14 percent ^{241}Pu is feasible for samples aged up to six months.

The isotopics analysis is also appropriate for the assay of low burnup materials. The plutonium foil is an example of this (0.022%, 93.71%, 5.95%, 0.293%, and 0.035% for the ^{238}Pu, ^{239}Pu, ^{240}Pu, ^{241}Pu, and ^{242}Pu weight percents, respectively). Thirteen passive assays on the foil give the results shown in Table II. Here again the experimental precision (scatter) agrees with the calculated precision for the 2000-s passive measurements. The calculated results are shown in Columns 2 and 3 as the percent of the isotopic fraction and the percent of total plutonium, respectively, for each of the five isotopes. Although the errors on the isotopic fractions other than f_{239} are larger than for the high burnup plutonium in the solutions, they translate into small uncertainties in total plutonium since these isotopes are now significantly lower in relative content.

It should be noted that the effect of the ^{241}Am grow-in is less pronounced for the isotopics analysis of low burnup material. The foil data in Table II were obtained from plutonium aged more than six months after americium separation.

TABLE II
ISOTOPIC FRACTION RESULTS FOR WEAPONS GRADE Pu FOIL

	CALCULATED 1σ	
	% of isotopic fraction	% of total plutonium
^{238}Pu	15%	0.003%
^{239}Pu	0.25%	0.237%
^{240}Pu	5%	0.29%
^{241}Pu	4%	0.01%
^{242}Pu	40%	0.02%

B. Calibration at Tokai-Mura

The recent calibration at Tokai-Mura was accomplished with solutions of high burnup plutonium provided as reference materials. Total plutonium concentrations were precise to +0.5 percent. Figure 8 shows these calibration results for densitometry plotted as the percentage deviation from the analytical chemistry values (used as reference values) versus plutonium concentration. The data were obtained for Pu solutions aged two weeks and one year after americium separation. The error bars reflect only the precision in the densitometry measurement as in Fig. 6. The error is significantly increased by inclusion of the precision in the reference concentrations. Furthermore, three of the four outlying data points agree with independent measurements obtained using a second NDA instrument.

Determination of the parameters for isotopics assay was accomplished using the fresh plutonium solutions. Reference values were obtained from mass spectrometric results. The experimental precisions in the isotopicsparameters are in agreement with the expected statistical precisionsin the measurements and are comparable to those quoted in Table I. The absolute results agree with those determined at LASL.

Further calibration data will be obtained at PNC before the first reprocessing campaign commences.

REFERENCES

1. T. R. Canada, D. G. Langner and J. W. Tape, "Nuclear Safeguards Applications of Energy-dispersive Absorption Edge Densitometry," Nuclear Safeguards Analysis (E. A. Hakkila, Ed.), ACS Symposium Series, No. 79 (1978).

2. K. J. Hofstetter and G. A. Huff, "On-line Isotopic Concentration Monitor," AGNS-1040-2.3-52 (October 1978).

3. J. L. Parker, "A Plutonium Solution Assay System Based on High Resolution Gamma Ray Spectroscopy," LA-8146-MS (November 1979).

4. R. H. Augustson and T. D. Reilly, "Fundamentals of Nondestructive Assay of Fissionable Material," LA-5651-M (September 1974), pp 27-31.

5. Private communication with S.-T. Hsue.

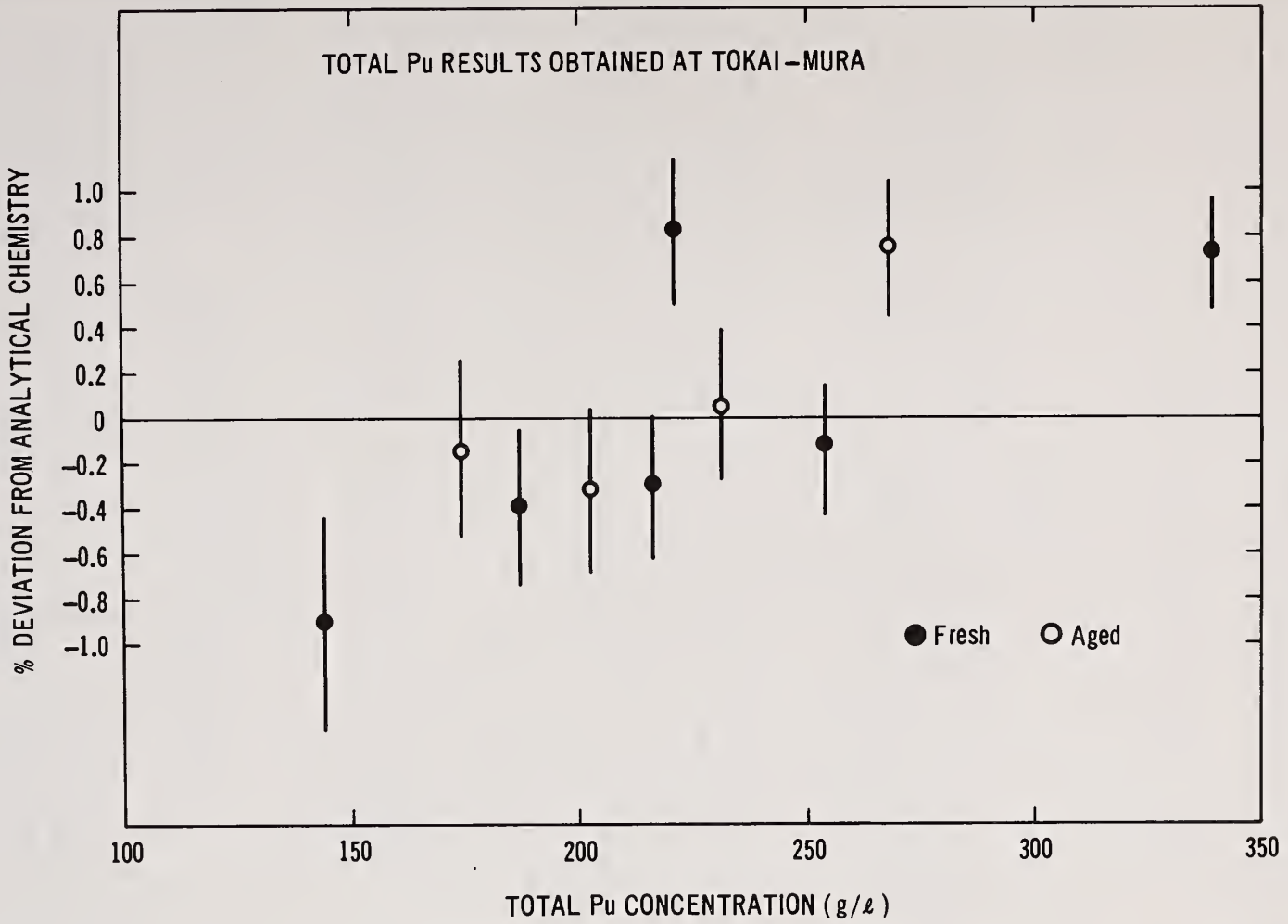

Fig. 8. Total Pu measurements of solution standards at Tokai. "Fresh" and "aged" correspond to two weeks and one year, respectively, after americium separation.

Nondestructive, Energy-Dispersive, X-Ray Fluorescence Analysis of Product Stream Concentrations from Reprocessed Nuclear Fuels*

by

David C. Camp and Wayne D. Ruhter
Lawrence Livermore Laboratory, Livermore, CA 94550

ABSTRACT

Energy-dispersive x-ray fluorescence analysis (XRFA) can be used to measure nondestructively pure and mixed U/Pu concentrations in process streams and hold tank solutions. The 122-keV gamma ray from ^{57}Co excites the actinide K x rays which are detected by a HPGe detector. A computer- and disk-based analyzer system provides capability for making on-stream analyses, and the noninvasive measurement is easily adapted directly to appropriate sized pipes used in a chemical reprocessing plant. Measurement times depend on concentration and purpose but vary from 100s to 500s for process control of strong to weak solutions. Accountability measurements require better accuracy thus more time; and for solutions containing plutonium, require a measurement of the solution radioactivity made with an automatic shutter that eclipses the two exciting sources. Plutonium isotopic abundances can also be obtained. Concentrations in single or dual element solutions from less than 1 g/l to over 200 g/l are determined to an accuracy of 0.2% after calibration of the system. For mixed solutions the unknown ratio of U to Pu is linearly related to the net U/Pu K x-ray intensities. Concentration values for ratios different than the calibration ratio require only small corrections to the values derived from a calibration polynomial. Minor fission product contamination does not prevent concentration determinations by XRFA. The computer-based system also allows real-time dynamic concentration measurements to be made.

KEY WORDS: X-ray fluorescence analysis, nondestructive measurements; uranium, plutonium concentration and isotopics determinations; reprocessing plant process control, accountability, inventory control, dynamic concentration measurements, on-line real-time measurements; computer-based system.

INTRODUCTION

Product Accountability and Process Control

In the event that spent nuclear fuel is reprocesssed to reclaim uranium or plutonium, several nondestructive analytical techniques can be used to obtain process control and product accountability information. Generally, reprocessing begins with dissolution of the spent fuel followed by separation of the fission products; and finally purification of the desired actinide elements, uranium and plutonium. These two elements may appear in separate streams or may occur together as a coprocessed stream. The single and/or dual element streams will usually be concentrated and sent to a hold tank for accountability. Throughout the separation there is a need to control the process, that is, to monitor and regulate the actinide concentrations in order to satisy chemical engineering or criticality safety considerations.

*Work performed under the auspices of the U.S. Department of Energy by the Lawrence Livermore Laboratory under contract number W-7405-ENG-48.

Input concentrations into the various process, hold, and final accountability tanks will encompass a wide range of concentrations. Values from less than 1 g/l to perhaps more than 200 g/l can be expected. Furthermore, a wide range in the uranium to plutonium ratio may occur in coprocessed streams. These various process streams and tank concentrations can be monitored on-line, rapidly, nondestructively, and quantitatively using the analytical technique of energy dispersive x-ray fluorescence analysis (XRFA). The technique also provides sufficient accuracy for Safeguards accountability purposes over the entire range of single or dual element stream concentrations expected at a reprocessing facility.

Eventually, the coprocessed product may be precipitated and converted to a powder blend of uranium and plutonium oxide. This mixed oxide (MOX) product may be packaged in standard amounts, e.g. canisters containing 2000 g of MOX. Since spent fuel received from different reactors will not have the same burnup, the elemental and isotopic compositions of various MOX batches will differ. Thus, for accountability, inventory control, and subsequently fuel fabrication purposes, there is a need to know the percentage of plutonium enrichment. Furthermore, the isotopic composition of the product is required for fissionability information. These two measurements, enrichment and isotopics can be made by the nondestructive technique of gamma-ray spectrometry. Descriptions of these measurement procedures[1] and techniques[2] can be found elsewhere. This paper is limited to a discussion of how energy dispersive XRFA can be used to quantitatively measure actinide solution concentrations that are encountered throughout reprocessing facilities.

Overview of XRFA

The analytical technique of XRFA depends upon the ability to excite atoms within a sample, and to measure accurately the characterisitic x rays emitted from the excited atoms. The atoms may be excited in many different ways. These include the use of ordinary x-ray tubes, with or without filtered anodes; irradiation by α, β, γ, or x rays from radioisotopes; bombardment by charged particles from accelerators; bombardment by electrons, as in electron microprobes; irradiation by secondary x rays from a selected target element, or by polarized x or γ rays such as from synchrotron radiation; self-excitation, if the sample contains radioactivity; and by observing x rays that follow certain nuclear decay modes.

Phenomenologically, XRFA can be understood as follows. Assume that a flux of exciting radiation composed of photons of energy, E_p, is incident on a sample. A small part of the incident radiation flux may not interact with the sample at all; another part may scatter, either with or without some energy loss; and part of the flux may be completely absorbed by the sample. A simplified representation of one interaction is illustrated in Fig. 1. If the incident quantum is totally absorbed, and if E_p(keV) is greater than the binding energy of one of the atom's electrons, then one of the shell electrons will be ejected. This creates a vacancy in one of the atomic shells, which leaves the atom in an excited state.

If the vacancy created is in the K-shell, then it may be filled by a transition of an electron from an outer shell into the inner shell vacancy. This results in either the emission of one of the atom's characteristic x rays or an Auger electron (which rarely escapes the sample). If an x ray is emitted and escapes the sample, it is available for spectroscopic analysis. Since all of the characteristic x rays associated with an element are well-known, it is possible to identify most of the elemental constituents of a sample through x-ray fluorescence analysis. A more detailed discussion of the technique can be found elsewhere.[3]

The next section describes the experimental equipment, including the computer-based analytical support instrumentation, and the procedures used in obtaining and reducing the data. The section entitled "Experimental Results" will present results obtained on single and dual element nitrate solutions for a range of concentrations. This section also discusses the effects that any fission product activity in the process streams will have on the determination of actinide concentrations.

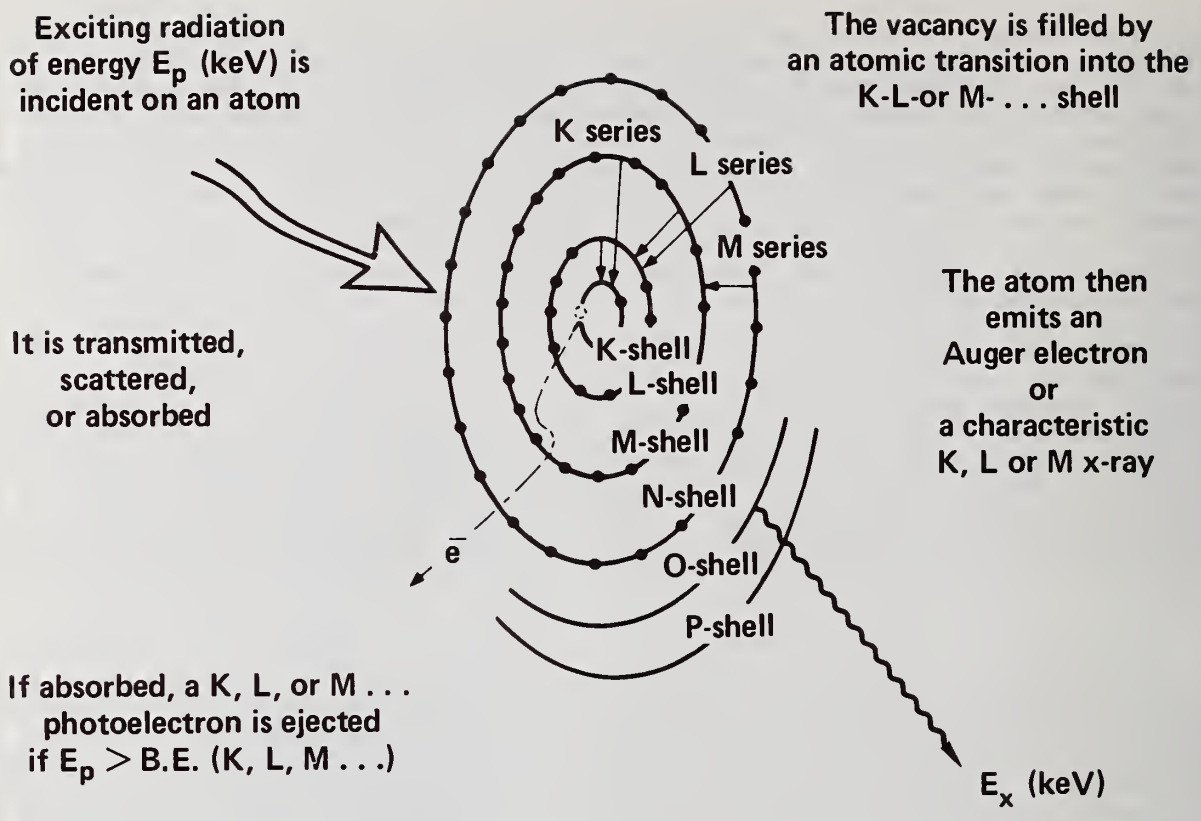

Fig. 1. A representation of energy-dispersive x-ray fluorescence analysis (XRFA). The number of electrons within a shell and the number of shells depend on the particular atom.

EXPERIMENTAL EQUIPMENT AND PROCEDURES

Excitation Source Requirements

Gamma rays can be used to excite x rays from atoms within a sample. The binding energies of K electrons in uranium and plutonium are 115.59 and 121.72 keV, respectively. Since the primary gamma ray emitted by ^{57}Co has an energy of 122.05 keV, it is an optimum exciting radiation for these two actinide elements. The exciting radiation is usually collimated in some fashion that depends on the geometry of the sample. This reduces the radiation fluorescence of, or the scatter from, nonsample materials. In the application of interest here the sample was a solution contained within a cylindrical geometry, usually a stainless steel cell. The collimated 122-keV gamma rays interact with atoms in the solution, creating x rays characteristic of those elements dissolved in the solution. A portion of the emitted x rays strike the detector, and from the energies and intensities detected the elemental concentrations in the solution can be determined.

Lithium-drifted silicon, Si(Li), is an excellent radiation detector for x rays with less than 30 keV of energy, but it becomes very inefficient for radiation detection above 60 keV. Since the K x-ray energies of uranium and plutonium extend from 94 to 122 keV, a lithium drifted or high-purity germanium detector, Ge(Li) or HPGe, is used. For this work a 10-mm deep, 200-mm^2 HPGe detector was used. It had an energy resolution of 515 ev FWHM for the 122.05-keV gamma-ray peak of ^{57}Co. Since ^{57}Co also emits 570- and 692-keV gamma rays with branching intensities of about 0.16%, as well as other weaker gamma rays above 300 keV, their intensities must be strongly attenuated by introducing shielding between the source and the detector.

Clearly, the x-ray intensity recorded by the detector increases as the sample to detector distance decreases. However, as the distance is decreased, less shielding is possible between the intense ^{57}Co sources and the detector. The higher energy gamma rays, which pass through Hevimet shielding (a tungsten alloy) and interact with the HPGe detector, create a Compton continuum that appears as a constant, energy independent background beneath the U and Pu x rays. This background contribution increases with decreasing amounts of shielding, degrading the x-ray signal-to-noise ratio. Additional high Z shielding is required around the detector housing (above the cryostat) to reduce background radiation detected from the local environment and source-air sampling. X rays from lead and Hevimet can also be excited by the source gamma rays; hence, absorbers of cadmium and copper are used as liners on the top and bottom surfaces to eliminate these x rays. A central 12.5-mm collimation hole lined with cadmium allows part of the x rays released within the sample to strike the detector.

The source-detector collimation assembly is shown in Fig. 2. It is 7.5 cm in diameter and 5.0 cm thick. Two ^{57}Co sources are collimated to create two beams. The radioactivity was electroplated onto a 1.6-mm-diameter spot on nickel foil and encased in a welded stainless steel capsule* 4.8 mm in diameter and 3.2 mm thick. The 0.37-mm thick stainless steel plate indicated in Fig. 2 is part of the bottom of a glove box, which was used when handling all of the solutions. The source-detector collimation assembly and liquid-nitrogen (LN) dewar are separate from, and located below, the glove box. It was used when handling solutions containing plutonium so that contamination would be confined in the event of a spill.

Computer-Based Analysis System

X rays emitted from the solution samples were detected by the HPGe detector, and their corresponding pulses were preamplified and routed to a Canberra 1413 amplifier and 1468A pile-up rejector. Valid output pulses were processed by a Nuclear Data ND600 pulse height analyzer (PHA). The PHA, with its own LSI-11 microprocessor, was coupled to an LSI-11 microcomputer that had a 32K 16-bit-word memory. A dual floppy disk was coupled to the LSI-11 and each disk has a 216K-byte (108K-word) capacity. Also, a dual hard disk system with a 10M-byte capacity was coupled to the LSI-11. Other system peripherals included a Hazeltine video teletypewriter terminal, an LA-180 high-speed line printer, and a Tektronix digital data plotter.

The computer and disc-based PHA capability adds a considerable amount of versatility to the experimental system. In fact, in an actual reprocessing installation a computer-based data analysis system would be essential, and probably linked to the plant's centralized computer center. This particular system allowed successive spectra to be stored on disk and permitted spectral analysis to be carried out simultaneously with data acquisition. Whatever automatic analysis sequence is desired, appropriate software can be written and stored on floppy or hard disk.

EXPERIMENTAL RESULTS

Spectra and Concentration Ranges

Pure Uranium Solutions. The present work focussed on pure uranium solution concentrations in the range from 0.6 g U/l to 180 g U/l. Earlier work[4] investigated solutions from less than 1 to almost 400 g U/l. The top spectrum shown in Fig. 3 is the result of an x-ray fluorescence analysis of 3M uranium nitrate solution at 176 g U/l concentration contained in a 25.4-mm diameter stainless steel cell with 1.7-mm wall thickness. Total analysis time was 200 live time seconds at 26% analyzer dead time using two 8.5 mCi ^{57}Co sources. The energy region extends from 0 to about 225 keV (55 eV/channel). The broad, intense peak centered at about channel 1570 is a result of the primary exciting radiation (122.05-keV gamma rays) incoherently or Compton scattering through a mean angle of 140°. The cadmium $K\alpha$ and $K\beta$ x rays appear below channel 500 and result from fluorescence of the inner wall

*Available from Isotopes Products Laboratories, Burbank, CA. Reference to a company or product name does not imply approval or recommendation of the product by the University of California or the U. S. Department of Energy to the exclusion of others that may be suitable.

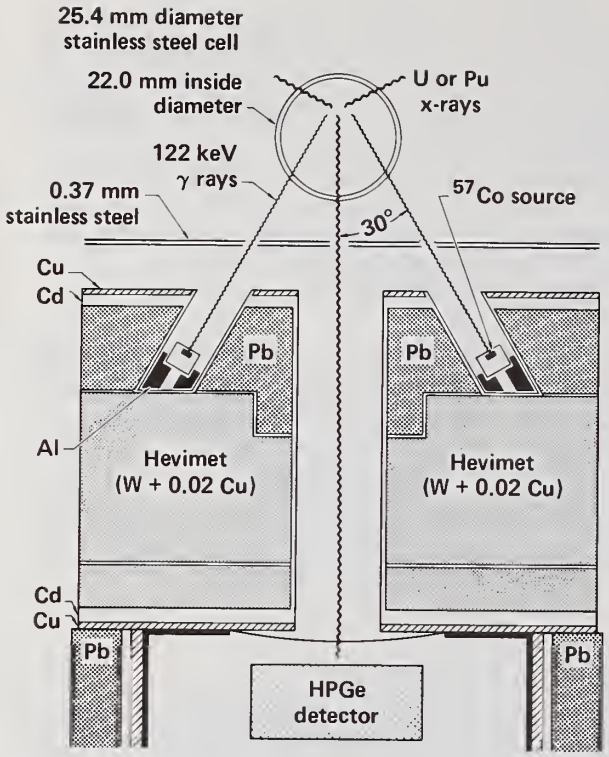

Fig. 2. A cross section of the cylindrical source-exciter and detector-collimator assembly. The stainless steel plate is part of the bottom of a glove box assembly.

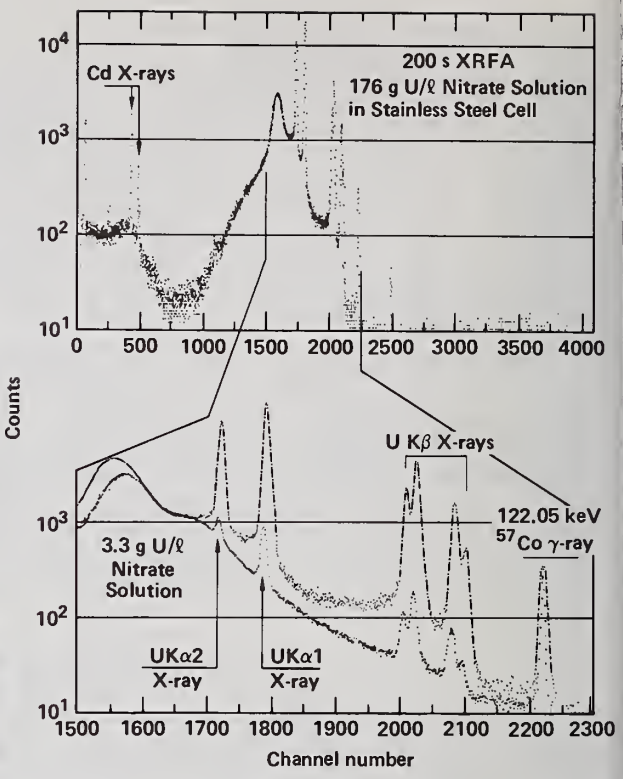

Fig. 3. The top spectrum is a 200 second, 4096-channel, XRFA of uranium nitrate solution at 176 g U/1. The solution was in a 25.4-mm diameter stainless steel cell with 1.7-mm thick walls. The lower two spectra show the 80- to 125-keV region expanded. The more intense peaks represent 176 g U/1; the less intense ones 3.3 g U/1. The broad incoherently scattered peak at 85 keV is more intense for the weaker solution.

liner (Cd) of the detector collimation shielding. Gain and zero stabilizers were used for all data obtained. The Kα Cd x ray was used for zero stabilization, while usually, the uranium Kα1 x-ray (or Kα1plutonium) was used for gain stabilization. The 122.05 and 136.40-keV gamma-ray peaks result from coherent scattering of the ^{57}Co source emissions. A nearly flat plateau of 10 counts or less exists above channel 2200. This plateau results from the Compton distribution of higher energy gamma rays (340-, 352-, 570- and 690-keV, et al.) which penetrate the Heavimet shielding and Compton scatter out of or into the HPGe detector.

The lower section of Fig. 3 shows an expanded view of the 80- to 130-keV region of two spectra, one representing 176 g U/1, the other 3.27 g U/1. The data are shown as if equivalent counting times (200s) were used for the two concentrations. Note that as the solution concentration increases, the x-ray peak intensity increases as expected, but the intensity of the incoherent scattering peak decreases. The intensity of the coherently scattered 122.05-keV peak also increases with concentration; however, most of the coherent scattering observed here occurs off of the stainless steel cell. The singlet Kα2 and Kα1 uranium x ray peaks appear at about channel 1720 and 1790, respectively; while the

Kβ x ray multiplets: (Kβ1 + Kβ3 + Kβ5) and (Kβ2 + Kβ4 + Kδ) appear near channels 2000 and 2100, respectively. Only the intensities of the Kα x rays are determined and usually only the Kα1 peak is used in establishing a calibration relationship (discussed below). The Kα1 x-ray peak contains 2.0×10^5 counts for the 176 g U/l solution; while for the 3.27 g U/l solution the Kα1 peak contains 7600 counts. This latter figure corresponds to an accuracy of 1.15% from statistics alone for a 200-second counting analysis (4-minutes clock time) through stainless steel pipe.

Pure Plutonium Solutions. The concentration range examined for pure plutonium solutions extended from 3.3 g Pu/l to 60.4 g Pu/l. The top spectrum shown in Fig. 4 is the result of an x-ray fluorescence analysis of 3M plutonium nitrate solution with 60.4 g Pu/l contained in the 25.4-mm stainless steel cell with 1.7-mm wall thickness. Total analysis time was 200 live time seconds at nearly 45% deadtime. The energy region is the same as that for Fig. 3, i.e. 0-225 keV. Note however, that the natural radioactivity arising from the plutonium isotopes and their decay products adds numerous gamma rays throughout the spectrum. The broad, intense, Compton scattered peak from the 122.05 keV exciting radiation is still prominent, but no longer dominates the spectrum. The very strong peak just above channel 1000 is the 59.53-keV gamma ray from the decay of ^{241}Am, a daughter activity of ^{241}Pu. This peak would not be nearly so intense in freshly reprocessed solutions.

The top spectrum in the lower section of Fig. 4 shows an expanded view of the 80- to 130 keV region of the 60.4 g Pu/l solution spectrum. The other spectrum is a 200s count of the solution radioactivity. It was obtained using an automatic shutter that can totally eclipse the two ^{57}Co exciting sources. The first two peaks in the radioactivity spectrum (at channels 1720 and 1760) are the Kα2 x rays of uranium and neptunium (UKα1 at 1790 and NpKα1 at 1835), which are results of the α-decays of ^{238}Pu and ^{240}Pu to ^{234}U and ^{236}U, and ^{241}Am to ^{237}Np, respectively. The complex multiplet located between channels 1865 and 1900, is a composite of the ^{241}Am 102.97-keV, ^{239}Pu 103.02-keV, ^{241}Pu 103.68-keV, and ^{240}Pu 104.24-keV gamma rays. The presence of the ^{239}Pu 98.78 keV and the ^{241}Am 98.95 keV gamma rays on the upper energy side of the uranium Kα1 x ray at channel 1790 is also clearly evident. The weak satellite located at about channel 1910 is from the Kα2 x-ray of plutonium and the 99.86-keV gamma ray from ^{238}Pu. The plutonium x ray is a result of the gamma-ray activity within the solution self-fluorescing the resident plutonium.

All of this additional x- and gamma-ray activity adds considerable complexity to the spectrum. Clearly, the complexity added will depend both on the plutonium isotopics and the age of the solution since reprocessing. Because it is impossible to know this contribution a priori, the experimental procedure, that leads to the most accurate quantitative results, is to subtract the solution radioactivity data from the XRFA data to obtain the net, externally excited, plutonium x-ray intensities. This requires two counting periods, one for solution fluorescence, a second for solution radioactivity. The length of each measurement period will be governed by the desired purpose of the measurement and the solution concentration. That is, process control concentration values need not be determined as accurately as those to be used for accountability or inventory purposes. As a general rule, if equal counting times are used for the XRFA and solution radioactivity measurements, sufficiently accurate concentration values can be obtained.

Fig. 5 shows the Kα2 and Kα1 x rays of uranium and plutonium obtained in two separate XRFA spectra, one taken of pure 60.5 g U/l; the other a result of the net (total XRFA minus solution radioactivity) XRFA spectrum from 60.4 g Pu/l. Only the 90- to 107-keV region of the spectra are shown. Both are 200s counts; however, the plutonium solution was excited 34 days after the uranium solution and has not been corrected for decay of the ^{57}Co sources. Including corrections for both the concentration difference and the half-life, the fluoresced intensity for plutonium is 2.2% greater than that for uranium. This arises primarily from the fact that the K edge of plutonium (121.72 keV) is nearer the exciting radiation (122.05 keV) than is the uranium K-absorption edge (115.59 keV). The careful observer will note near channel 1850 that the plutonium spectrum in Fig. 5, which is the difference between the two spectra shown in Fig. 4, shows more counts, yet more statistical fluctuation, than the uranium spectrum.

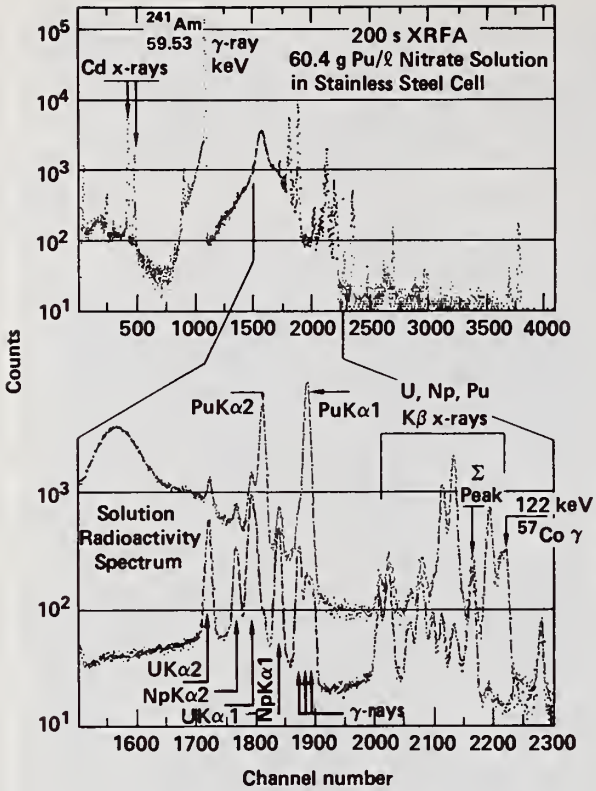

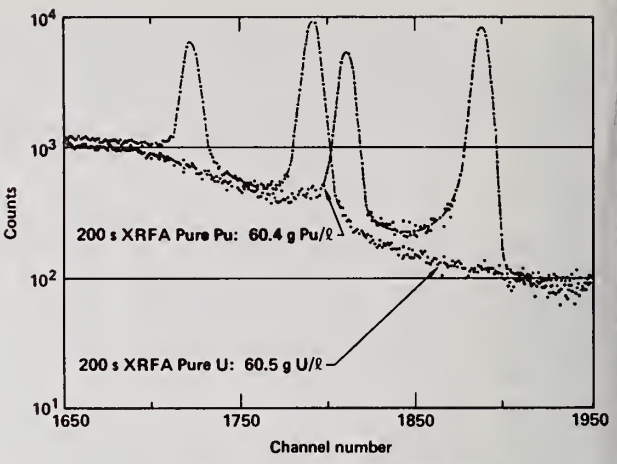

Fig. 5. Two individual spectra are superimposed for the 90- to 107-keV region. The two left most peaks are Kα2 and Kα1 of uranium, respectively; the two right most peaks are these same x rays for plutonium. The solution concentrations are nearly equal; however, no correction for exciter half-life has been applied to either spectrum. The plutonium spectrum is the difference spectrum (XRFA - activity) of the two spectra shown in the lower part of Fig. 4.

Fig. 4. The top spectrum shows an XRFA of plutonium nitrate with 60.4 g Pu/l in the stainless steel cell. The lower two spectra show an expansion of the 80- to 125-keV region for the XRFA spectrum and its natural radioactivity (two exciting sources eclipsed). The difference between the two yields the net XRFA spectrum (see Fig. 5).

Spectrum Analysis. The number of counts in an x-ray line must be determined to calibrate the XRFA technique, or deduce an unknown solution concentration once the system is calibrated. For pure uranium solutions the total or gross number of counts within a fixed channel window surrounding the Kα1 x ray can be used to calibrate[4] the system. For pure plutonium or mixed uranium-plutonium solutions this method will not yield quantitatively accurate concentrations. Instead, the net counts above the background continuum must be determined.

The peaks of interest in XRFA spectra are x rays which have a more complicated shape[5] than gamma rays. Gamma-ray peak shapes arising from germanium detectors consist of a gaussian distribution, plus short and long-term tailing components on the lower energy side of a peak. The gaussian term arises because of the statistical sharing of energy deposited between electron-hole production and phonon production (vibration or heating of the germanium crystal structure). The full width at half the maximum peak height (FWHM) of this gaussian depends on the detector capacity, peak energy, and pulse amplifying electronics. The short-term tail is a result of the intrinsic charge collection capability of a detector, which depends primarily on the germanium material quality and detector configuration (planar, coax, 5-sided). For a given detector the energy dependence of the gaussian FWHM and short term tail components is defined by measuring strong singlet gamma rays throughout the spectral region of interest. The long term tail is sample dependent, e.g. massive samples give rise to more small angle, forward scattered gamma rays than do point sources.

An x-ray peak shape includes all of the effects arising for gamma rays plus an intrinsic Lorentzian line shape, which extends symmetrically to both lower and higher energies about the peak centroid. For the U and Pu Kα x rays, the Lorentzian widths vary from 106

to 114 eV. The distribution observed in a spectrum, then, is a convolution of the Lorentzian, gaussian, and short-and long-term tailing components. Figure 6 shows the form all of these components take for the Kα2 and Kα1 x rays of uranium.

The gamma- and x-ray fitting algorithms were combined into a code called GRPANL (group analysis).[6] To determine the energies and/or intensities of one or more peaks within a spectral region, the user must specify (1) the number of peaks in that region; (2) whether they are gamma or x rays; (3) if x rays, their Lorentzian widths; (4) their approximate peak positions; (5) their intensities, or specify if they are to be determined; (6) the background slope over the region, if any; and (7) the approximate (or exact) values for the peak shape parameters (gaussian FWHM, short-and long-term tailing amplitudes and slopes). Generally, the latter are known from strong singlet gamma rays that were recorded and analyzed earlier. The energy calibration for the region is specified by entering the conversion gain (eV/channel) and the intercept energy, or by entering the energies of two strong peaks in that region. Thus, GRPANL is a code used to determine the intensities of peaks with known positions, and is not a general purpose code designed to resolve multiplets of unknown complexity.

For an analysis of the pure uranium solutions the same channel region (from 1696 to 1812) was used for all of the concentrations measured. Similarly, for pure plutonium solutions, the region from 1780 to 1910 was used, and for mixed solutions, the region 1696 to 1916 was used. A somewhat wider window was used when carrying out an isotopic analysis of the natural radioactivty spectrum.

Calibration. Sets of solution standards have been prepared using ACS grade natural uranium (for pure uranium) and plutonium metal (for the pure plutonium solutions). Sufficient HNO_3 acid was used to adjust the acid concentration to 3.0M. At least two runs and generally three were made for each concentration. All data were obtained using the same 25.4-mm stainless steel cell, which was thoroughly rinsed and dried between solution changes. A fiducial line was inscribed lengthwise on the outside of the cell. Two lucite "feet" captured and positively positioned the cell on the stainless steel floor of the glove box. These "feet" and the fiducial line on the cell allowed the cell to be accurately repositioned above the source-exciter, and detector-collimation housing.

Figure 7 shows the net counting rate (left ordinate scale) for the uranium or plutonium Kα1 x ray as a function of solution concentration (top scale). The plutonium count rate is 2.2% greater than uranium for a given concentration when corrected for half-life (the two curves are not resolved in Fig. 7). As the concentration increases, there is less than a linear increase in the count rate. This decrease in the count rate slope is a combination of increasing self-absorption of the Kα1 x ray within the solution and an effective decrease in the solution volume (penetration of the exciting radiation) as the concentration is increased. Clearly, the net count rate observed will depend on the ^{57}Co source strength ($T_{1/2}$ = 270 d), the experimental geometry, the cell or pipe wall thickness, and the HPGe detector efficiency. Furthermore, at 150 g U/l the rate of change of count rate with concentration becomes less sensitive, i.e. a 1% change in count rate corresponds to almost a 3% change in concentration for the 25.4-mm cell. The observed count rate is also sensitive to changes in geometry, and to changes in the system dead time which varies with concentration. Air bubbles in a flowing stream would also affect the observed count rate. Thus, it is not desirable to use the count rate vs concentration curve to define a calibration relationship. Rather, it is better to define one that is independent of the source half-life and system dead time; that is insensitive to minor changes in geometry and stream flow conditions; and, that is more sensitive to concentration changes with increasing concentration.

It was noted in the two spectra shown in the lower portion of Figure 3 that as the x-ray intensity increases, the 140° incoherently scattered 122-keV radiation peak intensity near 86 keV decreases. A ratio of the net Kα1 x-ray intensity to a portion of the spectrum that includes the incoherent peak is more sensitive to concentration than the count rate. The concentration in g/l can be related to this ratio through the relationship:

$$C = K\left(\frac{NK\alpha 1}{GI}\right) \qquad (1)$$

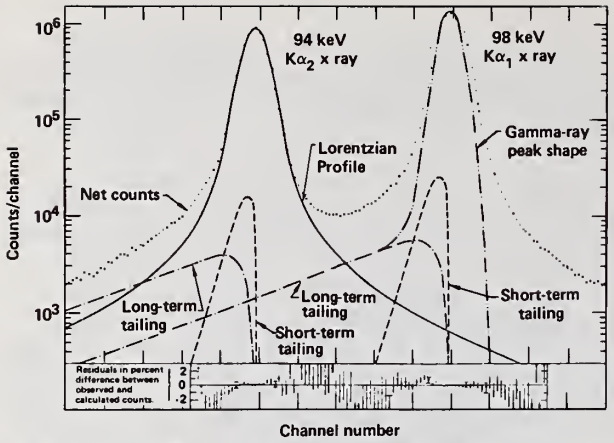

Fig. 6. The Kα2 and Kα1 x-ray peak distributions of uranium observed with a germanium detector. The x ray peaks are fit with a convolution of four mathematical functions, short and long term exponential tailing, a Lorentzian profile, and gaussian distributions.

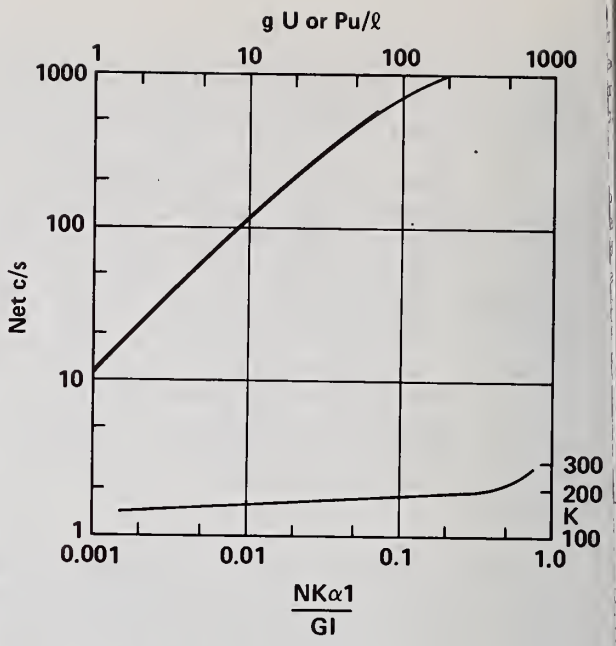

Fig. 7. A log-log plot of count rate (left) vs solution concentration (top) for single element solutions. The curve for plutonium is 2% greater than that for uranium, which is not resolved from uranium (thin line) on this plot. The lower curve shows the behavior of K (right) vs the experimental ratio (bottom). The K curves for uranium and plutonium are similar but not identical.

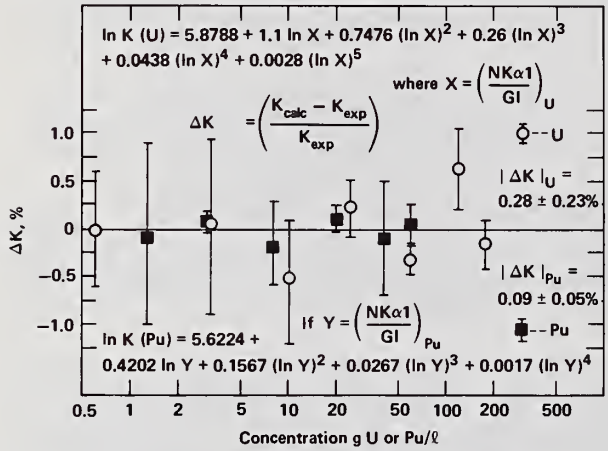

Fig. 8. A semilog plot for the residual in ΔK vs concentration for U (open circles) and Pu (filled squares). The polynomials representing K for both elements are shown as well as the average absolute value differences between the polynomial expression and the experimental data. Error bars indicate relative precision at each concentration.

where NKαl is the net number of counts in either the uranium or plutonium Kαl x-ray peak, GI is the gross number of counts in the incoherent peak channel 1500-1640, and K is a nonlinear calibration parameter having units of g/l. This ratio is independent of source exciter half-life, changes in dead time, and small changes in geometry.

The lower portion of Figure 7 shows the behavior of K (right ordinate scale) vs this ratio (lower scale) for the stainless steel cell containing a uranium nitrate solution. A similarly shaped relationship exists for the plutonium K calibration parameter. The increase in K at higher concentrations is effectively a result of increasing self-absorption of the U or Pu Kαl x rays and decreasing fluoresced volume as the solution concentration increases. A least squares fit to ln(K), expresssed as a polynomial function of the natural logarithm of the parenthetical ratio, results in the equations shown as insets in Fig. 8 at the top for uranium, and at the bottom for plutonium. Also shown is the percentage deviation between the calculated and experimental K as a function of solution concentration in the cell. The mean absolute value difference is 0.28% with a

root mean square deviation of 0.23% for uranium, and 0.09%±0.05% for plutonium. The error bar shown at each individual concentration calibration value represents the reproducability or precision obtained for 3 runs. The counting statistics obtained for the Kα1 x ray for any single run varied between 0.2% and 0.5%.

Mixed Uranium-Plutonium Solutions. The probable range of solution concentrations of interest for mixed U-Pu solutions extends from several grams per litre to perhaps several hundred grams per litre. The uranium to plutonium ratio may have almost any value but for this study was confined from 2.3 to 1 to 7.0 to 1. Table I lists the range of solution concentrations measured for three different uranium to plutonium ratios, and indicates in parentheses the estimated concentration error made in solution preparation. Both stock solutions were 3M nitrate solutions. The estimated errors vary from 0.1% for the most concentrated solution to just over 1% for the weakest solution.

TABLE I. RANGE OF MIXED SOLUTION CONCENTRATIONS MEASURED

2.33:1		3.5:1		7.0:1	
U (g/l)	Pu	U (g/l)	Pu	U (g/l)	Pu
		3.51(4)	1.00(1)		
10.49(6)	4.50(3)	10.53(5)	3.00(2)	10.08(7)	1.46(1)
35.00(12)	15.01(5)	35.10(6)	10.01(4)	41.94(13)	6.05(4)
70.00(26)	30.02(9)	70.20(23)	20.02(6)	69.81(24)	10.07(7)
		105.3(3)	30.02(8)		
		140.4(4)	40.03(10)		
		175.5(2)	50.04(5)		

a) The maximum estimated error made in the solution preparation is shown in parentheses.

Three 90- to 107-keV spectra are shown in Figure 9. The top spectrum represents a 1000s XRFA of a nitrate solution containing 175.5 g U/l and 50 g Pu/l. The middle spectrum represents a 1000s spectrum of the solution radioactivity obtained by eclipsing the two excitation sources. This complicated spectrum contains a total of 16 gamma and x rays within a 10 keV region and suggests why an accurate quantitative analysis of the top spectrum is very difficult. The lower spectrum is the difference between the top two spectra, that is, the net fluoresced intensities of the uranium and plutonium Kα x-rays. Note that the neptunium x rays seen in the upper spectrum are completely absent in the lower spectrum. Their presence in the upper spectrum is solely a result of the solution radioactivity being counted simultaneously with the fluoresced activity. It is necessary to use GRPANL on the lower spectrum to correctly resolve UKα1 from PuKα2 seen near channel 1800. For all mixed solutions the same region (channel 1696 to 1916) was analyzed.

The top two spectra shown in Figure 9 were accumulated for counting times that might be used for an accountability measurement. The total clock time required for both measurements was about 45 minutes, and the resulting accuracy in the peak area determinations for the difference spectrum is under 0.3% for UKα1 and about 0.4% for PuKα1. Thus, results accurate to better than 0.5% can be obtained for high concentration solutions in less than one hour, and without the necessity of doing any off-line analyses. In the event process control information were needed for such a concentrated mixture, an entire measurement would require no more than ten minutes, i.e. a 100s live time fluorescence count and a 100s radioactivity measurement, plus analysis time. The overall accuracy of the concentrations determined would then be of the order of 1%.

The top spectrum shown in Figure 10 represents a 500s fluorescence of a mixture containing 35.1 g U/l plus 10 g Pu/l. Once a solution's total actinide concentration falls below 50 to 60 g/l, the spectral region containing the U-Pu x rays of interest cannot be accurately analyzed by GRPANL unless a distribution for scattered radiation from pure nitric acid is subtracted from the fluoresced data. The intensity distribution of the incoherently scattered exciting radiation in the vicinity of the uranium and plutonium x rays decreases by more than a factor of ten within 12 keV, and does so with a steep, compound exponential

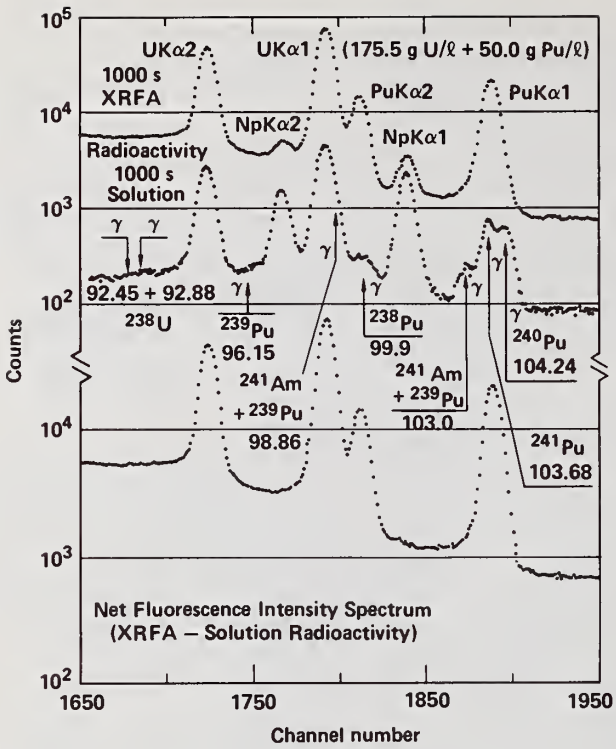

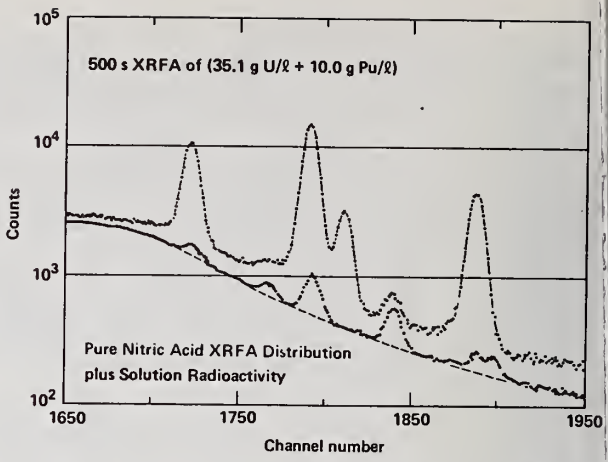

Fig. 10. Two 90- to 107-keV region spectra of a mixed U-Pu nitrate 35.1 g U/l plus 10.0 g Pu/l. Analysis of the top spectrum alone may yield concentration values sufficiently accurate to control the process chemistry. The lower spectrum is a sum of the solution's natural radioactivity plus a 450s spectrum of pure nitric acid (dashed line continuum).

Fig. 9. Three 90- to 107-keV region spectra of mixed U-Pu nitrate with 175.5 g U/l plus 50.0 g Pu/l. The top spectrum would provide sufficient accuracy for an accountability measurement. The middle spectrum shows the solutions natural radioactivity. The top spectrum minus the central spectrum results in the lower spectrum, the net XRFA of the mixture.

slope (see also Figure 3, the 3.2 g U/l spectrum). The shape resulting from the scattered exciting radiation for pure nitric acid is represented by the continuum level (dashed lines) in the lower spectrum.

The peaks that appear in the lower spectrum of Figure 10 are a result of adding the 500s solution radioactivity spectrum to a pure nitric acid distribution. GRPANL was used to determine the net uranium and plutonium x-ray intensities on a spectrum (not shown) which is the difference between the upper and lower spectra shown. The statistical accuracy in the channel to channel data in the difference spectrum (not shown) will not be the same as that of the original data, particularly in non-peak regions, e.g. above channel 1900. Thus, in order to obtain a realistic chi squared value from the GRPANL fit, a constant is added to the entire region. The constant added has a standard deviation equal to the mean value of the standard deviations for the average number of counts in the pre- and post-background regions (i.e. 1686-1695 and 1917-1926).

The 500s live-time XRF spectrum shown in Figure 10 represents the amount of time that might be used for a process control measurement of solutions having median value uranium-plutonium concentrations. If the typical 20% analyzer dead time is included, the XRFA measurement would require 10 minutes (clock time), and would yield concentration values accurate to about 2%, even without making a quantitative correction for the solution radioactivity. That is, in order to control the chemical process it may be sufficient to determine the solution concentration to only a few percent. This assumes that the plutonium isotopics do not vary widely from day to day (or batch to batch). However, for accountability or inventory control measurements where better accuracy is required, the solution radioactivity must be measured and the more exact quantitative procedures described above used. Accountability measurements cannot be done as quickly as those for process control; and generally, will also require replicate analyses.

Calibration of Mixed Solutions. Just as was done for the pure uranium or plutonium solutions, it is possible to determine a calibration parameter, K, for the mixed solutions. However, because the U/Pu ratio can vary, K will be valid only for a single value of the uranium to plutonium ratio. Seven of the 13 solutions measured (see Table I) had a concentration ratio of 3.5 to 1, thus K was evaluated for this ratio. The smooth curve shown in the top portion of Figure 11 shows the behavior of K versus the ratio of the net counts contained in both the uranium and plutonium Kα1 x rays to the area of the gross incoherent peak (channels 1500-1640). Note that the numerator of the abcissa now contains the total actinide Kα1 x-ray intensity. The resulting polynomial for ln(K) is shown as an inset in the top most graph of Figure 11. The fit of this expression to the experimental data is shown in the lower graph of Figure 11. The mean for the absolute values of the differences is 0.18±0.27%. The error bars shown for each point represent the reproducibility obtained for 3 runs; while for any single run of any mixture, better than 0.6% counting statistics were obtained in NPuKα1, and better than 0.3% for NUKα1.

The uranium to plutonium ratio is not always 3.5. Nevertheless, the total actinide concentration may be obtained from the calibration parameter polynomial after a small correction is applied. The necessity for this correction depends on the U/Pu ratio. Clearly, for solutions containing unknown concentrations of U and Pu, their ratio is also unknown. However, because their fluorescence efficiencies, their Kα1 x-ray energies, and their absorption coefficients are very nearly equal, their actual concentration ratio is nearly equal to the ratio of their experimental count rates. The top graph in Figure 12 shows that the observed U/Pu count rate ratio increases linearly with the ratio of concentration of U/Pu. This linear relationship holds true over the range from U/Pu = 2.3 to U/Pu = 7, the concentration ratios range examined in this study. That is,

$$[U/Pu]_{conc.} = 1.046 \left(\frac{NUK\alpha 1}{NPuK\alpha 1} \right) \tag{2}$$

The approximate total actinide concentration can be determined from the calibration polynomial shown at the top of Figure 11. Then, a small correction is applied. That correction in percent is given by ΔP, and its behavior vs concentration ratio is shown in the lower graph of Figure 12. This correction is positive for all U/Pu ratios greater than 3.5 (i.e., K yields too small of a total actinide concentration) or negative for all ratios of U/Pu less than 3.5. Thus, the total actinide concentration is given by

$$C(U + Pu) = K \left[\frac{NUK\alpha 1(U+Pu)}{GI} \right] \left(1 + \frac{\Delta P}{100} \right) \tag{3}$$

where

$$\Delta P(\%) = -1.98 + 0.59 \left(\frac{NUK\alpha 1}{NPuK\alpha 1} \right) \tag{4}$$

The individual plutonium and uranium concentrations are given by

$$C(Pu) = \frac{C(U+Pu)}{\left[1 + 1.046 \left(\frac{NUK\alpha 1}{NPuK\alpha 1} \right) \right]} = \frac{C(U+Pu)}{(1+R)} \tag{5}$$

and

$$C(U) = \frac{R}{(1+R)} \left[C(U+Pu) \right] \tag{6}$$

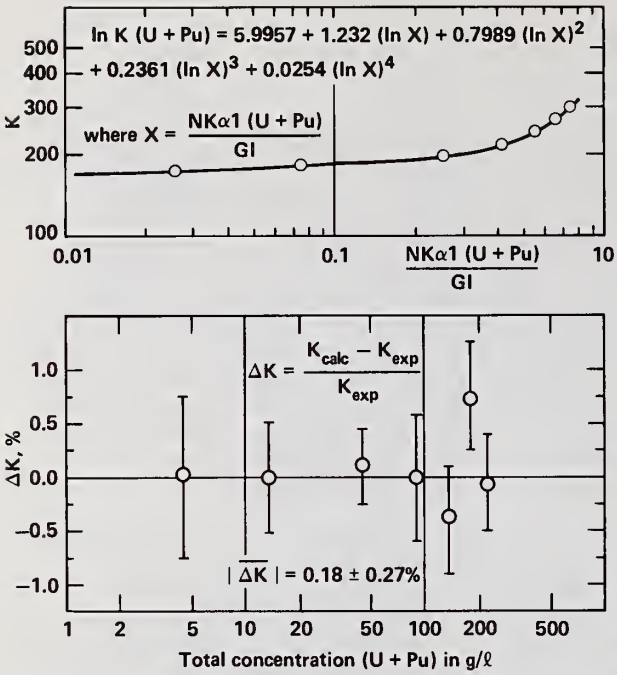

Fig. 11. The upper graph shows the K calibration parameter vs experimental ratio for mixed solutions having U/Pu = 3.5/1. Note that the polynomial expression is based on the sum of the net x ray peak intensities of uranium and plutonium. The individual error bars indicate reproducibility resulting from three individual runs.

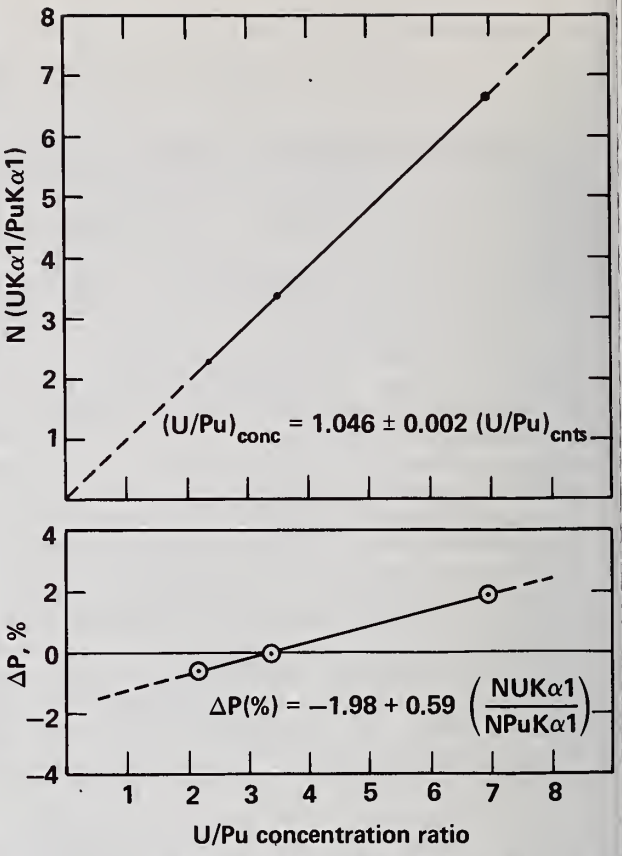

Fig. 12. The upper graph shows a linear relationship between observed U/Pu net counts and actual U/Pu concentration. The lower plot shows the correction factor ΔP that must be applied to the concentration value vs the U/Pu concentration ratio.

It is clear that the linear relationships shown in Fig. 12 will not necessarily hold for very large ratios (greater than 20/1) or very small ratios (less than 1). To insure validity of the XRFA method, it must be calibrated over the entire range of concentrations and elemental ratios that are expected to occur.

Dynamic Concentration Measurements. One of the advantages offered by the nondestructive XRFA technique is its ability to yield concentration values for flowing streams. Appropriate precautions must be taken to insure that the stream will not be subject to foam or sporadic air bubbles at the measurement location. In the earlier work[4] detailed experiments were carried out to demonstrate the techniques ability to make dynamic concentration measurements. Here, only a summary of those results will be presented.

The top section of Figure 13 shows a set of 24 measurements. The first and last six measurements were made with the solution static, while the central 12 measurements were made with the solution flowing at 80 1/h. The static and flow results overlap well within the precision of their standard errors. The flow system consisted of a reservoir and tygon tubing connected to a 25 mm diameter pyrex cell and a peristaltic pump. The pump forced the solution to circulate through the tubing and cell and return to the reservoir by a cylical squeezing action. Once a known volume of a specific concentration is introduced into a dry cell and tubing system, additional small volumes of pure acid or of a more concentrated solution will change the initial concentration accordingly.

The lower section of Figure 13 illustrates a dynamic concentration measurement. Initially, 100.0 ml of the 100.0 g U/l standard solution was introduced into the flow system with the cell and tubing dry. Appropriate volumes of 3M HNO_3 were calculated and measured out, then introduced at regular intervals into the flow system. This caused a concentration reduction of exactly 1.0 g U/l for each of five times. Then, appropriate volumes of more concentrated uranium nitrate solutions were introduced to increase the solution concentration 2.0 g U/l for each of three steps. This brought the concentration to about 101 g U/l, whereupon a final calculated volumetric addition of 3M HNO_3 returned the solution to its original 100.0 g U/l concentration.

The pause time of 100s was selected on the basis of earlier dynamic concentration runs. It was somewhat longer than the time required for the solution volume to reach equilibrium after introduction of an additional volume. Each 100s analysis had approximately the same statistical accuracy of $\pm$0.53%; however, the mean values and precisions indicated at each successive concentration are determined from just the measurements made within that interval. Note that the mean of the first and last five dynamic concentrations measurements is 100.05$\pm$0.63 g U/l, in excellent agreement with the mean value of 100.13$\pm$0.40 g U/l from the first 24 static/flow cycle measurements.

Fission Products in Product Streams. It is possible that additional levels of radioactivity might be associated with the reprocessed actinide products. These activities might be purposely added (e.g. ^{60}Co or ^{238}Pu), or they could be fission products, which were not completely separated during the earlier stages of chemical purification. It is beyond the scope of this report to discuss the relative advantages or disadvantages of adding such spikes. Suffice it to say that if significant levels of activity are found in the process stream and product forms - solutions or oxides, then many of the nondestructive analytical techniques, which have required years of development time and at significant costs, may not be useable. For the purposes of this study, a simple experiment was conducted in order to evaluate the behavior of the XRFA technique to additional levels of activity in the process or product streams.

In order to simulate fission product activity in the stainless steel cell, 4.8 mCi of ^{137}Cs activity was chemically prepared in nitric acid solution, and loaded into the same cell as that used to count the pure and mixed actinide solutions. For the counting geometry used throughout these experiments, this activity represented very nearly the limiting count rate that the non-optimized commercial electronics could process. The system dead time approached 70%. The lower spectrum in Fig. 14 shows a 500s XRFA of the 90- to 107-keV region of a 10.5 g U/l plus 4.5 g Pu/l mixed solution. The top spectrum represents a 500s count of this solution plus 4.8 mCi of ^{137}Cs activity. Thus, assuming that there were no fission product gamma rays within the 90- to 107-keV region, the major effect of fission product activities on XRFA in process or product streams is to raise the background continuum level in the region of the x-ray peaks of interest, but the x rays can still be analyzed accurately. The top spectrum, then, corresponds to a solution containing 10.5 g U/l, 4.5 g Pu/l, and 27.7 mCi/gPu of fission product gamma-ray activity. Since the system's counting electronics were very near their maximum count rate limit, any further increase in the stream's uranium or plutonium concentration would lock-up or shut-off the electronics. Therefore, if higher plutonium solution concentrations were expected, then the decontamination factors in the earlier stages of separation would have to be improved. That is, a solution containing about 150 g U/l and 45 g Pu/l could be counted if it contained less than 2.8 mCi of fission product activity per gram of plutonium.

Relative Isotopic Abundances. The absolute abundance of each of the plutonium isotopes, except ^{242}Pu, can be determined from measurements of the solution radioactivity and concentration. A radioactivity measurement is made when an automatic, horseshoe shaped shutter is activated to eclipse the two exciting sources. The ultimate purpose of, and thus the accuracy required from, the isotopic abundance measurement will govern the measurement time. For example, a 1000s XRFA and solution radioactivity measurement of a 175 g U/l plus 50 g Pu/l solution was sufficiently long enough to accurately determine its concentration for accountability or inventory control purposes (see discussion above).

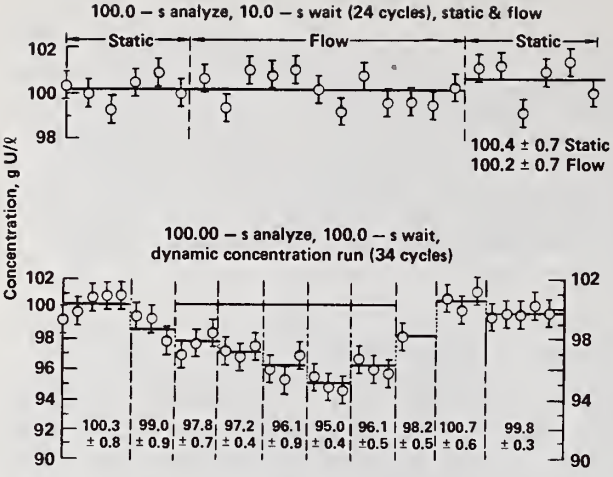

Fig. 13. Two plots of solution concentration vs time. Analysis and pause times vary. The first and last six measurements were made with the solution static, the center 12 with it flowing. The lower set is a dynamic concentration run (see text). The error bars indicate 1 σ statistical counting accuracy only

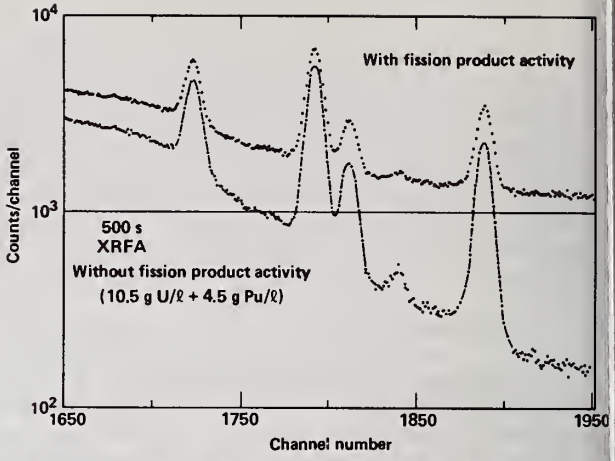

Fig. 14. Two 90- to 107-keV spectra with (upper spectrum) and without (lower spectrum) fission product activity within the solution. The mixed U-Pu solution has a concentration of 10.5 g U/l plus 4.5 g Pu/l. Nearly 30 m was required to record the upper spectrum because of excessive dead time caused by the fission product radioactivity (28 mCi/g Pu).

However, if the isotopic abundances of the same solution were also desired to an equivalent accuracy (sub 0.5%), then the 1000s radioactivity measurement time is insufficient. This arises not because of a lack of solution radioactivity, but because the HPGe detector is almost an order of magnitude further away from the sample than it need be, a result of the shielding required for the XRFA measurement. If an additional detector were located immediately adjacent to the pipe, the activity count rate would be considerably greater. Thus, an optimum system for an on-line accountability measurement of the final product might consist of two detectors, one devoted to XRFA, the other optimized to determine the relative isotopic abundances from the solution radioactivity. The computer-based analyzer system could be programmed to control both detector systems, their measurements times, and all data reduction required for both analyses.

SUMMARY

The experimental results discussed above have demonstrated that energy dispersive x-ray fluorescence analysis (EDXRFA) can determine the concentration of uranium, plutonium, or mixed uranium-plutonium solutions in flowing or static streams. The EDXRFA technique is nondestructive and can be adapted directly to pipelines in facilities that have process or product streams containing these actinide elements. The technique can also be used to make off-line measurements. By using an automatic shutter to eclipse the exciting radiation, the natural radioactivity of the solution mixture can be measured. Thus, the relative plutonium isotopic abundances can be determined for plutonium solutions; while for uranium solutions, the degree of enrichment in ^{235}U can be deduced after calibration of the system.

The time required for the measurement depends on the purpose of the measurement and the concentration of the solution. Generally, measurements made to control or monitor the process chemistry need not be made as accurately as those for accountability and inventory control. Typical analysis times for process control information are from 100 to 500 seconds for solution concentrations from several hundred to a few grams per liter, respectively. Longer measurement times are required for inventory control purposes where accuracies better than 1% are desired. The XRFA method is capable of yielding such accuracy if it is carefully calibrated and reproducible counting geometry is maintained.

For concentrated solutions containing mixed uranium and plutonium, the contributions to the uranium x-ray intensities from plutonium decay and to the plutonium x-ray intensities from its gamma-ray activities must be removed. This is accomplished by subtracting (via the computer) the solution radioactivity spectrum from the XRFA spectrum. Then, the unknown uranium to plutonium concentration ratio is determined from the net intensities of their x rays, and the individual concentrations are calculated from simple expressions. Thus, accountability measurements may require from one to two hours, the longer times being required for the weaker concentrations. But, since on-line results can be obtained automatically, and without any personnel-sample interaction, the method should still be cost-effective.

Finally, actinide solution concentrations can be measured, even if a small amount of fission product radioactivity exists in the product solution. The limiting factor is the maximum count rate that the electronics can handle. The actinide x-ray intensities stimulated by the 122-keV exciting radiation from ^{57}Co are sufficiently intense to be seen above low levels of fission product background continuum; and the x-rays can be analyzed without a sacrifice in measurement accuracy, even for relatively low solution concentrations. In conclusion then, this technique should prove to be of great interest to enrichment facilities and to spent nuclear fuel reprocessing facilities in which single or dual element actinide solutions must be measured or monitored for concentration and isotopic content.

REFERENCES

1. W. D. Ruhter and D. C. Camp, "Nondestructive Assay of Mixed Uranium Plutonium Oxides by Gamma-Ray Spectrometry," UCRL-52625 (1979).

2. R. Gunnink, J.B. Niday, A. L. Prindle, W. D. Ruhter and D. C. Camp, "Determination of Plutonium Isotopics by Gamma-Ray Spectrometry," UCRL - Publication in preparation (1980).

3. D. C. Camp, "An Introduction to Energy Dispersive X-Ray Fluorescence Analysis," UCRL-52489 (1978).

4. D. C. Camp, W. D. Ruhter, and S. Benjamin, "Nondestructive, Energy Dispersive X-Ray Fluorescence Analysis of Product Stream Concentrations from Reprocessed LWR Fuels," UCRL-52616 (1979).

5. R. Gunnink, "An Algorithm for Fitting Lorentzian-Broadened, K-Series X-Ray Peaks of the Heavy Elements," UCRL-78707 (1976).

6. R. Gunnink and W. D. Ruhter, "A Generalized Computer Code for Resolving Overlapping Gamma-Ray and X-Ray Peaks - GRPANL," UCRL Report in Preparation (1980).

Discussion:

Canada (LASL):

XRF has been around for a long time and people know it works. It's nice to see that one can get a signal both into and out of a pipe; however, the traditional problem with XRF has been sample preparation. That is, knowing what the sample self-attenuation is for the ingoing and outgoing channels. Certainly, if this is going to be a Safeguards tool, you have not addressed that problem. That is, with nice clean solutions you can obtain a calibration curve that will work for those solutions. However, if you start changing the sample matrix by adding other ions or changing the plutonium to uranium ratio, your calibration curve will no longer apply.

Camp (LLL):

You have raised two points. First, sample self-absorption; and second, unexpected changes in sample matrices. First, the calibration parameter, K, that I described does, in fact, account for attenuation in the input exciting radiation and for sample self-absorption in the emitted x-rays. Therefore, for a reprocessing plant's final product solution that is relatively stable in its day to day output form, including being free of sedimentation, I believe the EDXRFA technique as I have described it, and calibrated it with working standards, will be applicable for Safeguards accountability purposes.

Your second point is well made. In a real-life processing plant environment, there may be day to day variations in the process chemistry that will lead to variations in acid stream molarity sedimentation, changing fission fraction content, and other unexpected changes in the solution matrix form. Admittedly, the experimental work we have done so far has been done with "controlled" laboratory solutions. We are already aware of how certain variables affect the concentrations obtained by EDXRFA; and in fact, have reported on them (see reference 4).

We are looking forward to the offline test of our technique to be conducted on JB line solution samples at the Savannah River Plant in calendar year 1980. We may encounter just the kind of variable sample matrix effects you allude to during those tests. If so, we will simply have to deal with them, that is, try to understand them; and seek appropriate corrections for their effects on the concentration values obtained from the calibration equations.

Canada:

May I just add one more comment. The measurement techniques we develop in Safeguards must not take the operator's word for what, in fact, is or is not in a solution. That is why it is important that the measurement techniques developed be as matrix independent as possible, or that we know what the matrix effects are and how to correct for them analytically.

Harlan (Rockwell-Rocky Flats):

If we had a clean solution for the application of your technique at a much lower concentration, say 10^{-2} to 10^{-3} grams per liter of plutonium, with americium concentrations from 20% to 100% of the plutonium concentrations, would your technique be usable?

Camp:

Quantitatively, we have focused on solution concentrations from a half a gram per liter, up. Clearly, with this technique, you excite atoms that are in the solution stream, and the less atom density you have in the stream, the less x-ray signal you are going to get. If you want to count long enough, yes, you could obtain positive results for those small concentrations. However, I don't believe it would be very effective with K x-ray excitation. Perhaps it could be done more efficiently using L x-ray excitation.

On the other hand, I think there are a lot of techniques being developed now which are much better suited to measure 10^{-2} to 10^{-3} gram per liter concentrations. These are concentration levels that you might expect to find in a waste stream or an aqueous or organic process recirculating stream. As far as the americium content goes, their K-x-rays are not excited by the 122 keV Co^{57} radiation. If americium is present we must introduce cadmium absorbers to attenuate the 59.53 keV gamma-ray in order to prevent pileup effects, and bring the deadtime to reasonable levels.

Brodda (NRC-Juelich):

Did I understand correctly that, in case of the simultaneous determination of uranium and plutonium, you consider the plutonium $K\alpha_1$ line and unfold the plutonium $K\alpha_2$ and uranium $K\alpha_1$ lines for the uranium determination?

Camp:

That is correct. In the case of mixed solutions, we determine the $K\alpha_1$ x-ray intensity for both uranium and plutonium intensity. In order to get the $K\alpha_1$ of uranium, we must unfold the $K\alpha_2$ of plutonium.

Brodda:

Why don't you just use the $K\alpha_2$ of uranium? It seems to be without interference.

Camp:

There is no reason you cannot do as you say. For these x-rays the intensity ratios are about 0.6 of a unit for $K\alpha_2$ to one unit for $K\alpha_1$. In fact, you could use them both in order to create a calibration curve if you wanted to. There is no reason you can't. It is just that you obtain better counting statistics with lower background for the $K\alpha_1$ uranium x-ray.

Experimental U-233 Nondestructive Assay With a Random Driver

by
Paul Goris
Hanford Engineering Development Laboratory, Richland, Washington

ABSTRACT

Nondestructive assay (NDA) of U-233 in quantities up to 15 grams containing 7 ppm U-232 age 2 years was investigated with a random driver. A passive singles counting technique showed a reproducibility within 0.2% at the 95% confidence level. This technique would be applicable throughout a process in which all of the U-233 had the same U-232 content at the same age. Where the U-232 content varies, determination of U-233 fissile content would require active NDA. Active coincidence counting utilizing a Pu-238, Li neutron source and a plastic scintillator detector system showed a reproducibility limit within 15% at the 95% confidence limit. The active technique was found to be very dependent on the detector system resolving time in order to make proper random coincidence corrections associated with the high gamma activity from the U-232 decay chain.

KEYWORDS: U-233 decay chain; random coincidence corrections

INTRODUCTION

The Hanford Engineering Development Laboratory (HEDL) is operated by the Westinghouse Hanford Company for the United States Department of Energy, Richland, Washington, under contract DE-AC14-76FF02170. Operations include a fast breeder fuels development and fabrication laboratory, analytical chemistry laboratories, a safeguards facility, and other supporting activities. A Fast Flux Test Facility (FFTF) which is the primary test facility for development of the Fast Breeder Reactor (FBR) for electrical power generation is nearing start-up. A Fuels and Materials Examination Facility (FMEF) is under construction. The FMEF will examine irradiated fuel and test material specimens from FFTF operations and provide the technical base for economic production of large quantities of fast breeder reactor fuel. These facilities will also be operated by HEDL.

Fissile materials associated with HEDL operations include PuO_2 and enriched UO_2 feed, mixed oxide powder and pellets, fast breeder reactor fuel pins, fuel bundles, and fissile scrap and waste. Investigation of alternate fuel cycle Source Nuclear Materials (SNM) will require handling of U-233 with significant quantities of U-232, spiked fuels, and incompletely reprocessed (CIVEX) fuels.

A number of existing NDA instruments and techniques applied for safeguards measurements in the uranium-plutonium fuel cycle will find very limited use in alternate fuel cycles. Consequently, further development of NDA techniques and instruments is required for safeguards accountability in alternate fuel cycle programs.

Alternate fuel cycle NDA evaluations at HEDL were initiated with U-233 assay by means of a random driver. $^{233}UO_2$ (7 ppm U-232, 2 years since purification) standards were prepared ranging from 1 to 15 grams for this work. These evaluations were undertaken from an experimental standpoint in anticipation of FMEF operational requirements. The intent was not to emphasize any particular NDA instrument, but to become familiar with those techniques and instruments which may find use in alternate fuel cycle programs.

U-233 NDA RESTRICTIONS

Nondestructive assay of U-233 is complicated due to a low spontaneous fission factor limiting passive coincidence counting techniques; low thermal energy release limiting calorimetry

and intense gamma radiation due to U-232 daughters. The latter restriction is very significant when employing NDA techniques dependent on gamma sensitive detection systems.

Figure 1 gives a gamma ray spectrum of U-233 containing 250 ppm U-232 ten years after purification.[1] All of the peaks indicated result from the U-232 decay chain. Of particular concern is the 2.61 MeV Tl-208 peak which accounts for essentially all of the intense gamma radiation associated with U-232.

The spectrum of Figure 1 was observed with a GeLi detector having a total volume of 54 cc, efficiency of 9%, and a resolution of 2.3 keV at 332 keV.

None of the principal gamma peaks of U-233 are visible in this spectrum. NDA of U-233 by direct measurement of its gamma ray peaks would be quite difficult in the presence of U-232 gamma rays even if the U-232 content and purification history are known.

The buildup of gamma activity due to U-232 daughter growth can be seen in Table I. These data are based on cylindrical geometry with contact at the bottom of a thin iron container.

TABLE I

BUILDUP OF U-232 CHAIN GAMMA ACTIVITY PER GRAM U-233

U-232	Rad/Hr at Contact			
ppm	Zero	25 d	1 yr	10 yr
10	0.002	0.020	0.195	0.575
100	0.005	0.158	1.90	6.50
1000	0.006	1.52	18.90	56.50
5000	0.140	7.65	94.20	282

In high gamma radiation fields, detector systems show saturation. Plastic scintillator detectors of the HEDL random driver are reasonably linear at count rates up to $\sim 10^6$ cps corresponding to ~30 mrad/hr. Experience at the Los Alamos Scientific Laboratory indicates that gas proportional neutron detecting tubes begin to show bias and saturation effects as gamma intensity approaches ~1 rad/hr.[2] Reasonably accurate NDA in high gamma radiation fields can be dependent on adequate sample shielding.

RANDOM DRIVER NDA

Earlier NDA investigations with random drivers are indicated by the references.[3,4,5,6,7] A random driver ordinarily employs ^{238}PuLi or ^{241}AmLi (α,n) neutron sources to induce fissions in the fissile material within a sample; hence, it "drives" the sample. Since the neutrons emanating from the source have energies below the fission threshold of fertile materials, the technique is insensitive to ^{232}Th and ^{238}U content in a sample. However, the source energy is high enough to achieve the penetrability required for assaying samples of high fissile mass, i.e., the problem of sample self-shielding is minimized.

The "randomness" of the driver pertains to the nature of the source, i.e., alpha-decay is purely random in time, and since one neutron only is emitted per (α,n) reaction with Li, the neutrons produced are also random and therefore not correlated with one another. This characteristic enables multiple fast neutron scintillation detectors to distinguish noncorrelated source neutrons from fission-produced neutrons which have high probabilities of being detected within a short coincidence interval, typically 35 nanoseconds.

In addition to the activation mode described above, commercial random drivers may also include passive singles and passive coincidence counting modes.

The HEDL random driver built by the National Nuclear Corp. of Redwood City, California, is illustrated by Figure 2. The instrument utilizes a ^{238}PuLi (α,n) neutron source providing 10^6 neutrons per second. Radially adjustable detector and source housing mounts enable well diameter variations from 4 to 19 inches.

U-233 GAMMA RAY SPECTRUM

250 PPM U-232 10 YEARS AFTER PURIFICATION

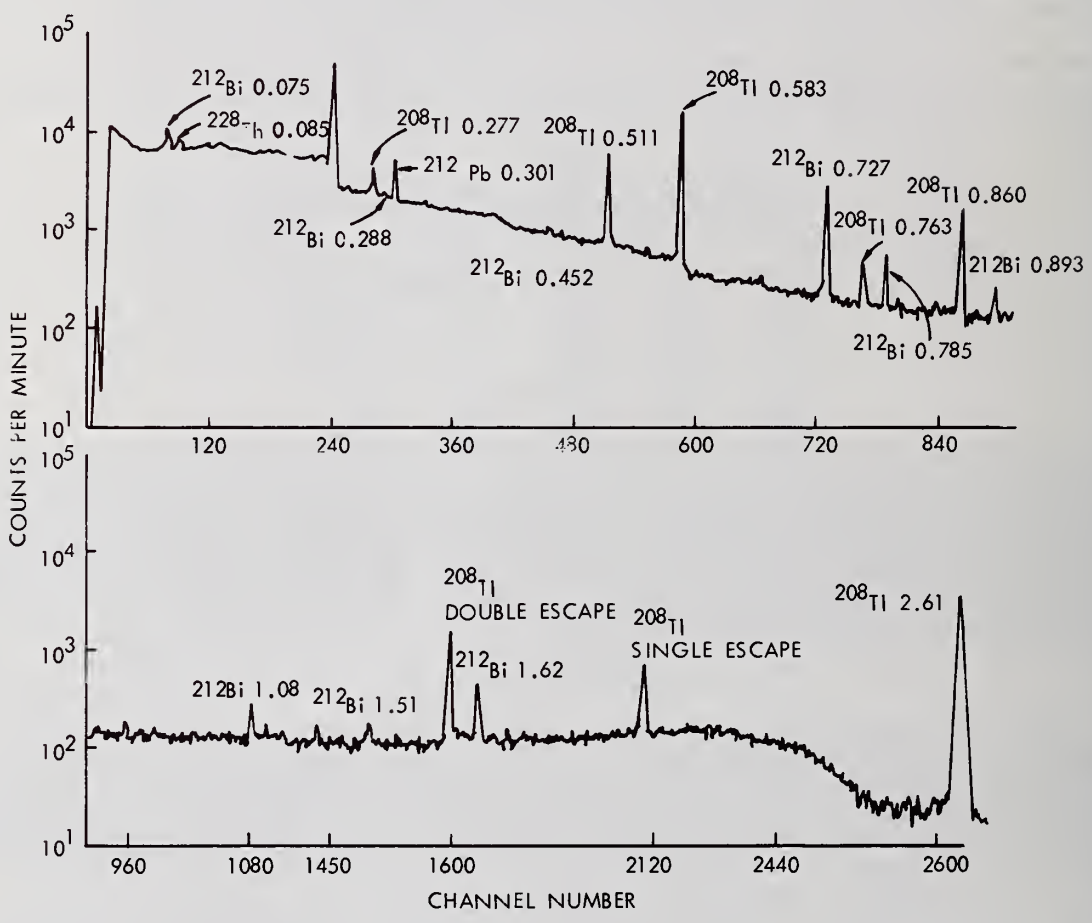

Fig. 1. U-233 Gamma Ray Spectrum Showing Dominance of U-232 Decay Chain Gamma Emitters.

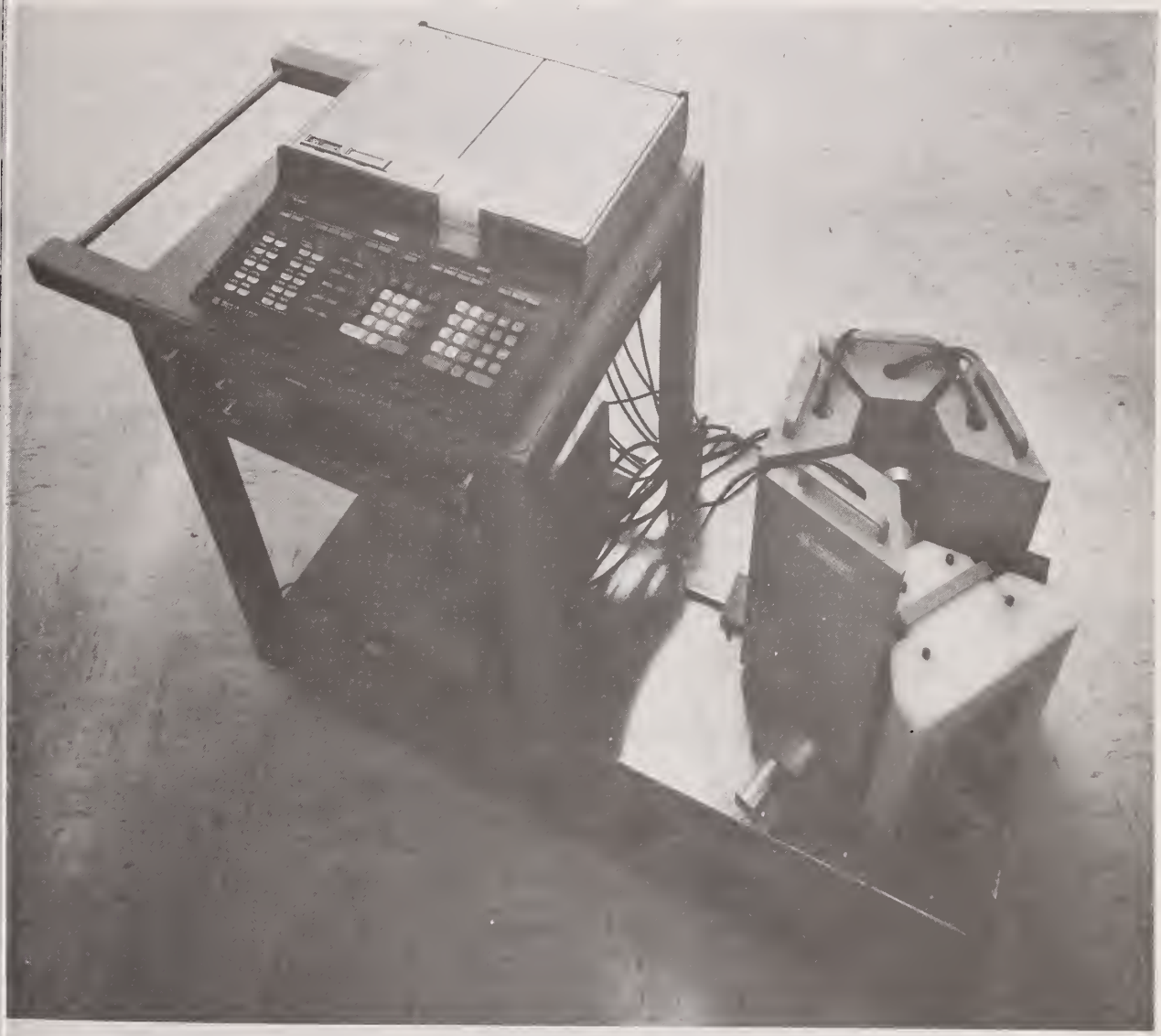

Fig. 2. HEDL Random Driver.

The instrument was designed as a versatile assay machine, capable of measuring plutonium and uranium quantities over a wide range. Its primary function is to measure milligram to gram quantities of Pu fissile, Pu-240, U-235, and U-233 contained in cans with outer dimensions of 3-1/2 inches in diameter and 3-1/3 inches in height. These dimensions are associated with the majority of SNM containers used throughout HEDL operations.

The HEDL instrument is capable of singles counting modes involving 1 to 4 detectors, and coincidence counting modes of (2 of 2, 3, 4), (3 of 3, 4), and (4 of 4) where the first figure in parenthesis is the number of coincidences and the last figures the number of detectors. In the singles counting mode, a count is registered if any one of the plastic scintillator detectors senses an event. In coincidence counting modes, the indicated number of detectors must sense an event within the extremely small gated time period of about 50 nanoseconds. The coincident count is related to gamma and neutron emissions from the nucleus in an extremely short period following a fission event.

Plastic scintillator detectors of the instrument are sensitive to both gamma rays and neutrons, and are responsive to very high count rates. The complete detector system exhibits reasonable linearity up to $\sim 10^6$ counts per second. Sensitivity to both gamma rays and neutrons is an important factor in applications as a small sample assay unit.

Figure 3 indicates well configurations associated with the HEDL instrument.

Detectors and neutron source housing are positioned on radially adjustable mounts to accommodate container diameters up to 19 inches. When a lead sample shield is used, container diameters are limited within the 4-inch ID of the shield and detectors are positioned at the shield perimeter. A lead sample shield was utilized to study NDA response as a function of gamma ray shielding.

U-233 NDA STANDARDS

A series of six U-233 NDA experimental standards was prepared from $^{233}UO_2$ powder containing 7 ppm U-232 at about 2 years since purification. These standards are described by Table II.

TABLE II

U-233 NDA EXPERIMENTAL STANDARDS

Grams, U-233	Isotopic Distribution	
0.99	U-232	0.0007 w/o
2.56	U-233	98.026
4.20	U-234	1.194
7.26	U-235	0.078
10.66	U-236	0.018
15.06	U-238	0.683

RESULTS

U-233 experimental NDA was carried out with the HEDL random driver utilizing passive singles counting, passive coincidence counting, and active coincidence counting. It was concluded from these observations that passive singles, and active coincidence counting modes may find applicability in U-233 NDA. Passive coincidence counting is not recommended due to nonlinearity and an apparent high random coincidence count rate. Random coincidences are corrected for in active coincidence counting.

Passive Singles Counting

Figure 4 indicates response of the passive singles counting mode with respect to the U-233 standards. A count is registered in this mode when any one of the detectors senses a gamma ray or neutron.

This counting mode would be quite useful for samples from a process in which the U-233 material is the same throughout. NDA standards prepared from this material would experience

RANDOM DRIVER WELL CONFIGURATIONS

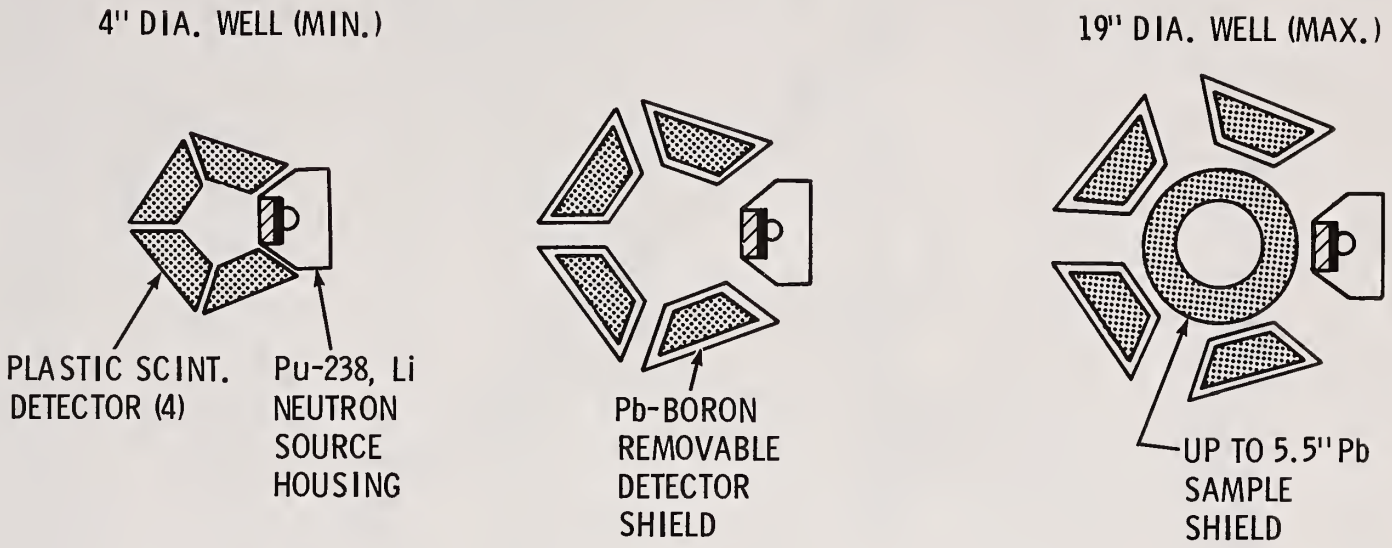

Fig. 3. HEDL Random Driver Well Configurations.

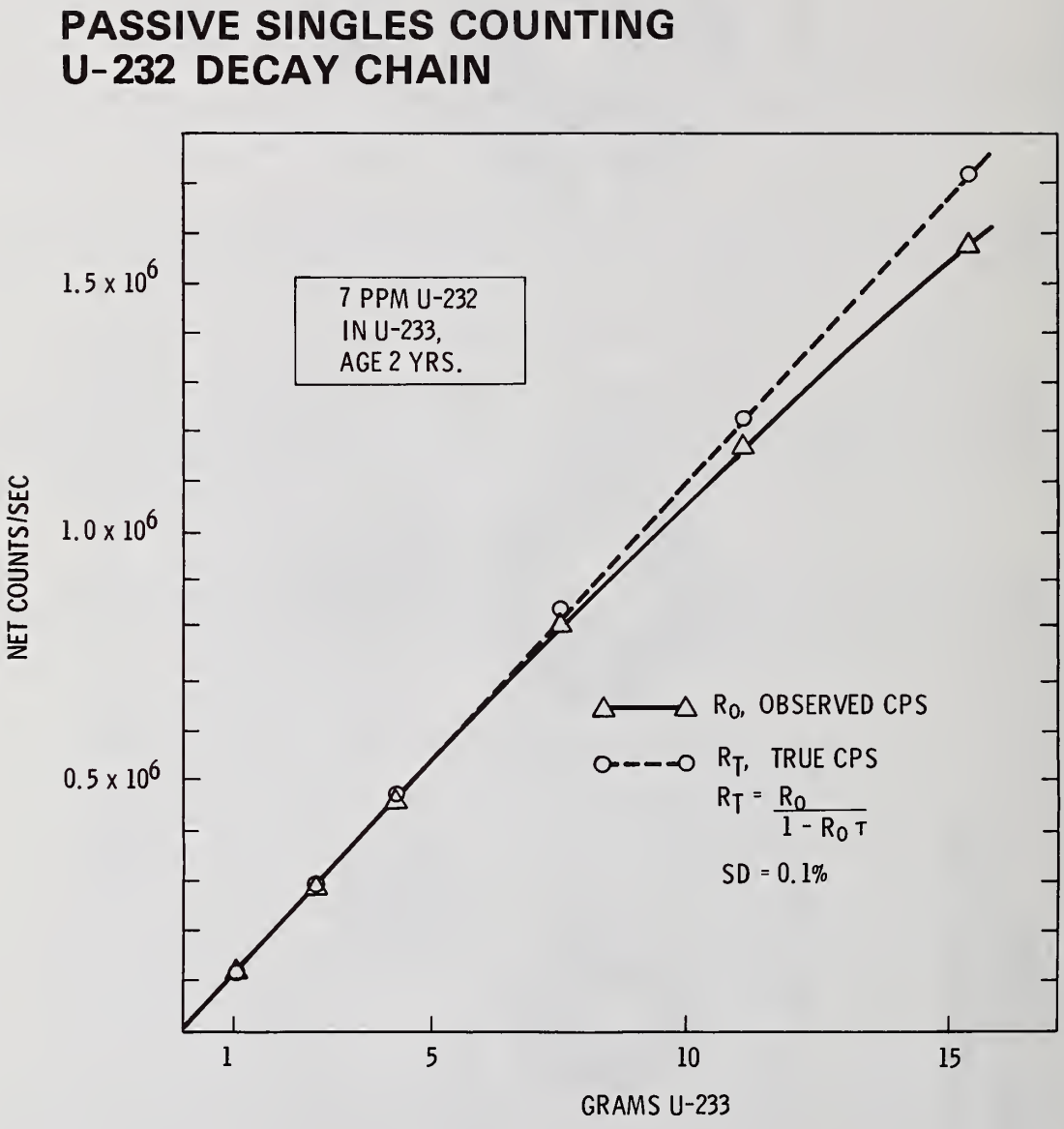

Fig. 4. HEDL Random Driver Singles Response Corrected for Dead Time.

the same time dependent changes associated with the U-232 decay chain. Accordingly, the gross gamma and neutron counting technique of the passive singles counting mode could be applied throughout the process to assay waste, intermediate, and bulk quantities of material. The experimental precision of the passive singles technique is within 0.2% at the 95% confidence limit. Reliable passive singles counting is also very important in active coincidence counting since random coincidence corrections depend on the singles count rate.

Passive Coincidence Counting

Theoretically, little or no basis exists for passive coincidence counting of U-233. The low U-233 spontaneous fission factor of 4.6×10^{-4} d/s/g should eliminate passive coincidence counting for U-233 NDA. However, a passive coincidence response was observed with the random driver as indicated by Figure 5.

Two unusual conditions were noted: (1) the level of coincidence counts in view of the very low U-233 mass, (2) the nonlinear increase with increasing U-233 mass. In an attempt to identify mechanisms relating to the passive coincidence response of Figure 5, U-233 standards were counted passively in a neutron well coincidence counter with BF_3 neutron detecting tubes. Results are summarized by Table III.

TABLE III

PASSIVE NEUTRON WELL COINCIDENCE COUNTING
OF U-233 STANDARDS

Counts	Background	1 Gram	7 Gram	15 Gram
Gross	14792	15626	18588	22409
Real	31	40	48	68
Acc.	35	30	45	70

As expected, gross neutron activity shows a definite relation to U-233 mass, and is believed to be (α,n) neutrons. U-233 is an alpha emitter with a half life of 1.62×10^5 years, and the U-232 decay chain produces 7 alpha emitters whose intensity increases in accordance with the decay of 1.91 year Th-228, the daughter of U-232. (α,n) reactions would occur with oxygen in $^{233}UO_2$ and low Z impurities. The major low Z impurities include phosphorous 325 ppm, aluminum 175 ppm, iron 85 ppm, sulfur 62 ppm, silicon 45 ppm and a number of others at lower levels.

The net neutron coincidence count is given by (Real - Acc.). These values from Table III show an insignificant neutron coincidence count level substantiating the very low level of U-233 spontaneous fission, and also indicating that (α,n) induced fission in U-233 must be quite low.

In view of nonlinearity, plastic scintillator detectors are not recommended for passive coincidence counting of U-233 as a function of U-232 decay chain gamma activity. Passive counting of this gamma activity can be carried out much more reliably by singles counting which can be corrected for dead time to give a very good linear response according to Figure 4.

ACTIVE COINCIDENCE COUNTING

Active coincidence counting utilizing plastic scintillator detectors depends on reasonably accurate corrections for random coincidence backgrounds. This requirement is particularly important in active assay of U-233 containing U-232 with its decay chain gamma activity. A few ppm U-232 depending on age since purification may result in a random coincidence background count rate many times higher than the induced fission count rate. Corrections for random coincidence background may be made by (1) delay circuitry which cuts out gamma counts enabling essentially neutron counting in fast coincidence, (3) delay lines which interrupt the gamma ray pattern enabling evaluations of random to true coincidence ratios, (3) resolving time correction formulas. The particular random driver in use at HEDL is not equipped with delay circuitry, and use of delay lines has not yet been investigated. Consequently, this study is based on resolving time correction formulas. This subject is covered in detail by Gozani.(8)

U-233 ASSAY, RANDOM DRIVER

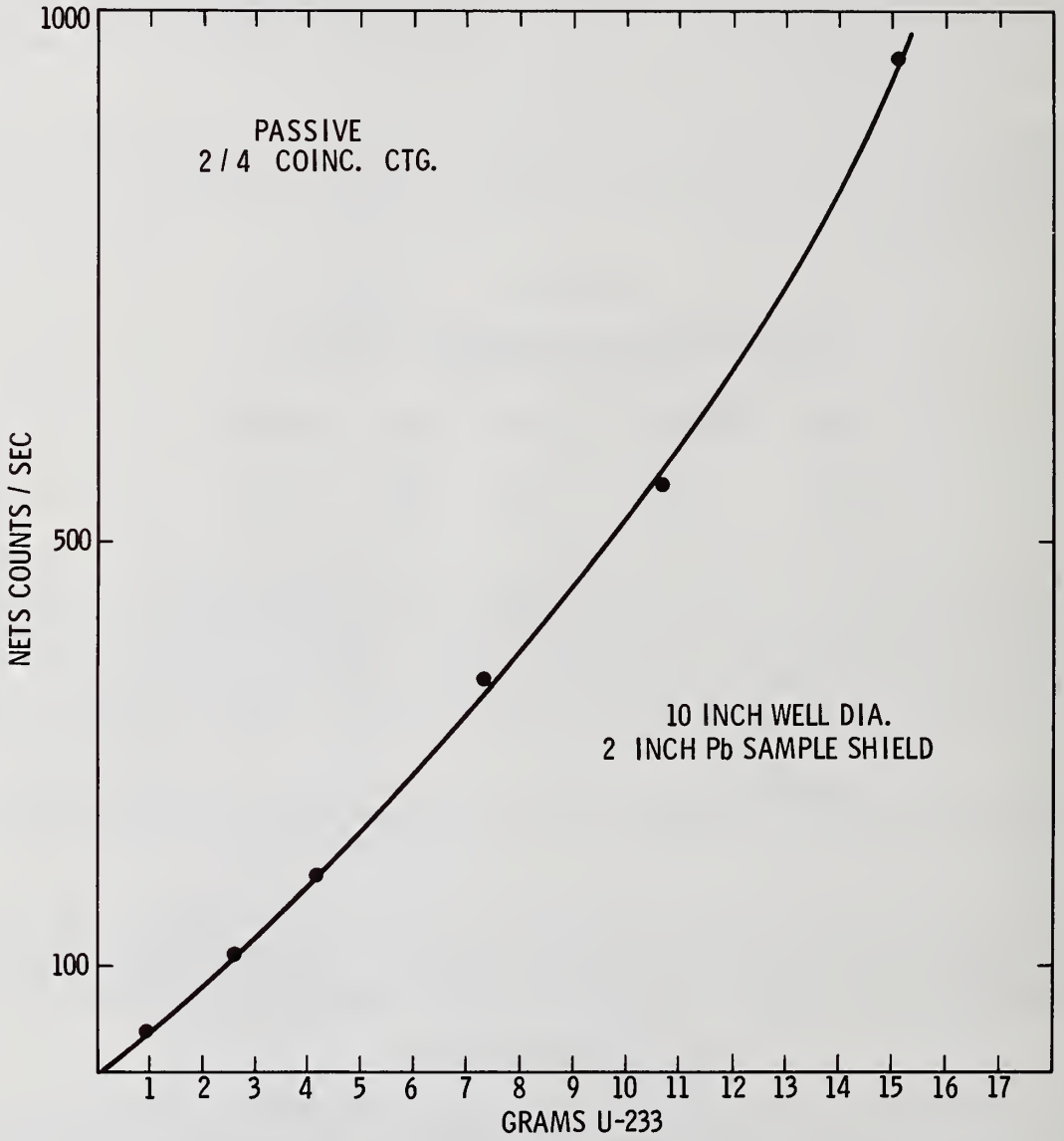

Fig. 5. Passive Coincidence Counting of U-233 with U-232 Decay Chain Gamma Emitters.

Active coincidence counting of U-233 can be somewhat complicated with plastic scintillator detectors depending on the U-232 decay chain gamma activity. The random gamma coincidence rate is quite high and increases nonlinearly as indicated by Figure 5. Table IV indicates the effect of combining random gamma coincidences. Two gamma sources A and B were measured separately in positions 1 and 2, respectively. The sum of the individual count rates was 7748 cps. The two sources were then measured simultaneously in respective positions; however, the combined random coincidence count rate was then 14112 cps representing an increase greater than 80% over the individual sum.

TABLE IV

RANDOM GAMMA COINCIDENCE COMBINATION

	Gamma Coincidence Cps
Gamma Source A	6750
Gamma Source B	998
Individual	7748
Combined	14112

The combining of random gamma coincidences must be taken into account when using plastic scintillator detectors in active coincidence counting. Essentially the sample and the source are measured simultaneously; the sample, the source, and the environmental background are measured separately. When the latter three backgrounds are accounted for, the result is a combined active coincidence component (Acc.) plus a random coincidence component (Rcc.). The component (Rcc.) must be evaluated in order to express (Acc.). (See Table V.)

TABLE V

ACTIVE COINCIDENCE COUNTING COMPONENTS

X = Sample Background
S = Source Background
B = Environmental Background
Acc. = Active Induced Count Rate
Rcc. = Random Coincidence Count Rate

$$X + S + B + (Acc. + Rcc.)$$
$$- (X + B)$$
$$- (S + B)$$
$$\frac{B}{NET = (Acc. + Rcc.)}$$

Table VI lists typical data associated with the U-233 standards containing 7 ppm U-233, 2 years old. The net count rate representing the U-233 fissile content is 126 cps. Note by column 2 that a count rate of 1142 cps results before the random coincidence correction is made.

TABLE VI

U-233 ACTIVE NONDESTRUCTIVE ASSAY

	Counts per Second			
	Singles	Coincidence	Random Coincidence Correction	
Sample + Source	441,000	6,140	2,722	
Sample	333,000	3,632	1,549	
Source	106,000	1,376	157	
Environmental Background	400	10	0	
		1,142	1.016	(126 cps) NET

For uranium and plutonium associated with very little gamma activity, corrections indicated by column 2 of Table VI suffice since the random coincidence rate is negligibly small. Because the random coincidence rate is quite high for the U-233 with 7 ppm U-232 at age 2 years, random coincidence corrections indicated by column 3 are very necessary.

Figure 6 summarizes U-233 data based on a one-inch lead sample shield. The lead sample shield serves to reduce the singles count rate to levels not severely affected by saturation. Alternatively, the singles count rate could also have been reduced by radial movement of the four detectors outward. The setup with lead shielding is described to demonstrate that the technique does work when the intense gamma rays from the U-232 decay chain are shielded. Although the one-inch lead shield reduces the gamma activity to more ideal levels for NDA, the induced activation count rate is also reduced, in particular, the fission gamma response. The induced gamma, neutron total fission count rate is reduced by an approximate factor of five when a one-inch lead sample shield is used.

The data of Figure 6 represent a family of curves related to resolving times in making random coincidence corrections. Resolving times determined electronically may vary by a few nanoseconds and could lead to significant error in making random coincidence corrections. This would be particularly true if the net active count rate is undercorrected. (Overcorrecting is not so serious since values remain in proportion to induced fission rates.) In this case, the residual random coincidence count rate of the U-232 decay chain would be misconstrued as a reflection of the induced active count rate.

The correct resolving time is that which results in approximately the same net active count rates for standards with and without the U-232 decay chain gamma activity. The calibration point indicated in Figure 6 was determined by the count rate associated with a 15-gram unirradiated U-235 standard which has very little random coincidence background. A resolving time of 49 nanoseconds resulted in very nearly the same count rate for U-233 with high gamma activity as for the U-235 on a gram-for-gram basis. The U-235 response was adjusted to the expected count rate for U-233 in proportion to thermal neutron fission cross sections. Count rates for U-235 and plutonium by active assay have been found to agree very well in proportion to their respective thermal neutron fission cross sections with use of a (Pu-238,Li) neutron source. In practice, resolving time calibration would best be carried out with two U-233 standards of equal fissile content. One of these standards would contain a few ppm of U-232 to provide a high random coincidence background. A resolving time is determined which then results in approximately equal net active count rates for both standards. Since pure U-233 was not readily available at the time, unirradiated U-235 served as a suitable substitute. Table VII describes factors in making random coincidence corrections.

TABLE VII

RANDOM COINCIDENCE CORRECTIONS

$$\text{Random Coincidence Corrections} = F\left(\frac{Rs}{N}\right)^{A}\tau^{A-1}$$

where:

- F is related to the number of detectors (not always the same as the number of detectors) F = 3 for 2 of 3 coincidences since 3 detectors provide 3 combinations for coincidences to occur. F = 6 for 2 of 4 coincidences since 4 detectors provide 6 combinations for coincidences to occur. Coincidence corrections become more complicated for 3 or more coincidences according to Gozani.[8]
- Rs is the singles count rate for N detectors
- $\frac{Rs}{N}$ is the singles count rate per detector
- A is the number of coincidences out of N detectors
- τ is the resolving time

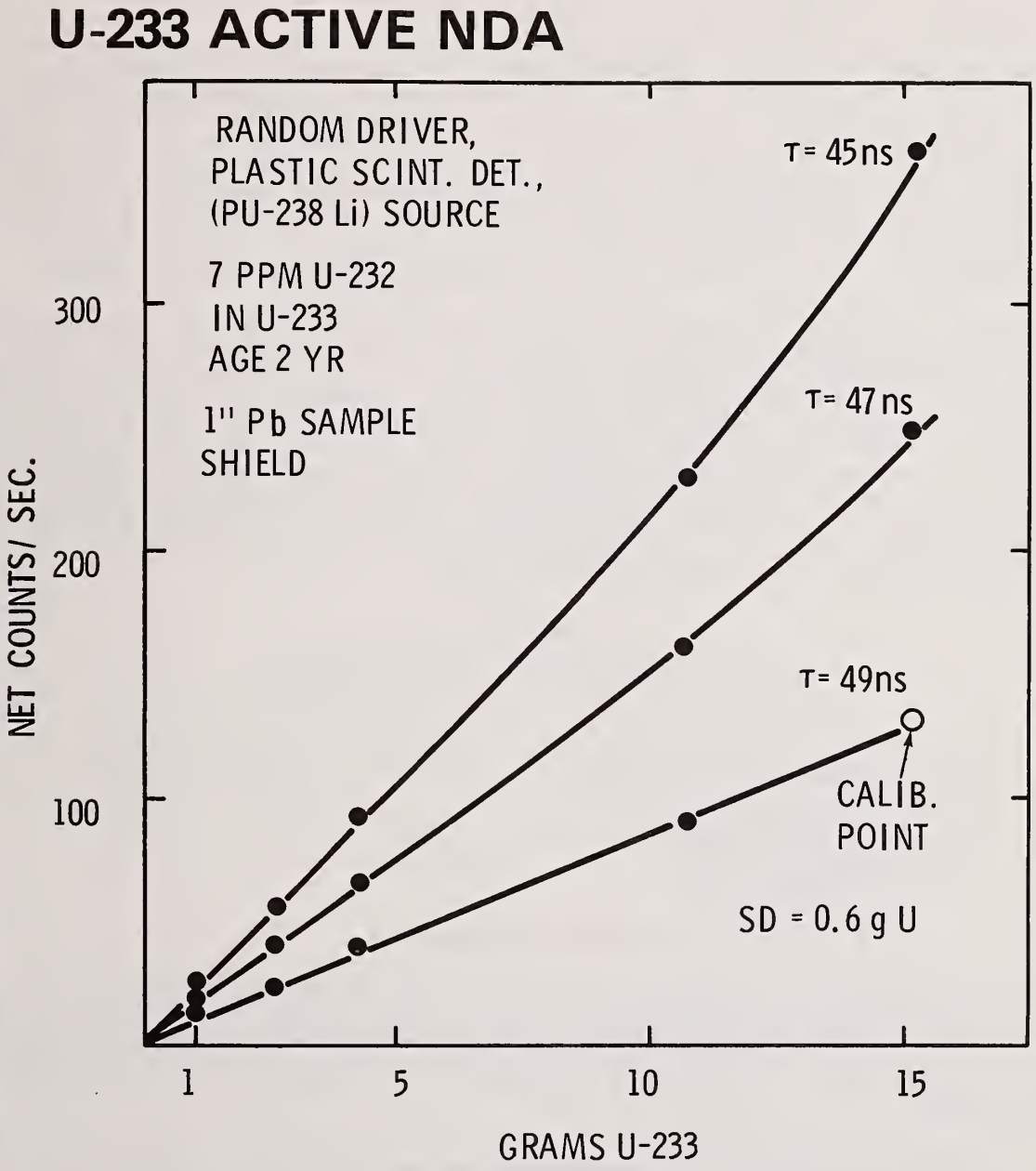

Fig. 6. The Effect of Resolving Time of Random Coincidence Corrections for Active NDA.

The calibration curve of Figure 6 associated with a resolving time of 49 nanoseconds is reasonably linear. A linear fit of the data gives an average standard deviation of ∿0.6 g uranium or 4% at the 15 gram level. The standard deviation is much wider at the lower gram levels; however, calibration over a wide range can be misleading. The recommended calibration procedure is a two-point technique closely bracketing the level of fissile material to be assayed. In this case, count rate levels for a two-point calibration involving one and two gram standards, for example, could be adjusted and would result in a standard deviation of ∿4% as well. The practice of multiple calibration points over a wide range should be avoided as much as possible in nondestructive assay particularly for this reason. An additional benefit is the fact that more counting time can be associated with a minimum number of points on a curve thereby improving reliability from a statistical counting standpoint. The ultimate precision attainable in active assay of uranium and plutonium with the HEDL random driver is a standard deviation of ∿1.5% based on a two-point calibration technique. This level of precision is associated with fissile standards essentially free of random coincidence background. Figure 7 shows a two-point calibration based on unshielded samples.

Since active coincidence counting for fissile material associated with high gamma activity depends on small differences between large numbers, instrument performance must be very stable. Frequent high voltage checks and evaluation of the resolving time should be made. Plastic scintillator detectors should be conditioned by continuous counting of a source in the range of samples to be assayed. The basis for this requirement is given by Table VIII. Detectors were individually adjusted to give very nearly the same reading with a given gamma source after overnight inactivity. One detector was then disconnected and a gamma source of 1.7×10^6 cps was counted over a 1-hour period. Note the count rate increase with the active detectors. Ultimately, the active detectors "cool off", so to speak, and return to the initial adjusted count rate. Because of this condition, detectors should be activated for a period prior to use in high precision NDA work.

TABLE VIII

PLASTIC SCINTILLATOR DETECTOR CONDITIONING

Detector No.	1	2	3	4
Initial Adjusted Count Rate with Gamma Source	3.1×10^4	3.1×10^4	3.1×10^4	3.1×10^4
Count Rate after 1-Hour Counting with 1.7×10^6 cps Gamma Source	4.2×10^4	3.1×10^4 (turned off)	4.2×10^4	4.2×10^4

SUMMARY AND CONCLUSIONS

HEDL investigation of U-233 NDA with a random driver was undertaken to gain experience in activation assay of proliferation resistant fuels. Results of this study are presented primarily from the standpoint of providing information that may be useful in development of associated NDA techniques. Promotion of random drivers for this purpose was not a principal goal; however, random drivers may prove to be competitive in NDA of proliferation resistant fuels.

Restrictions on U-233 NDA including low spontaneous fission factor, limited gamma ray signatures, and low thermal energy release indicate that activation techniques should be used for U-233 NDA. In order to apply active NDA utilizing plastic scintillator detectors, a high random coincidence rate due to gamma activity from the U-232 decay chain must be corrected for. Corrections were found to be very dependent on resolving times. The proper resolving time was determined experimentally by comparison with an unirradiated U-235 standard.

The standard deviation for active assay of U-233 with a high random coincidence background is ∿7%. In comparison, the standard deviation for U-235 with very low random coincidence background is ∿1.5%. The difference in precision is due to the accuracy with which random coincidence corrections can be made.

A two-point calibration technique with standards bracketing levels of fissile material samples as closely as possible is recommended for most accurate results.

U ACTIVE NDA

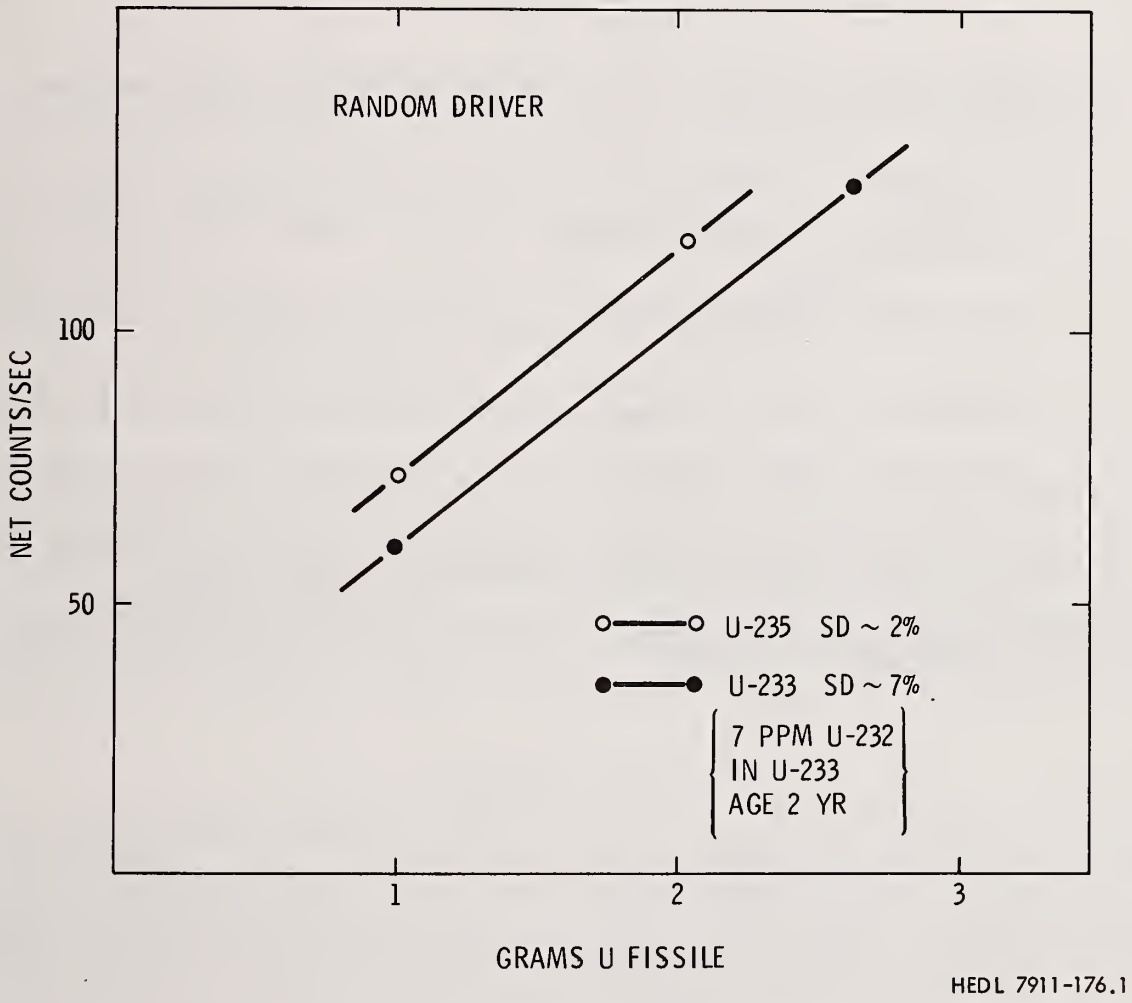

Fig. 7. Two-Point Calibration Technique for Active Random Driver NDA.

Passive singles counting was found to be a very accurate technique for high gamma U-233 samples. This technique would be very useful in a process whereby all of the material contained the same U-232 content and purification history. When the counts per second per gram fissile is established in such a process, the technique could be applied to all categories of material including waste. The standard deviation for passive singles counting based on a two-point calibration is ∿0.1%.

The study concluded that passive coincidence counting has no practical application in U-233 NDA since the observed coincidence count rate is essentially all random coincidences due to U-232 decay chain gamma activity.

REFERENCES

1. J. D. Jenkins, et al, "Conceptual Design of the Special Nuclear Material Nondestructive Assay and Accountability System for the HTGR Fuel Refabrication Pilot Line," ORNL-TM-4917, 1975, p 49.

2. R. B. Walton, (LASL Correspondence Q-1-79-161).

3. J. E. Foley, "Random Source Interrogation System," Los Alamos Scientific Laboratory, Report LA-4883-PR, p 9, 1971.

4. J. E. Foley, "Random Driver Measurements at the LASL Uranium Recovery Facility (CMB-9)," Los Alamos Scientific Laboratory, Report LA-5431-PR, p 5, 1973.

5. J. E. Foley, "Application of the Random Source Interrogation System at the Oak Ridge Y-12 Plant, Preliminary Results," Los Alamos Scientific Laboratory Report LA-5078-MS, 1972.

6. T. L. Atwell, et al, "NDA of HTGR Fuel Using the Random Driver," Los Alamos Scientific Laboratory, Report LA-UR-74-977.

7. K. H. Czock, et al, "Evaluation of the Versatile Passive-Active Counting System (Verpacs) for Nondestructive Assay of Plutonium," IAEA/STR-43, September 1973.

8. T. Gozani, "Corrections for Accidental Coincidence in Fission Detectors," Trans., Americ Nuclear Society, Vol 17, p 84, 1973.

MEASUREMENT OF PLUTONIUM AND AMERICIUM IN MOLTEN SALT RESIDUES *

by

Francis X. Haas, James L. Lawless, Wayne E. Herren, and Marvin E. Hughes
Rockwell International, Energy Systems Group, P.O. Box 464, Golden, Colorado 80401

ABSTRACT

The measurement of plutonium and americium in molten salt residues using a segmented gamma-ray scanning device is described. This system was calibrated using artificially fabricated as well as process generated samples. All samples were calorimetered and the americium to plutonium content of the samples determined by gamma-ray spectroscopy. For the nine samples calorimetered thus far, no significant biases are present in the comparison of the segmented gamma-ray assay and the calorimetric assay. Estimated errors are of the 10 percent and is dependent on the americium to plutonium ratio determination.

KEYWORDS: Waste assay, plutonium, americium, nuclear safeguards, nondestructive assay.

INTRODUCTION

A segmented gamma-ray scanning device has been installed at Rocky Flats for measurement of Waste residues in small, less than one gallon, containers. Initially, the system has been programmed to assay crushed molten salt residues for plutonium and americium. The americium assay is required to account for the decay of the isotope 241-Pu. The salt residues are generated in the plutonium recovery process by a molten extraction procedure. The spent chloride salt media from the extraction contains all of the americium and some of the plutonium present in the plutonium feed material. Plutonium content of the salts ranges up to 400 grams and americium content to 30 grams. Typically, the ratio of americium to plutonium is 5- to 10 percent. Matrix weights are of the order of 2 kilograms.

MEASUREMENT PROCEDURE

The measured salts are doubly contained in stainless steel cans: A Volrath 8801 can inside a volrath 8802 can. The outside dimensions of the sample cylinder are approximately 4.25 inches in diameter and 5.5 inches tall. A commercially available counting system, Canberra Industries Model 2220C, (Ref. 1) is used to assay the salts. The sample can is divided into five segments and each segment is counted for 200 seconds. The plutonium is measured using the area of the 414-keV peak; the americium is measured using the area of the 662-keV peak. We also monitor the intensity of the 393-keV peak due to 239-Pu.

Gamma ray attenuation corrections are made for all of these gamma rays using the 400 keV gamma-ray peak from an external 75-SE transmission source. The relative attenuation correction for the 400 keV gamma ray to that occuring at the 662-keV americium gamma ray was measured by recording the transmission of gamma rays from the 72-SE source and an external 137-CS source, energy 662 keV, through a molten salt cake containing no radioactive contaminants. The measured ratio of the mass attenuation coefficients at 662 keV is 0.78.

* Operated by Rockwell International for DOE under Contrace DE-AC04-76DP03533.

Figure 1 shows a gamma-ray spectrum of the 400 keV energy region from a sample containing approximately 10 percent americium relative to plutonium. High count rates from the sample required that we incorporate pulse pile-up rejector electronics into the system. This reduced the high energy tailing on the accumulated peaks and the amount of coincident summing in the crystal of the 208 keV peak from the decay of 237-U and 241-Am. This latter peak, 416 keV, is now seen as only a slight "bump" on the high energy base of the 414-keV peak. The pile-up rejector electronics has allowed us to maintain a simple background subtraction procedure for the areas of the peaks. By monitoring the area of the 393-keV peak relative to the area of the 414 keV peak, we have ascertained that this model of area determination is adequate for americium levels below 15 percent relative to plutonium. The ratio of 393-keV assay to that obtained from the 414-keV assay range from 0.97 to 1.03 with the uncertainty of each determination being of the order of 4 percent or less.

CALIBRATION

The system has been calibrated for plutonium by fabricating salt standards containing 100-, 200-, and 400 grams of plutonium. These standards contain no americium and have been calibrated by calorimetric techniques. Agreement of the gamma-scan values with those obtained from calorimetry were less than 3 percent. System reproducibility for these samples was +/- 2 percent.

The americium calibration was obtained by preparing two salt samples into which weighed quantities of americium of 6 and 29 grams, respectively, were added. Both of these samples were contaminated with about 25 grams each of plutonium. This was verified by both the calorimeter and the gamma-ray spectra. It was these samples that called our attention to the interferences present at 416 keV due to pile-up of the 208 keV gamma-ray and at 419 keV due to the americium in the samples. To investigate the extent of these interferences three samples were prepared having approximately 5-, 10-, and 20 percent americium relative to plutonium. Again, contamination of the samples occurred as indicated.

By comparison of the calorimetric assay with the assigned weights, however, the agreement between the calorimetric assay and the segmented gamma assay was within 5 percent. The calorimetric determination in this latter case was calculated using the americium to plutonium ratio determined by gamma-ray spectroscopy using the 125 keV peak from americium and the 129 keV peak from plutonium. Five spectra are summed, one spectrum from each segment, and the ratio determined from the summed spectrum.

Calibration of the system was also undertaken using samples selected from inventory. The Department of Energy, Albuquerque Operations Office, Division of Safeguards and Security (DOE/ALO-DSS) requested that the molten salt waste category undergo an inventory verification study for their most recent audit. Nine samples were chosen. Each sample was calorimetered and the americium/plutonium ratio determined as above. All of the packages were chosen on a highly selective basis because of the limited calibration range, less than 3 watts, of the calorimeters used for the study. In addition, the selection involved the handling of a minimum number of drum storage containers to minimize the health hazards to the operating personnel.

RESULTS AND DISCUSSION

Figure 2 shows the results of the comparison of the plutonium values obtained by calorimetry versus those measured by the segmented gamma-ray system. The points represented

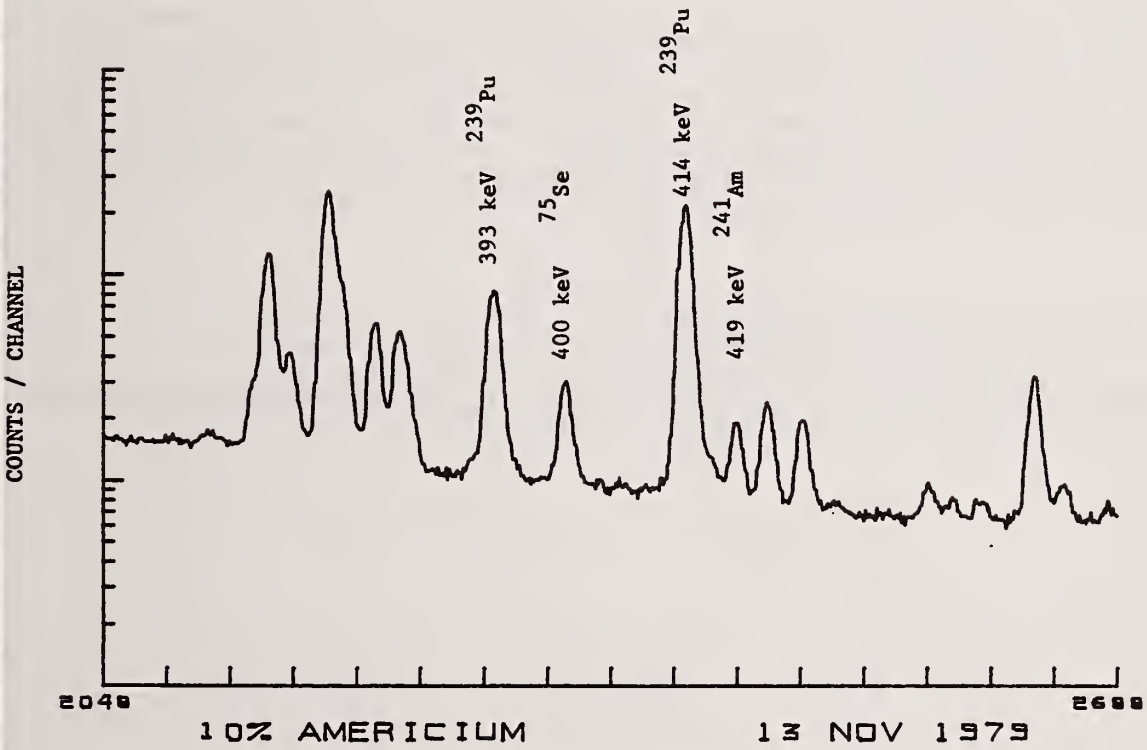

Figure 1. Spectrum of the 400 keV energy region used for segmented gamma-ray assay. Peaks used in the analysis are the 393- and 414-keV peaks from the decay of 239-Pu.

by x's are the points measured for the prepared standards. The dots represent the data for the DOE/ALO-DSS verification samples. Figure 3 shows the corresponding data for the americium values. The straight line indicates the locus of points where the segmented gamma scan values equal the calorimetry values. The predominant error in this technique is that propagated by the uncertainty in the americium/plutonium ratio determination applied the calorimetry values. This error is estimated to be 7- to 10 percent based on comparisons with the same ratio obtained using the 419-keV and 414-keV gamma rays and previous results relative to the verification program (Ref. 2) since the americium contributes 30- to 90 percent of the heat in all of the samples, except the pure plutonium samples, the overall uncertainty in the plutonium determination by calorimetry is then of the order of 3- to 10 percent. Error bars on all the points overlap the line of equality in the figures, except those points with the error bars indicated.

A statistical study of the comparison of the results from the gamma-ray segmented scan with calorimeter results for the nine inventory samples indicate a standard bias for the samples of -5.1 percent with an error of 6.2 percent. For the small number of samples studied, the relative biases are not statistically significant at the 95 percent confidence level. The study of biases is continuing at the present time, four samples per month will be taken from inventory, calorimetered, and counted at least once per week for the month. This process will continue until a statistically significant number of samples are verified and biases, if any, determined.

REFERENCES

1. Canberra Industries, Inc., Meridan, Ct.

2. John F. Lemming, Francis X. Haas, and Jack Y Jarvis, "Gamma-ray Isotopic Measurements for the Plutonium Inventory Verification Program," MLM-2312 (Aug. 25, 1976)

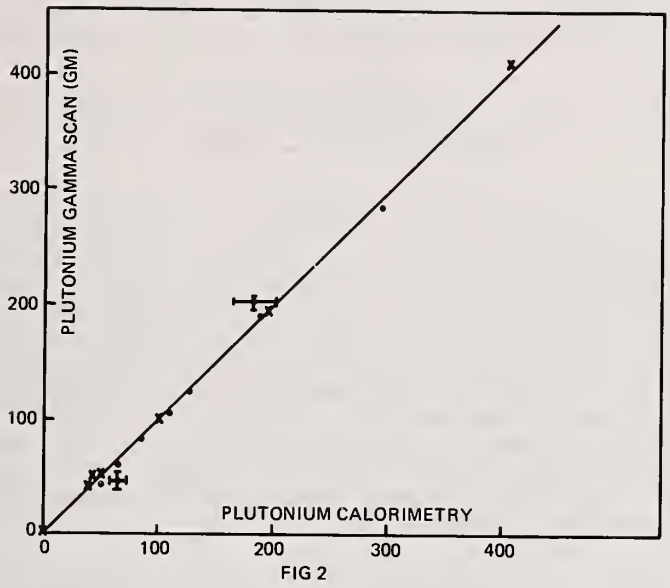

FIG 2

Comparion of plutonium values obtained by calorimetry and segmented gamma scan. Dots represent values from inventory samples. x's represent values from artificially made salts. See text.

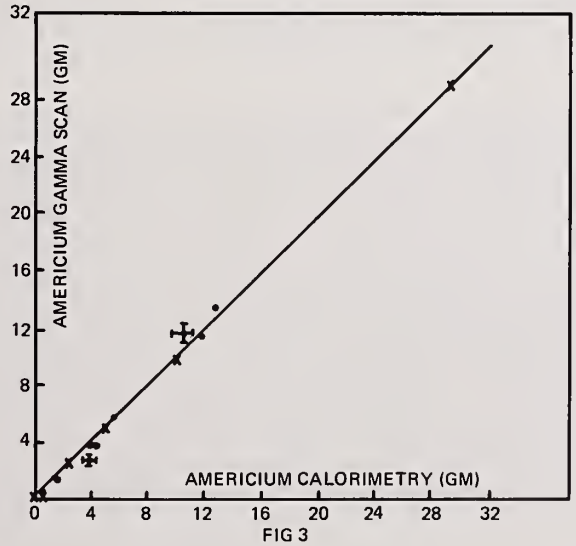

FIG 3

Comparison of americium values obtained by calorimetry and segmented gamma scan. Dots represent values from inventory samples. x's represent values from artificially made salts.

URANIUM AND PLUTONIUM ASSAY OF CRATED WASTE BY GAMMA RAY, SINGLES NEUTRON, AND SLOW NEUTRON COINCIDENCE COUNTING*

by

Ronald A. Harlan
Rockwell International, Energy Systems Division, Rocky Flats Plant,
Golden, Colorado 80401

ABSTRACT

Nuclear counting techniques were applied to plutonium contaminated waste in 4-ft by 4-ft by 7-ft wooden crates sealed with a fire retardant polyester plus fiberglass overcoat. The counting systems were proven to be useful for safeguards verification measurements and to some extent for accountability measurements. Neutron and gamma ray measurements both are recommended. The latter serve to double check the neutron results and provide a capability for estimating uranium and other radionuclides that may be in the waste but that do not emit usable amounts of neutrons. About 5 grams (g) of plutonium or uranium can be detected in 20 minutes.

KEYWORDS: Counter, estimates, gamma rays, neutrons, nondestructive assay, plutonium waste, safeguards, uranium waste, verification.

INTRODUCTION

The Rocky Flats Plant has disposed of a large portion of its contaminated waste by putting waste in 4-ft by 4-ft by 7-ft (1.22 by 1.22 by 2.13 m) wooden crates. Before shipment to retrievable or irretrievable storage, the crates were sealed with a fireresistant fiberglass reinforced polyester coating. These large containers were and presently are used for their economy relative to disposal in smaller containers.

A crate counter was built to estimate the plutonium content in waste.[1] The counter responded only to neutron events counted singly (singles neutrons). It was intended to provide a safeguards verification measurement for waste, and possibly an accountability value in addition. The wastes expected were primarily metallic matrices which had been partially decontaminated in a water wash operation. In recent times, dry combustible wastes assayed in 55-gallon drums were subsequently dumped into crates as were drum counted high efficiency particulate air (HEPA) filters. Practice did not bear out the author's original hope for an oxide or hydroxide chemical form of plutonum in the waste. The results of these disposal practices were large and variable neutron outputs from (α,n) reactions on waste matrix materials in addition to the desired spontaneous fission neutrons from plutonium-240. If the $^{241}Am/Pu$ ratio exceeds 0.01, additional (α,n) neutrons become important because of americium's high specific activity. Gamma ray detectors were placed at the crate-counting facility not only to double-check neutron counting results, but to provide a means to estimate the amounts of uranium or other radionuclides which could be in some wastes.

*This work was supported by the USDOE under Contract DE-AC04-76DP03533.

The crate counter now serves as a verifier of values assigned via drum counters for combustibles and HEPA filters and by scans of metallic parts with hand-held survey meters in light metal waste. As an assay device, the crate counter cannot equal the more accurate performance of small package counters or drum counters because of the geometric and absorption problems of large crates.

EXPERIMENTAL

Equipment

The neutron counting portion of the crate counter consisted of 10 lithium loaded zinc sulfide screens 12 in. (305 mm) in diameter coupled by Lucite light pipes to 5-in. diameter (127 mm) photomultiplier tubes. The tubes were connected in turn through standard nuclear preamplifiers, amplifiers, and discriminators to printing scalers. Discriminators were set to eliminate gamma ray response by choosing a setting well above that where response to ^{60}Co gamma rays was stopped. Unfortunately, this also reduced the neutron counting efficiency considerably. The detectors were mounted outside a polyethylene cave with 2-in. thick (51 mm) walls.

Crates placed by fork lift on a table, which was moved by roller conveyor, were totally enclosed when rolled inside the cave. Figure 1 shows the counter being loaded and Figure 2 shows the counter in its counting configuration. Detector placement may be noted in Figures 1 and 2. The detectors are the dark devices on top and underneath the cave and are inside conical covers on the sides.

An external monitor box is visible in Figure 2. The small white polyethylene box contained one detector identical to those on the main counter and was constructed with alternating polyethylene and cadmium except for the face opposite the main counter. The detector was mounted inside on 2-in. thick polyethylene and faced the crate and drum storage area of the building. The five sides with cadmium effectively decoupled this detector from neutrons originating in crates in the counter. If higher throughput were desired, one crate could be counted every 20 minutes, and background could be estimated by multiplying the external monitor count by an experimentally measured factor.[1] This was usually not done in practice because additional error was introduced into the background measurements. This additional error effectively doubled the minimum detectable amount of plutonium.

The chosen neutron counting sequence alternated background measurement and crate measurement always terminating in a background measurement. This sequence was chosen so that backgrounds measured immediately before and after each crate can be averaged. The averaging procedure gave a better estimate of changing room backgrounds than the external monitor described above.

Another monitor, not shown in Figures 1 and 2, was provided. All incoming crates or drums pass by the counter through a door just off the right-hand edge of Figure 2. The NaI(Tl) detector in this monitor at the door senses gamma rays from incoming shipments. When a preset level is reached, any crate count in progress is automatically stopped until the local radiation field is returned to an acceptably low level. Counting is then resumed.

A slow neutron coincidence counter (SNCC) unit was borrowed from Los Alamos Scientific Laboratory for testing with the neutron portion of our system. This unit has its own shift register logic and signal processing and has been described else-

Fig. 1. Crate Counter Being Loaded with Standards Crate; Note Standards Crate and cf. Fig. 3.

Fig. 2. Crate Counter with Crate and Table Rolled into Position.

where.[2,3] The unit was connected to our system to use only the logic processing portion presenting data in the forms: time, total count, real coincidence plus accidental count, and accidental count.

Gamma ray assay capabilities were added after the original installation.[1] For evaluation purposes, two 4-in. diameter x 2-in. thick (102 x 51 mm) NaI(Tl) detectors were placed on top of the counter adjacent to neutron detectors already there. These were shielded from crates with 0.25 in. (6.4 mm) of lead and 0.06 in. (1.5 mm) of cadmium. This shielding eliminated 60 keV radiation and reduced the count rate from plutonium gamma rays to permit reasonable multichannel analyzer (MCA) deadtimes. Lead shielding 2 in. thick was also placed in the horizontal plane around the NaI(Tl) detectors.

A high-purity germanium detector was placed on a movable cart, which could be rolled into position when desired. This detector was placed 6 ft (1.8 m) from the edge of a crate in the counter cave and centered longitudinally. The germanium detector had an efficiency of 15% of that of a 3- x 3-in. NaI(Tl) cylinder for the cobalt-60 1.33 MeV gamma ray. It was shielded on its circumference by 2 in. of lead and at its face by 0.06 in. of cadmium and 0.01 in. of copper sheet, again to reduce deadtime at the MCA.

Pulses from the NaI(Tl) detectors entered a pair of amplifiers, adjusted to match the gains, and the outputs passed through a summing amplifier to an MCA. Alternatively, the output from the germanium detector after amplification was sometimes passed to the MCA. At times, two MCA's were available. Data were collected simultaneously from all three counting systems whenever possible.

Calibration

The counter was first calibrated with PuO_2 sources for neutron counting. Four sources with 25 g each of plutonium were placed in a specially built crate with 35 "through" tubes. Figure 3 diagrams the standards crate. One end of the real crate is visible in Figure 1. The crate has been used only with a combustibles matrix at this writing. Two PuF_4 sources, each containing 25 g of plutonium, were also used to evaluate problems and test gamma ray detection systems.

After this calibration, 10 crates of combustibles were accepted that had been filled with drum counted material. The summed drum counts were taken as a standard value. The counter response to these crates was then compared to the plutonium oxide calibration. A similar procedure was followed for eight HEPA filter crates. Mean neutron counting connection factors were derived from these results. These crates were used to derive a gamma ray calibration, assuming drum count results were correct.

Samples

Over 200 crates have been counted and distributed approximately as 50% combustibles, 29% HEPA filters, and 21% light metals categories. All were neutron counted and 33 were also gamma ray counted. Crates were not routinely gamma ray counted for production unless neutron results were over 100 g and disagreed violently with the originators value which was assigned before movement to the preshipment storage building. These data may be used for further calibration adjustments. Several crates with smaller gram values were gamma ray counted for research purposes.

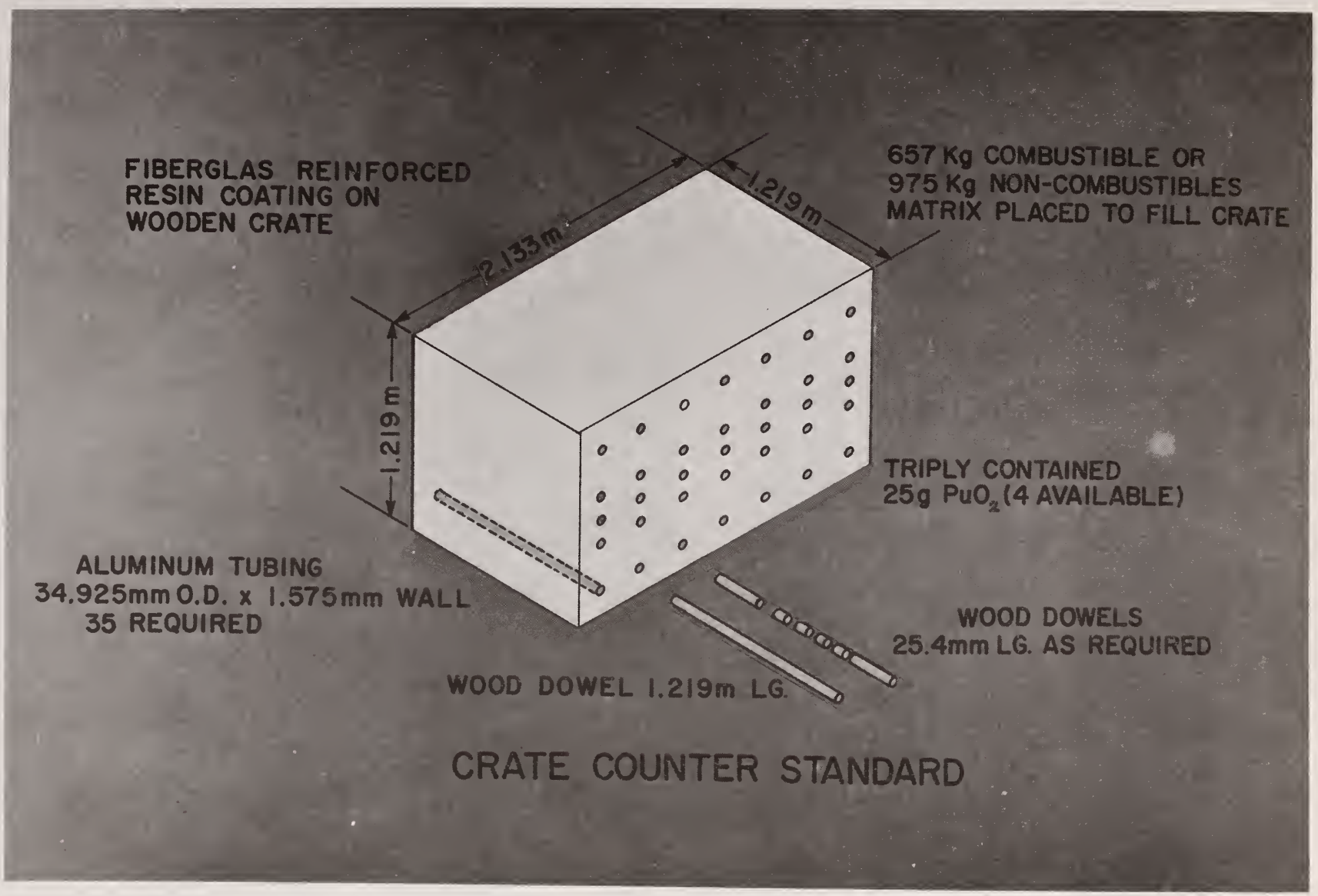

Fig. 3. Illustration of Method of Loading Sources in a Crate for Calibration.

RESULTS AND DISCUSSION

Neutron Counting Responses

Response to PuO_2 neutron sources are given in Table I for a bare source and for sources moved throughout the standard crate to derive an average response. The counting efficiency for a bare source was 0.22%, and for a distributed source in the average combustibles crate was 0.11%. These efficiencies are much smaller than the theoretical value of 1% because of the high discriminator thresholds used.

Table II summarizes data on average minimum detectable amounts of plutonium as oxide and in the real waste. These data were derived using summed drum counter results. One can see that the (α,n) reactions make an important contribution toward larger count rates and therefore lower minimum amounts. A detraction is the large range of responses within a category of waste. Geometrical variations coupled with (α,n) production variations have caused disagreements usually less than a factor of 4, but ranging up to a factor of 10 when comparing results within a category. The crate counter tended to overrespond more often than it underresponded. In any case, a confirmatory gamma ray count is essential for semiquantitative work.

The SNCC trials were unsuccessful. Because the detection efficiency was low, the coincident signal was totally lost in the accidental coincidences and real coincidences in the background. Also, it appeared that the neutron dieaway times were much longer than the 128 μsec gate on the SNCC. This 128 μsec gate was the longest available.

Gamma Ray Responses

Count rates were adequate with the Ge detector and more than adequate with the NaI(Tl) detectors. The former detector was favored because of its superior resolution. After the initial calibration with production crates, agreement with summed drum count results was good, in most cases within $\pm$40%.

Both NaI(Tl) and Ge data were examined to seek (α,n) and (α,p) reaction gamma rays up to 5 MeV energy with negative results for 20-minute counts. Had these been detectable, they could potentially have provided a means to correct neutron responses.[4] Tests with the PuF_4 sources easily showed the 1275 keV gamma ray of ^{22}Na. It was concluded that PuF_4 does not occur to any great extent in the plants waste crates, but it must be remembered that all crates did not receive a gamma ray count. In only one very "hot" crate counted for 6 hours were any possible reaction gamma rays observed. Such long count times are considered impractical for routine use. Gamma ray counting can detect high americium-241 to plutonium ratios and potentially could explain some high neutron count rates in this way.

Gamma ray counting served to confirm the presence and amounts of uranium-235 in some crates. Also, uranium-233 was sought in some crates containing very old glove box lines being discarded. None was detected. Neutron counting would not detect these radionuclides.

One may conclude from data obtained that gamma ray assay was essential to good verification operations and gave generally more reliable estimates of plutonium contents than did singles neutron counting. The latter was essential, however, since gamma rays are easily shielded. Both techniques are needed for verification.

Table I. Response of Rocky Flats Crate Counter to PuO_2 Sources.

Configuration	Counts per second per gram	Standard error
Bare Source, Empty Counter	0.269	0.004
Average of 4 ea. 25 g PuO_2 moved to 24 locations "mapping" crate volume.	0.131	0.046
Background	99.1([a])	1.4

([a])Independent of special nuclear material, but influenced slightly by mass of waste matrix. Units are counts per second only.

Table II. Detection limits for plutonium by singles neutron counting under current counting parameters, in an average crate with 1200 sec. count.

Plutonium form([a])	Limit at confidence level 0.95 (g)
PuO_2 with no matrix (α,n) reactions, but in combustibles matrix.	8
PuX in combustible waste	1.6
PuX in HEPA filters	0.8
PuX in light metals	0.6 ([b])

([a]) "X" means chemical form unknown.
([b]) Subject to further study.

Examples of Verification Usefulness

The crate counter neutron measurements from the start of production waste measurements consistently indicated more plutonium than was being reported in the light metal category. As an example, one crate was sent back to the originator, opened, and its contents rescanned by a collimated hand-held gamma ray survey meter. When the new estimate was made, it agreed within 5% with crate counter gamma ray measurements. This led to a review of administrative control of crate packing operations and subsequently to tightening procedures. Use of the counter has led to improved normal operating loss (NOL) accountability.

In another case, gamma ray counting found a small amount of uranium in a crate which should have had none, and no uranium in a crate which should have had some. The crates were sequentially numbered indicating a probable clerical error in numbering the two crates. Incidentally, the gamma ray measurements at the crate counter, assuming a labeling mixup, was almost exactly the amount of uranium reported by the originator of the crates.

A Second Generation Counter

Thought has been given to improving crate counter design. It is believed that slow neutron coincidence counting must be included in an improved design. In order for it to work, better neutron efficiency (10 to 30%) is needed. Shielding is essential to reduce the correlated neutron background induced by cosmic rays. The counting facility preferably should not be too near the crate traffic and storage area or must be heavily shielded.

It was estimated that 200 1-in. dia., 4-atm helium-3 neutron detectors ≈ 3 feet long can do the job adequately. Fewer detectors of larger size could be used. For safeguards purposes, it is not necessary to make the background essentially zero; therefore a few feet of earth or concrete could suffice for shielding purposes.

The good penetrability of neutrons makes this concept attractive for verification at the irretrievable waste activity level of 10 nCi Pu/gram of waste. To do this, one would want all of the detection efficiency one could reasonably design into the system and very effective shielding. Safeguards gamma ray measurements of crates, perhaps on a rotating table, are essential for complete verification if special nuclear material other than plutonium will be present. SNCC development activities for large waste containers are planned at Los Alamos Scientific Laboratory and the author will look forward to those results.

SUMMARY

The crate counter has proven its value as a safeguards verification tool. It can provide fair accountability, relying more heavily on gamma ray counting for quantitative estimates in its present form. While single measurement errors may be large, results averaged over many crates provide good NOL values. The crate counter has led to improved accountability at one point of origin, and one may speculate that further improvements may be forthcoming, particularly when the light metals waste category data are digested fully. Experience gained will aid design of a second generation crate counting facility, should one be funded.

ACKNOWLEDGEMENT

Many people contributed to the ultimate success of this project. Especially notable were contributions in physical construction by E. D. Frantz and in electronic setup and troubleshooting by W. E. Herrens. K. B. Gerald helped with calibration data collection. The Rocky Flats Chemistry Standards Laboratory constructed the PuO_2 and PuF_4 sources and provided the standards crate. The Rocky Flats Waste Management organization has been cooperative and helpful. Thanks are also due R. N. Chanda for encouragement and to B. T. Cross and S. A. Schuler for production of this manuscript. I am also indebted to the Los Alamos Scientific Laboratory for loan of an SNCC and to N. Ensslin and H. O. Menlove for discussions.

REFERENCES

1. R. A. Harlan, Nuclear Materials Management VI No. III (1977) p. 457.

2. J. E. Swansen, N. Ensslin, M. S. Krick and H. O. Menlove, Nuclear Safeguards Research Program Status Report, J. L. Sapir, compiler, USERDA Report LA-6788-PR, Los Alamos Scientific Laboratory, June 1977, p. 4.

3. N. Ensslin, M. L. Evans, H. O. Menlove and J. E. Swanson, Nuclear Materials Management VII No. III (1978) p. 43.

4. H. R. Martin Reaction Gamma Rays in Plutonium Compounds, Mixture and Alloys, USERDA Report, RFP-2382, Dow Chemical U.S.A., Rocky Flats Division, June 16, 1975.

FIGURE CAPTIONS

Figure 1. Crate Counter being loaded with standards crate; note standards crate and cf. Figure 3.

Figure 2. Crate Counter with crate and table rolled into position.

Figure 3. Illustration of method of loading sources in a crate for calibration.

Discussion:

Eccleston (LASL):
Can you tell me the advantages you realized by using a lithium-loaded zinc sulfide detection system rather than ^3He detectors?

Harlan (Rockwell-Rocky Flats):
I think today I would use ^3He, but at the time we were designing this counter we had just installed a drum counter, and it had BF_3 detectors. We were having a lot of trouble with instability. It turned out that there was just water vapor coming of the new concrete pit, and that was causing the high voltage to break down. In any case, we were suspicious of building another system right at that point that might give us a lot of trouble. Also, one would need very many ^3He or BF_3 detectors, perhaps one hundred or more, to get a high efficiency. And, since you can't gang too many of these together, they would require a lot of preamps. We only used four detectors ganged onto one preamp, which goes to an amplifier and thus to a discriminator. Thus, we only used three amplifiers in this sytem. The electronics would have been more complicated and expensive to use ^3He detectors. As I said, for a second generation counter, I think I would use ^3He detectors.

Eccleston:
What sort of an efficiency did you have with your lithium counters?

Harlan:
At the discriminator points at which I am operating, the efficiency is only one-tenth of a percent, roughly.

Eccleston:
Why do you think you would need one hundred ^3He counters, then? What kind of an efficiency would you have with one hundred ^3He counters?

Harlan:
I don't know. That would be getting near that 10% number.

Eccleston:
Are you familiar with the work that Q-2 has done with their tunnel detectors?

Harlan:
Yes. In fact, in the written paper, I comment right at the end that I know that LASL is working on developing counters for large containers such as these. They are being funded through the transuranic waste program. I will be watching with great interest to see what they design.

Evaluation of an L_{III} X-ray Absorption-Edge Densitometer For Assay of Mixed Uranium-Plutonium Solutions

by

W. C. MOSLEY, M. C. THOMPSON, and L. W. REYNOLDS

Savannah River Laboratory
E. I. du Pont de Nemours and Company
Aiken, South Carolina 29801

ABSTRACT

An L_{III} x-ray absorption-edge densitometer (XRAED), designed and built at Los Alamos Scientific Laboratory, has been evaluated at Savannah River Laboratory for the assay of uranium and plutonium in process solutions. For 2000-second data collection, the precisions (95% confidence level) for uranium assays varied ± 1.04% at 10 g of uranium per liter to 0.34% at 45 g/L, and plutonium assays varied from ± 6.7% at 2 g of plutonium per liter to ± 2.2% at 10 g/L. Hydroxylamine nitrate, a reducing agent used in solvent extraction tests, affect the accuracies of both uranium and plutonium assay by densitometry, and plutonium analysis by coulometry. It appears that the XRAED could be used to control the SRL miniature mixer-settlers, but additional testing will be needed to demonstrate that XRAED accuracy is sufficient for accountability of special nuclear materials.

KEYWORDS: X-ray absorption-edge densitometry, uranium and plutonium solutions assay, densitometer evaluation

INTRODUCTION

Rapid, on-line, nondestructive assay of uranium and plutonium concentrations in nuclear fuel reprocessing streams may be used to control the process and maintain accountability of special nuclear materials (SNM). An x-ray absorption-edge densitometer (XRAED) designed and built by Los Alamos Scientific Laboratory[1] (LASL) has been evaluated at Savannah River Laboratory (SRL) for accurate assay of uranium and plutonium in process solutions. XRAED precision was determined from multiple assays of individual samples. Accuracy was determined by comparing XRAED assays to highly accurate chemical analyses. An initial 6-month evaluation of the XRAED for assay of 20-100 g/L of uranium process solutions showed results to be accurate within ± 0.6 g/L (95% confidence level). This paper reports the results of the XRAED evaluation during the following 10 months for assay of process solutions containing both plutonium and uranium.

EXPERIMENTAL METHODS

X-Ray Absorption-Edge Densitometer

Description

LASL designed the XRAED to assay solutions with uranium to plutonium ratios (U/Pu) between 4 and 10 and Pu concentrations between 2 and 10 g/L.[1] The densitometer (Figure 1) consists of four basic components:

1. The x-ray source and beam tube
2. The sample cell
3. The Si(Li) detector
4. A computer-based multichannel analyzer

The x-ray source has a tungsten target and molybdenum filter and operates at 20.6 kV to produce an x-ray spectrum with relatively constant intensity near the L_{III} edges of uranium and plutonium (17.168 and 18.057 keV, respectively) and with a sharp cut-off above the plutonium edge. The x-ray beam is collimated to 5 mm.

The sample cell used at SRL was made of stainless steel with Kel-F® (registered trademark of the 3M Company) windows. It was connected by a stainless steel loop to filling and sampling equipment in an adjacent glove box containing miniature mixer settlers used for studies of coprocessing solvent extractions. The sample cell was enclosed in a secondary containment cabinet maintained at negative pressure with respect to the room. An alpha monitor in the cabinet exhaust was used to detect any leakage from the sample cell. No leakage occurred during the evaluation.

The Si(Li) detector was 30 mm square with a resolution of 155 eV, full width at half maximum at 5.7 keV. The optimum detector count rate for data collection was 20,000 counts per second.

A TN-1700 multichannel analyzer based on a Data General Supernova® computer was used for data acquisition. Software in BASIC language was developed by LASL for data collection and analysis. Input and output were made via a General Electric TermiNet® equipped with a cassette tape unit for recording assay results and x-ray spectra.

Theory of Operation

In absorption-edge densitometry, uranium and plutonium concentrations are determined by comparing the sample-attenuated x-ray spectrum with the spectrum of a 0.5M HNO_3 reference solution.[1] X-ray transmission through a sample of thickness x at energies just above and below the L_{III} absorption edge are, respectively:

$$T_1 = T_m e^{-\mu_1 \rho x}$$

$$T_2 = T_m e^{-\mu_2 \rho x} \qquad (1)$$

where, ρ is the sample elemental concentration of interest and the μ is the mass attenuation coefficient. T_m includes any matrix contribution to the transmission. The ratio of these transmissions removes the matrix effects from the concentration measurement:

$$R = T_1/T_2 = e^{-\Delta\mu\rho x} \qquad (2)$$

and

$$\rho = \ell n\ R/k \quad (\text{where } k = \Delta ux) \qquad (3)$$

The calibration factor, k, can be evaluated empirically using standard solutions of known ρ.

The reduction of data begins with a normalization (channel by channel division) of the sample spectrum to the reference spectrum to remove matrix effects. A first-difference spectrum is generated from the normalized data. The difference spectrum displays peaks, the centroids of which coincide with the absorption edges in the normalized data. The background-subtracted integral under the peak is the ratio, R, defined in Equation 2.

The first-difference spectrum is analyzed by determining the background-subtracted integrals with specified regions of interest containing the uranium peak, the plutonium peak, or backgrounds. For the mixed U-Pu samples, the background between the two peaks cannot be used, so only the background regions on either side of the peaks are calculated. Backgrounds at the peaks are determined by linear extrapolation. Background in the peak regions are determined with a straight-line extrapolation of these. The background-subtracted integrals, which are the experimental values of R, are used to determine the assay using stored calibration constants according to Equation 2.

Calibration

The calibration constants in equation 3 for the XRAED were determined at LASL using mixed standard uranium-plutonium solutions with compositions representative of the range for process solutions. These calibration standards were stored and assayed in sample cells which were geometrically identical to the flow-through cell used at SRL.

LASL personnel verified these calibrations for the XRAED installation at SRL using mixed solutions made from nonstandard materials. These solutions were made from reagent grade uranyl nitrate and nonstandard plutonium metal and contained 0.5M reagent grade hydroxylamine nitrate (HAN) and 2M nitric acid to simulate process solutions. The solutions were characterized with highly accurate chemical analyses (described later) before and after the XRAED assays that were used to verify the calibration.

XRAED Operation

XRAED operation required a daily visual check of the stored x-ray spectrum for the 0.5M HNO_3 reference solution. This spectrum was usually remeasured once a week. The software also required a daily check of the transmitted x-ray spectrum for a standard uranium foil. If results fell within prescribed limits, normal operation continued. If results were outside the limits, a recheck of the foil spectrum was required. If results were still outside the prescribed limits, the normal assay sequence was interrupted until the problem was corrected.

After successful completion of the foil check, the cell was emptied, rinsed with a portion of sample, and another portion loaded and assayed. The x-ray tube current was adjusted to produce a detector count rate of 20,000 per second. Count times of 1000 seconds had been used for assay of 20-60 g/L of uranium solutions. However, LASL specified a 2000 second count time for mixed solutions, because the uranium reduced the x-ray intensity in the regions of the Pu L_{III} absorptions edge. Assay results were printed out on the TermiNet. X-ray spectra were recorded on cassette tape for transmittal to LASL for further evaluation.

Each sample was usually assayed three times. The sample was then withdrawn from the sample cell and portions submitted for chemical analysis and determination of solution density.

Chemical Analyses

Samples were tightly sealed in polyethylene bottles for chemical analysis, usually performed within one week after assay. Evaporation was found to cause about a 0.2% increase in concentration in a week. Weighed sample aliquots were used in both uranium and plutonium analyses.

Uranium Analysis

A method based on a modified Davies-Gray titration was developed for highly precise and accurate determinations of uranium in process solutions to support the XRAED evaluation. This method is not affected by plutonium, thorium, iron, nitric acid or tributylphosphate which may be present in process streams. HAN, which interferes with uranium analyses, was reduced to acceptable levels by treatment with cold, concentrated nitric acid. Uranium is selectively reduced from U(VI) to U(IV) and then quantitatively reoxidized by weight-titration with National Bureau of Standards (NBS) potassium dichromate solution to a potentiometric end point. The apparatus consisted of a tin oxide-treated glass electrode with a commercial calomel reference electrode. A blank sample and a primary standard solution made from NBS uranium were analyzed daily to check on the quality of reagents and operation of the equipment. With the modified Davies Gray method, uranium concentrations in process solutions were determined within 0.1% of the actual concentrations (relative standard deviation).

Plutonium Analysis

A coulometric method for the accurate analysis of plutonium in process solutions was developed to support the XRAED evaluation. Plutonium was quantitatively oxidized on a gold electrode in nitric acid at a controlled potential which eliminated uranium interference.

Accurate plutonium determinations in process solutions required special sample pretreatment to remove the large amounts of HAN which severely interfered with the Pu^{+3}/Pu^{+4} redox pair. The HAN was effectively destroyed in a sample aliquot by treatment with hot concentrated nitric acid.

During the evaluation, it was discovered that the HAN in process solutions contained unexpectedly high levels of iron which interfered with plutonium analyses. Tests showed that 80% of the iron was oxidized and reduced at the potentials used for the plutonium analysis. Subsequently, the iron content in each process solution sample was determined colorimetrically using 1, 10-phenanthrolene (17 µg/mL). The charge transfer associated with the iron redox process was then subtracted from the total sample charge transfer to correct the plutonium analysis. Daily analysis of a blank sample was used to determine the background charge transfer. A periodic analysis of a primary standard solution was used to check the operation of the equipment. Extensive testing indicated that plutonium analyses of process solutions should be accurate within 0.5% (relative standard deviation).

Solution Density Measurement

Uranium and plutonium concentrations in grams per liter were calculated from the potentiometric and coulometric analyses using solution densities measured with a Mettler-Paar DMA 45 density meter and DMA 401W remote cell at room temperature. The measuring principle is based on the change of the natural frequency of a hollow oscillator when filled with different liquids or gases. Air and distilled water were used as the calibrating fluids. The density of a spectroscopic grade sample of cyclohexane was within 0.0001 g/cm^3 of the literature value. Duplicate samples were reproducible to ± 0.0001 g/cm^3.

Evaluation Method

The difference in percent between XRAED assays (X) and the chemical analyses (C) for both uranium and plutonium is

$$(\%) = \frac{(X - C)}{C} \times 100. \qquad (4)$$

These values were used to determine the accuracy (bias) of the XRAED assays. The standard deviation in multiple assays of each sample indicated the precision of XRAED measurements.

XRAED Samples

Process Solutions

Process solutions containing uranium and plutonium were produced during solvent extraction tests in miniature mixer-settlers at the rate of 0.3 to 0.6 mL/min (Table 1). During the evaluation, the XRAED was used to monitor the progress of several of these tests by assaying samples collected sequentially in 60 mL increments. Unfortunately, many of these process solutions contained plutonium at concentrations less than 2 g/L, which is the lower design limit of the XRAED. Larger volumes of several composite solutions collected in earlier mixer-settler tests were also used to provide samples for evaluation. In addition to uranium and plutonium, the process solutions also contained 0.2 to 1.5M nitric acid and 0.2 to 0.8M HAN. One mixer-settler experiment produced process solutions with hydrazine rather than HAN.

TABLE 1

PROCESS SOLUTIONS USED IN XRAED EVALUATION

Solution	*No of Samples*	*Uranium* ρ_U *(g/L)*	*Plutonium* ρ_{Pu} *(g/L)*	HNO_3 *M*	*HAN M*
BP1	14	16.1 - 41.9	2.2 - 4.7	0.5	0.5 - 0.8
BP2	9	7.7 - 20.8	0.5 - 3.9	1.5	0.2
BP3	8	7.7 - 34.7	0.5 - 3.5	1.4	0.2
BP4	6	8.4 - 35.7	3.5 - 8.7	<0.5	0.3
BP5	7	14.2 - 27.9	0.3 - 2.2	1.0	0.35
BP6	2	9.6 - 14.2	2.9 - 4.7	2.7	0[a]
BP7	15	14.3 - 35.2	1.2 - 4.6	1.0 - 2.3	0.15 - 0.3
BP Composite #1	10	11.0 - 22.4	2.0 - 4.0	-	-
BP Composite #2	3	15.8	4.0	-	-

a. Contained 0.1M Hydrazine Nitrate.

TABLE 2

CALIBRATION VERIFICATION SOLUTIONS USED IN XRAED EVALUATION
2.0M HNO_3 - 0.5M HAN

Calibration Solution	*Uranium* ρU *(g/L)*	*Plutonium* ρ_{Pu} *(g/L)*
CS1	13.1	3.1
CS2	21.9	4.0
CS3	40.2	10.0
CS4	20.2	5.0
CS5	35.0	4.9
CS6	36.6	4.0

Prepared Solutions

A series of six solutions containing 13.1-40.5 g/L uranium and 3.1-10.2 g/L plutonium with U/Pu equal to 4.0 to 9.1 was prepared to verify the LASL calibration of the XRAED (Table 2). These solutions were prepared from reagent grade uranyl nitrate and plutonium metal (99.9% purity) and contained 2M nitric acid and 0.5M HAN to simulate process solutions. Portions of these solutions remaining from the calibration verification were used in the XRAED evaluation.

Four primary standard solutions were prepared from NBS standard #960 uranium metal and #949d plutonium metal. Two of the solutions contained HAN. For these primary standard solutions, the XRAED assays and chemical analyses were both compared to the weighed values.

When unexpected iron impurity in the HAN was found to interfere with plutonium analyses, another series of eleven solutions containing 14.4-44.9 g/L uranium and 2.4-9.5 g/L plutonium with U/Pu equal to 4.1 to 10.2 was prepared without HAN for XRAED evaluation (Table 3). These solutions were made from residual uranium standard solutions and dissolved nonstandard plutonium metal and contained $\sim$ 2M HNO_3.

RESULTS

Densitometry Precision

The standard deviations from the mean uranium and plutonium assay values for multiple (3-6) assays of the various types of solutions are shown in Figure 2 and 3. Linear regression analysis results did not accurately describe the data over the ranges of concentrations for uranium and plutonium. However, second order regression analyses did describe the nonlinear variations in the standard deviations for uranium ($\bar{\sigma}_U$) and plutonium ($\bar{\sigma}_{Pu}$) by

$$\bar{\sigma}_U(\%) = 0.75 - 0.0250\ (\rho_U) + 0.000271\ (\rho_U^2) \qquad (5)$$

for $10\ g/L \leq \rho_U \leq 45\ g/L$

and

$$\bar{\sigma}_{Pu}(\%) = 4.41 - 0.606\ (\rho_{Pu}) + 0.0276\ (\rho_{Pu}^2) \qquad (6)$$

for $2\ g/L \leq \rho_{Pu} \leq 10\ g/L$

Since densitometer users will probably rely on the results of a single assay, precision should be considered in terms $2\bar{\sigma}$ (95% confidence level). Thus, the precision in uranium assay varies from ± 1.04% at 10 g/L to ± 0.34% at 45 g/L and the precision in plutonium assay varies from ± 6.7% at 2 g/L to ± 2.2% at 10 g/L. The precision of the uranium assay for mixed U-Pu solutions is the same as that for uranium.[1]

Densitometer Accuracy

Assay of the mixed U-Pu solutions prepared with 0.5M reagent HAN for confirmation of the densitometer calibration (Figure 4 and 5) showed a ± 0.18% bias for uranium and a ± 1.5% bias for plutonium. However, in subsequent assays of process solutions, the uranium results were too scattered for interpretation (Figure 6). Solutions with $\sim$ 8 g/L of plutonium showed a bias of $\sim$ + 2.1% (Figure 7). At lower plutonium concentrations, the plutonium bias varied with process HAN concentration from $\sim$ - 2% for 0.2M HAN to $\sim$ + 8% for 0.8M HAN.

Primary standards with and without reagent HAN were assayed and analyzed, and results were compared with weighed values to help resolve the uncertainties about the effects of HAN. Results are given in Table 4. Chemical analyses agreed well with the weighed values in the standards that contained no HAN. Densitometer results for plutonium showed good agreement with chemical analysis and weighed values, but uranium assays showed a bias of

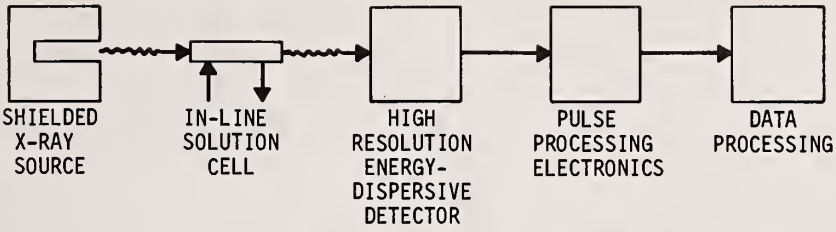

FIGURE 1. Block Diagram of XRAED

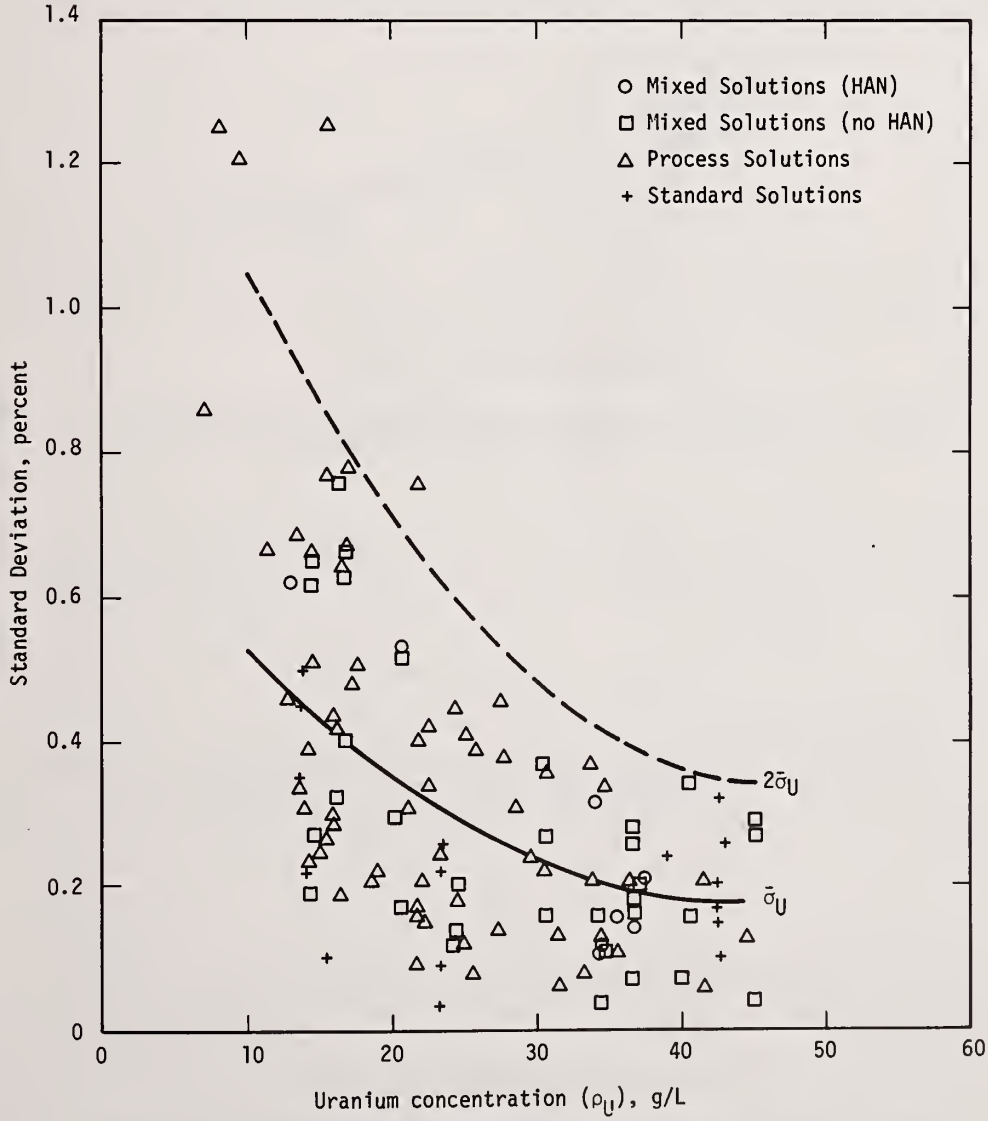

FIGURE 2. Precision in XRAED Assay of Uranium in Mixed U-Pu Solutions with 2≤Pu≤10g/L and 4≤U/Pu≤10

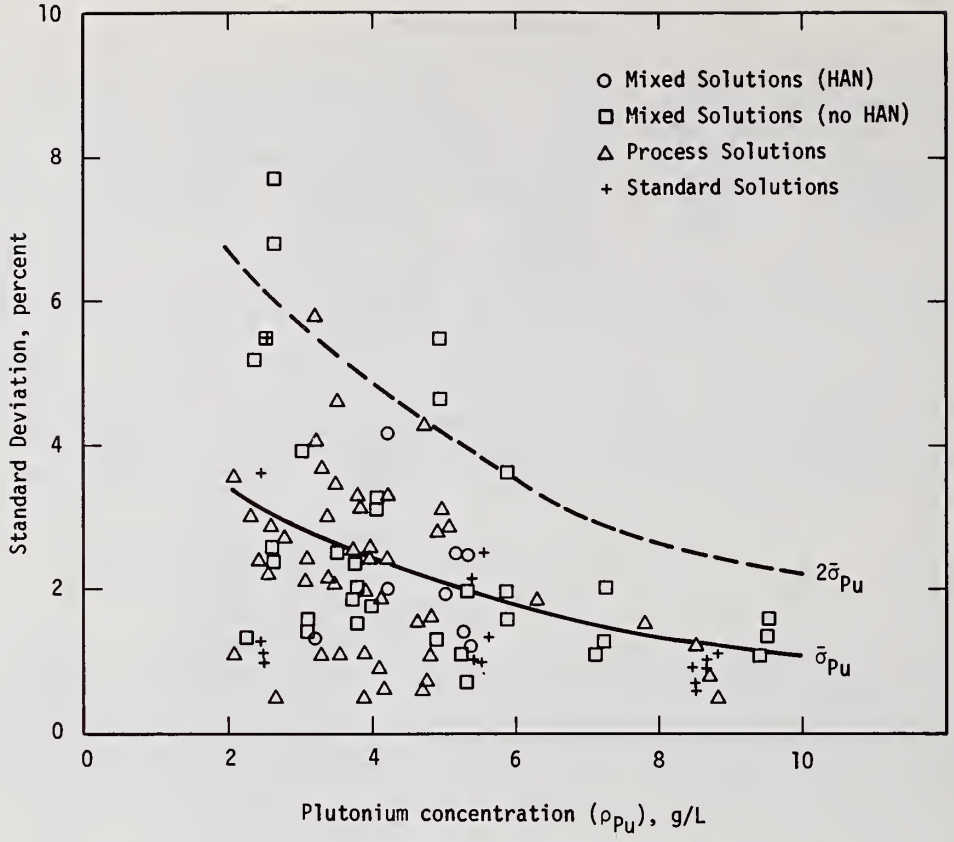

FIGURE 3. Precision in XRAED Assay of Plutonium in Mixed U-Pu Solutions with 2≤Pu≤10g/L and 4≤U/Pu≤10

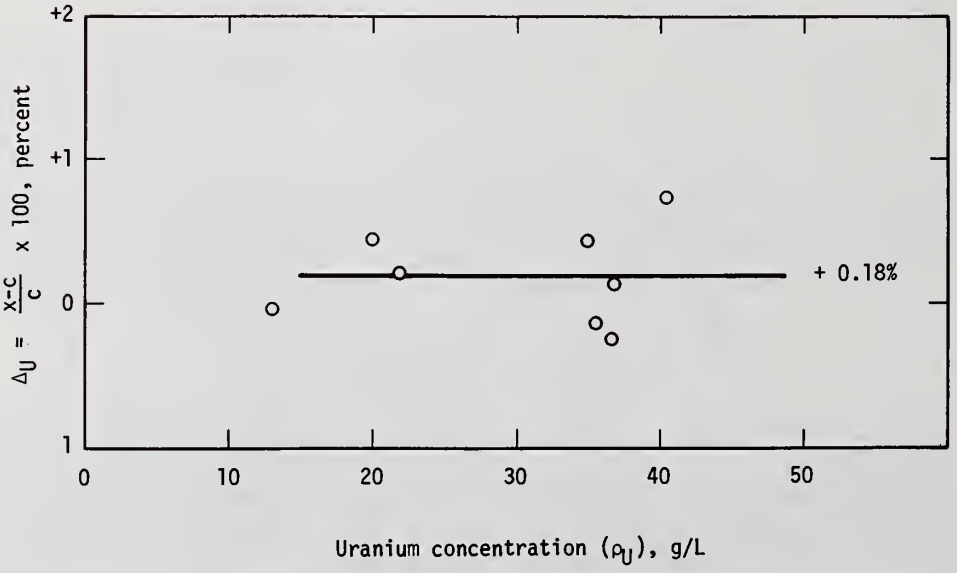

FIGURE 4. Difference Betweem Uranium Assay and Chemical Analysis of Mixed U-Pu Solutions Containing HAN (Calibration Solutions)

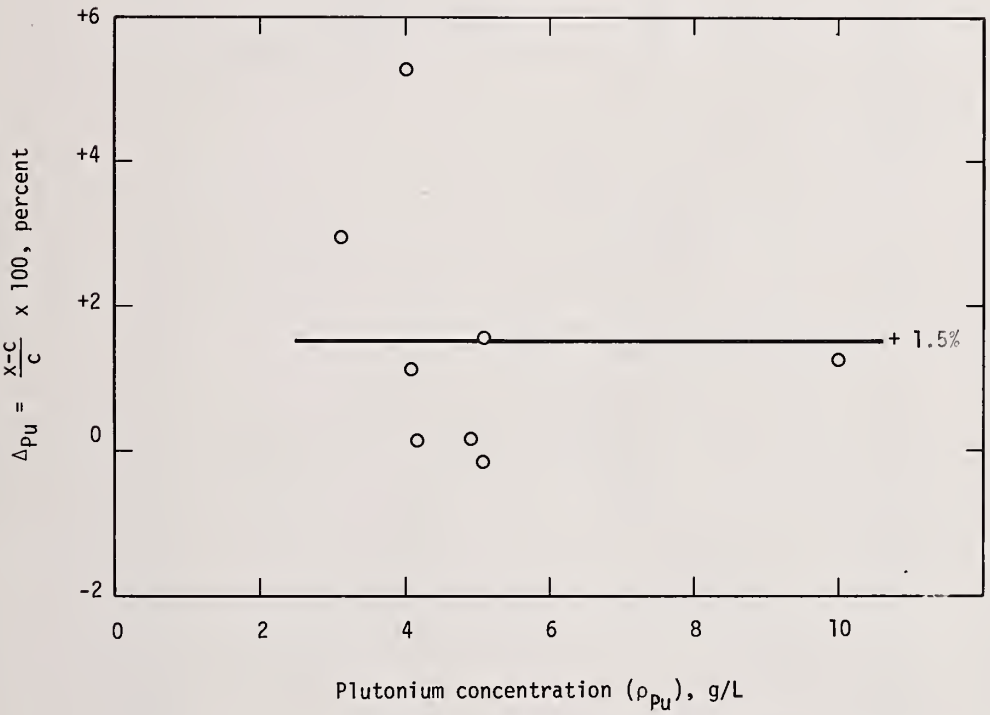

FIGURE 5. Difference Between Plutonium Assay and Chemical Analysis of Mixed U-Pu Solutions Containing HAN (Calibration Solutions)

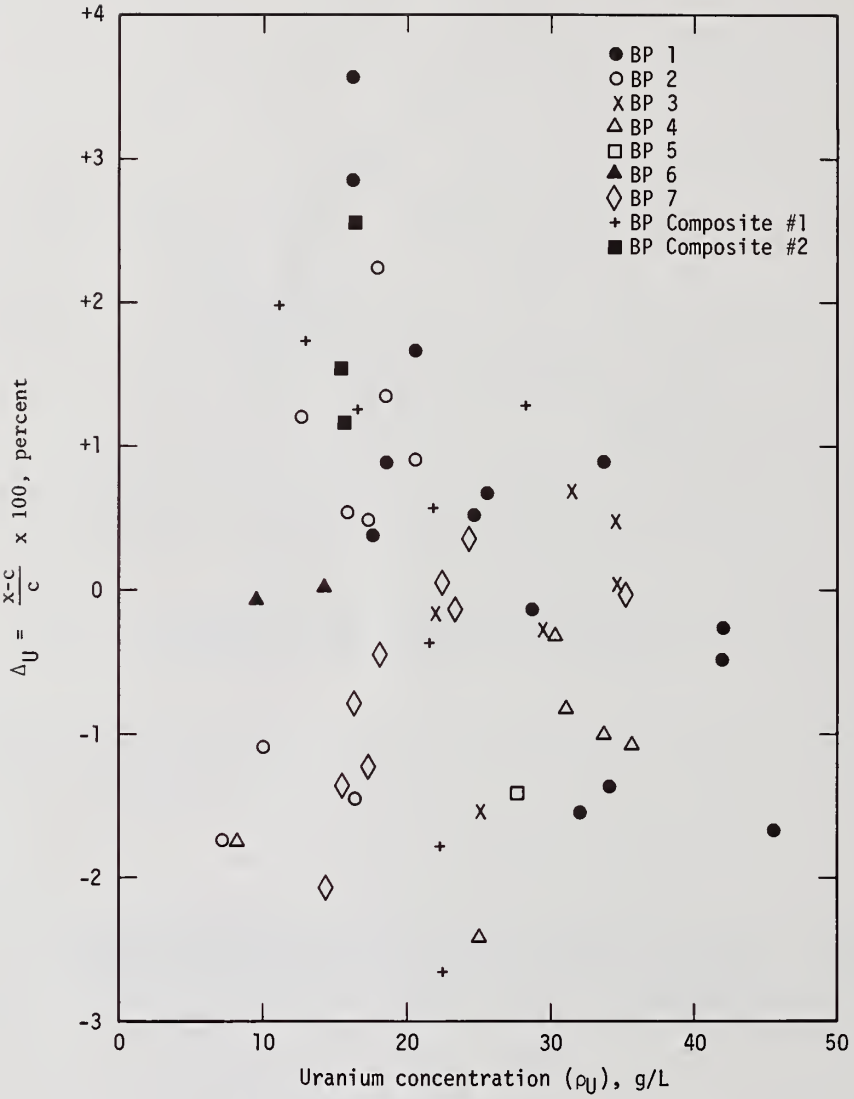

FIGURE 6. Difference Between Uranium Assay and Chemical Analysis of Process Solutions

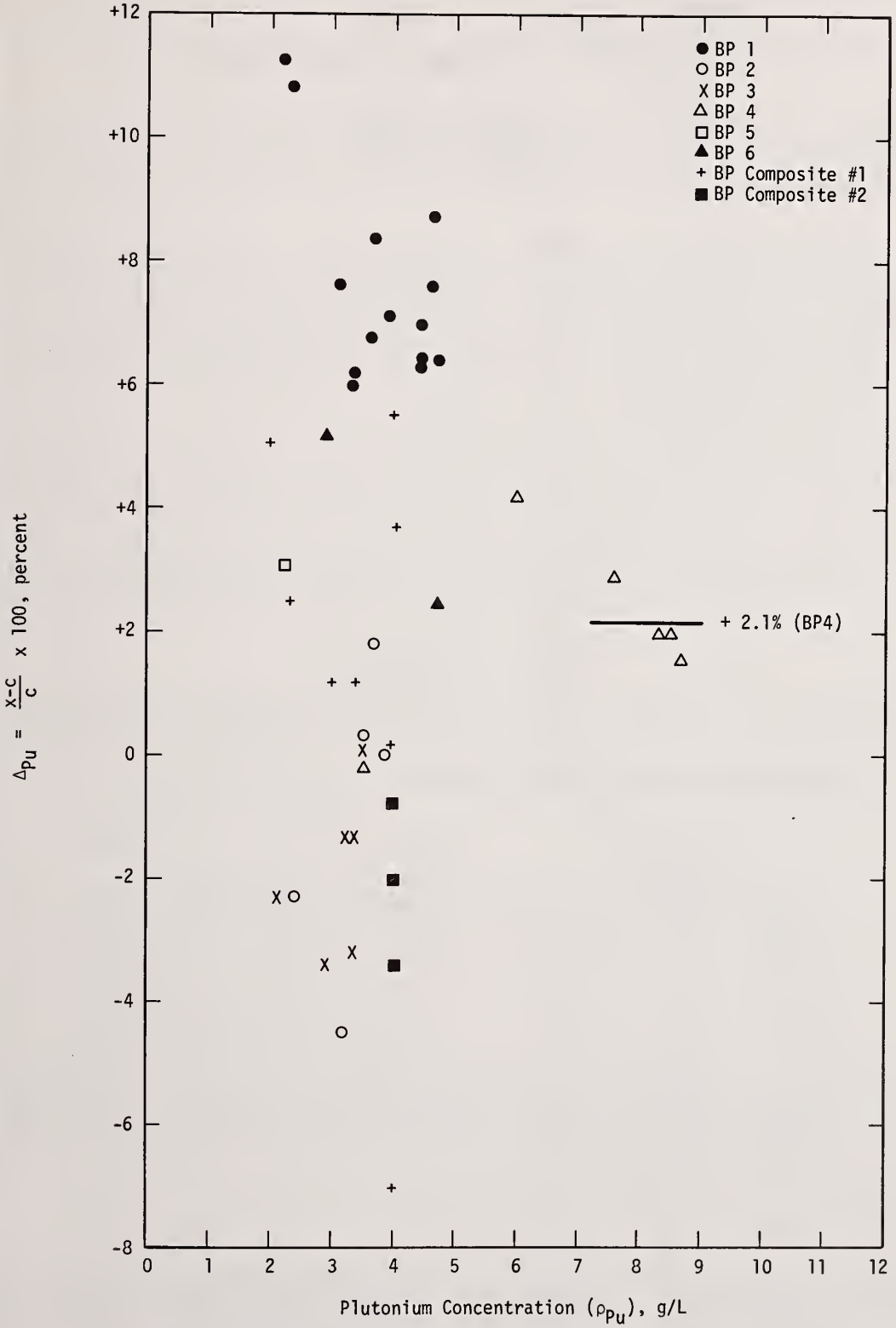

FIGURE 7. Difference Between Plutonium Assay and Chemical Analysis of Process Solutions

TABLE 3

MIXED SOLUTIONS (no HAN) USED IN XRAED EVALUATION
2.0M HNO_3

Mixed Solution	*Uranium* ρU *(g/L)*	*Plutonium* ρ_{Pu} *(g/L)*
MS1	14.2	2.4
MS2	44.6	5.8
MS3	16.1	3.9
MS4	30.4	2.9
MS5	36.2	4.9
MS6	33.9	5.1
MS7	24.3	3.6
MS8	39.8	9.2
MS9	15.8	3.7
MS10	20.4	2.4
MS11	36.5	7.0

TABLE 4

Chemical and Densitometer Results for Primary Standards

Standard		*W Weighed Values g/L*	*C Chemical Analysis of Standard g/L*	*X Densitometer Assay g/L*	*Cx Chemical Analysis of Sample After Assay g/L*	*Differences C-W / W %*	*X-W / W %*	*X-C / C %*	*X-Cx / Cx %*
PS #1	U	42.195	42.269	42.745	42.181	+ .18	+1.30	+1.13	+1.34
	Pu	8.449	8.439	8.486	8.431	- .12	+ .44	+ .55	+ .65
PS #2	U	22.989	23.018	23.377	23.018	+ .12	+1.69	+1.56	+1.56
	Pu	5.435	5.416	5.462	5.411	- .36	+ .50	+ .85	+ .94
PS(HAN) #1	U	16.569	16.594	16.630	-	+ .15	+ .36	+ .22	-
	Pu	2.273	2.256	2.411	-	- .70	+6.09	+6.87	-
PS(HAN) #2	U	38.779	38.935	38.910	-	+ .52	+ .33	- .06	-
	Pu	5.307	5.246	5.590	-	-1.14	+5.34	+6.56	-

∿ + 1.5%. Chemical analyses of primary standards containing HAN did not agree as well with weighed values as the pure standards did. A possible bias for plutonium of ∿ 0.9% may have been caused by loss of plutonium through effervescence during the destruction of the HAN prior to coulometric analysis. The densitometer assays for plutonium showed a bias of ∿ + 6% because of the HAN.

Figures 8 and 9 show the differences between assays and chemical analyses for the series of mixed U-Pu solutions prepared without HAN. Uranium assays had a ± 0.63% bias for concentrations greater than 20 g/L. Results for solutions with ∿ 16 g/L uranium had a + 1.66% bias. Plutonium assay results were scattered about an average bias of + 2.3%.

XRAED assays and chemical analyses for a mixed solution (MS6A) prepared with the same uranium and plutonium concentrations as MS6, but containing 0.8M process HAN, are compared in Table 5. The process HAN had no effect on the uranium or plutonium assays or the uranium analysis. However, the plutonium analysis values for MS6A were 5.3% higher than those for MS6 because iron impurity in the process HAN interfered with the coulometric analysis. The iron level in MS6A was determined colorimetrically and the plutonium analyses corrected to give a + 3% bias compared with + 4.8% for MS6.

Results for two process solutions (BP6) from a solvent extraction test with hydrazine nitrate instead of HAN showed a bias in uranium assay of - 0.02% (Figure 6), and a bias in plutonium assay of + 3.8% (Figure 10).

Plutonium analyses for five process solutions (BP7) were corrected for the effects of iron impurity. Comparison of XRAED assays with these corrected chemical analyses (Figure 10) show a bias of + 5.5%.

Densitometer Reliability

The XRAED was operational about 95% of the time. The malfunctions experienced during the fourteen months of XRAED evaluation were:

MALFUNCTION	DOWN TIME (days)
Oil leak in X-ray power supply	7
Broken part in Terminet	3
Computer loss of software statement	2
Intermittent malfunction in x-ray interlock circuit	12

During XRAED operation, 85% of the initial daily foil checks were accomplished. The second foil check was accomplished 9% of the time. The rest of the time, the 0.5 M HNO_3 reference spectrum had to be remeasured before the foil check was accomplished. For this last situation there was a delay of several hours before the XRAED was ready to assay samples.

CONCLUSIONS

The XRAED precisions for uranium and plutonium determined in the SRL evaluation agreed with the testing, evaluation, and calibration of LASL. At the 95% confidence level, the precision for uranium assays varied from 1.04% at 10 g/L to ± 0.34% at 45 g/L and the precision for plutonium assays varied from + 6.7% at 2 g/L to ± 2.2% at 10 g/L.

Table 6 summarizes the differences between XRAED assays and chemical analyses for uranium and plutonium in the various type of solutions used in the XRAED evaluation.

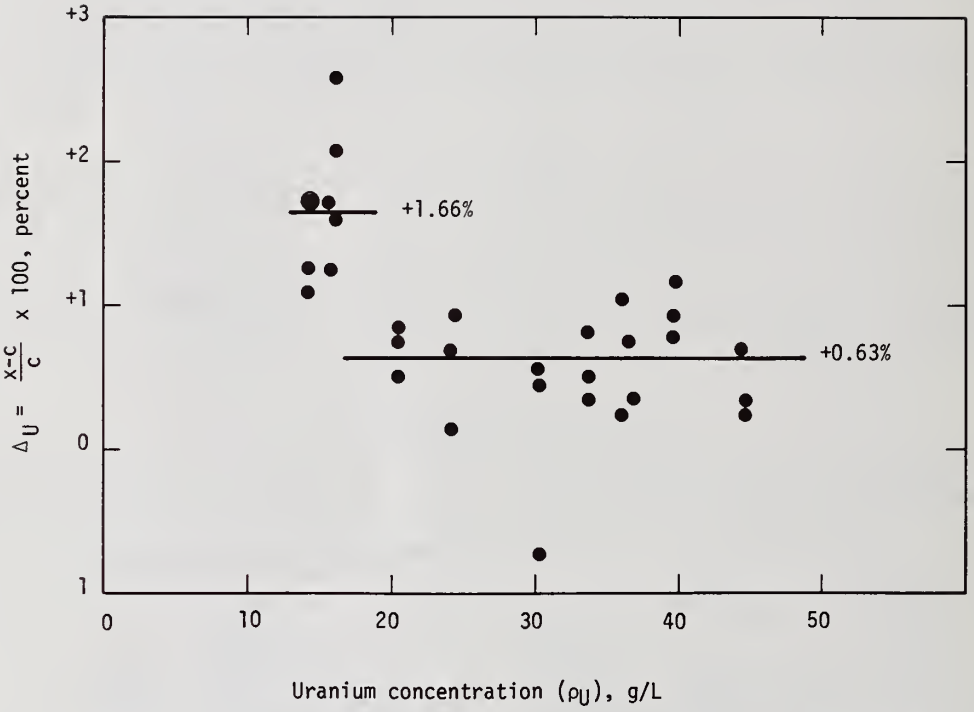

FIGURE 8. Difference Between Uranium Assay and Chemical Analysis for Mixed U-Pu Solutions with No HAN

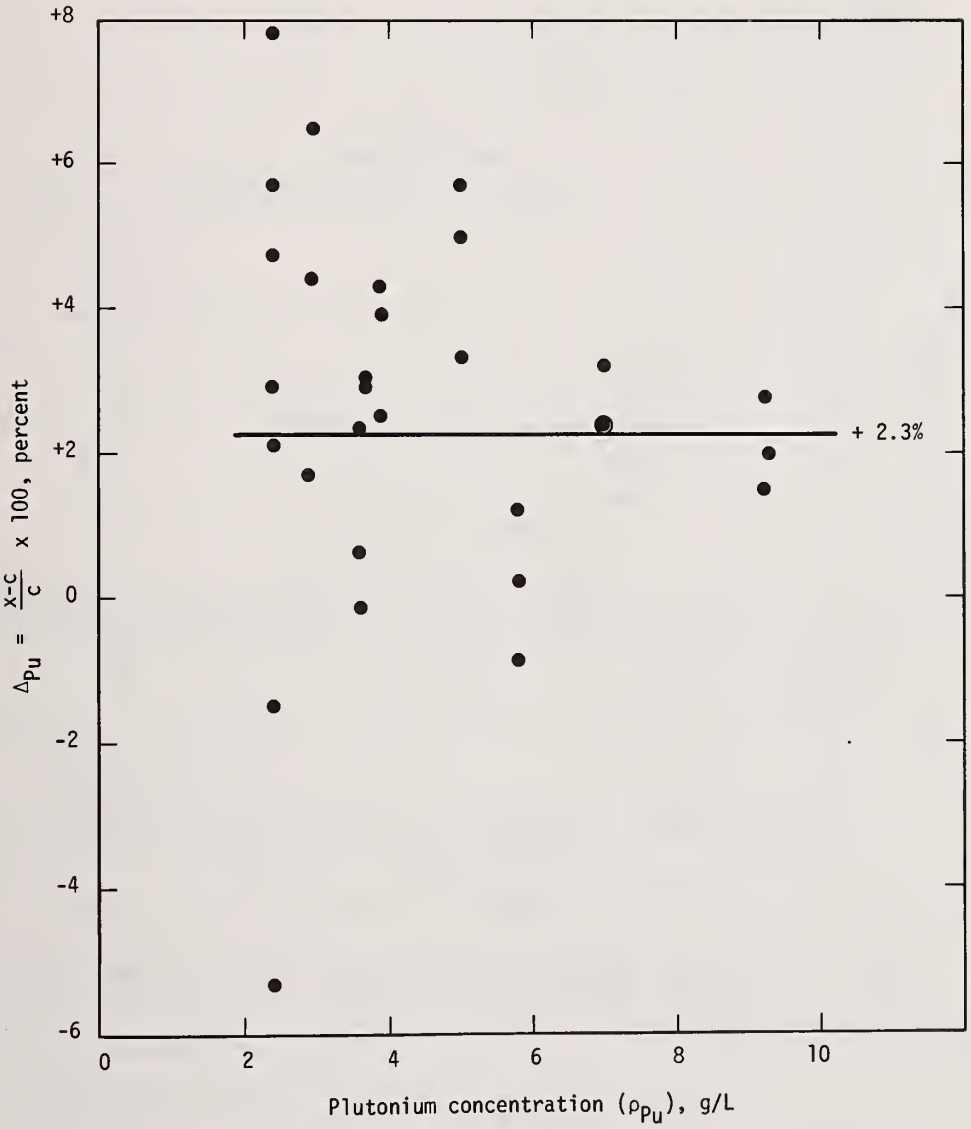

FIGURE 9. Difference Between Plutonium Assay and Chemical Analysis of Mixed U-Pu Solutions with No HAN

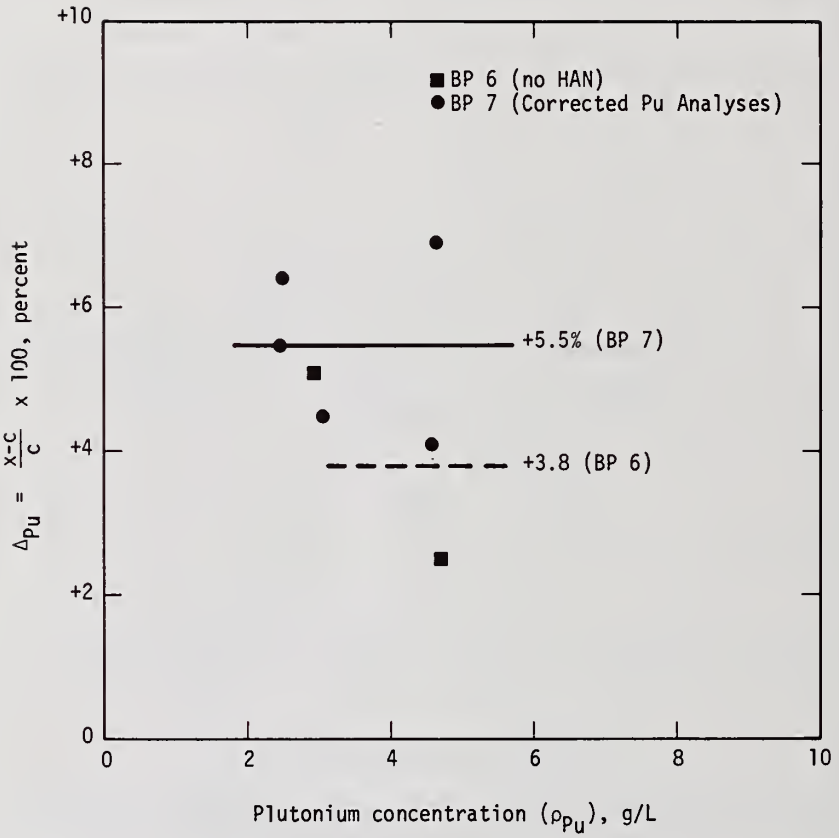

FIGURE 10. Difference Between Plutonium Assay and Chemical Analysis of Process Solutions BP6 and BP7

TABLE 5

XRAED ASSAYS AND CHEMICAL ANALYSES OF MIXED U-ρu
SOLUTIONS CONTAINING NO HAN (MS6) AND 0.8M PROCESS HAN (MS6A)

	XRAED		*Chemistry*		*Differences*	
	ρU (g/L)	ρ_{Pu} (g/L)	ρU (g/L)	ρ_{Pu} (g/L)	ΔU(%)	ΔPu (%)
MS6						
(no HAN)	34.00	5.29	33.82	5.05	+0.53	+4.8
MS6A	34.07	5.24	33.90	5.32	+0.50	-1.9
(0.8M Process HAN)						+3.6[a]

a. Corrected for Fe in Process HAN

TABLE 6

DIFFERENCES BETWEEN XRAED ASSAYS AND CHEMICAL ANALYSES OF URANIUM
AND PLUTONIUM CONCENTRATIONS IN SOLUTIONS USED IN EVALUATION OF THE LASL XRAED

Solution	*Uranium Bias, Δ* %	*Plutonium Bias, ΔPu* %
Primary Standards (PS) (no HAN)	+ 1.35	+ .70
Mixed Solutions (MS) (no HAN)	+ 0.63 (ρ_U > 20 g/L) + 1.66 (ρ_U ≈ 15 g/L)	+ 2.3
Calibration Solutions (CS) (0.5M HAN)	+ .18	+ 1.5
Primary Standards (PS-HAN) (0.5M HAN)	+ .08	+ 6.7
Process Solutions (BP 1-5)	?[α]	(+ 2.1 for BP 4 with ρ_{Pu} ≈ 8 g/L)
Process Solutions (BP 6) (no HAN)	- .02	+ 3.8
Process Solutions (BP 7) (corrected Pu analysis)	?	+ 5.5

a. Results too scattered for interpretation.

Assessment of the accuracy of XRAED assays of process solutions was complicated by HAN apparently interfering with both the XRAED assays and plutonium analyses. The interference with the coulometric analysis was caused by iron impurity in the HAN. Iron was present in much higher levels in the process HAN, which was used as a reducing agent in solvent extraction tests, than in the reagent HAN used to prepare calibration verification solutions and primary standards.

The results for the primary standards and mixed solutions with no HAN are considered the most reliable. These results show a uranium bias of + 0.6 to 1.7%, and a concentration dependence with the bias becoming more positive with decreasing uranium concentration. A bias in plutonium of + 0.7 to 2.3% is indicated, but no apparent concentration dependence could be deduced from these results. Changes in the XRAED assay software can be made to correct for these biases and concentration dependence.

The results for the primary standard solutions indicate that HAN in a solution causes the uranium assays to be $\sim$ 1% lower than that of a solution with no HAN. Also, the plutonium assay of a solution with HAN is $\sim$ 5% higher than that of a solution with no HAN. Time did not permit an investigation of these effects of HAN on densitometry during the SRL evaluation.

The XRAED provided timely assays of uranium-plutonium process solutions to support solvent extraction experiments in the SRL miniature mixer settlers. It appears that the XRAED could be used to control reprocessing in the SRL miniature mixer-settlers. However, because of possible effects of some components in the process solutions on densitometer accuracy, further testing will be needed to demonstrate that the XRAED accuracy is sufficient for SNM accountability.

ACKNOWLEDGEMENTS

The authors would like to thank C. D. Ouzts for operating the densitometer and B. M. DeWeese for performing the chemical analyses in support of the densitometer evaluation at SRL.

REFERENCES

1. P. A. Russo, T. R. Canada, D. G. Langner, J. W. Tape, S. Hsue, L. G. Cowder, W. C. Mosley, L. Reynolds, and, M. C. Thompson, "An X-Ray L_{III}-Edge Densitometer for Assay of Mixed S.N.M. Solutions." CONF 790430-9, First Annual Symposium on Safeguards and Nuclear Material Management, Brussels, Belgium, (1979).

2. M. S. Okamoto and M. C. Thompson, "Coprocessing Solvent Extraction Studies," *Nuclear Technology* 43, 126 (1979).

Discussion:

Walton (LASL):

Additional comments about the test and evaluation appear to be appropriate. Because the budget for this work at SRL was expended and the course of this work has changed, the evaluation of this instrument was terminated before it was completed. For this reason and because of the difficulties SRL experienced in the chemical analysis of uranium and plutonium, this instrument will be transferred to the New Brunswick Laboratory for continuation of its evaluation. We will check the instrument at LASL and review the data analysis software prior to putting it through its paces at NBL. To the best of our knowledge, there is no physical basis for the sensitivity attributed by Mr. Mosley to variations in HAN concentration.

The Goals of Measurement Systems for International Safeguards*

by

J. M. de Montmollin
Sandia Laboratories, Albuquerque, NM

E. V. Weinstock
Brookhaven National Laboratory, Upton, NY

ABSTRACT

The safeguards applied by the International Atomic Energy Agency are based on technical performance goals and criteria that have been developed, but not officially adopted by the Agency. The goals derive in part from the external consequences that safeguards are intended to prevent and in some cases on internal considerations of feasibility. To the extent that these goals may not be attainable, as may be the case with large-throughput bulk reprocessing plants, the Agency is placed in a difficult position. In this paper safeguards goals and criteria and their underlying rationales are critically examined. Suggestions for a more rational and workable structure of performance goals are offered.

KEYWORDS: International Atomic Energy Agency; international safeguards; safeguards performance criteria; safeguards objectives

International Atomic Energy Agency safeguards have been the subject of much attention in recent years, since concerns over nuclear-weapon proliferation have come to have a predominant influence on US policies affecting nuclear power. The performance criteria and goals that are being developed for the technical safeguards system are reflected in the perceptions of the policymakers and the reliance they are willing to place on IAEA safeguards. Technical performance criteria therefore have an impact on policy objectives, and they must be considered in that broader context. In this paper we address the problem of the specification of goals and criteria that are both practical from the technical standpoint and that will support the attainment of non-proliferation policy objectives.

IAEA SAFEGUARDS

Let us begin with a brief description of IAEA safeguards, and how they relate to domestic safeguards such as those administered by NRC. They differ in important respects, and form complementary but distinct elements in the overall structure.

As shown in Figure 1, the two systems include both common and separate elements. The IAEA system relies in an essential way on the State System of Accounting and Control, or SSAC. The Agency provides general guidelines for the SSAC that the State is expected to operate, and it avoids duplication of SSAC data, making independent measurements only for verification of the State's records.[1] The Agency cannot impede or obstruct the movement of materials in any way, and it relies on the containment -- walls, shielding, barriers, containers -- that is available. The Agency performs independent audits of records required by the State, as well as independent measurements, observations, and surveillance of containment and certain operations.

*The views expressed herein are those of the authors, and do not necessarily reflect those of Brookhaven or Sandia Laboratories or the Department of Energy.

While the Agency system provides only a capability to detect unauthorized activities, the State system covers control and response functions as well. It includes physical protection -- the monitoring and control of personnel and the exclusion of those not authorized, and means to respond to any attempted violation while it is in progress. It protects against sabotage, as well as misuse or diversion of materials and facilities.

The two systems differ further in that the State system is backed by the legal authority of the State, and is directed against threats to State interests by subnational groups or individuals. The IAEA system is intended to promote that protection by the State, but principally to provide assurance that the State itself does not violate its commitments pledging not to misuse materials or facilities. IAEA safeguards are applied only with the consent of the State, with the technical details subject to negotiation. While the State is the nominal adversary, there is a common interest in providing assurance that legitimate activities are not a cover for weapon production. The credibility of the assurance provided by IAEA safeguards depends in large measure on the capability to detect a diversion, should it occur. Since an actual attempted diversion of nuclear material would be a rare and unique event, the perception of the IAEA capability, rather than a history of successful detections, is the basis for the reliance on IAEA safeguards. Performance criteria and the ability of the IAEA to meet them are the basis for those perceptions.

THE OBJECTIVE OF SAFEGUARDS

The agreement establishing the IAEA states that the purpose of safeguards is

> ". . . to ensure that special fissionable and other materials, services, equipment, facilities, and information . . . are not used to further any military purpose . . ."[4]

The authority of the Agency to prevent misuse is limited to monitoring, and not direct control or sanctions.* The first document describing the IAEA safeguards system was more specific:

> "The purpose of safeguards inspections shall be to verify compliance with safeguards agreements and to assist States in complying with such agreements . . .."[5]

The NPT[2] obligated non-weapon-State signatories to accept IAEA safeguards. A group of technical consultants was convened by the IAEA for the purpose of drafting a new document covering safeguards under the NPT.[6] The group considered the problems of how a system could operate so as to provide assurance with positive measures of performance that diversion did <u>not</u> occur.[7,8] The solution that they arrived at was to state the objective of safeguards in positive terms:

> ". . . the objective of safeguards is the timely detection of diversion . . . of nuclear material . . . and the deterrence of such diversion by the risk of early detection."[9]

Although that definition of safeguards objective is widely cited and accepted, it differs from that stated in the safeguards document covering non-signatories of the NPT[10] and in the NPT itself in that it states that the objective is the detection of diversion rather than verification of compliance with non-proliferation obligations.** The problem of providing assurance that diversion has <u>not</u> occurred is not really solved by stating safeguards objectives in terms of detection of diversion. Safeguards operations

---

*There is limited additional authority in connection with Agency-supplied materials or Agency-sponsored projects, but that is of little practical significance.

**Article III of the NPT states in part that safeguards are ". . . for the exclusive purpose of verification of the fulfillment of obligations assumed under this treaty . .."

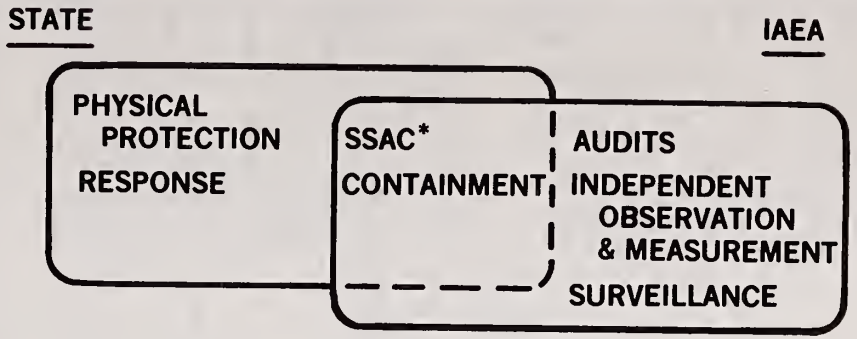

STATE SYSTEMS

MONITOR AND CONTROL
RESPONSE ACTION

--

STATE REGULATION AND ENFORCEMENT

AUTHORITY

NATIONAL LAWS

IAEA SAFEGUARDS

MONITOR BY MUTUAL AGREEMENT
VERIFICATION
GUIDELINES FOR PHYSICAL PROTECTION

AUTHORITY

IAEA STATUTE
- ART III
  - NPT[2]
  - TLATELOLCO[3]
  - BILATERAL AGREEMENTS
- ART XII
  - IAEA PROJECTS & MATERIALS

*STATE SYSTEM OF ACCOUNTING AND CONTROL

FIGURE 1. RELATIONSHIP OF IAEA SAFEGUARDS TO DOMESTIC SYSTEMS

lead to periodic findings by the IAEA that compliance is verified or not verified, and that is the objective as stated in INFCIRC/66 Rev. 2 and the NPT. The credibility of that verification depends on a capability to detect any diversion that might be attempted. A capability to detect diversion is a means to the end objective of verification. In the general case where no diversion occurs the objective is verification, and the problem of proving non-diversion remains.

VERIFICATION, NOT DETECTION

If the findings generated by the safeguards system could be so conclusive and unambiguous that we could always expect either hard evidence of diversion or convincing assurance of no diversion, the definition of safeguards objective would have less significance. That is, if the two cases were mutually exclusive, so that the absence of one condition necessitated the other, the objectives would be equivalent. However, in the real world there is a third state: a condition of uncertainity in which it can neither be stated that compliance with obligations is verified, nor that diversion has been detected. That situation may be due in part to other factors besides the imperfect performance of the technical safeguards system. Negotiated safeguards arrangements are neither perfect nor all-embracing; the safeguards operations can go no further than to verify that the agreements were complied with and that no indications of possible diversion were detected in the process. Failure to verify compliance may or may not be related to an actual diversion. It makes considerable difference whether the safeguards operation is intended to meet some required probability of detecting any diversion that might be attempted or whether it is expected only to detect indications of apparent violations and hence to reach a finding of inability to verify compliance.

Figure 2 diagrams the relationships between detection of diversion and verification of compliance as they are generally idealized and as they actually are in safeguards operations. The horizontal axis represents a scale of varying degrees of assurance or confidence. On the basis of the safeguards data that is collected and analyzed, a finding is reached with some degree of assurance represented by point A or B. A, for example, might be based on a more intensive sampling plan, smaller MUF, or fewer anomalous indications. As we move to the left, assurance diminishes to the point where we are unable to verify compliance with a degree of assurance deemed to be adequate. Current safeguards criteria recognize some small band of uncertainty, represented by the 95 percent confidence limits, wherein there is a risk of false alarm or failure to detect. No data are collected that would establish a point on the left side (except in the rare case of actual diversion), and therefore no statement could be made on the basis of available data other than verification or inability to verify. Inability to verify, unless it could be dismissed as being within the allowable margin for error represented by the statistical confidence limits, is often assumed by many in the technical safeguards community to be tantamount to detection of diversion.

The uncertainty is not limited only by the precision of the technical safeguards system. As Figure 2(b) indicates, detection of diversion and verification of compliance do not form a continuum, since agreements are not perfect or all-encompassing, and non-compliance is not necessarily associated with diversion. Agreements must accomodate practical considerations, often after hard negotiations, including such things as intrusiveness and operational impact, proprietary rights, costs, and political constraints. Material accounting, the principal safeguards measure, can only be implicitly assumed to approximate reality because of IAEA resource limitations and the possibilities of undeclared streams and the falsification of records. Finally, the safeguards systems' technical performance is limited by coverage and reliability as well as measurement precision.

The relatively large uncertainty band that separates assured detection from assured verification in Figure 2(b) is the reason why detection and verification cannot be accepted as being effectively mutually exclusive. A finding of verification can be made only if there is supporting data at some point such as A or B. If such a point cannot be established, and if there is no direct evidence to substantiate an actual diversion, the only finding that can be made is that compliance cannot be verified. If there is an

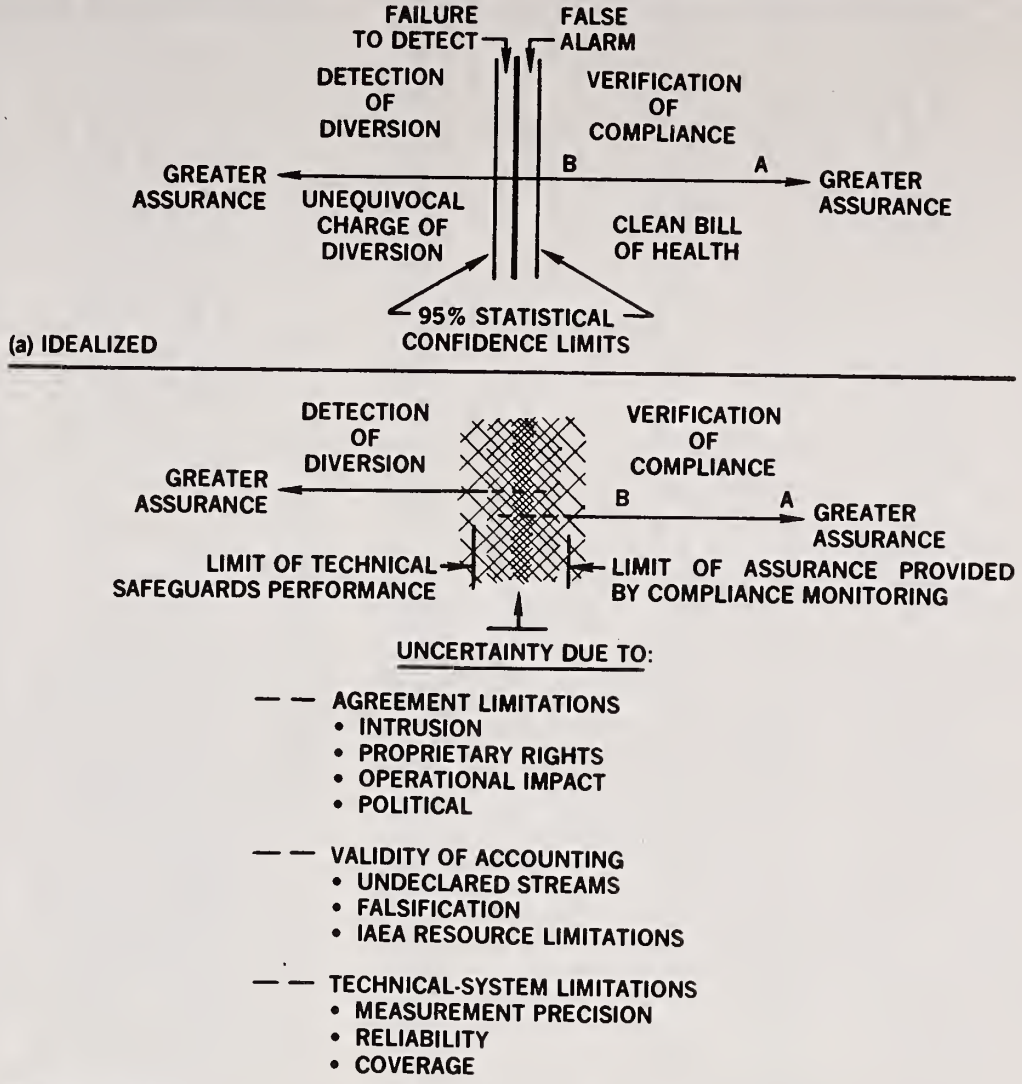

FIGURE 2. RELATIONSHIP OF DETECTION OF DIVERSION TO VERIFICATION OF COMPLIANCE

actual diversion and an effort is made to conceal it, the diverter is likely to be able to make it sufficiently ambiguous so that the information falls into the region of uncertainty with inadequate assurance to support a direct confrontation.

THE CONSTRAINT OF ACCEPTABILITY TO THE SAFEGUARDED

The IAEA Statute does not obligate any State to accept safeguards.* A commitment to accept safeguards must be otherwise motivated, usually from participation in some regional or international agreement such as the NPT or the Treaty of Tlatelolco or because it was a condition imposed by an exporting State. Typically the commitment is only to submit to "IAEA safeguards," with the actual arrangements to be subject to negotiations within general guidelines proposed by the Agency. While the State is committed to accept some kind of IAEA safeguards, the specific arrangements are confidential between the IAEA and the State. The guidelines for the agreements are provided in INFCIRC/66 Rev. 2 and INFCIRC/153. They have no legal force in themselves; for example, INFCIRC/66 Rev. 2, states specifically that its provisions will become legally binding only when, and to the extent that, they become incorporated into an individual agreement[11,12]. Similarly, the title page of INFCIRC/153 contains the following statement:

> "The Board of Governors has requested the Director General to use the material reproduced in this booklet as the basis for negotiating safeguards agreements between the Agency and . . . States . . . "[6]

Since what constitutes IAEA safeguards is not specified in the basic agreement such as the Statute or the NPT, in which the State agrees to accept them, the IAEA cannot unilaterally impose its own performance criteria. The agreement will in the end be based principally on a commonality of interests, bounded by the Agency's need to maintain credibility and the State's willingness to accept some intrusion on operations and national sovereignty. In setting performance goals and criteria, the Agency is motivated to press for greater effectiveness, striving for further improvements in the future.[13] At the same time, the impact on the State's nuclear activities must be reasonable.[14]

EXTERNAL AND INTERNAL GOALS

The distinction between external goals -- wherein performance goals are specified in terms of quantities related to prohibited uses of the diverted material -- and internal goals based on current or reasonable extensions of state-of-the-art capabilities, is an important one. Current goals are ambivalent in this respect: threshold quantities and timeliness goals are based at least in principle on the time and amounts required for a diverter to fabricate a single explosive device, while detection and false-alarm probabilities are based on statistical limits of measurement precision and not on deterrent value or consequences of failure.

If goals could be set which are both reasonably achievable, now or in the near future, and which would be effective as deterrents and in limiting the consequences of diversion, the distinction between external and internal goals would be unimportant. That is the case with many safeguards applications: external goals can be met with measures that are reasonable and acceptable. However, that is not true for large-throughput bulk processing plants. Acceptance of external goals as requirements that cannot be met will in the end diminish confidence in the entire safeguards institution, as the inability to meet stated goals becomes more widely apparent.

The IAEA has the mission of applying the most effective safeguards that it can, subject to the constraints of impact on operations, limited resources, and acceptability to the State. It is therefore bound by internal constraints, however desirable it may be to meet more difficult external goals.

---

*With the unimportant exception of Agency-sponsored materials or projects.

GOALS VS. REQUIREMENTS

If goals are not immediately attainable, we must distinguish between goals and requirements, or what might more accurately be called current standards of performance. Standards that are currently achievable with reasonable effort and impact form a reference point for negotiating ageements, Requirements,* in the sense that an IAEA system that does not meet them is considered inadequate, should be based on what is currently achievable, and hence on internal goals.

Since the basic agreements obligate the Agency to apply safeguards without specifying what performance constitutes adequate safeguards, there can be no requirements based on external goals that are not immediately attainable. From the Agency's standpoint, there is no question of the "adequacy" of safeguards beyond its internal performance standards --"adequate" is doing the best it can with what it has.

On the other hand, external goals are all that matter to the outside world, and to States whose actions are influenced by safeguards. They can certainly set performance levels in terms of the function they hope IAEA safeguards will accomplish for them, and they are free to judge whether safeguards are "adequate" to them or not on the basis of those requirements. However, if the Agency adopts external requirements which it cannot meet, it is caught in a serious dilemma. It would be in a position of having to apply safeguards which by its own criteria it must concede to be inadequate, or to apply no safeguards at all on the grounds that adequate safeguards were infeasible. Either choice would be detrimental to the IAEA and the non-proliferation effort.

US REQUIREMENTS

The example of the US Nuclear Non-Proliferation Act of 1978[15] is a good illustration of the different forces that influence national and IAEA safeguards policies. We will concentrate here on the important single issue of timeliness.

There is a view held by some in the US that there should be a rigid requirement that timeliness of detection should be enough shorter than conversion time** so as to allow preventive action to be taken before the first explosive device could be fabricated. The preventive action is understood to be some form of diplomatic pressure sufficient to cause immediate cessation of the conversion operation, but the time that is to be allowed for the action is not specified. In any case, since the conversion time for plutonium in any form that is free of fission products is stated by the IAEA to be on the order of one to three weeks (days for metal), there is little time for the IAEA to reach a finding that is unambiguous enough to generate any kind of immediate action that could be expected to stop the conversion operation in its tracks. Furthermore, the available time is stated by advocates such as Wohlstetter to be a matter of hours,[16] or even "practically zero" (Gilinsky).[17]

The official US position on the timeliness requirement is written into the Nuclear Non-Proliferation Act. With regard to whether reprocessing of US-exported spent fuel is to be permitted, the Act states:

> "Sec 303(b)(2) . . . foremost consideration will be given to whether or not the reprocessing or retransfer will take place under conditions that will ensure timely warning to the United States of any diversion well in advance

*Requirements can only be self-imposed by the Agency, and there is no authority to require States to accept safeguards measures merely because they are claimed to be necessary to meet the IAEA's stated performance goals.

**The time required to convert material to a weapons-usable form.

of the time at which the non-nuclear state could transform the diverted material into a nuclear explosive device."

In the floor debate on the bill, Senator Glenn explained that, while there might be circumstances in which the timely warning requirement might be relaxed somewhat, those circumstances would be very unusual:

". . . there is no part of this bill that is of more significance for the prevention of nuclear proliferation than the elevation of the 'timely warning' standard to statutory force.

"I think it is important to note that the concept of timely warning, the basic concept upon which the entire international safeguards program rests, is strictly a measure of whether the warning of a diversion will be received far enough in advance of the time when the recipient could transform the diverted material into an explosive device to permit an adequate diplomatic response."

". . . the bill requires that foremost consideration be given to the question of timely warning. This implies that the latter will receive the greatest weight among all factors. Although this does not require denial of a request when timely warning is not clearly determinable, the language suggests that, in the absence of a clear determination that timely warning will indeed be provided, a strong combination of other factors would be necessary to compensate for this weakness in safeguards. It then follows that a decision to approve reprocessing in the absence of such a clear determination would be an unusual event . . ."[18] (underlining added).

Senator Glenn subscribes to a view of the function of IAEA safeguards, as indicated in the underlined passages, that Gilinsky and others have held since as early as 1970.[19] Commissioner Gilinsky, whose views closely parallel those of the Carter Administration, reiterated the point in his statement to the Senate Energy Committee:

"Safeguards . . . are an alarm that warns of illicit activity. To be effective the warning has to come in time for us to do something about it."[17]

It is important to recognize the difference between the US position and IAEA objectives. The US position is that reprocessing should not be permitted if safeguards cannot provide "timely warning" of diversion, as defined by Senator Glenn. Where the US has control, such as in the approval of the reprocessing of US-origin spent fuel, the consequence of inability to meet the US requirement for timely warning is to forbid reprocessing. The consequences for the IAEA are entirely different. It is obligated to apply safeguards to the best of its ability under the current state of the art. It may adopt the "timely-warning" criterion as an ultimate goal, but it can hardly adopt it as a requirement that must be satisfied before safeguards can be considered adequate, if the requirement cannot be met. Unlike the US, the IAEA cannot prohibit reprocessing, and it must safeguard those operations as it is best able to do so. The views as to what constitutes "adequate" safeguards that are reflected in the Non-Proliferation Act can form a basis for action by the US, if it chooses to adopt them as criteria for approving exports. They are not valid, and are in fact counterproductive for the IAEA in discharging the responsibilities assigned to it, if the requirements cannot be met.

THE NEED FOR A MORE RATIONAL BASIS FOR IAEA SAFEGUARDS GOALS

The performance criteria currently used by the IAEA in the design of safeguards arrangements are rationalized in part by external objectives and in other instances by internal considerations. The external objectives have a superficial logic which upon closer examination is much less compelling. As the safeguards tasks become more difficult, with the advent of large-throughput bulk processing plants involving plutonium, a critical reexamination of the present criteria seems appropriate.

Let us preface the discussion by recalling the point made earlier that the objective of safeguards is to verify compliance with safeguards agreements, and that the assurance provided by that verification depends in part on the perceived capability to detect a diversion if it should be attempted. The perceived capability also has value as a deterrent. Finally, the capability defines an alarm level upon which States can plan their response, which may be to seek confirmatory information from other sources or to take more direct action to counter the diversion. The criteria we are discussing here apply to the capability for detection, which is a function that supports the primary objective of verification.

Before specific criteria are considered, the roles of external and internal goals for the IAEA should be clarified. Internal performance goals are necessarily related to feasibility; they are technical, and they govern the performance of the technical system in providing the capability for detection. External goals are political; they are determined by the broader purposes that the safeguards operation is intended to serve: providing assurance that non-proliferation commitments are honored and deterring violations of them.

We suggest the following structure for technical-system performance criteria:

1. Current and near-term performance standards should be based on what it is feasible to do. The current standard is the reference point for negotiation of an agreement, and the IAEA is obligated to apply whatever measures current technology will permit. It can do no more.

2. The standards should not be static. To stimulate improved capabilities and to enhance future safeguards performance, standards could be scheduled for higher levels in the same way that progressively-tighter air quality and automobile economy standards are scheduled by law to become effective at future dates.

3. External goals are needed to guide the evolving internally-driven performance standards and to drive R&D. Quantitative external goals need not be universal, fixed values. There are no clear limits for external goals that are based on external considerations alone;* the ultimate goal is perfection. The significance of a diversion sufficient for one explosive depends to a large extent on who the diverter is. It must be recognized that any threshold of detection capability would in principle allow a sufficient amount of material for the fabrication of one or more explosive devices to escape detection, if long-protracted or multiple diversions are assumed. External goals can, however, provide a logical basis for balancing performance goals in the planning of R&D programs.

INTERACTIONS AMONG QUANTITATIVE PERFORMANCE GOALS

Various measures of performance interact so that improvement of one is often at the expense of another that is of possibly greater importance. While we have suggested that performance standards should be based on what is feasible, external consequences should be considered in balancing tradeoffs.

Consider the example of allowable probabilities of failure to detect and false alarm. These are the uncertainties shown in Figure 2a. There is no mention of allowable uncertainty in the safeguards documents, INFCIRC/66 Rev. 2 or INFCIRC/153. The Safeguards Manual[20] addresses uncertainty in the statistical terms of "probability of detection" and "confidence level of detection", cites recommendations of experts from member States

*For example, if the goal is to detect a single diversion of one significant quantity, what about two diversions of half that threshold? Or, a protracted diversion of 13 months rather than 12 months?

of values between 90% and 99% for each, and states that in most cases 95% will be used. As shown in Figure 3, those goals require a capability to detect a diversion of 3.3 times the combined standard deviation of the State's and the IAEA's measurements. For a given diversion (expressed in units of the standard deviation--in the present case, 3.3σ), a point on the curve represents a particular combination of false alarm and detection probability. Tradeoffs between them can be made by sliding along the curve. The actual size, in kilograms, of the diversion that can be detected with a given probability and false alarm rate depends on the internal capability of the safeguards system--i.e., on the precision of the measurement system. The selection of a particular operating point on a curve, however, should be based on external consequences; that is, on the relative consequences of a false alarm and of a failure to detect a diversion of a given magnitude.

It is not apparent that the 95%/95% criteria have any relation to external consequences. Such cutoff limits are appropriate, for example, for quality-control limits in a manufacturing operation, where the consequences of a "false alarm"--rejection of an acceptable item--can be readily assessed and accepted in terms of economic cost. In the case of international safeguards, however, if a false conclusion of diversion is reached and immediate action is taken in response, driven by US concerns over timeliness, for example, the resulting political impact on the IAEA could be very serious indeed. The potential magnitude of the problem is illustrated by projections for the international nuclear industry, according to which between 50 and 100 large reprocessing, fabrication, and enrichment plants may be in existence by the year 2000. A material accountability system with a positive alarm limit of 2σ would then produce one to two false alarms per year, purely on the basis of statistics. From the past history of US plants handling strategic special nuclear material, the actual alarm rate can be expected to be much higher, due to human failures, blunders, unanticipated processing conditions, unsuspected sources of error, etc. Even the purely statistical rate, however, would probably be intolerable.

Another consideration is that the need to avoid the consequences of what may be a false alarm would increase the uncertainty in concluding that an actual diversion had occurred. The resulting uncertainty would necessarily raise the threshold of detection, which would tend to reduce the deterrent value. At the same time, insistence on too-stringent goals for detection probability is likely to result in compromise of other goals on the basis of subjective judgment.

For these reasons, it would probably be desirable eventually to reduce the false alarm probability substantially below the 1 to 10% rates cited in the Safeguards manual.[20] From Figure 3, reducing the false alarm probability from 5% to, say, 0.1% would reduce the detection probability for a 3.3σ diversion from 95% to 48%. A further reduction of the false alarm rate to 0.01% would reduce the detection probability to 34%, but at a slightly higher diversion level of 4σ the detection probability at this same very low false alarm rate would be as high as 60%.

Some have suggested that the statistical false-alarm rate resulting from measurement uncertainties could be reduced by containment and surveillance. That is, an apparent MUF would not be assessed as a diversion unless it were confirmed by indications from surveillance. While a positive indication might reinforce a conclusion from the MUF that a diversion had occurred, it appears unlikely that the absence of such an indication could provide sufficient basis to reject a conclusion based on MUF. Such confidence in the reliability and completeness of containment and surveillance, to detect any diversion, is not justified. Apparent diversions can be identified as false alarms only by a determination that the material is actually present, which leaves us with the statistical false-alarm rate of the measurement system as the irreducible minimum, short of additional sampling and measurement.

Sanborn[21] has pointed out another problem with low false alarm and high detection probabilities, namely that they are hard to demonstrate in a rigorous mathematical manner. There are two reasons. First, the central limit theorem, on which the assumption of normality of the sample distribution is based, cannot be relied on in the region of the tails of the distribution, for small sample sizes. Second, the data for the distribution are being supplied by the diverter himself, and hence any assumption of normality may be invalid.

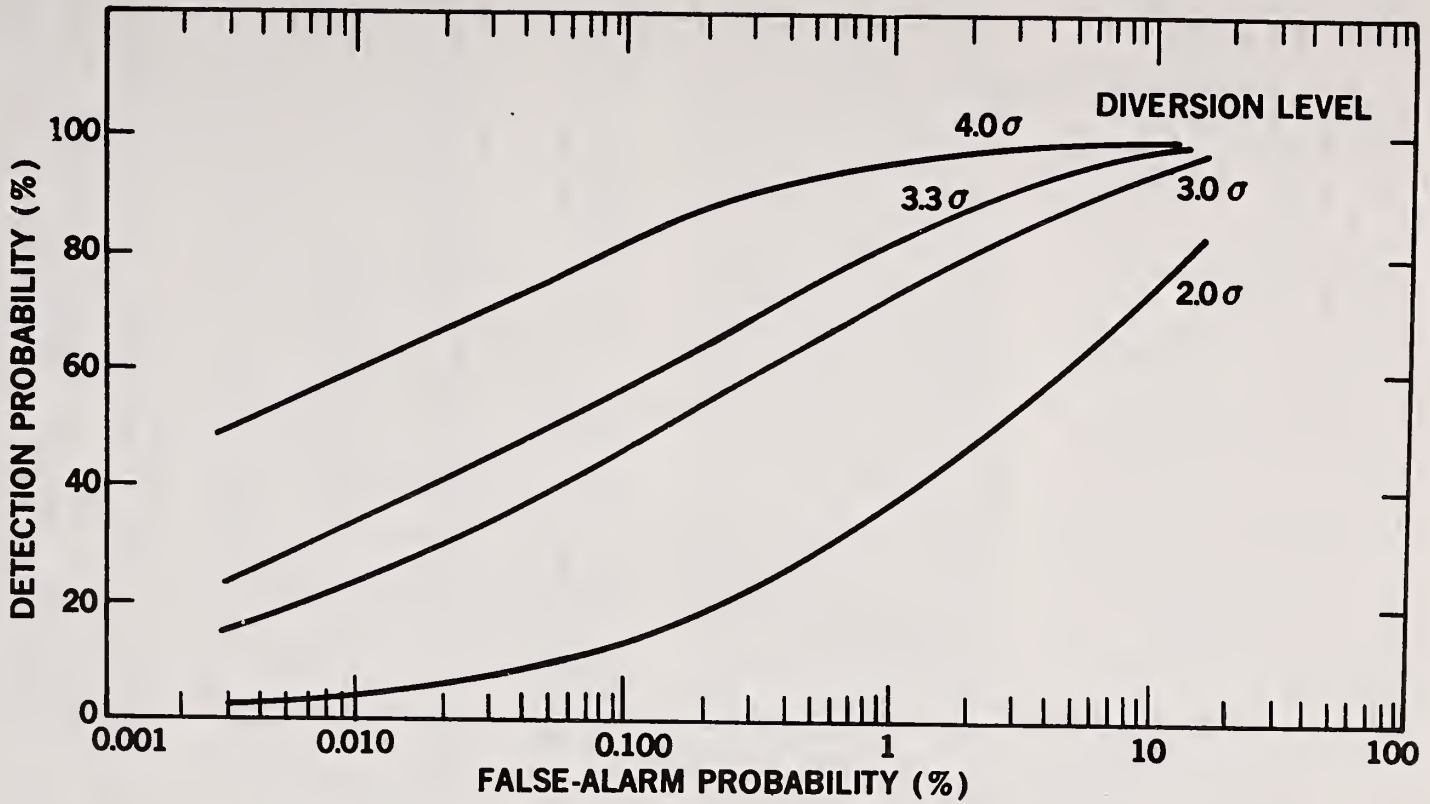

FIGURE 3. DETECTION PROBABILITY VS ONE-SIDED FALSE-ALARM PROBABILITY FOR VARIOUS DIVERSION LEVELS

If the measurement precision cannot be improved, lower false-alarm rates can be achieved only at the expense of some other, externally-derived, goal: the threshold quantity to be detected or the probability of detection.* What is the consequence of accepting a lower probability of detection for diversion of a threshold quantity?

Let us first consider probability of detection for a specified minimum quantity to be detected. What are the consequences of a too-low probability of detection? The perceived capability of detection affects the deterrent value of safeguards, and less directly, the degree of assurance that compliance with non-proliferation agreements is verified. Deterrent value depends on the disincentives that are the consequence of being caught, as well as the probability of detection. What sanctions might be imposed as a consequence of an IAEA finding of diversion is beyond the scope of safeguards. We may assume, however, that the consequences of a State being detected in a deliberate attempt to secretly violate its non-proliferation pledges would be sufficiently grave that the State would not take any significant risk of detection. For that reason, it seems very unlikely that a State that would be deterred by a 95% probability of detection would accept a risk on the order of 50% or even less. The external consequences of detection and false alarm are entirely different, and much lower probability of detection than probability of no false alarm could be accepted.

The consequences for the IAEA of requiring high probabilities of detection must also be considered, in view of the increased sampling requirements. In Figure 4, from Sanborn[21], the fraction of the total population required to be sampled by the inspector is plotted as a function of detection probability and the number of items F falsified by the diverter. Consider, for example, the curve for F=8 falsified items. For a detection probability of 0.5, approximately 8% of the total population must be sampled; for a detection probability of 75% the sample size must be 15%, and for detection probabilities of 95 and 99%, the sample sizes must be approximately 30 and 43%, respectively. Increasing the detection probability from 50 to 95% therefore quadruples the sample size, while going to 99% increases it, overall, by a factor of more than five. These are very considerable increases in inspection effort, and one may well question whether they are worth it, in view of the cost in limited IAEA resources and the dubious value of high probability of detection.

As Figure 3 shows, the probability of detection is related to the size of the diversion, for a fixed probability of false alarm. Let us examine the question of the minimum quantity that must be detected in terms of external consequences of failure to detect and internal constraints on the ability to detect.

IAEA safeguards are based on the "significant quantity" of material necessary to fabricate a single explosive device, which they define as 8 kg of plutonium or 25 kg of highly-enriched uranium. Goals are based tentatively on the detection of one "significant quantity" in a single, abrupt diversion or in a protracted diversion spread over one year. As we have suggested, there is no rational basis for a detection capability based on a minimum quantity corresponding to a single explosive device, insofar as diversion by the State is concerned. In the case of subnational diversion it has more significance, and it is possible that thinking based on subnational diversion has been carried over. The external consequences of national diversion that are important arise from the detection of <u>any</u> diversion that indicates covert violation of non-proliferation agreements, and the actual amount has less significance than is generally supposed.

From the practical standpoint, it is necessary to establish some threshold quantity of detection, not on the basis of external consequences, but as a measure of system sensitivity. The threshold should therefore reflect system capability rather than any external consequence of diversion. The IAEA's "significant quantity" may be satisfactory, provided that it is in the range of feasibility. Feasibility limits will be exceeded, however, in the case of large-throughput bulk processing plants. A significant quantity represents a very small fraction of the quantities that must be measured, as indicated in

*These two goals can be balanced against each other. They are not independent, and both are measures of detection limit.

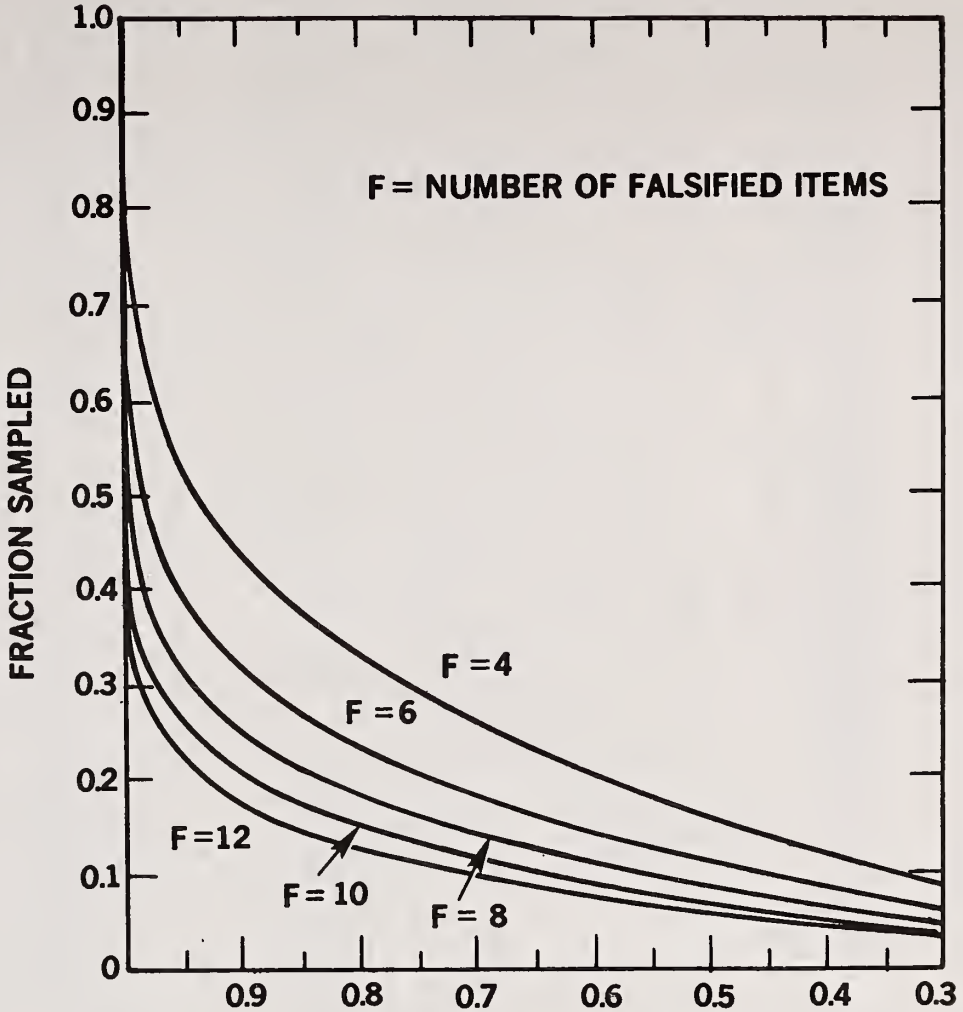

FIGURE 4. PROBABILITY OF DETECTION OF A FALSIFIED ITEM AS A FUNCTION OF SAMPLE SIZE

Table I. It is assumed here that present US NRC regulatory requirements for commercial reprocessing plants, namely that LEMUF(Pu) $\leq 1\%$ of throughput for material balances every 6 months, can be met. It is also assumed that the uncertainties in the successive material balances add randomly, so that the uncertainty for a year is just $\sqrt{2}$ times the uncertainty for 6 months, which understates the actual error. The plutonium fraction is assumed to be 1% and 8%, respectively, for LWR and LMFBR spent fuel. A 200-te/yr LMFBR reprocessing plant is comparable to a 1500 te/yr LWR plant in terms of plutonium flows, and each is a likely size for economic operation.

Table I

UNCERTAINTIES (2σ)* IN THE
MATERIAL BALANCES OF LWR AND LMFBR REPROCESSING PLANTS
AS A FUNCTION OF THROUGHPUT

te HM/yr	Uncertainty (kg Pu per year) LWR	LMFBR
10	0.7	5.7
100	7	57
200	14	114
300	21	
1500	105	

As can be seen, for LWR reprocessing plants of ≥ 100 te/yr throughput the annual uncertainty is about equal to a significant quantity, while for a plant the size of the NFS West Valley plant it amounts to two or three significant quantities. These may be regarded as in the pilot-plant range, or typical of what a small industrialized or fairly large semi-industrialized country might want to support recycle. On the other hand, a 1500-te/yr LWR reprocessing plant would have a material balance uncertainty at least an order of magnitude larger than a significant quantity. It is therefore these large economically-sized plants that are the problem, as far as material accountancy is concerned, not the smaller ones in which some developing countries have expressed an interest.

ABSOLUTE VS. RELATIVE GOALS

The preceding discussion raises the important question of whether, in plants like the ones considered, safeguards measurement goals should be expressed in terms of absolute or of relative quantities. There are two difficulties with absolute goals, one of which is the inability to meet them with large plants. The second difficulty is a related one. A rigid insistence on the ability to detect the diversion of one significant quantity over a period of one year would favor the building of small, relatively-uneconomical reprocessing plants. Plants of this kind could be ordered by developing or semi-industrialized nations with a weapons program in mind, and justified on the grounds that they meet safeguards measurement requirements. On the other hand, a large industrialized country, if it wanted to reprocess, would be forced to build a number of small plants, each capable of meeting the requirements but in the aggregate providing essentially the same opportunities for diversion as a single economical plant of the same total size. So in the first case the policy of absolute requirements would favor the very situation the US is most concerned about; that is, the spread of small reprocessing plants to developing countries, while in the second case it would favor an economically-irrational development without appreciably reducing the risk of undetected diversion. Insistence on absolute goals could be regarded, in fact, as discriminatory against large nations, since it imposes much more stringent measurement requirements on them--requirements that cannot even be met by present technology--than on small nations.

*Assuming two material balances per year with random measurement errors only, and 2σ = 1% of throughput.

The consequences of the "significant-quantity" limit, when applied in the US export-approval conditions, will be contrary to US policy objectives. The large processing plants that fail to meet the measurement goals will, for the foreseeable future, all be located in large industrial countries. A credible nuclear weapons program in such a country would have to involve tens and probably hundreds of weapons. A mere half dozen or so weapons in the hands of a country like West Germany or Japan, for example, would not be very useful to it. Furthermore, such countries are quite capable, if they considered it necessary, of developing a large clandestine military program tailored to their specific needs. It is therefore highly unlikely that they would take the risk of diverting material from a safeguarded facility when the amounts to be gotten this way are so limited.

On the other hand, small semi-industrialized or developing countries are likely, for the foreseeable future, to operate only the smaller plants, in which the detection goal for material accountability can be met. The effect will therefore be to permit reprocessing of spent exported fuel in countries the US is most concerned about, while forbidding reprocessing by western-European States and Japan, where proliferation risks are minimal.

The proper balance of emphasis in reprocessing safeguards could be accomplished by defining limits of detection capability on the basis of a fraction of throughput rather then in absolute, "significant" quantities. In small plants, where it is feasible, the significant-quantity limit could be retained. A limit expressed as a small fraction of throughput would provide good assurance that the major countries having such plants did not divert, since, although the detection limit might not allow enough for several explosives to be detected, the quantity would be insignificant in military terms and would therefore provide credible assurance that no diversion at all had been attempted.

TIMELINESS GOALS

Risks of false-alarm/detection failure can be balanced against timeliness as well as threshold-detection levels. Up to times on the order of a few months, improved timeliness in safeguards findings can only be achieved at the expense of uncertainty. A goal of extremely short "detection" time displays an oversimplified view of what "detection" really is. As discussed above, "detection" of diversion by the safeguards system is a final conclusion of a process that begins as an attempt to verify compliance with the safeguards agreement. A finding of diversion, if there is any serious attempt by the State to conceal the diversion, is arrived at by a process of elimination. Any abnormalities must be investigated to see if there are other causes than diversion. While strong indications might lead the inspectors to report directly, as provided for in the agreement, it seems unlikely that with covert diversion there would be sufficient basis for immediate and vigorous responsive action until all available information had been thoroughly assessed.

What is loosely referred to as "detection" is the conclusion of a process of analysis and investigation, beginning usually with routine inspection and collection of samples for analysis, and ending after a number of alternative explanations have been investigated and rejected. There is no single indication or event short of the final decision that could be called "detection". Rather, from the first indication there is the possibility of diversion, but with a high degree of uncertainty. As the assessment progresses, uncertainty diminishes but time passes. It is as if a kind of Heisenberg uncertainty principle were at work: as detection time is reduced the "detection" becomes more ambiguous, and the resolution of uncertainty is at the expense of timeliness. The provisions contained in INFCIRC/153[1] to resolve any uncertainties, which could require considerable time, illustrate the tradeoff between time and uncertainty.

Thus it appears that detection time can be reduced to the extreme degree considered necessary by some US policymakers only if it is done at the expense of increased false-alarm probability or if the diversion is very large. Since the purpose of very short detection times is to allow immediate diplomatic action to be taken before conversion to weapon components could be completed, a high degree of confidence in the

finding of diversion would also be necessary. False-alarm limits would have to be more stringent, not less, if timely detection is to lead directly to responsive action.

The logical basis that rationalizes the need for extremely short detection times calls for closer examination. Implicit in the timeliness requirement, as stated in the Nuclear Non-Proliferation Act, is the assumption that when conversion time for one explosive is completed some kind of point of no return is reached, after which corrective diplomatic action is pointless or ineffective, and the diverting State must henceforth be accepted as a member of the nuclear club. It is not at all apparent or self-evident why that should be so. We are aware of no discussion of that fundamental assumption in all the voluminous literature on non-proliferation. It is accepted as a rule of some kind of game, which defines winning or losing in terms of who wins the race at the end of conversion time. A number of arguments against that point of view are offered:

(1) The non-proliferation objective is the prevention of the acquisition of nuclear armament by another State, and the threshold is a nuclear-weapon capability with effective delivery systems, not the final assembly of unit no. 1. This process affords considerably more time and opportunity to detect a clandestine weapons program, through both international safeguards and national intelligence activities.

(2) An important and officially stated objective of the IAEA is to deter diversion, a function which depends on the perception of the risk of detection and the probable consequence of discovery and not on the time at which a violation is discovered. Since the nature of the response of the international community to a violation would probably not be any different whether or not conversion had occurred (even assuming that there was some way of knowing whether it had), the deterrent value should be the same in either case. This point can be illustrated by the example of India. There, knowledge of preparations before the test explosion did not lead to the application of effective response measures, and pressures to restrain them continue more than five years later. If the detection-time/conversion-time dependency were correct, such pressures after the test explosion would be pointless. In fact, it would be harmful to US objectives to convey the impression to a potential diverter that once he converts the material into a weapon he is "home free".[22]

(3) The objective of diplomatic pressure would presumably be to restore the status quo ante; that might include return of the diverted material and assurance that the weapon program itself had in fact been terminated. The accomplishment of neither of these objectives depends on whether the material has been fabricated into a weapon, since, clearly, it can be returned at any stage and, at least in principle, there is no clearly delineated point or threshold beyond which a weapons program cannot be terminated.

(4) The claimed shortness of conversion times robs the first weapon assembly of much of its significance, since it implies that the fabrication of a weapon is easy, even for a nation with no prior experience. If so, it cannot have great significance as a threshold.

(5) The concern over a single explosive is much more valid in the case of subnational diversion, where the threat is more immediate and the significance of additional numbers of weapons relatively less. The preoccupation with the minimum time to fabricate a single explosive seems to be the result of a blurring of the distinction between physical protection against subnational groups and safeguards against national diversion.

Thus, while timely warning is certainly of value, there is no apparent logical basis for requiring that detection time--the time from diversion to detection--not exceed conversion time, or that there is necessarily any direct, quantitative relationship.

SUMMARY

Currently, the tentative goals for IAEA safeguards performance lack internal consistency and a sound logical basis. In particular, it is argued that there is no rational foundation for the claimed connection between detection time and conversion time; that present goals for false-alarm probability will most likely be unacceptable for the expanded nuclear industry of the future, while goals for detection probability are set unnecessarily high; and further, that rigid insistence on absolute thresholds for detection that are unattainable in high-throughput bulk processing facilities may be counterproductive.

A distinction must be made between external safeguards goals, based on the consequences of diversion, and internal goals that govern IAEA operations, if attainment of the external goals is not feasible. The IAEA should adopt quantitative performance goals that are clearly feasible, and upgrade them as the state of the art advances. This can be done in accordance with a prearranged schedule as is done in some US environmental regulations. External goals can provide balance in the establishment of IAEA goals, but they should not be adopted as quantitative requirements unless they are feasible.

IAEA safeguards are too often viewed in negative terms, a view that is more appropriately applied to domestic safeguards. Domestic safeguards agencies are regulatory agencies; the IAEA is not. The IAEA, like other international agencies, is based on respect for agreements that are accepted voluntarily. IAEA safeguards are a great step forward in the widespread acceptance of in-country monitoring of compliance with agreements. Expectations of what IAEA safeguards can accomplish, as reflected in stated performance goals, should be in terms of positive assurances that non-proliferation commitments are respected, and not in terms of a regulatory body that can compel compliance.

A capability to detect diversion is an essential element in the safeguards system; it establishes the level of credibility of assurance that safeguards provide. It is not reasonable, however, to expect that a detection capability that combines a high probability of detection with extremely short detection times can at the same time provide hard enough information to justify immediate and drastic diplomatic response. Such an expectation would appear to be based on a grossly-oversimplified view of what constitutes detection of diversion. Externally-derived performance goals should anticipate more realistic responsive actions. Those might include verification from other sources of early, ambiguous alarm signals, or more deliberate actions on the basis of carefully-assessed findings that require longer times.

In practice, the IAEA must be governed by internally-derived goals--what it is possible to do, now and in the future. The ability of the IAEA to accomplish what safeguards can do must not be compromised by striving for unattainable external goals, which can only lead to system distortions and less-than-optimum performance. External goals are needed to guide safeguards R&D, but not to define requirements that safeguards must meet in order to be considered adequate.

References

1. The Structure and Content of Agreements Between the Agency and States Required in Connection with the Treaty on Nuclear Weapons, INFCIRC/153, IAEA, May 1971, par. 7, 31, 32.

2. Treaty on the Non-Proliferation of Nuclear Weapons, 1968.

3. Treaty for the Prohibition of Nuclear Weapons in Latin America, 1967.

4. Statute of the International Atomic Energy Agency, 1956, Article III.

5. The Agency's Safeguards System (1965, As Provisionally Revised and Extended in 1966 and 1968), INFCIRC/66, Rev. 2, IAEA, September 16, 1968, par. 46.

6. INFCIRC/153.

7. Rometsch, et. al., "Safeguards -- 1975-1985", IAEA-SM-201/103, Safeguarding Nuclear Materials, Proceeding of a Symposium, Vienna, 20-29 October, Vol. I, p. 5.

8. Paul C. Szasz, "The Law and Practices of The International Atomic Energy Agency", Legal Series No. 7, IAEA, 1970, Note 6, p. 637 and Note 67, p. 639.

9. INFCIRC/153, par. 28.

10. INFCIRC/66 Rev. 2, par. 46.

11. INFCIRC/66 Rev. 2, par. 14.

12. Szasz, p. 558.

13. INFCIRC/153, par. 6.

14. INFCIRC/153, par. 4, 5.

15. The Nuclear Non-Proliferation Act of 1978, Public Law 95-242.

16. Prof. Albert Wohlstetter, as quoted in the Congressional Record, February 2, 1978, p. S1077.

17. NRC Commissioner Gilinsky, Statement before the Senate Energy Committee, Congressional Record, February 21, 1978, p. S1077.

18. Senator John Glenn, Congressional Record, February 7, 1978, p. S1310.

19. Gilinsky and Hoehn, "Non-Proliferation Treaty Safeguards and the Spread of Nuclear Power, R-501, Rand Corporation, May 1970, p. 9.

20. International Atomic Energy Agency, IAEA Technical Safeguards Manual, IAEA-174, 1976, par. 5.1.3.

21. Jon Sanborn, Brookhaven National Laboratory. Personal communication.

22. Myron B. Kratzer, International Energy Associates Limited. Personal communication.

Discussion:

Persiani (ANL):

There is a timeliness to Table II, where the standards could be made progressively more restrictive. The more technically advanced countries can develop systems with less restrictive guidance. As the LDC's countries become more technically sophisticated and want to develop their own dependent nuclear power economy, they are subjected to more restrictive conditions on their uranium. That struck me as something you could talk about.

deMontmollin (Sandia):

Right, that was our point. As the technology improves and the acceptability of safeguards grows in the future, the people and the system become more adapted to it. The system shouldn't settle for what goals are presently feasible, but rather the goals can improve in the future. The idea of goals that are presently attainable doesn't need to restrict the progress in the future toward better goals that, at the same time, are more politically acceptable and technically feasible.

Franklin (EURATOM):

If I have understood you correctly, you are saying that, if we abandon a very narrow technical definition of goals and incorporate the political values into a safeguards system, it is possible to achieve these external objectives. But if you start trying to implement that in practice, what kind of political problems do you think you run into when you say that a plant of a particular kind should meet one set of technical criteria if it is in a friendly country, and a different set of technical criteria if it is in a country which is perceived as less friendly? How, at the level of international organization, do you think that is going to be operational?

deMontmollin:

Well, I don't think it would be on the basis of considering countries or classes of countries, but rather as a function of throughput. As one example, the 8 kg limit in a reprocessing plant. If it were a function of throughput rather than a fixed quantity, it would tend to be more generally feasible. That is, the feasibility would be more nearly the same for all sizes of plants. It just happens that these large-throughput plants are in sectors that, for diversion to be credible, would require a large diversion. That is a fortunate circumstance, and I don't think it could ever be set up on a basis of discrimination or classifying of countries.

The Evolution of Safeguards Systems Design

by

J. P. SHIPLEY, E. L. CHRISTENSEN, and R. J. DIETZ
Los Alamos Scientific Laboratory, Los Alamos, New Mexico 87545

ABSTRACT

Safeguards systems play a vital detection and deterrence role in current nonproliferation policy. These safeguards systems have developed over the past three decades through the evolution of three essential components: the safeguards/process interface, safeguards performance criteria, and the technology necessary to support effective safeguards. This paper discusses the background and history of this evolutionary process, its major developments and status, and the future direction of safeguards system design.

INTRODUCTION

The 1968 Treaty on the Non-Proliferation of Nuclear Weapons[1] emphasizes the need for effective safeguards systems. Articles I and II of the treaty prohibit signatories from transferring nuclear weapons or explosives devices, control, or assistance between nuclear weapons states and non-nuclear weapons states. Article III, paragraph 1 requires that each non-nuclear weapons state, according to the treaty, accept safeguards "for the exclusive purpose of verification of the fulfillment of its obligations assumed under this Treaty with a view to preventing diversion of nuclear energy from peaceful uses to nuclear weapons or other nuclear explosive devices." Thus, the objective of safeguards, as an instrument of nonproliferation policy, is "the timely detection of diversion of significant quantities of nuclear material ... and deterrence of such diversion by the risk of early detection."[2]

For nearly 35 years since the first nuclear weapons explosion, three questions have been continuously debated: what effects do safeguards have on nuclear facilities, how well should safeguards perform, and how well can safeguards perform? We shall examine the background, history, and status of these three questions by considering three evolutionary aspects of safeguards systems: (1) the safeguards/process interface, (2) safeguards performance criteria, and (3) safeguards technology. Our point of view will be primarily that of materials accounting, recognizing that physical protection and containment/surveillance are vital parts of an effective, complete system.

THE SAFEGUARDS/PROCESS INTERFACE

A Historical Example

The following example, drawn from the early history of the nuclear age and the Los Alamos Scientific Laboratory, illustrates the evolving thinking of facility operators concerned about nuclear materials accounting. Beginning in 1943, the first work with plutonium was done on a small scale with a distinct flavor of experimentalism. Each experiment always led to quantitative analyses of feed, product, and sidestreams because of the chemist's desire for understanding. These comprehensive analyses were frequently used to draw materials balances, but the procedures were not called accountability.

As the quantity of plutonium increased, more detailed accounting systems became necessary. A bookkeeping system was established, and radioactive material was transferred from one area to another, from one person to another, as if the radioactive material were capable of being counted like pennies in a bank. But it wasn't. Discrete items or items amenable to precise chemical analyses were transferred without too much difficulty. Residues and

*Work performed under the auspices of the US Department of Energy, Office of Safeguards and Security.

wastes in a heterogeneous matrix were a different matter because of the impossibility of obtaining a representative sample. There were, of course, no instruments for quantitative nondestructive assay.

Because wastes could not be assayed, it was always possible that some significant amount of plutonium might go out in a box of waste or trash. Consequently, in 1949 LASL designed, built, and installed a neutron counter using BF_3 tubes to detect neutrons emanating from each box and container leaving the plant. Although the measurement wasn't quantitative, it did give assurance that only small amounts (less than 0.5 gm) were in the containers. In addition, no portable, quantitative gamma survey instruments were available, so that the guards had to rely on visual examination of people and items leaving the facility.

The plutonium content of process residues was another matter of great concern because of accounting requirements imposed by LASL and the USAEC. The plutonium content of heterogeneous residues was difficult to measure; consequently, it was decided early in 1949 to keep residues segregated according to generator. The residues were stored in segregated groups until a process unit could be dedicated to processing a block of these residues. Each group of residues was designated as a "receipt area" so that data could be properly credited to the group by referring to that receipt area number.

The process data were recorded in log books, and transfers of plutonium were recorded on receipts. It was a slow and laborious process to make the final evaluation and to calculate inventory differences, and there was no practical way to obtain interim numbers.

In 1958 and 1959 as a result of a study of the data gathering and analysis process, several conclusions were reached: (1) Accountability data and process data were often the same. (2) The shipper and receiver were documenting the transfer by each recording the same data. (3) Compilation and evaluation of hand-logged data was slow and subject to error. (4) Good process data, criticality control data, and accountability data could not exist independently. It was then decided to design and establish an automated data processing system to address the above considerations. The data necessary to document each transfer were selected. The number of fields had to be restricted so that all the data would fit the 80-column format normally available at that time on punched cards. After many iterations, a format was chosen and a system was put into operation in 1960. The initial printouts are described in LA-2662.[3] This system was used as a recording document virtually unchanged for more than 17 years. There were, however, the development and use of an increased number of sorting programs and printouts that served many coincident process and accountability needs.

As interest in safeguards increased, it was realized that quick recall and analyses of data were necessary for the timely review of inventory differences. The main drawback was that data recall had to await the bi-weekly printout, although special printouts could be obtained on 4 hours notice, but at the expense of accumulating huge stacks of paper. Timely access and review was also the desire of process accountability and criticality managers.

The desire for timeliness led to the dedication of a computer to data acquisition and handling, with remote terminals in the plant connected to the computer. The result was a dynamic materials accounting system that collected process and accountability data and immediately updated the inventory file. The system would be invaluable to process people, and when NDA equipment could be developed and installed between materials balance areas, it would be invaluable for improved safeguards. Such a system is now being installed, tested, and improved at TA-55, the new plutonium processing facility at Los Alamos.[4,5]

From this example, we can see four main reasons, other than for safeguards, why facility operators are keenly interested in materials accounting: (1) production control, (2) supplier/customer interactions, (3) safety, including criticality control, and (4) regulatory requirements imposed to meet externally generated criteria. Thus, materials accounting is intimately related to both process control and safeguards, and both sets of considerations must be taken into account in any cogent safeguards systems design.

Integrating Materials Accounting and Process Design

Good materials accounting depends on the ability to draw materials balances having acceptably low uncertainties. That is, the nuclear material must be measurable, which has important implications for process design. For example, process equipment must be constructed so that significant amounts of material are not "hidden" in locations inaccessible for measurements. In the past, equipment was often not designed with this constraint in mind and instrumentation for measuring material residing inside process vessels was unavailable. These limitations have forced the materials accounting system to rely on cleaning out the process, i.e., doing a physical inventory, before a materials balance could be drawn.

Oftentimes, process operating procedures have significant impacts on the performance on the materials accounting system. For example, buffer tanks occasionally have input and output transfers that occur simultaneously, which severely limits the ability to infer the transfers from level and concentration measurements made on the tank. On the other hand, if input and output transfers do not occur simultaneously (e.g., if the tank is "batched"), then obtaining the transfer measurements is relatively straightforward.

The examples show that a great deal of thought must be given to designing the process for improved safeguards and process operations, two compatible and mutually supportive requirements. This is a relatively simple matter at the design stage of the process, but much more difficult and costly after the facility has been built. It is imperative, therefore, that the safeguards and process viewpoints be integrated at the earliest stages of facility design. Furthermore, it is often true that features important to materials accounting are the "designer's choice" with respect to the process and could have been changed had safeguards been a factor.

International Safeguards Considerations

The implementation of international safeguards contributes additional complexities to the safeguards/process interface. By statute, the IAEA performs independent verification activities to arrive at a technical conclusion on "the amount of material unaccounted for over a specific period, giving the limits of accuracy of the amounts stated."[2] These activities are based on the "use of material accountancy as a safeguards measure of fundamental importance, with containment and surveillance as important complementary measures."[2] Thus all the process design features relevant to safeguards discussed above are important, and there are several additional factors, such as proprietary information and questions of national sovereignty.

To fulfill its verification responsibilities, the IAEA is both allowed and required to take samples, make independent measurements, check standards, and examine records and reports. These activities require that the IAEA have access to the so-called strategic points, which include key measurement points used by the Agency for drawing materials balances and points where containment/surveillance measures may be executed. That is, the IAEA's activities may be considered, by some at least, to be intrusive. The degree of intrusiveness to a large extent will depend upon the capability of the facility's materials accounting system and on the inspector's confidence that he can ascertain whether or not the facility is being operated as declared. Both of these criteria depend heavily on the process design and must be incorporated early in the design stage.

PERFORMANCE CRITERIA

Performance criteria for materials accounting systems have also evolved. We will consider first the US domestic requirements and then discuss the proposed IAEA goals.

US Domestic Requirements

In recognition of the limitations of materials accounting, regulatory requirements in the US have specified that materials balances should be drawn immediately following a shutdown-cleanout physical inventory. A minimum physical inventory frequency has also been specified depending on the type of facility. For example, reprocessing plants must take a physical inventory and draw a materials balance at least once every six months. In addition, the uncertainty associated with the materials balance is also specified. In the reprocessing plant example, the materials balance uncertainty (the limit of error of the material unaccounted for) must be less than 1% of throughput.[6] Although these requirements have been deemed adequate in the past, the advent of large, high-throughput facilities requires that new criteria be considered.

Clearly, the current regulations have limitations in timeliness and sensitivity. In a 1500-metric ton/year reprocessing plant, a diversion of 75 kg of plutonium is the nominal amount that should be detected, and that only after 6 months. In addition, the merits of specifying detection sensitivity as a fraction of throughput are still being debated. On the one hand, a relative criterion seems inappropriate if the diversion quantity of interest is in absolute terms. On the other hand, an absolute criterion appears to favor small facilities, which are economically less attractive.

These changing perceptions have indeed resulted in increasing reconsideration of both the forms and the values of performance criteria. It is a continuing struggle to formulate performance requirements that both meet our perceived needs and are achievable with reasonable extrapolations of current technology.

IAEA Requirements

At the current time, performance criteria for IAEA safeguards are still being developed. However, criteria have been proposed for "timely detection" and "significant quantities" and have been authorized by the Director General of the IAEA for use by the Agency in its safeguards system.[7] The definition of significant quantity is related to the quantity of special fissionable material required for a single nuclear explosive device. For example, a significant quantity of plutonium is generally taken to be eight kilograms.[7,8] Timely detection depends on the "conversion time" for a particular material and has been defined as the minimum time required to convert different forms of nuclear material to metallic components of a nuclear explosive device. Thus, for plutonium oxide, nitrate or other pure compounds, the estimated conversion time is on the order of one to three weeks.[7,8]

The IAEA assumes that proliferation occurs when a single nuclear explosive is acquired. Therefore, to counter the range of possible diversion scenarios the proposed IAEA criteria have been set at detecting 8 kg of plutonium diverted over any period of time from one to three weeks up to one year.[7,8] That is, the Agency must treat both abrupt and protracted diversion scenarios, and the time allotted to detect these diversion scenarios is one to three weeks following completion of the diversion.

Given the current capabilities of the IAEA safeguards system and the facilities it has to safeguard, which currently are all low-throughput facilities, these are reasonable and achievable criteria. However, the large-throughput facilities on the horizon require continued attention to technology development.

TECHNOLOGICAL DEVELOPMENTS

Improved Instrumentation

We have seen that in the early days very little instrumentation, particularly NDA, was available. However, tremendous strides have been made in recent years.* New NDA instruments routinely make measurements of much better than 1% precision and accuracy on many types and forms of nuclear materials.[9,10] Large improvements have been made in the ability to assay such difficult items as waste containers and spent fuel.[11,12] In addition, these measurements can be made in a timely fashion and on the spot.[13] To satisfy the needs of IAEA inspectors, portable versions of these instruments have been developed, such as a high-level neutron coincidence counter that folds up into a suitcase.[14,15]

At the same time measurement capabilities are being improved, the instruments are being tested, evaluated, and demonstrated in operating environments. For example, an absorption-edge densitometer is being installed at the Japanese reprocessing plant at Tokai, and IAEA inspectors routinely use a multitude of portable hand-held units in their inspection activities.

Near-Real-Time Accounting

To meet the changing performance criteria discussed above, near-real-time accounting concepts and systems are being developed in preparation for the construction of new high-throughput facilities.[16-19] The essential feature of near-real-time accounting is the ability to obtain an estimate of the inventory of nuclear material in the process without having to resort to a physical inventory. This ability is desirable because it greatly improves timeliness and sensitivity, and it is made possible by the ongoing instrumentation development work discussed previously. In conjunction with near-real-time accounting, sophisticated data analysis methods, which we call decision analysis,[20-23] make most effective use of the vast amount of new information that will be available. The decision analysis techniques treat the data as an aggregation rather than as individual materials

*The references cited in this section are only examples of those available. A complete list would be much too long for this paper. See the cited works for additional references.

balances to provide the best achievable sensitivity to diversion in any scenario. The decision analysis techniques also provide quantifiable measures of systems performance and a defensible basis for action.

The costs of these improvements, surprising though it may seem, are not large. It is often true that near-real-time materials accounting can be accomplished with very few additional instruments, including upgrades of process control measurements, added to that instrumentation already necessary for properly performing conventional materials accounting. Likewise, the advanced data analysis techniques merely make better use of the information that should already be available for the more traditional analysis methods.

Systems Design Approach

All these technological developments must be folded together to form a coherent safeguards system. That is, we must have a systematic approach to safeguards and facility design. This approach has been developed through numerous interactions with the safeguards community and the process designers, and has been reported in several documents.[16-19,24,25] Although many steps must occur in a successful system design, one step stands out as both the most difficult and the most useful: computerized modeling and simulation of the facilities and safeguards systems. This is true for a host of reasons, including cost, time, and unavailability and inflexibility of operating facilities. This approach allows the investigation of ideas that would be impossible to try in actual facilities. We must constantly keep in mind that the results are only as good as the information we put in. For this reason, any modeling and simulation activity must be based on a specific reference process and must, of necessity, involve the cooperation and participation of the process designers.

For materials accounting, the modeling and simulation approach requires a detailed dynamic model of the process based on actual process design data. Design concepts are evolved by identifying key measurement points and appropriate measurement techniques, comparing possible materials accounting strategies, developing and testing appropriate data analysis algorithms, and quantitatively evaluating the capability of the proposed materials accounting system to detect losses. By using modeling and simulation techniques the effects of process and measurement variations over long operating periods and for various operating modes can be studied in a short time.

CONCLUSION

Examination of these three aspects of safeguards makes evident their dynamic, evolutionary, and interrelated natures. Facility operators are always interested in making the best use of available materials accounting capability. Performance criteria are changing to provide better protection against perceived threats and to make the most effective use of current technology. Both these aspects have spurred the development of the third: technological advances in safeguards. All three aspects must play a major role in safeguards system designs for future high-throughput facilities.

At the conceptual level, future activities will be aimed at international safeguards. The implementation of these concepts in the international context, however, must await demonstration and evaluation of advanced safeguards systems in a benign but realistic environment.

REFERENCES

1. "Treaty on the Non-Proliferation of Nuclear Weapons," reproduced in International Atomic Energy Agency document INFCIRC/140 (April 1970).

2. "The Structure and Content of Agreements Between the Agency and States Required in Connection with the Treaty on the Non-Proliferation of Nuclear Weapons," International Atomic Energy Agency document INFCIRC/153 (corrected) (June 1972).

3. E. L. Christensen, J. A. Leary, J. P. Devine, and W. J. Maraman, "A Punched-Card Machine Method for Management of Nuclear Materials," Los Alamos Scientific Laboratory report LA-2662 (January 1962).

4. G. R. Keepin and W. J. Maraman, "Nondestructive Assay Technology and In-Plant Dynamic Materials Control--DYMAC," in Safeguarding Nuclear Materials, Proc. Symp., Vienna, October 1975 (International Atomic Energy Agency, Vienna, 1976) Paper IAEA-SM-201/32, Vol. I, pp. 304-320.

5. R. H. Augustson, N. Baron, R. F. Ford, W. Ford, J. Hagen, T. K. Li, R. S. Marshall, V. S. Reams, W. R. Severe, and D. G. Shirk, "A Development and Demonstration Program for Dynamic Nuclear Materials Control," Proc. Safeguards Symp., Vienna, Austria, October 2-6, 1978 (International Atomic Energy Agency, Vienna, in press), IAEA-SM-231-110.

6. Title 10 Code of Federal Regulations, Part 70.51.

7. C. G. Hough, T. Shea, and D. Tolchenkov, "Technical Criteria for the Application of IAEA Safeguards," Proc. Safeguards Symp., Vienna, Austria, October 2-6, 1978 (International Atomic Energy Agency, Vienna, in press), IAEA-SM-231/112.

8. IAEA Safeguards Technical Manual, Part A, International Atomic Energy Agency technical document IAEA-174 (Vienna, 1976).

9. R. H. Augustson and T. D. Reilly, "Fundamentals of Passive Nondestructive Assay of Fissionable Material," Los Alamos Scientific Laboratory report LA-5651-M (September 1974).

10. T. D. Reilly and M. L. Evans, "Measurement Reliability for Nuclear Material Assay," Los Alamos Scientific Laboratory report LA-6574 (January 1977).

11. D. F. Jones, L. R. Cowder, and E. R. Martin, "Computerized Low-Level Waste Assay System Operating Manual," Los Alamos Scientific Laboratory report LA-6202-M (February 1976).

12. S. T. Hsue, T. W. Crane, W. L. Talbert, Jr., and J. C. Lee, "Nondestructive Assay Methods for Irradiated Nuclear Fuels," Los Alamos Scientific Laboratory report LA-6923 (January 1978).

13. T. R. Canada, S. T. Hsue, D. G. Langner, E. R. Martin, J. L. Parker, T. D. Reilly, and J. W. Tape, "Applications of the Absorption-Edge Densitometry NDA Technique to Solutions and Solids," Nucl. Mater. Manage. VI(III), 702-710 (1977).

14. M. S. Krick and H. O. Menlove, "The High-Level Neutron Coincidence Counter (HLNCC): Users' Manual," Los Alamos Scientific Laboratory report LA-7779-M (June 1979).

15. J. E. Foley, "Field Manual for the High-Level Neutron Coincidence Counter (HLNCC)," Los Alamos Scientific Laboratory report LA-7729-M (to be published).

16. J. P. Shipley, D. D. Cobb, R. J. Dietz, M. L. Evans, E. P. Schelonka, D. B. Smith, and R. B. Walton, "Coordinated Safeguards for Materials Management in a Mixed-Oxide Fuel Facility," Los Alamos Scientific Laboratory report LA-6536 (February 1977).

17. E. A. Hakkila, D. D. Cobb, H. A. Dayem, R. J. Dietz, E. A. Kern, E. P. Schelonka, J. P. Shipley, D. B. Smith, R. H. Augustson, and J. W. Barnes, "Coordinated Safeguards for Materials Management in a Fuel Reprocessing Plant," Los Alamos Scientific Laboratory report LA-6881 (September 1977).

18. H. A. Dayem, D. D. Cobb, R. J. Dietz, E. A. Hakkila, E. A. Kern, J. P. Shipley, D. B. Smith, and D. F. Bowersox, "Coordinated Safeguards for Materials Management in a Nitrate to Oxide Conversion Facility," Los Alamos Scientific Laboratory report LA-7011 (April 1978).

19. H. A. Dayem, D. D. Cobb, R. J. Dietz, E. A. Hakkila, E. A. Kern, E. P. Schelonka, J. P. Shipley, and D. B. Smith, "Coordinated Safeguards for Materials Management in a Uranium-Plutonium Nitrate-to-Oxide Coconversion Facility: Coprecal," Los Alamos Scientific Laboratory report LA-7521 (February 1979).

20. J. P. Shipley, "Decision Analysis in Safeguarding Special Nuclear Material," invited paper, Trans. Am. Nucl. Soc. 27, 178 (1977).

21. J. P. Shipley, "Decision Analysis for Nuclear Safeguards," invited paper presented at the Spring Meeting of the American Chemical Society, March 12-17, 1978; in Nuclear Safeguards Analysis, Nondestructive and Analytical Chemical Techniques, E. A. Hakkila, Ed. (American Chemical Society, Washington, DC, 1978).

22. James P. Shipley, "Decision Analysis for Dynamic Accounting of Nuclear Material," in Analytical Methods for Safeguards and Accountability Measurement of Special Nuclear Material, H. T. Yolken and J. E. Bullard, Eds., NBS Special Publication 528 (November 1978), pp. 83-97.

23. J. P. Shipley, "Efficient Analysis of Dynamic Materials Accounting Data," Nucl. Mater. Manage. VII, 355-366 (1978).

24. J. P. Shipley, "Conceptual Design of Integrated Safeguards Systems," Nucl. Mater. Manage. VI(III), 111-124 (1977).

25. H. A. Dayem, "Modeling and Simulation for Safeguards Systems Design," ESARDA Symposium on Safeguards and Nuclear Materials Management, Brussels, Belgium, April 25-26, 1979.

Discussion:

Skinner (SRL):
You said that we should have near-real-time accounting. Does that include chemical separation plants?

Shipley (LASL):
We ought to consider the possibility of using near-real-time accounting and investigate what good it will do us. We have, in fact, done a study of near-real-time accounting as applied to a chemical separations facility, and Arnie Hakkila will talk about the results of that study this morning.

Skinner:
It was my interpretation of 5630.2 that material in solution is category 1B, which requires a balance every 30 days. If you are doing a dynamic inventory, you can close the balance in 30 days without near-real-time accounting.

Shipley:
I would preempt that by saying that we also call that dynamic materials accounting. Dynamic materials accounting means, to me, the fact that you can draw a materials balance without necessarily having to take a physical inventory. I would call that near-real-time accounting, and you will hear some more about that this morning in Hakkila's paper.

Schleicher (EURATOM):
You have shown in one of your slides that IAEA inspectors have access to two types of strategic points, namely key measurement points and points for containment and surveillance. In practice these points are often not sufficient to achieve the proposed Agency goals for short detection times and significant quantities. This gave rise to considerable difficulties in the negotiation of Facility Attachments for some European plants, the Agency requiring access to strategic points or areas which are not covered by the two categories foreseen, which you mentioned. Practical solutions have had to be found and IAEA inspectors have obtained extended access. Experience will show if such solutions can in the long term be considered as satisfactory by all parties concerned.

Monte Carlo Simulation of MUF Distribution for Application to Euratom Safeguards

by

FLAVIO ARGENTESI and MICHAEL FRANKLIN
Commission of the European Communities, Joint Research Centre,
Dept. A, Ispra Establishment (VA), Italy

ABSTRACT

A statistical material accountancy system (NUMSAS) has been developed by the Joint Research Centre. This system is designed for implementation within the framework of Euratom Safeguards. As well as developing NUMSAS, the J.R.C. has developed a computer code to provide a Monte Carlo simulation of the activity of NUMSAS. This simulation code is being used to study the statistical properties of MUF and MUF variance as estimated by NUMSAS. This paper presents simulation results describing the propagation of skewness through a set of plant accounts. It also illustrates the effect of skewness on detection and false alarm probabilities.

KEYWORDS: Euratom Safeguards, MUF simulation, MUF statistical inference.

BACKGROUND

A statistical nuclear material accountancy system for fabrication plants has been developed by the Joint Research Centre (J.R.C.) of the Commission of the European Communities at Ispra. This accountancy system (NUMSAS) is designed for use in the context of Euratom Safeguards and has been developed in collaboration with the Euratom Safeguards Directorate. The Euratom regulations (1) envisage MUF evaluation based on detailed accounting records and a knowledge of the plant measurement system. Any simpler approach is unlikely to provide an adequate basis for international safeguards. NUMSAS offers a rigorous basis for implementing these requirements since it provides the techniques for a LE-MUF calculation based on the statistical characteristics of the plant measurement system and the measurement histories of the batches of nuclear material involved.

NUMSAS is a complete accountancy system providing facilities for,

- the detection and correction of clerical errors in accountancy declarations supplied to the Safeguards Authorities
- automatic interpretation of Euratom accountancy declarations describing inventory changes
- a wide variety of accountancy reports
- statistical analysis of MUF and the plant measurement system.

The system is described in a paper (2) and in a J.R.C. report (3). With the cooperation of plant operators NUMSAS has been used by the Euratom Safeguards Directorate in analysing the accountancy declarations from a fabrication plant (4). Work is in progress in implementing NUMSAS in other plants coming under Euratom Safeguards.

In the context of international safeguards the evaluation of accounting information involves a variety of interdependent considerations. These include,

- the level of confidence in the clerical accuracy of the accountancy data
- the level of trust existing between the safeguards authority and the operator. This will involve factors such as the inducement to falsification inherent in the particular case
- the percieved level of effectivness of the plant system of containment and surveillance
- the risk of error inherent in any safeguards response. This would encompass factors such as the probabilities of both false alarm and failure of detection as well as the gravity of any mistaken action by safeguards authorities.

In this respect, the safeguards evaluation of MUF is unlike the routine quality control applications of statistics. In the quality control philosophy, the "MUF" is accepted or rejected on the basis of precise quantitative criteria. These criteria are determined by required probabilities of false alarm and detection. In the quality control approach the probabilities can be justified by optimisation of purely financial costs. Moreover this optimisation is underpined by probability models which can be validated directly. In the international safeguards context however, the probabilistic criteria are only one element in a decision process which must take into account other non-quantifyable information.

Safeguards Authorities have been discussing the effects of establishing explicit statistical targets for safeguards in present-day plants (5). This approach would strengthen the role of detection and false alarm probabilities in the evaluation process. NUMSAS offers the possibility of basing LE-MUF calculations on such probabilistic criteria. The NUMSAS calculation of LE-MUF is based on a statistical model of measurement error propagation within a plant accountancy system. This type of model is one which has already been applied by J.L. Jaech (6) to the accountancy of nuclear material. It has also been accepted by the IAEA Manual F. Simple and straightforward techniques for calculating LE-MUF when using an accountancy system such as NUMSAS are outlined in (6). This paper describes work undertaken by J.R.C. Ispra to study the robustness of these techniques. For this study the J.R.C. has developed a computer code to provide a Monte Carlo simulation of the activity of NUMSAS. This simulation code (MUFSIM) can be used to estimate the false alarm and detection probabilities inherent in using these techniques in any specific case. This simulation activity is designed to provide technical support to the implementation of NUMSAS within Euratom Safeguards.
Before describing some results of these simulations it is necessary to outline the statistical methods underlying the NUMSAS LE-MUF calculation.

THE NUMSAS STATISTICAL MODEL

The NUMSAS statistical model assumes that the measured value for the isotope content of an individual batch of nuclear material is calculated as the product of three independent measurements. These are,

- the bulk weight or volume
- the element factor value, e.g. the proportion of uranium per unit bulk weight
- the isotope factor value, e.g. the proportion of U^{235} per unit weight of uranium.

Each of these measurements is assumed to be contaminated by errors of measurement. The NUMSAS model allows for five kinds of error sources which may be involved in the measurement of a single batch. These are,

- weighing scales or volume determination techniques
- sampling techniques for element factor determination

- analysis techniques for element factor determination
- sampling techniques for isotope factor determination
- analysis techniques for isotope factor determination.

For each error source in the plant measurement system, the model takes account of both systematic and random errors. The model equations for error propagation in weighing and in element and isotope factor determinations are given briefly below.

The model of measured weight is,

$$\hat{W} = W\ (1 + \lambda_i + \bar{\epsilon}_i(n)); \quad \ldots\ldots\ldots\ldots\ldots \qquad (1)$$

$$\text{with} \quad \bar{\epsilon}_i(n) = \frac{1}{n} \sum_{j=1}^{n} \epsilon_{ij}$$

where W is the true weight of the batch,

λ_i is the value of the systematic error for scale i

n is the number of replicate weighings

ϵ_{ij} is the value of the random error of the j^{th} weighing of this item using scale i.

The model equation describing element factor determination is more complicated since there are both sampling and analysis errors. The model of measured element factor is,

$$\hat{P} = P\ (1 + \theta_i + \bar{\eta}_i(m) + \xi_j + \bar{\nu}_j(d)); \quad \ldots\ldots \qquad (2)$$

where P is the true value of the element factor for the batch

θ_i and ξ_j are the values of the systematic errors for the i^{th} sampling method and j^{th} analysis technique respectively

$\bar{\eta}_i(m)$ and $\bar{\nu}_j(d)$ are the averages of random errors in sampling and analysis respectively.

The model equation for isotope factor determination ($\hat{Q}$) is similar in structure to that for element factor. Both the random and systematic errors are assumed to be zero mean stochastic variables.

This model is capable of representing two kinds of correlations between the measured values of different batches. Batches whose measurement has involved a common error source will incorporate a common systematic error. The second kind of correlation will occur in batches which have been treated as a group for determination of element or isotope factor. The measurements of such batches will have certain random errors in common.

The above model is the one which is implemented in the current release of NUMSAS. It is a relative error model in which the systematic and random effects of measurement are assumed to be linear functions of the true value being measured. For some error sources alternative models may be desirable. For example, the random and systematic effects of a scale may be represented in the form of absolute errors. In this case the LE-MUF calculation would be based on an equation of the form

$$\hat{W} = W + \lambda + \bar{\epsilon}(n); \quad \ldots\ldots\ldots\ldots \qquad (3)$$

as an alternative to equation 1 above. Future releases of NUMSAS will offer

the user a choice between absolute and relative error models for each error source.

MUF STATISTICAL INFERENCE BASED ON NUMSAS

The NUMSAS system is designed to evaluate whether or not the plant MUF can be accounted for as an accumulation of measurement error. To do this, NUMSAS provides a calculation of the standard deviation of MUF ($\hat{\sigma}_{MUF}$). The standard deviation formula is a first order Taylor series approximation based on equations (1) and (2). The formula is described in the USAEC publication (6). To carry out this calculation NUMSAS uses quantitative information about the plant measurement system as well as the accountancy declarations. The data required about the plant measurement system are the standard deviations of the stochastic variables in the model equations. Since the MUF standard deviation calculation involves the measured values in the accountancy declarations it is also contaminated by measurement errors and is itself an estimate of the true standard deviation of MUF.

Basing LE-MUF on the standard deviation estimate and the desired probabilities of detection and false alarm can be done by using tables of the Normal distribution (6). The LE-MUF or alternatively the statistical significance of MUF can be calculated in this way provided the t_{MUF} statistic follows a standardised Normal distribution. If this assumption is not met, the LE-MUF may lead to more false alarms than is deemed desirable in the light of Safeguards objectives. Alternatively it may lead to failure to react to what is really a significant MUF.

The simulation code MUFSIM is being used to study the statistical distributions of MUF, the MUF standard deviation estimate ($\hat{\sigma}_{MUF}$) and the t_{MUF} statistic (t_{MUF} = measured MUF minus true MUF, all divided by $\hat{\sigma}_{MUF}$). Assuming that the measurement system is described by equations of the kind (1), (2) and (3) the simulation can provide a calculation of the real false alarm and detection probabilities of any specific LE-MUF. In this way, cases can be identified in which the actual false alarm and detection probabilities differ from the nominal ones. The magnitude of this difference can be related to factors in the measurement activities of a plant. As a result Safeguards Authorities have a more accurate basis for their judgements about the significance of a given MUF.

THE MUF SIMULATION CODE (MUFSIM)

The MUF simulation code simulates the activity of the accountancy system NUMSAS. To do this, MUFSIM simulates the action of a measurement system throughout the balance period of a plant. It then does a NUMSAS evaluation of the MUF derived from the simulated accountancy records. This NUMSAS evaluation can then be compared with the known true situation on which the simulation is based. In the MUFSIM code, the processing and measurement activities of the plant are represented purely in terms of the accountancy declarations which they generate. More strictly, MUFSIM simulates the propagation of measurement errors through a set of plant accounts.

The MUFSIM code requires the following inputs:

- a list of pseudo material accountancy declarations specifying the true weight, true element content and true isotope content of the batches and also their measurement histories
- a list of measurement error source declarations specifying the statistical parameters of the error sources making up the plant measurement system.

The code simulates the action of the measurement system on the true material values and then calculates the MUF and the MUF-variance which would be estimated by NUMSAS on this observed data. Based on a sample of such results, MUFSIM provides a variety of statistics describing the distributions of

observed MUF, estimated MUF variance and the t_{MUF} statistic (it also calculates the true MUF and true MUF variance). The Kolmogorov test (7) is applied automatically by MUFSIM to test hypotheses about the distribution of MUF, and the t_{MUF} statistic. The code simulates statistical accountancy in terms of element MUF and isotope MUF simultaneously and provides all the output results for each approach. The code is capable of simulating scale measurement errors according to either of the two error propagation equations (1) and (3) above.

Unlike most statistical simulation codes, the MUFSIM code has as input a large amount of data. These are the pseudo accountancy records for the material balance period. Since many of the records refer to common events in measurement histories, opportunities exist for complex data inconsistencies which are difficult to detect. Each record in the plant accounts must be self-consistent but this is not enough. Each record must also be consistent with all other records in the accounts which refer to common events. For this reason, MUFSIM incorporates a phase of consistency checking of the accountancy records before commencing simulation. This is designed to relieve the user of as much as possible of the checking of input data.

The MUFSIM code is modular and can easily be adapted to alternative models of measurement structure or alternative distributional assumptions for systematic and random errors. The ability to simulate any pattern of correlations implicit in the measurement histories is implemented by the use of multilinked list structures applied to the accountancy declarations (8). With this approach sublists are used to link items sharing common systematic or random errors. The simulation of correlations in nuclear accountancy measurements can be treated very efficiently by means of list processing techniques. Figure 1 below illustrates the processing activities of the simulation code.

THE SIMULATION EXPERIMENTS

The simulation experiments using MUFSIM are designed to study the factors affecting the quality of the Normal approximation to the distribution of the t_{MUF} statistic. The simulations are intended to focus on the degree to which the normality of t_{MUF} is sensitive to

- increases in the standard deviations of measurement errors in all or part of the measurement system
- the number of batches of nuclear material involved in the balance calculation
- the distributional assumptions about the basic measurement errors in the plant measurement system
- changes in the form of the model equations representing measurement error propagation.

In this way the simulations can identify those situations, of measurement history, material volume or measurement system, for which the use of Normal tables can lead to operational error probabilities different from those intended.

The objective in this work is not to replace the normal approximation by anything more refined. Instead the objective is to gain some idea of the possible differences between nominal and actual detection probabilities which might occur. This knowledge can form a basis for judgements about the degree of uncertainty attaching to calculated figures. It is not a practical proposition to envisage a statistical accountancy system for Safeguards which would use information about the higher moments (skewness etc.) of the plant error sources. It is difficult enough to get valid information about the variances.

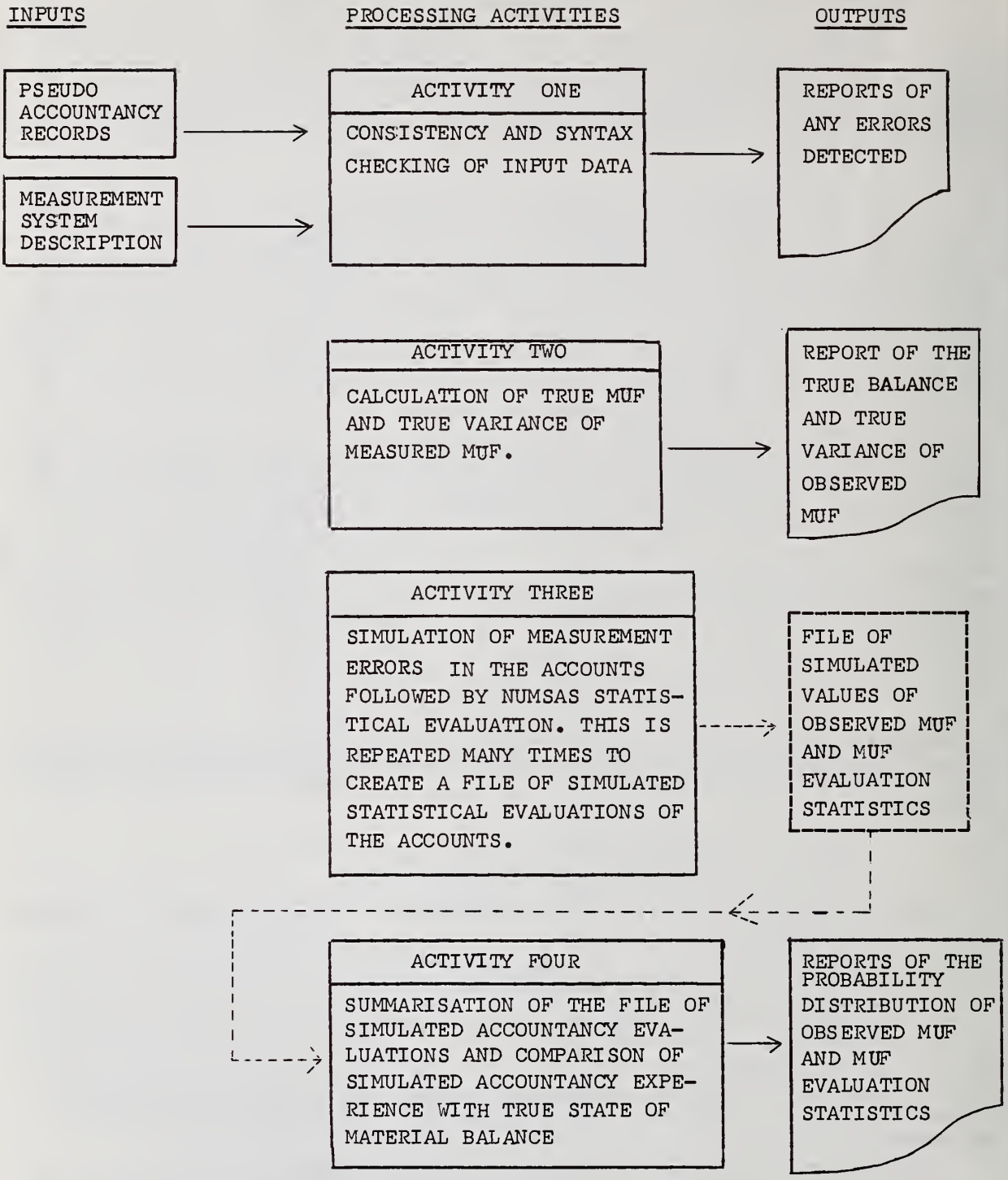

FIG. 1 THE MAJOR PROCESSING ACTIVITIES OF MUFSIM

The findings which are presented here are concerned with the propagation of skewness throughout a plant accountancy. In particular they examine the effect of a skew systematic error on the tail probabilistic associated with t_{MUF}. The input data which has been used for the simulation results presented here have been published in the USAEC report (6) (pp. 200-208). They represent the accountancy of a small scale fuel fabrication facility for a 1 month balance period. For full details of the data the reader should consult (6). For the purposes of this paper a brief summary is given here. The error sources making up the measurement system are listed in Table I.

ERROR SOURCE TYPE	MATERIAL USAGE	ERROR SOURCE CODE
Scale	Weighing UF_6 cylinders	SC01
Scale	Weighing cans of UO_2 powder and scrap	SC02
Scale	Weighing boats of sintered pellets	SC03
Sampling	Sampling UF_6	ES11
Sampling	Sampling UO_2 powder	ES12
Sampling	Sampling UO_2 pellets	ES13
Sampling	Sampling dirty powder	ES14
Sampling	Sampling sludge	ES15
Sampling	Sampling Ammonium diuranate scrap	ES16
Analysis	Uranium analysis for UF_6	EA21
Analysis	Uranium analysis for UO_2 powder	EA22
Analysis	Uranium analysis for UO_2 pellets	EA23
Analysis	Uranium analysis for scrap items	EA24
Sampling	Sampling of UF_6, UO_2 powder and UO_2 pellets for isotope enrichment determination	IS31
Analysis	Analysis of UF_6, UO_2 powder , UO_2 pellets for isotope enrichment	IA41

TABLE I : Plant Measurement Error Sources.

The accountancy records for the balance period give a picture of the begining inventory, inputs, outputs and ending inventory. This material movement information is summarised for different types of material in Table II.

Material Type	Begining Inventory	Input	Output	Ending Inventory
UF_6 cylinders	5	7	0	2
Cans of UO_2 powder	13	0	0	35
Boats of sintered pellets	0	0	0	97
Cans of hard scrap	0	0	0	2
Cans of green scrap	5	0	0	7
Cans of dirty powder	4	0	0	6
Cans of grinder sludge	0	0	0	2
Cans of ADU scrap	8	0	0	26

Table II : Material Flow during Balance Period.
(Figures in the table are numbers of items)

The material balance data given in (6) represents measured values of batch weights, element and isotope factors. These values have been used with a changed meaning for the purposes of the simulation. For the simulation they are taken to be the true values on which simulated measurement errors are imposed. The different error sources listed in Table I are of differing degrees of importance for the statistical accountancy. Some contribute very little to the total MUF variance either because they have small standard deviations or because they are involved in the measurement of only a small proportion of the material affecting MUF variance. Table III shows the relative importance of these error sources for the balance period in question. For Table III the MUF accountancy has been carried out in terms of total uranium. The variance of uranium MUF is broken down into a systematic and random component for each error source.

Table III shows that sampling of ammonium diuranate scrap for determination of uranium content is by far the largest source of uncertainty in the accountancy. In particular, the systematic error accounts for approximately 58% of the MUF variance. This is because the determination of uranium content of such scrap has a large relative standard deviation. Examples in which a single error source can dominate the uncertainty are not purely academic cases. Experience with NUMSAS (9) has shown that this can occur even in plants whose accountancy involves many thousands of batches with physical inventories at six monthly intervals. The simulation results presented here illustrate the effect on MUF evaluation if this dominant systematic error should have a skew distribution. Two aspects of this situation are presented. The first is effect on uranium t_{MUF} of varying the degree of skewness of the systematic error while allowing it's dominance (percentage of MUF-variance) to remain unchanged. This effect is illustrated by simulation results in Figures 2, 3 and 4. The effect on t_{MUF} is shown in three ways. These are,

- the skewness of the sampling distribution of t_{MUF} (Fig. 2)
- the degree to which the simulated t_{MUF} sample is fitted by the standardised normal distribution. This is measured by the Kolmogorov statistic (Fig. 3)

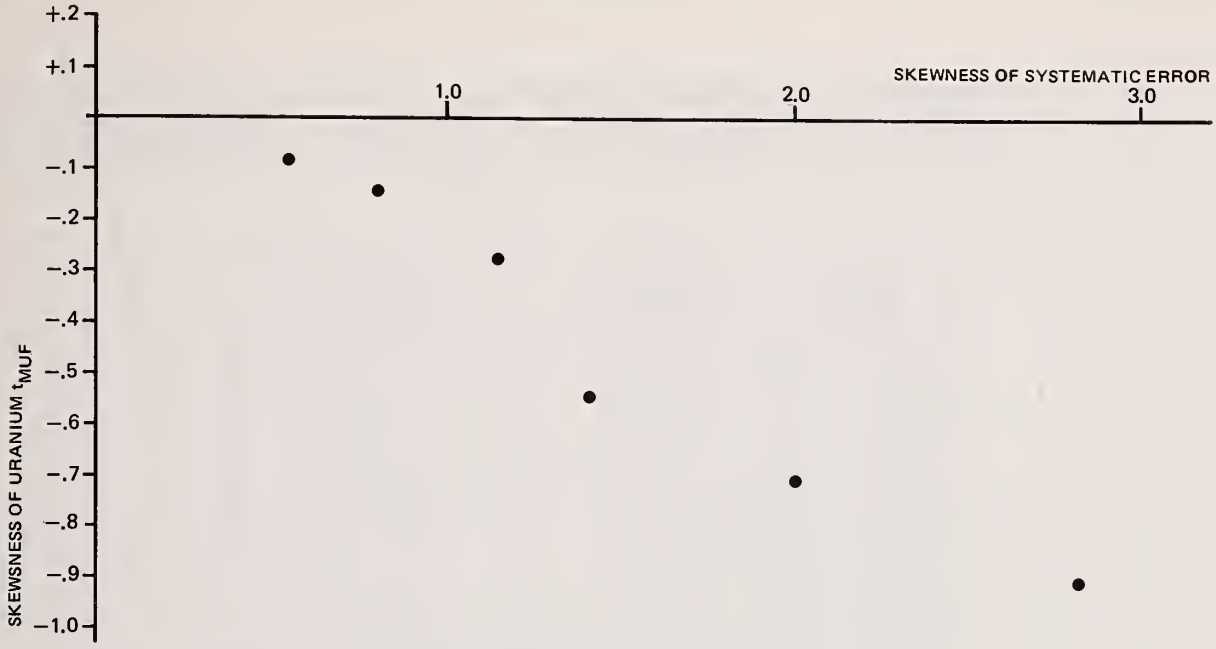

Fig 2 Systematic Error Skewness affecting Skewness of t_{MUF}

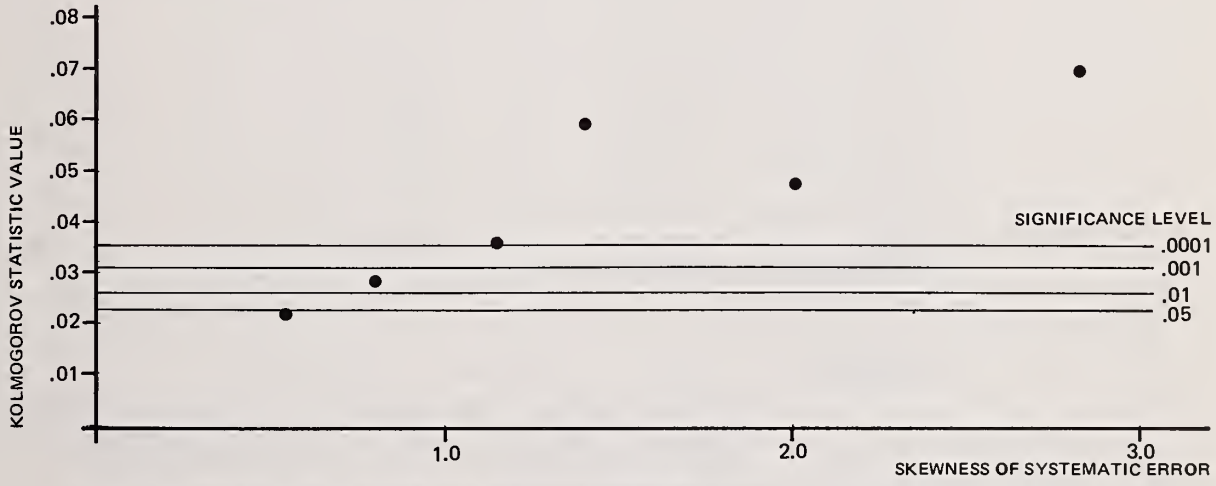

Fig 3 Systematic Error Skewness affecting Kolmogorov Statistic

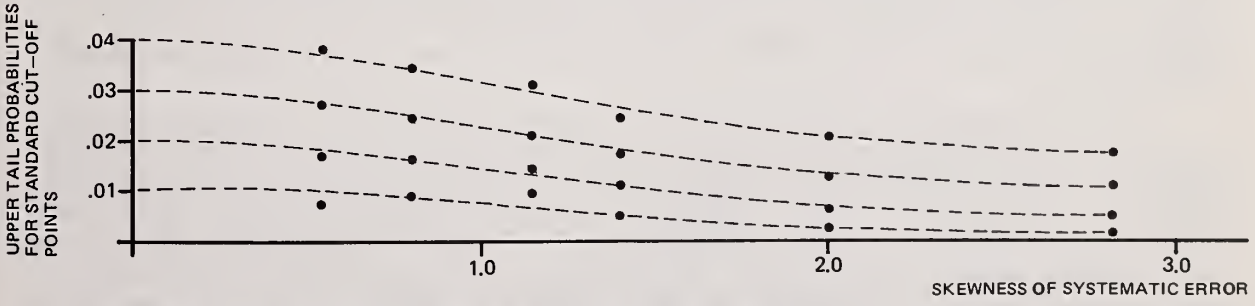

Fig 4 Systematic Error Skewness affecting t_{MUF} Tail Probabilities
(For each value of skewness the graph shows estimates of the probabilities that t_{MUF} exceeds 1.75069', 1.88079, 2.05375, and 2.32635).

- the estimated probabilities of t_{MUF} exceeding standard test cut-off points. In particular the cut-off values corresponding to the upper 1%, 2%, 3% and 4% of the standardised normal curve (Fig. 4).

ERROR SOURCE	RANDOM (GMS SQUARED)	SYSTEMATIC (GMS SQUARED)
SC01	1000.960	250240.058
SC02	1845.345	23779.712
SC03	34.789	3374.561
ES11	120323.616	62668.550
ES12	93.743	2372.872
ES13	80.616	11608.751
ES14	14989.011	487.990
ES15	41630.162	6723.442
ES16	4154636.038	6773246.756
EA21	120323.616	84326.801
EA22	374.972	5741.765
EA23	270.960	28090.311
EA24	2996.272	2341.311

Table III : Uranium MUF Variance Components.

(These figures are based on equations of the form (2) and (3); apart from this they are derived from the data of USAEC publication (6)).

The second aspect which is presented is the effect of the dominance of the skew systematic error. In this case the value of the skewness is held fixed and the relative standard deviation of the systematic error is varied. The effect of this on uranium t_{MUF} is again shown in the same three ways (Figures 5,6 and 7). The sample size for all of the simulations presented here is 4000.

In these examples, the systematic error for sampling of ammonium diuranate scrap has been simulated with positive skewness. Most of the ammonium diuranate scrap however has entered into the MUF equation for this balance period with a negative sign. Hence the positive skewness in the systematic error is propagated to give a negative skewness in the distribution of t_{MUF}.

Figures 2 and 5 illustrate the fact that the skewness of t_{MUF} depends both on the degree of skewness of the systematic error as well as the dominance of that error. A systematic error whose skewness is small produces negligible skewness in t_{MUF}. Similarily a systematic error which is highly skew but which has a relatively small contribution to the MUF variance will produce a negligible skewness in t_{MUF}. Figures 3 and 6 show how the fit of the standardised normal distribution is affected by the skewness of t_{MUF}.

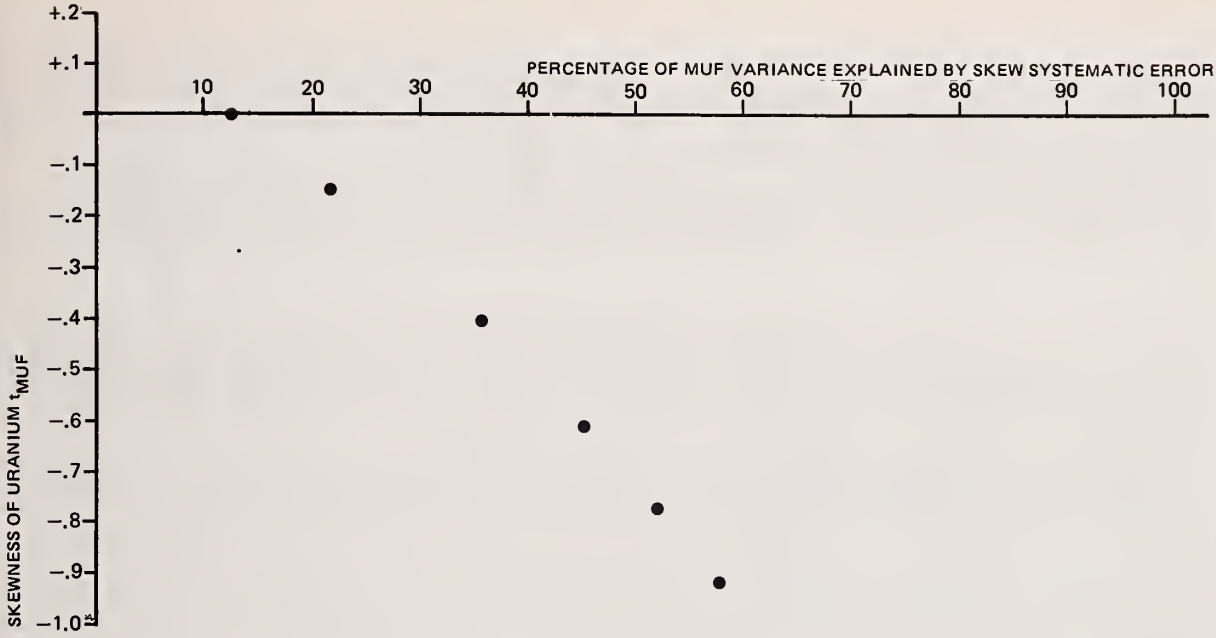

Fig 5 Dominance of Skew Systematic Error affecting Skewness of t_{MUF}

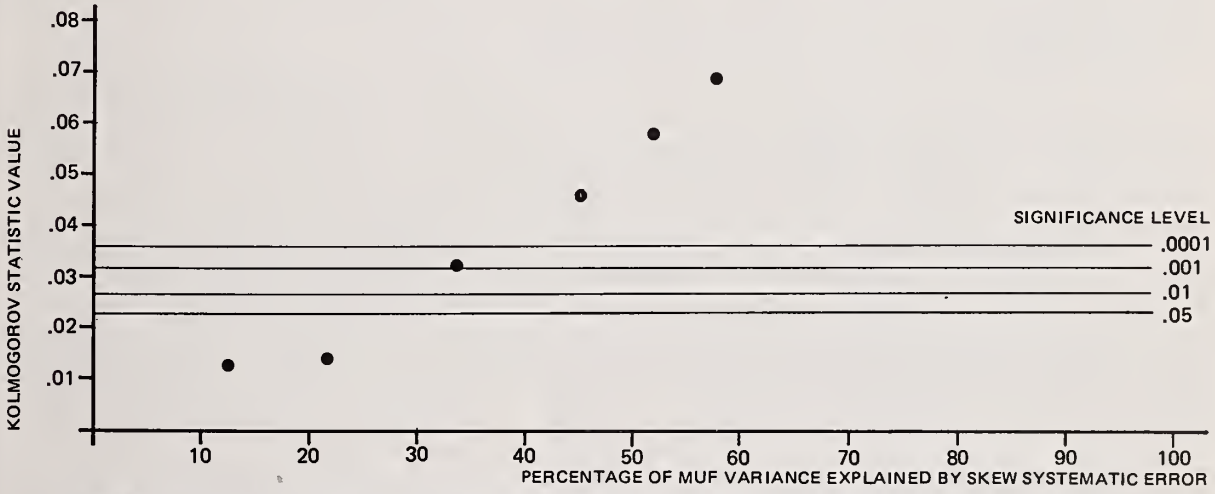

Fig 6 Dominance of Skew Systematic Error affecting Kolmogorov Statistic

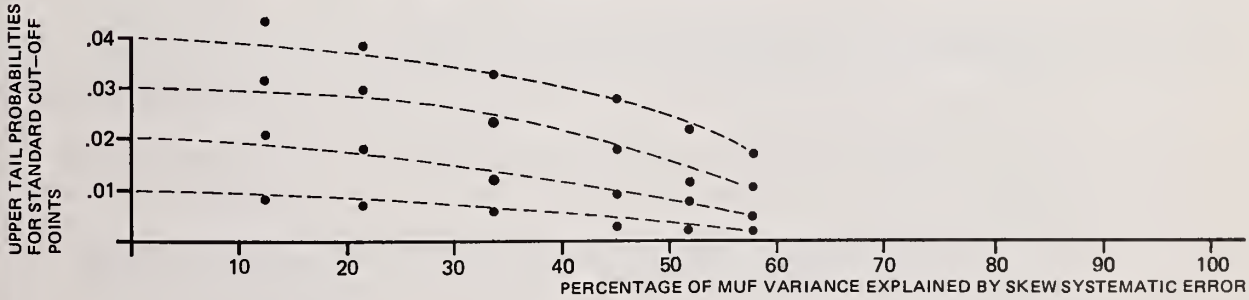

Fig 7 Dominance of Skew Systematic Error affecting t_{MUF} Tail Probabilities
(For each value of skewness the graph shows estimates of the probabilities that t_{MUF} exceeds 1.75069, 1.88079, 2.05375 and 2.32635).

Figures 4 and 7 show how the upper tail probabilities of the actual t_{MUF} distribution differ from those of a standardised normal distribution. Generally the negative skewness of t_{MUF} results in smaller tail probabilities than would be the case if t_{MUF} were normally distributed.

The simulations which produced Figures 2-7 give essentially similar graphs for the skewness, normality and tail probabilities of t_{MUF} for isotope.

CONCLUSION

The evaluation of accountancy declarations involves the Safeguards Authorities in the interpretation of large volumes of data. The use of EDP and statistical data processing are necessary tools in coming to grips with the detail and complexity of this information. On the other hand, the evaluation of MUF by Safeguards Authorities can never be reduced to a blind mechanical use of statistical rules. The administrative process of evaluation involves a variety of considerations, both statistical and non-statistical which have been mentioned already. As in any other administrative decision process the Safeguards Authorities will exercise judgement about the quality of the information available in respect of each dimension of the problem. In this regard the statistical dimension is no exception. The use of statistical techniques must always be tempered by a knowledge of the assumptions and approximations involved in calculating statistical indices. For example, any statistical inference about MUF must reflect the uncertainty, if any, about the validity of the error propagation equation (1), (2) and (3) as an adequate description of the plant measurement system. Similarity it must reflect any uncertainty about the accuracy of the error source standard deviation estimates since these play a central role in determining the statistical significance of MUF.

The program of simulation; some of which has been presented here, can be viewed as refining a third such area of judgement, the quality of the normal approximation for assigning a significance level to observed MUF. The simulation results reported here show that skewness, for example, can effect the quality of the normal approximation. In the example presented, the actual false alarm probability would be less than the nominal one and there would be a corresponding decrease in the detection probabilities. If the balance period had been one in which the ammonium diuranate scrap had appeared in the accounts with a positive sign the effect would have been to give a false alarm probability greater than the normal one and a corresponding increase in detection probability. Thus in the case where a single error variable dominates the MUF uncertainty and where there is doubt as to the normality of this error, the statistical significance of MUF as calculated using normal tables may be a little larger or a little smaller than the true value.

M.G. Kendall and A. Stuart (10) discuss factors affecting the robustness of the classical t-statistic. Work on this topic provides insights as to when the normal approximation to the distribution of t_{MUF} is likely to be good. The conditions for adequacy are likely to include

- that the linearisation of MUF contained in the Taylor's series approximation is a good enough approximation
- that the number of independent random variables in the MUF calculation is not too small
- that no single variable whose distribution is not Normal should dominate the MUF variance in the sense we have discussed in this paper
- that the measurement system does not create any strong correlation between observed MUF and $\hat{\sigma}_{MUF}$ for the balance period in question.

The purpose of this simulation study is to quantify these aspects in a practical way for safeguards purposes. The results presented in this paper are initial results and it would be premature to make any quantitative generalisations at this stage.

REFERENCES

1. Commission Regulation (Euratom) N° 3227/76 of 19 October 1976 concerning the application of the provisions on Euratom Safeguards; published in the Official Journal of the European Communities, Vol. 19, N° L363, 31 December, 1976.

2. Argentesi F., Casilli T., and Franklin M. - NUMSAS : A Statistical Nuclear Material Accountancy System in the EURATOM Framework.
Proceedings of the 1st Annual ESARDA Symposium on Safeguards and Nuclear Material Management.
Brussels, Belgium, April 25-27, 1979.

3. Argentesi, F., Casilli, T. and Franklin, M. - Nuclear Material Statistical Accountancy System (EUR 6471 EN) published by the Commission of the European Communities, Joint Research Centre, Ispra-Establishment, Italy, 1979.

4. Cuypers M., Schinzer F., and Van der Strict - Development and Application of a Safeguard System in a Fabrication Plant for Highly Enriched Uranium.
Proceedings of the IAEA Symposium on Nuclear Materials Safeguards.
Vienna, Austria, Oct. 2-6, 1978.

5. Hamlin A.G. - The Effects of Establishing Statistical Targets for Safeguards on Nuclear Material Accountancy.
Proceedings of the 1st Annual ESARDA Symposium on Safeguards and Nuclear Material Management.
Brussels, Belgium, April 25-27, 1979.

6. Jaech J.L. - Statistical Methods in Nuclear Material Control.
Published by the Technical Information Centre, Office of Information Services, US Atomic Energy Commission, 1973.

7. Noether, G.E. - Elements of Nonparametric Statistics, published by John Wiley and Sons, Inc., New York, 1967.

8. Knuth D.E. - The Art of Computer Programming, Vol. I, Fundamental Algorithms, published by Addison Wesley Publishing Company, London, 1979.

9. Argentesi, F. and Cullington, G. - Sensitivity Analysis of the MUF Variance with respect to the Measurement System Performances of a Large HEU Fabrication Plant.
Proceedings of the ANS Topical Meeting on Measurement Technology for Safeguards and Material Control, Charleston, South Carolina, USA, Nov. 26-29, 1979.

10. Kendall, M.G. and Stuart, A. - The Advanced Theory of Statistics, Vol. II, Inference and Relationship, published by Charles Griffin and Company Ltd, London, 1967.

SENSITIVITY ANALYSIS OF A MATERIAL BALANCE DECLARATION WITH RESPECT TO MEASUREMENT ERROR SOURCES

FLAVIO ARGENTESI

Joint Research Centre, Commission of the European Communities, Ispra, Italy

and

GEOFFREY R. CULLINGTON

Euratom Safeguards, Commission of the European Communities, Luxembourg

ABSTRACT

A sensitivity analysis of the variance of MUF, with respect to the basic statistical properties, in terms of variances for random and systematic errors of the measurement system's components, has been performed for an actual material balance of a high enriched uranium fabrication plant. The material balance considered in this study contains several thousand batches.

1. INTRODUCTION

A material balance declaration of a high enriched uranium fabrication plant has been studied to evaluate the sensitivity of MUF Variance with respect to measurement error sources.

The estimation of the MUF variance for the various combinations of standard deviations of the measurement errors sources has been performed with the NUMSAS programme (ref.1).

The nominal values for the standard deviations used are those provided by the plant operator according to his evaluations and are shown in Table I as relative standard deviations (i.e. Kg/Kg) because NUMSAS assumes a measurement errors model of multiplicative type.

The material balance considered in this study was composed of 1237 batches in the beginning inventory, 530 as inventory changes and 1275 in the ending inventory.

The quantity of U involved in the material balance is large amounting to 3000 Kg in inventory. The sensitivity analysis study refers only to the total quantity of U and not the fissile part.

NUMSAS programme calculates the composition of MUF variance in terms of the systematic and random contribution of each error source. Therefore from the variance components table of NUMSAS (see Table II) it is possible to determine which measurement errors sources are important contributors to the MUF variance.

In this case seven measurement error sources appear of major importance.

Three refer to random component of scales involved in measurement of UF_6, $U_3O_8 + UO_2$ powder and pellets respectively. the other four sources refer to the chemical analysis of UF_6, UF_4, $U_3O_8 + UO_2$, and platelet NDA measurement.

TABLE 1 MEASUREMENT SYSTEM as used in this STUDY

MEASUREMENT METHOD	STANDARD DEVIATIONS		REMARKS
	Random	Systematic	
SC01	0.002	0.00001	Scale for weighing UF_6 bottles
SC03	0.0001	0.00001	Balance with range 0 to 10 Kg used for UF_4
SC05	0.0001	0.00001	Like SC03 but used for U_3O_8+UO_2
SC06	0.004	0.00001	Balance used for U_3O_8 and UO_2 for batches $>$ 10 Kg
SC07	0.0005	0.00001	Balance used for UO_2 pellets
SC09	0.001	0.00001	Like SC03 but used for U/UAl swarf
SC10	0.001	0.00001	Like SC03 but used for U/Th mixtures
SC11	0.004	0.00001	Like SC06 but used for U/Th mixtures
SC12	0.0015	0.0015	Balance used for U/ThO_2 mixtures
EA01	0.00025	0.0003	U content of UF_6
EA02	0.001	0.002	U content of UF_4
EA03	0.0005	0.001	U content of U_3O_8, UO_2 and pellets
EA04	0.0025	0.0025	γ absorption in U-Al platelets
EA05	0.005	0.001	U content of U-Al swarf
EA06	0.005	0.001	U content of U-Th mixtures
EA07	0.002	0.001	U content of U-lx powders
EA08	0.0008	0.001	U content of U-ThO_2 particles
EA09	0.0025	0.0025	γ-ray emission of U-Alx (cermets) platelets

NOTE: - This is not the complete plant measurement system but that part of it which relates to the present study.

2. DESCRIPTION of the PLANT

The operations which take place in this plant are briefly as follows:

- The starting point for the main fabrication lines is highly enriched uranium hexafluoride
- There is a scrap recovery unit in which campaigns are also run for clients.
- Chemical, metallurgical and mechanical treatment of various types of uranium are possible.
- Large stocks of uranium of all enrichments are at hand in a variety of forms and dimensions
- The stock of uranium is split into thousands of accountancy units.
- Part of the uranium stock is mixed with thorium, the latter being the major component.

The main production lines are

- Chemical processing areas
- The MTR line (alloy and cermet)
- The HTR line (Kernels, particles and pebbles)
- The UO_2 line (pellets and pins)

Fig. 1 shows a simplified flow diagram of the processes of the plant with all the measurement points used in this material balance marked.

The weighing scales are all of the digital read out type and all the readings are recorded by hand.

The U content analysis measurement methods EA01, 02 and 03 are destructive chemical analyses using the modified Davies-Gray method of titration with the end point determined potentiometrically. The difference between the 3 methods is the preparation from the starting point of the material in the sample. The plant operators state that any errors due to sampling are incorporated in the standard deviations of the measurement method itself. EA04 is an NDA method which measures the absorption of TM-170 γ rays through the coupon of U-Al alloy. The coupon is moved past the source and the total count is integrated and compared with a standard.

EA05 is a calculation of the U content based on the constituents of the alloy.

EA06, 07 and 08 are destructive analyses like EA01, 02 and 03, the difference being dependent on the different chemical preparative work required to prepare the aliquot for the titration.

EA09 is a direct determination of the U^{235} content of the cermet platelets before they are rolled out by measuring the 185 Kev γ -ray using a Na I (Tl) detector. Each measurement is compared with a standard and the U content is calculated using the enrichment which is based on a mass spectrometer measurement at an earlier stage in the process.

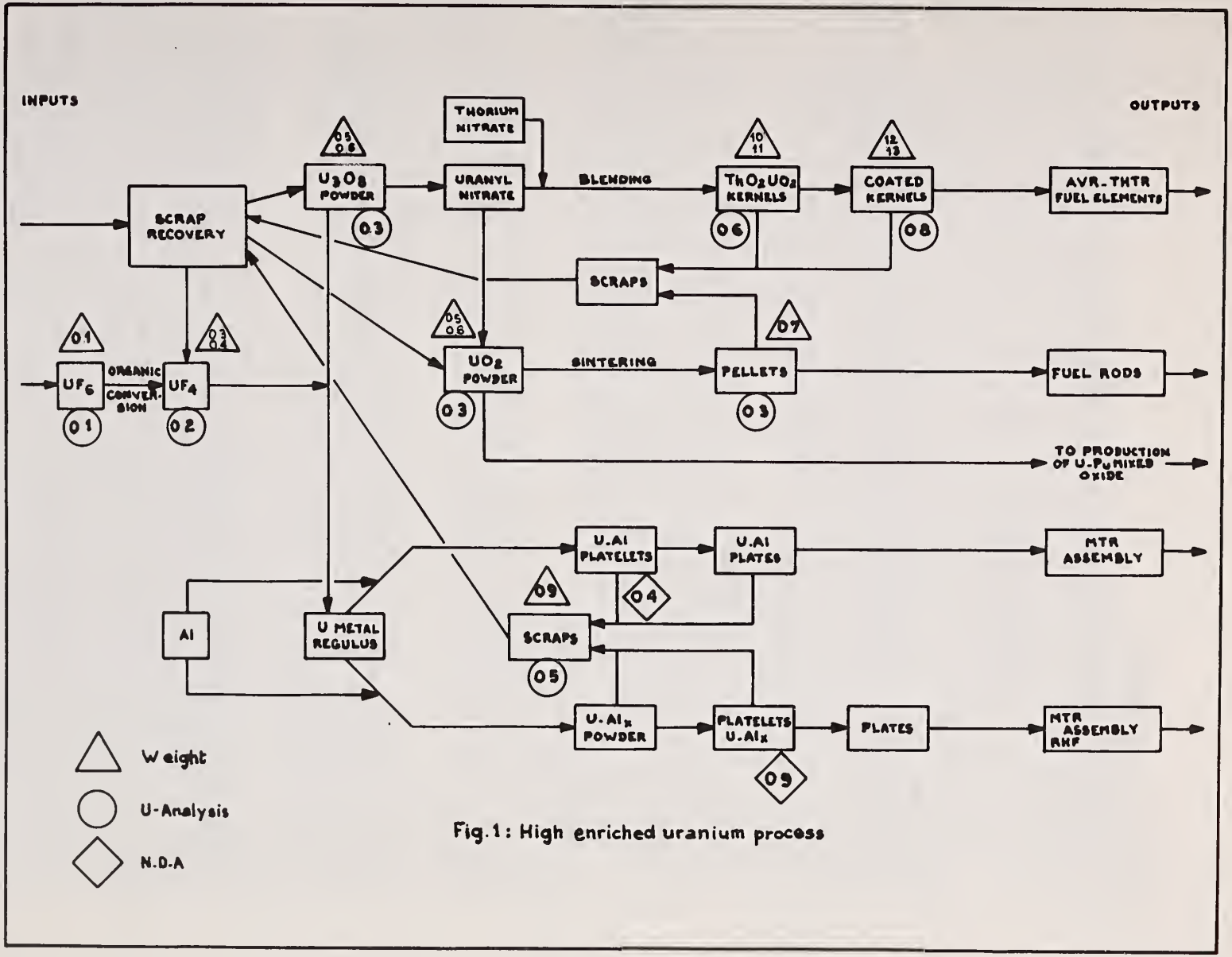

Fig. 1: High enriched uranium process

3. INPUT DATA to the ANALYSES

The input data to a NUMSAS calculation is the data for a material balance period consisting of

Beginning Inventory	BI
Inventory Changes	ICs
Ending Inventory	EI

The input data for this study consists of 3042 lines of data some of which are single items but others are grouped into batches where the items are identical. The total number of lines in the BI is 1237 and in the EI 1275 corresponding to 3021 Kg and 2685 Kg of high enriched uranium respectively. Each line of data contains all the information required for reporting the PIL (Physical Inventory Listing) to the Euratom and IAEA safeguards authorities. In addition a code for the error path is added which provides the key to the sources of error, which are quoted as relative standard deviations as given by the operator as a result of his evaluations (see Table I).

The data for the inventory changes is taken directly from the reports sent into the EURATOM safeguards authority by the operator with the addition of the error path. The amount of material involved is 432 Kg as input and 768 Kg as output and covers a 6 month period.

The data used is real and refers to a European high enriched fuel fabrication plant.

4. BRIEF DESCRIPTION of NUMSAS

The basic purpose of NUMSAS is to provide additional information for safeguards authorities or plant managers who wish to evaluate a non-zero material balance (MUF) at the end of a balance calculation in order to judge whether it can reasonably be accounted for as an accumulation of measurement errors in the balance calculation.

The statistical approach on which NUMSAS is based views the measurement error component of MUF as having a probability distribution which can be calculated if the plant measurement system is known. For this reason NUMSAS uses information about the errors arising in each of the measurement activities of the plant. In addition to this, NUMSAS requires information about the measurement history of each batch of nuclear material involved in the balance calculation.

As well as being a tool for material control, NUMSAS can be used by plant operators to study the performance their plant measurement system. The separate elements of the measurement system will contribute in differing degrees to the variance of MUF. NUMSAS can be used to quantify the contribution of each element of the measurement system and this information can be used to identify the principal sources of uncertainty. It can also be used to provide a basis for judging the cost-effectiveness of any proposed improvements in the measurement system.

The measurement system is taken to mean any instrument or procedure used in the plant to measure the nuclear material content of a batch. This includes weighing scales, volume determination instruments, sampling methods as well as analytical instruments or techniques. In the plant being studied there are 9 weighing scales, 2 non destructive analysis techniques, 8 sampling techniques and 7 chemical analysis techniques. The value of the standard deviations of the sampling techniques have been taken to be zero so there is no contribution to σ MUF from them. Table I gives the details of these measurement methods each of which is referred to a measurement error source. Each source is defined as having 2 components of error, a systematic error and a random error.

To use the NUMSAS system it is necessary to know (or have estimates of) the standard deviations of random error and systematic error for each measurement error source. It is important that the estimates used are representative of plant operating conditions. In general special measurement experiments will be necessary to estimate these quantities for a particular plant. Estimates quoted by instrument manufacturers or estimates achieved in research laboratories may be of little value for material control purposes. The present study is devoted to establishing the effect of changes in the values of the standard deviations of the random and systematic errors for each error source.

The NUMSAS model assumes, in the most complex case, that the measured value for the isotope content of an individual batch is calculated as the product of three distinct measurements. These are

- the bulk weight or volume
- the element factor value, e.g. the proportion of uranium per unit bulk weight
- the isotope factor value, e.g. the proportion of U-235 per unit weight of uranium.

Each of these three measurements is made with it's appropriate measurement instrument or method. The NUMSAS measurement model is for both random and systematic types a multiplicative model, i.e. the standard deviations for each error source are relative standard deviations. For example the recorded weight of a batch will use a scale and may be the average of several weighings. In this case the recorded weight $\hat{W}$ will be:

$$\hat{W} = W\,(1 + \lambda_i + \bar{\varepsilon}_i\,(n));$$

$$\text{with } \bar{\varepsilon}_i\,(n) = \frac{1}{n} \sum_{j=1}^{n} \varepsilon_{ij}$$

where W is the true weight of the batch,

λ_i is the value of the systematic error for scale i

n is the number of replicate weighings

ε_{ij} is the value of the random error of the j^{th} weighing of this item using scale i.

The case of element factor determination is more complicated since there are both sampling and analysis errors. However this is not the only complication. In determining isotope or element factor, batches which were weighed separately may be treated as a single batch. This is done by taking a number of samples in a representative way throughout the batch. Subsequently, each sample may be subjected to several replicate analyses (case I) or alternatively the samples may be merged and the resultant sample may be subject to replicate analyses (case II). The factor value of the batch is taken as the average of the values in the different replications. Thus while each weighed batch will have an associated factor determination value the factor determination may be common to a group of weighed batches. The NUMSAS model of measured element factor $\hat{P}$ can be represented as

$$\hat{P} = P\,(1 + \theta_i + \eta_i(m) + \zeta_j + \bar{\gamma}_j\,(d))\,;$$

$$\text{with } \bar{\eta}_i(m) = \frac{1}{m} \sum_{k=1}^{m} \eta_{ik} \quad \text{and} \quad \bar{\gamma}_j(d) = \frac{1}{d} \sum_{k=1}^{d} \gamma_{jk}$$

where P is the true element factor value for the batch

θ_i is the value of the systematic error for the i^{th} sampling method

ξ_j is the value of the systematic error for the j^{th} analysis instrument or technique

m is the number of replicate samples

η_{ik} is the value of the sampling random error of the k^{th} sample using the i^{th} sampling method

d is the total number of replicate analyses i.e. the total over all the samples

γ_{ik} is the value of the analytical random error of the k^{th} analysis replication using the jth analytical method. In case II these are the random errors of the d analyses on the merged sample. In case I they are the random errors of $\frac{d}{m}$ replicate analyses on each of m samples.

The model presumes that isotope factor determination is based on a separate sampling and analysis from that of the element factor determination. The model is similar to that for element factor in that the measured isotope factor $\hat{Q}$ is represented in the form,

$$\hat{Q} = Q\,(1 + \alpha_i + \bar{\beta}_i(m) + \delta_j + \bar{\nu}j(d)\,);$$

with $$\bar{\beta}_i(m) = \frac{1}{m} \sum_{k=1}^{m} \beta_{ik} \quad \text{and} \quad \bar{\nu}_j(d) = \frac{1}{d} \sum_{k=1}^{d} \nu_{jk}$$

where Q is the true element factor value for the batch

α_i is the value of the systematic error for the i^{th} sampling method

δ_j is the value of the systematic error for the j^{th} analysis instrument or technique

m is the number of replicate samples

β_{ik} is the value of the sampling random error of the k^{th} sample using the i^{th} sampling method

d is the total number of replicate analyses i.e. the total over all the samples

ν_{jk} is the value of the analytical random error of k^{th} analysis replication using the j^{th} analytical method. In case II these are the random errors of the d analyses on the merged sample. In case I they are the random errors of $\frac{d}{m}$ replicate analyses of each of m samples.

The measured value of the isotope content of an individual item is represented in the model as $Z = \hat{W}\,\hat{P}\,\hat{Q}$. This formula is the NUMSAS model of a single material balance declaration. The NUMSAS model also assumes that all the error random variables are statistically independent with zero means. In this case the means and variance of $\hat{W}$, $\hat{P}$ and $\hat{Q}$ are given by the formulae,

$$E(\hat{W}) = W \quad ; \quad \mathrm{Var}(\hat{W}) = W^2 \left(\sigma_\lambda^2 + \frac{\sigma_\varepsilon^2}{n} \right) \quad ;$$

$$E(\hat{P}) = P \quad ; \quad \mathrm{Var}(\hat{P}) = P^2 \left(\sigma_\theta^2 + \frac{\sigma_\eta^2}{m} + \sigma_\xi^2 \frac{\sigma_\gamma^2}{d} \right) \quad ;$$

$$E(\hat{Q}) = Q \quad ; \quad \mathrm{Var}(\hat{Q}) = Q^2 \left(\sigma_\alpha^2 + \frac{\sigma_\beta^2}{m} + \sigma_\delta^2 + \frac{\sigma_\nu^2}{d} \right) \quad ;$$

In this notation the variances of the measurement errors are specified in terms of relative standard deviations which are denoted by the symbol σ.

5. DERIVATION OF THE SENSITIVITY EQUATION

We assume m error sources, each source being a generator of both random and systematic variance.

The variance of MUF; σ^2 MUF will be given by the sum of 2 m independent variances m of random origin and m of systematic origin

$$\sigma^2_{MUF} = \sum_{i=1}^{m} Ki\, \sigma_i^2 + \sum_{i=m+1}^{2m} \gamma i\, \sigma_i^2 \quad \ldots\ldots\ldots \quad (1)$$

The calculation of the Ki and γi will be different according to the different properties of random and systematic errors see (Ref 1).

For the purpose of the present study equation (1) can be written without distinguishing between random and systematic component:

$$\sigma^2_{MUF} = \sum_{i=1}^{2m} \alpha_i\, \sigma_i^2 \quad \ldots\ldots\ldots\ldots\ldots\ldots \quad (2)$$

and

$$\sigma_{MUF} = \left(\sum_{i=1}^{2m} \alpha_i\, \sigma_i^2 \right)^{1/2} \quad \ldots\ldots\ldots\ldots\ldots \quad (2a)$$

The scope of our study is that of evaluating the sensivity coefficient of the σ MUF with respect to the 2 m errors sources.

These sensitivity coefficients S_K can be conveniently derived as follows:

$$S_K = \frac{\delta \sigma_{MUF}}{\delta \sigma_K} = \frac{1}{2} \left(\sum_{i=1}^{2m} \alpha_i\, \sigma_i^2 \right)^{-1/2} 2\alpha_K\, \sigma_K \quad \ldots\ldots \quad (3)$$

Substituting equation (2a) into (3) we have

$$S_K = \frac{\delta\sigma_{MUF}}{\delta\sigma_K} = \alpha_K \frac{\sigma_K}{\sigma_{MUF}}$$

For the Kth error source we have

$$\sigma^2_{ECK} = \sigma^2_K \quad \alpha_K$$

Where the σ^2_{ECK} are the various components into which NUMSAS separates σ^2_{MUF}. is the variance of the Kth source. By substituting equation (5) in (4) we have:

$$S_K = \frac{\sigma^2_{ECK}}{\sigma_K \ \sigma_{MUF}}$$

Equation (6) is the sensitivity equation used in this study.

6. SENSITIVITY COEFFICIENT EVALUATION

The NUMSAS programme for specific set of nominal values σ_i (i = 1 ..... 2m) provides σ MUF and the table of σ^2_{ECK} . By using equation (6) the Si (i = 1...2m) sensitivity coefficients can be easily evaluated.

These sensitivity coefficients represent the variations of MUF standard deviation per unit of variation in the corresponding error source.

The numerical values of the S_K depend on two conditions:

- the specific material balance structure of the plant with respect to the measurement system
- the numerical values of the relative standard deviations associated with the error source to which the sensitivity coefficient refers.

In this study the role of the material balance structure seems to be the major factor for the ranking of the sensitivity coefficients. Different error sources can show the role of the two conditions previously mentioned.

Table II gives the following data for the balance

- the sensitivity coefficients
- the normalised contributions of the different error sources to the variance of MUF
- the weight of material which has been measured by each measurement method (also shown in Table I).

Scale SC01 for instance used for the measurement of a total amount of 2057 Kg of U, and measures with a relative standard deviation for random errors of 0.002.

The contribution of scale SC01 to the σ MUF is 77.2% of the σ MUF value and its S_K is 288600.

On the other hand scale SC 06 with a relative standard deviation for random errors of 0.004 (twice that of scale SC 01) contributes only 3.9% to the σ MUF. The total amount of U measured by this scale is only 37 Kg.

Table II Sensitivity Coefficients

MEASUREMENT METHOD	SENSITIVITY COEFFICIENTS		NORMALISED CONTRIBUTION TO σ^2 MUF		RELATIVE STANDARD DEVIATIONS		Kg U
	Random	Systematic	Random	Systematic	Random	Systematic	
Weighing Scales							
SC 01	288600	799	77.2	< 0.1	0.002	0.00001	2057
SC 03	342	72	< 0.1	< 0.1	0.0001	0.00001	347
SC 05	576	213	< 0.1	< 0.1	0.0001	0.00001	439
SC 06	7240	18	3.9	< 0.1	0.004	0.00001	37
SC 07	< 1	< 1	< 0.1	< 0.1	0.0005	0.00001	0.3
SC 09	99	117	< 0.1	< 0.1	0.001	0.00001	38
SC 10	2	< 1	< 0.1	< 0.1	0.001	0.00001	4
SC 11	1	< 1	< 0.1	< 0.1	0.004	0.00001	1
SC 12	3108	2994	0.6	0.6	0.0015	0.0015	274
Uranium Analaysis Methods							
EA 01	36070	23970	1.2	1.0	0.00025	0.0003	2057
EA 02	865	19710	0.1	5.3	0.001	0.002	148
EA 03	5061	30230	0.3	4.0	0.0005	0.001	676
EA 04	1221	483	0.4	0.2	0.0025	0.0025	175
EA 05	66	116	< 0.1	< 0.1	0.005	0.001	17
EA 06	10	15	< 0.1	< 0.1	0.005	0.001	5
EA 07	171	559	0.1	0.1	0.002	0.001	20
EA 08	1658	1996	0.2	0.3	0.0008	0.001	274
EA 09	1334	12160	0.4	4.1	0.0025	0.0025	182

7. DISCUSSION AND CONCLUSIONS

The presence of the large random component associated with the operation of scale SC 01 is in part due to the presence of an unusually high quantity of UF_6 in this particular balance. In any case the role of the random error associated with this scale will be important because almost all the input material to the plant is UF_6 and is therefore weighed on this scale. It is worth noting here once again the misleading nature of the widely held belief that random errors "cancel out" and are consequently of little

importance in the material balance of a large plant. The effect of a random error in a measurement can of course be reduced by replication of that measurement. The analysis of the numerical values of the sensitivity coefficients S_k shows that this system is sensitive to only a few error sources, i.e. the random components of SC 01, SC 06 and EA 01 and the systematic components of EA 01, EA 02, EA 03 and EA 09 which together account for 96.7% of the variance of MUF. SC 01 weighs the bottles of UF_6 and EA 01 analyses the U content of the UF_6. SC 06 is used for weighing UO_2 and U_3O_8. EA 02 is used for the U content of UF_4 and EA 03 is used for the U content of UO_2, U_3O_8 and pellets. EA 09 is the non destructive γ assay of the U-AL cermet platelets.

Any project oriented to the improvement of the performance of the plant measurement system from the point of view of the statistical analysis of a material balance should concentrate on the above seven measuring equipments and/or procedures.

It is not necessary to proceed to a full cost of benefit analysis to see that a major reduction in the σ MUF can be achieved if the methods of measurement of the UF_6 could be improved. On the other hand it is clear that many of the measurement techniques make only a very minor contribution to the σ MUF and it is likely that they will continue in this way for future balances in this plant.

For such error sources one can infer that less precise and accurate measurements equipment and procedures could be used without any significant effect on the MUF-LEMUF analysis of a material balance.

Future safeguards requirements about measurement systems should take into account such properties of material balance. The sensitivity study presented in this paper can be performed for other plants in different parts of the fuel cycle. Such a generalized evaluation of the role of the measurement systems in various parts of the fuel cycle could help in defining the properties of measurement systems.

8. REFERENCE

1) F. Argentesi, T. Casilli and M. Franklin
Nuclear Material Statistical Accountancy System
EUR 6472 EM (1979) pp. 92.

Discussion:

Persiani (ANL):

You made a very good point that you were not able to verify or scrutinize the sampling technique of the operator. Isn't that really the weakest link in our safeguards system? If we cannot impose an international system, impose sampling techniques, the study you have made, the sensitivity, and what goes on in the processing plant, may not be on a one-to-one level.

Cullington (ISPRA):

Perhaps I have misled you a bit. We are certainly able to examine the sampling technique and see what this technique is. What is difficult, is to allocate random and systematic errors to the technique itself. The final thing is, that it is just incorporated into the analytical technique, and this is a problem we have had in more than one plant. I think our regulation requirements are perhaps a little less precise and a little less fixed than the American requirements, which require a full presentation of all these data in a much more defined format.

Gordon (BNL):

Could you describe the method used in this plant for the elemental analysis of UF_6?

Cullington:

Only in very simple terms because I am not a chemist. Basically the chemistry is the modified Davies-Gray method of titration with end point determined potentiometrically.

Heinberg (LASL):

I have a couple of questions addressing the first vu-graph that showed scrap coming in external to the plant. I don't think you addressed how that was measured. I also noticed that there were waste streams indicated. Is that a true statement?

Cullington:

The scrap material comes in on an estimated value and is then treated and measured after the material has been processed. This is normally done in the presence of the plant operator so that the input figure is corrected to the results of this scrap process. The NUMSAS program also has a feature in it that correlates items that appear on the plus and minus side of the MUF equation. So, if some scrap has been delivered in a period as an input and appears on the ending inventory with a plus and a minus equation, it has been untouched and it is not included in the LEMUF analysis because it cancels itself out. In fact, any scrap material appears as an input of UO_2, UF_4, or U_3O_8, according to the more precise and pure chemical technique. The other question of the scrap: yes, there are some scraps produced. They were very small amounts in this particular balance, and they have not been included in it, so in that respect the balance has been made slightly artificial. In this particular period, it was not an important amount, but it is a valid point to say it has not been included.

Deviations from Mass Transfer Equilibrium and Mathematical Modeling of Mixer-Settler Contactors

by

A. L. BEYERLEIN, J. F. GELDARD, H. F. CHUNG,
Department of Chemistry and Geology,
Clemson University, Clemson, SC 29631

and

J. E. BENNETT
Department of Electrical and
Computer Engineering, Clemson
University, Clemson, SC 29631

(Work was supported by Los Alamos Scientific Laboratory, Q-4 Systems, Under Contract N28-9750D-1).

ABSTRACT

This paper presents the mathematical basis for the computer model PUBG of mixer-settler contactors which accounts for deviations from mass transfer equilibrium. This is accomplished by formulating the mass balance equations for the mixers such that the mass transfer rate of nuclear materials between the aqueous and organic phases is accounted for. Mass transfer equilibrium or SEPHIS limit can be achieved with this model in the limit of a large mass transfer area between the two phases. Concentration profiles calculated with PUBG in the SEPHIS limit agree with those calculated using SEPHIS-MOD3 or -MOD4. (For a description of SEPHIS models see S. B. Watson and R. H. Rainey, "Modifications of the SEPHIS Computer Code for Calculating the Purex Solvent Extraction System", ORNL-TM-5123, Dec. 1975 and A. D. Mitchell, "A Comparison Between SEPHIS-MOD4 and Previous Models for the Purex Solvent Extraction System", ORNL-TM-6565, Feb. 1979). Comparisons with Thompson and Shankle's measured uranium concentration profiles (M. C. Thompson and R. L. Shankle, "Calculation of Uranium Inventories in Mixer-Settlers During Solvent Extraction with 7.5% TBP", Savannah River Laboratory, DP 1357, August 1974) on the 1D and 1E contactors indicated good agreement between PUBG calculations and measured data is obtained by adjustment of the mass transfer area to values which indicate there are significant deviations from mass transfer equilibrium. PUBG calculations in the SEPHIS limit on the 1D and 1E contactors predict a steady state uranium holdup that is 10.8% and 16.3% lower, respectively, than the experimental values. This is consistent with the expectation that deviations from equilibrium will lower the efficiency of the contactor and increase its nuclear material holdup.

KEYWORDS: Mathematical models, mixer-settlers, chemical contactors, mass transfer rates, mass transfer equilibrium, uranium holdup, plutonium holdup.

INTRODUCTION

The chemical modeling of the steady state operation of mixer-settler contactors for solvent extraction processes has been investigated by a number of workers (1-5). It was not until safety requirements demanded in the reprocessing of nuclear fuels during startup and shutdown that models for predicting both the transient as well as the steady state behavior of mixer-settler contactors were developed (6-13).

The SEPHIS computer models (8-12) developed at Oak Ridge National Laboratory and Hanford Engineering Development Laboratory are very frequently used for simulating both the transient and steady state behavior of mixer-settler contactors used in nuclear reprocessing facilities. These models have been continuously upgraded by introduction into the model improved distribution coefficient correlations (9, 10, 14), the extension of the applicability of the model to partitioning of plutonium and uranium (9), and improved numerical integration methods (11, 12). The modifications of A. D. Mitchell (11, 12) in the most recent version of SEPHIS, called SEPHIS-MOD4, have considerably improved the predictions of transient behavior and account for inhomogeneities in the settlers by the introduction of three well mixed zones.

Excepting TRANSIENTS(7) and SOLVEX(13), the models for mixer-settlers developed so far assume mass transfer equilibrium for the distribution of uranium and plutonium between the aqueous and organic phases. Some comparisons between model predictions and measured data indicate mixer-settler contactors operate very close to mass transfer equilibrium (8,10). However, recent data of Thompson and Shankle (15) on uranium purification appears to show that operating conditions for mixer-settler contactors may occur which produce significant deviations from mass transfer equilibrium. These workers compared their measured data with the predictions of the computer model TRANSIENTS, developed by J. T. Lowe (7). This model accounted for deviations from mass transfer equilibrium in terms of the mass transfer efficiency which is the ratio of the mass of nuclear material transferred relative to that which would have been transferred if the process were at equilibrium. The mass transfer efficiency is input into this model. The mass transfer efficiency is also input into SOLVEX.

Deviations from mass transfer equilibrium in solvent extraction contactors are determined by the rate of mass transfer between the aqueous and organic phases. Mass transfer equilibrium or the SEPHIS limit is achieved with very rapid mass transfer rates. If the mass balance equations used to describe the solvent extraction processes include the mass transfer rate as in the case of L. E. Burkhart's model for pulsed column contactors (16), deviations from mass transfer equilibrium are automatically accounted for. In view of possible deviations from equilibrium in mixer-settler contactors (15), it was a goal of this work to develop a model PUBG (plutonium-uranium-Beyerlein-Geldard) for mixer-settler contactors which accounts for deviations from mass transfer equilibrium by including in the model the effects of mass transfer rates.

Another motivation for the development of PUBG is the generation of input-output data to be used with modern system identification methods to devise mathematical estimators for solvent extraction processes. Such estimation techniques are useful with in-process inventory procedures for nuclear material accountability as well as for optimization and control of solvent extraction processes in chemical contactors. The use of chemical models in this way requires that they simulate the fluctuations occurring in the operation of a real plant and the random error associated with the measurement of output data. These fluctuations are obtained in PUBG with a random number generator.

MODELING THE MIXER-SETTLER CONTACTOR

Descriptions of mixer-settler contactors have been given in previous reports and publications (7, 8, 10, 11). They consist of a sequence of stages which are given a numerical designation from 1 to N, N being the total number of stages. The aqueous and organic phases flow countercurrently from one stage to another. By convention it is assumed the aqueous flow is from stage 1 to stage N and the organic flow is in the opposite direction

from stage N to stage 1. The countercurrent flows enter each stage at the mixer where they are rapidly stirred in order to provide a large interfacial area between dispersed and continuous phases which will facilitate the mass transfer of nuclear materials between the two phases. The phases are then pumped from the mixer to the settler portion of the stage which only serves to separate the two phases so that they may be pumped to their next respective stages. The feed stream containing the nuclear materials may enter the contactor at any of the stages depending upon the application.

The basis for a mathematical model of the transient and steady state behavior of a mixer-settler contactor are the following mass balance equations,

$$\frac{d(V_j^o S_\alpha^o(j))}{dt} = O_j^m M_\alpha^o(j) - O_j^s S_\alpha^o(j), \tag{1}$$

$$\frac{d(V_j^a S_\alpha^a(j))}{dt} = A_j^m M_\alpha^a(j) - A_j^s S_\alpha^a(j), \tag{2}$$

$$\frac{d(V_{Mj}^o M_\alpha^o(j))}{dt} = O_{j+1}^s S_\alpha^o(j+1) - O_j^m M_\alpha^o(j) + O_j^f F_\alpha^o(j) - R_\alpha, \tag{3}$$

$$\frac{d(V_{Mj}^a M_\alpha^a(j))}{dt} = A_{j-1}^s S_\alpha^a(j-1) - A_j^m M_\alpha^a(j) + A_j^f F_\alpha^a(j) + R_\alpha, \tag{4}$$

Equations (1) and (2) are the mass balance relations for the settlers whereas Eqs. (3) and (4) are the mass balance relations for the mixers. The quantities S_α, M_α, and F_α are the concentrations in grams per unit volume of species α in the settler, mixer, and feed stream, respectively; O_j and A_j are the flow rates of the organic and aqueous phases, respectively, at the jth stage; V_j and V_{Mj} are the phase volumes in the settler and mixer respectively, at the jth stage; and R_α is the rate of mass transfer of species α from the organic to aqueous phase. The superscripts o, a, m, s, and f refer to the organic phase, aqueous phase, mixer, settler, and feed stream, respectively.

Equations(1) to (4) assume that the phases in the settlers are uniform or well mixed. The computer models SOLVEX (13) and SEPHIS-MOD4 (11) account for non-uniformity by dividing the phases in the settlers into well-mixed zones. For such models the mass balance equation must be modified to account for the contributions of each zone.

The mass transfer rates R_α may be expressed in terms of the deviations of mixer concentrations from their equilibrium values. The simplest such expression is given by,

$$R_\alpha = K_\alpha A(M_\alpha^o - M_\alpha^o(eq)), \tag{5}$$

$$M_\alpha^o(eq) = D_\alpha M_\alpha^a. \tag{6}$$

where K_α is the mass transfer coefficient for species α, A is the interfacial area between the aqueous and organic phases available for mass transfer, $M_\alpha(eq)$ is the concentration which would be obtained in the mixer if mass transfer equilibrium were obtained, and D_α is the distribution coefficient for species α. The computer model PUBG of this work uses correlations of G. L. Richardson (14) as modified by Watson and Rainey (10) for estimating D_α.

Mass transfer equilibrium requires that $M_\alpha^o = M_\alpha^o(eq)$. This condition can be approached by letting K_α or A approach large values which forces $M_\alpha^o - M_\alpha^o(eq)$ to have small values. Very few measurements of K_α have been made. A reasonable method of estimating both K_α and A is a variation method which matches model calculations with selected data from real mixer-settler contactors.

The computer model PUBG assumes that the transient behavior for the mixer is on a much shorter time scale than the transient behavior of the settlers. As a consequence of this assumption the mixer concentrations will approach a quasi-steady state, i.e.,

$$\frac{dM_\alpha^o(j)}{dt} \simeq 0 \tag{7}$$

$$\frac{dM_\alpha^a(j)}{dt} \simeq 0. \tag{8}$$

much more rapidly than the settler concentrations approach their steady state values.

Equations (7) and (8) neglect contributions to the time rate of change of the mixer concentrations that are produced by the settlers feeding the mixer. These equations require that one assume that the settlers contain most of the total stage volume and that the contribution of the mixers to the stage volume is negligible. This assumption is made in the earlier SEPHIS models (8-10), TRANSIENTS (7), and SOLVEX (13). Equations (7) and (8) and assumptions under which they are valid do not affect steady state predictions but will affect transient predictions.

SEPHIS-MOD4 (12) accounts for the transient behavior of the mixers with a Runga Kutta integration procedure and therefore comparisons of transient predictions of PUBG for the settler concentrations with predictions of SEPHIS-MOD4 will provide a test of the steady state assumption for the mixers, Eqs. (7) and (8), provided that the PUBG calculations are for the SEPHIS limit. Such comparisons indicate that when the ratio of the settler volume to mixer volume ranges from 1.5 to 3, the concentrations of SEPHIS-MOD4 are about 10% lower than those of PUBG when they have achieved about half their steady state values. For ratios greater than 3, the comparisons indicate that Eqs. (7) and (8) become a very good approximation. Currently efforts are being pursued to remove this approximation from PUBG for the purpose of improving its transient predictions for the lower settler to mixer volume ratios. Although effects of the approximation on transient predictions are significant for lower settler to mixer volume ratios they are not large. This fact and the simplicity achieved with the approximation justifies its use for many applications.

Equations (7) and (8) are not equivalent to mass transfer equilibrium conditions assumed in the various SEPHIS models (8-12). In order that mass transfer equilibrium is obtained the mass transfer rate must be much greater than the reciprocal of the residence time of the nuclear materials in the mixer, i.e.,

$$K_\alpha A >> \frac{O_{j+1}^s}{V_{Mj}}, \tag{9}$$

$$K_\alpha A >> \frac{A_{j-1}^s}{V_{Mj}}. \tag{10}$$

Conditions (9) and (10) are obtained in practice by obtaining large values of the interfacial area A. The value of A can be optimized by rapid mixing which produces a finely dispersed phase.

For a particular stage j the steady state equations, Eqs. (7) and (8) may be rewritten in the following manner if recycle flows are neglected,

$$M_\alpha^o(j) = \frac{\Lambda}{\pi}\left(O_{j+1}^s S_\alpha^o(j+1) + O_j^f F_\alpha^o(j)\right) + \frac{1}{\pi A_j^m}\left(A_{j-1}^s S_\alpha^a(j-1) + A_j^f F_\alpha^a(j)\right), \quad (11)$$

$$M_\alpha^a(j) = \frac{1}{A_j^m}\left(O_{j+1}^s S_\alpha^o(j+1) + O_j^f F_\alpha^o(j)\right) + \frac{1}{A_j^m}\left(A_{j-1}^s S_\alpha^a(j-1) + A_j^f F_\alpha^a(j)\right) - \frac{1}{A_j^m} O_j^m M_\alpha^o(j), \quad (12)$$

where

$$\Lambda = \left(\frac{1}{K_\alpha D_\alpha A} + \frac{1}{A_j^m}\right), \quad (13)$$

$$\pi = \frac{O_j^m}{K_\alpha D_\alpha A} + \frac{1}{D_\alpha} + \frac{O_j^m}{A_j^m} . \quad (14)$$

Since the distribution coefficients D_α depend on the mixer concentrations $M_\alpha^o(j)$ and $M_\alpha^a(j)$, Eqs. (11) and (12) do not represent a solution of the mixer steady state approximation (Eqs. (7) and (8)). They are however a convenient form to use for obtaining the solution by an iterative method. The mixer concentrations obtained by iteration are then substituted into the mass balance equations (Eqs. (1) and (2) for the settlers and the resulting expressions are integrated by a fourth order Runga Kutta numerical procedure to generate the transient behavior of the settlers.

The initial version of PUBG assumed mass balance equations in which the flow rates and volumes referred to the solution volume per unit time and solution volume, respectively. Concentrations and the distribution coefficients were assumed to have units of grams per liter of solution and molarity based units, respectively. The SEPHIS-MOD2, MOD3, and MOD4 models assume flow rates and volumes whose units refer to the volume of solvent required to prepare the solution, concentrations in units of grams per liter of solvent, and distribution coefficients based on units of grams per liter of solvent (solute free units). Consequently, there are small differences between steady state PUBG calculations in the SEPHIS limit and the calculations of the SEPHIS models, particularly for processes where a high proportion of the TBP is complexed by nuclear materials (uranium and plutonium). Recently PUBG has been modified so that the mass balance calculations assume solute free units. This latterversion of PUBG (called PUBGS to distinguish it from the earlier version of PUBG) for calculations performed in the SEPHIS limit is equivalent to the SEPHIS models. The differences between these two versions of PUBG are inconsequential for calculations presented in this paper.

DISCUSSION OF MODEL CALCULATIONS

Comparisons of PUBG with Measured Data

Generally deviations from mass transfer equilibrium will reduce the efficiency of a contactor, thereby causing higher nuclear material holdup and higher stage concentrations, particularly in the extraction sections of the contactor. Exceptions to this rule may occur in the scrub bank of a contactor, extracting nuclear materials from an aqueous to an organic phase, where under some conditions sufficiently small deviations from equilibrium

may produce slightly lower aqueous phase concentrations than are obtained at mass transfer equilibrium. The mass transfer equilibrium limit or SEPHIS limit is obtained with PUBG for sufficiently high interfacial areas between the aqueous and organic phases. In a real contactor high interfacial areas are obtained with mixer conditions (stirring rate, phase ratio, etc.) that produce fine dispersions of the phase of lesser volume. Significant deviations from mass transfer equilibrium can result from (i) entrainment of one solvent in the other (7) and (ii) thermodynamic conditions which result in small mass transfer coefficients.

Comparisons of chemical model calculations with measured data reported by Groenier(8) and Watson and Rainey(10) on the coextraction of uranium and plutonium (1A contactor) show that the mixer-settler contactors from which the data were obtained operated very close to mass transfer equilibrium(17). More recently Thompson and Shankle(15) reported relatively complete sets of data on the 1D contactor (uranium extraction from the aqueous to organic phase) and 1E contactor (strips uranium from the organic phase) which indicate significant deviations from the mass transfer equilibrium may occur in mixer-settler contactors. In the case the 1D contactor the experimental uranium holdup 4990 grams differed from the value 4478.5 grams, calculated in the SEPHIS limit, by about 10.9%. Complete agreement between the calculated and measured uranium holdup is obtained by adjustment of the mass transfer area A to values representing deviations from mass transfer equilibrium in the calculated data. This adjustment of A produces some improvement in the agreement between the calculated and measured concentration profiles. In the case of the 1E contactor the difference between the measured uranium holdup, 3532, grams and that calculated in the SEPHIS limit, 2969 grams, is 16.3% . Substantial improvement in the agreement between predictions and experiment are obtained for both the uranium holdup and concentration profile by adjustment of the mass transfer area A, thus providing strong evidence that deviations from equilibrium may affect mixer-settler contactors.

Detailed comparisons of measured concentration profiles and uranium holdup for the 1E contactor studies by Thompson and Shankle(15) with data calculated using PUBG are shown in Table 1 and Figures 1 and 2. Table 1 also contains the concentration profiles calculated with SEPHIS-MOD4 and the concentration profiles calculated by Thompson and Shankle using TRANSIENTS(15). The latter calculation accounts for deviations from mass transfer equilibrium in terms of the mass transfer efficiency(7).

Table 1. Calculated uranium concentration profiles and holdup for the 12 stage 1E stripping contactor compared with the experimental measurements of Thompson and Shankle. The organic phase contains 7.12 g/liter of uranium, 0.037 M HNO_3, and 7.5% TBP. The aqueous phase is 0.04 M HNO_3. The relative flow rates of the organic and aqueous phases are 3.0 and 1.0, respectively. The concentrations in stages 2 to 5 (not shown) are small. Concentrations are in grams/liter.

Stage	Experimental Data	PUBG A = 4.8	PUBG SEPHIS Limit	SEPHIS-MOD4	TRANSIENTS
			Aqueous Phase		
1	< 0.005	7.1×10^{-7}	2.3×10^{-16}	0.0	< 0.001
7	0.005	0.021	6.4×10^{-6}	4.8×10^{-6}	0.098
8	0.005	0.110	3.5×10^{-4}	2.8×10^{-4}	0.299
9	0.065	0.581	0.019	0.017	0.916
10	2.020	2.831	0.819	0.759	2.800
11	11.570	10.181	8.636	8.397	8.426
12	21.500	21.360	21.360	21.115	21.360

(Table 1 continued on the next page.)

Table 1. Continued from previous page

Stage	Experimental Data	PUBG A = 4.8	PUBG SEPHIS Limit	SEPHIS-MOD4	TRANSIENTS
			Organic Phase		
1	< 0.001	5.3×10^{-8}	1.4×10^{-18}	0.0	0.001
7	0.053	0.001	3.9×10^{-8}	2.8×10^{-8}	0.011
8	0.018	0.007	2.2×10^{-6}	1.6×10^{-6}	0.033
9	0.180	0.037	1.2×10^{-4}	9.5×10^{-5}	0.100
10	0.105	0.194	0.006	0.0055	0.305
11	0.731	0.944	0.273	0.254	0.934
12	Not Analyzed	3.394	2.879	2.815	Not Considered
Total Uranium Holdup* Grams	3532	3542	2969	2914	3468.6

* In accordance with Thompson and Shankle (15) the organic phase concentration of stage 12 was not included in the holdup calculation.

Figure 1 shows the significantly improved agreement between the measured aqueous phase uranium concentrations and the calculated concentrations that is obtained as the mass transfer area is decreased toward a value of 4.8. In Table 1 one notes that a mass transfer area of 4.8 also results in good agreement between the measured and calculated organic concentration profile. The calculations assume the mass transfer coefficient is a constant and the units of mass transfer area are selected so that the mass transfer coefficient is unity. A more sophisticated model would account for the concentration dependence of the mass transfer coefficient. However for deviations from mass transfer equilibrium which are no larger than those represented by this data, Figure 1 appears to show that assuming the mass transfer coefficient is a constant is a reasonably good approximation.

A number of calculations with PUBG were performed as a function of mass transfer area. The uranium holdup obtained from these calculations is shown in Figure 2. One notes that holdup decreases with increasing mass transfer area and asymptotically approaches the SEPHIS limit. The holdup for a mass transfer area of 4.8, which is selected on the basis of comparisons of calculated and experimental concentration profiles, yields a uranium holdup that is within 0.86% of the experimental value. Therefore a suggested method of selecting the most appropriate mass transfer area for a particular contactor is by matching the calculated concentration with that of one of the stages.

Chemical Models and System Identification Studies

Modern system identification methods (18) may be used to obtain accurate estimates of nuclear material holdup from measured input-output data on a real contactor. However adequate measurements of input-output data have not been obtained for the development of such methods. Consequently input-output data that has been calculated from chemical models is being used to investigate the applicability of modern system identification methods to nuclear material holdup estimation. In order that chemical models can be used for this purpose, they must be capable of simulating the transient behavior of a real extraction

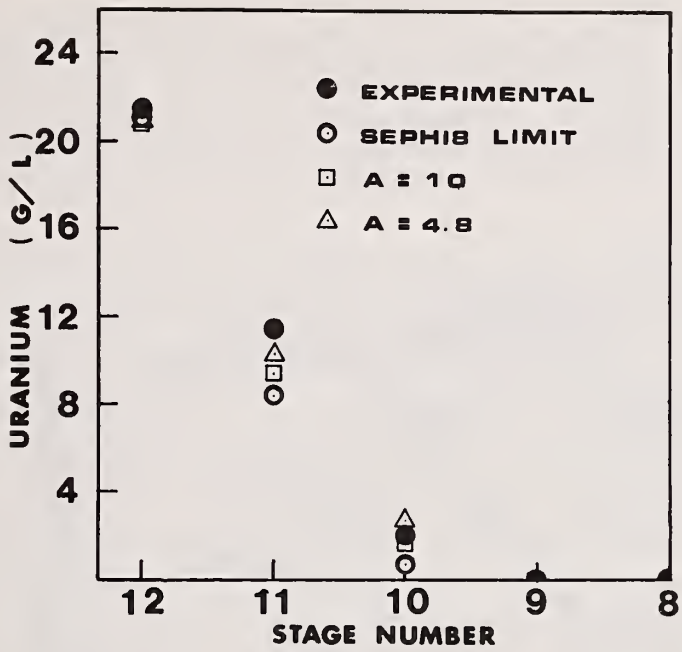

Figure 1. Comparisons of PUBG calculations of aqueous uranium concentrations on the 1E mixer-settler contactor at various mass transfer areas with experimental data(15).

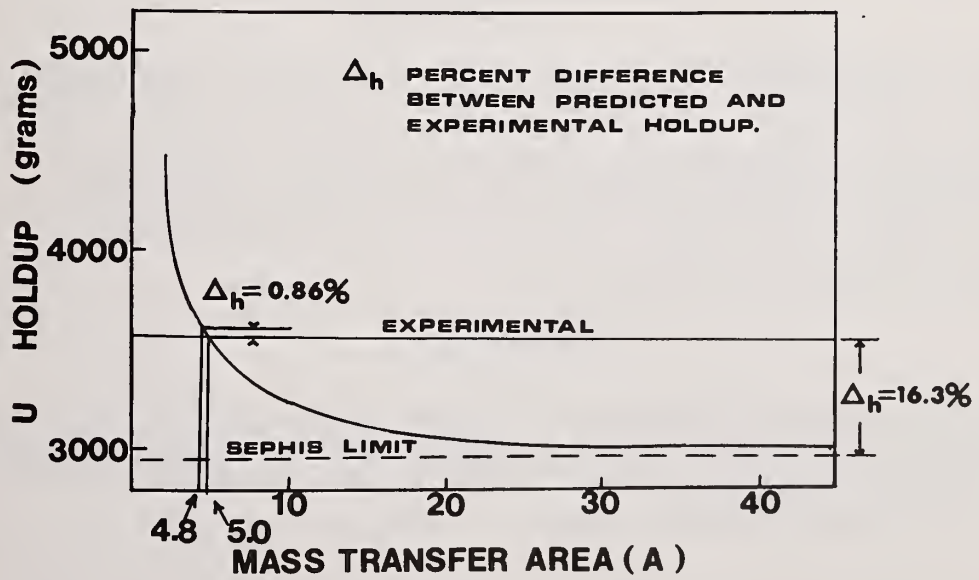

Figure 2. Calculated uranium holdup in the 1E contactor as a function of mass transfer area compared with values obtained from experimental data(15).

process during startup or shutdown. They must also include fluctuations in feed stream concentrations and flow rates and variations in the stage concentrations which could result from the deposit or dissolution of nuclear material on the walls of the contactor.

Figure 3 shown the transient behavior obtained using PUBG for the aqueous plutonium concentration in the feed stage of a 1A contactor whose feed stream concentrations fluctuate with a 10% standard deviation. The fluctuations in the feed stream are obtained with a random number generator. The magnitude and frequency of the fluctuations may be adjusted by appropriate input into the program. The calculated plutonium holdup and the results of a identification delay system calculation (17) are also shown.

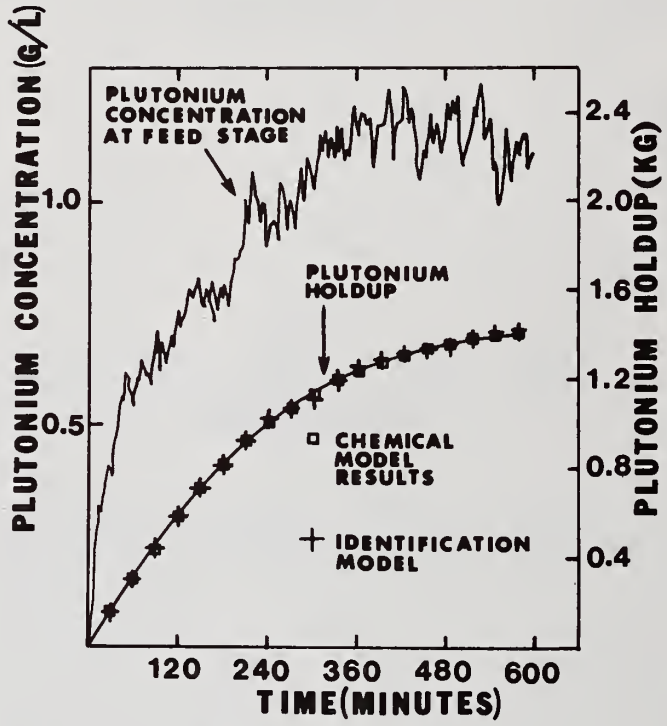

Figure 3. An illustration of the aqueous phase concentration calculated with PUBG or the feed stage (stage 8) of a 16 stage 1A contactor having a total stage volume of 150 liters. The feed stream concentrations fluctuate with a 10% standard deviation and have average values of 285.0 g/1 U, 2.66 g/1 Pu and 2.55 M HNO_3. The organic phase is 30% TBP and the aqueous scrub solution is 3.0M HNO_3. The flow rates are 1.0, 5.01, and 1.67 liters/min for the scrub solution, organic phase, and feed stream, respectively, and the aqueous to organic phase ratio is 0.19.

ACKNOWLEDGEMENTS

The authors gratefully acknowledge the financial assistance of Los Alamos Scientific Laboratory through the Q-4 Systems group. The many helpful discussions with D. D. Cobb and C. A. Ostenak of Los Alamos Scientific Laboratory and L. E. Burkhart of Iowa State University are also acknowledged.

REFERENCES

1. R. E. Treybal, Liquid Extraction, (McGraw Hill, New York, 1951).

2. W. O. Haas, Chemical Reprocessing of Reactor Fuels, Edited by J. F. Flagg (Academic Press, New York, 1961).

3. B. A. DiLiddo and T. J. Walsh, Ind. Eng. Chem., 53, 801 (1961).

4. D. R. Olander, Ind. Eng. Chem., 53, 1(1961).

5. W. R. Burton and A. L. Mills, Nucl. Engr., 8, 248 (1962).

6. I. D. Eubanks and J. T. Lowe, I and EC Process Design Develop., 7, 172 (1968).

7. J. T. Lowe, I and EC Process Design Develop., 7, 362 (1968).

8. W. S. Groenier, "Calculation of the Transient Behavior of a Dilute-Purex Solvent Extraction Process Having Application to the Reprocessing of LMFBR Fuels", Oak Ridge National Laboratory Report, ORNL-4746, April 1972.

9. G. L. Richardson and J. L. Swanson, "Plutonium Partitioning in the Purex Process with Hydrazine Stabilized Hydroxylamine Nitrate", Hanford Engineering Development Laboratory, HEDL-TME 75-31, June 1975.

10. S. B. Watson and R. H. Rainey, "Modifications of the SEPHIS Computer Code for Calculating the Purex Solvent Extraction System", Oak Ridge National Laboratory, ORNL-TM-5123, December 1975.

11. A. D. Mitchell, "A Comparison Between SEPHIS-MOD4 and Previous Models for the Purex Solvent Extraction System", Oak Ridge National Laboratory, ORNL-TM-6565, Feb. 1979.

12. A. D. Mitchell, "SEPHIS-MOD4: A User's Manual to a Revised Model of the Purex Solvent Extraction System", Oak Ridge National Laboratory, ORNL-5471, May 1979.

13. W. C. Scotten, "SOLVEX--A Computer Program for Simulation of Solvent Extraction Processes", Savannah River Laboratory, DP-1391, September 1975.

14. G. L. Richardson, "Effect of High Solvent Radiation Exposures on TBP Processing of Spent LMFBR Fuels", Hanford Engineering Development Laboratory, HEDL-TME 73-51, June 1973.

15. M. C. Thompson and R. L. Shankle, "Calculation of Uranium Inventories in Mixer-Settlers During Solvent Extraction with 7.5% TBP", Savannah River Laboratory, DP 1357, August 1974.

16. S. M., Yih and L. Burkhart, "State-of-the-Art Simulation of a U-Pu Partitioning Column for Nuclear Fuel Reprocessing", ANS Proceedings of the Winter Meeting, TANSAO, 30, 328 (1978).

17. J. E. Bennett, A. L. Beyerlein, J. K. Bryan, J. J. Komo, and J. F. Geldard, "Improved Chemical Contactor Models Using Modern System Identification Techniques in Nuclear Accountability", Final Report to be submitted to Los Alamos Scientific Laboratory, Q-4 Systems Group on Contract No. N28-9750D-1.

18. Pieter Eykhoff, System Identification: Parameter and State Estimation, (John Wiley & Sons, New York, 1974).

19. K. K. Bixwas and G. Singh, IEEE Transaction on Automatic Control, AC-23, No. 3 (1978).

Dynamic Materials Accounting for Solvent-Extraction Systems*

D. D. Cobb and C. A. Ostenak
Los Alamos Scientific Laboratory, Los Alamos, New Mexico

ABSTRACT

Methods for estimating nuclear materials inventories in solvent-extraction contactors are being developed. These methods employ chemical models and available process measurements. Comparisons of model calculations and experimental data for mixer-settlers and pulsed columns indicate that this approach should be adequate for effective near-real-time materials accounting in nuclear fuels reprocessing plants.

KEYWORDS: Dynamic materials accounting; solvent-extraction contactors; in-process inventory; chemical modeling

I. INTRODUCTION

A. Background

All commercial nuclear fuels reprocessing plants use the Purex process for the separation and purification of uranium and plutonium from spent nuclear fuels. Separation and purification are achieved with a series of solvent-extraction contactors in which uranium and plutonium are selectively transferred between relatively immiscible countercurrent aqueous and organic streams. To optimize the sensitivity of near-real-time accounting for nuclear materials in reprocessing plants, estimates of the in-process inventories in the solvent-extraction contactors are required.

The importance of contactor in-process inventory to dynamic accounting systems for reprocessing plants is highlighted in recent safeguards systems studies.[1-4]** Contactor-inventory uncertainty is especially significant over relatively short accounting periods, having a smaller effect over longer periods as throughput-measurement errors accumulate, so that the availability of good estimates of the contactor inventory would improve the system's sensitivity for detecting short-term losses of in-process materials. The goal of the current study is to develop techniques for estimating contactor inventories to 5-10%, because the safeguards systems studies indicate that such estimates should be adequate for effective near-real-time accounting.

Currently, techniques for high-quality direct measurements of contactor inventory are not available. Their development would likely require substantial instrumentation costs, and their implementation could result in costly process design modifications. The development of indirect methods for estimating contactor inventory using chemical models and available process measurements appears to be more promising at present.

Many process monitoring instruments are installed in a nuclear reprocessing plant to monitor and control the operation of solvent-extraction contactors. Typically, the compositions, flow rates, and temperatures of inlet and outlet streams, the aqueous-organic interface levels, and, for pulsed columns, the pulse amplitudes and frequencies are monitored and controlled. Sample lines may be available from selected mixer-settler stages or from pulsed-column phase-disengagement sections. Where present, such sample lines, coupled with appropriate nondestructive assay (NDA) or conventional chemical techniques, could provide useful data for estimating contactor inventories.

*This work was performed as part of the US Department of Energy-Office of Safeguards and Security research and development program.

**See paper by E. A. Hakkila et al., Los Alamos Scientific Laboratory, in these Proceedings.

Of particular interest for contactor-inventory estimation would be the availability of high-quality flow and concentration measurements for contactor feed, product, and waste streams. If the separations process is designed so that the contactors are separated by buffer tanks, then the stream flows and concentrations can be obtained by combining volume measurements with chemical analyses of the tank contents. By contrast, if the contactors are closely coupled without intermediate measurements, it may be necessary to estimate the combined in-process inventory of a series of contactors bounded by the available input-output accounting measurements. This would complicate the inventory-estimation algorithm and would probably degrade the quality of the estimates.

B. Current Study

The LASL Safeguards Systems Group (Q-4) has initiated a modest effort to develop techniques for estimating contactor inventories. Under LASL sponsorship, researchers at Clemson University are studying the effects of mass-transfer dynamics and chemical kinetics on contactor behavior and modern systems identification techniques that can be used for real-time estimation of contactor inventory. Researchers at Iowa State University and the DOE-Ames Laboratory are developing state-of-the-art theoretical models of pulsed-column behavior. The General Atomic Company (GA) is providing experimental data on pulsed-column uranium inventories from process development work at their Solvent-Extraction Pilot Plant. Allied-General Nuclear Services (AGNS) is supplying pulsed-column data from their Engineering Laboratory. Such data, virtually nonexistent in the open literature, are essential for model verification.

II. MODELING TECHNIQUES FOR CONTACTOR IN-PROCESS-INVENTORY ESTIMATION

The most widely used computer model for solvent-extraction process development is SEPHIS (solvent extraction processes having interacting solutes).[5-8] SEPHIS was originally developed to predict the transient and steady-state behavior of solvent-extraction contactors operating with a dilute Purex (15% TBP) LMFBR flow sheet.[5] SEPHIS has since been modified for standard Purex (30% TBP) flow sheets, incorporating changes in the computer-program structure and in the mathematical modeling of the system.[6-8]

In addition to SEPHIS, other computer models for different contactor types are being developed to simulate the solvent-extraction portions of the Purex process.[9-12] These computer models are discussed below.

A. Mixer-Settler Models

SEPHIS performs a stage-wise, iterative calculation of the approach to steady-state of the uranium, plutonium, and HNO_3 concentrations in a multistage contactor. In the most recent version, SEPHIS-MOD4, the contactor is modeled as a series of ideal mixer-settler stages with equilibrium end points, which more nearly describes the operation of mixer-settlers than of continuous differential contactors (columns). The required number of ideal stages is selected to match the desired overall separation efficiency and throughput.

Researchers at Clemson University are developing a chemical model, PUBG, for estimating the in-process inventories of mixer-settlers.* By contrast with SEPHIS, the major feature of this new model is that the effects of departures from equilibrium can be simulated by allowing the user to specify the effective mass-transfer area (A). For example, varying the mass-transfer area between $A \to \infty$ (the SEPHIS equilibrium limit) and $A = 10$ (a large departure from equilibrium) causes the calculated in-process plutonium inventory to increase significantly (Table I).

In practice, it may be possible to "calibrate" the model predictions for a mixer-settler by choosing an appropriate value for the A parameter. Calculations indicate that the value of A, and hence the departure from equilibrium, is very sensitive to the plutonium concentration in the waste stream (Table I). This concentration is commonly measured for process control, and the A parameter therefore might be determined from the measured waste stream concentration.

*See companion paper by A. L. Beyerlein et al., Clemson University, in these Proceedings.

TABLE I

PLUTONIUM INVENTORIES AND AQUEOUS WASTE STREAM CONCENTRATIONS CALCULATED FOR DIFFERENT MASS-TRANSFER AREAS (15-STAGE EXTRACTION/SCRUB MIXER-SETTLER)

Model	Plutonium Inventory (g)			Plutonium Concentration (g/L)
	Aqueous	Organic	Total	Aqueous Waste Stream
SEPHIS-MOD4	94.9	521.4	616.3	5.31×10^{-6}
PUBG: $A \rightarrow \infty$	89.1	523.5	612.6	4.44×10^{-6}
A = 100	96.2	530.7	626.9	3.54×10^{-5}
A = 40	114.0	548.6	662.7	2.58×10^{-4}
A = 20	150.9	585.5	736.5	1.40×10^{-3}
A = 10	214.6	648.3	862.8	5.63×10^{-3}

A comparison of the inventories of uranium and plutonium determined by experiment[6] and calculated by SEPHIS-MOD4 and PUBG (at the SEPHIS equilibrium limit) is given in Table II. The experimental values shown are for a laboratory-scale batch-extraction process using an 11-stage mixer-settler operating with a dilute (15.3% TBP) Purex flow sheet. Although SEPHIS-MOD4 and PUBG are capable of simulating various Purex process flow sheets, validation of the computer models with LWR (30% TBP) Purex flow sheets is not yet possible because of the lack of corresponding experimental data.

A few comparisons of calculated and experimental stage profiles and inventories have been published by Savannah River Laboratory (SRL) for their 12-stage miniature mixer-settlers.[9] A modified version of the computer model TRANSIENTS[10] was used to calculate the total in-process uranium inventory in each mixer-settler bank. Modifications were necessary to accommodate a 7.5%-TBP flow sheet consisting of two cycles to recover and purify uranium.

In Table III, SRL's calculated and experimental uranium inventories for their 12-stage stripping mixer-settler are compared with PUBG and SEPHIS-MOD4 calculations. The TRANSIENTS calculations agree with the experimental data nearly as well as PUBG (A = 4.8) because an efficiency factor of 70% is used in TRANSIENTS to account for departures from mass-transfer equilibrium.

TABLE II

EXPERIMENTAL PLUTONIUM AND URANIUM INVENTORIES VERSUS SEPHIS-MOD4 AND PUBG (11-STAGE EXTRACTION/SCRUB MIXER-SETTLER)

	Plutonium Inventory		Uranium Inventory	
	Aqueous	Organic	Aqueous	Organic
Experiment[6]	18.9	14.9	81.0	183.5
SEPHIS-MOD4	23.3	16.6	88.5	173.3
PUBG: $A \rightarrow \infty$	20.0	15.7	78.9	173.3

TABLE III

EXPERIMENTAL URANIUM INVENTORIES VERSUS SEPHIS-MOD4, PUBG AND TRANSIENTS (12-STAGE STRIPPING MINIATURE MIXER-SETTLER)

	Uranium Inventory (g)		
	Aqueous	Organic	Total
Experiment[9]	3327	206	3533
SEPHIS-MOD4	2865	49	2914
PUBG: $A \rightarrow \infty$	2917	53	2970
$A = 4.8$	3318	224	3542
TRANSIENTS[9]	3207	262	3469
Eff. = 0.7			

B. Pulsed-Column Models

A state-of-the-art computer model for simulating pulsed-column operation incorporates several improvements over SEPHIS.[11] This model is based on a critical review of about 160 papers and an extensive survey of design and operating features of full-scale pulsed columns throughout the world. Calculations are performed stage-wise, using finite-difference equations that include the effects of reaction kinetics, nonequilibrium mass transfer, back-mixing, and correlations of phase volumes with phase flow rates.

Comparisons of the Burkhart pulsed-column model with experimental data provided by GA and AGNS are in progress. Data from these two independent sources are being used for the development of theoretical correlations relating in-process inventory to observable process parameters.

A comparison of AGNS experimental uranium concentration profiles with profiles calculated by SEPHIS and the Burkhart model is shown in Table IV. The experimental data were supplied by AGNS for one of their laboratory-scale pulsed columns operating with a 30%-TBP uranium-extraction flow sheet. The aqueous and organic concentration profiles from the Burkhart model closely fit the experimental data, and agree better with experiment than does SEPHIS. Similar comparisons of experimental and theoretical plutonium concentration profiles also are needed, if empirical values for the plutonium mass-transfer rate and back-mixing coefficient are to be determined.

III. CONCLUSION

To optimize the benefits of dynamic materials accounting in reprocessing plants, it will be necessary to estimate the in-process inventory of solvent-extraction contactors. Contactor-inventory-estimation techniques are now being developed because direct measurements of the quantities of uranium and plutonium in contactors are not practicable during process operations. Any inventory-estimation technique probably will require experimental validation (or calibration) for each contactor system.

The following list summarizes the conclusions of this study to date.

- Contactor-inventory estimates to 5-10% will be useful for near-real-time accounting in reprocessing plants.
- Contactor-inventory estimation, based on model predictions and process measurements, appears to be the most promising technique; however, more theoretical and experimental work is necessary to develop this technique for plutonium recovery processes.

TABLE IV

EXPERIMENTAL URANIUM CONCENTRATIONS VERSUS SEPHIS AND THE BURKHART MODEL (2-IN.-I.D. EXTRACTION/SCRUB PULSED COLUMN)

Distance (ft) from Column Bottom	Uranium Concentration (g/L)					
	SEPHIS		Experiment		Burkhart Model	
	Aq	Org	Aq	Org	Aq	Org
24 (scrub)	0	52.5	0	54.0	0	54.0
21	17.2	65.0	15.0	62.7	15.0	62.7
18	25.0	71.0	19.7	67.5	19.8	67.5
15 (feed)	25.0	71.0	20.0	68.5	21.4	69.0
12.8	10.0	32.5	9.0	38.0	9.1	39.2
12.2	1.5	6.2	1.5	20.1	1.5	17.6
11.2	0.4	1.0	0.4	8.0	0.4	7.0
9	0	0	0	1.0	0	1.0
7	0	0	0	0	0	0

- SEPHIS-type modeling assumptions may not be suitable for adequate estimation of in-process inventories.
- Some adaptation and validation of models will be required for each contactor system.
- Improved experimental plutonium distribution coefficients over a range corresponding to commercial fuels reprocessing flow-sheet conditions are needed.

ACKNOWLEDGMENTS

The authors gratefully acknowledge the contributions to this work from J. E. Bennett and A. L. Beyerlein (Clemson University), L. E. Burkhart (Iowa State University), A. F. Cermak and R. G. Spaunburgh (Allied-General Nuclear Services), and D. R. Engler (General Atomic Company).

REFERENCES

1. E. A. Hakkila, D. D. Cobb, H. A. Dayem, R. J. Dietz, E. A. Kern, E. P. Schelonka, J. P. Shipley, D. B. Smith, R. H. Augustson, and J. W. Barnes, "Coordinated Safeguards for Materials Management in a Fuel Reprocessing Plant," Los Alamos Scientific Laboratory report LA-6881 (September 1977).

2. K. Ikawa, H. Ihara, H. Sakuragi, H. Nishimura, and M. Hirata, "Study of the Application of Dymac Principles to Safeguarding Spent Fuel Reprocessing Plants," Japan Atomic Energy Research Institute report JAERI-Memo-8241 (April 1979).

3. E. A. Hakkila, D. D. Cobb, H. A. Dayem, R. J. Dietz, J. T. Markin, J. P. Shipley, J. W. Barnes, and L. A. Scheinman, "Materials Management in an Internationally Safeguarded Fuels Reprocessing Plant, Vol. I," Los Alamos Scientific Laboratory report LA-8042 (in press, December 1979).

4. D. D. Cobb, Ostenak, J. E. Bennett, A. L. Beyerlein, L. E. Burkhart, D. R. Engler, and A. F. Cermak, "Estimation of In-Process Inventory in Solvent-Extraction Contactors," in "Materials Management in an Internationally Safeguarded Fuels Reprocessing Plant, Vol. II," Los Alamos Scientific Laboratory report LA-8042 (in press, December 1979), App. C.

5. W. S. Groenier, "Calculation of the Transient Behavior of a Dilute-Purex Solvent Extraction Process Having Application to the Reprocessing of LMFBR Fuels," Oak Ridge National Laboratory report ORNL-4746 (April 1972).

6. S. B. Watson and R. H. Rainey, "Modifications of the SEPHIS Computer Code for Calculating the Purex Solvent Extraction System," Oak Ridge National Laboratory report ORNL-TM-5123 (December 1975).

7. G. L. Richardson, "Effect of High Solvent Irradiation on TBP Processing of Spent LMFBR Fuels," Hanford Engineering Development Laboratory report HEDL-TME-73-51 (June 1973).

8. A. D. Mitchell, "A Comparison Between SEPHIS-MOD4 and Previous Models of the Purex Solvent Extraction System," Oak Ridge National Laboratory report ORNL/TM-6565 (February 1979).

9. M. C. Thompson and R. L. Shankle, "Calculation of Uranium Inventories in Mixer-Settlers During Solvent Extraction with 7.5% TBP," Savannah River Laboratory report DP-1357 (August 1974).

10. J. T. Lowe, "Calculation of the Transient Behavior of Solvent Extraction Processes," Ind. Eng. Chem. Proc. Des. Dev. 7, 362-366 (1968).

11. S. M. Yih and L. Burkhart, "State-of-the-Art Simulation of a U-Pu Partitioning Column for Nuclear Fuel Reprocessing," ANS Proc. Winter Meeting, TANSAO 30, 328 (November 1978).

12. W. C. Scotten, "SOLVEX - A Computer Program for Simulation of Solvent Extraction Processes," Savannah River Laboratory report DP-1391 (September 1975).

Materials Accounting Considerations for International Safeguards in a Light-Water Reactor Fuels Reprocessing Plant

by

E. A. HAKKILA, D. D. COBB, H. A. DAYEM,
R. J. DIETZ, E. A. KERN, and J. P. SHIPLEY
Los Alamos Scientific Laboratory, Los Alamos, New Mexico

ABSTRACT

This paper summarizes the requirements and functions of materials measurement and accounting systems applicable to large (1500 metric tonnes heavy metal per year - MTHM/yr) future reprocessing facilities as well as small (210 MTHM/yr) plants that are presently under IAEA safeguards. The effectiveness of conventional and proposed improved measurement and accounting systems were compared using modeling, simulation, and analysis procedures. The study showed that conventional accountability can meet IAEA goal quantities and detection times in these reference facilities only for low-enriched uranium. Dynamic materials accounting may meet IAEA goals for detecting abrupt (1-3 wks) diversion of 8 kg of plutonium. Current or projected techniques cannot meet the one year protracted diversion goal for plutonium if this goal is based on an absolute 8 kg quantity.

KEYWORDS: Nuclear safeguards; dynamic accounting; fuel reprocessing

I. INTRODUCTION

This study attempts to identify problems and proposes solutions involved in nuclear materials accountability for internationally safeguarding light-water-reactor spent fuel reprocessing plants. The problem was addressed by studying a large reprocessing facility that may be on stream in the 1990s time frame as well as a small plant representative of facilities presently under IAEA safeguards. Near-real-time materials measurement and accounting concepts previously proposed for a State's accounting system[1] were extended to include the problems associated with international verification.

II. BASIS FOR INTERNATIONAL SAFEGUARDS

The basis for most current international safeguards agreements is the 1968 Treaty on the Non-Proliferation of Nuclear Weapons (NPT) agreed to by over 100 signatory nations. The detailed terms and conditions under which specific facilities are safeguarded are negotiated with the International Atomic Energy Agency (IAEA) in accord with the general conditions of Article III of the NPT as set forth in the IAEA document INFCIRC/153.[2]

The objective of international safeguards, as declared by these documents, is the "...timely detection of diversion of significant quantities of nuclear material from peaceful nuclear activities... ." The emphasis is on "...the use of materials accountancy as a safeguards measure of fundamental importance, with containment and surveillance as important complementary measures... ."

INFCIRC/153, para. 31 also requires that the IAEA "shall make full use of the State's system of accounting for and control of all nuclear material subject to safeguards under the Agreement, and shall avoid unnecessary duplication of the State's accounting and control activities." In the case of reprocessing plants, the materials balance closing is determined by computing the material unaccounted for and its limit of error based on a measured,

verified materials balance. The uncertainty associated with the nuclear materials balance depends fundamentally on the measurement system uncertainties, on the plant throughput, and on the beginning and ending inventories for the materials balance period.

The application of international safeguards is negotiated between the IAEA (Agency) and the State (operator) on a case-by-case basis. "Goal quantities" for the detection of diversion have been proposed by the IAEA, but have not been generally accepted by Member States. These "goals" are related to the quantities of nuclear materials required to produce an explosive device and the time necessary to convert these materials to that purpose. The goals include the detection of the diversion of:

- o 75 kg of uranium-235 contained in low-enriched uranium over a period of one year.
- o 8 kg of plutonium in 1-3 weeks ("abrupt diversion").
- o 8 kg of plutonium over an entire year ("protracted diversion").

The agency verification of the State's accounting system consists of three steps:

- o Examination of the information provided in the Design Information Questionaire and in subsequent routine and special accounting reports;
- o Collection of independent information by the IAEA in inspections;
- o Evaluation of the information provided by the State and collected in inspections for the purpose of determining the completeness, accuracy, and validity of the information provided by the State.

Inspection activity as defined in INFCIRC/153 permits approximately 3700 man hours (18 man years) and 1400 man hours (7 man years) of annual inspection, respectively, for plants having annual throughputs of 1500 and 210 MTHM.

III. REFERENCE FACILITIES

In this study we have used the Allied-General Nuclear Services (AGNS) Barnwell plant as a reference facility for the high-throughput plant and the PNC pilot facility at Tokai-mura, Japan (Tokai) as the reference facility for the smaller plant. Both reprocessing plants use conventional Purex technology to reprocess LWR reactor fuel having a nominal plutonium concentration of approximately 1%. The following differences in process design or operation could be important for materials accounting.

- o The AGNS plant uses a centrifugal contactor for initial fission product decontamination, with pulsed columns for all subsequent extraction, scrub, and strip operations. The Tokai facility employs mixer-settlers throughout.
- o The centrifuge for solids removal (fission product metallic ingots, Zircaloy fines) is located between the accountability tank and process feed tank at AGNS and between the dissolver and accountability tank at Tokai.
- o An additional scrub section in the Tokai plant between the fission product decontamination and the uranium-plutonium partition steps provides an additional 10 to 100-fold improvement in fission product decontamination before the plutonium purification cycle.
- o Buffer tanks are included between the decontamination and partition cycles and between the partition and plutonium purification cycles in the Tokai design.

IV. MBA STRUCTURE FOR CONVENTIONAL AND DYNAMIC MATERIALS ACCOUNTING

Both the State's system of accounting and control and the international safeguards system depend fundamentally on the definitions of process areas about which materials balances are to be drawn. We have examined several strategies for drawing these balances for the large and small reprocessing facilities and the conversion process.

We term conventional any materials accounting scheme in which balances are drawn solely on the basis of physical inventories. Under this kind of strategy, the facility customarily is divided into a number of materials balance areas (MBAs) such as those shown in Fig. 1. A balance is drawn about each MBA coincident with a physical inventory of that MBA. Thus, the timeliness of a conventional accounting system is limited by the physical inventory frequency, which in turn is severely constrained by the economics of process operation.

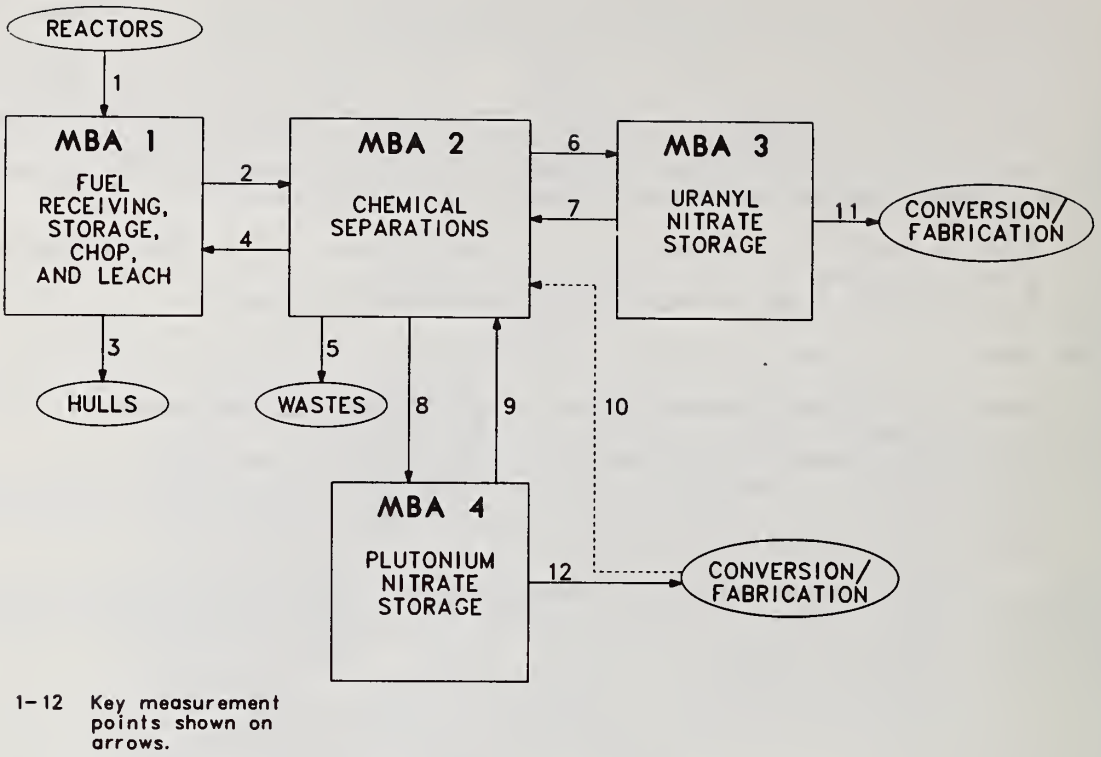

Fig. 1. MBAs for reprocessing facilities.

Near-real-time (or dynamic) materials accounting may be thought of as an augmentation of conventional materials accounting in which additional materials balances are drawn between physical inventories. The physical inventory measurements are replaced by measurements, or estimates, of the in-process inventory using on-line or at-line instrumentation and sophisticated data analysis methods. The drawing of such dynamic materials balances sometimes is facilitated by subdividing the MBAs into unit process accounting areas (UPAAs) that are closely related in time and space through process structures and operating procedures. The use of near-real-time accounting based on the UPAA subdivision generally provides improved sensitivity, in time, location, and amount, to diversion of nuclear material. We have considered mixtures of these strategies for the reference facilities.

A. Large Reference Facility

High-throughput facilities, such as the AGNS plant, will be of increasing safeguards interest in the next few years. Therefore, we have studied the safeguards aspects of such a reference facility based on the AGNS design as the best example currently available.

1. Conventional Materials Accounting

Conventional materials accounting relies on discrete-item counting and materials-balance closure following periodic shutdown, cleanout, and physical inventory. For this study, the baseline facilities are divided into four MBAs. An MBA is generally a physical area that is identified such that the quantity of nuclear materials moving into or out of the MBA can be measured. The input, output, and inventory measurement points for these MBAs are called key measurement points (KMPs).

As shown in Fig. 1, the four MBAs are fuel receiving, storage, chop, and leach (MBA 1), separations process area (MBA 2), uranium product storage area (MBA 3), and plutonium-nitrate storage area (MBA 4). MBAs 1, 3, and 4, are shipper/receiver MBAs while MBA 2 is a process MBA. Each of the MBAs is described in the following text.

a. MBA 1--fuel receiving, storage, chop, and leach. The fuel receiving, storage, chop, and leach MBA includes the cask-unloading and spent fuel pools, the shearing operation, and the dissolution process. The flow KMPs are:

KMP 1 - receipt of irradiated fuel,
KMP 2 - transfers from MBA 1 to MBA 2 (chemical separations MBA),
KMP 3 - measured discards (hulls), and
KMP 4 - recycle from MBA 2.

The inventory KMP is located in the spent fuel pool.

A shipper/receiver difference can be closed about MBA 1 after each campaign (approximately every 5 days) when the dissolver tanks, hull-rinse tanks, and associated piping are drained and flushed into the accountability tank. This flush-out between batches from different customers results in a more accurate shipper/receiver difference because it minimizes contamination from previous customer batches. The shipper/receiver difference is obtained by adding the shipper's values for a number of fuel batches (KMP 1) to the corresponding number of batches of recycled acid (KMP 4) and subtracting the accountability tank and laboratory vial batches (KMP 2) and the leached hull batches (KMP 3). Inventory verification in MBA 1 is based on piece count and identification of the fuel assembly fabrication serial numbers.

b. MBA 2--chemical separations process. This MBA includes the solvent-extraction operations from the accountability tank to the uranyl-nitrate and plutonium-nitrate product sample tanks. The flow KMPs are:

KMP 2 - transfers to MBA 2 from MBA 1,
KMP 4 - recycle to MBA 1,
KMP 5 - measured discards and retained waste,
KMP 6 - transfers from MBA 2 to MBA 3 (uranyl-nitrate storage),
KMP 7 - recycle from MBA 3,
KMP 8 - transfers from MBA 2 to MBA 4 (plutonium-nitrate storage),
KMP 9 - recycle from MBA 4, and
KMP 10 - transfers to MBA 2 from the conversion process.

The inventory KMPs are the analytical laboratory and those tanks in which reliable volume measurements can be made when the process is drained and flushed.

A physical inventory in MBA 2 includes a shutdown and flushout of the separations process area, and a cleanout of extraneous samples and a piece-count verification of remaining materials in the laboratory. The process line is drained and flushed into approximately 26 primary accountability tanks that have been calibrated so that reliable volume measurements can be made and samples can be taken for analysis.

A materials balance is taken after each physical inventory by adding all measured receipts (KMPs 2, 7, 9, and 10) to the initial inventory and subtracting all measured removals (KMPs 4, 5, 6, and 8) and the final inventory.

c. MBA 3--uranyl nitrate product. The uranyl-nitrate product MBA is a shipper/receiver MBA. The shipper's value is accepted under KMP 6 and is obtained from chemical analysis of a sample and volume measurement of the uranium product sample tank. The receiver's value is accepted under KMP 11 and consists of chemical analysis of a sample and volume measurement of the uranyl nitrate accountability tank at the headend of the UF_6 facility. This MBA has no inventory because solution is transferred directly from the uranium product tank in the chemical separations area (MBA 2) to the collocated UF_6 facility.

d. MBA 4--plutonium nitrate product storage. The plutonium nitrate product storage MBA contains slab tanks that are capable of storing 42 000 L of plutonium nitrate at a concentration of 250 g Pu/L. This MBA is a shipper/receiver MBA. The plutonium-nitrate solution transferred from the plutonium-product measuring tank to the plutonium-nitrate storage-facility slab tanks through KMP 8 constitutes the shipper's value. The nitrate product transferred to the receipt tanks in the collocated oxide-conversion plant constitutes the output of MBA 4. The receiver's value is determined by volume measurements and samples taken for chemical analysis in the receipt tanks. Alternatively, plutonium-nitrate product that does not meet specifications can be recycled through KMP 9 from the slab tanks back through the separations process area (MBA-2) on a campaign basis. In this case, the receiver's value is determined in the plutonium rework tank in MBA 2 using volume measurements and chemical analysis.

A physical inventory in MBA 4 requires volume measurements, sampling, and analysis of all solutions in the storage area or, alternatively, confirmation that tamper-safe seals are intact and the prior measurements are still valid.

2. Dynamic Materials Accounting

Dynamic materials accounting can provide significant improvement in the chemical separations process MBA. The chemical separations process area can be treated either as a single UPAA or as two UPAAs: a codecontamination-partitioning process UPAA (UPAA 1) and a plutonium-purification process UPAA (UPAA 2). This UPAA structure is complementary because dynamic materials balances can be taken about the chemical separations area in two ways.

a. UPAA 1 2--chemical separations process. The chemical separations process MBA can be treated as a single UPAA (UPAA 12) if measurements of the in-process inventory are made on each of the major process vessels in the process area. The inventory measurements must be added to the inventory KMPs.

In-process inventory measurements can be combined with flow KMPs 2, 4, 5, 6, 7, 8, 9, and 10 to form a dynamic materials balance approximately every two days. Because most of the material is transferred through the feed and product KMPs, the frequency of taking materials balances is governed by the feed and product batch frequencies. Under normal operating conditions, two and one-half accountability batches and one product batch are processed every day. Therefore, process logic dictates that a materials balance can be taken every two days to include an integral number of feed and product batches. Smaller batches, for example waste batches to high-level waste, are included in the materials balances when the measurements become available.

Alternatively, a materials balance could be taken around UPAA 1 2 after each feed batch (approximately every 9.6 h) if an on-line plutonium product measurement is added. The product measurement would consist of flow and concentration measurements.

b. UPAA 1--codecontamination-partitioning processes. A separate UPAA can be formed around the codecontamination-partitioning processes if flow and concentration measurements are added to the 1BP, 1SP, and POR streams. A dynamic materials balance can be taken about UPAA 1 for each feed accountability batch (every 9.6 h) by combining measurements of the concentration and volume of the feed batch, the concentration and flow in the 1BP, 1SP, and POR streams, the initial and final in-process inventories in the process vessels, and the concentration and volume of the high-activity waste (HAW) sample tank solution.

c. UPAA 2--plutonium purification process. Dynamic materials balances can be taken about the plutonium purification process if flow and concentration measurements are added to the aqueous and organic recycle streams (2AW, 2BW, 3AW, 3BW, and 3PD), and in-process inventory in contactors and the evaporator can be estimated. The balances can be taken using one of two product measurements, the daily batch in the plutonium sample tank or the on-line flow and concentration measurements on the concentrator product (3PCP) stream. Contactor in-process inventory may be estimated using process operating data.[3]

B. Small Reprocessing Plant

Many commercial reprocessing plants that are currently operating have capacities of less than 300 MTHM/year. Therefore, a materials measurement and accounting system that would be more typical of presently operating reprocessing plants was evaluated using the Tokai reprocessing plant as the reference facility.

1. Conventional Materials Accounting

The physical inventory accounting system structure in a small plant is identical to that of the large plant.

2. Dynamic Materials Accounting

Near-real-time accounting of plutonium can be applied to the chemical separations area, as a single UPAA, without additional measurement points by periodically sampling for chemical analysis and measuring the volume of each of the process vessels, and estimating the in-process inventory in each mixer-settler bank. These measurements are necessary for

determining the in-process inventory. The UPAA boundaries are the accountability tank, the plutonium receiver tank, and the waste and recycle acid tanks. A dynamic materials balance can be drawn after any integral combination of feed and product batches; i.e., a materials balance could be taken as often as once a day (two feed batches and one product batch).

As shown in Fig. 2, the near-real-time accounting system could be extended to include three UPAAs, and combinations thereof, within the chemical separations area. The UPAAs within the chemical separations area would be codecontamination-partitioning, UPAA 1; codecontamination, UPAA 1A; partitioning, UPAA 1B; and plutonium purification, UPAA 2. The codecontamination-partitioning can be divided into two UPAAs because of the buffer tanks that are between the first and second extraction cycles. This option is lacking in the large chemical separations plant where such a division is not possible. Added measurements include flow and concentration in the streams between the UPAAs, as well as on-line or at-line concentration measurements for determining in-process inventories. The feed and product batch measurements rely on the traditional installed volume measurements coupled with chemical analysis. In-process inventory volume measurements are also in place.

V. MODELING, SIMULATION, AND ANALYSIS TECHNIQUES

A. Modeling and Simulation Approach

The design and evaluation of the accounting systems are based on computer simulations of the reference facilities because these facilities have either not been built or have not been operated in a full production mode. Additionally, alternative operating, measurement, and accounting strategies can be readily compared.

The modeling and simulation approach requires (1) a detailed dynamic model of the process based on actual design data and operator experience; (2) simulation of the model process on a digital computer; (3) a dynamic model of each measurement system based on best estimates of instrument performance and behavior; (4) simulation of accountability measurements applied to nuclear materials flow and in-process inventory data generated by the model process simulation; and (5) evaluation of simulated materials balance data from various materials accounting strategies.[4]

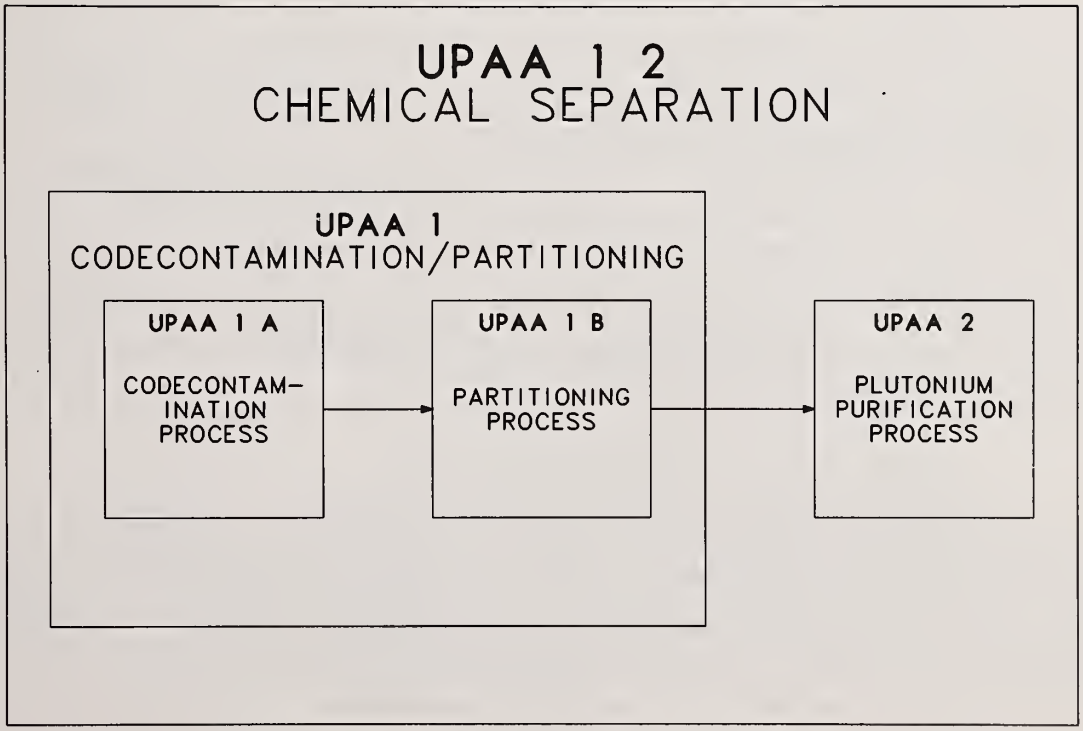

Fig. 2. UPAAs in the reference small chemical separations facility.

B. Data Analysis Techniques

Analysis of materials accounting data for detection of possible nuclear materials diversion is one of the major functions of the MMAS. Diversion may occur in two basic patterns: abrupt diversion (the single theft of a relatively large amount of nuclear materials) and protracted diversion (repeated thefts of nuclear materials on a scale too small to be detected in a single materials balance because of measurement uncertainties).

The use of unit-process accounting and dynamic materials balances enhances the ability to detect such diversions, but it also means that the operator of the safeguards system will be inundated with materials accounting data.

Decision analysis (see Refs. 5-9), which combines techniques from estimation theory, decision theory, and systems analysis, has been developed as a logical framework of tools for statistical treatment of the dynamic materials accounting data that become available sequentially in time. Its primary goals are (1) detection of the event(s) that nuclear materials has been diverted, (2) estimation of the amount(s) diverted, and (3) determination of the significance of the estimates.

The decision analysis algorithms include the Shewhart chart, cusum, uniform diversion test (UDT), sequential variance test (SVT), smoothed materials balance test (SMBT), and Wilcoxon rank sum test. The algorithms for the Shewhart chart, cusum, UDT, SVT, and SMBT are structured to account for correlated data (so-called systematic errors) so that correct variances are computed for the associated decision tests.

C. Data Analysis Graphic Aids

The decision tests must examine all possible sequences of the available materials balance data because, in practice, the time at which a sequence of diversions begins is never known beforehand. Furthermore, to ensure uniform application and interpretation, each test should be performed at several levels of significance. Thus, a graphical display that indicates those sequences that cause alarms, specifying each by its length, time of occurrence, and significance, is essential. One such tool is the alarm-sequence chart,[10] a type of pattern recognition device that has proven very useful for summarizing the results of the various tests and for identifying trends.

D. Systems Performance Analysis

One essential part of designing nuclear materials accounting systems is analyzing their expected performance in detecting losses of nuclear material.[11] Systems performance analysis, in turn, implies the definition of suitable performance measures that can be easily related to externally established criteria. Thus, there are two aspects of the analysis problem: first, defining performance measures, and second, relating those measures to established, quantitative performance criteria.

Performance measures for any nuclear materials accounting system embody the concepts of loss-detection sensitivity and loss-detection time. Because of the statistical nature of materials accounting, loss-detection sensitivity can be described in terms of the probability of detecting some amount of loss while accepting some probability of a false alarm. Loss-detection time is the time required by the accounting system to reach some specified level of loss-detection sensitivity. Note that the loss scenario is not specified; that is, whether the loss occurs in an abrupt or in a protracted fashion, the total amount of loss is the measure of performance. Note also that loss-detection time only refers to the internal response time of the accounting system.

Intuitively, the performance of any accounting system is describable by some function

$$P\ [L,N,\alpha] \quad , \tag{1}$$

where P is the accounting system's probability of loss detection, L is the total amount of loss over a period of N balances, and α is the false-alarm probability. Thus, a convenient way of displaying system performance would be a three-dimensional graph of the surface P versus L and N for some specified value of α. These graphical displays, called performance surfaces, portray the expected performance of an accounting system as a function of the three performance measures, loss, time, and detection probability, rather than as a single point.

VI. EFFECTIVENESS OF THE OPERATOR'S MATERIALS MEASUREMENT AND ACCOUNTING SYSTEM

The operator's material measurement and accounting system for an internationally verifiable safeguards system, including location and types of flow and concentration sensors, has been described previously.[1,12,13] The effectiveness of the accounting system that uses conventional and dynamic accounting for detecting abrupt and protracted diversion of uranium and plutonium were evaluated for the MBA structures described in Sec. III using modeling, simulation, and analysis techniques discussed in Sec. IV.[13]

Table I lists materials balance standard deviations for conventional materials accounting in the process MBAs of the reference facilities. These materials accounting sensitivities will be degraded if high-quality measurements cannot be obtained. Conversely, the sensitivities could be improved if measurement errors can be controlled. Measurement errors can be controlled by identifying the dominant error sources and establishing effective measurement control procedures. Note that the diversion detection sensitivity is at least 3.3 times the materials balance standard deviation for a 95% detection probability and a false alarm probability of 5%. From our analysis, we conclude that:

- For ^{235}U the proposed IAEA criteria for diversion sensitivity and timeliness probably are attainable by conventional materials accountability if rigorous materials measurement control programs are instituted.
- For plutonium, the proposed IAEA criteria for sensitivity and timeliness cannot be met by conventional materials accountability.

Near-real-time materials accounting techniques were applied to the process MBAs in an effort to meet the proposed IAEA criteria. Materials balance uncertainties for the reference facilities are summarized in Table II. In each case, a range of uncertainties is given for the largest UPAA that was considered--the entire process area for each facility. The cases considered range from best-case estimates of contactor in-process inventories with two-day recalibrations of input-output flow and concentration measuring instruments, to worst case estimates of contactor in-process inventories with no recalibrations within the accounting periods. Note that the diversion detection sensitivity is at least 3.3 times the materials balance standard deviation for a 95% detection probability and a false-alarm probability of 5%.

In examining both the conventional (Table I) and the dynamic (Table II) materials accounting sensitivities, we further conclude that for plutonium:

- In the large chemical separations process area, the proposed IAEA criteria for detecting abrupt diversion can probably be met if a rigorous measurement control program is undertaken.
- In the large chemical separations process area, the proposed IAEA criteria for detecting protracted diversion cannot be met by any known system; the goal quantity is only 0.05% of the annual plant throughput.

TABLE I

CONVENTIONAL MATERIALS ACCOUNTING IN THE REFERENCE FACILITIES

Accounting Period (months)	Materials Balance Standard Deviations (kg)			
	Large Reference Facility		Small Reference Facility	
	U-235	Pu	U-235	Pu
3	10.4	13.4	1.4	1.9
6	20.3	26.2	2.8	3.7
12	40.1	52.1	5.7	7.3

TABLE II

DYNAMIC MATERIALS ACCOUNTING IN THE REFERENCE FACILITIES

Accounting Period	Materials Balance Standard Deviations (kg Pu)	
	Large Reference Facility[a]	Small Reference Facility[b]
1 balance[c]	2.0-2.3	0.26-0.37
1 day	---	0.26-0.37
2 days	2.1-2.4	---
1 week	2.5-3.4	0.32-0.43
2 weeks	3.0-5.3	0.37-0.57
1 month	3.9-9.5	0.53-0.83

[a]Ranges are given from two-day recalibration, 5% estimates of contactor in-process inventories to no recalibration, 10% estimates of contactor in-process inventories.

[b]Ranges are given from two-day recalibrations, 10% estimates of contactor in-process inventories to no recalibrations, 20% estimate of contactor in-process inventories.

[c]A materials balance is taken every 9.6 h in the large chemical separations process and one day in the small chemical separations process.

- In the small chemical separations process area, proposed IAEA criteria for abrupt diversion probably can be met.
- In the small chemical separations process area, the proposed IAEA criteria for protracted diversion may be achievable.

REFERENCES

1. E. A. Hakkila, D. D. Cobb, H. A. Dayem, R. J. Dietz, E. A. Kern, E. P. Schelonka, J. P. Shipley, D. B. Smith, R. H. Augustson, and J. W. Barnes, "Coordinated Safeguards for Materials Management in a Fuel Reprocessing Plant," Los Alamos Scientific Laboratory report LA-6881 (September 1977).

2. "The Structure and Content of Agreements Between the Agency and States Required in Connection with the Treaty on the Non-Proliferation of Nuclear Weapons," Intenational Atomic Energy Agency document INFCIRC/153 (June 1972).

3. D. D. Cobb and C. A. Ostenak, "Dynamic Materials Accounting for Solvent-Extraction Systems," American Nuclear Society Topical Conference on Measurement and Technology for Safeguards and Materials Control, Kiawah Island, SC, November 26-29, 1979.

4. D. D. Cobb and D. B. Smith, "Modeling and Simulation in the Design and Evaluation of Conceptual Safeguards Systems," Nucl. Mater. Manage. VI (3) 171-184 (1977).

5. J. P. Shipley, "Decision Analysis for Nuclear Safeguards," in Nuclear Safeguards Analysis - Nondestructive and Analytical Chemical Techniques, E. A. Hakkila, Ed., Am. Chem. Soc., Washington, DC (1978), pp. 34-64.

6. James P. Shipley, "Decision Analysis for Dynamic Accounting of Nuclear Material," in Analytical Methods for Safeguards and Accountability Measurement of Special Nuclear Material, H. T. Yolken and J. E. Bullard, Eds., NBS Special Publication 528 (November 1978), pp. 83-97.

7. J. P. Shipley, "Efficient Analysis of Dynamic Materials Accounting Data," Nucl. Mater. Manage. VII, 355-366 (1978).

8. R. E. Kalman, "A New Approach to Linear Filtering and Prediction Problems," Trans. ASME J. Basic Eng. 82D, 34-45 (March 1960).

9. R. E. Kalman and R. S. Bucy, "New Results in Linear Filtering and Prediction Theory," Trans. ASME J. Basic Eng. 83D, 95-108 (March 1961).

10. J. P. Shipley, D. D. Cobb, R. J. Dietz, M. L. Evans, E. P. Schelonka, D. B. Smith, and R. B. Walton, "Coordinated Safeguards for Materials Management in a Mixed-Oxide Fuel Facility," Los Alamos Scientific Laboratory report LA-6536 (February 1977).

11. D. D. Cobb and J. P. Shipley, "Performance Analysis of Nuclear Materials Accounting Systems," Nucl. Mater. Manag. VIII (2), 81-92 (1979).

12. E. A. Hakkila, R. J. Dietz, J. P. Shipley, "The Role of Near-Real-Time Accounting in International Safeguards for Reprocessing Plants," Nucl. Mater. Manage. VIII, 654-665 (1979).

13. E. A. Hakkila, D. D. Cobb, H. A. Dayem, R. J. Dietz, J. T. Markin, J. P. Shipley, J. W. Barnes, and L. A. Scheinman, "Materials Management in an Internationally Safeguarded Fuels Reprocessing Plant, Vol. I," Los Alamos Scientific Laboratory report LA-8042 (in press).

Discussion:

Suda (BNL):

I would like to comment on your presentation of the conventional accounting system and some of the numbers you have derived in handling these numbers. The limits of error on MUF that you quoted on the conventional system are high by at least a factor of three. What you have shown does not agree with my discussions with the AGNS technical staff. They think the uncertainties on MUF and LEMUF for the first year may be as high as 30 kg on the plutonium and could be perhaps half that after two years of collecting data. The bases you are comparing yourself with are published regulations that reflect 1966 data, and everything that has happened in measurement technology since then has been ignored in that report.

Hakkila (LASL):

Actually, we have tried to be realistically conservative about the errors that we used for both the conventional and dynamic accounting systems, and we have used numbers that were arrived at both from the literature and from consultations with the AGNS staff and other reprocessors. I don't know why we have such a large discrepancy between the numbers that you are quoting. Our diversion sensitivities are probably better than would be achieved with the relative standard deviations that are used in some of the AGNS reports.

Ehinger (AGNS):

A lot of the numbers that were used are those published in the safety analysis report and in some of the original submissions. We have demonstrated that a tenth of a percent in volumetric measurements is attainable. It is attainable and is routinely attainable. This is a big factor in some of the numbers that were published in your slides. We feel that there should be some revisions in those. It is very difficult to quantify exactly, but we can do significantly better than the conventional accountability slides shown. I kind of agree with Syl. There should be some reassessment of those things.

Hakkila:

The calibration data you refer to were obtained in cold runs and have not been demonstrated with reprocessing samples. I think one of the largest sources of error in the accountability tank measurement is not the volume measurement, but rather the chemical analysis of the dissolver solutions.

Ehinger:

True, but if we can do the volume analyses to a tenth of a percent, we can begin to look at those biases and the level of biases you were talking about. You were saying you don't feel we can ever attack biases and systematic errors at the 0.05% level, but we feel that now we can. Granted, we can't make an assessment of the analytical capabilities because we don't have the true hot solutions. We like to throw back and say that when the analytical people can match the performance of volumetric measurements, then you can begin to deal with these levels down at what we are talking about.

Hakkila:

The numbers we have used on the chemical analyses, I think, reflect some of the experience of the European operators, and we have tried again to be realistic with the numbers that are quoted to us from say, Karlsruhe. Our data for the accountability tank are more conservative than those used by the Japanese in JAERI-Memo-8241.

Suda:

If these are Karlsruhe numbers, then I think they should be presented as something that reflects measurements over there and not what is currently capable here.

Hakkila:

We realistically try to reflect measurements that can be obtained from actual process samples. I think it is one thing to obtain one or two tenths of a percent precision on analysis of weapons-grade plutonium, and altogether something else to do it on an actual dissolver solution. Once it can be demonstrated to us that it can be done on a dissolver solution, we will be more than happy to go back and use those numbers in our modeling and simulation programs. They would improve the diversion sensitivity of both the conventional and dynamic accountability schemes.

Discussion:

Persiani (ANL):

You said that you could not adopt the Los Alamos DYMAC system because of contamination with active plutonium. Was it because you could not physically implement the system or was it because there were some differences in fundamental concepts?

Ikawa (JAERI):

We concluded that it is impossible or very difficult because the Los Alamos concept mainly depends on the flow measurement. In the Tokai plant no accurate flow measurement system is installed. If we try to install flowmeters, there is a possibility of plutonium contamination.

Hakkila (LASL):

I would like to comment on that. I think the problem arises from the definition of dynamic materials accounting. We consider your approach as dynamic materials accounting. In fact, in our study of the Tokai facility we did not include flow measurements; rather we used batching in and out of tanks, with a materials balance period of one day. This is equivalent to two input accountability tank and one product tank batches. The main idea behind near-real-time or dynamic materials accounting is to be able to draw material balances around a unit process accounting area within some period of time that will provide the desired detection sensitivity and timeliness. The length of the materials balance will depend on the throughput of the facility. For Tokai, which has a fairly low throughput, the materials balance time can be longer than for AGNS, which has seven times the Tokai throughput.

Study of the Application of Semi-Dynamic Material Control Concept to Safeguarding Spent Fuel Reprocessing Plants

by

KOJI IKAWA, HITOSHI IHARA, HIDEO NISHIMURA and MITSUHO HIRATA
Japan Atomic Energy Research Institute, Tokai, Ibaraki, Japan

and

HIROTAKA SAKURAGI
Nippon Computer Bureau Ltd., Tokyo, Japan

and

MASAYUKI IWANAGA, NAOHIRO SUYAMA and KEN-ICHI MATSUMOTO
Power Reactor and Nuclear Fuel Development Corporation, Tokai, Ibaraki, Japan

ABSTRACT

This report presents a result of the feasibility study of the application of the dynamic material control concept to existing small spent fuel reprocessing facilities, using the Tokai Reprocessing Plant as a model. A semi-dynamic material accounting and control system was examined corresponding to the detection time of ten days. This accounting system would be achieved by weekly measured material balances with a maximum delay of three days for analyses. Comparative studies of diversion sensitivity suggest that such a system could be meet control objectives currently discussed relating to the quantitative sensitivity and timeliness. The proposed system uses existing plant instrumentations and capabilities of the laboratoty, and therefore it could be back-fitted to the exsisting small facilities.

I. INTRODUCTION

In the Spring of 1978 the government of Japan, U.S. and France agreed to pursue a program for the improvement of safeguards techniques as applied to spent fuel reprocessing plants, with emphasis on applicability of these techniques to the Tokai facility, Japan. This joint program has been called as TASTEX, and includes thirteen individual tasks (A~M). This paper describes a preliminary result on the Task-F; 'Study of the application of DYMAC principles to safeguarding spent fuel reprocessing plants'.

This study was directed to limited questions summarized as follows:

(1) It is not necessary true that an effective dynamic material control system can be back-fitted at an acceptable cost into those facilities such as three existing reprocessing facilities either currently operating under IAEA safeguards or planned for future operation.

(2) The only existing study of the effectiveness of dynamic material control for reprocessing facilities [1] assumed a large scale facility of 1500 t/a and a safeguards objective is measured in hours. This is really required to control a large in-process plutonium holdup effectively. For current facilities of 300 t/a or smaller, however, it is expected that safeguards objective could be measured in a more relaxed time-base, e.g., 1~10 days. There has been no study of effectiveness for such facilities, however.

(3) There has been little work on the important question of verification of dynamically prepared material balances on the part of international safeguards inspectors.

Therefore, in our study, an emphasis is placed on the feasibility study of the application of the basic concepts of dynamic material control to existing small (300t/a or smaller)

spent fuel reprocessing facilities, using the Tokai Rerocessing Plant as a model plant. 'DYMAC' system at the TA-55 plutonium facility of the Los Alamos Scientific Laboratory was reviewed and discussions with LASL's people were made on problems relating to the dynamic material control concepts and techniques of evaluation of effectiveness of a dynamic material accounting system.

As a result of those preliminary studies, we reached to a conclusion that it is very difficult to apply the same concept assumed in the LASL's paper for the BNFP model plant, because processes of the reference plant had been already contaminated with active plutonium.

As an alternative system a model of semi-dynamic material accounting and control system was examined corresponding to the detection time of ten days. This model was originally proposed by J. E. Lovett, System Studies Section, Department of Safeguards, IAEA, during his consultation on this study in Japan in the summer of 1978, and has been called as "the ten day detection time model".

II. CHARACTERISTICS OF THE MODEL PLANT

The reference plant is a small scale plant of about 210 ton/a or 0.7 ton/day, using the Purex recovery process with a mechanical chop-leach headend and mixer-settler contactors. The schematic diagram of process flow is shown in Fig. 1, in which three formal material balance areas are indicated. These are used to draw a formal (or traditional) material balance after which the facility is shut down and the physical inventory is measured. Measurement methods being adopted for the accountability purpose are summarized in Table I.

TABLE I MEASUREMENT METHODS FOR MAIN KMP'S [4, 5]

KMP	Measurement point	Chemical analysis		Sampling	Volume or weight measurement
		Uranium	Plutonium		
FKMP-Q_1	Input accountability vessel	Isotopic dilution -Mass spectrometry	Isotopic dilution -Mass spectrometry	Circulation using air lift and vacuum line	Pneumatic bubble system using dip tube
FKMP-Q_6, Q_R	Waste solution	Solvent-extraction -DBM spectrophotometry	Solvent-extraction -α counting	Circulation using air lift and vacuum line	Pneumatic bubble system using dip tube
FKMP-Q_8	UO_3 product	$K_2Cr_2O_7$ titration	-	Proposional sampler	Weighing by a large scale
FKMP-Q_9	Plutonium product accountability vessel	-	$Ce(SO_4)_2$ titration	Using vacuum	Pneumatic bubble system using diptube
IKMP	In-process inventory vessels	Case by case, methods same as FKMPs	Case by case, methods same as FKMPs	Case by case, methods same as FKMPs	Case by case, methods same as FKMPs

In-process inventory and its fluctuation due to different fuel type is indicated in Table II. These values were obtained by simulations using a flow simulation code, DYSAS-R[2].

III. SEMI-DYNAMIC MATERIALS ACCOUNTING AND CONTROL SYSTEM

Basic Concept of Ten Day Detection Time Model

In general, the objective of dynamic materials control is to use a combination of computer data processing, in-, on-, or at-line non-destructive measurement equipment, improved facility design, and advanced statistical techniques to prepare and evaluate a large number of material balances or modified material balances, each covering both a small portion of a large bulk processing facility and a short period of time. In case of existing facilities, however, adoption of some of these elements can not be made without significant modifica-

tions of the plant itself. It is, of course, desirable to limit such a modification as small as possible. From this point of view and basing upon the preliminary study on the plant characteristics of the reference model plant, followings were taken into account as elements to construct a possible dynamic materials control;

(1) The dynamic physical inventory should be taken weekly during plant operation and the analysis and evaluation should be made within three days after the inventory cut-off point.

(2) Existing plant instrumentations should be used whenever they could satisfy the minimum requirement for timeliness and sensitivity.

(3) Wet chemical analytical techniques shown in Table I should be chosen so long as the laboratory could keep capability to get results by them within three days after sample taking.

(4) The most effective statistical data-analysis techniques combined with supportive computer technology should be fully utilized.

The dynamic material balance equation shown below is solved weekly.

$$MUF_d = BI_d + I_d - P_d - W_d - EI_d$$

where, BI_d is beginning inventory, which is identical to the measured ending inventory from the preceding dynamic material balance period (DMBP), I_d is input dissolver batches, P_d is product batches, W_d is waste discard batches, EI_d is ending inventory at the end of DMBP, and, MUF_d is dynamic material unaccounted for, including variations in the unmeasured portion of the in-process inventory.

It is important to recognize that EI_d does not include entire physical inventory but includes materials in the main equipment. Thus during initial startup operations MUF_d includes the unmeasured in-process inventory, the quantity of which will be 1~3 kgs of plutonium or 9~15% of the total plutonium inventory in the MBA 2. Under steady-state conditions only the fluctuations in this in-process inventory appear in MUF_d. For the evaluation of MUF_d, CUSUM statistics and Kalman filter estimates are adopted as the primary evaluation tool.

Measurements in the Ten Day Detection Time Model

A. Input quantities: The reference model facility will generate approximately thirteen input dissolver batches during the course of one week's normal operation, each containing 1.7~3.6 kgs plutonium. Since some of these batches will be generated 8~10 days before the analytical data is required, it can be assumed that the normal high quality input measurement data will be available for these batches.

B. Output quantities: Product solution The reference model facility will generate approximately five batches of plutonium product solution during the course of one week's normal operation, each containing about 8 kgs Pu. It is assumed that since the three days are allowed for the completion of measurements and the statistical evaluation of dynamic material balance data, all of these batches can be analyzed by the normal high precision methods.

Waste materials Under normal operating conditions the Pu contained in discarded waste material is small, and the NDA measurements performed normally are completed rapidly. In the ten day model it is assumed that each material balance will be credited with the Pu contained in all waste generated and measured during the material balance period.

C. Physical inventory: The inventory cut-off point is chosen at some adequate time point when the evapolator becomes empty. This is because of the difficulty to measure the volume and density of solution in the evaporator. At the designated inventory cut-off point, the model plant may be expected to have the materials shown in Table II. No attempt is made to measure the relatively small quantity of minor equipment items shown in the table.

Buffer storage vessels All four vessels are equipped with level recorders, density

recorders, temperature indicators, and sample lines, so in principle weekly inventory measurements should present no problem.

TABLE II In-process plutonium inventory and its fluctuation in MBA 2

Fuel Type	BWR	BWR	BWR	PWR	PWR	PWR
Burnup (MWD/ton)	10000	15000	20000	10000	20000	27500
Input Accountability Vessel (3)	1657	2154	2454	1978	3015	3598
Buffer Vessel (4)	1152	1910	2790	2131	3614	2481
Buffer Vessel (8)	495	854	871	660	1102	1330
Buffer Vessel (12)	468	534	705	521	833	950
Buffer Vessel (16)	364	481	545	421	699	1083
Pu Product Reception Vessel (18)	8320	8394	6357	8229	9493	8134
Sub-total of major inventory	12456	14324	13724	13954	18755	16721
Extraction I (5)	328	423	500	389	608	720
Extraction II (6)	48	62	74	57	89	106
Extraction III (9)	241	313	368	285	445	528
Extraction IV (10)	163	211	248	192	299	355
Extraction VIII (14)	232	300	351	274	428	511
Extraction IX (15)	135	175	203	158	248	298
Others (7,11,13)	148	192	226	176	275	328
Evaporator (17)*	0	0	0	0	0	0
Sub-total of minor inventory	1295	1676	1970	1531	2392	2846
Total Inventory in MBA 2	13751	16000	15694	15485	21147	19567
Ratio of Main to Total	91 %	90 %	87 %	90 %	89 %	85 %

(* at the time when Evaporator became empty)

Product evaporator Because of difficulties of measurement, no attempt was made to measure the material in the product evaporator, and it is scheduled to choose the seven day material balance period such that the ending physical inventory is always taken immediately after the evaporator has been discharged, and before evaporator feed is resumed.

Mixer-settler extraction systems The inability to perform meaningful physical inventory measurements (other than by cleanout) imposes a basic limitation on the effectiveness of any dynamic material control system. For the relatively small facilities considered here this limitation is not serious because of small quantities in these systems.

In the proposed system no measurement of the inventory in these systems is assumed. There may be one other alternative, however, in the form of an adaptation of the computer simulation technique using a code, SEPHIS [6]. It has been used in this study to estimate holdups in the mixer-settler system.

IV. EFFECTIVENESS OF SEMI-DYNAMIC MATERIAL ACCOUNTING AND CONTROL

Evaluation Method and Simulated Operation Modes

A dynamic model of the reference reprocessing plant, DYSAS-R (Dynamic Safeguards Simulation Code for Reprocessing Facility), have been developed. The model includes almost all major processes associated with plutonium in the reprocessing plant. The simulated data represent in process material flows and inventories under normal operating conditions including plant-start-up, flush-out, and clean-out operations. The simulated process flow data are treated as "true values" for measurements, which are also simulated according to the measurement procedure being associated respective uncertainties. For this purpose a code "SIMAC" (Simulation of Measurements and Accountancy) was developed.

The simulated material balance data are analyzed by powerful data-analysis and sequential-detection techniques. A general framework of these techniques have been developed by J.P.Shipley[1]. We used them without any modification. The procedure of sequential-decision analysis based on CUSUM and Kalman filter are used to develop a code, "SADAC" (Safeguards Data Analysis Code).

Table IV to VI show input elements of the simulation study. These elements correspond to plant operation schedule (mode), fuel type, type of measurement error, and, type of recalibration frequency. Combinations of these elements are represented by "Simulation Study Cases (S.S.)" and shown in Table VII.

Summary of Results

(1) The value of MUF_d of the first dynamic material balance period after a clean-out physical inventory taking includes unmeasured in-process holdup, the quantity of which varies from 1.3 to 3.3 kg Pu depending upon concentrations of input dissolver batches.

(2) The measurement accuracy of dynamic physical inventory taking has a small influence on the value of MUF_d, because the in-process holdup is at most 3.3 kg Pu in comparison with the total throughput in a dynamic material balance period (42.6 kg Pu in the corresponding case).

(3) In general, the result shows that the sensitivity of detection of diversion will be about 1 σ_{MUF_d} for a week material balance. The summary of the results is shown in Tables VIII and IX. The quantity of plutonium assumed to be diverted within a dynamic material balance period (7 days) is 0.25 σ_{MUF_d} for S.S.1-5-2, 1.5 σ_{MUF_d} for S.S.1-9 and S.S.1-10, and 1 σ_{MUF_d} for all the other cases.

(4) Twenty-two cases of flow-simulations and their measurement-simulations, and additional ten cases of measurement sinulations for the purpose of evaluating normal operating conditions have been carried out. A lot of data have been obtained and much of them have been expressed graphically to make understanding easy and sure. Numeric results are summarized in Table VIII and Table IX, which are also convenient to recognize why the traditional material accounting is not always effective for the safeguards purpose, and why the dynamic material accounting is expected to be effective and robust even it is based on the 'ten-day-detection-time model'. From these tables following description can be done.

(5) In case of the traditional material accounting, LEMUF ranges from 6.9 to 14.7 kg Pu for the 6-month-material-balance period and from 6.9 to 7.7 kg Pu for the 4-month-material-balance period. This means that the traditional material accounting can not detect the quantity of safeguards significance (8 kg Pu) in most cases.

(6) When the dynamic material accounting is adopted, accounting data are processed and analyzed using a computer system, and then the statistical analysis and the sequential-decision analysis can be fully utilized. From the simulation study it has become clear that these techniques will provide us a powerful ability to detect any significant diversion assumed under the preliminary IAEA criteria.

(7) All cases in Table IX assumed protracted diversions. Diversion rate is defined as a quantity to be diverted within a dynamic material balance period (a week). In case of a traditional material accounting, a diversion rate is equal to a sum of weekly diversions within a traditional material balance period (6 months). It is indicated as 'total diversion' in the table.

In case of the traditional material accounting, a simple magnitude comparison between MUF and LEMUF is only a way to decide whether any diversion had occurred or not within the spcefied material balance period.

(8) In our simulation studies, six cases* in eleven (total) cases show that observed MUF's exceed their limit of error, LEMUF. It means that the traditional material accounting succeeds to detect occurrence of diversions in these cases, even though these detections will be made after the 'total amount' (in the table) of plutonium will have already been diverted. [* S.S.1-1, 2, 5-1, 6, 9, 10]

(9) On the contrary, five cases* (a half of the total cases) show that observed MUF does not exceed their limit of error. These are the cases that the traditional material accounting failed to detect occurrence of diversions of the amounts shown in the table. Some of these diversions are greater than 8 kg, the quantity of safeguards significance. [* S.S.1-3, 4, 5-2, 7, 8]

(10) When the dynamic material accounting is adopted, however, all of these diversions except S.S.1-5-2 could be successfully detected by the sequential decision analysis technique probably within about five dynamic material balance periods after such a diversion was initiated, although the detection time depends upon the probability to commit an error of the first kind,

Fig. 3 shows an example of sequential-decision analysis. In alarm charts letters A to G indicate possibility of occurrence of diversion while letter T or blank indicates no decision should be made at that point.

(11) The only one exception is the case S.S.1-5-2 in which very small diversion rate, i.e., 0.25 MUF_d is assumed. This corresponds to 100 grams of plutonium per a week. In this case, the detection of diversion will be made at the 21st material balance or 140 days after the initiation of such a diversion. The total diversion of plutonium amounts to 2 kgs.

(12) It must be emphasized that in the dynamic material accounting, a simple magnitude comparison between MUF and LEMUF has little meaning. It should be emphasized also that the Kalaman filter estimate for MUF_d presents good estimate of assumed diversion rate.

(13) As a preliminary conclusion, semi-dynamic material accounting system based upon the 'ten-day-detection-time model' can be recognized as feasible and effective system for the model reprocessing plant.

REFERENCE

[1] E.A. Hakkila et al, LA-6881, Vol. I,II (1977)
[2] K. Ikawa et al, JAERI-memo 8241
[3] K. Ikawa et al, JAERI-memo 8242
[4] K. Nakajima et al, IAEA-SM-231/34 (1978)
[5] K. Nakajima et al, Final Report of IAEA Research Contract No. 796/RB (1971)
[6] S.B. Watson et al, ORNL-TM-5123 (1975)

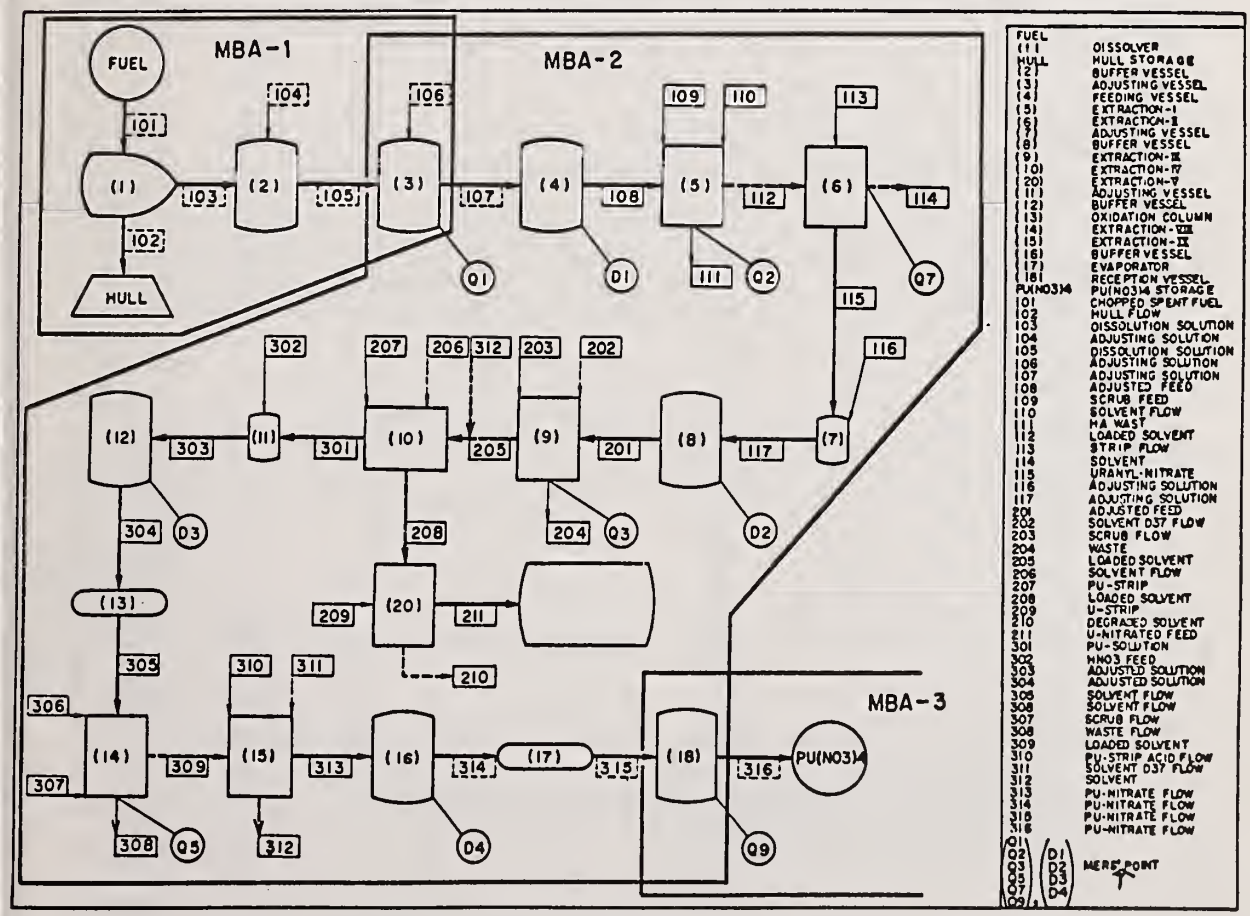

Fig. 1 MODEL REPROCESSING PLANT PROCESS FLOW

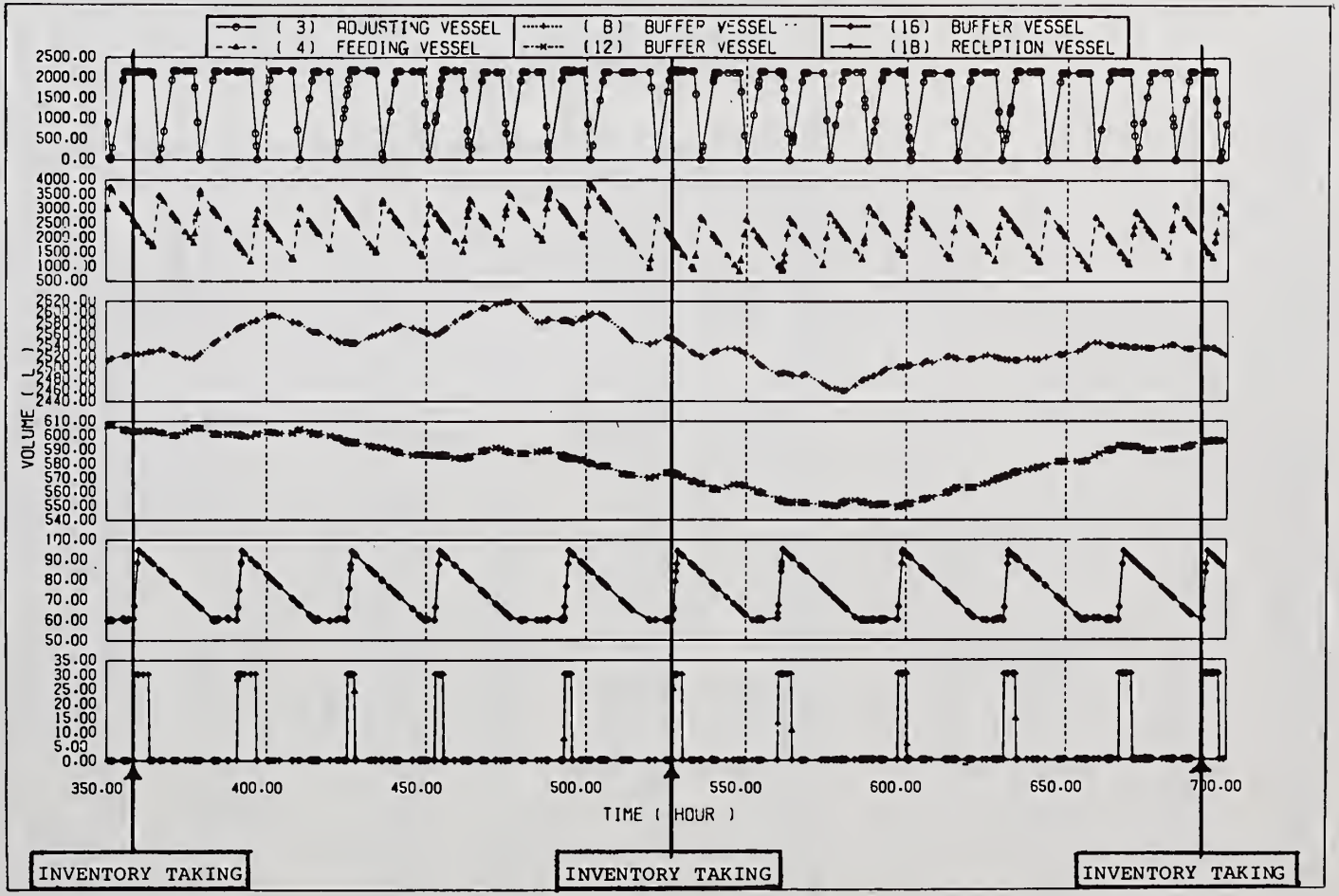

Fig. 2 Graphic representation of variations in volume of solution in the major measurement points. Three inventory cut-off points are also indicated. Each point is chosen at a particular point of time immediately after the evaporator become empty and before evaporator feed is resumed. This figure is drawn by the flow simulation code, DYSAS-R.

TABLE III Simulated Operation Modes

Operation Mode	Pattern (Unit: day)	Number of Dissolver Batches
1	Run 150 → PIT 30	250 + 6 + 50 Fu C P
2	Run 70 → F 10 → Run 70 → PIT 30	120 + 16 + 114 + 6 + 50 Fu F Fu C P
3	Run 30 → F 10 → Run 30 → F 10 → Run 30 → F 10 → Run 30 → PIT 30	52 + 16 + 52 + 16 + 52 + 16 + 46 + 6 + 50 Fu F Fu F Fu F Fu C P
4	Run 90 → PIT 30	146 + 6 + 50 Fu C P
5	Run 40 → F 10 → Run 40 → PIT 30	68 + 16 + 62 + 6 + 50 Fu F Fu C P

* Fu : Fuel , F : Fliush-out, C : Clean-out, P = PIT

TABLE IV Fuel Type

Fuel Type	Reactor Type	Burn-up (MWD/T)	Total Heavy Metal Weight(kg)	Uranium of Fresh Fuel (kg)	Uranium (kg)	Plutonium (kg)
1	BWR	10,000	550	400	394.0	1.656
2	BWR	15,000	550	400	391.2	2.128
3	BWR	20,000	550	400	389.2	2.496
4	PWR	10,000	550	400	394.0	1.968
5	PWR	20,000	550	400	388.0	3.040
6	PWR	27,000	550	400	384.8	3.576

TABLE V Type of Measurement Error

Type	
1	Meas't system 1, standard inventory meas't
2	Meas't system 1, optimistic inventory meas't
3	Meas't system 2, standard inventory meas't
4	Meas't system 2, optimistic inventory meas't

TABLE VI Type of Recalibration Frequency

Type	Frequency
1	weekly
2	every third week
3	monthly
4	no

TABLE VII Cases of Simulation Studies

Case No.	Operation Mode	Fuel Type	Type of Measurement Error	Type of Recalibration Frequency
S.S.1-1	1	1	1	2
S.S.1-2		2		
S.S.1-3		3		
S.S.1-4		4		
S.S.1-5		5		
S.S.1-6		6		
S.S.1-7	2	5	1	2
S.S.1-8	3			
S.S.1-9	4			
S.S.1-10	5			
S.S.2-1	1	5	(1)	2
S.S.2-2			2	
S.S.2-3			3	
S.S.2-4			4	
S.S.3-1	1	5	1	1
S.S.3-2				(2)
S.S.3-3				3
S.S.3-4				4
S.S.4	3	4/5/6	1	2

TABLE VIII Summary of the Simulation Studies
- In case of no diversion -

(these values are for plutonium)

		Dynamic Material Accounting						Traditional Material Accounting			
			Average			Kalman filter Estimate					
Case	Total feed (kg)	Div. rate (g/DMB)	$\overline{MUF_d}$ (g/DMB)	σ_{MUF_d} (g/DMB)	LEMUF $=2\sigma_{MUF_d}$ (g/DMB)	MUF_d (g/DMB)	σ_{MUF_d} (g/DMB)	LEMUF $=2\sigma_{MUF_d}$ (g/DMB)	Total Div. (kg/TMB)	MUF (kg/TMB)	σ_{MUF} (kg/TMB)	LEMUF $=2\sigma_{MUF}$ (kg/TMB)
S.S.1-1	414.00	0	99	224	448	32	44	88	0	2.171	3.398	6.796
S.S.1-2	532.00	0	112	294	588	-68	58	116	0	2.470	4.364	8.728
S.S.1-3	624.00	0	142	354	708	110	76	152	0	2.988	5.122	10.244
S.S.1-4	492.00	0	76	267	534	-58	55	110	0	1.662	4.036	8.072
S.S.1-5	760.00	0	152	417	834	137	93	186	0	3.352	6.234	12.468
S.S.1-6	894.00	0	256	506	1012	261	113	226	0	5.630	7.332	14.664
S.S.1-7	711.36	0	162	399	798	161	83	166	0	3.567	5.844	11.688
S.S.1-8	614.08	0	98	363	726	239	67	134	0	2.165	5.063	10.126
S.S.1-9	443.84	0	140	383	766	78	123	246	0	2.107	3.851	7.702
S.S.1-10	395.20	0	169	361	722	139	98	196	0	2.537	3.447	6.894

TABLE IX Summary of the Simulation Studies
- In case of diversion -

		Dynamic Material Accounting							Traditional Material Accounting			
			Average			Kalman Filter Estimate						
Case	Total feed (kg)	Div. rate (g/DMB)	$\overline{MUF_d}$ (g/DMB)	σ_{MUF_d} (g/DMB)	LEMUF $=2\sigma_{MUF_d}$ (g/DMB)	MUF_d (g/DMB)	σ_{MUF_d} (g/DMB)	LEMUF $=2\sigma_{MUF_d}$ (g/DMB)	Total Div. (kg/TMB)	MUF (kg/TMB)	σ_{MUF} (kg/TMB)	LEMUF $=2\sigma_{MUF}$ (kg/TMB)
S.S.1-1	414.00	226	325	226	452	228	44	88	4.742	7.153	3.381	6.762
S.S.1-2	532.00	292	416	290	580	324	60	120	6.133	9.154	4.341	8.682
S.S.1-3	624.00	343	483	348	696	492	76	152	7.205	10.136	5.096	10.192
S.S.1-4	492.00	268	361	263	526	281	55	110	5.637	7.984	4.017	8.034
S.S.1-5-1	760.00	418	577	420	840	625	92	184	8.780	12.695	6.204	12.408
S.S.1-5-2	760.00	100	267	419	838	269	94	188	2.107	5.881	6.229	12.458
S.S.1-6	894.00	492	700	496	992	689	111	222	10.332	15.400	7.300	14.600
S.S.1-7	711.36	391	526	403	806	538	81	162	8.217	11.579	5.820	11.640
S.S.1-8	614.08	355	372	365	730	255	71	142	7.096	8.187	5.039	10.078
S.S.1-9	443.84	614	652	376	752	791	121	242	7.978	9.778	3.813	7.626
S.S.1-10	395.20	560	590	365	730	376	88	176	7.274	8.843	3.417	6.834

DMB : Dynamic Material Balance Period = 7 days

TMB : Traditional Material Balance Period = {6 months for S.S.1-1~S.S.1-8
4 months for S.S.1-9, 10

Div : Diversion

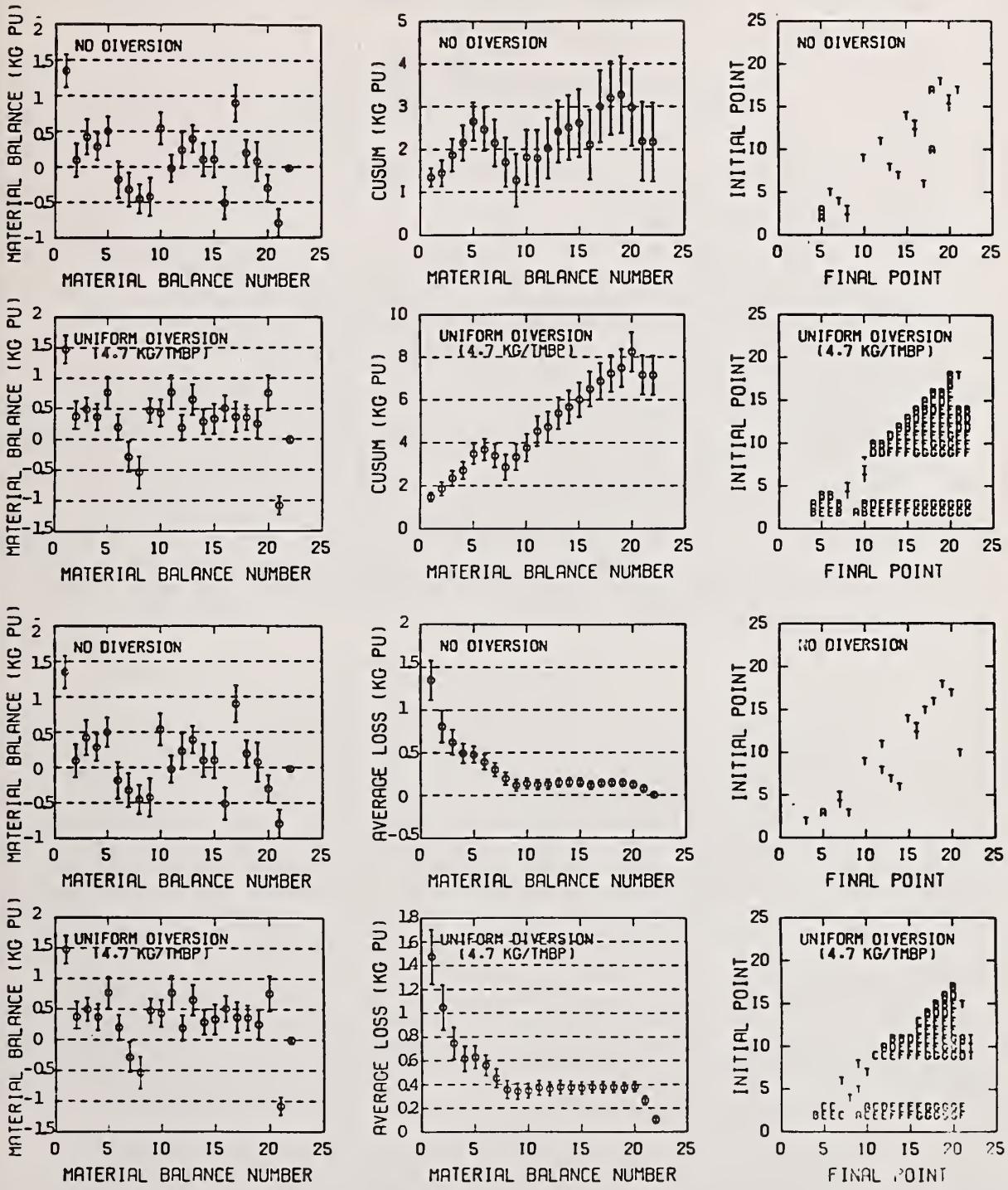

S.S.1-1 , 6 months : material balance, cusum, Kalman filter estimates and alarm charts.

Fig. 3 Sequential Decision Analysis for Case S.S.1-1

Safeguards System of Backend Facilities with Emphasis on Waste Management

by

Y. Akimoto, T. Ishii, and S. Yamagami
Mitsubishi Metal Corporation, Tokyo, Japan
and
T. Shibata
Power Reactor and Nuclear Fuel Development Corporation, Tokyo, Japan

Safeguards system for the collocated backend facilities is discussed. According to the assessment using evaluation function for CS (containment and surveillance) and MA (material accountancy), proposed here, CS should play a very important role to increase the safeguards effectiveness for the industrial scale facilities. Diversion of nuclear material through an abnormal route can be avoided by multiple devices of CS, installed to every possible diversion path along the nuclear material flows. Nuclear materials, shipped or received at each facility, should be itemized as much as possible, so that CS may effectively complement the function of MA. For a section recovering plutonium from dirty scrap and α waste, an independent MBA is recommended to be set up with enhanced safeguards system.

KEYWORDS: Containment and surveillance, evaluation of safeguards effectiveness, detection probability, backend facilities, waste management.

INTRODUCTION

One of the major problems for industrial scale plutonium recycling is to establish an effective safeguards system for a series of chain backend facilities of fuel cycle which accept spent fuels from reactor and send refabricated MOX (mixed oxide) fuels to reactor. Here, international safeguards system for these facilities is discussed.

In accordance with INFCIRC-153, MA (material accountancy) is defined as a safeguards measure of fundamental importance and CS (containment and surveillance) as an important complementary measure. The current implementation, however, has been performed with much emphasis on MA, of which limitation is drawn gradual attention along with the growth of the process capacity.

Although the information of material quantity is essential in the MA system, the real important value in the safeguards is not the quantity itself, but the detection probability of diversion.

In fact, even the results of MA or MUF verification are valuable only after it is converted to the detection probability to find the significant quantity of materials diverted. On the premise that the objective of the safeguards is timely detection of diversion, it is reasonable to consider the detection probability, as well as time, as an essential factor. This means that the efforts in the advanced safeguards should be directed to the improvement of detection probability and the reduction of detection time.

As is schematically shown by vectors in Fig. 1, one of the efforts to these direction is the development of advanced MA system to approach the real time detection and to pursue more accurate and precise measurement. Other is the trial of systematic application of CS system in order to reach the higher detection probability. The situation indicates the importance of coordination of MA and CS, which has so far been treated independently. Authors have already proposed[1] the idea of evaluation method, which are commonly applicable to both MA and CS, and usable to a large backend facilities.

In this paper the idea is further clarified and the safeguards system for large

backend facilities is discussed based on the proposed evaluation method. Safeguards for a facility of waste treatment and scrap recovery is specially investigated.

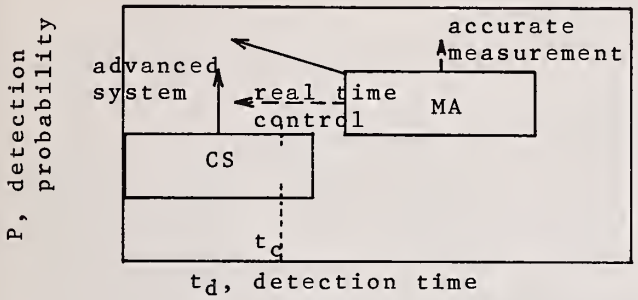

Fig.1 Schematic relationship between detection time and detection probability of diversion

EVALUATION METHOD OF SAFEGUARDS EFFECTIVENESS

The safeguards effectiveness in the improved system is to be evaluated based on common criteria which are applicable both to CS and MA systems. In this chapter the derivation method of the diversion detection function is briefly described.

Evaluation of the detection probability, P(t), will take the following steps:

(1) Evaluation of a single unit of instrument,

(2) Evaluation along with every possible diversion path for the CS devices, and

(3) Evaluation along with the nuclear material flows for the MA devices.

Combining these evaluation steps, the evaluation data are piled up, so that whole system within a single MBA or a unit facility can be evaluated.

The diversion detection probability for the whole system can be expressed as a function of the detection time, t, for a total amount of diverted material, M, and given as:

$$P(t)_M = 1 - \{1 - P_{CS}(t)_M\}\{1 - P_{MA}(t)_M\} \quad \ldots\ldots\ldots (1)$$

where P_{CS} and P_{MA} are the detection probabilities by CS and MA, respectively.

This equation allows to evaluate seals and item-detection devices with the same criteria, which are not related directly to amount of diverted material. The results of the calculation procedure are described in Appendix.

In present non-proliferation criteria the time required to manufacture the parts for a nuclear weapon, called conversion time, t_c, is given as standard for detection time and no worth is recognized for detection after t_c. However, it is realistic to consider the continuous connection between the earliness of detection and its worth, although the validity of diversion detection after t_c should be drastically discounted, as the principle of non-proliferation is to detect any single nuclear weapon before it is produced.

For this purpose, continuous weighting function, such as Fermi function, is introduced which decreases with time and has inflection point at time t_c. The worth of early detection can be correctly evaluated by this function.

Consequently the safeguards effectiveness E_M will be expressed by integral of a continuous function which shows the higher value with shorter detection time and higher detection probability, as,

$$E_M = \int_o^T P(t)_M \, w(t) dt \quad \ldots\ldots\ldots\ldots\ldots\ldots (2)$$

Here, T is an external parameter, $P(t)_M$ is the total detection probability of diversion described in the Appendix and suffix M corresponds to threshold amount of nuclear material. w(t) is a Fermi type function,

$$w(t) = \frac{1}{\exp \frac{t-tc}{\tau} + 1} \quad \ldots\ldots\ldots\ldots\ldots\ldots (3)$$

where τ is a factor to decide curve configuration of Fermi function, i.e. in case τ=0 the curve configuration is similar to the present way of evaluation and with increase of τ, curves are changing as in Fig. 2 (2). Quantity of τ depends deeply on the situation of a nation and the character of a diverter and a controller.

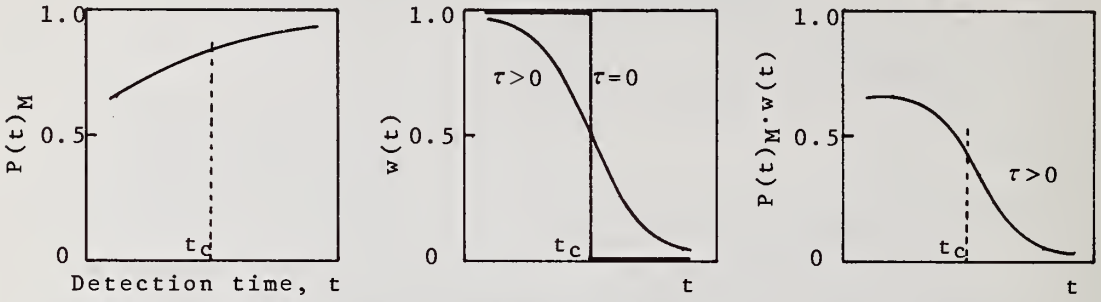

(1) Detection probability (2) Weighting function (3) $P(t)_M \cdot w(t)$

Fig.2 Schematic curves of safeguards evaluation function

SAFEGUARDS SYSTEM IN THE BACKEND FACILITIES

Criteria to Evaluate the Safeguardability

In order to allow maximum safeguards effectiveness in the backend facilities, the following criteria are considered.

Collocation. Backend facilities are collocated so as to unify each facility from the viewpoint of CS. This allows the completion of a closed loop for plutonium recycling as chain facilities from the point of spent fuel receiving to the point of MOX fuel shipping. In this type of system, the inflow/outflow of plutonium to and from the backend fuel cycle center take place only in the form of completely itemized fuel assemblies.

Itemization. At the input/output of sensitive facilities nuclear materials flow should be itemized as much as possible. By sealing every item and applying CS, the sensitivity of MA can be complemented.

Optimum application of CS and MA. CS and MA devices should be systematically arranged in the facility so that they could achieve, at minimum expense and with minimum disturbance to operations of the facility, a level of safeguards effectiveness, which is difficult to achieve with any of these alone. Introduction of evaluation function, described before, makes it possible to analyse and pursue the most suitable coordination of both devices to attain the proposed safeguards effectiveness.

CS system. In facilities with large material throughput or inventory, it is very difficult to get the high detection probability by MA system even if strenuous efforts are exercised. These difficulties will be solved by arranging multiple levels of CS devices, applied to all possible diversion paths from nuclear materials flow. The degree of multiplicity should be such that even in the event of failure of any single CS device, detection probability of the total system does not decline appreciably and also that the false alarm rate is negligible for all practical purposes. CS devices with a high probability of failure should be backed up by redundant installations to improve reliability. The collocation discussed above brings in increasing the degree of multiplicity with CS barriers and lengthening diversion paths, thus improving detectability and reliability.

Safeguards at sensitive sections. In sections like analysis and waste recovery

process where, even though the material throughput is low, operation schemes are always changing, the danger of making a clandestine facility is relatively high. For such sections an enhanced safeguards system with advanced CS and MA should be applied.

Material Balance Area

According to the above criteria, following concept for safeguards in the backend facilities are proposed.

Collocation

Figure 3 shows the MBAs in the collocated backend facilities. On the premise that spent fuel storage is built in the same building with reprocessing plant, the storage is included in a same MBA (MBA-I) with headend and dissolution process, although strategic point should be prepared between these processes to observe a transfer of spent fuel. Quantity of nuclear material in the fuel cannot be confirmed before it is dissolved and accounted.

In MBA-II, fission products, uranium and plutonium are separated in nitrate forms by extraction method. High active liquid waste and hull, as well as β-γ waste are also processed and solidified in this MBA. Uranium nitrate is purified and converted to oxide or fluoride form in the same MBA and shipped to uranium storage, MBA-III.

Purified plutonium nitrate, which is very attractive to diverter, is sent to a specially prepared MBA (MBA-IV), plutonium conversion process, where plutonium is converted to oxide form.

Independent MBA (MBA-V) is also alloted to plutonium storage which is operated in item accountancy implementation so as to allow operation by an independent organization.

MOX fuel fabrication facility is separated into three MBAs which are located in the same building. MBA-VI is prepared for a buffer storage of PuO_2 and UO_2 for MOX fuel fabrication facility. MBA-VII corresponds to the fabrication facility including such processes as powder preparation, pellet formation and fuel element fabrication. Fuel assembling process and the storage of finished assemble belong to MBA-VIII.

Dirty scrap of nuclear material and low level α waste, generated from all the backend facilities are collected together to specially prepared MBA (MBA-IX), i.e. α waste treatment and nuclear material recovery process, which are discussed later.

Itemization

As shown in Fig. 3 and Table I, many parts of transportation of nuclear material between MBAs can be itemized. There are some cases, however, that the item transportation is not considered. In cases of material transfer from MBAs I to II and MBAs II to IV, nitrate solution is transported through pipe lines. But the transportation in these cases can be fully guarded, because buildings of those MBAs are mutually connected.

α bearing waste solution is also transported through pipe lines from MBAs II, IV and VII to IX. However, only the solution with low α concentration is released through pipe line, and the concentrated α waste solution is transported by itemized form using special bottle.

Optimum Application of CS and MA

In MBAs where large MUF value is considered, such as MBAs II, IV and VII, high detection probability by MA system cannot be expected. Therefore, these MBAs should rely intensively on the CS system. MBAs III, V, VI and VIII, where material is treated only by itemized form, are also guarded by CS devices in addition to item accountancy.

MBA-IX, which has significant importance in view point of safeguards, should be guarded by coordinated MA and CS system, as is discussed later.

CS System

As an example, detection probability by CS system for plutonium conversion facility is calculated with equation (1). About 60 sets of CS devices are arranged throughout the special designed facility.[2] Detection probability on the whole facility is given as functions of quantity of material diverted and the time to be detected, as shown in Table II.

Safeguards at Sensitive Sections

It is clear that nuclear material storage with large inventory, located in various MBAs should be strategically inspected. Besides the large storage, there are some important sections where various kinds of operation are conceivable, such as waste treatment process or sampling bench. Sampling points in each MBA should be strategically checked. Waste treatment system is discussed in the following section.

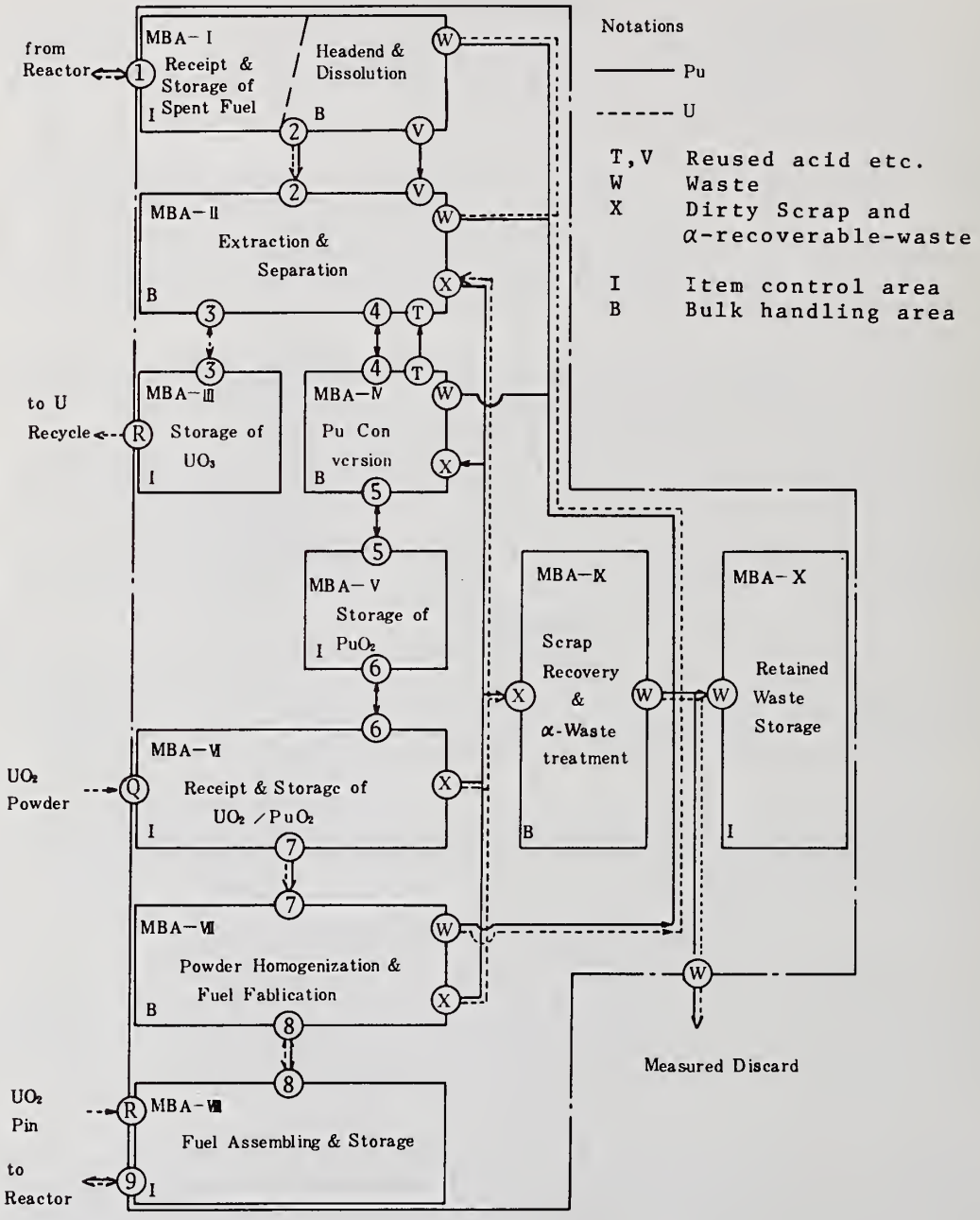

Fig.3 MBAs in the collocated backend facilities

Table I Itemization of nuclear material between MBAs at transportation

	Transportation between MBAs			Forms of nuclear material	Transportation means	Itemization
①	out	→	I	spent fuel assembly	spent fuel cask	yes
②	I	→	II	spent fuel nitrate solution	pipe line	no
③	II	→	III	UO_2 or UO_3 powder (or U-fluoride)	container	yes
Ⓟ	III	→	out	UO_2 or UO_3 powder (or U-fluoride)	container	yes
④	II	→	IV	Pu-nitrate	pipe line	no
⑤	IV	→	V	PuO_2 powder	can + container	yes
⑥	V	→	VI	PuO_2 powder	can + container	yes
⑦	VI	→	VII	PuO_2 powder	can + container	yes
Ⓠ	out	→	VI	UO_2 powder	container	yes
⑧	VII	→	VIII	MOX fuel element	carriage	yes
⑨	VIII	→	out	MOX fuel assembly	fuel cask	yes
Ⓡ	out	→	VIII	UO_2 fuel element	carriage	yes
Ⓧ	IV, VII	→	IX	dirty scrap (U + Pu)	can + container	yes
	II, IV, VII	→	IX	α solid waste	container	yes
				α liquid waste	bottle	yes
					pipe line	no
	IX	→	II	U-nitrate	pipe line	no
	IX	→	IV	Pu-nitrate	vessel	yes

Table II Detection probability by CS system at plutonium conversion plant

Amount of Pu / Time	Detection Probability			
	$m>1000^g$	$1000>m>100$	$100>m>10$	$10>m$
$t > 7$ days	1.00	1.00	1.00	1.00
$7 > t > 1$	1.00	1.00	0.94	0.82
$1 > t$	1.00	0.995	0.93	0.79

WASTE TREATMENT AND NUCLEAR MATERIAL RECOVERY PROCESS

In the process like intermediate and low level waste treatment, and nuclear material recovery, the operation schemes are changeable and possibility of diversion is relatively high, even though the nuclear material throughput is small. Therefore these processes are collected to a special sections with a single MBA, where enhanced safeguards are applied.

Facility Description

Liquid and solid α wastes, dirty α scraps and analytical residues are transported to this facility from plants as reprocessing, plutonium conversion and MOX fuel fabrication. These materials received are processed as follows;

(1) Dirty scraps and solid analytical residues, transported by a canned form, are accounted and dissolved. The solution is filtered and the filtrate including nuclear material is sent to the solvent extraction process, where plutonium and uranium are separated, purified and recovered as nitrate forms.

(2) α solid wastes, received by drum or container, are treated to remove α nuclides and to reduce the total waste volume with methods as calcination, crushing, acid leaching and so on. Acid solution with α material thus produced, is sent to the solvent extraction process.

(3) α liquid waste, transported by pipe line or special bottle, is accounted and classified into two categories; evaporation line and precipitation-filtration line. Nitric acid with concentrated α material which is the product of these lines, is also sent to the solvent extraction process.

An example of typical material flow is shown in Fig. 4.

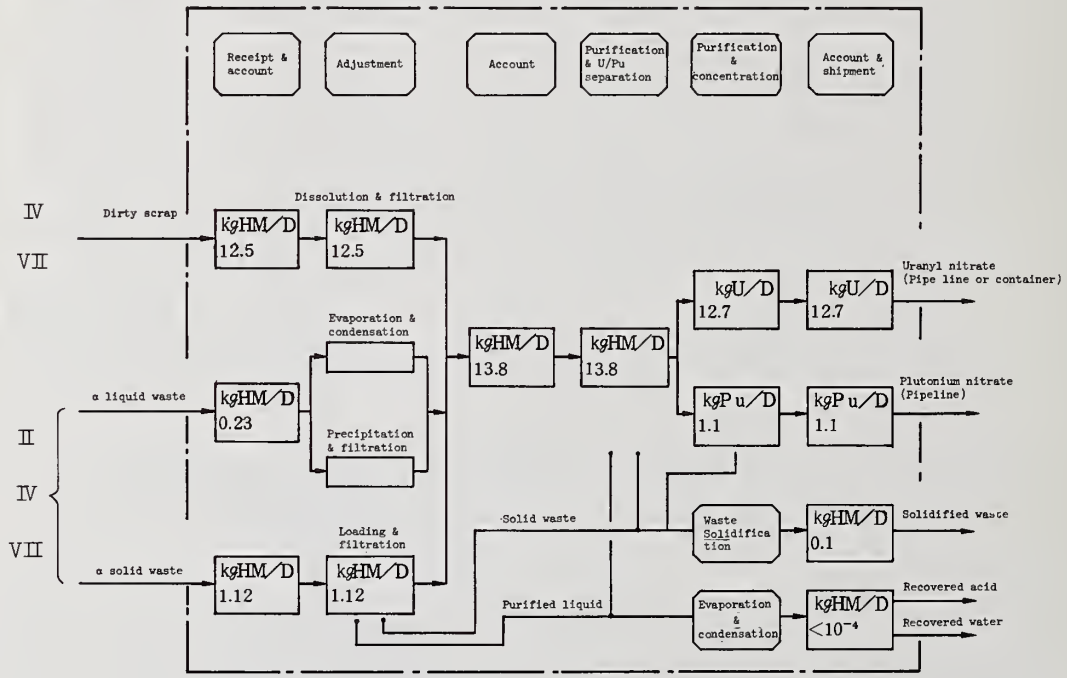

Fig. 4 Materials flow in MBA Ⅸ for α waste treatment and nuclear material recovery process

Material Accountancy

Accuracy of materials accounting for dirty scrap and solid analytical residues, and α liquid waste is reasonably well, whereas quantitative identification of α material in the α solid waste in a drum is comparatively poor.

On the assumption that measurement accuracy is about 1% for scrap and analytical residues, and 20% for waste in the drum, MUF of plutonium in the annual operation reaches to 1.7kg, which satisfies the quantitative criteria of MA.

In addition to these results all the inventory in this facility is found to be restricted within 8 kg.

Containment and Surveillance

As the materials are mainly treated in glove boxes, there are many possibility for a man to access to nuclear materials. Therefore, special care will be paid to isolate an operator from nuclear material. The concept of the facility is schematically shown in Fig. 5.

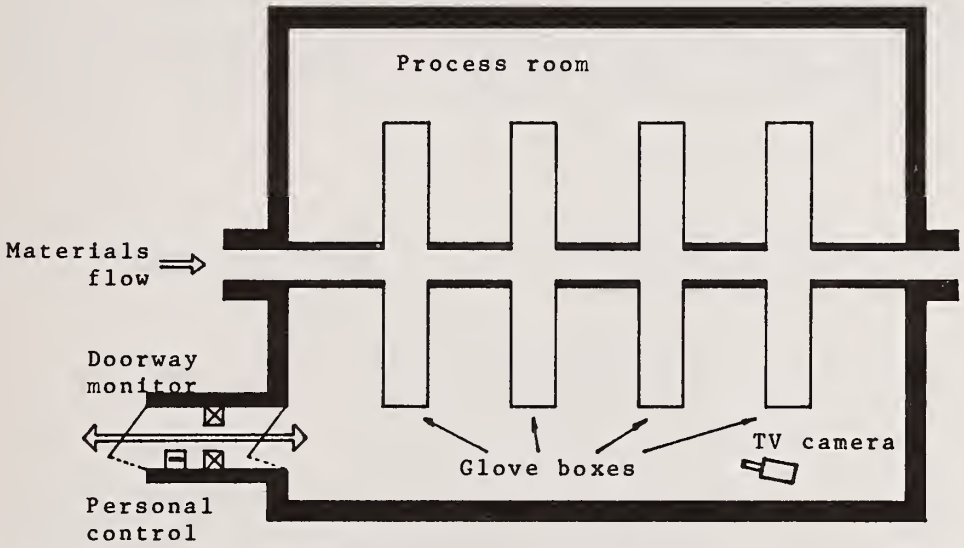

Fig.5 Concept of waste treatment and scrap recovery facility

REFERENCES

[1] "An improved safeguards system and its application to large backend facilities", Japanese contribution to INFCE WG 4, Co-chairman/WG 4/81 (A, B), Nov. 1978.

[2] Y. Akimoto et al. "A quantitative evaluation of the effectiveness of safeguards with emphasis on CS" 1st Annual Symposium on Safeguards and Nuclear Material Management, Brussels, Apr. 1979.

APPENDIX

Derivation Method of Detection Probability Formulae

Detection probability of diversion is derived with the coordination of CS and MA. Derivation steps are summarized in Fig. 6.

Basic philosophy of the CS detection system in order to increase the detection probability, is to install plural and redundant CS devices at the same position and to set multiple stages of CS devices along all possible diversion paths. The calculation of detection probability was carried out by the successive 6 steps in Fig. 6.

Detection probability by each device, which is expressed S(t) for seal, O(t) for optical monitor, R(t) for radiation monitor and so on, is denoted to $P^{I}_{ijkl}(m)$ in the calculation. This is the detection probability of nuclear material at amount m by each CS device at position l, which is installed in the "k"th stage along possible diversion paths from the "j"th box. If the reliability of each device is not enough, the plural numbers of the device will be installed as a group to increase the reliability as a whole. The reliability of the single device or the group at a certain position is expressed as P^{II}_{ijkl}, so that the detection probability of this position is given as P^{I}_{ijkl}.

$P^{II}_{ijkl} = P^{III}_{ijkl}$.

There are l kinds of diversion paths by each stage k for the material to be diverted from box j. Formula of the 4th step in Fig. 6 gives the detection probability when the material is diverted from a certain box to the outside through combination of the easiest paths at every stage.

Formula of the 5th step shows that detection probability of a whole facility is governed by the lowest value of probability among that obtained from all boxes. Up to this step, the case of a single theft is described, while in the 6th step formula $P^{V}(t)_{M}$ expresses the detection probability for a certain amount of nuclear material M, which can be obtained by i times of thefts.

As the similar formula of detection probability, $P^{V}(t)_{M}$, can be obtained in the MA system, detection probability of CS-MA coordinated system against diversion of a certain amount of nuclear material M, is given by:

$$P(t)_{M} = 1 - \{ 1 - P^{V}(t)_{M} \}\{ 1 - P^{VI}(t)_{M} \}.$$

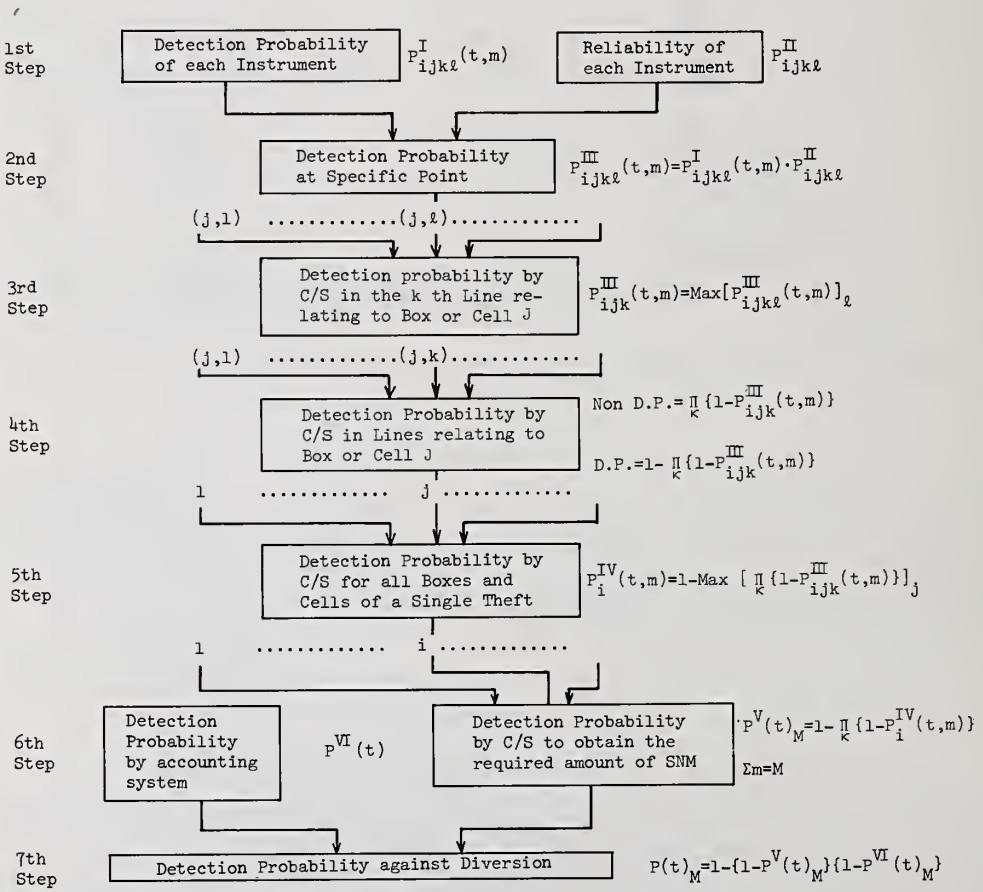

Fig. 6 Calculation Method of Detection Probability

Discussion:

Persiani (ANL):

I know this is a controversial point. I do agree that the coupling of containment/surveillance systems and materials accountancy would add up to a very effective safeguards system. However, I don't quite see containment/surveillance being used as a system to detect diversion. It could detect abnormal flows of material or personnel through certain boundaries. The effectiveness of containment/surveillance will depend on identifying all of the diversion paths, which to me appears to be an exhaustive, if not impossible, effort. Materials accountancy, on the other hand, is independent of diversion paths. So when you formulate functions as you indicated, the weighting of these probabilities that you associate with containment/surveillance and that you associate with materials accountancy must really be different, if not uncorrelated. I don't know how you come up with a function.

Mr. Ishii (Mitsubishi Metal Corp.):

To make the containment/surveillance effective, I think it is necessary to consider it from the design state of the process. Doing that, I think we can get satisfactory results by applying containment/surveillance systems. Many people have said that the important point is how to overcome the safeguards problem for large-throughput facilities. Of course, I know that I cannot give you the complete answer now, but with this effort, I think we can make progress towards that point.

LIST OF ATTENDEES
November 26-30, 1979, Kiawah Island

Adams, G. Anthony
Westinghouse-Advanced Reactor Div.
Cheswick Avenue
Cheswick, PA 15024
412/363-8700, X641

Ahmed, Hassan J.
Westinghouse NFD
P.O. Drawer R
Columbia, SC 29250

Alvar, Kenneth R.
IRT Corporation
7650 Convoy Court
San Diego, CA 92138

Armento, W. J.
Oak Ridge National Laboratory
P.O. Box X
Oak Ridge, TN 37830
615/574-6547

Atwater, Henry F.
Los Alamos Scientific Laboratory
P.O. Box 1663, MS 562
Los Alamos, NM 87545
505/667-4724

Baloga, Stephen M.
National Bureau of Standards
Building 245
Washington, DC 20234
301/353-3691 (DOE)

Bambas, K. J.
Allied-General Nuclear Services
P.O. Box 87
Barnwell, SC 29812

Bäumel, Siegfried
Dornier System GmbH
Postfach 1360
7990 Friedrichshafen
West Germany

Baxman, Horace R.
Los Alamos Scientific Laboratory
P.O. Box 1663
Los Alamos, NM 87545
505/667-5864

Behrens, James W.
National Bureau of Standards
Rad. Physics B119
Washington, DC 20234
301/921-2386

Belew, Wendell L.
U.S. Department of Energy
Savannah River Operations Office
P.O. Box A
Aiken, SC 29801
(FTS) 239-3856

Bennett, J. E.
Riggs Hall-Elec. & Computer Eng.
Clemson University
Clemson, SC 29631
803/656-3376

Beyerlein, Adolph
Clemson University
Dept. of Chemistry & Geology
Clemson, SC 29631
803/656-3490

Beyrich, Wolfgang
Nuclear Research Center Karlsruhe
Postfach 3640
7500 Karlsruhe
Fed. Rep. of Germany

Biggerstaff, G. E.
Nuclear Fuel Services
Box 218
Erwin, TN 37650
615/743-9141

Bingham, Carleton D.
U.S. DOE-New Brunswick Lab.
9800 South Cass Ave.
Argonne, IL 60439
312/972-2446

Blakeman, Edward D.
Union Carbide Corporation
Oak Ridge National Lab.
Bldg. 3500, X-10
Oak Ridge, TN 37830
605/574-4670

Bostick, Debra T.
Oak Ridge National Lab.
Analytical Chemistry Div.
Oak Ridge, TN 37830
615/574-4920

Bowersox, David F.
Los Alamos Scientific Lab.
P.O. Box 1663, MS 505
Los Alamos, NM 87545
505/667-2327

Bowman, Charles D.
National Bureau of Standards
Rad. Physics B119
Washington, DC 20234
301/921-2234

Brauer, Fred P.
Battelle NW Laboratory
P.O. Box 999
Richland, WA 99352
509/942-3722

Brodda, Bert G.
Nuclear Research Center
Juelich GMBH/ICT
P.O. Box 1913, D-5170 Juelich
Federal Republic of Germany

Brumbach, Stephen B.
ANL
Box 2528
Idaho Falls, ID 83901
208/526-7506

Brutus, André A.
Compagnie Générale des Matières
Nucléaires Establishment de Marcoule
B.P. 170, Bagnols-sur-CEZE
France 30200

Busquet, Pierre
CEA
75 Rue Dutot
Paris, France F7,5015

Camp, David C.
Lawrence Livermore Laboratory
University of California
Livermore, CA 94550
(FTS) 532-6680

Campbell, Milton H.
Exxon Nuclear Company
12119 Beech
Richland, WA 99352
509/375-7309

Canada, Thomas R.
Los Alamos Scientific Lab.
P.O. Box 1663, MS 539
Los Alamos, NM 87545
505/677-6779

Canody, Karen
Babcock & Wilcox CNFP
P.O. Box 800
Lynchburg, VA 24505
804/384-5111, X6202

Carpenter, B. Stephen
National Bureau of Standards
Physics Bldg., Room B320
Washington, DC 20234
301/921-3868

Casabona, Lewis F.
Teledyne-Isotopes
50 Van Buren Avenue
Westwood, NJ 07675
201/664-7070

Cathey, Susan S.
DuPont Corp.
Savannah River Plant
Aiken, SC 29801
803/450-4245

Chanda, R. N.
Rockwell-Rocky Flats
Box 464
Golden, CO 80401
303/497-2727

Chastagner, P.
DuPont Corp.
Savannah River Plant
Aiken, SC 29801
803/725-3293

Cheng, Yu-Tarng
National Bureau of Standards
Reactor A106
Washington, DC 20234
301/921-3634

Chiles, M. M.
Oak Ridge National Lab.
P.O. Box X, Bldg. 3500, MS 5
Oak Ridge, TN 37830
615/574-5603

Chinault, John
Westinghouse NFD
112 Lamar Lane
W. Columbia, SC 29169
776-2610

Clay, W. T.
Oak Ridge National Lab.
P.O. Box X
Oak Ridge, TN 37830
615/574-5600

Cobb, Donald D.
Los Alamos Scientific Lab.
P.O. Box 1663, MS 541
Los Alamos, NM 87545
505/667-7777

Cooper, John H.
Oak Ridge National Lab.
P.O. Box X
Oak Ridge, TN 37830
615/574-7063

Cowder, Leo
Los Alamos Scientific Lab.
P.O. Box 1663, MS 540
Los Alamos, NM 87545
505/667-6141

Croarkin, Mary C.
National Bureau of Standards
Physics A341
Washington, DC 20234
301/921-2805

Cullington, Geoff R.
Commission of European Communities
Kirchberg, Luxembourg
Great Britain
352/4301-2282

Cuypers, Marc
Commission of European Communities
Joint Research Centre, CEC
ISPRA, Belgium
0332/780135

DeBievre, Paul
C.B.N.M.
B-2440, Geel
Belgium
32-14-589421

De Montmollin, J. M.
Sandia Labs - Div. 1760A
P.O. Box 5800
Albuquerque, NM 87185
505/264-7682

Dempsey, Thomas J.
Princeton Gamma Tech.
Box 641
Princeton, NJ 08540
609/924-7310

Dodgen, Mary S.
DuPont Corp.
Savannah River Plant
Aiken, SC 29801
803/725-2699

Dowdy, E. J.
Los Alamos Scientific Lab.
9910 Walker House Road, Apt. #4
Gaithersburg, MD 20760
301/353-3362

East, Larry V.
Canberra Industries, Inc.
70 Gracey Avenue
Meriden, CT 06450
203/238-2351

Eccleston, G. W.
Los Alamos Scientific Lab.
P.O. Box 1663, MS 540
Los Alamos, NM 87545
505/677-2185

Eddelmon, Joe D.
Pulcir, Inc.
P.O. Box 357
Oak Ridge, TN 37830
615/483-6358

Edelson, Martin
Ames Laboratory
29 Spedding-Iowa State Univ.
Ames, IA 50011
515/294-4922

Ehinger, Michael H.
Allied General Nuclear Services
P.O. Box 87
Barnwell, SC 29812

Ellis, John H.
Allied General Nuclear Services
P.O. Box 87
Barnwell, SC 29812
259-1711

Embry, Gene
EGH ORTEC
Route 1
Morrisville, NC 27567
919/467-8028

Erkkila, Bruce H.
Los Alamos Scientific Lab.
Los Alamos, NM 87545
505/667-6202

Fager, Jon E.
Battelle Northwest
P.O. Box 999
320 Bldg., 300 Area
Richland, WA 99352
509/942-3722

Fainberg, Anthony
Brookhaven National Lab.
197-C
Upton, NY 11973

Fehlau, Paul E.
Los Alamos Scientific Lab.
P.O. Box 1663, MS 562
Los Alamos, NM 87545
505/667-5372

Fellers, Curtis L.
Monsanto
Mound Avenue
Miamisburg, OH 45342
513/865-3689

Filby, Evan E.
Exxon Nuclear Idaho
P.O. Box 2800
Idaho Falls, ID 83401
208/526-3748

Fleissner, John G.
Monsanto Corp.
Mound Avenue
Miamisburg, OH 45342
513/865-3766

Fleming, Thomas B.
Reutor Stokes, Inc.
7755 Holyowe Drive
Hudson, OH 44236
216/475-3434

Franklin, Michael T.
EURATOM
Bat. 36, EURATOM
21020 ISPRA
Prov. Varese
Italy

Freeman, Brian P.
U.S. DOE
9800 S. Cass Avenue, D-350
Argonne, IL
312/972-2466

Garner, Ernest L.
National Bureau of Standards
Room A219, Chemistry Bldg.
Washington, DC 20234
301/921-2078

Geldard, John F.
Clemson University
Dept. of Chem. & Geol.
Clemson, SC 29631
803/656-3089

George, Kenneth D.
Union Carbide Corp.
P.O. Box 324
Tuxedo, NY 10987
914/351-2131

Goldberg, Paul F.
National Research Council
1717 H Street, N.W.
Washington, DC 20555
202/634-3295

Gordon, David M.
Brookhaven National Lab.
Building 197
Upton, NY 11973
516/345-2943

Goris, Paul
Westinghouse Hanford
P.O. Box 1970
Richland, WA 99352
509/942-3427

Gottschalk, Gary P.
Westinghouse Hanford
2152 Baker
Richland, WA 99352
509/942-3716

Gould, Donald J.
Sandia Labs
Albuquerque, NM 87185
505/264-3435

Green, Bob E.
Canberra
6729 Bonneville Drive
Knoxville, TN 37921
615/521-1964

Green, Leon
Brookhaven National Lab.
Cornell Ave., Bldg. 197C
Upton, NY 11973
516/345-2944

Guay, Pm
Service CM-Boite Postale No. 14
Dijon
France

Haas, F. X.
Rockwell International
Systems Energy Group
P.O. Box 464
Golden, CO 80401

Hakkila, E. A.
Los Alamos Scientific Lab
P.O. Box 1663, MS 541
Los Alamos, NM 87545
505/677-7777

Hamilton, Richard A.
Rockwell Hanford Operations
234-5 Bldg., 200 West Area
Richland, WA 99352
509/942-2584

Hamman, Robert D.
Allied Gen. Nucl. Services
236 Fairway Lane
Barnwell, SC 29812
803/259-1711, X466

Harlan, R. A.
Rockwell International
Energy Systems Group
P.O. Box 464
Golden, CO 80401
303/497-4751

Hartwell, Jack K.
EG&G Idaho, Inc.
TRA652
Idaho Falls, ID 83401
208/526-4187

Hawkins, Ron L.
NUSAC, Inc.
7926 Jones Branch Drive
McLean, VA 22101
703/893-6004

Heinberg, Milton
Los Alamos Scientific Lab.
P.O. Box 1663, MS 324
Los Alamos, NM 87545
505/667-5886

Henderson, B. C.
Allied General Nuclear Services
P.O. Box 847
Barnwell, SC 29812
803/259-1781

Hess, W. Bascom
DuPont Corp.
Savannah River Plant, Bldg. 232-H
Aiken, SC 29801
803/725-6712

Hoffmann, Ronald L.
Babcock & Wilcox
P.O. Box 1260
Lynchburg, VA 24505
804/384-5111

Holland, Michael K.
New Brunswick Laboratory
9800 South Cass Ave., D-350
Argonne, IL 60525
312/972-2466

Hopwood, W. H. (Jr.)
Union Carbide Corp.
P.O. Box Y
Oak Ridge, TN 37830
615/574-2421

Hsue, Sin Tao
Los Alamos Scientific Lab.
P.O. Box 1663, MS 540
Los Alamos, NM 87545
505/677-6141

Hsue, Faye
Los Alamos Scientific Lab.
P.O. Box 1663
Los Alamos, NM 87545
505/667-2334

Hudgens, Claude R.
Mound Laboratory
Miamisburg, OH 45342
503/865-3303

Hurt, Robert D.
Union Carbide Corp.
Oak Ridge National Lab.
Bldg. 7601
Oak Ridge, TN 37830
615/574-7137

Ikawa, Koji
JAERI
Tokai-Mura, Naka-Gun
Ibaraki-Ken
Japan 319-11

Ishii, Tamotsu T.I.
Mitsubishi Metal Corp. 100
1-5-2, Ohtemachi, Chiyodaku
Tokyo, Japan
03-270-8451

Jackson, Darryl D.
Los Alamos Scientific Lab.
P.O. Box 1663, MS 740
Los Alamos, NM 87545
505/667-6308

Jain, Mahavir
Los Alamos Scientific Lab.
Q3, MS 539
Los Alamos, NM 87545
505/667-6202

Jenkins, L. M.
Oak Ridge National Lab.
Box X, Bldg. 3019
Oak Ridge, TN 37830

Jean, Guy Pierre
Commissariat a l'Energie Atomique
B.P. No. 6
92260 Fontenay-aux-Roses
France

John, Dr. Joseph
IRT Corp.
P.O. Box 80817
San Diego, CA 92138
214/565-7171

Johnsen, Edwin G.
National Bureau of Standards
Technology A130
Washington, DC 20234
301/921-3475

Johnson, C. E.
Exxon Nuclear Idaho
P.O. Box 2800
Idaho Falls, ID 83401
208/526-2281

Johnson, S. J.
Rockwell Hanford Operations
222-S, 200-W
Richland, WA 98352
509/942-2452

Jones, Frank E.
National Bureau of Standards
Physics B252
Washington, DC 20234
301/921-2148

Joseph, Charles
AGNS
P.O. Box 87
Barnwell, SC 29812
803/259-1711

Joy, Donald R.
U.S. Nuclear Regulatory Comm.
SS-881
Washington, DC 20555
301/427-4043

Keepin, G. Robert
Los Alamos Scientific Lab.
MS 550
Los Alamos, NM 87545

Kotani, Fumio
Nuclear Materials Control Center
2-3-4 Akasaka Minato-ku
Tokyo
Japan
03-583-5355

Larsen, Robert P.
Argonne National Lab.
1150 Oak Hill Road
Downers Grove, IL 60515
312/972-4173

Lee, David M.
Los Alamos Scientific Lab.
P.O. Box 1663, MS 537
Los Alamos, NM 87545
505/667-2183

Lemming, John F.
Monsanto Research Co.
Mound Lab.
Miamisburg, OH 45342
513/865-3494

Lewis, Kenneth
U.S. Dept. of Energy
9800 S. Cass Ave.
Argonne, IL 60439
312/972-2461

Li, T. K.
Los Alamos SScientific Lab.
MS 539
Los Alamos, NM 87545
505/667-6202

Lipsett, John J.
AECL Research Co.
CRNL, Stn. 30
Chalk River, Ontario K0J1P0
Canada
613/584-2651

Lynch, R. Larry
NUSAC
7426 Jones Branch Dr.
McLean, VA 22102
703/893-6004

Lysne, Eric J.
Norland/Ino. Tech.
3001 Velkommen WA
Stoughton, WA
414/563-8456

MacDougall, C. Sue
Oak Ridge National Lab.
P.O. Box X
Oak Ridge, TN 37830
615/574-4878

MacMurdo, Kenneth W.
DuPont Corp.
Savannah River Plant
Aiken, SC 29801

Mallett, Gavin R.
General Electric Co.
P.O. Box 780
Wilmington, NC 28402
919/343-5659

Marsden, Philip S.S.F.
UKAEA, NMACT
Bldg. 10-30, AERE, Harwell
Didcot, Oxfordshire OX11 ORA
England
0234-24141

Martin, Walter G.
USNRC, Region I
Office of Inspection & Enforcement
631 Park Avenue
King of Prussia, PA 19406
215/488-1230

Mason, D. L.
Union Carbide Corp.
Nuclear Division
P.O. Box Y
Oak Ridge, TN 37830

McDowell, W. Jack
Union Carbide Corp.
P.O. Box X
Oak Ridge National Lab.
Oak Ridge, TN 37921
615/574-6714

Menlove, Howard O.
Los Alamos Scientific Lab.
P.O. Box 1663, MS 537
Los Alamos, NM 87545
505/667-6754

Meyers, Thomas
Nuclear Data, Inc.
Golf at Meacham Rds.
Schaumburg, IL 60196
312/884-3627

Michel, Charles J.
Nuclear Fuel Services, Inc.
P.O. Box 218
Erwin, TN 37650
615/743-9141

Mitchell, Wanda G.
Department of Energy
2208 Prentiss Dr., #312
Downers Grove, IL 60515
312/972-2493

Molen, Gary F.
Allied General Nuclear Services
P.O. Box 87
Barnwell, SC 29812
803/259-1711

Mosley, W. C.
DuPont Corp.
Savannah River Lab.
Aiken, SC 29801

Mrus, Stanley T.
Burns & Roe Industrial Svcs.
283 Route 17 South
Paramus, NJ 07652
201/265-8710

Mullins, W. T.
Union Carbide Corp.
Oak Ridge Gaseous Diffusion Plant
P.O. Box P, MS 458
Oak Ridge, TN 37830
615/574-9616

Nakano, Hiromasa
PNC
202/338-3770

Nartowicz, Robert F.
Pulcir
2551 West Beltline
Middleton, WI 53562
608/831-6511

Nilson, Roy
Exxon Nuclear
2955 Geo. Wash. Way
Richland, WA 99352
509/375-7286

Oh, Ki Hoon
Los Alamos Scientific Lab.
P.O. Box 1663, MS 537
Los Alamos, NM 87545

Olson, William M.
Los Alamos Scientific Lab.
P.O. Box 1663
Los Alamos, NM 87545
505/667-2336

Parker, John E.
Savannah River Plant
Aiken, SC 29801
803/725-4245

Parnell, Robert I.
General Electric Co.
P.O. Box 780
Wilmington, NC 28401
919/343-6007

Persiani, Paul J.
Argonne National Laboratory
245 S. Charles St.
Naperville, IL 60540
312/972-4870

Peters, Frank
NSF
Box 218
Erwin, TN 37650
615/743-9141, X138

Pietri, Charles E.
U.S. DOE - NBL
8253 Lakeside Drive
Downers Grove, IL 60515
312/972-2448

Piper, Dennis G.
IRT Corporation
P.O. Box 80817
San Diego, CA 92071
714/565-7171, X334

Plummer, Kenneth E.
Allied General Nuclear Svcs.
P.O. Box 87
Barnwell, SC 29812
803/259-1711

Ragan, George L.
Oak Ridge National Lab.
103 Albright Rd.
Oak Ridge, TN 37830
615/574-5571

Ramalho, Antonio J.G.
IAEA
Vienna International Centre
P.O. Box 200, A-1400
Vienna
Austria
2360-1959

Reed, William P.
National Bureau of Standards
Materials B354
Washington, DC 20234
301/921-2761

Reilly, T. Douglas
Los Alamos Scientific Lab.
P.O. Box 1663, MS 537
Los Alamos, NM 87545
505/667-6754

Robertson, Baldwin
National Bureau of Standards
FM 105
Washington, DC 20234
301/921-3681

Roche, C. T.
Argonne National Laboratory
9700 S. Cass Avenue
Argonne, IL 60439
312/972-3431

Rodenburg, W. William
Monsanto Research Corp.
Mound Laboratory
Miamisburg, OH 45342
513/865-3136

Rodrigues, Claudio
Instituto de Pesquisas
Energeticas en Nuclear
Sao Paulo
Brazil
211-6011

Rogers, Donald R.
Monsanto Corp.
P.O. Box 32
Miamisburg, OH 45459
513/865-3754

Ruhter, Wayne D.
Lawrence Livermore Lab.
Mail Code L-233
Livermore, CA 94550
(FTS) 532-5762

Russo, Phyllis
Los Alamos Scientific Lab.
P.O. Box 1663, MS 540
Los Alamos, NM 87545
505/667-2160

Sanborn, Jonathan B.
Brookhaven National Lab.
Building 197
Upton, NY 11973
514/345-3698

Savage, Allen L.
Combustion Engineering R 21-A
Hermatite, MO 63047
319/296-5640

Schleicher, Hans W.
Commission of European Community
Luxemburg-Kirchberg
Luxemburg
Germany
43011

Schrack, Roald A.
National Bureau of Standards
Rad. Physics B119
Washington, DC 20234
301/921-2677

Shipley, James P.
Los Alamos Scientific Lab.
P.O. Box 1663, MS 541
Los Alamos, NM 87545
505/667-7777

Sinclair, R. E.
Nuclear Data, Inc.
Rt. 1, Box 92
Six Mile Ridge Road
Cumming, GA 30130
404/887-0274

Skinner, Albert J.
DOE-SROO
P.O. Box A
Aiken, SC 29801
(FTS) 239-2064

Smathers, Douglas C.
Sandia Laboratories
P.O. Box 5800
Albuquerque, NM 87185
505/264-4941

Smith, Craig S.
USDOE
P.O. Box 13523
Albuquerque, NM 87192
(FTS) 264-8254

Smith, Gerald W.
Sandia Laboratories
Albuquerque, NM 87185
505/264-6452

Smith, Hastings
Los Alamos Scientific Lab.
P.O. Box 1663, MS 540
Los Alamos, NM 87545
505/667-6141

Smith, Julia M.
Brookhaven National Lab.
Building 197
Upton, NY 11973
516/345-2942

Smith, Warren H.
Monsanto
Mound Lab.
Miamisburg, OH 45342
513/865-3572

Sprinkle, James K.
Los Alamos Scientific Lab.
P.O. Box 1663, MS 540
Los Alamos, NM 87545
505/667-7903

Stevens, Dwane
Pulcir
501 Oak St.
Sweetwater, TX 79556
915/235-5494

Stirling, A. J.
Atomic Energy of Canada
Chalk River Nuclear Lab.
Chalk River, Ontario
Canada K0J IJ0

Strohm, Walter W.
Monsanto
Mound Lab.
Miamisburg, OH 45342
513/865-3462

Studley, Robert V.
E. I. duPont de Nemours
1108 Parsons Lane
Aiken, SC 29801
803/725-2018 or 2876

Suda, Sylvester C.
Brookhaven National Lab.
Building 197
Upton, NY 11973
516/345-2925

Suwala, Matthew C.
Babcock & Wilcox - Apollo
609 N. Warren Avenue
Apollo, PA 15613
412/842-0111, X680

Trahey, Nancy M.
DOE - NBL
9800 S. Cass Ave.
Bldg. 350
Argonne, IL 60439
312/972-2485

Turel, Stanley P.
National Research Council
Office of Standards Development
Washington, DC 20555
301/443-5904

Ulbricht, William H.
U.S. DOE - NBL
9800 S. Cass Ave.
Argonne, IL 60439
312/972-2490

Van Raaphorst, J. G.
ECN
Westerduinwec 3
Petten (N.H.)
The Netherlands 1755ZG

Voeks, Anna M.
DOE - NBL
9800 S. Cass Ave.
Bldg. 350
Argonne, IL 60439
312/972-2487

Voss, Frank S.
Goodyear Atomic Corp.
P.O. Box 628
Piketon, OH 45661
614/289-2331

Vronich, John J.
Argonne National Lab.
9700 S. Cass Ave.
Argonne, IL 60439
312/972-3435

Wachter, John W.
Oak Ridge National Lab.
P.O. Box X, Bldg. 7601
Oak Ridge, TN 37830
615/574-7137

Wagner, Raymond P.
Los Alamos Scientific Lab.
P.O. Box 1663, MS 505
Los Alamos, NM 87545
505/667-3172

Walker, Alan C.
U.S. Dept. of Energy
P.O. Box 550
Richland, WA 99352
(FTS) 444-6918

Walker, Raymond L.
Oak Ridge National Lab.
P.O. Box Y
Oak Ridge, TN 37830
615/574-2449

Walsh, William P.
Battelle Pacific NW Lab.
P.O. Box 999
Richland, WA 99352
509/375-2818

Walton, Roddy B.
Los Alamos Scientific Lab.
P.O. Box 1663, MS 540
Los Alamos, NM 87545
505/667-4393

Weh, Rudolf
Wiederaufarbetung von
Kernbrennstonen mbH
Postfach 1407
3000 Hannover 1
Fed. Rep. of Germany

Weinstock, Eugene V.
Brookhaven National Lab.
197-C
Upton, NY 11973
516/345-2943

Yamamoto, Tadashi
National Bureau of Standards
Inorganic Analytical Res. Div.
Washington, DC 20234
301/921-2142

Zimmer, W. H.
EG&G Ortec
100 Midland Road
Oak Ridge, TN 37830
615/842-4411

Zook, Alan Creig
New Brunswick Lab., DOE
1404 Canterbury
Joliet, IL 60436
312/972-2480

Zucker, M. S.
Brookhaven National Lab.
197
Upton, NY 11973
516/345-2929

U.S. DEPT. OF COMM. BIBLIOGRAPHIC DATA SHEET	1. PUBLICATION OR REPORT NO. NBS SP 582	2. Gov't. Accession No.	3. Recipient's Accession No.

4. TITLE AND SUBTITLE

Measurement Technology for Safeguards and Materials Control

5. Publication Date
June 1980

6. Performing Organization Code

7. AUTHOR(S) (Editors)
Thomas R. Canada (LASL) and B. Stephen Carpenter (NBS)

8. Performing Organ. Report No.

9. PERFORMING ORGANIZATION NAME AND ADDRESS

NATIONAL BUREAU OF STANDARDS
DEPARTMENT OF COMMERCE
WASHINGTON, DC 20234

10. Project/Task/Work Unit No.

11. Contract/Grant No.

12. SPONSORING ORGANIZATION NAME AND COMPLETE ADDRESS *(Street, City, State, ZIP)*
American Nuclear Society (ANS) Isotopes and Radiation Division; Institute of Nuclear Materials Management (INMM); and NBS

13. Type of Report & Period Covered
Conference Proceedings 1979

14. Sponsoring Agency Code

15. SUPPLEMENTARY NOTES

Library of Congress Catalog Card Number: 80-600072

☐ Document describes a computer program; SF-185, FIPS Software Summary, is attached.

16. ABSTRACT *(A 200-word or less factual summary of most significant information. If document includes a significant bibliography or literature survey, mention it here.)*

This publication contains the proceedings of the American Nuclear Society's Topical Conference entitled, Measurement Technology for Safeguards and Materials Control. The meeting, co-sponsored by the Office of Measurements for Nuclear Technology of the National Bureau of Standards and the Institute of Nuclear Materials Managemnt, was held at Kiawah Island, South Carolina, on November 26-30, 1979. The objective of the conference was to provide a forum for reports of current work and for information exchanges on technical subjects that are relevant to measurement technology for nuclear safeguards and material control.

The presentations were applications oriented and offered a good balance between chemical analysis, nondestructive assay techniques, bulk measurement techniques, inspection techniques, and integrated systems for material measurements and control. Reports discussing preparation and use of reference materials and measurement traceability were included. Examples of measurement requirements and techniques used for both national and international safeguards are given. Approaches to various analysis of materials throughout the fuel cycle from enrichment and fuel fabrication to spent fuel and reprocessing are considered.

17. KEY WORDS *(six to twelve entries; alphabetical order; capitalize only the first letter of the first key word unless a proper name; separated by semicolons)*
Accountability; accuracy; gamma spectrometry; mass spectrometry; nondestructive assay; nuclear safeguards; precision; reference materials; special nulcear materials; x-ray fluorescence.

18. AVAILABILITY ☒ Unlimited

☐ For Official Distribution. Do Not Release to NTIS

☒ Order From Sup. of Doc., U.S. Government Printing Office, Washington, DC 20402, _____

☐ Order From National Technical Information Service (NTIS), Springfield, VA. 22161

19. SECURITY CLASS (THIS REPORT)
UNCLASSIFIED

21. NO. OF PRINTED PAGES
769

20. SECURITY CLASS (THIS PAGE)
UNCLASSIFIED

22. Price
$11.00

USCOMM-DC

NBS TECHNICAL PUBLICATIONS

PERIODICALS

JOURNAL OF RESEARCH—The Journal of Research of the National Bureau of Standards reports NBS research and development in those disciplines of the physical and engineering sciences in which the Bureau is active. These include physics, chemistry, engineering, mathematics, and computer sciences. Papers cover a broad range of subjects, with major emphasis on measurement methodology and the basic technology underlying standardization. Also included from time to time are survey articles on topics closely related to the Bureau's technical and scientific programs. As a special service to subscribers each issue contains complete citations to all recent Bureau publications in both NBS and non-NBS media. Issued six times a year. Annual subscription: domestic $17; foreign $21.25. Single copy, $3 domestic; $3.75 foreign.

NOTE: The Journal was formerly published in two sections: Section A "Physics and Chemistry" and Section B "Mathematical Sciences."

DIMENSIONS/NBS—This monthly magazine is published to inform scientists, engineers, business and industry leaders, teachers, students, and consumers of the latest advances in science and technology, with primary emphasis on work at NBS. The magazine highlights and reviews such issues as energy research, fire protection, building technology, metric conversion, pollution abatement, health and safety, and consumer product performance. In addition, it reports the results of Bureau programs in measurement standards and techniques, properties of matter and materials, engineering standards and services, instrumentation, and automatic data processing. Annual subscription: domestic $11; foreign $13.75.

NONPERIODICALS

Monographs—Major contributions to the technical literature on various subjects related to the Bureau's scientific and technical activities.

Handbooks—Recommended codes of engineering and industrial practice (including safety codes) developed in cooperation with interested industries, professional organizations, and regulatory bodies.

Special Publications—Include proceedings of conferences sponsored by NBS, NBS annual reports, and other special publications appropriate to this grouping such as wall charts, pocket cards, and bibliographies.

Applied Mathematics Series—Mathematical tables, manuals, and studies of special interest to physicists, engineers, chemists, biologists, mathematicians, computer programmers, and others engaged in scientific and technical work.

National Standard Reference Data Series—Provides quantitative data on the physical and chemical properties of materials, compiled from the world's literature and critically evaluated. Developed under a worldwide program coordinated by NBS under the authority of the National Standard Data Act (Public Law 90-396).

NOTE: The principal publication outlet for the foregoing data is the Journal of Physical and Chemical Reference Data (JPCRD) published quarterly for NBS by the American Chemical Society (ACS) and the American Institute of Physics (AIP). Subscriptions, reprints, and supplements available from ACS, 1155 Sixteenth St., NW, Washington, DC 20056.

Building Science Series—Disseminates technical information developed at the Bureau on building materials, components, systems, and whole structures. The series presents research results, test methods, and performance criteria related to the structural and environmental functions and the durability and safety characteristics of building elements and systems.

Technical Notes—Studies or reports which are complete in themselves but restrictive in their treatment of a subject. Analogous to monographs but not so comprehensive in scope or definitive in treatment of the subject area. Often serve as a vehicle for final reports of work performed at NBS under the sponsorship of other government agencies.

Voluntary Product Standards—Developed under procedures published by the Department of Commerce in Part 10, Title 15, of the Code of Federal Regulations. The standards establish nationally recognized requirements for products, and provide all concerned interests with a basis for common understanding of the characteristics of the products. NBS administers this program as a supplement to the activities of the private sector standardizing organizations.

Consumer Information Series—Practical information, based on NBS research and experience, covering areas of interest to the consumer. Easily understandable language and illustrations provide useful background knowledge for shopping in today's technological marketplace.

Order the **above** *NBS publications from: Superintendent of Documents, Government Printing Office, Washington, DC 20402.*

Order the **following** *NBS publications—FIPS and NBSIR's—from the National Technical Information Services, Springfield, VA 22161.*

Federal Information Processing Standards Publications (FIPS PUB)—Publications in this series collectively constitute the Federal Information Processing Standards Register. The Register serves as the official source of information in the Federal Government regarding standards issued by NBS pursuant to the Federal Property and Administrative Services Act of 1949 as amended, Public Law 89-306 (79 Stat. 1127), and as implemented by Executive Order 11717 (38 FR 12315, dated May 11, 1973) and Part 6 of Title 15 CFR (Code of Federal Regulations).

NBS Interagency Reports (NBSIR)—A special series of interim or final reports on work performed by NBS for outside sponsors (both government and non-government). In general, initial distribution is handled by the sponsor; public distribution is by the National Technical Information Services, Springfield, VA 22161, in paper copy or microfiche form.

BIBLIOGRAPHIC SUBSCRIPTION SERVICES

The following current-awareness and literature-survey bibliographies are issued periodically by the Bureau:

Cryogenic Data Center Current Awareness Service. A literature survey issued biweekly. Annual subscription: domestic $25; foreign $30.

Liquefied Natural Gas. A literature survey issued quarterly. Annual subscription: $20.

Superconducting Devices and Materials. A literature survey issued quarterly. Annual subscription: $30. Please send subscription orders and remittances for the preceding bibliographic services to the National Bureau of Standards, Cryogenic Data Center (736) Boulder, CO 80303.

U.S. DEPARTMENT OF COMMERCE
National Bureau of Standards
Washington, D.C. 20234

OFFICIAL BUSINESS

Penalty for Private Use, $300

POSTAGE AND FEES PAID
U.S. DEPARTMENT OF COMMERCE
COM-215

U.S.MAIL

SPECIAL FOURTH-CLASS RATE
BOOK